AD-785 898

PROCEEDINGS OF THE THIRD INTERNATIONAL CONGRESS ON MARINE CORROSION AND FOULING HELD AT GAITHERSBURG, MARYLAND, ON OCTOBER 2-6, 1972

NATIONAL BUREAU OF STANDARDS

PREPARED FOR
OFFICE OF NAVAL RESEARCH

1974

DISTRIBUTED BY:

NTIS
National Technical Information Service
U. S. DEPARTMENT OF COMMERCE

Best
Available
Copy

AD785 898

Proceedings of the

THIRD INTERNATIONAL CONGRESS ON MARINE CORROSION AND FOULING

October 2-6, 1972
National Bureau of Standards
Gaithersburg, Maryland, U.S.A.

N00014-72-C-0281 NR 306-057

DDC
RECEIVED
SEP 30 1974
B

PREFACE

United States representatives to the Permanent International Committee for Research on Preservation of Materials in the Marine Environment were asked in 1969 if it would be possible for the United States to host the Third International Congress on Marine Corrosion and Fouling. Subsequent official inquiry showed that the United States could serve. This position was confirmed between Monsieur V. Romanovsky, Chairman of the Permanent International Committee, and Dr. Robert F. Acker, speaking for the United States' representatives. The National Bureau of Standards in Gaithersburg, Maryland, was selected as the meeting site.

An Executive Committee was named, key chairmen were appointed, and the business of organizing the essential components of the Congress was initiated late in 1970. A series of monthly meetings through 1971 and 1972 culminated in the gathering of participants and conduct of the Congress in October of 1972.

The fields of corrosion and marine biology are known to overlap significantly in that the only metals resistant to colonization by marine organisms in quiescent sea water are those which corrode and produce toxic corrosion products. Measures taken to prevent the corrosion (such as cathodic protection) cause these metals to foul, and a common antifouling measure -- the electrolytic production of hypochlorous acid -- may alter substantially the corrosive character of sea water. As is reported in several papers of the Third Congress, marine algae may penetrate and cause deterioration of marine coatings and anaerobic bacteria may alter the corrosion behavior of steel in a marine environment. These are examples of the complex interplay between biological factors, corrosion, and the measures used to control both fouling and corrosion. These kinds of interactions document the need for a Congress which included coverage from the sometimes disparate disciplines of biology, chemistry, physics, and engineering.

Several policy decisions were made during the deliberations of the Executive Committee and the Program Committee which are reflected in the format and the content of these Proceedings. First, a decision was made to address problems of marine biology along with the problems of physical corrosion, as described above. Second, investigators were encouraged to submit papers dealing with both fundamental and applied kinds of research. Third, the manuscripts were prepared in a format ready for the printer's camera. The photo-offset method of printing was selected in order to speed delivery and reduce cost of the publication. Finally, discussions which followed the individual papers were organized in two different ways. One type of discussion is unabridged in this volume and shows the name of the discussant or discussants. The other form is a summary of more lengthy discussion; it omits names of discussants and is condensed from tape recordings and notes.

The members of the Executive Committee feel that their efforts in planning and organizing the Congress have been amply rewarded. Knowledge of biological and physical processes in the ocean have been enhanced, along with understanding of practical problems and solutions. Most important, ties between colleagues throughout the world have been strengthened. Through sharing of ideas, through discussion of common concerns, new bonds of friendship have been formed.

Robert F. Acker
B. Floyd Brown
John R. DePalma
Warren P. Iverson

Editors of the Proceedings

ACKNOWLEDGEMENTS

The Executive Committee gratefully acknowledges contributions of funds toward support of the Third International Congress on Marine Corrosion and Fouling from the following sponsors:

American Iron and Steel Institute
American Wood Preservers Institute
Maritime Administration
M & T Chemicals, Inc.
National Bureau of Standards
Naval Facilities Engineering Command
Naval Oceanographic Office
Naval Ships Systems Command
Office of Naval Research
Oceanographer of the Navy
U.S. Coast Guard

The Committee expresses its appreciation for staff, secretarial, and technical support from the above as well as the following organizations:

American Society for Testing and Materials
Centre Belge d 'Etude de la Corrosion,
Brussels
Centre de Recherches et d'Etudes Oceanographiques,
Paris
Marine Technology Society
National Association of Corrosion Engineers
Northwestern University
Society for Industrial Microbiology
Society of Naval Architects and Marine Engineers

The members of the Executive Committee thank Mr. W.W. Kirk of the Sea Horse Institute and the International Nickel Company, Wrightsville Beach, North Carolina, for mailing of announcements; Mrs. Julian Anastasio and Mrs. John H. Ring of the Bureau of Standards for typing, correcting, and assembling of manuscripts; Mrs. Gordon H. Rosberg, Jr. of Northwestern University for preparing agendas for meetings and typing all materials exclusive of the manuscripts in camera-ready form; Mrs. Elio Passaglia and Mrs. Edward L. Brady for scheduling and arranging special social events; Miss Kathy J. Crosby and others from the National Bureau of Standards for their services in registration, publication of a list of participants, and in handling of a myriad of details in connection with actual conduct of the Congress.

Those who served with Dr. B. Floyd Brown wish to particularly acknowledge his contribution to the success of the Congress in conceiving, developing, and producing an outstanding scientific program.



The Executive Committee

Left to right, front row: Sara Torrence, B. Floyd Brown, Ruth D. Turner, Warren P. Iverson, Robert F. Acker, John R. DePalma, Allen C. Jewett
back row: Frederick W. Fink, John D. Costlow, Irving Poretz, Allen L. Alexander, Thomas P. May, Ronald B. Johnson, Robert T. Cook
Absent: Jerome Kruger, Dale Miller, Elio Passaglia, Harry C. Burnett

COMMITTEES

Third International Congress on Marine Corrosion and Fouling

Executive Committee
Co-Chairmen:

Robert F. Acker
Northwestern University

John R. DePalma
Naval Oceanographic Office

Warren P. Iverson
National Bureau of Standards

Allen L. Alexander
Naval Research Laboratory

Allen Jewett
Office of Naval Research

Irving Poretz
Maritime Administration

Jerome Kruger
National Bureau of Standards

Dale Miller
National Association of Corrosion Engineers

Elio Passaglia
National Bureau of Standards

Committees Functioning as Part of the Executive Committee:

Program Committee
Chairman:

B. Floyd Brown
Naval Research Laboratory

John D. Costlow
Duke University

Frederick W. Fink
Battelle Memorial Institute

Thomas P. May
International Nickel Co.

Ruth D. Turner
Harvard University

Arrangements Committee
Co-Chairmen:

Robert T. Cook
National Bureau of Standards

Sara Torrence
National Bureau of Standards

Registration Committee
Chairman:

Harry C. Burnett
National Bureau of Standards

Finance Committee
Chairman:

Ronald B. Johnson
National Bureau of Standards



Dr. John D. Hoffman
Welcoming Address

WELCOMING ADDRESS

TO

THIRD INTERNATIONAL CONGRESS ON MARINE CORROSION AND FOULING

John D. Hoffman

Director, Institute for Materials Research

It is a pleasure to welcome you this morning to the Third International Congress on Marine Corrosion and Fouling. This Congress provides a forum for presenting theoretical and applied information on the technology affecting the corrosion and fouling of materials in the sea. Included are all phases of design, development, applied engineering, and economics, which may influence the construction and operation of ships and underwater installations. It is an area of technology that is of interest to numerous scientific and technical organizations as evidenced by the fact that this forum is co-sponsored by some eight different government agencies with the active support of seven different private professional societies.

We at NBS are particularly pleased to be the host of a forum that is truly international in nature. In looking through the abstracts, I note that over forty of the papers to be presented are by foreign researchers. There are 22 different countries represented among the attendees.

I am also pleased that this forum will cover the complete spectrum of research on marine fouling from that which is very basic to that which is very applied. Your main concern, of course, is with materials used in the marine environment. However, the data and information that will be presented at this meeting could have great impact not only with respect to solving problems concerned with the use of materials in the sea, but also with respect to the use of materials throughout society. The corrosion and fouling of materials affects all of us. We did an issue study here at NBS a few years ago which was concerned with corrosion. We learned that corrosion costs the U. S. economy more than 10 billion dollars a year for consumer products alone. We have all heard stories of disasters which have resulted in the loss of life when structures have failed due to corrosion. Our most notable failure analysis study at NBS involved the analysis of the collapse of the Silver Bridge over the Ohio River in 1967 in which 46 people lost their lives. It was found that stress-corrosion cracking, which resulted in a brittle fracture in an eye-bar of the bridge, may have been the cause of this tragic example of a materials failure.

It is also interesting to note that human body fluids have similar salt content as the sea. The preservation of metallic implant materials in a corrosive environment is indeed a serious problem that is not unrelated to the theme of this forum.

The continuing dialogue provided by forums such as these cannot help but to point the way to some solutions to the very complex problems involved in the preservation of materials and should also help to insure the safe and efficient use of materials in service throughout society.

Once again welcome to you all and have a good meeting.



Monsieur V. Romanovsky
Opening Address

NATIONAL BUREAU OF STANDARDS SPECIAL PUBLICATION , Proceedings of the 3rd International Congress on Marine Corrosion and Fouling, Held October 2-6, 1972, Gaithersburg, Maryland (Issued)

Opening Address

V. Romanovsky

President, Comité International Permanent pour
la Recherche sur la Préservation des
Matériaux en Milieu Marin

Il m'est extrêmement agréable d'avoir l'occasion de parler devant vous.

Il est extrêmement rare qu'un francais soit appelé comme Président International d'un Congrès qui se tient aux Etats-Unis. J'en suis très fier et très honoré.

Je ne pensais pas en 1964, lorsque, sans aucun moyen matériel, j'avais décidé d'organiser le 1er Congrès International sur la Corrosion Marine et les Salissures, que le 3è Congrès aurait lieu à Washington, que mon initiative et mon idée de l'époque auraient, en 8 ans, traversé l'Atlantique.

Lorsqu'il y a 4 ans nous avons, dans le cadre du Comité International Permanent pour la Recherche sur la Préservation des Matériaux en Milieu Marin, accepté la candidature de la délégation des Etats-Unis pour que ce Congrès ait lieu à Washington, nous avons pris cette décision parce qu'il est normal que ce Congrès traverse l'Atlantique, il est normal que l'organisation de ce Congrès accueille tous ceux qui, pour des raisons budgétaires ne peuvent malheureusement pas venir nous voir en Europe.

Je vois que l'assistance ici est déjà très nombreuse, malgré que beaucoup de congressistes ne soient pas encore arrivés.

Je suis persuadé que l'occasion qui nous est ainsi offerte de faire ce Congrès aux Etats-Unis sera excellente, car elle permettra une meilleure compréhension entre ce que l'on fait en Europe et ce que l'on fait aux Etats-Unis.

Après le Congrès de Cannes, le Congrès suivant a eu lieu à Athènes et c'est notre Ami le Professeur SKOULIKIDIS qui a bien voulu se charger d'en faire l'organisation.

Je ne veux pas vous entretenir pendant longtemps, car je vois que l'heure tourne et que, après l'interruption, vous avez encore beaucoup de travail, les communications commencant tout de suite après cette interruption.

Je voudrais simplement vous remercier au nom de notre Comité, appelé à promouvoir l'organisation de ces Congrès; je voudrais donc exprimer ma reconnaissance d'être venus si nombreux et je voudrais souhaiter un plein succès à ces travaux. Je voudrais également, avant de terminer, remercier les organisateurs. Déjà la semaine dernière pendant laquelle nous avons eu des réunions de notre Comité International Permanent, nous avons pu apprécier la qualité de l'organisation, la gentillesse des organisateurs, les attentions délicates dont ces organisateurs nous ont entouré et je suis persuadé, qu'ici, vous allez également apprécier cette gentillesse et cette compétence. Lorsqu'à la fin de ce Congrès, j'aurai l'occasion de

venir devant vous pour quelques instants, prononcer quelques mots pour faire une sorte de synthèse rapide et que j'aurai l'occasion d'exposer les résultats, je ne pourrai certainement pas tarir d'éloges vis-à-vis des organisateurs.

TABLE OF CONTENTS

	Page
Photograph of F.L. LaQue, Keynote Lecturer	1
Corrosion and Fouling. Keynote Lecture by F.L. LaQue	2
A Study of the Importance of the Ship's Hull Condition. An Approach to Improving the Economy of Shipping. A.M. van London	14
Maintaining a Smooth Ship Bottom. R.P. Devoluy, W.H. Briggs, and J. Marra	33
Observations on the Breakdown of Paint Surfaces by Ship-Fouling Algae. B.L. Moss	39
Corrosion and Fouling of an Instrumented Array at a Six Hundred Foot Ocean Site. J.R. Padilla and J.S. Muraoka	48
The Corrosion of Mild Steel by a Marine Strain of Desulfovibrio. W.P. Iverson	61
The Biologist's View of the Teredinidae and their Control. R.D. Turner and J.L. Culliney	83
The Role of the Biologist in Anti-Fouling Research. D.J. Crisp	88
Préparation des Tôles de Construction Naval avant Application de Peintures. G. Dechaux	94
Protection of Steel Piles in a Natural Seawater Environment. Part 1 M. Romanoff, W.F. Gerhold, W.J. Schwerdtfeger, W.P. Iverson, B.T. Anderson, L.L. Watkins, and R.L. Alumbaugh	103
Steelmate - An Underwater Protective Coating for Steel and Wood. P.C. Trussell and T.P. Clark	120
Experiments with Coated Aluminum in Seawater. J.R. Saroyan	125
Corrosion Prevention with Thermal-Sprayed Zinc and Aluminum Coatings. F.N. Longo and G.J. Durmann	158
Electrochemical Properties of Magnesium, Zinc, and Aluminum Galvanic Anodes in Sea Water. T.J. Lennox, Jr.	176
Studies on the Design of Cathodic Protection Systems for Cargo/ Ballast Tanks of Crude Oil Tankers. W. Posch, C. de Waard, and W. Smit	191
Cathodic Protection of Alcan's Port Alfred Harbor Facilities. B.H. Levelton and G. Reidl	202
Steel, Concrete and Salt Water. I. Carnet	215
New Technology for the Preventive Protection and Maintenance of Submerged Reinforced Concrete Structures. A. Montefusco	226

How to Make Use of Corrosion Data. H.H. Uhlig 234

Influence of Minor Alloy Additions on the Passive Behavior of Binary Cu-Ni Alloys. E.D. Verink, Jr., and T.S. Lee, III 241

The Influence of Chromium on the Corrosion Behavior of Copper-Nickel Alloys in Sea Water. D.B. Anderson and K.D. Efird 264

The Influence of Composition upon the Structure and Properties of A Cast Cu-Ni-Mn-Fe-Al Alloy for Marine Applications. B.N. Hall and R.A. Farrar 277

Corrosion Behavior of Copper-Base Alloys with Respect to Seawater Velocity. R.J. Ferrara and J.P. Gudas 285

A Review of Corrosion Resistant Alloy Developments and Recent Marine Corrosion Studies in the United Kingdom Ministry of Defense. J.F.G. Conde, G.C. Booth, J.C. Rowlands and B. Angell 299

No More Dezincification of Hot-Forging and Free-Cutting Brass. The ENKOTAL Principle. B. Lunn and M. Schmidt 311

Condenser Tube Test Apparatus Incorporating Impingement, Crevice, and Heat Transfer Conditions. H.S. Campbell 313

Cathodic Protection, Iron Injection and Chlorination in Marine Heat Exchangers. J.H. Morgan 322

Electrochemical Aids in Corrosion Control in Anti-Fouling and in Scale Prevention. J.B. Cotton 331

Impressed Current Cathodic Protection as Applied to Desalting Plants. G. Dittmeier and P. Byrne 338

Methods of Controlling Marine Fouling in Desalination Plants. D.C. Mangum, B.P. Shepherd, and J.C. Williams 357

Les Bases Electrochimiques de la Corrosion Localisée en Eau de Mer. M. Pourbaix 365

On the Electron-Configuration Theory of Marine Corrosion. L.H. Bennett, L.J. Swartzendruber, and M.B. McNeil 410

A Study of the Corrosion Products of Copper, Zinc and Some of Their Alloys, E.D. Mor and A.M. Beccaria 427

Erosive Damage-Processes Due to Cavitation. F. Erdmann-Jesnitzer and H. Louis 439

Short Time Testing of Cavitation Resistance by Liquid Impact. E.F. Beutin, F. Erdmann-Jesnitzer, and H. Louis 448

New Testing Chamber for Cavitation Erosion. F. Erdmann-Jesnitzer and H. Louis 454

Corrosion- and Creep-Induced Instability-Modeling of Fatigue-Cracking in Various Alloys. J.M. Kraff, C.L. Lamb and K.E. Simmonds 462

Protection Contre la Corrosion Marine sous Tension d'Alliages d'Aluminium par des Revêtements d'Oxydes d'Aluminum Hydratés ou non et des Aciers par des Revêtements de Fe_3O_4. I. Alliages d'Aluminium. T. Skoulikidis et A. Karageorgos 499

Stress Corrosion Cracking in Marine Environments. J.C. Skully 514

The Development of a High Strength Ductile Stainless Steel of Improved Corrosion Resistance in Marine and Chemical Environments. W.H. Richardson, P. Guha, and R. Machin 528

Special Light Metal Alloys and Their Electrochemical Protection for Construction and Decorative Elements Used in Sea-River-Ships. P. Csokan 538

Alleviation of Corrosion Problems in Deep Sea Moorings. R.L. Morey and H.O. Berteaux 549

The Relationship Between the Concentration of Oxygen in Seawater and the Corrosion of Metals. F.M. Reinhart and J.F. Jenkins 562

Etude de la Protection des Structures Sous-Marines. C. Bugeia et C. Louis 578

Corrosion Resistance of Metals in the Black Sea Water. F. Tavadze, S. Manjgaladze and M. Vashakidze 594

Microfouling: The Role of Primary Film Forming Marine Bacteria. W.A. Corpe 598

Role of Surface Chemical Composition on the Microbial Contribution to Primary Films. G.E. Sechler and K. Gundersen 610

The Role of Chemotactic Responses in Primary Microbial Film Formation. L.Y. Young and R. Mitchell 617

Mechanism of Adhesion of Marine Bacteria to Surfaces. K.C. Marshall 625

Influence of the Initial Surface Condition of Materials on Bio-adhesion. R.E. Baier 633

Marine Fungi: Spore Dispersal, Settlement and Colonization of Timber. E.B.G. Jones 640

Fundamental Aspects of the Problem of Antifouling. H. Barnes 648

Chemical Bonding in Cirriped Adhesive. E. Lindner and C.A. Dooley 653

Spore Settlement in Relation to Fouling by Enteromorpha. A.O. Christie 674

The Effect of Water Velocity on the Settlement of Swarmers of Enteromorpha spp. D.R. Houghton, I. Pearman, and D. Tierney 682

Mechanisms of Adhesion of Fouling Organisms. D.J. Crisp 691

Molecular Fouling of Surfaces in Seawater. R. Neihof and G. Loeb 710

Ship-Fouling as an Evolutionary Process. G. Russell and O.P. Morris 719

Larval Transport, Settlement, and Population Structure of Offshore Biofouling Assemblages in the Northeastern Gulf of Mexico. W.E. Pequegnat and L.H. Pequegnat 731

Crustecdysone Action and the Effects of Light During the Post-Breeding Condition of the Cirripede Balanus balanoides (L). D.J. Tighe-Ford and D.C. Vaile 744

Biological Studies on Fouling Problems in Italy. G. Relini and G. Dabini-Oliva 757

Metabolism of Mercury Compounds by Bacteria in Chesapeake Bay. J.D. Nelson, Jr. and R.R. Colwell 767

The Role of Celluloytic Bacteria in the Digestive Processes of the Shipworm. F.A. Rosenberg and J. Cutter 778

The Effects of Temperature and Other Factors on the Tunnelling of Lyrodus pedicellatus and Teredo navalis. P.A. Board 797

Inhibition of Calcium Secretion by Chemical Inhibitors in Shell Dwelling Organisms. A.A. Karande and K.B. Menon 806

On the Nutritional Requirements of Wood-Boring Crustacea. H. Kühne 814

Settling of Larval Shipworms, Teredo navalis L. and Bankia gouldi Bartsch, Stimulated by Humic Material (Gelbstoff). J.L. Culliney 822

Deep Water Wood-Boring Mollusks. R.D. Turner 836

Neuroendocrine Regulation of Reproductive Cycle in Martesia striata R. Nagabhushanam 842

Studies of the Fouling Communities Along Argentine Coasts. R. Bastida 847

Fearless Fouling Forecasting. J.R. DePalma 865

Control of Marine Fouling in a Water Cooling System in Tropical Australia. D. Straughan 880

The Problem of Marine Fouling in the Coastal Waters of India and its Economic Implications with Special Reference to Fishing Fleet Management. R. Balasubramanyan, N. Unnikrishnan Nair and A.G. Gopalakrishna Pillai 898

Succession and Seasonal Progression in the Fouling Community at Beaufort, North Carolina. J.P. Sutherland and R.H. Karlson 906

Study of Some Variables Affecting Antifouling Paints' Performance. V. Rascio and J.J. Caprari 930

New Methods of Screening Test of Antifouling Toxicants and Coatings. S. Mawatari 956

Ship Hull Anti-Fouling System Utilizing Electrolyzed Sea Water. J. Shibata, M. Kimura, K. Ueda and Y. Seike 964

Marine Fouling Control by Electrolytic Hypochlorite. T.J. Lamb 995

A Study of the Performance of Selected Premium Marine Coatings Systems. R.J. Dick and W.M. Lawall 1005

Summary of the Congress. Monsieur V. Romanovsky, Rapporteur Générale 1022



Dr. F. L. La Que
Keynote Lecturer

Corrosion and Fouling

F. L. La Que

The International Nickel Co., Inc.
1 New York Plaza
New York, N. Y. 10004

The inter-relationship between corrosion and fouling has a characteristic commonly encountered in other corrosion phenomena. This is that anyone dealing with this matter can expect to encounter many contradictions and instances of apparently anomalous behavior.

For example, macro-fouling organisms can protect metals from corrosion under some circumstances while they can promote severe attack under similar circumstances. Similarly, bacterial slimes which are important in the early stages of macro-fouling which may be harmful to some metals, can exert a protective effect on other metals as a shield against effects of turbulence. Certain metal ions released by corrosion will prevent attachment of fouling organisms while others can inhibit the desired effects of anti-fouling coatings. Toxic ions incorporated in coatings applied to prevent fouling can cause destructive corrosion of the underlying metal.

This paper will review the background of what has been mentioned and present some illustrative data.

It is easy to understand that a heavy accumulation of fouling organisms which can become several inches thick can suppress a corrosion reaction controlled by access of oxygen to cathodic surfaces. Such accumulations will also eliminate the corrosion accelerating effect of high flow velocities by reducing the velocity to practically zero at the interface with the metal at the base of the fouling, even though the velocity of flow at the outer edge of the fouling may be very high.

This was illustrated by experience with the sea water intake piping at the former Ethyl-Dow bromine extraction plant at Kure Beach, North Carolina.

Here, sea water was pumped into the plant reservoir pond thru ordinary steel pipes about six feet in diameter. When the pumps were running the velocity of flow thru the pipes was about eight feet per second (2.4 m per sec.). Test of the effect of velocity of flow on corrosion of steel by sea water in the absence of attached fouling organisms indicate a rate of corrosion of steel of about 0.025 inch (0.06 cm) per year. However, inspection of these steel pipes after service for ten years showed a rate of thinning less than 0.005 inches (0.013 cm) per year. This is the rate commonly observed on steel specimens immersed in quiet sea water in the presence of fouling organisms. The effect of the accumulation of fouling on the surfaces of the steel pipes completely eliminated the effect of the velocity of flow thru the pipes.

Incidentally, it was noted that the manually arc welded joints made in the field on these steel pipes showed no evidence of accelerated attack on either the weld beads themselves or in the adjacent heat affected zones.

The cathodic reaction in the corrosion of steel under heavy marine growths, which create an anaerobic condition, is evidently supported by sulfate reducing bacteria (spiro vibro desulfuricans). Several years ago, Dr. R. L. Starkey of Rutgers University, took cultures from beneath corrosion products on heavily fouled steel specimens immediately after they had been taken from clean unpolluted sea water. He found a very large population of these sulfate reducing bacteria on the steel surfaces which were corroding at a rate of about 0.005 in. (0.013 cm) per year. From this it can be concluded that these bacteria can account for what is considered to be the normal rate of corrosion of steel in sea water under anaerobic conditions. Bacteriologists should not be tempted to conclude that when they find such anaerobic bacteria, an abnormally high rate of corrosion of steel should be expected or should be attributed to the presence of these bacteria.

Cultures from corrosion products on other metals disclosed that alloys that released copper ions in corrosion products didn't show high populations of sulfate reducing bacteria which, evidently, are suppressed by copper ions.

However, sulfur compounds and particularly hydrogen sulfide released by sulfate reducing bacteria can have a severely accelerating effect on corrosion of copper base alloys as observed frequently when these alloys are exposed to polluted sea water. The sulfide corrosion product films which replace the more usual basic carbonate films are quite cathodic to the underlying metal and are likely to promote severe pitting at the inevitable discontinuities in such films. Continuous sulfide films provide protection against impingement attack which becomes less important than pitting in limiting the life of brass condenser tubes handling sulfide polluted water.

Other types of bacteria encountered in polluted waters lead to the formation of ammoniacal compounds which accelerate corrosion of copper alloys and can lead to stress corrosion cracking when present in the vapor phase, especially when the ammonia becomes concentrated in accumulations of non-condensible gases.

The iron modified 10% and 30% cupro nickel alloys have been found to be superior to other copper base alloys in tolerating the presence of hydrogen sulfide and ammonia produced by bacteria under anaerobic conditions and in polluted waters.

In the presence of excessive amounts of either hydrogen sulfide or ammonia, or both, as encountered in abnormally polluted waters, e.g. in Havana Harbor and at New Haven, Connecticut, no copper base alloy is likely to be reliable. It will be necessary to go to ferrous or nickel base alloys containing high percentages of chromium and molybdenum or to titanium. These materials are not adversely affected by even high concentrations of hydrogen sulfide or ammonia in sea water.

While, as described in the case of the steel pipes, heavy marine growths protected the steel from the corrosion accelerating effect of a high flow velocity, fouling organisms can accelerate attack on some alloys by creating local shielding of the metal surfaces from the access of oxygen required to preserve passivity. This effect is illustrated by Figure 1, showing localized attack of an otherwise passive metal in the shape of the base of the barnacle under which the attack took place.

Such attack under marine organisms is commonly encountered on stainless steels with the straight chromium alloys such as AISI grade 410 being most susceptible and grade 317 being least susceptible among the common commercial grades. The more highly special alloys represented by Incoloy alloy

825* and Carpenter 20 cb* are superior to the 317 grade while the nickel base chromium molybdenum alloys Inconel 625* and Hastelloy C* and titanium are substantially free from attack under barnacles and other marine organisms.

Observations of attack of stainless steels under barnacles have shown that practically all the instances of attack occurred under dead barnacles with very few cases of similar attack under living organisms present on the same test panels. Evidently side effects of the bacterial and other products of deterioration of the macro-organisms play an important role in destroying passivity under the organisms.

The bad effects of fouling in promoting localized attack of stainless steels as compared with the good performance of duplicate specimens of the same steels in the absence of such organisms were demonstrated by some tests carried out at the Freeport, Texas, plant of the Dow Chemical Company.

One set of specimens was exposed in the sea water intake basin under conditions of low velocity flow which permitted the attachment of barnacles and other marine growths on the metal surfaces. A duplicate set was exposed in a flume thru which sea water was pumped from the basin at a velocity of about five feet (1.5 m) per second. This velocity plus treatment of the water with about 0.5 ppm of chlorine prevented any attachment of marine organisms. Under these conditions in the flume stainless steel specimens were able to retain their passivity and remained free from attack. Duplicate specimens exposed in the intake basin suffered severe localized attack under attached organisms, as shown by Figure 2.

There is very little evidence of any direct effect of macro-organisms on corrosion of metals in sea water. The nearest approach to this was a peculiar association of sea urchins with attack on steel piling used to support an off shore oil drilling pier near Santa Barbara, California.

Steel piling had suffered such intensive erosion by suspended sand in the breaker zone that it had to be replaced. When the eroded piling was removed it was found that the submerged surfaces had accumulated a large number of sea urchins, each of which occupied a hemispherical cavity of approximate size as shown by Figure 3.

There were suggestions that the cavities were the result of the action of some corrosive substance secreted by the sea urchins. It seems more likely that movement of the sea urchins where they rested on the steel surfaces prevented the steel from developing protective corrosion products so that while the sea urchins were active, the steel corroded at the relatively high rate characteristic of the early stages of corrosion of steel in sea water.

Macro-organisms and particularly barnacles can penetrate and destroy soft coatings such as coal tar enamels, as shown by Figure 4. They can also lift protective wrappings by working under the edges of laps, as shown by Figure 5. Certain species of teredo have been found to penetrate coatings and burrowing clams (martesia) are able to penetrate plastics and even some grades of concrete.

Some studies were made to determine the efficacy of different continuous and intermittent treatments of sea water with chlorine to prevent the growth of fouling organisms and bacterial slimes. The test set up included specimens in the form of pipes arranged as a sort of telescope which permitted observations of the combined effects of chlorine and velocity on the corrosion of the pipe materials.

---

* Trade marked alloys

So far as the effect of chlorine on the organisms was concerned it was found that a continuous addition of chlorine so as to leave a residual of from 0.25 to 0.5 ppm, as measured with orthotoledene, was more effective than intermittent additions of higher concentrations.

So far as the effect on corrosion of steel was concerned, as shown by Figure 6, there appeared to be no direct effect of the chlorine additions as shown by the results of tests at zero velocity. The principal effect appeared to be the result of the action of the chlorine in preventing attachment of protective slimes to the steel surfaces so that the corrosion accelerating effects of the higher rates of water flow could be demonstrated.

In the case of copper base alloys, the results covered by Figure 7, showed that chlorine additions capable of preventing the growth of slimes and fouling organisms would not be expected to have a significant effect in accelerating corrosion of these alloys.

Incidentally, exposure of specimens of pine wood to the chlorinated sea water showed that addition from 0.25 to 0.5 ppm of chlorine would serve to protect the wood from attack by teredo and other wood boring organisms.

Another series of tests showed that intermittent heating of sea water, e.g. to 100 to 110 degrees F. (40 to 45 degrees C) for thirty minutes each week was sufficient to prevent the growth of fouling marine organisms and wood borers.

Such intermittent heating had no significant effect on corrosion of metals.

It is well known that copper and a few copper alloys are able to release a sufficient concentration of copper ions in corrosion products to suppress the attachment of fouling organisms. This was the basis of the use of copper to sheath the hulls of wooden sailing vessels. Metal sheathing was replaced by the use of organic coatings loaded with sparingly soluble copper flakes or powders and, more commonly, cuprous oxide. More recently organic tin and lead compounds such as tributyl tin have been found to be effective pigments in anti-fouling coatings.

As is the case with the rate of release of copper from anti-fouling coatings, where the critical rate is about 10 micrograms per sq. cm. per day, there appears to be a critical rate of release of copper in corrosion products which must be exceeded if the attachment and growth of fouling organisms is to be suppressed.

An early indication of the existence of such a critical rate of corrosion was provided by experience with specimens of bare copper which were in galvanic contact with specimens of steel having exposed areas covering a range relative to the area of the copper to which they were attached.

When the area of the associated steel was large enough to give the copper sufficient galvanic protection to reduce its rate of corrosion below the critical rate, the copper lost its anti-fouling properties. These rather crude experiments indicated that the critical rate of release of copper in corrosion products was of the order of 5 mg per sq. dm. per 24 hours. This would be equivalent to a rate of thinning of copper slightly less than 0.001 in.(0.0025 cm) per year.

This critical rate was confirmed somewhat more precisely by tests of a number of copper alloys carried out by C. L. Bulow and reported in reference 1. An earlier study by F. L. La Que and W. F. Clapp made use of a series of alloys of copper with nickel, ranging from pure copper to pure

nickel thru a number of steps.

Several sets of these specimens were exposed simultaneously. They were inspected each day until there was visible evidence of fouling on the alloys at the high nickel end of the series. At that time a complete set of specimens was removed for weight loss determinations to measure corrosion rates.

Observations of fouling were continued until fouling occurred on the alloy having the next highest nickel content and so on until fouling was observed towards the higher copper end of the series.

This procedure yielded data from which the weight loss vs. time curves shown in Figure 8 could be constructed. By combining the rates of release of copper in corrosion products as indicated by the slopes of the weight loss vs. time curves with observations of fouling it was possible to confirm the indications that the critical rate of release of copper required for a copper alloy to be anti-fouling was about 5 mg per sq. dm. per day. This was illustrated further by the data in Table 1.

It is, of course, important to note that the apparently critical rate of release of copper as calculated from weight loss determinations applies only to alloys that corrode substantially uniformly over the whole surface. If attack is localized, as is often the case with bronzes containing substantial amounts of aluminum and iron, there will be large unattacked areas surrounding large or small islands of localized attack. Fouling will occur on the uncorroded surfaces.

If alloys that are normally anti-fouling are in glavanic contact with sufficiently large areas of less noble metals so as galvanically to reduce the rate of corrosion of the normally anti-fouling alloys below the critical rate, they will, of course, become fouled.

For some difficult to establish reason the critical rate of release of copper from corroding metallic surfaces is about five times greater than the critical leaching rate of copper from anti-fouling paints.

The copper nickel alloys are particularly interesting with respect to their anti-fouling properties. Exposure of a series of these alloys containing only nickel and copper indicated that the dividing line between the alloys that fouled and those that did not was around 45% nickel.

However, in order to give commercial alloys the desired high level of resistance to erosion and impingement attack by sea water moving at high velocity, as in condenser tubes and salt water piping, it is necessary to supplement the presence of nickel by the addition of an appropriate amount of iron, e.g. about 0.4% in the 30% nickel alloy, and 1.2% in the 10% nickel alloy. From the standpoint of resistance to fouling the effect of the iron addition to the 30% nickel alloy is to make it act like a 45% nickel alloy so that it is no longer completely resistant to fouling.

However, the addition of 1.2% iron to the 10% nickel alloy does not affect its anti-fouling properties. Thus, this alloy has the unique ability to withstand attack by sea water moving at high velocity while being able to corrode in quiet sea water at an acceptably low rate, still above the critical one required to prevent fouling. This characteristic is illustrated by Figures 9A and 9B.

Commercial advantage is being taken of this property of the 90:10 cupro nickel thru its use for the hull of a shrimp fishing boat shown in Figure 10. This boat has been in service for more than a year and has remained free from fouling. The absence of fouling organisms has resulted in significant improvements in fuel consumption and speed as compared with

sister ships with painted steel hulls, and put into service at the same time and on which there have been heavy accumulations of fouling organisms.

Reference was made previously to interactions between metals and anti-fouling coatings. It has been shown that not only can copper leached from anti-fouling paint accelerate corrosion of steel exposed at bare spots in the coating, but corrosion products of steel can inactivate an anti-fouling paint.

When steel is exposed at a bare spot in a coating system which includes a top layer containing either metallic copper or cuprous oxide, there can be serious galvanic acceleration of the corrosion of the exposed steel.

This is most likely to occur if the metallic copper loading of an anti-fouling paint is sufficiently high to achieve sufficient contact between the copper particles to make the coating electrically conductive.

In the case of anti-fouling coatings based on cuprous oxide the danger of attack at bare spots is minimized by using a good non-conductive anti-corrosive layer beneath the anti-fouling layer. This insulates the steel from the copper compounds in the top layer, and prevents cementation of copper onto the underlying steel which then could become an active cathode accelerating attack of steel at bare spots. The depth of attack at such bare spots increases as the ratio of the area of the coated surface to the area of the bare spot increases.

The danger of accelerated attack at bare spots in cuprous anti-fouling coatings is even greater with aluminum than with steel. Mercury compounds sometimes used along with copper in anti-fouling coatings can be expected to be particularly damaging to aluminum and should be avoided with this metal. The preferred anti-fouling coatings for aluminum are those based on organic tin compounds.

Anti-fouling coatings based on copper and copper compounds can become inactivated by contact with sufficiently large areas of bare steel, zinc or magnesium. The effect is most pronounced with coatings based on metallic copper but has been observed also with cuprous oxide paints applied over an inadequate anti-corrosive layer.

In addition to the presumed galvanic inactivation of an anti-fouling paint there is also an inactivation effect of iron corrosion products. This was demonstrated by tests with steel specimens having a large bare spot in an anti-fouling coating. These specimens were exposed in a channel thru which sea water flowed in only one direction.

Inactivation of the anti-fouling coating occurred only downstream of the bare spot source of iron corrosion products.

The examples cited from these early investigations illustrate the complexity of inter-related corrosion and fouling phenomena which, no doubt, will be demonstrated even further by the several other and more up to date contributions to this conference, which can be expected to throw much needed further light on the mechanisms involved.



Figure 1. Attack under barnacles on stainless steel specimen.

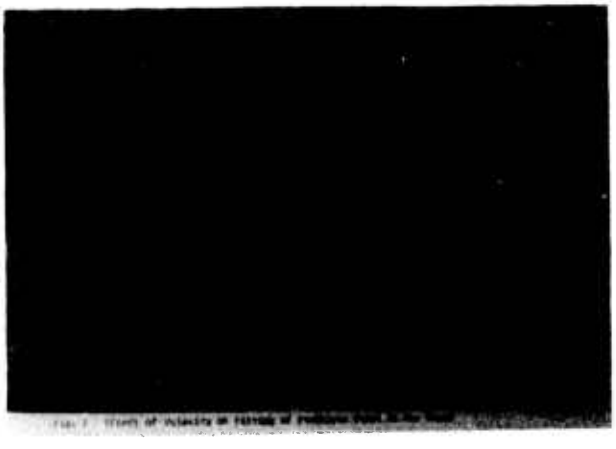


Figure 2. Effect of water velocity on localized attack of type 316 stainless steel.



Figure 3. Localized attack under sea urchins on steel piling.



Figure 4.



Figure 5.

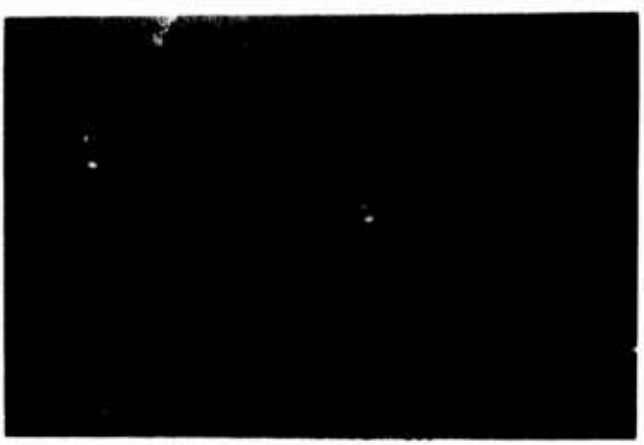


Figure 6.



Figure 7.



Figure 8. Weight Loss vs. time curves for copper nickel alloys in sea water.

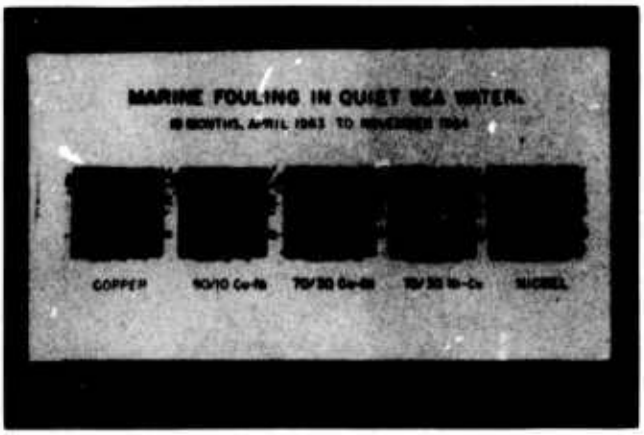


Figure 9A. Fouling of range of copper nickel alloys.

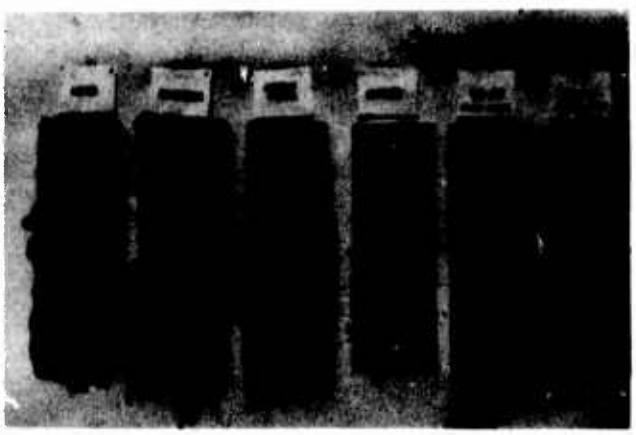


Figure 9B. Comparison of fouling of different alloys.



Figure 10. Shrimp fishing boat fabricated from anti-fouling 90:10 copper nickel alloy.

Table 1

Relationship Between Corrosion Rates and Fouling of Nickel Copper Alloys During Last Sixty-Two Days of Seventy-Eight Days Exposure in Sea Water at Kure Beach, N. C.

Alloy	Weight Loss in mg./sq.dm./day	Calculated Cu Content of Corrosion Products in mg./sq./dm./day	Fouling	Remarks
Copper	23	23	None	Uniform attack
20% Ni, 80% Cu	8.8	7	"	" "
30% Ni, 70% Cu	6.5	4.5	Incipient	" "
40% Ni, 60% Cu	9.3	5.6	Irregular	Fouling occurred on unattacked surfaces
50% Ni, 50% Cu	17	8.5	Irregular	Corrosion highly localized, fouling in unattacked areas
60% Ni, 40% Cu	7.2	2.9	Yes	Localized attack
70% Ni, 30% Cu	9.3	2.8	"	" "
80% Ni, 20% Cu	9.7	1.9	"	" "
90% Ni, 10% Cu	10	1.0	"	" "

A STUDY ON THE IMPORTANCE OF THE SHIP'S HULL CONDITION
An approach to improving the economy of shipping

A.M. van Londen
HEMPEL'S MARINE PAINTS
Lundtoftevej 150
DK-2800 Lyngby, Denmark

In the course of the last century the design of ships' hulls has become a technical science, and shipowners invest considerably in securing the most economic design. Surprisingly, a factor of even greater economic importance than the shape of the hull has up to now been neglected: the surface roughness of the underwater hull.The total resistance of a moving ship consists of residual resistance and frictional resistance. For most ships the frictional resistance is by far the more important part, viz. 70-80 percent of the total resistance. The frictional resistance is strongly affected by the surface roughness, not only by the macro-roughness, but also by the micro-roughness. The effect of the surface roughness on the flow pattern along the ship is discussed, and also its effect on the transport process perpendicular to the ship's hull. This transport process determines the effective life of an antifouling paint. Most of the poison in antifouling paints is released during the sailing period of a ship when there is no need for this release. Assuming that the flow along a ship could be altered, then it should not only be possible to reduce the drag, but also to extend the effective life of antifouling paints. Certain soluble polymers are known to have friction reduction properties. This phenomenon is explained by assuming that such polymers thicken the laminar sublayer. The use of such soluble polymers in practice is restricted by the costs involved. A new, virtually waterinsoluble, hydrophilic acrylic resin is claimed to have drag reducing properties. These properties can be explained by a thickening or stabilization of the laminar sublayer. Adopting this as a working model, laboratory tests by means of rotortests have been carried out to demonstrate drag reduction and decrease in the release of poison from antifouling paints. The drag reduction found is rather small, only 3,5 to 5 percent. However, the effect on the release of poison is very pronounced. Further two experiments made in towing tank laboratories showed a positive effect of the hydrophilic coating. However, these results cannot be extrapolated to actual ships. For this reason in an early stage of the research work some practical tests have been done with the help of two shipowners. The best practical test controlled by an independent ship research institute has shown a positive result of 4 percent on fuel consumption. Other tests have been less successful. The work is continuing, and this is certainly justified taking into account the econimics involved.

Key Words: ship resistance; surface roughness; drag reducing polymers; HYDRON ®; antifouling efficacy.

---

1. Introduction

Ever since the time man began building coats and ships for transportation on rivers, lakes, and seas, special attention has always been given to the underwater part of the hull. This attention is quite understandable. The submerged body of the vessel must be completely water-tight and must be kept in a good condition to make the ship a safe means of transport. Through the centuries attention has been concentrated on the preservation of the ship's hull material. Wooden ships have to be protected against penetration of water and wood-boring organisms. Steel ships need a protection against corrosion. Very early in the history of shipping a detrimental effect on the manoeuvrability and speed of the ships was observed caused by the settlement of organisms on the ships' bottoms. For centuries the only remedy was removal of the fouling organisms in frequent careening or drydocking. Later on copper sheathing came into use on wooden ships, developing into poisonous antifouling paints, which on steel ships are used in combination with anticorrosive paints. During the last century the design of the ship's hull has become a technical science, and shipowners invest considerably in the most economic design. Also the investment in protection against corrosion and fouling has increased. However, the care for the underwater part of the ship's hull is still insufficient. In this article the theoretical consideration will be given to emphasize this point of view. Laboratory and practical data will be presented in order to prove the technical and economical importance of an up-to-now neglected factor: the surface roughness of the ship's hull.

2. The resistance of a moving ship

The total resistance of a moving surface vessel is the sum of two components, viz. the frictional resistance and the residual resistance (1, 2, 3).[1] The frictional resistance is caused by tangential stresses due to the drag of the water moving parallel to the vessel's surface. This frictional resistance is a function of the Reynolds number[2] and the surface condition of the hull. The residual resistance is caused by the distribution of pressure around the hull developed by waves and eddies formed by the ship's motion. This resistance is strongly dependent upon the lines (form) of the hull. In Table 1 a survey is given of the resistance of a moving ship and the main factors involved. The air resistance has not been taken into consideration.

In Fig. 1 the relation between frictional and residual resistance is shown for ships of four different sizes operating at speeds between 10 and 35 knots. It is obvious that for most ships the frictional resistance is more important than the residual resistance. Only for relatively small ships operating at speeds over 25 knots the residual resistance becomes the predominant factor. This is confirmed by the practical results given in Fig. 2 (4).

---

[1] The numbers in parenthesis refer to the list of references at the end of this paper.

[2] The Reynolds number is a dimensionless number defined as:

$$Re = \frac{l.V}{\nu}$$

l = specific length (m)
V = speed ($m.sec.^{-1}$)
ν = kinematic viscosity ($m^2.sec.^{-1}$)

Other practical data have been published illustrating the influence of the surface roughness or condition of the ship's hull, viz.

- actual measurements of the surface roughness on the 34.800 t.d.w. tanker "FERNCREST" compared with oil consumption indicate that a 25 micron increase in surface roughness requires about 1.75% increase in H.P. (5),

- full scale trials on the "LUCY ASHTON" have shown a difference between an ironoxide pigmented paint versus an aluminium pigmented paint, the ironoxide paint giving 3% more total resistance corresponding to 5% difference in frictional resistance. Slight fouling (scattered small barnacles and a band of fine grass) increases the total resistance by 30% corresponding to a 50% increase in frictional resistance (2),

- measurements of the surface roughness on 68 new ships have shown an average roughness of 190 micron varying from about 100 up to 400 micron! Lackenby indicates an increase in total resistance on a large new ship by about 2½% for an average increase in surface roughness of 25 micron (2),

- in Fig. 3 and 4 the effect of surface condition on oil consumption is shown (6), and

- actual service records of the "LUBUMBASHI" over 5 years have shown an increase in total resistance of 17%, which is only due to the increase in frictional resistance caused by roughening of the hull independent of fouling (7).

Concluding it can be stated that the surface condition of the ship's hull is a major factor affecting ship performance (2), and that this surface condition merits intensive care.

3. Surface roughness and flow along the ship's hull

The surface roughness of the ship's hull can be divided into the macro-roughness and the micro-roughness. The macro-roughness is the roughness due to welding , poor application of the paint, corrosion, fouling, and disintegration of the paint coating. It is a roughness, which can easily be detected, and which can be prevented or minimized by modern protective means and methods. The micro-roughness can be defined as the intrinsic roughness of the paint coating, of which little is known. Its importance has, however, been demonstrated by the effect of the pigmentation of the paint on the resistance of the ship (2). It has been supposed that the micro-roughness plays a role in the processes taking place in the boundary layer between a ship's hull and seawater (8). The flow pattern along the ship's hull is dependent upon the Reynolds number. At increasing Reynolds number laminar flow will change to turbulent flow via the transition stage (Fig. 5). Under laminar flow the direction of the flow is exclusively parallel and in the same direction as the moving ship. Under turbulent flow the main direction of the flow is still parallel to the direction of the moving ship, however, flow in all possible directions will occur. Inasmuch as for ships only the laminar conditions (in ports at rest) and turbulent conditions (moving at sea) are of importance, the transition stage is not discussed here. For smooth surfaces the transition from laminar to turbulent flow takes place at a $Re = 5.10^5$-10^7. For a rough surface this transition takes place at a lower Reynolds number. A surface is considered to be rough if the peaks of the surface configuration transgress the laminar sublayer's thickness. If these peaks are smaller, the surface is considered to be hydrodynamically smooth (see Fig. 6). In general a ship at rest is hydrodynamically smooth because of the presence of a relatively thick laminar sublayer. A ship operating at normal speed has a very thin

laminar sublayer and will be hydrodynamically rough hence a turbulent flow along the hull exists under this condition.

The loss of energy caused by turbulence will reach a maximum at a certain Reynolds number dependent upon the surface roughness. In Fig. 7 the theoretical flow pattern along a ship's hull is given. However, due to the size and operational conditions of ships it is expected that the flow is fully turbulent over the whole wetted surface of a ship (9).

4. Laminar sublayer and transport processes along the ship's hull

At a low Reynolds number a relatively thick laminar sublayer is present. This layer is a thin continuous layer of water adjacent to the ship's hull more or less bound to the hull and moving along with the ship. With increasing speed the thickness of the laminar sublayer decreases, and at a certain Reynolds number the continuous laminar sublayer becomes discontinuous (see Fig. 5). In this stage the laminar sublayer still exists, but is disturbed by eddy currents and is consequently renewed regularly (Hanratty's surface renewal model) (10). This surface renewal model assumes that the fluid in contact with the wall is replaced at fixed time intervals by fluid of the bulk concentration. The eddies which are responsible for transmitting stress from the turbulent flow to the viscous regions close to the wall have a circumferential dimension approximately equal to their distance from the wall (11). This has been confirmed by Townsend who shows that cylindrical eddies of the same radial scale as the boundary layer thickness to a large extent govern the turbulence processes in the near wall region (12).

Transport to and from the continuous laminar sublayer takes place by diffusion only due to the molecular movement (see fig. 8). This is a slow process. Transport to and from the discontinuous laminar sublayer takes place mainly by transport of macromolecular masses (mixing). This is a quick process. In the area outside the laminar sublayer transport takes place by diffusion only in case of a laminar flow and by mixing in case of turbulent flow.

It is clear that the continuous laminar sublayer acts as a transfer resistance. For a discontinuous sublayer this barrier effect will be rather small. The transport processes in the near wall region along the ship's hull affect corrosion, cathodic protection, and the performance of antifouling paints. Especially the effect on antifouling paints is of great practical importance. The action of antifouling paints is based on the release of a bio-active material. However, this action is only needed during the laydays of ships. The release of bio-active material is quick when the ship is moving, and due to the fact that the period of moving is bigger than the period in ports only a small amount of the expensive bio-active material is used effectively (see Fig. 9). More than 90% is wasted during the travelling of the ship (13).

5. Drag reducing polymers

Since the discovery of the Thom's phenomenon of friction reduction properties of dilute polymer additives (14) and the effect of high molecular compounds on hydrodynamic testing (15) this phenomenon has been intensively investigated. Naturally also a lot of attention has been given to various polymers with drag-reducing properties such as Polyox, guar-gum, Carbopol, and CMC. The phenomenon is very complex and is certainly not fully understood. However, the mechanism of the frictional reduction has been explained simply and nearly satisfactorily by the assumption that the polymers thicken the laminar sublayer (16). The various studies have been compiled as follows (17):

for flow through cylindrical pipes:

- No drag reduction occurs until the flow characteristics change from laminar to turbulent.
- The amount of drag reduction increases with increasing Reynolds number and with increasing molecular weight of the polymer additive.
- The thickness of the viscous sublayer increases with the concentration of the polymer.

for experimental work with rotating discs:

- Confirmation of the results of pipe flow with respect to molecular weight and, in addition, demonstration that maximum drag reduction occurs with linear polymers. The longer the molecular weight the greater the corresponding drag reduction.

The results obtained with laboratory tests may well be used in studying the possible effect in practice on ships as actual sea-trials with H.M.S. "HIGHBURTON" using Polyox have shown that reductions in shaft horsepower can be achieved in the order of 12% corresponding to reductions of skin friction of the order of 22% (18).

All known polymers with drag-reducing properties are readily soluble in water. The dosage of the material is done by injection or dissolving in the bulk of the water although it is only of use in the near-wall region. This solubility and the uneconomical method of dosage restrict the practical use of such polymers due to the high costs. A new material - HYDRON ® - is available, which may offer a more economical solution.

6. HYDRON ®, a new polymer

HYDRON R is the trade name for a water insoluble hydrophilic acrylic resin. The hydrophilic characteristics of the resin can be programmed during the fabrication process, which is patented (19). The use of HYDRON ® in marine coatings is patented (20, 21, 22). It has been indicated that the capacity of HYDRON ® to take up water is related to its drag reducing properties (20 22). In this respect it is worth mentioning the resemblance between the HYDRON ® polymer and the dolphin's outer skin, which has been described by Kramer (23):

> "Dolphin's outer skin is so delicate that it can be scraped off with a finger nail. The surface layer consists of a highly pliable material. The entire outer skin is waterlogged. It dries out, becomes brittle, and turns soft again when put back into water. In dry state the outer skin weighs only one fifth of its wet weight, an indication of its high water content."

The drag-reducing properties of a HYDRON ® coating may be explained by:
- a damping effect of the coating, or
- an increase of the thickness of the laminar sublayer.

7. Working model

As a basis for investigation of the use of HYDRON ® as a shipbottom coating a simple working model has been adopted, based on the assumption that the HYDRON ® coating increases the thickness of the laminar sublayer and has a stabilizing effect on the laminar sublayer (see Diagram 2). The increase of the thickness of the laminar sublayer will decrease the surface roughness hydrodynamically seen. This means that the transition of

the laminar to turbulent flow will take place at a higher Reynolds number. In other words this will cause drag reduction. The increase in thickness of the laminar sublayer and the stabilization of the layer will decrease the release of poison from the antifouling coat under turbulent conditions, e.g. when the ship is in motion. This release is not affected under laminar conditions, e.g. when the ship is in port, due to the relatively thick laminar sublayer present under this condition. The decrease in the release of poison will be considerable in case the stabilization effect could prevent the transition from the continuous laminar sublayer into the discontinuous form; then the laminar sublayer will act as a very effective barrier under turbulent conditions.

8. Laboratory experiments

In the initial stage of research it is of crucial importance to demonstrate an effect of the polymer coating on drag. In case this is positive, according to the assumed working model at the same time a smaller release of poison from the antifouling coat must be found. In a later stage additional factors have to be studied such as wear of polymer coating, various curing mechanisms, application, different antifouling paints, etc. It is clear that these factors are all of great practical importance. Furthermore, the effect of the material must be optimized. The crucial experiment - the demonstration of the effects - is in fact a very simple test consisting of:

- aging on a rotor apparatus of a shipbottom paint system with and without a topcoat of the HYDRON ® polymer combined with
- energy measurements
- determination of rate of release of poison, and
- checking of antifouling performance after different aging periods.

This test also provides information on the physical performance of the coating like wear, resistance, adhesion, flaking, etc.

9. Description of testmethods

9.1. Rotor apparatus

A rotorapparatus consists in principle of a cylinder, which can be rotated in seawater. The apparatus has been designed to test and study the aging of shipbottom coatings and has shown a good correlation with practical results on ships (24).

9.2. Energy measurement

An energy measurement consists of measurement of
- the current consumption of the electromotor, and
- the increase in temperature of the seawater in the rotortank, which has been insulated to prevent heatlosses.

9.3. Antifouling performance

The performance of an antifouling paint is dependent upon the release of poison during aging and its effect on fouling organisms. A good test for antifouling paint performance consists of (24, 25):
- aging under turbulent conditions by rotortesting, combined with
- analysis for residual poison in the coating after various periods of aging, and
- checking of its biological activity after certain periods of aging by immersion tests in the sea under fouling conditions.

9.4. Wear of coating

Film thickness measurements after various periods of aging will indicate the wear of the coating. These measurements are done by microscopial examination of cross-sections.

10. Laboratory test data

Tests have been done on two rotor apparatuses with a circumferential speed of 33,75 knots. The application of the HYDRON ® coats has been done on the test area only and not on the braces used for fastening the test panels. This means that only a part of the cylinder is actually coated with HYDRON ® (less than 70%). The fouling test has been carried out in Bombay. The most relevant test data are given in Tables 1 and 2 and in Fig. 10. During the initial tests a deterioration of the HYDRON ® coating has been observed. This effect started in the brush marks. Further tests with spray-applied coatings have shown only minor break-down of the HYDRON ® coat, even at a circumferential speed of 54 knots. All further rotortesting has given positive results (Table 3).

11. Discussion of rotor test results

The test results on the energy consumption show a positive effect of the HYDRON ® coating. This effect is rather small, on an average only 3,5% (see Table 2). However, it must be kept in mind that the rotor cylinder is only partly (less than 70%) coated with HYDRON ®. The real effect may be approximately 5%.

The heat generated by the rotor body in the seawater also indicated a positive effect of the HYDRON ®. In case HYDRON ® is used less generated heat is indicating less friction. Again the difference is too small to establish a quantitative significant effect. Both energy consumption and generated heat demonstrate a qualitative positive effect of the HYDRON ® coating.

From the cross-sections (Table 1) a very pronounced effect of the HYDRON ® skin can be seen upon the release of poison from the antifouling coating during aging. As the antifouling performance is not impaired by the HYDRON ® coating (Table 1) this means prolongation of the effective life-time of the antifouling paint.

12. Tests by hydrodynamic laboratories

The Hydro- and Aerodynamic Laboratory, Lyngby, Denmark, has carried out a testing programme to determine the effect of a HYDRON ® coating. The test has been performed in a small tank in the laboratory with a model of a cargo liner (26). A small reduction in resistance has been found, which is within the limits of repeatability in the small tank. As it is supposed that the improvement is due to a shift in the transition area between laminar and turbulent flow an extrapolation to ships cannot be made.

The Naval Ship Research and Development Center, Washington D.C., U.S.A., has carried out tests with the NSRDC Friction Plane (27). A positive effect of 1½% has been found using a HYDRON ® coating. However, this difference lies within the probable band of repeatability for such tests.

The hydrodynamic specialitsts do not advise any model test, which could provide evidence about the practical performance of a special coating. For this reason practical tests have been initiated in an early stage of the research work.

14. Practical testing

Reliable data on the performance of ships in actual operation are very difficult to obtain. This is due to the variations in the practical conditions.

The most reliable is the so-called speed trial over the measured mile. Another possibility is to follow the performance and oil consumption over long periods of time. Possibly tests on sister ships operating on the same route could also provide reliable information. Consultation of various experts in hydrodynamics has given unexpected favourable reactions. The principle and the possible explanation of the effect seem to be scientifically acceptable.

The arrangement of practical tests on ships has turned out to be very difficult, indeed. First of all the selection of ships is limited by the following requirements:

- travel performance and oil consumption known over a period of time
- preferably 3-5 years old
- recording of travel performance and oil consumption
- preferably one out of a series of sister ships, and
- preferably travelling on one route

Secondly, practical tests introduce commercial interests such as change in antifouling paint, extra drydocking time for the application of the extra coat and the possible impact on the market as such. Besides some positive tests on small motor boats and sailboats a number of tests on big ships have been carried out. For these tests the co-operation and assistance of two important shipping companies are highly appreciated. The first shipowner is using a computerized system to follow the operational performance of the ships. In total five tests have been carried out (Tables 4 and 5), **of which four showed positive results.**
The second shipowner has carried out a test in the most reliable way, viz.:

- drydocking + application of the new coat of antifouling
- undocking and speed trials over the measured mile
- redocking + application of one coat of HYDRON ®, and
- undocking followed by speed trials over the measured mile.

The trials over the measured mile have been carried out by the IRCN (28). Although the application of the HYDRON ® coating was not up to desired standard the speed trials have given a 4% positive effect on required horsepower at a speed of 16 knot or an increase in speed of 0,15 knot at equal horsepower.

The original test results have also been analysed in Denmark using a Speed-Trial Analysis computer programme. This has shown a speed increase of 0,25 knots (29).

Both institutes underline the inaccuracy of such trials. However, both of them express categorically that there is no doubt as to the better performance of the ship after application of the HYDRON ® coating.

The ship has been painted with an antifouling paint of unknown performance. After 6,5 months fouling and rust-formation have been observed.

The interpretation of the practical results can be debated and the results may not be striking. However, they can be rated as positive and promising.

15. Economy

Accurate economic calculations on frictional resistance can only be made by the shipowners as they have all the necessary data available. The economy will depend not only on the type of the vessel, but on other factors such as size, operational speed, trading, days at sea versus lay-days, ballasted or loaded, etc.

Some examples of economic calculations have been given in the literature (30, 31, 32, 33, 34). They are summarized in Table 6. From these data an average earning can be calculated on fuel consumption alone of $0.133 per ton per year for one per cent reduction in total resistance. For the 1971 price of fuel oil ($19/ton) this figure is $0.20.

A 250.000 t.d.w. tanker with a 30.000 HP engine and 300 days at sea will annually use about 43.000 ton fuel oil. In case of a 3% gain in performance the saving on fuel will amount to $26.000 per year. This saving has to be considered low relative to the possible increase of earning capacity of the ship. This can be illustrated by the following example. A 300.000 t.d.w. tanker has an operational cost of approximately $30.000 per day. A 1 per cent increase in speed will give 3 more operational days per year, in other words a saving of $90.000. This does not include savings made possible by the prolongation of the effectiveness of antifouling paints.

16. General considerations

It is certainly too early to draw any definitive conclusions from this study and the preliminary investigations. The available knowledge on drag reducing polymers and the positive result obtained on an actual ship indicates the practical possibilities. The preliminary results with a HYDRON ® coating may be classified as promising. A qualitative effect on drag reduction has been found and a very pronounced effect on the release of poison from an antifouling coating. These findings correspond to the working model adopted for this research project.

As it is very difficult to extrapolate laboratory and towing tank test results to actual ships, testing in practice has been started. This may seem to be premature and not fully justified at this moment. However, the beneficial effect on the antifouling performance alone may make the use of HYDRON ® a cost saving treatment. Moreover, practical testing will once more focus attention on this interesting phenomenon and will stimulate the research efforts.

17. Remark

The barrier action of the increased sublaminar layer will also affect the corrosion rate, and in case cathodic protection is used, the current density needed for protection. The latter is under investigation in order to develop a reliable and quick test method.

Acknowledgement

In the first place I thank the Management of HEMPEL'S MARINE PAINTS for allowing this publication. I owe a special thanks to both Mr. G.J. Govers and Mr. J. Bjerregaard, who carried out the practical work in an enthusiastic and dedicated way. Further I thank all who have contributed actively or have given their valuable criticism. In this respect I should like to mention especially Mr. Børge Hansen, Mr. J.R. Stephenson, Mr. J.M. Barfoed, Mr. B. Bender-Christensen, Mr. G. Olesen, and Mr. J. van der Noordaa.

Literature

1. ANON: *Marine Fouling and its Prevention.* U.S. Naval Institute, Annapolis, Maryland, 1952.

2. H. LACKENBY: *Ship Performance and the Effect of Hull Surface Condition.* Corrosion, Prevention and Control, Vol. 91, No. 8, August 1962.

3. R.A. BOYNTON AND P.G. NEAL: *The Frictional Resistance of Ship's Hulls.* The Paint Journal, Vol. 13, No. 99, July 1961.

4. T. IZUBUCHI: *Increase in Hull Resistance through Shipbottom Fouling.* Zosen Kiokai, Vol. 55, December 1934.

5. B. MATZOW-SØRENSEN: *Maling og Beregning av Skipsruhet.* SFI Nyt, No. 2, 1967, NTH Trondheim.

6. BRITISH SHIP RESEARCH ASSOCIATION: *Hull Roughness and Ship Performance.* (Brochure). Wallsend, Northumberland.

7. G. AERTSSEN: *Sea Trials on Two Cross-channel Twin Screw Motor Ships.* Transactions Royal Institution Naval Architects. London, Vol. 103, 1961, page 181.

8. A.M. VAN LONDEN: *Corrosie-en aangroei-wering van de scheepshuid.* De Ingenieur, Chemische Techniek, Vol. 2, No. 17, April 1968.

9. S.B.S. UBEROI *Viscous Resistance of Ships and Ship Models.* Hydro- and Aerodynamic Laboratory, Lyngby, Denmark, Report No. Hy-13, Sept. 1969.

10. TH.J. HANRATTY: *Turbulent Exchange of Mass and Momentum with a Boundary.* A.I.Ch.E. Journal Vol. 2, No. 3, September 1956.

11. TH.J. HANRATTY *Study of Turbulence close to a Solid Wall.* The Physics and Fluids Supplement, 1967.

12. A.A. TOWNSEND: *The Structure of Turbulent Shear Flow.* Cambridge University Press, Cambridge 1966.

13. A.M. VAN LONDEN: *The Influence of Cathodic Protection on the Anti-fouling Action of Antifouling Paints.* 2nd International Congress on Marine Corrosion and Fouling, September 1968, Athens, Greece.

14. B.A. TOMS: *Some Observations on the Flow of Linear Solutions through Straight Tubes at Large Reynolds Numbers.* 1st International Congress on Rheology, Holland, Vol. 2, 1948, page 135.

15. J.W. HOYT *Microorganisms - Their Influence on Hydrodynamic Testing.* Naval Res. Rev. Vol. 21, No. 5, 1968.

16. FRANK M. WHITE: *An Analysis of the Effect of a Polymer Additive on Turbulent Wall Friction and Pressure Fluctuations.* Navy Underwater Sound Laboratories New London, Connecticut, December 1967.

17. M.H. FLETCHER: *Surface Wake of a Circular Cylinder in Dilute Aqueous Solutions of Poly(ethylene Oxide).* Report of Naval Postgraduate School, June 1969,

18. ANON: *Hull Friction Reduction.* Paint Technology Vol. 33, No. 6, June 1969.

19. BR.PAT. 1.192.663 *Hydrophilic Varnishes.*

20. U.S. PAT. 838.269: *Hydrophilic Polymer Coating for Underwater Application.*

21. BR. PAT. 1.205.768: *Marine Protective Coatings.*

22. US.PAT. 3.575.123: *Marine Structure Coated with an Acrylic, Insoluble, Waterswellable Polymer.*

23. M.O. KRAMER: *The Dolphins' Secret.* A.S.N.E. Journal, February 1961, page 103-107.

24. A.M. VAN LONDEN: *Testing and Investigation of Shipbottom paints.* J.O.C.C.A. Vol. 52, No. 2, February 1969.

25. A.M. VAN LONDEN: *Evaluation of Test Methods for Antifouling Paints.* Journal of Paint Technology, Vol. 42, No. 549, October 1970.

26. HYDRO- AND AERODYNAMIC LABORATORY: *Hya 7063, Report No. 1: Testing Drag Reduction by Polymer Coating.* February 1971. Lyngby, Denmark.

27. T.M. PEMBERTON: *An Evaluation of the Resistance Characteristics of HYDRON ® Paint Using Models 4125 and 4667-1.* Naval Ship Research and Development Center, Washington D.C., U.S.A., T & E Report No. P-351-H-01, September 1969.

28. INSTITUT DE RECHERCHES DE LA CONSTRUCTION NAVALE, Paris: *Essais de Vitesse les 28.11.71 et 1.12.1971 pour Etude de Peintures de Carene.*

29. HYDRO- AND AERODYNAMIC LABORATORY: *Hya 727. Fartpreveanalyser.* June 1972. Lyngby, Denmark.

30. OECD, DIRECTORATE FOR SCIENTIFIC RESEARCH, Report DAS/RS/64.85, April 1964: *Surface Roughness of Ships' Hulls and its Economic Implications.*

31. A.M. VAN LONDEN: *Behandlung und Schutz der Schiffs-Aussenhaut.* Schiff und Hafen, Jahrgang 22, 8. August 1970.

32. LOHR AND BARRY: *Prevention of Tanker Corrosion with Modern Coatings.* Am.Chem.Soc. 158th Meeting, September 1969.

33. H.J. LAGEVEEN-VAN KUYK: *Cost Relations of the treatment of Ship's Hulls and Fuel Consumption.* Shipping Worlds & Shipbuilder, July-August 1967.

34. H.O. LEBBINK AND G.P.A. HULSING: *Economische aspecten van het verven in de scheepshouw en scheepvaart.* Lecture VOM, 29th October 1970.

TABLE 1: Data on testpanels

Topcoat	Distance of aging in miles	Average thickness in micron of: HYDRON ® coat	Released layer	Antifouling coat[1]	Fouling resistance[2]
none	5.000	-	8.4	67	good
2 coats HYDRON ®	5.000	16	0	76	good
none	10.000	-	12.1	80	good
2 coats HYDRON ®	10.000	15	less than 1	80	good
none	20.000	-	16	95	good
2 coats HYDRON ®	20.000	16	5	98	good
none	40.000	-	19	92	good
2 coats HYDRON ®	40.000	21	6.7	91	good
1 coat HYDRON ®	5.000	5.8	0	79	good
1 coat HYDRON ®	10.000	6	0	66	good
1 coat HYDRON ®	20.000	5	6	82	good
2 coats HYDRON ®	5.000	13	0	75	good
2 coats HYDRON ®	10.000	14.5	0	96	good
2 coats HYDRON ®	20.000	15	5	89	good
4 coats HYDRON ®	5.000	40	0	75	good
4 coats HYDRON ®	10.000	38	0	79	good
4 coats HYDRON ®	20.000	38	5	85	good
2 coats HYDRON ®	0	14	-	87	good
none	0	-	-	79	good

[1] including released layer

[2] tested in Bombay

TABLE 2: Summary of energy calculations

aging in miles	total energy input in kcal/hr[1]			generated heat in kcal/hr[2]		
	without HYDRON (R)	with HYDRON (R)	difference in %	without HYDRON (R)	with HYDRON (R)	difference in %
0	4340	4224	2.7	2261	2210	2,3
5.000	4340	4209	3.0	2232	2145	3.9
10.000	4349	4195	3.5	2294	2201	4.1
20.000	4330	4140	4.4	2302	2236	2.9
40.000	4463	4286	4.0	2412	2304	4.5
average	4364	4211	3.5	2300	2219	3.5

[1] Energy input = $\sqrt{3} \times U \times I \times \cos \varphi \times 360 \times 0.24 \times 10^{-3}$ = 506 kcal, for I = 1 A.

[2] Generated heat = temperature increase in ^{o}C x 240 kcal (content rotortanks is 240 l).

TABLE 3: Some results of rotortests

test	number of repetitions	average energy input in kcal/hr.		
		without HYDRON (R)	with HYDRON (R)	difference in %
1	6	3250	3070	5,4
2	6	3040	2970	2,3
3	5	3220	3160	1,8
4	5	3230	3110	3,7
5	5	3040	2970	2,5
6	5	3200	3130	2,0
7	5	2960	2910	1,7
8	5	3040	2970	2,8

TABLE 4: Practical tests on ships of shipowner 1.

ship	tonnage (DWT)	in service since	test area in m2	condition of hull	type of antifouling paint	thickness HYDRON ® coat in microns	results			
							performance compared with preceding period (see Table 5)	effect on release of poison	fouling	remarks
1	46350	1966	8000 (bottom + sides)	rather rough	Cu_2O/vinyl-based	5 - 10	positive	HYDRON ® reduces release with appr. 50%	partly after 8 months	
2	79600	1967	5100 (sides only)	rough	Cu_2O/vinly-based	appr.10	positive	unknown	green algae after 7 months	
3	42950	1962	6050 (bottom + sides)	rather rough	Cu_2O/vinyl-based	appr.10	negative	unknown	not fouled after 5 months	sold after 5½ months
4	77450	1964	8300 (sides)		Cu_2O/vinyl-based	appr. 10	positive	unknown	unknown	
5	41780	1960	9100 (bottom + sides)	smooth	Cu_2O/vinyl-based	appr. 5	positive	see ship 1	not fouled after 6 months	sold after 6 months

TABLE 5: Sailing data of five ships with tests

ship	in-between drydocking period		date of leaving drydock	performance		
	number	time in months		after drydocking	end of period	characterization [1]
1	1	6.4	9. 7.66	99.8	94.9	-0.0254
	2	13.1	21. 1.67	96.2	88.0	-0.0209
	3	9.6	25. 2.68	93.8	89.7	-0.0142
	4	9.3	12.12.68	96.0	91.5	-0.0162
	5	19.6	20. 9.69	99.3	87.2	-0.0205
	6[2]	11.3	8. 5.71	98.1	93.0	-0.0151
2	1	5.3	28.10.67	98.9	94.8	-0.0258
	2	11.5	6. 4.68	96.7	82.9	-0.0400
	3	14.4	21. 3.69	95.6	82.7	-0.0299
	4	12.7	4. 6.70	96.2	85.2	-0.0289
	5[2]	9.7	24. 6.71	95.7	89.6	-0.0207
3	1	5.6	30. 3.62	100.0	99.9	-0.0008
	2	12.1	17. 9.62	100.0	97.5	-0.0070
	3	11.0	20. 9.63	99.9	96.0	-0.0118
	4	9.0	20. 8.64	100.0	94.3	-0.0211
	5	9.2	19. 5.65	100.0	93.4	-0.0240
	6	9.7	24. 2.66	99.6	95.5	-0.0140
	7	16.7	16.12.66	98.0	89.9	-0.0162
	8	20.8	7. 5.68	95.2	85.6	-0.0154
	9	24.0	31. 1.70	96.9	91.3	-0.0078
	10[2]	5.6	30. 1.72	100.0	96.9	-0.0185
4	1	9.4	8.10.64	99.9	95.0	-0.0175
	2	7.2	19. 7.65	94.9	93.1	-0.0085
	3	15.4	25. 2.66	98.6	85.8	-0.0278
	4	14.5	8. 6.67	100.0	94.3	-0.0132
	5	18.7	23. 8.68	99.1	88.9	-0.0181
	6	17.0	14. 3.70	96.3	86.2	-0.0198
	7[2]	8.1	14. 8.71	93.9	90.1	-0.0158
5	1	3.0	15. 7.60	100.0	99.9	-0.0013
	2	5.5	15.10.60	100.0	98.7	-0.0077
	3	10.2	31. 3.61	100.0	97.5	-0.0082
	4	10.5	7. 2.62	99.4	96.8	-0.0082
	5	7.7	21.12.62	100.0	99.2	-0.0035
	6	10.0	13. 8.63	100.0	99.4	-0.0020
	7	11.0	12. 6.64	100.0	95.4	-0.0140
	8	11.3	12. 5.65	99.8	93.0	-0.0202
	9	9.7	22. 4.66	100.0	94.6	-0.0185
	10	15.1	12. 2.67	99.2	88.5	-0.0237
	11	24.2	16. 5.68	95.1	88.5	-0.0091
	12	13.2	23. 5.70	100.0	90.0	-0.0253
	13[2]	5.6	29. 6.71	96.5	95.2	-0.0079

[1] decrease in performance per day (average in %)

[2] with Hydron ®

TABLE 6: Some examples of economic calculations on ship performance related to surface roughness.

ref.	assumptions				operation speed in knots	earnings per year on fuel [1]	earnings per year on fuel in $	total oil consumption in ton per year	savings in $ per ton per year for 1% reduction in total resistance
	reduction in total resistance in percent	days at sea per year	oil consumption in ton per day	cost of oil per ton					
27	20	300	43.3	£5.-	14.3	£13.000	31.600	13.000	0.122
28	15	150	35	?	18.5	$10.000	10.000	5.250	0.127
	15	275	95	?	16.5	$50.000	50.000	26.125	0.128
	15	260	100	?	22	$50.000	50.000	26.000	0.128
29	20	330	100	$13.-	?	$85.800	85.800	33.000	0.130
30	10	150	32	D.fl.50.-	16.5	D.fl. 24.000	6.860	4.800	0.143
31	10	310	150	?	?	D.fl. 232.500 [2]	66.500	46.500	0.143
	10	170	50	?	?	D.fl. 42.500 [2]	12.150	8.500	0.143

[1] the earnings are on fuel consumption alone
the gain in earning capacity of the ship will certainly be higher than the saving on the fuel bill (26,29)

[2] assuming a cost of oil D.fl.50.- per ton

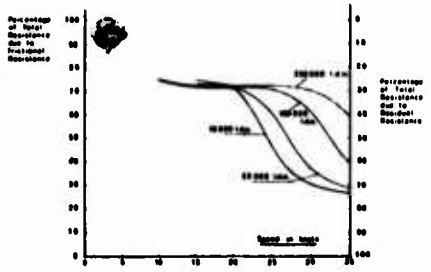


Fig 1

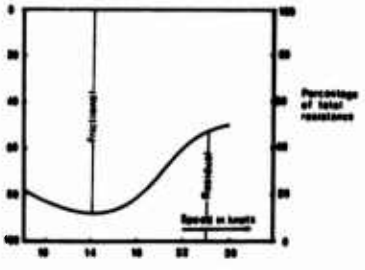


Fig 2 : Percentage of total resistance due to frictional and residual resistance at different speeds. From data of Iwabuchi.

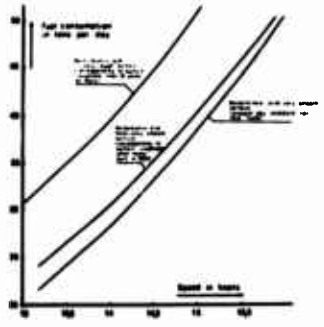


Fig 3 Performance of an 10000 t.dw. tanker influenced by different hull surface conditions

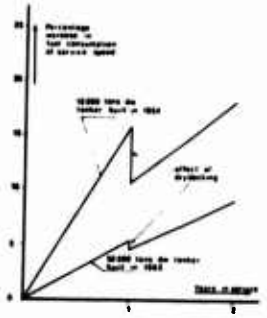


Fig 4 Effect of modern hull treatment upon the performance of ships

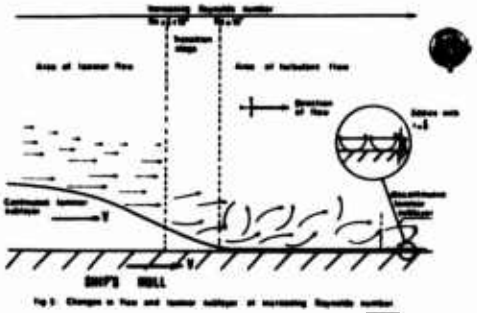


Fig 5 Changes in flow and laminar sublayer at increasing Reynolds number

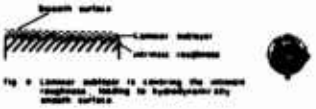


Fig 6 Laminar sublayer is covering the laminar roughness, leading to hydrodynamically smooth surface

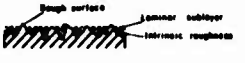


Fig 7 Peaks of laminar roughness are sticking out through the laminar sublayer, the surface remains rough

Fig 8 Rough and smooth surface

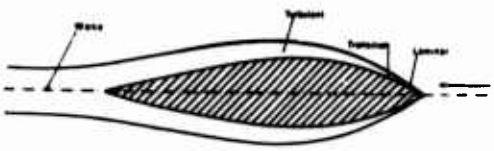


Fig 7 Theoretical flow pattern along ships hull.

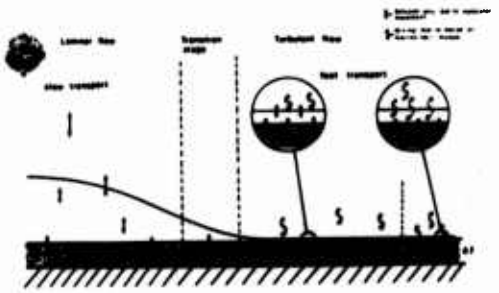


Fig 8 Perpendicular transport along the ships hull, dependent upon type of flow

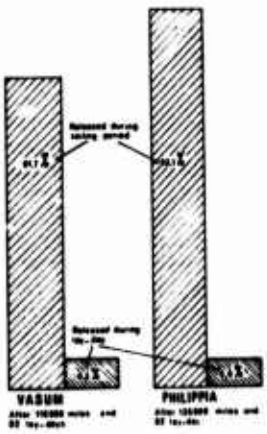


Fig. 9: Comparison of copper released during soiling period and lay-days.

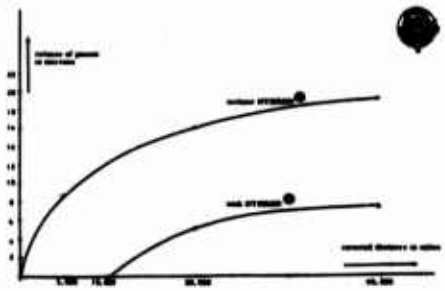


Fig. 10

Diagram 1 Resistance of a moving ship its components and main influencing factors



Diagram 2 Working model for the effect of a Hydron coating as a shipbottom skin

Discussion

Drs. Christie and Crisp: Did we correctly interpret Dr. Van Londen's explanation of reduced drag and leaching rate as being a direct result of the change in the velocity profile which was changed by diffusion of soluble polymer? We would question whether this can be the case since the equations for momentum transport and mass transport normal to the surface are of similar form except for the nondimensional coefficients involved. Since diffusion was more profoundly reduced than drag, we would suggest that the acrylic film merely interposed an additional diffusion resistance between the toxic pigment and the sea water. Whether the profile of the boundary layer is in fact altered by a resin layer did not appear to us to have been convincingly demonstrated in the patent literature since there was no attempt to employ true controls. We noted that a film of material without drag reducing property but of equal smoothness should have been applied to the control panel. Otherwise any observed reduction in drag may simply have resulted from the increased smoothness characteristic of any newly applied film compared with that of the original surface. We ask whether any published experiments with such controls have ever shown significantly reduced drag.

Dr. Van Londen: I apologize for having failed to explain sufficiently clear the drag reduction and the decrease in the release of poison under turbulent conditions. My assumption and working model is an increase in the thickness of the laminar sublayer or a stabilization of that layer. Our laboratory experiments have shown that the release of poison is independent of the thickness of the applied Hydron coating. This demonstrates that the Hydron coating does not merely act as an additional diffusion resistance. I do not know to which patent Drs. Christie and Crisp referred specifically. To my knowledge there is no patent on Hydron describing the theoretical background for the effect of Hydron. Laboratory tests with Hydron in comparison with control inert films are being carried out at the moment in a university laboratory. The practical test using measured miles trials have been done with newly applied coatings. It can hardly be assumed that the thin Hydron coating (less than 10 micrometer dry film thickness) decreased the intrinsic roughness of the hull. The ship was several years old, the hull was in a not too good condition and the application of the Hydron coating was not up to standard. Even so a 4% difference in H.P. has been reported.

MAINTAINING A SMOOTH SHIP BOTTOM

R. P. Devoluy, Woolsey Marine Industries, 201 E. 42nd Street, New York, N. Y. 10017
W. H. Briggs, Newport News S. B. & D. D. Co., Newport News, Va. 23607
John Marra, Sea-Land Services Inc., P. O. Box 1050, Elizabeth, N. J. 07207

This paper outlines the importance of ship bottom smoothness, summarizes the magnitude and the causes of surface roughness, and examines possible remedies for this problem.

Key Words: Shipbottom smoothness, magnitude and causes of roughness, remedies

1. Importance of Bottom Smoothness

The consequences of ship bottom roughness were recently summarized by the manager of a large tanker fleet (1)[1] who is concerned with the inadequacy of drydock space for the new generation of very large cargo carriers if the present 18 to 24 months drydocking interval cannot be extended by longer lasting anti-fouling paints and smooth anticorrosive coatings of greater longevity. For such vessels, on a popular run, the hull surface deterioration loss over 24 months is equal to 18 days ship time. This is worth $166,000 per year solely on the basis of lost speed.

This concern for bottom smoothness is not new. In 1951, U. S. Navy investigations (2) reported significant increases in frictional resistance between sister ships using the hot plastic system and the smoother vinyls. Both types of anti-fouling normally stay clean for at least two years and hence fouling was not a factor in these trials. The vinyls soon became the Navy specification system and they are still used on most American Naval Vessels and on many merchant ships.

In 1950 the owner of a T-2 tanker sought to reduce the bottom and boottop roughness by sandblasting and applying the vinyls. For the next two years it was reported (3) that the speed of the vessel had increased by 0.27 knots while the fuel consumption remained approximately the same. The owner concluded that the bottom treatment was worth seven days of ship time per year. Unfortunately the vessel suffered a severe grounding during the third year. The extensive replacement of plates ended the collection of meaningful data.

2. Causes of Bottom Roughness

These causes can be classified as the attachment of marine fouling due to the inadequacy of the anti-fouling paint for the period between drydockings and the deterioration of the anticorrosive coatings and subsequent corrosion of the steel surfaces. Ship bottom abrasion is a frequent contributor to the failure of both paints. This paper considers the ship bottom area to extend from keel to deep load line inasmuch as it is common practice on large cargo carriers to extend the anticorrosive and the antifouling to the deep load line in order to prevent algae attachments. Some species of algae cause severe loss of speed.

It is often impossible to separate roughness caused by fouling from that resulting from the deterioration of the anticorrosive coating and subsequent pitting of the steel. Fortunately, some observers have been meticulous on this point.

[1] The numbers in parentheses refer to the list of references at the end of this paper.

3. The Effects of Fouling

35% to 45% increases in fuel consumption at 20 knots were reported by earlier observers (4). More recently, and probably more accurately, an increase in fuel of 30% due to general fouling was observed (5). Also, attachments of certain species of algae on the sides of large tankers can cause 30% - 37% extra fuel consumption (6).

An excellent study (7) on the economics of bottom treatment concludes that the cost of the antifouling paint is of secondary importance provided that it reduces the rate of fouling. Obviously, the antifouling must also retain its smoothness. New requirements also include resistance to under water cleaning methods and compliance with the increasingly severe toxicity regulations being imposed by the environmental and labor protection agencies.

4. The Effect of Deterioration of the Anti-Corrosive Coatings and of the Steel Surface

Hydrodynamicists, naval architects and marine engineers have often recommended that more attention to the smoothness of the ship bottom surface would be economically rewarding. Service trials (8) conducted before and after blasting and recoating disclosed a 17% increase in a ship's resistance after five years due to paint roughness and pitting of the steel. Another 3% increase in resistance was attributed to fouling. Hydrodynamically, the surface was returned to essentially new ship condition by the blasting and recoating. The paint roughness was due to blisters and pitting. The blisters ranged from 0.1 inches (2500 μ) to 0.2 inches (5000 μ) in height and the corrosion pits were about 0.1 inches (2500 μ) deep. This investigator also suggested that the shape of the roughness was more important that its absolute height.

A classic paper (9) on the resistance of ships due to skin friction and hull surface condition states that the skin frictional resistance on merchant ships contributes up to 80% of the total resistance for lower speed vessels. The author reports that an 18,000 deadweight ton tanker suffered an increase of 40% in required power due solely to paint breakdown and corrosion products.

One British Ship Research Association report (10) presents a table of mean roughness versus approximate allowance from trials of two 18,000 DWT tankers. It is encouraging to note that there is zero allowance for surface roughness up to 5 mils (125 μ). The values range from 3% allowance for 6 mils (150 μ) up to 32% allowance for 20 mils (450 μ). There was very little fouling on these vessels.

The Norwegian Technical Institute (SFI) found (11) that a seven year old, 37,000 DWT tanker had its surface roughness reduced from an average of 29 mils (725 μ) down to 11 mils (275 μ) by blasting and applying a modern, high-build coating system. At 15 knots this reduction in roughness allowed a 25% decrease in shaft horsepower. Another SFI observer (7) states that a mean roughness of 4 mils (100 μ) corresponds to a 5% to 7% increase in resistance. The SFI has accumulated enough data to publish "Roughness Standards for Ships" (12). This excellent presentation includes plastic sheets reproducing fine degrees of bottom surface roughness. The roughness grades are then related to increases in shaft horsepower.

5. Obtaining a Smooth Bottom

Briefly, the ship owner must choose from the available modern coatings and select the ones which can be applied where his ships are built and where they are likely to be maintained. Unfortunately, it seems that the better coatings are often sensitive to surface moisture and to low temperatures during application.

The vinyl coatings were the first step towards smoother bottoms and are still widely used. They can be applied at very low temperatures but are sensitive to surface moisture.

They remain smooth if applied at the proper film thickness, but they will blister when abraded to a sub-standard thickness. The vinyl antifouling is outstanding and is also used over many other types of good anticorrosives.

The aluminum - bituminous paints were introduced at about the same time as the vinyls and still enjoy a good share of the market. They have good tolerance for adverse drydock conditions and maintain their smoothness unless abraded. They can only be topcoated with coal-tar-rosin types of antifouling and, unfortunately, this type has some tendency to check and crack as the film thickness builds up over the years.

The past decade has seen the development and use of epoxy, coal-tar-epoxy, chlorinated rubber and flakeglas-polyester anticorrosive coatings. To varying degrees these coatings feature low water vapor permeabilit which is judged by many corrosion engineers to be the most important property of an underwater anticorrosive coating. Also these coatings are available in "high build" formulations which permit application economies by obtaining the required film thickness in fewer coats than with traditional paints.

The chlorinated rubbers seem to blister less than the epoxies or the vinyls when abraded much below specified film thickness. However, the epoxies seem to be more abrasion resistant than the vinyls or chlorinated rubbers. Flakeglas-polyesters have the best abrasion resistance, the lowest permeability, and can be applied at 30 to 50 mils in one coat. At present, they cannot be applied below 50°F which is also about the lower temperature limit for epoxies and coal-tar epoxies. The coal-tar epoxies are normally applied as two 8 mil (200 μ) coats and feature good abrasion resistance, low permeability and good blistering resistance.

As previously mentioned, the bottom anticorrosive and antifouling is often carried up to the deep load line. This helps to maintain surface smoothness on this substantial area. As a parameter for the degree of bottom smoothness that can be expected on a new tanker, one owner (13) specifies a maximum average roughness of 5 mils (125 μ).

6. Maintaining a Smooth Bottom

Assuming that most ship owners will eventually invest in superior coatings that can be applied to a satisfactory degree of smoothness, what can be done to preserve the smooth surface by the ship owner and by the shipyards?

The ship owner can control the fouling problem by underwater cleaning techniques, such as scuba divers using rotary nylon brushes or by brush boats, when he finds that his drydocking schedule will exceed the expected service life of the antifouling paint. In addition the economics of such cleaning techniques may be decidedly attractive. For example, at a cost of $4400 U. S. (or less) for a 1100 ft. (340 M) of a large tanker (250,000 DWT), only 1/8 knot of speed needs to be restored to repay the cleaning cost over a 30 day voyage. (Based on low charter rates of about $18,000 per day). A speed regain of a half knot or more is common.

The ship owner can also control pitting at abraded areas and reduce underfilm corrosion by means of impressed current cathodic protection. The potential must be controlled so as not to damage the anticorrosive coatings (14)(15). Cathodic protection is not a substitute for good coatings, and in fact, performs best with high performance coatings that have low permeability and some alkali resistance. With a proper combination, the tendency for roughness to develop is limited to areas of damage or abrasion.

The shipyards can contribute significantly to the retention of bottom smoothness by changing from "sand sweeping" or "brush blasting" with dry sand or grit of irregular mesh size to the use of hydroblasting. It is known that "sand sweeping" to remove loose paint and light fouling roughens the old paint and that the penetration of sand to the substrate leads to underfilm corrosion and blistering of the new coats.

Hydroblasting, at 2400 pounds pressure with a 16 gallon per minute flow rate, removes algae and also barnacles up to 0.25 inches (6250 μ) in diameter. If heavy fouling has to be removed, fine sand can be injected into the high pressure water stream. The latter is much less harmful to the old coating than a dry blast with the variable particle size sand normally used. It has been observed that hydroblasting has a tendency to make the old painted surface smoother. Surprisingly, better antifouling performance was experienced on two hydroblasted ships.

7. Speed Regain

This term is being used to identify the economic rewards resulting from blasting and recoating a rough bottom. "Speed regain" is defined as that percent of loss from the ship's original speed which is recovered by blasting the bottom to remove all paint and corrosion products, and then recoating. It does not include the periodic speed recovery from removing fouling and loose paint, and by routine repainting, at regular drydockings.

Obviously, there are many variables and hence it is not surprising that many different values for "speed regain" have been reported. These variables include:

(a) Is the roughness mainly blisters? What is the height and intensity of the blisters?

(b) Is pitting corrosion the predominant cause of roughness? How deep and how wide are the pits? What is their intensity?

(c) Is the effect of roughness the same for fine form and full form ships?

(d) Does the ship's propeller and rudder have the same smoothness before and after blasting and recoating the bottom?

It is clear that the procedures for returning a blistered paint bottom to a smooth condition will differ from the measures prescribed for pitted bottom plates. A blistered surface, with little or no pitting, is simply blasted and recoated with the required film thickness of a good coating system. A pitted bottom depending on the age of the ship and the severity of the pitting, requires more selectivity in choosing a remedy. Most ship owners are aware that blasting an old bottom with deep pits can yield a rougher surface in spite of recoating with very good coatings. This is caused by the removal of thick rust scale from the deep pits by the blasting. Such deep pits cannot be filled except by troweling with special compounds, or by spray or roller application of thixotropic coatings such as the flakeglas-polyesters.

Recent unpublished data obtained on properly instrumented ships indicate a range of "speed regain" from seventy to ninety-five percent of the new ship speed. New instruments such as that developed by S. F. I. (a trade name is Monotester R) now provide superior surface roughness measurements under drydock conditions. Data can be more readily obtained for correlation with either skin friction or speed regain.

It is now evident that materials, cleaning methods, and technology are now available to improve bottom smoothness and to assess the economic and operational impact of surface roughness. However, the application of these new tools must also encompass environmental considerations as well as economic and operational factors.

References

1. I. B. BLACKWOOD "An Owner's View on Maintenance", Tanker and Bulk Carrier Vol. 18, No. 12, 1972, p. 32.

2. F. H. TODD "Skin Friction Resistance and the Effects of Surface Roughness", Transactions of SNAME Vol. 59, 1951, pp. 315-374.

3. R. P. DEVOLUY "Coating the Bottom with Glass", Marine Engineering/Log, June 1970, pp. 33-35.

4. WOODS HOLE OCEANOGRAPHIC INSTITUTION "Marine Fouling and its Prevention" published by U. S. Naval Institute, Annapolis, Md. 1952, Chapters 1 and 2.

5. G. AERTSSEN "Service-Performance and Trials at Sea", 12th ITTC 1969.

6. H. J. LAGEVEEN - VAN KUYK "Cost Relations of the Treatment of Ship Hulls and the Fuel Consumption of Ships", Netherlands Research Center TNO Report 93C, March 1967.

7. J. F. STORM "Economic Painting and Drydock Practice", SFI Meddelelse No. M.66 Nov. 1965.

8. G. AERTSSEN "New Sea Trials on the Sandblasted Lubumbashi", RINA Transactions 1959.

9. H. LACKENBY "The Resistance of Ships, with Special Attention to Skin Friction and Hull Surface Condition", Institution of Mechanical Engineers, 1962.

10. W. M. LYNN "Trial Performance Results and Hull Surface Roughness Measurements for 18,000 DWT Tankers" BSRA Report 267, 1958.

11. B. M. SORENSON "Measurements of Surface Roughness of Ship Bottoms Can Show the Way to Great Savings" SFI-NYTT (Norway) September 1963.

12. SFI (NORWEGIAN TECHNICAL INSTITUTE) "Roughness Standards for Ships", 1970.

13. I. E. TELFER "External Maintenance Assists Optimization of Hull Performance", Motor Ship, March 1972, pp. 537-539.

14. R. P. DEVOLUY "Behavior of Ship Bottom Paints Subjected to Cathodic Protection", Corrosion, Vol. 9. No. 1, 1953, pp. 2-10.

15. G. W. MOORE & J. H. MORGAN "Cathodic Protection, Its Application in Preventing Hull Roughness" RINA Transactions, 1967.

Written Contribution

After the Congress, Mr. J. H. Morgan wrote as follows:

There were several comments at the Congress on the effect of cathodic protection on paints, and these were mostly concerned with the breakdown of the paint under extreme conditions of cathodic protection. We have noted on ships that have been fully protected a considerable increase in the life of the paint and there have been several remarkable examples of this.

Firstly, on a tanker hull with a coal tar epoxy paint this lasted seven years without re-painting and the hull paint remained smooth and unaffected by its immersion in the sea. It was still possible, at the end of the seven year period, to bring up a shine on the surface by rubbing it. Secondly, we also found on two ships which operated under extreme conditions of scour, one group being ice breakers and the others operating in the Thames Estuary, that although part of the paint was physically removed, that which was not removed remained on the surface in good condition. Before the protection was applied the whole surface was completely clear of paint so that the cathodic protection had succeeded in preserving the paint that was left despite the heavy abrasion.

I believe this extension of the preservation of the paint is a very important aspect of ship impressed current cathodic protection which we are only just beginning to observe. It is only in the last decade that reliable impressed current systems have given continuous protection and this has only been applied to a significant number of ships in the last seven or eight years. We now have a lot of experience of ships protected during this period, and we are able to say without any doubt that cathodic protection in which the hull is held at or close to the accepted criterion of protection will extend the life of the hull paint when this is not adversely affected by alkalinity.

Observations on the breakdown of paint surfaces by ship-fouling algae

Betty L. Moss

Department of Botany
The University
Newcastle upon Tyne NE1 7RU, U.K.

Zoospores and zygotes have been grown on a variety of substrates. Their method of attachment has been studied, using both light and electron microscopy. The primary rhizoid is negatively phototactic and grows down into the substrate. If the substrate is hard, then lines of weakness, such as the microscopic cracks in a paint film, are penetrated. Rhizoid production continues throughout the life of the plant. The rhizoids radiate out from the base of the thallus and eventually penetrate the substrate for a considerable distance, so building up a firm anchorage. This rhizoid development results in the physical breakdown of the surface layers of the substrate. It is suggested that such algae, growing on the sides of ships or on wooden jetties, are active bio-deteriorants.

Key Words: Enteromorpha; germination; rhizoids; Scanning Electron-microscopy; substrate penetration; breakdown of substrate; bio-deteriorants.

---

1. Introduction

Species of marine algae which are concerned with ship-fouling require an extremely strong anchorage if they are to remain attached to the substrate of paint and corroded metal on the sides of a ship. Like all marine algae they have the continual battering of wave action to withstand, but in addition they have the movement of the ship to combat. Against these combined forces of water movement, plants of Enteromorpha and Ectocarpus have a remarkable tenacity.

Species of Enteromorpha and Ectocarpus reproduce by motile cells which swim around for a time and then settle on a substrate. Whether this be on a moving ship or on a wooden jetty, there must be an immediate and strong adherence of the cell to the substrate so that it is not washed away by the next wave. Evans and Christie[1] have demonstrated that the initial adhesion of zoospores of Enteromorpha is associated with

---

[1] Figures in parenthesis indicate the literature references at the end of this paper.

the production of extrafibrillar material, some of which is proteinaceous in character with a probable carbohydrate component. Following this initial adhesion, the zoospore or zygote soon shows signs of germination when a protuberance grows out on one side. This outgrowth is soon cut off by a cell wall from the rest of the cell. It continues to elongate and eventually it forms a long filament of cells with apical growth, constituting the primary rhizoid. While this rhizoid develops, the rest of the zoospore or zygote grows out in the opposite direction to form a filament of cells which subsequently differentiate into the thallus. The present study follows the growth of the primary rhizoid and its association with, and its effects upon, the substrate.

2. Method for obtaining cultures of Enteromorpha

Dense suspensions of zoospores or zygotes were obtained following the method described by Christie and Shaw[2] and Christie and Evans.[3] Adult thalli were originally collected from the coast of Northumberland about 3-5 days before the high spring tide of each month, transferred to the laboratory in plastic bags, and then set up in a dish of seawater receiving unilateral light. The zoospores which were liberated moved away from the light, whereas gametes and parthenospores aggregated on the side of the dish towards the light. Suspensions of these reproductive cells could then be pipetted into culture dishes containing either Erdschreiber solution, or seawater with added nitrates and phosphates. In the bottom of the culture dishes were placed glass coverslips, glass slides, or other substrates upon which the motile cells were allowed to settle in the dark. They were subsequently transferred to culture cabinets kept at constant temperature and illuminated from above by fluorescent tubes.

Material for examination under the Scanning E.M. was generally fixed, together with the substrate, in Langlet solution, and then dehydrated prior to being sprayed with gold for examination. This prefixed and predried material generally gave better results than when living material was sprayed straightaway.

3. The rate of germination of zoospores

Zoospores were allowed to settle on glass slides placed at the bottom of culture dishes containing Erdschreiber solution. The dishes were kept in a culture cabinet at 10°C and were supplied with light of approximately 4300 lux from overhead fluorescent tubes on an 16 hour/8 hour, light/dark period. At daily intervals the slides were removed and examined under a light microscope for visible evidence of germination. On settling, the zoospore is roughly spherical in shape, whereas on germination the primary rhizoid can be seen as a protuberance growing out from one side (Fig. 1a and b). Several hundreds of zoospores were counted on each slide and the percentage which had germinated was calculated. The slides were replaced in the culture medium and the same ones were examined and counted over a period of 14 days. The following results were obtained:

Time	% germination
5 days	43%
7 ,,	51%
10 ,,	60%
14 ,,	70%

This indicates that a population of zoospores which had been liberated simultaneously do not show synchronous growth and cell division when kept under constant culture conditions of light and temperature. A progressive increase in the numbers germinating occurred with time.

Simultaneously some culture dishes of settled zoospores had been covered with dark paper so as to obscure all light. These slides were again examined at intervals for visible signs of germination. After 14 days in total darkness, many zoospores were colourless and appeared to be disintegrating. A small number had put out a rhizoidal protuberance but in no case was this ever seen to be cut off by a distinct cell wall from the original parent cell. The viability of such cells which had been kept in total darkness was tested by transferring some of these same culture dishes to the light regime of the other dishes, at daily intervals. They were then left for twenty days under the light regime and at the end of these twenty days the number of young plants which had grown was counted. Assuming that these dishes originally would have yielded the same percentage germination as the previous ones, the percentage survival was calculated. After 10 days in continuous darkness, a survival rate of 16.7% was obtained. After more than 10 days in continual darkness, only an occasional thallus survived.

4. The effect of light upon the direction of growth of the primary rhizoid

Experiments were set up with zoospores plated out on glass slides which were placed in culture dishes kept at 10°C and illuminated from one side only. After one week the direction of the growth of the rhizoidal cell was determined from several hundred zoospores. The following percentages were obtained:

Growth towards the source of light	18.3%
Growth away from the source of light	61.3%
Growth perpendicular to the light source	20.4%

In a second series of experiments set up, the direction of growth of the primary rhizoid was determined at 5, 7, 10 and 14 days respectively. The following results were obtained:

Time	Towards the light source	Away from light source	Perpendicular to light source
5 days	6%	81%	13%
7 days	12%	73%	15%
10 days	6%	87%	7%
14 days	0%	96%	4%

These results show that the primary rhizoidal cell generally grows out from the side of the zoospore away from the source of incident light. When similar samples were examined over a longer period of time, those rhizoids,which at first had grown towards the source of light or perpendicular to it, soon curved round and grew away from the light, so that after 14 days' growth practically all the primary rhizoids were growing away from the light.

5. Growth of the rhizoids on various substrates

For the following observations made both with the light microscope and the Scanning E.M., zoospores and zygotes were allowed to germinate on various substrates so that the growth and the subsequent development of the rhizoidal system could be followed. Glass is commonly used as a laboratory substrate, but it differs from most natural substrates of these algae in that it is completely non-porous. Plants were grown on agar made up in sea water containing additional nitrates and phosphates. This was a soft substrate in which the course of the rhizoids could be clearly seen. Harder substances, such as films of paint, with and without antifoulants, were sprayed in

thicknesses of 1mm or 2mm directly onto the E.M. stubbs, and these were used as substrates on which the zoospores could settle and germinate. Nylon fabrics and glass fibre ribbon were found suitable substrates to examine under the Scanning E.M. as also too were shavings of wood. The latter could also be fixed and sectioned for examination under the light microscope.

As in most species of marine algae, growth of the primary rhizoid of Enteromorpha is associated with the production of extracellular mucilage. This seems to be produced at and around the growing apex. Under the light microscope it appears as a colourless layer surrounding the tip of the rhizoid and if sectioned and examined under the E.M. it appears as a light staining layer. Its thickness sometimes equates or even exceeds the diameter of the rhizoidal cell. That it probably serves as an adhesive is shown by the fact that when zoospores are plucked from a glass surface, it is the intimate contact of this mucilage with the glass which is broken. As a rhizoid grows and advances through a substrate, this mucilage gets left behind as a thin layer all around it.

If the zoospores are germinated on a soft clear substrate such as agar, with light coming from above, then the rhizoids, being negatively phototactic, grow straight down into it. In the early stages of growth, the rhizoids may penetrate far deeper into the agar than the thallus extends above it in the opposite direction. Rhizoids grown on agar are absolutely straight, unless they meet another rhizoid; the only solid obstacle to be encountered in such a substrate. Then there is an immediate twisting and coiling of the rhizoids around each other, suggesting perhaps that the rhizoids are sensitive to contact. Whatever substrate other than glass was used, the primary rhizoid always grew down into it. Figures 1,f and 2,a show primary rhizoids entering wood and nylon fabric respectively. Always the initial production of the primary rhizoid seems to raise the zygote or zoospore up above the substrate, suggesting that a great deal of physical force is essential for the initial penetration by that rhizoid. If the substrate is hard, so that immediate penetration is not possible, then the rhizoid may spread out over the surface, keeping very close contact with all its irregular contours, until a way in is found. In woven or knitted nylon fabrics, the primary rhizoid could be followed, pursuing a tortuous course and interweaving between the fibres of the fabric. In some experiments, the zoospores were grown on glass fibre ribbon approximately 1mm thick which was suspended in a dish of seawater. Light was supplied from above, while the sides and bottom of the dish were enveloped in black paper. The rhizoids grew straight through the fibre glass into the darkened medium and hung there just like a crop of roots developing from seedlings.

When grown on thin films of paint, the tips of the rhizoids frequently burrowed along under the surface (Fig. 1,c). Small cracks represented lines of weakness where the tip could penetrate (Fig. 1,e). Paint films containing antifoulants prevented germination of the zoospores (Moss and Woodhead)[4]. No growth of a primary rhizoid occurred and the smooth coat of the normal zoospore was thrown into irregular folds (Fig. 1,d). When grown on shavings of pine wood, the course of the primary rhizoid could be followed easily by sectioning the substrate and examining it under the light microscope. The rhizoid advanced along the cavity of a tracheid, and then penetrated through the pits into neighbouring tracheids, the pits being the obvious areas of weakness. The diameter of the rhizoid was generally restricted where it went through the pit and then it expanded again in the cavity of the next tracheid. Plants which had been growing for 2 or 3 weeks had their rhizoids penetrating well down inside the tracheids of the wood.

The growth of the primary rhizoid is soon followed by others which originate as tubular outpushings from cells near the upper end of the primary rhizoid and also from the basal cells of the young thallus (Fig. 2,c). They radiate out around the base of the young plant and eventually all of them penetrate the substrate (Fig. 2,b). This production of rhizoids continues throughout the life of the plant, so that eventually hundreds of them are developed by each thallus. They interweave and make a complex anastomosing system over the surface and penetrate down into the substrate. The fact that they do penetrate the substrate may have drastic effects. Young plants growing on wooden jetties can be seen to penetrate the vessels or tracheids of the wood for a

considerable distance. Breaking through the cell walls, or through the thinner regions of the pits in the wood, will result in the physical breakdown of the surface layers of the wood by the rhizoids. Samples from ships are generally so mixed up with thick layers of paint and corroded metal that the course of individual rhizoids is difficult to follow. But on a metal plate which had been coated with antifoulant and attached to a ship on the north-Atlantic run, the early stages of algal colonisation, and the damage this caused, were clearly visible. A sparse population of Ectocarpus had developed on the plate. By the time the plate was received, these plants had dried out and the thalli had been torn off. But the basal rhizoidal systems remained and the darkened circular areas in Figure 2,d show where the rhizoids had spread out from the base of each plant. As a result of this rhizoid penetration, the paint surface was raised and cracked, and under higher magnification with the Scanning E.M. it appeared irregular and extremely pitted (Fig. 2,e). The densely interweaving rhizoids had grown through the paint film and through the silver coloured primer which had been applied to the steel plate. Under this they had spread out in a rosette in close contact with the metal. Each rosette of rhizoids was surrounded by the obvious stainmarks of corrosion.

6. Discussion

The preliminary experiments showing that in a population of swarmers of Enteromorpha there is staggering in the timing of germination means that if they settle on the side of a ship whilst it is in port these same swarmers may show no macroscopic signs of growth until after the ship has made perhaps two voyages across the Atlantic. Whilst many zoospores appear to remain dormant for up to two weeks, even when supplied with the right temperature and light conditions, others germinate immediately. This would mean that in a first population on a freshly painted ship you would straightaway get a succession of development. If the ship passed through unfavourable conditions for the growth of Enteromorpha at one stage, then it is likely that some other developmental stages might persist. The fact that some zoospores could remain viable in the dark at 10°C for 10 days is an obvious advantage to a species colonising ships. If the ship is drawn up alongside a quay for several days where light to the algae is restricted, then this might temporarily restrict their growth. When the ship moved away again so that the algae were in direct sunlight, normal growth would be resumed. The length of time during which zoospores remain viable is considerably shorter than that recorded for many brown algae, e.g. Kain [5] reported that zoospores of Laminaria sp. remained viable up to 60 days in total darkness at 10°C and Moss and Sheader [6] found that germinating eggs of Halidrys-siliquosa remained viable in the dark for up to 120 days.

After the initial adherence of the reproductive cell to the substrate, the primary rhizoid grows out on one side, away from the source of incident light. This negative phototactic response is similar to that of the primary rhizoid of Fucus and many other marine algae. It means that the rhizoid behaves like the root of a higher plant, and grows away from the source of light, down into the substrate. At the same time, the young thallus, like the shoot of higher plants, grows out in the opposite direction towards the source of light and so makes for maximum photosynthetic efficiency. From the tip of the rhizoid, copious mucilage is produced, and undoubtedly this is concerned with adhesion to the substrate. But as the rhizoid advances through a substrate, this mucilage may get left behind as a thin outer coating. In addition to adhesion, perhaps it may also act as a lubricant and as a cementing filler lining the cavities through which the rhizoid is penetrating.

After the primary rhizoid penetrates the substrate, and as the thallus grows, so more basal rhizoids are produced. These spread out in a rosette-like system from the base of the young plant and eventually they too grow down into the substrate. The production of these basal rhizoids is a continuous process throughout the life of a plant so that eventually a single thallus may have many hundreds of rhizoids. Each rhizoid is only 10μm or less in diameter, but each one may penetrate several millimetres down into the substrate. How is this penetration achieved? The present observations suggest that mainly physical force is involved. The raising of the reproductive cell above the surface and the manner in which the rhizoid may burrow into the surface layers of paint films suggests this. Possibly it is the sensitivity to contact which enables the rhizoid to

closely adhere to and to follow the contours of an irregular hard substrate, until a crack or line of weakness is found for penetration. When growing on a substrate of wood, it was the pits, i.e. the weakest point in the cell wall thickening, which were used as the points through which the apical cell of the rhizoid could penetrate and so advance from tracheid to tracheid.

While individual rhizoids are microscopic in size, the combined growth of hundreds of them from a single plant may lead to "blistering" of the surface of the paint. They may penetrate through the paint film and down to the metal surface. If they are growing on wooden jetties or quay headings, then the rhizoids may penetrate several millimetres down below the surface of the wood. If growing on a ship, then the rhizoids may penetrate through the paint down to the metal. The effects of the rhizoids boring into a substrate may not be as dramatic or as obvious as is the action of some boring animals, but nevertheless the action of a dense population of algae will in time severely break down the surface layers of the substrate on which they are growing. In fact, these algae appear to be active bio-deteriorants.

The algae on a ship may also be the initial sites of corrosion. When the rhizoids penetrate the paint and meet the resistant hard metal, they may spread out over this in a rosette shape. When the thalli of such plants reproduce and disintegrate, the basal rhizoids will remain behind. Then they could act like a candlewick, absorbing seawater and carrying it down directly to the metal surface. If the rhizoids disintegrate completely, then the minute capillary channels which they formerly occupied would become filled with seawater. So that these sites of colonisation by the algae could become points for the initial corrosion of the metal below.

References

1. L. V. EVANS and A. O. CHRISTIE, Ann.Bot. 34, 452-482 (1970).

2. A. O. CHRISTIE and M. SHAW, Br.phycol.Bull. 3, 529-534 (1968).

3. A. O. CHRISTIE and L. V. EVANS. Nature, Lond. 193, 193 (1962).

4. B. MOSS and P. WOODHEAD. New Phytol. 69, 1025-1027 (1970).

5. J. KAIN. J.Mar.Biol. U.K. 49, 455-473 (1965).

6. B. MOSS and A. SHEADER. in press (1972).

The experiments described at the beginning of this paper were carried out by P. Woodhead during the tenure of a research studentship donated by British Paints Ltd.

Summarized Discussion

In reply to the question whether there was any evidence of penetration by other than mechanical effects, specifically enzyme attack, the author said that there was no evidence for this, and that the observations suggest that the penetration is purely physical. In answer to another question, the author stated that the mucillage was not analyzed--because of the small amount of material, analysis would be difficult--but one would expect differences among the green, brown, and red algae which synthesize different metabolites.

In reply to queries about the depth of penetration of rhizoids, the author said that no definite figure could be given since it depends on so

many factors. In substrates such as wooden piles and jetties one can find them several millimeters down, but not inches. They would penetrate a coat of antifouling paint; she would not like to put a definite figure to the thickness of the paint, but it was of the order of one millimeter.

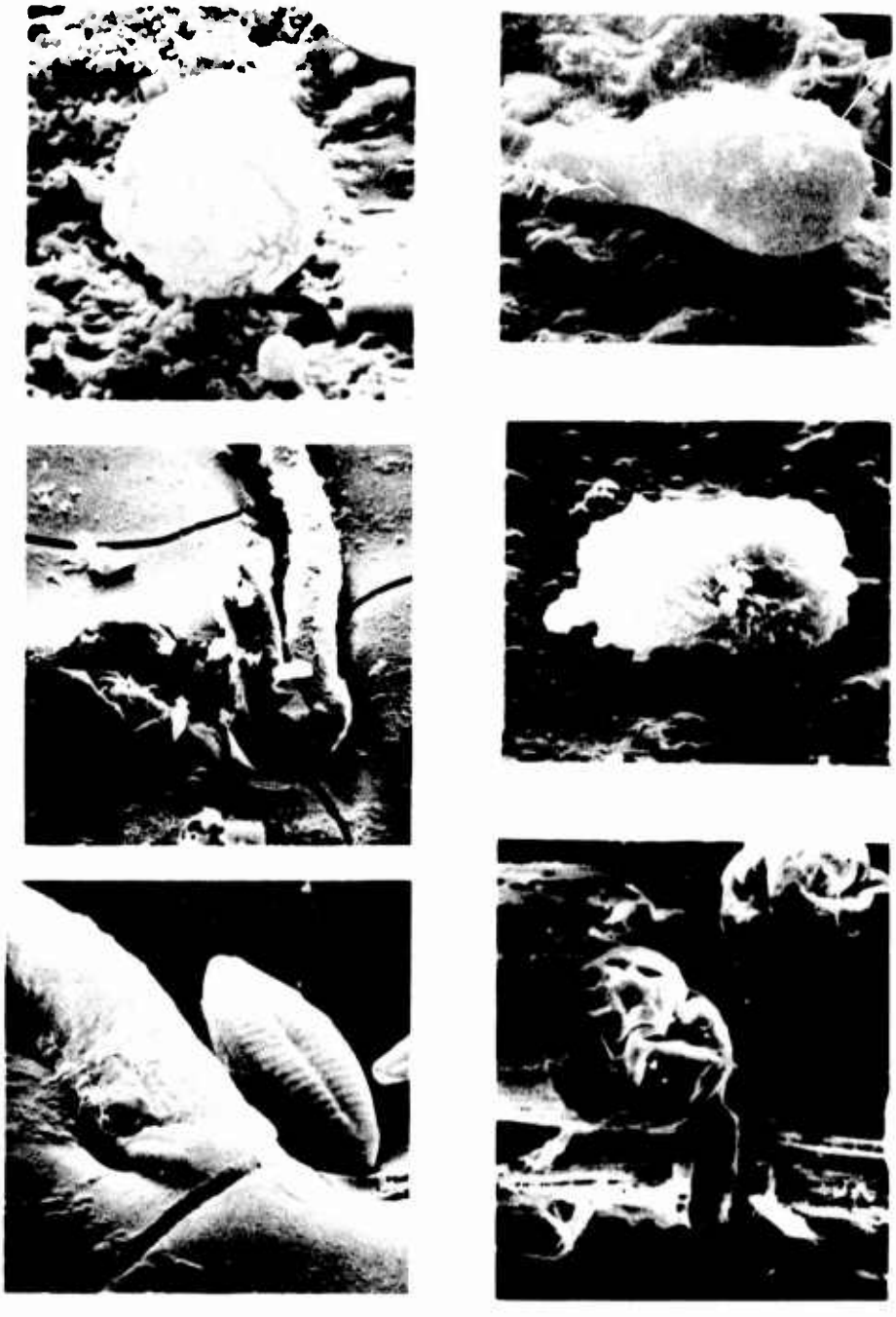


Figure 1. Development of the primary rhizoid. a) settled zoospore with rhizoid protuberance. b) rhizoid elongating. c) tip of rhizoid burrowing into surface of paint. d) irregular form of zoospore in contact with antifouling paint. e) tip of rhizoid entering paint. f) rhizoids penetrating tracheids of wood.

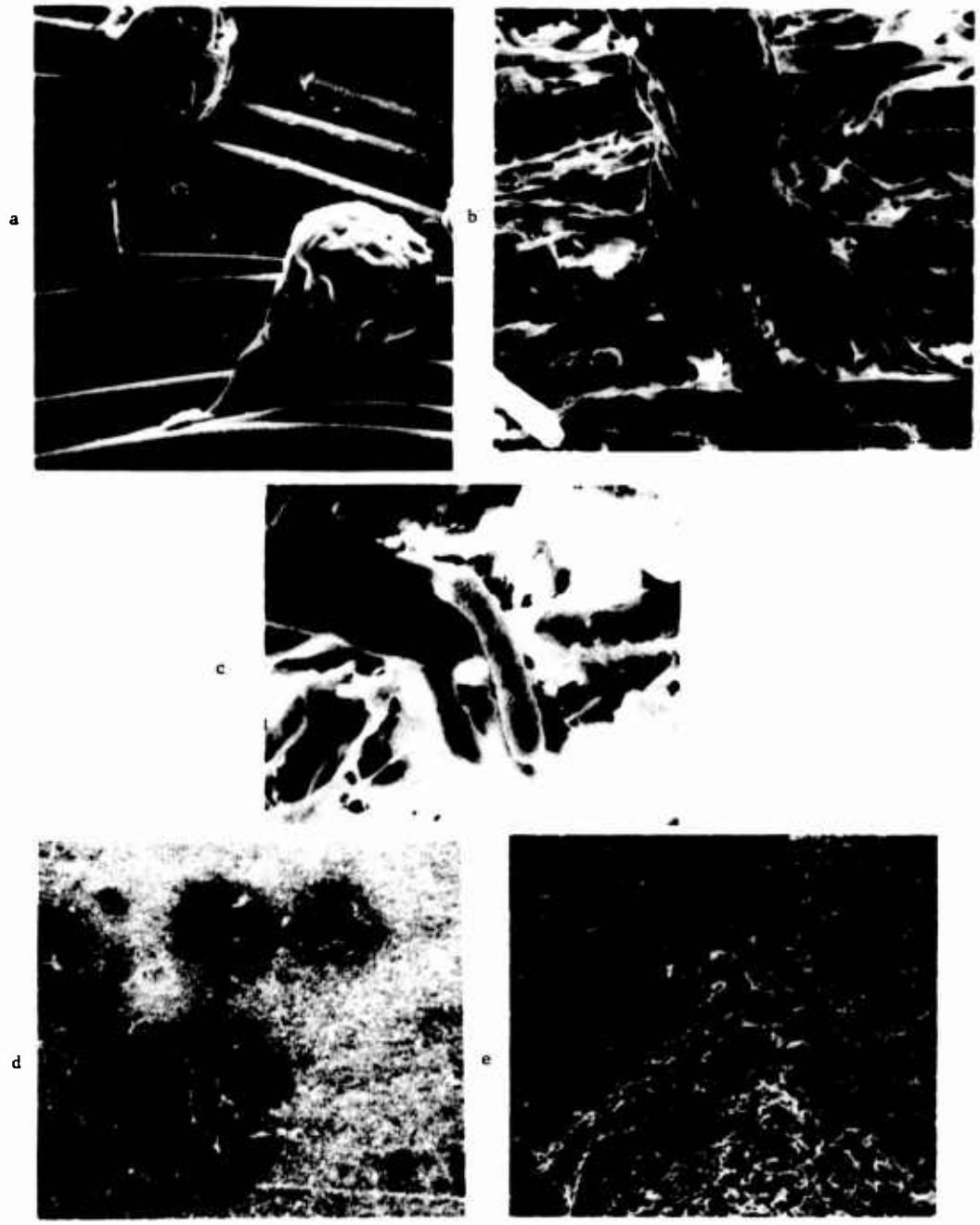


Figure 2. a) Entry of the primary rhizoid between nylon fibres
b) Development of two more rhizoids from base of the thallus. c) extensive rhizoid system of an older plant. a, b and c x approx. 1000. d) discolouration and blistering of paint surface by rhizoids from individual plants x approx. 30. e) portion of (d) showing "pitting" and damage to paint as seen under the Scanning E.M. x approx. 200.

Corrosion and Fouling of an Instrumented Array at a 600-Foot Ocean Site

Joseph R. Padilla and James S. Muraoka

Naval Civil Engineering Laboratory
Port Hueneme, California 93043

This report presents data obtained at a 183-meter site in the Santa Barbara Channel by the deployment of three instrumented arrays and discusses the effects of fouling and corrosion on the arrays. Each array consisted of three current meters placed at 182-, 90-, and 15.5-meter depths and supported by an aluminum buoy. Each array was anchored by a concrete block to which test panels of wood (Douglas fir), plastics, creosote-impregnated concrete, and rope specimens were secured. The arrays were deployed for 6-month periods starting in January 1970, August 1970, and August 1971. Severe corrosion occurred on the current meters of the first array. Fouling reduced the useful data from the 15.5-meter instrument to only 44 days; the other meters functioned throughout the deployment period. Corrosion of array number two was completely arrested by the use of zinc anodes. A new instrument was used on array number three at the 182-meter position to record current speed and direction, conductivity, pressure, temperature, and time for each 15 minutes throughout the deployment, but corrosion of this instrument prevented the collection of current data. Current speeds for all three arrays averaged 0.12 m/sec at 15.5 meters, 0.075 m/sec at 90 meters and 0.057 m/sec at 182 meters. Mean current direction varied between 270 and 299 degrees. Barnacles were found attached to the aluminum buoys and concrete anchor blocks; hydroids and other fouling organisms covered instruments that were not protected by antifouling paints but were not found on concrete panels or on instruments that were coated with antifouling paints. Wood panels were riddled by borers, including *Xylophaga washingtona* and *Bankia setacea*; plastic panels were free of growth but sustained damage from borers on parts adjacent to wood panels. Rope specimens were subjected to tensile strength tests. The strength of nylon rope decreased, that of polyester rope remained the same, and the strength of polyethylene and polypropylene rope increased.

Key Words: Fouling; sea water corrosion; marine borers; barnacles; *Xylophaga washingtona*; *Bankia setacea*; arrays; current meters.

Introduction

In 1970 the Navy undertook a project to evaluate the technology of underwater construction. The project, called SEACON (an acronym for SEAfloor CONstruction experiment), consisted of 20 different experiments to evaluate hardware and new techniques in use or under development at the Naval Civil Engineering Laboratory in the area of ocean engineering (1).[1] The goal was to emplace a concrete foundation on the seafloor and later, through a guideline system, place a concrete structure on top of this foundation. As in any construction experiment, a site investigation was necessary to choose a site; and once chosen, to predict and analyze the performance of the structure and foundation to be placed on the seafloor. The site chosen was in the Santa Barbara Channel, some 6 miles

[1] Figures in parentheses indicate the literature references at the end of this paper.

(11.1 km) south of Santa Barbara, California, at 34°17'11"N latitude, 119°42'47"W longitude. A water depth of 600 feet (183 m) was chosen in order to push the technology beyond scuba diving capability and beyond the 100- to 200-foot (approximately 30- to 61-m) depths which have seen so much construction that they can be considered state of the art. Figure 1 shows the location of the construction site.

Few environmental data existed in the literature for this site when the survey was started. In addition to collecting short-term data at the site by such means as bathythermographs, water sampling and visual observations of the sea conditions, NCEL decided to gather some long-term environmental data prior to, and during the period the concrete structure was on the bottom. This paper deals with the corrosion and fouling of instrumented arrays while deployed at the site over a 2-year period.

Materials and Method

Test Arrays

Array Number One. The first array, deployed on January 28, 1970, consisted of three Richardson type current meters programmed to record current speed and direction on film and on magnetic tape at 30-minute intervals for a 6-month period. The meters were placed at the bottom (182 meters), mid depth (90 meters), and near the top of the array (15.5 meters below the surface). The array with the meters was suspended with an aluminum subsurface buoy and held in place by a 2 x 3 x 3-foot (0.61 x 0.915 x 0.915-m) 1,783-pound (807-kg) concrete anchor block as shown in Figure 2. The meters are designed to take an in-line loading, but because of failures of the tie rods during retrieval the meters were mounted in specially designed brackets. Three-eighths-inch (9.52 mm) wire rope was used between the meter mounting brackets. Figure 2 shows a 38-inch (0.965 m) diameter, 6061-T6 aluminum buoy which was sand blasted and painted orange; the wire rope of 6 x 19 construction, greased; and the steel meter mounting brackets which were sand blasted and painted with zinc powder paint. The concrete anchor block was used also to support test samples for biodeterioration and fouling studies. On this first array only one slab of creosote impregnated concrete was tied to the lifting eye of the concrete anchor block.

Array Number Two. After consultation with the manufacturer of the meters, several steps were taken to improve upon the design of array number one. On 28 August 1970 the second array was deployed in essentially the same area (34°17'15.5"N, 119°42'47.5"W) 1,000 feet (305 m) from the site of the first array. Figure 1 shows the location of this array and the other two array locations. This array was basically the same design as array number one, with a subsurface buoy, anchor weight, and the three current meters.

One of the changes incorporated into the second array, as a result of array number one's performance, was to paint the same subsurface aluminum buoy with zinc powder paint. Because gray is difficult to distinguish by divers, two 6-inch (152.4 mm) white stripes were painted around the buoy. In addition, the meters were isolated from the steel brackets and shackles by nonferrous micarta-like isolators. Also, 1-pound (0.453-kg) MIL-SPEC zinc anodes were mounted on the meters, as shown in Figure 3. Mounting rods of aluminum were used to connect the major portions of the meter to the anode electrically. The anodizing on the meter case parts was machined off to permit metal-to-metal contact for electrical continuity for proper anode performance. A copper base antifouling paint was applied to the rotor and vanes and the housing surrounding these parts. This was done for the meter which would be placed at the top of the array only. The concrete anchor block was modified with aluminum brackets to permit the mounting of additional samples of wood, acrylic and creosote impregnated concrete test panels. These are shown in Figure 4.

Array Number Three. The acquisition of a new digitizing instrument capable of recording current speed, current direction, water temperature, pressure, and conductivity data influenced the design of array number three. This time the changes were minor because of the good results obtained from array number two. The new meter was placed at the bottom of the array to obtain the additional parameters which would be of more value at the level of the concrete structure. This meter was delivered with an anode mounted on one end of the meter. Anodes were also attached to the ends of the stainless steel tie rods. The use of anodes on the tie rods is questionable, especially if they are designed to protect the tie rods from crevice corrosion failures under rubber standoffs. This meter was not mounted in the special bracket for the deployment, but the isolators were used to separate it from the steel

hardware and wire. The mid-depth and top meters were the same ones used previously. The two top meters were programmed to record data at 30-minute intervals for 208 days, and the new meter at 15-minute intervals for 240 days. The meters and the buoy needed no refurbishment other than a washing to remove the previous biological growth. Wood, ropes, plastic, acrylic, and concrete test panels were again attached to the bottom concrete anchor block. Due to delays in the emplacement of the main experiment (the concrete structure), array number three was not deployed until 28 August 1971.

Test Panels for Fouling and Biodeterioration

The antifouling concrete test panels which were exposed at this site were prepared by saturating lightweight expanded shale aggregates with a chemical solution composed of a mixture of (1) creosote oil, (2) tributyltin oxide, (3) pentachlorophenol, and (4) malachite green (water and oil soluble). The chemically saturated expanded shale aggregates were then mixed in a cement mortar and cast in a wood mold to form a 1 x 6 x 12-inch (25.4 x 152.4 x 304.8-mm) panel (2). The concrete anchor block served as the control block.

The various plastic panels which were exposed at this site are listed in Table 1. A 1/4 x 2 x 3-1/2-inch (6.35 x 50.8 x 88.9 mm) wood piece (Douglas fir) was placed between each plastic panel to serve as a spacer and as a wood bait piece. The panels were fastened together with a type 316 stainless steel bolt. The assembled plastic and wood panels were then secured vertically to a 1/2-inch (12.7 mm) thick aluminum bar attached to the side of the concrete anchor block as shown in Figure 4. The panels were exposed approximately 1 meter above the bottom sediment. A hardness test was conducted before and after exposure using a Durometer (ASTM D1484). The results of this test are presented in Table 1.

The synthetic rope specimens exposed at this test site are listed in Table 2. An eye was spliced at each end of the rope specimens so that a tensile strength test could be performed upon recovery. These 2-foot (0.61-m) lengths of rope were secured to the concrete anchor block.

Results and Discussion

First Array (January 1970-July 1970)

Corrosion and Fouling. The first array was retrieved on 23 July 1970, 176 days after implant. This provided the first long-term corrosion and fouling data as well as current data for the site (Figure 5). Corrosion of the meters was severe at all depths, but the worst damage occurred on the top meter. The aluminum pressure cases did not leak, but several parts of each meter had to be replaced because the integrity of the part was questionable for another deployment. The severe pitting and corrosion was obviously due to the use of steel brackets, wire, and hardware directly connected to the aluminum meter cases. The screw-in anodes supplied with these meters failed to function. Figure 6 shows the area where the anode was screwed into the case. An analysis of the composition of these anodes showed them to be standard zinc castings with impurities rather than pure zinc, which may account for the poor performance and effect as shown in Figure 7.

The greatest detrimental influence on the primary function of the array, that is, the collection of environmental data, was from fouling. All three meters and the wire had some degree of hydroid growth when retrieved after 176 days. The current meter brackets, on the other hand, were free of growth. This is attributed to the zinc powder paint which was used to a greater degree in the second array as a result of the performance of the first array. The top meter (15.5 meters) experienced such severe fouling attachment of hydroids and barnacles that the direction indicator vane ceased to turn with changes in current direction (Figure 8). The complete "stop" condition occurred 54 days after implant, with the actual influence on the current data occurring only 44 days after implant. With Savonius rotors, the speed data from these meters was greatly influenced in the low velocity area by the marine growth which increased the weight and unbalanced the rotor. It should be noted that the rotor and vane of this top meter were not protected with antifouling paint, whereas the lower two meters were.

Fouling and Biodeterioration. Numerous barnacles (*Balanus tintinnabulum*, *Balanus concavus pacificus*, and *Balanus nubilus*) were found attached to the aluminum buoy which was exposed about 14 meters below the surface of the sea. During growth, the shells of several of these barnacles had penetrated the protective coating as shown in

Figure 9. The antifouling concrete test panels exposed near the seafloor were free of any marine growth. However, growing on the concrete anchor block, which served as the control block, were traces of hydroids and approximately 25 small goose barnacles, *Scalpellum osseum*.

Second Array (August 1970-December 1970)

Corrosion and Fouling. Ship schedules demanded an early retrieval of array number two after only 128 days. The corrosion and fouling performance of array number two was markedly improved over that of array number one. The aluminum subsurface buoy showed no further pitting, and the only growth was on the white stripes. The meters also were devoid of corrosion this time, and it was obvious from the shape of the zinc anodes that they were performing as they should. The growth on all three meters was less, which is a result of the shorter immersed time and the different time of year that the meters were in the water. The water was warmer during the period the second array was deployed than when the first array was deployed; the current patterns were essentially the same (Figure 10). The rotor and vane areas on all three meters were devoid of any growth of any consequences, even though the top meter again had considerable growth on other parts. The wire rope used in array number two was the same as in array number one. It was beginning to show some surface corrosion, but could conceivably have been used a third time.

Fouling and Biodeterioration. The antifouling concrete panels were free of any marine growth. The concrete anchor block which served as a control block was also free of marine growth except for a trace of hydroid attachment. Upon recovery, the surface of the chemically treated panels became covered with creosote oil. The oil oozed out of the expanded shale aggregate panels as they expanded when exposed to the warmer atmospheric condition aboard ship. The surface of a clear acrylic plastic panel was covered with a thin layer of slime growth together with a fine bottom sediment. The visibility was considered good through the plastic panel as shown in Figure 11. The information on fouling of acrylic plastic was of interest because this material was used as a window in the SEACON structure and on other undersea structures. Numerous molluscan wood borers, *Xylophaga washingtona*, were found inside a Douglas fir panel. The shells of the largest borer measured about 1/4-inch (0.635 cm) in diameter. Other species of fouling organisms normally found attached to materials exposed at the surface of the sea such as acorn barnacles, mussels, tubeworms, and bryozoans were not found on test panels exposed at this depth.

Third Test Array (August 1971-February 1972)

Corrosion and Fouling. The third array was retrieved on February 25, 1972, exactly 186 days after emplacement. The new current meter at the bottom provided at least 6 months' data of temperature, pressure (even though it remained at one depth), and conductivity for the site. These data are listed in Table 3. The current velocity data are questionable in view of past data and the problem is being looked into. Upon retrieval, the rotor was found to be loose in its housing, that is, no longer in the small screw-type cup bearings. A closer examination disclosed that the bearing on one end plate was missing, the end plate which had the anode mounted to the outer side. In spite of this, the area around the bearing corroded and the bearing fell out. The threads were no longer visible. Corrosion was not severe on the meter, but the housing around the rotor had some deep pitting on one of the rods. The other end of the meter, approximately 2 meters away from the anode, also showed some localized pitting. The refurbishment can be considered minor compared to the meters which were emplaced for almost the same length of time and at the same time of year on array number one. The other parts of the array were in excellent condition when retrieved. The top meter again had severe marine growth except on the rotor and vane housings end, which had been coated with antifouling paint.

Fouling and Biodeterioration. The general condition of the test specimens soon after recovery is shown in Figure 12.

Concrete Panels. The antifouling concrete test panels were again free of marine growth. The concrete anchor block which served as control was also free of marine fouling except for some hydroid growth. Goose barnacles which were found on this concrete block during the first test array were not found on it during this test period. Shortly after recovery of the treated panel the surface became covered with an oily coating of creosote.

Wood Panels. The wood panels (Douglas fir) which served as spacers between the plastic panels were riddled with two types of molluscan wood borers, *Xylophaga washingtona* and *Bankia setacea*. Finding *Bankia setacea* (Figure 13), a shallow water borer, in wood panels exposed at ~182 meters was surprising. The wood panels which were in contact with the antifouling concrete panels were free of borer attack. The wood had absorbed enough toxic chemicals from the antifouling panels to render these immune from any borer attack.

Plastic Panels. Exposed at ~182 meters, the plastic panels were free of marine growth such as barnacles, mussels, tube worms, and bryozoans normally found at the surface. However, the surfaces of the plastic panels were lightly covered with branches of thin, threadlike tentacles of hydroids. A thin layer of slime growth together with a fine bottom silt were present on the surface of these panels. The visibility through a 1/4-inch (0.635 cm) acrylic panel was considered good as is shown in Figure 14. Although the plastic panels were essentially free of marine growth, light to moderate borer damage was sustained by all of the panels under the area where a wood panel was in contact with the plastic surface. The borers present in the wood had continued to bore into the plastic producing numerous pit-like holes over the surface as shown in Figure 15. The result of a hardness test on plastic specimens after continuous submergence for 186 days, is presented in Table 1.

Rope Specimens. The rope specimens (nylon, polyethylene, polypropylene, and polyester) were essentially free of marine fouling except for some slime growth over the ropes. A tensile strength test was conducted on the recovered rope specimens (wet) to determine the effects of the ocean environment on synthetic rope fibers. The results of this test are presented in Table 2. The breaking strength data of ropes which had not been exposed in seawater (control) is also presented for comparison.

In general, the exposed nylon ropes decreased in tensile strength; the polyester ropes remained about the same; and the polyethylene and polypropylene ropes increased in strength. Similar results were obtained on synthetic ropes exposed for a period of 6 months at a depth of 2,500 feet (7.62×10^2 m) off the coast of Southern California (3).

Summary and Conclusions

Three current meter arrays were used as the source of data on corrosion, fouling, and biodeterioration of materials for the SEACON project. Very severe corrosion and fouling were found on the first array, deployed for 176 days. The corrosion of the aluminum current meter cases was arrested by using zinc anodes and isolators to separate the instruments from the steel brackets and wire. The fouling by marine organisms, most prevalent at the uppermost (15.5-meter depth) instrument, was arrested by using cuprous antifouling paint on the rotor and vane sections of the current meters. Zinc powder paint eliminated fouling of the aluminum subsurface buoy.

Current speed and direction data were recorded at three depths, 15.5 meters, 90 meters, and 182 meters. The mean speeds for these depths were 0.2 knot (0.1 meter/sec), 0.2 knot (0.1 meter/sec) and 0.1 knot (0.05 meter/sec, respectively. The mean direction of the current was within a 30^0 quadrant (270^0-300^0) at all depths. Long-term data collection with instruments having sophisticated electronics and external moving parts is a difficult task. The judicious use of cathodic protection and antifouling coatings is necessary in the ocean, especially in these relatively shallow depths.

It was found that materials and instruments exposed near the surface of the sea at this particular location will become fouled primarily with hydroids, barnacles, and tube-dwelling amphipods. Growth of these marine organisms on critical parts of oceanographic instruments such as rotor or vane sections of a current meter will result in malfunctioning of the instrument and the collecting of inaccurate data. Applications of antifouling coatings will protect instruments from fouling attachments.

Materials such as plastic, rope, wood, and antifouling concrete were exposed near the seafloor (182-meter depth) in the Santa Barbara Channel for varied periods of time to determine the effects of marine organisms.

Plastic, rope, and concrete specimens were essentially free of fouling growth when exposed at this location. However, wood panels were riddled by molluscan borers. These borers also caused damage to the plastic specimens in the areas where a wood panel was in direct contact with the plastic. The tensile strength of nylon decreased, and

polyester rope specimens remained about the same while the tensile strength of polypropylene and polyethylene specimens increased.

Acknowledgement

The authors wish to thank Dr. Ruth D. Turner, Harvard University, for identifying the wood borers and Dr. Dora P. Henry, University of Washington, for identifying the goose barnacles.

References

(1) *Navy Seafloor Construction Experiment (SEACON)—Plans and Operational Information*. Naval Civil Engineering Laboratory, Port Hueneme, Calif., April 1971.

(2) Naval Civil Engineering Laboratory Technical Note N-1211: *Antifouling Concrete*—Preliminary Report, by James S. Muraoka, Port Hueneme, Calif., Jan. 1972.

(3) *Deep Ocean Biodeterioration of Materials*, by James S. Muraoka, Ocean Industry, Feb/Mar 1971.

Table 1. Results of Tests on Plastic Panels Exposed at SEACON Site[1]

Size in Inches (mm)	Materials	Hardness Test[2]	
		Before Exposure (Dry)	After Exposure (Wet)
1/8 x 6 x 12 (3.175 x 152.4 x 304.8)	Acrylic, "G"	90.0	88.0
	Nylon, 6	79.3	63.0
	Polyethylene	47.6	47.6
	Polycarbonate	84.6	83.6
	Polypropylene	74.3	75.0
	Polyvinyl Chloride	85.0	85.0
	Polystyrene	84.0	83.0
	Phenolic Laminate Grade XXX	94.6	92.0
	Vinyl, pp, rigid	85.0	84.3
1/16 x 4 x 12 (1.587 x 101.6 x 304.8)	Polyurethane	95.0[3]	94.0[3]
	Tetrafluoroethylene	55.0	55.0
5/16 x 6 x 12 (7.94 x 152.4 x 304.8)	Vinyl, black, pp, rigid	81.3	81.3
1/16 x 6 x 12 (1.587 x 152.4 x 304.8)	Vinyl, pm, rigid	85.0	85.0

[1] Third Array Test.
[2] Durometer "D" ASTM D1484.
[3] Durometer "A" ASTM D1484.

Note: These panels were essentially free of marine growth except for deposits of primary film, fine silt and thin threadlike tentacles of hydroids. All of the test panels were damaged by borers under an area where a wood piece was in contact with the plastic.

Table 2. Results of Tests on Breaking Strength of Rope Specimens[1]

Rope Materials[2]	Breaking Strength in Pounds (kg)[3]	
	Unexposed Specimens	Exposed Specimens
Polypropylene	1137 (515)	1395 (632.5)
Polyethylene	1025 (468)	1190 (530)
Polyester	1535 (696)	1500 (680)
Nylon	1515 (687)	1262 (572)

[1] Exposed for 186 days.
[2] Average of two ropes.
[3] All ropes 1/4-inch (6.35 mm) diameter.

Table 3. Temperature and Salinity at 182-Meter Depth for 6-Month Period

Month (1971)	Temperature Range Kelvin	Salinity o/oo
September	282.3-282.7	34.65
October	282.1-282.8	34.75
November	281.9-282.7	34.50
December	281.6-282.6	34.55
January	281.6-282.9	34.50
February	278.3-282.6	37.0

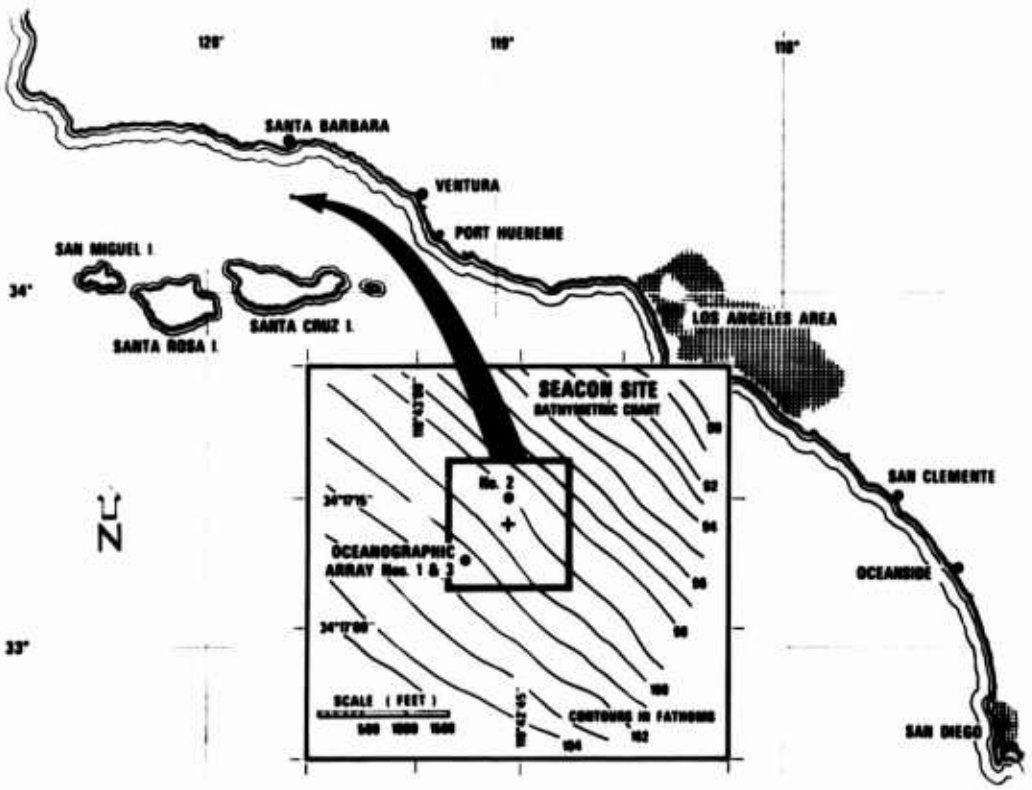


Figure 1. SEACON site—location of instrument arrays 1, 2 and 3.

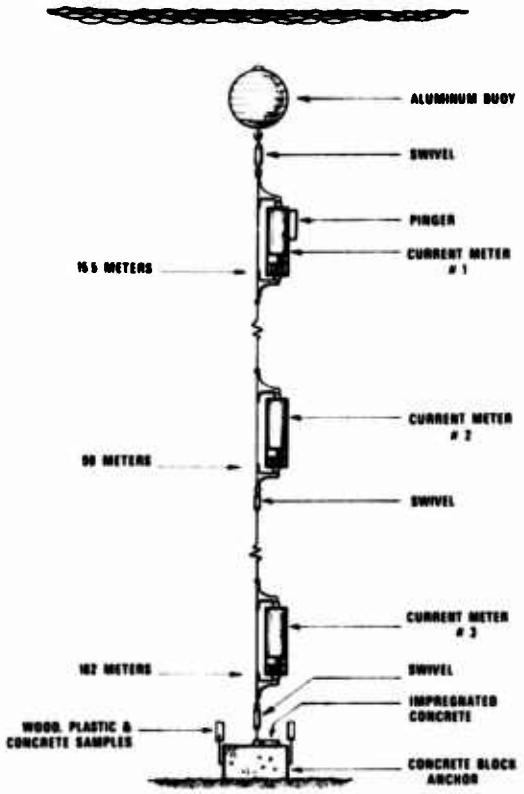


Figure 2. Instrument arrays as deployed.

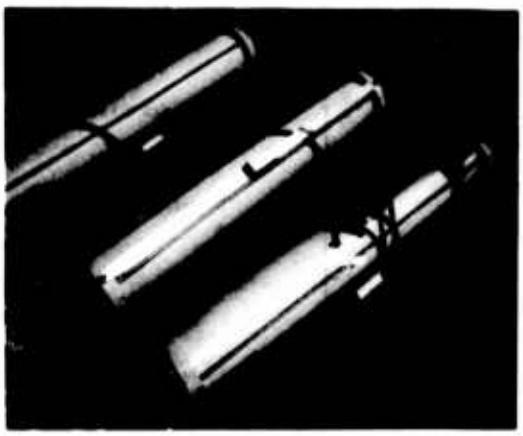


Figure 3. Current meters for array number two with 1 pound (0.434 kg) zinc anodes.

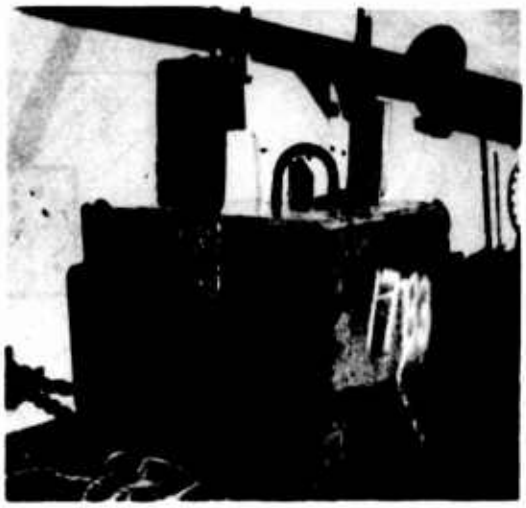


Figure 4. Plastic, antifouling concrete and wood specimens secured to a concrete anchor block. Recovered after 128 days at 600 feet (182 m).

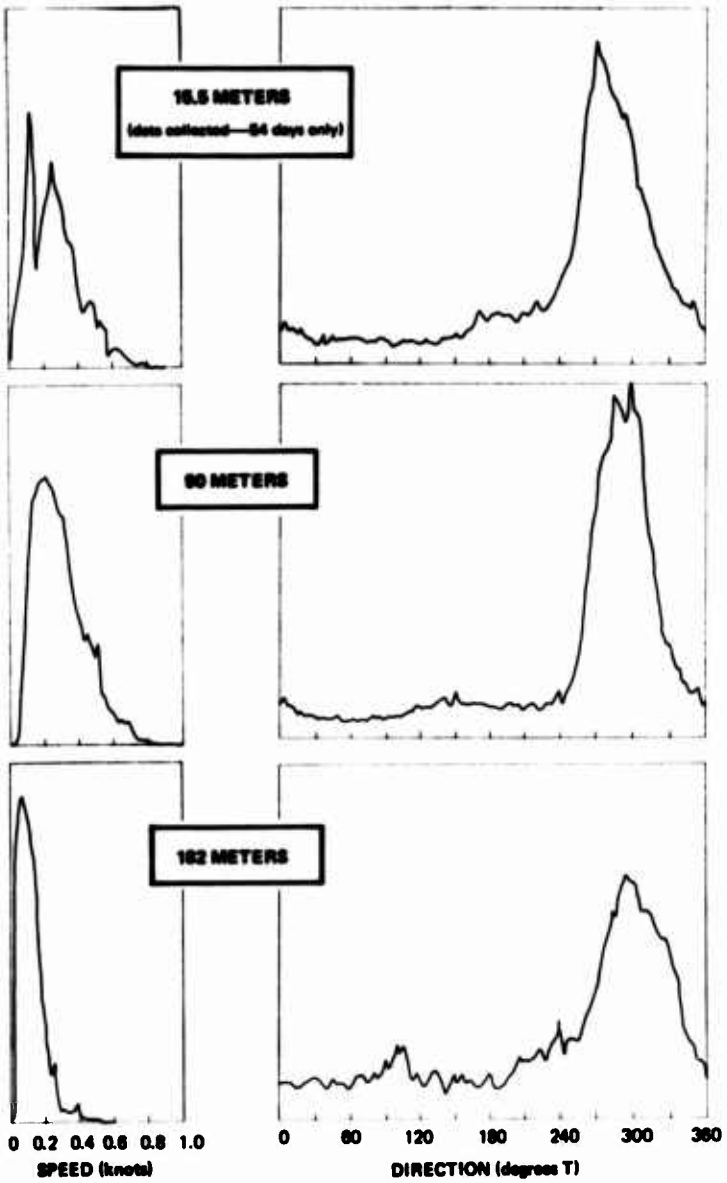


Figure 5. Current speed and direction for three meters deployed for 176 days on array number one.



Figure 6. Corrosion of current meter and plate around screw-in anode. Anode shown is approximately 30% expended after 176 days in-situ.

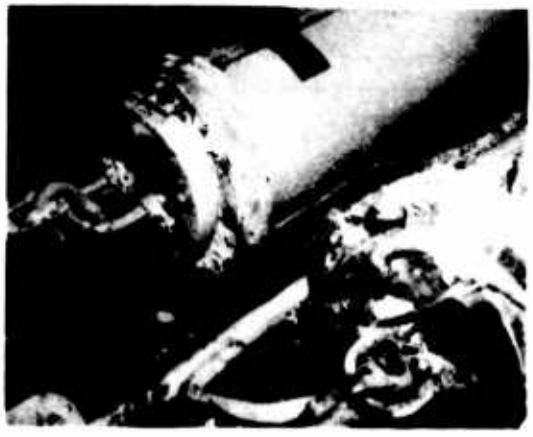


Figure 7. Corrosion products on current meter end plate deployed approximately 15 meters below surface after 176 days.

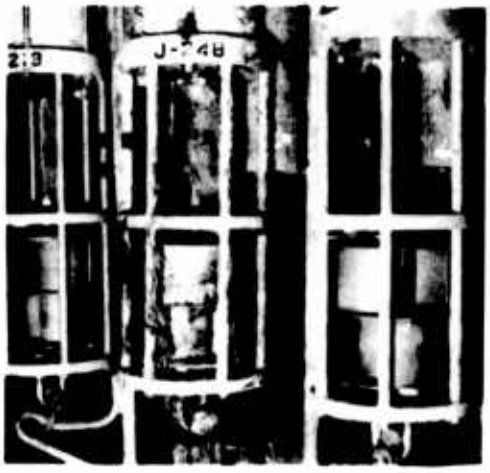


Figure 8. Hydroids and barnacles growing on rotor and vane sections of a current meter exposed near the surface of the sea (15.5 m).



Figure 9. Protective coating of an aluminum buoy penetrated by barnacle shells.

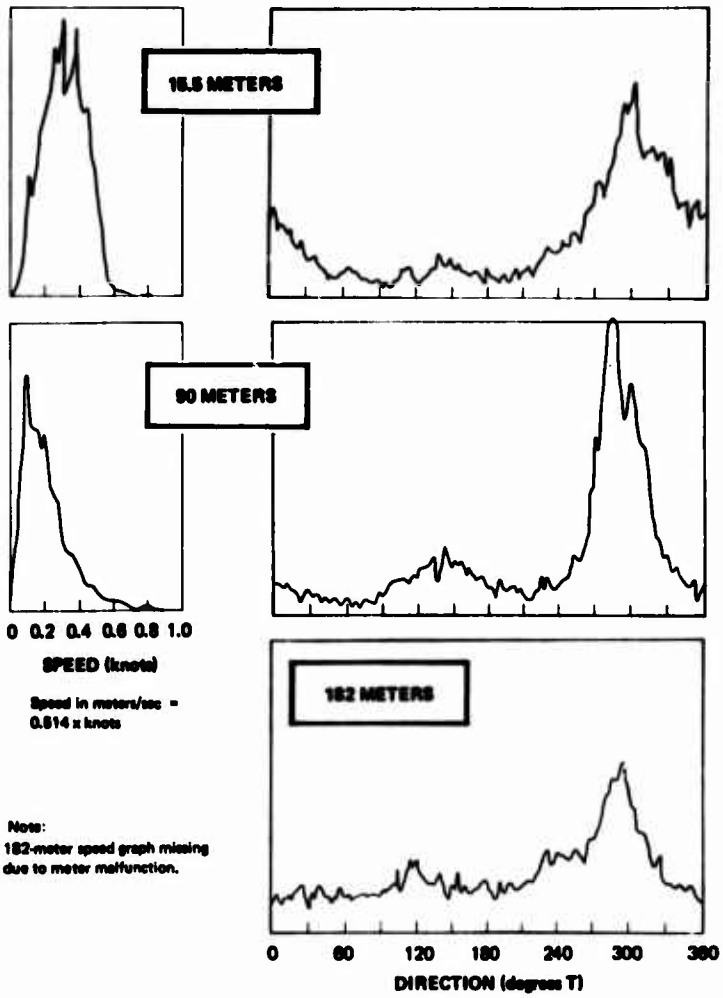


Figure 10. Current speed and direction data for three meters deployed 128 days at site number two.

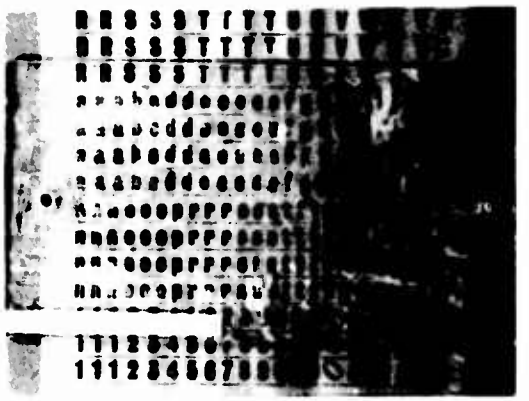


Figure 11. Visibility through a 1/4-inch (6.25 mm) thick acrylic plastic plate (128 days in-situ).



Figure 12. Plastic, antifouling concrete and rope specimens secured to a concrete anchor block. Recovered after 186 days in the sea.

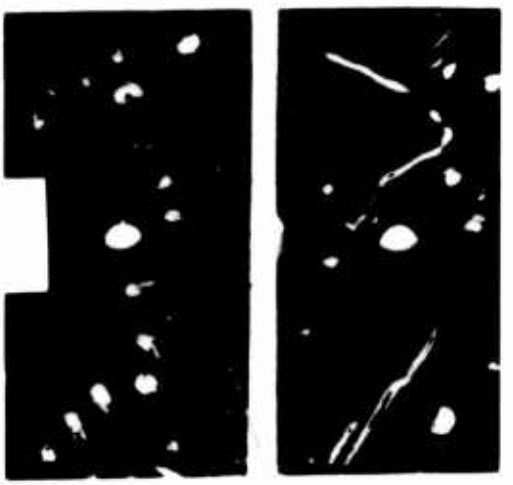


Figure 13. Fir panel riddled with molluscan wood borers, *Xylophaga washingtona*, and *Bankia setacea*, (two elongated tunnels) from 182-meter depth.

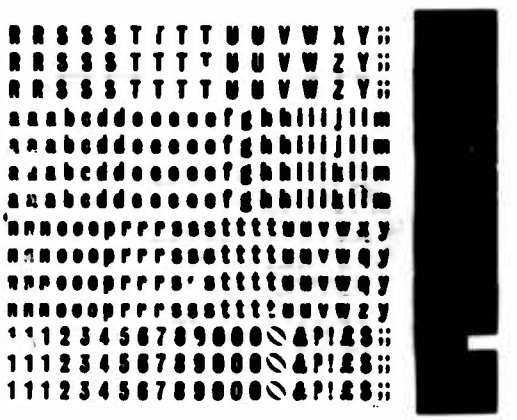


Figure 14. Acrylic test panel with visibility only partially marred by hydroid growth. Pit-like holes made by borers under a wood bait piece (186 days in-situ, 182 meters).



Figure 15. Pit-like holes caused by wood borers on the surface of a tetrafluoroethylene panel in contact with wood.

The Corrosion of Mild Steel by a Marine Strain of Desulfovibrio

Warren P. Iverson

National Bureau of Standards
Washington, D.C. 20234

A marine strain of Desulfovibrio was isolated from steel piling detritus at Dam Neck, Virginia. A medium which provided good surface growth on 2% agar plates in a hydrogen atmosphere was developed (Trypticase, 15 gm; Phytone, 5 gm; NaCl, 5 gm; seawater, 1000 ml). The corrosion rate of mild steel in this medium, with and without the addition of Fe^{++} ions, was investigated using polarization techniques. In the absence of added Fe^{++} ions, the corrosion rate was found to decrease and then either increase or remain at a low level. In one corrosion cell a high rate of corrosion was accompanied by the formation of a corrosion product or products in the shape of "stalactite" formations. Analysis indicated free sulfur and an iron sulfur compound with iron in the Fe^{+++} state.

In the presence of added Fe^{++} ions, the corrosion rate was found to increase to 255 mdd in one corrosion cell and then decrease. Chemically prepared FeS produced little change in the potential or the corrosion rate. Corrosion of mild steel in a bacteria-free culture filtrate, to which Fe^{++} ions were added in excess to remove the $S^{=}$ ions was extremely high. After an induction period of 3 days, the corrosion rate increased to a maximum of 1130 mdd 8 days after the start of the corrosion process. During the period of extensive corrosion, the potential of the steel dropped to more noble values.

When the black precipitate, formed upon the addition of Fe^{++} ions, was removed, the resulting filtrate was still highly corrosive, indicating that the depolarizing agent was water soluble and not the precipitate. The depolarizing agent appears to act as an electron carrier, removing electrons from the iron and transferring them to an acceptor which is thereby reduced. The action of this depolarizing agent could account for the high anaerobic corrosion rates observed in the field.

Inhibition of corrosion in cultures of Desulfovibrio appears to be due to the action of H_2S which reacts with the iron to form a protective film and prevents the actions of the soluble depolarizer.

Key Words: Marine corrosion, anaerobic corrosion, marine Desulfovibrio, depolarizing agent, polarization techniques, ferrous ions.

---

1. Introduction

There is ample evidence that corrosion by sulfate-reducing bacteria may, under certain circumstances, be of significant importance in the marine environment.[1,2,3,4] Most of

[1] Figures in parentheses indicate the literature references at the end of this paper.

the laboratory studies involving anaerobic corrosion by these bacteria have been made using non-marine strains. On the basis of these studies, a number of mechanisms have been proposed to account for this type of corrosion. These are: (a) stimulation of the cathodic area of the metal by the removal and utilization of the polarizing hydrogen by the bacterial cells;[5] (b) formation of FeS/Fe couples by the reaction of ferrous ions with sulfide ions produced by the bacteria;[6,7] (c) a combination of (a) and (b), namely removal and utilization of hydrogen by the bacteria from the ferrous sulfide of a FeS/Fe couple;[8] and (d) local acid cell formation.[9] A considerable portion of the literature has been concerned with mechanism (a), the so-called cathodic depolarization theory, and mechanism (b).[10] Difficulty has been found in assessing their relative contributions to the overall reaction, however.

It is quite definitely established that the microbiological anaerobic corrosion of mild steel is markedly stimulated by the presence of ferrous ions in the electrolyte.[11,12,13,14] Adams & Farrer[13] reported that the hard adherent coating of ferrous sulfide, often formed over the metal surface when steel is exposed to cultures of sulfate reducing bacteria, was not formed when the medium contained an excess of ferrous ammonium sulfate. The film has been shown by Booth and Tiller[14,15,16] to be protective but often temporary and that on prolonged exposure to bacterial cultures, the initially protective film may be removed progressively, with the acceleration of corrosion.[17,18] They also showed that the initial protective film was not found at all if sufficient ferrous ions were present in the medium to precipitate immediately all the sulfide produced by the bacteria. As a result of this inhibition of film formation, the initial corrosion rate was greatly increased. It was the purpose of this study to: a) isolate a culture of a marine strain of Desulfovibrio and develop a medium for its cultivation on agar plates; b) study the corrosion of mild steel in a similar medium using two electrochemical techniques for measurement of instantaneous corrosion - the linear polarization technique and the "polarization break" technique; and c) study the effects of corrosion in the medium as influenced by the presence of added ferrous ions.

2. Experimental

(1) Culture and Media

The culture of Desulfovibrio was originally isolated in API broth from detritus obtained from an off-shore piling at Dam Neck, Virginia.[19] In previous studies[20] to develop a medium for the agar surface isolation and cultivation of non-marine strains of Desulfovibrio under a hydrogen atmosphere, it was found that a Trypticase soy agar* plus salts medium (Trypticase soy agar, 40 gm; sodium lactate 60% sol, 4.0 ml; magnesium sulfate, 20 gm; agar, 5 gm; ferrous ammonium sulfate, 0.5 gm; distilled water, 1000 ml) gave satisfactory results. Cultivation of the marine strain on this medium was unsuccessful as might be expected. Increasing the sodium chloride concentration of the medium to 3% as well as the use of artificial seawater prepared from an ASTM sea salt mixture,+ in place of the distilled water, likewise showed no improvement. Substitution of aged seawater (34 ohm-cm resistivity) for the distilled water did, however, ensure good to excellent growth of the marine strain. Growth of contaminating organisms was considerably reduced by the elimination of sodium lactate from the medium. Magnesium sulfate was also eliminated, as it did not appear to have any effect in stimulating growth. The resulting medium (Trypticase, 15 gm; Phytone, 5.0 gm; NaCl, 5.0 gm; agar, 20 gm; ferrous ammonium sulfate, 0.5 gm; aged seawater, 1000 ml) was used for routine maintenance of the marine strain. The pH was adjusted to 7.0±0.1 with NaOH when necessary. The ferrous ammonium sulfate solution was sterilized by Seitz filtration and added to the autoclaved medium before pouring the plates. This was eventually omitted from the medium. Growth on this medium (in the presence of ferrous ammonium sulfate) was accompanied by darkening of the medium surrounding the colonies.

---

*Trypticase soy agar (Trypticase, 15.0 gm; Phytone, 5.0 gm; sodium chloride, 5.0 gm; agar, 15 gm). Certain materials are identified in this paper in order to adequately specify the experimental procedures. In no case does such identification imply recommendation or endorsement by the National Bureau of Standards nor does it imply that the material identified is necessarily the best available for the purpose.

+Sea Salt Formula A ASTM D-1141-52

The purity and identification of the culture as a species of Desulfovibrio was verified from time to time by microscopic observation of the cell morphology and visual observation of the colonies. Positive identification was made by flooding the agar surface on which growth was present with an alkaline solution (10% NaOH) and observing a bright red fluorescence of the colonies under ultraviolet light. This red fluorescence has been reported by Postgate[21] to be characteristic of cells of organisms in the genus Desulfovibrio. Transfers of the strain were usually made at monthly intervals.

The medium used in the corrosion studies contained the same materials as the agar platint medium except for the absence of the agar. When ferrous ions were introduced into the medium, 2.5 gm ferrous ammonium sulfate per liter were added.

(2) Electrochemical Studies

(a) Electrochemical cell

The electrochemical cell consisted of a 400-ml beaker (tall form) fitted with a rubber stopper to support two electrodes (test and platinum) and a Luggin capillary (Figures 1 and 2). The Luggin capillary was joined to a sat. cal. electrode immersed in saturated KCl solution by an agar bridge. The agar bridge consisted of transparent plastic tubing fitted tieh saturated KCl agar (30 gm KCl, 3 gm agar, 100 ml distilled water). A thick piece of string was also inserted from end to end of the tubing before filling with the KCl agar to insure a more permanent conductivity in event of bubble formation or drying of the agar. Several cells were often connected simultaneously to the saturated calomel electrode. Diffusion of air through the agar bridges was hindered by supporting the calomel electrode and the ends of the KCl bridges in a rubber stopper sealed to the beaker containing the saturated KCl solution. Initially the air above the saturated KCl solution was replaced with N_2, but this procedure was later omitted.

The working or test electrode consisted of a cylinder of cold rolled 1020 steel 1/4" in diameter and 1/4" in length supported by a threaded rod. Initially, the supporting rod and all of the surface of the cylinder except the end face were sealed off by heat shrinkable plastic tubing. In later studies, the cylinder was sealed in epoxy except for the end face and the supporting rod enclosed in a glass tube. A Teflon washer was used to seal the end of the tube against the epoxy coated cylinder. Tension was maintained by tightening a nut at the other end of the threaded rob which was separated from the other end of the glass tube by a second Teflon washer.

The exposed end of the steel cylinder was polished using progressively fine grades of emory paper (220, 320, 400, and 600) and degreased in acetone. Sterilization of the electrode assembly was usually accomplished by storing it in 95% ethanol until ready for use. Before using, the residual alcohol was removed by flaming. In a few cases, the electrode was sterilized by immersion in a 1:1 solution of conc. HCl and water and rinsed thoroughly in sterile distilled water. The steel surface was repolished with sterilized 600 grade emory paper. Mild steel nails (ca 38.0 mm long, 1.82 mm diam.) were treated in dilute HCl (1:1 water; conc. HCl), dried, degreased in acetone and kept in 95% ethanol until used. Before use the excess ethanol was removed by burning.

The platinum electrode (auxiliary electrode) consisted of a piece (6x7 mm) of platinum gauge (52 mesh) attached to a platinum wire sealed in glass tubing. The platinum electrode was cleaned by flaming, washing in conc. HCl and rinsing in distilled water.

In preparation of the cell, 200 ml of the Trypticase, Phytone seawater (TPSW) medium (346 mg of SO_4^{--}) was autoclaved in the beaker. If the medium contained Fe^{++} ions, a Seitz filtered solution of ferrous ammonium sulfate in seawater was added.

The stopper holding the platinum electrode and the Luggin capillary was also sterilized by autoclaving. Upon removal from the autoclave, the capillary tube was filled with sterile, saturated KCl agar using suction. After the agar hardened, the sterile iron electrode was inserted through a hole in the stopper and the stopper, with the two electrodes and the capillary inserted into the beaker.

To prevent oxygen from dissolving in the medium, sterile autoclaved (1 hr at 15 psi) melted vaspar (equal parts of petroleum jelly and paraffin) was poured on the surface of the medium through a hole in the stopper to a depth of about 1 inch. The hole was then stoppered, the cell placed in an incubator (27±0.1°C) and electric and agar bridge connections made. Electrochemical measurements were then initiated. When the cell was inoculated, a hole was made through the vaspar using a heated rod and a suspension of bacterial cells introduced into the medium via a sterile hypodermic needle and the hole sealed with vaspar. The bacterial suspension was prepared by scraping off the surface growth from one or two agar plates, using a bacteriological loop, and suspending the growth in a few ml of autoclaved seawater. 0.5 ml to 1.0 ml of the suspension was generally used to inoculate the medium.

(b) Electrochemical measurements

Potential measurements were made with an electronic potentiometer (pH meter). Redox potential measurements were obtained by adding +0.250 volts to the observed potential reading of the platinum electrode versus the saturated calomel half cell. No corrections for pH were made as the medium was initially adjusted to 7.0±0.2 and the pH of the medium after the electrodes were removed was within this range. Corrosion rates were determined by two polarization methods, the linear polarization method and the "polarization break" method. The linear polarization technique is based on the following relationship derived by Stern and Geary:[22]

$$\frac{\Delta E}{\Delta I} = \frac{1}{2.3\, I_{corr}} \left(\frac{Ba \cdot Bc}{Ba + Bc}\right) \qquad (1)$$

In this equation ΔE is the overvoltage of the corroding electrode produced by a polarizing current ΔI. $\Delta E/\Delta I$ is the slope of the polarization curve, Ba and Bc are the slopes of the anodic and cathodic polarization curves in the Tafel region, and I_{corr} is the corrosion current. The constants Ba and Bc were both assumed to be equal to 0.1 in this investigation. The error will usually be about 20% or less, as established by Stern and Weisert.[23] Substituting this value for Ba and Bc and solving for I_{corr} the following equation is derived:

$$I_{corr}(\mu A) = \frac{21.7 \Delta I(\mu A)}{\Delta E(mV)} \qquad (2)$$

The "polarization break" method originally proposed by Schwerdtfeger and McDorman[24] is based on the observation that anodic and cathodic polarization curves consist of straight-line segments having different slopes. The current value at which the change (break) in slope occurs is designated I_p for the cathodic and I_q for the anodic curve as in Figure 3. The corrosion current I_c can be calculated from the following relationship, which was derived by Pearson [25] and confirmed by Holler:[26]

$$I_{corr} = \frac{I_p \cdot I_q}{I_p + I_q} \qquad (3)$$

The corrosion rate in milligrams per square decimeter per day (mdd) was calculated from the corrosion current density using Faraday's law for Fe corroding to Fe^{++} (1 mdd being equivalent to 4.0×10^{-7} amp/cm^2).

The electrical circuit employed was essentially similar to that described by Schwerdtfeger[27] except for the bridge circuit which was omitted and a greater variable resistance (1.11 M ohm) used in series with the batteries. Current measurements were made with a multiple range micro-ammeter employing a chopper amplifier circuit. In addition to direct potential measurements of the steel electrode, overpotential measurements (the difference between the open circuit potential, and the potential after applying current) were made using a null circuit in series with a high impedance (10 megohms) chopper amplifier voltmeter.

In making the measurements, the open circuit potentials of the platinum electrode (redox potential) and the steel electrode were obtained first. An increment of current sufficient to polarize the electrode to an overpotential of 2 to 10 mV was then applied and

and the corrosion rate was calculated, using the ΔI and ΔE values in equation (2). The current was then cut off and after an interval of about 1/2 to 2 hours (usually sufficient for depolarization) a cathodic polarization curve plotted using the galvanostatic technique with 2-minute intervals between increasing equal increments of current. Previous calculation of the corrosion current was found to be helpful in deciding the equal current increments to be used. After a sufficient time interval to allow depolarization of the electrode to the original open circuit potential, ranging from 20 minutes to a day, the anodic polarization curve was plotted. As the values obtained by the two polarization techniques were usually comparable, the values obtained by the "polarization break" method are reported unless specifically mentioned.

Rapid potential fluctuations of the steel electrode which occurred during one of the experiments were measured using the circuit shown in Figure 4.

3. Results

(a) Corrosion in the absence of Fe^{++} ions

The results of the first experiment, shown in Table 1, were obtained in TPSW medium, without added Fe^{++} ions, inoculated with the marine strain of Desulfovibrio. The corrosion rate decreased on the 21st day after inoculation to a rate about 1/10 that of the rate before inoculation and then increased. No data were obtained from the 44th to the 50th day because of the instability of the open circuit potential. A drop in potential of the steel electrode to more noble (positive) values and then to more active (negative) values coincided with the decrease and increase in corrosion rates. The redox potential dropped to over 400 mV simultaneously with active growth of the culture. The polarization curves up to 1 day after inoculation were similar to those in Figure 3a where the slope in the anodic branch after the break was less than the slope of the curve before the break. In addition, the break in the cathodic branch occurred before the break in the anodic curve, indicating that the reaction was under cathodic control. From the second day until the conclusion at the end of 51 days the anodic curves were typical of those in Figure 3b and 3c with respect to the slopes after the breaks. The anodic slopes were always greater after the breaks than before. Where the break in the anodic curve occurs before the break in the cathodic curve, the corrosion rate is under anodic control (Figure 3b). Schwerdtfeger[28,29] usually found pitting to occur when the process was under anodic control. Under mixed control, the breaks occur in cathodic and anodic branches at equal applied current values. The polarization curves from the second day to the conclusion indicated that the corrosion process varied from one type of control (cathodic, anodic, mixed) to another.

The surface of the steel electrode at the conclusion of the experiment as shown in Figure 5 indicates areas where a dark film has broken away from the surface. Electron probe studies indicated the presence of sulfur in the film.

This experiment was repeated but electrochemical measurements were made over a longer period of time (495 days). The data for 280 days are shown in Figure 6. Again as previously, the corrosion rate was found to decrease along with a drop in potential to more noble values and reached a minimum value of 0.29 milligrams per square decimeter per day (mdd) on the seventh day after inoculation. From the ninth day until the 32nd day, the open circuit potential was unstable and linear polarization measurements could not be made (Figure 7b). It was possible to determine the corrosion rates using the "polarization break" method, however. Another period of instability also occurred from the 44th to the 53rd day. Previously[30] it had been found using the circuit shown in Figure 4 that corroding metals in the presence of oxygen produce a series of fluctuations in the absolute potential when measured across the resistor. These potential fluctuations are shown in Figure 8. The corrosion rate continued to increase until it reached a peak of 102 mdd on the 102nd day and then decreased to a level of 80 mdd, rising again to 312 mdd after 488 days. The potential of the steel electrode decreased in the noble direction (less negative) until it reached -0.401 V, rose again to -0.640 V on the 459th day and then decreased to -0.609 V at the conclusion of the measurements (495 days). The redox potential dropped from +0.160 V just before inoculation on the 26th day before inoculation to about -0.200 V. The slopes of the anodic polarization curves after the breaks again changed two days after inoculation, as previously, from that in Figure 3a to Figure 3b, indicating that a film was present on the metal surface. The corrosion process was then under cathodic, anodic, and mixed con-

trol until the termination of the experiment.

Several months after inoculation, a black "stalactite" formation of corrosion products was observed growing from the steel electrode (Figure 9). Periodically it dropped to the bottom of the corrosion cell when it was disturbed and a new one formed. At one time, the growth of the "stalactite" was in a lateral position from the electrode. When the cell was disassembled, the broken off fragments (Figure 10) produced a metallic sound when dropped to the bottom of a beaker. Upon drying in vacuo they had a tendency to crumble. X-ray diffraction analysis, indicated the material was in the amorphous state. An electron scanning micrograph of the material is shown in Figure 11. Analysis by the Mossbauer technique and a scanning electron microscope coupled with an energy dispersive x-ray spectrometer indicated the presence of an as yet unidentified compound of iron and sulfur. Iron was in the Fe^{+++} state. Free sulfur was also detected. The material was heated in vacuo to 1230°C for about 15 minutes and allowed to slowly cool to room temperature. X-ray diffraction studies and Mossbauer spectroscopy revealed the presence of 77% ferrite, 13% austenite, and 10% cementite. Bacteriological analysis revealed that the cell was contaminated with a gram positive non-sporulating rod. Viable Desulfovibrio cells were also present upon culturing of the medium.

In repeating the experiment a 3rd time, no increase in corrosion rate or development of corrosion products was noted. The results are indicated in Table II. The corrosion rate dropped to 0.07 mdd, rose to almost 0.22 and remained at this value for the duration of the experiment. Again the potential of the steel fell to more positive (noble) values. Although no polarization measurements were made, no "stalactite" formations were noted over a period of 10 months. The polarization curves indicated that a film on the steel surface was present and that the corrosion reaction was under mixed or slight cathodic control from the second day after inoculation.[7]

The experiment was repeated a 4th time but a Seitz filtrate (bacteria-free) was employed instead of the culture. The results are indicated in Table III. Again, no great increase in the corrosion rate was noted, and no "stalactite" formation occurred over a period of 10 months. The potential of the steel was found in general to increase to more negative (active) values during the period when the corrosion rate increased and then remained fairly constant at -0.572 V for the last 30 days of measurement. The corrosion process was under mixed control most of the time. Bacterial contamination of the culture filtrate was noted after the 10th day.

(b) Corrosion in the presence of added Fe^{++} ions

In the presence of Fe^{++} ions, the corrosion rate reached a peak value of 256 mdd and then dropped to values lower than in the medium without iron (Figure 6). It was of interest that the redox potential became more negative during the rapid increase in corrosion rate, from -0.150 V when the corrosion rate was 19 mdd to -0.305 V when the corrosion rate was 256 mdd and to-0.214 V when the corrosion rate dropped back to 9 mdd. The polarization curves before inoculation and up to the 39th day after inoculation were under cathodic control and typical of the curves in Figure 3a. From this time until the conclusion of the measurement (495 days) film formation occurred and the corrosion reaction was at various times under mixed, cathodic, and anodic control.

The results of a second experiment to attempt to duplicate these results are shown in Table IV. The potential of the steel electrode dropped about 10 mV in a more active (negative) direction immediately after inoculation and remained quite stable for 58 days after inoculation. The corrosion rate increased as previously but only reached a maximum of about 1/10 of the previous maximum on the 28th day after inoculation. A discernable decrease occurred after 74 days. As previously, the redox potential dropped very slightly to more negative values during the time when the corrosion rates were the highest. The polarization curves indicated that the corrosion reaction was under cathodic control before inoculation and through the 58th day after inoculation. From the 76th day through the final measurement the corrosion reaction was under mixed control with a film being present. Similar results were also obtained in a third cell.

(c) Effect of chemically prepared iron sulfide on the corrosion of mild steel

It appeared from the previous results that stimulation of corrosion by the marine strain of Desulfovibrio consistently occurred in the seawater medium when added ferrous ions were present. In view of the results by Booth[7] that FeS brought about cathodic stimulation of mild steel, the possibility that this compound might be responsible for the stimulation of corrosion seemed likely.

After measurements were made on a mild steel specimen in sterile (TPSW) medium with added ferrous ions (same concentration as used in the inoculated medium) sodium sulfide was added to form FeS and the measurements continued for fourteen days. From the results presented in Table V it appears that the chemically produced FeS had little if any effect on the corrosion rate or the potential of the steel. The polarization curves indicated that the corrosion reaction was under cathodic control before and after the addition of the S^{--} ions with no film formation.

(d) Effect of the addition of Fe^{++} ions to a TPSW culture filtrate on the corrosion of mild steel

As FeS had no effect on the corrosion rate, the possibility of another iron compound formed in the culture by the addition of Fe^{++} ions was suggested. Fe^{++} ions were added in excess to a Seitz filtered culture, the electrodes placed in the solution, and the surface sealed with vaspar. The amount of Fe^{++} ions added was determined in a previous experiment in which the culture filtrate was titrated with ferrous ammonium sulfate using a sulfide ion electrode. The results are indicated in Table VI. Corrosion current density reported in the table was obtained by the linear polarization method. After an induction period of 3 days during which the potential of the steel electrode decreased to more noble (positive) values, the corrosion rate increased greatly, reaching a maximum of over 1000 mdd on the 10th day after the initiation of the increase. This increase in corrosion rate was accompanied by a change in the redox potential to lower (more negative) values. A similar effect was noted previously in the TPSW culture containing Fe^{++} ions where a peak corrosion rate of 256 mdd was reported. The polarization curves indicated that the corrosion process was under mixed or anodic control after the 3rd day and that a film was produced on the surface of the steel. A black film which covered about 1/4 of the total surface area of the steel surface was observed when the electrode was removed.

To determine whether the corrosion of the steel was due to the black precipitate or a soluble component in the culture filtrate, Fe^{++} ions were added to a culture of the marine strain and the resulting organisms and black precipitate were removed by Seitz filtration. Five small mild steel nails were placed in the filtrate which was then sealed with vaspar. Five nails were also placed in sterile medium and sealed with vaspar to serve as a control. After an induction period of 3 days, the solution turned completely black. Twenty days after the solution had turned black, the nails were removed, the black corrosion products removed by wiping with paper tissue and the nails were weighed. The results are presented in Table VII. The average corrosion rate of the nails was about 30 times that of the control nails.

4. Discussion

It is evident from the results obtained that the marine strain of Desulfovibrio produces a strong depolarizing agent in the seawater medium and that the bacterial cells per se are not essential as originally proposed in the cathodic depolarization theory of von Wolzogen Kuhr and van der Vlugt.

From the high corrosion rates obtained, it appears as if the depolarizing agent removes electrons directly from the metal itself rather than through direct utilization of hydrogen. The corrosion rate of iron based on the rate of hydrogen formation by the direct reduction of water as a function of the electrode potential has been calculated by Nelson[31] to be from 0.05 to 0.4 $\mu A/cm^2$ (0.125 to 1.0 mdd), using potentials of steel in bacterial cultures within the range of -0.45 to -0.6 V (NHE). Such values would be too low to explain the high corrosion rates obtained by direct utilization of hydrogen. A highly reduced compound appears to be formed in the medium as indicated by the lowering of the redox potential. A black compound was also formed which is presently being identified. The possibility is

suggested that the depolarizing agent after removal of the electrons from the iron is in a highly reduced condition and transfers the electrons to an acceptor, in a manner similar to the electron transferring enzymes in biological systems. The black material may be the reduced acceptor.

Blackening of yeast extract broth, containing a steel coupon and inoculated with a non-marine strain of Desulfovibrio was reported previously.[32] The black corrosion product was initially amorphous but after heating in vacuo to 1230°C, Fe_2P was identified by x-ray diffraction studies.

As H_2S is also produced by Desulfovibrio the results presented in this paper as well as by others[13,14,15,16] appear to indicate that a film of iron sulfide is formed on the surface of the steel if there is no material (Fe^{++} ions) present to remove it. This film appears to act as a protective film thereby preventing corrosion. When this film becomes detached, the ensuing corrosion is probably a result of the action of the depolarizing agent also produced by Desulfovibrio. If this protective sulfide film is prevented from forming by previous removal of the sulfide, the depolarizing agent has access to the metal surface and can initiate the corrosion reaction. This appears to happen when Fe^{++} ions are present in the medium. The corrosion rate at first increases and then decreases (Figure 6 and Table IV). The decrease in corrosion rate may be due to additional H_2S which was produced from the ammonium sulfate after the sulfide ions initially produced were removed by the Fe^{++} ions. Although the depolarizing agent appears to be involved, the exact mechanisms for the formation of the stalactites remains to be determined. From the high corrosion rates obtained when the sulfide ions are removed, it appears likely that the depolarizing agent may be responsible for the high corrosion rates obtained in the field as a result of bacterial action.

REFERENCES

1. W. S. Patterson, *Trans. North East Coast Inst. of Eng. and Shipbuilders* 68, 93 (1952).

2. E. F. Corcoran and J. S. Ketredge, *Marine Corr. and Fouling Conf.*, Scripps Inst. of Oceanography, La Jolla, Calif. (1956).

3. G. H. Booth, A. W. Cooper, and A. K. Tiller, *J. Appl. Chem.* 13, 21 (1963).

4. C. A. Willingham and H. L. Quinby, *Dev. Ind. Microbiol.* 12, 78 (1970).

5. C. A. H. Von Wolzogen Kühr and L. S. van der Vlugt, *Water* 18 (16), 147 (1934).

6. R. Stumper, *Compt. Rend.* 176, 1316 (1923).

7. G. H. Booth, L. Elford, and D. S. Wakerly, *Br. Corr. J.* 3, 242 (1968).

8. R. A. King and J. D. G. Miller, *Nature* 233, 491 (1971).

9. B. H. Goldner and J. B. Dittman, *Amer. Petroleum Inst. Second Biennial Symp. Microbiol.* (1964).

10. W. P. Iverson, *Biological Corrosion, Advances in Corrosion Science and Technology* 2, New York (1972).

11. H. J. Bunker, *J. Soc. Chem. Ind.* (London) 58, 93 (1939).

12. *Chemistry Research HMSO* (London) p. 22 (1948).

13. M. E. Adams and T. W. Farrer, *J. Appl. Chem.* 3, 117 (1953).

14. G. H. Booth and A. K. Tiller, *Trans. Faraday Soc.* 56, 1689 (1960).

15. A. K. Tiller and G. H. Booth, *Trans. Faraday Soc.* 58, 110 (1962).

16. G. H. Booth and A. K. Tiller, *Trans. Faraday Soc.* 58, 2510 (1962).

17. G. H. Booth, P. M. Shinn, and D. S. Wakerly, *Congr. Inst. Corros. Marine et des Salisseeuree*, CREO (Paris) p. 363 (1964).

18. G. H. Booth, J. A. Robb, and D. S. Wakerly, *Proc. 3rd Int. Congr. on Met. Corr.* (Moscow) 2, 542 (1966).

19. R. C. Allred, *Prod. Month.* 22 (9), 32 (1958).

20. W. P. Iverson, *Appl. Microbiol.* 14 (4), 529 (1966).

21. J. Postgate, *J. Gen. Microbiol.* 9, 440 (1953).

22. M. Stern and A. L. Geary, *J. Electrochem. Soc.* 104 (1), 56 (1957).

23. M. Stern and E. D. Weisert, *Proc. ASTM* 59, 1280 (1959).

24. W. J. Schwerdtfeger and O. M. McDorman, *J. Electrochem. Soc.* 99, 407 (1952).

25. J. M. Pearson, *Trans. Electrochem. Soc.* 81, 271 (1950).

26. H. D. Holler, *J. Electrochem. Soc.* 97, 271 (1950).

27. W. J. Schwerdtfeger, *J. Res. Nat. Bur. Stand.* 70C, 187 (1966).

28. W. J. Schwerdtfeger, *J. Res. Nat. Bur. Stand.* 66C (3), 245 (1962).

29. *Nat. Bur. Stand. Rept. 10, 104, Corros. Res.* (1969).

30. W. P. Iverson, *J. Electrochem. Soc.* 115 (6), 617 (1968).

31. E. E. Nelson, *Corros.* 18, 247t (1964).

32. W. P. Iverson, *Nature* 217 (5135), 1265 (1968).

ACKNOWLEDGEMENT

This study was supported by the Office of Naval Research. Many of the electrochemical measurements were made by Joan Churney, formerly at NBS. X-ray diffraction studies were made by C. J. Bechtold, Mossbauer studies by L. Swartzendruber, scanning electron microscope studies by D. B. Ballard and H. Yakowitz and certain chemical analyses by J. Taylor, all of NBS. The discussions with W. J. Schwerdtfeger concerning the polarization break technique were most greatfully appreciated.

Table 1

Corrosion of Mild Steel in TPSW Culture
1st Cell

Time	O.C. Potential Steel	Redox Potential	Corrosion Current Density	Corrosion Rate
(days)	(V)	(V)	(uA/cm^2)	(mdd)
1	-0.717	+0.270	0.70	1.75
4	-0.711	+0.250	0.48	1.20
7	-0.699	+0.261	0.42	1.05
1*	-0.695	+0.271	2.30	5.86
7	-0.564	-0.199	0.28	0.70
14	-0.550	-0.200	0.13	0.32
21	-0.491	-0.194	0.04	0.10
25	-0.451	-0.197	0.22	0.55
42	-0.548	-0.183	1.73	4.32
43	-0.582	-0.180	2.56	6.40
44	-0.574	-0.180	-	-
49	-0.605	-0.178	-	-
50	-0.605	-0.180	-	-
51	-0.604	-0.180	3.20	8.00

*1st day after inoculation - inoculum 5 days old.

Table II

Corrosion of Mild Steel in TPSW Culture
3rd Cell

Time	O.C. Potential Steel	Redox Potential	Corrosion Current Density	Corrosion Rate
(days)	(V)	(V)	(uA/cm^2)	(mdd)
1	-0.715	+0.160	0.32	0.80
6*	-0.728	+0.182	0.11	0.27
1°	-0.750	-0.100	0.12	0.30
4	-0.710	-0.143	0.18	0.45
8	-0.684	-0.210	0.16	0.40
15	-0.671	-0.232	0.11	0.27
22	-0.631	-0.215	0.03	0.07
30	-0.605	-0.218	0.09	0.22
36	-0.599	-0.220	0.09	0.22
43	-0.572	-0.221	0.09	0.22
50	-0.569	-0.231	0.11	0.27
64	-0.561	-0.222	0.10	0.25

*Cell inoculated on 6th day with 11-day-old cells from TPSW agar surface without added Fe^{++} ions.

°Days after inoculation.

Table III

Corrosion of Mild Steel in TPSW Culture Filtrate

Time	O.C. Potential Steel	Redox Potential	Corrosion Current Density	Corrosion Rate
(days)	(V)	(V)	(uA/cm^2)	(mdd)
1	-0.642	-0.192	0.10	0.25
3	-0.683	-0.201	0.19	0.47
8	-0.746	-0.210	0.73	1.82
29	-0.582	-0.220	0.42	1.05
39	-0.569	-0.221	0.14	0.35
50	-0.619	-0.215	1.60	4.00
59	-0.632	-0.228	1.02	2.55
71	-0.633	-0.221	0.85	2.12
81	-0.589	-0.230	0.71	1.77
91	-0.579	-0.230	0.46	1.15
101	-0.573	-0.228	0.82	2.05
112	-0.580	-0.281	0.73	1.82

*Filtrate of a 6-day-old culture. PH filtrate 7.0.
Potential of sulfide ion electrode was -0.620 V.

Table IV

Corrosion of Mild Steel in TPSW Culture with Added Fe^{++} Ions*

Time	O.C. Potential Steel	Redox Potential	Corrosion Current Density	Corrosion Rate
(days)	(V)	(V)	(uA/cm^2)	(mdd)
2	-0.699	-0.101	0.92	2.30
6	-0.699	-0.189	1.06	2.65
12*	-0.692	-0.082	1.08	2.70
1*	-0.685	-0.155	2.20	5.50
7	-0.683	-0.191	3.52	8.81
14	-0.676	-	7.75	19.37
22	-0.674	-0.229	6.56	16.32
28	-0.678	-0.238	12.42	31.06
36	-0.681	-0.221	7.20	18.00
42	-0.682	-0.223	9.86	24.65
49	-0.688	-0.227	10.30	26.15
58	-0.668	-0.232	10.53	26.32
74	-0.617	-0.190	5.86	14.65
92	-0.620	-0.194	4.80	12.00
101	-0.610	-0.201	4.16	10.40

*Cell inoculated on 12th day with 7-day-old cells from TPSW agar surface without added Fe^{++} ions.

*Days after inoculation

*0.25%ferrous ammonium sulfate

Table V

Effect of FeS in Sterile TPSW Medium on the Corrosion of Mild Steel

Time	O.C. Potential Steel	Redox Potential	Corrosion Current Density	Corrosion Rate
(days)	(V)	(V)	(uA/cm^2)	(mdd)
0	-0.705	-0.000	-	-
1	-0.698	-0.012	0.33	0.82
2	-0.695	-0.003	0.38	0.95
6	-0.690	-0.001	0.28	0.70
0*	-0.702	-0.020	0.38	0.95
1	-0.705	-0.040	0.46	1.15
2	-0.705	-0.080	0.43	1.07
3	-0.705	-0.090	0.32	0.80
6	-0.703	-	0.51	1.25
14	-0.705	-0.100	0.38	0.95

*Immediately after addition of 0.3 gm $Na_2S.9H_2O$ added to 200 ml TPSW medium containing 0.5 gm ferrous ammonium sulfate. Ferrous ions were in excess. 23.6 mg (1.34 mM) FeS recovered.

Table VI

Effect of TPSW Culture Filtrate* to Which Fe^{++} Ions Were Added on the Corrosion of Mild Steel

Time	O.C. Potential Steel	Redox Potential	Corrosion Current Density		Corrosion Rate	
(days)	(V)	(V)	(uA/cm^2)		(mdd)	
			PB•	PL•	PB•	PL•
0	-0.695	-0.240	-	-	-	-
1	-0.796	-0.162	1.1	2.3	2.7	5.7
2	-0.784	-0.197	1.0	2.3	2.5	5.7
3	-0.762	-0.295	1.0	2.0	2.5	5.0
3-1/3	-0.662	-0.335	-	20.8	-	52.0
4	-0.595	-0.318	-	115.5	-	288.7
5	-0.589	-0.320	-	172.8	-	432.0
6	-0.578	-0.319	134.4	172.8	336.0	432.0
7	-0.574	-0.315	114.2	154.2	285.5	365.5
8	-0.570	-0.310	192.0	172.8	480.0	432.0
9	-0.565	-0.303	307.0	198.4	767.5	496.0
10	-0.562	-0.300	255.0	153.6	637.5	384.0
13	-0.548	-0.278	452.5	460.8	1131.2	1152.0
14	-0.550	-0.192	102.1	106.6	255.2	266.5
15	-0.542	-0.223	76.8	69.4	192.0	173.5

*8-day-old (TPSW) culture Seitz-filtered and 0.3835 gm $FeCl_2.4H_2O$ dissolved in 4 ml sterile seawater added.

PB• - Polarization break method

PL• - Linear polarization method

Table VII

Effect of Filtrate• of TPSW Culture to Which Fe^{++} Ions• Were Added on the Corrosion of Iron Nails after 20 Days

No. Nails+	Wt. Loss (mg)			% Original Wt. Lost			Corrosion Rate (mdd)		
	Min.	Ave.	Max.	Min.	Ave.	Max.	Min.	Ave.	Max.
5	9.7	15.1	19.6	1.20	1.92	2.50	22.2	32.3	39.7
				Control*					
5	0.4	0.6	0.7	0.05	0.07	0.09	0.92	1.29	1.62

•7-day-old culture

•0.3803 gm $FeCl_2.4H_2O$ added to 200 ml culture. pH 6.7 after addition and filtration. Fe^{++} ions in excess.

+Nails 1.82 mm dia.; Av. wt. 0.7778 gm.; Av. length 38.0 mm.

*Nails in uninoculated TPSW medium.

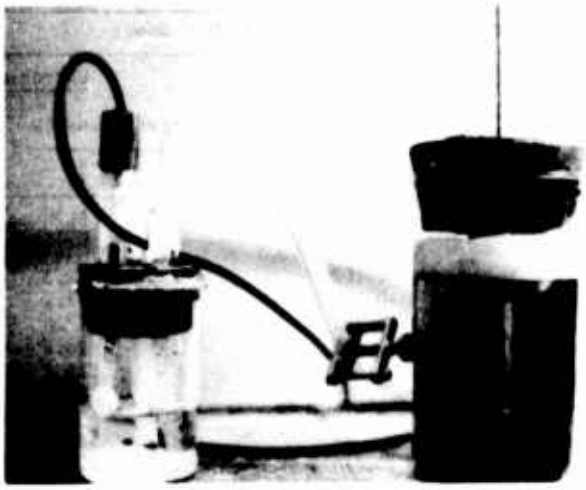
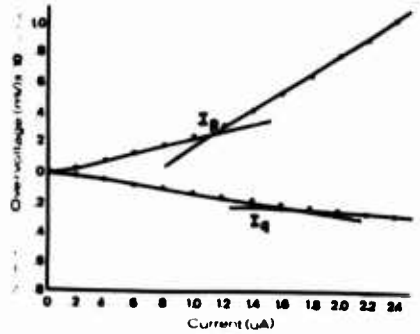


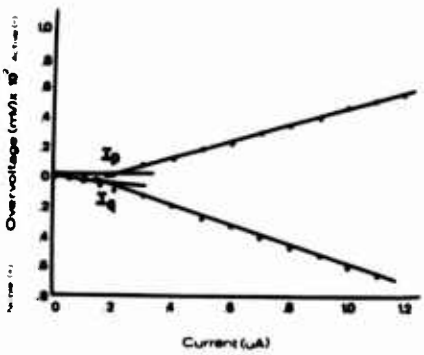
Figure 1. Polarization cell and calomel half-cell.



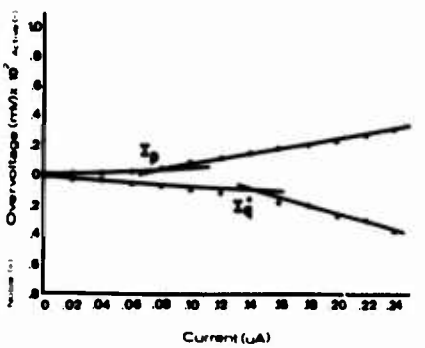
Figure 2. Polarization cell showing steel, platinum, and luggin capillary.



a



b



c

Figure 3. Polarization curves of mild steel in TPSW medium in the absence of added ferrous ions: a) 1 day after inoculation. Corrosion under cathodic control - open circuit potential -0.695 V; b) 3 days after inoculation. Corrosion under slight anodic control - open circuit potential -0.618 V; c) 9 days after inoculation. Corrosion under cathodic control - open circuit potential -0.518 V.

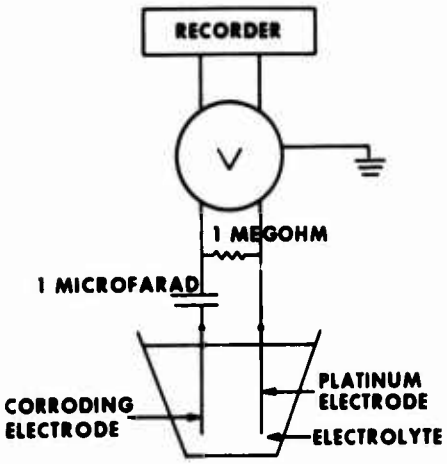


Figure 4. Schematic diagram of circuit used in obtaining rapid potential variations



Figure 5. Surface of mild steel electrode after removal from culture showing dark film and areas at the top edge where the film was detached. White area at bottom due to drop of KCl-agar which fell on specimen during drying of film (magnification ca 10X).

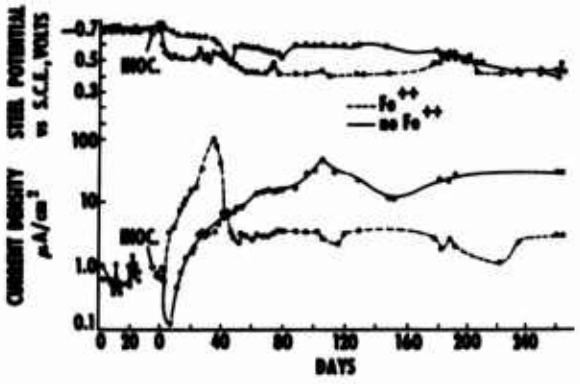


Figure 6. Corrosion rates and open circuit potentials of mild steel vs time in TPSW culture with and without added Fe^{++} ions (2.5% ferrous ammonium sulfate). The inoculum for each cell consisted of 6-day-old cells in 0.5 ml sterile seawater.

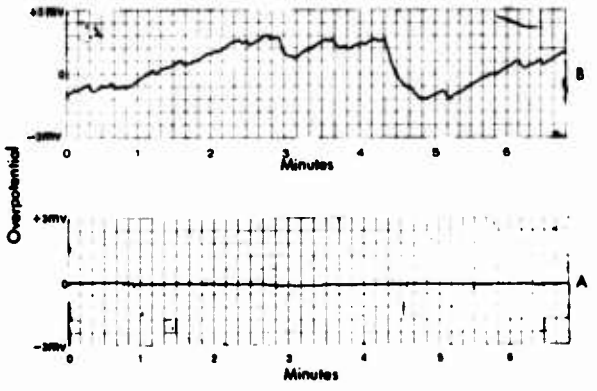


Figure 7. Variations in open circuit potential of mild steel electrode vs time in TPSW culture a) with and b) without added Fe^{++} ions. (18 days after inoculation).

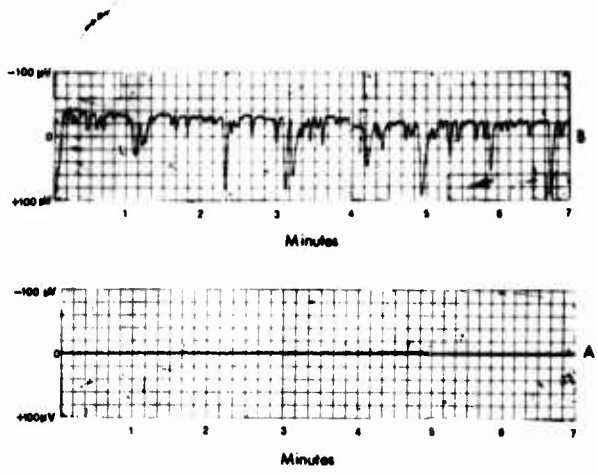


Figure 8. Potential variations of mild steel electrode (obtained with circuit in Figure 4) vs time in TPSW culture a) with and b) without added Fe^{++} ions (17 days after inoculation).



Figure 9. "Stalactite" formation from mild steel electrode in TPSW culture without added Fe^{++} ions.



Figure 10. "Stalactite" fragments obtained from electrode in Figure 9. (Magnification ca 7X).



Figure 11. Electron scanning micrograph of "stalactite" fragment. (Magnification ca 1050X).

Written Discussion

La Que: The calculations of corrosion rates were evidently based on the dimensions of the test specimen rather than on the area actually corroding which is affected by the application of current.

Iverson: The calculations were based on the dimensions of the test specimen. This, of course, may not represent the areas actually corroding, but at present the electrochemical techniques are the best available techniques for measuring the corrosion rates in lieu of disturbing the system by removing the specimen and determining the weight loss. In the case of the surface area of the electrode where the corrosion rate was extremely high, a black film was present over about 1/4 of the area with the remaining 3/4 of the surface area severely attacked. The corrosion rate would be even higher if the measurements were based on this area. The high corrosion rate was verified by weight loss measurements on the small nails. The surface area of the nails appeared to be uniformly attacked and the estimation of corrosion rates using weight loss data and surface area is probably close to reality.

Carlston: Your comments on the addition of Fe^{++} to the aged seawater media has to take into account the small solubility of Fe^{++} (and even smaller solubility of Fe^{+++}) in natural seawater because of the precipitating anions in the environment. Thus, on a practical basis in seawater, the added ions should have little effect.

Iverson: That would appear to be correct. The corrosion of the steel electrode in seawater without added ions, with the formation of the stalactite growths, would appear to be a more natural process. Ferrous ions were added to the seawater in an attempt to demonstrate the increased corrosion rate in the presence of these ions as noted by others and to possibly get a better idea of the mechanism involved. As it turned out, the ferrous ions removed the S^{--}, thereby preventing protective film formation of some form of iron sulfide at the surface and thereby permitting the depolarizer produced by the organisms to react directly with the metal surface.

Carlston: It should be made clear (as by other discussors) that the simultaneous presence of Fe^{3+} and S^{--} would indicate that the sulfur must be in an oxidized state (consistent with free sulfur).

Iverson: According to analysis using the scanning electron microscope coupled with an energy dispersive spectrometer, some free sulfur was detected. The results of the Mossbauer analysis, however, indicated the iron sulfur compound was close to but distinct from FeS_2 in its properties. It would appear from these results that some oxidation of the corrosion product had occurred.

Carlston: The resulting iron material after heating in a vacuum at 1200°C shows great enrichment of C over the nominal 0.2%. Thus, the cathode areas (Fe_3C) must grow appreciably during a run. This might be responsible for the changes in corrosion rate with time.

Iverson: It should be pointed out that the product after pyrolysis in this case was quite different from the original product. This was probably due to the fact that there was sufficient carbon (a bacterial contaminant) in the material to bring about reduction of the iron sulfur compound to iron and iron carbide upon vacuum heating.

Baber: In the medium, without ferrous ions, where the corrosion rate decreased and then increased to about 70 mdd along with an unstable fluctuation of the steel potential, what effect did the varied metallurgical properties of the ferrite, cementite, and austenite content contribute to

the reversible anodic and cathodic nature of the metal microstructure as evidenced by the unstable potential? Also, would this cause a breakdown of the sulfide film into ferric ions and sulfur?

Iverson: As previously mentioned, the ferrite, austenite and cementite are not the natural corrosion products. The unstable potential was probably due to a protective sulfide film which became disattached.

Baber: In the experiment where ferrous ions caused an increase and then decrease of the corrosion rate, what was the ferric content of the protective film and the ferrous content?

Iverson: This was not determined.

Baber: Were the ferrous ions converted to ferric ions which provided a protective film for the material?

Iverson: I would think not since conditions in the medium were highly anaerobic. The protective film was probably some form of iron sulfide.

Summarized Oral Discussion

In reply to a question concerning the composition of the stalactite material, the author stated that the Mössbauer spectrum of the material indicated it was close to but not identical to FeS_2 and that the material also could have been an oxidized form of the original material.

In reply to a question as to whether anaerobic corrosion could be influenced by temperature as well as water pollution, the author stated that both factors could influence anaerobic corrosion. One would generally expect the metabolic activities of the bacteria as well as the corrosion processes to increase with an increase in temperature. With an increase in pollution, one might expect an increase in the amount of organic material which would provide nutrients for the bacteria and hence an increase in their growth rate and metabolic activities.

In reply to a question concerning the valence change of iron during the corrosion process, the author stated that it was assumed to be 2 until further studies indicated otherwise.

In response to a question concerning the correlation between the electrochemical techniques used for measuring corrosion, the author stated that the results obtained with the two techniques generally were quite comparable.

In reply to a question concerning the position of the auxiliary electrode, the author stated that it was usually placed about 5 to 10 mm to the side of the specimen and that the position of the electrode probably would have little effect on the polarization as the currents were very small (usually in the nanno-Ampere range).

The biologist's view of the Teredinidae and their control (with a documentary film on teredo life histories)

Ruth D. Turner and John L. Culliney
Museum of Comparative Zoology
Harvard University
Cambridge, Mass. 02138

Research in medicine and agriculture has shown that effective control of pest species begins with their proper identification and a knowledge of their life histories. Until recently, however, research on the control of marine borers has centered largely on the material being attacked rather than the organisms involved, and this may be one reason for the lack of success.

Field and laboratory studies have shown that Teredinidae exhibit a great deal of variability, emphasizing the danger of generalization. It would appear, however, that one of the most vulnerable periods in the life history of all species is the time of settlement and metamorphosis. At this stage the young borer must be able to deposit calcium for its developing shell, tube and pallets. If this process is interrupted the borer dies before it can penetrate the wood deep enough to be of any consequence. Some natural woods have now been found which have this effect and cooperative research is now in progress to isolate the chemicals involved and determine their action.

The film, showing the three types of life histories found in the Teredinidae, was made primarily to document normal behavior, to form the basis for comparison of one species with another, and the behavior of larvae under experimental conditions.

Key words: wood borers, Teredinidae, life history, control.

As biologists interested in the life history and ecology of marine boring and fouling mollusks, it has long been our contention that the approach to the control of these mollusks, where they are pests, has not put sufficient emphasis on the biology of the animals. Rather it has emphasized the protection of the wood, metal or other material being used in the marine environment. Largely by a process

of elimination some reasonably effective means of protecting material in the sea have been developed. In most cases, however, the biological reasons for the results are unknown. Medical and agricultural literature is replete with reports of the successful control of diseases and pests which have resulted from first knowing in detail the organism to be controlled. We feel that this is the path which must be taken if boring and fouling organisms are to be eventually controlled.

A review of the literature has shown that most of the work on the systematics, distribution and biology of the Teredinidae has been confined to ports or other areas where man is concerned about his vessels, wharves, bridges or other structures. Relatively little is known about boring and fouling organisms where man is not involved and few people realize that the Teredinidae are important in the ecology of littoral and estuarine water where they play a major role in the recycling of woody plant material.

The first step in studying any phase of the biology of any organism is its proper identification. Consequently before beginning life history and ecologic studies it was necessary to put the systematics of the Teredinidae on a sound basis and this has been done (1)[1]. While working on life history studies of a given species in the laboratory we have, whenever possible, studied natural populations in the field at the same time. Such studies have shown for example that though the adults of some species may be able to extend their burrows into the living tissue of mangrove or other trees, the larvae apparently can only penetrate dead wood. When searching for borers in tropical waters, particularly in areas with extensive tides, it becomes obvious that only those larvae survive which settle in shaded, moist areas where they are not subject to intense heat, dessecation and extremely high salinities during the long hours of exposure at low tide. The sunbaked margin of mangrove forests or the sunny side of pilings are usually devoid of boring and fouling organisms in such areas. Using experimental collecting panels we have found that the spawning of a single species may be controlled in one area by the rainy season and in another by temperature (2). Laboratory experiments have shown that the free swimming larval stage of some species can be prolonged for several days or weeks by reducing the food or the temperature, or both, and that when conditions are returned to optimum the larvae will resume growth and settle (3). Culliney (4) reported on delayed settlement and metamorphosis in the calcareous rock, coral, and shell borer, Lithophaga bisulcata d'Orbigny, and suggested that this ability may occur in many species having specialized substrate requirements. Larvae capable of delaying metamorphosis could survive a drop in temperature locally or be carried long distances by ocean currents as shown by Scheltema (5). Such findings emphasize the danger of generalizations based on research involving a single species or on a limited number of experiments. One fact, however, common to all species of Teredinidae becomes increasingly obvious as work progresses and that

---

[1] Figures in parentheses indicate the literature references at the end of this paper.

is the importance to the settling larvae of the ability to extract calcium from sea water and deposit it in the form of shells, tubes and pallets. The valves of the larvae at the time of settlement are about 200 to 300 μ in length and are strong enough to excavate a small depression in the softened outer surface of the wood. Small particles scraped from the surface are formed into a ring and gradually work up the sides of the valves producing a cone over the larvae. By the time this is accomplished the larvae has come in contact with the harder wood surface beneath. Now, if penetration is to be successful, four events must take place all of which involve the deposition of calcium. 1) the impregnation of the cone with calcium to strengthen it and protect the metamorphosing larvae beneath, 2) the development of the denticulated ridges on the anterior end of the valves in order that the young borer can penetrate the wood and grow, 3) the development of the calcareous pallets used to plug the aperture of the burrow when the siphons are withdrawn and so protect the now imprisoned borer from predators or adverse conditions; 4) the production of a calcareous tube at the posterior end of the burrow which insures the proper fit of the pallets and to which the muscles of the pallets and siphons are attached. Considering the minute size of the newly settled borer this represents an incredible amount of calcium deposition within a very short space of time, in our observations about 6 to 10 hours. Failure to do any of the above means certain death for the young teredinid because it cannot grow if it is incapable of penetrating the wood, it cannot protect itself without pallets, nor can it effectively work the siphons and pallets without the burrow lining. Realizing this weak link in the life history of the borers, we are now cooperating with wood specialists and chemists at the U. S. Naval Research Laboratory testing the effects of various chemicals extracted from natural woods known to be resistant to borers and which our observations suggest affect the ability of the borer to deposit calcium. Some chemicals may act as chelating agents while others may work in quite a different way. We are doing bioassays using the chemicals in various concentration and some of these have proved rather effective. We are also observing the behavior of the larvae and their penetration using the natural wood as well as small pine discs impregnated with the extracted chemicals. These experiments are in progress so we cannot report results at this time. The purpose of citing this work is to illustrate the type of cooperative research we believe is essential to solving many of the marine boring and fouling problems.

The film which we have made is a documentary the purpose of which is to show: 1) diversity in the family Teredinidae; 2) the three types of life histories, e.g. oviparous or planktotrophic in which fertilization takes place in the sea and the entire larval life is planktotrophic lasting about 6 weeks to 2 months (example shown, Nototeredo knoxi Bartsch, but including species in all genera except Teredo and Lyrodus); short-term larviparous in which the young are held in the gills of the parent to the straight-hinge stage and the free swimming period is about 2 weeks (example shown, Teredo navalis Linnaeus, but including other species in the genera Teredo and Lyrodus); and the long-term larviparous in which the young are held by the parent to the pediveliger stage, with the free swimming stage reduced to a few hours or about a week (example shown, Lyrodus pedicellatus Quatrefages, but including other species in the genera Teredo and Lyrodus); 3) the settlement and crawling behavior of normal pediveligers and finally 4) the penetration of the larvae into the wood, the development of the siphons, calcification of the cone and the develop-

ment and function of the pallets.

Having a documentary film of the normal functioning of borers we can now make similar films of larvae placed on naturally resistant or treated wood and record and compare their behavior. This is one step toward understanding what and how these chemicals work. There are numerous other experiments where a knowledge of the normal behavior and the use of time-lapse movies will prove useful such as the study of the effects of the primary film, competition with settling larvae of other species, and the effects of currents on settling.

References

1. R. D. Turner, A Survey and Illustrated Catalogue of the Teredinidae (Mollusca: Bivalvia). Museum of Comparative Zoology, Harvard University, Cambridge, Mass. 265 pages, 64 plates, 25 text figures (1966).

2. R. D. Turner, Australian Shipworms, Australian Natural History 17 (4): 139-145, pls. 1-4. (1971).

3. R. D. Turner, Biology of Marine Wood-boring Molluscs. [in] Marine Borers, Fungi and Fouling Organisms of Wood edited by E. B. G. Jones and S. K. Eltringham. Organization for Economic Cooperation and Development, Paris. Chapter 13, pp. 259-301, figures 1-14. (1971).

4. J. L. Culliney, Laboratory rearing of the larvae of the mahogany date mussel, Lithophaga bisulcata. Bulletin of Marine Science 21 (2): 591-602, figures 1-8. (1971).

5. R. S. Scheltema, Dispersal of phytoplanktotrophic shipworm larvae (Bivalvia: Teredinidae) over long distances by ocean currents. Marine Biology 11: 5-11, figures 1-3. (1971).

Discussion

Bowen: You said you were not sure whether there was supplemental feeding of plankton. Have you compared the amino acid analysis of the tissue with that of the wood on which they were feeding?

Culliney: No. This was done some time ago by Dr. Charles Lane, or one of his colleagues, at Miami. I believe they found that there was not enough amino acids in wood to account for those found in the animal. They speculated that there must be some other source of amino acids and thought perhaps it could be from the fungus in the wood because the amino acid spectrum of the fungus filled in the gaps that were apparent between the wood and the teredo. Phytoplankton is very probably a source of food for these animals because they have a crystalline style and perfectly good lamellibranch gills and so are capable of filter feeding.

Trussel (Vancouver): You mentioned the attack on mangrove. Are live mangroves attacked?

Turner: My feeling is, after examining mangrove in Florida, Puerto Rico, Brazil, India, Australia, New Guinea and Panama, that initial penetration can occur only in dead wood, i.e., broken stubs of branches or twigs. Once in the dead wood and well established they can extend their burrows into the living part of the tree. I have never seen evidence of their going directly into living wood. At one time I tried growing small trees in tubes and introducing larvae but I always lost them. It was an almost impossible experiment.

Miller: Would Dr. Turner care to speculate on the significance of economic damage cost to man-made structures caused by teredine borers compared to that caused by crustacean borers?

Turner: That is a hard question to answer because it so often depends on the locality. There are areas in Puerto Rico where Martesia are more destructive than teredines and in Guam where Limnoria seem to be the most destructive. I did not believe Sphaeroma were really destructive until I went to Australia but at least one species there can cause incredible damage. In localities with a high Limnoria population they may 'control' the teredines by so disturbing the settling young that they cannot penetrate the wood; or they may so erode the surface of the wood that the entrance of adult burrows are enlarged, exposing them to predators. Generally if there is a consistent, very heavy Limnoria attack, the teredinid attack is light. Attack by Limnoria is more easily detected and controlled, therefore, I expect one could say that on a world-wide basis the costs due to teredinid activity are considerably higher. However, conditions vary and so one really cannot generalize.

Kuhne: When you observed such a large number of larvae, did you notice that the larvae preferred the autumn wood?

Culliney: We have not made any quantitative observations. You saw in the movie of the penetrating larvae that it did choose the less dense wood, the wood with a wider banding.

The role of the biologist in anti-fouling research

Dennis J Crisp

N.E.R.C. Marine Invertebrate Biology Unit
Marine Science Laboratories
Menai Bridge
Anglesey, North Wales, U.K.

Unlike most other forms of pest control, which are concerned with rather specific animal and plant groups such as insects, fungi or rodents, marine anti-fouling controls must contend with a great diversity of organisms drawn not only from a wide variety of animal groups but also from plants and micro-organisms. The formidable array of potential colonisers lying in wait to attach themselves to surfaces exposed to the sea is the result of many parallel lines of evolution leading to a sedentary existence. This particular luxury is available to marine organisms because they can rely on suspended or dissolved nutrients being carried to them by water currents in the sea. The number of known species involved in fouling was reported in 1950 (U.S. Navy 1952)(1) as reaching 2,000, and must now be in the region of 4,000-5,000, while the micro-organisms, whose study is in rudimentary state, must be seriously underestimated in this total.

It is clear that to obtain detailed information on the life history and settlement of all these organisms would be an unrealistic and unrewarding aim; concentration on certain species and groups has therefore been necessary. The organisms considered to be of prime importance to fouling have varied with circumstances - the particular fouling problem, the geographical region, current shipping practice and the state of the art have all had an influence.

In earlier days, when sailing ships were often becalmed for long periods, it was the attachment of the oceanic stalk barnacles (Lepas sp.) that caused concern; offshore buoys and rigs are still faced with the same problem. However, modern freighters and naval ships, as Visscher showed some fifty years ago (Visscher, 1928) (2), are not appreciably fouled when under way, but as they spend some time in port they may then accumulate the minute post-settlement stages of coastal organisms which then grow rapidly during the voyage. Acorn barnacles dominate the fouling of rich, estuarine areas where ports are usually to be found; tubeworms, Bryozoa and ascidians are abundant in clearer and less nutrient-rich waters. With a faster turn-round and improved copper-based paints capable of preventing most animal settlement, the research aim had to be focused on the green alga (Enteromorpha) which grows luxuriantly at the water line and is a serious problem for large tankers. As in medicine, however, overcoming one problem may only serve to throw another into relief. The virtual elimination of green filamentous algae by new organo-metallic toxics, revealed the presence of a brown alga, Ectocarpus. This alga appears particularly resistant and some varieties appear to have evolved a specific adaptation to copper (Russell and Morris, 1970) (3). Problems quite different from those of ships' hulls are encountered in seawater installations where pipes and conduits are used. Here the most troublesome organisms are mussels which cause blockages and bacteria which may accelerate corrosion. Since the water supply can be controlled, whereas the surfaces are inaccessible, the problem of internal fouling can be solved more satisfactorily by water treatment than by toxic paints. Continuous chlorine injection at a very low concentration or intermittent heating have been found satisfactory. Design is often the key factor in avoiding a shutdown of the plant for cleaning, but engineers are strangely reluctant to consult biologists on these problems in advance.

It is hard to see how any scientific or other investigation can proceed in the absence of an adequate background. In ordinary life, the conceptual framework

(Figures in parentheses indicate the literature references at the end of this paper)

which we build up from experience comes to be accepted so regularly that we lose awareness of its existence and importance. In performing every-day tasks, we pay attention only to the immediate object of our senses without recognising that the sensory information we use would be a meaningless jargon but for stored experience. Similarly, in our adult scientific society it is easy for bureaucrats, administrators and even research managers to imagine that they can select those programmes which have an immediate impact on current problems and finance them exclusively. They tend to forget that not only the interpretation of every experiment and observation, but even the plan of attack on an applied problem is dependent on maintaining the framework of knowledge which we call 'pure science'. Since biology is a more complex and less firmly established science than physics and chemistry, the role of the biologist in comparison with his physical counterpart must lie to a greater degree in putting down such foundations. It would seem inappropriate, therefore, that one should define rigidly the scope of biology in anti-fouling research, provided one recognises that the process of larval settlement is central to the problem. To give perspective to the part played by biologists, I must go back a century and a half when the physical sciences were making rapid progress and forty years before Darwin wrote his classic work on barnacles. The electro-chemical work of Davy and Faraday would never have ranked for a modern research grant in terms of current shipping problems, but it marks, nevertheless, the earliest rational achievements in the field of anti-fouling and anti-corrosion. Their work led them to appreciate that copper sheathing, though satisfactory for wooden ships, could never be used in conjunction with iron; they pioneered the use of zinc sacrificially to prevent corrosion and, most interesting of all, Davy showed the relationship between anti-fouling efficiency and the rate of leaching of copper from the metal surface. With the introduction of iron ships, the need to replace copper led to the development of paints made from various toxic ingredients and by purely empirical methods cuprous oxide was found to achieve the highest measure of success.

By the time biologists were introduced into anti-fouling research in the 1920's, fundamental advances in zoology and botany had already provided descriptions of the form, life histories and much of the behaviour of the many groups of fouling organisms. The area which biologists needed to explore was the use of new kinds of poisons and attempts to interfere with the process of settlement and adhesion, but success in these fields was at the time beyond the capacity either of biology or of the existing allied sciences. Since the conceptual framework for dealing with these problems was missing, little progress could be made. Biologists working in paint firms became subservient to paint technology; their prime purpose was to quantify and embellish with scientific names the crude testing methods employed. With so little challenge they sought an independent role and became more interested in the settlement of organisms on control panels than in the non-settlement on paint films. Studies of breeding cycles were useful in predicting settlement seasons and geographical comparisons of seasonal successions were made showing that at higher latitudes, as expected, the opportunities for testing were confined to the warmer months of the year. Following some of the principles developed by plant ecologists, they began to study the ecological successions as one animal replaced another on the panel surface, starting with primary films and ending usually with a climax cover of Mytilus (Sheer, 1945) (4). Although a side issue of no immediate relevance to fouling prevention, it was from this type of study that attention became directed towards larval behaviour and habitat selection.

Primary films begin to form by the adsorption of macro-molecules and the attachment of bacteria only a few hours after a clean surface has been placed in the sea, and they become fully developed within a week (Zobell, 1938, 1939) (5,6). It was noticed that these films were the forerunner of other fouling organisms. Though wrongly assumed that they were essential - an error corrected by Miller et al (1948) (7), and by Crisp and Ryland (1960) (8), it was nevertheless true that primary films encourage the settlement of most larvae (Daniel, 1955) (9). The conclusion that larvae could choose between different kinds of surfaces came initially as a surprise.

A similar enlightenment arose simulataneously among marine ecologists. It had been assumed that marine larvae developed according to a timetable, and therefore,

wherever they happened to alight when the moment for metamorphosis arrived, they were predestined to settle. Random settlement of this kind would be incredibly wasteful, particularly for animals with very specialised habitats. But the great interest in marine larvae stimulated by Gunnar Thorson (1946) (10) on larval polychaetes pioneered by Douglas Wilson (1952) (11) demonstrated that most, if not all, larvae could delay metamorphosis and so escape the consequences of a tightly-scheduled development. They would test various habitats until a suitable substratum was found. Their searching, though not necessarily 'intelligent', involved genuine choice. They could reject less attractive, though acceptable, sites and settle on the most attractive ones (Crisp and Meadows, 1963 (12), Crisp, 1973a (13), 1973b (14).

Larval choice experiments can be carried out in a simple apparatus in which a variety of test objects are placed at the periphery of a rotating dish and offered simultaneously to the larvae. It has been demonstrated by this means that many larvae settle in response to substances that represent important clues in the natural environment. Certain barnacles and oysters are gregarious and settle on surfaces that have been soaked in extracts of their own species (Crisp and Meadows, 1962) (15), Crisp, 1967 (16), Bayne, 1969 (17)), while some hydroids, Bryozoa, and species of the tubeworm Spirorbis prefer surfaces soaked with extracts of the marine alga on which they are usually found, (Crisp and Williams, 1960 (18), Williams, 1964 (19), 1965 (20)). It has been shown that the settling response of barnacle cyprids is mediated either by contact with an adsorbed film of protein extracted from the integument of its own species, or by contact with the integument itself. It does not require the diffusion of any material from the surface. The recognition of specific proteins at a surface must involve a novel sensory mechanism not yet understood. However, the fact that the larvae choose between surfaces independently of any diffusion process may offer a new dimension in anti-fouling research - the concept of a long-lasting repellent surface not requiring the leaching of limited reserves of toxic material.

A recent interest in larval biology has led to improved rearing techniques. These have yet to be applied to the testing of paint films, but there now exists the knowledge necessary to carry out tests under controlled laboratory conditions throughout the year with much greater precision than would be possible under raft conditions in the sea. Methods have also been developed in which porous materials have been used to imitate a paint surface through which toxic materials are allowed to diffuse at a controlled rate (Christie and Crisp, 1963 (21)). By dissociating the problems of paint formulation from those of screening candidate substances, a much larger number of new poisons can be tested in a given time.

So far, I have considered two biological approaches to the settlement problem; first, the time-honoured method of killing the larva by local concentrations of poison and, second, by discouraging it before it consummates the act of settlement. The third possibility is to interfere with the process of adhesion which takes place after settlement. Studies of these mechanisms and of the substances used are being vigorously investigated for algae (Evans and Christie, 1970 (22)) and for barnacles and other organisms (Lindner and Dooley, 1973 (23), Crisp, 1973a (13). A physical or chemical means of preventing adhesion could well lead to a novel solution of the fouling problem.

It is appropriate that much of this promising work is being done in universities and government laboratories, financed in part by progressive firms in the marine paint and shipping industries. For these studies have a much wider application; the discovery of settlement-inducing substances is of importance to the shellfish industry and has already found use in oyster hatcheries, while many industrial and medical applications are awaiting advances in the technology of underwater cements and adhesives.

Within the paint industry itself, the past forty years has witnessed a considerable improvement in the reliable life of cuprous oxide paints, but, apart from the recent introduction of some new organo-metallic based paints, very little progress

indeed on novel or imaginative lines. Much of the research has been repetitious on account of the numerous firms all engaged in parallel investigations on traditional materials and the progress achieved appears to me to have been unduly costly.

For the sake of future developments, it is worth considering the causes of this disappointing rate of progress. I would suggest three factors stand out. First, it has to be recognised that copper oxide as a basis for anti-fouling paint is difficult to improve upon. It has a high toxicity over a wide spectrum of groups of animals and plants. It is not difficult to prepare and formulate nor unduly expensive. Hence the tendency in the industry has quite understandably been to seek improvement in cuprous oxide paints rather than to search for other materials and methods. Secondly, the performance of ships' paints is notoriously variable even under raft conditions, let alone on ships. Sales cannot, therefore, be expected to rise sharply following the introduction of a marginally improved product; indeed, by the time a new product has proved itself, competitors will already be marketing compositions skilfully slipped through the net of the patent laws. In this situation, investment in exploratory science is difficult to justify against investment in sales and advertising. Thirdly, the structure of the industry mitigates against scientific progress. It consists of a number of relatively small competing units usually working on small profit margins; none of them are capable of sustaining a major research effort such as the problem needs. Nor is it possible to imagine their being able to co-ordinate their efforts within the existing commercial system.

During the war years, one had a glimpse of what co-ordination might achieve, both in Britain and in the United States, during a period when private gain could be subjugated to national enterprise. Rapid progress was made towards an understanding of the fundamentals of the fouling problem. The results were published in the Journal of the Iron and Steel Institute in the United Kingdom, and in the Wood's Hole book on marine fouling in the United States; the latter remains a classic on the subject. Once again, the problem demands a similar interdisciplinary approach, with full co-ordination of the scientists involved. Moreover, there are two new factors which are likely to reveal more clearly than hitherto the deficiencies of the present system. First, there is a distinct possibility that restrictions may be placed on the use of certain poisons. Mercury is almost certainly to be banned. There is little case to be made against the use of copper since it is a relatively abundant element in seawater in the ionic form and the contribution from ships' paints is negligible compared with that reaching the sea from natural drainage. Nevertheless, it is possible that its use may be resisted. Organo-tin derivatives, though rapidly degraded in seawater, may suffer a similar fate. If such legislation is applied, there will need to be concerted efforts to find new and acceptable materials or quite different methods of protecting ships.

The second and more fundamental reason why a new approach is required is the need for really long-lasting paints, perhaps of five or more years duration. The need arises as anti-corrosive paints improve and the possibility of underwater inspection and repair make dry-locking less frequent. The time scale precludes any possibility of such paints being developed empirically by the old methods of testing. More reliable tests, using continuously reared test organisms under laboratory conditions, plus accelerated methods of exposure, must be tried, but past experience indicates that rate processes are among the most difficult to scale up. The other alternative is to replace empiricism by design. For this purpose, we need to know the principles on which marine paints operate to such a degree of refinement that performance can be predicted. We need to know what characteristics of solubility and biodegradability in the paint film and in seawater are required for a toxin to work successfully. We need to know the diffusion properties of a wide range of paint matrices. We need investigation into two layer paints to find how far initial losses of toxic can be minimised. It is also essential that any alternative methods to the use of anti-fouling paints should be fully investigated.

It is likely that these needs are beyond the capacity of commerce, and it will be necessary for national and university laboratories to pioneer much of the

fundamental research.

Fortunately, much of the information on the physics, chemistry and biology of the settlement of fouling organisms which is required in order to seek new methods of fouling prevention is identical to the information required for marine cultivation, though the aims, so far as the organisms are concerned, may be the opposite. Governments are already aware of the need to promote research into the rearing of commercially exploitable animals and the findings of this research are quite like to be of value to the anti-fouling problem just as work on barnacles led to the production of substances useful for stimulating the settlement of oysters, (Crisp, 1967 (16), Bayne, 1969 (17)). It would be a mistake, therefore, to judge either the past work or the future potential of larval biology in terms of a single application.

Lest I have been too disparaging, a backward look over the past 350 years will serve to show how far biologists have advanced in their understanding of barnacle fouling and the biodegradation of wood. In Gerard's 'Herball' (1597), one can see how the absence of a basic scientific framework allows utter confusion between observation and interpretation:- 'for travelling upon the shores of our English coast between Dover and Rummey, I founde the trunke of an olde rotten tree, which (with some helpe that I procured by fishermens wives that were there attending upon their husbands returne from the sea) we drewe out of the water upon dry lande: on this rotten tree I founde growing many thousands of long crimson bladders, in shape like unto puddings newly filled before they be sodden, which were verie cleere and shining,at the neather end whereof did grow a shell fish, fashioned somewhat like a small Muskle, but much whiter, resembling a shell fish that groweth upon the rocks about Garnsey and Garsey, called a Lympit: many of these shels I brought with me to London, which after I had opened, I founde in them living things without forme or shape; in others which were neerer come to ripeness, I found living things that were very naked, in shape like a Birde; in others, the Birds covered with soft downe, the shell halfe open, and the Birde readie to fall out, which no doubt were the foules called Barnakles: howbeit that which I have seen with mine eies, and handled with mine handes, I dare confidently avouch, and boldly put downe for veritie'.

References

1. U.S. Navy Department, Marine Fouling and its prevention. Woods Hole Oceanographic Institution, Woods Hole, Mass. Published by U.S. Naval Institute, Annapolis, Maryland, 388pp. 1952.

2. VISSCHER, J.P. Bull. Bur. Fish. Wash. 43(2), 193-252. 1928.

3. RUSSELL, G. and MORRIS, O.P. Nature, Lond. 228, 288-89. 1970.

4. SHEER, B.T. Biol. Bull. mar. biol. Lab., Woods Hole 89, 103-121. 1945.

5. ZOBELL, C.E. The sequence of events in the fouling of submerged surfaces. Official Digest, Federation of Paint and Varnish Production Clubs. 8pp. 1938.

6. ZOBELL, C.E. Biol. Bull. mar. biol. Lab., Woods Hole 77, 302. 1939.

7. MILLER, M.A., RAPEAN. J.C. and WHEDON, W.F. Biol. Bull. mar. biol. Lab., Woods Hole 94, 143-157. 1948.

8. CRISP, D.J. and RYLAND, J.S. Nature, Lond. 185, 119. 1960.

9. DANIEL, A. J. Madras Univ. 25B, 189-200. 1955.

10. THORSON, G. Meddr Kommn Danm. Fisk.-og Havunders Serie: Plankton 4(1), 523pp. 1946.

11. WILSON, D.P. Annls Inst. océanogr., Monaco 27, 49-156. 1952.

12. CRISP, D.J. and MEADOWS, P.S. Proc. R. Soc. B.158, 364-87. 1963.

13. CRISP, D.J. Mechanisms of adhesion of fouling organisms. In: Proceedings 3rd International Congress on Marine Corrosion and Fouling, Gaithersburg, Maryland, U.S.A. 1972. (in press) 1973a

14. CRISP, D.J. Factors influencing the settlement of marine invertebrate larvae. In: Perspectives in Perspectives in Chemoreception by Marine Organisms. Ed. P.T. Grant. Academic Press, New York. (in press) 1973b

15. CRISP, D.J. and MEADOWS, P.S. Proc. R. Soc. B.156, 500-520. 1962.

16. CRISP, D.J. J. Anim. Ecol. 36, 329-335. 1967.

17. BAYNE, B.L. J. mar. biol. Ass. U.K. 49, 327-356. 1969.

18. CRISP, D.J. and WILLIAMS, G.B. Nature, Lond. 188, 1206-7. 1960.

19. WILLIAMS, G.B. J. mar. biol. Ass. U.K. 44, 397-414. 1964.

20. WILLIAMS, G.B. J. mar. biol. Ass. U.K. 45, 257-73. 1965.

21. CHRISTIE, A.O. and CRISP, D.J. Ann. appl. Biol. 51, 361-366. 1963.

22. EVANS, L.V. and CHRISTIE, A.O. Ann. Bot. 34, 451-466. 1970.

23. LINDNER, E. and DOOLEY, C.A. Chemical bonding in cirripedd adhesive. In: Proceedings 3rd International Congress on Marine Corrosion and Fouling, Gaithersburg, Maryland, U.S.A. 1972. (in press) 1973.

Préparation des tôles de construction navale avant application de peintures

G. Dechaux, Ingénieur en Chef Honoraire du Génie Maritime
Président de l'Association des Ingénieurs en Anticorrosion de France et de l'Union Française (1956 - 1972)

—

Constitution de la calamine d'après des travaux récents. Le FeO peut être confondu avec l'acier nu. Possibilité de le distinguer par exposition aux intempéries, essai au SO_4Cu, coupe micrographique. Inconvénients de ces procédés dans les processus industriels actuels. Inconvénient de la calamine. Description de deux méthodes rapides, non destructrices non polluantes : évaporation différentielle de W.S., relevé de la topographie électrochimique superficielle à l'aide d'une électrode Ag/Agce, l'électrolyte consistant en un papier imbibé d'alcool dénaturé.
Ce dernier procédé permet de vérifier le décalaminage et la décarburation locale.

—

Les risques d'aggravation de la corrosion dus à la présence de calamine sur les tôles de navire, et particulièrement sur les tôles de carènes, sont bien connus depuis longtemps. Il y a plus d'un siècle que M. Becquerel parlait de l'action néfaste de "l'oxyde des battitures" sur la corrosion des carènes. Aussi, depuis la mise en évidence de ce fait, a-t-on mis en oeuvre des procédés de plus en plus sûrs, rapides et perfectionnés, destinés à éliminer complètement cette calamine de la surface des tôles.
Mais est-on certain que les examens actuels courants permettent de vérifier que l'on a bien atteint le but ?
C'est ce sujet que nous allons traiter en décrivant d'abord la calamine et, après exposé - critique des divers contrôles courants de l'efficacité du décalaminage, nous proposerons deux essais <u>non destructifs</u> permettant <u>rapidement</u> de caractériser, sans doute possible, l'état de la surface soumise au décalaminage du point de vue corrosion. Nous soulignons "<u>non destructifs</u>" et "<u>rapidement</u>", car il est essentiel de suivre le rythme "industriel" de préparation de surface (et d'application de peinture), sans faire de prélèvements ni sans dénaturer ou polluer la surface à examiner.
La calamine est constituée d'une succession de couches d'oxydes de fer allant du moins oxydé au plus oxydé, à partir de la surface du métal : FeO Fe_3O_4 Fe_2O_3 .
La thèse de R. Collongues (1) a mis en évidence les lacunes, c'est-à-dire la composition non stoechiométrique de ces oxydes, en particulier de FeO.
Deux communications récentes permettent de voir un peu plus clair dans la constitution de ces couches.
Dans la première J. Manenc et G. Vagnard (2) étudient " à l'aide de la micro-
" graphie optique et de la spectrométrie, l'oxydation d'alliages Fe-C
" (C entre 0,1 % et 0,6 %) oxydés dans l'air ou dans un mélange H_2 et H_2O
" entre 700° et 900° C.
" Cette étude montre que la cinétique d'oxydation n'est influencée par la
" présence de carbone qu'à 800° et au-dessous. Cette oxydation est encore
" plus lente que pour le fer pur. Puisque, quelle que soit la température,
" un enrichissement en carbone au voisinage immédiat de l'interface a été
" constaté, l'activité du fer dans l'oxyde n'est pas modifiée à haute tempé-
" rature du fait de la présence de carbone dans l'alliage .....
" Enfin, la <u>décarburation</u> se produit localement, sans doute par voie gazeuse,
" à travers des fissures où la calamine s'est décollée et non par migration
" à l'état solide dans l'oxyde puisque le carbone y a une solubilité négli-
" geable " .
Dans la seconde communication, Philippe Delbourg (3) étudie la formation, la croissance et l'adhérence de la calamine sur quelques types d'aciers de construction à l'aide d'une thermobalance (à pesée continue) ou de pesées successives et d'une analyse des échantillons à la microsonde électronique de Castaing.
Dans le cas de l'acier extra doux (C = 0,13) en partant de la surface en contact avec l'atmosphère, on rencontre toujours les constituants suivants : une <u>très mince couche</u> de <u>Fe_2O_3</u> (hématite) souvent discontinue ou fragmentée, une

mince couche de Fe_3O_4 (magnétite) dont l'interface avec le protoxyde FeO sous-jacent est remarquablement rectiligne, une couche importante de FeO (protoxyde de fer) à cristaux basaltiques. Cette phase n'est jamais stoechiométrique (Fe_{1-xO}) ; elle est appelée wüstite par de nombreux auteurs. Dans cette couche d'oxyde se trouvent des granules de Fe_3O_4 qui ont précipité dans la partie supérieure (ou externe).

L'auteur appelle "calamine proprement dite" l'ensemble de ces trois couches d'oxydes de fer.

En contact avec le métal sain, on trouve une autre couche d'oxydation, que certains auteurs appellent "zone contaminée" et qui est composée d'une phase de FeO à cristallisation fine polyédrique dans laquelle les grains sont séparés par une phase plus foncée : le silicate de fer Fe_2SiO_4 (Fayalite).

"Selon la température d'oxydation (entre 1000° et 1300°C), le combustible,
" le facteur d'air($\frac{\text{air utilisé pour la combustion}}{\text{air stoechiométrique}}$), le pourcentage de l'é-
" paisseur de la zone contaminée par rapport à l'épaisseur de la calamine
" varie de 1,8 % à 16,1 % .....
" Dans le cas où l'adhérence de la calamine ne viendrait pas à être perturbée
" par une cause extérieure, les proportions des différents oxydes seraient de
" 1 % , 4 % et 95 % respectivement pour Fe_2O_3 , Fe_3O_4 et FeO " .

(Shreir donne 10 % 20 % 70 % - Hauffe 7 % 15 % 78 % - Fancutt et Hudson donnent pour FeO entre 40 et 95%).

La couche mixte (zone contaminée) en contact avec le métal est très adhérente. Mais le protoxyde de fer après sablage ou grenaillage a le même aspect (même couleur, même brillant) que l'acier. Comme ce point est le point essentiel de notre exposé, nous nous appuierons sur quelques références.

Après sablage ou grenaillage, on obtient "une surface de couleur grise,
" demi-mate due à l'oxyde de fer gris (FeO) qui subsiste à l'interface entre
" l'acier supposé idéalement propre et le solde de la croûte de calamine "
(4) (p.413).

Un excellent entrepreneur de peinture (4) (p.416) demande "qu'aucune peinture
" ne soit appliquée avant un intervalle de 24 heures après sablage. Toutes
" les parties présentant après ce laps de temps des taches bleuâtres, révélant
" la présence de calamine, seront à nouveau décapées et à 24 heures au moins
" avant mise en peinture ".

La même observation est effectuée dans un autre domaine (5) : la galvanisation à chaud. R. Souké signale que " le protoxyde de fer FeO ..... bien que mé-
"tastable à la température ordinaire n'en met pas moins un temps très long
" pour se transformer en oxyde magnétique. Son aspect est noir ou gris très
" foncé ; il cristallise dans le système cubique ; il est extrêmement dur
" si bien que son polissage peut être réalisé et le faire confondre avec
" l'acier " .

Enfin, nous rencontrons dans notre sujet précis : tôles de construction navale, le mémoire de R.W. Wilson et J.J. Zonsveld (6).

" Il est très difficile de distinguer entre la surface de l'acier "à blanc"
" et les couches profondes de la calamine caractérisées par un oxyde gris ".

Ceci explique ce que disent précédemment ces auteurs dans le même mémoire, à savoir " qu'à l'heure actuelle l'usage le plus courant est de laisser
" rouiller les surfaces décalaminées pendant la période de construction du
" navire puis de les brosser juste avant l'application des peintures " .

C'est ce que faisait l'entrepreneur dont nous avons donné l'avis et c'est le procédé que nous appliquions pour vérifier s'il subsistait de la calamine sur les carènes sablées à l'Arsenal de Toulon, il y a quarante ans.

En résumé : après grenaillage ou sablage, la simple appréciation de l'aspect de la surface ne permet pas de dire si l'on a affaire à l'acier "à blanc" ou au protoxyde de fer.

Pour déterminer le taux de décalaminage réalisé par grenaillage, nous sommes déjà en possession d'une méthode pratique qui s'applique à un ouvrage en cours de construction ou terminé : exposition aux intempéries naturelles qui donne de la fleur de rouille (en 24 heures) sur les surfaces mises à nu, les régions où subsiste FeO tendant à donner lentement des taches bleuâtres : Fe_3O_4. Cependant, ce délai de 24 heures est trop long pour une étude comme celle de Wilson et Zonsveld qui se proposaient comme but final l'application de primai-

re d'atelier (shop primer) sur tôles décalaminées par grenaillage industriel. Pour déterminer le taux de décalaminage réalisé, ils ont eu recours à deux méthodes : l'une de laboratoire, l'autre d'atelier.

Au laboratoire, ils examinent des coupes métallographiques. Le taux de nettoyage est obtenu par comptage et mesure. La coupe donnée dans leur mémoire (fig.9) montre que 90 % environ linéaire est recouvert de FeO c'est-à-dire $\frac{\text{ligne calaminée}}{\text{ligne non calaminée}} = 9$, ce qui donne pour le rapport des surfaces 81, c'est-à-dire que plus de 98 % de la surface est encore caliminé.

Au chantier, on applique un tampon contenant SO_4 Cu (4 % SO_4 Cu dans H_2SO_4 à 1 %) sur la surface à examiner. Le cuivre se dépose sur l'acier mis à nu et non sur la calamine qui apparaît alors en sombre sur fond de cuivre. Cette indication correspond à celle que donne l'exposition aux intempéries après 24 heures.

Rappelons ici quelques données sur les inconvénients de la calamine.

J.C. Moree (7) donne une micrographie qui met en évidence sous la peinture riche en zinc la formation de rouille autour d'une écaille de laminage qui n'avait pas été éliminée. Or, actuellement, en Europe, dans les chantiers importants, on prend sur parc toutes les tôles et profilés qui entrent dans la construction du navire, on les grenaille et on leur applique immédiatement une couche de peinture primaire d'attente ou d'atelier dans une machine automatique qui fait défiler la tôle à une certaine vitesse sous la grenailleuse et ensuite devant la machine à peindre, à moins que cette opération n'ait déjà été effectuée en aciérie. Et le primaire d'atelier est en général une peinture riche en zinc, séchant très rapidement. Nous voyons donc l'intérêt d'éliminer toute trace de calamine, même avec ces peintures qui fonctionnent comme protection cathodique, grâce à la poussière de zinc.

La différence de potentiel entre calamine et acier dans l'eau de mer est donnée dans plusieurs mémoires.

M. Paul Ffield (8) donne pour la d.d.p. entre acier nu et calamine dans l'eau de mer 26 mV, soit celle qui existe entre le cuivre et l'acier nu (25mV). Comme le fit remarquer le Dr. T.P. May (p.645 réf.8) la d.d.p. entre cuivre et acier est plutôt de l'ordre de 200 à 300 mV que 25 mV. La valeur trouvée par P. Ffield est due aux polarisations à l'anode et à la cathode produites par la circulation du courant (cf diagramme classique de Evans).

J.C. Rowlands (9) donne les potentiels de l'acier doux et de la calamine dans l'eau de mer à 20°C par rapport à une électrode de référence au calomel saturé. Elles sont respectivement - 650 mV et - 200 mV, ce qui donne une d.d.p. entre calamine et acier doux de 450 mV. Shreir donne 300 mV. Signalons que selon Vetter, les trois oxydes de fer connus ont par hasard des potentiels très voisins.

Dans sa communication (8) P. Ffield donne les résultats d'essais sur l'influence des rapports Surface calaminée/Surface d'acier nu. Il opère sur des éprouvettes de 12 pouces carrés en sablant 5, 10, 25, 50 et 100 % de la surface totale. Il a trouvé que, pour la même durée d'exposition dans l'eau de mer, la corrosion de la surface nue exprimée en pouces par an était respectivement 9 - 6,66 - 3 - 1,6 et 1 en prenant comme unité la corrosion de la surface entièrement sablée : 0,005 pouce par an. Mettons ces résultats sous forme de graphique (fig. 1) avec en abscisse le rapport Surface calaminée/Surface acier nu. On voit que jusqu'à près de 10 % de calamine restante, la corrosion est pratiquement proportionnelle au rapport de ces surfaces.

Retenons de ces chiffres qu'en circuit ouvert la calamine a à peu près la même différence de potentiel galvanique que le cuivre par rapport à l'acier, et que la corrosion qu'elle provoque est proportionnelle à la surface qu'elle occupe par rapport à l'acier nu lorsqu'elle est partiellement éliminée.

Pour assurer le succès d'un revêtement, la calamine doit donc être éliminée au maximum possible.

Mais outre la calamine, la surface de la tôle peut présenter d'autres hétérogénéités locales: inclusions, décarburation. La décarburation peut être plus sensible pour certains modes d'élaboration des aciers. Ces hétérogénéités crèent des micropiles, même si la calamine a été entièrement éliminée et comme elles font partie intrinsèque du métal, un grenaillage plus poussé revient à meuler l'acier. Nous avons rencontré des tôles dont la décarbura-

tion atteignait une profondeur de 152 µ. Il est également essentiel de connaître la présence de ces hétérogénéités car la corrosion locale qu'elles entraînent ne peut être évitée qu'en associant au revêtement une protection cathodique par anodes sacrificielles ou courant imposé. Nous avons vu en effet que la protection cathodique conférée par la peinture riche en zinc ne suffisait pas. Nous n'insisterons pas plus sur ces éventualités - mais nous devrons en tenir compte pour notre examen des tôles après grenaillage. Dans ce cas, seule la coupe micrographique peut donner une indication.

Nous en sommes donc arrivés au point suivant : avant d'appliquer un primaire sur une tôle grenaillée, il est essentiel de savoir si toute la calamine est éliminée et si l'on n'a pas affaire à un métal présentant des hétérogénéités superficielles.

Pour les préparations industrielles actuelles, nous éliminons les contrôles suivants :

1 - examen visuel (échelle suédoise par ex.) : inefficace
2 - exposition aux intempéries : trop long
3 - essai au sulfate de cuivre : polluant
4 - coupe métallographique et examen au microscope : destructeur et relativement long

Une critique n'est valable que si elle est positive, c'est-à-dire si l'on propose une solution meilleure correcte au problème posé.

Nous voulions, de plus, une solution non destructrice, non polluante et permettant d'explorer rapidement une surface ou une ligne de la surface. Nous avions envisagé des méthodes magnétiques par courant de Foucault, des essais de microdureté, par rayons X ou γ. Finalement, nous avons eu recours à des solvants qui s'éliminent simplement par évaporation. Les deux solutions que nous proposons permettant la première (en date) l'essai de toute la surface, la seconde l'exploration linéaire sur une ligne aussi longue que l'on veut.

Nous avions d'abord envisagé avec J. Frasch un examen basé sur la différence de vitesse d'évaporation, due à la différence d'adsorption du solvant entre les régions mises à nu et les régions encore calaminées. Il s'agissait de vérifier l'efficacité du décalaminage à la flamme. Comme solvant, nous avions utilisé le white-spirit (W.S.) - d'autres solvants pourraient également convenir. Le processus est simple : on répand et on projette sur la tôle à examiner un film mince de W.S., qui la recouvre entièrement. Ce W.S. s'évapore et à la fin de l'évaporation les zones où le métal est mis à nu se distinguent de celles où le métal est encore recouvert de calamine par la différence de brillant provoquée par la réflexion de la lumière sur le film liquide qui subsiste encore sur les zones calaminées plus adsorbantes (fig.2). On peut donc ainsi caractériser l'acier mis à nu et la calamine - mais seulement par comparaison, quand les deux coexistent, en présence de l'un et de l'autre.

Ce procédé est valable dans certains cas : décalaminage à la flamme, sablage d'un élément de coque, quand presque certainement une partie de la calamine a été éliminée. Mais dans le grenaillage automatique, industriel, très uniforme, nous nous sommes trouvés en présence de surfaces présentant le degré Sa3 de l'échelle suédoise mais entièrement recouvertes de la couche de FeO (ce que l'on pouvait vérifier par l'essai au SO_4Cu ou l'essai dont nous allons parler).

L'essai au W.S. ne peut distinguer entre une surface totalement calaminée et une surface totalement décalaminée. En effet, l'évaporation du W.S. dépend de très nombreux facteurs : vitesse de passage de la tôle, sa température (à la suite du grenaillage), la température, l'humidité, la pression atmosphériques, la vitesse de circulation de l'air. On ne peut donc mesurer avec précision la vitesse d'évaporation sur la calamine seule et sur l'acier nu, ce qui aurait permis de distinguer les deux cas limites - qui donnent une évaporation uniforme (homogène) mais pas à la même vitesse. Nous nous trouvons dans le cas du coloriste qui doit distinguer deux blancs : l'un jaunâtre, l'autre bleuâtre ; il est obligé de les mettre côte à côte.

Nous n'avions pas rencontré cet inconvénient dans l'essai aux intempéries (acier = rouille , calamine = pas de rouille) ni dans l'essai au SO_4Cu (acier = précipité de cuivre, calamine = pas de précipité de cuivre).

Il nous fallait donc avoir recours à un autre essai qui ne nous entraîne pas à confondre une surface entièrement décalaminée avec une surface entièrement calaminée.

Or, nous avions mis au point un essai non destructif permettant de vérifier les hétérogénéités superficielles d'un acier de construction navale, en l'espèce la décarburation superficielle, hétérogénéités qui conduisaient à une corrosion anormale. Rappelons ce procédé décrit à la fin de notre communication au 3ème Congrès de la Fédération Européenne de la Corrosion (Bruxelles juin 1963).

On applique sur la tôle à examiner un papier filtre très pur de 14x22x0,5 cm (type électrophorèse). Si la surface est verticale ou au plafond, on maintient le papier sur la tôle à l'aide de petits aimants permanents. Le papier est imbibé d'alcool dénaturé 90/95° (en France : alcool éthylique avec 3,5% de méthylène et 1 % d'alcool isopropylique). L'alcool pur ne convient pas. Une fois imbibé, le papier colle bien sur la tôle. Ce papier imbibé d'alcool sert d'électrolyte et l'on mesure (ou enregistre) la différence de potentiel qui existe entre une électrode sonde en Ag/AgCe que l'on déplace sur le papier imbibé et, soit la masse du métal, soit une électrode identique fixe appliquée sur le papier à un endroit qui peut être considéré sans calamine : par exemple un coin de tôle ou l'extrémité d'un biseau effectué à la meule (fig.3). Si dans ce dernier cas (2 électrodes) on ne prend pas cette précaution, on retombe dans la même difficulté que précédemment : sur une tôle entièrement recouverte de FeO on trouve des d.d.p. entre électrodes aussi faibles que sur une tôle entièrement mise à nu.

L'électrode mobile est déplacée à la vitesse de 3 à 4 cm/sec par exemple selon deux tracés en dents de scie ou en sinusoïde, l'un d'axe de symétrie parallèle au manipulateur, l'autre perpendiculaire au manipulateur. On effectue ainsi un quadrillage. Les d.d.p. sont lues ou mieux enregistrées : les d.d.p. entre les deux tôles (masse/électrode, électrode fixe/électrode mobile) sont partout supérieures à 60 mV pour une tôle recouverte totalement de FeO et localement $>$ 60 mV pour une tôle partiellement décarburée. Pour une tôle parfaitement mise à nu, les d.d.p. sont partout $<$ 60 mV.

La valeur de 60 mV ne résulte pas de considérations théoriques mais d'essais pratiques sur plusieurs centaines d'éprouvettes et de tôles que l'on pouvait laisser rouiller - ce qui est la méthode la plus sûre (mais la plus longue) de la vérification de l'absence de calamine.

Notons que les d.d.p. que nous mesurons ne correspondent pas aux d.d.p. dans un électrolyte minéral comme l'eau de mer.

A chaque série de relevés de ces d.d.p. (topographie électrochimique), on renouvelle les feuilles de papier filtre car il peut se produire un léger dépôt d'argent (noir) du côté de l'électrode mobile (mais pas de dépôt de fer ou de ses composés du côté acier). Le papier humide donne les mêmes résultats que s'il est gorgé d'alcool. La pression sur l'électrode n'intervient pas.

Nous avons choisi une épaisseur de papier assez forte : 5 mm pour absorber les irrégularités mécaniques superficielles provoquées par le grenaillage. Les écarts de potentiel ($\leq$60 mV) d'une tôle parfaitementdécalaminée et sans décarburation superficielle correspondent, à notre avis, aux régions plus ou moins écrouies de la surface grenaillée. Notons qu'un papier filtre trop mince est arraché par l'électrode qui se déplace sur le papier mouillé.

Le tableau fig. 5 résume les possibilités des différents procédés d'atelier qui permettent d'apprécier l'état de surface de la tôle tant du point de vue calamine que décarburation.

Nous avons fait figurer dans le tableau la valeur absolue de la d.d.p.,ce qui conduit à confondre la décarburation partielle d'une tôle parfaitement calaminée avec un décalaminage partiel, c'est-à-dire localement $|d.d.p| > 60$ mV. Mais la calamine est cathode par rapport à l'acier, alors que les zones décarburées sont anodiques par rapport à l'acier de base. Pour distinguer ces deux cas, il suffit de faire un trait au crayon de graphite sur la tôle. Quand l'électrode mobile passe sur ce trait, la déviation est dans le même sens quand il s'agit de calamine et en sens opposé quand il s'agit de décarburation. Nous ne parlons pas de + et de - car sur le chantier

avec les manipulateurs occasionnels, il peut se produire des erreurs.
Remarquons, ici, que nous avons simplement cité en passant, dans les défauts de surface de l'acier, les inclusions superficielles qui sont mises en évidence par les coupes micrographiques. C'est volontairement, car l'étude de C.E. Homer (10) montre que, sur des surfaces rugueuses (comme celles des tôles sablées et grenaillées) s'il est possible que les inclusions puissent être à l'emplacement des débuts de corrosion, ce ne sont pas les facteurs décisifs et qu'une vérification expérimentale est pratiquement impossible.
Le tableau fig. 6 représente quatre résultats obtenus par la mesure des d.d.p.
La figure 4 donne deux enregistrements obtenus dans l'exemple 1.
Le papier se déroulait à la vitesse de 60 mm/min, l'électrode mobile étant déplacée à la vitesse de 3-4 cm/sec. Sur un enregistrement de 12 cm, on a donc en 2 minutes sondé environ 4 mètres linéaires de la surface. Ceci permet d'apprécier la rapidité de la méthode qui donne tous les renseignements intéressants, du point de vue corrosion, que l'on peut obtenir par l'exécution d'une coupe micrographique.
Les résultats de la fig. 6 montrent que si Sa2½ peut suffire dans le cas 3, Sa3 ne suffit pas dans les cas 1 et 4 et qu'il n'y a aucune corrélation entre les images de sablage et l'état réel de la surface de l'acier.
Notons que les résultats sont parfaitement reproductibles : on peut recommencer les mesures ou les enregistrements autant de fois que l'on veut à condition de prendre à chaque fois un carton filtre neuf (comme déjà dit).
Nous avons dit que ce procédé a été mis au point à l'occasion de la vérification d'une corrosion anormale d'une tôle (n° 5 du tableau fig. 6). Cette corrosion, due à la décarburation, ne se présentait que sur une face de la tôle et localement, sur cette face, on obtenait 180 mV. La décarburation superficielle en forme de cigare qui intéressait 150 µ d'épaisseur existait sur la seule face incriminée. Notons que les essais avaient été effectués sur l'acier ayant déjà subi 5 sablages successifs Sa3.
Quelle est la marche à suivre pour vérifier le décalaminage d'une tôle ?
Si l'on décalamine au chalumeau ou par sablage manuel, on peut employer l'essai d'évaporation au W.S. qui a des chances de conduire à une évaporation hétérogène. Il suffit de recommencer jusqu'à obtention d'une évaporation homogène. L'on sera alors en présence d'une tôle certainement totalement décalaminée, mais qui pourra être décarburée superficiellement - ce que l'on ne saura qu'en mettant en oeuvre le procédé de mesures de topographie électrochimique. Il est intéressant de connaître ce point car pour éviter la corrosion des zones décarburées en immersion complète il faut avoir recours à une protection cathodique, comme nous l'avons déjà dit.
Dans le cas de grenaillage automatique, il est plus simple de recourir à ce dernier procédé qui nous donne une physionomie exacte de l'état de la tôle en quelques minutes.
Si l'on est en présence de calamine, totale ou partielle, on réduit la vitesse de passage de la tôle de la grenailleuse jusqu'à obtention en une seule passe d'une surface parfaitement décalaminée. Il suffit donc de faire l'essai sur les premières tôles jusqu'à ce que l'on obtienne la vitesse de passage sur la machine la plus rapide donnant le décalaminage complet. Naturellement, les tôles qui ont servi aux essais de mise au point sont grenaillées de nouveau.
Qu'avons-nous constaté ? Sur les nombreux essais que nous avons effectués il y a en moyenne 20 % de tôles qui correspondent à Sa3 mais ne sont pas complètement décalaminées (ex. 1) mais souvent avec des d.d.p. maximales de l'ordre de 120 mV. Cependant, l'on peut avec un sablage Sa2½ obtenir un décalaminage total (ex. 3). Le même aspect de tôle (Sa2½) donne des résultats différents pour une même coulée et une même épaisseur de tôle selon le traitement (recuit ou non) : ex. 2 et 3.
Nous pensons apporter une contribution intéressante à ce problème essentiel de la vérification de la préparation de surface.Les résultats d'exploitation des carènes et des ouvrages immergés pourront donner lieu à des déboires,qui ne seront pas à attribuer à la conception,la fabrication ou l'application du produit,mais à une appréciation incorrecte de la préparation de surface.

Nous adressons nos remerciements à MM.Parsis,d'Hayer,Bouden,Souské & Bonfante.

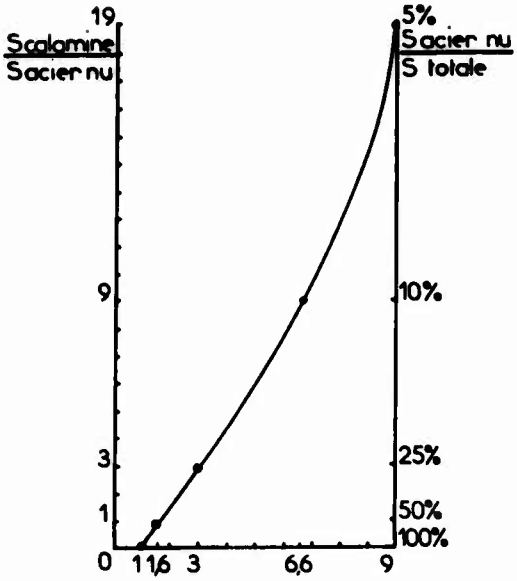
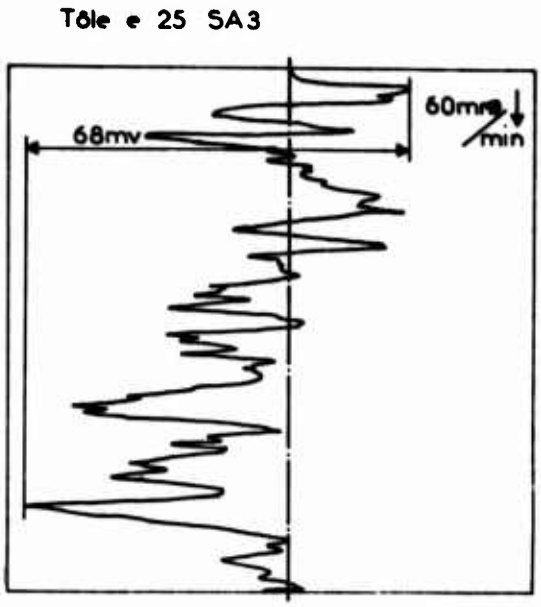


FIG.1



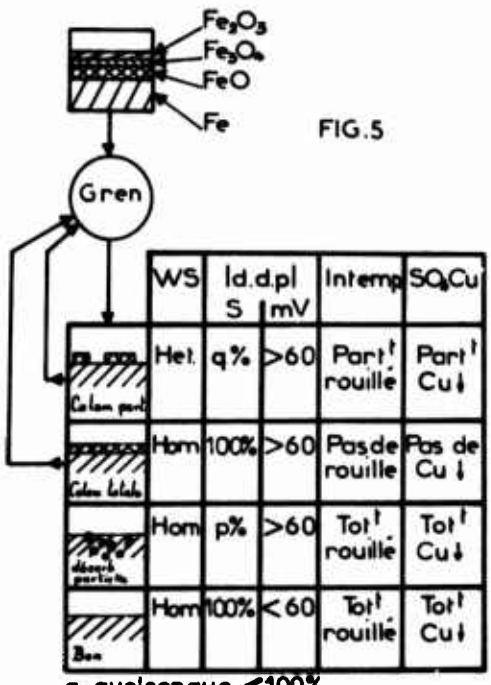


FIG.5

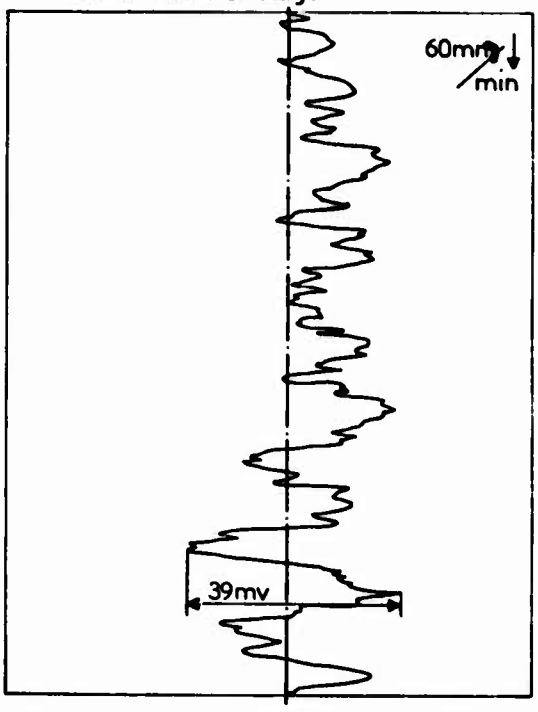


FIG.4



FIG.2

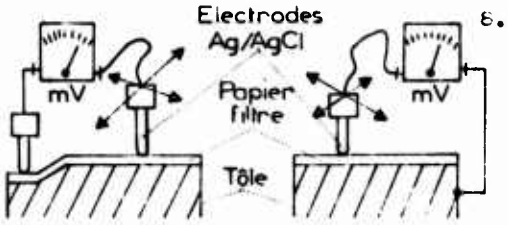


FIG 3

	épaisseur tôle mm	SA1½	SA2	SA2½	SA3	Sablage Complem
1	25**				68mV	39mV
2	12***	95mV		91mV		50mV
3	12****	117mV		60mV		
4	25*		60mV		100mV	45mV
5	12*****				180mV	180mV

x les 2 electrodes sur la surface de la tôle xx fig4 xxx recuit industriel xxxx etat brut xxxxx décarburation locale après 5 sablages SA3 successifs

FIG.6

Références

1. R. Collongues - Thèse 1954 Pub.Sci.et Techniques du Ministère de l'Air Paris 1957
2. J. Menenc et C. Vagnard - Corrosion Science 1969 Vol.9 p.857-868
3. Philippe Delbourg - Congrès 1970 de l'Association Technique du Gaz de France (A.T.G.)
4. - Editorial. Travaux de peintures Vol.14 n° 11 nov. 1959
5. R. Bouské - La galvanisation à chaud -Dunod-1963-p.17
6. R.W.Wilson et J.J.Zonneveld - North east coast Institution of Engineers and Ship builders 16 mars 1962
7. J.C. Moree - Protecting Steel with zinc dust paints. Zinc Development Association p.30 fig.7
8. Paul Ffield - Communication du 10 nov.1950 à The Society of Naval Architects and Marine Engineers à New York
9. J.C. Rowlands - Journal of Iron and Steel Institute déc. 1961
10. C.H. Romer - Second Report on the corrosion committee. Iron and Steel Institute 1934 p.256

Discussion

Question: Do you put anything in the denatured alcohol to increase its conductivity at all?

Dechaux: Non, avec l'alcool pur vous n'obtenez rien, vous n'avez pas de conductibilité. J'avais essayé beaucoup de liquides et j'en suis arrivé à l'alcool dénaturé, c'est une chance d'avoir réussi il y a 10 ans et je vous fais profiter de cette trouvaille.

Question: Do you have any test data which show the performance of, let's say, a primer is over the three different surfaces and how significant is this difference in primer performance?

Dechaux: Je vais vous montrer une figure extraite de la revue "Zone Development Association" qui indique la formation de rouille autour d'une écaille de laminage restant sur l'acier. C'est pour cela qu'il faut que l'acier soit complètement débarrassé de calamine, je vous ai épargné, étant donné que le temps est limité, l'examen des études très intéressantes qui avaient été faites par M. Paul FIELD, montrant que dans l'eau de mer la corrosion est à peu près proportionnelle à la quantité d'écailles de laminage sur l'acier.

Question: Did you use this method automatically or was it automated?

Dechaux: Cette méthode n'a jamais été automatisée parce que ce n'est pas nécessaire. Mais on peut très bien imaginer un petit moteur, quelque chose qui glisse, la tôle qui passe, c'est facile. On peut très bien mettre un dispositif pour automatiser et pour avoir une pression plus constante : c'est inutile. La méthode a été appliquée dans le midi de la France, à Dunkerque, au Havre, à côté de Nantes, par des hommes différents et par des appareils enregistreurs différents et on a toujours trouvé les mêmes résultats. Depuis 10 ans des milliers d'essais ont été faits. Je n'ai pas fait les essais exprès pour ce Congrès, j'ai voulu faire constater une expérience de 10 ans.

Question: Do you take one sample of every plate or just samples at random?

Dechaux: Non, on ne fait pas un prélèvement de chaque tôle, on met le papier filtre sur la tôle à examiner. L'intérêt de la méthode est de mettre le carton sur la tôle. On applique le procédé en général, les tôles viennent d'une gaine coulée, c'est-à-dire que les oxydes qui sont en proportion différentes sont toujours à peu près les mêmes. Sur la première tôle qui passe on fait la mesure : on trouve 80, on réduit la vitesse de passage de la tôle et on vérifie que sur la 2ème tôle on est dans la limite de 60, et on peut faire après cà une vérification à chaque changement de coulée, c'est l'avantage du procédé. Une fois que vous avez réglé votre machine pour une coulée déterminée et pour une épaisseur déterminée, elle est réglée définitivement.

Protection of Steel Piles in a Natural Seawater Environment - Part I

M. Romanoff,* W. F. Gerhold, W. J. Schwerdtfeger, W. P. Iverson
B. T. Sanderson, and E. Escalante

National Bureau of Standards
Washington, D. C. 20234

L. L. Watkins

U.S. Army Coastal Engineering Research Center
Washington, D. C. 20016

R. L. Alumbaugh
U.S. Naval Civil Engineering Laboratory
Port Hueneme, California

In a joint research effort between the National Bureau of Standards, the U.S. Army Corps of Engineers, and the U.S. Naval Civil Engineering Laboratory, the corrosion behavior of protected carbon and low alloy steel piling in seawater is being investigated. Nine-three "H" and pipe pile specimens, 35 feet long, were jetted into the Atlantic Ocean floor off the coast of Dam Neck, Virginia. The results of this study, which will take about 15 years to complete, will demonstrate which of the systems tested are best for protecting steel piles in seawater. Many types of protective methods are included in the investigation consisting of coating systems (coal-tar epoxy, hot-dip zinc, flamesprayed aluminum and zinc, zinc-rich paints, epoxies, etc.), cathodic protection by zinc and aluminum sacrificial anodes, and combinations of coatings and cathodic protection. At one-year intervals, polarization measurements and visual observations are made on the piles to determine the effectiveness of the coating systems and to measure the rates of corrosion. Potentials of cathodically protected piles are also measured. These data will be correlated with physical determinations made on the piles when they are removed from exposure. The first removal of one set of piles (31 in number) is scheduled for October, 1972, after exposure for approximately 5 years.

Key Words: Cathodic protection; coating index; corrosion rates; marine environment; polarization techniques; protective coatings; steel piling.

---

1. Introduction

Steel piling, in the form of pipe and tubing has been used since the latter part of the 19th Century and steel H-piling for buildings, bridges, and other foundations came into use during the early 1900's. While much of the tonnage comprises land installations, a very important proportion is in shoreline environments. A considerable amount of money has been

---

*Deceased

[1]Figures in parentheses indicate the literature references at the end of this paper.

spent to maintain the integrity of coastal structures while allowing for corrosion. Design engineers have in the past and still have a dire need for more accurate information on the rates of corrosion of steel piling in the wide variety of marine environments encountered. More long-term information is also needed on methods of protecting steel piling from corrosion.

Previous reports on the corrosion of steel piling in seawater include those by Ayers and Stopes,[1] Brouillette and Hanna,[2] Ryaner,[3] and Ross.[4] The literature has been recently reviewed by Watkins.[5] Reports on the use of protective coatings for steel piles include those by Alumbaugh,[6,7] Alumbaugh and Brouillette,[8,9,10] and Alumbaugh and Curry.[11] A collection of papers by Schwerdtfeger and Romanoff on the Corrosion of steel pilings in soils has recently been published.[12,13]

In view of their common interests and need for better corrosion data and means for protecting steel piling in the marine environment, a joint cooperative field test project involving the National Bureau of Standards (NBS), the U.S. Army Coastal Engineering Research Center (CERC), and the U.S. Naval Civil Engineering Laboratory (NCEL) was established in 1967. Electrochemical measurements for determining potentials, corrosion rates, and coating deterioration indices are carried out by NBS with assistance of CERC, test site environmental studies by CERC, and visual coating evaluation by NBS, CERC, and NCEL. Annual inspections involving these studies have been carried out since the piles were installed in June, 1967, and will be carried out for 10 more years. A preliminary report on this project appeared in 1971.[14] The objective of this paper is to describe the results, primarily electrochemical, obtained for the past 5 years. The complete results of the 5th year await final observations of a set of pulled piles. They will be reported when the observations and measurements on the removed piles have been completed.

2. Experimental

a. Scope

The field test consisted of observing and analyzing the condition of steel H-piles and cylindrical piles installed at a shallow-water site exposed to ocean waves. Some piles were installed without protection, others with cathodic protection, others with protective coatings, and still others with both protective coatings and cathodic protection. The piles were installed in sets of three; one pile from each set will be pulled every 5 years (15-year test duration). Inspections are made annually while a more detailed examination is made of the piles removed at the 5-year intervals.

b. Test site

The pile test site is located in the Atlantic Ocean off-shore from Dam Neck, Virginia (Figure 1). The shore fronting the site is a relatively long straight beach. The distance from the mean low water shoreline to the center of the site is approximately 125 feet (37.5 m), but varies according to the seasonal accretion and erosion of the shore. The water depth prior to the installation of the piles was approximately 4 feet (1.2 m). The tide ranges of the test site should be nearly equal to those at Virginia Beach, which has a mean tide range of 3.4 feet (1.0 m) and a spring tide range of 4.1 feet (1.2 m). There are many factors involved in the selection of a suitable site for a marine pile corrosion test. Some of the factors which influenced the use of the Dam Neck site are: (a) It can provide all of the primary marine corrosion zones, i.e., buried, sand, abraded, submerged, tidal (very little data is available on corrosion of steel exposed to ocean surf), splash and atmospheric zones; (b) The location is about midway along the United States Atlantic coast and the mean water temperature is approximately midway of the maximum and minimum mean seawater temperatures which have been recorded near the United States Atlantic coast; (c) Sheltered water for floating equipment used for installation and extraction of piles is reasonably near in the event of storm warnings; (d) The long-term water depth should be relatively stable; (e) The test piles should be relatively free from vandalism or abuse by the general public.

Water salinity and temperature data from the nearby U.S. Coast and Geodetic Survey station at Virginia Beach[15] show a mean salinity of 26.8 parts per thousand and a mean water temperature of 57.9°F (14.4C). The salinity has ranged from 18.2 to 37.5 parts per

thousand, and the temperature has varied from 33.8°F (1.0C) to 82.4°F (28.0C) over the 7 years of record.

Bottom elevation surveys made during annual inspections with transit and rod with the assistance of scuba divers have shown the bottom elevation to vary from -2.5 feet (0.76 m) to -7.0 feet (2.3 m) referenced to mean low water. Since these differences in bottom elevation have been noted at annual inspections, it is likely that the range of bottom elevations would be greater with more frequent measurements. Bottom elevation changes are considered to be due to seasonal bottom profile changes, i.e., "northeaster" storm waves tend to erode the bottom during the winter, and long period swells accrete the bottom during the summer. The bottom profiles are shown in Figure 2.

The piles are subjected to the impacts of breaking waves and splashing water a majority of the time. Occasionally storms may occur which produce wave crests to the top of the piles. Such occurrences, however, are infrequent. The occasional existence of waves at the top of the piles negates the existence of a purely atmospheric zone on the piles.

Borings made near the low water line fronting the site indicate that bottom material at the site consists primarily of fine sand. Relatively thin strata of blue-gray clay and silt, less than 3 feet (0.9 m) in thickness, exist near the surface. The median diameter of sand particles on the bottom as sampled in September, 1967, was 0.15 mm. The sand is easily carried into suspension by the surf and should have a tendency to abrade the pile surfaces.

c. Test piles

The piles were emplaced in three rows parallel to the shoreline giving 31 systems of three piles each (Figure 3). Of these 31 systems, five were bare carbon or low alloy steel having no protection, three were bare carbon or low alloy steel with cathodic protection [either zinc (military spec A-18001G) or aluminum-zinc-mercury alloy (99.9% purity Al+ 0.045% Hg + 0.45% Zn) sacrificial anodes], and 23 were coated with protective coatings, two of which were also cathodically protected (zinc sacrificial anodes). The "H" piles were primarily of mild carbon steel (ASTM A36+66T), 8 inches by 8 inches (20.3 cm by 20.3 cm) by 35 feet (10.7 m) in length, and weighing 48 pounds (21.6 kg) per linear foot (71.6 kg/linear m). The pipe piles of carbon steel (ASTM A252) were 8 in (20.3 cm) diameter, schedule 80 pipe, 35 feet (10.7 m) in length with a cone shaped tip welded to the bottom end to facilitate installation. Stainless steel rods (Type 316 ELC) were welded between the inside flanges on one side of the "H" piles so that one would be 2 feet (0.6 m) above and one about 2 feet (0.6 m) below mean high water, as contact points for electrical measurements. These may be seen in Figure 6. Stainless steel (Type 316 ELC) rods were butt welded to the surface of the pipe piles at about the same elevation as those on the "H" piles.

d. Protective systems

Some of the protective coating systems included in this series were selected on the basis of screening tests conducted by NCEL, where the coatings had been evaluated on 10-foot (3.0 m) test panels. A number of other coating systems that appeared to have merit for this type of application were selected and included in the investigation. The systems included metallic coatings, nonmetallic coatings, and zinc-rich coatings with topcoat. The metallic coatings included hot-dipped zinc (galvanized, 4 to 5 oz/ft^2), flamesprayed zinc with polyvinylidene chloride and vinyl topcoats, and flamesprayed aluminum with and without vinyl topcoat. The nonmetallic coatings included coal-tar epoxy, aluminum pigmented coal-tar epoxy, phenolic mastic, polyvinylidene chloride and glass-flake-filled polyester. The zinc-rich primers were of two types, organic and zinc inorganic silicate. Top coatings for the zinc inorganic primers included polyamide cured coal-tar epoxy, polyamide cured epoxy, vinyl mastic, and high-build vinyl. The top coating for the organic rich primer was a polyamide cured coal-tar epoxy. Prior to application of the coatings, the piles were sandblasted to near white metal in accordance with the Steel Structure Painting Council Specification SSPC-SP-10-63T. With the exception of the hot-dip galvanized, the flamesprayed metallic, and the glass-flake-filled polyester, the coatings were applied by airless paint spray with brush touchup. The glass flake coating required rolling to orient the glass flakes after the air-spray application. Flamesprayed coatings were applied by the use of a wire-type metalizing gun. A description of the coating systems, the number of coats and coating thicknesses are presented in Table 4 appendix.

The sets of piles are identified by a number, and the piles within a set by a letter (A, B, or C). The A piles (facing the shore) were completely coated except for six 1-inch (2.5 cm) by 6-inch (15.2 cm) bare "windows" located at pertinent intervals on the outer face of one flange, and the exterior face of the pipe piles. The windows were facing the ocean in all cases. The purpose of the "windows" is to determine the capability of the various coatings to resist undercutting by rust at various areas of exposure (partial atmospheric zone, splash zone, tidal zone, water zone, and sand zone). The B piles (center) were completely coated for their full length and the C piles (facing the ocean) were coated on the top 23 feet (6.9 m) with the bottom 12 feet (3.6 m) uncoated (Figure 4). If the corrosion on the area below the mudline is slight, savings can be realized by not coating the buried portion of piles in future structures.

The sacrificial anodes employed in some sets were of zinc and aluminum. The zinc anodes, 4x4x36 inches (10.2x10.2x91.4 cm) each weighed 150 lbs (68.2 kg) and the aluminum anodes, 2 inches (5.1 cm) longer weighed 60 lbs (27.2 kg) each. Two anodes were installed on each pile (Figure 5).

e. Installation of piles

Prior to installation, the piles were positioned on the beach. A rubber-tired crane carried them onto a 3-section floating causeway. A crawler crane with a single-pipe jetting rig then installed the piles off the side of the causeway. The floating causeway was usually repositioned after 3 sets of piles were installed. The piles were jetted through about 19 feet (5.8 m) of bottom material. The anodes of the middle pile (pile B) of each of the 5 cathodically protected series were attached at a lower level on the piles so that they were buried in the bottom sand. This was done to check the effectiveness of the buried anodes vs the anodes in the seawater attached to the A and C piles. The rows of piles were spaced 10 feet (3.0 m) apart with a spacing of 5 feet (1.5 m) between the sets of coated piles and 10 feet (3.0 m) between the sets of the cathodically protected piles. The piles after installation are shown in Figures 6 and 7.

f. Visual inspection above water

Visual observations include an estimate of the percent of intact coating and whether coatings are blistering, undercutting, checking, cracking, or peeling in accordance with ASTM Standard Methods for Evaluating Paint Coatings, when possible. Because of the heavy fouling attachment in the tidal and immersed zones of the piles, the visual observations and ratings are of necessity restricted to the upper tidal splash zones. These data are to be correlated with physical determinations and visual observations to be made on the first set of piles (31 in number) that are scheduled to be removed in the fall of 1972 after approximately 5 years exposure.

Photographs are taken of each pile set during the annual inspections using an underwater camera. Aluminum ladders with protective padding were constructed to facilitate close-up inspection and photography and electrical connections.

g. Electrochemical measurements

Electrical connections to the piles were made using two 3-wire electrical cables supported by a wire rope connected to the top of a pile on one end and the top of a beach-based truck on the other end. Electrical contact to the stainless steel rods on the piles was made by a vise-clamp connected to the cable wire. The vise clamps were coated with silicone rubber.

Potential measurements of the cathodically protected piles were made with a potentiometer using both a Ag-AgCl half-cell and a Cu-$CuSO_4$ half-cell. The Cu-$CuSO_4$ half-cell was positioned in the damp sand on the beach and covered to prevent light and heat effects. The Cu-$CuSO_4$ half-cell was the most convenient to use. The Ag-AgCl half-cell, submerged in the water, served as a check electrode.

The circuit used for obtaining the polarization curves is similar to that reported by Schwerdtfeger[12] except the Holler bridge circuit was omitted as the electrolytic IR drop was negligible. One or two 12-volt storage batteries supplied the polarizing current. A

bare pile was used as the auxiliary electrode in determining the coating indices. For corrosion rate measurements simultaneous measurements were often made on two piles, one being the cathode and the other the anode, the order then being reversed. Two wires in each cable were used to supply the current and the third wire for measuring potential, thus eliminating any IR drop as a result of the polarizing current in the wire.

Coating indices on piles A and B with nonmetallic coating were obtained by measuring the current required to polarize the pile to -0.85 V after a 5-minute interval using the C pile as an auxiliary electrode. The ratio $\Delta V/\Delta I$ was designated as the coating index and used as a measure of the coating effectiveness. This ratio is used as a measure of the coating resistance relative to uncoated steel and is similar to the method described by Parker.[16] Piles with metallic coatings were generally polarized to cathodic (active) overpotentials of 150 mV (approximately equal to overpotentials on piles with nonmetallic coatings). For these measurements on the A and B piles of each series, pile C again served as the auxiliary electrode.

Corrosion rate measurements on all the coated piles as well as the piles whose corrosion rate was determined using the "polarization break" were made using the linear polarization method based on the Stern-Geary equation:[17]

$$\frac{\Delta E}{\Delta I} = \frac{1}{2.3\, I_{corr}}\left(\frac{B_a \cdot B_c}{B_a + B_c}\right)$$

In this equation ΔE is the overvoltage of the corroding electrode produced by a polarizing current ΔI; B_a and B_c are the slopes of the anodic and cathodic polarization curves, respectively, in the Tafel region, and I_{corr} is the corrosion current. The constants B_a and B_c were both assumed to be equal to 0.1 in this equation. According to Stern and Weisert[18] the error when this assumption is made can be about 20%. This assumption results in the following equation:

$$I_{corr(mA)} = \frac{21.7\Delta I(mA)}{\Delta E(mV)}$$

The "polarization break" method was used to determine the corrosion rate on many of the uncoated as well as some of the coated piles. This technique originally proposed by Schwerdtfeger and McDorman[19] is based on the observation that anodic and cathodic polarization curves consist of straight line segments having different slopes. The current at which the "change" in slope (break) occurs is designated I_p for the cathodic and I_q for the anodic curve. The corrosion current I_c can be calculated from the following relationship, which was derived by Pearson[20] and confirmed by Holler[21]:

$$I_c = \frac{I_p I_q}{I_p + I_q}$$

The cathodic and anodic polarization curves were obtained galvanostatically using either one- or two-minute intervals between each increase in the current increment. The equal current increments used were based on the corrosion current obtained by the linear polarization method (viz. the applied current necessary to change the potential from 2 to 10 mV). The data were plotted on linear coordinate paper simultaneously with the acquisition of current-potential values to insure that the "break" was obtained. Polarization curves were usually run simultaneously on the "cathodic" pile and the "anodic" pile.

On the cathodically protected piles, only the cathodic curves were obtained. The current value at the "break" in this curve has been determined to be approximately the cathodic protection current supplied by the sacrificial anode.[22]

3. Results

a. Visual observations

Due to the heavy fouling in the tidal and immersed zones of the piles, the visual observations and ratings were of necessity restricted to the upper tidal and splash zones. A full visual coating evaluation of the piles including these zones will be made and

published after one row of the piling has been removed for the 5-year inspection.

b. Electrochemical measurements

Potential and galvanic currents on the cathodically protected piles are presented in Table 1. Although the potentials of the steel piles vs a Ag-AgCl half-cell and a Cu-$CuSO_4$ half-cell were both measured, only the potentials vs the Cu-$CuSO_4$ half-cell are indicated. In general the potentials of the piles having anodes in the sand were less negative (more noble) than those of the piles having their anodes in the water. Over the years the potentials of piles with anodes in the sand had a tendency to rise to more protective values. The galvanic current densities from the anodes buried in the sand were generally lower than the current densities from the anodes in the seawater.

The coating indices and the corrosion currents of the coated piles are presented in Table 2. As would be expected, the piles having lower corrosion currents have higher coating indices. The indices after 5 years range from about 0.05 for the uncoated piles to 1.38 for the coal-tar epoxy coated pipe pile. The polyvinylidene chloride over flame-sprayed zinc, the phenolic mastic and a coal-tar epoxy over a zinc inorganic silicate coating have relatively high coating indices while the lowest index is found for the polyvinylidene chloride coating over bare steel.

An indication of the general deterioration of all the coatings over the years is shown in Figure 8. All of the coating indices including those of the controls (uncoated bare piles) are plotted for each year. The average (arithmetical mean) of the indices for the coated piles is indicated by a horizontal dash connected by the curve. A coating effectiveness scale is also indicated. Zero on the scale is based on the average coating index for the bare piles. One hundred on the scale is based on the best coating index obtained, that for pile 7B in 1967 (Table 2). The value of coating effectiveness between 0 and 100 is based on the relation between the corrosion currents and the coating indices for the bare and coated piles A and B. The coating effectiveness is based on the best curve (not indicated) of the relationship. Thus a coating effectiveness of 80% means that the corrosion current measured for the coated pile represents only 20% of the possible corrosion current for the bare piles (average), that is, 60 mA out of a possible 300 mA.

The corrosion rates of the steel piles calculated from the "polarization break" method are shown in Table 3. With the exception of the galvanized steel piles, the corrosion rates of the steel piles remained fairly constant during the years of measurement. Corrosion rates on the galvanized piles continue to decrease from year to year, being about 1/20 the initial rate after 4 years. As might be expected, the corrosion rates for the piles coated, except for the bottom 12 feet, are lower than for the bare piles. The corrosion rate in the water zone was calculated when the length of the piling exposed to sand and tidal water was 28 feet (8.5 m), 21 feet (6.4 m) of the piling being buried in the sand (7 feet or 1/4 of the piling being exposed to the water). Thus in the following relationship:

$$3 = \frac{1.4+1.4+1.4+x}{4} \text{ or } x = 7.8 \text{ mils per year (0.2 mm per year).}$$

x is the corrosion rate in the water zone, 3.0 mpy (0.08 mm per year) is the corrosion rate in sand + water (see pile #1) and 1.4 mpy (0.035 mm per year) is the corrosion rate in the sand only (based on early exposure) (see piles 17C and 27C). According to Hunter and Horton[23] 5 mpy (0.12 mm per year) is the worldwide average corrosion rate in seawater.

4. Discussion

From the results of the electrochemical measurements which have been obtained so far on the coated piles, it appears as if some coating systems are performing much better than others. The value of the polarization tests enables early and objective data to be obtained on the coating systems before the piles are removed. Although this test evaluates the coating systems in the water and sand, visual observation, made so far on the coatings above the water, appeared to agree quite well with the electrochemical results. A full correlation can only be made when the piles are removed and examined quite carefully. As the area below and in the splash zones is heavily encrusted with fouling, some of the coating may be removed when the fouling is scrapped off. However, the protective nature of the

coating can still be determined.

Of interest is the observation that whereas the overall corrosion on most of the coated piles tends to increase, the corrosion rate of the galvanized piles tends to decrease during 4 years. Corrosion rates measured the 5th year indicate that this tendency has ceased, the rate once again approaching that of uncoated steel. This observation has also been reported for galvanized pipes in an underground environment[24] and is believed to be due to the increased corrosion resistance of a zinc-iron alloy, lasting underground 13 years or perhaps longer.

The galvanic current data on the cathodically protected piles thus far obtained appear to indicate that the most efficient location of the anodes may be in the sand rather than in the water.

Electrochemical measurements coupled with visual observations thus may afford an invaluable means of evaluating protection systems on pilings long before they are removed for final inspection. As the protection systems are subjected to a natural environment the value of such observations is of considerable significance. The environment in this test represents a temperate-water site. Eventually a warm-water site and a cold-water site will be used for testing the protective systems. CERC already is evaluating protective systems in a warm-water site using the technique described in this paper.

Acknowledgement

NBS participation in this test was sponsored by the American Iron and Steel Institute; CERC was funded by the U.S. Army Corps of Engineers Engineering Studies Program; and NCEL was funded by the Naval Facilities Engineering Command. Appreciation is expressed to the U.S. Navy Amphibious Construction Battalion No. 2, Little Creek, Virginia, for installation of the test piles; to the U.S. Navy Fleet Anti-Air Warfare Training Center for access and protection of the site and other assistance; and to the Commander U.S. Atlantic Fleet for making teams of divers from Explosive Ordinance Demolition and Underwater Demolition Units available to assist in making electrical connections to the piles and bottom depth measurements. Appreciation is also expressed to the coating manufacturers who provided technical and material assistance to this project. Surface preparation and coating operations were carried out primarily by industrial corporations. The assistance of James L. Fink and John T. Hill (Corrosion Section, NBS) and Michael Dickey, John Jones, Andre Szuwalski, and particular scuba divers (CERC) in the inspections is greatly appreciated.

The views and opinions expressed in this paper are those of the authors and are not to be construed as an official Department of the Army position unless so designated by other authorized documents.

References

1. J. R. AYERS and R. C. STOKES, *J. Waterways, Harbors Div. ASCE*, 87, Proc. Paper 2886, 95 (1961).

2. C. V. BROUILLETTE and A. E. HANNA, *U.S. Naval Civil Eng. Lab. Tech. Rept.* R-467 (1966).

3. A. C. RAYNER, *U.S. Army Corps of Eng. Beach Erosion Bd. Tech. Memo* No. 10 (1948).

4. C. W. ROSS, *U.S. Army Corps of Eng. Beach Erosion Bd. Tech. Memo* No. 10 (1948).

5. L. L. WATKINS, *U. S. Army Coastal Eng. Res. Center Tech. Memo* No. 27, Washington, D.C. (1969).

6. R. L. ALUMBAUGH, *U.S. Naval Civil Eng. Lab. Tech. Rept.* R-194, Port Hueneme, California (1962).

7. R. L. ALUMBAUGH, *Mat. Protect.* p. 34, July (1964).

8. R. L. ALUMBAUGH and C. V. BROUILLETTE, *U.S. Naval Civil Eng. Lab. Tech. Rept.* R-490, Port Hueneme, California (1966).

9. C. V. BROUILLETTE and R. L. ALUMBAUGH, *U.S. Naval Civil Eng. Lab. Tech. Rept.* R-397, Port Hueneme, California (1965).

10. R. L. ALUMBAUGH and C. V. BROUILLETTE, *Mat. Protect.* 6, 37 (1967).

11. R. L. ALUMBAUGH and A. F. CURRY, *U.S. Naval Civil Eng. Lab. Tech. Rept.* R-711, Port Hueneme, California (1971).

12. W. J. SCHWERDTFEGER and M. ROMANOFF, *U.S. Nat. Bur. Stand. Monograph* 127, 54 p. (1972).

13. W. J. SCHWERDTFEGER and M. ROMANOFF, *U.S. Nat. Bur. Stand. Monograph* 128, 12 p. (1972).

14. L. L. WATKINS, *J. Waterways, Harbors & Coastal Eng. Div., ASCE*, 97, Proc. Paper 8292, 549 (1971).

15. *U.S. Dept. of Commerce ESSA, Coast and Geodetic Surv. Pub.* 31-1 (1968).

16. M. E. PARKER, *Mat. Protect.* 6, 25, Aug. (1967).

17. M. STERN and A. L. GEARY, *J. Electrochem. Soc.* 104 (1), 56 (1957).

18. M. STERN and E. D. WEISERT, *Proc. ASTM* 59, 1280 (1959).

19. W. J. SCHWERDTFEGER and O. N. McDORMAN, *J. Electrochem. Soc.* 99, 407 (1952).

20. J. M. PEARSON, *Trans. Electrochem. Soc.* 81, 485 (1942).

21. H. D. Holler, *J. Electrochem. Soc.* 97, 277 (1950).

22. W. J. SCHWERDTFEGER, *ASTM Mat. Res. and Stand.* 10, No. 3, 22 (1970).

23. A. D. HUNTER and C. H. HORTON, *Underwater Eng.* Nov. 15 (1960).

24. M. ROMANOFF, *NBS Circular* 579 (1957).

Table 1 - Potentials and Galvanic Currents on Cathodically Protected Steel Piles Over a Period of 5 Years of Exposure (Offshore) in The Atlantic Ocean at Dam Neck, Virginia.

Pile	Pile[1] Description	Anode[2] System	Potential of Pile, V-Ref-Cu-$CuSO_4$ Positioned Remote - On The Beach						Galvanic Current Density, mA/ft^2-Based on Break in the Cathodic[5] Polarization Curve			
			1967[4] Intermediate Tide	1968 Low Tide	1969 High Tide	1970 High Tide	1971 High Tide	1972 High Tide	Tide H, High; L, Low; I, Intermediate 1969	1970	1971	1972
2A	Bare Steel	Zn, in water	-1.04	-1.03	-1.08	-1.07	-1.08	-1.04	6.4(L)	7.7(I)	5.7(I)	5.4(I)
2B	" "	Zn, in sand	0.700	0.725	0.910	0.832	0.979	0.93	6.9(H)	4.1(L)	3.9(L)	6.0(I)
2C	" "	Zn, in water	1.05	1.05	1.05	1.04	1.07	1.06			5.6(I)	4.0(I)
3A	Bare Steel	Al, in water	1.04	1.03	1.04	1.04	1.05	1.03		3.3(L)	4.0(L)	7.8(L)
3B	" "	Al, in sand	0.710	0.730	0.920	0.823	0.943	0.87			6.6(H)	8.3(L)
3C	" "	Al, in water	1.04	1.04	1.04	1.03	1.05	1.04	8.1(I)			5.4(L)
5A	[3] Coated Steel	Zn, in water	1.10	1.07	1.12	1.09	1.05	1.07			4.6(H)	3.5(L)
5B	" "	Zn, in sand	1.09	1.07	1.10	1.08	1.03	1.09	1.9(I)	1.4(H)	1.4(H)	2.7(L)
5C	" "	Zn, in water	1.09	1.08	1.11	1.09	1.04	1.00	4.9(L)	4.2(H)		5.3(L)
11A	Galv. Steel	Zn, in water	1.08	1.06	1.08	1.08	1.02	1.03		5.6(I)	4.4(H)	6.3(I)
11B	Hot-Dipped	Zn, in sand	1.05	0.990	1.01	0.977	0.980	0.98				1.8(I)
11C	3oz Coat	Zn, in water	1.08	1.06	1.08	1.07	1.02	1.06	5.7(L)		6.7(L)	6.1(I)
24A	Bare	Zn, in water	1.07	1.05	1.07	1.07	1.01	1.03		5.9(H)	7.1(I)	4.7(L)
24B	Low Alloy	Zn, in sand	0.860	0.925	1.00	0.919	0.940	1.00		3.5(I)		4.0(L)
24C	Steel	Zn, in water	1.05	1.05	1.07	1.07	1.01	1.05	5.1(I)			5.6(L)

[1] All piles, except system 24, are mild carbon steel, all are H-piles, 8in.x8in.x48 lbs/ft.-35ft. long. In all cases, the sand line was from 19 to 21 ft. measured from the bottom of the pile, in general the row of C piles having the more sand. The length of a pile exposed to sand and water varied between 24 ft. and 28 ft., depending on the normal tide.

[2] Zinc anodes are 4in.x4in.x36in. weighing 150 lbs. Aluminum anodes are 4in.x4in.x38in. weighing 60 lbs. Each pile is protected by two anodes permanently mounted on opposite flanges at the same elevation. On the A and C piles, the anodes are mounted in the water zone between the sand line and the mean low water line. On the B piles, the anodes are mounted in the sand zone, the tops of the anodes being about 6 ft. below the sand line.

[3] Piles are coated with coal tar epoxy. Pile A has 5 windows (bare area, 1in.x6in.). Pile B was completely coated, and pile C was completely coated except for the lower 12 ft. in the mud zone.

[4] Initial measurements - Made in 1967, 4 months after installation.

[5] Galvanic current includes the local action current on the anodes which on the bare piling systems might account for about 10 percent.

Table 2 - Performance of Coated Piles, Based on Electrical Measurements, Over a Period of 5 Years of Exposure Offshore in The Atlantic Ocean at Bam Neck, Virginia.

Pile No.	Description Pile and Coating [a]	Tide [b] 1967	1968	1969	1970	1971	1972	Corrosion Current, [c] mA 1967	1968	1969	1970	1971	1972	Coating Index, [c] V/I (mV) 1967	1968	1969	1970	1971	1972
23A	Low Alloy	I	H	-	H	L	H	-	-		360	186	362	0.11	0.061	-	-	0.11	0.07
23B	Steel			-	-	L	H	-	-		-	300	354	-	-	-	-	0.08	0.05
4A	Coal tar epoxy	H	H	I	H	I	H	-	-	82	78	62	91	0.1	1.1	0.5	0.37	0.37	0.27
4B	" " "	H	H	I	H	I	H	-	-	65	76	75	113	7.3	0.97	0.45	0.44	0.39	0.27
3A	Coal tar epoxy and Al oxide armor	H	H	I	I	I	I	-	-	76	65	81	97	12.3	1.0	0.65	0.43	0.34	0.29
7B	Coal tar epoxy and Al oxide armor	H	H	I	I	I	I	-	-	65	61	71	104	43.0	1.4	0.82	0.47	0.36	0.27
8A	Al-pigmented epoxy tar	H	H	I	L	I	I	-	-	56	52	68	91	3.0	1.1	0.58	0.56	0.41	0.34
8B	Al-pigmented epoxy tar	H	H	I	L	I	I	-	-	49	48	63	78	21.6	1.5	0.64	0.61	0.95	0.34
9A	Al-pigmented coal tar epoxy	H	I	I	L	H	I	-	-	72	76	80	105	6.8	0.60	0.36	0.30	0.30	0.22
9B	Al-pigmented coal tar epoxy	H	H	I	L	H	I	-	-	76	105	176	135	5.0	0.92	0.32	0.27	0.26	0.21
6A	Coal tar epoxy	H	H	I	L	I	I	-	-	96	80	59	130	5.0	0.63	0.34	0.30	0.25	0.19
6B	" " "	H	H	I	L	I	I	-	-	90	83	68	265	9.4	0.75	0.38	0.29	0.25	0.20
12A	Polyvinylidene	I	H	I	H	I	I	-	-	130	304	100	182	0.56	0.22	0.20	0.13	0.10	0.12
12B	Chloride (White)	I	H	I	H	I	I	-	-	101	107	170	270	0.37	0.10	0.15	0.11	0.12	0.09
13A	Al flame spray (clear vinyl topcoat)	I	H	I	H	I	I	-	-	34	109	49	89	0.65	0.55	0.60	0.41	0.37	0.23
13B	Al flame spray (clear vinyl topcoat)	I	H	I	H	I	I	-	-	28	63	64	98	1.1	0.70	0.82	0.63	0.48	0.40
14A	Al flame spray wire	I	I	I	H	L	H	-	-	54	90	54	109	1.0	0.49	0.46	0.40	0.36	0.25
14B	" " " "	I	I	I	H	L	H	-	-	54	39	56	102	1.0	0.53	0.48	0.44	0.33	0.24
15A	Zn flame spray Polyvinylidene	I	I	H	I	L	H	-	-	43	22	30	33	0.96	0.37	0.53	0.71	0.99	0.75
15B	Chloride (White)	I	I	H	I	L	H	-	-	37	30	22	21	1.3	0.43	0.60	0.60	0.93	0.85
16A	Zn flame spray (vinyl topcoat-replaced)	I	I	H	I	L	H	-	-	46	106	48	176	0.48	0.30	0.49	0.30	0.25	0.15
16B	Zn flame spray (vinyl topcoat-replaced)	I	I	H	I	L	H	-	-	28	124	87	302	0.50	0.36	0.80	0.35	0.23	0.13
17A	Phenolic mastic (gray finish)	I	I	H	L	I	H	-	-	36	37	24	35	7.0	1.9	1.1	0.81	0.68	0.64
17B	Phenolic mastic (gray finish)	I	I	H	L	I	H	-	-	14	15	18	47	30.0	5.5	2.1	1.6	1.14	0.76
1A	Bare carbon steel	I	I	-	L	I	H	-	-	-	270	190	325	0.07	0.067	-	0.064	0.064	0.07
1B	" " "	-	-	H	L	I	H	-	-	367	293	380	470	-	-	0.072	0.075	0.069	0.06
10A	Coal Tar Epoxy over Organic Zn Rich	H	I	H	H	I	H	-	-	39	35	28	90	5.9	2.2	0.88	0.69	0.67	0.62
10B		H	I	H	H	I	H	-	-	33	30	28	37	30.0	3.6	1.2	1.0	0.85	0.76
19A	Vinyl over Inorganic Zn rich	H	I	I	H	I	I	-	-	82	97	68	121	1.7	0.58	0.38	0.25	0.33	0.23
19B	Vinyl over Inorganic Zn rich	H	I	I	H	I	I	-	-	76	80	68	87	3.5	0.53	0.44	0.33	0.35	0.26
20A	Epoxy polyamide over inorganic Zn rich	L	I	I	H	I	I	-	-	50	43	31	60	5.1	2.0	0.70	0.59	0.58	0.43
20B	Epoxy polyamide over inorganic Zn rich	L	I	I	H	I	L	-	-	37	33	35	64	7.9	3.7	1.1	0.94	0.58	0.42
21A	Epoxy tar over Inorganic Zn rich	L	L	I	I	I	L	-	-	39	37	22	48	4.6	1.9	1.1	0.75	0.76	0.73
21B	Epoxy tar over Inorganic Zn rich	L	L	I	I	I	L	-	-	18	16	18	38	15.7	6.7	2.3	1.7	1.25	1.00
22A	Vinyl mastic over inorganic Zn rich	L	I	L	I	L	I	-	-	84	102	37	130	2.4	0.65	0.38	0.24	0.38	0.20
22B	Vinyl mastic over Inorganic Zn rich	L	I	L	I	L	L	-	-	72	87	37	135	3.0	0.60	0.39	0.28	0.39	0.21
25A	Coal tar epoxy Mariner steel	I	I	L	I	L	I	-	-	65	87	24	95	1.7	0.60	0.40	0.28	0.43	0.26
25B	Coal tar epoxy Mariner steel	I	I	L	I	L	I	-	-	60	76	28	83	4.1	0.72	0.49	0.37	0.45	0.46
29A	Polyester glass flake	I	I	I	I	L	I	-	-	51	61	26	48	6.8	1.7	0.64	0.66	0.57	0.50
29B	" " "	I	I	I	I	L	I	-	-	41	33	24	58	12.0	2.6	0.79	0.80	0.67	0.58
5A	Bare carbon steel	-	-	I	L	L	I	-	-	298	278	176	390	-	-	0.073	0.070	0.092	0.06
5B	" " "	-	-	I	I	L	I	-	-	369	455	190	334	-	-	-	0.049	0.077	-
26A	8-inch Bare	-	-	H	I	I	-	-	-	217	-	-	-	-	-	0.082	-	-	-
26B	Carbon Steel Pipe	-	-	-	I	I	I	-	-	-	390	201	325	-	-	-	0.05	0.073	0.06
27A	Coal tar epoxy (inner 8 in. pipe)	-	I	I	H	I	H	-	-	24	20	16	34	-	1.8	1.2	1.0	0.94	0.91
27B	Coal tar epoxy (outer 8 in. pipe)	-	I	I	H	I	H	-	-	15	20	13	24	-	2.6	1.9	1.5	1.38	1.33
28A	Coal tar epoxy Al oxide armor, 8 in. pipe	-	H	I	H	H	H	-	-	43	26	18	33	-	1.2	0.91	0.86	0.85	0.79
28B	Coal tar epoxy Al oxide armor, 8 in. pipe	-	H	I	H	H	H	-	-	33	22	20	32	-	2.1	1.1	0.92	0.81	0.86

[b] L, low tide; H, high tide; I, intermediate between tide changes. Variation of water level between low and high tides was between 3 and 6 ft.

[c] Instantaneous corrosion current $= \frac{\Delta\theta}{.0023} = \frac{\Delta\theta}{\theta_a - \theta_c} = \frac{IR}{V}$, assuming $\theta_a - \theta_c = 0.1$ volt and 25°C to 10mV.

[d] Based on cathodic polarization from the normal corrosion potential for a period of 5 minutes to -0.95 volt (Ref. $Cu-CuSO_4$), except for piling systems 13, 14, 15 and 16. Systems 13, 14, 15 and 16, having corrosion potentials affected by the metallic coatings, were polarized by about 150mV regardless of the corrosion potentials.

[a] All piles are H piles (8in.x8in.x35ft. long), except for systems 26, 27, and 28 which are pipe piles (8in.x35ft. long). Bare piles are included as controls. In all cases, the sand line was approximately 14ft. from the bottom of the pile at time of installation in 1967. Length of pile exposed to water and sand varied between 2 ft. and 8 ft., depending on the tide and movement of sand around the pile. Coated H piles are 2 windows (bare areas, 1 in. x 1 in.) exposed to the sand and 2 or 3 windows, depending on the tide, exposed to the water. The coated 8 piles were completely coated (no bare areas) when installed in 1967.

Table 3 - Corrosion Rates on Steel Piling Over a Period of 5 Years of Exposure (Offshore) in the Atlantic Ocean at Dam Neck, Virginia - Based on Yearly Polarization Measurements.

Pile	Pile 4/ Description	Avg. Corrosion Current Density mA/ft² 1/ Tide H. high; L. low; I. intermediate						Corrosion Rate-Avg. Penetration mpy 2/ Tide H. high; L. low; I. intermediate					
		1967 3/	1968	1969	1970	1971	1972	1967 3/	1968	1969	1970	1971	1972
1	Bare low carbon steel H pile 8 in.x8 in.	5.9(I)	4.4 (L)	4.8 (L)	5.9 (H)	5.7 (I)	5.9H	3.0(I)	2.2 (L)	2.4 (L)	3.0 (H)	2.9 (I)	3.0H
4C	Low carbon steel coated with coal tar epoxy except for bottom 12 ft. H pile	-	3.0 (L)	3.3 (L)	3.9 (L)	3.3 (I)	5.0H	-	1.5 (L)	1.7 (L)	2.0 (L)	1.7 (I)	2.5H
17C	Low carbon steel coated with phenolic mastic except for bottom 12 ft. H pile	-	-	-	-	2.6 (H)	4.6H	-	-	-	-	1.3 (H)	2.3H
10	Galvanized low carbon steel H pile. Hot-dipped coating	4.5(I)	0.48(I)	0.39(I)	0.31(L)	0.24(L)	3.0L	2.3(I)	0.24(I)	0.20(I)	0.16(L)	0.12(L)	1.5L
23	Bare Low Alloy Steel H Pile	4.6(I)	7.8 (I)	5.0 (L)	4.5 (H)	4.6 (I)	5.5I	2.3(I)	3.9 (I)	2.5 (L)	2.3 (H)	2.3 (I)	2.9I
26	Bare low carbon steel 8 in. pipe pile	-	5.0 (I)	5.1 (L)	5.9 (I)	8.6 (L)	9.5I	-	2.5 (I)	2.6 (L)	3.0 (I)	4.3 (L)	4.8I
27C	Low carbon steel 8 in. pipe pile coated with coal tar epoxy except for bottom 12 ft.	-	2.7 (L)	2.7 (L)	8.0 (L)	7.4 (H)	5.1I	-	1.4 (L)	1.4 (L)	4.0 (L)	3.7 (H)	2.6L

1/ Based on average of corrosion current densities calculated from breaks in the rectangular and semi-logarithmic plots of cathodic and anodic polarization curves. Note: To convert mA/ft² to uA/dm² (approx), multiply by 107.5.

2/ Based on corrosion current densities shown in this table and Faraday's law, assuming that the electrochemical equivalent K = 2.8938×10^{-4} g/C. Note: To convert mpy (mils per year or thousands of an inch per year) to μmpy (micrometers per year) aprox, multiply by 25. Corrosion rate, mpy = 0.5x Corrosion current density (mA/ft²), approx.

3/ Initial measurements - Made in 1967, 4 months after installation.

4/ All piles, except 23, are mild carbon steel. All H-piles are 8 in. x 8 in. x 48 lbs./ft. The piles are 35 ft. long and the sand line was from 19 to 21 ft, measured from the bottom of the pile. The length of piling exposed to sand and tidal water varied between 24 and 28 ft., the remainder being exposed to atmosphere and spray. Thus, of the length of piling exposed to sand and tidal water, approximately 75 percent is exposed to sand.

NOTE: The calculations of corrosion current density and corrosion rate are based on the area of bare steel originally exposed to sand, water, or both. Thus, for the coated piles, 4C, 17C, and 27C, where the bottom 12 feet were uncoated, the early calculations can be attributed to corrosion in sand only. An increase in the corrosion rates of the coated piles with time is probably due primarily to a deterioration of the coating.



Figure 1. Location map of piling test site, Dam Neck, Virginia.

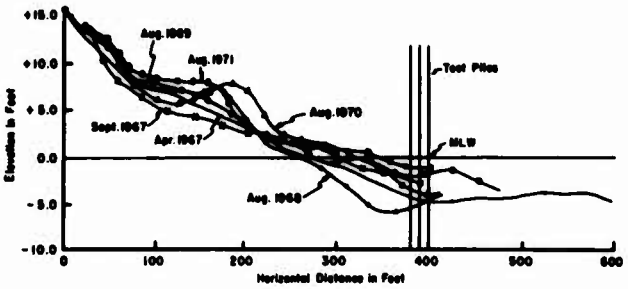


Figure 2, Bottom profiles, piling test site, Dam Neck, Virginia.

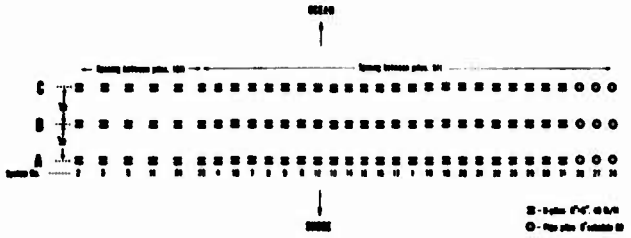


Figure 3. Piling installation plan.

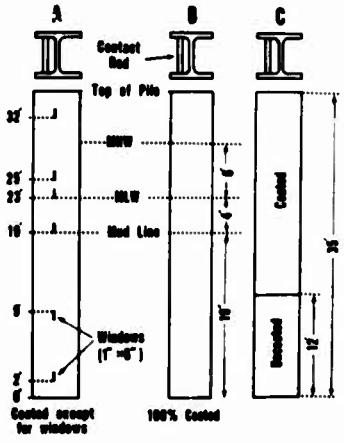


Figure 4. Diagram of pile-coatings. MHW (mean high water), MLW (mean low water).



Figure 5. Close-up view of anodes installed on piles.



Figure 6. Close-up view of piles.



Figure 7. Distant view of pilings, showing electrical cable used to make electrochemical measurements.

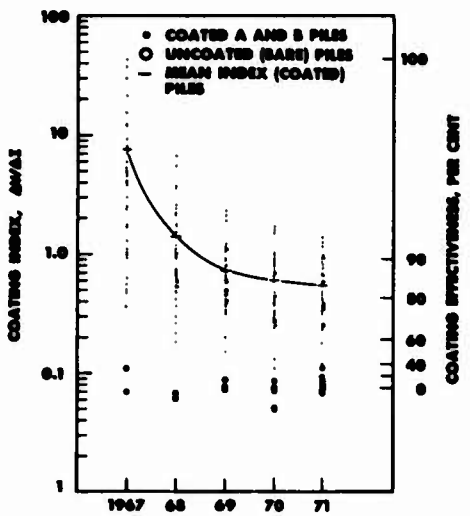


Figure 8. Graph showing decrease in coating effectiveness and coating indices.

APPENDIX

(Table No. 4)

Description of coating systems on Steel Piling Exposed to Atlantic Ocean at Port York, Virginia[a][b]

Piling System Number	Coating Description	Number of Coats	Coating Thickness on Each Pile[c] (in mils)	Remarks
4	Formula C-200, Polyamide-Cured Coal-Tar Epoxy	2	A-16 B-16 C-16	
5	Formula C-200, Polyamide-Cured Coal-Tar Epoxy	2	A-20 B-20 C-16	Protected beneath waterline with two zinc anodes[d]
6	Polyamine-Cured Coal-Tar Epoxy	2	A-16 B-16 C-16	
7	Formula C-200, Polyamide Cured Coal-Tar Epoxy Formula C-200 and Cornets	2 1	A-16(32)[d] B-32(36) C-31(36)	Third coat and cornets applied between 16' and 22' from bottom of piles only.
8	Aluminum Pigmented Coal-Tar Epoxy Amine-Cured, Red-Lead Pigmented, Coal-Tar Epoxy Primer Amine-Cured Coal-Tar Epoxy Intermediate Amine-Cured, Aluminum-Pigmented, Coal-Tar Epoxy Finish	1 1 1	A-27 B-25 C-28	
9	Aluminum-Pigmented Coal-Tar Epoxy Primer Amine-Cured Coal-Tar Epoxy Intermediate Amine-Cured, Aluminum Pigmented, Coal-Tar Epoxy Finish	1 1 1	A-10 B-10 C-10	
10	Hot-Dipped Zinc (Galvanized)	1	A-9 B-9 C-9	
11	Hot-Dipped Zinc (Galvanized)	1	A-7 B-9 C-7	Protected beneath waterline with two zinc anodes[d]
12	Polyvinylidene Chloride, Formula 113/54, Mil-L-19189 (Alternate Orange and White Coats)	7	A-7 B-5 C-7	
13	Flamesprayed Aluminum Wire	1	A-9 B-9 C-9	Aluminum precoated with a flamesprayed steel wire flash bonding coat and oil thick
14	Sealed Flamesprayed Aluminum Flamesprayed Aluminum Wire Wash Prime, Formula 117, Mil-P-15328D Clear Vinyl Sealcoat	1 1 2	A-10 B-9 C-9	Aluminum precoated with a flamesprayed steel wire flash bonding coat and oil which.
15	Coated Flamesprayed Zinc Flamesprayed Zinc Wire Polyvinylidene Chloride, Formula 113/54, Mil-L-19189 (Alternate Orange and White Coats)	1 7	A-12 B-12 C-13	
16	Coated Flamesprayed Zinc Flamesprayed Zinc Wire Vinyl Red-Lead Primer, Formula A110 Mil-P-15929	1 3	A-8 B-8 C-8	
17	Phenolic Mastic Amine-Cured, Red-Lead Pigmented, Phenolic Mastic Primer (with Mica Filler) Amine-Cured Phenolic Mastic Finish	1 1	A-13 B-16 C-16	
18	Coated Zinc Rich Epoxy Zinc Rich Epoxy Primer Formula C-200, Polyamide-Cured Coal-Tar Epoxy Finish	1 2	A-19 B-21 C-22	
19	Coated Zinc Inorganic Silicate Zinc Inorganic Silicate Primer High-Build Vinyl Finish	1 1	A-12 B-10 C-12	
20	Coated Zinc Inorganic Silicate Zinc Inorganic Silicate Primer (Half-Cured) Polyamide-Cured High-Build Epoxy Finish	1 1	A-10 B-10 C-12	
21	Coated Zinc Inorganic Silicate Zinc Inorganic Silicate Primer (Half-Cured) Amine-Cured Coal-Tar Epoxy Finish	1 1	A-21 B-22 C-19	
22	Coated Zinc Inorganic Silicate Zinc Inorganic Silicate Primer (Post-Cured) Strontium-Chromate, Iron-Oxide, Vinyl-Phenolic Primer Vinyl Mastic Finish	1 1 1	A-10 B-8 C-13	
26	Formula C-200, Polyamide-Cured, Coal-Tar Epoxy	2	A-17 B-16 C-17	"H" piles were of low alloy steel.
27	Formula C-200, Polyamide-Cured Coal-Tar Epoxy	2	A-20 B-17 C-20	Carbon steel pipe piles
28	Formula C-200, Polyamide-Cured Coal-Tar Epoxy Formula C-200 and Cornets	2 1	A-21(36)[d] B-21(32) C-30(36)	Carbon steel pipe piles. Third coat and cornets applied between 16' and 22' from bottom of piles only
29	Flakeglass-Filled Polyester	1	A-32 B-30 C-30	

[a] All piles were carbon steel "H" piles unless noted otherwise.
[b] Piles in each system were coated as follows:
A-Piles - Completely coated except for six 4"x6" bare windows located at intervals along the outside face of the outer flange of piles.
B-Piles - Completely coated.
C-Piles - Top 23 feet completely coated, bottom 12 feet left uncoated.
[c] Number on A-and C-piles indicates coating on water below MLW, number on B-piles located in the sand.
[d] Values in parentheses indicate total thickness after application of third coat of C-200 and cornets between 16 and 22 feet from bottom of piles.

Summarized Discussion

In reply to a question concerning the galvanized piling, it was stated that the galvanizing (4-5oz) was still providing protection after 4 years but was showing signs of deterioration after the 5th year.

It was commented that the corrosion current on a coated pile was about the same as for uncoated piles. In reply to this comment, it was stated that this pile was a polyamide cured coal tar epoxy pile which was not coated on the bottom (bottom 12 feet). (On re-examination of the original data, it was found that the high value reported (6.5 mA/ft^2) was in error and that the proper value should be 4.6 mA/ft^2 as indicated in Table 1 for pile 5A).

It was commented that at the location of the piling where there was a lot of sand erosion, the results obtained would be less indicative of corrosion than of erosion and therefore have restricted application. (Author's comment: This site was chosen principally for its erosive effect by the American Iron and Steel Institute, the National Bureau of Standards and the Army Corps of Engineers, since many offshore installations by the Army Corps of Engineers are in such environments. Further tests of the systems in quiescent waters are now in progress or being planned.)

A comment was made that in a study of current requirements of cathodically protected piles without coating in quiet water, great difficulty was experienced in measuring current consumption. With variations in water level of a few inches, very different measurements of current consumption were obtained. On the coated piles, coating deterioration was noted primarily at the water-air interface.

In reply to a question as to whether the area of the pile down in the mud was considered in calculating the corrosion rates by the polarization method, the authors stated that it was.

A comment was made that the average corrosion rates would not reflect the possible differences in the performance of the low alloy piling and the ordinary carbon steel piling in the splash zone where the low alloy steel piling shows an advantage. The author's reply was that in the beginning, the low alloy steel seemed to corrode at a lower rate than the carbon steel. Also the current requirements for cathodic protection of the low alloy steel were lower than for the carbon steel. As time progressed, however, these differences were not too obvious.

It was commented that it would be of interest to measure the potential profile from the sand line up to the high tide line and compare these readings with the measured corrosion observed when the piles are pulled. Also, it would be of interest to compare these data with the data obtained in quiet waters.

STEELMATE - An Underwater Protective Coating for Steel and Wood

P.C. Trussell & T.P. Clark

B.C. RESEARCH
3650 Wesbrook Crescent
Vancouver 8, Canada.

Protection of Steel and Wood in Humid and Submerged Environments

The advent of this research institute into the field of protecting materials in the marine environment was an outgrowth of applied work on the protection of wood against wood borers. Research initiated in 1949 lead to systems of protecting saw-logs transported and stored in sea water (1), pontoons of floating wood and dry docks, floating dolphins and a variety of wooden marine installations. Later a non-destructive sonic method for determining the soundness of marine piling was developed. By the mid 1950's, however, no satisfactory technique had been developed for the protection of standing wooden piles.

In 1957 this institute undertook two approaches in an attempt to develop a method for protecting standing piling: the mechanized wrapping of piling from the mud line to beyond the high-tide level using heavy-duty, plastic tape; and the development of a mastic-type coating applicable to piling both below and above water. Within a year the first approach was abandoned because of difficulties forseen with obstructions in the wrapping of piles, such as the close proximity of brace piles to standing piles in pier bents. The mastic coating first showed very promising results but on subsequent field testing failed because of inadequate adhesion to wooden piles. This coating was eventually abandoned.

A re-evaluation of the problem lead to placing a priority on a protective coating for steel over one for wood in the marine environment. Two reasons for this decision were the increasing use of steel over wood in the sea and greater technical feasibility. Steel, after proper cleaning, provides a much more consistant and receptive substrate for coating than does submerged wood. Subsequent work has lead to the development of a protective coating for steel (2), referred to as STEELMATE, a modification of which is applicable to wet or submerged wood. Most of the work that has been done and which will be referred to in this paper, relates to two formulations which have been used for protecting steel.

Requirements for an Underwater Coating:

The underwater or intertidal environment presents a completely new set of conditions with different demands for the application and life of a coating compared with those in air, and particularly those on dry surfaces. The coating first must adhere to wet surfaces, and this is achieved in part by displacement of most of the water during application by brush or roller, and then of absorption and reaction with the remaining film of water lying between the applied coat and its substrate. The coating must be compatible

[1] Figuires in parentheses indicate the literature references at the end of this paper.

with the salts in sea water as well as perform in the presence of fresh water. Desirably the coating should be a high-build one that will provide a reasonably thick single coat for the sake of economy, since underwater painting is costly compared to that in air. For the same reason, the coating should preferably be self-sufficient, and require no undercoating or topcoating.

To meet application requirements, the coating must grip the substrate readily and set fairly quickly so as to resist disassociation from the substrate by wave action. The coating must also be amenable to application over a fairly wide temperature range, and particularly at lower temperatures since bodies of water on average are much cooler than the atmosphere when coatings are applied. The coating must protect the steel against corrosion, accordingly its water and oxygen permability must be low. Since it exists in an aqueous environment it must withstand freeze-thaw action.

A number of other attributes must be built into the coating if it is to meet practical marine applications. For example, sand-blasted steel readily forms a thin oxide coating which often becomes visible in 15 or 20 minutes. The coating must be able to penetrate the newly formed oxide film and grip the steel underneath. If the coating is to be applied to ship bottoms, it must have a resistence to cold flow. One of the requirements which has presented considerable difficulties has been overcoming attack and damage by barnacles (3). Impurities in the water, or on the surface of waters can interfere with the application and curing of coatings. For example, surface oil pollution in industrial harbours will readily contaminate the surface of sand-blasted steel, at or near the intertidal zone, thereby interfering with adhesion of the coating to the steel.

From the requirements set forth above it can be seen that the demands on an underwater coating are rigorous. This can be appreciated more when it is realized that the cost of preparation and application of a coating underwater is substantially higher than that for one in air, and consequently the protective life of the coating underwater is desired to be moderately long.

Properties of the Coating:

STEELMATE has a polyester base in combination with other resins and additives. It is prepared in three parts - the vehicle, powder (pigment) and catalyst which are combined immediately before application. The pot-life is forty-five to fifty minutes. The specific gravity is 1.18 so that it responds to gravity underwater. It requires twelve hours for drying in air, forty-eight hours underwater. The separate constituents have a shelf life of over a year. Coverage in air is about 120 square feet per gallon at 10 mil, underwater about 60 square feet per gallon taking into account practical losses. Application can be made in water over the range of 33° to 100°F by adjusting the amount of catalyst. At 150°F does not set well. Tests undertaken on initial formulations of STEELMATE at 30°C (36°F) and 30 knots water current showed that the "cold flow" was too high for application to ships' bottoms within the first 24 hours (4). Subsequent modifications are now under test.

Laboratory Assessment:

Laboratory evaluation using weatherometer, salt-spray and freeze/thaw tests were made using well-known cold-tar epoxy, zinc-rich polyamide-epoxies and vinyl systems on steel for comparison. The STEELMATE was applied as one coat and the others as two-or three-coat system according to the manufacturers' specifications. In the salt-spray test, the cold-tar epoxy, the polyamide-epoxy and the aluminum vinyl coatings showed undercutting from score marks across the coated steel specimens whereas both aluminum and red-brown samples of STEELMATE were free from undercutting. In the weatherometer test the cold-tar epoxy performance began to drop after the equivalent of three years exposure,

whereas the polyamide-epoxy, aluminum vinyl and STEELMATE were in excellent condition after the equivalent of 12 years. The red-brown STEELMATE was tested to the equivalent of 30 years at which some fading but no breakdown of the coating occurred. In the freeze/thaw tests, the cold-tar epoxy failed after 16 cycles and polyamide-epoxy after 30 cycles; the aluminum vinyl and the STEELMATE coatings were still in excellent condition after 100 cycles. A summary of the data on STEELMATE are set forth in Table 1.

The laboratory results have shown that STEELMATE applied as one coat is equivalent or superior to two and three coat systems considered of high servicability for terrestrial applications.

Field Applications to Steel:

Applications have been made in the field using STEELMATE over the past two years. At Groton, Conn. two 18-member steel mooring dolphins were coated in August, 1970. The dolphins were cleaned by sand-blasting and painted by using coarse-textured rollers and paint brushes. The coating was applied from -1 foot to +9 foot mean low water. In the Spring of 1971 it was reported that the paint was becoming detached on about 10% of the overall area. Subsequent examination in August, 1971 combined with laboratory examinations on samples detached coating established that loss of bond was caused by incomplete removal of mill scale during sand blasting. In the remaining areas, the coating was still firmly attached and the steel substrate was free of corrosion.

In the Fall of 1970 structural steel fenders at the Seatrain Dock, Newark, N.J. were coated with STEELMATE from mean low water to plus three feet, partly over cold-tar epoxy which had been applied earlier and partly over clean steel. An inspection on October 8, 1971 disclosed that some of the coating was failing where it had been applied over the epoxy coating due to disbonding of the epoxy coating but in all cases the STEELMATE was intact where it had been applied directly to steel.

On March 1, 1971 seal tanks at the Oak Bay Marina at Victoria, B.C. were drained, sand-blasted and coated with STEELMATE by spraying both inside and out. The tanks were refilled twelve hours after application of the coating and the seals returned to them. More than one year later, no sign of peeling, pin-holing or loss of adhesion was detected.

In the Summer and Fall of 1971, H-piles supporting a structure in Baltimore were coated. These piles were capped about one foot above water level. After one year examination revealed that the STEELMATE had completely disbonded in the top 15 inches of all piles, but where properly applied, had cured and was in good condition below that point. Presumably, oil on and near the surface of the water had interfered with the application and curing of the coating. Experimentation and testing is continuing on this field application.

Attempts to apply STEELMATE to sheet piling in the Neches River at Beaumont, Texas, in June 1972 ran into difficulties with adhesion due to river pollutants. This problem was overcome by the addition of a surfactant to the coating. This enabled quick and intimate contact of the coating with the steel despite the rapid rate of oxidation of sand-blasted steel taking place under the high-temperature, humid conditions.

Our experiences to date have clearly demonstrated the need for caution in applying protective coatings to wet or submerged steel. Water, with all the materials for which it can be a vehicle, both solids and solutes, presents a hostile environment and it is obvious that there must be a limit to the hostility that any coating can withstand.

Application to Wood:

The coating for wood varies in composition and in properties to that for steel. The steel coating is relatively impervious to the transmission of air and moisture vapour, that for wood is required to "breathe" so that in areas where the coating is applied to wood above the water level, the moisture would not be locked into the wood providing conditions for dry-rot to occur.

One of the practical difficulties confronting the development of a coating for wood was to have the coating adhere to submerged wood despite the presence of a fine coating of slime over the wood. Despite careful cleaning of the surface of submerged wood, some slime either persists or readily reforms over the surface of the wood, and any coating that is to be applied must be able to accommodate this coating of slime. In compounding a coating to meet this requirement, the coating for wood does not set to the same degree of hardness as that for steel.

Sea water exposure carried out at San Diego and at Vancouver have shown that underwater wood coating, cured for two weeks in air prior to exposure, can prevent attack of Douglas Fir by marine borers. Such coatings have resisted marine-borer attack for two and one-half years to date.

REFERENCES:

(1) TRUSSELL, P.C., WALDEN, C.C., and ALLEN, I.V.F., Protection of Wood Against Marine-Borer Damage with Sodium Arsenite. Materials Protection 5, No's. 5,6,7; May, June, July, 1966.

(2) CLARK, T.P., Underwater Paint. Presented at National Association of Corrosion Engineers - Corrosion/72. Annual meeting, March 20-24, 1972. St. Louis.

(3) DRISKO, R.W. and BROUILLETTE C.V., Maintenance Painting of Steel Structures Between Tides and Below Water. Materials Protection and Performance 10 (No. 4), April, 1971.

(4) VAN LONDEN, A.M. 1972. Private communication.

TABLE 1

LABORATORY TEST RESULTS ON STEELMATE

	Results
Salt Spray Tests, 3300 hours (ASTM - B - 117-64)	Discolouration and fading with slight corrosion in cuts but no under-cutting.
Weatherometer equivalent 30 years (ASTM E-42-64)	Fading at surface, condition good, bond firm.
Freeze/Thaw, -20°F for 24 hours, alternated 140°F for 24 hours: 100 cycles	Excellent condition, bond firm.

Oral Discussion

Miller: How is the underwater portions of steel cleaned in preparation for application of the coating?

Trussell: We have been recommending sandblasting to white steel.

Miller: Why is it necessary to completely exclude water from an underwater surface that is going to be coated?

Trussell: We feel that without intimate contact, the adhesion of the coating is poor and it will eventually debond.

Question: Are the brushes and rollers used to apply the coating standard equipment?

Trussell: The brushes have bristles slightly stiffer than those used for painting in air. (The coating is paintable but is fairly viscid.) The roller is coarse-textured, something like wall-to-wall carpeting. Brushes and rollers are of special design but can be purchased in the market.

Clark: Are there any special preparations made at the mud line?

Trussell: No, aside from having to cover as much of the pile as possible, which might mean moving some of the earth from the base and later refilling.

Collins: Could the author tell us a little more about your novel approach for preventing barnacles?

Trussell: We add toxic organic chemicals to the coating which will diffuse through the coating to the surface to prevent attachment of barnacles for 6 to 9 months, after which the coating is hard enough to maintain its integrity against barnacle attack.

Experiments With (Coated) Aluminum in Seawater

John R. Saroyan

Mare Island Naval Shipyard
Vallejo, California 94592

Aluminum generally will withstand atmospheric exposure as long as an adherent oxide film forms and remains over the surface. If, however, the oxide layer is disrupted and cannot heal, corrosion can take place. Immersed in seawater, disruption of the oxide film can occur. Besides the presence of chloride ion causing discontinuity in the formation or healing of the oxide layer, other factors can interfere. These include crevices (depletion of oxygen), fouling attachments and wear actions.

Experiments with bulk paint pigments, their corresponding epoxy coatings and the effect on aluminum alloys have been studied. It appears that inhibitive chromates can help solve many of the corrosion problems involving aluminum alloys in seawater. The most effective inhibitive pigment is strontium chromate in an epoxy binder at a PVC of 20-25% in the dry film, with a total PVC of 25-35%.

Key Words: Seawater; aluminum; aluminum alloy; galvanic series; negative potential; cathodic protection; anodic reaction; corrosion; exfoliation corrosion; pitting corrosion; crevice corrosion; fouling and corrosion; chromate ion; inhibitive pigments; protective oxide layer (aluminum); protective coatings.

---

1. State of the Art

When lightweight structures are planned, usually aluminum alloys are considered. Such structures include aluminum craft, boat hulls, and topside structures such as deck houses, masts and radar antennas.

Once the choice is made to use aluminum alloys, the problems which are associated with aluminum and the environment must be identified and coped with.

Aluminum as a pure metal is highly reactive as indicated by its position in the electromotive series of metals. Likewise, aluminum alloys are similarly reactive in seawater or marine atmosphere.

Most structural materials coupled with aluminum, such as steel, will become cathodes. Then, the aluminum being anodic, deteriorates under galvanic corrosion, when an electrolyte such as seawater is present.

Uncoupled, generally aluminum alloys do quite well in the atmosphere. Where there is sufficient oxygen present, an adherent thin film of oxide forms on the surface and serves as a protective coating. This is quite different from the corrosion of steel or rusting, where the reaction can continue until the metal is consumed.

In seawater, aluminum may not do as well where conditions are not right to form the protective oxide layer. For one condition, the presence of the chloride ion interferes

with the formation of a continuous oxide film. Besides the chloride causing film disruption, such factors as crevices, stagnant low oxygen containing seawater, wear actions and fouling attachments can all contribute to destroying the oxide protective film and invite corrosion. Aluminum in seawater can suffer various types of corrosion. These include general surface corrosion, stress corrosion, pitting corrosion, crevice corrosion, intergranular and exfoliation type corrosion. The exfoliation type corrosion is quite destructive as it weakens the physical strength of the structure.

Two aluminum alloys are used primarily for aluminum craft and boat hulls (1).[1] These are alloys 5086 and 5456. Although both contain magnesium (5086-4% and 5456-5%) (2) as the primary alloying ingredient, they differ in strength. Alloy 6061 is a general purpose structure material using a combination of magnesium and silicon as the chief alloying ingredients.

The chemical composition limits are given below for the above three aluminum alloys (3): (Also included are No. 1100 and No. 356 (cast) for information on panel evaluations).

Alloy Designation	Silicon	Iron	Copper	Manganese	Magnesium	Chromium	Nickel	Zinc	Titanium	Others Each	Others Total	Aluminum Min.
5086	0.4	0.5	0.1	0.2-0.7	3.5-4.5	0.05-0.25	--	0.25	0.15	0.05-	0.15	Remainder
5456	0.4Si+Fe	--	0.1	0.5-1.0	4.7-5.5	0.05-0.2	--	0.25	0.2	0.05-	0.15	Remainder
6061	0.4-0.8	0.7	0.15-0.4	0.15	0.8-1.2	0.04-0.35	--	0.25	0.15	0.05-	0.15	Remainder
1100	1.0Si+Fe	--	0.2	0.05	--	--	--	0.1	--	0.05-	0.15	99.0
356	6.5-7.5	0.6	0.25	0.35	0.2-0.4	--	--	0.35	0.25	0.05-	0.15	Remainder

Besides chemical identity, aluminum alloys are also classed as to the temper resulting from mechanical, strain hardened or heat treatments. The following tempers (H and T value) are available for the three alloys: 5086-H32, 5456-H321, and 6061-T6.

Because the temper produces certain properties, more than one temper may be available for a given aluminum alloy.

The alloy 6061-T6 being a general purpose structure alloy, is used for railings, non-welded structures and piping (plumbing) such as for radar antennas. Although most such uses have been successful, certain radar antennas in way of stack gases and subject to marine atmosphere have shown serious corrosion of the plumbing network.

Figure 1 photograph shows an antenna plumbing section badly corroded, resulting from dissimilar metals (6061-T6 aluminum and stainless steel) in stack gas and marine environments.

The alloys 5086 and 5456 have given very good service in the marine environment. The particular tempers arrived at, as indicated above, are what is referred to as "quarter-hard" (2) and this is designated as "H32" for 5086 and "H321" for 5456. The initial marine uses of these alloys were for superstructures and portions of ships and boats other than

[1] Figures in parentheses indicate the literature references at the end of this paper.

hulls. Here, because of location, accessibility and cosmetic reasons, such surfaces were usually painted. As a result, no major corrosion problems developed with either alloy.

As the use of these two alloys become generally accepted for marine use, it was believed that the introduction of aluminum hull craft and boats would pose no serious problems (1). However, there have been several instances where serious corrosion has resulted particularly with the use of alloy 5456-H321 for boat hulls. The most severe corrosion has occurred in unpainted bilge areas where alternately stagnant water (low oxygen content) and dry conditions prevail. In such unpainted bilges, pitting corrosion soon results which leads to two other types of corrosion within the "interior metallurgical structure" (2): namely, intergranular and exfoliation corrosion.

The exfoliation type corrosion is illustrated and shown in the Fig. 2 photograph. This photograph shows a hull section of an aluminum boat made of 5456-H321 alloy. The pitted and somewhat delaminated surface was the interior of the bilge area and was not painted, permitting this severe corrosion to take place. The opposite side of the plate was the exterior hull and was protected by painting.

Figure 3 shows another hull section where delamination or exfoliation corrosion has resulted. The exfoliation type of corrosion gets started from some initial penetration of the aluminum either from an edge or a pit. Then the exfoliating corrosion action starts in a linear path, parallel to the main axis of the plate. These linear paths, "highly directional structure of flattened and elongated grains" (4), may be identified as continuous stretches of an aluminum-magnesium precipitate (34% magnesium in aluminum) (5). Such a composition which is anodic is readily attacked, for example, by seawater. This metallurgical structure is characteristic of rolled plate and shapes. Today, exfoliation resistant 5086 and 5456 alloys are available and are designated by tempers of H116 and H117. Mechanical working (or strain hardening) of these alloys in two directions breaks up the continuity or layers of the precipitate compound (34% Mg in Al) and hence eliminates the exfoliation potential.

2. Background

A. Hull Coatings - Bilges, Tanks, Underwater Areas.

In some instances, aluminum alloy hulls of craft and boats made of 5086-H32 and particularly 5456-H321 have shown exfoliation type corrosion, along with pitting, in bilge areas. To arrest any further corrosion by providing means for repairing the corroded areas, certain studies were initiated on a more or less expediency basis. These studies were pursued prior to some of the experiments which are reported further on in this paper.

To evaluate both the aluminum metal and the coating system which was to provide the protection against all types of corrosion, an accelerated test had to be implemented. For evaluation, the following aluminum alloys were available: 5456-H321, 5086-H32, 5456-H116 and 5086-H116.

The particular accelerated test, that was suggested, is known as "SWAACT" (seawater-acetic acid test). It was developed by Reynolds Metal Company (6) and is essentially a modification of the conventional salt spray test, Federal Test Method Standard 141A, of 1 September 1965, "Salt Spray (Fog) Test, Method 6061. The test employs an intermittent (30 minutes on, 120 minutes off) synthetic sea salt-acetic acid spray at pH3 for one or two weeks at 120°F (49°C).

Figure 4 illustrates the results of evaluations under the "SWAACT." The photograph shows various aluminum alloy coupons after one week exposure to the test.

Although the coatings used in these evaluations were not specifically designed to withstand acetic acid, some such coatings did well after being subjected to the "SWAACT Test." Figure 5 shows coated 5456-H321 (cold worked) aluminum alloy; system: (1) acid cleaner ("DICO," Diversey Corporation, Chicago, Illinois); MIL-P-23377 strontium chromate (12%) epoxy-polyamide and MIL-P-24441, Formula 156, Red. After two weeks exposure to the "SWAACT Test" the scribed coating system was considered satisfactory as a means of prevent-

ing exfoliation of an aluminum alloy that is prone to exfoliation. However, the actual scribe was 50% full of corrosion products, such that the edges of the coating at the scribe lifted.

Also, immersion tests were conducted using the method of Alcoa Research Laboratories (7) and a synthetic seawater immersion at 175°F (80°C) for one week.

From the results of these initial, expedient studies (8), the following conclusions were arrived at:

Optimum protection was afforded by coating systems consisting of:

a. Chemical conversion coating under MIL-C-5541 (i.e., Alodine 1200 or 1200S of Amchem Products, Inc., Ambler, Pa. 19002).

b. High inhibitive strontium chromate (12%) primer conforming to MIL-P-23377.

c. Finish coat, epoxy-polyamide, MIL-P-24441 Formula 156 (formerly 1B40) or Devoe Marine coatings, Formula 209 Devran No. 27 Exterior Coating--Celane, Riverside, California 92502.

d. In some instances, with high chromate primer, the chemical conversion coating of MIL-C-5541 may not be required.

e. When the MIL-P-23377 high chromate primer was replaced with a lead-silico chromate primer, the performance was lowered after one week in the "SWAACT Test."

f. Also replacing both the conversion coating and the strontium chromate primer with only a lead-silico chromate primer, still lowered corrosion resistance resulted.

g. Replacement of MIL-P-23377 strontium chromate primer with No. 117 "wash primer" (MIL-P-15328) showed somewhat lowered performance.

h. Replacement of MIL-P-23377 primer with Mare Island 1B30 primer, nonchromate (MIL-P-24441, Formula 150) showed less corrosion resistance.

B. Radar Antennas

Certain previous studies on protection of "equipment subject to stack gas and marine environment" (9) revealed information pertinent to protection of aluminum alloys in seawater. This report established the chemical conversion treatment as a means for improving corrosion resistance of 6061-T6 aluminum alloy. Also the procedure serves as an automatic and photographic method to identify clean aluminum surfaces prior to painting. If the surface is not clean prior to the conversion coating step, the resulting deposited conversion coating will not be uniform. It will be spotty and discolored rather than uniform golden in color.

The current coating system applied over the conversion coating for 6061-T6 radar antenna plumbing is epoxy, pigmented with lead silico chromate followed by exterior epoxy. It appears that this system could be improved by incorporating effective, corrosion inhibitive pigments.

C. Maintenance and Repair of Aluminum Craft and Boat Hulls.

Certain craft that have displayed pitting and exfoliation types of corrosion undergo the following repair and maintenance process:

When the hull plating is replaced use the following:

5456-H116 or 5456-H117 to replace 5456-H321

5C86-H116 or 5086-H117 to replace 5086-H32

Repair Painting of Bilges

When repainting bilges that show pitted and visible exfoliation corrosion, the following procedure has been established:

1. Remove all loose paint and corrosion by light sandblasting, power brushing, or orbital sanding. Do not use any ferrous metal tools on aluminum.

2. Remove all grease, oil and other contaminants using a water emulsion type cleaning compound (i.e., MIL-C-22543).

3. Flush thoroughly with fresh water.

4. Apply one coat of pretreatment coating, Formula No. 117, MIL-P-15328 (0.5 mil dry film) on bare areas.

5. Then apply two coats of MIL-P-23377 (2 mils dry film).

6. Topcoat with one coat of MIL-C-22750 (3 mils dry film).

As an alternate, an epoxy system in accordance with MIL-P-23236 may be applied over the cleaned metal. (For example, Devran 202-215 (Devoe and Raynolds Celanese, Amercoat 81-82 (Ameron); Intergard 4421/4423 (International).

D. Underwater Painting

The underwater hull is painted with a system utilizing an approved non-copper or non-mercury bearing antifouling coating. The following are approved Antifouling Systems:

Glidden System	Dry Film Thickness
1-coat Nupon Primer 287-G-500/122-C-62	2 mils (50.8 microns)
1-coat Vinyl-Cote AC Brown 178-D-1	2 mils (50.8 microns)
1-coat Vinyl-Cote Metallic Mastic 178-E-9	4 mils (101.6 microns)
1-coat Vinyl-Cote No-Cop AF 178-R	2 mils (50.8 microns)

USS Chemicals (Porter Paint Co.)

Standard System	
2-coats Shipyard Primer	1 mil/coat (25.4 microns)
1-coat Tarset 305 A.F.	12 mils (304.8 microns)
Heavy Duty System	
1-coat Shipyard Primer	1 mil (25.4 microns)
1-coat C-200	6 mils (152.4 microns)
1-coat Tarset 305 A.F.	12 mils (304.8 microns)

E. Exterior Boottopping and Above

Generally the exterior aluminum topside surfaces are repainted because of appearance. Blistering, crazing, cracking and chalking are some of the signs that repainting is required. The painting procedure outlined below is generally effective for topside aluminum surface, except for such units as radar antennas in way of stack gases plus the normal marine atmosphere. As previously reviewed, for these surfaces a special preservation process is used. The following steps are suggested for general topside maintenance:

1. Remove all loose paint by light sandblasting, power brushing or orbital sanding. Do not use any ferrous metal tools on aluminum.

2. Clean surface with a liquid detergent cleaner such as MIL-D-16791, Type I, and thoroughly rinse with fresh water.

3. Touchup bare metal areas with "wash primer" Formula No. 117, MIL-P-15328 (0.3-0.5 mils dry film) (7.6-12.7 microns).

4. Within 24 hours, apply 2-coats of Formula No. 84 Zinc Chromate Alkyd (TT-P-645) of Formula 120 Zinc Chromate Vinyl Primer (MIL-P-15930).

5. After a minimum of eight hours dry, apply two coats of 27 Haze Gray (TT-E-490). Dry film 1.5 mils per coat (38.1 microns).

F. Deck Paint

Heavy traffic areas can be painted with a non-skid coating system. The following procedure is given:

1. Scrape, clean and apply No. 117 to bare metal as discussed previously. Apply other primers as recommended by vendor of nonskid material.

2. Apply finish coat of non-skid specified under MIL-D-23003, Type II. The color should match Formula 20 of JAN-P-699.

G. Cathodic Protection

Aluminum marine alloys under the proper care are said to be resistant to seawater corrosion. Also, it is stated that there are commercial aluminum hull boats which have been in salt water service for several years with no paint on the hull, but with proper cathodic protection. Regardless, painting does provide adequate resistance to corrosion, provided, of course, the paint film is continuous and formulated correctly for the specific environment.

Because of dissimilar metal connections, stray electrical currents, improper grounding and other sources of electrolytic corrosion, most aluminum boats are equipped with sacrificial anodes. The preferred anode is zinc since the potential difference between zinc and aluminum is not as great as that between magnesium and aluminum.

3. Introduction

Probably a more difficult task than evaluating metals and coatings in an accelerated test is to find the specific laboratory test that will simulate or duplicate the natural environment.

For many years the immersion cycle test of specification MIL-P-23236 (see below) has been used as a screening test for tank coatings (fuel and seawater). It seems once a coating system passes this year-long test it can be used practically anywhere seawater is in contact.

In the experiments to follow, simple seawater (synthetic and natural) immersions have been used extensively. The cycle test of MIL-P-23236 was used when evaluating complete scribed coating systems.

Immersion Cycle Test of MIL-P-23236

Test Procedure for Tank Coatings. For many years the U. S. Navy paint laboratories have utilized methods of MIL-P-23236 to evaluate anticorrosive coatings for use in tanks. The test procedure is quite severe, but coatings that successfully pass this cycle test are suitable for severe service use, for example, on underwater structures.

The procedure comprises four operations carried out in the following order:

1. Salt-water immersion: Immerse panels totally for one week in a 3 percent salt-water solution* of commercial table salt dissolved in distilled water, at a temperature of 70 to 90°F (20.1-30.2°C).

* Natural seawater is used by some organizations.

2. Aromatic-fuel immersion: Following salt-water immersion, immerse panels totally for one week in a 40 percent aromatic synthetic gasoline made up of a blend of 60 volumes of aliphatic petroleum naphtha (TT-N-95A), 20 volumes of toluene (TT-T-548A), 15 volumes of xylene (TT-X-916), and 5 volumes of benzene (VV-B-231A) at a temperature of 70 to 90°F (20.1-30.2°C).

3. Hot-seawater immersion: Following fuel immersion, immerse panels totally in hot synthetic seawater* for two hours at 175°F (80°C).

4. Hot-seawater spray: Following the hot-synthetic-seawater immersion, place each panel within a suitable closed container and opposite a 3/16 in. (.45 Cm) spray nozzle set at a distance of 2-1/2 ft. (0.76M) from the panel face. At a nozzle pressure of 25 psi, spray each panel dead center with a blast of hot (175°F) (80°C) synthetic seawater for a period of 10 seconds.

Note: Operations 1 to 4 constitute one complete test cycle. This cycle is repeated, and coating deterioration is reported after each complete cycle.

If the coating is still satisfactory after 20 cycles, wipe the panel lightly with a soft cloth and fresh water, allow 48 hours for it to dry thoroughly, then recoat the central upper third of one side of each panel, masking the portion from the edge to 1/2 in. (1.27 Cm) inward, with one coat of the finish coating of the coating system. Allow one week of dry time and complete the immersion test with five additional test cycles; inspect the coating for failure.

4. Scope of Experiments

The experiments conducted included sequence studies of pigments, individual coatings incorporating the candidate pigments, and finally complete coating systems utilizing the specially pigmented coatings as primers. As control, bare aluminum panels were included in the series of tests.

Preliminary tests included immersion of five aluminum alloys--6061-T6, 5086-H32, 5456-H321, 1100-H14 and 5086-H116 in both synthetic (See Table A for composition) and natural seawater. Figure 6 photograph shows the condition of the five aluminum alloys (6061-T6, 5086-H32, 5456-H321, 1100-H14 and 5086-H116) after 30 days immersion in the dark in synthetic seawater. All panels darkened and showed various degrees of mostly pitting corrosion; 6061-T° showed the most corrosion attack. Figure 7 shows the five alloys after 30 days immersion in the dark in the ocean. Here again, there is mostly pitting type corrosion. 6061-T6 is the least resistant to the ocean immersion. Figure 8 photograph, a welcomed error in test design, showed accelerated galvanic corrosion induced by a monel panel holding rod. None of these panels showed any exfoliation corrosion. Only pitting type corrosion was evident.

In some instances, the accumulation of fouling growth on aluminum has not been considered a major problem from the viewpoint of causing corrosion. For example, discussion by A. Guilhaudis (France) and C. P. De et al. paper (10) "Corrosion Behavior of Metals and Alloys Immersed Conditions in Indian Harbour" -- "------have you found a relation between the formation of pitting and fouling?" C. P. De replied: "On the basis of present exposure, no correlation can be drawn between the formation of pitting and fouling."

Other information indicates corrosion caused by fouling attachment. Walker et al (11) indicates that "Alloy 7039-T64 showed only very minor degree of pitting on one of the two exposed panels (maximum pit depth of 8 mils, 203.2 microns) which appear to have occurred under localized marine fouling."

Further, Saroyan (12) indicates that "fouling causes corrosion."

Galler (13) supports pitting corrosion by fouling attachment. He states that "an important auxiliary problem of hard fouling--that is the shelled forms, such as barnacles--may be accelerated corrosion. Not infrequently, the dead-water pocket between the base of

* Natural seawater is used by some organizations.

the barnacle and the metallic surface may become a galvanic cell owing to the growth of anaerobic bacteria and other microorganisms which bring about a sufficient change in the pH of the water in the pocket to generate an electrical current. The result may be pitting of the metal plates. Often, after a ship's bottom has been scraped and older barnacle shells removed, depressions show up in the steel plates which coincide with the outline of the base of the shell."

Recent immersion experiments conducted at the Point Reyes, California test site explored the subject of corrosion caused by fouling.

Figure 9 photograph shows fouling after 60 days immersion on all five aluminum alloys: 6061-T6, 5086-H32, 5456-H321, 1100-H14 and 5086-H116.

To illustrate crevice corrosion or oxygen concentration cell, certain well-formed, attached barnacles (on 5086-H116 aluminum alloy), as shown in the Fig. 10, photomicrograph, were dislodged and the base plate carefully removed without abrading the aluminum.

Figure 11 photomicrograph shows the surface of the aluminum after the barnacle was removed. Pitting caused by crevice corrosion can plainly be seen.

Experiment Series 1 and 2 following explored the inhibitive effect on the aluminum alloys of sodium chromate in synthetic seawater. With some yardstick values of chromate concentration necessary to prevent corrosion, subsequent tests with pigments and pigmented coatings and system were performed.

The effect of bulk inhibitive type pigments, suspended in synthetic seawater, on aluminum alloys was studied. Also the leached material as well as the increased aluminum content of the seawater was determined. These same pigments were incorporated into epoxy-polyamide coatings; and then these coatings were tested as to their effect on aluminum alloys. The cured epoxy coatings applied on glass panels were immersed in synthetic seawater along with aluminum panels. The effect on the aluminum panels of the leached matter from the various coatings was noted.

Finally, the pigmented epoxy coatings were utilized as primers in a coating system. The cured coating system was scribed and subjected to the immersion cycle test of MIL-P-23236. The comparative performances at the scribes for two periods (3 months and 6 months) of time were noted.

Experiment 1 -- Effect on Aluminum Alloy 6061-T6 When Immersed in Synthetic Seawater and in Synthetic Seawater with Varying Amounts of Sodium Chromate.

Aluminum alloy 6061-T6 panels (1/8" x 3-1/2" x 5-1/2") (.3 x 9 x 14 cm) were immersed in 950 ml of synthetic seawater (See Table A for composition.) with or without sodium chromate added. The solutions were identified as to various cation concentrations initially and also after the aluminum panels had been immersed in the solutions for 30 days.

Table 1 summarizes data obtained including pH values and condition of aluminum panels after 30 days immersion. The cation concentrations are given in micrograms per milliliter (µg/ml).

It will be noted for Beaker No. 1, (seawater control) the panel showed corrosion. (See Fig. 12, photomicrograph showing pitting of 6061-T6 aluminum alloy.) This is also supported by an increase of Al in solution from .5 to 2.00. Beaker No. 2 showed a few spots of corrosion. The Al in solution increased from .5 to 1.00. Also a concentration of 2µg/ml for Cr was present. The corrosion decidedly drops off in Beaker No. 3 where Cr is 11.7 µg/ml and the Al remains at the initial value of 0.5.

Experiment 2 - Effect on Aluminum Alloy 1100-H14 when Immersed in Synthetic Seawater and in Synthetic Seawater with Varying Amounts of Sodium Chromate.

This experiment is a repeat of experiment No. 1 for the reason that Alloy 6061-T6 contains some chromium and as such values for Cr could have been in error. With the 1100-H14 alloy, chromium can be accounted for as coming solely from the sodium chromate. Also it was

desired to learn if there was a surface effect of the chromate on the aluminum. The procedure followed was as in Experiment No. 1. Smaller aluminum alloy 1100-H14 1/8" x 2" x 4" (.3 x 5.1 x 10.2 cm) panels were used. The panels were immersed in synthetic seawater with or without sodium chromate added.

Table 2 summarizes the immersion data obtained. It is estimated that chromate, analyzed as 10-15 ppm as cation Cr (10-15 ppm), is sufficient to inhibit corrosion of 6061-T6 and 1100-H14 aluminum alloy. Other data suggest that aluminum is passivated by 1% sodium chromate (3) in a 3.5% NaCl solution.

Experiment No. 3 - Effect of Pigments in Seawater on Aluminum Alloy 6061-T6

Excessive amounts (about 10 Gms) of various pigments were stirred into 500 ml of synthetic seawater and permitted to remain in quiescent condition (except for one stirring a day) for about a month (18 May-21 June 1972).

Samples of the seawater and dissolved pigment portion were taken for analysis. Following the sampling, 1/8" x 3-1/2" x 5-1/2" (.3 x 9 x 14 cm) 6061-T6 aluminum panels were [illegible]d to half their areas in the solutions. Effects of the derived solutions on the aluminum panels were noted.

Table 3, Part A summarizes the data from the pigment solution experiment. Concentrations of cations and pH originating from the solutions of pigments in the seawater were determined.

Table 3, Part B summarizes the data obtained after immersing the 6061-T6 1/8" x 3-1/2" x 5-1/2" (.3 x 9 x 14 cm) aluminum panels in the pigment-seawater solutions. The effect of these solutions on the aluminum is indicated after 15 days immersion. Certain panels were left in the solutions for a total period of 33 days. Selective areas of these panels were photographed as close-ups and the following photomicrographs show these magnified areas:

Figure 12 shows as a control a panel of 6061-T6 immersed in synthetic seawater. Photomicrograph shows pitting corrosion after 33 days immersion.

Figure 13 is a photomicrograph showing a selected area of the surface of the 6061-T6 aluminum panel after 33 days immersion in synthetic seawater containing bulk strontium chromate pigment. There is no evidence of corrosion.

Figure 14 is a photomicrograph showing a magnified area on the surface of a 6061-T6 aluminum alloy panel immersed 33 days in synthetic seawater containing basic lead silico chromate pigment (shows pitting corrosion).

Figure 15 is a photomicrograph showing a selected area on the surface of a 6061-T6 aluminum alloy panel immersed 33 days in synthetic seawater containing bulk zinc chromate pigment. There is no evidence of corrosion.

Figure 16 is a photomicrograph showing a selected area on the surface of a 6061-T6 aluminum alloy panel immersed 33 days in synthetic seawater containing bulk lead chromate pigment. Shows pitting type corrosion.

Figure 17 is a photomicrograph showing a selected-magnified area on the surface of a 6061-T6 aluminum alloy panel immersed 33 days in synthetic seawater containing bulk red lead pigment. Shows pitting type corrosion.

Experiment 4 - Effect of candidate pigments on aluminum alloys when incorporated in epoxy coatings, applied to glass slides and immersed in synthetic seawater with aluminum alloys.

The various pigmented epoxy coatings were applied on 2-1/4" x 3" (5.7 x 7.6 cm) glass panels (one side only) cured 10 days and immersed in 450 ml synthetic seawater to include a wetted area of 6-3/4 sq. inches (43.3 sq. cm). The aluminum panels were either 1/8" x 3-1/2" x 5-1/2" (.3 x 9 x 14 cm) (6061-T6) or 1/4" x 3-1/2" x 5-1/2" (.6 x 9 x 14 cm) (5086-H32). The immersed surface was 2-1/4" x 3-1/2" (5.7 x 9 cm).

Table 4 tabulates the results of this immersion test. Also listed below are photographs of some of the aluminum panels after the 30 days immersion. Figure 18 photograph shows condition of the 6061-T6 aluminum alloy panel after 30 days immersion in synthetic seawater previously containing a glass panel coated with strontium chromate pigmented epoxy coatings (PVC 2-1/2%, 5%, 10% and 15%)--shows varying performance from slight corrosion to very slight corrosion.

Figure 19 shows condition of 6061-T6 aluminum alloy panels after 30 days immersion in synthetic seawater, previously containing glass panels coated with epoxy coatings pigmented respectively with tributyltin fluoride, strontium chromate and lead silico chromate. The tributyltin fluoride (45% PVC) panel shows pitting and anodic areas of bright metal. The strontium chromate (MIL-P-23377) panel shows no corrosion on one side but 30 spots of filiform type corrosion (black areas) on the other side. The lead silico chromate (commercial epoxy) shows pitting and anodic areas of bright metal. The two seawater control panels (5086-standing; 6061, flat) had slight edge and surface corrosion. 6061 had two pits. Included is a control panel immersed in synthetic seawater.

Figure 20 shows condition of 6061-T6 aluminum alloy panels after 30 days immersion in synthetic seawater, previously containing glass panels coated with epoxy coatings pigmented with cuprous oxide and tributyltin fluoride--25% and 45% PVC Cu_2O, surface darkened, edge corrosion, a few pits, filiform dark pitting areas; 15% and 25% TBTF panels turned black, pits, anodic areas of bright metal, some edge corrosion.

Experiment 5 - Performances of aluminum alloys (356 cast - 1/8" x 6" x 12") (.3 x 15.2 x 30.4 cm) and No. 1100-H14 (1/8" x 4-1/2" x 12") (.3 x 11.4 x 30.4 cm) panels coated with epoxy coating systems, scribed and subjected 18 months to the immersion cycle of MIL-P-23236 are summarized here in Table 5.

The panels were thoroughly cleaned using the process of alkaline cleaner (Diversey 202, Diversey Corp.) and (Desmutter, Deoxidizer, Amchem Deoxidizer No. 1). The panel was divided into four areas lengthwise. The first top quarter consisted of only a topcoat epoxy with no inhibitive pigments. The second quarter consisted of candidate epoxy primer with the topcoat epoxy. The third quarter consisted of conversion coating (MIL-C-5541, i.e., Alodine 1200, Amchem Co.), the candidate epoxy primer followed by the epoxy topcoat. The bottom quarter consisted of the conversion coating and the epoxy topcoat. All quarters were scribed down to the bare metal before being subjected to the immersion cycle of specification MIL-P-23236.

Alodine 1200 conversion coating improved performances of "poor" or low performing primers. Strontium chromate primers are improved only slightly by the conversion coating treatment (MIL-C-5541). In such cases, if clean aluminum surfaces can be assured, Alodine conversion treatment may be eliminated.

The most effective inhibitive pigment tested here is strontium chromate, used in an epoxy binder in the amount of 20-25% PVC, with a total pigmentation of 25-35% PVC. Possibly, depending on use, acceptable performance may be derived from compositions of 15-20% PVC strontium chromate, with total PVC of 25-35%.

Typical performances are shown in the following photographs:

Figure 21 photograph showing condition of system coated-scribed 356 Cast aluminum alloy panel after 18 months immersion in the cycle test of MIL-P-23236. (Basic zinc chromate pigmentation, 25% PVC; overall average of 4 ratings is 80% performance for basic zinc chromate and 90% with Alodine conversion treatment.)

Figure 22 photograph showing condition system of coated-scribed 356 cast aluminum panel after 18 months immersion in cycle test of MIL-P-23236. (Strontium chromate pigmentation, 25% PVC; performance is 95% for the pigment and 97% with the Alodine 1200 treatment.)

Figure 23 photograph showing condition of system coated-scribed 356 cast aluminum panel after 18 months immersion in cycle of MIL-P-23236. (Asbestine 3X pigmentation, 25% PVC; performance is 0% for the pigment and 60% with the Alodine 1200 treatment.

Figure 24 photograph showing condition of system coated-scribed 356 cast aluminum panel after 18 months immersion in cycle of MIL-P-23236. Primer, pretreatment coating, Formula No. 117, MIL-P-15328. 40% for #117 and 80% with alodine 1200 treatment.

Experiment 6 - Performance of 1/8" x 6" x 12" (.3 x 15.2 x 30.4 cm) aluminum alloy panels (6061-T6, 5086-H32 and 5456-H321) coated with epoxy coating systems, scribed and subjected for rating periods of three months and six months to the immersion cycle of MIL-P-23236 are summarized in Table 6.

The panels were thoroughly cleaned as described previously (Diversey 202 and Deoxidizer No. 1). The top third of the panel was coated with green epoxy primer, U.S Navy Formula No. 150, followed with gray epoxy (Formula 151) and a finish coat of white epoxy (Formula No. 152) both of MIL-P-24441. The bottom two-thirds was coated with the candidate primer coating followed by the gray epoxy (151) and topcoated with white epoxy (Formula No. 152). Just prior to immersion, the top third areas and the bottom third areas, both sides of the panel, were scribed down to bare metal. Three months later, the middle area was scribed (for the three months ratings).

Typical performances are shown in the following photographs:

Figure 25 photograph showing condition of system coated-scribed 6061-T6 aluminum panel (#437) after 3 and 6 months immersion in cycle test of MIL-P-23236 (2-1/2% PVC strontium chromate pigment). Performance of Scribe No. 2 (101) 3 months is 9.8 rating. Scribe No. 3 (102) and No. 5 is 3.3 rating (6 months).

Figure 26 photograph showing condition of system coated-scribed 6061-T6 aluminum panel (#442) after 3 and 6 months immersion in cycle test of MIL-P-23236 (25% PVC strontium chromate pigment). Performance of Scribe No. 29 (B) 3 months is 10 rating. Scribes No. 28 (C, 11) and No. 30, 6 months 10 rating.

Figure 27 photograph showing condition of system coated-scribed 6061-T6 aluminum panel (#449) after 3 and 6 months immersion in cycle test of MIL-P-23236 (15% lead silico chromate pigment). Performance of Scribe No. 63, 3 months is 9 rating. Scribes No. 64 (110) and No. 66, 6 months, 6.7 rating.

Figure 28 photograph showing condition of system coated-scribed 6061-T6 aluminum panel (#484) after 3 and 6 months immersion in cycle test of MIL-P-23236 (MIL-P-23377, 12% PVC stontium chromate). Performance of Scribe No. 241, 3 months, is 9.9 rating. Scribes No. 242 (121) and No. 241, 6 months, 7.5 rating.

Figure 29 photograph showing condition of system coated-scribed 6061-T6 aluminum panel (#485) after 3 and 6 months immersion in cycle test of MIL-P-23236. Commercial epoxy system primer - lead silico chromate pigmentation. Performance of Scribe #246, 3 months is 8.5 rating. Scribe Nos. 247 (122) and 249, 6 months, are 6.7 and 5 ratings.

Figure 30 photomicrograph showing condition of Scribe No. 1, area No. 100, system coated-scribed 6061-T6 aluminum panel (#437) after 6 months immersion in cycle test of MIL-P-23236. Coating system MIL-P-24441, 1-coat each Formulas 150, 151 and 152. Performance is 2.5 rating.

Figure 31 photomicrograph showing condition of Scribe No. 3, area No. 102, system coated scribed 6061-T6 aluminum panel (#437) after 6 months immersion in cycle test of MIL-P-23236. Coating system epoxy primer, 2-1/2% PVC strontium chromate pigment; Navy formulas 151 and 152. Performance is 3.3 rating.

Figure 32 photomicrograph showing condition of Scribe No. 28, area No. 11, system coated-scribed 6061-T6 aluminum panel (#442) after 6 months immersion in cycle test of MIL-P-23236. Coating system epoxy primer, 25% PVC strontium chromate pigment; Navy formulas 151 and 152. Performance is 10 rating.

Figure 33 photomicrograph showing condition of Scribe No. 54, area No. 110, system coated-scribed 6061-T6 aluminum panel (#449) after 6 months immersion in cycle test of MIL-P-23236. Coating system epoxy primer, 15% PVC lead-silico chromate; Navy formulas 151 and 152. Performance is 6.7 rating.

Figure 34 photomicrograph showing condition of Scribe No. 242, area #121, system coated-scribed 6061-T6 aluminum panel (#484) after 6 months immersion in cycle test of MIL-P-23236. Coating system epoxy primer, 12% PVC strontium chromate pigment - MIL-P- 23377; Navy formulas 151 and 152. Performance is 7.5 rating.

Figure 35 photomicrograph showing condition of Scribe No. 247, area #122, system coated-scribed 6061-T6 aluminum panel (#485 after 6 months immersion in cycle test of MIL-P-23236). Coating system commercial epoxy primer, lead-silico chromate pigmentation; Navy formulas 151 and 152. Performance is 6.7 rating.

Table A

Table of Composition of Synthetic Seawater

Instant Ocean Chemical Analysis
Aquarium Systems, Inc.
1450 East 289 Street
Wickliffe, Ohio 44092

September 1967

Directions for final preparation of the synthetic sea water are given on the packages. When tap waters are deficient, or special culture problems call for them, fluoride, silicate and other substances may be substituted for tap water for culturing delicate forms.

Component	% by Weight
$NaCl$	65.226
$MgSO_4 7H_2O$	16.307
$MgCl_2 6H_2O$	12.762
$CaCl_2$	3.261
KCl	1.737
$NaHCO_3$	.4963
KBr	.07206
H_3BO_3	.06214
$SrCl_2 6H_2O$	.04689
$MnSO_4 H_2O$	.009379
$Na_2HPO_4 7H_2O$	.009379
$LiCl$	.002343
$Na_2MoO_4 2H_2O$	.002343
$Na_2S_2O_3 5H_2O$	.002343
$Ca(C_6H_{11}O_7)_2 H_2O$	.001669
$Al_2(SO_4)_3 18H_2O$	.001202
$RbCl$	.0004005
$ZnSO_4 7H_2O$	.0002563
KI	.0002403
EDTA NaFe	.0001936
$CoSO_4 7H_2O$	.0001335
$CuSO_4 5H_2O$	.00002670

Table 1

Analysis* Before and After 30 Days of Solutions of Synthetic Seawater with Varying Amounts of Sodium Chromate and Immersed Aluminum Panels, 6061-T6

1.

Beaker	1	2	3	4	5	6	7
pH							
Before	8.5	8.5	8.5	8.5	8.5	8.5	8.5
After	8.2	8.4	8.5	8.5	8.5	8.5	8.5
Cr, µg/ml							
Before	<0.1	2.00	11.7	110	227	1120	2240
After	<0.1	2.00	11.7	110	227	1120	2240
Na, µg/ml							
Before	9600	9600	9700	9820	10000	10500	12000
After	9600	9600	9700	9820	10000	10500	12000
Mg, µg/ml							
Before	1000	1000	1000	1000	1000	1000	1000
After	1000	1000	1000	1000	1000	1000	1000
Ca, µg/ml							
Before	380	380	380	380	380	380	380
After	380	380	380	380	380	380	380
K, µg/ml							
Before	290	290	290	290	290	290	290
After	290	290	290	290	290	290	290
Sr, µg/ml							
Before	4.30	4.30	4.30	4.30	4.30	4.30	4.30
After	4.35	4.40	4.30	4.39	4.37	4.30	4.30
Cl, µg/ml							
Before	15500	15500	15500	15500	15500	15500	15500
After	15500	15500	15500	15500	15500	15500	15500
SO_4, µg/ml							
Before	2000	2000	2000	2000	2000	2000	2000
After	2000	2000	2000	2000	2000	2000	2000
Al, µg/ml							
Before	<0.5	<0.5	<0.5	<0.5	<0.5	<0.5	<0.5
After	2	1	<0.5	<0.5	<0.5	<0.5	<0.5

2. Sediment taken from Solutions 1, 3 and 7 after exposure was identified as aluminum corrosion products.

3. Condition of panels after 30 days immersion is summarized as follows:

Beaker	1	2	3	4	5	6	7
Panel Condition	General Corrosion	Few spots of Corrosion	No Corrosion	No Corrosion	No Corrosion	No Corrosion	No Corrosion

Note: Analysis for aluminum (above) correlates directly with the observed corrosion. Panel in Beaker No. 1 showed corrosion. Aluminum content went from <0.5 to 2.0 µg/ml. Panel in Beaker No. 2 showed a few spots of corrosion. The aluminum content went from <0.5 to 1.0 µg/ml. Panel in Beaker No. 3 showed no corrosion. The aluminum content remained at <0.5 µg/ml.

4. Conclusion: Chromate calculated as chromium in the amount of about 12 µg/ml prevented 6061-T6 aluminum alloy from corroding in seawater after 30 days.

*Analysis by the Mare Island Naval Shipyard Chemistry Laboratory

Table 2

Part A - 24 Hours

Immersion Data of Aluminum Alloy 1100-H14 (1/8" x 2" x 4") (.3 x 5.1 x 10.2 cms) In Synthetic Seawater and Sodium Chromate

Beaker	Na_2CrO_4 Added Per Liter of Synthetic Seawater (Gms)	Calculated Cr Con. µg/ml (ppm)	Condition of Panels After 24 Hours Immersion
1	None	--	Darkened Surface; white edge corrosion.
2	.003	1	No change
3	.006	2	No change
4	.015	5	No change
5	.03	10	No change
6	.045	15	No change
7	.06	20	No change
8	.075	25	No change
9	.15	50	No change
10	.30	100	No change

Part B - 15 Days

Beaker	pH	Actual Cr Con. (ppm)	Condition of Panels after 15 Days Immersion
1	8.5	<.2	Surface darkened; white corrosion only on edges and hook hole.
2	8.6	0.9	Metal surface bright; very minute amount of corrosion.
3	8.6	1.3	Metal surface bright; very small amount of edge corrosion and crevice in hook hole.
4	8.6	4.3	Few local spots of corrosion; four spots of corrosion on edges; one spot in hook hole; surface bright.
5	8.6	8.9	Surface bright; only a few spots of surface corrosion.
6	8.6	13.3	Surface bright. No surface corrosion; one corrosion spot in hook hole.
7	8.6	17.4	No change
8	8.6	21.4	No change
9	8.6	46	No change
10	8.6	87	No change

The effect Cr Con. for corrosion protection for aluminum alloy 1100-H14 may be estimated at about 15 ppm for the 15 day immersion period in the silent water condition and contained chromate.

Part C - 30 Days

Beaker	Panel Condition after 30 Days Immersion
1	Considerable edge and surface corrosion. Surface darkened. Corrosion in hook hole surface.
2	Surface shiny. Some edge corrosion. Corrosion in hole.
3	Surface shiny. Some edge corrosion. Corrosion in hole.
4	Surface shiny. Some corrosion edge and hole. Few minute surface corrosion spots.
5	Surface shiny. Few spots corrosion on edge. Corrosion in hole.
6	Surface shiny. Few spots corrosion in hole.
7	Surface shiny. One spot corrosion edge. Some corrosion in hole.
8	Surface shiny. One spot edge corrosion. Some corrosion in hole.
9	Surface shiny. One spot corrosion on edge.
10	Surface shiny. No corrosion.

For a period of 30 days, 15-20 ppm Cr should give adequate corrosion protection to aluminum alloy 1100-H14 under silent water conditions and contained chromate.

Table 3

Part A

Pigments in Synthetic Seawater

A. Pigments added to seawater 18 May 1971 (pH of synthetic seawater, 8.5)
B. Solutions sampled 21 June 1971 (34 days).
C. Aluminum alloy 6061-T6 placed in pigment-seawater 19 August 1971 (93 days from 18 May).
D. Solution sampled on 2 September 1971.
E. Aluminum panels removed and examined on 21 September 1971.

	Pigment	Element Determined	Solutions of B Conc. µg/ml	Solutions of D Conc. µg/ml	pH
1.	Seawater	--	--	--	8.5
2.	Strontium Chromate #2821-02	Strontium	260	290	8.4
	Harshaw Chemical Co.	Chromium	160	180	8.4
3.	Basic Lead Silico Chromate	Lead	<1	<1	8.3
	Oncor M-50	Chromium	1.5	0.8	8.3
	National Lead Co.				
4.	Barium Meta Borate	Barium	<5	<5	8.4
	Busan 11-M1				
	Buckman Laboratories				
5.	Zinc Chromate #45-228	Zinc	35	29	7.0
	Reichhold	Chromium	230	230	7.0
6.	Lead Chromate O-1924, 04-5	Lead	<1	<1	8.4
	4908 - Reichhold	Chromium	1.8	1.5	8.4
7.	Yellow Iron Oxide	Iron	<0.2	<0.2	8.5
	Charles Pfizer & Co.				
8.	Organokrome "A"	Chromium	340	370	8.2
	Charles Pfizer & Co.				
9.	Zinc Oxide #427W (lead free)	Zinc	0.7	0.2	8.5
	Eagle Picher				
10.	Basic Zinc Chromate J1345	Zinc	0.8	0.2	8.5
	MPC - Mineral Pigment Corp.	Chromium	4.3	4.3	8.5
11.	Red Lead 97% Type I. Grade B	Lead	<1	<1	8.4
	Lead TT-R-191				
	National Lead Co.				
12.	Zinc Dust #555	Zinc	0.4	0.4	8.0
	American Smelting & Refining Co.				
13.	Alodine 1200 S	Chromium	860	860	2.5
	Amchem Products				
14.	Cuprous Oxide	Copper	0.8	0.6	8.5
	C.K. Williams				
15.	Tributyltin Fluoride	Tin	<10	<10 (Determined later to be 0.6 ppm)	8.3
	M&T Chemical Co.				

Conclusions:

1. Chromates yielding large amounts, several hundred ppm's or µg/ml as Cr, prevent corrosion. Low values such as 1.5, 1.8, etc. ppm Cr, show corrosion.

2. Pigments such as Red Lead, Cuprous Oxide, Tributyltin Fluoride cause accelerated corrosion of aluminum 6061-T6. Barium Meta Borate, Yellow Iron Oxide and Zinc Oxide pit aluminum.

Table 3

Part B

Panel No.	Condition of Panel After 15 Days Immersion
1 (Fig. 12)	(Control: In seawater) Panel turned black - both sides; white corrosion spots 1/16"-1/8" (.15-0.3 cm); pitting. Face - 20 spots; Back - 10 spots.
2 (Fig. 13)	Excellent; no corrosion (surface yellow chromate stain which washes off with water).
3 (Fig. 14)	Face and back spots of white corrosion; face - 5 spots 1/8" (0.3 cm), numerous 1/16"-1/32" (.15-.075 cm) spots; back - 10 1/8" (0.3 cm) spots of corrosion. Also 1/16"-1/32" (.15-.075 cm) spots.
4	Panel turned black both sides. Face - 5 spots 1/8" (.3 cm) corrosion; Back - 12 spots 1/8" (.3 cm) corrosion.
5 (Fig. 15)	Excellent; no corrosion.
6 (Fig. 16)	Panel turned black, both sides. Face - 12 1/32" (.075 cm) spots of corrosion; Back - 8 1/32" (.075 cm) spots of corrosion.
7	Panel turned black. Face - 10 spots corrosion 1/32"-1/8" (.075-0.3 cm); Back - 25 spots corrosion 1/32"-1/8" (.075-0.3 cm).
8	Excellent; no corrosion.
9	Turned black both sides. Face - 30 spots corrosion (1/8" (0.3 cm); Back - 20 spots of corrosion - 1/8" (0.3 cm)
10	Considerable dark areas at and near waterline.
11 (Fig. 17)	Turned black both sides. Face and Back over 50 spots of corrosion 1/8" (0.3 cm) and larger.
12	Turned dark both sides; slightly golden; numerous spots etched or pitted.
13	Both sides surface etched uniformly and a golden deposit formed.
14	Very extensive corrosion - 60% face surface, 50% back surface.
15	Extensive corrosion - 40% face and back surfaces.

Table 4

Part A

Performance and Data on Aluminum Panels Immersed in Synthetic Seawater Containing Glass Panels Coated with Pigmented Epoxy Coatings

Beaker	Aluminum Panel	Primer	Performance of Panels - 40 Hours
1A (Fig. 18)	6061	2-1/2% $SrCrO_4$	Slight corrosion; clear solution
2A (Fig. 18)	"	5% $SrCrO_4$	Slight corrosion; clear solution
3A (Fig. 18)	"	10% $SrCrO_4$	Slight corrosion; solution: Very slight tint of yellow.
4A (Fig. 18)	"	15% $SrCrO_4$	Very slight corrosion; solution: distinctly yellow.
5A	"	20% $SrCrO_4$	Very slight corrosion; solution: more yellow than 4A.
6A	"	25% $SrCrO_4$	OK - No corrosion; solution: more yellow than 5A.
7A	"	2-1/2% Ins.$ZnCrO_4$	Some scattered white corrosion; clear solution.
8A	"	5% Ins. $ZnCrO_4$	Some scattered white corrosion; solution: clear water white.
9A	"	10% Ins. $ZnCrO_4$	Some scattered white corrosion; solution: clear water white.
10A	"	15% Ins. $ZnCrO_4$	Some scattered white corrosion; solution: water white solution.
11A	"	20% Ins. $ZnCrO_4$	Some scattered white corrosion; solution: water white.
12A	"	25% Ins. $ZnCrO_4$	Some scattered white corrosion; solution: water white.
13A	"	15% M-50	Two deep pits; surface corrosion (back-side scratched places); solution: water white.
14A	"	25% M-50	Several pits; surface corrosion; solution: water white.
15A	"	15% 11M1	Surface turned black; many pits and surface corrosion especially near lower edge; solution: water white.
16A	"	25% 11M1	Surface turned black; many pits and surface corrosion over surface; solution: water white.
17A	"	15% Reg. $ZnCrO_4$	Slight corrosion; solution: yellow tint.
18A	"	25% Reg. $ZnCrO_4$	Very slight corrosion; solution: yellow tint.
19A	"	15% $PbCrO_4$	A few pits at lower edge; some surface corrosion; solution: water white.
20	5086	25% $PbCrO_4$	Alloy is 5086-H32; few spots filiform type corrosion; solution: water white.
21	"	15% Fe Oxide	Seems OK; slight etched spots but no white corrosion; solution: water white.
22	"	25% Fe Oxide	One fairly large pit; a few black, filiform type corrosion areas; slight etched spots but no white corrosion; solution: water white.
23	"	15% Organokrome	One filiform shape pit (black); solution: water white.
24	"	25% Organokrome	Minor filiform black areas; one pit; solution: water white.
25A	"	15% ZnO	Panel turned black; two pits; extensive surface etched areas; some white in beaker; solution: water white.
26A	"	25% ZnO	Panel turned black; spots of corrosion with white product; etched areas; solution: water white.
27A	"	15% Red Lead	Panel turned black; few pits; some dark areas; seem to be some white product; solution: water white.
28A	"	25% Red Lead	Panel turned black; few pits; few dark spots; some white products; solution: water white.
29A	"	15% Zn Dust	Panel turned dark; black areas; few pits; areas of bright etched metal; solution: water white.
30A	"	25% Zn Dust	Panel turned dark; black areas; few pits; areas of bright metal; white products; may not be corrosion; solution: water white.
31A	"	45% Zn Dust	Panel turned dark; few bright metal areas; solution: water white.

Table 4 - Part A (Cont.)

Beaker	Aluminum Panel	Primer	Performance of Panels - 40 Hours
32A	5086	15% Cu_2O	Surface darkened; white corrosion edges; several pits; black filiform depressed areas; etched areas; hemisphere droplets milky product; solution: water white.
33A (Fig. 20)	"	25% Cu_2O	Surface darkened; white corrosion edges; few pits; black, filiform depressed areas; hemisphere droplets milky product; solution: water white.
34A (Fig. 20)	"	45% Cu_2O	Surface darkened; white corrosion edges; a few pits; black filiform depressed areas; hemisphere droplets milky product; solution: water white.
35A (Fig. 20)	"	15% TBTF	Panel turned black; several deep pits; areas bright metal; some edge corrosion; solution: water white.
36A (Fig. 20)	"	25% TBTF	Panel turned black; few pits; areas bright metal; some edge corrosion; solution: water white.
37A (Fig. 19)	"	45% TBTF	Panel turned black; several pits; elongated areas of bright metal; some edge corrosion; solution: water white.
38A (Fig. 19)	"	MIL-P-23377B	One side OK; no corrosion; other side 30 filiform type corrosion spots; solution: slight yellow tint.
39 (Fig. 19)	"	Devran 202	Panel turned black; several pits; etched bright metal metal areas; slight edge corrosion; solution: water white.
40 (Fig.19) (Fig. 19)	6061 5086	Seawater Control	Panel turned black; few etched areas; bright metal; some surface corrosion; some slight edge corrosion; (6061 has 2 pits); solution: water white.

Conclusion:

1. With chromate pigmented coatings, a distinct yellow color solution must result for effective corrosion protection of the aluminum.

2. At 3.9 µg/ml as Cr and a slight yellow colored solution (10% strontium chromate PVC), panel shows slight corrosion.

3. At 15.2 µg/ml as Cr (15% strontium chromate PVC), with a distinct yellow colored solution, the aluminum panel shows only very slight corrosion (practically nil).

4. About 15 µg/ml Cr seems to be a minimum value to show some evidence of corrosion protection of the aluminum.

5. Coatings pigmented with red lead, cuprous oxide and tributyltin fluoride cause accelerated pitting corrosion of aluminum.

6. Coatings pigmented with barium meta borate, yellow iron oxide, and zinc oxide cause some pitting of aluminum.

Table 4

Part B

Beaker	Coating		Concentration in µg/ml or ppm 48 Hr. Value	30 Days
1A	2-1/2% $SrCrO_4$	Cr =	0.2	0.3
2A	5% $SrCrO_4$	Cr =	0.4	0.5
3A	10% $SrCrO_4$	Cr =	3.9	12.4
4A	15% $SrCrO_4$	Cr =	15.2	55.0
5A	20% $SrCrO_4$	Cr =	27.0	95.0
6A	25% $SrCrO_4$	Cr =	35.0	128.
7A	2-1/2% Insoluble $ZnCrO_4$	Cr =	1.0	1.6
8A	5% Insoluble $ZnCrO_4$	Cr =	<0.1	<0.1
9A	10% Insoluble $ZnCrO_4$	Cr =	<0.1	<0.1
10A	15% Insoluble $ZnCrO_4$	Cr =	<0.1	<0.1
11A	20% Insoluble $ZnCrO_4$	Cr =	0.2	0.2
12A	25% Insoluble $ZnCrO_4$	Cr =	<0.1	<0.1
13A	15% Lead Silico Chromate	Cr =	<0.1	<0.1
14A	25% Lead Silico Chromate	Cr =	<0.1	0.2
15A	15% Barium Borate	Ba =	<5	<5
16A	25% Barium Borate	Ba =	<5	<5
17A	15% $ZnCrO_4$	Cr =	8.2	10.1
18A	25% $ZnCrO_4$	Cr =	12.2	14.4
19A	15% $PbCrO_4$	Cr =	4.1	0.2
20A	25% $PbCrO_4$	Cr =	4.1	0.2
21A	15% Fe Oxide	Fe =	<0.2	<1
22A	25% Fe Oxide	Fe =	<0.2	<1
23A	15% Organokrome	Cr =	0.1	<0.1
24A	25% Organokrome	Cr =	4.4	14
25A	15% ZnO	Zn =	0.1	0.1
26A	25% ZnO	Zn =	0.1	0.1
27A	15% Red Lead	Pb =	<1	<1
28A	25% Red Lead	Pb =	<1	<1
29A	15% Zn Dust	Zn =	0.1	0.1
30A	25% Zn Dust	Zn =	0.1	0.1
31A	45% Zn Dust	Zn =	0.1	0.1
32A	15% Cu_2O	Cu =	0.1	0.1
33A	25% Cu_2O	Cu =	0.2	0.1
34A	45% Cu_2O	Cu =	0.3	0.1
35A	15% Tributyltin Fluoride	Sn*=	<10	0.2
36A	25% Tributyltin Fluoride	Sn*=	<10	0.2
37A	45% Tributyltin Fluoride	Sn*=	<10	0.4
38A	MIL-P-23377B Epoxy $SrCrO_4$	Cr =	6.3	38
39A	Devran 202 Lead Silico Chromate	Cr =	<0.1	<0.1

Note: *(Sn) tin determined by emission spectroscopy all others by atomic absorption spectroscopy.

Table 5

Performance Data of System Coated-Scribed #356 (Cast) and 1100-H14 Aluminum Panels After 18 Months Immersion in Cycle Test of Specification MIL-P-23236

Performances are Averages on Both #356 and 1100 Alloys

Panel No.	Scribed Areas #2 and #3 Primer Plus Topcoat Scribe #2	Scribe #3	Performance* at Scribes #2	#3	Panel No.	Scribed Areas #2 and #3 Primer Plus Topcoat Scribe #2	Scribe #3	Performance* at Scribes #2	#3
1	Zn 25/10	A	70	90	13	Sr 25/10	A	85	90
2	Zn 25/15	A	80	90	14	Sr 25/15	A	90	95
3	Zn 25/20	A	80	90	15	Sr 25/20	A	95	95
4	Zn 30/10	A	40	80	16	Sr 30/10	A	90	95
5	Zn 30/15	A	70	85	17	Sr 30/15	A	90	97
6	Zn 30/20	A	87	90	18	Sr 30/20	A	95	97
7	Zn 35/10	A	50	77	19	Sr 35/10	A	90	95
8	Zn 35/15	A	65	77	20	Sr 35/15	A	87	95
9	Zn 35/20	A	85	90	21	Sr 35/20	A	95	97
10	Barytes 25	A	0	70	22 (Fig.23)	Asbestine (3x)25	A	0	60
11 (Fig.21)	Zn 25	A	80	90	23 (Fig.24)	#117 Wash Primer	A	40	80
12 (Fig.22)	Sr 25	A	95	97	24	Commercial Lead Silico Chromate Epoxy	A	0	75

Coatings:

Zn - Basic Zinc Chromate
Sr - Strontium Chromate
A - Conversion Coating Alodine 1200
Topcoat - Epoxy

*Rating Method: 100 to 0 (10) - no defects; 0 - complete failure)

Total PVC/PVC of inhibitive pigment, i.e., Zn: 25/10

Defects include: Corrosion, undercutting, blisters, film lifting.

Conclusion:

1. Alodine 1200 conversion coating (MIL-C-5541) improves performances of "poor" or low performing primers. Strontium chromate primers are improved only slightly. In such cases, if clean surfaces can be assured, alodine conversion treatment may be eliminated.

2. The most effective inhibitive pigment tested here is strontium chromate, used in an epoxy binder in the amount of 20-25% PVC, with a total pigmentation of 25-35% PVC. Possibly depending on use, acceptable performances may be derived from compositions of 10-20% PVC strontium chromate, with total PVC of 25-35%.

Table 6

Performances of Coated-Scribed Aluminum Panels

Panel No.	Aluminum Alloy	Experimental Coating Total PVC = 35%	Performance Rating* at Scribe			
			Scribe No.	3 Months	Scribe No.	6 Months
		(Control)			1	2.5
437 (Fig.25)	5086-H32	2-1/2% PVC Strontium Chromate	2	9.8	3 (Fig. 31)	3.3
					5	3.3
438	"	5% Strontium Chromate	7	9.9	8	5
					10	7.5
439	"	10% Strontium Chromate	12	10	13	6.7
					15	6.7
440	"	15% Strontium Chromate	17	10	18	9
					20	9
441	"	20% Strontium Chromate	22	10	23	9
					25	9
442 (Fig.26)	"	25% Strontium Chromate	27	10	28 (Fig. 32)	10
					30	10
478	6061-T6	2-1/2% Strontium Chromate	211	10	212	7.5
					214	5
479	"	5% Strontium Chromate	216	9.9	217	8.5
					219	7.5
480	"	10% Strontium Chromate	221	9.9	222	8.5
					224	9
481	"	15% Strontium Chromate	226	10	227	9.7
					229	9.7
482	"	20% Strontium Chromate	231	9.8	232	9.9
					234	9.9
483	"	25% Strontium Chromate	236	10	237	9.9
					239	10
443	5086-H32	2-1/2% Insoluble Zinc Chromate	32	9.7	33	3.3
					35	3.3
444	"	5% Insoluble Zinc Chromate	37	9.9	38	5
					40	5
445	"	10% Insoluble Zinc Chromate	42	9.9	43	5
					45	5
446	"	15% Insoluble Zinc Chromate	47	10	48	6.7
					50	7.5
447	"	20% Insoluble Zinc Chromate	53	9.9	54	8.5
					56	8.5
448	"	25% Insoluble Zinc Chromate	58	9.9	59	9
					61	8.5
453	"	15% Zinc Chromate	83	10	84	9.8
					86	9.8
454	"	25% Zinc Chromate	88	10	89	9.9
					91	9.9
455	"	15% Lead Chromate	93	7.5	94	5
					96	5
456	5456-H321	25% Lead Chromate	98	9	99	5
					101	5
449 (Fig.27)	5086-H32	15% Lead Silico Chromate	63	9	64 (Fig.33)	6.7
					66	6.7
450	"	25% Lead Silico Chromate	68	9	69	7.5
					71	7.5
451	"	15% Barium Meta Borate	73	9.5	74	6.7
					76	6.7
452	"	25% Barium Meta Borate	78	9.5	79	6.7
					81	6.7
457	5456-H321	15% Yellow Iron Oxide	103	9	104	6.7
					106	6.7

Table 6 (Cont.)

Panel No.	Aluminum Alloy	Experimental Coating Total PVC = 35%	Performance Rating* at Scribe			
			Scribe No.	3 Months	Scribe No.	6 Months
458	5456-H321	25% Yellow Iron Oxide	108	9.3	109	6.7
					111	7.5
459	"	15% Organokrome	113	10	114	7.5
					116	9
460	"	25% Organokrome	118	9.8	119	9.8
					121	9
461	"	15% Zinc Oxide	123	8.5	124	6.7
					126	5
462	"	25% Zinc Oxide	128	7.5	129	9
					131	9
463	"	15% Red Lead	133	5	134	2.5
					136	2.5
464	"	25% Red Lead	138	3.3	139	2.5
					141	2.5
465	"	15% Zinc Dust	143	9	144	6.7
					146	6.7
466	"	25% Zinc Dust	X	8	148	6.7
					150	6.7
467	"	45% Zinc Dust	152	9	153	6.7
					155	5
475	5086-H32	1. MIL-C-5541 Chrome Treatment	195	0	196	2.5
					198	5
		2. 5% Strontium Chromate				
476	5456-H321	Same	200	3.3	201	0
					203	0
477	6061-T6	Same	206	9.9	207	9
					209	7.5
484 (Fig.28)	"	MIL-P-23377 (12% Strontium Chromate, Total PVC = 27%)	241	9.9	242 (Fig.34)	7.5
					244	7.5
474	5456-H321	MIL-P-23377 (12% Strontium Chromate, Total PVC = 27%)	190	6.7	191	5
					193	5
485 (Fig.29)	6061-T6	Commercial Epoxy Lead Silico Chromate	246	8.5	247 (Fig.35)	6.7
					249	5

*Rating of Scribe: 0 = Scribe completely filled with white corrosion products. Scale 0-10; 10 = No corrosion products - bright metal.



FIG. 1 - DISSIMILAR METAL CORROSION OF 6061-T6 ALUM. RADAR ANTENNA PLUMBING. (OFFICIAL U.S. NAVY PHOTOGRAPH)

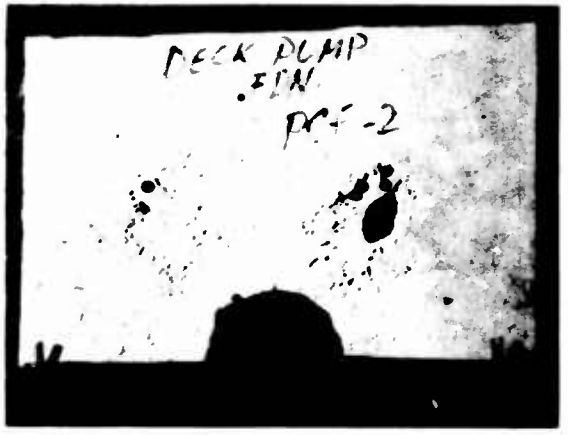


FIG. 2 - PITTING CORROSION OF 5456-H321 ALUM. HULL SEGMENT. (OFFICIAL U.S. NAVY PHOTOGRAPH)



FIG. 3 - EXFOLIATION CORROSION OF 5456-H321 ALUM. HULL SECTION. (OFFICIAL U.S. NAVY PHOTOGRAPH)

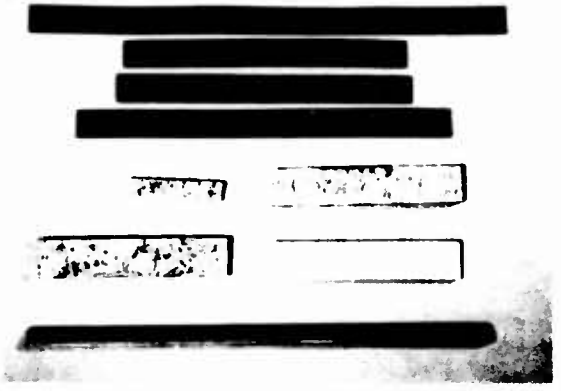


FIG. 4 - ALUM. ALLOYS SUBJECTED TO ONE WEEK SEAWATER-ACETIC ACID TEST. (OFFICIAL U.S. NAVY PHOTOGRAPH)

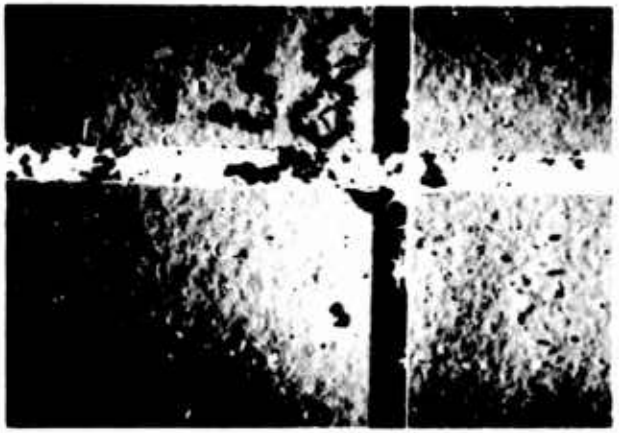


FIG. 5 - COATED AND SCRIBED 5456-H321 ALUM. SUBJECTED TO ONE WEEK SWAACT TEST. (OFFICIAL U.S. NAVY PHOTOGRAPH)

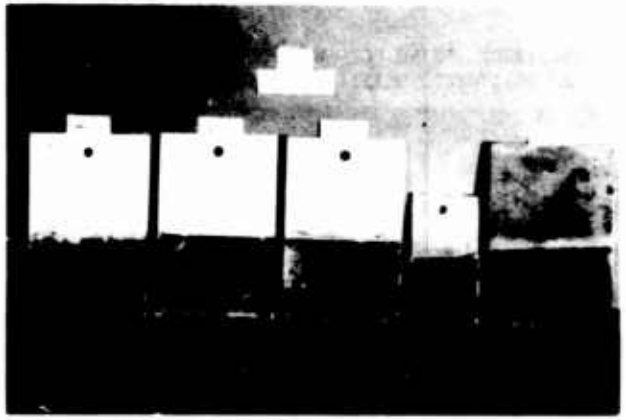


FIG. 6 - ALUM. ALLOYS IMMERSED IN SYNTHETIC SEAWATER-30 DAYS IN THE DARK. (OFFICIAL U.S. NAVY PHOTOGRAPH)



FIG. 7 - ALUM. ALLOYS IMMERSED IN THE OCEAN-30 DAYS IN THE DARK. (OFFICIAL U.S. NAVY PHOTOGRAPH)



FIG. 8 - ALUM. ALLOYS IMMERSED IN THE OCEAN-30 DAYS IN THE DARK - GALVANIC CORROSION. (OFFICIAL U.S. NAVY PHOTOGRAPH)



FIG. 9 - FOULING ON ALUM. ALLOYS AFTER 60 DAYS IMMERSION IN THE OCEAN. (OFFICIAL U.S. NAVY PHOTOGRAPH)



FIG. 10 - BARNACLE ATTACHED ON 5086-H116 ALUM. ALLOY. (OFFICIAL U.S. NAVY PHOTOGRAPH)



FIG. 11 - PITTING CORROSION RESULTING UNDER BARNACLE DUE TO OXYGEN-CONCENTRATION CELL. (OFFICIAL U.S. NAVY PHOTOGRAPH)



FIG. 12 - CLOSE-UP SHOWING PITTING CORROSTION OF 6061-T6 ALUM. IN SYNTHETIC SEAWATER - 33 DAYS. (OFFICIAL U.S. NAVY PHOTOGRAPH)

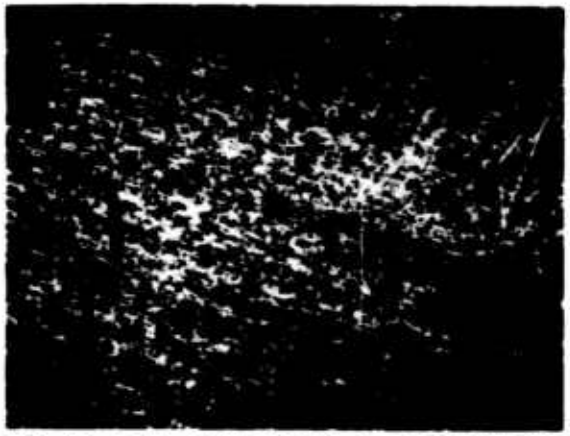


FIG. 13 - ALUM. ALLOY 6061-T6 AFTER 33 DAYS IMMERSION IN SYNTHETIC SEAWATER WITH BULK STRONTIUM CHROMATE PIGMENT. (OFFICIAL U.S. NAVY PHOTOGRAPH)

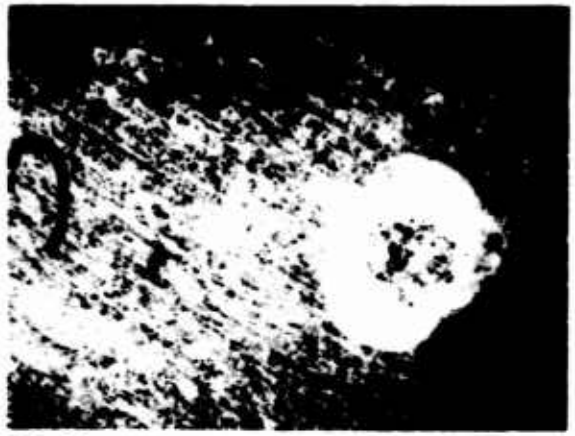


FIG. 14 - ALUM. ALLOY 6061-T6 AFTER 33 DAYS IMMERSION IN SYNTHETIC SEAWATER WITH BULK LEAD SILICO CHROMATE PIGMENT. (OFFICIAL U.S. NAVY PHOTOGRAPH)

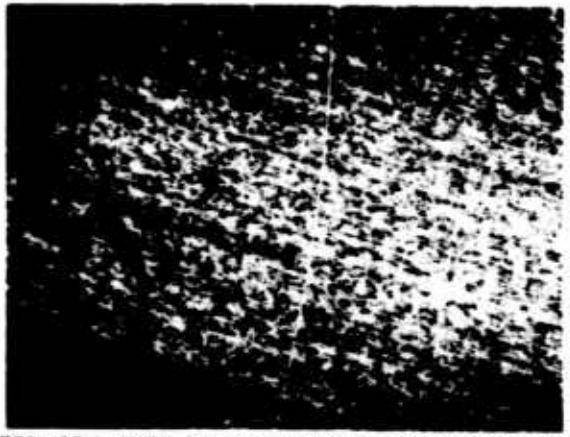


FIG. 15 - ALUM. ALLOY 6061-T6 AFTER 33 DAYS IMMERSION IN SYNTHETIC SEAWATER WITH BULK ZINC CHROMATE. (OFFICIAL U.S. NAVY PHOTOGRAPH)

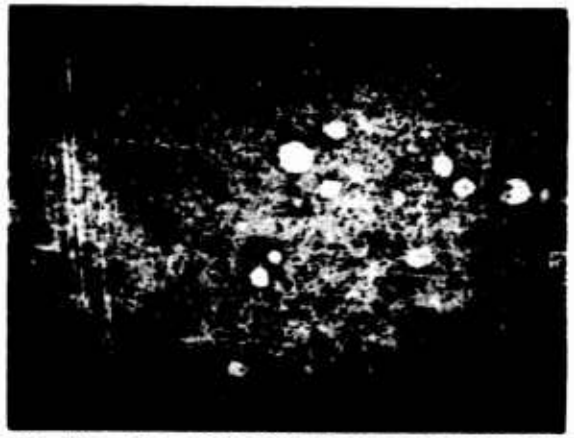


FIG. 16 - ALUM. ALLOY 6061-T6 AFTER 33 DAYS IMMERSION IN SYNTHETIC SEAWATER WITH BULK LEAD CHROMATE. (OFFICIAL U.S. NAVY PHOTOGRAPH)

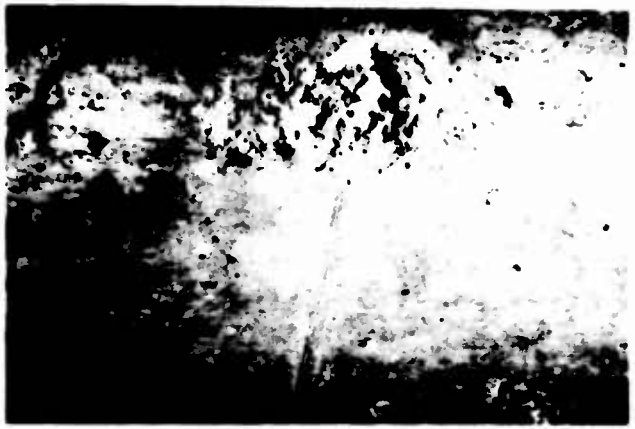


FIG. 17 - ALUM. ALLOY 6061-T6 AFTER 33 DAYS IMMERSION IN SYNTHETIC SEAWATER WITH BULK RED LEAD PIGMENT. (OFFICIAL U.S. NAVY PHOTOGRAPH)



FIG. 18 - CONDITION OF ALUM. ALLOY 6060-T6 AFTER 30 DAYS IMMERSION IN SYNTHETIC SEAWATER WITH PREVIOUSLY IMMERSED GLASS PANELS COATED WITH EPOXY COATINGS, PIGMENTED WITH VARYING STRONTIUM CHROMATE (2-1/2%, 5%, 10% and 15% PVC). (OFFICIAL U.S. NAVY PHOTOGRAPH)



FIG. 19 - CONDITION OF ALUM. ALLOY 6061-T6 AFTER 30 DAYS IMMERSION IN SYNTHETIC SEAWATER WITH PREVIOUSLY IMMERSED GLASS PANELS COATED WITH EPOXY COATINGS, PIGMENTED WITH TBTF (45% PVC), STRONTIUM CHROMATE (12% PVC, MIL-P-23377) AND LEAD SILICO CHROMATE (COMMERCIAL EPOXY). (OFFICIAL U.S. NAVY PHOTOGRAPH)

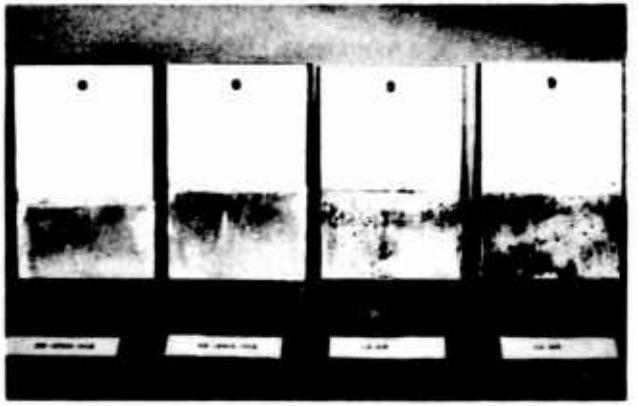


FIG. 20 - CONDITION OF ALUM. ALLOY 6061-T6 AFTER 30 DAYS IMMERSION IN SYNTHETIC SEAWATER WITH PREVIOUSLY IMMERSED GLASS PANELS COATED WITH EPOXY COATING PIGMENTED WITH CUPROUS OXIDE (25, 45% PVC) AND TBTF (15, 25% PVC). (OFFICIAL U.S. NAVY PHOTOGRAPH)

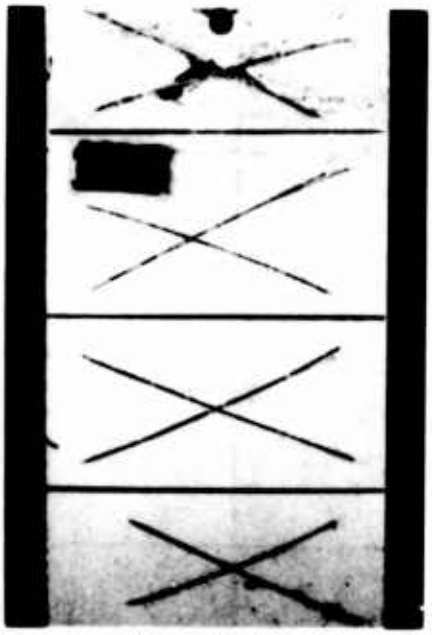


FIG. 21 - CONDITION CAST ALUM. #356, COATED AND SCRIBED, AFTER 18 MO'S CYCLE TEST MIL-P-23236. EPOXY, BASIC ZINC CHROMATE, 25% PVC (PERFORMANCE 80% AND 90%) (OFFICIAL U.S. NAVY PHOTOGRAPH)

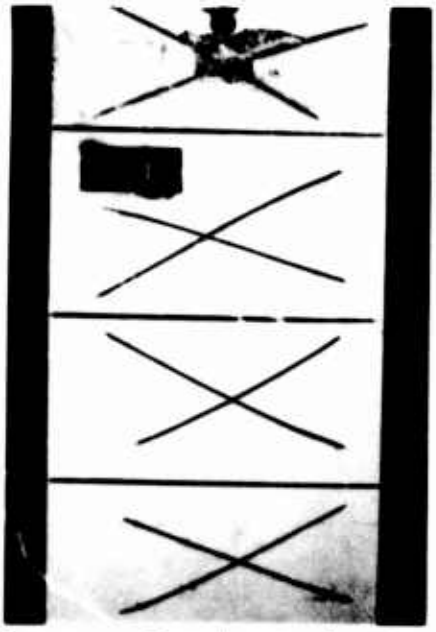


FIG. 22 - CONDITION CAST ALUM. #356, COATED AND SCRIBED, AFTER 18 MO'S CYCLE TEST MIL-P-23236. EPOXY, STRONTIUM CHROMATE, 25% PVC (PERFORMANCE 95% AND 97%) (OFFICIAL U.S. NAVY PHOTOGRAPH)

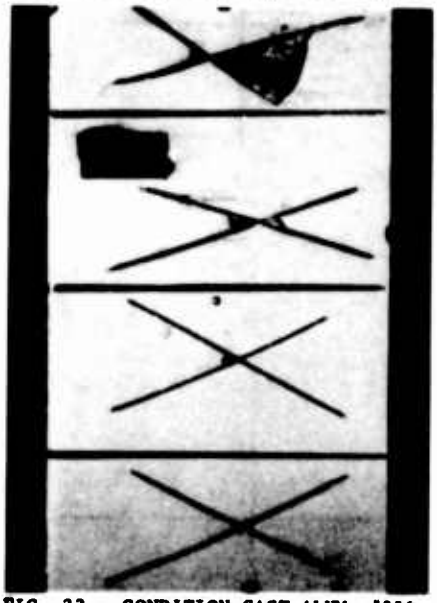


FIG. 23 - CONDITION CAST ALUM. #556, COATED AND SCRIBED, AFTER 18 MO'S CYCLE TEST MIL-P-23236. EPOXY, ASBESTINE 3X, 25% PVC (PERFORMANCE - 0% AND 60%) (OFFICIAL U.S. NAVY PHOTOGRAPH)

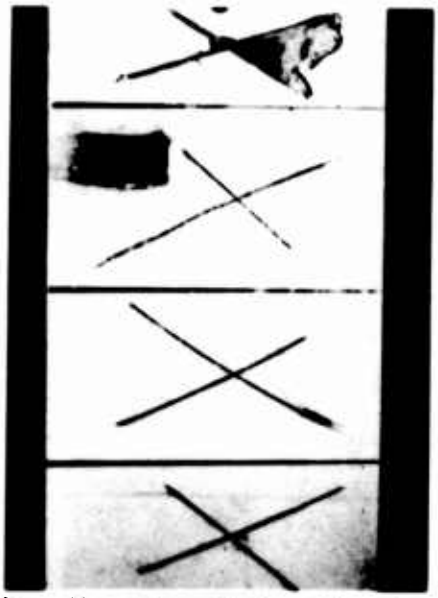


FIG. 24 - CONDITION CAST ALUM. #356, COATED AND SCRIBED, AFTER 18 MO'S CYCLE TEST MIL-P-23236. FORMULA #117 (MIL-P-15328) (PERFORMANCE - 40% AND 80%) (OFFICIAL U.S. NAVY PHOTOGRAPH)

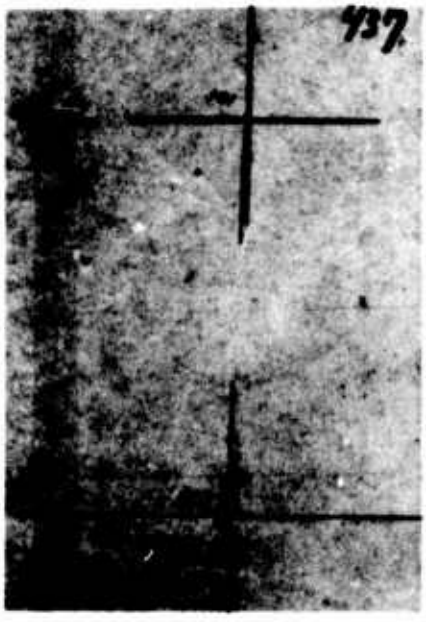


FIG. 25 - CONDITION 6061-T6 (#437) COATED SCRIBED, 3 AND 6 MO'S IN 23236. SCRIBE #2 (101) - 3 MO, RATING 9.8. SCRIBE #3 (102) RATING 3.3 (2-1/2% STRONTIUM CHROMATE) (OFFICIAL U.S. NAVY PHOTOGRAPH)

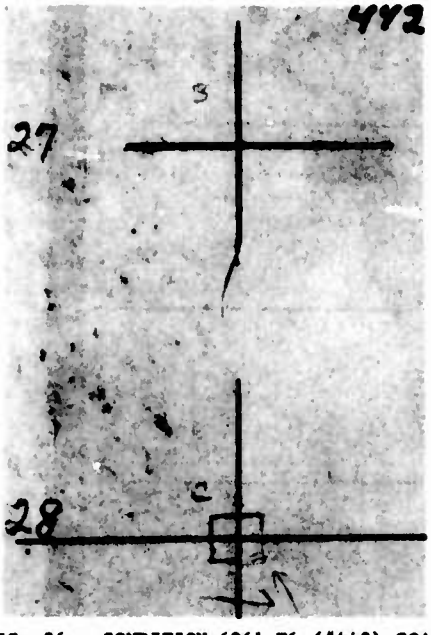


FIG. 26 - CONDITION 6061-T6 (#442) COATED SCRIBED, 3 AND 6 MO'S IN 23236. SCRIBE #27 (B) 3 MO, 10 RATING. SCRIBE #28 (C, 11) 6 MO'S 10 RATING (25% PVC STRONTIUM CHROMATE). (OFFICIAL U.S. NAVY PHOTOGRAPH)

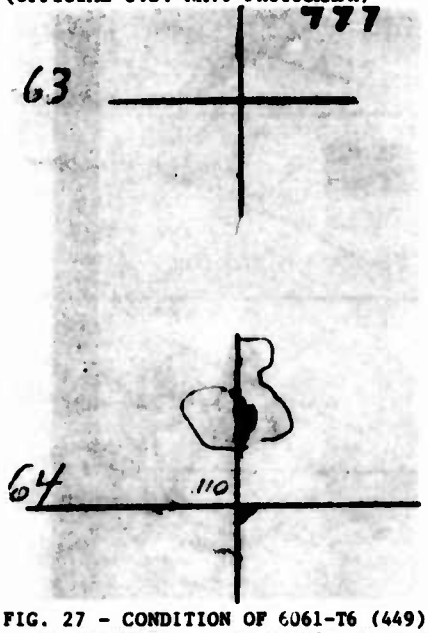


FIG. 27 - CONDITION OF 6061-T6 (449) COATED-SCRIBED, 3 AND 6 MO'S IN 23236. SCRIBE #63, 3 MO RATING 9. SCRIBE #64 (110) 6 MO'S RATING 6.7. (15% LEAD SILICO CHROMATE) (OFFICIAL U.S. NAVY PHOTOGRAPH)



FIG. 28 - CONDITION OF 6061-T6 (484), COATED-SCRIBED, 3 AND 6 MO'S IN 23236. SCRIBE #241, 3 MO RATING 9.9. SCRIBE #242 (121) 6 MO 7.5 RATING. (12% PVC STRONTIUM CHROMATE, MIL-P-23377) (OFFICIAL U.S. NAVY PHOTOGRAPH)



FIG. 29 - CONDITION OF 6061-T6, COATED-SCRIBED 3 AND 6 MO IN 23236, SCRIBE #246, 3 MO RATING 8.5. SCRIBE #247 (122) 6 MO RATING 6.7 (COMMERCIAL EPOXY, LEAD SILICO CHROMATE). (OFFICIAL U.S. NAVY PHOTOGRAPH)



FIG. 30 - CONDITION OF 6061-T6, COATED-SCRIBED 6 MO'S IN 23236. SCRIBE AREA 100 PERFORMANCE 2.5 RATING (MIL-P-24441 SYSTEM - 1 COAT EACH 150, 151 AND 152) (OFFICIAL U.S. NAVY PHOTOGRAPH)



FIG. 31 - CONDITION OF 6061-T6, COATED-SCRIBED, 6 MO'S IN 23236, #3 (102) 6 MO'S 3.3 RATING (2-1/2% PVC STRONTIUM CHROMATE) (OFFICIAL U.S. NAVY PHOTOGRAPH)



FIG. 32 - CONDITION OF 6061-T6, COATED-SCRIBED 6 MO IN 23236, SCRIBE #28 (11), 6 MO 10 RATING. (25% PVC STRONTIUM CHROMATE) (OFFICIAL U.S. NAVY PHOTOGRAPH)



FIG. 33 - CONDITION OF 6061-T6, COATED-SCRIBED, 6 MO IN 23236, SCRIBE AREA 110, 6 MO RATING 6.7 (15% PVC, LEAD SILICO CHROMATE) (OFFICIAL U.S. NAVY PHOTOGRAPH)

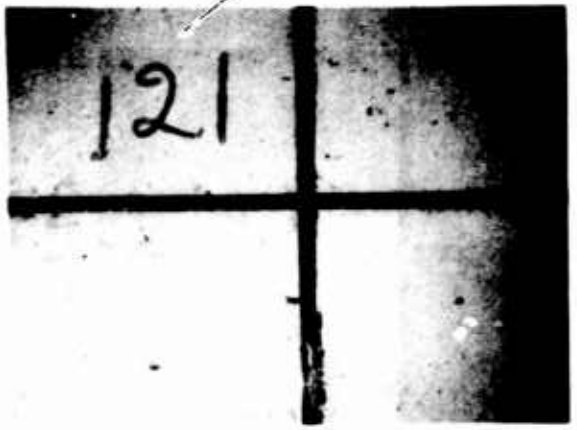


FIG. 34 - CONDITION OF 6061-T6, COATED SCRIBED, 6 MO IN 23236, SCRIBE AREA 121, 6 MO RATING 7.5 (12% PVC STRONTIUM CHROMATE, MIL-P-23377) (OFFICIAL U.S. NAVY PHOTOGRAPH)



FIG. 35 - CONDITION OF 6061-T6, COATED-SCRIBED, 6 MO IN 23236, SCRIBE AREA 122, 6 MO RATING 6.7. (COMMERCIAL EPOXY, LEAD SILICO CHROMATE) (OFFICIAL U.S. NAVY PHOTOGRAPH)

References

1. U.S. Naval Ship Systems Command Notice 4700 of 16 May 1969 (NAVSHIPS Note 4700 6101D:TCW:an Ser 22), Enclosure (1).

2. Carson L. Brooks, "Aluminum-Magnesium Alloys 5086 and 5456-H116," Naval Engineering Journal, pp. 29-32, August 1970.

3. Booklet, "Aluminum Alloys in the Plastics and Resins Industries, p. 14. The Aluminum Association - Machinery and Equipment Committee (2nd Ed.).

4. Paper, "Exfoliation Corrosion of Aluminum Alloys," S.J. Ketcham and I.S. Shaffer, Naval Air Dev. Center, Warminister, Pa. Given at ASTM Annual Meeting at Atlantic City, N. J., June 1971 (Committee G-1 on Corrosion of Metals).

5. W. L. Fink and L. A. Willey, Aluminum Research Laboratory, New Kensington, Pa., "AL-MG Aluminum-Magnesium Constitution of Binary Alloys," p. 1163, Metals Handbook, American Society for Metals, 1948 Edition.

6. H. B. Romans, "Standard Method for Exfoliation Testing of Aluminum Alloys MRD STP-AC7" in "Standard Testing Methods for Applied Corrosion Studies in Stress Corrosion Cracking and Exfoliation Corrosion of Aluminum Alloys," Reynolds Metal Company, 16 April 1968.

7. Report by Alcoa Research Laboratories, New Kensington, Pennsylvania, "Tentative Immersion Type Exfoliation Test Procedure; Exfoliation Test for AL-MG Alloys for Boat and Ship Hull Construction."

8. F. W. Breuer, "Evaluation of Anticorrosive Coatings for Aluminum Alloy Hulls. Test Methods and Preliminary Results," Unpublished report of the Mare Island Paint Laboratory, Mare Island Naval Shipyard, Vallejo, Ca. 94592. Report No. 69-5, Nov 1969.

9. J. R. Saroyan, "Equipment Subject to Stack Gas and Marine Environment," Progress Report on Chemical Conversion Coatings on Aluminum, Report No. 58-12, 3 Dec 1958.

10. "Corrosion Behaviour of Metals and Alloys Under Immersed Conditions in Indian Harbours" by C. P. De, V. M. Kelkar and M. D. Vora, Naval Chemical and Metallurgical Laboratory, Naval Dockyard, Bombay, India, presented at the 2nd International Congress on Marine Corrosion and Fouling, Athens, Greece, Sep 1968.

11. George A. Walker and Huai-Pu Chu, "Some Observations on the Stress Corrosion Characteristics of High Strength Aluminum Alloys in Marine Environment." Corrosion, Vol. 28, No. 6, June 1972, pp. 233-242.

12. John R. Saroyan, "Countdown for Antifouling Paints," p. 2, Table 2, presented at The 2nd International Congress on Marine Corrosion and Fouling, 20-24 Sep 1968, Athens, Greece.

13. S. R. Galler, "Boring and Fouling," pp. 7-18, Publication, Handbook of Ocean and Underwater Engineering. Myers, Holm and McAllister, McGraw-Hill Book Co., New York (1969).

Oral Discussion

Carson: Have you ever tried aluminum pigmented vinyl as an anti-corrosive?

Saroyan: We are trying it in the U.S. Navy now, yes, not only on panels but on ships.

Corrosion Prevention with Thermal Sprayed Zn & Al Coatings

American Welding Society Committee on Thermal Spraying

c/o Longo, F. N. and Durmann, G. J.
METCO, Inc.
1101 Prospect Ave.
Westbury, N. Y. 11590

This paper presents the results of eighteen years testing, undertaken by the American Welding Society, to evaluate flame sprayed zinc and aluminum coatings, sealed and unsealed, applied to low carbon steel.

Panels were exposed to sea water at mean tide and below low tide levels at two different locations. Panels were also exposed to atmospheric conditions at six different locations including rural, industrial, salt air and salt spray environments.

The results indicate that low carbon steel can be protected from the corrosive effects of these environments for eighteen years or more by the application of flame sprayed zinc or aluminum coatings.

Introduction

This paper reports the results of an eighteen year study of the corrosion protection afforded by wire flame sprayed aluminum and zinc coatings applied to low-carbon steel. The program was initiated in July 1950 by the Committee on Metallizing of the American Welding Society (now the Committee on Thermal Spraying). The first panels were exposed in January, 1953. This report is a presentation of the results of an inspection of the metallized coated steel panels made after all panels had been exposed for eighteen years.

Originally, exposure periods of 1, 3, 6 and 12 years were scheduled. At the end of each of the above periods, a complete set of panels, consisting of three identical panels of each type, was to be removed from the exposure racks for laboratory examination. At the same time, the panels of each type remaining on site were to be inspected and their condition recorded. However, early inspections indicated that nearly all coatings would last for more than twelve years, at all exposure sites. Accordingly, the panels scheduled for removal at six years were left on exposure for twelve years, and the twelve year set was left exposed for eighteen years. Results of the 6 year and 12 year inspections are reported in AWS publications C2.8-62 and C2.11-67 respectively.

The initial program details discussed here, with minor deletions, were taken directly from the AWS 12 year report C2.11-67.

Test Sites

Test sites were selected to provide a wide variety of environmental conditions. These exposure sites and the exposure dates for the panels in this program are listed in Appendix 1. All sites are recognized ASTM test areas. No really mild, rural exposures were included; some degree of atmospheric contamination, either saline or industrial, exists at all sites. Sea water tests include full and half-tide immersion in quiet sea water, and full immersion in flowing sea water (approximately 3 knots).

Test panels for atmospheric exposure are mounted on racks in a position which is 30 degrees from the horizontal.

Panels for sea water immersion are mounted in a vertical position.

Test Panels

Test panels were made of low-carbon steel sheet (carbon - 0.08 percent, manganese - 0.30 percent, phosphorus - 0.008 percent, sulfur - 0.03 percent, silicon - 0.003 percent, copper - 0.30 percent). The sizes of steel panels for atmospheric and sea water exposure were 4 x 6 x 1/8 in. (102 x 152 x 3.2mm) and 4 x 12 x 1/8 in. (102 x 305 x 3.2mm) respectively.

The aluminum and zinc wire flame sprayed coating thicknesses for atmospheric exposure tests were 0.003, 0.006, 0.009, 0.012 and 0.015 inches (.08, 0.15, 0.23, 0.34 and 0.41mm). In addition to these, a coating thickness of 0.018 in. (0.49mm) was included in the sea water exposure tests.

Panel Preparation

The as-supplied panels were hot rolled steel which had been pickled to remove mill scale. Surfaces were inspected and panels showing gross defects were rejected.

The panels were then thoroughly blast cleaned using a forced-feed blast generator and a minimum pressure of 90 psi (620 Kg/m^2) at the generator with the types and mesh sizes of abrasives as shown in Appendix 2.

The flame spraying operation was done on a special automatic machine on which 36 panels were flame sprayed at one time. The speeds of rotation and traverse of both panels and wire flame spray gun across the surface were automatically controlled in order to obtain uniformity of coating thickness.

Three types of wire were used:

1. 1/8 in. (3.2mm) dia. aluminum - 99.0 percent min. purity
2. 1/8 in. (3.2mm) dia. zinc - 99.9 percent min. purity
3. 1/8 in. (3.2mm) dia. steel, SAE 1010 grade; carbon - 0.08/0.12 percent, phosphorus - 0.04 percent max., sulfur - 0.05 percent max.

The steel wire was used for a flash bonding coat on some specimens, and was applied automatically to a thickness of 0.001 inches (.03mm). This bonding coat is not considered as part of the coating thickness.

Sealing treatments, where used, were applied by spraying. Appendix 3 shows the composition of the sealing materials. These formulations were thinned sufficiently to insure good penetration and were applied sparingly. The purpose was to fill the surface and subsurface pores of the sprayed metal, rather than to overcoat. By actual measurements the sealers used, added little or nothing to the coating thickness.

The types of aluminum and zinc coated panels are listed in Appendices 4 and 5; Types 14 to 28, inclusive, were included in order to determine the effect of preparation of the steel on the life of the coating. All of these panels had a coating thickness of .009 in. (0.23mm) and are located at only two of the tests sites: Kure Beach, North Carolina (80-ft. (24m) lot) for atmospheric exposure and Wrightsville Beach, North Carolina (mean tide) for sea water exposure.

Conclusions

1. Aluminum coatings .003 in. to .006 in. (.08mm to .15mm) both sealed and unsealed give complete base metal protection from corrosion in sea water, and also in severe marine and industrial atmospheres.

2. Unsealed zinc coatings require .012 in. (.34mm) for complete protection in sea water for eighteen years. In severe marine and industrial atmospheres .009 in. (.23mm) of unsealed zinc or .003 in. to .006 in. (.08mm to .15mm) of sealed zinc are needed for eighteen years protection.
3. The application of one coat of wash primer plus one or two coats of aluminum vinyl enhances the appearance and extends the life of aluminum and zinc coatings.
4. Thin coats of aluminum perform better because they have less tendency to develop pits and blisters.
5. The corrosion protection afforded by zinc and aluminum coatings is not affected by method of steel preparation. Specifically, a steel flash is not essential as a bond coat.
6. The use of flame sprayed aluminum and zinc coatings must be considered as a means to extend the life of iron and steel structures and thereby help to conserve these natural resources.

Results

The following results are divided into three separate sections:

1. Sea Water Exposure - Total Immersion & Mean Tide
2. Marine Atmosphere
3. Industrial Atmosphere

It should be kept in mind that these results pertain primarily to the overall general condition of the test panels at each of the above three types of exposure sites.

SEA WATER EXPOSURE - TOTAL IMMERSION & MEAN TIDE

Wrightsville Beach, North Carolina - Mean Tide

Aluminum Coated Panels

Unsealed aluminum coated panels at this site show a few blisters which originate at the coating: steel interface. The heavier the coating the larger the blisters, in some cases 5/16 in. (8mm) diameter. In those cases where a blister has broken open, the exposed steel is relatively free of corrosion. A layer of iron oxide is present but no measurable loss of steel is evident. While the aluminum surrounding these broken blisters probably contributed to the protection of the steel there is no significant evidence of corrosion of the aluminum. See Fig. 1 for the typical aluminum structure. Scraping the aluminum surface presents a bright, metallic lustre.

All vinyl sealed panels are in excellent condition including those which were coated with only .003 in. (.08mm) of aluminum. See Fig. 2. A few small blisters are present on some of the sealed panels but considerably smaller than on the unsealed aluminum panels. Breaking open these blisters reveals typical voluminous aluminum corrosion products and a thin layer of rust on the steel. No measurable loss of steel is evident. This is also true where the coatings were mechanically damaged at the edges by the ceramic mounting insulators. Areas as large as 1/2 in. (13mm) X 1/8 in. (3mm) of exposed steel show no significant loss of steel. No progressive corrosion of the aluminum surrounding these areas is evident.

There is no noticeable difference in coating performance as a function of the variations in surface preparation methods tested (see Appendix 2).

Zinc Coated Panels

All unsealed zinc coated panels of less than 0.012 in. (.34mm) in coating thickness have failed. The 0.012 in. (.34mm), 0.015 in. (.41mm) and 0.018 in. (.49mm) thick unsealed zinc coatings show little or no rust but the coatings have been almost completely converted to corrosion product. See Fig. 3.

Chlorinated rubber sealers on zinc did not perform satisfactorily. The steel is deeply pitted where coatings have failed, and the appearance indicates that the residual zinc

corrosion product has become cathodic to the exposed steel. There is no evidence to show that there is any difference in coating performance as a result of the surface preparation methods tested.

Wrightsville Beach, North Carolina - Total Immersion

Aluminum Coated Panels

Unsealed aluminum coatings at this site appear to blister slightly more than those at the mean tide level. The steel is still being protected, even where the blisters have broken open, as in the case of the aluminum coated panels exposed at the mean tide level.

The vinyl sealed panels are in excellent condition, showing a few small unbroken blisters. The coatings on these panels are in a condition similar to aluminum sealed panels exposed at the mean tide level.

Zinc Coated Panels

The performance of zinc coatings in this exposure is very similar to those exposed at the mean tide level.

Zinc coatings sealed and unsealed, less than 0.012 in. (.34mm) thick have failed. Zinc coatings of 0.012 in. (.34mm), 0.015 in. (.41mm) and 0.018 in. (.49mm) sealed and unsealed have protected the base metal, but it appears that the zinc has been converted to corrosion products. See Fig. 3. This tightly adherent mixture of white rust and foulants appears to be providing the corrosion protection to the base metal. All panels which have failed are very deeply pitted.

Sea Water Exposure - Freeport, Texas

Panels at this site were lost in a hurricane. The only documented test information available at this site can be obtained by reference to the AWS Twelve Year Report. AWS C2.11-67.

MARINE ATMOSPHERE

Kure Beach, North Carolina 80-ft. (24m) Lot

At this site the specimens face the surf in a south easterly direction at an average distance of 80-feet (24m) from the normal mean tide level, exposing them to the Atlantic Ocean's spray, salt air and the weather.

Aluminum Coated Panels

All unsealed panels have a dull gray-brown blotchy appearance, with evidence of blistering of the aluminum in thicknesses greater than .003 in. (.08mm). Unsealed .006 in. (.15mm) thick panels have approximately 6-20 blisters, per sq. inch, less than 1/8 in. (3.2mm) diameter. Unsealed aluminum panels .009 in. (.23mm) thick have over 20 blisters per sq. inch up to 1/8 in. (3.2mm) diameter. Blisters do not appear to be as prevalent on the groundward surfaces.

One coat of aluminum vinyl sealer on .003 in. (.08mm) of aluminum appears slightly duller than two coats. Aluminum vinyl sealed panels seem to be in excellent condition, See Fig. 4. There is evidence of a few blisters in coatings thicker than .003 in. (.08mm) sealed with one and two coats of aluminum vinyl. The groundward side of these panels have a slightly blotchy appearance but no evidence of any blisters of metal.

No difference in general appearances or tendency to blister could be observed as a function of surface preparation method.

Zinc Coated Panels

Zinc coatings .003 in. (.08mm) unsealed, exhibited heavy rusting of the base metal. See Fig. 5.

Aluminum vinyl sealer has completely deteriorated on the .003 in. (.08mm) zinc with rusting of the base at the edges and encroaching on the faces. Both skyward and groundward surfaces are covered with white rust. Unsealed .006 in. (.15mm) zinc are exhibiting rusting of the base metal at the edges with the flat surfaces covered with small nodes of heavy white rust.

Zinc coatings sealed with chlorinated rubber are similar in appearance to unsealed zinc.

Unsealed coatings of zinc .009 in. (.23mm) or greater are covered with many small nodes of white rust with no evidence of the base material rusting.

The aluminum vinyl is gone from the skyward surface of most of the panels to which it was applied. Heavy white rust is evident. The groundward surfaces have very little evidence of aluminum vinyl remaining.

The fact that the aluminum vinyl sealer has deteriorated completely on the zinc panels in this severe marine atmosphere appears to justify the decision not to use the vinyl sealer on the sea water test panels. Early laboratory tests with vinyl sealed, zinc coated panels exposed in the sea waters off Long Island, N. Y. indicated failure of the vinyl as a sealer for zinc. This may be a function of the chloride ion since vinyl sealed zinc has performed very well in the industrial atmospheres where there are less chlorides available.

No difference in the condition of panels as a function of surface preparation method is apparent.

Kure Beach, North Carolina 800-ft. (245m) Lot

Aluminum Coated Panels

All panels are in excellent condition at this site. See Fig. 5. Unsealed aluminum panels .003 in. (.08mm) thick are light gray in color on the skyward surface with a slightly darker gray stain and some light rust staining on the groundward surface. No rust staining is evident on the heavier unsealed aluminum coatings.

All aluminum vinyl sealed panels are excellent. Those with one coat of sealer have a dark mottled appearance over 95% of the skyward surface while those with two coats have the mottled appearance on 20 - 25% of the area. The groundward surfaces have their original appearance.

Zinc Coated Panels

The .003 in. (.08mm) unsealed zinc panels are dark blue in color with horizontal stripes of white rust that appear to conform to the spray pattern. See Fig. 5. This condition is apparent on both surfaces with the groundward surface having a slightly darker blue color.

The one coat of aluminum vinyl sealer on the .003 in. (.08mm) zinc has 10 - 20% of the skyward surface appearing mottled, with a few pinpoint blisters of the aluminum vinyl. Groundward surfaces are in very good condition with the exception of one panel that has approximately 5% deterioration of the sealer. The chlorinated rubber sealer has long since disappeared leaving those panels very similar to the unsealed panels with slightly less evidence of the horizontal striping.

Panels with coating thickness greater than .003 in. (.08mm) appear to have absorbed the aluminum vinyl sealer to a greater degree than the .003 in. (.08mm). The groundward surfaces are in very good condition. There is no evidence of rusting of the base metal on any of the panels in the 800-ft. (245m) lot.

Brazos River, Texas

Aluminum Coated Panels

This test site cannot be considered a very severe marine atmosphere. All panels are in very good condition with no evidence of the base metal corroding. All panels have a light tan discoloration which appears to be the color of the dust in the area. The groundward surfaces of unsealed aluminum in the .006 in. to .015 in. (.15mm to .41mm) types show some evidence of blisters which is not apparent on the skyward surfaces. The .003 in. (.08mm) aluminum panels, unsealed, had no evidence of blistering on either side. The aluminum vinyl sealer has developed a blotchy appearance on most of the panels. Vinyl sealed .003 in. (.08mm) aluminum is in excellent condition with the groundward surface having an as new appearance. Panels in the .009 in. to .012 in. (.23mm to .34mm) groups with one coat of aluminum vinyl have developed a blotchy appearance on the groundward surface. Those with two coats of vinyl sealer are excellent.

Zinc Coated Panels

Zinc coated panels at this site are in good condition. A tan discoloration on all panels is particularly evident at the edges. There is no evidence of the base metal rusting. Unsealed zinc panels have taken on a light blue color.

The aluminum vinyl sealer shows some deterioration, as much as 25% of the skyward surface on some of the panels, with zinc corrosion products evident. The groundward side of the panels sealed with aluminum vinyl is in good condition.

Panels sealed with chlorinated rubber are similar in appearance to the unsealed panels except that a horizontal striping effect is more evident. There is no evidence of any chlorinated rubber remaining.

Point Reyes, California

Aluminum Coated Panels

Unsealed aluminum, .003 in. (.08mm), have developed a black discoloration over 25 - 75% of the skyward surfaces, with no evidence of nodes or blisters. The groundward surfaces have a slight rust stain evident. Heavier coatings of unsealed aluminum are lighter and do not have as much discoloration.

All panels sealed with one coat of aluminum vinyl have a mottled appearance, while those with two coats are excellent.

There is no evidence of rusting of the base on any of the panels.

Zinc Coated Panels

Unsealed zinc panels have a blue color on the skyward surfaces with the familiar horizontal stripes more evident on the .003 in. (.08mm) than on heavier coatings. The groundward surfaces on all unsealed panels are a dark blue color.

The .003 in. (.08mm) zinc panels sealed with one coat of aluminum vinyl exhibit blistering of the sealer 5-10% on the skyward surfaces. The remaining area is bright and in excellent condition. It is apparent that the aluminum vinyl sealer is deteriorating to a greater extent on the heavier coatings of zinc than on thinner coatings. This deterioration is accompanied by corrosion of the zinc. Since heavier coatings absorb more, two coats of vinyl sealer would be in order.

Panels sealed with chlorinated rubber have a tan discoloration, a combination of zinc corrosion product and deteriorated sealer. This is true of both surfaces.

INDUSTRIAL ATMOSPHERE

New York City Area (Kearny, New Jersey)

Aluminum Coated Panels

Unsealed .003 in. (.08mm) aluminum coatings show many nodes of corrosion on the skyward surface that are black in color due to retained contamination. The groundward surface is gray to black in color with some indication of nodular corrosion. No rusting of the base is evident.

Unsealed .006 in. (.15mm), .009 in. (.23mm), and .012 in. (.34mm) aluminum coatings show heavy blistering of aluminum on the skyward surface. The groundward surfaces exhibit nodular type corrosion.

Aluminum vinyl sealed coatings show evidence of a few scattered nodes of corrosion product on the skyward surface of the .003 in. (.08mm) panels. Heavier coatings show indications of a few scattered blisters. Groundward surfaces are all excellent.

All coating thicknesses sealed with two coats of aluminum vinyl are in excellent condition on both surfaces.

Zinc Coated Panels

Unsealed .003 in. (.08mm) zinc coatings failed completely on the skyward surface and approximately 75% of the groundward surface. The .003 in. (.08mm) zinc coatings sealed with chlorinated rubber also failed completely on the skyward surface and about 10% on the groundward surface. Zinc coatings .003 in. (.08mm) sealed with aluminum vinyl are in excellent condition and appear brighter and cleaner than aluminum with the equivalent amount of sealer. It is interesting to note that the vinyl is in better condition on the .003 in. (.08mm) coatings than on the heavier zinc coatings where it has deteriorated 10-30% in some cases. This is probably because .003 in. (.08mm) coatings are smoother and do not absorb as much sealer as the heavier coatings.

Unsealed .006 in. (.15mm) zinc coatings exhibit some rusting on the skyward surface and less on the groundward surface. Unsealed .009 in. (.23mm) and .012 in. (.34mm) coatings are blue in color with some deposit staining. No rusting of base metal evident.

Columbus, Ohio

Aluminum Coated Panels

All unsealed sprayed aluminum panels have a black nodular type of corrosion product with the size of the nodule increasing with the thickness of coating. There is no evidence of the base metal corroding. Panels sealed with one coat of aluminum vinyl are beginning to show some indications of these black nodes forming. Panels with two coats of aluminum vinyl sealer are in excellent condition.

Zinc Coated Panels

Unsealed .003 in. (.08mm) zinc coated panels lost approximately 90% of the zinc on the skyward surfaces and the base metal is rusting. Edges also show rusting. The groundward side of the panels is covered with white rust that appears stained with red rust. All zinc coated panels sealed with aluminum vinyl are in good condition. One panel in each of the .006 in. (.15mm) and .009 in. (.23mm) group, sealed with aluminum vinyl, is exhibiting a 5-10% deterioration of the sealer with some white rust evident. Unsealed .006 in. (.15mm) panels show some red rust at the edges of the identifying notches. Some black nodes are evident which are probably white rust with deposit stain.

East Chicago, Indiana

Aluminum Coated Panels

This is a very heavy industrial environment with all panels having a dark brown discoloration. All unsealed aluminum panels of .006 in. (.15mm) or more have evidence of blistering of the aluminum on the skyward surfaces. Unsealed aluminum .003 in. (.08mm) has a more nodular type of corrosion on the skyward surface with less evidence of aluminum corrosion on the groundward surface. Aluminum vinyl sealed panels have a very heavy deposit stain on both surfaces. Two coats of aluminum vinyl appear slightly better than one coat. No corrosion of the sprayed aluminum is evident.

Zinc Coated Panels

Sprayed zinc panels sealed with aluminum vinyl are in very good condition with some deposit staining on the vinyl sealer.

Appendix 1

Test Site Data

Test Site and Environment	No. Of Panels		Date Exposed
Atmospheric Exposure	**Aluminum**	**Zinc**	
Brazos River, Texas (salt air)	156	156	March 1954
Columbus, Ohio (urban)	120	120	November 1953
East Chicago, Indiana (industrial)	120	120	November 1953
Kure Beach, North Carolina			
*80-ft (24m) lot (severe marine)	336	336	January 1953
**800-ft (240m) lot (salt air)	156	156	January 1953
New York City Area (industrial)	120	120	November 1953
Point Reyes, California (salt air)	156	156	December 1953
4 x 6 in. (102mm x 152mm) panels reserved	156	156	
Sea Water Exposure			
Freeport, Texas	156	156	October 1953
Wrightsville Beach, North Carolina			
below-low-tide	156	156	October 1953
mean-tide	336	336	October 1953
4 x 12 in. (102mm x 305mm) panels reserved	156	156	
Total	2124	2124	

*80-ft (24m) from shoreline
**800-ft (240m) from shoreline

Appendix 2

Types of Abrasive Used For Blast Cleaning Specimens In This Test Program*

Types of Abrasive	Mesh Distribution	Description
Coarse Silica Sand	Tyler Screen Sieve Analysis +14 mesh 5% -14+20 " 48% ±10% -20+28 " 40% ±10% -28+35 " 10% ±10% -35 " 5%	Abrasive is washed angular silica sand, dry and free of feldspar, clay or other friable constituents.
Fine Silica Sand	U.S. Standard Screen Analysis +20 mesh 5% -20+30 " 67% ±10% -30+40 " 24% ±10% -40 " 10%	Abrasive is washed angular silica sand, dry and free of feldspar, clay or other friable constituents.
Chilled Iron Grit	Conforms to SAE specification for G-25 angular chilled iron grit.	Abrasive is angular chilled iron grit.

*Note: It should be noted that the precise mesh distributions shown would probably not be obtainable in all areas, and they should not be used for specification purposes.

Appendix 3

Composition and Description of Seal Coats

Seal Coat	Composition		Description
Wash Primer	Resin component:		An air drying, two-part, acid-zinc chromate wash coat primer.
	Pigment: Insoluble type, inert, zinc chromate	8.2%	
	Nonvolatile vehicle: Polyvinyl butyral	9.5%	
	Volatile vehicle: Butyl and isopropyl alcohol	82.3%	
	Acid component:		
	Phosphoric acid	16.0%	
	Ethyl (or isopropyl) alcohol plus water	Balance	
Mix four parts of the resin component with one part of the acid component to obtain final primer composition.			
Aluminum Vinyl	Pigment: Non-leafing aluminum flake	10%	A vinyl copolymer aluminum flakes, air-drying type of coating material
	Nonvolatile vehicle: Vinyl copolymer and plasticizer	20%	
	Volatile vehicle: Toluene and ketones	70%	
Clear Vinyl	Pigment: None		A clear, vinyl copolymer, air-drying coating material.
	Nonvolatile vehicle: Vinyl chloride-acetate		
	Resin	16%	
	Plasticizer	1.4%	
	Volatile vehicle: Ketones	37.6%	
	Aromatic hydrocarbons (Toluene, benzol, xylol)	45.0%	
Chlorinated Rubber	Solids: Chlorinated rubber -- plus two types of chlorinated paraffins plus a stabilizer	34%	A clear, air-drying, chlorinated rubber type coating material
	Solvents: Aromatic petroleum solvents	66%	

Appendix 4

Panel Types For Atmospheric Exposure

Aluminum Flame Sprayed Panels				Zinc Flame Sprayed Panels			
Panel Type	*Panel Preparation	Coating Thickness, in. & mm	**Seal Coat	Panel Type	*Panel Preparation	Coating Thickness, in. & mm	**Seal Coat
1	1	0.003(.08mm)		1	1	0.003(.08mm)	
2	1	" "	WP+AV-1	2	1	" "	WP+AV-1
3	1	" "	WP+AV-2	3	1	" "	CR-2
4	1	0.006(0.15mm)		4	1	0.006(0.15mm)	
5	1	" "	WP+AV-1	5	1	" "	WP+AV-1
6	1	" "	WP+AV-2	6	1	" "	CR-2
7	1	0.009(0.23mm)		7	1	0.009(0.23mm)	
8	1	" "	WP+AV-1	8	1	" "	WP+AV-1
9	1	" "	WP+AV-2	9	1	" "	CR-2
10	2	0.012(0.34mm)		10	2	0.012(0.34mm)	
11	2	" "	WP+AV-1	11	2	" "	WP+AV-1
12	2	" "	WP+AV-2	12	2	" "	CR-2
13	2	0.015(0.41mm)		13	2	0.015(0.41mm)	
14	2	0.009(0.23mm)		14	2	0.009(0.23mm)	
15	2	" "	WP+AV-1	15	2	" "	WP+AV-1
16	2	" "	WP+AV-2	16	2	" "	CR-2
17	4	" "		17	4	" "	
18	4	" "	WP+AV-1	18	4	" "	WP+AV-1
19	4	" "	WP+AV-2	19	4	" "	CR-2
20	6	" "		20	6	" "	
21	6	" "	WP+AV-1	21	6	" "	WP+AV-1
22	6	" "	WP+AV-2	22	6	" "	CR-2
23	3	" "		23	3	" "	
24	3	" "	WP+AV-1	24	3	" "	WP+AV-1
25	3	" "	WP+AV-2	25	3	" "	CR-2
26	5	" "		26	5	" "	
27	5	" "	WP+AV-1	27	5	" "	WP+AV-1
28	5	" "	WP+AV-2	28	5	" "	CR-2

*Types of Surface Preparation
1. Coarse silica sand
2. Coarse silica sand and steel flash
3. Fine silica sand
4. Fine silica sand and steel flash
5. Chilled iron grit
6. Chilled iron grit and steel flash

**Types of Seal Coat
WP-Wash Primer
AV-Aluminum Vinyl
CR-Chlorinated Rubber
-1-One Coat Of Specified Seal Coat
-2-Two Coats Of Specified Seal Coat

Appendix 5

Panel Types For Sea Water Exposure

Aluminum Flame Sprayed Panels				Zinc Flame Sprayed Panels			
Panel Type	*Panel Preparation	Coating Thickness, in. & mm	**Seal Coat	Panel Type	*Panel Preparation	Coating Thickness, in. & mm	**Seal Coat
1	2	0.003(.08mm)	WP+CV-1	1	2	0.003(.08mm)	CR-1
2	2	" "	WP+CV-2	2	2	" "	CR-2
3	2	0.006(0.15mm)		3	2	0.006(0.15mm)	
4	2	" "	WP+CV-1	4	2	" "	CR-1
5	2	" "	WP+CV-2	5	2	" "	CR-2
6	2	0.009(0.23mm)		6	2	0.009(0.23mm)	
7	2	" "	WP+CV-1	7	2	" "	CR-1
8	2	" "	WP+CV-2	8	2	" "	CR-2
9	2	0.012(0.34mm)		9	2	0.012(0.34mm)	
10	2	" "	WP+CV-1	10	2	" "	CR-1
11	2	" "	WP+CV-2	11	2	" "	CR-2
12	2	0.015(0.41mm)		12	2	0.015(0.41mm)	
13	2	0.018(0.49mm)		13	2	0.018(0.49mm)	
14	1	0.009(0.23mm)		14	1	0.009(0.23mm)	
15	1	" "	WP+CV-1	15	1	" "	CR-1
16	1	" "	WP+CV-2	16	1	" "	CR-2
17	3	" "		17	3	" "	
18	3	" "	WP+CV-1	18	3	" "	CR-1
19	3	" "	WP+CV-2	19	3	" "	CR-2
20	5	" "		20	5	" "	
21	5	" "	WP+CV-1	21	5	" "	CR-1
22	5	" "	WP+CV-2	22	5	" "	CR-2
23	4	" "		23	4	" "	
24	4	" "	WP+CV-1	24	4	" "	CR-1
25	4	" "	WP+CV-2	25	4	" "	CR-2
26	6	" "		26	6	" "	
27	6	" "	WP+CV-1	27	6	" "	CR-1
28	6	" "	WP+CV-2	28	6	" "	CR-2

*Types of Surface Preparation

1. Coarse silica sand
2. Coarse silica sand and steel flash
3. Fine silica sand
4. Fine silica sand and steel flash
5. Chilled iron grit
6. Chilled iron grit and steel flash

**Types of Seal Coat

WP-Wash primer
CV-Clear vinyl
CR-Chlorinated rubber
-1-One coat of specified seal coat
-2-Two coats of specified seal coat



Figure 1

"a": 250X. Nital etch. Flame sprayed aluminum coating, .006 in. (.15mm) thick, no sealer, over a flash coat of carbon steel. This illustrates the condition of the aluminum coating after exposure for 18 years at Wrightsville Beach, N.C. in sea water at mean tide level.

"b": Same area as above, except under polarized light and showing the amount of coating which has converted to aluminum corrosion product (white) and remaining aluminum (black).

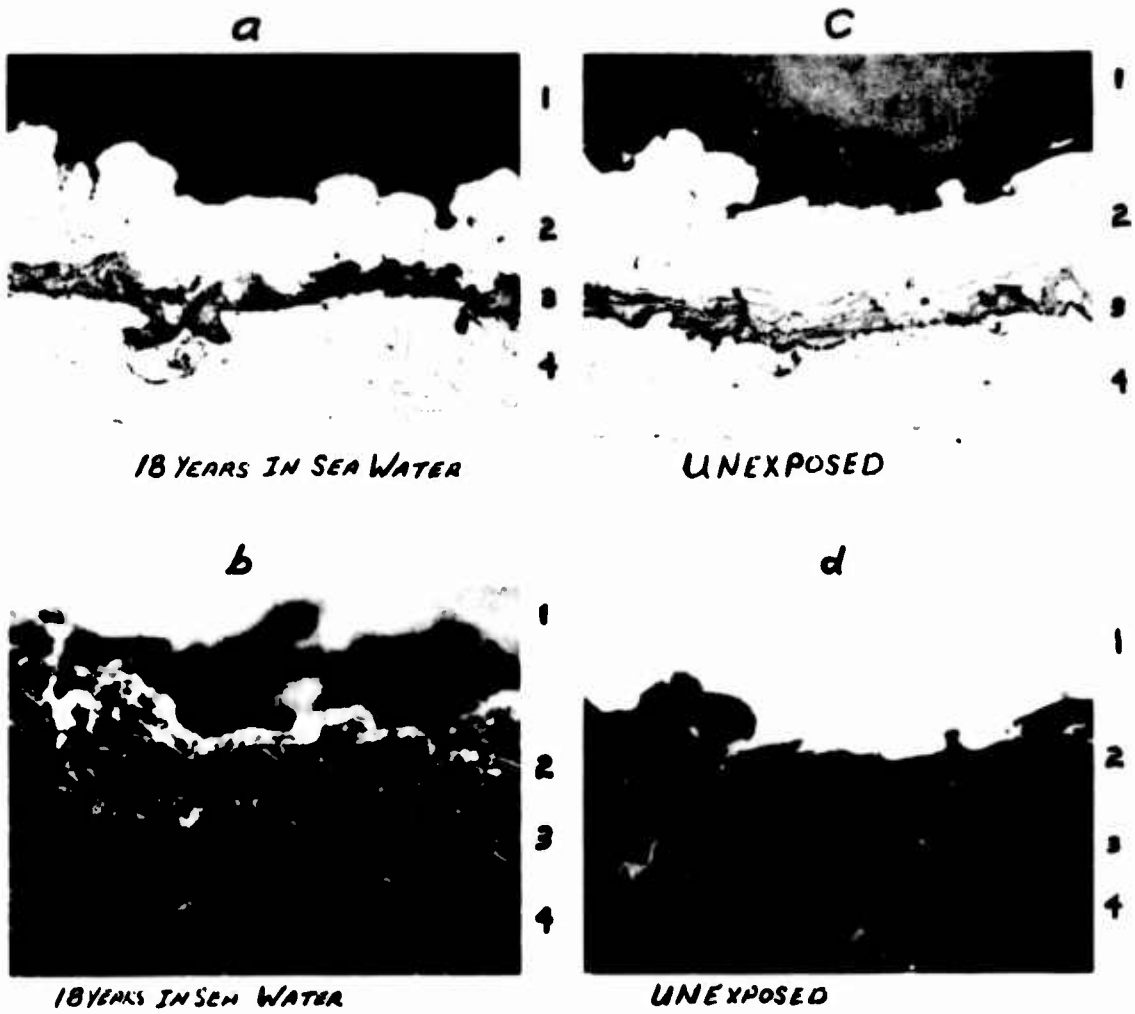


Figure 2

"a": 250X. Nital etch. Flame sprayed aluminum coating .003 in. (.08mm) thick plus one coat primer and two coats of vinyl. Exposed for 18 years below low tide at Wrightsville Beach, N.C. This photo illustrates the overall condition of the aluminum coating. Compare with photo "c" which shows the same coating, Nital etched on a reserve panel which was never exposed.

"b": Same area as "a", but under polarized light to illustrate the relatively small amount of aluminum corrosion. For comparison, see photo "d", showing unexposed aluminum.



Figure 3

"a": 60X. .012" (.34mm). Flame sprayed Zn, no sealer, exposed for 18 years at Wrightsville Beach, N.C. in sea water at mean tide level. This photo illustrates remaining zinc and zinc corrosion product.

"b": Same area as above, however, under polarized light. The zinc corrosion product appears white and the zinc is black.

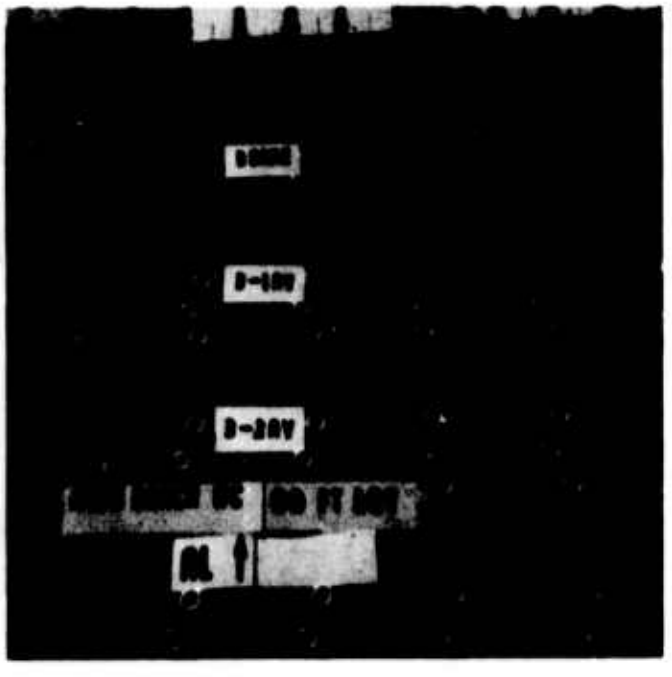


Figure 4

This photograph was taken at Kure Beach, N. C., 80 feet (24m) from the normal mean tide level, facing the surf. It shows the condition of flame sprayed aluminum with and without sealers after 19 years exposure.

The top left three panels have .003 in. (.08mm) aluminum without a sealer.

The center left three panels have .003 in. (.08mm) aluminum, a wash prime and one coat of aluminum vinyl.

The lower left three panels are the same except for two coats of aluminum vinyl.

The remaining unidentified panels are .006 in. (.15mm), .009 in. (0.23mm) aluminum with and without sealers.



Figure 5

This photograph was taken at Kure Beach, N.C., which is a marine environment, 80 feet (24m) from the normal mean tide level, facing the surf. It shows the condition of flame sprayed zinc with and without sealers after 19 years exposure.

The top left three panels show what remains of .003 in. (.08mm) zinc without a sealer.

The center left two panels have .003 in. (.08mm) zinc, a wash prime and one coat of aluminum vinyl.

The lower left two panels were .003 in. (.08mm) zinc with chlorinated rubber sealer.

The two upper right panels are .006 in. (.15mm) zinc with chlorinated rubber.

The remaining panels are .009 in. (0.23mm) zinc with and without sealers.

Oral Discussion

May: Did you identify the chemical composition of the zinc and aluminum used here?

Schriber: The zinc was 99% pure, and so was the aluminum.

Electrochemical Properties of Magnesium, Zinc, and Aluminum Galvanic Anodes in Sea Water

T. J. Lennox, Jr.

Code 6325
Naval Research Laboratory
Washington, D.C. 20390

Over the last thirty years several improved galvanic anode alloys have been introduced for cathodic protection systems in sea water. Magnesium anodes conforming to MIL-A-21412A and zinc anodes conforming to MIL-A-18001H have been used successfully over sufficiently long periods that their electrochemical characteristics and service performance are well established. On the other hand, over the past decade aluminum anodes have been in a state of flux with the introduction of new alloys every few years. However, the enhanced electrochemical properties of some of the more recently developed aluminum anodes have made them attractive economically.

Data have been presented on the critical parameters for magnesium, zinc, and aluminum alloy anodes. The closed-circuit electrochemical potentials, current output characteristics, current capacity, and corrosion characteristics have been summarized. Comparative data on some of the newer and older aluminum alloy anodes and the advantage of galvanic anodes over other type cathodic protection systems have been discussed.

The protective potentials for steel to four different types of reference electrodes have been presented, and a nomogram of reference electrode potentials in chloride solutions of various resistivities has been included.

It is concluded that the presently available magnesium, zinc, or aluminum anodes procured to the proper specifications have dependable electrochemical characteristics and are suitable for cathodic protection systems in sea water.

Key Words: Galvanic anodes; sea water; magnesium anodes; zinc anodes; aluminum anodes; electrochemical properties; relative metal costs; reference electrodes; corrosion characteristics.

1. Introduction

Until approximately forty years ago corrosion protection on submerged structures relied almost entirely on the application of protective coatings. Although the principles of cathodic protection have been applied to ship hulls for approximately 150 years (3)[1], it was not until the 1940's (4)

[1] The numbers in parentheses refer to the list of references which make up the Bibliography at the end of this paper.

that concern developed over the variable performance of the zinc anodes which were routinely placed on the stern of a ship to prevent corrosion accelerated by the nonferrous metal propellers and appendages.

Cathodic protection to mitigate corrosion is generally used in conjunction with prctective coatings by establishing a sufficiently negative potential on a submerged structure to make the entire structure cathodic. Cathodic protection may be obtained using either relatively inert anodes with an impressed voltage from an external power source or from sacrificial galvanic anodes such as magnesium (1,2), zinc (3-11), or aluminum (12-21). Galvanic anodes depend on their inherent electrochemical activity for driving voltage and are a self-contained power source when coupled to a more noble (cathodic) metal.

This paper is prepared with the thought that it should serve as a guide to the use of galvanic anodes in sea water and is based on the author's and other's experience on studies of the electrochemical properties of magnesium, zinc, and aluminum anodes in service and field-service type experiments. A bibliography of pertinent references (1-22) on the subject is included.

The primary considerations in establishing the useful properties of a galvanic anode are based on reliable performance associated with the following parameters: 1) closed-circuit electrochemical potential, 2) long-term current output characteristics, 3) current capacity per pound, and 4) corrosion characteristics. The economics of any cathodic protection system should be based not only on cost of anode material, but should include actual installation costs. These latter costs may be quite variable from one shipyard to another, and the cost per pound of anode metal will vary with the source; for these reasons only relative costs per ampere year for galvanic anode materials will be discussed.

It should also be pointed out that the author and his associates (18,19) have not tested all existing anode alloys, especially alloys that may have been developed in the last several years. Therefore, the comments and statements in this paper are not meant to limit the use of unmentioned alloy anodes. As a precaution to users of galvanic anodes, however, any anode material should not be considered for long-term installation until the intended user has had demonstrated to him by in-service test data or data from long-term field-service tests that the materials being considered do indeed fulfill his requirements technically as well as economically.

Of necessity in a paper of this type general or typical data will be presented. In summarizing, however, more specific data are presented.

Closed-Circuit Potentials

The closed-circuit electrochemical potentials to a silver/silver chloride (Ag/AgCl) reference electrode of the presently used magnesium and zinc anodes for which a U.S. Military specification exists are shown in Fig. 1. Also shown in Fig. 1 are the potentials of several aluminum alloy anodes. A military specification does not exist for aluminum galvanic anodes, but one is in preparation by the Naval Ships Engineering Center, Hyattsville, Maryland.

Magnesium anodes have the most negative (anodic) potential of the common galvanic anode alloys. Zinc and aluminum anodes have similar potentials which are positive (cathodic) to magnesium anodes by approximately 0.5 volt. None of the anode alloys has a specific potential in sea water. Therefore a range and typical potential values have been shown in Fig. 1. The zinc anode appears to have the narrowest range of potentials of any of the galvanic anodes studied.

Current Output Characteristics

Typical current output versus time characteristics for magnesium, zinc, and several aluminum alloy anodes are shown in Fig. 2. Generally, galvanic anodes of the proper specification or identity can be relied upon to supply galvanic current for a cathodic protection system over long time periods, i.e., they do not anodically polarize in sea water. An exception to this is some of the aluminum-zinc-tin alloy anodes which have shown a continual decrease in current output with time indicating anodic polarization. Anodes which polarize significantly with time cannot be considered as suitable galvanic anodes for long-term cathodic protection systems.

Current Capacity

The current capacity in ampere hours per pound as a function of anode current density for magnesium, zinc, and several aluminum alloy anodes is shown in Fig. 3. The aluminum-zinc-mercury alloy anode has consistently produced the highest current capacity, and the high capacity for this alloy was maintained over the anode current density range from 200 to 1000 ma/sq ft. The aluminum-zinc-tin alloy anodes are also capable of producing a high current capacity, but in many instances the capacity is well below that of magnesium anodes (500 ampere hours per pound) especially at anode current density levels below approximately 700 ma/sq ft. The low current capacity observed on some of the aluminum-zinc-tin anodes may be the result of improper heat treatment, as these alloys generally require post casting heat treatment to obtain a high current capacity. The aluminum-zinc-indium alloy anodes have a current capacity approximately midway between the best and poorest performing aluminum anodes. Zinc anodes have a current capacity of approximately 370 ampere hours per pound at all current density levels, and zinc anodes are essentially 100% efficient in sea water.

Reding (20) has shown, Fig. 4, that the current capacity of the aluminum-zinc-mercury alloy anode can be detrimentally affected in an environment such as anaerobic mud covered with sea water. In this environment the current capacity of aluminum-zinc-mercury anodes can be as low as 400 ampere hours per pound. Increasing the zinc content to 4% resulted in increasing the current capacity to over 1000 ampere hours per pound. Table 1 shows a comparison of current capacities for aluminum alloy anodes and for zinc anodes in the anaerobic mud sea water system. The zinc anode current capacity was not detrimentally affected in this environment.

Corrosion Characteristics

The corrosion characteristics in sea water of magnesium, zinc, and several aluminum alloy anodes are shown in Table 2. Both the magnesium and zinc alloy anodes usually show uniform attrition and are essentially self cleaning of anodic corrosion products. The magnesium anodes may tunnel at ferrous cores especially under velocity conditions. This tunneling which can result in electrical isolation of the anode from the structure being protected can be reduced or eliminated with the use of porcelain coated steel cores or by covering the entire anode except for one surface with a thick (approximately 1/8 inch) adherent PVC type coating. The attrition of zinc anodes will generally be less uniform at low anode current density.

None of the aluminum alloy anodes are self cleaning, and generally the attrition pattern is less uniform than for either magnesium or zinc anodes in sea water. It has also been noted that some surface areas on the aluminum-zinc-mercury alloy anodes remain essentially inactive. In long-term use, the inactivity of these areas could perhaps result in some segments of the anodes being lost without ever producing any useful current.

Specific Galvanic Anode Properties

A summary of specific properties for galvanic anodes is shown in Table 3. This summary includes the nominal composition of the anodes, closed-circuit potential to the Ag/AgCl reference electrode, current capacity in ampere hours per pound, anode consumption rate in pounds per ampere year, and density of the alloys.

Magnesium anodes have a typical potential of -1.52 volts and a current capacity of 500 ampere hours per pound. Zinc anodes have a potential of -1.04 volts and will provide 368 ampere hours per pound.

The most consistent electrochemical properties for aluminum alloy anodes has been obtained from anodes containing zinc and mercury. Typically these anodes have a potential of -1.06 volts and a current capacity of 1250 ampere hours per pound in full strength sea water.

Aluminum anodes with alloying elements of zinc and tin, and which generally require a heat treatment to obtain optimum electrochemical characteristics, have shown quite variable properties. A typical potential for this class of alloy anode is -1.03 volts, and the current capacity can vary from as high as 1100 to as low as 400 ampere hours per pound. With a current capacity of only 400 ampere hours per pound from an aluminum anode the advantage of using aluminum over zinc anodes is lost for most long-term cathodic protection installations.

The aluminum anodes alloyed with zinc and indium have a typical potential of -1.1 volts and a current capacity ranging from 750 to 900 ampere hours per pound.

Relative Costs and Advantages

The relative metal costs per ampere year for zinc, magnesium, and aluminum anodes are summarized in Table 4. These data are based on actual ampere hour per pound values obtained from each anode alloy as shown in Table 3 and the nominal U.S. prices for each of the alloys in anode form.

The relative cost per ampere year of the aluminum-zinc-mercury anodes is approximately two thirds that of zinc anodes and approximately one half that of magnesium anodes. With the price per pound used in this comparison the aluminum-zinc-tin alloy anode would be less costly than the aluminum-zinc-mercury anodes if a high current capacity could be consistently realized from the aluminum-zinc-tin anodes. The relative cost of the aluminum-zinc-indium anodes is somewhat greater than that of the aluminum-zinc-mercury anodes and slightly less than for zinc anodes.

Table 5 shows some of the advantages of galvanic anodes as a class for cathodic protection systems. The advantages for galvanic anodes over other systems can be summarized by pointing out their simplicity in use and the relatively low initial cost.

Protective Potentials

The protective potentials for steel in sea water measured to four different reference electrodes are shown in Table 6.

A nomogram for correcting the potentials observed to the Ag/AgCl reference electrode to potentials on the saturated calomel (SCE) or saturated copper/copper sulfate ($Cu/CuSO_4$) electrode scale in waters of varying resistivity is shown in Fig. 5. This nomogram will be useful in establishing the potential to either the saturated calomel electrode (SCE) or the $Cu/CuSO_4$

electrode when the potential has been determined to a Ag/AgCl reference electrode, for example, on the hull of a ship which traverses full strength sea water and brackish water. As discussed by Peterson, Groover (22) "... the Ag/AgCl reference electrode is an almost ideal reference cell for full sea water because it requires no salt bridge and has a low temperature coefficient. If the resistivity of the water in question is known, the range of this electrode is extended to cover almost any brackish water whose principal dissolved solid is sodium chloride."

Example a) in Fig. 5 shows that if a potential of -0.79 volts is measured to the Ag/AgCl reference electrode in 20 ohm-cm water (full sea water) the potential would be -0.79 volts to the SCE and -0.85 volts to the $Cu/CuSO_4$ electrode. In 1500 ohm-cm water (example b) in order to have a potential of -0.85 volts to the $Cu/CuSO_4$ (-0.79 volts to the SCE) one must measure a potential of -0.91 volts to the Ag/AgCl reference electrode.

Conclusions

1. By using magnesium anodes conforming to MIL-A-21412A, zinc anodes conforming to MIL-A-18001H, or aluminum anodes of the proper identity, one can readily obtain dependable electrochemical properties from galvanic anodes for sea water service. Aluminum alloy anodes containing small percentages of zinc and mercury have consistently given satisfactory electrochemical characteristics, but the current capacity may be lowered considerably if the anodes are used in anaerobic muds covered by sea water.

2. The aluminum-zinc-mercury alloy anodes have the lowest relative metal cost per ampere year compared to magnesium, zinc, or other aluminum alloy anodes studied.

3. The Ag/AgCl reference electrode appears to be an ideal reference cell for use in sea water, and potentials observed with it in brackish water whose principal dissolved solid is sodium chloride can readily be converted to the SCE or $Cu/CuSO_4$ electrode scale by use of the nomogram.

Acknowledgment

The author is indebted to Dr. B.F. Brown, former Head of the Physical Metallurgy Branch, Metallurgy Division of NRL, and M.H. Peterson for their encouragement to present this paper. He is also indebted to Messrs. R.E. Groover and C.W. Billow of the NRL Marine Corrosion Research Laboratory, Key West, Florida, where much of the data on the aluminum alloy anodes was developed.

Note: The views expressed in this paper are those of the author and are not to be construed as being the official opinion of the Naval Research Laboratory or the Department of the Navy.

Bibliography

Magnesium Anodes:

1. R. A. Humble, "Cathodic Protection of Steel in Sea Water with Magnesium Anodes," Corrosion 4,7, 358-370 (1948).

2. L. J. Waldron and M. H. Peterson, "Magnesium Anodes for the Cathodic Protection of Naval Vessels," Corrosion 17,7, 373t-375t (1961).

Zinc Anodes:

3. Sir Humphrey Davy, "On the Corrosion of Copper Sheathing by Sea Water, and on Methods of Preventing this Effect; and on their Applications to Ships of War and Other Ships," Phil. Trans. Roy. Soc. (London).

114, 151-158 (1824); "Additional Experiments and Observations on the Application of Electrical Combinations to the Preservation of the Copper Sheathing of Ships, and to Other Purposes," ibid 114, 242-6 (1824); "Further Researches on the Preservation of Metals by Electrochemical Means," ibid, 115, 328-46 (1825).

4. T. P. May, G. S. Gordon, and S. Schuldiner, "Anodic Behavior of Zinc and Aluminum-Zinc Alloys in Sea Water," Cathodic Protection - A Symposium by Electrochem Soc. and Nat. Assoc. Corrosion Engrs., p. 158-69, Nat. Assoc. of Corrosion Engrs., Houston, Texas (1949).

5. R. B. Teel and D. B. Anderson, "The Effect of Iron in Galvanic Anodes in Sea Water," Corrosion 12,7, 343-349 (1956).

6. J. T. Crennell and W. C. G. Wheeler, "Zinc Alloy Anodes for Use in Sea Water," J. Applied Chem. 6,45, 415-421 (1956).

7. E. C. Reichard and T. J. Lennox, Jr., "Shipboard Evaluation of Zinc Galvanic Anodes Showing the Effect of Iron, Aluminum and Cadmium on Anode Performance," Corrosion 13,6, 410t-416t (1957).

8. J. T. Crennell and W. C. G. Wheeler, "Zinc Alloy Anodes," J. Applied Chem. 8, 571-576 (1958).

9. L. J. Waldron and M. H. Peterson, "Effect of Iron, Aluminum and Cadmium Additions on Performance of Zinc Anodes in Sea Water," Corrosion 16,8, 375t (1960).

10. J. A. H. Carson, "Zinc as a Self-Regulating Galvanic Anode for Ship Hulls," Corrosion 16.10, 491t-496t, (1960).

11. T. J. Lennox, Jr., "Characteristics and Applications of Zinc Anodes for Cathodic Protection," Materials Protection 1,9, 37-45 (1962).

Aluminum Anodes:

12. R. L. Horst, "Latest Developement with Aluminum Alloy Anodes," A paper presented at the South Central Regional NACE Conference, October 24-26, 1962, Houston, Texas.

13. T. Sakano and K. Toda, "Studies on Al-Zn-In Alloy Anodes for Cathodic Protection," Corrosion Engineering 11,11, 486-492 (1962).

14. R. A. Hine and M. W. Wei, "How Effective are Aluminum Anodes in Sea Water?" Materials Protection 3,11, 49-55, (1964).

15. T. Sakano, K. Toda, and M. Hanoda, "Tests on the Effect of Indium for High Performance Aluminum Anodes," Materials Protection 5,12, 45-50 (1966).

16. J. J. Newport and J. T. Reding, "The Influence of Alloying Elements on Aluminum Anodes in Sea Water," Materials Protection 5,12, 15-18 (1966).

17. C. F. Schrieber and J. T. Reding, "Field Testing a New Aluminum Galvanic Anode for Sea Water Service," Materials Protection, 6,5, 33-36 (1967).

18. T. J. Lennox, Jr., M. H. Peterson, and R. E. Groover, "A Study of Electrochemical Efficiencies of Aluminum Galvanic Anodes in Sea Water," Materials Protection 7,2, 33-37 (1968).

19. T. J. Lennox, Jr., R. E. Groover, and M. H. Peterson, "Electrochemical Characteristics of Six Aluminum Galvanic-Anode Alloys in the Sea," Materials Protection and Performance, 10,9, 39-44 (1971).

20. J. T. Reding, "Sacrificial Anodes for Ocean Bottom Applications," Materials Protection and Performance, 10,10, 17-19 (1971).

Other:

21. G. L. Doremus and J. G. Davis, "Marine Anodes - The Old and New - Cathodic Protection for Offshore Structures," Materials Protection 6,1, 30-39 (1967).

22. M. H. Peterson and R. E. Groover, "Tests Indicate the Ag/AgCl Electrode is Ideal Cell in Sea Water," Materials Protection and Performance 11,5, 19-22 (1972).

Summarized Discussion

In reply to queries the author stated that the mercury content of the special aluminum anode alloy is only 0.05% (nominally), and the tolerability of the marine environment for an alloy of this composition can only be finally settled when the environmentalists set a standard; he noted that marine organisms have been observed growing directly on and around working Al-Zn-Hg anodes. Concerning a conjecture that alkali formation on a working anode might be responsible for keeping the anode free from fouling, the author noted that marine fouling can be found directly on magnesium anodes.

Where hydrodynamic drag or noise is a factor, it was pointed out that ranking of anode materials should be based on ampere-hours per unit volume rather than per unit weight. On the basis of volume, zinc and aluminum anodes are comparable. Where submerged weight is critical, as perhaps on a sub-surface buoy, it is the apparent weight in sea water rather than the weight in air that is important, and on such basis the aluminum alloys are even more attractive than when compared on the basis of weight in air.

There are no known effects of depth on the performance of galvanic anodes; all experiments with cathodic protection from zinc anodes at great depths appear to have confirmed the effectiveness of the anodes, but such experiments are lacking for magnesium and aluminum anodes.

Table 1. Laboratory Current Capacities of Aluminum and Zinc Anodes in Saline Electrolytes

Alloy	Current Capacities (amp hr/lb)[1]		
	Sea Water	Anaerobic Mud Covered with Sea Water	Sand Covered with Sea Water
Al,0.4Zn,0.04Hg	1270	550	1250
Zinc (MIL-A-18001H)	360	360	360
Al,7Zn,0.03Sn	760	510	-
Al,1.5Zn,0.03Sn	870	500	-

[1] current density approximately 100 ma/sq ft.

[after Reding (20)]

Table 2. Corrosion Characteristics; Galvanic Anodes

Anode Alloy	Description
Mg (MIL-A-21412A)	Self cleaning, uniform attrition, may tunnel at ferrous cores unless precautions to prevent.
Zn (MIL-A-18001H)	Self cleaning, uniform attrition; less uniform at low anode current density.
Al-Zn-Hg	Not self cleaning, striated attrition; some areas relatively inactive.
Al-Zn-Sn	Not self cleaning, uniform to irregular attrition; dependent on alloy and heat treatment.
Al-Zn-In	Not self cleaning, uniform to irregular attrition; dependent on anode current density.

Table 3. Galvanic Anode Properties Summary

Anode	Composition (nom.%)	Typical potential to Ag/AgCl Ref. (volts neg.)	Driving Pot. to cathode at -0.8V to Ag/AgCl Ref. (volts)	Current capacity (amp hr/lb)	Nominal anode consumption (lb/amp yr)	Density (lb/cu in)
Magnesium (MIL-A-21412A)	Al 5.0-7.0 Zn 2.0-4.0	1.52	0.72	500	17	0.063
Zinc (MIL-A-18001H)	Al 0.10-0.50 Cd 0.025-0.15	1.04	0.24	368	24	0.258
Aluminum Zn-Hg	Zn 0.35-0.5 Hg 0.035-0.05	1.06	0.26	1250	7	0.0984
Zn-Sn	Proprietary, several alloys available, some heat treatable	1.03	0.23	400-1100	22-8	0.1
Zn-In	Zn 2.5 In 0.02	1.10	0.30	750-900	12-10	0.1

Table 4. Galvanic Anodes - Relative metal cost/ampere year

Anode Material	Relative Cost* (dollars)
Zinc (MIL-A-18001H)	1.00
Magnesium (MIL-A-21412A)	1.31
Aluminum	
Zn-Hg	0.67
Zn-In	0.77 to 0.93
Zn-Sn	0.62 to 1.70

*Based on actual ampere-hours/lb, not theoretical values.

Table 5. Galvanic Anode Advantages Over Other Type Systems

Item	Description
Current source	Self contained
Current direction	Always correct for protection
Stuffing glands	Not required
Hull penetrations	Not required
Isolation from hull	Must not be isolated
Lead wires	Generally not used
Dielectric shield	Required only for Mg anode
Damage (mechanical)(electrical)	Not very susceptible. No concern when properly shielded and cast-in bonded cores used
Maintenance	None required, other than periodic replacement of anodes
Initial cost	Relatively low

Table 6. Protective Potentials of Steel Measured Against Four Reference Electrodes in Sea Water

Reference Electrode	Electrolyte	Protective Potential in Volts (68°F)
Calomel	Saturated KCl	-0.79
Ag/AgCl	Sea water	-0.79*
$Cu/CuSO_4$	Saturated $CuSO_4$	-0.85
Zinc (MIL-A-18001H)	Sea water	+0.25

* These are practical values in full strength uncontaminated sea water.

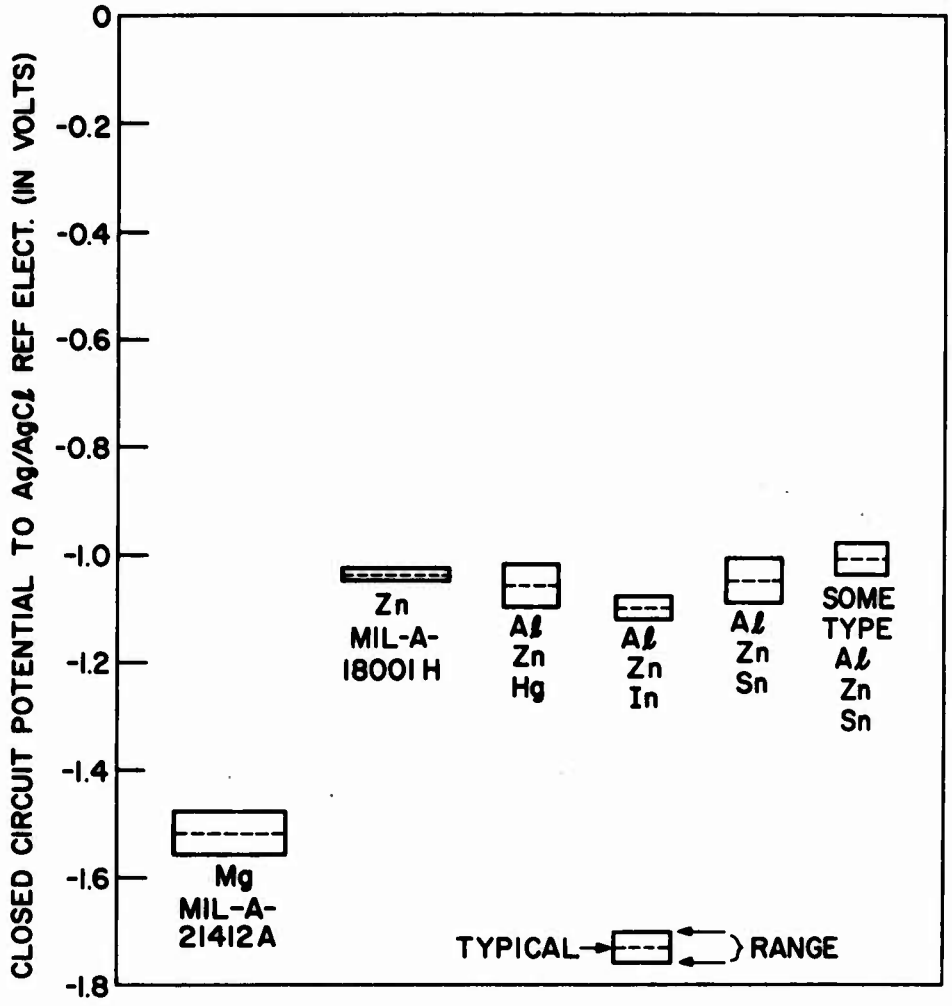


Fig. 1--Closed circuit potentials of galvanic anodes in sea water.

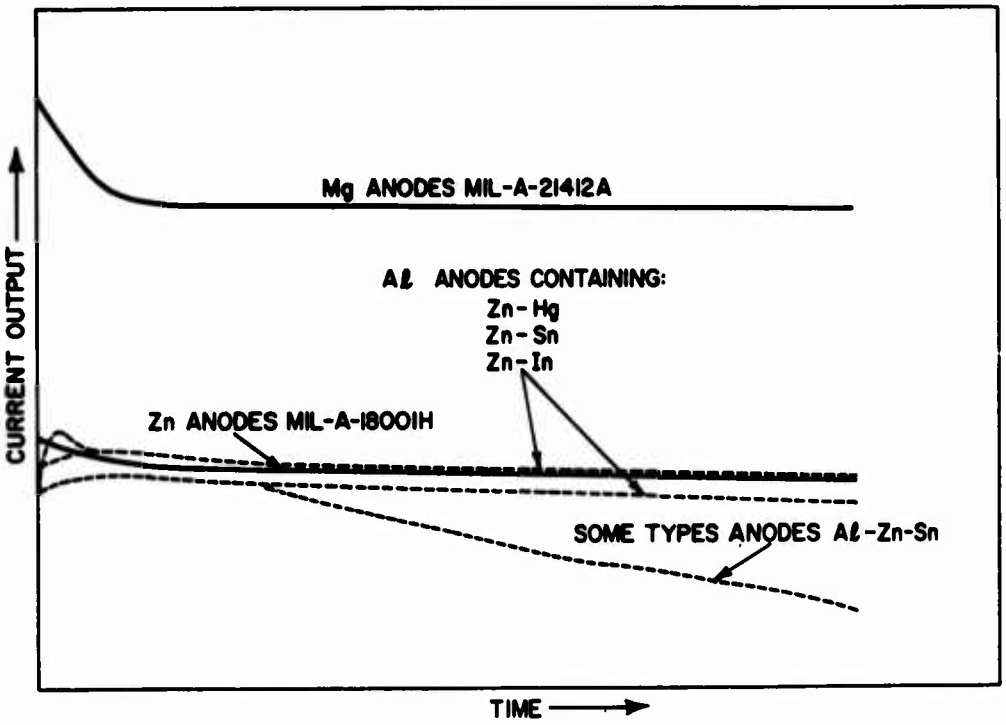


Fig. 2--Current output-time characteristics for magnesium, zinc, and aluminum galvanic anodes in sea water.

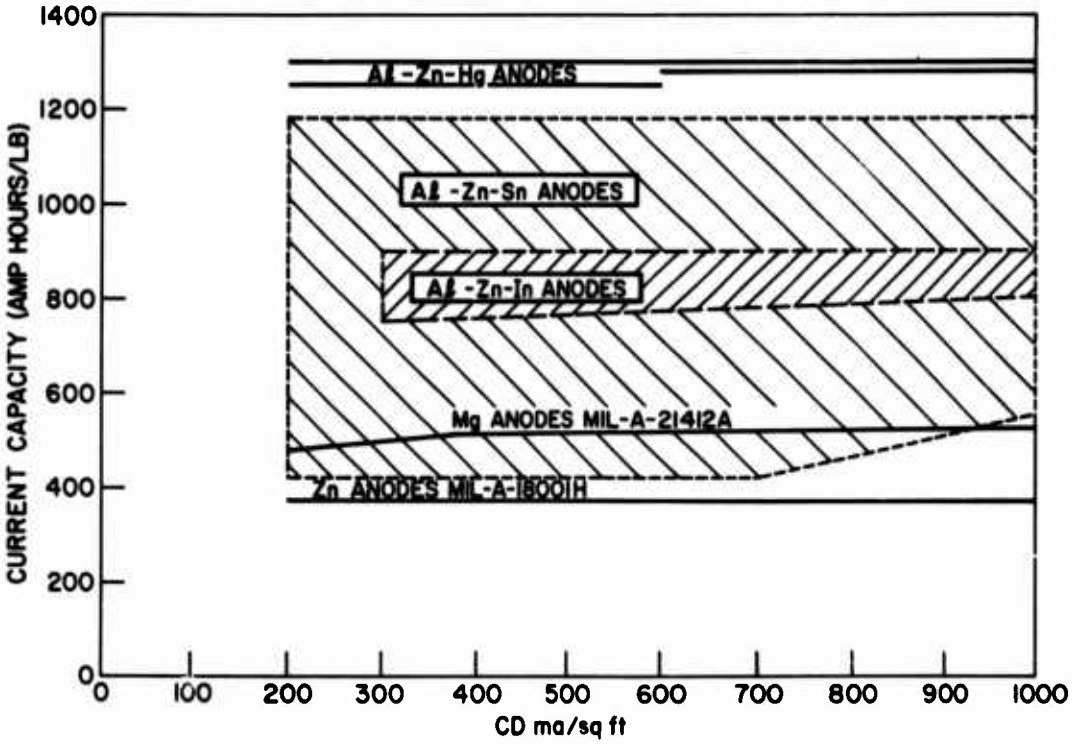


Fig. 3--Current capacity of galvanic anodes as a function of anode current density.

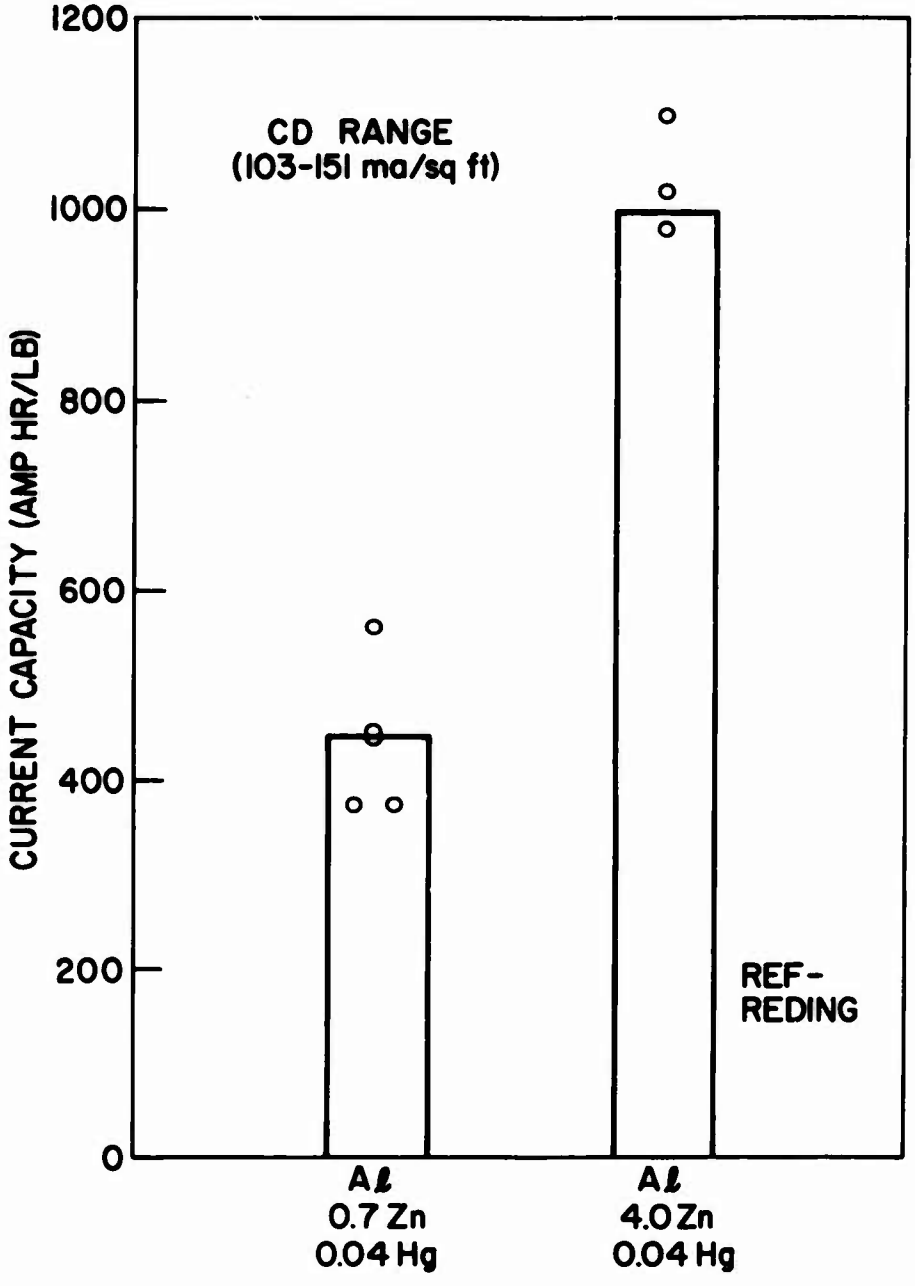


Fig. 4--Current capacity of low and high zinc content aluminum-mercury galvanic anodes in anaerobic mud covered with sea water.

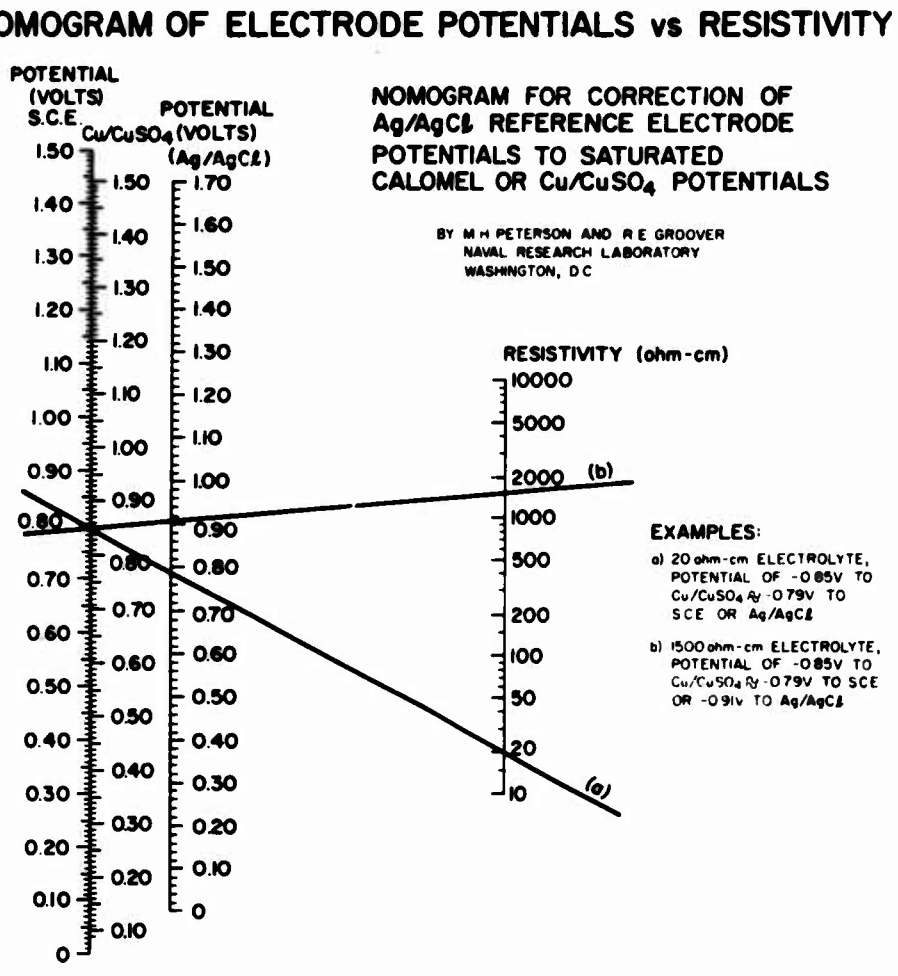


Fig. 5--Nomogram of electrode potentials vs resistivity.

Proceedings of the 3rd International Congress on Marine Corrosion and Fouling, held October 2-6, 1972, Gaithersburg, Maryland

Studies on the design of cathodic protection systems for cargo/ballast tanks of crude oil tankers

W. Posch, C. de Waard and W. Smit

Koninklijke/Shell-Laboratorium, Amsterdam
(Shell Research N.V.)

Cathodic protection of the cargo/ballast tanks of large crude carriers is complicated owing to sheer size and the fact that steel covered with waxy sludge stimulates pitting corrosion. Data necessary for the appropriate design of cathodic protection systems have been collected in three ways: by monitoring currents and potentials on board tankers over a service period of two years, by in-situ measurements of current distributions in such tanks and by model studies and theoretical calculations of current distributions.

Der kathodische Schutz von Ladung/Ballast Tanks von sehr grossen Rohöl-Tankern ist bedingt durch deren Grösse und die den Lochfrass begünstigenden Ablagerungen von wachsartigen Rohöl-rückständen keine einfache Aufgabe. Die für eine richtige Auslegung des kathodischen Schutzsystemes notwendigen Daten wurden aufgrund von jahrenlangen Messungen von Schutzströmen und Potentialen auf Tankern sowie Stromdichtemessungen in derartigen Tanks und aufgrund von Modellstudien und theoretischen Berechnungen ermittelt.

La protection cathodique des réservoirs charge/lest des grands pétroliers à brut est compliquée par leurs grandes dimensions et par le fait que l'acier couvert de boues paraffineuses stimule la corrosion par piqûre.
Les données nécessaires pour arriver à des systèmes efficaces de protection cathodique ont été recueillies de trois façons: en enregistrant continuellement les courants et les potentiels à bord des pétroliers pendant deux années, en mesurant sur place les distributions de courant dans ces réservoirs et en faisant des études sur modèles et des calculs théoriques concernant les distributions de courant.

Key Words: crude oil tankers; cargo/ballast tanks; corrosion; cathodic protection; designs.

Introduction

The problem of "bottom pitting" in cargo/ballast tanks of crude oil tankers has received increasing attention in recent years. Operational factors, such as longer ballast voyages and the considerably larger size of the tanks in the very large crude carriers (VLCC's) of today, may have favoured this nasty and serious type of corrosion. On the other hand, more stringent requirements for corrosion control have to be met due to the permission of reduced scantlings. We have shown already (1)[1] that this pitting corrosion is the result of a purely electrochemical corrosion, that waxy sludge layers - contrary to general belief - do not act as insulators but instead stimulate localized corrosion and that areas of different waxy sludge coverage can interact electrochemically over rather large dis-

[1] Figures in parentheses indicate the literature references at the end of this paper.

tances (giant corrosion cells). It is in particular the latter phenomenon that places the problem in the proper perspective, because it indicates that any partial protection system - such as selective painting - is bound to fail. It has become clear that if cathodic protection is the solution - as suggested by ourselves and many others - the entire surface of the tank has to be reckoned with in a cathodic protection design, mere protection of those surfaces subject to pitting not being sufficient.

The application of cathodic protection in cargo/ballast tanks of VLCC's is much more complicated than for other marine purposes. To be able to come to a proper evaluation of the technical problems involved and to anticipate what degree of protection can be achieved at reasonable cost, we had to have full knowledge of the parameters governing corrosion and protection in these tanks. To this end we pursued a number of possibilities. In a first approach we collected data on existing cathodic protection systems. Highlights of this experience are given. The second - also rather pragmatic - approach was mapping the protective current distribution pattern in a cathodically protected ballasted tank. In this method the current densities were measured in situ with the aid of a novel type of probe, positioned by a diver. The third way was assessing the protective current distribution pattern by model experiments. These model experiments were supplemented with a theoretical study, in which, in addition to such factors as tank geometry and anode positioning, the polarization resistance of the steel surface to be protected was taken into account.

Electrochemical data from monitoring existing cathodic protection systems in cargo/ballast tanks

Electrochemical data about cathodic protection installations with zinc anodes were collected by monitoring over a service period of two years anode current outputs, protective current densities and potentials in cargo/ballast tanks of two tankers. In the one vessel all horizontal tank surfaces were painted, in the other no paint had been used at all. The experimental set-up and results have been reported in detail elsewhere (2). Two features considered important for the design of cathodic protection systems, viz. the anode current output versus time relationship and the protective current demand, will be discussed here.

At the beginning of a clean ballast voyage, the anode current output was considerably larger than that at the end of the run. The current output often decreased exponentially with time, according to the equation

$$i_t = i_\infty + (i_o - i_\infty) \cdot e^{-\frac{t}{\tau}} \qquad (1)$$

The time constant τ varied quite a bit from run to run, but appeared to be of the order of 1 - 2 days. Typical examples of experimental curves are shown in Fig. 1.

According to Vetter (3) the current response to a potentiostatic pulse can be described by a sum of exponential functions when transport of the electrochemically active species is controlled by diffusion and convection. Eq. (1) is compatible with this, though, strictly speaking, we are not dealing with a potentiostatic pulse. Nevertheless we can conclude that the dynamic behaviour of the anode output is probably controlled by the formation of an oxygen-depleted layer of the ballast water near the cathode, i.e. the surface area to be protected. In other words, if such a current output pattern is obtained, the anodes are doing their utmost to protect the steel.

In dirty ballast, however, such peak values were very seldom obtained. In general current output curves had the shape as shown in Fig. 2. Even after a considerable time of protection the current output sometimes still increased. This and the fact that rather noble potentials were measured in the vicinity of the anode indicate that anodes were largely incapacitated by sludge deposits, and the protective current demand was not satisfied.

From the current densities and potentials measured at the same location polarization curves could be constructed. A typical curve for a bulkhead obtained on the computer - used to process the huge amount of data - is shown in Fig. 3. This curve exhibits the feature characteristic of a corrosion process controlled by diffusion of dissolved oxygen, viz. a current plateau. The magnitude of this current represents the protective current requirement.

The current density required for full protection can also be derived from the corrosion current density of the steel in the unprotected condition, i.e. from the relation between corrosion current and polarization resistance. The slope of the polarization curve at $i = 0$ then gives the polarization resistance. As shown in Table 1, a reasonable consistency was found between the current densities derived by these two independent methods.

From Table 1 it appears that the current density requirement for verticals is about 40 mA/m^2. For bare horizontals this is about 100 mA/m^2, while for bare areas (defects) in painted horizontals an average of 650 mA/m^2 is found.

It is quite clear from these figures that in the case of horizontals the current density for damaged spots in a coating is much higher than for steel without a coating. Nevertheless one has to assume that the total current required for a coated horizontal surface should require less current than or at least as much current as the same area of bare steel. Eq. (2) gives the function describing the current demand of painted horizontals:

$$i_{hor} = 100 + \frac{1}{0.0015 + \left(\frac{d_{O_h}}{O_v}\right)^2} \ (mA/m^2) \qquad (2)$$

where d_{O_h} is the fraction of damaged horizontal surface area and O_v is the (bare) vertical area. We have plotted eq. (2) in Fig. 4, where the full line represents the current densities in the damaged area only, and the dashed one gives the current for the total area, i.e. coated + damaged areas.

Protective current density measurements in ballasted tank with the aid of a diver

It was felt necessary to get supplementary information about the current density distribution in a ballasted tank, since in the above experiments densities had been measured in a limited number of places only. To this end we devised a new method based on the following principle. The current flowing from the anodes to the steel surfaces to be protected will do so according to a certain pattern, the shape of which is governed by the current requirements of the relevant surfaces. The potential with respect to the electrolyte along the current lines will change when current is flowing. Two reference electrodes positioned along the lines will show a potential difference, which can be measured. This potential difference, $\vec{V}$, is related to the vector component, $\vec{I}$, of the current flow along the line between the two electrodes according to:

$$\vec{V} = \rho \,.\, \vec{I} \,.\, \vec{l} \ , \qquad (3)$$

where ρ = specific resistivity of the electrolyte and
$\vec{l}$ = distance between the electrodes.
It follows from this equation that from a potential difference measurement the current flow can be calculated;

$$\vec{i} = \frac{\vec{V}}{\rho \,.\, l_{eff}} \ . \qquad (4)$$

In this equation l has been replaced by l_{eff}, which is found by calibration for a fixed reference electrode arrangement.

When l is small compared with the dimensions of the steel parts on which the measurements are done, $\vec{I}$ parallel to the steel surface may be assumed to be zero. In that case only the component perpendicular to the steel surface need be measured.

When using a method based on this principle, the small, but varying offset between the two nominally equal electrodes must be compensated for. This can be done either by interchanging the electrodes in each set of measurements and eliminating the offset by taking the average of the two readings, or by measuring the offset separately in the same electrolyte, but shielding the system from external currents. With the probe used, which is shown in Fig. 5, the latter method was adopted. The probe consists of a U-shaped body of rigid PVC tubes, which was attached perpendicularly to the steel wall by a strong permanent magnet. Two standard calomel electrodes were installed inside the legs of the U. The leads of the electrodes ran through the bottom of the U and were connected outside the electrolyte to a sensitive microvoltmeter.

The tiny holes in the legs of the tubes positioned at the height of the electrodes, by which connection with the electrolyte was achieved, were shielded from outside currents by a water-filled tube. In Fig. 5A, the probe is in the measuring position, in Fig. 5B in the offset reading position.

The probe was calibrated in the laboratory. The factor by which a mV reading was converted to mA/m^2 turned out to be 30.6 for ballast water with a resistivity of 23.4 Ωcm.

The measurements were carried out with the aid of a diver who positioned the probe and made the necessary changes for determination of the offset. Series of measurements were taken, first in a number of locations on the bottom and then going up the bulkhead in the same bay. The distance between two successive measuring points was about 1 m.

A typical profile of current densities and potentials for a longitudinal bulkhead is shown in Fig. 6. It can be seen that up to 4 m the current density is almost constant; then it decreases smoothly until, at 9 m, some peaks appear which are not reflected in

the potentials. Differences in surface conditions of the steel, i.e. coverage with waxy sludge. are possibly the reason for this. It is interesting to note that the potential does not follow this trend, which permits the conclusion that potentials alone are not necessarily an adequate yardstick for measuring the degree of protection.

When the measured current densities are plotted versus the potentials for one large area, an impression can be obtained about the polarization characteristics of this surface. Such a plot is shown in Fig. 7, which reveals a striking difference between the points relating to the vertical bulkhead and those to the bottom. The points for the bulkhead are on or fairly close to the curve expected for oxygen diffusion controlled corrosion. From the limiting diffusion current a current demand of about 40 mA/m^2 can be derived. The results for the bottom, however, do not show any saturation effect, the potential hardly changes over a wide range of current densities. Obviously bottoms require a considerably higher current density to obtain protection.

Another interesting phenomenon occurred when doing measurements on pipeline sections in a tank. Pipelines in large crude carriers are nowadays often made of nodular cast iron. To obtain the flexibility necessary in view of the movements a ship makes, joints with rubber glands, etc., are employed. As a result electrical contacts are rather poor, and if no additional anodes are placed on the pipelines, the effect of cathodic protection leaves much to be desired. In Fig. 8 it is shown that the top side of such a pipe section not only receives less protective current than the bottom, but is sometimes even sacrificed to the protection of the bottom. This example proves clearly how a difference in sludge coverage can lead to interaction between surfaces and that it stimulates and sustains local corrosion. It has become quite evident that the cathodic protection of such pipelines should receive special attention so as to prevent premature failure by pitting.

Model studies and theoretical calculations on current distribution

Rounding off our study, we attempted to collect additional data on the protective current distribution in a cargo/ballast tank by model studies and a theoretical treatment of the problem. In particular it was thought that by these methods a better understanding of the influence of geometry and anode arrangement can be obtained.

The protective current distribution is governed by the resistance between the electrodes. When the resistance of the anodes is considered to be constant, there are two variables which contribute to the total resistance:

(1) The resistance of the ballast water between anodes and any part of the tank, which depends on tank geometry and water conductivity;
(2) the polarization resistance of the surface to be protected, because the steel itself sets an upper limit to the current it accepts.

The influence of geometry and anode arrangement was assessed in scaled models. The contribution of the polarization was made negligible by using alternating instead of direct current. The conductivity of the water used was adapted to the scaling factor of the model. Our model represented a part of a tank where the current distribution etc. had been monitored, so that model tests could be compared with field data.

Typical current distributions near bulkheads are shown in Fig. 9. It appeared that with the anode arrangement as in this case - i.e. all anodes on the bottom, the bottom and lower part of the bulkheads only receive sufficient protective current. Moving the anodes to a somewhat higher level only marginally improves the current distribution with respect to bulkheads. In Table 2 field and model current densities are compared. In view of the fact that this was a simplified model, the agreement is very good.

In order to account for the effect of the polarization resistance, a more definite idea of the essential role of the geometrical parameters was needed. To this end the effect of anode geometry and location was investigated theoretically for a sphere and for an infinitely long cylinder, above an infinitely large steel plate. These cases were solved analytically via the Green function approach to the Laplace equation. There was a fairly good agreement between the current densities calculated with the aid of a computer program and those obtained from model experiments. Subsequently, the effect of a potential-independent polarization resistance was studied on the basis of an extension of the above-mentioned analysis. Fig. 10 shows the dependence of anode output on anode/cathode distance, with the polarization resistance as a parameter. For a number of polarization resistances, the anode output shows a maximum at a certain distance, whereas for large distances the output does not depend any more on the anode/cathode distance. The output is then nearly equal to the output controlled by the anode resistance, which is completely determined by the shape of the anode. The relative insensitivity of the anode output as a function of the polarization resistance indicates that similar results are to be expected when the polarization resistance is no

longer independent of the potential. In contrast with the anode output, however, the distribution of the current depends very much on anode/cathode distance as well as on polarization resistance. In Fig. 11 an example is given of the relation between the anode/cathode distance and the area receiving a current density which is greater than or equal to a certain fraction of the initial corrosion current. It shows that this area yields a slight maximum for a certain distance, which is caused by a decrease of the current density at larger anode/cathode distances, and a decrease of anode output for small distances.

Amsterdam, 6th September 1972
DS

REFERENCES

1. W. POSCH and J. JACKSON, "Waxy sludge deposits, a cause of pitting corrosion in cargo tanks of crude oil tankers", paper presented at 2nd International Congress on Marine Corrosion and Fouling, Athens, September 1968.
2. C. DE WAARD and W. POSCH, "Cathodic protection of cargo/ballast tanks of crude oil tankers", paper presented at the Conference on Corrosion and Fouling of Metals by Sea and Brackish Waters, Travemünde, March 22-24, 1972.
3. K.J. VETTER, "Electrochemical Kinetics", Academic Press, New York, 1967, p. 218.

Summarized Discussion

The author's interpretation of some of the data presented was questioned: the potential drop onto the steel surface at a frontal current density of 200 ma/sq m is 60 mv/m and controls the current density onto the steel, it was asserted. If the steel surface is painted, this control no longer exists, and at a break in the film the cathode accepts all of the current available and polarizes to a more cathodic potential. This reasoning would explain the current/potential curve at various degrees of paint damage. The model presented by the author was said to be scaled ignoring the foregoing facet of the control, so it is a model of the theory, not necessarily of the tank. The corrosion of the pipes in the tanks was attributed to an electrolysis effect caused by potential variations.

In reply, the author pointed out that the model studies considered only unpainted conditions; for damaged spots on a painted surface he would concur with the reasoning above. He was aware of a number of cases in which electrolysis (or stray current) was the obvious cause of pitting of pipelines, but some cases could not be so attributed; in such cases he is inclined towards a macro-corrosion-cell theory.

TABLE 1

ESTIMATED CURRENT DENSITY REQUIREMENTS (mA/m^2) DURING A NUMBER OF BALLAST VOYAGES

Bulkhead		Unpainted bottom		Painted bottom with defects
from R_{pol}	from limiting current	from R_{pol}	from limiting current	from R_{pol}
50	65	20	60	600
30	-	80	200	600
50	60	180	-	700
40	40	50	-	200
60	50	50	120	300
30	-	80	60	400
30	30	170	180	1250
40	-	80	-	1000
30*	35			750
40	40			
50	35			
Average 40	45	90	120	650

TABLE 2

PROTECTIVE CURRENT DENSITIES

Location	Derived from model mA/m^2	From field test mA/m^2
on transverse bulkhead 1.5 m above bottom	42.5	50
" " " 2.6 m " "	20	20
" " " 3.6 m " "	8.5	10
on bottom 0.75 m from transverse bulkhead	20	39
" " 1.33 m " " "	150	54

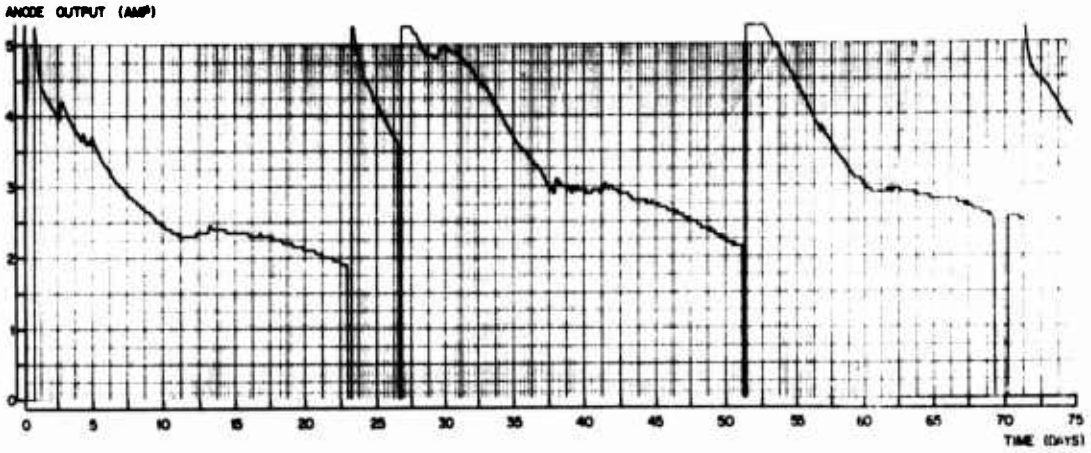


FIGURE 1
ANODE OUTPUT FOR A NUMBER OF CONSECUTIVE CLEAN BALLAST VOYAGES

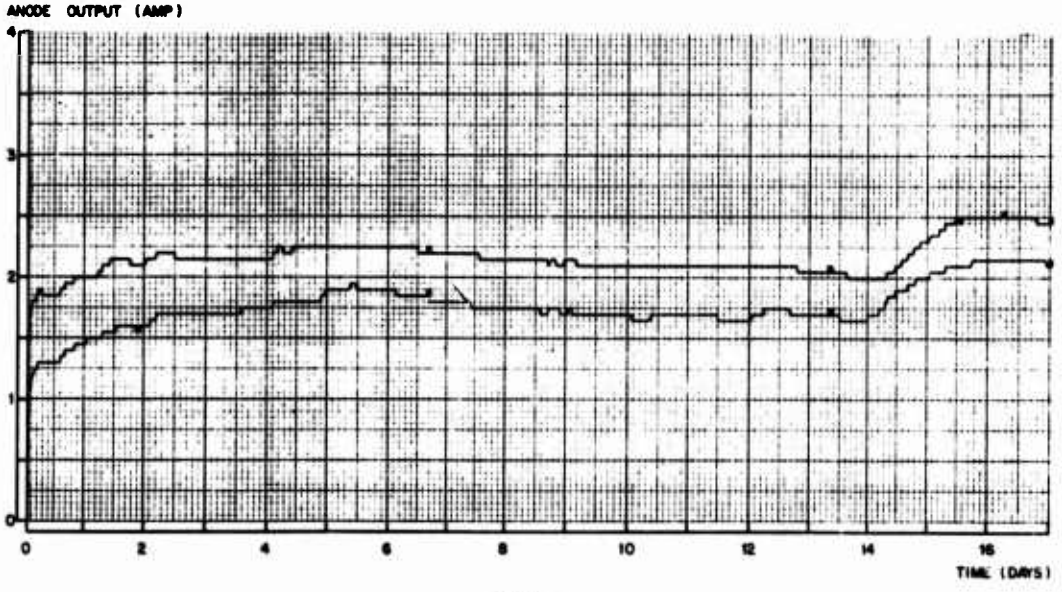


FIGURE 2
ANODE OUTPUTS DURING A DIRTY BALLAST VOYAGE

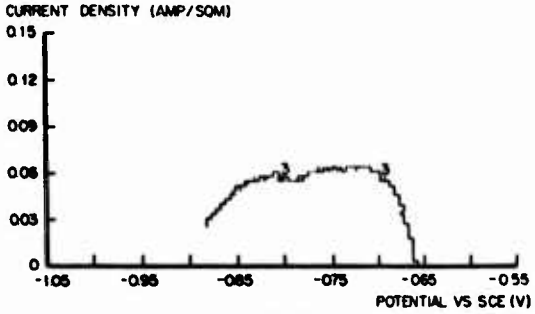


FIGURE 3
EXAMPLE OF AN EXPERIMENTAL POLARIZATION CURVE
OF A BULKHEAD

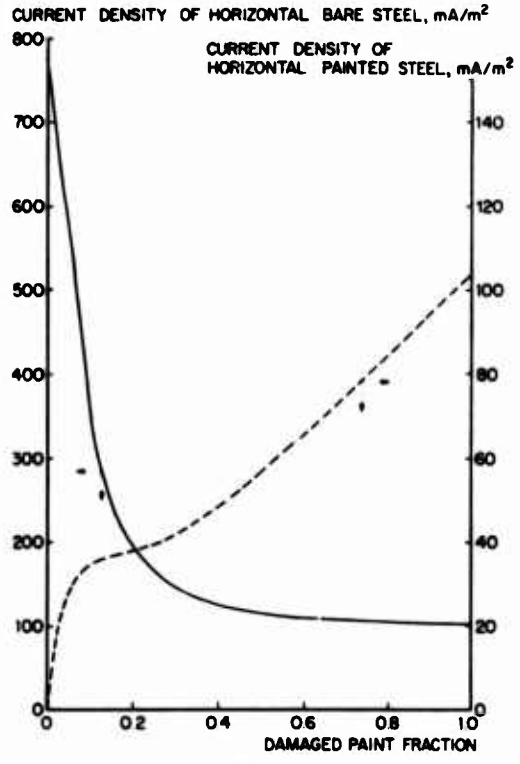
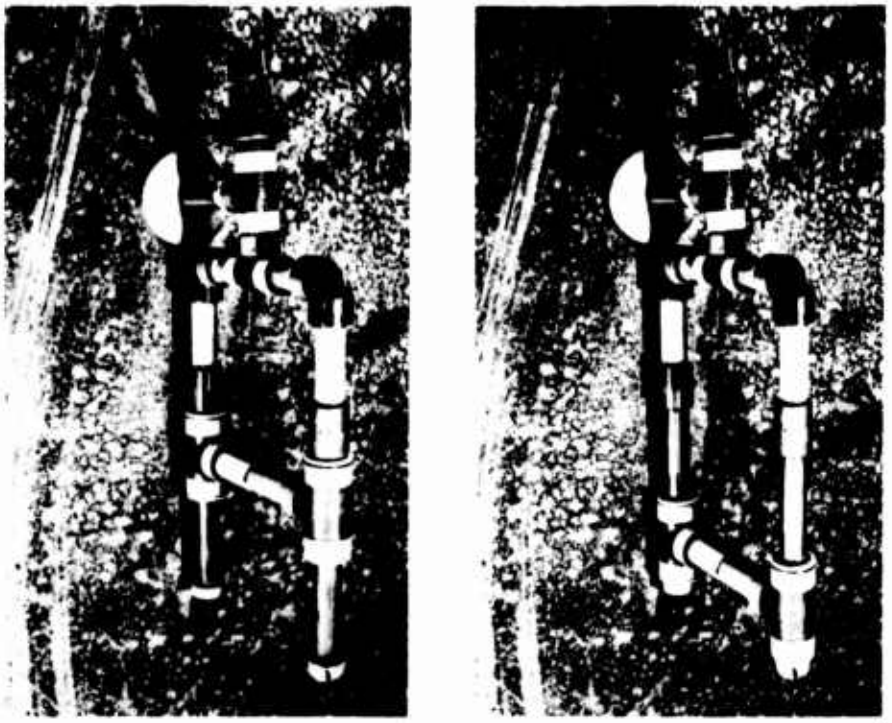


FIGURE 4
CURRENT DENSITY VERSUS PAINT DAMAGE
OF HORIZONTAL PAINTED STEEL
RATIO HORIZONTAL/VERTICAL AREAS = 1/2



A B

FIGURE 5

CURRENT DENSITY PROBE

A = MEASURING POSITION

B = POSITION FOR DETERMINATION OF OFF - SET

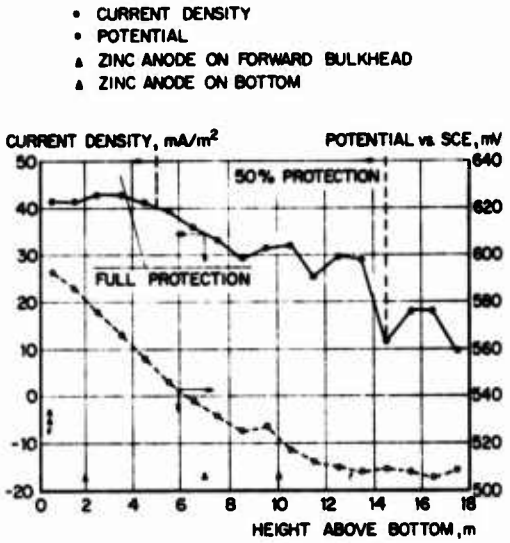


FIGURE 6
CURRENT DENSITIES AND POTENTIALS
ON LONGITUDINAL BULKHEAD

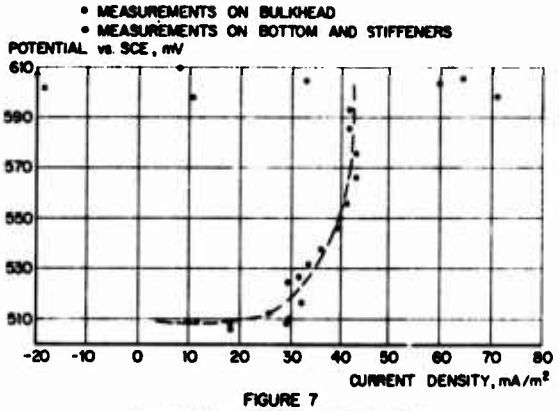


FIGURE 7
POTENTIAL/CURRENT-DENSITY PLOT

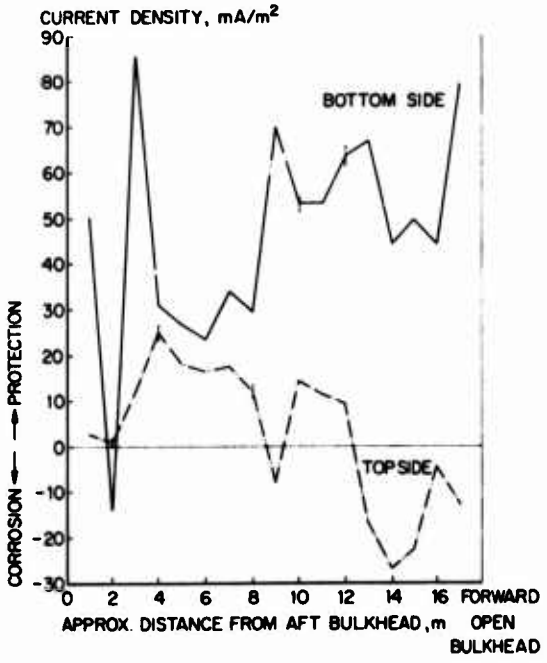


FIGURE 8
CURRENT DENSITIES ON TOP AND BOTTOM
OF A CARGO LINE

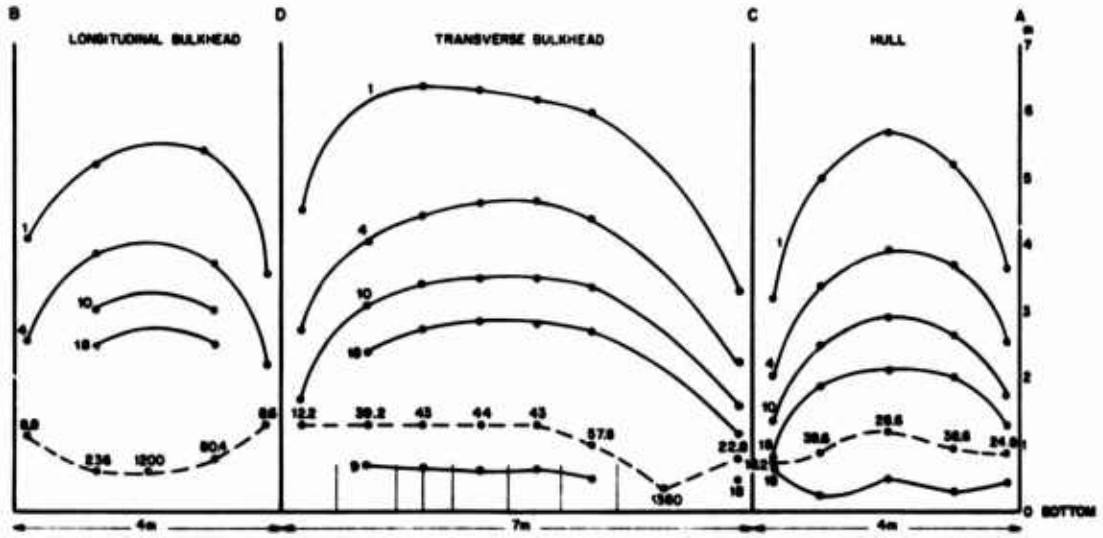


FIGURE 9

CURRENT DISTRIBUTION ON WALLS OF TANK MODEL (mA/m^2)

---- HIGHEST CURRENT DENSITIES

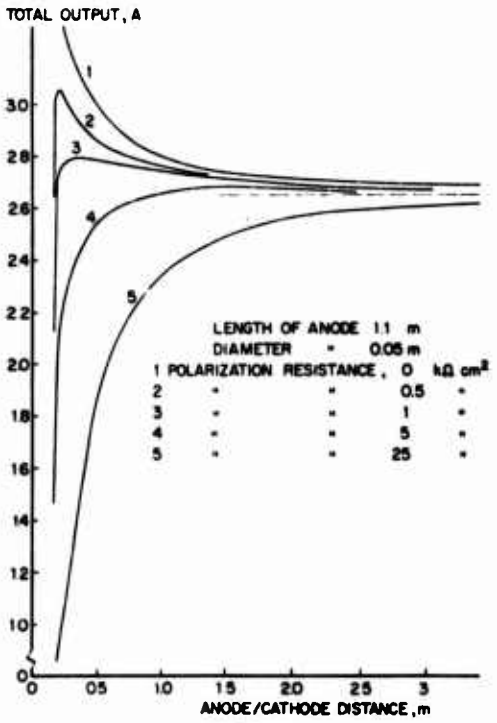


FIGURE 10

TOTAL OUTPUT OF ANODE VERSUS ANODE/CATHODE DISTANCE

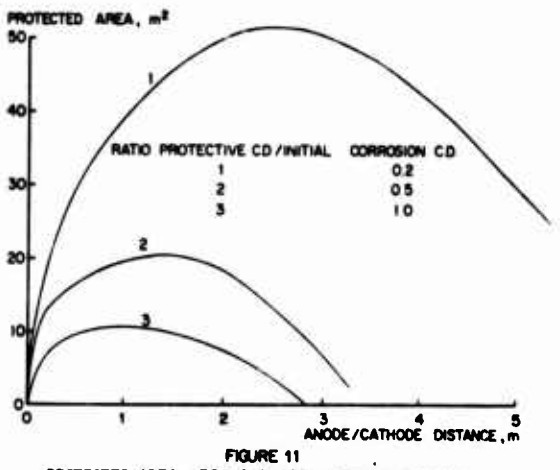


FIGURE 11

PROTECTED AREA VERSUS ANODE/CATHODE DISTANCE

Cathodic Protection of Alcan's Port Alfred Harbor Facilities

B. H. Levelton

President
B. H. Levelton and Associates Ltd.
Vancouver, Canada

G. Riedl

Senior Engineer
Alcan Engineering Services
Montreal, Canada

A. Location of Facilities

Port Alfred Harbor is located at the end of a nine-mile-long bay on the Saguenay River, 66 miles upstream from the St. Lawrence River. Figure 1 shows the location of the harbor.

B. Harbor Facilities and Design

Originally, the harbor had two wooden wharves. New Powell Wharf Berth No. 1, 2 and 3 were erected during 1947-48. It consists of a concrete deck supported by 2300 steel H-piles arranged in 105 bents 10-11 feet apart. Berth No. 4, built in 1954-55 has 366 steel H-piles. The average wetted length of piles during high tide is 40 feet. Powell Wharf is used for the handling of metal, paper, oil, caustic and miscellaneous cargoes.

Frodingham sheet piles (281) were used for 362 feet of Bulkhead south of Powell Wharf.

The wooden structure of Duncan Wharf was replaced in four sections between 1953-64. Sections No. 1 - 4 consist of 866 steel H-piles. During the winter of 1971-72, the wharf was extended by the addition of Section No. 5 built on 148 tubular steel piles 30 inches in diameter. Simultaneously part of Section No. 3 and 4 was reinforced by two rows of 30 inches diameter piles. Duncan Wharf is used for the unloading of bauxite, coke, salt and other bulk materials.

The 260 feet long bulkhead between Duncan and Powell Wharves consists of 190 Frodingham sheet piles.

Figure 2 shows the harbor layout.

C. Environmental Conditions

1. Water

The bay is characterized by two distinct strata, the upper layer 20 to 25 feet thick consisting of river water contaminated to some extent by seawater, and the lower layer consisting of seawater diluted to a degree by fresh water. The compositions of the fresh water stratum varies with time of year, tides and winds. The seawater stratum does not change significantly throughout the year.

The temperature of both strata remains between 36 and 38°F. throughout the year.

Typical salinity profiles for various times of the year are shown in Figure 3.

Discharge of effluents from the neighboring pulp mill have led to deposition of large amounts of fine organic matter within the harbor. Under Powell Wharf this organic material forms a layer several feet thick. Water analyses at the bottom have shown hydrogen sulfide levels as high as 3000 ppm. The pH of this bottom water was as low as 5.8, a marked decrease from the normal seawater pH of 8.1 measured further out in the bay.

Tidal levels in the bay may vary as much as 24 feet, and strong tidal currents occur.

The bay and the Saguenay River are basically free from marine fouling. In the past two years there is evidence that minor fouling by a bryozoan organism is increasing. Occasionally ships bring in mussels which will live for a short while in the saline layer, but these are rare. The fouling that does exist leads to a slimy formation which does not offer a significant barrier to protective current.

2. Ice

Port Alfred experiences climatic extremes. During the brief summer the temperature may reach 90°F with high humidity, while in winter, which lasts four to five months, the temperature may stay below 40°F for several weeks.

During winter months the bay freezes over with ice thicknesses up to 3½ feet. Beneath wharves all piles are covered with ice in the intertidal zone with thicknesses up to 6 feet. In addition, tidal action leads to formation of spherical lumps of ice which may range up to 5 feet in diameter. At high tide these spheres tend to bridge the space between piles, forming arches which become cemented together in time.

Figure 4 shows typical conditions beneath the wharves.

Tidal currents and wind action lead to an accumulation of pack ice up to 25 feet thick in various areas.

Since the harbor must be operated year round, two icebreakers are stationed at Port Alfred.

The onset of warmer weather, occurring approximately in the middle of April, causes the accumulation of ice to drop in large pieces. These pieces may weigh several tons (Figure 5).

D. Early Cathodic Protection Designs

Recognition of the corrosivity of water and examinations of piling indicated the need for a cathodic protection system. Accordingly in the fall of 1954, a cathodic protection system was designed and installed on Powell Wharf Berth No. 1 and 2 by an outside consultant. It consisted of 955 graphite anodes, 3 inches diameter x 60 inches long and 62 aluminum ingots. The anodes were installed in strings at the mudline between the bents. The current was supplied by 16 rectifiers, 240 amps, 12 volts each.

Although protective potential was achieved in some sections of the wharf, visual inspection indicated unabated corrosion in many areas.

In December 1955, the cathodic protection for Powell Wharf Berth No. 4

was energized. It consisted of 3 rectifiers, 400 amps, 12 volts each, supplying current to 15 steel piles 3000 lbs. installed in Pond No. 1 and 2, and 16 large carbon blocks installed on the north side of the berth.

The above designs were based on the assumption that 5 ma/sq. ft. for the area exposed to water and 1 ma/sq.ft. for the section of piles below the mudline would be sufficient to protect the wharf.

After several years of operation and continuous difficulties with the maintenance of anodes and rectifiers it became obvious that to stop corrosion a much higher current density was required. Consequently 16 new rectifiers, 400 amps, 15 volts each, were installed in December 1964. This modification greatly increased current on the main Powell Wharf but did not improve significantly the pile-to-water potential.

On Duncan Wharf each new section replacing the wooden structure was cathodically protected. The first system installed on Section No. 2 consisted of 131 graphite anodes, divided into 6 ground beds, and one rectifier, 400 amps, 12 volts. The anodes 4 inches diameter x 80 inches long were maintained on 6 large steel racks 100 feet north of the wharf.

It soon became obvious that the protective current was not going beyond the first 2 rows of piles located nearest the graphite beds. Consequently, this design was abandoned in favor of anodes installed in strings at the mudline between bents.

The entire protection of the 4 new sections of Duncan Wharf consisted of 11 rectifiers supplying 3700 amps, 12 volts, and 426 graphite anodes, 4 inches diameter x 80 inches long.

The annual loss of anodes or strings was extensive. During the 14 years of operation between 1954-68, 1474 anodes were installed with the original design and additional 1986 anodes due to maintenance for a total of 3466 anodes or 260,000 lbs. of graphite. None of this graphite could be recovered.

The failure of anodes and strings was due to mechanical damage by ice, turbulence of water, breakage and general deterioration of cables. Most damage occurred in shallow water where the ice or debris simply broke or ripped off the anodes. The anode-cable connection was not strong enough to take the continuous movement and rolling of anodes due to tides and propeller wash. Some anodes contained hidden defects which could not be detected before installation. The cable insulation was too thin and too weak to take the mechanical abuse due to movements of debris at the mudline and low temperature of water.

Because of differences in salinity and in the level of the mudline, anodes attached to the same string were operating at greatly different current densities. Anodes located at the low end of a string, where the water was deeper and had higher salinity, were discharging many times the amount of current discharged by anodes of the same string but located at higher ground where the salinity and the conductivity of water were lower. This caused rapid consumption of anodes in the deeper end of the wharf which has longest piles and requires more protection.

The average cost of installation and of maintenance of the cathodic protection from 1954-66 was approximately $35,000 per year.

E. Re-Assessment of Protection Requirements

A detailed survey of piling beneath the wharves in 1967-68 indicated severe metal loss immediately below the capping beam and in the zone around low tide. (Fig. 6) Accordingly, a long-term rehabilitation program was

instituted.

The upper ends of piles (splash zone), where severe localized corrosion occurred, were built up by welding, reinforced with steel plates, sand-blasted and coated with a tar-epoxy underwater curing compound formulated for this application.

The experience encountered in weaknesses of earlier designs and the observed corrosion of piling in immersed areas led to the formulation of new criteria for a cathodic protection system:

1. It must withstand the action of pack ice and ice build-up on piles beneath the wharves.

2. It must withstand turbulence from tidal action and propeller thrust.

3. It must distribute current uniformly in both fresh and saline layers.

4. It must be easily replaceable and/or repairable.

5. It must give a 15-year minimum life.

6. It must be effective immediately.

F. Field Studies to Determine Design Parameters

During the summer of 1968, a program was initiated to establish variations in salinity and thickness of the two water strata. Early results showed conclusively the need for two separate protection systems, one at or near the bottom in seawater, and the other near low tide generally in fresh water. To determine the vertical and horizontal distribution of anodes in these two systems an experimental cathodic protection system was installed on Powell Wharf Berth No. 3. It consisted of several anodes located at the bottom and several more at low tide level fed from two separate rectifiers. Individual anodes were moved by pulleys both vertically and horizontally to determine the configuration providing optimum protective potentials on all surrounding piles.

These tests led to the design of a complete system for Powell Berth No. 3 consisting of one rectifier supplying current to 25 carbon anodes (750 lb. each) on the ocean bottom and a second rectifier feeding 25 lead-silver plate-type anodes (17 x 17 inches, 56 lbs.) mounted on anchored plastic floats (Fig. 7). This system was considered to be experimental for the purpose of evaluating the effects of ice and currents.

The inspection of this system in the spring of 1969 revealed excellent protection of piling to essentially full tide and good condition of floating anodes. No anodes were lost in spite of several bottom anodes and floats with anchors being moved from their original positions by tides and propeller wash. The consumption of carbon anodes was high and records of subsequent years have shown that they are not practical cathodic protection anodes.

The lead-silver anodes, while performing adequately, have shown over the years a localized wastage near the center (close to the cable attachment) and require a higher driving potential than graphite.

G. Design for Powell Wharf Berth No. 4

Experience after one year's operation of Powell Berth No. 3 showed that improvements in anode material, cable, connectors, conduits and wiring techniques were necessary. The design for Powell Berth No. 4 incorporated Alcan-Grade high-density resin-saturated graphite anodes (12 inch diameter,

10 inches high, 75 lbs.) for both upper and lower levels.

1. Upper System

This system consisted of 103 anodes, 91 of them rigidly fixed on horizontal continuations of 2½ inch pipe conduit, one foot below zero water level (-1.0 ft.) and 12 on new cylindrical glass-fiber/polyester floats. These floats were anchored by ropes to horizontal sections of conduits located at -8.0 ft. These anodes were served by two rectifiers.

The decision to install only 12 floating anodes was made because of the high cost of floats and concern about their resistance to ice surrounding them at low tide.

2. Lower System

It consisted of 102 anodes installed on 2½ inch conduit at the bottom. These were served by two rectifiers. The overall design is shown in Exhibit 40.

The first winter's operation demonstrated clearly that the decision to use rigidly fixed upper level anodes was a mistake. All 91 anode assemblies were damaged to some extend, whereas the 12 floating anodes on Powell Berth No. 4, and 25 on Powell Berth No. 3 were undamaged. The 91 rigidly fixed anodes continued to operate in spite of the conduit being bent downward and some anodes being ripped off the brackets and holding plates (Fig. 8).

It was obvious that damage resulted from direct impact of large masses of ice, not from downward thrust of pack ice. Significantly, the floats yielded under impact without incurring damage. This experience showed that it was futile to design a rigid structure to withstand ice impacts--it was necessary instead to design an assembly which yielded and then sprang back.

Excellent protection was afforded by the system to piling. Measurement of potentials and observation of pile surfaces indicated full protection to half tide level with significant protection even at high tide level. The provision of an upper level of anodes gave good protection to steel whenever it was immersed and residual polarization reduced corrosion of steel exposed when the tide dropped.

All upper level anode assemblies are gradually being replaced by floating-type anodes, tethered by ropes to the piling. The excellent experience with the cylindrical plastic floats has lead to their general use where space is not a problem.

The float design is based on a number of considerations:

1. It must permit the anodes to be mounted on the top to "throw" the current upward.

2. It must have a low center of gravity to prevent the assembly from turning upside down, hence, some counterweighting is necessary.

3. It must be adequately buoyant to hold the 75 lb. anode and to provide at least another 25 lb. upward thrust to hold itself in position.

4. It must be robust enough to withstand buffeting by ice.

The details of this instrumentation are outside the scope of this paper.

H. Designs for Remaining Wharves

The remaining wharves not protected as of the spring of 1970 were: Powell Wharf, Berths No. 1 and 2; Duncan Wharf, Sections No. 1 through 4; and Duncan Wharf Extension, or Duncan Section No. 5.

Of these, the Duncan Extension was different in that it was constructed from 30 inch pipe piles filled with concrete rather than H-piles. Since it was not completed until late in 1971, it was the last section to receive a measure of protection.

The designs proven on Powell Berths No. 3 and 4 were extended to the remaining structure, viz. use of two levels of anodes, the top supported on floats anchored just below low tide level. These designs worked extremely well in those areas where there was deep water (10 feet at least) even at low tide.

The in-shore ends of both Powell and Duncan Wharves posed new problems. At low tide much of the area is dry or covered by only a few feet of water principally on the west sides of Powell Berth No. 1 and Duncan Sections No. 1, 2 and 3 where ships do not moor at any time. Since floating anodes would clearly be of no use here, and since heavy abuse from ice was anticipated, a new design was developed using a 12 inch diameter by 36 inch graphite electrode. This was buried two-thirds in the ground with the anode lead entering the bottom end, protected by a wooden box, and laid in a trench to conduit on the nearest pile. These "shallow-water" anodes have withstood two winters without damage by ice. The graphite has proved to be remarkably tough and strong. Figure 9 shows typical installations.

In those areas with about five feet or less of water at low tide, a conventional anode rigidly fixed to a bracket set at the mudline was adopted. This arrangement is necessary where the ground slopes and a "shallow" water anode could not be placed, or where the cost of working under water to place an anode was prohibitive.

Other anode assemblies on Powell Berth No. 1 and 2 and Duncan Berths No. 1 through 5 utilized a 12 inch diameter by 15 inch graphite anode rather than the 12 x 10 inch anode used previously. This size was selected to lower circuit resistance and to ensure a longer life (Fig. 10).

The ice damage beneath Duncan Wharf exceeded all expectations. Even though the smallest conduit used was 1½ inch pipe securely strapped to piles, the weight of ice ripped off, broke and bent it. Figure 11 shows typical damage resulting from the winter of 1970-71. As a consequence, it is now standard practice to use 2½ inch pipe as conduit attached every 30 inches to piling with welded steel straps, and constructed to conform to the profile of piles and capping beams. No fillets where ice can collect are permitted. The damage perhaps is not surprising in view of ice build-up.

The damaged conduits were re-installed using the new criteria, and they, and other conduits placed in the summer of 1971, survived the winter of 1971-72 with negligible damage.

I. Rectifiers

All rectifiers are oil-immersed with either selenium oxide or silicon dioxide plates. The original rectifiers used for the early protection systems have proven to be adequate for the new system and no purchase of new units is anticipated. Routine maintenance by the Port electrical personnel ensure continued efficient operation.

The following numbers and capacities of rectifiers are installed:

Location	Quantity	Total Amperes
Powell Berths No. 1 and 2	16	6400
Powell Berth No. 3	2	1050
Powell Berth No. 4	4	1610
Duncan Sections No. 1-4	11	3710
Duncan Section No. 5	5	1360
Bulkhead (between wharves)	1	240
	39	14,370

J. Bonding of Piles

All piles within one bent are bonded by means of reinforcing steel within the capping beam. Bonding between bents has been achieved by installing a continuous four-square-inch steel bar on the outside piles immediately below the capping beam. Each pile is welded to the bar, and each wharf, in effect, is ringed by the bar. This bonding is essential to good current distribution. The bond is coated with a heavy coal-tar-epoxy paint.

K. Wiring System

1. Positive Leads

The positive leads on the wharves are two 500 MCM copper cables, each looped for the wharf length. These are carried in aluminum pipe conduit well above deck level. Each loop is served by a separate set of rectifiers floating on it. One loop serves high-level (floating, etc.) anodes while the other serves deep-water anodes. The two levels, therefore, can be adjusted independently.

On all of the Powell Wharf Berths, individual anode leads are run back to the appropriate positive busbar and attached in a series of junction boxes (Fig. 12). Current measuring shunts are installed in each lead or provision is made for breaking the circuit and inserting an ammeter. If necessary, current regulating resistances can be inserted in each anode lead (this is considered improbable).

On Duncan Wharf, lateral positive leads run beneath each bent containing anodes. One lateral serves high-level and the other deep-water anodes. Each anode lead is attached to a positive lateral and a current-measuring shunt is encapsulated in the splice. Fine potential wires lead directly from each splice to the junction box where current to each anode can be ready directly.

2. Negative Leads

The negative lead from each group of rectifiers consists of a 500 MCM stranded copper cable installed in its own conduit. This negative busbar is cross-connected at intervals to the side of the wharf remote from the rectifiers and busbars. This is normally the deep-water side of each wharf. This procedure has been followed to ensure that the maximum amount of current flows to the deep area. The precaution may appear to be trivial, but experience has shown that on a low-voltage system of this type (4.5

volts at rectifier) even minute differences in network resistance markedly affect current distribution.

L. Criteria for Protection

A pile potential of minus 0.85 volts referred to a saturated copper-copper sulfate half cell is considered to represent protection. A potential of minus 0.95 volts is preferred. All potentials are measured with the half cell as close as possible to the pile to ensure that a "point" potential is obtained.

Experience by Riedl and Levelton elsewhere has shown that a heavy fouling layer can lead to erroneous potential values (generally too high). Tests were made at Port Alfred with a diver holding an electrode at various distances less than one foot from the pile. On cleaned and uncleaned piles (at Port Alfred fouling is insignificant)no significant differences in potential was found with the electrode held directly against the pile and held at distances up to one foot away.

Extreme caution in areas near anodes is essential. A significant potential gradient exists in the water near anodes so that an electrode remote from the pile yields fallacious readings.

The presence of a so-called calcareous deposit in those areas continuously receiving high current density is common and is indicative of effective cathodic protection. Generally, such deposits tend to form in the vicinity of anodes where current density is high and potential is also high as a consequence. These deposits consist principally of magnesium hydroxide, precipitated from seawater by the caustic developed at the cathodes (piles), with lesser amounts of calcium salts.

At Port Alfred, the appearance of well protected piles is unmistakable. After something more than one year of full protection old corrosion scales, tubercles, and the like fall off, leaving a clean gray surface which shows in detail all past corrosive attack. The metal almost appears to have been acid cleaned except that the surface is dull.

The protective current density developed by studies on all systems is approximately 10 milliamperes per sq. ft. There are distinct hazards in arbitrarily selecting an average or mean current density for design of systems. Unless excellent current distribution is planned for and achieved, an average value is of little value because some areas may well be below the protective current density while others are overprotected.

M. Monitoring

In order to ensure that the wharves are being protected and to detect damage to anodes, rectifiers, and leads, routine monitoring by Port personnel has been instituted. This involves:

1. Automatic recording of potential year round at permanent reference electrodes mounted on Duncan Wharf and Powell Wharf.

2. Complete potential surveys of all wharves during the summer, using a boat and portable reference cell.

3. Checks of rectifier operation every month.

4. Recording of individual anode current outputs every two months.

This program not only ensures that wharves are protected but it indicates the location of failed components and allows for a planned maintenance program.

N. Instrumentation

Concurrent with the design and installation of cathodic protection systems was the development of an instrumentation system to gather data on their performance. This instrumentation was not intended to supplant routine pile-to-water potential surveys, but rather to record in detail the conditions at a number of selected sites. These detailed findings could then be extrapolated to other areas by means of data obtained by routine surveys.

In essence, the instrumentation program was:

1. Aim

   To automatically record pile potentials and anode current outputs at predetermined times at a number of locations.

2. Method

   (a) Timer - Programmed punched-tape timer with a three month capacity, capable of actuating four scanners.

   (b) Scanners - Two installed with 20 and 50 channels--multi-range channels.

   (c) Potential recorders - These consist of a modified recording chart potentiometer and an automatic vertical potential profile scanner.

O. Operating Data for the System

The system has been designed so that 20% of anodes can be lost without impairing protection (this assumes general rather than localized loss). Trials to date have shown that the safety factor may actually be higher because, in addition to good current distribution, extra rectifier capacity is available. While the system in its entirety has not been operative for an adequate time to establish maintenance requirements, there are indications that less than 5% anode loss per year will be experienced.

By the end of 1973, some 1900 anodes of all kinds, served by 39 rectifiers and delivering 14,370 amperes will be operative. The maximum area of steel protected is in the order of 1,000,000 sq. ft. It is anticipated that the cost of the six-year rehabilitation program will be approximately 2.5 million dollars.

The steel piling beneath the wharves are fully protected to half tide level, and the very serious corrosion occurring near low tide level has been completely arrested.

The program at Port Alfred represents a significant contribution to cathodic protection design and installation under unusual conditions. It has been achieved through a major evaluation of materials and a detailed study of water and ice conditions at the harbor.



Figure 1: Wharves at Port Alfred

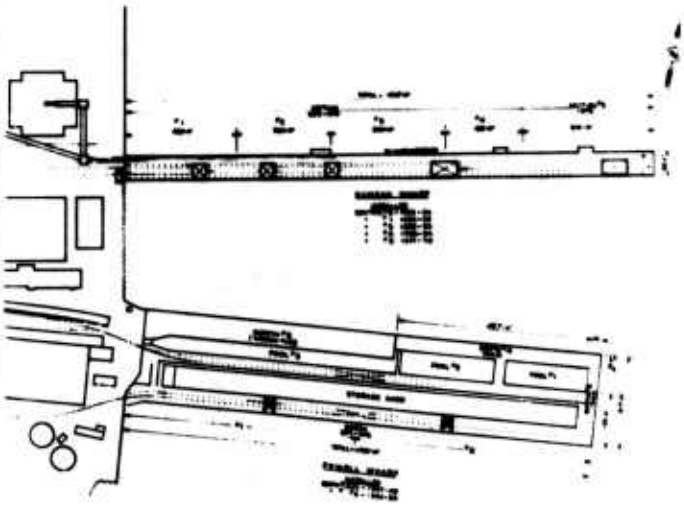


Figure 2: Plan of Wharves at Port Alfred



Figure 3:
Salinity of Water Vs. Depth



Figure 4:
Pool 1, Powell Wharf in Midwinter,
Low Tide



Figure 5:
Ice Fallen Beneath Powell Berth 1

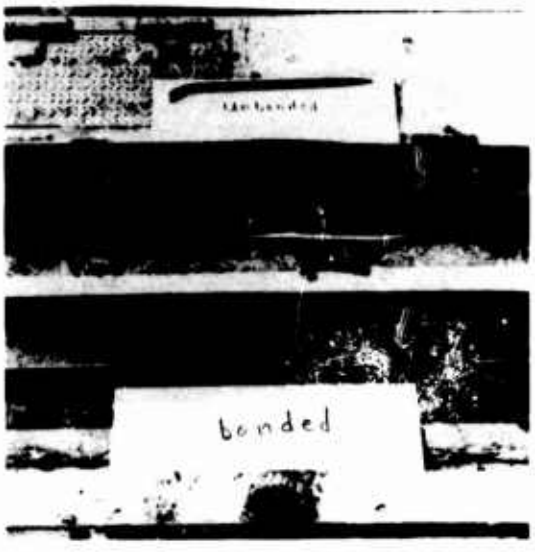


Figure 6:
Two H-Piles, Bottom Bonded to Cathodic Protection System, Top Unprotected, Approximately 15 Years Service.

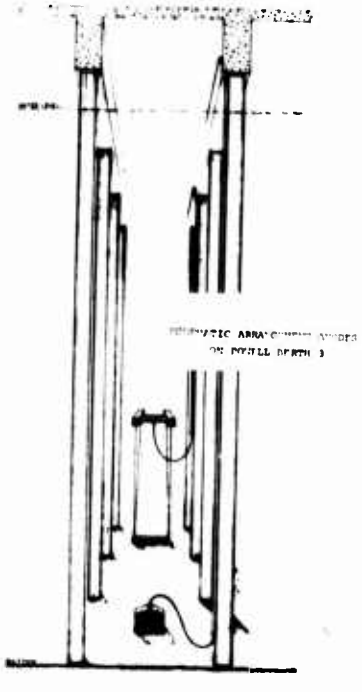


Figure 7:
Schematic Arrangement Anodes on Powell Berth 3.



Figure 8:
Anode Torn from Mounting Plate by Ice, Still Operative.

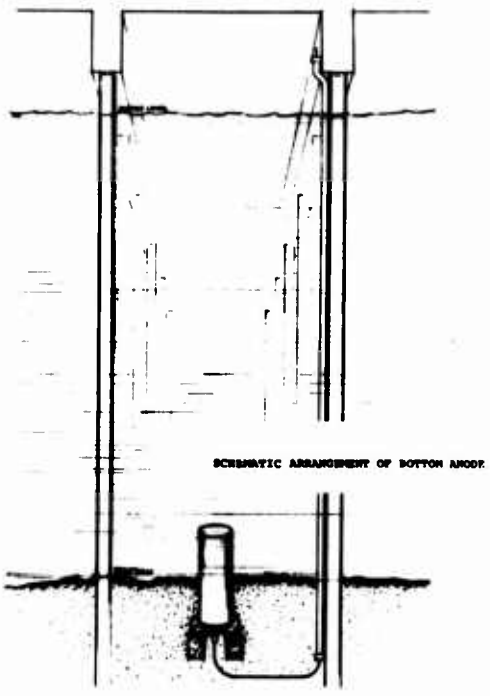


Figure 9:
Schematic Arrangement of Bottom Anode.



Figure 10:
Bottom Anode Used on Powell Berths 1 and 2 where Bottom Sediments Preclude Digging.



Figure 11:
2½-inch Conduit Ripped From Brackets, Duncan Wharf.

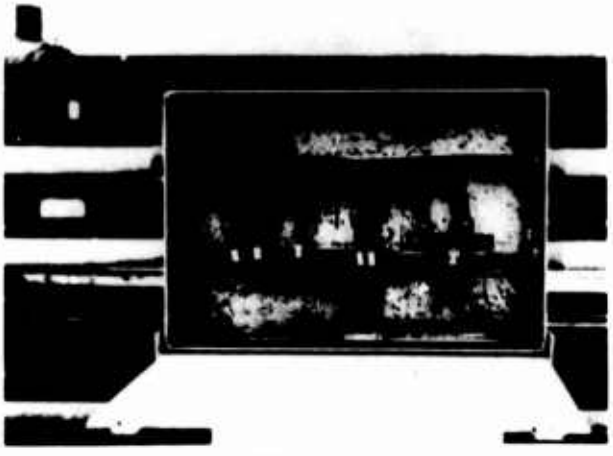


Figure 12:
Anode Connections and Current-Measuring Shunts, Powell Berth 4.

Summarized Discussion

In reply to a question, the authors reported that in zones where anerobic conditions exist, protection of steel piling was achieved at -0.85 to -0.90 V. They also explained that although foamed glass would probably have been better to use for anode floats, the foaming had to be done on the site; in consideration of this, they selected foamed polyurethane inside polyester for the floats.

Replying to other questioning, the authors explained that the areas of most severe localized corrosion were at the concrete caps and at mean low tide. The caps were not of the highest quality, they were in the true splash zone, and consequently, they were always wet. The concentration of attack near the low tide level was attributed to the fact that the piling in the tidal zone tended to be cathodic, drawing current from and causing corrosion of the steel near the low tide level. It was from such considerations that the positioning of the anodes was determined.

Steel, Concrete and Salt Water

Israel Cornet

Department of Mechanical Engineering
University of California, Berkeley
Berkeley, California, 94720

Steel in concrete structures is vulnerable to corrosion when appreciable concentrations of chloride ion reach the steel surface. Concrete of proper composition, sufficient thickness of cover, and proper placement is essential for protection, but even such concrete may not be sufficient to give adequate maintenance-free performance in severe exposures.

High strength steel under high stress in concrete may require precautions such as exclusion of sulfide-containing aggregate.

Sometimes steel in concrete structures is subject to damage by stray current from cathodic protection of pipelines or other sources. Prestressed concrete piling may present special problems if stray currents are present.

Galvanized reinforcement, or possibly cathodic protection of the steel may be of interest.

Key words: Steel; concrete; salt water; corrosion; cathodic protection; stress cracking; hydrogen sulfide embrittlement.

1. Introduction

Steel is passive in a saturated aqueous solution of calcium hydroxide (1, 2)[1] A film of saturated hydrated iron oxide coats the steel and prevents further oxidation. Cured portland cement concrete has a pH about 12.4, and resembles the chemical characteristics of a saturated calcium hydroxide solution sufficiently that such solutions are often used to simulate a concrete-water environment (1-3).

If sodium chloride in sufficient quantity is added to a saturated calcium hydroxide solution, or to concrete, the film formed on steel in such media loses some of its protective quality. There is a shift of electrochemical potential and the steel becomes susceptible to pitting and to general corrosion (4). The concentration of chloride ion at which steel becomes vulnerable to corrosion in saturated calcium hydroxide solution is 0.02 molal (aerated solution) (1, 2) to 0.08 molal (nitrogen saturated solution) (5). This corresponds to a range of 1200 to 5000 parts per million of sodium chloride. Concentration limits may be a function of temperature and relative humidity also. It has been demonstrated that there is a critical relative humidity for steel in concrete, so that corrosion will be stifled if the relative humidity is low enough (6). On the other hand it should be noted that corrosion of steel in concrete can occur although no standing water is present and the relative humidity is less than 100% (7).

Although concrete cover be of good quality and thickness, it still possesses some permeability to water, salt, and oxygen. In an aggressive marine environment it is only a question of time before corrosion attacks steel in concrete. Deterioration processes may be considered in steps. Imagine a reinforced concrete pile to be driven into a saline water. There is an induction time, say 1 year for 1 inch of ⅚ sack concrete cover, during which chlorides must diffuse through the concrete (8). During this period the steel displays a passive potential. When chloride ion at the metal-concrete interface reaches a high enough concentration, the protective film of iron oxide breaks down, and the steel is no longer passive. The half cell potential of the steel shifts to an active value. In field structures there would be zones where there are concentration cells, due to differences in chloride ion and especially differences in oxygen concentration. There can thus be a quarter to a half volt difference in potential between different parts of the steel, and this galvanic cell can drive the corrosion reaction.

[1] Figures in parentheses indicate the literature references at the end of this paper.

The chloride ion at high concentration has several effects in concrete. It reduces the electrical resistivity of concrete (8), thus decreasing the total resistance of the electrochemical circuit and increasing the corrosion current (which is equivalent to increasing the rate of corrosion). Sodium chloride added to calcium hydroxide solution will itself lower the pH (9). In concrete the chloride ion not only renders steel active or anodic, but as the anodic reaction progresses the local pH drops drastically to 4, or even to 3 in local pits. Ferrous ion at this pH is soluble, and diffuses away from the steel surface to precipitate where the pH is higher and build up a hydrated oxide corrosion product, beneath which the corrosion reaction continues. The corrosion product is lower in density than the steel corroded away, in fact the volume of the product may be double the volume of the steel replaced. Pressure builds up due to the confined corrosion product, putting concrete in tension and causing the concrete to crack and spall.

The corrosion of steel in concrete tends to be a problem in marine environments, particularly where there is exposure to salt spray, to alternate wetting and drying as in a tidal zone, to repeated freezing and thawing, where deicing salts are used, and where air conditioning is used (10).

Experience has shown that certain concrete structures are more durable and require less maintenance than others in an agressive marine environment. Quality of the construction materials, mix proportions of the concrete, proper curing, and particularly the thickness of cover over the steel and the quality of workmanship affect the durability.

Before we examine the effect of thickness of cover in detail, let us review other factors which affect quality and durablity.

2. Construction Materials

Water used in concrete mixing should be potable and free of harmful corrosive elements (11, 12). Tests have shown that concrete mixed with sea water corrodes more quickly than concrete mixed with pure water (9). When water quality is in doubt, a comparison is usually made of mortar made with pure water and mortar made with the water to be tested. The basis of comparison is most often the setting time and the 14 day compressive strength (12). However, these test results can sometimes be misleading.

Aggregate should be clean (12) (washed with pure water), non-reactive (13, 14), and well-graded (15). Depending on intended use, abrasion resistance should also be taken into consideration. The usual size of maximum coarse aggregate used in marine construction (covering steel reinforcement) is between 3/4 in. and 1-1/2 in. Other studies have shown improved results when the coefficient of thermal expansion of the aggregate is near to that of the mortar (16, 17).

Portland Cement type V (or type II as a second choice) is considered the most suitable for marine environments. Studies have shown that these cements, and others with low C_3A content, usually give the best results. It has been observed that sulphate resistance decreases with increased C_3A content, although there have been exceptions (13, 18, 19). For construction in marine environments, the recommended maximum limit for C_3A content is 5% to 8% (13). Addition of pozzolan has been shown to increase the life expectancy (mix proportions might be something like 2 parts portland cement to 1 part pozzolan) (18, 20).

The use of air entraining agents increases the durability of concrete, especially when it is to be exposed to freezing and thawing (16, 18, 20-24). It also shows increased resistance to the effects of deicing chemicals. Recommended air content is between 2% and 6% (25-27). Too much air decreases the strength of the concrete and its resistance to abrasion (28). The optimum air content will be influenced by the size of the largest aggregate used (25, 28). Also, if galvanized steel is used, the air entraining agent selected must be compatible with this type of steel (29). The use of air entraining agents reduces the amount of water required to produce a mix of the same cement factor and workability (30).

3. Concrete Mix Proportions

To offer greater resistance to the diffusion of environmental elements, it is desir-

able to obtain a dense, non-porous concrete.

Porosity increases with increased water to cement ratio, so the lowest water to cement ratio which gives a concrete of good workability would be most suitable. Best results have been obtained with a water to cement ratio of .4 to .45, or about 4-1/2 to 5 gallons per sack (15, 19, 28, 31). If an air entraining agent is used, this value will be somewhat less (30).

Density increases with increased cement content, so a high cement content would be best. For construction in marine environments, the recommended value for cement content is 6 to 7 sacks of cement per cubic yard (14, 23, 28).

Recommended slump value is about 3 in maximum (32, 20, 33). The mix should be plastic.

4. Curing

Proper curing is an important part of obtaining high quality concrete. Recommendations include moist curing for at least 14 days (15, 28). Also, more favorable results are obtained with concrete which has been thoroughly dried before exposure to freezing and thawing (20, 26).

5. Thickness of Cover

The purposes of obtaining a sufficiently thick concrete cover over the reinforcement are: weight, prevention of buckling under compression, protection from a corrosive environment, and resistance to the expanding force of the corrosion product. In the United States, the standard recommendation for thickness of cover is 3 in of 6 to 7 sack concrete. Some have stated that any thickness, even as little as 1/4 in (6) as long as the concrete is of high quality, will be sufficient. Though in some cases this may be true, there have been many failures both in laboratory tests and in practice, of high quality concrete where the coyer was on the order of 1-1/2 in. Many feel that 2 in is insufficient (18, 19, 34), and cite examples of corrosion of reinforcing steel under a concrete cover of 2 in (33, 35, 36). Some suggest a minimum limit of 2-1/2 in of cover (31), and it is interesting to note that one of these suggestions is accompanied by a recommendation of at least 7-1/2 sacks of cement per cubic yard (15), a stricter recommendation than that mentioned above. Most authorities recommend at least 3 in of cover with a cement meeting the recommendations discussed above (13, 28, 34, 37, 38). Others have suggested increasing the cover to 4 in at corners (14), where the concrete is subject to stronger abrasive forces. Some authorities suggest a minimum of 4 in of cover (13, 32). It is also recommended that the thickness of cover be at least twice the diameter of the largest aggregate used (to prevent surface cracks from propagating too quickly to the reinforcement) (13), and at least one to two times the diameter of the reinforcing bar it covers (20). It is extremely important that the concrete cover be uniform in thickness (9, 14). It must be kept in mind that the thickness requirement is closely related to the specifications for the concrete materials and mix proportions; an extra inch of cover will not necessarily make up for too porous concrete.

Most authorities would agree that by following the above specifications, one could obtain a reinforced concrete capable of lasting more than 50 years in a marine environment (37).

Some practical questions may be raised. If 3 in cover were specified, but only 1-1/2 in were furnished, how much would the durability be reduced? Or if one has the option of getting 4 -1/2 in of cover, what premium is it worth? One must turn to theory or to empirical relations to answer such questions. Four test models have been presented to account for the effect of thickness of mortar coatings, in the range of 3/8 in to 1-1/2 in of mortar over the steel (39). The test models are modified here for concrete, with 3 in cover being selected as a reference base, in Figure 1. Curves are normalized, and relative resistance to corrosion is compared for various thicknesses of concrete cover.

The Thickness model is based on the premise that corrosion protection is directly proportional to the thickness of concrete.

The diffusion model assumes that concrete acts as a barrier to diffusion of oxygen, or salts, to the metal surface, just as a thermal insulation restricts heat transfer. On a flat slab, the resistance to corrosion is again a linear function of thickness. On a cylindrical surface a logarithmic function is obtained:

$$N_A = D_A \frac{2L(c_1-c_2)}{\ln(r_2/r_1)}$$

where N_A is the number of mols of species A diffusing, D_A is the diffusivity, L is the cylinder length, (c_1-c_2) is the concentration difference, r_2 is the outer radius and r_1 is the inner radius of the concrete cylinder, and $r_2 = r_1 + t$ where t = thickness. Thus N_A at thickness 3 in/N_A at thickness $t = R_t/R_{3\ in}$, where R is the resistance to corrosion.

The Volume model assumes that the quantity of concrete cover is important in protecting steel. For example, under the influence of stray currents the pH of concrete at the steel surface decreases, and the more hydrated cement there is present, the greater the resistance to pH change and the longer corrosion is prevented. Again the resistance to corrosion is directly proportional to thickness, for a flat slab. However, for a cylinder the protection depends on the volume of concrete around the steel, $V = \pi(r_2^2-r_1^2)\,L$, where r_2 = outer radius, r_1 = inner radius, $r_2 - r_1 = t$ = thickness, and L = length. In this model concrete is considered to neutralize acid. The model is consistent with experience that Portland cement is more protective than aluminate cement.

The California State Division of Highways has presented a formula $R_T = f(t^{1.22})$, where R_T is the probable number of years to deterioration of steel in 70% of the structures placed in a normal highway bridge environment, and $f(t^{1.22})$ is a function of the thickness of cover to the 1.22 power. This empirical formula is based on maintenance inspection and repair data on 239 bridge substructures with reinforced concrete with covers ranging from 1 in to 3 in thick.

Examination of the curves in Figure 1 shows that 1-1/2 in of cover would give only 43 to 55% of the protection 3 in cover would give. 4-1/2 in of cover would give 1.38 to 1.65 times the protection that 3 in cover would give. The curves are so close to each other, that a simple thickness model is probably sufficient for ordinary estimates. In fact the curves show that one would have to go to large depths of cover, and correspondingly long exposure time to get data which would indicate which model best fits the facts. The empirical California State Division of Highways formula and the Volume model are reasonably close to each other. The Diffusion model is the most conservative in estimating the benefits of additional cover.

All of these curves pass through the origin when extended, but of course they should all terminate at a thickness about double the maximum aggregate size.

There is evidence that if steel is coated with a neat cement slurry, substantial improvement in corrosion resistance will be obtained. Presumably if there are voids or air bubbles around the steel much poorer performance will result. Analysis of the effect of concrete cover will not account for such variables.

Theoretically a sigmoid equation should be obtained for deterioration, ranging from zero to 100 percent, versus time, ranging from zero to complete deterioration. There would be an induction time during which corrosion would be virtually zero. The unrealistic models presented, therefore, compare remarkably well with maintenance experience.

6. Cracks

There is evidence that cracks in the concrete, even when they do not extend to the reinforcing steel, may serve to localize and to accelerate corrosion (40, 41).

7. High Strength Steel

In some structures high strength reinforcement is being used. Even higher strength

steel is used as rods or wires in prestressed or in post-tensioned structures, in rock anchors, beams, panels and slabs. Such high strength steel is susceptible to damage by stress corrosion cracking, by hydrogen sulfide embrittlement, as well as by pitting and general corrosion attack. When steel starts to corrode in concrete exposed to chloride ions, the pH drops in pits and other locally anodic areas. Sulfides in the concrete may then form H_2S, even though the corrosion attack be minimal. Since sulfides specifically impede the formation of hydrogen molecules from atomic hydrogen, a high strength steel may be charged with hydrogen and embrittled locally. Structures normally are subject to elastic deformations, expansions and contractions due to changes in temperature, in static and in dynamic loading. In some cases the embrittled steel fails after a period of time under the imposed stress condition. This is identified as a delayed failure, a brittle fracture probably due to a hydrogen embrittlement mechanism.

In one project light weight concrete slabs about 185 ft x 185 ft x 9-1/2 in were post-tensioned by seven-wire stranded cables or tendons, 0.6 in (5/8 in nominal) in diameter. The wires were about 0.2 in diameter, and 270,000 psi ultimate strength, 220,000 psi yield strength. They were loaded to 0.8 ultimate strength, and the load then backed off and locked at about 0.70 ultimate strength. They relax and creep to 0.6 ultimate strength. Several wires and tendons failed after 40 days to 14 months. Investigation showed that several factors were present. Failures were not uniformly distributed in the slabs. Each slab had six pours of concrete. Failures tended to occur in certain pours, even though the same tendon extended through other pours. The tendons were encased in protective grease and wrapped in a paper tubular tape. The tendons went over and under reinforcing rods and other tendons in the slab, with tendons approximately 6 to 18 inches apart. Failures tended to occur more frequently over columns, in areas of high positive moment. Strand in the failure area showed ductility reduced to 2 to 3%, with 15 to 20% loss of ultimate strength. Strand four or five feet from the failure area often showed normal strength (58.6 Kips) and ductility over 5% in 24 inches. Concrete cores analyzed 180 parts per million of sulfide sulfur. (Analyses of 500 to 9000 parts per million were also obtained, but were subject to question.) The concrete had used 5/8 inch light-weight aggregate. Samples of aggregate were found to be quite variable. Some aggregate samples were reddish in color, other samples were brown with a darker or even black interior. The aggregate varied in size of pores and in hardness. Some samples of aggregate with dark interiors gave an odor of hydrogen sulfide when moistened with hydrochloric acid solution. The aggregate generally had a hard glazed exterior, but in bulk it showed dusting, and there were broken pieces of aggregate present.

Paper wrapped tendons present a corrugated exterior to the concrete surrounding them. When tendons are tensioned the movement of strand may cut through the paper tape and crush aggregate protruding into the corrugation. This would expose high strength steel directly to pulverized aggregate. In one building it was estimated that stressing a strand to 0.8 ultimate strength required 9 inches of extension of strand under high stress. A concrete beam section was made and tendons stressed to 0.8 ultimate strength were pulled about 9 inches under constant stress. The beam was then sectioned and it was found that aggregate had been crushed.

Experiment and experience confirmed that a plastic tube was less likely to be damaged than paper wrap during construction. Tendons in plastic tubes showed a lower coefficient of friction during tensioning, which is advantageous.

Some differences in potential were observed between tendons in the slabs where failures were encountered.

Numerous metallurgical examinations, by many laboratories, failed to give definitive answers. Some samples of broken wires had enough evidence of corrosion to warrant labelling the failures stress corrosion cracking. Other samples did not show evidence of corrosion pits or surface attack (Figure 2). An interesting feature of some of the brittle failures was fracture at an angle of about 45° to the long axis of the wire. It has been shown in the laboratory that high strength steel wire stressed in H_2S solutions forms cracks which tend to be aligned at 45 degrees to the direction of tensile stress (42). The preferred crystallographic orientation of the steel in the wire causes this unusual crack orientation. It was therefore concluded that hydrogen sulfide embrittlement of the high strength steel caused these delayed failures. A hydrogen embrittlement

mechanism is involved(43).

Improved quality control of the aggregate, tighter control of construction techniques, closer inspection of the installation before placing concrete, and substitution of plastic tubes for paper wrap, have eliminated the delayed failure problem. It is recommended that sulfides be excluded from concrete where prestressing or post-tensioning is involved. Chlorides such as calcium chloride are also excluded.

8. Stray Current Corrosion

Even if a steel reinforced concrete structure is properly designed and properly constructed, it may still be subject to accelerated corrosion attack in marine environments. There is a hazard encountered with increasing frequency in coastal installations. We refer to stray current corrosion, also called interference effects, from neighboring cathodic protection systems. In the USA regulations of the Dept. of Transportation require that pipelines must be protected cathodically. The regulations even specify that such pipe be polarized cathodically -0.85 volts relative to a saturated copper-copper sulphate reference electrode. In many cases this results in a pipeline being protected by an impressed current anode at 18-25 volts, with currents of several hundred amperes. The current flowing from such an anode may actually go many miles. Steel reinforcement positioned vertically some distance from the protected pipeline may be but little affected by this current. However, if a long steel structure is in the potential field, current may be picked up at one end of the structure and discharged at anotherend. For every ampere year of current leaving the steel, about 20.1 pounds (9.1 kilograms) of steel is consumed. This corrosion of steel can result in cracking of concrete in the areas of current discharge. If high strength steel under high stress is subject to this current discharge, there may be ductile failure of the stressed steel due to reduction in section (44), but more likely there will be stress corrosion cracking of the steel due to localized corrosion and pitting.

An example of situations to be watched is at the eastern end of the San Francisco-Oakland Transbay Tube, a link in the new San Francisco Bay Area Rapid Transit System (45). This 19,000 foot long tube employs an impressed current cathodic protection system, using 16 rectifiers and anodes spaced at approximately 1000 foot intervals and 250 feet away from the tube. Each anode distributes about 250 amperes of current to protect the 3/8 inch thick outer shell of bare steel of the tube.

A survey of the western end of this tube has been published (45). In that survey it was concluded that 500 feet away from the anodes, or 750 feet away from the tube, the potential difference to the tube reaches zero, and foreign structures outside this range should be free of interference.

At the eastern end, the tube passes between two pre-existing wharf structures of the Port of Oakland Seventh Street Marine Terminal (Fig. 3). These wharves have reinforced concrete decks on prestressed concrete piles. The first stage wharf, on the east, is about 1300 feet long and 200 to 400 feet from the tube subsurface easement. The second stage wharf, on the west, is 1500 feet long and 100 to 700 feet from the tube subsurface easement.

On September 11, 1972, a potential survey was made in the San Francisco Bay close to the Port of Oakland Seventh Street Marine Terminal. At that time the anode operating nearest to the wharves was Anode No. 50. This anode is located 3 feet off the bottom, about 14 feet deep, about 1000 feet from where the pier line extended crosses the Transbay Tube easement. About 33 volts is applied at the rectifier, but potential drop through 1000 feet of 4-0 cable brings the potential at the lead-platinum anode to 19 to 20 volts; the current is 250 amperes. A launch moving at 2+ knots trailed two silver-silver chloride electrodes on electrical cables, the first electrode 20 meters behind the launch, the second electrode 20 meters behind the first. Difference in potential between the electrodes was recorded as a function of time. These data give $\Delta(mv)/\Delta x$, where Δx is 20 meters, at a given time. Integrating this curve gives the ΔV in millivolts, relative to a point at infinity, versus time. The integrated curve is shown in Figure 4. Traverse 6 passes over Anode No. 50, Traverse 8 is about 50 feet from the second stage wharf. Both traverses are parallel to the wharf. Note that even at the surface of the water there may be ΔV exceeding 100 millivolts 1500 feet from the anode. The results of this survey

show current effects at greater distances than reported in the earlier survey of the western area of the Transbay Tube (45). The anodes in the western end were about 75 feet deep; Anode No. 50 is 14 feet deep. In the three years that some of the anodes have been operating, the Transbay Tube has been polarized so that current is thrown to a greater distance from the anodes.

Polarization measurements are being made at selected points on the Port of Oakland wharf structures, and changes in potential are being observed. There are indications that one end of the wharf is picking up current; the current travels along deck steel and then is discharged at piling closest to the protected Transbay Tube.

Similar potential fields are observed in the vicinity of a ship which is cathodically protected by impressed current anodes. In busy marine terminals which have ships loading and unloading much of the time there may be effects anticipated on steel and concrete in the vicinity.

Subway tube installations are cathodically protected under water in San Francisco, Boston, New York and other metropolitan areas. Underwater tunnel steel casings for automobile and other vehicular structures are similarly protected in some areas.

9. Corrosion Protection

In an aggressive marine environment some protection against corrosion may be obtained by using galvanized steel reinforcement. This is particularly useful where the exposure may cause reinforcement to rust heavily before concrete is placed around the steel (44, 46).

Protective coatings for sealing concrete have been used successfully in water tanks. Where high strength steel under high stress is to be used, care should be taken that sulfide-containing material is excluded.

Cathodic protection of piling and foundations should be considered if stray current effects are present or anticipated. This will call for a design which has electrical continuity, to permit bonding and the application of protective current. An alternative design calls for insulation and isolation, so that long line currents or cathodic interference effects are avoided.

Design, construction, inspection, and maintenance should be guided by the fact that structures which have steel in concrete in marine environments are susceptible to corrosion and deterioration.

10. Acknowledgment:

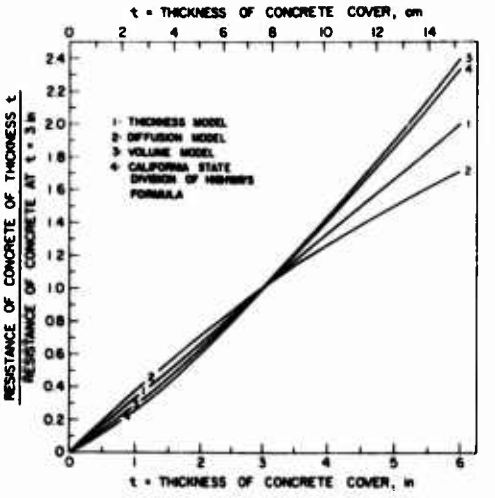
Technical assistance by Gail Kendall is gratefully acknowledged. The potential survey of Figure 4 is by Robert Corwin. Data on anode location, potential and current are by Peter Todd.

References

1. I. Cornet, T. Ishikawa and B. Bresler, *Materials Protection*, 7, 3 (1968).
2. Gordon N. Scott, *American Pipe Construction Co.* (1962).
3. D. A. Hausmann, *Materials Protection*, 6, 11 (1967).
4. Marcel Pourbaix, *Basic and Applied Corrosion Research - NACE* (1969).
5. T. Ishikawa, I. Cornet and B. Bresler, *Proceedings of the Fourth International Congress on Metallic Corrosion* (1969).
6. D. H. Pletta, E. F. Massie and H. S. Robins, *ACI Proceedings*, 46, 33 (1950).
7. D. Spector, *Materials Protection*, 4, 2 (1965).
8. D. Spellman and R. Stratfull, *State of California, Division of Highways, Research Report No. M & R HRB 635116-6* (1972).
9. R. Shalon and M. Raphael, *ACI Proceedings*, 55, 76 (1959).
10. D. F. Griffin, *Materials Protection*, 4, 11 (1965).
11. Imre Biczok, *Concrete Corrosion Concrete Protection* Budapest (1964).

12. Standard Specifications, *State of California Business and Transportation Agency - Department of Public Works - Division of Highways* (1969).
13. C. M. Wakeman, E. V. Dockweiler, H. E. Stover and L. L. Whiteneck, *ACI Proceedings*, 54, 46 (1958).
14. J. D. Mozer, A. C. Bianchi and C. E. Kessler, *ACI Proceedings*, 62, 54 (1965).
15. Howard F. Finley, *Corrosion*, 17, 3 (1961).
16. Thomas B. Kennedy and Katharine Mather, *ACI Proceedings*, 50, 9 (1953).
17. Albert Weiner, *ACI Proceedings*, 43, 30 (1947).
18. R. F. Blanks, Chm. Advisory Committee, *ACI Proceedings*, 49, 42 (1953).
19. I. L. Tyler, *ACI Proceedings*, 56, 45 (1960).
20. Walter H. Price, Chm., ACI Committee 210, *ACI Proceedings*, 52, 18 (1955).
21. Bruce E. Foster, Chm., ACI Committee 212, *ACI Proceedings*, 60, 64 (1963).
22. Edwin C. Roshore, *ACI Proceedings*, 61, 47 (1964).
23. J. R. Castleberry, Managing Editor, *Materials Protection*, 7, 3 (1968).
24. T. B. Kennedy, *ACI Proceedings*, 52, 61 (1956).
25. F. H. Jackson, *ACI Proceedings*, 47, 3 (1950).
26. Inge Lyse, *ACI Proceedings*, 57, 69 (1961).
27. R. C. Robinson, *Materials Performance*, 11, 3 (1972).
28. Hubert Woods, Chm., ACI Committee 201, *ACI Proceedings*, 59, 57 (1962).
29. B. Bresler and I. Cornet, *Report to International Lead Zinc Research Organization, Inc.* Report #TS-69-4. Contract #T-47460 (1969).
30. H. J. Gilkey, *ACI Proceedings*, 54, 34 (1958).
31. Rudolph Szilard, *ACI Proceedings*, 66, 5 (1969).
32. American Association of State Highway Officials, *Spec. for Highway Bridges* (1969).
33. J. L. Beaton, D. L. Spellman and R. F. Stratfull, *Highway Research Record #204, National Research Council* (1967).
34. S. Halstead and L. A. Woodworth, *The South African Institution of Civil Engineers* (1955).
35. R. F. Stratfull, *Corrosion*, 13, 3 (1957).
36. J. L. Beaton and R. F. Stratfull, *State of Calif. - Dept. of Public Works - Division of Highways* (1963).
37. L. L. Whiteneck and C. M. Wakeman, "Problems with Marine Concrete?" *Paper, Presented NACE, Los Angeles Section* (September 16, 1966), and personal communication.
38. Shu-T'ien Li and Chen-Yeh Liu, *ACI Proceedings*, 67, 10 (1970).
39. I. Cornet, *Materials Protection*, 6, 3 (1967).
40. I. Cornet and B. Bresler, *Materials Protection*, 5, 4 (1966).
41. C. A. de Bruyn, *Symposium of Bond and Crack Formation in Reinforced Concrete - Stookholm, Summaries*, 4 (1957).
42. H. E. Townsend, Jr., *Corrosion - NACE*, 28, 2 (1972).
43. C. F. Barth and A. R. Troiano, *Corrosion - NACE*, 28, 7 (1972).
44. I. Cornet, *Materials Protection*, 3, 1 (1964).
45. H. E. Bomar and R.H. Marchand, *Materials Protection*, 9, 4 (1970).
46. D. Hunt, *Galvanized Reinforcement for Concrete, Appendix A*, Zinc Institute, Inc. International Lead Zinc Research Organization, Inc. (1970).

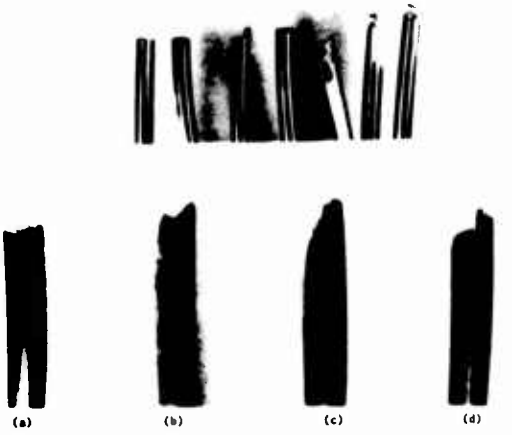
FIGURE 1



EFFECT OF CONCRETE COVER THICKNESS IN RESISTING CORROSION OF STEEL REINFORCEMENT

CYLINDRICAL PILE, STEEL 6 in FROM CENTER, OUTER DIAMETER = 12 in + 2t

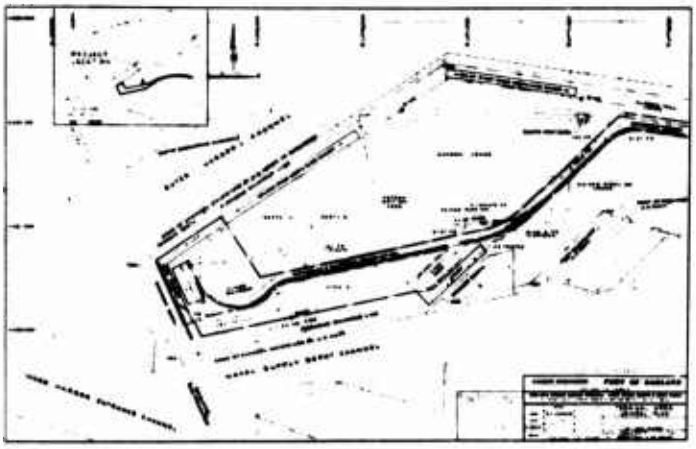




The close-up views of the wire ends of brittle fracture

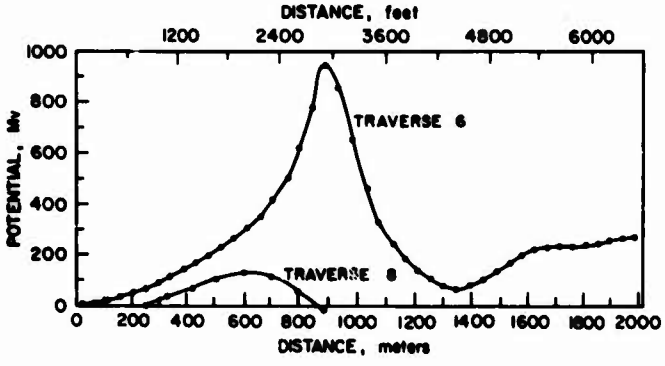
STRESS CORROSION AND OTHER BRITTLE FRACTURES

FIGURE 2



PORT OF OAKLAND, SEVENTH STREET MARINE TERMINAL

FIGURE 3



POTENTIAL DIFFERENCE FROM REMOTE ANODE

FIGURE 4

Summarized Discussion

In reply to various questions, the author amplified his presentation as follows: the permissible emf change to protect steel in concrete has not been established. There is also some disagreement as to the preferred method for fabricating prestressed concrete; the few failures of prestressed concrete which have occurred in the U. S. were attributed in the grouting method of incorporating the prestressed wires into the concrete. According to a reference cited in the paper, there is a difference of opinion concerning whether a crack in the concrete has to extend all the way to the steel before the steel commences to corrode locally. The number of sacks of concrete per cubic yard appear in U. S. standards which are referenced in the paper; 7-1/2 sacks, with the concrete covering the steel to a depth of 3 inches, exceeds the standard but is preferred by some.

New Technology for the Preventive Protection and Maintenance of Submerged Reinforced Concrete Structures

Alberto Montefusco

Chevron Oil Italiana S. p. A.
Via Cristoforo Colombo 149 - 00147 Roma - Italy

The maintenance work on concrete piles in submerged structures, as usually performed with conventional methods, involves many drawbacks and often results in poor and unreliable performance. Rather recently, epoxy-polyamide compounds (1)[1] have proved to be effective in providing protective coatings on submarine structures. The present report describes a new method of repair experimented recently on the damaged sections of reinforced concrete piles supporting and old jetty in the Savona bay (Italy) in the Mediterranean sea. Many piles, severely damaged, have been fully reconstructed by injecting under pressure an epoxy resin compound which has been specially developed for this particular technology.
After having explained the main reasons for decay in submerged marine structures, information is given on the physical properties of the product utilized as well as on its behaviour in the presence of the concrete and reinforcing steel-rods. The application of the resin requires new methods of inspection with subsequent data interpretation. The technology for carrying out the repair work is also different from the previous ones. In fact, the very short pot life of the resin after mixing gives many advantages but, on the other hand, many new problems must be faced. These were successfully overcome while the work progressed as fully described in the report. Special emphasis has been paid to the planning of the job and to the equipment used.
As a conclusion, statistical data and some results obtained two years after application are furnished.

Key Words: erosion; submerged concrete structures; piles; jetty; inspections; injection; epoxy resin.

1. Introduction

The scope of this report is to describe a new method of reconstruction of the submerged concrete structures as experimented by Chevron Oil Italiana maintenance organization on a pier for mooring of small tankers.

[1] Figures in parentheses indicate the literature references at the end of this paper.

Many piers and submerged marine structures built in recent years are provided, in some way, with passive protection against erosion and corrosion and, when necessary, are also provided with active protection against corrosion but, at the time our pier was built in the Savona bay in the Mediterranean Sea, the problem had not yet been faced.
Our observations led to the conclusion that the submarine structures of this pier had been damaged more by the effect of erosions than by corrosive agents. This factor of deterior ation, which acquires greater or lesser importance, depending on the circumstances, is always present in constructions in shallow waters.
In the particular case we want to deal with, the erosive attack on the piles of a pier can act in two ways:

- attack by waves and submarine currents caused by heavy meteomarine perturbations.
- attack by micro-biological marine flora and fauna which finds its most favourable habi tat in the microscopic porosities of the material, in this case concrete, to which it clings tenaciously with the result of crushing it very slowly but gradually and inexor- ably.

We started with the idea of applying a special product and, as the work progressed, we realized it was necessary to completely modify our method of work.
This is why I thought it would be interesting to inform my colleagues in the field, by means of this report, about the process with which we tried to perfect the new method.

2. Description of the structure in need of repair

The construction, realized in 1932 by an outstanding Italian Constructor, was the first construction of that type in the Savona Harbour and one of the very first in Italy.
We have no suitable data on hand to make a comparison with similar constructions of the same age but, from what we know about more recent works, the Savona pier appears to have shown an exceptional resistance.
In order to introduce the subject of its maintenance a brief description might be helpful:
It is about 450 meters long and consists of 30 pairs of octagonal shaped reinforced con- crete piles driven deeply into the sandy sea bed. The two piles of each assembly are 15 mt. apart and are linked together by parallelepiped headers at sea level. The frame- work, supporting a cat-walk beam and piping, rests on these headers.
At the offshore end of the catwalk beam, a wharf-head is installed, also supported by reinforced concrete piles submerged for 9.50 meters.
We have no precise information regarding maintenance works carried out before and im- mediately after the second world war as the pier, like all petroleum installations of stra_ tegical importance was, at that time, competence of the CIP (Italian Petroleum Commit- tee). However, it has been ascertained that some aircraft bombs, which exploded in the immediate vicinity of the central section, caused a lowering of this section of about 1 me ter and permanent deformation of the catwalk beam with consequent damage to the piles.
Other cracks have apparently been caused by scale formation on the reinforcing rods, displacing the concrete skin between the rods and the adjacent beam face.

3. Considerations on conventional methods of repair

The usual method of repair was to remove this loose concrete skin and gunite the affected areas after sand-blasting the exposed reinforcing rods. This is a precarious job to do underwater and, as an alternative in the most serious cases, some piles were renewed by cutting them off near their top and foot and connecting a new piece to the old stumps by steel-clamps coated with concrete.

However, the deformed state of the pier caused considerable alarm and it was doubted whether it could continue to be operated in its precarious condition.
Accurate checks, carried out since then at regular intervals did not show further yields but, at the same time, they gave a sound idea of the damage caused by the erosions and of the necessity to make good the decay of the structures.
The most efficient way of repairing it was the afore mentioned one, that is the subtitution of the central section of the pile with a new one.
As a consequence, the underwater inspection was limited to finding out the extent of damage to each pile and scheduling the substitution priorities.
By using this method about 50% of the piles were replaced in slightly over 10 years and it was planned to renew the balance by the same method when necessary.
Findings of the last inspections were discouraging:

1^ 30% of the replaced piles, show evident decay 15 years after their substitution.

2^ Even if the new replaced pile sections are in good condition the process of deterioration of the stumps, between which the new sections are fitted, does not stop because the reinforcing rods remain exposed. This could eventually cause the stumps to yield and the consequent collapse of the structure.

In addition to that, deep erosions were found in the lower face of the braces in the tidal zone, even though many of them had been recently repaired. Therefore, the information about a new more efficient protective material composed of epoxy resins (1)[1] has been taken into consideration by us with utmost attention but with those reservations one must have when facing a completely new technology.

4. New possibilities stemming from the use of epoxy resins

The use of epoxy resins had already been experimented by us for other repair works, such as the internal coating of tank bottoms subjected to corrosions and internal lining of short runs of pipelines. After some years results have been appreciably positive therefore we decided to use this material also for the maintenance of our pier.
In order to dispel some doubts as to the behaviour of the new proposed products when under stresses, we asked that the relative tests be carried out by an officially recognized laboratory. Said tests have been executed by the material testing laboratory at the Politechnique in Milan and gave us the following results:

- compression strength for specimens without inerts = 13,000 psi = 900 kg/cm^2
- compression strength for specimens with 15% to 30% of fine sand = 10,000 psi=700 kg/cm^2
- tensile strength = 3,200 psi = 220 kg/cm^2

It should be remembered that even a very good concrete has a very low tensile strength and the compression strength can approach the above values only after 28 days curing, whilst the epoxy resin under study reaches its maximum values only a few hours after having been applied even when immersed in water, which is most important for this particular type of application.
Furthermore, the possibility of an efficient binding with inerts gave us a measure, even if only an indication, about the capacity of the resin to bind itself to the old concrete.
We had no doubts as to an efficient linkage to the reinforcing rods, since this was already proven by the results of previous applications.
Having ascertained the convenience of adopting this new material from the technical stand point, the problem arose as how to keep the cost of the work within acceptable limits.

---

[1] Figures in parentheses indicate the literature references at the end of this paper

The cost of the new product is very high compared to that of concrete, very high too is the cost of manpower which consists of a frogman crew highly skilled in this type of work. The problem then was to set up a working procedure which was completely new compared to that used in the past .

5. Remarks on the inspections

To begin with, the generic inspection, as it used to be conducted, with the purpose of ascertaining whether or not the pile had to be renewed, was no-longer valid.
Hence we reviewed the criteria with which inspections had to be carried out and it was decided that the exact levels of the damaged points and the extent of the damage should be indicated. In the most serious cases also a photograph proof had to be provided.
It has been demonstrated, that even a very accurate preliminary inspection does not supply so precise an idea of the extent of the damage as that which will be found during the course of the actual repair work.
The first obvious deduction was that two inspections are needed:
- a preliminary one to locate roughly the damaged points to be taken care of;(Exhibit 1)
- a second one, to find out with the utmost precision, from the stand points of quantity, the work to be done (Exhibit 2).

In fact, as can be deducted from the photographs, during the first inspection it is not a good practice to completely remove the layer of marine fauna and flora, as these cling tenaciously to the concrete, one cannot scrape them off without danger of additional damage to the concrete itself.
The most careful cleaning must, on the other hand, be done immediately prior to the actual repair because, if even a short time elapses between the cleaning and the repair, the marine micro-organism starts to grow again.
Hence, the detailed inspection must be followed within a few days by the repair work otherwise it results only in wasted time. The detailed inspection will supply the following precise data necessary before the start of work:
- determination and supply of the right quantity of material needed;
- time calculation and working schedule with decisions about priorities;
- method to be followed for preparation of the structure to be repaired and set up of the related equipment.
- preparation beforehand of the forms to be used;
- preparation of the equipment for injecting the resin.

When this data is to hand one can proceed with the actual phase of application being reasonably confident that any unforeseen problems can be coped with.
This is important from the committent's standpoint as it represents the means of controlling costs within the limits of the budget.
To achieve this in an efficient manner good communications are necessary, during the whole duration of the work, between the product supplier, the contractor and the committent.
This was done in our case and, therefore, the main features of each of the above listed phases are briefly described here below:

6. Pre-work inspection

The preliminary inspection had already been carried out by an independent Company before awarding the contract and the recorded data were transmitted to the contractor.
The contractor carried out immediately the cleaning of all piles we pointed out and recorded the length, width and depth of each damaged point.

At the same time all photographs were taken with a 360° lens camera which showed up even the smallest shadings.
A small tag with the relevant identification number was kept beside the pile being photographed to avoid mistakes.
This inspection required 10 calendar days of work by the whole team of 5 frogmen, which proves the importance of this phase. They have in addition, supplied us verbally with information about other useful elements of evaluation, such as the state of the surfaces and the condition of the steelrods.
In this connection we noticed that most rods, even when exposed and, obviously, lacking their protective skin for a long time, did not show a high degree of corrosion.

7. Evaluation and supply of the required material

The data from the survey was entered on a form showing the levels, the measurements, the volume of spaces to be filled and the quantity of material to be supplied.
In order to provide for unavoidable losses and a safety margin in the quantity of material the volumes were calculated on the developed circumscribed solid instead of on the cylindrical one.
This recorded data, as well as allowing us to evaluate the quantity of material needed, gave us the opportunity to make the following useful statistical observations :
- the east-ward row of piles shows 55% more erosion than the west-ward row, this depends presumeably on the direction of the prevalent wind;
- the first half of the pier starting from the beach shows prevailing damage in the upper section of the piles while the second half of the pier shows prevailing erosions in the lower section. This corresponds with the tidal zone.

In doing this we did not consider the damage tothe headers, the repairing of which with the new technology is still under study.

8. Timing - Scheduling - Priorities

Timing seaworks is obviously much affected by meteo-marine conditions. Each calendar day of fine weather we can plan to use two squads composed of two frogmen working in shifts of three hours submerged and the rest of the day at the surface. A frogman foreman supervises the work while a carpenter helps in getting the forms and the equipment ready.
When the work is running smoothly we can estimate to get an average of 1.5 damaged points repaired per day, but taking into account some unexpected shut-down, due to weather conditions, it is safer to keep to a slightly lower figure.
Priorities are fixed by giving precedence to the most damaged points. However, some freedom must be left to the men to allow them to select the depth at which to work according to the condition of the sea. It is well known, in fact, that one can work near the surface only when the sea is quite calm, whilst when the sea is rough it is better to work at a deeper level. Also the visibility, when immersed, can be limited by currents and winds even when the sea is very calm.

9. Preparation of surfaces to be repaired and setting up of equipment.

The scraping off of the decayed material down to a sound surface must be performed efficiently, and, as previously said, immediately before the pouring of the resin.

It can be done by using pneumatic scrapers or hydrodynamic guns followed by an accurate sanblasting. In all cases it is necessary to provide on site a source of energy such as electric power line or engine driven machines.
It is of course, necessary to provide sets of operating tools, spare parts and miscellaneous materials in order to avoid costly interruptions.

10. Preparation of the resin

The product is supplied in two components to be thoroughfully mixed together to obtain a compound which must be poured immediately, because its pot-life is limited to 30 minutes at normal ambient temperature. The resultant density is about 1.5. Epoxy-resins of this type have in the past been utilized for the preventive protection of structures, applying them by hand to provide a thin layer of coating. In our case we were dealing with a different kind of job involving the reconstruction of old piles by the application of much higher quantities of new material. The work, if performed manually, could have led to problems due to the very short pot life of the material, so we decided to inject the resin under pressure into forms clamped to the damaged sections of the piles.

11. Preliminary set-up of the required forms

On the basis of the surveyed measurements it is wise to have ready beforehand some forms having similar sizes and different lengths so that they can be used on more than one pile.
The form must be slightly longer than the erosion to be repaired without being excessively long in order not to waste costly product. In the case of two erosions very close together on the same pile, it may be convenient to use a single long form so that the two repairs can be effected in one operation.
The forms are supplied with a set of threaded holes. They are used for injecting the resin and for expelling the water by injecting the product in sequence, starting from the bottom hole and proceeding upwards as soon as the resin comes out of the next hole.
The seal between pile and form edges is obtained by use of synthetic rubber gaskets.

12. Resin injection equipment

The injection guns, normally found in the market, are of limited capacity, usually no more than 2 kilos at a time; therefore it can be easily understood that for major works there is a substantial loss of time and waste of material because the gun must be sent up to the surface every time for careful cleaning before filling it again.
Therefore the dimension and capacity of the guns must be consistent with the extent of the work to be done; in our case we used two specially made pneumatically operated injectors with which we obtained fairly good results.

13. Execution of the work

Pneumatic chisels were used to scrape off the damaged concrete; the exposed rods were then grinded and the forms applied. At the end of each cleaning operation the frog man leadman inspected the job and gave his o.k. for putting on the forms. The injection job was effected using alternatively the two guns previously prepared and, after a few hours, we proceeded to dismantle the forms because the drying time is, as previously said, very short.
As shown by the photograph, the piles after repair, appear completely new (Exhibit 3).
At the end of all repair work we carried out, as an experiment, the complete coating of a pile, applying the resin by hand. On the basis of the results we will decide in future, if it is wise to adopt the same treatment on all piles. We also coated one full header with the same object.

The following summarizes the work completed in 57 working days:
- pre-work inspection on 33 piles
- injection applications on 57 piles
- coating of a full pile
- complete repair and coating of a header

The average time losses for meteo-marine reasons was 25% of the total.
The average cost was 380,000 Lire (= U.S.$ 650) per injection.

14. Results and considerations

An accurate check was carried out in August 1972, two years after the repair work, by a different contractor.
The piles were carefully cleaned and the examination gave these results:
- the bonding between fouling and resin is much weeker than between fouling and concrete. In fact, the only organisms which tenaciously clung to the resin were the borers (exhibit 4). They are not dangerous because they are not able to penetrate more than a few millimeters.
- In some cases families of muscles had grown under the edges of the coating, giving the impression of inefficient linkage between resin and concrete at the edges.

We chipped out with hammer and chisel these edges and found that after a few centimeters the linkage between the materials was sound and it was not possible to proceed in cutting out the resin without damaging the concrete.
The possible explanation of the absence of linkage at the edges can be found reading the daily reports written at the time of the work:
- some piles had not been injected immediately after the cleaning but only the following day.
- in other cases the forms were wider than the interested area so that the injected resin was spread out on a surface larger than the well prepaired one.

We found no sign of deterioration in the coatings above sea level. As a conclusion, owing to the limited time elapsed since the application, we cannot pronounce yet decisively in favour of the new technology but the first results are extremely promising.

1. ROBERT M. JORDA, "Applying Protective Epoxy Coatings to Submerged Metal, Wood, and Concrete Structures". Paper presented at the International Congress on Fouling and Marine Corrosion - June 8-13, 1964.

Discussion

Some participants expressed concern that the resin, without a filler, would not afford any structural strength, and specifically unless its elastic modulus matched that of concrete. The author did not have elastic modulus data, but pointed out that hardening time--about 30 minutes--is of great importance in getting the resin in place and hardened before it is washed away by wave action; it would have been difficult to apply and cure concrete patching in sea water under the conditions described.



EXHIBIT 1
Preliminary Inspection



EXHIBIT 2
Pre Work Inspection



EXHIBIT 3
Pile After Repair Work



EXHIBIT 4
Repaired Area After Two Years

How To Make Use of Corrosion Data

Herbert H. Uhlig

Department of Metallurgy and Materials Science
Massachusetts Institute of Technology
Cambridge, Massachusetts 02139

The marine engineer in choosing materials of construction to resist sea water attack can rely on weight loss data for non-passive metals like copper, iron, steels, and zinc. In applying passive metals e.g. stainless steels, nickel, nickel alloys, aluminum and aluminum alloys, the prevailing potential should be maintained below the critical potential for pit initiation, and crevices should be avoided in any structural design. Under conditions of high velocity, the passive metals are better resistant than are the non-passive metals. The effect of heat treatment on sensivity to intergranular attack should be evaluated in all metals that are to be welded or are to be heat treated for stress relief and other purposes. Applied or residual tensile stress is important to sensivity to cracking in sea water particularly for titanium, aluminum and magnesium-base alloys at ordinary temperatures, and of austenitic and ferritic stainless steels at elevated temperatures. A critical potential exists for some of these alloys, and probably for most other metals as well, below which cracking does not occur. All high strength metals and alloys including carbon steels, maraging steels and stainless steels may crack in presence of moisture alone. Adequate designs, therefore, often call for a thicker section of a medium strength metal rather than the use of a high strength metal to sustain a given load.

Key Words: Galvanic Coupling, Pitting Corrosion, Welding, Velocity Effects, Stress Corrosion Cracking, Corrosion Fatigue.

Corrosion data are usually expressed as weight loss or metal penetration for a given period of exposure. For uniform attack, both in time and dimensions, such data supply useful design information. For example, an average corrosion rate of a carbon steel in sea water of 0.010 cm/year indicates that an H beam 0.5 cm thick will lose half its cross sectional dimensions within (0.5/0.01) x 1/2 x 1/2 or 12.5 years, the extra factor 1/2 coming in because of corrosive attack from two sides. Since the rate of weight loss usually decreases with time, the corrosion rate extrapolated to long periods of exposure may be unduly pessimistic, and the predicted life may be actually short of what is experienced. For example, reported immersion data in tropical sea water[1] (Panama) show that the average corrosion rate of carbon steels after one year exposure is 0.015 cm/year, but after 16 years, primarily because of rust accumulation and organic fouling, the rate may average only 0.007 cm/year. Rates in this particular sea-water environment become relatively steady after one to two years. The actual required time for steady-state probably depends on local variations in the ocean temperature, salinity, velocity, etc. as well as on the metal or alloy. In any event, using average rates fortunately includes a factor of safety in design calculations.

Although steels corrode relatively uniformly over their surface, corrosive attack of other metals may not be uniform. The passive metals, for example aluminum or stainless steels, exposed to sea water lose less weight than do carbon steels in the same time, but they are subject to localized or pitting type of attack which may penetrate deep sections of the metal in a matter of months. Hence, only tables of weight loss data for non-passive metals are apt to supply useful data to the design engineer, and these are an

important part of his stock-in-trade. The category of metals for which such data are useful include iron and carbon steels, low-alloy steels, tin, cupro-nickel alloys (<40% Ni),brasses (<15% Zn), zinc and zinc-base alloys. For these metals, it is often possible to measure uniform corrosion rates employing electrochemical techniques such as is recommended by M. Stern and A. Geary[2], or by change in electrical resistance of wire or strip specimens.

Galvanic coupling of non-passive metals to more noble metals (as indicated by the Galvanic Series) accelerates corrosion of the non-passive metal, the maximum effect of which as illustrated for Cu-Fe couples is given by Rate (coupled) = Rate (uncoupled) $(1 + \frac{\text{Area Cu}}{\text{Area Fe}})$. For more noble metals which polarize cathodically more than does Cu, e.g. Pb or Sn or stainless steels, the rate is accelerated somewhat less than the equation predicts. The important factor is the relative area of active (anodic) to noble (cathodic) metal when coupled; the ratio should always be kept large otherwise rapid penetration of anodic metal results. Weld metal that is active (negative) in potential to ship plates can lead to rapid penetration by corrosion of the welded seams.

How does one handle metals that undergo pitting corrosion? What sort of data can be relied upon to replace overall weight loss measurements that are relatively useless for estimating time of metal penetration? Other than to avoid environments or conditions which breakdown passivity, or to choose metals which are not passive (some are listed above) and hence are not subject to deep pitting, conditions must be chosen to prevent pits from initiating. This is best done by ensuring a prevailing potential of the metal structure always below the critical potential required for pitting. Applied cathodic protection is useful, as is galvanic coupling to metals having sufficiently active corrosion potentials. For example, the critical pitting potential of 18-8 stainless steel in sea water (3% NaCl) is 0.21 volt on the hydrogen scale (SHE). If sufficient area of zinc or iron (corros. potential, SHE =-0.8 and -0.4V respectively) is coupled to it so as to depress the overall potential below this value, pits will not initiate. An 18-8 propeller mounted on a steel ship and in electrical contact with it does not experience pitting corrosion. In the case of aluminum, the corresponding critical potential is more active (-0.45V) and therefore zinc, but not iron, is a satisfactory sacrificial metal.

Pitting of aluminum or stainless steels can also be avoided by reducing the dissolved O_2 concentration (deaerating) of sea water. The corrosion potential of the metal is thereby depressed below the critical value. Also, because passivity is thereby altered or perhaps destroyed, damaging electrochemical cells (passive - active cells) are avoided which account for pit growth. Along the same lines, pitting inhibitors like nitrates (for Al or 18-8) or hydroxyl ions (for 18-8) can be added to saline solutions(Fig. 1,2); their action is to shift the critical pitting potential to values that are noble to the prevailing corrosion potential of the metal. The marine engineer, in other words, should have available a table of critical pitting potentials for passive metals,[5] as well as of corrosion potentials of the common sacrificial metals, in order to properly design marine structures incorporating pit-sensitive passive metals.

Although pit initiation can be avoided as described, it is still possible for some passive metals to undergo localized corrosion at crevices (crevice corrosion) at potentials below the critical values. The reason for this is that stagnant electrolyte in crevices becomes deficient in dissolved O_2 resulting from continuing slight uniform corrosive attack of the metal. The resultant differential aeration cell between metal inside and outside the crevice builds up acid corrosion products within the crevice accompanied by increased Cl^- concentration. Eventually passivity breaks down within the crevice and the resultant passive-active cell of large potential difference causes marked continuing corrosion of active metal. The larger the area of passive metal outside the crevice, the greater is the galvanic current and corresponding localized attack. To avoid crevice corrosion, it is good practice, of course, to rigorously avoid all crevices in the design of equipment and structures exposed to aqueous solutions, a rule that is well known to corrosion engineers. Existing crevices should be avoided by filling them with weld metal or with insulating cements, or avoiding surface films such as are formed by fouling organisms. Stirring of the electrolyte sometimes helps by equalizing composition of solution inside and outside the crevice. Cathodic potection may also be employed. Metallurgically, crevice corrosion

is minimized, but not eliminated, by choosing alloys that tend to retain their passivity in solutions of low pH and low partial pressures of dissolved oxygen. Adding a few tenths percent Pd to titanium is helpful, as is the addition of molybdenum to 18-8 stainless steels (type 316). Further advances of this kind in the development of passive alloys are much needed in order to avoid a troublesome and often serious type of damage in saline environments.

Welded Structures

If structures are to be welded, it is necessary to know the effect of heat treatment on corrosion rates. For commercially pure metals e.g. copper, nickel, titanium and aluminum, heat treatment has no appreciable effect. Carbon steels can also be welded without damaging effect in sea water if recognition is taken of the proper galvanic relations between weld metal and base steel, and any mill scale, which acts as a cathodic surface, is removed. But for many aluminum-base alloys, austenitic and ferritic stainless steels, Hastelloys, Inconels and similar alloys, welding operations may induce accelerated corrosive attack at grain boundaries either at the weld area or near it (weld decay). To avoid sensitivity to such attack, the structure can sometimes be heat treated after welding, or alloys can be employed that resist the responsible heat-induced composition change along grain boundaries e.g. use of "stabilized" austenitic stainless steels. The marine engineer, therefore, should also have complete data on the effect of heat treatment at all temperatures on corrosion resistance of alloys before specifying materials for a welded joint or the conditions of stress-relief heat treatment.

Effect of Velocity

High velocity conditions accelerate corrosive attack of some metals more than others. In general, passive metals are better resistant to so called impingement attack or corrosion-erosion than are the non-passive metals. Copper, for example, is especially sensitive to attack by high velocity sea water despite its good corrosion resistance in slow moving sea water. Alloying copper with Zn, Al, or Ni makes it more resistant, accounting for the prevailing compositions of condenser tube alloys used commercially for sea-water heat exchangers. The stainless steels are more resistant than iron, and Monel (70% Ni-Cu), being passive, is more resistant than are the cupro-nickel alloys (10-30% Ni-Cu). The passive alloys, however as mentioned earlier, tend to undergo pitting corrosion which makes them unattractive for condenser tube applications despite their good resistance to high velocity waters. Hence cupro-nickels and aluminum brasses, although not quite as resistant to impingement attack, are preferred for sea-water exposures. Titanium and titanium-base alloys resist both high velocity conditions and pitting corrosion, making them expecially useful for condenser tubes and similar applications. Some of the available alloys (but not pure titanium low in alloyed oxygen) are subject to stress corrosion cracking, and this factor must be taken into account. At temperatures above the boiling point of sea water,the critical pitting potential of titanium or of titanium alloys in dilute chloride solutions approaches the neighborhood of normal corrosion cell voltages (approximately 1 volt) and hence under these conditions are subject to pitting attack. This is not usually a factor at atmospheric pressures, except for very concentrated hot chloride solutions e.g. boiling $CaCl_2$. However, crevice corrosion of titanium occurs in hot sea water at atmospheric pressure.(6)

Effect of Stress

Contrary to general impressions, a stressed metal or one that is severely cold-worked does not usually corrode more rapidly in sea water compared to an unstressed or annealed metal. The corrosion rates of metals like copper, lead, iron and carbon steels depend on the rate of diffusion of dissolved oxygen to the metal surface, and hence corrosion rates are not affected by the structure of the underlying metal. Only in acids, like hydrochloric, is attack of cold-worked carbon steels more rapid than for annealed steels. The corrosion product is now hydrogen gas, the rate of formation of which depends on the number of lattice imperfections (produced by plastic deformation) occupied by carbon atoms and of low overvoltage. This same factor is not important to the corrosion rates in hydrochloric acid of cold-worked pure aluminum, copper or nickel.

The pitting behavior of passive metals is also not appreciably affected by stress or cold-work under conditions where the temperature of plastic deformation does not rise above a point permitting metal diffusion and localized composition changes within the alloy. The critical pitting potential of cold-worked 18-8 type 304 stainless steel in 0.1 N NaCl is about 0.1 V more active than that of annealed, quenched 18-8[7]. Uniform corrosion rates of passive metals in sea water in general remain small or negligible whether the metal is cold-worked or annealed.

However, the main effect of a tensile stress (not compressional) is to cause cracking of some alloys in specific chemical environments (stress corrosion cracking). Iron, and low or moderate strength steels are fortunately resistant to this type of attack in sea water, but they fail by cracking in nitrate solutions, hot or cold, or in hot alkaline solutions. Pure metals are resistant or immune to this type of attack in all environments, the degree of required purity varying with the metal and the environment. Many commonly used austenitic (<45% Ni) and ferritic stainless steels (e.g. those containing 2% Ni or a few tenths percent Cu) are sensitive to cracking in hot saline solutions. High-strength titanium alloys are sensitive to cracking in sea water either hot or cold, as are high strength aluminum alloys and magnesium alloys. Copper-base alloys are normally resistant to sea water; they may crack however in ammonia or amine atmospheres or in ammoniacal aqueous solutions. Interestingly, they are not susceptible in absence of dissolved oxygen, accounting for their successful use as condenser tube alloys for steam boilers despite the often intentional addition of ammonia or amines to boiler water in order to control corrosion of the steel boiler or of steam return lines. The marine engineer, obviously, should have complete information on environments that cause stress corrosion cracking of structural metals.

The evidence accumulated so far indicates that stress corrosion cracking occurs only above a critical potential which varies with the metal and its environment. For austenitic stainless steels, which are among the alloys that have been studied most so far, the critical potential of 18-8 in concentrated $MgCl_2$ boiling at 130°C is -0.128V (SHE) for annealed quenched alloy[8] and -0.145V (SHE) for 36% cold reduced alloy [9] (Fig. 3). Analogous potentials have been reported for the 18% chromium ferritic stainless steels, (Fig. 4)[10], and for carbon steels in nitrates[11][12]. Similar measurements are still to be accumulated for other metal systems. They are important to structures adequately designed to avoid failure by stress corrosion cracking under specific conditions of exposure.

For example, because of the influence of the critical potential on failure, certain galvanic couples can be employed to avoid failures by stress corrosion cracking. Examples of some of these are listed in Table I. As in pitting corrosion, inhibitors can also be added to the environment to shift the critical potential to more noble values thus avoiding the damaging potential range, or in certain instances rate of crack growth can be retarded.

A special comment is needed with respect to high strength steels, which probably also applies to high strength aluminum, copper, nickel and titanium alloys as well. Here the damaging environment above a critical stress level can be water alone. For carbon steels, including the low alloy carbon steels, martensitic and precipitation-hardening stainless steels, and maraging Ni steels, the critical yield strength is about 180,000 psi,[13]. Any steel above this strength level stressed to 75% of its yield strength and exposed to the normal atmosphere will fail within weeks or months. Cathodic protection although useful for some metals is less reliable for high strength steels including martensitic stainless and maraging steels because generation of hydrogen at the metal surface may cause hydrogen cracking which is fully as damaging as stress corrosion cracking. Cathodic protection has more promising utility for protecting the high strength copper-base or aluminum-base alloys which are not subject to hydrogen cracking. In practice, high strength steels are insulated from contact with moisture by use of greases or a cadmium electroplate. Cadmium is preferred because it has about the same corrosion potential as steel, and hence any galvanic cells that are set up at defects in the coating generate less damaging hydrogen than would a coating which is more active in potential than steel, such as zinc. Because high strength steels are sensitive to both moisture and hydrogen, it is often advisable to use a lower strength steel of thicker cross section to sustain a

given load.

If the applied stress is cyclic or repeated, metals whether of low or high strength fail by fatigue. The fatigue life is typically shorter the more corrosive the environment to which the metal is exposed. All corrosive environments tend to be damaging in contrast to only specific environments that cause damage by stress corrosion cracking under conditions of static stress. Although fatigue resistance in air is typically greater the higher the strength of the metal, the property of corrosion resistance is usually more important to the fatigue resistance of any cyclically stressed metal in sea water. For example, copper or cupro-nickel alloys which corrode uniformly at low rates have longer fatigue life in sea water than do medium or high strength carbon steels which are stronger but corrode at higher rates. Similarly, stainless steels in sea water are usually more resistant to fatigue than are low-alloy steels of the same or higher tensile strength.

It has been found that the damage to fatigue life caused by a corrosive environment exists only if the uniform corrosion rate lies above a specific value which varies with the metal.[14-16] For mild steel or high strength steels the specific rate is about 5 mdd, and for copper it is 285 mdd. Hence the fatigue limit of carbon steels in deaerated sea water, in which the corrosion rate lies below 5 mdd, is the same as that in air (Fig. 5). Cathodic protection effectively increases fatigue life to the value in air at any potential which reduces the uniform corrosion rate below the specific value. It is not necessary, in other words, to reduce the corrosion rate to zero. The normal corrosion rate of copper in aerated sea water lies below the specific rate corresponding to a fatigue life of 10^7 cycles, accounting for the observed good resistance of copper to corrosion fatigue. Present data indicate in addition that effective inhibitors for any metal are those that reduce the uniform corrosion rate below the specific corrosion rate.

High strength steels up to approximately 300,000 psi tensile strength when fatigued in dry air have a fatigue limit equal to about 1/2 the tensile strength (Fig. 6). However, the fatigue life falls below normal dry-air values at tensile strengths in the order of 170,000 psi or above in presence of atmospheric moisture or of water whether deaerated or not. Their behavior in this respect overlaps their sensitivity to stress corrosion cracking in presence of moisture.

Acknowledgement

Research results summarized in this paper have been made possible by support of the U.S. Army Research Office-Durham; the Office of Saline Water, U.S. Department of Interior; the American Iron and Steel Institute; and the Inland Steel Co.

September 28, 1972

Discussion

Reference was made to the author's experiments in which coupling equal areas of 17 Cr - 2 Ni steel to 16 Cr iron increased resistance to cracking from 0.7 hours to 200 hours, and the question was asked whether much smaller anode/cathode ratios such as are common in cathodic protection. The author replied that there are few quantitative data on this point, but that a very small ratio can be effective. In reply to another question, the author said that there is a critical potential for SCC of 18/8 stainless steel in magnesium chloride boiling at 130°C, and the value of this potential is 0.15 v (SHE). In reply to a question concerning the effect of stirring on crevice corrosion, the author noted that crevice attack is accelerated for deep crevices but that stirring is beneficial for shallow crevices.

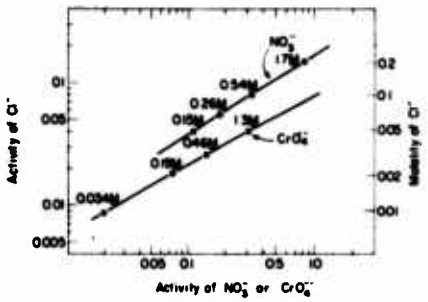


Fig. 1 Inhibiting Effect of Nitrates and Chromates on Pitting Corrosion of Aluminum in Chloride Solutions. No pitting is observed at inhibitor concentrations lying to the right of the respective lines., 25°C (3)

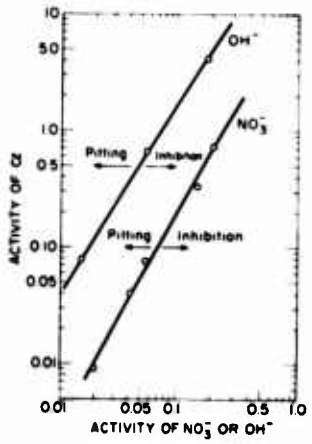


Fig. 2 Inhibiting Effect of Nitrates and Hydroxyl Ions on Pitting Corrosion of 18-8 Stainless Steel in Chloride Solutions(4), 25°C

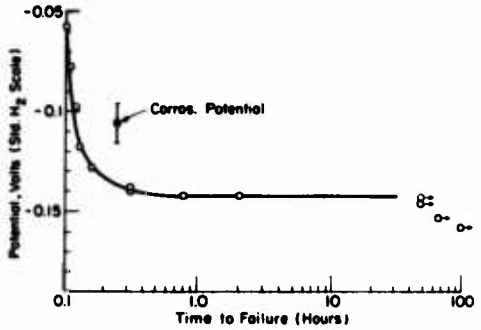


Fig. 3 Effect of Cathodic Polarization of Cold-rolled 18-8 Stainless Steel on Stress Corrosion Cracking in $MgCl_2$ Solution, 130°C. Critical potential below which failure does not occur is -0.145 V. (9)

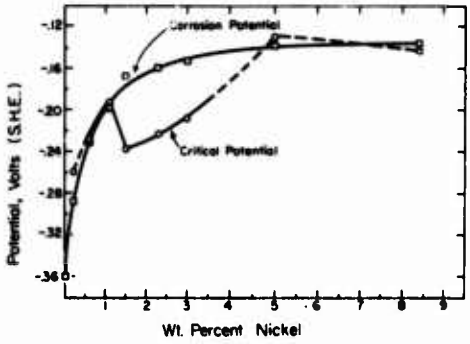


Fig. 4 Effect of Alloyed Nickel in Cold-Rolled Ferritic Stainless Steels on Critical and Corrosion Potentials in $MgCl_2$, 130°C. (10)

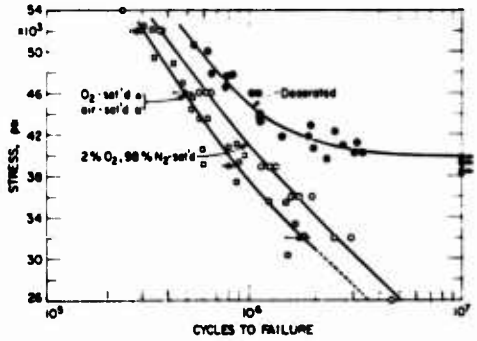


Fig. 5 Effect of Dissolved Oxygen Concentration or Corrosion Rate in 3% NaCl Solution on Fatigue Life of 0.18% C Steel, 25°C (13)

Influence of Minor Alloy Additions on the Passive Behavior of Binary Cu-Ni Alloys

Ellis D. Verink, Jr. and T. S. Lee, III

Department of Materials Science and Engineering
University of Florida, Gainesville, Florida 32601

Electrochemical hysteresis methods have been employed to construct experimental potential vs pH diagrams for a series of eight iron-free alloys ranging from pure copper to pure nickel in chloride-free and in 0.1M NaCl electrolytes at room temperatures. Interconnecting corresponding features of these diagrams produces a three-dimensional potential vs pH vs composition diagram which defines domains of corrosion and noncorrosion and delineates electrochemical conditions for existence of stable species. The compositions of the solid species are confirmed by x-ray analytical methods where possible. Interconnecting corrosion velocity contours for each diagram generates surfaces in three dimensions which provide relative information regarding the influence of alloy additions on corrosion kinetics. The three-dimensional diagram for iron-free Cu-Ni provides a "base line" for assessing the influence of minor solute additions to the binary Cu-Ni alloy system. Data are presented for five different iron levels in 90-10 Cu-Ni; four iron levels in 80-20 Cu-Ni and three iron levels in 70-30 Cu-Ni.

Experimental potential vs pH diagrams of alloys rich in one constituent tend to have many features in common with the equilibrium Pourbaix Diagram for the major alloy constituent. In the Cu-Ni system, the experimental diagrams for the Cu-rich alloys tend to resemble those for pure copper in varying degrees. Likewise at the nickel-rich end, the experimental diagrams for the alloys tend to resemble that of pure nickel. In the case of pure nickel, however, the experimental potential vs pH diagram bears little resemblance to the equilibrium Pourbaix Diagram constructed from thermodynamic data.

In nil-chloride solutions the change in the experimental potential-pH diagrams with increasing nickel is gradual over the entire compositional range. The general corrosion region "shrinks" to a small pH range, but the "immunity" line seems to remain more or less unchanged up to 45-55 Cu-Ni. As nickel increases beyond 55% the immunity line moves to more active potentials in the acid region. In the alkaline region, as nickel increases above 55%, the position of the metal/oxide coexistence line shifts from the expected position of the Cu/Cu_2O coexistence to the expected position of the $Ni/Ni(OH)_2$ coexistence. Increasing nickel also widens the pH range of passive behavior in chloride-free solutions.

By contrast, in .1M NaCl solutions there is a relatively abrupt change in the character of the potential vs pH diagrams at about 50-50 Cu-Ni. On the copper-rich side of this composition the diagrams tend to resemble the Cu-Cl-H_2O equilibrium Pourbaix Diagram (for .1M Cl^-) in many respects. On the nickel-rich side they tend to resemble the pure nickel diagram for .1M NaCl.

Key Words: Electrochemical corrosion, protection potential, Pourbaix Diagram, potential, pH, pitting potential, copper-base alloys, Cu-Ni, cupronickel, chlorides, copper, nickel, iron modified cupronickel, hysteresis.

---

1. Introduction

Copper-base alloys enjoy wide usage throughout industry, particularly in sea water applications, where they generally exhibit a low corrosion rate and an inherent resistance to marine fouling. Copper-nickel alloys are used extensively in surface condensers and salt water lines on shipboard, and for heat exchanger tubes in oil refineries. Among the alloys enjoying the widest usage are 90-10 cupronickel, 70-30 cupronickel and Monel[1]. While various investigations have reported the general effect of nickel content in binary copper-nickel alloys (1-10)[2] and the effect of iron in cupronickels (11-15) on their resistance to corrosion, little has been published relating electrochemical observation with corrosion behavior. This investigation presents electrochemical aspects of the corrosion behavior of the alloys of the binary copper-nickel system and organizes experimental observations into potential vs pH diagrams.

2. Experimental

Electrochemical hysteresis methods (16,17) have been employed to construct experimental potential-pH diagrams for a series of binary copper-nickel alloys (Table 1) ranging from pure copper to pure nickel in chloride-free and in 0.1M Cl^- hydrogen-deaerated electrolytes at room temperature. These diagrams provide a "base line" for assessing the influence of minor solute additions to the binary copper-nickel alloys, notably iron additions to cupronickels (Table 1). Figure 1 shows a flow chart for the organization of this electrochemical investigation.

The experimental method and the equipment used in this investigation have been discussed elsewhere (18). In establishing the details of the experimental technique for this study, it was necessary to qualify and standardize the following procedures so as to avoid spurious configurations in the polarization curves:

1. Sample polishing procedure
2. Sample cleaning procedure
3. Selection of electrolyte buffers
4. Polarization scan rate
5. Alloy microstructure

These procedures and the method in which they were derived are also discussed elsewhere (18).

---

[1]Trade name, International Nickel Company, Inc.
[2]Figures in parentheses indicate the literature references at the end of this paper.

3. Results

Copper-Nil Chloride Solutions

Figure 2 shows a comparison between the equilibrium Pourbaix Diagrams for the system copper-water (ionic species at a = 10^{-6}) (19) and the experimental E-pH diagram for pure copper in nil chloride solutions. Figure 2(a) is the equilibrium diagram considering CuO, while 2(b) considers $Cu(OH)_2$ as the stable solid species. There is reasonably good agreement between the various features of the equilibrium diagrams and the experimental diagram. The immunity line, that is, the line separating the immunity region from the corrosion region appears to correspond to an equilibrium between Cu and Cu^{++} in nil chloride solutions.

The zero current potentials (on the upward potential scan) in the neutral and alkaline pH ranges correspond closely to an equilibrium between Cu and Cu_2O. Primary passivation corresponds to the expected position of the Cu_2O/CuO coexistence, while secondary passivation occurs close to the expected position of the $Cu_2O/Cu(OH)_2$ coexistence. The vertical line separating corrosion from passivation is at a somewhat lower pH than that predicted by the equilibrium diagrams.

Copper-Chloride Solutions

The effect of chloride ion in solution is shown in Fig. 3. With increasing chloride content, the immunity line shifts to more active potentials, the corrosion region extends to a higher pH, and pitting occurs at more active potentials.

A comparison between equilibrium Cu-Cl-H_2O diagrams (20) and the experimental diagram for copper in 0.1 molar chloride solutions (Fig. 4) once again shows considerable similarity. The immunity line corresponds closely to the equilibrium between Cu and $CuCl_2^-$ (at $a_{CuCl_2^-} = 10^{-6}$). Zero current potentials in alkaline solutions occur at the predicted position of the equilibrium between Cu and Cu_2O. Primary passivation corresponds to the predicted position of equilibrium between Cu and hydrated Cu_2O, while secondary passivation corresponds closely to the expected potentials for the formation of $3Cu(OH)_2.CuCl_2$ from Cu_2O.

Nickel-Nil Chloride Solutions

In the case of nickel, the agreement between theory and practice is not as satisfying. Figure 5 compares the equilibrium Pourbaix Diagram for the Ni-H_2O system (ionic species at a = 10^{-6}) (19) with the experimental diagram for nickel in nil chloride solutions. The only obvious agreement is the correspondence between the zero current potentials in neutral and alkaline pH's with the equilibrium between Ni and $Ni(OH)_2$. The region of general corrosion is restricted to a much lower pH and more noble potentials than thermodynamics predict. The passivation process forming the upper (noble) bounds of the corrosion region occurs at much more active potentials than predicted. Potentiostatic tests for as long as 270 hours were performed to verify the lack of dissolved nickel in solution in ranges of immunity and passivation as predicted from the experimental diagram.

In his presentation of the equilibrium Ni-H_2O diagram, Pourbaix recognized the discrepancies between theory and experimental results. Pourbaix presented a tentative experimental diagram (19) which, while closer in appearance to the diagram obtained in this study, still indicates a much larger region of general corrosion than observed herein. Under similar experimental conditions other researchers (21-24) have found results similar to those presented herein.

Sato and Okamoto (21) have related the passivation forming the upper bounds of the corrosion region to an equilibrium between $NiOH^{++}$ and Ni_3O_4 in

the case of a large concentration of nickel ions. This appears appropriate in the present case as high current densities, thus high corrosion rates, are attained within the corrosion region.

De Gromoboy and Shrier (22) have suggested the possibility of higher oxides forming by direct oxidation of the metal. The Ni/Ni_3O_4 equilibrium is given by the relation, $E = 0.31 - 0.059$ pH. This corresponds closely to the primary passivation potential in neutral and alkaline solutions for the experimental diagram. They also have shown that at certain stages of the polarization of nickel, the reaction $Ni \rightarrow NiO$ is kinetically easier than $Ni \rightarrow Ni^{++}$, and subsequently that the $Ni \rightarrow Ni_3O_4$ reaction is favored kinetically over $Ni \rightarrow NiO$.

It seems possible that kinetic effects combined with possible inaccuracies in the thermodynamic data for the $Ni \rightarrow Ni^{++}$ reaction may account for the discrepancies between equilibrium calculations and experimental results. The thermodynamic inaccuracies may be due to the difficulty in attaining a reversible equilibrium between Ni and Ni^{++} (25).

Nickel-Chloride Solutions

Figure 6 shows the effect of chloride ion in solution on the experimental E-pH diagram for nickel. This effect manifests itself in an enlargement of the corrosion region to a higher pH and more active potentials. Corrosion also extends to more noble potentials due to the absence of a passive film in acid chloride solutions. While the same equilibria which occur in nil chloride solutions appear to be evident in neutral and alkaline pH's, the rupture potentials shift to more active values.

Attempts at correlating the zero current potentials in acid solution with the formation of some known chloride complex were unsuccessful. Consequently, no thermodynamic basis for this behavior has been established.

Copper-Nickel Alloys-Nil Chloride Solutions

The influence, on experimental E-pH diagrams developed in nil chloride solutions, of increasing nickel in binary copper-nickel alloys is shown in Fig. 7. The general trend is to decrease the pH range of corrosion and shift line V (immunity line) to more active potentials. This shift appears to occur in a gradual fashion over the entire compositional range. The critical transition range from general "copper-like" to "nickel-like" behavior occurs in the composition range between 80-20 and 55-45 copper-nickel. This range encompasses the critical alloy composition for passivity as defined by the electron configuration theory suggested by Uhlig (4).

The 80-20 alloy, while still exhibiting a larger corrosion region than nickel, has a zero current line (X) approaching that of the $Ni/Ni(OH)_2$ equilibrium. Primary passivation (line Y) occurs at nearly the same potentials as nickel, but is confined within a narrower range of pH. Secondary passivation (line Z) coincides with primary passivation (line Y) in the Cu diagram indicating a copper-oxide equilibrium. However, identification of this film in situ was not possible using conventional techniques because of the extreme thinness of the films. Persistence of this equilibrium continues until the pure nickel experimental E-pH diagram.

The experimental E-pH diagram for the 55-45 alloy exhibits a general shape similar to that of pure nickel. The corrosion region encompasses the same pH range; however, corrosion exists at more noble potentials than in pure nickel. The pH range of primary passivation (line Y) is greater than in the 80-20 alloy and continues to increase with increasing nickel content.

The 45-55 alloy diagram shows the appearance of an upper (noble) boundary on the corrosion region. The electrochemical potential range of general corro-

sion region. The electrochemical potential range of general corrosion continues to decrease with increasing nickel, while the onset of corrosion (line V) occurs at progressively more active potentials.

The current density contour diagrams for alloys exposed to nil chloride solutions (Fig. 8) show, with increasing nickel content, an increase in the corrosion rate within the general corrosion region and a decrease in corrosion rates within the region of passivation.

Copper-Nickel Alloys-Chloride Solutions

Figure 9 shows a composite of experimental E-pH diagrams for alloys exposed to 0.1 molar chloride solutions. The general shape of the diagrams remains similar to that of copper through the 55-45 diagram. The immunity line (V), the zero current line (X), and primary passivation (Y) are essentially unchanged as nickel is added up to about 45%. Secondary passivation (Z) is no longer evident after about 10% nickel. The vertical line (W) separating general corrosion from pitting and passivation, is shifted to progressively lower pH's as the nickel content in the alloy is increased.

The existence of the "corrosion boot" in the copper-rich alloys has been verified by potentiostatic test.

The change from "copper-like" to "nickel-like" behavior at approximately 50% nickel is in good agreement with results obtained by LaQue in sea water (1,2). The decrease in corrosion at nickel concentrations greater than approximately 50% can probably be attributed to the disappearance of a corrosion region in the neutral pH range of sea water for alloys containing greater nickel concentrations.

The nickel-rich alloys exhibit a general behavior similar to that of nickel. The 45-55 diagram has the general shape of the nickel diagram but the immunity line (V) still appears to be at the same potential as the copper immunity line. Line X (zero current line) coincides closely with the $Ni/Ni(OH)_2$ equilibrium, while line Y (primary passivation) corresponds to line Y in the nickel diagram.

The vertical line (W) shifts to the same pH as for pure nickel in the 25-75 alloy diagram, while the immunity line (V) shifts to a more active potential approaching that for nickel.

The current density contour diagrams for alloys exposed to 0.1 molar chloride solutions (Fig. 10) show no appreciable changes in corrosion rate from that of pure copper as nickel is added to the alloys.

Copper-Nickel-Iron Alloys-Chloride Solutions

The effect of iron additions to cupronickels on their electrochemical behavior is very slight. The immunity potential shifts slightly with varying iron content as is shown in Fig. 11. Assuming that the optimum solute concentration coincides with the most noble value of immunity potential, the optimum iron concentration for 90-10 is 1.4% iron; for 80-20, it is 1.2% iron; and for 70-30, it is 0.9% iron.

It also appears that the rupture potentials are shifted to slightly more noble potentials at the optimum iron concentrations for all three cupronickels (Fig. 12).

For the 90-10 and 70-30 cupronickels, all other characteristics of the experimental E-pH diagrams apparently remain virtually unaffected. The addition of 1.2% or 2.3% Fe to the 80-20 cupronickel results in the manifestation of a secondary passivation, which is not evident in the alloys containing <0.05 and 0.7% Fe.

Using chronoamperometric techniques, it was found that the rate of formation of the primary passive film on 90-10 alloys was quickest for the 1.4% Fe-containing alloy. Table 2 shows that a steady-state current density was reached within one minute for the alloy containing 1.4% Fe. The alloy containing 1.4% Fe also showed the lowest steady-state current indicating that this film was not only formed most rapidly but also was more protective than films on alloys containing less iron.

A similar study at secondary passivation potentials indicates that the 1.4% Fe alloy forms a secondary passive film as protective as that formed on the iron-free alloy after 30 minutes. This is evident by comparing circled values within Table 3. Once again, the degree of "protectiveness" appears to be greatest at the 1.4% Fe level.

Tables 4 and 5 show results of chronoamperometric studies on 80-20 and 70-30 alloys containing various iron concentrations. In Table 4, it can be seen that the greatest "protectiveness" is afforded by the alloy containing 1.2% Fe. Table 5 shows that the time required for formation of the primary passive film on the 0.9% Fe alloy is one-sixtieth that of the iron-free alloy and that the film on the 0.9% Fe alloy affords the greatest "protectiveness".

The optimum iron concentrations found in this study are in the same general range as those reported previously for increased impingement resistance (11-14).

4. Conclusions

From a systematic electrochemical study of binary copper-nickel alloys the following conclusions appear justified:

1. The experimental potential-pH diagrams for pure copper are in good agreement with the equilibrium Pourbaix Diagrams for the systems Cu-H_2O and Cu-Cl-H_2O.

2. The effect of chloride ion on the potential-pH diagram for pure copper in aqueous solutions is:

   a. to increase the potential and pH range of general corrosion,
   b. to lower the "rupture" potentials to more active values,
   c. apparently to favor the formation of chloride-containing, passive films.

3. The "general corrosion" region of the experimental potential-pH diagram for the Ni-H_2O system is restricted to a much smaller potential and pH range than that predicted by the equilibrium Pourbaix Diagram.

4. Chloride ion additions in aqueous solution have the following influences on the experimental potential-pH diagram for nickel:

   a. enlarges the "general corrosion" region to a higher pH and more active potentials,
   b. inhibits passive film formation at noble potentials in acid solutions,
   c. shifts "rupture" potentials to more active values,

5. The effect, on experimental potential-pH diagrams developed in nil chloride solutions, of increasing the nickel content in binary copper-nickel alloys is to shift the "immunity line" to more active potentials and to decrease the pH range of "general corrosion".

6. The transition range from "copper-like" to "nickel-like" behavior in nil chloride solutions occurs in the composition range of the 80-20 and 70-30 cupronickels. In acid solutions, these alloys behave as copper, whereas, in neutral and alkaline solutions, they behave as nickel.

7. The experimental potential-pH diagram for 55-45 copper-nickel alloy exposed to nil chloride solutions has more characteristics of the experimental nickel diagram than of the experimental copper diagram.

8. The current density contour diagrams for alloys exposed to nil chloride solutions show, with increasing nickel content, an increase in the corrosion rate within the "general corrosion" region and a decrease in corrosion rate within the region of passivation.

9. In 0.1 molar chloride solutions:

   a. The transition from "copper-like" to "nickel-like" behavior occurs in the composition range of the 55-45 and 45-55 copper-nickel alloys.
   b. In the compositional range from copper to the 55-45 copper-nickel alloy, the general shape of the experimental potential-pH diagram remains virtually unchanged. However, there is a restriction of "general corrosion" to a slightly smaller pH range.
   c. As nickel content increases from 55% to 100% there is further restriction of the pH range of "general corrosion". However, the "immunity line" shifts to more active potentials in this same range.
   d. As the nickel content increases, the current density contour diagrams for the alloys show no appreciable changes in corrosion rates from that of pure copper.

10. Chloride ions in aqueous solution shifts the "immunity line" and "rupture" potentials for all alloys examined to more active potentials and increase the pH range of "general corrosion". This effect is similar to that observed for pure copper and pure nickel.

11. Iron additions to cupronickel alloys exert a slight influence on the electrochemical behavior of the alloys. This effect is manifested in the following ways:

   a. The "immunity" potentials and the "rupture" potentials shift to slightly more noble values with optimum iron concentration in the alloys.
   b. The "rate" of formation and the relative "protectiveness" of the passive films is optimized with optimum iron concentrations in the alloys.

12. Based on electrochemical techniques, the optimum iron contents appear to be 1.4 w/o for 90-10 cupronickel; 1.2% w/o for 80-20 cupronickel; and 0.9 w/o for 70-30 cupronickel.

References

1. F. L. LaQue, Journal of the American Society of Naval Engineers, 53, 29 (1941).
2. F. L. LaQue, Discussion in Transactions of the Electrochemical Society, 85, 320 (1944).
3. R. Landau and C. S. Oldach, Transactions of the Electrochemical Society, 81, 521 (1942).
4. H. H. Uhlig, Zeitschrift fur Elektrocheme, 62, 700 (1958).
5. N. D. Stolica and H. H. Uhlig, Journal of the Electrochemical Society, 110, 1215 (1963).
6. J. Osterwald and H. H. Uhlig, Journal of the Electrochemical Society, 108, 515 (1961).
7. F. Mansfeld and H. H. Uhlig, Journal of the Electrochemical Society, 117, 427 (1970).
8. G. Trabanelli, F. Zucchi and L. Felloni, Corrosion Science, 5, 211 (1965).
9. R. B. Niederberger, R. J. Ferrara and F. A. Plummer, Materials Protection and Performance, 9, 18 (1970).
10. T. J. Lennox, Jr., M. H. Peterson and R. E. Groover, Materials Protection and Performance, 10, 32 (1971).
11. A. W. Tracy and R. L. Hungerford, Proceedings of ASTM, 45, 591 (1945).
12. F. L. LaQue, Discussion in Proceedings of ASTM, 45, 613 (1945).
13. G. L. Bailey, Journal of Institute of Metals, 79, 243 (1951).
14. W. C. Stewart and F. L. LaQue, Corrosion,8, 259 (1952).
15. P. A. Parrish, M.S. Thesis, University of Florida, 1970.
16. M. Pourbaix, Corrosion, 26, 431 (1970).
17. E. D. Verink, Jr. and M. Pourbaix, Corrosion, 27, 495 (1971).
18. T. S. Lee, III, M.S. Thesis, University of Florida, 1972.
19. M. Pourbaix, Atlas of Electrochemical Equilibria in Aqueous Solutions, First English Edition, Pergamon Press, 1966.
20. J. Van Muylder, N. de Zoubov and M. Pourbaix, Cebelcor RT 101 (1961).
21. N. Sato and G. Okamoto, Journal of the Electrochemical Society, 110, 605 (1963).
22. T. S. de Gromoboy and L. L. Shreir, Electrochimica Acta, II, 895 (1966).
23. J. R. Myers, F. H. Beck and M. G. Fontana, Corrosion, 21, 277 (1965).
24. T. Tokuda and M. B. Ives, Corrosion Science, II, 297 (1971).
25. W. M. Lattimer, Oxidation Potentials, Second Edition, Prentice-Hall, 1952.

5. Acknowledgements

The research reported herein was supported by the U. S. Department of the Interior under Contract Number 14-30-2600 administered by the Office of Saline Water, Washington, D. C., with partial support by the Department of the Navy under Contract Number N-14-68-A-0173-0015 administered by the Office of Naval Research, Washington, D. C. Pure nickel used in preparing certain of the alloys was supplied by the International Nickel Company, Inc., New York, New York.

Discussion

Noting that the position of any particular line on a Pourbaix diagram depends upon the stoichiometry of a particular species, the question was asked whether the author intended to pursue this question; in reply the author said that a great deal more work needs to be done both on more alloys and on better analyses of corrosion products. A question was asked concerning interpretation of results of studies such as the author's in terms of practical experience. For example, if the iron content of cupro nickel is increased, the resistance to impingement attack is increased, but the resistance to pitting worsens. The author replied that the studies reported represent early developments in this line of attack, that enlistment of other workers to help build up the body of scientific knowledge was important, that liason with practical experience was also important, and that these important aspects were slowly being addressed. In reply to a question concerning the effects of metallurgical structure, the author said that some effect should be detected depending upon whether iron was in or out of solution, but that other variables (e.g., grain size) would not affect the result. The author noted, in response to another question, that predictions had been checked with respect to crevice attack, and that with copper-zinc alloys the theoretical data superimposed on practical results gave good agreement; agreement was not so good with nickel alloys.

Table 1

Alloy Compositions

Cu - 99.999Cu
90-10 0 Fe - 87.8 Cu, 11.8 Ni, <0.05 Fe, 0.35 Mn
90-10 0.5 Fe - 87.5 Cu, 11.7 Ni, 0.53 Fe, 0.27 Mn
90-10 1.0 Fe - 86.87 Cu, 11.6 Ni, 1.05 Fe, 0.48 Mn
90-10 1.4 Fe - 87.34 Cu, 11.3 Ni, 1.36 Fe
90-10 2.0 Fe - 86.23 Cu, 11.3 Ni, 1.99 Fe, 0.48 Mn
80-20 0 Fe - 77.13 Cu, 22.2 Ni, <0.05 Fe, 0.67 Mn
80-20 0.7 Fe - 76.23 Cu, 22.5 Ni, 0.67 Fe, 0.62 Mn
80-20 1.2 Fe - 76.02 Cu, 22.3 Ni, 1.20 Fe, 0.48 Mn
80-20 2.3 Cu, 21.1 Ni, 2.26 Fe, 0.61 Mn
70-30 0 Fe - 68.63 Cu, 30.7 No, <0.05 Fe, 0.62 Mn
70-30 0.3 Fe - 68.45 Cu, 30.7 Ni, 0.32 Fe, 0.53 Mn
70-30 0.9 Fe - 68.51 Cu, 30.2 Ni, 0.90 Fe, 0.39 Mn
55-45 - 54.2 Cu, 45.8 Ni
45-55 - 45.9 Cu, 54.1 Ni
25-75 - 25.2 Cu, 74.8 Ni
Ni - 99.98 Ni, 0.01 C, 0.001 Mn, 0.001 Fe, 0.001 Cu, 0.001 Cr, 0.001 S, 0.001 Si, 0.001 Mg

Table 2

Current Density as a Function of Exposure Time of 90-10 Alloys in 0.1 Molar Chloride Solutions at Primary Passive Potentials ($E = -0.180V_{sce}$)

Time (minutes)	Current Density ($\mu A/cm^2$)				
	0 Fe	0.5 Fe	1.0 Fe	1.4 Fe	2.0 Fe
0	+160.0	+145.0	+155.0	+135.0	+125.0
1	4.0	4.0	4.0	1.9	2.0
5	3.0	2.0	3.0	1.9	2.0
10	3.0	2.0	2.5	1.9	2.0
30	3.0	2.0	2.5	1.9	2.0
60	3.0	2.0	2.5	1.9	2.0

Table 3

Current Density as a Function of Exposure Time of 90-10 Alloys in 0.1 Molar Chloride Solutions at Secondary Passive Potentials ($E = +0.025V_{sce}$)

Time (minutes)	Current Density ($\mu A/cm^2$)				
	0 Fe	0.5 Fe	1.0 Fe	1.4 Fe	2.0 Fe
0	+200.0	+200.0	+200.0	+200.0	+200.0
1	6.5	12.0	8.5	2.7	15.0
5	4.0	9.0	6.0	1.7	12.0
10	3.3	8.0	4.5	1.5	11.0
30	2.7	7.0	2.5	1.0	8.0
60	2.7	7.0	1.5	0.8	6.0
90	2.7	7.0	0.8	0.8	5.0
120	2.7	7.0	0.8	0.8	2.0
180	2.7	7.0	0.8	0.8	2.0

Table 4

Current Density as a Function of Exposure Time of 80-20 Alloys in 0.1 Molar Chloride Solutions at Primary Passive Potentials ($E = -0.180V_{sce}$)

Time (minutes)	Current Density ($\mu A/cm^2$)			
	0 Fe	0.7 Fe	1.2 Fe	2.3 Fe
0	+130.0	+135.0	+135.0	+130.0
1	3.0	3.0	2.5	2.5
5	2.6	1.7	1.4	2.0
10	2.7	1.8	1.4	1.7
30	2.7	1.8	1.3	1.5
60	2.9	1.8	1.3	1.5
90	2.9	1.8	1.3	1.5

Table 5

Current Density as a Function of Exposure Time of 70-30 Alloys in 0.1 Molar Chloride Solutions at Primary Passive Potentials ($E = -0.180V_{sce}$)

Time (minutes)	Current Density ($\mu A/cm^2$)		
	0 Fe	0.3 Fe	0.9 Fe
0	+160.0	+145.0	+115.0
1	4.0	5.5	1.2
5	3.0	3.2	1.0
10	2.5	2.5	0.8
30	2.0	2.0	0.7
45	1.6	1.6	0.7
60	1.2	1.2	0.7
90	1.2	1.2	0.7

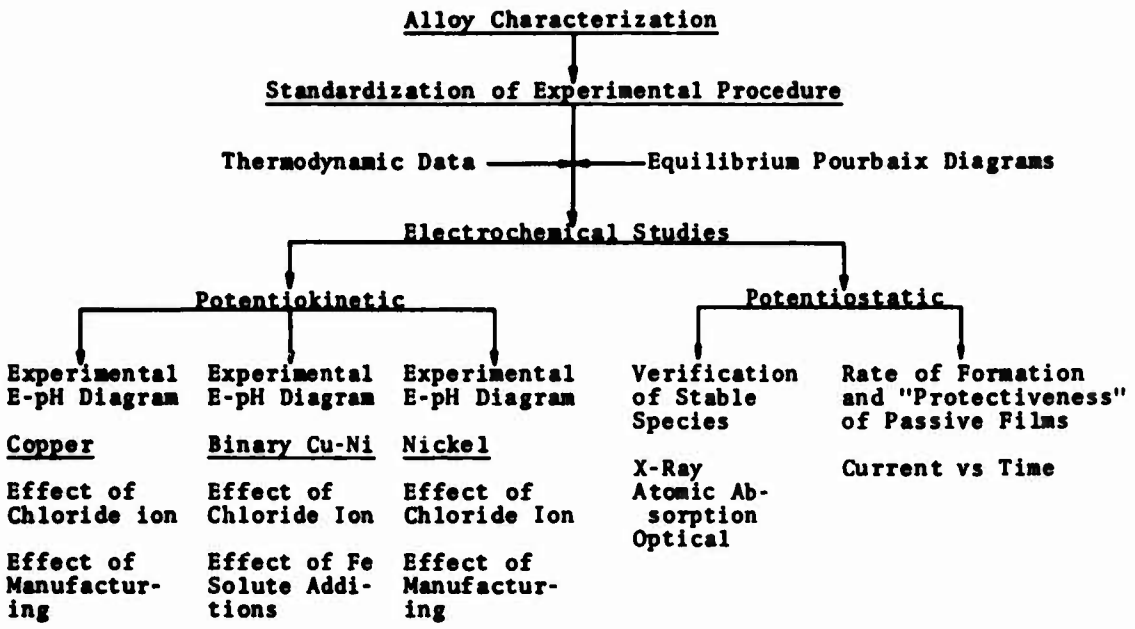


Figure 1: Activity flow chart for the present electrochemical investigation.

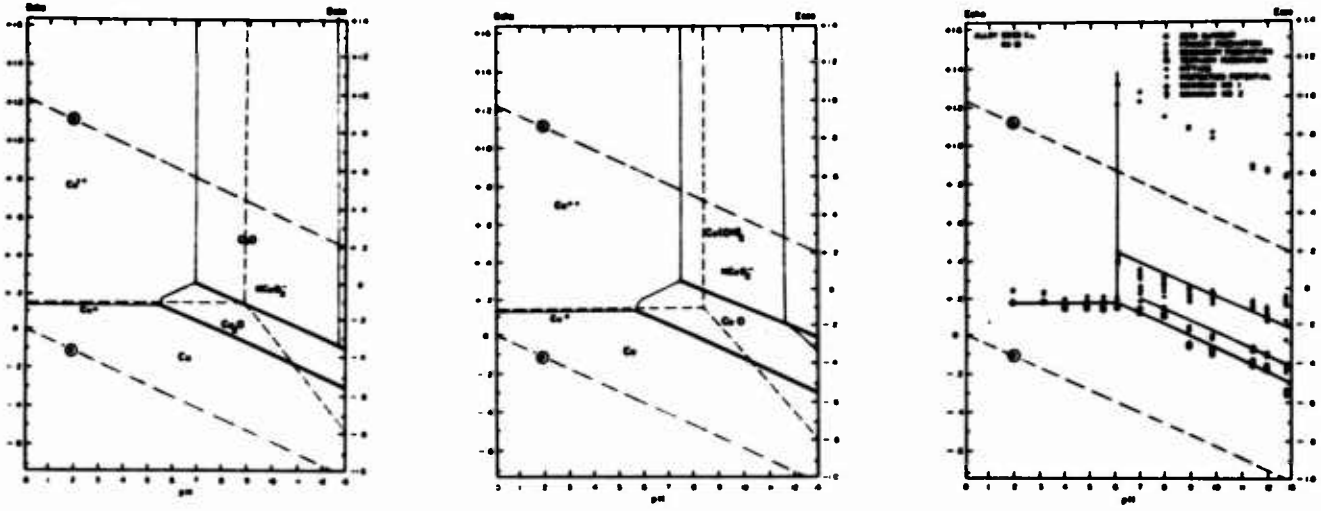


Figure 2: A comparison between the equilibrium Pourbaix Diagram for the system Cu-H_2O (23) [(a) considering CuO, (b) considering $Cu(OH)_2$] and the experimental potential-pH diagram for Cu in nil chloride solutions. The equilibrium diagrams were constructed for ionic species activity = 10^{-6}.

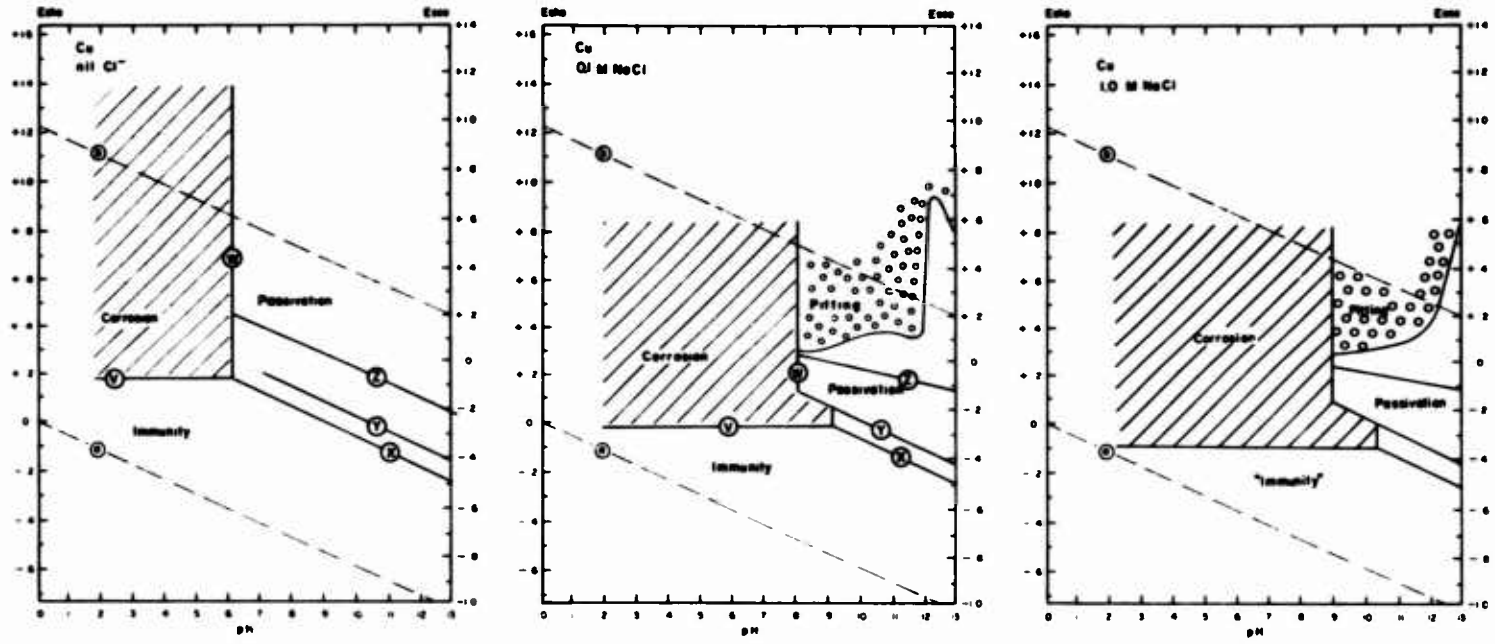


Figure 3: A comparison of experimental potential-pH diagrams for pure copper developed in electrolytes containing nil chloride (left), 0.1 molar chloride (center), and 1.0 molar chloride (right).

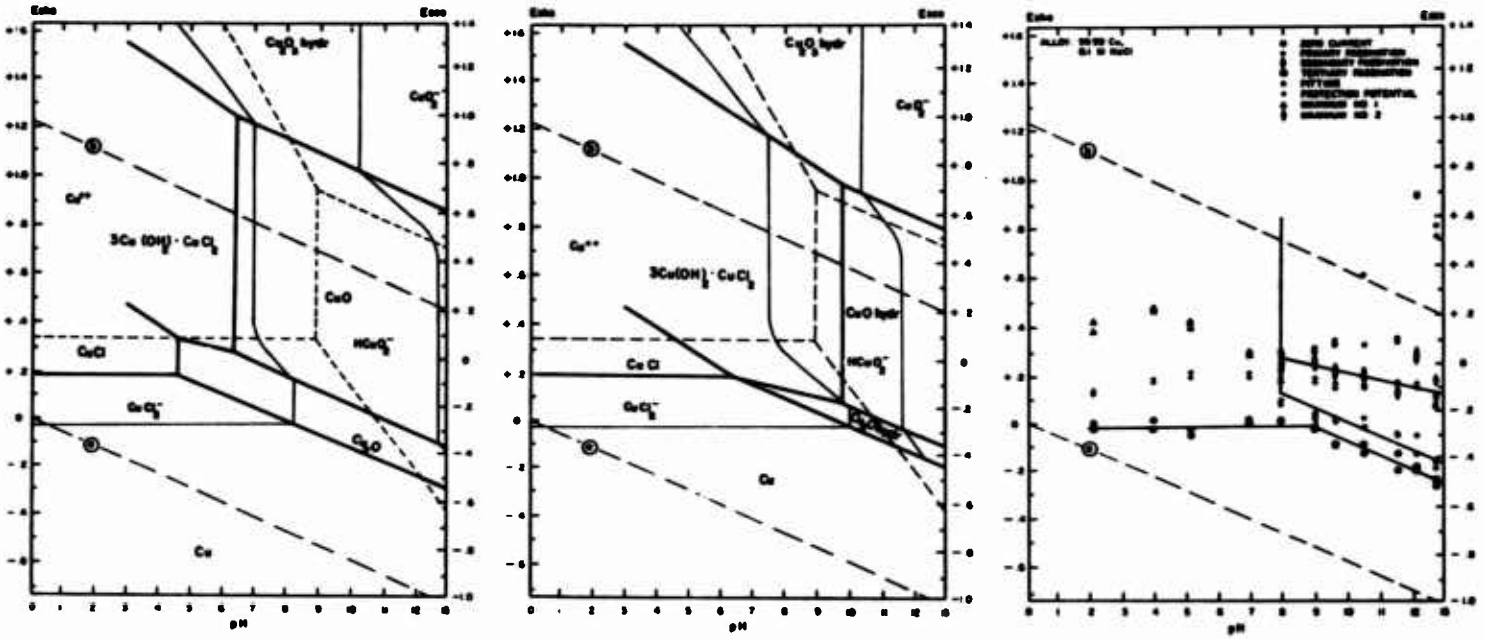


Figure 4: A comparison between the equilibrium Pourbaix Diagram for the system Cu-Cl-H_2O (24) [(a) considering Cu_2O and CuO, (b) considering hydrated Cu_2O and CuO] and the experimental potential-pH diagram for Cu in 0.1 molar chloride solutions. The equilibrium diagrams were constructed for ionic species activity = 10^{-6}.

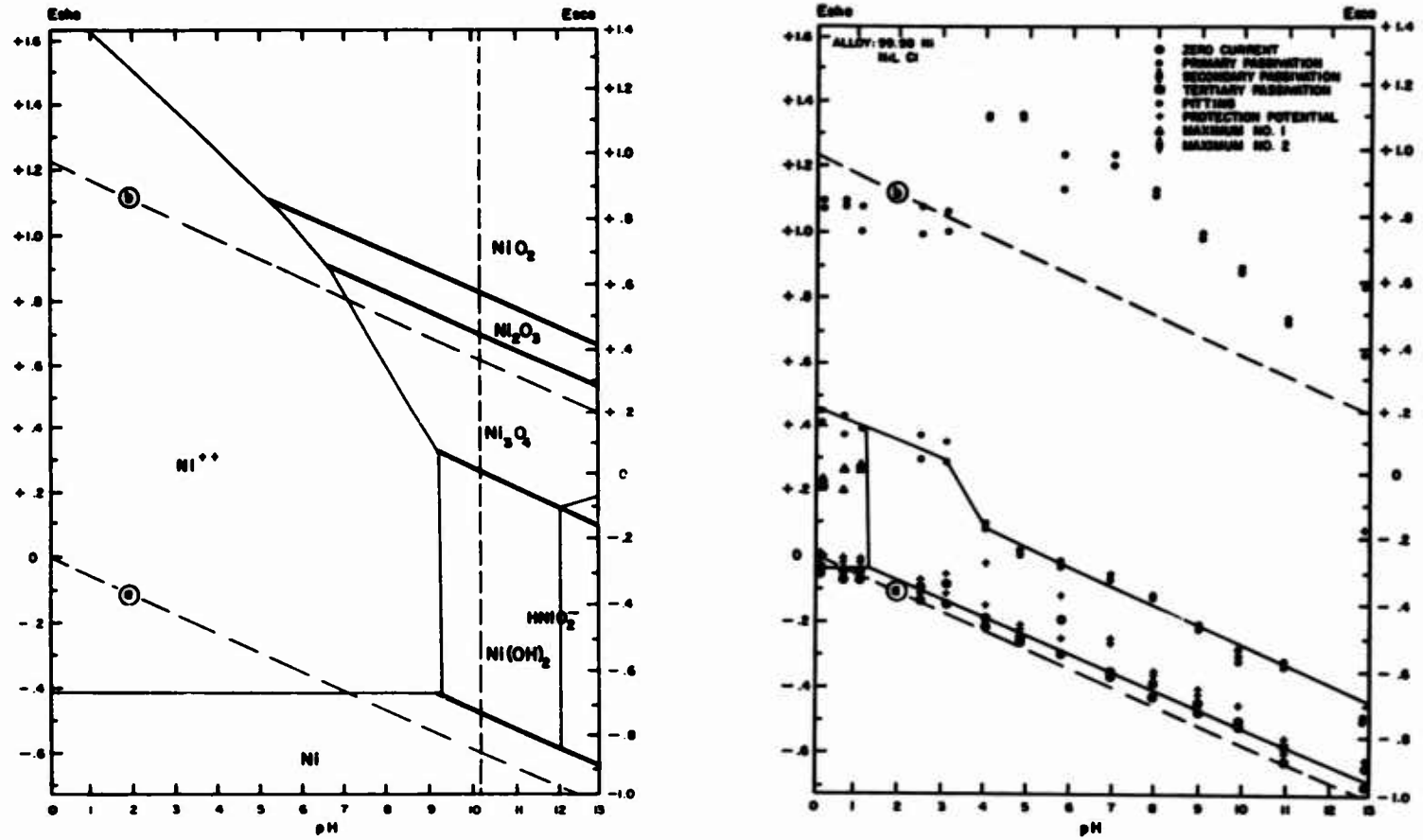


Figure 5: A comparison between the equilibrium Pourbaix Diagram for the system Ni-H_2O (23) and the experimental potential-pH diagram for Ni in nil chloride solutions. The equilibrium diagram was constructed for ionic species activity = 10^{-6}.

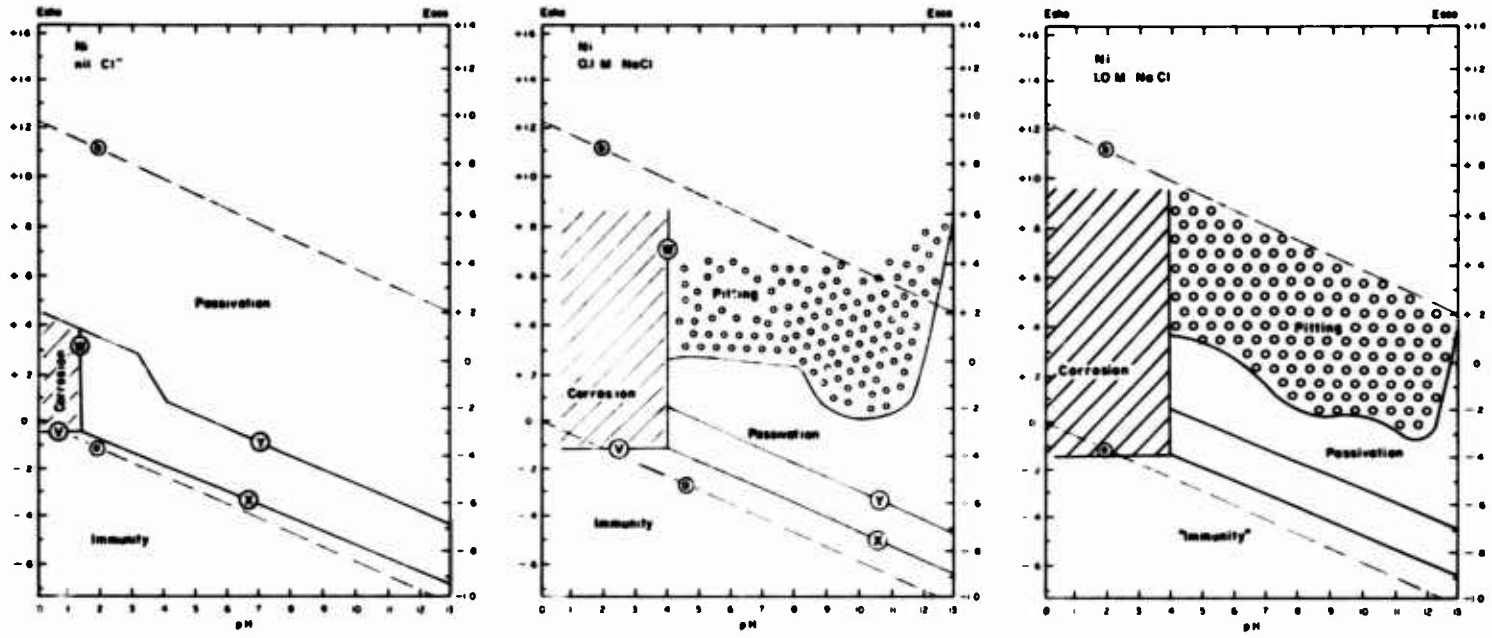


Figure 6: A comparison of experimental potential-pH diagrams for pure nickel developed in electrolytes containing nil chloride (left), 0.1 molar chloride (center), and 1.0 molar chloride (right).

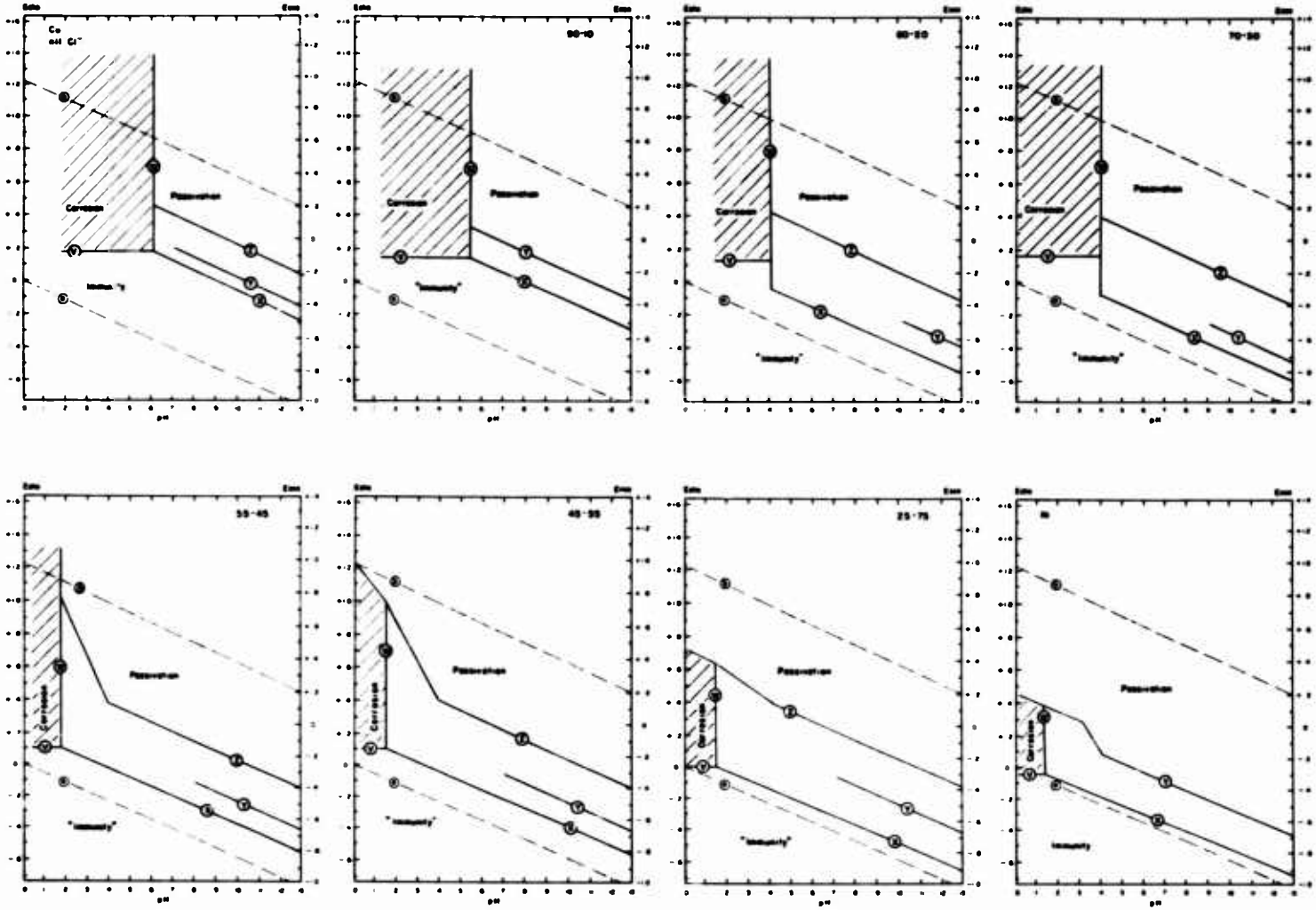


Figure 7: A comparison of experimental potential-pH diagrams for binary Cu-Ni alloys exposed to nil chloride solutions.

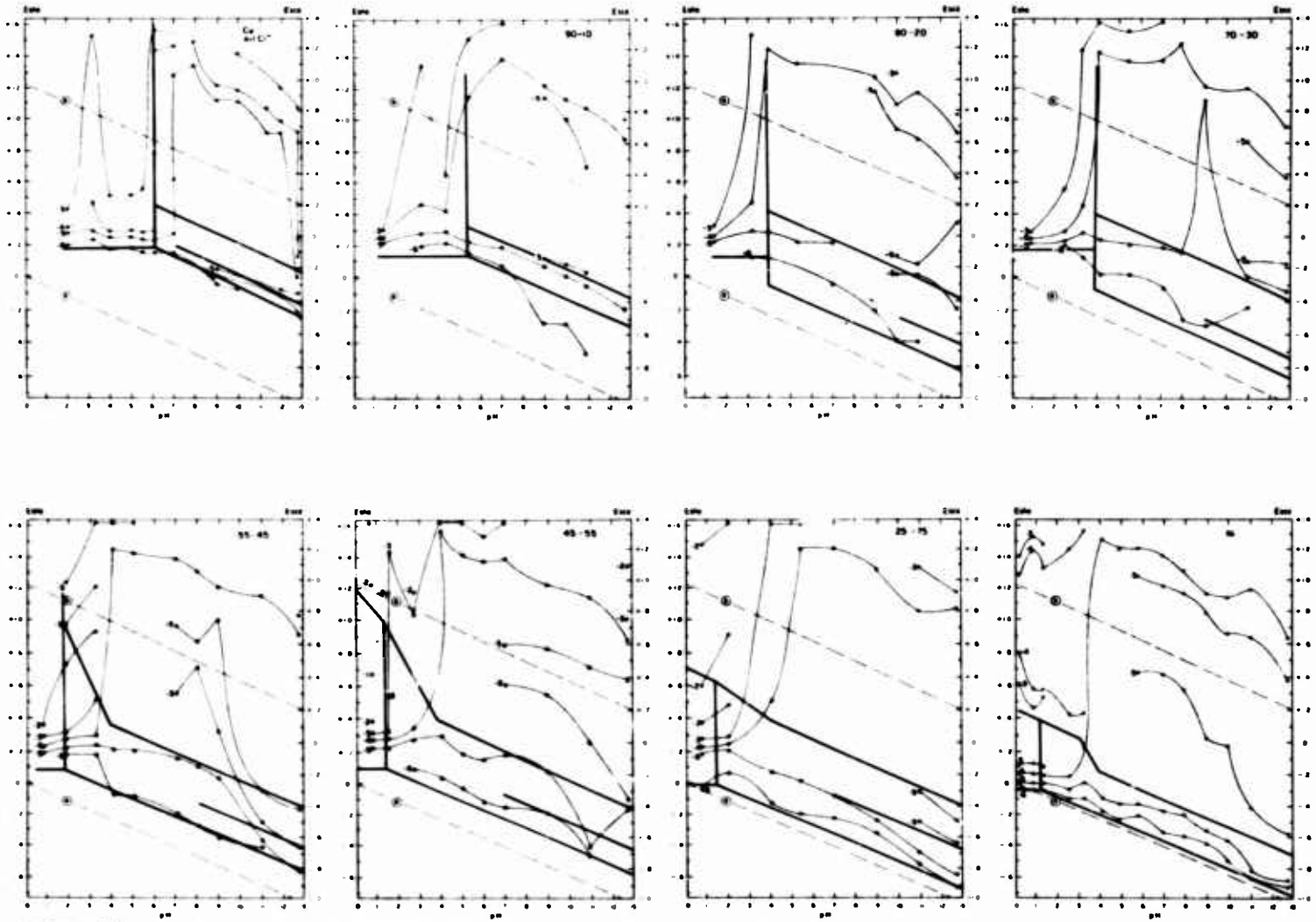


Figure 8: A comparison of current density contour diagrams for binary Cu-Ni alloys exposed to nil chloride solutions.

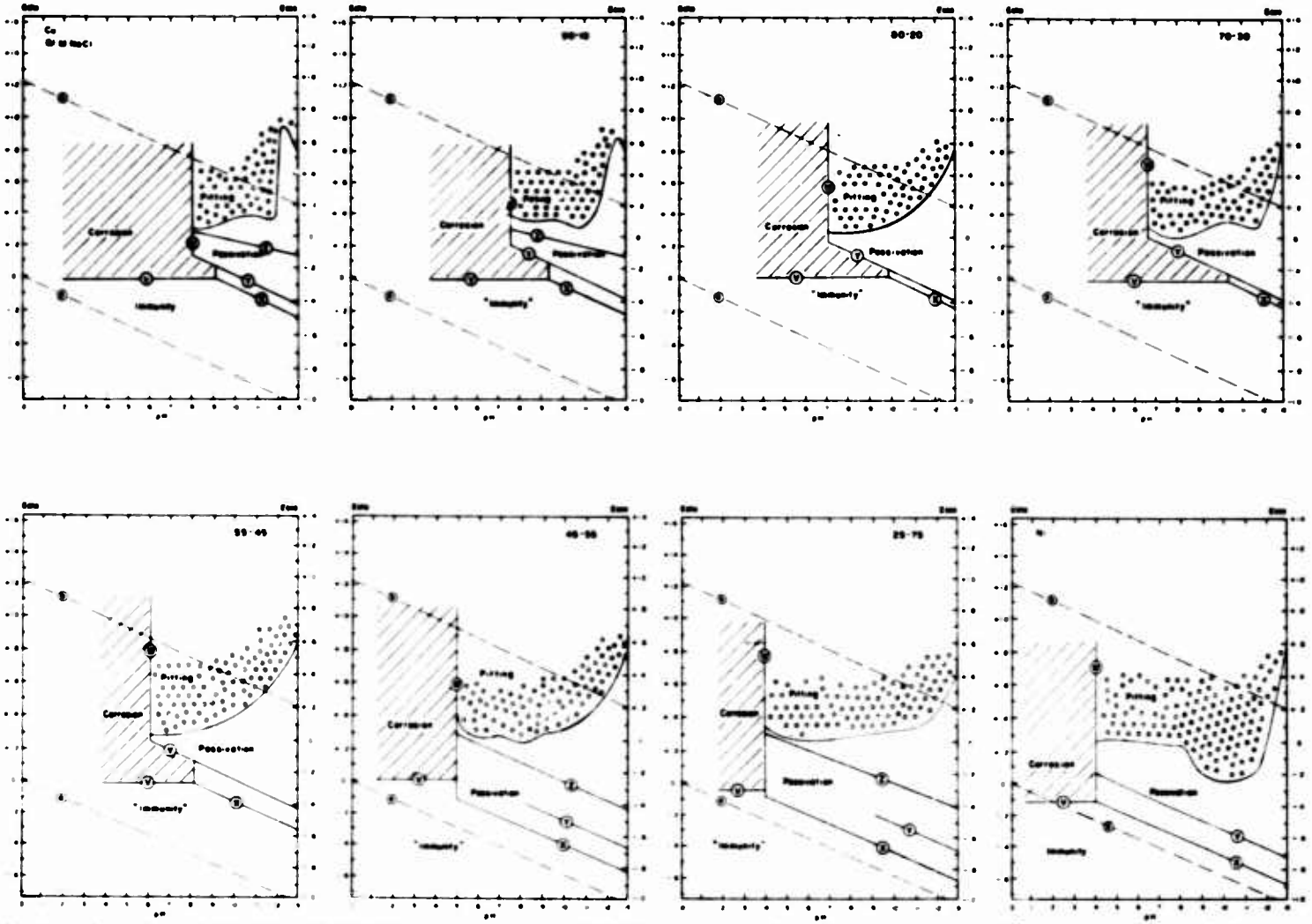


Figure 9: A comparison of experimental potential-pH diagrams for binary Cu-Ni alloys exposed to 0.1 molar chloride solutions.

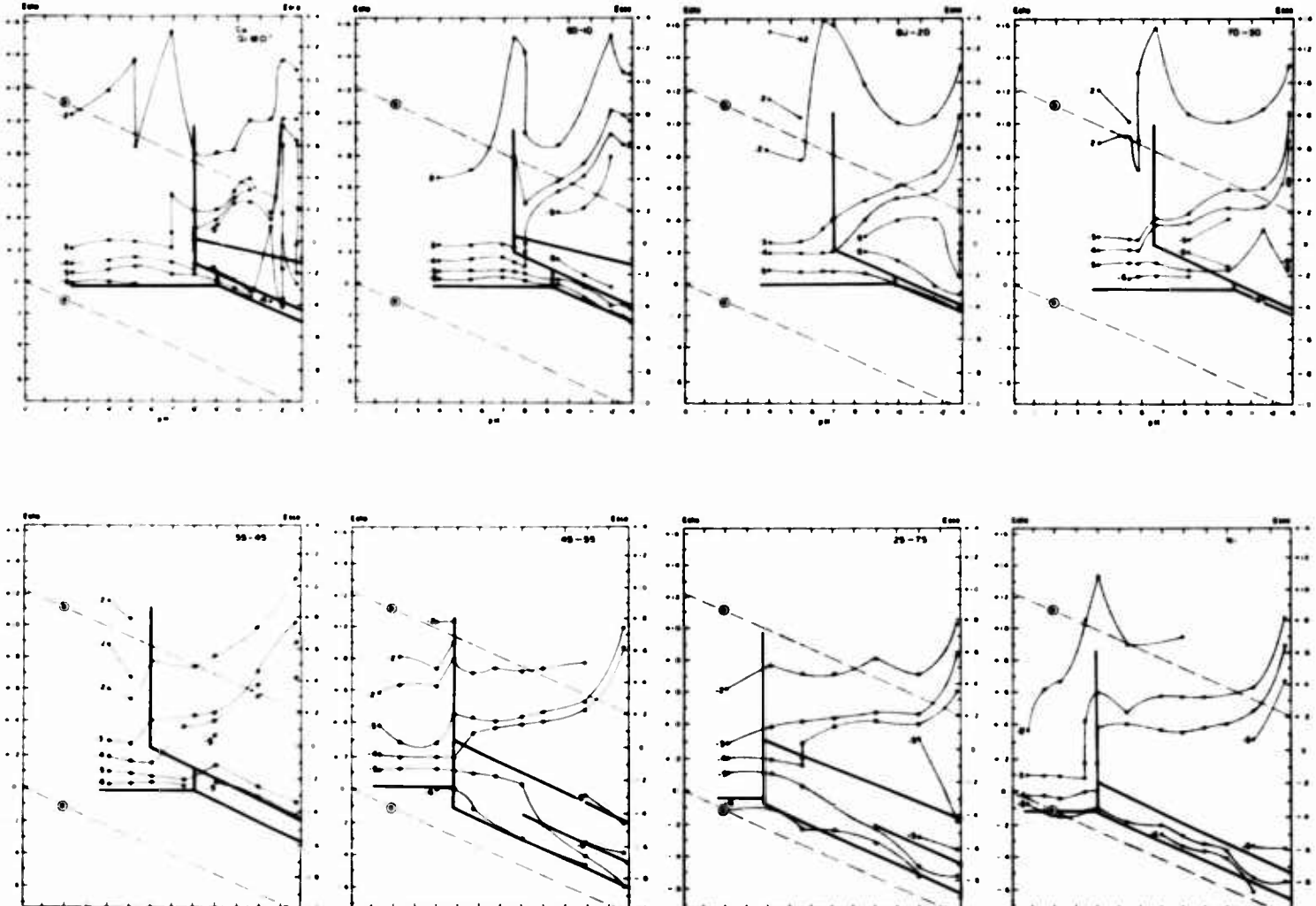


Figure 10: A comparison of current density contour diagrams for binary Cu-Ni alloys exposed to 0.1 molar chloride solutions.

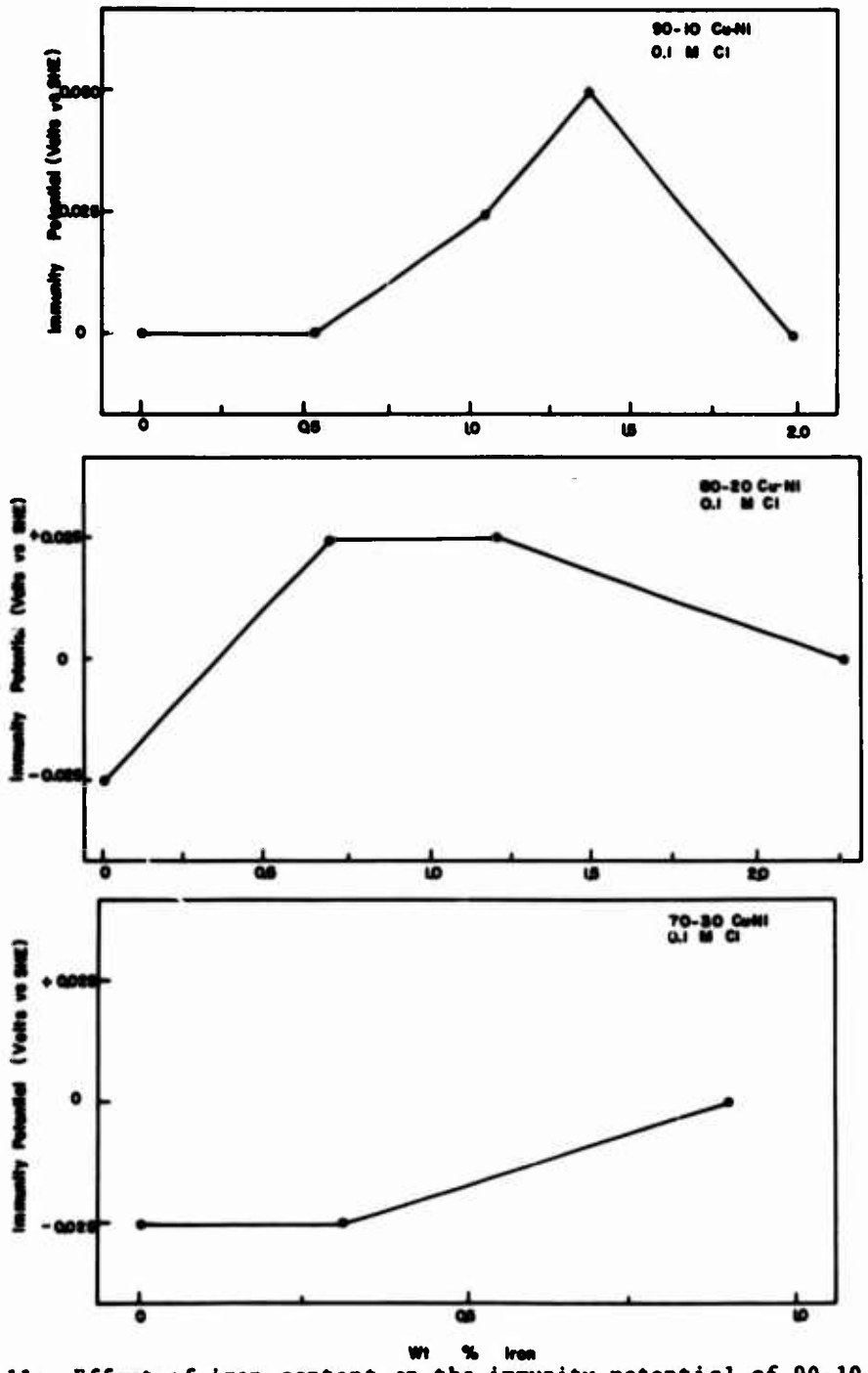


Figure 11: Effect of iron content on the immunity potential of 90-10 (top), 80-20 (center)and 70-30 (bottom) cupronickels exposed to 0.1 molar chloride solutions.

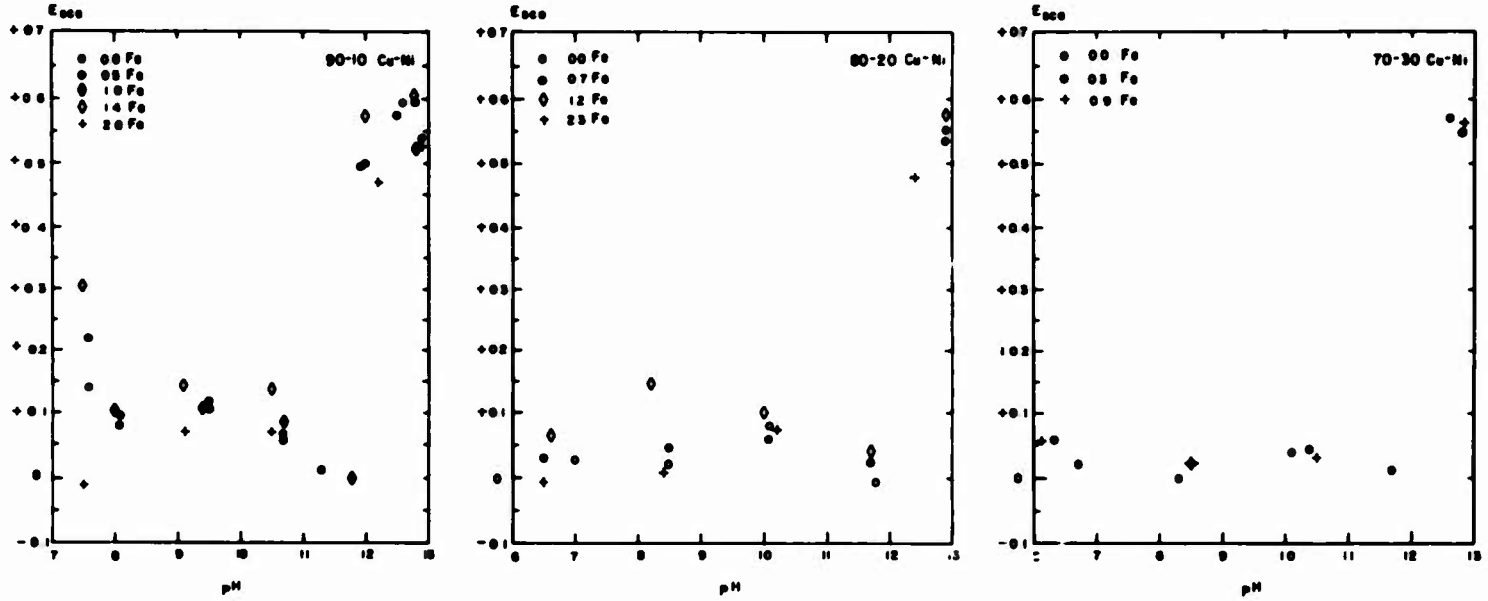


Figure 12: Effect of iron content on the rupture potential of 90-10 (left), 80-20 (center) and 70-30 (right) cupronickels exposed to 0.1 molar chloride solutions.

The Influence of Chromium on the Corrosion Behavior of Copper-Nickel Alloys in Sea Water

D. B. Anderson and K. D. Efird

The International Nickel Co., Inc.
Francis L. LaQue Corrosion Laboratory
P. O. Box 656
Wrightsville Beach, N. C. 28480

Extensive studies have shown the effectiveness of chromium (0.5-3%) in copper-nickel alloys for both strengthening and increasing sea water velocity limitations for turbulent flow conditions without adversely affecting other properties of this alloy system which are particularly attractive for marine service. Low velocity (0.3 to 0.6 m/s) sea water tests indicate a slight increase in susceptibility to localized attack for chromium modified alloys. Under high velocity conditions (to 40 m/s) chromium additions provide improved corrosion resistance and extend the upper velocity limits for the copper-nickel alloys in sea water.

Key Words: Sea Water Corrosion; Copper-Nickel Alloys; Chromium Additions; Velocity Effects; Impingement.

1. Introduction

New alloy developments often respond to what are believed to be clearly defined needs for better materials for specific problem areas. The true merits of a new material can best be judged by its acceptance for the intended application and, as is often the case, acceptance for a wide diversity of other applications requiring a similar combination of unique properties.

The widespread introduction of steam turbines to provide power for ship propulsion in the early 1900's provided the clearly defined need for condenser tube alloys with good corrosion resistance. "Condenseritis" became a recognized 'disease' which often played a major role in naval operations and inspired a series of alloy developments which are continuing today.(1-5)[1]

A number of new condenser tube alloys were developed between 1920 and 1950, initially in the United Kingdom and shortly thereafter in the United States. The most widely used alloys included Admiralty brass (70Cu-20Zn-1Sn), aluminum brass (78Cu-20Zn-2Al), copper nickel-30%, Fe modified copper nickel-30%, Fe + Mn modified copper nickel-30% and finally Fe modified copper nickel-10%. Admiralty brass and copper nickel-30% without appropriate iron additions quickly lost favor for marine applications and today aluminum brass and the iron modified copper nickel alloys dominate the marine heat exchanger tube market and are widely accepted for sea water piping and a variety of other applications.

The mechanical properties of non age-hardening copper nickel alloys are attractive for fabrication of tubular products with ease of welding permitting both seamless and seam-welded manufacturing without difficulty. As with most copper-base alloys, the copper nickels provide inherent anti-fouling properties which can minimize blockage and other problems associated with fouling growths. However, the primary advantage unique to the copper nickel alloys is their demonstrated corrosion resistance for a wide variety of flow conditions

[1] Figures in parentheses indicate the literature references at the end of this paper.

- ranging from stagnant sea water, where a variety of localized corrosion processes can limit the usefulness of many materials, to turbulent flow conditions where resistance to impingement corrosion and erosion corrosion become critical factors. Surveys of operating experience with tubing where sea water is used as a coolant in heat exchanger service - or more recently with tubing and other critical components in desalination service - invariably identify the copper nickels as premier alloys.(6-8)

Age-Hardenable Alloy Systems

The tensile properties of the copper nickel alloys described have generally restricted their use to comparatively low pressure systems. There are a number of ocean engineering applications (e.g. sea water piping in submarines and high speed pumps) where higher strength alloys possessing the unique fabrication and corrosion resisting properties of the copper nickels would be ideally suited. Several age-hardened 30% Ni alloys have been introduced,(9) but fabrication problems and difficulties in maintaining optimum strength and corrosion resistance in as-welded structures have limited their overall usefulness.

Development of Chromium Modified Copper Nickel Alloys

Recent research efforts have resulted in the introduction of three chromium modified copper nickel alloys - two wrought and one cast - a combination of alloys that provides a significant expansion of the areas of usefulness for the copper nickels in sea water systems.

Initial studies centered on the ability of chromium to exert substantial hardening in a 30% Ni alloy.(10) Hardening occurs through a spinodal decomposition mechanism as the alloy is cooled from the annealing temperature or from the melt, thus spontaneous hardening is not significantly affected by welding, a distinct advantage over age-hardened alloys. This alloy in wrought form is nominally 30% Ni - 3% Cr. Composition and properties are detailed in Tables 1 and 2 respectively.

In support of the introduction of this Cu-Ni-Cr alloy for sea water piping, a companion cast alloy was developed for pipe fittings, valve bodies, etc., to provide matching corrosion resistance and assurance of galvanic corrosion compatibility.(11) This alloy has been designated IN-768.

Initial sea water corrosion studies with these alloys indicated exceptional impingement corrosion and erosion resistance for flowing sea water systems. Realization that this property, without the companion hardening effect could provide the basis for an attractive condenser tube alloy for critical applications involving excessive turbulence, a third alloy was subsequently developed. This alloy, nominally 15% Ni - 0.5% Cr has been designated IN-838.(12) With its lower strength, this alloy matches the fabricability of CA-706 and CA-715.

2. Sea Water Corrosion Evaluations

Chromium modified copper nickel alloys, along with the standard 30% Ni (CA-715) and 10% Ni (CA-706) alloys, have been subjected to a variety of natural sea water corrosion tests at the Francis L. LaQue Corrosion Laboratory to fully characterize their corrosion behavior over a range of exposure conditions. A characterization of the sea water at the laboratory is given in Table 3. In the course of these corrosion studies, careful attention has been given to the delineation of the specific effects of chromium additions over a wide range of compositions within the copper nickel alloy system.

Low Velocity Sea Water Corrosion

Although the primary applications for copper-nickel alloys generally involve flowing sea water systems, flow interruptions must be considered and corrosion behavior for stagnant or low velocity flow conditions characterized. Corrosion data developed during a number of panel exposures in a sea water channel (tidal flow of <0.3 m/s) and a wooden flume where a constant flow of 0.6 m/s is maintained are summarized in Figures 1 and 2. The band for each alloy encompasses the range of data developed and reflects differences in specimen size, shape and surface conditions, sea water temperature (short-term ex-

posures), and to a lesser extent, minor compositional variations. Characteristically, corrosion rates for the copper nickel alloys decrease with time for undisturbed exposures of this type, requiring many years to stabilize. These data indicate an average corrosion rate of approximately 1 micron/year (<0.05 MPY) is achieved for CA-706 and CA-715 after the fifth year of exposure for both flow conditions studied. This is a much lower value than is generally cited for these alloys when corrosion rates are calculated from weight losses over comparatively short exposure periods which do not reflect the changing slope of the weight loss versus time curves.

Time has not permitted development of long-term data for the chromium modified alloys. Initial corrosion rates (six-month exposures) are generally slightly higher for alloys containing 1-3% Cr while the 0.5% addition has little effect. The modified alloys, however, demonstrate the same trend toward decreasing corrosion rates with time, and for long-term exposures it is doubtful whether any significant differences will be observed.

The short-term exposures also indicate a slight reduction in resistance to localized corrosion penetration with the 1-3% Cr alloys developing a characteristic shallow cratering type of attack and the 0.5% Cr alloy showing increased sensitivity to corrosion in tight crevices. The extent of this attack is relatively minor and - as with most copper-base alloys - the rate of localized penetration decreases sharply with time following the same general pattern as the average corrosion rates.

Effects of High Velocity Sea Water

With the interest in applications involving pipe, tubing and associated components for sea water systems, velocity effects have received the primary emphasis in the corrosion studies. Although final evaluation must involve practical flow systems with fabricated components - trials which are now in progress - various laboratory tests have been used for detailed assessments of the effects of Cr additions as a basis for determing optimum alloy compositions for subsequent development. In all cases direct comparisons have been made with CA-706 and CA-715 as standards of performance.

A jet apparatus adapted from a test device developed by the British Non-Ferrous Metals Research Association(13) was used to study impingement corrosion resistance as a function of velocity and alloy composition. This device permits exposure of coupon specimens in quiescent sea water while at the same time each specimen is subjected to a 1 to 2 mm diameter jet of aerated sea water impinging directly against a small area of the specimen surface. This creates a localized area of controlled turbulence, a primary factor in the impingement corrosion mechanism.

Series of 15% and 30% Ni alloys with varying Cr additions have been compared with jet impingement velocities of 7 and 15 m/s. These velocities were chosen to assure a high degree of turbulence of sufficient severity to clearly define composition ranges for optimum impingement corrosion resistance in flowing sea water systems. The results of these tests are shown in Figures 3 and 4. These data provide a clear indication of the effectiveness of Cr additions over the range of 0.5-3% in providing a marked increase in impingement corrosion resistance.

Typical jet impingement data for one- to two-month tests with jet velocities ranging from 1 to 15 m/s are summarized in Table 4. The usefulness of this test method in detecting velocity limitations for useful corrosion resistance is evident, a limit of 5 m/s for CA-706 and CA-715, 7 m/s for IN-838 and greater than 15 m/s for Cu-Ni-3% Cr and IN-768 being indicated. In comparison, limited impingement corrosion resistance is indicated for CA-443 (Admiralty brass) for velocities as low as 1 m/s while CA-687 (aluminum brass) consistently fails to match the performance of any of the copper-nickel alloys.

Companion studies have been conducted with a velocity flow system in which coupon specimens are positioned parallel to the flow direction (Figure 5). Specimens are placed in individual nozzles with appropriate orifice plates to permit a range of velocities in simultaneous tests. Table 5 summarizes data obtained in this manner for several of the alloys of interest. Velocities in this type of test are limited only by the available sea water pressure. Data in Figure 6 were developed with this test to show the effects of Cr additions

in 30% Ni alloys for sea water velocities of 15 and 40 m/s, velocities frequently encountered in sea water pumps. The effectiveness of the 2-3% Cr levels in the Cu-Ni-3% Cr alloy and IN-768 is clearly defined.

Galvanic Relationships

Introduction of new alloys into sea water systems requires careful consideration of galvanic relationships which can accelerate corrosion of critical components, regardless of their apparent merits based on isolated exposures. Compilation of extensive corrosion-potential data developed in flowing sea water has been used as a basis for a galvanic series which serves as a useful guide for predicting galvanic relationships.(14) Comparative data for the chromium modified copper nickel alloys are shown in relation to several common marine alloys in Figure 7. Increasing Ni and Cr levels generally result in more noble potentials with the Cu-Ni-3% Cr alloy and IN-768 being slightly cathodic to virtually all other copper-base alloys. The indicated relationship between CA-706 and IN-838 suggests that CA-706 would be an ideal tube sheet material where IN-838 tubes are used. The Cu-Ni-3% Cr alloy and IN-768 have exhibited similar corrosion potentials, a useful relationship where these alloys are used for various components in sea water piping systems.

Weld Studies

Engineering usefulness of any material requires weldability, and for materials designed for use in corrosive environments with no external protection (e.g. coatings, cathodic protection), the definition of weldability must include freedom from corrosion problems associated with welded joints. Preferably, no post-weld heat treatment should be required to insure optimum joint efficiency and corrosion resistance so that field repairs can be accommodated.

Of all the copper-base alloys, the copper nickels perhaps have the highest degree of weldability. Because they are solid solution alloys, there are no metallurgical transformations during the welding process to alter material properties in heat affected areas to induce potential weld corrosion problems.

Wrought and cast alloys can be welded by all of the conventional methods. Standard copper nickel-30% filler metal is ideal for the lower strength alloys, providing sound welds with desirable galvanic relationships. A proprietary Cr-containing electrode is available for the hardened alloys and generally permits full joint efficiency.

Extensive weld corrosion studies have been undertaken for a variety of sea water exposure conditions. Typical specimens from several of these studies are illustrated in Figures 8 & 9. All of these tests have been conducted with as-welded specimens without benefit of post-weld heat treatments and in no instance has there been any evidence of localized corrosion associated with the welds or heat affected zones.

3. Summary

The versatility of copper-nickel alloys for marine service is expanded through controlled additions of chromium. These chromium additions to the copper-nickel alloy system significantly influence both mechanical and corrosion properties of the system. Mechanical properties are affected primarily by the occurrence of a spinodal region in the ternary alloy. Significant hardening has thus been achieved in cast and wrought 30% Ni alloys. The effect on corrosion properties, however, does not depend on the spinodal decomposition.

The effect of chromium on the sea water corrosion properties of copper-nickel alloys is most dramatic under velocity conditions. These additions greatly extend the upper velocity limits of the alloys in sea water.

As a result of these studies, three alloys have been selected for development. They provide a combination of properties which extend the range of usefulness of the copper-nickel alloy system in marine applications.

4. References

1. A. W. Tracy and R. L. Hungerford, "The Effect of Iton Content of Cupro-Nickel on its Corrosion Resistance in Sea Water", Proceedings ASTM Vol.45, pp. 591-617(1945).
2. W. C. Stewart and F. L. LaQue, "Corrosion Resisting Characteristics of Iron Modified 90-10 Cupro-Nickel Alloy", Corrosion Vol.8, pp.259-277(1952).
3. P. T. Gilbert, "The Resistance to Failure of Condenser and Heat Exchanger Tubes in Marine Service", Trans. Institute of Marine Engineers, Vol.66, p.1(1954).
4. C. Breckon and J. Baines, "The Significance of Apparently Minor Factors in Corrosion Problems Affecting Condenser and Cooler Tubes", Trans. Institute of Marine Engineers Vol.67, No.10(Oct.1955).
5. D. H. Osborn and D. A. Sudrabin, "Copper Base Alloys: The Logical Choice for Marine Structures and Equipment", Proceedings 25th NACE Conference(1969).
6. H. A. Todhunter "Condenser Tubes in Sea Water Service", Power,(March 1967).
7. "Survey of Condenser Tube Life in Salt Water Service", OSW R&D Report #278 (1967).
8. E. H. Newton, J. D. Birkett and J. M. Ketteringham, "Survey of Materials Behavior in Large Desalination Plants Around the World", Report to OSW, March 1972.
9. J. N. Bradley, "Recent Developments in Copper-Base Alloys for Naval Marine Applications", International Metallurgical Reviews, Vol.17(1972).
10. F. A. Badia, G. N. Kirby and J. R. Mihalisin, "Strengthening of Annealed Cupro-Nickels by Chromium" ASM Transactions Quarterly, Vol.60, No.3, pp. 395-408 (1967).
11. F. J. Ansuini and F. A. Badia, "Development of a Cr-Si Hardened Cast Copper-Nickel", Trans. A.F.S.(1969).
12. D. B. Anderson and F. A. Badia, "Chromium Modified Copper-Nickel Alloys for Improved Sea Water Impingement Resistance", ASME Transactions (submitted for publication).
13. R. May and R. Stacpoole, "The Jet Impingement Apparatus for the Assessment of Corrosion by Moving Sea Water", Journal of the Institute of Metals, Vol. 77, No.4, p.331(1950).
14. J. R. Hunt and M. D. Bellware, "Ocean Engineering Hardware Requires Copper-Nickel Alloys", Transaction Third Annual MTS Conference,(1967).

Discussion

The authors stated in reply to query that the solid solubility of chromium in the 30% Ni-Cu alloy is 1.4%.

Table I

Nominal Compositions of Copper-Nickel Alloys

Alloy	% Ni	Cr	Fe	Mn	Cu
CA-706	10	-	1.4	0.4	bal.
CA-715	30	-	0.6	0.8	"
IN-838	16	0.4	0.8	0.5	"
Cu-Ni-3Cr	30	2.8	0.3	0.7	"
IN-768	30	1.6	0.7	0.6	"

Table 2

Nominal Mechanical Properties of Copper-Nickel Alloys

Alloy	Temper	Yield Strength (0.2% offset) KSI	Yield Strength (0.2% offset) MN/m^2	Tensile Strength KSI	Tensile Strength MN/m^2	% Elongation in 2" (51mm)
CA-706	Annealed	15	103	44	303	40
	Hard	62	427	69	476	5
CA-715	Annealed	21	145	57	393	43
	Hard	73	503	80	552	5
IN-838	Annealed	18	124	46	317	40
	Hard	66	455	70	483	6
Cu-Ni-3Cr	Annealed	50	345	80	552	30
	Hard	107	738	113	779	8
IN-768	As-cast	50	345	75	517	20*

*elongation in 1" (25.4mm)

Table 3

Sea Water Chemistry at The Francis L. LaQue Corrosion Laboratory

Major Variables

	max.	min.	avg.
pH	8.1	7.8	8.0
T,°C	29	6	18
Cl,g/L	19.8	18.1	19.0
O_2,mg/L	9.3	5.0	6.4

Average Analysis, mg/L

cations		anions	
Na	10,006	SO_4	2510
Ca	398	HCO_3	133
Mg	1204	NO_3	1.2
K	369	PO_4	.01
Cu	.015	F	1.5
Fe	.001	Br	61
Zn	.012	I	.16
Hardness,$CaCO_3$		5970	
Dissolved Solids		38,255	

Table 4

Summary of Jet Impingement Test Data

1-2 month tests, 10-26°C sea water

	Impingement attack - mm/mo				
Alloy	1.2 m/s (4 FPS)	4.6 m/s (15 FPS)	6.8 m/s (22 FPS)	9.8 m/s (32 FPS)	15.3 m/s (50 FPS)
CA-443	.18-.26	.15-.48	-	-	-
CA-687	.06-.15	.03-.25	-	-	-
CA-706	.08-.10	.01-.18	.03-.13	.13	.43-1.5
CA-715	.01-.03	.01-.09	.03-.57	.14-.17	.68-1.2
IN-838	-	-	.01-.03	.09-.12	.11-.69
Cu-Ni-3Cr	-	-	.01	-	.01
IN-768	-	-	.01	-	.01-.13

Table 5

Summary of Parallel Flow Sea Water Corrosion Tests

30 day exposures

Alloy	Avg. Sea Water Temp.	Localized Attack - mm			
		3 m/s (10 FPS)	6 m/s (20 FPS)	11 m/s (35 FPS)	15 m/s (50 FPS)
CA-706	10°C	.10	.10	.08	.08
CA-715	10°C	.03	.03	.08	.13
IN-838	20°C	<.03	.03	.10	.13
Cu-Ni-3Cr	10°C	<.03	<.03	<.03	<.03

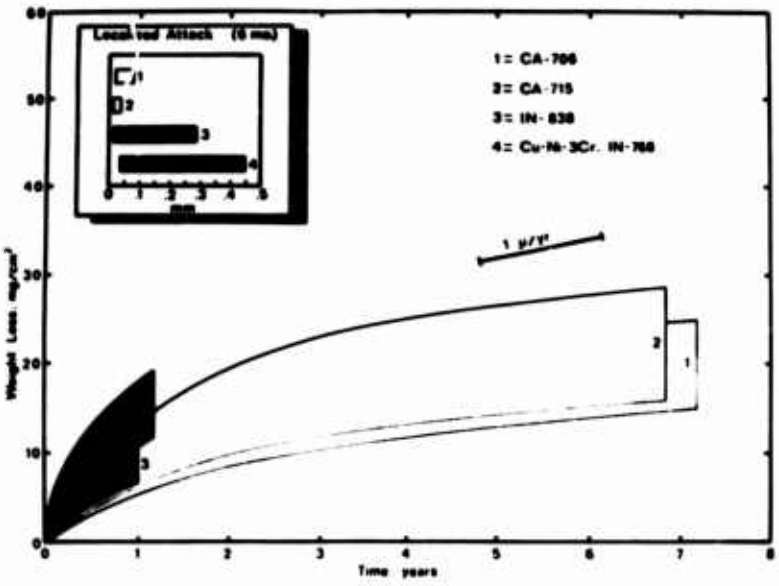


Figure 1. Corrosion of copper-nickel alloys in quiet sea water.

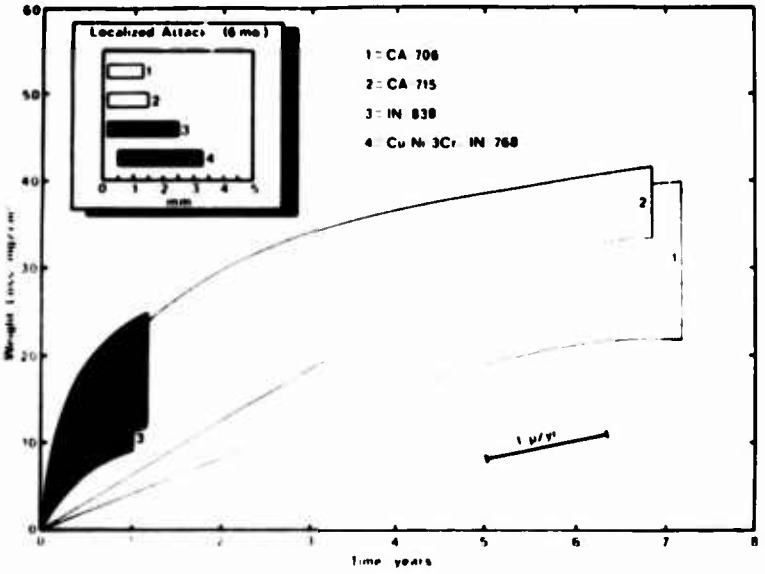


Figure 2. Corrosion of copper-nickel alloys in flowing sea water (0.6 M/Sec).

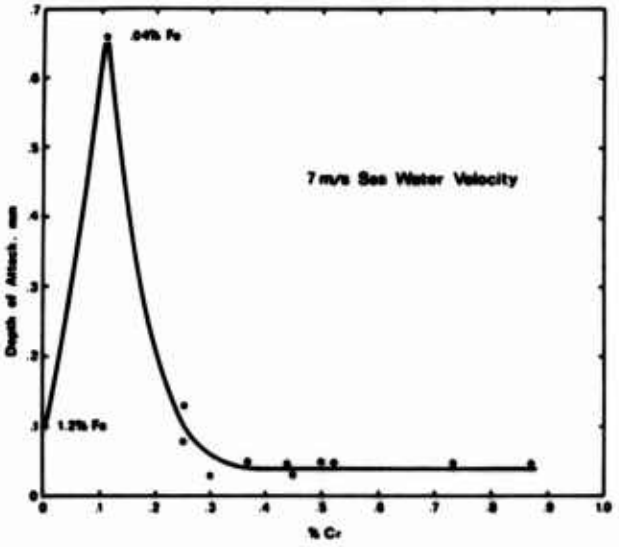


Figure 3. Effect of Cr additions on sea water impingement corrosion resistance of copper nickel alloys containing 15-18% Ni. Two-month tests with jet velocity of 6.8 m/s (22 FPS).

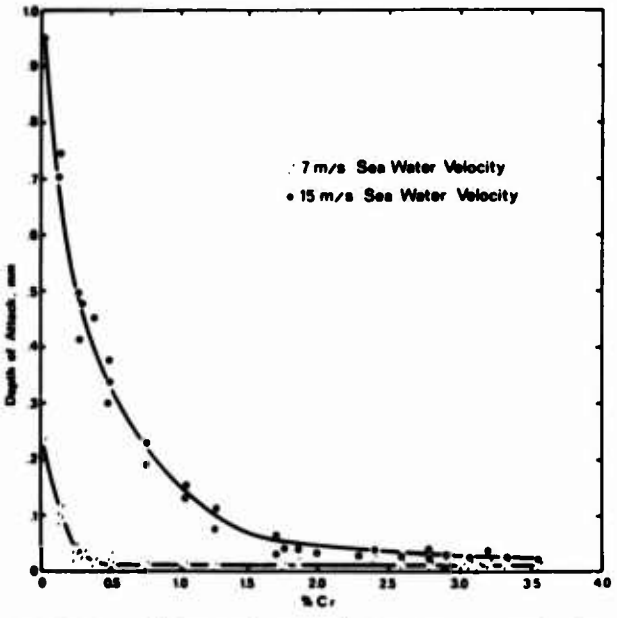


Figure 4. Effect of Cr additions on sea water impingement corrosion of copper nickel - 30% (one and two month tests).

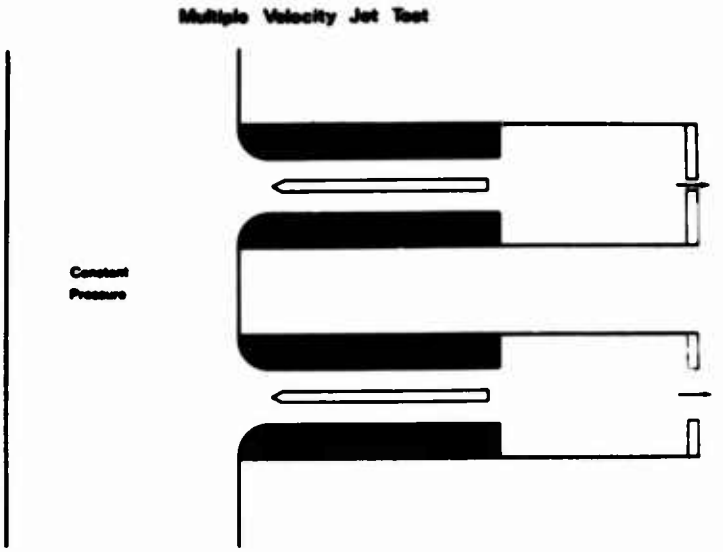


Figure 5. Parallel flow sea water corrosion test device.

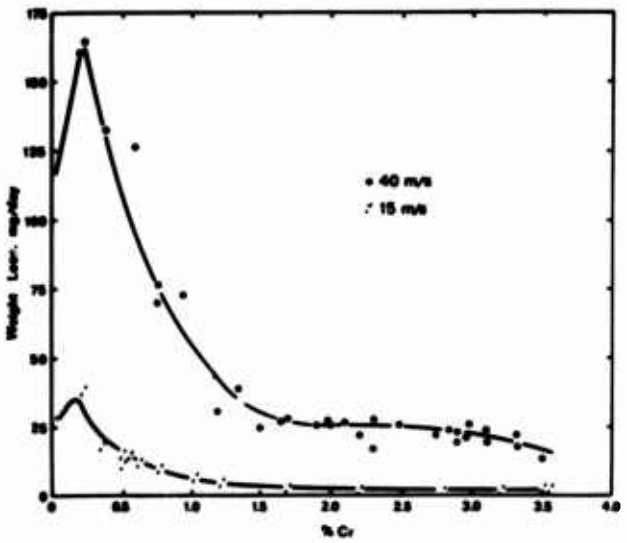


Figure 6. Effect of Cr additions on corrosion of copper nickel - 30% in high velocity sea water (one month, parallel flow tests).

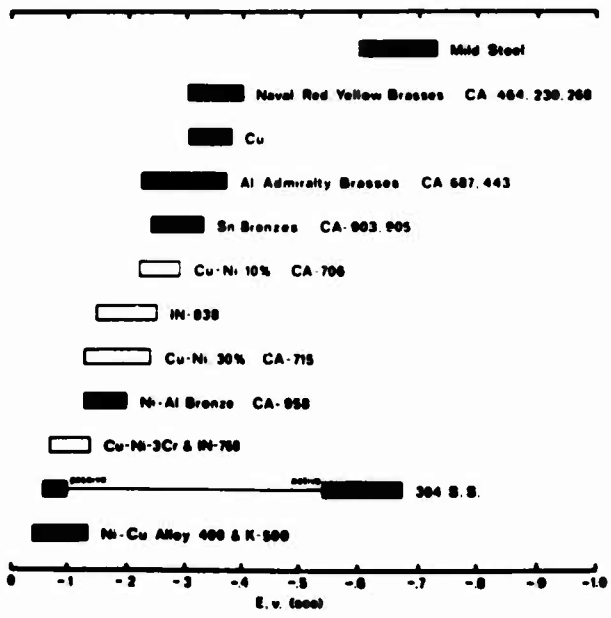


Figure 7. Corrosion potentials in flowing sea water at 2-4 m/s and 10-27°C.

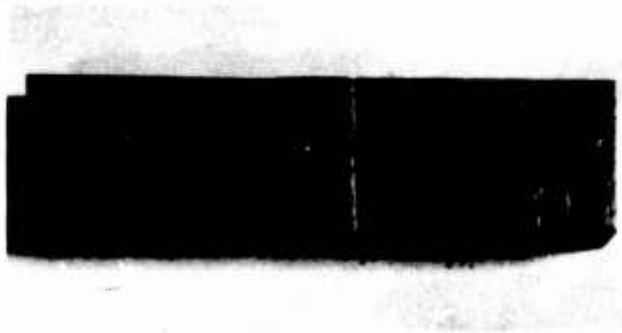


Figure 8. Welded joint after six-month sea water exposure. Joint combines 1/2" plate wrought Cu-Ni-3% Cr alloy (left) with IN-768. Manual gas tungsten and weld with proprietary Cr containing copper nickel-30% electrode.

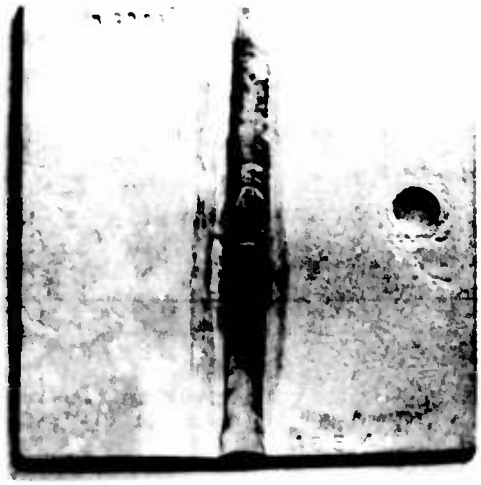


Figure 9. Welded joint combining IN-838 (left) and CA-706, four month sea water exposure. Gas tungsten are weld with 70-30 Cu-Ni filler metal.

The Influence of Composition upon the Structure and Properties of a Cast Cu-Ni-Mn-Fe-Al Alloy for Marine Applications

B N Hall and R A Farrar

Ministry of Defence
Ship Department
Foxhill, Bath UK
BA1 5AB

The University of Southampton
Southampton UK
SO9 5NH

The system Cu-Ni-Mn-Fe-Al has been investigated to obtain an understanding of the influence of composition upon structure and properties and to assess the suitability of the cast alloy for marine applications. This paper gives an outline of the alloy development and structural studies and an assessment of the marine corrosion resistance of the cast quinary alloy.

Structural studies on the ternary Cu-Ni-Al and quarternary Cu-Ni-Fe-Al systems built up an understanding of the quinary alloy. The essential features of the alloy include a cored Cu-Ni matrix containing stable γFe + Ni cuboids concentrated in the Ni rich dendrites; this phase derives from the basic Cu-Ni-Fe spinodal reaction and contributes to the matrix hardening. A second precipitate is the Ni-Al phase which can exist in several geometric forms and is considered to be the principle hardening precipitate in the system. It occurs in both grain boundary and interdendritic regions. Although susceptible to heat-treatment optimum properties are obtained in the 'as cast' condition.

Sea immersion tests showed the self-corrosion rate to be low and crevice corrosion resistance to be good. Galvanic coupling to 90/10 and 70/30 Cu-Ni showed galvanic compatibility. Jet impingement resistance is comparable to conventional cupro-nickels. The alloy has high resistance to stress-corrosion.

The overall characteristics of the alloy are good over a wide range of composition and it is considered to be very suitable for marine applications.

Key Words: Copper casting alloy, Cu-Ni-Mn-Fe-Al, microstructure, γ Fe + Ni, Ni-Al, mechanical properties, marine corrosion resistance.

1. Introduction

The Royal Navy have a requirement for a medium-high strength copper-base casting alloy for sea-water applications. A Cu-Ni-Mn-Fe-Al alloy was among those alloys considered capable of meeting the mechanical requirements. Preliminary corrosion assessment of experimental casts showed good resistance to jet-impingement attack while 'ad hoc' structural investigations by Dewey(1)[1] and Dennis (2) revealed complex microstructural features. A detailed investigation was therefore carried out at Central Dockyard Laboratory, Portsmouth and Engineering Materials Laboratory, University of Southampton to relate the effects of compositional variables to the structure and properties of the alloy.

[1] Figures in parenthesis refer to the list of references at the end of this paper.

2. Experimental Procedures

(i) Structural Investigations

Laboratory and Foundry castings were used, the former being mainly sand cast although a small number of melts were chill cast. The foundry melts were produced using oil fired furnaces in HM Dockyard, Portsmouth and sand cast by Durville and semi-Durville techniques; others were prepared in commercial foundries.

Additions of aluminium to 90/10 copper-nickel were investigated first followed by examination of the Cu-Ni-Fe-Al alloy and the quinary alloy containing manganese, in sequence. Compositions are given in Table 1.

Electron microscope, microprobe analyser and stereoscan techniques were used for structural examination in addition to conventional metallography. Qualitative microprobe results were obtained using X-ray photographs, semiquantitative results by line scans and quantitative analysis by comparative methods. Appropriate correction procedure was applied (3) (4).

(ii) Corrosion tests.

Self corrosion rates, crevice corrosion susceptibilities and galvanic compatibilities were determined on specimens 3" x 1" x $^{3}/_{16}$" immersed in Langstone Harbour. Specimens were clamped in Perspex jigs to simulate crevice conditions and others galvanically coupled to 90/10 and 70/30 copper-nickel. Jet impingement resistance was assessed using a modified Brownsdon-Bannister test (5) (6) best regarded as a sorting test giving comparative results on alloys tested at the same time. Stress corrosion resistance was assessed using constant load 'Unisteel' machines modified to make use of an available 'once through' sea-water supply at the Exposure Trials Station, Eastney, Portsmouth. Tensile type specimens used for preliminary tests had a $^{1}/_{80}$th sq in cross-section area. Specimens with $^{1}/_{40}$th sq in cross-section area were used for later tests, this size being easier to machine. Some welded specimens were tested using specimens machined from castings welded using Hiduron 191 as a filter wire.

3. Results

(i) Cu-Ni-Al. An alloy with 10% nickel and 2.5% aluminium (Cast 125-Table 1) was solution treated at 900°C for 1 hour, water quenched and precipitation hardened at temperatures between 500°C - 700°C; maximum hardening occurred after 1 hour at 650°C. Mechanical properties assessment of Cast 125 in the 'as cast'; solution treated and fully heat-treated conditions showed that optimum properties of 37.5 tons/sq in tensile (578 MN/m^2) and 10.5% elongation occurred in the 'as cast' condition. Microstructure consisted of cored nickel-rich dendrites and additionally, in the fully heat-treated material, a globular grain boundary precipitate. Microprobe analysis indicated this precipitate to be $Ni Al_3$.

(ii) Cu-Ni-Fe-Al. Nominal additions of 1% and 5% iron lead to a small reduction in strength and a noticeable increase in ductility both in 'as cast' and heat-treated conditions. As with the ternary alloy, optimum properties occurred in the 'as cast' condition. The increase in ductility was related to the iron content, the 1% iron alloy (Cast 126) giving 14% elongation in the 'as cast' state and the 5% iron alloy (Cast 127) showing 24.5%; the respective reductions in area being 20% and 25%.

Microprobe examination showed that iron was concentrated in the nickel rich dendrites. Carbon replica examination revealed a cuboid phase in the dendrites (Figure 1) and electron diffraction of an extracted region indicated a cubic lattice, a = 3.6 Å, corresponding to γ Fe + Ni.

Further quaternary alloys were made and examination of their properties showed that a simple ageing treatment of 4 hours at 550°C to be better than the full solution heat-treatment. This resulted in a slight increase in strength and a corresponding reduction

in ductility. The presence of the cuboid phase was noted in all casts; its distribution and size was not changed by heat-treatment. The lattice parameter was determined and confirms the suggested γ Fe + Ni phase reported by Dewey (1) and Dennis(2).

(iii) Cu-Ni-Mn-Fe-Al. The known commercial practice of adding chromium to the alloy as a grain refiner was repeated in the first experimental quinary alloys until its possible adverse effects were observed; this has been reported elsewhere (7).

The first series of quinary alloys were chill cast with variations in manganese and aluminium content. The properties of Cast No 7 (Table 2) demonstrated the considerable effect of aluminium content and Casts A1, A2 and A3 were prepared to examine its influence further. Examination of the mechanical properties (Table 2) show that increase in aluminium has a proportional effect upon strength. The properties in general reflect the benificial effect of chill casting. Further alloys, Casts 134, 135 and 136, were cast in sand moulds and show properties (Table 3) more typical of those expected from actual foundry castings.

Optical examination of cast 134 showed 'stringers' of a needle shaped phase present in interdendritic regions; some needles had broadened out to become diamond shaped flakes (Figure 2). Electron diffraction indicated the phase to be a nickel-aluminide with a composition approximating to Ni Al or $Ni_2 Al_3$; positive identification was not possible and no evidence was seen of the globular $Ni Al_3$ noted in the ternary alloy. The small phase noted in Figure 2 is the γ Fe+ Ni seen in the earlier alloys. The needle phase developed in size and quantity with heat-treatment (Figure 3) and was noted in further castings, for example in the Foundry cast plate, Cast 143, and again developing with heat-treatment. A thin foil from this cast also showed evidence of strain fields around unresolved precipitates (Figure 4). This was the only evidence which indicated the presence of a fine, sub-microscopic, precipitate. A second feature of Figure 4 is the areas where the cuboid γ Fe + Ni phase has fallen from the foil during specimen preparation. The cubes were strongly orientated in this cast and many others. Commercial vacuum cast No 7203 contained orientated cubes in addition to a stubby elongated nickel-aluminide phase in the grain boundaries Figure 5 and diamond shaped flakes in the interdendritic areas (Figure 6).

(iv) Corrosion test results.

Crevice and general corrosion specimens, from the alloys listed in Table 2, were examined after 1 year sea-immersion. The weight losses for the plain specimens are reported in Table 4. Crevice specimens were free from attack in the crevice area but some attack had occurred just outside the crevice area on a number of specimens (Figure 7, right hand specimen). This effect was also noted on a plain specimen (Figure 7, left hand specimen) just outside the area around the bolt hole which had been covered with a Tufnol insulator which in itself forms a crevice. Microscopic examination of a corroded area showed slight 'coppering' but this was not extensive.

Galvanic corrosion. Alloys L21, L25, E217 and E218 (experimental casts of a commercial alloy (8)) were coupled to 90/10 and 70/30 copper-nickel. Corrosion losses after one year immersion are included in Table 4; weight losses for the 90/10 and 70/30 alloys are not given in the Table but were similar to those for the alloys to which they were coupled.

Jet-impingement test results of the alloys used both for the plain/crevice tests and the galvanic tests are also reported in Table 4.

Preliminary stress-corrosion tests to determine suitable stress levels for further work were carried out on welded and unwelded specimens from Cast 38 at a stress level of 95% of 0.1% proof stress (19 tons/sq in). The welded specimens failed after periods ranging from 2209 hours to 3651 hours. Only one unwelded specimen failed and that after 3673 hours. Failure in the welded specimens occurred in the parent material approximately 0.25" away from the filter material following necking on either side of the weld.

Transcrystaline corrosion was prominent along the length of the parent metal. Figure 8 shows a typical transcrystaline crack propagating normal to the applied stress with branching secondary cracks. Further stress-corrosion tests were carried out on unwelded specimens of Cast 143, Cast DGS and Cast 7203. These materials represented a range of qualities; from low grade (Cast 143 which was contaminated with an embrittling iron-silicide phase), to typical commercial quality (Cast DGS) and high quality vacuum cast (7203). Specimens of the latter were subjected to between 75% and 120% of 0.1% proof stress. No failures had occurred after 6100 hours. Cast DGS was exposed at stresses ranging from 85% to 120% of 0.1% proof stress. Failure occurred after 4,600 hours at the highest stress level and metallographic examination showed numerous small, predominently transcrystaline, stress-corrosion cracks. No failures at the lower stress levels (110% of proof stress and below).

The poor quality material, Cast 143, was stressed at levels from 75% to 110% of proof stress. No failures occurred at the 75% and 85% stress levels after 6,800 hours; the remainder failed after periods varying upon stress level and the results are given in Table 5.

4. Discussion

(i) Alloy structure. Jones, Pfeil and Griffiths (9) indicated that 2.0-2.5% aluminium would provide optimum hardening of a copper -10% nickel alloy and this formed the basis of Cast 125. The ternary system is of little practical interest because of its low ductility (10.5% in 'as cast' condition) although the hardening mechanism after full heat-treatment would be expected to occur in the more complex alloys. The addition of iron results in a significant improvement in ductility and this contrasts with the observation by Weldon (10) that iron has little influence upon the mechanical properties of cupro-nickel although Weldon was discussing aluminium-free cupro-nickel with iron contents of 1-2%. It is apparent that 5% iron in the quaternary system will double the ductility obtained in the ternary system. This increase is due to the formation of the γ Fe + Ni cuboid phase which removes nickel from solution. It is significant that the increase in ductility is only accompanied by a small decrease in strength thus indicating that the cuboids assist in strengthening the matrix and compensate for the reduction in nickel content. In order to be effective as a hardening precipitate, the cube spacing would need to be in the region of 100 Å in order to interfere with dislocation movement. The nickel-aluminide phase was also present in the quaternary alloys.

The structure of the quinary alloys consisted of the γ Fe + Ni phase and various forms of the nickel-aluminide phase. This sometimes occurred in the form of needles or diamond flakes (Figure 6) although Cast 7203 also showed the stubby nickel-aluminide phase (Figure 5). Although it is possible that this latter phase is some intermediate stage between globular and needle forms of a nickel-aluminide complex a more probable explanation is that the grain boundary has moved and the globular nickel aluminide has acted as a nuclei for further nickel-aluminide precipitation. Thus the elongated, stubby phase is located between the original and final grain boundary positions.

The stability of the Fe + Ni cubes present in the quaternary and quinary was a constant feature, being unaffected by any of the heat-treatments. The alignment of the cubes was consistant with the findings of Butler and Thomas (11) regarding the spinodal decomposition of ternary Cu-Ni-Fe alloys. The lattice parameter (3.6 Å) confirms the observation of Dewey (1) that the phase is γ Fe + Ni.

Although the alloy is a precipitation hardening system and amenable to solution and ageing treatment some increase in strength can be achieved by a single heat treatment. The 'as cast' properties would be more satisfactory for general requirements.

(ii) Corrosion tests. The weight losses on the plain specimens reported in Table 4 are favourable for cupro-nickels, variations from specimen to specimen being within normal scatter. The alloy does not suffer attack within crevice areas but is susceptible to slight attack adjacent to crevices. The degree of corrosion on the specimens coupled to 90/10 and 70/30 cupro-nickel was comparable to that on uncoupled material and there would thus be no danger of galvanic corrosion if castings of the alloy were to be built into a

cupro-nickel sea-water system. The results of the Brownsdon-Bannister impingement tests were very favourable and May-type tests carried out independently by British Non-Ferrous Metals Research Association gave similar results (12). In service the quinary alloy should perform at least as well as conventional cupro-nickels.

The stress-corrosion tests were designed to obtain an assessment of susceptibility and establish confidence in the use of the alloy in practice. The choise of stresses was arbitrary but was considerably in excess of those found in service. The 'once through' sea-water facility avoided possible metallic ion contamination effects. Low susceptibility to stress-corrosion was established on all alloys and whilst the immunity of cast 7203 at stresses up to 120% proof after 6000 hours might reflect the quality resulting from vacuum melting, the good performance of commercial cast DCS and the fair performance of poor quality material, 143, endorse the opinion that stress-corrosion susceptibility is very low.

5. Conclusions

The structure of the cast quinary alloy consists of a cored copper-nickel solid solution containing a stable β Fe + Ni cuboid phase which contributes some strength and a nickel aluminide which considerably increases matrix strength. The alloy has good resistance to jet-impingement attack, crevice corrosion and stress-corrosion and no significant galvanic corrosion occurs when coupled to conventional cupro-nickels. The self corrosion rate is low.

It is considered that an alloy within the composition limits 10-13% Ni, 7-8% Mn, 4-6% Fe, 2-2½% Al balance Cu, in the 'as cast' condition is suitable for marine applications where medium to high strength is required.

Acknowledgments: This paper is published by permission of the Ministry of Defence although the views expressed are those of the authors. The authors wish to express their thanks to the Ministry and to colleagues who gave helpful advice.

References

1. M A P DEWEY, Fulmer Research Insitute. Report No E5397/1/1966.

2. P DENNIS, Aeon Laboratories Report No 460/8/11 (1966).

3. J ADLER and J GOLDSTEIN, U S Nat Aeronaut Space Admin Note D02984-1965.

4. S J B REED, Brit J Appl Phys 1965, 16, 913.

5. W H BROWNSDON and L C BANNISTER, J Inst Metals 1932 (49) 123.

6. B N HALL, Corrosion 1964, (20), 12, 379.

7. B N HALL and R A FARRAR J Inst Metals. 1969, (97), 190.

8. Langley Alloys Ltd.

9. D G JONES, L B PFEIL and W T GRIFFITHS, J Inst Metals. 1933(52), 139.

10. B A WELDON. Castings in Copper-Nickel Alloys. Foundry Symposium Dusseldorf April '67.

11. E P BUTLER and G THOMAS Acta Met 1970 (18) pp 347-365.

12. V CARTER, Private communication.

CAST IDENTIFICATION	Ni %	Al %	Fe %	Mn %	Cr %	OTHERS %	Cu %
125	9.98	2.45	0.05	-	-	-	BAL
126	9.98	2.26	1.14	-	-	-	BAL
127	9.14	2.38	5.26	-	-	-	BAL
2	11.78	1.86	5.95	1.95	0.45	-	BAL
4	11.78	2.04	5.95	4.07	0.48	-	BAL
5	11.86	2.00	6.14	4.87	0.45	-	BAL
6	11.75	2.00	6.00	5.79	0.45	-	BAL
7	10.64	1.02	6.14	7.02	0.70	-	BAL
8	11.89	2.00	6.09	7.88	0.49	-	BAL
10	12.04	2.12	6.15	9.66	0.30	-	BAL
A1	11.63	1.57	5.86	5.43	0.45	-	BAL
A2	11.60	2.36	6.00	5.45	0.25	-	BAL
A3	11.52	2.89	6.15	5.32	0.49	-	BAL
134	12.61	2.80	4.69	6.97	-	-	BAL
135	12.40	2.82	4.94	6.97	0.28	-	BAL
136	12.43	2.19	6.05	6.53	0.18	0.14 Sn	BAL
143	10.87	2.55	6.27	8.73	-	(0.13 Si 0.008 S)	BAL
7203	12.38	2.46	5.42	7.18	-	-	BAL
L21	11.60	1.93	4.46	5.00	0.50	-	BAL
L24	11.60	1.80	5.97	5.00	-	-	BAL
E217	10.80	1.53	4.37	2.95	0.17	-	BAL
E218	14.65	1.94	8.35	4.60	0.13	-	BAL
38	12.60	2.13	4.80	10.20	0.61	-	BAL
DGS	14.75	2.10	4.95	9.98	0.05	0.029 C 0.032 Si	BAL

Table 1 Composition of Alloys.

CAST NO	Mn %	Al %	TS MN/m^2	TS TONS/SQ IN	ELONG %	RA%
2	1.95	1.86	646	42.0	19	20
4	4.07	2.04	646	42.0	20	25
5	4.86	2.0	639	41.5	22½	25
6	5.79	2.0	646	42.0	25½	25
7	7.02	1.02	508	33.0	34½	50
8	7.88	2.0	554	36.0	18½	22½
10	9.66	2.12	616	40.0	24½	22½
A1	5.43	1.57	495	32.2	20	23
A2	5.44	2.36	622	40.4	27	30
A3	5.32	2.89	640	41.6	20	23

Table 2 Mechanical Properties of Chill Cast Cu-Ni-Mn-Fe-Al Alloys with varying Mn & Al contents. HT 1 hour at 550°C.

CAST NO	CONDITION	TS MN/m^2	TS TONS/SQ IN	ELONG %	RA %
134	AS CAST 4 HOURS AT 550°C	497 554	32.25 36.0	24 11½	25 12½
135	AS CAST 4 HOURS AT 550°C	592 592	38.5 38.5	24½ 9½	24 8
136	AS CAST 4 HOURS AT 550°C	473 504	30.75 32.75	28½ 16	30 22½

Table 3 Mechanical Properties of Sand Cast Cu-Ni-Mn-Fe-Al Alloys.

CAST NO	2	4	5	6	7	8	10	A1	A2	A3	L 21	L 45	E 217	E 218
General attack mdd	3.4	5.2	2.1	1.5	1.0	0.15	2.7	1.2	1.2	0	-	-	-	-
Impingement attack (mils)	3.0	1.75	3.0	1.5	3.5	1.0	2.0	5.75	1.5	1.75	1.1	1.0	1.75	1.25
Coupled to 90/10 mdd	-	-	-	-	-	-	-	-	-	-	4.8	4.0	1.7	4.9
Coupled to 70/30 mdd	-	-	-	-	-	-	-	-	-	-	3.3	1.0	1.6	4.4

Table 4 Results of Impingement, General and Galvanic Corrosion Tests.

% PROOF STRESS	TIME TO FAIL (HOURS)
75	Removed, unbroken after 6800
85	Removed, unbroken after 6800
85	Removed, unbroken after 6800
90	3738
90	575
95	455
95	479
100	215
100	335
110	192

Table 5 Endurance of low grade material to stress-corrosion failure.



Figure 1. Fe-Ni cubes in dendritic region of Cast 127.

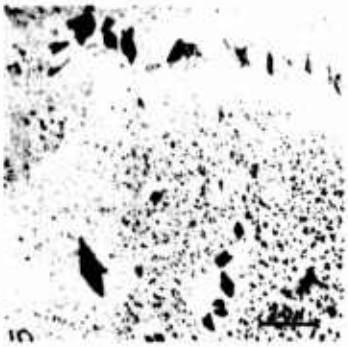


Figure 2. Nickel-aluminide needles and flakes in interdendritic region of Cast 134.



Figure 3. Nickel-aluminide needles in Cast 134 after heat-treatment at 550°C.



Figure 4. Thin foil of Cast 143.



Figure 5. Elongated nickel-aluminide phase in grain boundary. Cast 7203.



Figure 6. Diamond shaped flakes in interdendritic region. Cast 7203.



Figure 7. Plain and crevice corrosion specimens after 1 year immersion.



Figure 8. Transcrystaline crack on stress-corrosion specimen.

Corrosion Behavior of Copper-Base Alloys with Respect to Seawater Velocity

Robert J. Ferrara and John P. Gudas

Naval Ship Research and Development Center
Annapolis Laboratory
Annapolis, Maryland 21402

Interest in the corrosion behavior of metals over an expanding realm of sea-water velocity has been generated in response to the requirements of high-performance marine vehicles and associated subsystems. Historically, sea-water velocity corrosion testing has been conducted at discrete velocities within a relatively narrow range (2-45 feet per second). Efforts to expand this range to include velocities up to 120 feet per second have resulted in new approaches and a reassessment of available test techniques. This investigation deals with the behavior of copper-nickel alloys in the velocity range 9-120 feet per second. Four different test techniques were employed, including two rotating specimen tests, one impingement, and one multivelocity jet test. Results indicate the importance of third element additions to copper-nickel alloys to improve their resistance to corrosion-erosion and impingement damage. Secondary corrosion modes are also shown to significantly effect evaluation of velocity behavior.

Key Words: Copper-nickel alloys; corrosion-erosion testing; high velocity tests.

---

1. Introduction

Present design requirements for machinery and piping systems place emphasis upon resistance to corrosion and mechanical shock damage as well as the lightest weight possible, consistent with good design. The effects of sea-water corrosion and corrosion-erosion are particularly critical as evidenced by the present sea-water velocity limit of 15 fps for piping systems. (1) [1] To develop better alloys for present machinery and piping systems as well as to respond to future requirements of high-performance marine vehicles and associated subsystems, corrosion studies have been carried out with respect to the effects of sea-water velocity. (2-5) Historically, sea-water velocity testing has been conducted at discrete intervals within a relatively narrow range. Efforts to expand this range to include velocities in excess of 120 fps have resulted in new approaches and a reassessment of available test techniques. This investigation deals with the behavior of eight copper-nickel alloys tested in the velocity range of 9-120 fps. The results of three test techniques, including two rotating specimen tests and one impingement test, which have been employed extensively in past programs are presented and compared with those obtained in a new multivelocity jet test. Characterization of sea-water corrosion-erosion behavior of alloys tested is carried out with respect to both test

---

[1] Figures in parentheses indicate the literature references at the end of this paper.

technique and metallurgical variables. Correlation and applicability of the multivelocity jet test data is discussed with respect to the complete test program.

2. Material Description

Seven copper-nickel alloys and pure copper were tested in this investigation. Table 1 presents the chemical composition and conditions of each alloy tested. The list of alloys includes many candidates for seawater piping systems. Furthermore, this group of alloys represents a broad sampling of alloy content and composition.

3. Investigation

As has been stated, this investigation involves four test techniques. Not all alloys were tested completely, but a representative sample of complete test series does exist.

Multivelocity Jet Test

The jet test was designed to extend the range of test velocities to 100 fps and beyond. The test was originally conceived to produce high velocity flow past a stationary specimen mounted in a nylon nozzle. (5) The main advantage of this test is the fact that the velocity of water over the specimen surface can be controlled and measured with considerable precision. Originally, the high velocity jet tests were carried out at the singular test velocity of 120 fps relative to the specimen. This design was subsequently modified to enable multivelocity tests to be performed simultaneously. By varying the orifice size of each nozzle the range of available test velocities was changed to include 9.5 to 51.5 fps. Figure 1 is a schematic of the modified nozzle and specimen assembly. This program included tests carried out with both high velocity and multivelocity setups. Test duration in all cases was 30 days.

Rotating Disk Test

This test procedure consists of a series of specimen bars mounted on a disk which can be rotated in a tank full of sea water. The controls in this test include sea-water velocity, depth, and temperature. Flat bar specimens are attached to Micarta disks using insulated fasteners. Figure 2 is a description of the disk and test specimen assembly for this test. For this study, the specimens were tested in the range 26.3-28.9 fps outer tip velocity for 60 days. Corrosion rate was determined from weight-loss calculations.

BNFMRA[2] Impingement Test

This test consists of an aerated sea-water jet impinging on a stationary specimen which is totally immersed in sea water. The controls for this test include jet velocity, sea-water temperature, and oxygen content of the jet. For purposes of this study, the tests were run for 60 days with a peak jet velocity of 25 fps. The air content of the sea water was maintained at 3%. The specimens for this test consist of bars which are attached to a holder a fixed distance from the nozzle of the jet. Figure 3 is a drawing of the impingement jet and specimen holder for the BNFMRA jet impingement test. Both weight loss and depth of attack at the nozzle were determined from each test.

---

[2] BNFMRA - British Nonferrous Metals Research Association.

Rotating Spindle Test

The rotating spindle test consists of specimens in the form of disks mounted on and insulated from a spindle which is rotated in a tank of sea water. Clean sea water flowed continuously through the tank during the tests. There was no vortex around the spindle and the sea water remained free from entrained bubbles. The velocity achieved at the periphery of the specimens ranged from 24-26 fps, and the tests were run for 60 days. Figure 4 is a drawing of the rotating spindle specimen.

4. Results and Discussion

The results of the multivelocity jet tests and high velocity jet tests are plotted in figure 5. In examining this figure, it is seen that four alloys, CA 706, CA 719, CA 716 and pure copper exhibit excellent resistance to corrosion-erosion attack over the entire range of test velocities. Figure 6 indicates the slight degree of surface erosion damage which is typical of these alloys. The remaining alloys show generally higher corrosion rates at lower test velocities, and undergo significant corrosion-erosion damage as the high velocity limit is reached. Figure 7 shows general surface erosion which occurred with CA 715. As is seen, a reasonable degree of damage occurred at all test velocities. It must be noted in analyzing the results of the jet tests that these data describe resistance to corrosion-erosion attack caused by highly aerated seawater flowing over a smooth surface. Modes of attack such as impingement and cavitation have been essentially eliminated. Furthermore, only negligible crevice corrosion attack occurred at support points thereby minimizing that type of secondary mode uncertainty in corrosion rate determination.

Figure 8 presents the results of the rotating disk tests. It is seen that at the single test velocity, CA 716, CA 719 and 60/40 Cu-Ni showed superior resistance to corrosion-erosion damage. Typically, damage occurred by accelerated erosion at the leading edges and at the line of intersection of the mounting bracket and specimen surface. In figure 9, CA 719 is shown to suffer slight but observable edge and surface erosion whereas CA 717 displayed more severe local and overall surface degredation. In observing the 60/40 Cu-Ni specimens, it is seen that although surface erosion was negligible, moderate crevice attack took place when the specimen is attached to the disk. This test was seen to promote complicated secondary corrosion modes to a significantly greater degree than the jet tests.

Figure 10 presents the results of the BNFMRA jet impingement tests with respect to both weight loss and depth of attack criteria. The latter is the most applicable for this strict impingement test mode. CA 716, CA 719 and 60/40 Cu-Ni again display superior resistance to this type of attack. However, copper and CA 706 show reduced resistance as compared to the corrosion-erosion modes while CA 715 and 70/30 Cu-Ni (Low Fe) are consistantly poor in performance. Figure 11 shows typical specimens after completion of the jet impingement test.

The results of the rotating spindle tests presented in figure 12 indicate some agreement with other erosion type tests. However, the poor resistance of pure copper and good resistance of CA 715 to this mode of erosion attack does not agree with previously described results.

The analysis of results from the four test series of high velocity corrosion tests reflects many of the variables of this type of testing. Factors such as flow conditions, velocity range, degree of turbulence, seawater oxygen content, length of test and existance of velocity gradients directly effect modes and severity of attack. Furthermore, these factors strictly limit the description of corrosion behavior. However, certain conclusions can be drawn from this compilation of test results. The beneficial effects of iron additions on the corrosion-erosion behavior of copper-nickel

alloys is illustrated by the superior behavior of 60/40 Cu-Ni, CA 716 and to some extent, CA 706. In reviewing table 1, it is seen that these alloys have from 3 to 10 times the iron content of CA 715. It has been shown that both CA 715 and 70/30 Cu-Ni (Low Fe) display relatively poor resistance to corrosion-erosion and impingement attack. The beneficial effects of chromium additions are illustrated by the superior corrosion behavior of this alloy in all test modes. Beryllium additions made to copper-nickel alloys to promote precipitation strengthening appear to be detrimental from a corrosion standpoint.

The interpretation of the results from all of these tests is, as stated earlier, complicated by the variables introduced by each test format. The results have shown that alloys which exhibit superior resistance to corrosion-erosion attack in, for example, the jet tests, do not strictly or necessarily reflect this behavior in other test modes. However, the multivelocity jet test is seen to possess advantages of severity, applicability and accuracy over other corrosion-erosion test modes. The ranges of available test velocity, control of parameters and minimal introduction of secondary modes of corrosion are seen to be distinctly advantageous. The possibility further exists of incorporating cavitation damage into this format with simple specimen modification. However, application of the results presented here should be limited to situation where corrosion-erosion predominates and should not be projected directly to situations where turbulence, impingement, velocity gradients and/or cavitation contributes significantly to flow conditions.

5. Conclusions

The following conclusions may be reached from results derived in this program:

- o Additions of third element iron or chromium enhances resistance of Cu-Ni alloys to corrosion-erosion and impingement damage independent of level of nickel content.

- o CA 716 (solution annealed) CA 719 and 60/40 Cu-Ni show superior resistance to corrosion-erosion and impingement over the velocity range 9-120 feet per second.

- o The multivelocity jet test possesses significant advantages of severity, accuracy, and applicability when considering susceptibility to corrosion-erosion. The evaluation of test results should be done on the basis of corrosion-erosion phenomenon, and should not be projected to situations where impingement, velocity gradient, and/or cavitation are produced by flow conditions.

6. References

1. "Piping Systems," NAVSHIPS Tech Manual, Ch. 9840, (Mar 1970).

2. LaQue, F.L., and J.R. Mason, Jr., "The Behavior of Iron Modified 70-30 Cupro-Nickel Alloy in Salt Water and in Some Petroleum-Industry Environments," Paper presented to a Corrosion Session during the 15th Mid-Year Meeting of the American Petroleum Institute's Division of Refining, Cleveland, Ohio, (2 May 1950).

3. Stewart, W.C., and F.L. LaQue, "Corrosion Resisting Characteristics of Iron and Modified 90:10 Cupro Nickel Alloy," Corrosion, Vol. 8, pp. 259-277 (Auf 1952).

4. LaQue, F.L., "Corrosion Resistance of Cupro Nickel Alloys Containing 10-30 Percent Nickel," paper presented at the 10th Annual Conference, National Association of Corrosion Engineers, Kansas City, Mo., (Mar 1954).

5. Danek, G.J., Jr., "The Effect of Sea Water Velocity on Corrosion Behavior of Metals," Naval Engineers Journal, (Oct 1966).

CHEMICAL COMPOSITION AND CONDITION OF ALLOYS TESTED

ALLOY	Cu	Ni	Fe	Mn	Cr	Be	Condition
Cu	99.95	-	0.05	-	-	-	UNKNOWN
CA706	87.60	10.62	1.45	0.44	-	-	HALF HARD
CA715	67.20	31.42	0.60	0.72	-	-	HOT ROLLED
CA716	64.1	29.59	5.38	0.08	-	-	SOLUTION ANNEALED
CA719	66.41	29.7	0.21	0.58	3.10	-	HOT ROLLED+ANNEALED
70/30 Cu-Ni (Low Fe)	68.96	30.02	0.06	0.44	-	-	UNKNOWN
60/40 Cu-Ni	54.98	42.36	2.19	1.35	-	-	DRAWN AND STRESS RELIEVED
CA717	65.56	32.55	0.75	0.55	-	0.58	SOLUTION ANNEALED AND AGED

Table 1

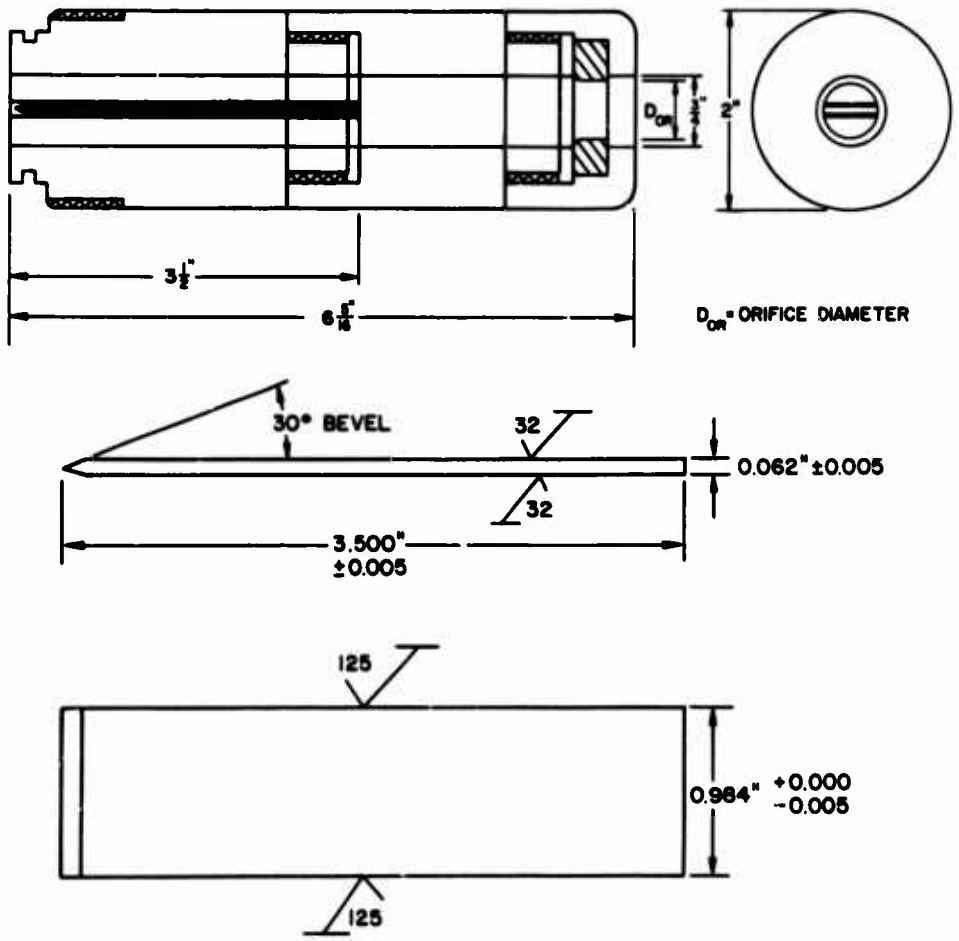


Figure 1.
Schematic of Multivelocity Jet Test Nozzle Assembly and Specimen Configuration.

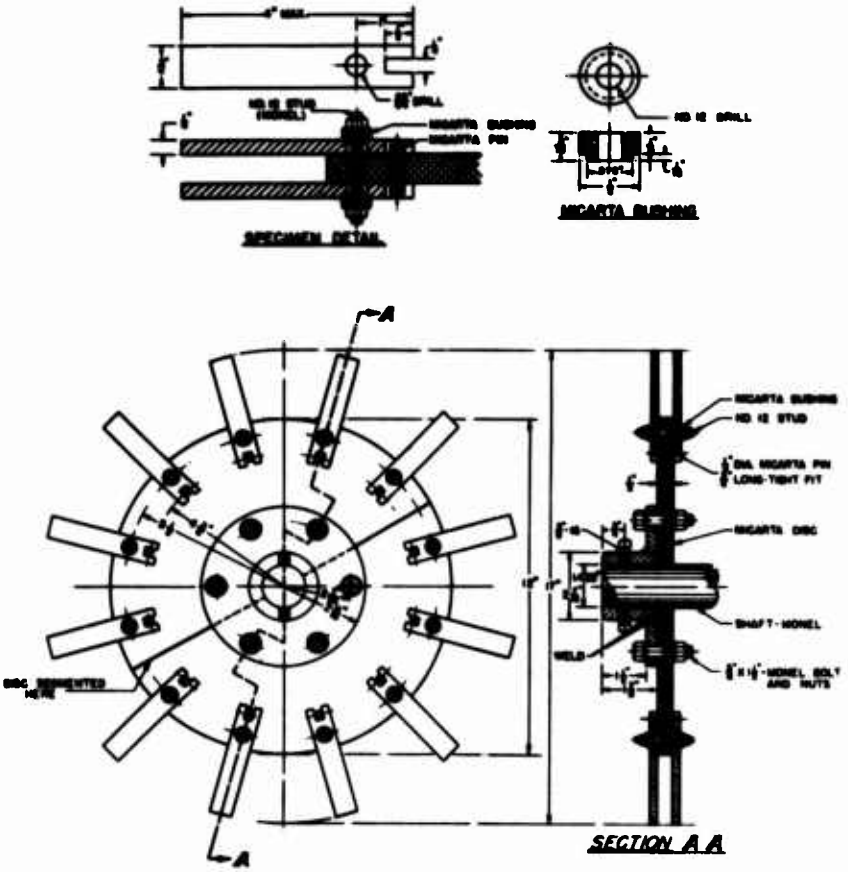


Figure 2
Micarta Disk and Test Specimen for
Rotating Disk Corrosion-Erosion Apparatus

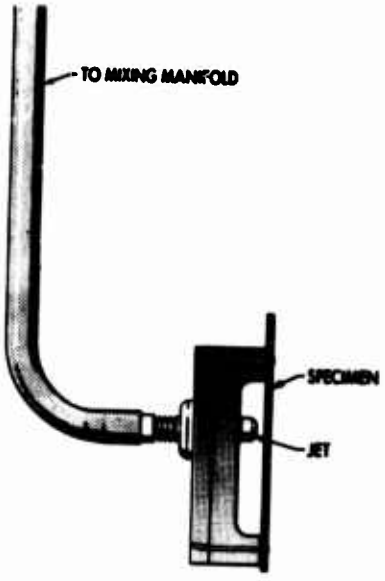


Figure 3
Impingement Jet and Specimen Holder
for BNFMRA Jet Test

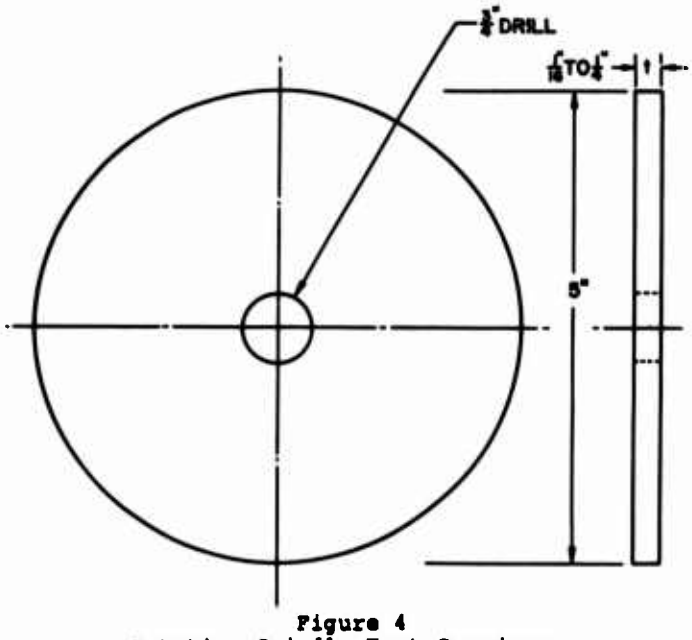


Figure 4
Rotating Spindle Test Specimen
Configuration

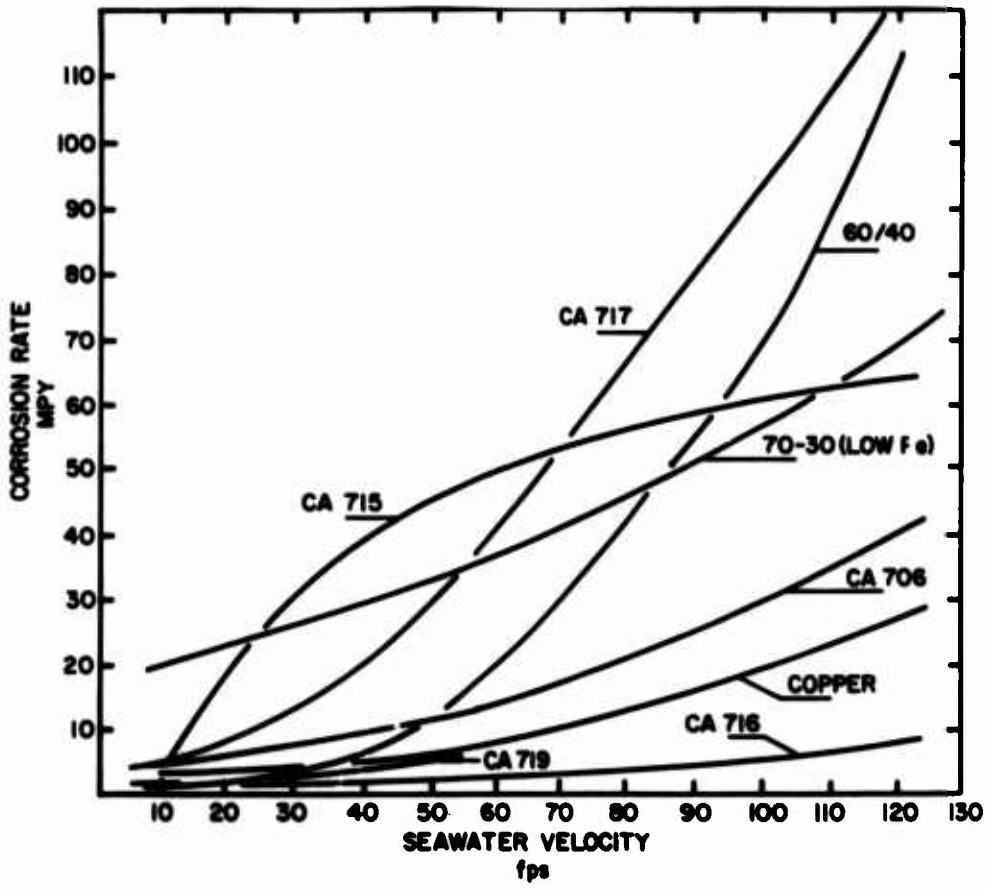
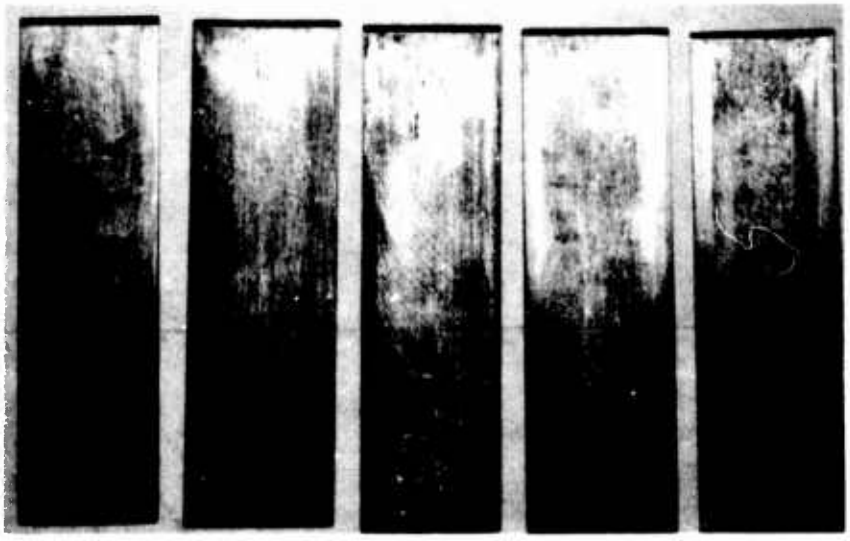


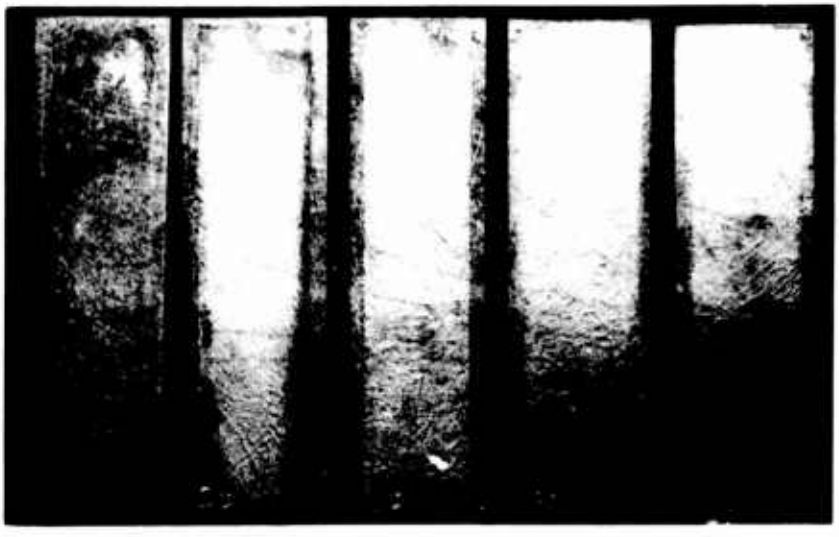
Figure 5
Results of Multivelocity and
High Velocity Jet Tests



9.5 16.9 26.3 38.0 51.5

VELOCITY, FPS

Figure 6
CA 716 (Solution Annealed) Specimens After Testing
in Multivelocity Jet Test Apparatus



9.5 16.9 26.3 38.0 51.5

VELOCITY, FPS

Figure 7
CA 715 Specimens After Testing in
Multivelocity Jet Test Apparatus

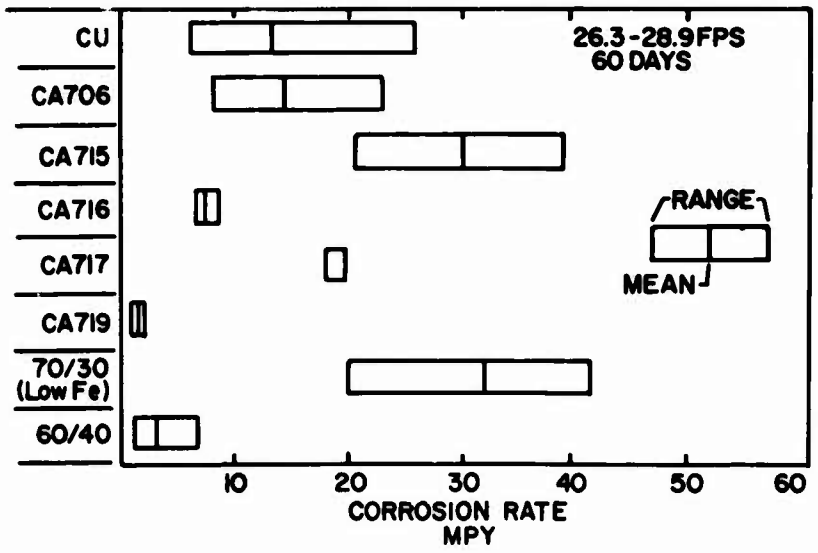


Figure 8
Results of Rotating Disk Tests



CA719 60/40 Cu-Ni CA717

Figure 9
Rotating Disk Specimens After Test

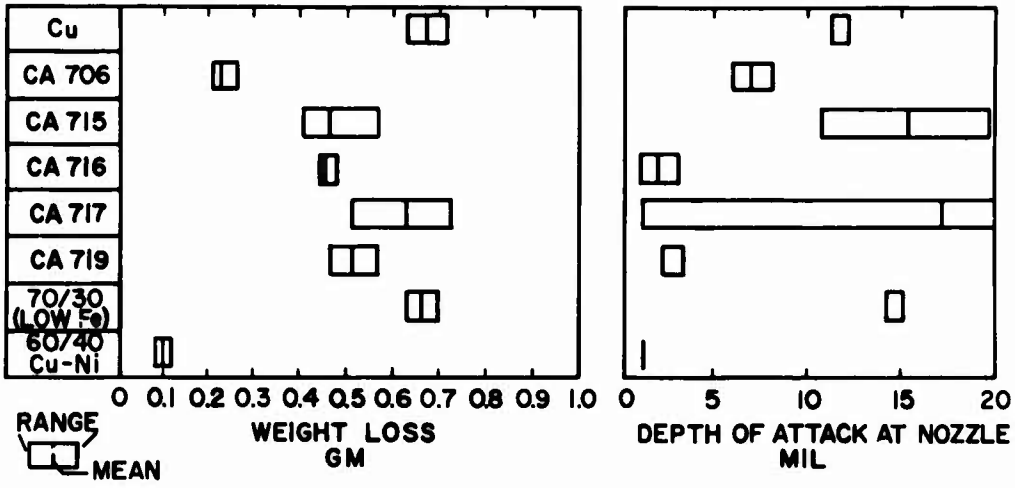


Figure 10
Results of BNFMRA Jet Impingement Tests

Surfaces Facing Jets Backsides

Item (a) - CA 706



Item (b) - CA 715



Figure 11
CA 706 and CA 715 BNFMRA Jet Impingement
Test Specimens After Test

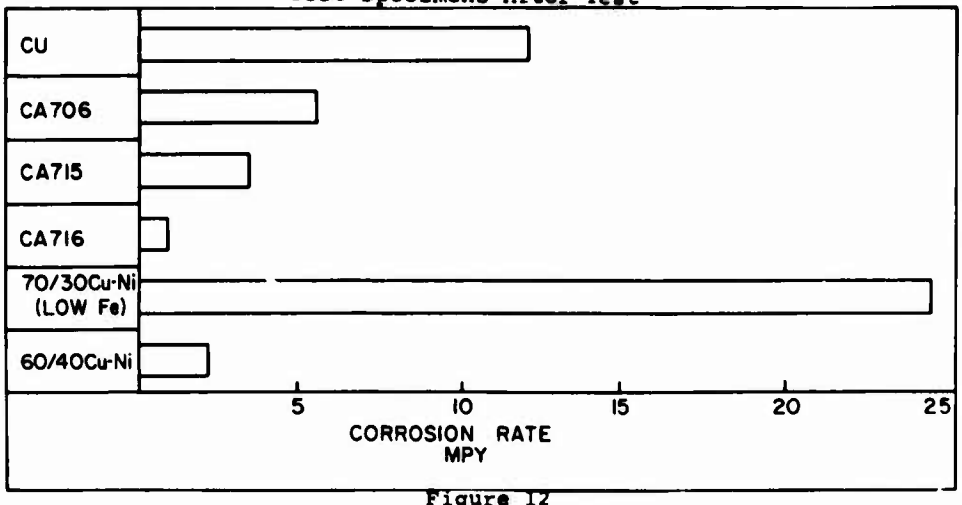


Figure 12
Results of Rotating Spindle Tests

Written Contribution by J. B. Cotton:

Mr. Campbell has already printed out the apparently anomalous low results obtained with copper as compared to those obtained with various types of cupro nickel. This is particularly noticeable when one compares the performance of copper with that of conventional 70/30 cupro nickel, CA 715 type, at the highest water speeds of 26 and 51 feet per second.

In the rotating spindle test and in the multivalent jet test at 9.5 feet per second, the order of merit more nearly accords with that expected from experience in service, although even in those tests the corrosion rate for copper is lower than would have been expected from service behaviour at more usual rates of flow. In any event one would normally have expected the performance of copper to have been inferior to almost any form of cupro nickel.

This departure of copper from the normally expected performance certainly requires some explanation and some further investigation and it should not be assumed that such results would never occur under service conditions at very high rates of flow, as the following example will demonstrate.

In 1957-8, the writer operated an experimental tube bundle (investigations at the former Metals Division of Imperial Chemical Industries) on once through flow of Brixham (Devon) sea water, at speeds of flow of 10 feet and 30 feet per second, the test condition at 30 feet per second being aggravated by the addition of 3% air. The tests ran for twelve months, virtually continuously, except for brief stoppages for maintenance of equipment--no stoppage being longer than five hours' duration. The tube dimensions in this test were 10 feet length, 0.5 ins outside diameter and 0.040 ins wall thickness.

At 10 feet per second, with no added air, copper performed as would be expected from known service behaviour, the tubes perforating (0.040 ins) within three feet from the inlet end in test periods that varied from six to fifty weeks. Cupro nickel CA 715 type suffered pitting only to a maximum depth of 0.0005 ins; 10% cupro nickel CA 705 type to a maximum depth of 0.020 ins; 2% aluminum brass suffered inlet end attack to a maximum depth of 0.021 ins while Admiralty Brass had virtually perforated.

At 30 feet per second, with 3% added air, the results were quite different. The maximum depths of attack on copper was 0.015 ins, that on CA 715 type cupro nickel was 0.012 ins, that on 705 type cupro nickel was 0.028 ins, that on Admiralty Brass 0.018 ins, while 2% aluminum brass had suffered highly localised perforation (0.040 ins).

The explanation for the apparent anomalous performance of these materials at very high speeds of flow appears to lie in the behaviour of the surface films. For cupro nickel and 2% aluminum brass tested at 30 feet per second, the surface films remained intact over more than 90% of the surface, the attack occurring in the form of very localised pitting, while for copper and Admiralty Brass there was much more overall removal of metal--the Admiralty Brass, for example, suffering from what was virtually a "carpet" of "horse shoe" type pits over the whole of its surface--but none of the pits penetrating more than two-fifths into the tube wall.

It is simple to postulate that results such as those for cupro nickel and 2% aluminum brass can be explained in terms of the establishment of electrochemical cells involving small anode at areas where the protective film has been only locally removed, the locally bared areas being coupled with a larger surrounding air-depolarised cathode. This needs to be confirmed by appropriate electrochemical investigations, and unfortunately, at the time the tests were made there was no opportunity of doing that.

Summarized Discussion

In reply to questions, the authors stated that the water in their experiments was recirculated, that there was no control over turbidity, that the surface roughness of the specimens was controlled at 30 rms, but that metallurgical features such as grain size were not controlled. There was general agreement that the performance of copper in the authors' tests was different from its performance in structural components and flow rate conditions commonly met in practice.

A Review of Corrosion Resistant Alloy Developments and Recent Marine Corrosion Studies in the United Kingdom Ministry of Defence

J. F. G. Condé, G. C. Booth, J. C. Rowlands and B. Angell

Admiralty Materials Laboratory
Holton Heath, Poole, Dorset, BH16 6JU, UK

Recent research on materials for marine engineering purposes has been aimed at improved reliability and reduced life cycle costs. Electrochemical studies of selective phase corrosion and other alloy development work have led to improved materials including two new precipitation hardened cupro-nickel alloys with 0.1% proof stress levels of 286 MN/m^2 and 463 MN/m^2. A static beam type fracture test has shown promise of discriminating between alloys in terms of their likely resistance to shock loading in service. The use of clad overlays on steel provides an alternative technique for achieving higher strength components, eliminating certain corrosion problems and reducing costs. Large scale pipe system experiments have been used to investigate the influence of hydrodynamic factors on corrosion-erosion of copper alloys and the mechanism of inpingement attack on condenser tube inlets has been studied electrochemically. An instrument for monitoring corrosion test electrodes has been developed and several techniques for detecting the incidence of impingement attack are being examined. A simple portable eddy current instrument for inspecting heat-exchanger tubing in-situ has been built and is being evaluated.

Key Words: marine corrosion; copper alloys; cladding impingement; cavitation; stress corrosion; electrochemistry; corrosion testing; corrosion monitoring; non-destructive testing.

---

1. Introduction

Recent research and development on copper based alloys and other materials for marine engineering purposes has been oriented towards achievement of maximum reliability and lowest life cycle costs in seawater systems and propulsion machinery in Naval vessels. This research on both the basic and technological levels has led in particular to a greater understanding of the corrosion behaviour and properties of copper base alloys. Escalation of the costs of alloying additions, such as nickel, which have a beneficial influence on marine corrosion resistance has led to interest in the development of precipitation hardened cast cupro-nickel alloys with 10 to 15% nickel in order to achieve high load carrying ability without increase in costs. An alternative approach to higher strength has been the use of clad steels. To prevent costly, adventitious failures, it has been necessary to consider possible techniques of corrosion monitoring and non-destructive testing of components in-situ.

2. Alloy Development

Studies have been aimed at improvement of resistance to certain specific forms of corrosion and also to achieving higher strengths without loss of weldability, toughness or corrosion resistance.

To obtain an understanding of the mechanism of preferential attack of individual phases in duplex alloys, electrochemical studies have been made on electrodes consisting of the individual phases of the copper-zinc, copper-tin and copper-aluminium systems. This work

has enabled prediction of the corrosion behaviour of more complex alloys with a larger number of metal components. In 90/10 aluminium-bronze the structure may be either $\alpha + \beta$ or $\alpha + \gamma 2$ according to heat-treatment. The α and β phases are of nearly equal potential when in seawater the beta being slightly anodic, but with the $\alpha + \gamma 2$ structure the $\gamma 2$ is significantly anodic by approximately 250 mV(1)[1]. It was known that the addition of up to 3% manganese prevented the formation of the $\gamma 2$ phase, but this results in the β phase becoming considerably less noble and consequently preferential attack of the β phase occurs. However, additions of silicon do not have this effect and a very successful aluminium-silicon-bronze (6 Al/2.2 Si/1 Fe/remainder Cu) has been developed(2). The nomenclature of the phases in this alloy being $\alpha + \kappa$ (Figure 1). This alloy has been used in both the wrought and cast forms with considerable success, it is readily welded, but there are limitations on mechanical properties (0.1% proof, 170 MN/m^2 (11 tonf/in^2)), tensile strength 525 MN/m^2 (34 tonf/in^2), elongation 36%), and the resistance to impingement attack is slightly inferior to 90/10 aluminium-bronze. With manganese addition to the 90/10 aluminium-bronze the resultant selective phase corrosion of the β phase is considerably slower than the corrosion of the $\gamma 2$ phase in the 90/10 alloy. For higher strength castings nickel-aluminium-bronze is now extensively used, and is essentially to British Standard 1400AB2C , with a restricted chemical composition, Al 8.5-10.0/Fe 4.0-5.5/Pb 0.02 max. This alloy has an $\alpha + \beta$ structure with varying forms of the κ phase. The κ phase is more noble than the alpha phase, and consequently selective attack of the alpha phase can occur when a lamellar kappa phase is present in a semi-continuous form, but this results in pitting which is readily observed visually. Selective attack in the 90/10 type aluminium-bronzes occurs with re-precipitation of copper retaining the original form and shape of the material, but with negligible mechanical strength. This latter form of corrosion is very dangerous by virtue of being largely undetectable both visually and by non-destructive testing using ultrasonic and eddy current techniques. A similar examination has been carried out on the higher strength alloy to BS1400CMA1 (Mn 13/Al 8/Fe 3/Ni 3/remainder Cu), which is an $\alpha + \beta$ alloy with very attractive mechanical properties, especially with respect to ductility where it is superior to most high strength copper-base casting alloys. Unfortunately, unless this alloy is cathodically protected, it is highly susceptible to selective phase corrosion of the β phase, especially under crevice conditions. The rate of attack is very dependent on the heat-treatment which the material has received, and it has been shown that heat-treatment at 600°C reduces the rate of corrosion. Commercial developments of this alloy with tin additions produced a marked improvement in reducing selective phase corrosion with some slight loss in mechanical properties, but rates of attack of the β phase have been reduced to about 0.3 mm/year as opposed to up to 4 mm/year with the tin free alloy. The variable corrosion behaviour of the tin free alloy was attributed to the variation in nickel distribution between the α and β phases according to the thermal history of the material.

Corrosion trials are frequently undertaken in conjunction with the alloy developers. Currently the main interest is centred around improvement in mechanical properties of the cupro-nickel alloys based on 70/30 and 90/10 compositions, whilst maintaining their excellent corrosion performance. The presence of iron and to a lesser extent manganese, in the cupro-nickels to obtain resistance to impingement attack is well known. However, a recent development(3) has been the replacement of iron with chromium, the wrought alloy being designated IN732 (30% Ni, 2% Cr, remainder Cu). Typical mechanical properties are:- 0.2% proof stress 372 MN/m^2 (24.1 tonf/in^2), tensile strength 607 MN/m^2 (39.3 tonf/in^2), elongation 30%. AML experience along with other potential user trials is that this material is very promising, but an unusual corrosion characteristic was found in that one sample had significant impingement attack on the leading edge where it was exposed under full immersion conditions in a flowing tide. Metallographic examination showed that this attack was associated with a precipitate in the grain boundary, which has not been positively identified but is possibly zirconium nitride, but there was evidence to suggest that the working of this particular sample was inadequate to break down the cast structure.

As noted above, a nickel-aluminium-bronze, broadly similar to BS1400 AB2C, is employed for high strength castings where shock resistance is a criterion. Experience has shown

[1]Figures in parentheses indicate the literature references at the end of this paper.

that whilst gunmetal and nickel aluminium-bronze have comparable Charpy Vee notch or Izod impact properties (13.5-27 J (10-20 ft.lb)), gunmetal has inferior shock resistance because its yield and fracture stresses are much lower than those of aluminium-bronze. If notched bar impact properties are relevant to shock resistance it is apparent that improvement can be obtained by increasing the yield strength at the same impact level or by increasing the impact value at the same yield level. To explore both of these possible approaches, research has been sponsored by AML into alloys based on a cupro-nickel matrix which has inherently greater toughness than the copper-aluminium matrix of the BS1400AB 2C type of alloy. The two approaches to alloy development were based on a nickel content of less than 15% to facilitate foundry production by the use of conventional non-ferrous melting practice. A further constraint on the development was that the alloys should have no undesirable skin forming properties to avoid casting problems, should be readily castable, weldable and possess adequate resistance to marine corrosion. It was essential that the alloys should be weldable to enable repair of defective castings and to permit greater versatility by ensuring that components of complex geometry and/or large size which might be difficult to make sound as a single casting could be fabricated by welding together a number of smaller sound castings of simple shape.

Two alloys have been developed which substantially match the target property levels. The lower strength alloy is a silicon-niobium hardened cupro-nickel with typically 10% Ni, 1.0% Mn, 1.5% Fe, 0.4% Si, 0.4% Nb, remainder copper, and has typical mechanical properties of 0.1% proof stress 286 MN/m^2 (18.5 $tonf/in^2$), tensile strength 420 MN/m^2 (27.5 $tonf/in^2$), elongation 21% and Izod 45J (33 ft. lb). The high strength alloy has a preferred composition of 12.5% Ni, 10-12% Mn, 5-7% Fe, which yields mechanical properties of 0.1% proof stress 463 MN/m^2 (30 $tonf/in^2$), tensile strength 664 MN/m^2 (43 $tonf/in^2$), elongation 13% and Izod 16J (12 ft. lb). Both alloys are precipitation hardened, the lower strength alloy achieving its properties during natural cooling in a 25 mm thick section in a sand mould. The high strength alloy depends on the presence of iron and/or manganese to form ordered precipitates which act as strong barriers to dislocation movement under stress[4]. The ordering reaction is advantageous in that casting and welding can be carried out prior to the hardening heat-treatment which involves heating at around 450°C for about 24 hours and thus avoids the quenching stresses and accompanying distortion which are associated with normal quenching and ageing methods. The use of beryllium as a hardening addition was discarded in view of the likely health hazard associated with melting beryllium containing alloys under conventional foundry conditions in the UK.

The silicon niobium alloy has good resistance to impingement attack as assessed by jet impingement tests with sea water in which it was compared with two 70/30 cupro-nickel alloys (CN107 and a low iron 70/30) and 90/10 cupro-nickel (CN102)[5] sea water exposure tests on the raft facility in Langstone Harbour are in progress and results will be available in the near future. Full scale tests in flowing sea water remain to be carried out in conjunction with larger scale foundry tests on the alloy. The weldability appears to be rather better than that of the 70/30 Si-Nb hardened high tensile cupro-nickel. The corrosion behaviour and weldability of the higher strength alloy remain to be assessed.

3. Toughness

Tests designed to assess the shock resistance of cast copper alloy components are expensive and produce results which do not identify separately the effects of the inherent shock toughness of the material per se, poor design or metallurgical defects. As noted earlier, impact values are not necessarily a reliable and discriminating guide to shock resistance. Thus effort has been devoted to an examination of alternative techniques for assessing this property in terms of some measurable parameter to enable new casting alloys to be compared with existing well characterised materials without recourse to empirical shock testing of components in the new material. A static fracture mechanics test similar to the procedure employed in studies of linear elastic fracture mechanics[6] has been found to give good discrimination. A three point notched and fatigue cracked bend test §0.8 x 25.4 mm (2 x 1 in) in cross section has been employed in a study at AML (Figure 2). In general copper base alloys are too ductile to provide valid K_{IC} values in small sections and fail by general yielding. The values obtained in tests on the specimens described are termed pseudo K_{IC} denoted by $\bar{K}_{IC}$. However the specimen does provide appreciable constraint at the tip of the sharp fatigue crack which supplies a realistic element in the test. The bending load to produce the first extension of the fatigue crack as detected by visual

observation of the flanks of the specimen, or by a sensitive potential difference technique, is some function of the fracture stress. Thus such a test combines features not simultaneously present in conventional impact tests and is considered realistic in spite of the pseudo nature of the parameter which is measured in the test. This parameter, K_{IC}, although somewhat artificial is found to be greater for larger specimens and has been shown to vary as $L^{0.6}$ where L is any linear dimension for geometrically similar specimens differing only in size. This relationship based on practical data is close to the value $L^{0.5}$ to be expected on theoretical grounds(7). Thus a small 50.8 x 25.4 mm (2 x 1 in) specimen provides pessimistic values in relation to the behaviour of thicker sections. Values of K_{IC} obtained for nickel-aluminium-bronze and gunmetal are 40 $MN.m^{-3/2}$ and 23 $MN.m^{-3/2}$ respectively. Values obtained on silicon, niobium hardened, high tensile 70/30 cupro-nickel are appreciably higher than for nickel-aluminium-bronze. The proprietary casting alloy Hiduron 501(8) (14% Ni, 5% Fe, 10% Mn, 2% Al, remainder copper) which has a 0.1% proof stress of 293 MN/m^2 (19 tonf/in^2) and an Izod value of 47.5 J (35 ft.lb) and the newly-developed 90/10 cupro-nickel alloy hardened with silicon and niobium both give values comparable with nickel aluminium-bronze.

None of the materials considered would be expected to show any pronounced strain rate effects associated with the higher rates of strain in shock loading as compared with static loading at low rates of strain but to establish that this is a valid assumption further tests are planned at higher rates of strain employing a pneumatic loaded bend test facility.

4. Metal Cladding

For specific components where the mechanical properties of steel are required and protection with organic coatings is not practical, cladding with various copper base alloys has been investigated. Further considerations have been the need to economise in the use of expensive copper base alloys in thick sections and the desire to improve the corrosion protection of inaccessible components such as sea tubes where painting is not effective.

Sea tubes, which are the inlets and discharges to seawater systems from a ship's hull are normally considered as part of the steel hull, and fabricated accordingly in steel. Some sea tubes are of a very complex shape, and others of small diameter, making access for appropriate abrasive blasting of the surface and protection with paint systems very difficult. For a number of years an alternative system has been to galvanise these pipes, but the life of such protection can be rather limited, due to bimetallic corrosion. A more effective and viable system is to line the sea tubes either with a weld overlay to give a "fusion clad" surface, or "skin clad" tubes with a thin alloy liner welded at intervals to the base steel pipe. The skin cladding may be formed in-situ by explosive forming. For this application the advantage is that the resultant corrosion from the bimetallic system is brought on to the steel hull, where it is readily observed at refits and measures can be taken for adequate surface preparation and application of high duty coatings. Thus the non-ferrous seawater system is effectively continued through to the ship's hull. The metal cladding technique has been considered for a number of other applications, including flash chambers of pre-multi-stage flash distillation plant, heat-exchanger tube plates and water boxes. Laboratory trials are currently in hand to determine the effects of cyclic pressurisation of "skin clad" tubes to assess any resultant disruption of the clad layer and possible corrosion-fatigue of the ply welds. In the same trial the performance of fusion clad, skin clad and explosively bonded cupro-nickel alloys to a steel are being assessed for resistance to water flows of 4.5 m/sec. Certain details of the welding and fabrication techniques have already been published and further information is to be published shortly(9,10). As the metal cladding techniques have been considered principally for systems subjected to flowing seawater, the prime consideration has been the use of 70/30 or 90/10 cupro-nickels, but both fusion and clad welding techniques can be used with other copper-base alloys such as nickel-aluminium-bronze.

5. Corrosion/Erosion Studies on Cupro-Nickel Alloys

Seawater systems in HM Ships have for many years been constructed from cupro-nickel alloys containing optimum levels of iron and manganese to improve resistance to impingement corrosion. The 5% cupro-nickel alloy is prone to impingement corrosion where flow velocities exceed about 2 m/sec and the superior resistance of the 10% and 30% nickel alloys has been demonstrated in service by the rare instances of failure since their introduction. However, tests have shown that these cupro-nickels can suffer impingement corrosion and

cavitation attack under adverse hydrodynamic conditions produced for example by increases in velocity, the use of short radius bends to conserve space, misalignment of flanges, etc. To study these effects large scale, long term pipe system experiments are carried out at the Admiralty Materials Laboratory[11]. A typical pipe and components test system in shown in Figure 3.

Experiments are in progress to determine the operating limits of cupro-nickels in seawater systems. Situations under examination include sharp bends and branches, pipe bore misalignment at flanged joints and the effects of pressure reducing and flow control devices. The "once-through" seawater facility at Portland Harbour[11] is being used to study the effect of 1, 2 and 3D bends and "T" branches on 10% cupro-nickel. Sub-systems having bores of 38, 76 and 127 mm are being employed to investigate size effect. The flow velocity in these experiments is 4.5 m/sec. AML experiments have shown that flange joints displaced by up to 3.2 mm produced no significant attack in straight pipe runs of 10% and 30% cupro-nickel in 5000 hours at 3 m/sec. The behaviour of the 10% cupro-nickel alloy with 2 mm and 4 mm misalignments at 4.5 m/sec and two distinct line pressures is now being examined. Flange misalignment combined with 1 and 2D bends is also being studied using five identical 38 mm bore sub-systems operating at 3 m/sec.

6. Hydrodynamic Characterisation

A study of the turbulence patterns associated with a pipe bend of radius 1.5 times the bore was undertaken at AML following an experiment in which impingement corrosion attack to a depth equivalent to 10% of the pipe wall thickness occurred with 10% cupro-nickel. The bend was constructed within a transparent block and the paths of plastic visualiser particles were observed, using an interrupted light source. This work was terminated prematurely but sufficient data were obtained to conclude that this technique combined with quantitative hydrodynamic measurements held considerable promise as a method of characterising pipework components known to produce potentially damaging turbulence patterns. Experimental evidence to date indicates that data of this nature combined with electrochemical studies are required if significant progress is to be made in explaining the complex mechanisms involved. A research is being sponsored in which the hydrodynamic characteristics of four common pipework situations will be investigated in a transparent recirculating loop of 50 mm bore[12]. Initial work will be carried out on simple orifice plates having an area ratio (d^2/D^2) of 0.36. This will be followed by the examination of a sharp bend ($\frac{R}{D} = 1.0$), a flange connection with 2 mm misalignment and a diaphragm control valve. The orifice plate was chosen to develop the characterisation method because more hydro-dynamic data are available for this device. Six identical sub-systems have been built at AML similar in geometry to the transparent loop and containing all four situations of interest so that the hydrodynamic conditions are reproduced as closely as possible. The effect of seawater velocities up to 5.5 m/sec is being assessed on the 5% and 10% cupro-nickel alloy test sections strategically placed downstream of the components mentioned earlier.

7. Electrochemical Examination of the Mechanism of Impingement Attack

The mechanism of impingement attack has been examined[13] using electrochemical techniques. Polarisation curves were determined for a model tube inlet (Figure 4) subjected to various water flows. The results showed that there was a significant change in the open circuit potential between the stagnant and turbulent flow conditions. This change could be attributed to the change of copper ion concentration, which would be significantly higher under static conditions than with flow, and therefore the metal would be more noble. However, from the slopes of the anodic polarisation curves under static and flowing conditions there is a change in gradient by a factor of two, indicating that under impingement conditions the metal dissolution process could be a single electron transfer (cuprous ion formed), whereas under static conditions it is a double electron transfer process (cupric ion formed). The flow in the model test system was examined using dye injection for flow visualisation and was found to be a very complex hydrodynamic situation which could not be simply represented in conventional flow equations. In the practical heat-exchanger situation, the actual rate of impingement attack will be determined by the extent to which the active or anodic site is polarised, which will in turn be dependent on the area of the surrounding cathode comprised of the water box and tube plate. Assuming a typical water box potential of about -0.20 V (SCE), the anodic current density required to polarise the

model tube inlet to the potential of -0.20 V was of a reasonable magnitude to explain the rate of attack experienced in practice. The anodic current densities required to polarise impinged tube inlets of copper, aluminium-brass and 70/30 (1% Fe) cupro-nickel were in the order expected from practical experience. Although this study was related to impingement attack at heat-exchanger tube inlets, the results are equally applicable to other hydrodynamic conditions in seawater pipe systems, such as misaligned flanges and sharp bends.

It is intended to examine the onset of impingement attack in relation to laminar sub-layer thickness; in these experiments, the laminar sub-layer thickness for water flow over a test electrode inserted in uniform flow conditions is determined by the bulk velocity, the wall friction factor and viscosity. The rates of impingement attack will be determined using a zero resistance ammeter connected between the test electrode subjected to high flow and a surrounding auxiliary electrode, not subjected to flow.

8. Corrosion/Erosion Resistance of Complex Copper Alloys

New materials are currently being developed to overcome problems in casting pump and valve bodies and to produce alloys with good mechanical properties combined with corrosion resistance. As part of the overall programme an assessment was required of the performance of high strength cupro-nickels and bronzes in the "as cast" condition and with simulated weld repair against seawater at varying levels of turbulence. This was accomplished by casting the materials of interest into pipes of 64 mm and 76 mm bore and 600 mm in length. The pipes, in the "as cast" condition were cut 100 mm and 410 mm from one end and butt welded together again with full penetration welds. The pipes were then bored out to the machined finish necessary for the observation of corrosion/erosion effects. Using a constrictive orifice plate (area ratio = 0.36) at the upstream (datum) end, the two welds were placed strategically in two distinct zones of turbulence. At the nominal bulk velocity of 4.6 m/sec the first weld and the adjacent heat-affected area were subjected to a high speed (15 m/sec) stream of mildly cavitating seawater, whilst the second experienced a decreasing velocity gradient as the flow returned to the bulk velocity. The results of the 5000 hour duration test showed that measurable wastage attack was produced on a cupro-nickel containing 17% Ni, 5% Mn, 2% Al, 0.8% Fe, and a high strength 30% Ni alloy containing 1.2% Nb + Ta, 0.3% Si. Silicon-aluminium-bronze (6% Al, 2% Si), and nickel-aluminium-bronze (BS1400 AB2) also suffered this type of attack in addition to the 30% Ni alloy used as a control. Under the conditions of this test the cupro-nickel had greater resistance than the silicon-aluminium-bronze but less than the nickel-aluminium-bronze. The welded areas were not significantly attacked with the exception of those in the high strength cupro-nickel in which isolated pitted regions were visible.

In order to assess the cavitation resistance of these alloys, 25.4 mm diameter bars were subjected to 100 hours exposure in the AML cavitation damage tunnel. This is a Venturi type flow test where the specimen is centrally located at the minimum cross section where the water flow reaches 35 m/sec and cavitation damage occurs on the downstream face. This is a more severe cavitating condition than the test described previously in that corrosion has little influence on the weight loss and damage is entirely as a result of mechanical forces. The results of this experiment showed that the cupro-nickels were less resistant than the bronzes as might be expected and the latter were comparable in their resistance. This result confirms earlier cavitation work on these alloys[11].

9. Corrosion Monitoring and NDT of Heat-Exchanger Tubes

At present the occurrence of impingement attack is rather unpredictable and the possibility of detecting its occurrence as it occurs in seawater systems is being investigated. One possible technique being explored is the use of Hall probes, which are semi-conductor devices, which give an output voltage when placed in a magnetic field. If sufficient sensitivity can be achieved for a portable instrument, such devices could be used to detect the anode to cathode current flowing in the metallic path of the electrochemical cell between the impingement site anode and surrounding cathode. The order of field strength required to be detected is 10^{-4} gauss, which will require effective screening of the probe to eliminate stray magnetic fields. With simulated cells and a commercial gauss meter, and utilising the Hall probes, as would be expected the field strength falls off inversely as the distance squared from the surface of the pipe, and the field decreases proportionally to the distance from the anode site.

Failures of aluminium brass heat-exchanger tube and pipe systems caused by sulphide pollution due to fitting out new construction ships in polluted estuarine waters, have been overcome by intermittent injection of an inhibitor, sodium dimethyldithiocarbamate (SDD), into the seawater system. Difficulties in regulating the frequency of inhibitor injection to avoid excessive over treatment were overcome using polarisation resistance measurements. For this purpose, a corrosion meter (Figure 5), operating on an alternating current low frequency (10 Hz) square wave signal technique, has been developed[15]. Electrode probes are positioned at representative positions in the seawater system and the corrosion rate is determined daily. When the inhibitor film begins to break down, an increase in corrosion rate is observed and the system is redosed with inhibitor. The corrosion meter can also be employed for assessing the "corrosivity" of particular aqueous environments to individual alloys by making the test electrode of the material for which corrosion rate data are required.

A conventional steam turbine warship would have two main condensers and some 30-40 auxiliary heat-exchangers. Once a failure of a heat-exchanger tube in the stack has occurred the NDT requirement is essentially to determine which tubes are likely to fail before the next refit, so that the offending tubes can be plugged and the required life obtained without further attention. Most heat-exchanger failures are attributed to impingement attack at the tube inlets which can be detected visually. However, other failures due to impingement do occur along the length of the tube caused by partial blockage with either foreign matter or marine biological fouling. For instances such as this and attack due to steam impingement, or hot spot corrosion, there is a requirement for a simple eddy current instrument to determine the location and extent of attack. Commercial instruments for this purpose are available, but they are sophisticated electronic instruments which require very specialised use and extensive training of operators. To overcome this problem a simple portable instrument operating on conventional eddy current techniques has been developed. The eddy current inspection of heat-exchanger tubes is carried out by passing a sensing probe along the length of the tube. For simple one-man operation the probe cable is threaded through a length of nylon tubing reinforcement rigidly fixed to the probe so that the probe can be readily moved in and out of the tube. The probe containing two coils is fed with an AC current signal which induces eddy currents in the tube wall. At a defect the eddy current field is disturbed, putting an AC bridge containing the two probe coils out of balance. This out of balance signal is then amplified for display on a meter or lamp read-out system. The depth of eddy current penetration of the tube wall is determined by the frequency of the signal fed into the probe. In order to avoid detecting baffles and support plates an operating frequency of 1 MHz is required for aluminium-brass and cupro-nickel tubes. Consequently, the sensitivity to steam impingement attack which occurs on the external surface of the tube is considerably reduced. A prototype instrument is shown in Figure 6. The electronic circuitry has been reduced to the minimum, using integrated circuit techniques, and it is powered by dry cells, giving a total instrument weight of 3.3 kg.

10. Concluding Remarks

Within the scope of this paper it has been possible to present only a cursory account of certain aspects of the broadly based and on-going programme of marine corrosion studies in the United Kingdom Ministry of Defence of which those relating to copper base alloys form an important element. The objective of achieving reliability in service and reducing through life costing is a challenging one which is gradually being attained. The application of the complementary approaches of basic electrochemistry and technological research has been found eminently suitable for the solution of short term service problems and for longer term research leading to improved materials and also more informed and effective application of existing and new materials in service.

11. Acknowledgments

This paper is published by permission of the Procurement Executive, Ministry of Defence, but the views expressed are those of the authors. The authors are indebted to Dr R G H Watson, Director, AML, for advice and encouragement and to Mr G Newcombe, of CDL, and Mr J M Short of AML for provision of certain previously unpublished data.

12. References

1. J. C. ROWLANDS, *Corr. Sci.* 2, 89 (1962).

2. B. UPTON, *Corrosion*, 19, 204t (1963).

3. F. A. BADIA, G. N. KERBY AND J. R. MIHALISIN, *Trans. ASM*, 60, 395 (1967).

4. G. B. BROOK, *Unpublished work, Fulmer Research Institute Ltd* (1971).

5. D. W. TOWNSEND, *Unpublished work, B.N.F.M.R.A.* (1971).

6. W. F. BROWN AND J. E. SHRAWLEY, *ASTM S.T.P.* 410 (1966).

7. J. M. SHORT, *Unpublished work, AMI* (1971).

8. P. GUHA, D. BROWN AND G. LITTLEWOOD, *International Conference on "Copper and Its Alloys", Amsterdam*, (1970).

9. J. N. BRADLEY AND G. NEWCOMBE, *International Conference on "Copper and Its Alloys", Amsterdam*, (1970).

10. G. NEWCOMBE, *To be published* (1972).

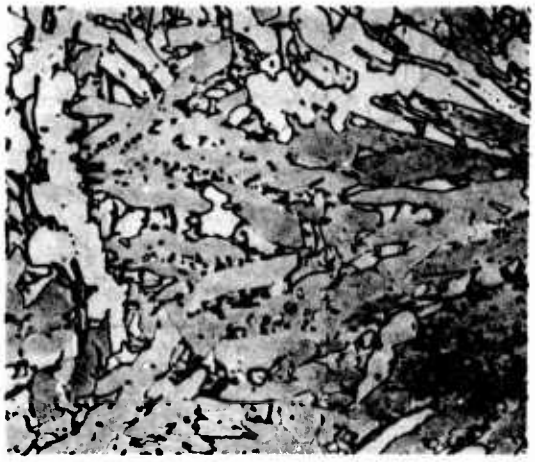
11. D. J. GODFREY, B. ANGELL AND A. F. TAYLOR, *International Conference on "Copper and Its Alloys", Amsterdam*, (1970).

12. S. P. HUTTON AND D. AU, *Unpublished Work, University of Southampton.*

13. J. C. ROWLANDS, *Proc. Localised Corrosion Conference, Williamsburg*, (1971).

14. J. C. ROWLANDS, *J. Appl. Chem.* 15, 57 (1965).

15. J. C. ROWLANDS AND M. N. BENTLEY, *Br. Corr. J.* 7, 42 (1972).



x 200

Figure 1. Microstructure of aluminium-silicon-bronze showing the alpha (dark) and kappa (light) phases.

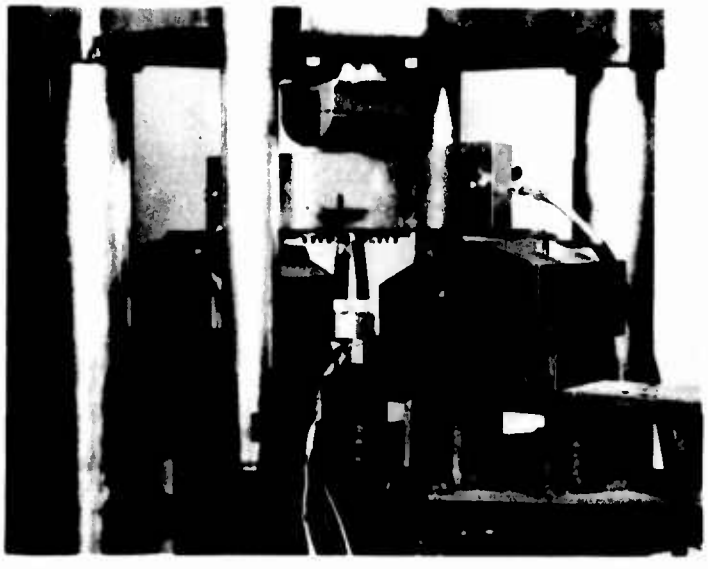


Figure 2. Fracture test on cast copper alloy specimen.

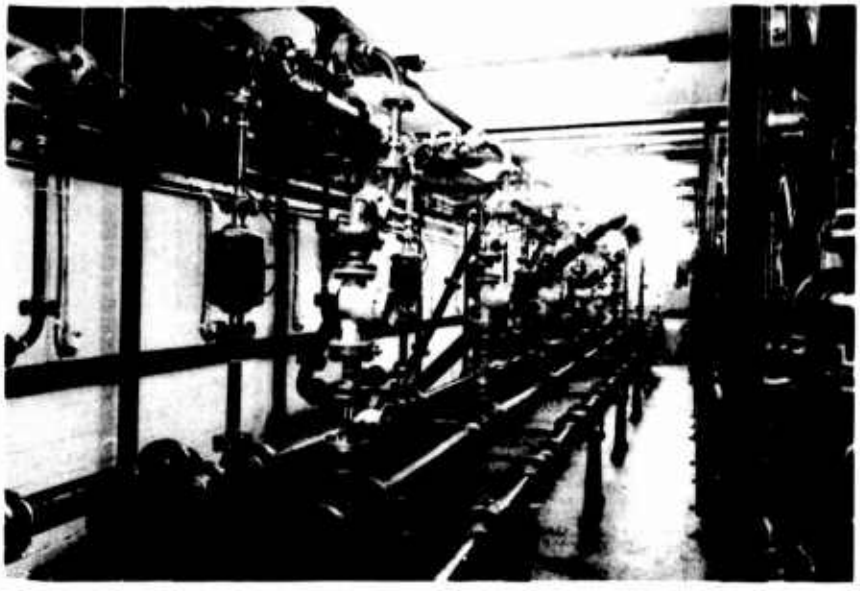


Figure 3. Typical seawater pipe and components test system.

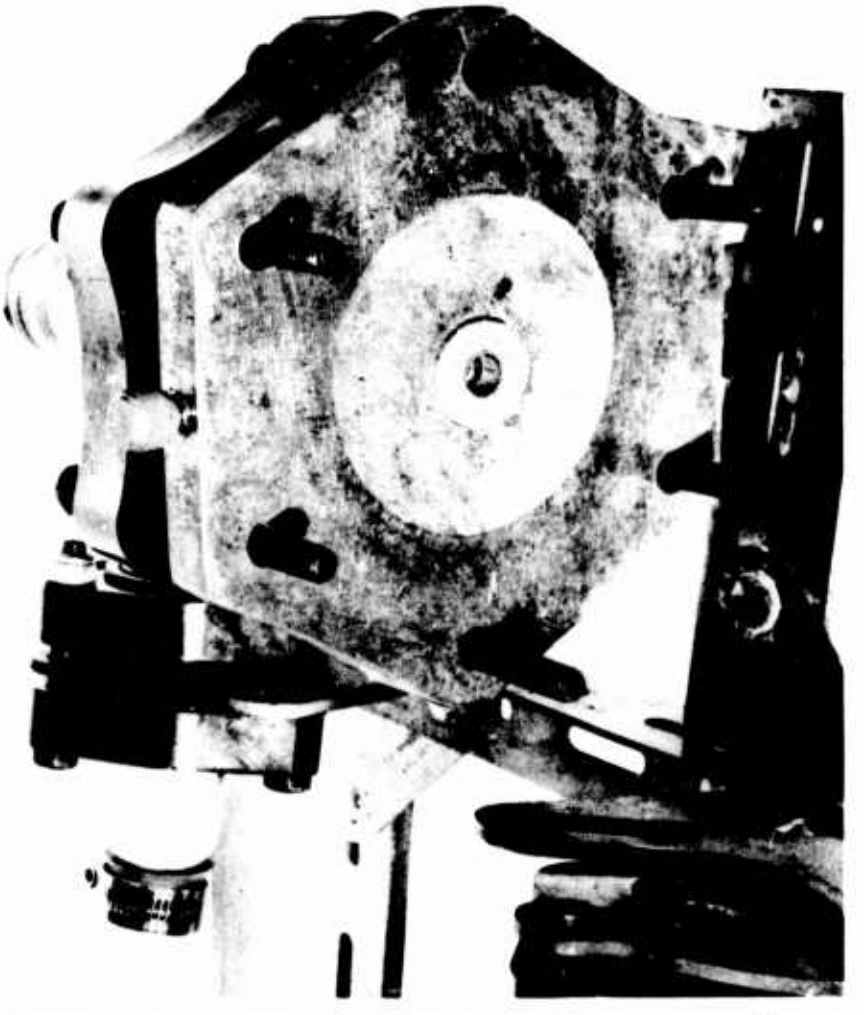


Figure 4. Model heat-exchanger tube inlet for electrochemical studies.

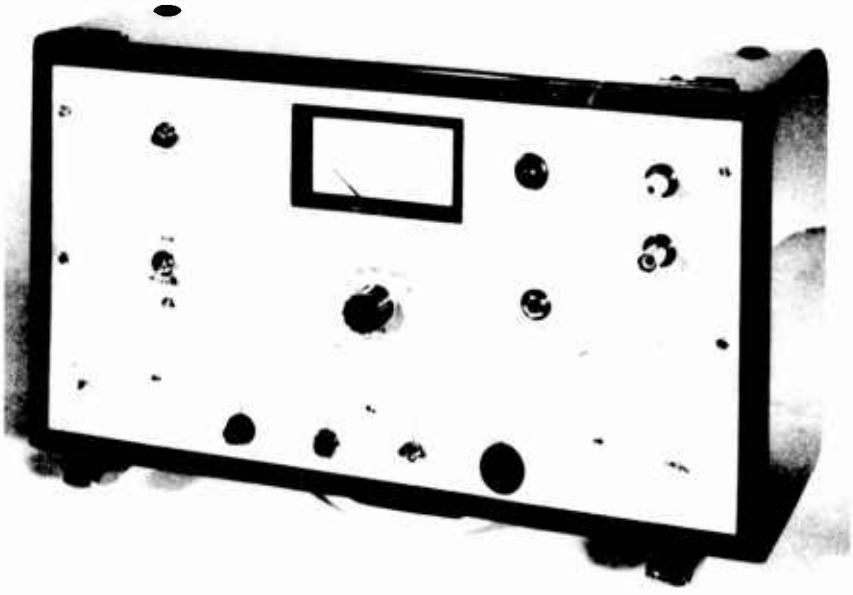


Figure 5. Corrosion meter



Figure 6. Eddy current heat-exchanger tube testing instrument.

No More Dezincification of Hot-Forging and Free-Cutting Brass.

The ENKOTAL* Principle

Dr. B. Lunn and M. Schmidt

A/S NKT
Copenhagen, Denmark

Dezincification of brass is a type of corrosion which occurs in chloride containing soft water supply and also sea water, especially when the waters are hot. The dissolved zinc leaves a porous copper sponge with no strength, causing breaks and leakage in the attacked brass part. In brass alloys used for sheet, tube and wire this process can be prevented by the addition of arsenic to the alloy, but in brasses used for hot-stamping and free-machining it has been impossible to prevent this type of corrosion, because they contain a structural element, beta crystal, which cannot be inhibited, as can the alpha crystal, which is the main structural element in the ductile brasses for sheet, tube and wire.

Many attempts have been made to improve the resistance to dezincification of the beta-containing brasses by the addition of alloying elements such as aluminum, silicon, manganese and tin, but the results are generally unsatisfactory with regard to resistance to dezincification, when good hot-stamping or free-cutting properties still are required.

The ENKOTAL principle is firstly to use a leaded brass of ordinary purity with a copper content slightly above that which is used in ordinary hot-stamping and free-cutting brasses. The copper content is kept within narrow limits, so that when the alloy is heated to the hot-stamping or extrusion temperature it contains adequate beta in the structure to make the hot material sufficiently ductile for the hot-stamping or extrusion operation. When cooled however some beta will still be left, which might corrode and make parts useless through dezincification.

Therefore, the second principle of ENKOTAL is to re-heat the extruded or hot-stamped part to a temperature lower than the hot-stamping or extrusion temperature, and keep it there for a sufficient length of time to break up the connection between the beta crystals in the structure rendering the remaining metal a homogeneous, continuous alpha structure, which, by its inhibition by arsenic, is resistant to dezincification. This heat-treatment has to be carried out in a rather narrow temperature and time interval.

The Properties of ENKOTAL

ENKOTAL is easy to hot-stamp into ordinary valve bodies, and the free-machining properties are good. The alloy is well suited for soft soldering, brazing and all common methods of surface-treatment such as plating, colouring, etc.

---

*ENKOTAL is a registered trademark of A/S NKT.

Heat-treated ENKOTAL has far greater resistance to dezincification. The same alloy without heat-treatment, is equal to all the many complex-brass alloys which have appeared during the last few years. ENKOTAL has been tested by a method published by the Swedish Authority, Planverket. It has been exposed to a very aggressive water supply used by the British Non-Ferrous Metals Research Association in their test procedure, and by a potentiostatic test developed by the Danish Corrosion Centre.

	Swedish test (metallographic examination)	Danish test (potentiostatic dissolution)	British test (metallographic examination)
	Depth of penetration	Z value *	Depth of penetration
ENKOTAL without heat-treatment	0,60 - 2,50 mm	1.4 - 1.8	0,40 - 2,20 mm
ENKOTAL properly heat-treated	0,02 - 0,20 mm	1.0	Nil

* $Z > 1.0$: Dezincification. $Z \leq 1.0$: No dezincification.

ENKOTAL has been developed during the last five-six years as NKT's answer to an increasing demand in Europe for a non-dezincifiable brass perfect for hot-stamping and free-machining.

Patent protection for the ENKOTAL principle is pending in several countries.



Fig. 1. Structure of ENKOTAL before heat treatment. Note stringers of ß-crystals in the direction of extrusion.



Fig. 2. Properly heat treated ENKOTAL. ß-crystals have been transformed to α-crystals.

CONDENSER TUBE TEST APPARATUS INCORPORATING IMPINGEMENT, CREVICE AND HEAT TRANSFER CONDITIONS

Hector S. Campbell

The British Non-Ferrous Metals Research Association
Euston Street, London, NW1 2EU, England

An apparatus is described for testing ten 200 mm lengths of condenser tube under conditions that include impingement, heat transfer, and crevices to stimulate shielded area attack. Details are given of the construction and operation of the apparatus and examples of its use. The apparatus is cheap to construct and easy to use. It can be installed on site to assist the selection of heat-exchanger tube materials, or to monitor seasonal changes in corrosivity of the cooling water. The information that it yields is much more comprehensive than is provided by any other existing apparatus for corrosion tests on condenser tubes and it is therefore particularly suitable also for assessing new materials or effects of surface condition arising from changes in methods of manufacture.

Key Words: Corrosion testing; condenser tubes; impingement; heat transfer; crevice corrosion; material selection.

1. Introduction

The method most commonly used for testing condenser tube materials is the May jet impingement test (1)[1] in which small strips, cut from the condenser tubes and abraded to a standard surface finish, are immersed in sea water and subjected to the effect of an underwater jet of sea water with air-bubbles in it. This is a good test for resistance to impingement attack and gives some incidental information on resistance to shielded area attack since ill-defined crevices exist between the specimen and the specimen holder. Resistance to impingement attack is also commonly assessed by the Brownsdon and Bannister test (2) in which a stream of air-bubbles is directed onto the surface of the test samples immersed in sea water or sodium chloride solution. Special tests for resistance to corrosion under localized heat transfer conditions (hot-spot corrosion tests) have been described - for example by Breckon and Gilbert (3) and by Bem and Campbell (4) - but temperature effects are usually ignored when comparing condenser tube materials.

To make valid comparisons between different condenser tube materials a test apparatus is required that will include all the principal corrosion hazards likely to be met by tubes in actual service:- impingement conditions, slow moving water conditions, heat transfer conditions and shielded area conditions. It is also important that it should use test pieces with the original "as manufactured" internal surface of the condenser tube intact. Breckon and Baines (5) have drawn attention to the deleterious effect of carbon films produced in heat exchanger tubes during manufacture and it is probable that other differences in surface condition may also effect corrosion resistance. Tubes may be supplied with the surface as-drawn and stress-relief annealed, pickled, abrasively cleaned or deliberately oxidized and it is desirable, therefore, to test them in the condition in

[1] Figures in parentheses indicate the literature references at the end of this paper.

which they are supplied and will be used in practice. An apparatus meeting these requirements has been constructed and its value proved in tests with a variety of condenser tube materials during the past two to three years. Details of the apparatus, its method of use and some examples of results obtained with it are given below.

2. Description of apparatus

The general arrangement of the apparatus is shown in Figure 1. It accommodates ten vertical 200 mm lengths of condenser tube spaced equally round a 125 mm diameter circle. Water enters the bottom of each tube through an inlet nozzle (Part No. 6 in Figure 1) which fits inside the tube and also locates it. The nozzle has a 5 mm diameter blind hole up the centre connecting with a 2.4 mm diameter hole, set at 45° to the vertical, through which the water emerges at a velocity of 10 metres per second to impinge on the wall of the tube. The water then rises up through the tube at a mean velocity of 0.1 metres per second (in a 1" or 22/24 mm condenser tube) and leaves through an outlet nozzle (Part No. 1) fitted into the top end of the tube. Half the length of each nozzle has a 2° taper on the outside to provide a reproducible annular crevice between it and the inside of the condenser tube. Neoprene 'O' rings (Part No. 3) provide seals between the tube and the top and bottom nozzles and the tubes are held in place by a common clamping plate (Part No. 2) at the top. The ten inlet nozzles are fed with water through a distributor (Part Nos. 7, 8, 15) of the design used in the May jet impingement apparatus, which ensures equal distribution of water between them. The distributor and nozzles are all of non-metallic materials. The part of each test piece between 40 and 65 mm from the top is fine-machined externally to fit a semi-circular notch in a 15 mm thick brass heater block (Part No. 4) - the tubes being held in contact with the block by a circumferential clip (not shown) to ensure efficient and equal heat transfer between the block and each tube. The diameter of the inlet and outlet nozzles and that of the semi-circular notches in the heater block are made to suit the size of condenser tube to be tested.

The heater block originally designed was fitted with electric heating elements on each side of it, but this quickly failed in the environment of continuous wet spray of the position in Asnaesvaerket power station in Denmark where the apparatus was installed and it was replaced by a steam heated block designed by the power station staff. The detailed construction of the heater block is shown in Figure 2. A 1.5 mm diameter vertical hole for a thermocouple was drilled in the block very close to the contact surface with one of the test tubes and the rate of passage of steam through the heater block was adjusted to give a temperature of 95°C at the thermocouple with the apparatus running. This arrangement worked well for about the first year of operation of the apparatus but after that time the particularly corrosive environment in which it was situated produced sufficient corrosion of the heat transfer surfaces of the notches in the heater block for significant differences of heat transfer conditions to develop between one tube and another. In later versions of the apparatus, installed at Kyndbyvaerket power station, the heater block was replaced by separate short heating jackets for each tube. The construction of the heating jacket is shown in Figure 3. The 'O' ring seals permit the jacket to be slipped over the tube. Oil, from a steam-heated heat exchanger, is circulated through the ten heating jackets in parallel, the outlet from each being fitted with a thermocouple and the inlet with an oil regulating valve which is adjusted to give an oil outlet temperature of 95°C. This heating arrangement, which was designed by the Danish power station staff, not only eliminated the corrosion effects that had been experienced with the heater block but also eliminated the necessity to machine part of the outside of the tubes.

The test rigs are run on a once-through system - the inlet being connected to the power station cooling water system and the outlet running to waste. A modification introduced into the later versions of the apparatus was to connect the tubes from the outlet nozzles to short lengths of metal pipe welded through the base of a cylindrical vessel with an outlet to waste at its centre. This makes it easy to check quickly that all ten test tubes are receiving their proper share of the incoming water by seeing that the height of the "fountain" at the top of each of the vertical outlet tubes is the same. Any blockage of the inlet nozzles can thus quickly be detected and rectified. This modification was introduced by the staff of Kyndbyvaerket power station.

3. Method of use

The 200 mm lengths of condenser tube forming the test pieces are cut off and the ends machined square with the axis of the tube; the lengths of all the test pieces must be the same within ± 0.1 mm. If the apparatus is the type with a heater block, a 25 mm length of the outside surface of the tube must be machined to fit the notches in the block - the dimensional tolerances being +0.00, -0.05 mm; if oil-filled heating jackets are being used this step is omitted. The samples are washed with acetone to remove any oily deposits but are not cleaned up in any other way. The apparatus is assembled and the rate of flow of water through it is adjusted to 25 litres per minute (total). The temperature of the heater block or the oil in the heating jackets is adjusted to 95°C and the apparatus is then left to run; the only attention that it requires is an occasional check that the water is flowing freely from all of the ten outlets and that the oil or heater block temperature is correct.

On the first two or three tests for which the apparatus was used the samples were taken off and cut up for examination after 4 weeks but it is generally better to run the test for 8 weeks. This gives more opportunity for the protective or partially protective films, that develop initially on the interior surface of the tubes, to thicken and blister if this is likely to occur in service with the particular combination of tube material and water concerned. For materials, such as titanium, which show a very high degree of resistance to corrosion the test can be run for longer periods.

At the end of the test period the tubes are cut open longitudinally for detailed examination. It is convenient when examining tubes from a test rig with a heater block to cut the tubes through first at their mid-point before slitting the two halves; this makes it easier to ensure that the cut does not run through the impingement area immediately opposite the incoming water jet nor through the heat transfer area that was in contact with the heater block. When examining tubes from a rig with oil-filled heating chambers the heat transfer area extends right round the tube and only the impingement area has to be avoided in slitting the tube for examination; there is therefore no need to cut it into two halves first.

A preliminary examination of the test pieces is made after slitting, with any deposits, etc. in situ, and the half-sections of tube then washed with water to remove loose deposits before more detailed examination. For recording the results four different areas are considered:- (a) the impingement area opposite the jet in the entry nozzle, where water velocity and turbulence are highest during the test; (b) the slow-moving cold water area extending from the impingement area up to the region where heat transfer occurs; (c) the heated area, including the heat transfer area itself and the warm water area above it; (d) the cold-water and hot-water crevices formed by the inlet and outlet nozzles. Assessment after washing off loose deposits is visual, using a low-power binocular microscope and looking particularly for impingement attack, pitting, and blistering or flaking of the corrosion product film. The tubes are next cleaned with cold 10% sulphuric acid and the depth of any impingement attack, pitting or other localized corrosion is recorded according to the area on the specimen on which it occurs.

4. Examples of use of the apparatus

The apparatus has been used for three purposes. The first is the selection of materials for condenser tubes to replace those in an existing condenser that have given unsatisfactory service, or for new condensers that are to be installed in the future. For these tests duplicate samples of five different materials, or materials with the same nominal composition but manufactured by different firms and with different internal surface conditions, have been tested in each run. The reproducibility of the results for the duplicate samples in any one run has been remarkably good. The materials on test have varied from run to run, though one or two standard materials have been included in every run as controls.

The second use made of the apparatus is to monitor changes in the corrosive characteristics of the cooling water at one site throughout the year. For such tests only

results for standard condenser tube materials are required and the same materials must obviously be included in every run. In practice it has proved possible to derive information on changes in the corrosive nature of the cooling water from examination of the control samples of standard alloys included in the runs made to compare different condenser tube materials. Where there are known to be, or are likely to be, seasonal changes in the character of the cooling water, comparisons should always be made at different times of the year since the materials that appear best in tests in winter when the water is cleanest may not be the best in tests under polluted conditions in summer.

The third use made of the apparatus is to assess the probable performance in service of new condenser tube materials. Tests are now in progress in which samples of tube of the 30% Ni, and 18% Ni, cupro-nickels containing 0.4% chromium (IN 848 and IN 837) recently developed by International Nickel Company, are being compared with standard 70/30 cupro-nickel, 70/30 cupro-nickel with 2% iron and standard 90/10 cupro-nickel.

5. Some results from the new apparatus

The first test rig to be constructed was installed in a power station in Denmark where the cooling water was somewhat unusual - it is taken from a fjord at the end furthest from the open sea and has a salinity approximately half that of normal sea water. Traces of ammonia (0.7 ppm with peak values of 2-3 ppm) are commonly present in the water although the source of this contamination is not known. 90/10 cupro-nickel tubes installed in condensers at this station have failed rapidly as a result of general corrosion accompanied by redeposition of large amounts of copper - the copper redeposition being extremely unusual in that it was not restricted to hot-spots or even to the hottest sections of the condenser. In experiments at the station with the new type of test rig 90/10 cupro-nickel has usually suffered rather widespread impingement attack in the impingement area to a depth of 0.1 to 0.2 mm in 8 weeks and has developed a moderately adherent protective film on the slow-moving cold water area. In the heat transfer area, however, and in the warm water area above it, the film has been loose and non-protective with widespread shallow general corrosion beneath it and frequently some copper redeposition. Redeposition of copper in the heat transfer area in hot-spot corrosion tests is well known and not surprising, but in these tests it occurred also on the cooler (warm water) area between the heat transfer area and the top outlet. Copper redeposition was also associated with general attack in the warm water crevice formed between the tube and the outlet nozzle.

70/30 cupro-nickel in the station has behaved much better than 90/10 but not so well as aluminium brass. The condenser tubed with aluminium brass was, however, in service for some time before the pollution of water with ammonia commenced and it was possible that the material owed its good performance to protective films developed during its early days of service. In the experiments with the new test rig, aluminium brass and 70/30 cupro-nickel generally suffered impingement attack to about the same depth as the 90/10 cupro-nickel and developed adherent protective films in the slow-moving cold water area. In some runs, in which the water was somewhat more corrosive than usual, the 70/30 cupro-nickel suffered slight attack beneath small blisters in the film in this area. In all the tests, however, it developed only a semi-adherent film in the warm water area, with slight etching and copper redeposition occurring beneath it and especially in the warm water crevice. In the tests with the more corrosive water localized pitting with copper redeposition occurred in the heat transfer area. Aluminium brass consistently developed a more protective film than cupro-nickel in the heat transfer and warm water areas. The film was not fully adherent but did not blister and only slight etching of the underlying metal occurred; no redeposition of copper occurred on aluminium brass either in the heat transfer area or in the warm water crevice.

Materials included in the experiments with the test rig but not previously used in condensers at the station included Cu-30% Ni-2% Fe-2% Mn (Yorcoron); Fe-18% Cr-10% Ni-Mo-Ti (SSH 2); Fe-18% Cr-12% Ni-Mo-low carbon (SSH 3); Cu-8% Sn-1% Al (AP Bronze) and commercial purity titanium.

Yorcoron proved significantly more resistant to impingement attack than the other cupro-nickels tested and formed a protective film in the slow-moving cold water area.

The film formed at the heat transfer and warm water area was less protective; attack in these regions was greater than on aluminium brass but still only slight and the Yorcoron showed less tendency than 70/30 cupro-nickel to copper redeposition. Its tendency to crevice corrosion was similar to 70/30 cupro-nickel and slightly less than for aluminium brass.

The stainless steels - SSH 2 and SSH 3 - suffered no impingement attack or attack in the slow-moving cold water area but proved liable to pitting in the heat transfer area and in the crevices. The pits in SSH 2 were of minute cross-section and consequently difficult to measure but appeared to be deep. The pits in SSH 3 were somewhat broader and shallower but, since only a few tests were carried out on these materials, and no one test included both, it would be unwise to make any generalization about their relative resistance to pitting. AP Bronze, which is an alloy developed particularly for service with polluted cooling waters, showed a very high degree of resistance to impingement attack, developing a dark and highly protective film in the impingement area. It showed, however, very high susceptibility to pitting in the crevices and in the heat transfer area. In some tests it formed an adherent protective film in the slow-moving cold water area but in others this part of the specimen developed extensive shallow pitting corrosion. The titanium samples tested included solid-drawn and seam-welded tube neither of which showed any corrosion whatever in 8 weeks.

6. Discussion

The results of the tests summarised above accord well with practical experience of the relative suitability of aluminium brass, 70/30 cupro-nickel and 90/10 cupro-nickel for condenser tubes in the station where the tests were conducted. They also give much more information about the probable relative performance of other alloys than could be obtained from a jet impingement test or any other existing condenser tube corrosion test. They indicate, for example, that Yorcoron would probably be a suitable condenser tube material for the station concerned but that AP Bronze, in spite of its resistance to impingement attack, would be totally unsatisfactory there because of its susceptibility to pitting and general corrosion. It also shows that the stainless steels tested, whilst having excellent resistance to impingement attack, would not be safe because of their liability to suffer pitting corrosion in shielded areas and possibly under heat transfer conditions. Titanium, because of its high resistance to all forms of corrosion, would probably require a considerably longer test period for there to be any possibility of its showing any attack at all.

7. Conclusions

The new apparatus is cheap to construct and easy to use. It can be installed on site to assist the selection of condenser or heat-exchanger tube materials, or to monitor seasonal changes in corrosivity of the cooling water. The information that it yields is much more comprehensive than is provided by any other existing apparatus for corrosion tests on condenser tubes and it is therefore particularly suitable also for assessing new materials or effects of surface condition arising from changes in methods of manufacture.

8. References

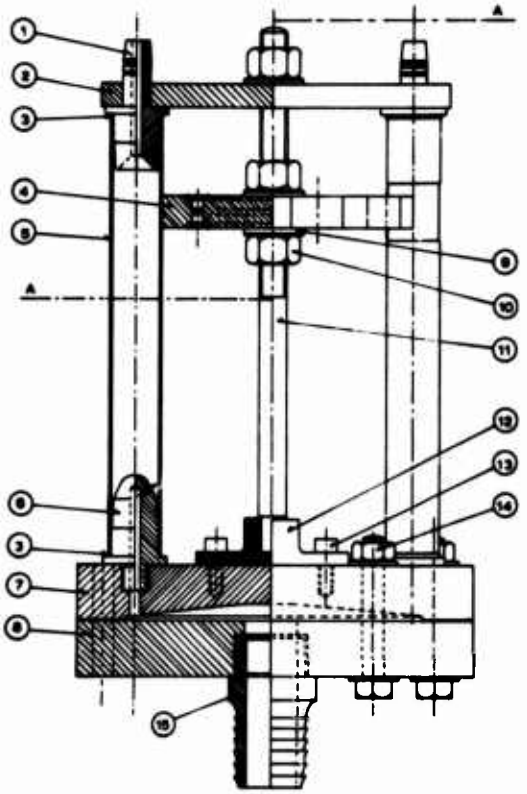
1. R. MAY and R.W. DE VERE STACPOOLE, J.Inst.Metals. 77, 331 (1950).

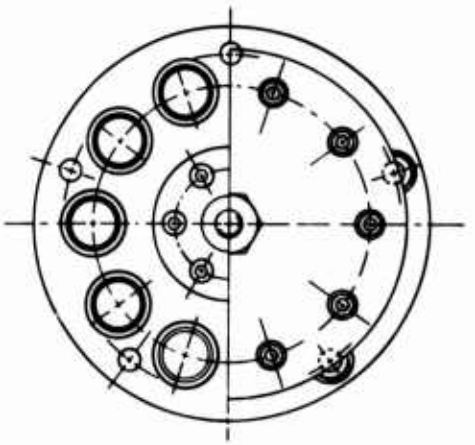
2. H.W. BROWNSDON and L.C. BANNISTER, J.Inst.Metals. 49, 123 (1932).

3. C. BRECKON and P.T. GILBERT, First International Congress on Metallic Corrosion, p. 624. Butterworths London (1962).

4. R.S. BEM and H.S. CAMPBELL, First International Congress on Metallic Corrosion, p. 630. Butterworths London (1962).

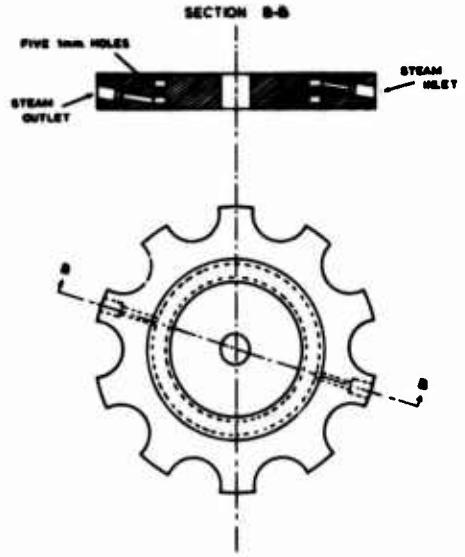
5. C. BRECKON and J.R.T. BAINES, Trans.Inst.Mar.Engrs. 67, 1 (1955).





SECTION A-A

Figure 1. General arrangement of condenser tube test apparatus.



SECTION B-B

Figure 2. Steam-heated heater block.

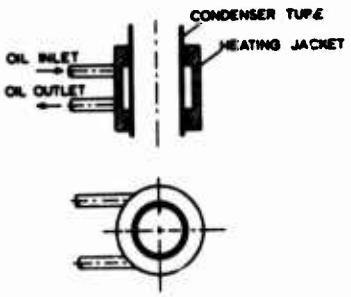


Figure 3. Oil-heated heating jacket.

Pourbaix: Je trouve cette expérience très astucieuse mais je voulais demander pourquoi on a mis les tubes verticaux alors que, dans les condenseurs, ils sont en général horizontaux. Vous avez quelquefois des effets de dépôts sur la génératrice inférieure du tube, c'est-à-dire vous avez un effet dissymétrique de la pesanteur, alors que çà me semblait aussi simple de les mettre horizontalement.

Campbell: The reason for having them vertical is really a matter of convenience. If you have your tubes horizontal in a rig like this it is very difficult getting even water distribution between them and it is quite essential that you should have equal flow otherwise your heat transfer conditions are different on the tubes. I agree that in a condenser in service you do get deposits on the bottom. What I hope in this is that the principal effect of the deposits is to produce a shielded area and I have provided a controlled shielded area in this by this two degree tape on the plugs on the top and the bottom. The attack that I am getting in those regions at the top and the bottom of the tube does, I think, represent the sort of attack one would get on the deposits in the tubes.

Pourbaix: Have you made any potential measurements of the tubes?

Campbell: I have not made any such measurements because about three years ago I stopped doing any research work and I am doing sort of consultancy work now so I am more interested in knowing what is the answer to a specific problem and the apparatus was designed for that, but there is no reason at all. I think the apparatus would lend itself well to this sort of use. I feel perhaps that I have been introducing it a little like a salesman, but I assure you that the designs are there and that you are free to make use of it and I hope that some people will feel that at least it's a good basic design. They may wish to modify it. If anybody wants its details of its construction I shall be pleased to provide them if they contact me and also if anyone uses it for taking its stages further, I would be most interested to hear and I hope perhaps that Professor Pourbaix will make use of it himself.

Smith, Copenhagen: Some years ago I know we supplied tubes to the power stations you were talking about. Have you tested this type tube in your test rig?

Campbell: No, we have not.

Smith: I will entrust you with some tubes.

Campbell: Well, the position really is that the test rigs are being run by the power station people, by the power company, and that within reason I think any tubes that are likely to be of use to them, they will be happy to put in. There are two sets of test apparatus now. One is made to take the standard imperial measure tube which is a one-inch tube and one is made to take the metric measure tube or two are made to take metric measure tubes. I think it would be worth testing these. I did not mention that we did also include in some of these tests tubes of the same nominal composition from different manufacturers. We have had aluminum brass from three different manufacturers and we have had 90-10 copper-nickel from two or three different manufacturers, I am not sure which, and there were some consistent differences, oh very small ones, between one manufacturer's and another in their performance in this. These are differences I am sure would not have shown up in an impingement test or something where you took it and you abraded the surface or you pickled the surface or something before you started. I am not going to say whose tube was better or worse.

Cotton: Professor Campbell, I would like to ask one if I may, in fact, I would like to go back to Professor Pourbaix's comment about potential measurement because he seemed to relate this to crevice attack and I think, Hector, perhaps would you like to say a little word about crevice attacking copper-base alloys because it is rather different than crevice attack in ferrous materials, stainless steel for example?

Campbell: I think the thing that is often not realized is how different the two situations are between crevice corrosion in a ferrous alloy or in aluminum on the one side and with the copper-base alloy on the other side. The attack occurs not inside the crevice as you would find if it were attacked due to a differential aeration cell. The attack occurs typically about here and you have got a cathodic region inside. In fact, you will quite often find copper being deposited on the inside there. This is because it is more in the nature of a copper-ion concentration cell and in fact it can go further and form a membrane there and you get then conditions to set up localized pitting here quite independent of the crevice that actually set it up.

Cotton: It really had quite a bit of relevance to what Professor Pourbaix said because if you are going to measure potentials, where do you measure them?

Pourbaix: Je suis bien d'accord avec ce que vous avez dit. La seule chose que je voudrais dire est que nous avons étudié les questions de corrosion caverneuse, corrosion par piqûres pour des laitons à l'aluminium, pour du cuivre, pour des aciers inoxydables et pour des aciers galvanisés. C'est un travail que nous n'avons pas encore publié. Je suis d'accord avec M. CAMPBELL pour dire que, dans chaque cas, le mécanisme de la corrosion caverneuse est différent. Mais je voudrais aussi dire que, dans chaque cas, les mesures de potentiel aident à la compréhension du phénomène et permettent de trouver des remèdes. Mais comme vous l'avez très bien dit la question de corrosion par crevasse dans les cuivres et dans les alliages de cuivre est un phénomène tout à fait différent, du point de vue de l'aération différentielle par exemple, de ce que l'on peut trouver dans les aciers ordinaires et les aciers inoxydables. Mais tous ces phénomènes sont sensibles à des variations de potentiel d'électrodes.

Campbell: One of the things that one has to remember when using potential measurements for this and this is something that Professor Pourbaix with his experience would, but perhaps I should mention it. That is, that you are getting film build-up over a long period and then you can get the film building up to such a point that the stresses within the film itself probably cause it to break down and to lose adhesion. This was why, as I mentioned, we found that it was advisable to extend our test period from one month to two months. If one were using measurements of potential, one would similarly have to conduct these over correspondingly long periods to allow the films to form and then to reach the stage where they were going to break down if they are going to.

Cathodic Protection, Iron Injection and Chlorination in Marine Heat Exchangers

John H. Morgan, Morgan Berkeley & Co. Ltd.,
Moorside Road, Winchester, Hants., U.K.

Marine heat exchangers, particularly condensers on steam turbine ships, can be protected against corrosion by impressed current cathodic protection in the waterboxes and by iron injection to reinforce the film on the aluminium brass tubes. Electrolytic dissolution of iron appears to be several orders more efficient than injection of ferrous sulphate solution. Chlorination will prevent fouling and sodium hypochlorite can be produced within the pipe/waterbox circuit.

Key words: Cathodic Protection; Impressed Current; Iron Injection; Ferrous Sulphate; Electrolytic Chlorination; Marine Heat Exchangers; Ship Condensers.

Introduction

A decade ago corrosion in marine heat exchangers was a matter of material selection coupled with coating of the sections which were not involved in heat transfer. On land-based power stations and refineries cathodic protection, mainly by impressed current, had been applied to similar equipment, and a simple impressed current scheme was fitted to a 40,000 DWT tanker. This coincided with the operation of a series of larger tankers up to 100,000 DWT where the problem was aggravated and the simple arrangement first tried was extended to these larger vessels.

Early systems. The initial installations were made with $\frac{1}{4}$" diameter platinised titanium rod anodes mounted into steel holders which were screwed through the wall of the waterbox. In cast iron boxes a back nut was used for sealing and in steel boxes a pipe boss was welded into place to take the anode holder. Reference electrodes of anode purity zinc, $\frac{3}{4}$" diameter, were mounted in a similar fashion. The anodes and electrodes were placed in the waterbox in an even pattern in anticipation that this would spread current to the whole of the tube plate and the waterbox. The current was supplied from a manually controlled transformer rectifier and on the third and later models this also had a built-in reference electrode monitoring facility. There was no experience of the current densities that were required so the capacity was based on a current of a $\frac{1}{4}$ amp per square foot of tube plate and the units were run so that there was a 300 millivolt change in the reference electrode potential.

The anodes were connected in groups of three via a local junction box to a fused outlet on the transformer rectifier. In one ship two transformer rectifiers were used, one of which fed the inlet and outlet of the condenser and the other the return end. The cathodic protection effectively reduced the corrosion and where there

had been deep pitting of the steel and tube ends this was stopped. The installation was not entirely successful and full protection was not achieved in all areas. There were also some unusual aspects to the operation of the protection and as the system had been based on hull techniques it was decided to analyse what was happening in the condenser waterbox.

Firstly, the current demand varied very much more than was anticipated although the water velocities remained reasonably constant; there were almost as large changes in current as were found with the hull system. The systems operated on a fixed output voltage which could be varied by a 15 step transformer tapping and it was decided to try automatic control using a standard hull controller.

Secondly, when a single automatic controller was used it was found that all the areas did not vary together and that separate automatic control was required at least between the inlet and the outlet.

Thirdly, the positioning of the reference electrodes was critical as was the selection of the reference electrodes used for control. Unlike the hull system, the anodes inside the condenser waterbox, and particularly in the pipes, did not back up each other and a reference electrode was almost completely influenced by the anodes next to it. It also became apparent that the reference electrode potential was influenced by the coating on the waterbox and could give a false reading of the potential if located in an area that was well coated. This led to a re-arrangement of the positions of the reference electrodes, a change in the selection technique for the control electrode and the need to monitor several reference electrodes even in a single waterbox.

Up-Dated Engineering. In addition to the fundamental problems of cathodic protection, a great deal of trouble was experienced with the anode design although this had been used successfully for many years in industrial plant. The problem was caused by vibration and the platinised titanium rods failed in hard mountings, possibly by oxygen starvation, and when softly mounted in a neoprene bush water was able to travel along the rod surface back into the cable joint assembly. An encapsulation technique was developed using a glassfibre resin tape wrapped around the anode as an insulator, machining this to be a good fit into the anode holder and cementing it in with an epoxy resin. The shape of the glassfibre cladding reduced the vibration fatigue on the rod, it covered the bare titanium area so that there was no breakdown from overpotential, and sealed the cable to anode joint preventing corrosion if water entered the head of the anode assembly. These anodes have now been in service for five years with less than 1% failure rate. The electrodes are made in a similar manner. An anode and holder is shown in Fig. (1).

With the introduction of inlet scoops fuel tanks prevented the mounting of anodes through the scoop wall and a triangular section anode was used, the cable being carried inboard along the pipe surface in a 2" x 2" angle which also held the anode. The back of the anode was shaped to allow a further cable to be carried beyond it so that two could be fed from a single entry point.

Control. In protecting the hull it is reasonable to control to within 20 to 30 millivolts, whereas in the condenser a much higher gain is required to respond to failure of a more distant anode. It is also necessary to use smaller control units in order that the various sections, the scoop, the inlet sea chest, the pump and the inlet and outlet boxes of the condenser can all be separately protected. A modular control system feeding a bank of transformer rectifiers was developed and also a small transistor

controller that could operate off a smooth d. c. output. The module system proved to be the more practical and these now are standardised with a 40 amp output. A two-module unit is shown in Fig. (2).

The higher gain has led to a much more positive indication of correct operation, and monitoring of the potential in various sections of the equipment can be carried out in the individual modules independent of the control electrode selection. This allows the operator to check the distribution of potential, and infer the distribution of the current, using different control electrodes; most hull systems monitor and control from the same electrode. The modular system uses the same plug-in electronics cards as the hull system and servicing is straightforward.

Iron Injection. Almost immediately the early systems were successful in suppressing corrosion (and these were all fitted to ships that already had hull cathodic protection) there was a spate of down-tube failures. This was also reported on ships which had full hull protection and non-ferrous pipes and a coated waterbox. At first there appeared tobe no correlation until it was realised that the soft iron pieces had either been removed to accommodate the impressed current anodes or, where they remained, they were cathodically protected with the rest of the waterbox. It was suggested that iron in solution was needed to repair the film on condenser tubes and this had been supported by Breckon[1] who had reported failures on condensers associated with cathodic protection. Steel anodes were installed and driven so that they dissolved despite the cathodic protection in the waterbox. The dissolution rate was arranged to be twice the corrosion rate of the soft iron pieces, for example, a consumption of 50lbs of iron a year on a large tanker. This brought about a dramatic reduction in the corrosion rate and the tubes were in excellent condition. The amount of iron supplied to the subsequent ships was increased by 50%.

The criterion of protection that had now been established was very vague in that it was three times the amount of iron that was dissolved from the condenser soft iron pieces. New condensers were not designed to have any soft iron and no formula could be found for calculating their size. There are two condenser perameters, the area of the tubes and the amount of water which could influence the rate of dissolution. As the cathodic protection was successfully preventing impingement attack on the tube ends it was felt that the more realistic criterion, though we are not to this day sure, would be the amount of water flowing, and the results of our work were correlated to this. A not very clear picture emerged and it would appear that a large tanker is more than adequately protected by dissolution of 70lbs of iron per year.

Ferrous Sulphate. Contemporary with our work other people, principally the tube and condenser manufacturers and the C. E. G. B., were experimenting with injecting ferrous sulphate into the water stream. At power stations fine crystals were thrown into the cooling water culvert once a day to provide a 1 p. p. m. iron dose for one hour. It was not possible to use this technique on board ship so mixing tanks were installed and the awful job of mixing sea water with ferrous sulphate crystals was undertaken by the crew. This is a hazardous business, the crystals are very fine and contain free acid, they should not be inhaled, they can cause inflammation of the eyes, and the dust that settles quickly becomes ferric chloride in the marine atmosphere, one of the more corrosive chemicals.

System Comparison. It is interesting to compare the two systems. 1 p. p. m. of ferrous sulphate crystals for one hour a day is recommended, although after a period of operation the same dosage every other day is found to be adequate, an average of 0. 02 p. p. m. as an integrated dose. With the electrolytic iron system the dosage

Figures in parentheses indicate the literature references at the end of this paper.

rate is very much lower, 0.5×10^{-3} p. p. m. and this is $2\frac{1}{2}\%$ of the practical ferrous sulphate injection a day. This order of difference must be capable of being explained as both techniques work equally well, and the reason could rest in a number of points.

Firstly, the intermittent injection of iron could be highly inefficient and that a smaller quantity continuously injected would give the same result. The technique of mixing by hand, and of hand dosage in the power station, would not readily lend itself to continuous operation except at great expense, and it would be very much cheaper to use a heavy shock overdosage for a short time. It would be difficult, using simple mixing techniques, to ensure a slow rate of flow as there would probably be blockages with undissolved crystals.

Secondly, 1 p. p. m. for an hour is recommended but this could be well in excess of the dosage required, though the consistency with which this criterion is recommended makes this doubtful.

Thirdly, it is possible that there is inadequate mixing in the water ream during injection and iron may not be well dispersed; certainly not as well as the corrosion product from 12 anodes placed around the pipe.

Fourthly, there is some evidence to suggest that the ferrous sulphate solution when mixed with sea water is partly converted to ferric chloride and exists in the pipe in macromolecular form as an anionic charged group. Cathodic protection would tend to keep the colloidal particles away from the tube surfaces, whereas the dissolved iron would most probably produce cationic particles which would be attracted to the cathode.

An improved system of dosage is under development in which a cationic solution of ferrous sulphate is used and when this completes sea trials it may show whether a lower rate of continuous dosage produces the same results and whether cationic ferrous sulphate will be more efficient than normal ferrous sulphate/ferric chloride complex.

Practical Operation. A system based on all this experience was fitted to a ship and the unit adjusted to the normal cathodic protection criterion, that is 250 millivolts to a zinc electrode. The chosen ship had experienced considerable trouble with its condenser waterbox which had been welded just before the system was fitted. After two months the waterbox was examined; there was no sign of calcareous deposit around the anodes, as had been expected, and although there had been no measureable corrosion, the metal did not have the appearance generally associated with cathodic protection, there being no dull grey bloom to the cathodic areas. The potential of the waterbox was depressed by a further 75 millivolts, and three months later appeared to be fully protected with a remarkable change in the appearance of the tube ends and tube plate. The extra depression of potential was very necessary and subsequent observations have shown that about 100 millivolts overprotection is required in the turbulent areas in the condenser and in the pipe work.

There was heavy fouling in the condenser with the exception of an area close to the anodes, and a similar effect occurred on several ships; this included an area of the tube plate. It was not clear what was having this effect as the areas were both those of maximum potential and the areas that might be affected by the anode products in the anolyte. This was cleared up when the other end of the tube bundle was examined and there was a similar, though smaller, fouling-free area, which showed that this anti-fouling effect was caused by anode product and this could only be sodium hypochlorite that was formed in the sea water.

In-line Chlorine Generation. An area of approximately 2 sq. ft. appeared clear and there was a current of 2 amps flowing from the anode at a water velocity of about 1 foot per second, so that 2 cubic feet of water were being treated by 1 amp second of electricity. This is the equivalent of a dosage rate of 0.01 p.p.m. of chlorine and is much lower than normally suggested for this type of work. It appeared that if instead of the 60 amps that was being used in the whole system to provide cathodic protection, the current could be increased six fold in the inlet half, then on a purely area basis all of the condenser tubes and tube plate would be kept free of fouling.

A study of the literature showed that complete anti-fouling had been achieved at between 0.1 and 0.2 p.p.m. of chlorine on a continuous basis and a series of anode/cathode configurations were tried in an effort to bring about an increase in chlorine generation without excessive overprotection. After a series of frustrated attempts with concentric tubes; with spaced rods and with rods and plates, it was decided to concentrate on the use of parallel plates. A simple arrangement of these that would screw into the condenser through a 2" hole was tried, but the efficiency of the process was very low. It was therefore decided to revert to the classical parallel plates and not attempt to mount these through the wall, but to fix them as a unit inside the condenser waterbox or pipe. At the slow flow rate that could be expected the parallel plates would quickly stifle by a calcareous build-up on the cathode. Some years earlier experiments were made using a switched output and these were found to be very successful, although the polarity switching arrangement that had been used in the laboratory was not suitable in a larger application. Bigger thyristors were now cheaply available and a solid-state switching system was developed which would automatically change the polarity of the plates.

The original idea had been to provide chlorine from the cathodic protection anodes and it was now decided to obtain the cathodic protection current from the chlorine generator. This was done by building a ring of guard electrodes near the ends of the parallel vanes, as shown in Fig. (3). These were connected to the positive output and not switched with the plates which had their polarity changed every few minutes. As the main protection in the condenser was automatically controlled some of the cathodic protection current was fed into a centre tapped transformer and the whole unit then gave out current in sympathy with the cathodic protection. This led to some difficulties in the electronics, particularly with the residual polarisation that occurred. These were overcome and the system is being successfully operated on four units at sea.

The automatic cathodic protection units in the condenser have proved, however, to be capable of providing sufficient variation that the chlorination units are now being built to give a constant, as opposed to an automatically regulated, supplementary cathodic protection current. This simplifies the construction of the electronics for the chlorination unit. The units that are in service operate at close to the predicted efficiency and in its operation to date 90% of the projected chlorine generated by the system has been found in the outlet.

Pollution. Impressed current protection is a complete non-pollutant. Electrolytic iron injection at 1 p.p.b. is of the order of the corrosion rate of a small structure in sea water. Ferrous sulphate injection which will turn to ferric salts in sea water could be a serious pollutant in a port where the water is already sufficiently noxious for dosing twice a day to be recommended. The presence of a few large ships could mean that a ton of ferrous sulphate is emptied into the harbour each day.

Electrolytic chlorine in the form of sodium hypochlorite is a non-pollutant and a discharge of 0.2 to 0.5 p.p.m. of chlorine would be absorbed rapidly.

The chlorine will act as an oxidising agent and would be a cleansing agent reducing other oxygen absorbing pollution.

We have therefore now equipped a ship with a system which protects its cooling water circuit against corrosion by cathodic protection, effectively brings about film repair and re-inforcement on the tubes by electrolytic iron injection, and we have integrated this with a chlorine anti-fouling system which is contained entirely within the pipes and waterboxes without any toxic effluent.

(1) BRECKON C. Cathodic Protection may Boost Corrosion. Pet. Refiner. 37, 189-190. Mar. 1958.

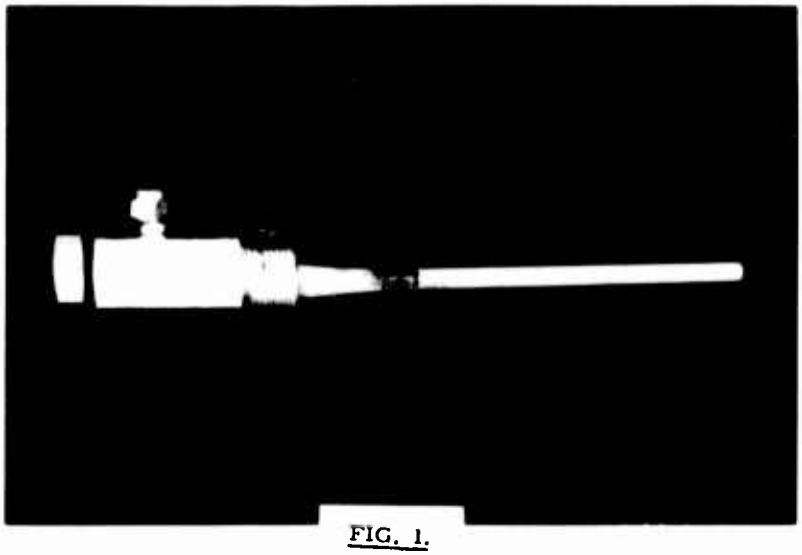


FIG. 1.

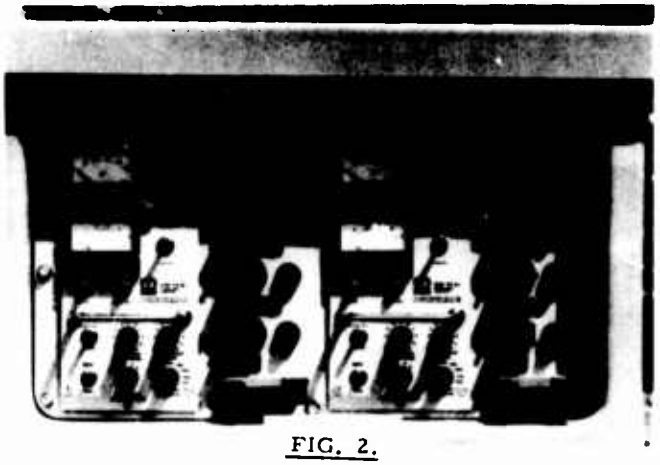
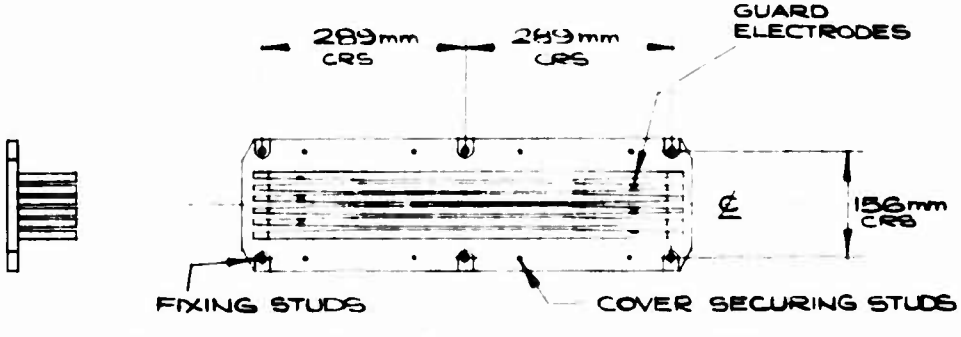


FIG. 2.



MAC1 CHLORINATOR WITH COVER REMOVED

FIG. 3.

Discussion

Shone: About eight years ago, several failures of aluminum brass tubes occurred on the new larger tankers, which we attributed to erosion, corrosion, or impingement attack. We carried out investigations and found that the systems were completely non-ferrous. They were usually made from aluminum brass with small amounts of copper nickel, and the waterboxes were rubber lined. We believe that this type of damage is associated with turbulent aerated high velocity sea water. Frequently, the design of these condensers was such that it promoted excessive turbulence. Mr. Morgan says that the earlier attempts to cathodically protect the tubes were not successful because of the unreliability of the platinized titanium anodes. We agree with this and at that time we were forced to look for alternative solutions. One of these solutions was the injection of ferrous sulfate in the sea water circulating systems. At that time, no simple system was available commercially for use on board ship and we designed and evaluated our own. This system is very simple. It consists of a mixing tank with a stirrer. The ferrous sulfate is fed from the mixing tank to a manifold and then to injection probes. We can feed lube oil coolers, the main condenser, the pumps, and any other such component in the ship. In some cases we are using the ferrous sulfate additions in conjunction with plastic inserts and wrought iron anodes. The wrought iron anodes corrode very slowly because of the natural current set up between the tubes and the iron. In your paper, you say that it is hazardous for the crew to mix the ferrous sulfate solution. In answer to this, I can only say that in two years we have had no complaints from the ship's personnel who carry out this operation. They are made aware of the fact that the crystals may contain small amounts of free acid and take the appropriate precautions. On the point of dosage, while we have not yet established the optimum dosage, we believe it is considerably less than the one part per million for one hour per day usually recommended. It seems likely that this figure is used because that was the amount recommended by Bostwick in his paper when he referred to the tubes at Jacksonville. Mixing is not a problem in our system and if the injectors are correctly sited, then the turbulence in the system is sufficient to provide all the mixing required. We find that this ferrous sulfate injection has prevented tube failure on about 20 of our vessels now that we have these units fitted on. On the subject of pollution, I would like to point out that our vessels do not use the large quantities of ferrous sulfate mentioned in your paper. We believe that corrosion control in marine heat exchangers may still be a matter of material selection and in some cases we have started to use 70-30 with about 2% iron for the tube materials. This is very successful. Unfortunately, we have run into one snag. We haven't got time to change the tube plates and we are getting some corrosion of tube plates now. In the future, we are seriously considering using titanium as a heat exchanger material.

Morgan: I would just like to thank you for what you have said. Two or three things I probably did not make clear. First of all, it was not the platinized titanium anode that failed. It was our techniques of mounting them. I think I ought to make that clear. It was not a failure of material. I would not be against any system of using ferrous sulfate, and when I mentioned it was hazardous, I was really putting this out as a warning to some unsophisticated operator. I am only too delighted that you had no troubles on your ships. I am very glad that you are finding the lower dosage satisfactory. It means that all those people we sold our electrolytic system to will now not come back and ask us to upgrade it.

Carson: I would like to ask Mr. Morgan if he mentioned that he got differences in, I gather, current requirements in different parts of the condenser. Did you find that the current requirements were considerably higher on the cold side than on the warm side? We have found in the use of galvanic anodes that there is much more corrosion of the anode on the cold side than on the warm side. I am talking about zinc in particular.

Morgan: We found this on some ships and we think it is associated with the fact that on the cold side, there is a lot of turbulence and that on the warm side, the water already having gone through the tubes, is better distributed. We have also found a lot of sand erosion on big ships where when a large ship goes along, it seems to put a pressure wave into a sandy bottom and sand comes up into the scoop. This causes very heavy damage to any coating and it is this sort of thing that we found to give much higher currents and it is this sort of thing that threw us when we thought we had a simple system that we could control manually and it would not need adjustment.

Carson: The introduction of iron into cooling water systems is really quite old. It is over 50 years old. Cumberland designed an electrolytic method of introducing iron into condenser systems back in the 1920's. Your methods of introducing iron and providing cathodic protection seem to me overly complicated. What is the matter with using galvanic iron anodes to do both jobs?

Morgan: On the historic note, I believe the first proper installation of this type was done by Mertz in the Dundee Power Station. On the question of using an iron anode that simply corrodes away, it does not give anything like enough current. Using iron anodes and corroding them away with power to provide the cathodic protection, there is not enough volume or space to go the two and a half years that a large ship would want to go; between dry-dockings, you would have to replace the iron anodes much more frequently.

Cotton: I should have thought that your answer to that question would be that the demand for cathodic current varies so enormously between a ship in dock and a ship moving in the sea, and that an iron anode just simply cannot cope with this variation in current demand. Am I right or wrong there?

Morgan: Right. A typical 260,000 ton tanker may take 60 or 70 amps on the average, and this might vary between 30 and 100 during a voyage. Now to get 100 amps out of sacrificial iron anodes and protect a steel water box would not be a very practical proposition.

Carson: I would like to comment on that. I do not have experience with the large type of heat exchangers you are talking about, but we have had very excellent results with using mild steel anodes in small ones. But I would also like to say that when people started putting rubber coatings on their steel water boxes, they removed the cathodic protection which was doing them the benefit. I am personally convinced without actually having tried it that you could get plenty of galvanic steel anodes in there to do the job.

Morgan: The boxes are made quite differently on a big ship.

Arup: Both the author and Mr. Shone seem to agree that the iron should be introduced very shortly before the condensers. In fact, have you evidence that this is necessary? In many installations, it would be of course much easier to introduce the iron at an earlier point and thus feed several units at one time.

Morgan: No, we have in fact done several systems where we introduced the iron very early on and we have produced systems where the anodes are perhaps a hundred feet or more from the condenser. This is to protect the cooling water circuit for other pieces of equipment. We have since put it further back. I do not think there is any problem there, and in the power station they throw the ferrous sulfate in into the sea alongside.

Electrochemical Aids in Corrosion Control in Anti-Fouling and in Scale Prevention.

J.B. Cotton

Imperial Metal Industries Ltd.,
Witton, Birmingham B6 7BA, England.

One of the basic problems associated with impressed current anodes used in cathodic protection of steel structures immersed in sea water is to provide a strong durable anode to conduct the protective current into the water. Over the past fifteen years, one advance in this direction lies in the development of platinised titanium anodes. For this type of anode the durability aspects relate to the precautions necessary to prevent pitting of the uncoated titanium support structure, the evaluation of the rate of loss from the platinum surface, and the definition of the conditions under which such loss occurs. The results from controlled practical tests at a sea water site in U.K. are summarised and examples of many forms of titanium-based anodes are illustrated.

The control of marine infestation of sea water cooling systems of coastal power stations by use of either chlorine or sodium hypochlorite has been practised for many years, the supply of disinfestant usually being in the bulk liquid form. Because of the inconvenience attendant upon bulk storage, such systems are not readily acceptable for use on board ship and even for land based systems, provision of bulk supplies can involve appreciable transport costs. Over the past fifteen years, there has been considerable development of in-situ production of sodium hypochlorite by the electrolysis of sea water, and the paper describes the development of compact electrolytic cells for this purpose. The design features of both monopolar or bipolar cells, employing coated titanium electrodes are summarised and the operating factors necessary to achieve an acceptable performance are indicated.

In the thermal desalination of sea water, a problem arises in the deposition of water deposited scale on heat exchange and evaporator surfaces. Scale deposition is usually controlled by adjustment of the pH value of the seawater, by acid dosing from bulk supplies of sulphuric, hydrochloric, and citric acids or by an addition of ferric chloride. By suitable selection of materials and design of equipment it has now been demonstrated that it is possible to generate the necessary acidity by electrolysis of sea water. The cell arrangement involves the discharge of hydrogen at a cathode and the transfer of the hydrogen to an anode which functions as a fuel-cell type electrode in converting the gaseous hydrogen to hydrogen ions. The operation of a prototype cell over a continuous period of 6000 hours is described and the economic aspects are summarised. Finally the possible application of electrochemistry to the production of pure oxygen from sea water is foreshadowed.

Introduction

Although the commercial or industrial use of electrochemistry in conjunction with sodium chloride brine has its roots in the birth of the alkali industry in the mid 1800's, and although rather earlier than that, Sir Humphrey Davy had, in fact, applied electrochemical principle to the cathodic protection of ferrous materials in the sea, it is only in the past twenty years that any significant attempt has been made to exploit the considerable advantage to be gained from commercial application of electrochemical processes to sea water.

In the past twenty years there has been a great deal of advance in the application of cathodic protection to sea water systems and some of the sophisticated control techniques now employed are described in other papers delivered to this Congress. Such systems could not achieve their full potentiality without improvement in corrosion resistance of applied - current anodes and there has been significant development in this direction. One of these has resulted in the use of platinised titanium anodes. Even platinum is not completely immune to corrosion under these conditions and the first part of this paper records some relevant experience in this development and summarises the results of some controlled tests instituted to define the rate of wear of platinum as an anode material.

The use of impressed current for cathodic protection is however likely to prove to be only the first of several systems in which electrochemistry can be applied in practical fashion to sea water systems. Thus although corrosion monitoring, in several forms, is making rapid headway for the corrosion control of chemical plant, its use in sea water systems is still in its infancy.

Significant progress has been made in the design and operation of small electrolytic cells for the in situ production of sodium hypochlorite from sea water for marine disinfestation purposes. Indeed, in this application practical experience has been accumulating over several years, during which the advent of platinised titanium electrodes has significantly facilitated the commercial development of such systems. The second part of this paper summarises some of the features involved in the practical behaviour of such electrodes.

Sea water is such an obvious source of hydrogen and oxygen that it is perhaps a little surprising that little attempt seems to have been made to separate and use these elements in appropriate circumstances. In desalination, for example, scale control is effected by pH adjustment of the primary sea water supply, and hydrochloric, sulphuric or citric acids are used as to replace the carbonic acid ion. By operating a sea water cell under specific conditions it has been demonstrated that the requisite level of acidity can be obtained by utilising cathodic hydrogen, from which an electron is extracted in a fuel-cell type electrode. A summary of developments in this direction appears in the third section of this paper.

Finally by restricting access of sea water in a cell system, it is possible to pass through all the oxidation states of chlorine to perchlorate and from this it is possible to produce fairly pure oxygen, virtually uncontaminated with chlorine.

A paper having as broad a scope as already indicated, would become unduly unwieldy by the inclusion of too much detail. Indeed, the main objective of the paper is to demonstrate the possibilities arising from the wider application of electrochemistry to sea water systems in the hope that some of the existing developments may receive further commercial impetus and that some of the possibilities might become commercial possibilities.

Platinised Titanium Anodes in Cathodic Protection

The basic development of the use of a thin film of platinum upon a supporting structure of titanium as a composite anode material was first described in 1958[1],[2]. Its success depends upon the fact that titanium will conduct electronically to the platinum, but that at any pores or defects in the surface film the titanium substrate will passivate, even in halide solutions.

(The numbers in parentheses refer to the list of references at the end of this paper).

This ability to passivate has, however, its limitations and when the applied potential difference between uncoated titanium and the environment in immediate proximity, attains a value of between nine and twelve volts, breakdown in passivity can occur and corrosion ensues. For this reason it is usual to limit the voltage when applied to a partially-coated titanium anode, to a value of nine volts, although under some circumstances higher values than this can be tolerated.(3)

Since 1958 many thousands of platinised titanium anodes have been employed in cathodic protection systems, the advantages of employing titanium as a strong versatile support being demonstrated by the wide range of shapes and sizes used. Thus anodes are produced in the form of plate, sheet, mesh, tube, rod and wire.

The ability of uncoated titanium to passivate and become non-conductive in the anodic sense to the electrolyte, is of advantage where long thin anodes are required to conduct only from an extremity. In such circumstances only the extremity is coated with platinum. Where long wire anodes are required, these can be produced from low-resistance copper-cored titanium, and the titanium sheath can be skip-coated to conduct only from the requisite areas.

One of the prime advantages of such anodes is that they can operate at high current densities - 100 amps per square foot and even, on occasion at 500 amps per square foot. In performing such duty platinum coated titanium should function, in theory, as adequately as solid platinum and with certain reservations experience has shown that they do so in practice. Even solid platinum has some solubility when anodically energised at high current densities, and the relative performance of solid platinum and of platinum plated titanium has formed the subject of an investigation by the corrosion team at IMI. Apart from simple anodic dissolution there are three further circumstances that can result in loss from the platinum surface. They are, dissolution, probably due to chelation, in certain water soluble organic derivatives; the superimposition of an A.C. ripple upon the D.C. source and what is believed to be the effect of local acidity beneath deposits.

The details of laboratory investigation and simulated performance at a marine site in U.K. were provided in a paper given to the British Joint Corrosion Group in London in February 1971 by P.C.S. Hayfield and M.A. Warne. That paper is in course of preparation for publication in the British Corrosion Journal.

Summarising the results obtained it has been shown that in moderately clean sea water at Brixham, Devon, the rate of dissolution of solid platinum operating at 120 amp/ft^2 with three phase full wave unsmoothed D.C. was 1.0 microgram per amp hour. When the current density was raised to 460 amp/ft^2 the rate of wear increased to 1.5 micrograms per amp. hour. For platinum plated titanium the rate of wear varied with the process used, and values from 0.36 to 1.34 micrograms per amp hour were recorded at current densities that varied from 30 to 300 amps/ft^2. Most wear rates fell below 1.0 micrograms per amp hour and it was concluded that this represents a conservatively high figure upon which to base the practical durability of platinised titanium under service conditions. In practical terms this provides a service life of two years for an anode carrying 100 micro inches thickness of platinum, operating continuously at 300 amp/ft^2 or a service life of 10 years for a similar anode operating at 50 amp/ft^2. That these figures can be related to practice is demonstrated by the fact that anodes prepared over ten years ago with a 100 micro inch coating of platinum are still operating satisfactorily at current densities of several tens of amp/ft^2.

There is little doubt that a superimposed A.C. ripple, upon the D.C. source can result in activation of platinum, and this effect has now been shown to be dependent upon the frequency of imposed A.C. Simusoidal frequencies of 50 Hz and lower are known to accelerate dissolution rate, but frequencies of 100 Hz and higher appear to have little effect(4). Tests at Brixham with various types of rectifying equipment including a thyristor controlled silicon rectifier, have shown that any aggravation of the wear rate over that of a fully smoothed supply is only marginal.

In practice unduly rapid failure of platinum plated anodes has occurred on one or two occasions when the anodes have been buried in mud or have acquired fairly heavy surface

(The numbers in parentheses refer to the list of references at the end of this paper).

deposits, the form of failure being by "undermining" of the platinum coating. The full explanation for this type of occurrence has yet to be determined; it appears to be associated with high local acidity developed under the blanket of deposit, and is possibly associated with pores in the coating. At all events modification of the coating process to produce an impervious layer seems to provide a remedy, although this still has to be demonstrated in really long term tests.

The chelation type of platinum dissolution in the presence of organic species related to sugars, has mainly occurred in metal plating baths and it is doubtful whether similar effects have been observed in sea water.

Despite some statistically low incidence of unduly short life under the circumstances summarised, the practical value of platinised titanium anodes has been amply demonstrated over the past twelve years. This type of anode should be regarded as the first of a series of composites based on titanium and carrying a variety of conducting surfaces, some of them specifically designed to combat difficult operating conditions.

Generation of Sodium Hypochlorite

The electrolysis of sea water in a cell in which anolyte and catholyte can easily mix allows the normal chemical reactions to take place in which chlorine formed at the anode reacts with sodium hydroxide at the cathode to produce sodium hypochlorite. The other main cathodic product is gaseous hydrogen. With dilute brine other side reactions can occur and in particular with sea water, the soluble impurities such as magnesium and calcium, when in contact with the alkaline catholyte, can precipitate, usually as hydroxides and this can complicate the operation of the cell.

The first commercial cells to demonstrate the feasibility of this process were developed about fifteen years ago. They employed graphite anodes, which were quite bulky and being subject to relatively rapid wastage, they had to be replaced at fairly frequent intervals. The advent of platinised titanium facilitated the design of neater cells with much longer periods of operation between maintenance shut down. The potentialities inherent in this system may perhaps be judged by the fact that in U.K. there are four different designs of cell available with some parallel development proceeding both in U.S. and Japan.

Such cells may operate in the monopolar principle, sometimes employing a steel cathode with a platinised titanium anode or they may function in a bipolar system in which isolated electrodes suspended in an appropriate electrical field gradient, acquire the ability to collect electrons on the anodic side to discharge chlorine ions and to pass electrons on the cathodic side to discharge hydrogen ions.

Bipolar cells have the advantage of a neater construction for a given load, and they have less complicated electrical connections, but care is needed to ensure that the fairly high electrical field and the distribution of electrolyte in narrow electrode passageways are correctly handled. The majority of commercial cells appear to operate on the bipolar principle.

The electrodes for a bipolar cell are usually of titanium, platinised on one surface only and this perhaps requires some explanation.

As already described for anodes used in cathodic protection, uncoated titanium will not readily pass current in the anodic sense i.e. it will not accept electrons from negatively charged solvated ions - hence the need to employ a surface film of platinum to discharge chlorine. In contrast to this titanium will readily pass electrons outwards in the cathodic sense to discharge positively charged ions e.g. hydrogen. Thus the bipolar electrodes discharge hydrogen from the uncoated cathodic surface and produce hypochlorite at the platinum coated anodic surface.

Because titanium readily forms a hydride and because titanium hydride is brittle, it is at first sight, rather surprising that titanium can be employed in this fashion. The facts are that only a thin surface layer of titanium hydride is formed and this discharges hydrogen readily. At sea water temperature, the hydrogen does not diffuse and the strength of the electrode is not materially impaired. The titanium hydride does however occupy a volume greater than the titanium from which it was formed and in the first designs of cell this resulted in some bowing and short circuiting of the sheet electrodes. This occurrence can be successfully countered by modified design of sheet, to contain the tendency to bowing or even by use of more robust electrodes.

It would, of course, be possible to avoid hydriding on the cathode side by use of a composite anode of, say, steel bonded to titanium but this raises complications. For example, in a sheet anode construction there is a rapid change from the anodic to the cathodic reaction at the edge, resulting in edge corrosion. This complication can be countered by redesign of cell at the sacrifice of some compactness, but further advances may be envisaged in which the cathodic surface of titanium can be treated to avoid hydriding while maintaining a low overpotential for hydrogen release.

Early experience in operation of bipolar systems clearly demonstrated that if cathodic deposits of magnesium hydroxide etc. were allowed to build up, such that they bridged the narrow anode-cathode gap, this could cause stripping of the platinum from the anode surface. The mechanism is believed to be that of "undermining" as previously described. The remedy is to ensure that inter-electrode spaces are adequately swept by proper distribution of sea water, moving at appropriate speeds.

One further possible hazard is the impingement of cathodic hydrogen on to the platinum surface. The extent to which this can result in rapid wear of the platinum is difficult to prove, but at least it is a sound principle to eliminate the hydrogen from the cell with as little delay as possible.

At all events, the early experience in the design and use of this form of cell has resulted in various cells of several different designs that appear to provide quite adequately reliable performance.

The in situ production of sodium hypochlorite for the prevention of the growth of marine organisms has obvious advantages especially for ship use and for power stations and desalination plant sited at locations to which transport of bulk chemicals carries a significant cost premium. The actual economic advantage to be gained from the use of in situ hypochlorite cells will obviously depend upon individual circumstances. One early figure[5] suggests that even for power stations where long distance transport was not a factor there could be substantial saving over that of bulk purchase of chemicals. In one more recent exercise involving a 37,000 ton tanker it was estimated that the saving in elimination of maintenance costs and in improved speed could amount to rather more than £3,000 p.a.

Electrolytic Acidification of Sea Water

In thermal desalination systems employing a sea water intake, it is necessary to adjust pH to an acid value to control scale formation in the evaporator sections. pH adjustment is usually effected by an addition of sulphuric, or hydrochloric acids. Ferric chloride and citric acid may also be employed.

For ship board use and in remote locations where desalination of sea water is often a necessity, there is much merit in the possibility that acid sea water could be generated electrolytically, in situ. This possibility arises from the suggestion that in a sea water electrolytic cell, in which chlorine is generated at the anode and hydrogen at the cathode, the gaseous hydrogen can be pumped over the anode and induced to part with electrons in a fuel-cell type reaction to produce hydrogen ions and provide the equivalent of ionised hydrochloric acid.

(The number in parenthesis refers to the list of references at the end of this paper)

Such a system was investigated at the IMI laboratory in 1965 and demonstrated to be feasible[6]. Independently a similar system was being investigated in US at the American Machine and Foundry Company, Stamford, Conn. (7), and subsequently L.H. Shaffer and R.A. Knight presented a paper to the Electrochemical Society in Boston May 5-9th 1968[8], in which the US development is comprehensively recorded.

In both systems it is essential to employ a porous catalytic membrane as the anode through which gaseous hydrogen is forced so that it ionises on the electrolyte side. In the U.S. version this membrane consisted of a polyethylene-sulphonated styrene base carrying a layer of platinum - 10% rhodium and activated with platinised platinum. In the British version it was a porous P.V.C. base carrying a layer of gold and activated with platinum-carbon- a fuel cell electrode developed for other purposes by the Shell Company. Both membranes have given successful operating lives, but it is probable that further improvements can be introduced.

It is clearly necessary to separate the acidic anolyte from the alkaline catholyte and in the U.S. system this was done by employing an anion exchange membrane to allow the selective diffusion of chlorine ions to the anode, to balance the hydrogen ions produced there. A cation membrane was used in front of the stainless steel cathode to allow selective diffusion of sodium ions to the cathode compartment. The use of the cation membrane facilitates the production of an alkaline stream from the cathode compartment and this stream can be used to soften the sea water intake to the cells and prevent fouling of the electrode compartments by precipitated magnesium and calcium salts. By 1969, the American system was in commercial operation, two cells having been developed with capacities of 6,000 and 30,000 gallons per day of product with an acidity equivalent to about 0.15 normal hydrochloric acid, at a power consumption of 2.5 Kw hr/1000 gallons.

The British cell is still in the development stage, the development being shared between IMI Ltd., Marston Excelsior Ltd. and Constructors John Brown Ltd. It adopts a simpler system in that anolyte and catholyte are separated only by a woven glass cloth screen. No attempt is made to produce a useable alkaline catholyte. Fouling of the cathode compartment is avoided by selecting a suitable geometry, with no stagnant areas and with high rates of flow of electrolyte. As already indicated, it employs a different catalytic anode membrane from the American cell. A small development sized cell has operated successfully for 6000 hours, producing an acid electrolyte at a pH of between 2.5 and 3.0 at a volume of 160 gpd Based upon this British experience it is estimated that commercial quantities of acid electrolyte at a volume of one million gallons per day could be produced at a cost of rather less than 2½ new pence per thousand gallons, including capital amortisation of the plant.

This system of acid production from sea water is clearly still in the early stages of development and improvement in the design and operation of the cells are certainly possible and would be encouraged as the commercial advantages become more appreciated.

The Production of Pure Oxygen

Although, as yet, there seems little commercial demand for the in situ production of pure oxygen from sea water, the increasing use of the sea may ultimately require this sort of development. Virtually as an exercise in the versatility of the application of electrochemistry to sea water systems, an experimental cell was constructed at IMI Witton, in which access of fresh sea water to the cell is restricted, allowing the anodic oxidation of chlorine to proceed quickly through all the oxidation states to perchlorate i.e.

$$Cl^- \longrightarrow ClO^- \longrightarrow ClO_3^- \longrightarrow ClO_4^-$$

Once the final oxidation process to ClO_4^- is complete, the oxygen current efficiency rises to 100%.

The cell, of fairly simple construction, consists of a low-voltage platinised titanium anode separated from a stainless steel gasket and divided into two compartments by means of a glass cloth screen to separate oxygen from hydrogen. A temperature of 60°C is maintained and the cell operated at a current density of 40-50 amps/dm^2 at 20 V. The hot electrolyte is pumped continuously around the circuit and cooled before re-injection into the cell.

(The numbers in parentheses refer to the list of references at the end of this paper)

The volume of this experimental cell is 170 ml and electrolyte is replenished at a rate of 7 mls per hour.

Oxidation of Cl^{1} to ClO_4^{1} is restricted by some chemical reduction at the cathode and to a large extent this can be countered by the addition of dichromate. Such an addition certainly increases the speed at which gaseous impurities in the oxygen are brought to a low level. The main gaseous impurities are chlorine and ozone and with a dichromate addition of 2 gm/litre these are brought down to a level of 0.01% v.v. within twelve minutes. The very small amount of residual chlorine can be removed by use of the conventional alkaline absorbents and ozone by passage through a DEOXO catalyst. During the first hour operation of the cell, the pH value of the electrolyte rises to a level of about 11, and there is some precipitation of calcium and magnesium salts, which will have to be removed in further development of the system. Although clearly, much further development is required this preliminary investigation into oxygen generation from sea water demonstrates that a feasible system for the production of pure oxygen from sea water is possible.

Conclusion

There is much evidence of an increasing impetus to take advantage of the natural resources available in the oceans, and it is to be hoped that the information summarised in this broad survey has pointed the direction in which there are likely to be further uses of electrochemistry in the marine field. The existing experience with hypochlorite cells could constitute the fore-runner of further vigorous developments and it could well be that a new industry in marine electrochemical engineering is taking root.

References

1. J.B. COTTON, Chem. Ind., London, 28th April 1958, p. 68.
2. J.B. COTTON, Pat. Metals Rev. 1958, 2, 45.
3. I. DUGDALE and J.B. COTTON, Corrosion Sci., 1964, 4, 397.
4. R. JUCHNIEWICZ and P.C.S. HAYFIELD, Proc. of 3rd Int. Congress on Metallic Corrosion, Moscow (1966).
5. A.F. ADAMSON et al, J. Appl. Chem., Nov. 13th (1963).
6. British Patent 1184791, 15.6.66.
7. Can. Pat. 756595 (1967).
8. L.H. SHAFFER and R.A. KNIGHT, J. Electro Chem. Soc., Electrochemical Technology, November (1969).

Impressed Current Cathodic Protection as Applied to Desalting Plants

G. Dittmeier and P. Byrne
Burns and Roe, Inc.
P.O. Box 663
283 Route #17 South
Paramus, N.J. 07652

The Clair Engle desalination plant located in Chula Vista, California, is a multi-stage, multi-effect flash distillation plant operating up to 280°F (137.78°C). The first effect steel recycle line carries hot, concentrated brine from various parts of the I Effect at temperatures around 225°F (107.22°C) and velocities of 2-1/2 - 6 ft/sec (.762 - 1.83 meters/sec). The corrosion rate in this pipe is about 60 mils (1.538 millimeters/year) per year with much greater corrosion at impingement points, especially elbows. Accordingly, this 133 feet (40.54 meters) of 16 inch (.406 meters) nominal diameter piping is subject to numerous corrosion failures at impingement points after around two years of operation. Also, the general corrosion will approach the maximum allowable for piping carrying 225°F water at 40 psi (2.8 kgm/sq cm) pressure in this time.

It was decided to evaluate the effectiveness of an impressed current cathodic protection system to protect this pipe after intermittent operation for 1-1/2 years. An impressed current system is the only type of cathodic protection that would provide sufficient current density to adequately protect the above piping. Impressed current cathodic protection systems have been successfully applied to marine environments in the past (1,2,3,4).[1] Application of this technique to hot brine in desalination plants has had limited application due to the estimated high current requirements. (3,4)

Equipment

The importance of constant protection and low maintenance costs has resulted in the selection of the automatic potential control (APC) system for protection of steel in a hot brine environment. This system has been described in the literature (3) and consists of a DC power supply, inert anodes, reference cells, and a potentiostatic controller as shown in Figure 1b. These components are interrelated as follows to achieve the objective of maintaining a protection fixed potential on the steel surface (vs. the $Ag/AgCl_2$ reference cell): the potentiostatic controller is fixed at the desired automatic control setting (usually 0.85-0.9 V vs. the $Ag/AgCl_2$ reference cell); the DC current supply furnishes sufficient current to the "inert" platinized titanium electrodes to maintain the above potential setting; the $Ag/AgCl_2$ control reference cell electrode signals the potentiostat so that the correct current is supplied to maintain the potential setting; the auxiliary reference cell electrode checks on protective voltage conditions down the line.

[1] The numbers in parentheses refer to the list of references at the end of this paper.

Environment

The above automatic potential control system was installed in 133 feet of 16 inch diameter carbon steel piping in the Clair Engle (desalination) plant (CEP) located in San Diego, California. A portion of this installation is shown in Figure 1a. The brine conditions are as follows: temperature 202-241°F (94.44-116.11°C), concentration 1.2 that of sea water, velocity 2-6 ft/sec (.610-1.83 meters/sec). Detailed data on the six applications are given in Table 1. The sea water chemical composition, pertinent to its corrosivity was: O_2-10 ppb[2], Cu-0.75 ppm, Fe-0.6 ppm. The brine was treated to achieve low alkalinity (i.e., low carbonate content) at a final pH in a range close to neutral (6.8-7.1).

Purpose

The purpose of the APC CP installation in the above plant and environment was to establish: a) the effectiveness of the system in reducing the prevalent high steel corrosion; b) the operating and maintenance characteristics of the unit; c) the economics of the unit vs. other means of protection--based on (a) and (c) and cost background.

Preliminary Design Studies

Preliminary to the design of the above installation, certain laboratory studies were conducted which showed that the initial polarizing current densities for steel range from 8 to above 200 ma/sq decm. Curve "a" in Figure 3 shows laboratory data on the effect of velocity on current density requirements for protecting steel with a potentiostatically controlled potential of 0.9 V (vs. the $Ag/AgCl_2$ cell). These conditions were on new steel at about 85°F (29.44°C) in artificial sea water. Note the sharp rise in current requirements above velocities of 1 ft/sec (.3048 meters/sec). For comparison, similar data cupro-nickel and aluminum were plotted in a similar fashion, as shown in curves b and c in Figure 3. Note the lower current density requirements to protect aluminum alloys vs. more noble metals. Conditions were the same as for the steel specimen. Figure 5 shows the effect of different control potential levels on current density requirements vs. velocity. Here, it is interesting that again above 1 ft/sec there is little difference in current requirements at various potential settings. Figure 4 is a plot of data obtained on the effect of brine temperature on current density requirements for steel under 0.9 V potentiostatic control. Here, the effect of temperature on current density requirements for steel becomes very significant above 150°F (65.56°C). Figure 2 shows the effect of salinity on current density requirements. The effect of salinity is less marked than that of temperature velocity.

Design Details, Initial Operation Characteristics

Based on the above data (Figures 2-5) for steel, design estimates were made on the current density requirements on new steel for the various units. These estimates are illustrated in Table 1 which gives data on each application along with environmental background information. The actual current density requirements, after a break-in period, are shown in Table 2. Overall, the initial design estimates for current density requirements were 1150 ma/sq ft to 2,460 ma/sq ft (123.79 to above 264.8 ma/sq decm). As can be seen in Table 2, design estimates of current were on the order of two times too high. This is to be expected since the polarizing effect of cathodic coating depositions is not predictable.

---

[2]parts per billion

Table 1, also presents data on rectifier sizing (maximum and minimum amperage capacity at 12.5 V). Other design criteria were number and type of anodes, spacing of anodes, and the location of the reference cells. The laboratory data on steel shown on Figures 1-4 plus proprietary data derived from experience formed the basis for the CP design: anode spacing of two feet, reference cell to nearest anode distance of about 20 inches (.508 meters). Too great a distance results in over-protection. The inert anode selected was platinized titanium with a large area to achieve low resistance. Laboratory tests showed low abrasion damage at prevalant sea water velocities (5 ft/sec or 1.524 m/sec) even in the presence of silica grit which ruined a pump. Among common anode materials, graphite, high silican iron, lead-silver, platinum surfaced anode materials have an operating cost of about 1/4 that of the nearest competitor (lead-silver).

The $Ag/AgCl_2$ reference cell was selected based on experience in sea water cathodic protection applications as this cell is least affected by pollutants such as organic matter normally found in sea water.

The rectifiers incorporated excess capacity to allow for current demand surges during startups. A breaker system and a current limiter were incorporated to prevent damage to rectifier components when current demand was unusually high.

Operation and Assessment

Figure 1a shows a typical configuration of piping being protected with anode and reference cell spacing, and coupon locations shown. Assessment of corrosion was done by three methods: ultrasonic wall thickness measurements, weight loss on steel coupons (coupled and insulated), and instantaneous corrosion rates by polarization current measurements. The last method was later abandoned due to current interferences.

The APC cathodic protection apparatus as shown in Figure 1b schematic was operated as follows: the protection setpoint (automatically controlled) was established at 0.8-0.9 volts, initially. The current limiter was adjusted so that the circuit breakers would operate at the capacity level of the rectifiers. The system is only operated when the pipelines are flooded. With switches on, the APC system automatically controls the setpoint voltage supplying the necessary current. The six applications in the system are monitored 3-4 times a day as follows: a) the control setpoint voltage is checked; b) the actual control reference cell and the auxiliary reference cell readings are taken and, c) the amperage drawn is recorded. The reference cell readings will often vary from that of the control voltage setting, particularly the auxiliary cell which is positioned further away from the control reference cell. Differences indicate degrees of under overall protection and, accordingly, these are indications of how well the automatic potential control system is functioning. Occasionally, reference cells must be cleaned or replaced, otherwise operating and maintenance labor is low on the APC compared to manual systems.

However, although the operating costs are lower than the manual type cathodic protection system, the capital cost is higher because of the extra electronic equipment required for automation. On balance, the APC unit is less costly than a manual system due to labor savings and better cathodic protection control providing the system is operated 8 years or longer.

Results - Operational

The experience with the equipment after 1-3/4 years operation has been on the overall satisfactory. Specifically, the following operating experiences was had on each component:

a. Anodes - No problems or replacements to date.

b. Reference Cells - The most bothersome malfunction in the system (as described above) is where control conditions are not maintained due to reference cell pluggage or deterioration. Here, reference cell potential is much below the control setting and current draw consequently is much too great. This situation is correctable by cleaning or replacing the reference cell. It is hoped that re-designing of the reference cell will overcome this problem. At the minimum, retractable type cells are required.

c. Often reference cell and resulting control malfunctions, particularly after startups, were self-correcting requiring none of the work described under (b) above.

d. Only one type of malfunction, premature breaker tripping or failure, was experienced with the rectifier system. This problem was temporarily overcome by raising the set potential gradually. The faulty breakers will be replaced.

Current Requirements vs. Time - Figure 6

Figure 6 shows current draw vs. time for Application 12 for eleven months. These data indicate the following: current requirements after startup drop with time to values 1/2 - 1/6 these at startup; each shutdown and restartup greatly increases current demands which again drop to much lower values; the final current after eleven months' demand is not any lower than a minimum point after one month.

Operating Data

Table 2 summarizes some typical operating data on the APC cathodic protection system. Minimum operating current densities after three and six months reflect the drop in current requirements due to polarizing scale build-up. However, as can be seen in Figure 6, operating currents vary widely depending on how soon after a shutdown the data is taken.

Corrosion

The corrosion prevention results of operating the cathodic protection system are shown in the following three tables. Table 3a shows the corrosion results for the first period at the potential setpoints illustrated. The methods of assessment are by ultrasonic wall thickness and coupon weight loss. Here, the corrosion protection given by the CP system was excellent, a reduction in weight loss from 50 mpy to 5-8 mpy (1.282 to .128-.205 millimeters per year). The current density requirements ranged between 870 and 1420 ma/sq ft (93.65 and 152.85 ma/sq dm) (vs 1150 and 2460 ma/sq ft (123.79 and 264.80 ma/sq dm) in the original estimate).

The corrosion results during the second phase were not as favorable. Here, as shown in Table 3b, the potential setpoint was lowered in accordance with the assumption that the heavy scaling found would be protective. The weight loss data was practically useless due to semi-conductive scale bridging between the coupon and the pipe wall. The ultrasonic thickness results, as shown in Table 3b, indicate poorer corrosion protection than with the higher potential setpoints. The setpoints were then raised back to close to the original points. The corrosion results are shown in Table 3c. Here it is apparent that the higher setpoints are not consistently more protective. The results from this experiment were inconclusive. There appears to be no advantage to operating at lower potentials particularly when there was no consistent drop in current density requirements. As can be seen by Figure 4 mentioned earlier, a higher potential does not increase current requirements greatly at velocities

above 4 ft/sec (1.219 m/sec).

The effect of various achieved steel potentials vs. $Ag/AgCl_2$ cell on pipe corrosion is summarized in Figure 7. Potentials below 730 mv do not achieve adequate protection whereas potentials above about 900 mv do not achieve increased protection.

Scale

The heavy scale deposition on all the steel surfaces resulted from reduction of dissolved Cu and Mg components in the sea water (levels were 0.75 and 4250 ppm, respectively). The scale composition was 68% Cu and 24% $Mg(OH)_2$ at an average thickness of 3/8 inches (.114 meters) after 1-1/2 years of operation of the CP unit. It was thought that this scale was formed due to over-protection on the unit initially (setpoint voltages of 0.9 V) and that the protection could be reduced as a result of this scaling. This has not proven to be quite the case although the scaling appears to be continuous. The scale is conductive, however, with a resistance of only 100 ohms on a 3/8 inch thick, 1 inch (.0254 meters) square distilled water saturated specimen.

Summary and Conclusions

Corrosion Protection

Overall, the unit has provided excellent protection of the steel piping as evidenced by the UT wall thickness measurements and the notable lack of piping failures at high velocity points (e.g., elbows). There have been many failures on unprotected steel piping in a similar environment.

Operational Problems

As can be seen in the below conclusions on economics, maintenance was a major economic factor. This was due to:

a. The need for a once per day minimum monitoring.

b. Periodic reference cell cleaning or replacement (labor a large factor here). The reference cells fouled every 3-4 months. One electrode failed in 1-1/2 years.

c. Occasional electrical work--usually circuit breakers and wiring repair.

Effect of Cathodically Deposited Coating

The coating (Cu and $Mg(OH)_2$ deposited on the cathodic (pipe wall) did not materially reduce cathodic protection power requirements. However, the data does indicate that the coating formed during the initial operation of the CP unit did reduce current density requirements.

Use of Steel Coupons to Monitor Corrosion

Due to the above coating deposition, weight loss data from steel coupons no longer were a valid method of measuring the effectiveness of C.P. after eight months of operation. This left ultrasonic measurement of pipe wall thicknesses as the only useful method.

Current Density Requirements

Current density requirements were very high, as expected, but not as high as originally predicted based on laboratory work. Current density drops gradually with operating time but reverts to much higher values after

a shutdown of more than 2-3 days.

Economics

A preliminary economic analysis was carried out to complete this study. In summary, the cathodic protection system described above is uneconomical compared to substituting a proven corrosion resistant material piping material such as copper-nickel for steel. However, the economical study made is based on a custom built experimental unit. The capital costs of this system do not necessarily reflect the true cost of an optimum commercial unit which would incorporate the benefit of design and maintenance economics derived from the operating experiences described above.

The results of this economic study are given in Table 4. The cost of protection, based on a 20 year amortization, is $4.66/sq ft/yr ($50.16/sq meter/yr) compared to $1.35/sq ft/yr ($14.53/sq meter/yr) for copper-nickel 10 piping substituted for steel. The principal cost factor for the CP unit was initial capital cost, including installation, closely followed by maintenance costs. Power costs proved to be of considerably less importance--a surprising development since current density requirements were unusually high.

References

1. J. A. H. Carson, "Principles of Design of Cathodic Protection Systems for the Hulls of Active Ships," Defense Research Board of Canada, Pacific Naval Laboratory Report 64-2.

2. G. G. Page, Corrosion Prevention and Control, (February 1964).

3. P. B. Byrne, "Automatic Anode Cathodic Protection for Marine and Offshore Structures," Materials Protection and Performance, p. 21, Vol. 10, No. 3 (March 1971).

4. G. H. Shroff, et. al., "Analysis and Summary of Reports and Data from the Freeport, Texas Test Bed Plant" (1961-1969), p. 247-249, U. S. Department of the Interior, Office of Saline Water, R & D Progress Report 759, December 1971.

Bibliography

J. H. Morgan, Cathodic Protection, Leonard Hill, Ltd., London (1959).

W. Matthewman, "More Developments in Automation of Cathodic Protection," Anti-Corrosion Methods and Materials, (August 1966).

TABLE 1

Design and Environmental Criteria - 16 Inch Applications Under C.P.

Appl. No.	Description	Temp.	Conc. Factor Conc. F. 1.0= 34,000 ppm Salinity	Velocity M/Sec.	Wetted Area sq. met. (Pipe Length, M)	Estimated Polarizing Current Density MA/ Sq. Dem.	Design Amps	Installed Amp Output Max.	Min.	# of Anodes	# of Reference Electrode
9	Recycle brine line to V-103 waterbox	91.1°C to 115.6°C	1.18	1.45	5.5 (4.3)	186	102	200	20	11	2
11	Salt water makeup to V-103	91.1°C to 115.6°C	1.0	1.91	7.7 (6.0)	264	204	150	15	10	2
12	Salt water makeup to V-103	91.11°C to 115.6°C	1.18	1.91	11.2 (9.0)	264	296	400	40	20	2
13-1 and 13-2	Flashing brine make-up from V-104 waterbox	91.1°C to 112.8°C	1.4 (est)	1.45	14.9 (12) 7.43 (5.5)	177	264 132	300 150	30 15	31 (Tot)	4 (Tot)
14	Flashing brine between V-105A and V-104	91.1°C to 112.8°C	1.4	0.78	4.9 (3.81)	123	61	100	15	8	2

TABLE 2

Design and Operating Data - CP System

Appl. No.	Wetted Area sq. Met	Design Amperes	Design Current Density	Operating Amperes After: 3* Mos.	Operating Amperes After: 16** Mos.	Operating Current Density, ma/sq After: Decim. 3 Mos.	Operating Current Density, ma/sq After: Decim. 16 Mos.	Control Potential Setting MV 3 Mos.	Control Potential Setting MV 16 Mos.	Actual Potential, MV 3 Mos.	Actual Potential, MV 16 Mos.
9	5.5	102	186 ma/ sq dem.	55	60	101	107	800	820	800	900
11	7.7	204	265 ma/ sq dem.	110	35	143	45	900	820	760	830
12	11.2	296	265 ma/ sq dem.	110	30	99	27	800	840	830	1000
13-1	14.9	264	178 ma/ sq dem.	140	50	95	34	940	710	790	1130
13-2	7.4	132	178 ma/ sq dem.	70	30	95	40	920	810	910	880
14	4.9	61	124 ma/ sq dem.	75	30	152	61	950	800	910	1100
TOTAL		1059		580	235 (61% reduct.)						

*March 1971
**July 1972

TABLE 3a, b and c

Cathodic Protection System - Corrosion Data

	a				b				c			
Time Per.	4/28/71-8/24/71				8/24/71-3/7/72				3/7/72-8/2/72			
Applic. No.	Set Point mv	Potent. Obt. mv	Operat. Amps. (Curr. Dens.)	Corros. Rate MM/Yr	Set Point mv	Potent. Obt. mv	Amps (Avg. Curr. Dens)	Pipe Corros. Rate MM/Yr	Set Point	Potent Obt. mv	Amps (C.D.)*	Pipe Corros. Rate MM/Yr
9	800	800	55 (970)	.15-.20**	650	660	120 (1710)	.26	820	820	40 (680)	.39
11	900	760	110 (1320)	0-.14**	700	680-1050	120 (780)	0	820	820	50-65 (700)	.25
12	800	830	110 (920)	0-.12	800	790	105 (766)	.26 .61	830 840	860	25-35 (250)	.05 .21
13-1	940	790	140 (873)	.12	710	710	140 (560)	---	710	1000	40-45 (270)	---
13-2	920	910	75 (1420)	----	800	760	75 (730)	---	810-830	810-830	25-35 (375)	---
14	950	910	75 (1420)	----	700	1050	30 (570)	---	800	1001	30 (565)	---

Unprotect. 1.39 mmpy

*Avg. Curr. Density
**Coupon

TABLE 4

Economic Analysis of Impressed Current
C.P. System Vs. Cu-Ni 10 Piping

Basic Assumptions

Piping Area Protected - 51.6 sq. meters
Total Length of .48 M Nom. Piping - 40.5 meters
Length of Amortization - 20 years
Cost of Electricity - 1¢ per Kw Hr.
C.P. System Voltage - 11V
Conversion Factor, AC to DC - 1.21
% of Operation/Yr - 80% or 6960 Hours Oper/Yr

Operational Data/Year

Avg. Current Draw per Unit - 50 A
No. Units - 6
Cost of Maintenance/Yr: (a) Manpower (6% man) = $ 800
(b) Materials = 200
Total $1,000

Amortized Cost of Installation - $\frac{\$26,000}{20\ Yrs.}$ = $1,300/Yr.

Power Costs

60 A x 11 V x 1.21 x 6 units x 6960 Hr. x 1¢/Kw Hr = = $300

Total Costs/Year

C.P. Unit	Cu-Ni Replac. (cost above steel)
$1,000	$\frac{\$15,000}{20\ Yrs.}$ = $7,500/Yr or
1,300	
300	
$2,600 or $50.16/sq meter/yr	$14.53/sq meter/yr

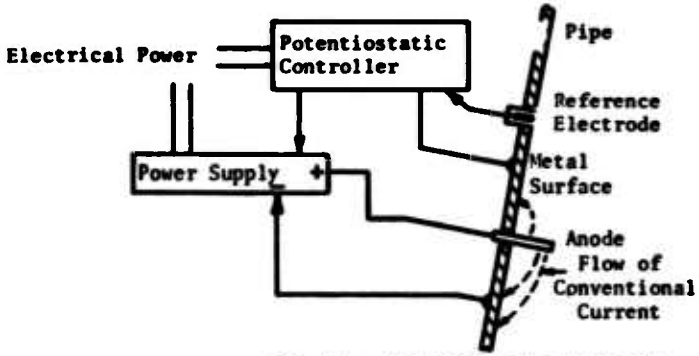


Fig. 1b. Schematic of a Cathodic Protection Unit (One Each Application)

Fig. 1a. Front View of Vessels V-103 and V-104 Showing Piping Application Under Cathodic Protection.

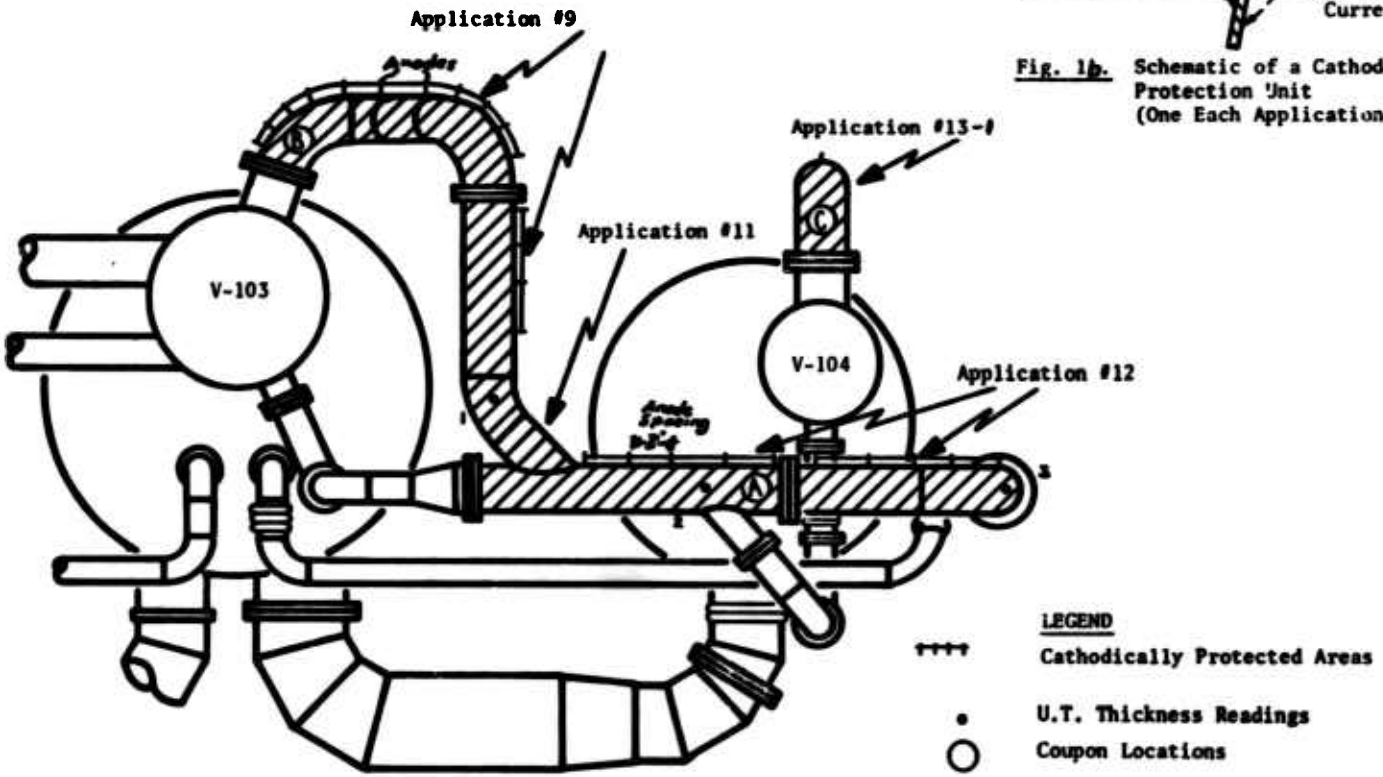


FIGURE 2

CURRENT DENSITY VS. SALINITY

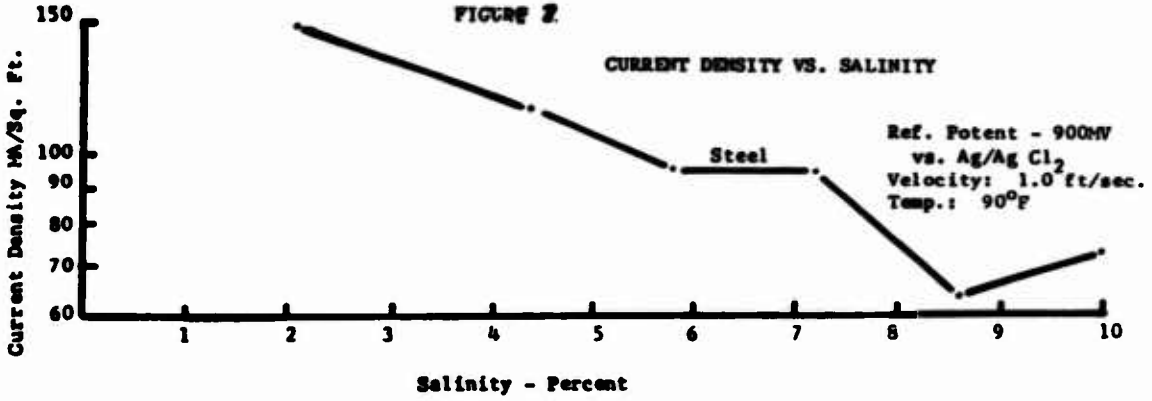


FIGURE 9

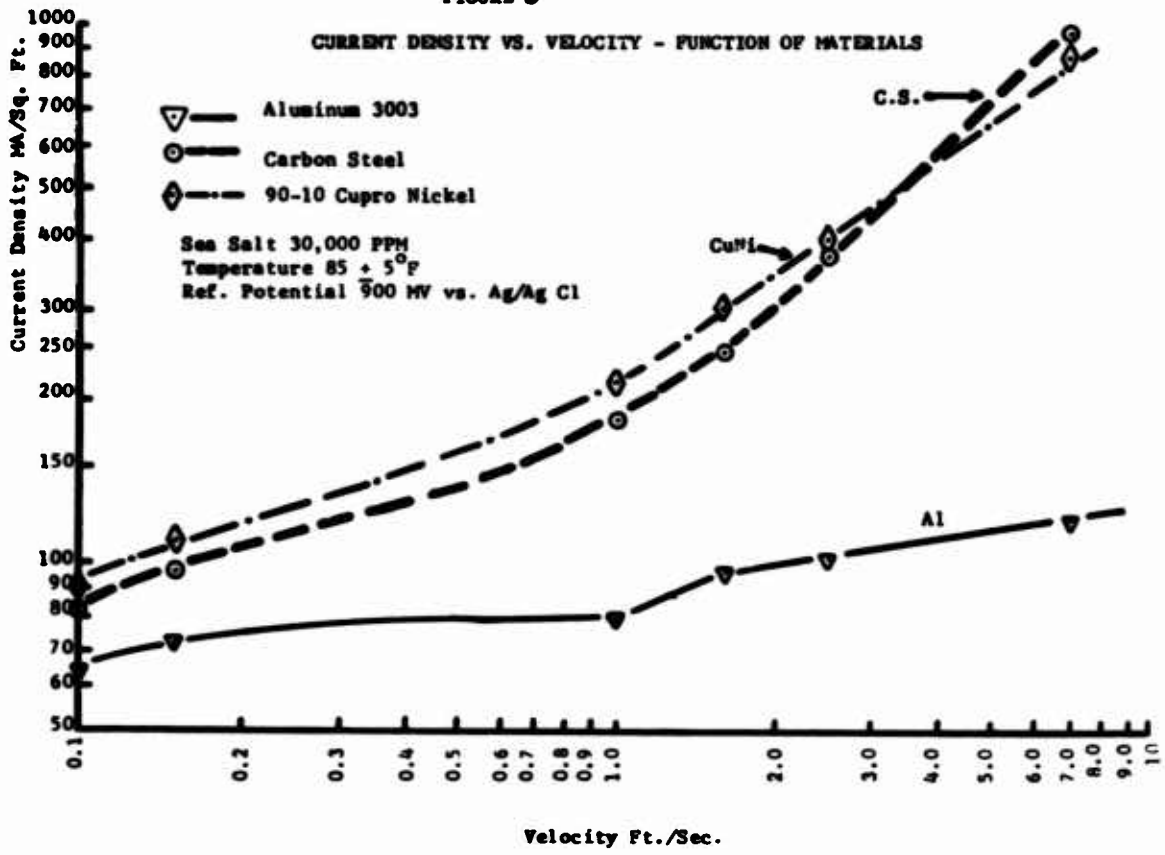
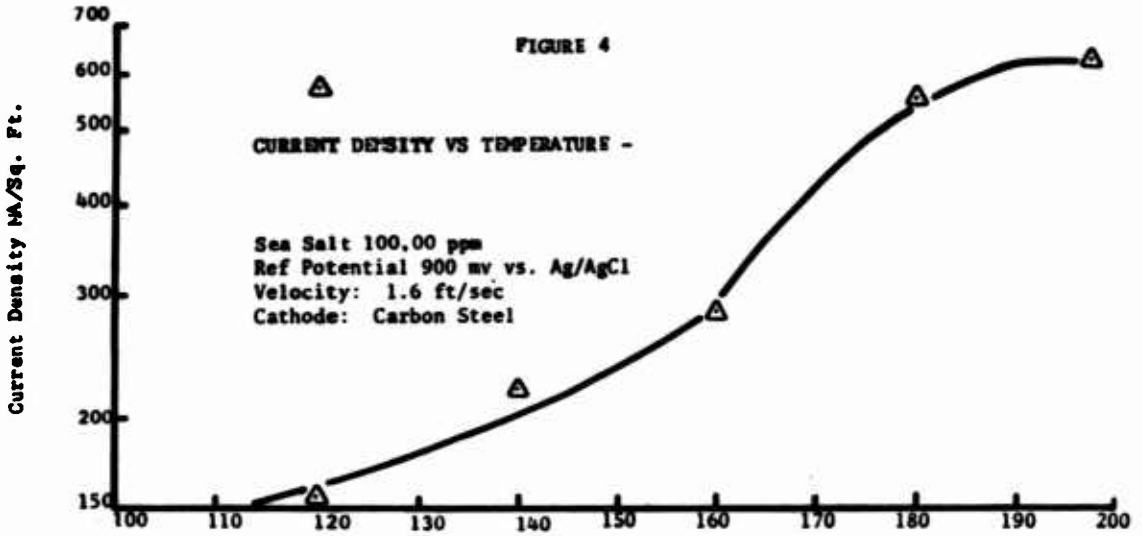

CURRENT DENSITY VS. VELOCITY - FUNCTION OF MATERIALS
Aluminum 3003
Carbon Steel
90-10 Cupro Nickel
Sea Salt 30,000 PPM
Temperature 85 ± 5°F
Ref. Potential 900 MV vs. Ag/Ag Cl
C.S.
CuNi
Al
Current Density MA/Sq. Ft.
1000
900
800
700
600
500
400
300
250
200
150
100
90
80
70
60
50
0.1
0.2
0.3
0.4
0.5
0.6
0.7
0.8
0.9
1.0
2.0
3.0
4.0
5.0
6.0
7.0
8.0
9.0
10
Velocity Ft./Sec.

FIGURE 4


CURRENT DENSITY VS TEMPERATURE -
Sea Salt 100,00 ppm
Ref Potential 900 mv vs. Ag/AgCl
Velocity: 1.6 ft/sec
Cathode: Carbon Steel
Current Density MA/Sq. Ft.
700
600
500
400
300
200
150
100
110
120
130
140
150
160
170
180
190
200

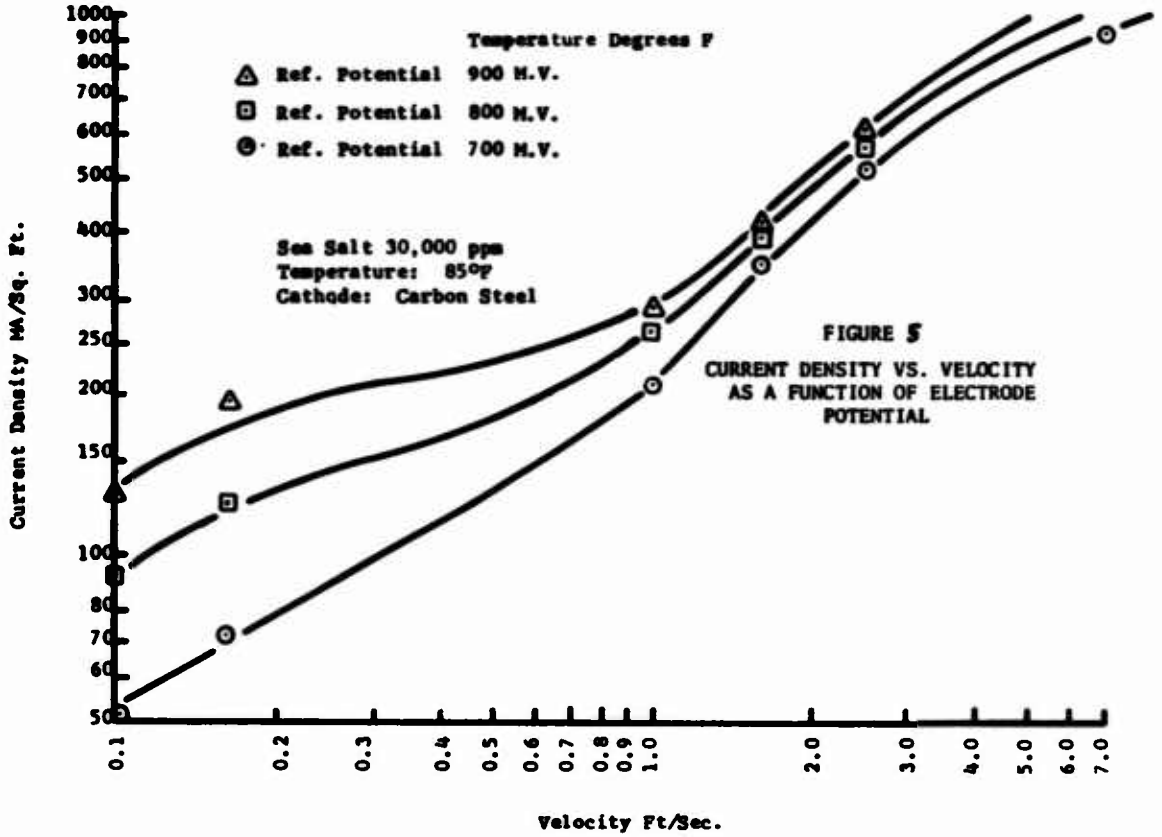


FIGURE 5

CURRENT DENSITY VS. VELOCITY AS A FUNCTION OF ELECTRODE POTENTIAL

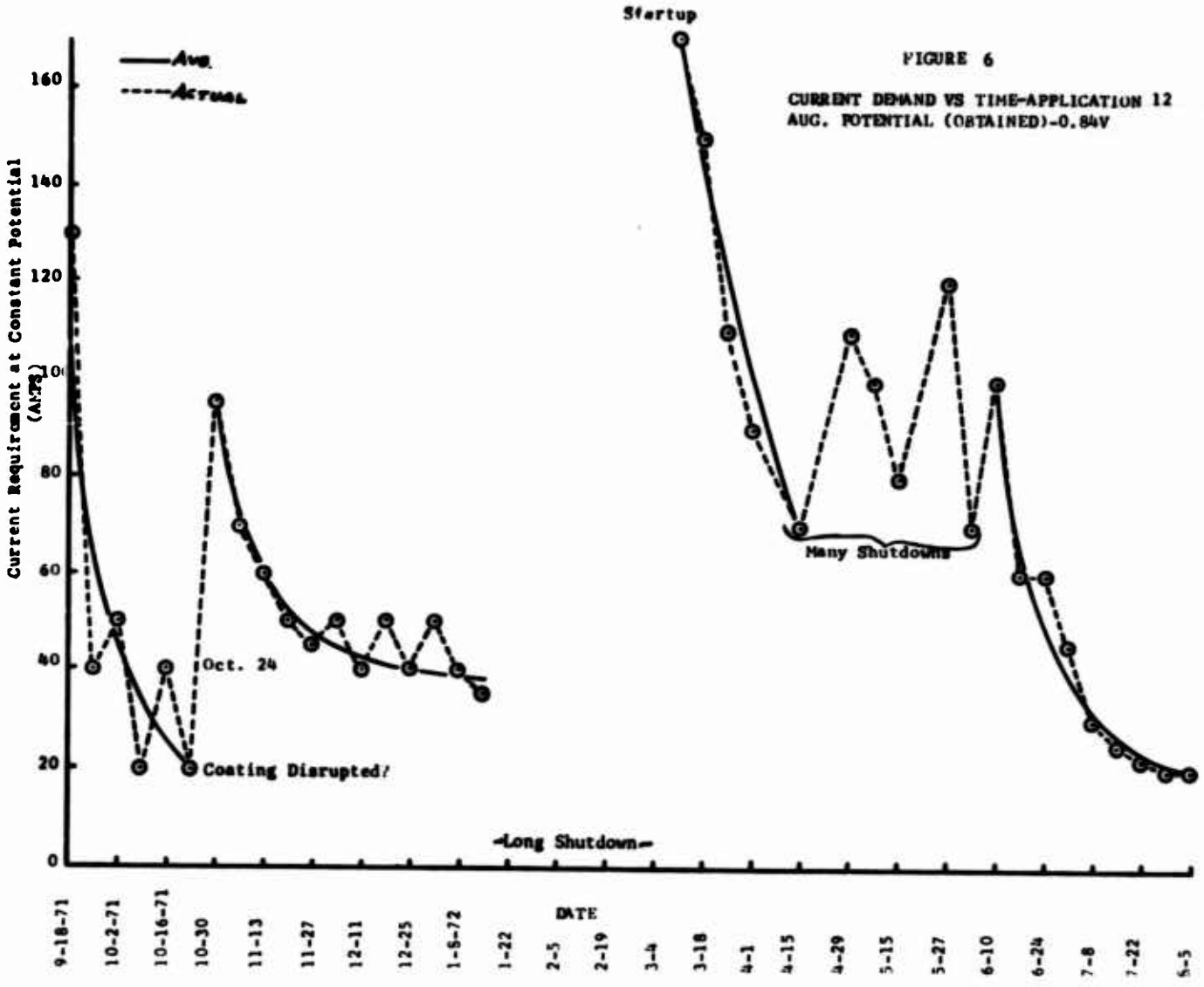
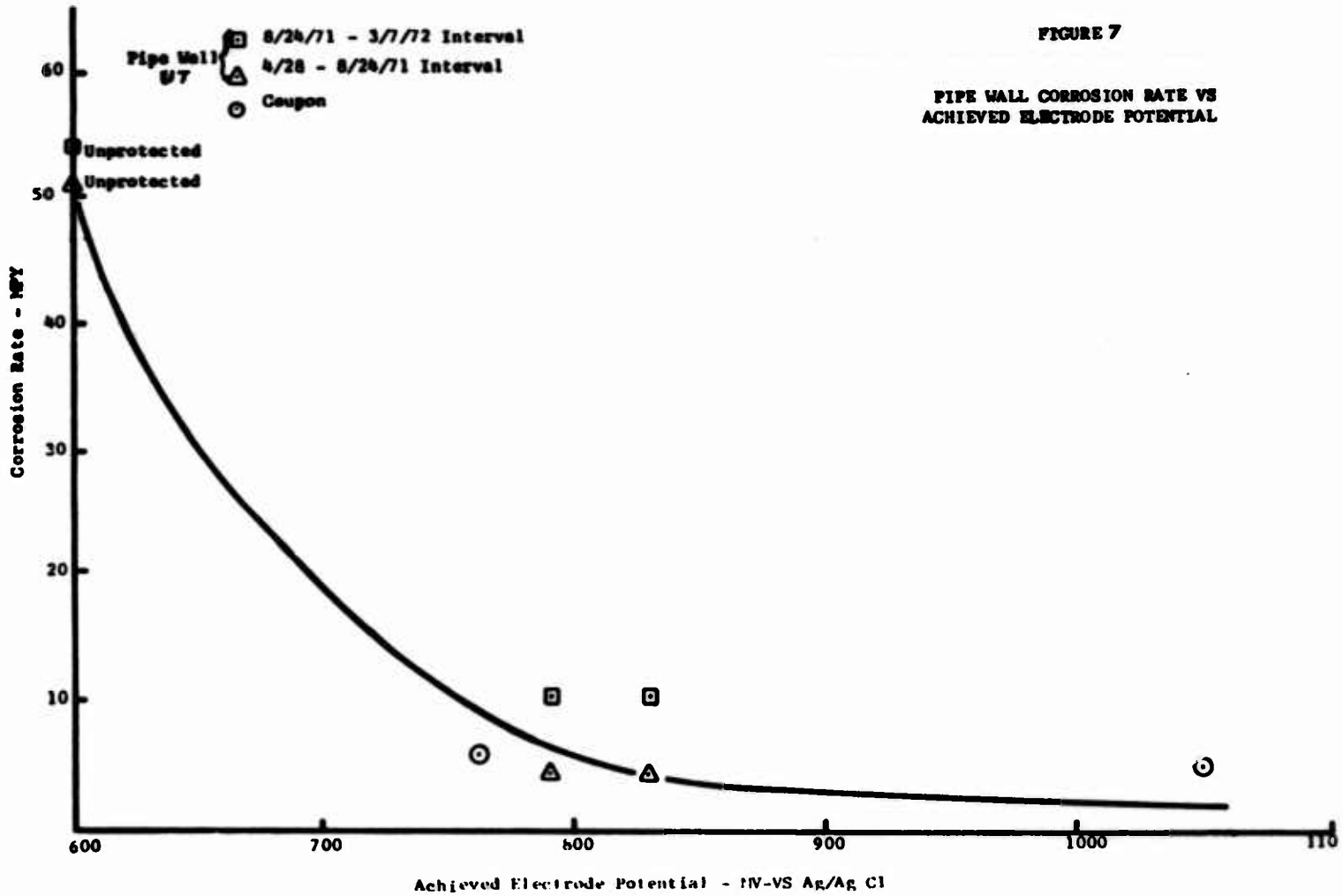


FIGURE 6

CURRENT DEMAND VS TIME-APPLICATION 12
AUG. POTENTIAL (OBTAINED)-0.84V

FIGURE 7

PIPE WALL CORROSION RATE VS
ACHIEVED ELECTRODE POTENTIAL



Discussion

Agawall: What would be the economics if you scale it up?

Dittmeier: Well, the economics would improve to some degree. I frankly do not think that it would be economical even on a larger scale compared to replacing the copper nickel pipe. It would just go in improving direction, that's all.

Morgan: In installing this system, you installed a very large capacity to get immediate polarization and the cost of this current is related to the amount of current it will deliver and not the continuous charge that comes out. It seems to me that you could have effected an economic saving by--and reduced the cost of the plant--to about a third. Why did you place the anodes so close together in such low resistivity sea water and why did you install capacity for immediate polarization?

Dittmeier: I would prefer that Mr. Byrne answer that question because he is the designer.

Byrne: We have had previous experience with LSW desalting plants and they are primarily designed for experimental evaluation. It is quite common to have the plants start up and shut down several times a day. The plants are drained. If you do not have a system that is going to achieve a polarization within a relatively short period of time, you don't get anywhere near the 90% reduction corrosion rate. Secondly, the data that had been available indicated very high current densities and we installed a number of anodes with the possibility then of removing anodes once they were in service. The initial data taken in aerated sea water indicated that at a 240°F and seven or eight feet per second you needed something of the order of 2000 milliamps per square feet in order to achieve immediate polarization. It is true the system did operate at roughly one-third the installed capacity, but the installation cost equalled the cost of the system and would not have been greatly reduced by reducing the amount of amperage installed. If you look at the paper, you will see 6% of a man-year is worth $1,000. Labor costs for installation and maintenance of this system are very high in the United States. I do not believe this may be true all over the world. So this essentialiy was a plant that was installed with the idea of achieving a 90% reduction because previous installations have always been installed on a lower capacity and for one reason or another could not achieve polarization and could not in fact prove that cathodic protection is at all practical at 240°F and seven or eight feet per second.

Cohen: I wonder if we can have Table 4 repeated which was the last slide. I think there was an arithmetical and based on that, I wonder if that affected the last number which you disclosed.

Dittmeier: That number has been corrected. The final number has been corrected. I know there were errors in it.

Walsh, Naval Ship Engineering Center: I have one question. You had stated earlier, this was a thousand gallon per day. Isn't this a thousand gallon per minute?

Dittmeier: I'm sorry, a million gallons per day.

Walsh: The other question would come up. You said you need instantaneous polarization because of the saline water office start ups and shut downs. On that basis, if you go into a real plant that is going to be producing for 24 hours a day for 20 years you do not need this sort of cathodic protection and it would be cheaper in the long run if you could go to the long term passivated system. So it could be economically feasible. Right?

Dittmeier: Yes. You could reduce the sizing of rectifiers and number of anodes in a continuously operating plant because you would not need such a high current demand all the time at each new start up. That is correct, but unfortunately most of the desalination plants in the world do not work very long before they shut down.

METHODS OF CONTROLLING MARINE FOULING IN DESALINATION PLANTS

D. C. Mangum, B. P. Shepherd, and J. C. Williams
Dow Chemical U. S. A., Texas Division 77541

Preliminary results have been obtained from a study of the feasible and economical methods of preventing marine fouling in desalination plants. The study is being done under contract with the Special Projects Division, Office of Saline Water, U. S. Department of the Interior. Experimental assessment of fouling is being made under simulated operating conditions employing control by water velocity, intermittent chlorination, intermittent heating, and toxic surfaces.

Velocity tests are being made by running seawater taken from the Gulf of Mexico through 3, 4, 5, and 6- inch pipes in series. Each pipe has one section of bare steel pipe and one of saran-lined pipe. The velocities are 1.7 to 6.8 fps. When the flow rate in the pipe is near the maximum at which organisms attach, which has been determined as approximately 3.5 fps, the lined pipe is fouled much less. The exfoliation of the unlined pipe produces areas where the surface velocity is less, thus permitting larvae to settle.

The other tests are being conducted by placing 3" by 12" asbestos-cement panels in troughs containing flowing seawater with appropriate experimental conditions. For the intermittent chlorination tests, four factors are being investigated: chlorine residual, cycle time, chlorination time, and water velocity. Initial results show that shorter cycle time and increased chlorination time are important factors in effective control. Another important feature is that continuous or frequent exposure results in a brown residue forming on the surface. This residue inhibits the fouling organism larvae from attaching. Three variables are being evaluated with the heat tests: cycle time, heating time, and water temperature. Results of the first phase show that cycle time and the time in the heated water are more important than the comparative water temperatures, as long as it is 30°F above ambient. Three materials are being used as toxic surfaces: 90-10 copper-nickel sheeting and two antifouling paints. The copper-nickel sheeting shows the most effective fouling control. Recommendations are made for operating procedures that will prevent fouling.

Introduction

A study to investigate the feasible and economical methods of preventing marine fouling in desalination plants is currently in progress at Dow Chemical U. S. A. at Freeport, Texas. The study is being done under contract with the Special Projects Division, Office of Saline Water, U. S. Department of the Interior. Experimental assessment of fouling control is being made under simulated operating conditions by employing water velocity, intermittent chlorination, intermittent heating and the introduction of toxic surfaces. Studies are being made on the chemistry of chlorine in seawater and the biological effects of chlorine in seawater. Upon completion of analysis and assessment of the experimental data, recommended optimum operating conditions will be outlined with consideration given also to the ecological impact.

Chlorine is an effective method of fouling control that has been in use for at least 50 years. A continuous residual of from 0.5 to 1.0 ppm will permit complete fouling control. Recent

studies show that chlorine may be deleterious to plankton when used in large amounts (1)[1]. Chlorine introduced into water where there are organic wastes can, by reaction, produce chloramines, which have been shown to be harmful to living organisms. Chlorination also apparently helps to stimulate attack on aluminum alloys, copper alloys and mild steel. Elevated temperatures will kill marine fouling organisms and heat has been used as a fouling control procedure. The effect of heated effluents on the environment has been the subject of much study and debate. Antifouling paints or toxic surfaces that do not foul rely primarily on the presence in solution of certain metal ions for their toxic effect. This method of control is facing increasing regulation because of the introduction into the water of these materials. Swifter flowing waters will prevent the settling of embryonic forms. The use of velocity has no extended effect on the environment, but power requirements to move the water are increased.

Any procedure or combination of procedures used to control fouling requires knowledge of the particular environment and careful planning in the design and application of the control systems.

The Gulf Coast, the Southern Pacific coast and the Caribbean area are the areas of greatest potential for shore installations of desalting plants (2). It is therefore appropriate that a study of fouling control be undertaken in the Gulf coast region.

Fouling occurs the year around at the Freeport, Texas, test site. The particular types of fouling organisms that are dominant depend upon the season and the location. Marine organisms of the Gulf of Mexico consist of species that are found in the temperate Atlantic and the tropical Caribbean waters. Less than ten percent of the species are endemic. The oyster Crassostrea virginica, the mussel Brachidontes recurvis, serpulids, and amphipods are predominant in the summer months. Barnacles, bryozoans, and hydroids are abundant in the winter months.

Test Facility

A test facility was built at The Dow Chemical Plant A location at Freeport, Texas, as part of the Office of Saline Water contract. Feed seawater to the facility was drawn from a large existing seawater canal by a stainless steel supply pump through a 6-inch suction line. The seawater was pumped through a 6-inch line to an open distribution box 14 feet long by 1-1/2 feet wide by 2-1/2 feet deep. This box served as a constant head source of seawater for the test channels. Construction was of plywood and lumber; the inside was epoxy coated. A lateral takeoff from the 6-inch supply line furnished seawater under pressure to the velocity test section. The flow rate varied from 150 to 300 gpm as required to produce the desired velocity.

The test channels were constructed of plywood and lumber and epoxy coated inside. They were 4 inches wide by 8 inches high, constructed in pairs and provided with covers. The 3" by 12" test specimens were placed on the bottoms of the channels and moved from one channel to the other as called for in the test schedule. Test channels were at a 3-foot height. Each set of channels was sloped slightly, with suitable flow straightening vanes, and weirs and baffles to control velocity. The toxic material specimens were the last specimens in each of the seawater channels. At the end of the troughs the seawater velocity was 4 fps. The test facility is shown in Figure 1.

Chlorine was supplied, by cylinder, through a standard chlorinator. Chlorine from the chlorinator passed to an injector - one for each of the 2 streams - where seawater from the injection pump forced the concentrated solution into the mixing pump where the solution is thoroughly mixed with additional seawater. This mixing reduced the time for the chlorine demand to be satisfied and for a stable point of chlorine residual to be reached. Each mixing pump discharged into a plastic reaction tank where an average holdup time of seven minutes permitted the chlorine demand to be satisfied. With the chlorine residual then stabilized, the chlorinated seawater flowed by gravity to the test channels. Two hot-water heating tanks with pumps which circulated water through the troughs were supplied so that

[1]Figures in parenthesis indicate the literature references at the end of this paper.

test specimens could be exposed to two different temperatures.

In Phase I of the study which lasted for five months, the chlorine and heat studies were done on a 2-level and 3-level multifactorial design, respectively. Information from these studies made it possible to go to a 2-level factoral design for both chlorine and heat studies. In this way, those areas of control that seem to be most promising could be examined more closely.

The test specimens were 3" by 12" boards. In Phase I these were ABS samples. In Phase II, now underway, they were black epoxy coated asbestos. These were moved from one trough to another at appropriate intervals. The effect of various control methods on the fouling organisms was determined by examining the 3" by 12" specimen plates. Each of the specimens was examined and an assessment made of the kind and amount of fouling. The following features were also noted about the growth of the specimens: the number of different species, the total number of individuals, the number of individuals per square inch, range of size of individuals, and whether they were dead or alive. The velocity pipes were disassembled and inspected. The final evaluation was then assessed by computer.

Chlorine Studies

In the studies of the effect of chlorine addition, four factors were evaluated: chlorine residual, cycle time, chlorination time and water velocity. During Phase I, two residuals were used: 0.5 and 3.0 ppm. Three water velocities were used: 1, 2, and 4 fps. Chlorination times were 6, 18, and 48 percent of the total cycle time of 4, 84 and 336 hours. During Phase II, two residuals were used, 0.25 and 1.0 ppm. Water velocity was 2 and 4 fps. Chlorination times were 7.5 and 15 percent of the total cycle time of 24 and 84 hours. The water velocities of 2 and 4 fps that was maintained in the troughs would vary as the specimen panels were added and as the level in the distribution box changed; even so, it did provide a different set of conditions to use with the chlorine tests.

Results from Phase I chlorine tests showed that the cycle time and interval length were the most important features. The shorter the intervals and the longer the treatment, the more effective the fouling control. Also, the computer analysis showed that the concentrations of chlorine (in this instance 0.5 ppm and 3.0 ppm) did not show much difference in their effect. The higher water velocity of 4 fps, in contrast with the 2 fps velocity, seemed to enhance the effect of chlorine. The results of the chlorine tests are shown in Table I, and two sample panels are shown in Figure 2.

The 4-hour and 84-hour cycle times were much more effective in controlling fouling than the 336-hour cycle time. In the 4-hour cycle, control resulted when the plates were exposed 18 and 48 percent of the time. Six percent exposure at a 4-hour cycle did not result in complete fouling control. For the 84-hour cycle time, fouling control resulted from exposure for 18 and 48 percent of the time. However, at 6 percent of the time at 1 fps, there was a growth of barnacles that was moderate to heavy. For the 336-hour cycle time, fouling control resulted from the 48 percent exposure and even by 6 percent exposure, with the flow at 4 fps. However, overall the 336-hour cycle time did not appear to be satisfactory.

During Phase II of the tests, as seen in Figure 3, oysters were the dominant fouling organism. Their growth was not prevented by the 1-3 hour exposure to chlorinated seawater every 24 hours. The most effective method of control was the 12 hour exposure every 84 hours in conjunction with 4 fps velocity. However, there are variations to the flow as the panel is added to the stream, as would be true in actual practice, since there would be velocity variations at the joints and dead spots in the pipes.

Experiments were run to determine if there was a periodicity to the barnacle activity that might be interrupted by an appropriate chlorination cycle. However, the barnacle, Balanus eburneus, has a continuous pumping-rest-pumping cycle that did not exhibit a diurnal or tidal periodicity. Addition of chlorine at any time would effect its activity. Also, an experiment was run to determine the specific effect of the addition of chlorinated seawater on the rhythmic pumping movements. When the chlorine was added the pumping did continue but the rhythmicity was altered and the pumping stroke changed. The barnacle did not, however, close its shell and retreat from the hostile environment.

An unusual aspect to the chlorine studies appeared after several weeks. A brown residue formed in the chlorine troughs and on the specimen boards that were put into the chlorine frequently, or for long periods of time. The barnacles did not settle on these boards. There was a period of several weeks when the troughs that had been used for the 3 ppm and 0.5 ppm chlorine did not have chlorinated seawater in them. Natural seawater was run through all of the troughs. After the first week, there were no barnacles in the troughs that had been used with the chlorinated seawater. There was a very noticeable brown residue on the sides of the troughs. The brown residue from the surfaces of several specimen boards, and some of the residue collected from the chlorine troughs were analyzed. The first analysis was made by infrared spectroscopy, and revealed that the brown residue contained silicon dioxide and an inorganic carbonate. Further tests made with a scanning electron microscope showed a comparatively high amount of manganese as shown in Figure 4. Manganese in the brown residue was much in excess of any other substance other than silicon.

The chemistry of chlorine in seawater is very complex and not fully understood, but the presence of the brown residue may be explained as follows. When chlorine is introduced into seawater, there is a slight shift in pH, and the smaller particles of the silt tend to coagulate and settle out. This silt is a montmorillonite clay and contains a certain amount of aluminum and magnesium. Manganese is present in seawater in the divalent form. The strongly oxidizing hypochlorite oxidizes the divalent manganese to the less soluble tetravalent form, and it precipitates out with the coagulated clays.

The exact reason why the residue deters the settling of the fouling larvae has not been determined. The residue did form under varied conditions of water turbidity. If it is a usual feature of the chlorination of seawater, it would mean that a deterrent surface can be formed on intake surfaces by continuous chlorination for a period of several weeks and then if conditions warrant it, intermittent treatment would control the fouling.

Temperature Effects

Heated water has been used in a number of instances to control fouling. It is most often utilized as an intake-outfall reversal in power plants where there is an abundant supply of heated water. Heat would be an appropriate control measure at a desalination plant built in conjunction with a nuclear reactor.

In the heat test, three variables were evaluated: temperature, cycle time, and heat time. For Phase I the temperatures were 102, 111, and 120°F. Cycle times were 336, 168, and 84 hours with 1/2, 2 and 8 hour exposure times. The ambient temperature during Phase I varied from 60°F to 70°F. Phase II of the heat experiments involved two levels of temperature, 104 and 112°F. The heat cycles were 84 and 168 hours and the exposure times 1/2 and 2 hours. The ambient temperature during these tests ranged from 75 to 84°F.

The results from the Phase I experiments were analyzed by computer. The amount of time exposed to the heated water is more important than the particular temperature if it is 30°F above ambient. The shorter cycle time is more effective. For the 102°F heat, the 336-hour cycle did not give effective control of the barnacles. However, the cycle time of 168 hours and 84 hours at 102°F, with exposure times of 2 and 8 hours were effective in controlling the fouling. The results with the 111°F and 120°F temperatures were nearly identical for comparable cycle and exposure times. The 336-hour cycle resulted in light fouling, but the 168 and 84-hour cycles, even with 1/2-hour exposure, resulted in control of fouling. Two panels from Phase I are shown in Figure 5.

Results from the first three months of the Phase II tests showed that the water temperature must be at least 30° above ambient for control. In these tests the panels that were exposed to the 104°F water, which was 20°F above ambient, were fouled by a number of oysters that are growing quite well. In fact, it seemed that the occasional immersion in the warmer water helped to remove the amphipod tubes and permit the oysters to grow even better. The panels that were exposed to the 112°F water were not fouled as shown in Figure 6. Other studies (4) have shown that for effective fouling control water temperature should be at least 30° above ambient.

Velocity Studies

If water is moving fast enough fouling is completely prevented because the organisms cannot settle and are torn off by the surface turbulence. This requires a velocity at the surface of at least 3.4 fps. In practice a velocity in excess of this would be required and the structure of the system has to be such that joints and elbows do not provide dead spaces where the larvae can attach.

Experiments with barnacle larvae showed that attachment cannot take place if the water velocity at the interface surface is in excess of one meter per second. However, once the cyprid is attached it cannot be pulled from the surface by much faster velocities.

Velocity tests were performed by running seawater through 3, 4, 5, and 6-inch pipes in series at a rate sufficient to provide the desired velocities. Two types of pipe were used, bare steel and plastic-lined pipe. A turbine flow meter was located between the 3 and 4-inch pipe and the rate of flow was monitored.

During Phase I of the velocity tests, there was a flow of 300 gallons per minute through the pipes with resulting velocities of 3.4 fps to 13.6 fps. Virtually no fouling occurred. After the second inspection the flow rate was reduced by half to 150 gallons per minute. This produced a velocity of 1.7 fps in the 6-inch pipe and 6.8 fps in the 3-inch pipe. The fouling was controlled by a velocity of 3.8 fps or more and there was no fouling in the 3-inch pipe. However, in the 4-inch pipe, which had a flow rate of 3.8 fps, fouling built up in the unlined section. The lined section of this pipe at the same velocity was not fouled. The unlined pipe had begun to rust, and as exfoliation occurred, an uneven surface was produced where the velocity was reduced and larvae could attach. In the 5-inch pipe, with a velocity of 2.4 fps, the lined section had much less fouling than did the rusted unlined part. For the 6-inch pipe, where the flow rate was 1.7 fps, the lining showed no advantage. Both parts of this pipe, lined and unlined, showed heavy fouling with a growth of barnacles, byrozoans, hydroids, and anemones, and all of the minor fouling species. These studies show that smooth plastic surfaces are able to help control fouling when the water velocities are in the range of 3.5 fps and greater.

Results from the tests using toxic materials revealed that at least two types of antifouling paint tested did not prevent the attachment of barnacles after the first month, as shown in Figure 7. The 90-10 copper-nickel plates prevented fouling except for a build up of amphipod tubes.

Application of Fouling Control

Fouling should be anticipated in the design of any seawater desalination plant and provisions should be incorporated in the design for the control of fouling. Depending upon the biological conditions encountered at a particular site, either chlorination or heating will likely be the control methods of choice, possibly assisted by an increase in velocity.

Chlorination systems should be equipped for continuous monitoring of chlorine residuals and should be installed in such a way that complete mixing of, and diffusion of, the chlorine in the intake water is achieved. Stagnant areas and pockets are to be avoided as these areas aid the attachment of fouling organisms. Smooth plastic lined pipe would help to prevent fouling if the water velocity is over 4 fps. The smooth surface of the lined pipe would also tend to accumulate the inhibiting residue that is often formed when seawater is chlorinated.

Test blocks and, perhaps, glass sight ports placed in pipelines will permit a monitoring of the degree of fouling present. Forecasts of fouling conditions at a site, based on fouling communities already present on submerged structures, or on the fouling experience of existing plants in the vicinity, are all subject to great inaccuracies. Many instances are cited of plants located close together with very different fouling problems. The growth rate of organisms in an intake tunnel can be many times that in quiescent waters nearby. There is even the possibility that the effluent from the plant being designed can alter the temperature regime of an area enough to make possible the luxuriant growth of a fouling organism not otherwise native to the area. The incorporation of provisions for fouling controls in the initial construction can avoid costly corrective construction later.

Any proposed method for controlling fouling in an intake pipe should assure that fouling growths never get started. This control would need to start during the construction phase when residual water in the partially installed portion of the line should always be maintained with a chlorine residual sufficient to prevent fouling growth. Upon completion of construction and start of operation, the seawater would be chlorinated at the inlet end on a continuous basis for at least two months, with a residual of about 0.5 ppm. When steady plant operation is assured, chlorination could be reduced to an intermittent basis. Treatment would depend on the season, but 12 to 24 hour treatment with 1.0 ppm every 84 hours would control barnacle fouling. Mussel or oyster fouling would require 12 hours out of 24 for complete control. Use of intermittent heated water has been an effective measure of control in many powerplant intakes. If ample heated water is available, weekly or biweekly flushing of the intake pipe with water approximately 50°F above ambient, would control fouling. Any water temperature that is used should allow for heat loss and still maintain a temperature of at least 30°F above ambient.

Test panels in the intake should be watched carefully and at the first sign of fouling, the frequency of chlorination should be increased until the maximum time interval between chlorination cycles which would prevent fouling had been determined. It will be necessary to watch the test panels for at least a year in order to determine changing needs for the periods and lengths of chlorination based on the possible seasonal appearance of different fouling organisms. Even after a complete seasonal cycle, test panels should be watched.

These studies are still in progress. More experiments will be undertaken on the fouling organisms and their response to various antifoulants. However, it appears that until new non-metallic antifoulants are developed, intermittert chlorine used in conjunction with a pipe velocity in excess of 4 feet will be the most effective method of control both from an environmental and an economical viewpoint.

References

1. A. J. Brook and A. L. Baker, Science. 176, 1414 (1972)

2. U. S. Department of the Interior, Saline Water Conversion Summary Report. p. 45. Supt. Documents (1972)

3. W. L. Chadwick, F. S. Clark and D. L. Fox, Trans. of the ASME. 72, 127 (1950)

Discussion

Question : Did you determine the chlorine demand curve?

Mangum: We did determine the chlorine demand. Ordinarily in those waters it was about four parts per million and it varied with the silt load from time to time, but in the winter sometimes now they say this has gone as high as twelve parts per million for a demand, but I haven't seen it that way.

Campbell: I am very interested in this brown scum and your finding that it had quite a lot of manganese in it. Now since it was produced by the clorination, I suspect that the manganese is probably there as manganese dioxide. If it is, it will be highly cathodic and may cause quite a lot of corrosion. So it may be a good thing from the point of view of keeping it clean, it may prove to be quite a bad thing from the corrosion point of view, and it is something that may be or need a bit of looking at.

TABLE 1

RESULTS OF CHLORINATION TESTS
Phase I

Cycle Time Hours	Chlorine Residual ppm	Chlorination Time (percent of total)	Water Velocity fps	Fouling Intensity Inspection Dates 1-4	2-1	3-1	3-29	4-26
4	0.5	6	1	0*	0*	0*	4	5
	3.0	6	2	0	3	2	2	2
	0.5	18	4	0	0	0	0	1
	3.0	18	1	2	2	0	2	2
	0.5	48	2	0	1	0	1	1
	3.0	48	4	0	0	0	0	0
84	0.5	6	4	1	1	1	1	1
	3.0	6	1	3	7	6	7	7
	0.5	18	2	1	1	2	3	3
	3.0	18	4	2	2	0	0	1
	0.5	48	1	0	1	0	1	2
	3.0	48	2	2	1	0	0	0
336	0.5	6	2	5	8	8	7	7
	3.0	6	4	0	0	0	0	0
	0.5	18	1	2	4	7	7	5
	3.0	18	2	3	3	3	3	2
	0.5	48	4	0	1	0	0	0
	3.0	48	1	3	2	2	1	2

*Flipper mechanism had been reversed

NOTE: Fouling Intensity Scale: 0 - 10 = none - heavy



Figure 1. Fouling test facility at The Dow Chemical Company, Freeport, Texas. Velocity test loop of lined and unlined pipe is shown to the right. The trough in the center holds panels for intermittent exposure to the heated water circulating in the troughs in the foreground. The troughs on the left have one stream of raw seawater and one stream of chlorine treated seawater. Test panels are moved manually or mechanically from one trough to another.



Figure 2. Chlorine test panels: 3ppm residual; No. 19, 84 hour cycle 6 % exposure; No. 23, 4 hour cycle 48 % exposure



Figure 3. Chlorine test panels: 84 hour cycle; 7.5 % exposure; velocity: 4 fps. No. 19, 0.25 ppm; No. 20, 1.0 ppm residual. One or two oysters are shown.

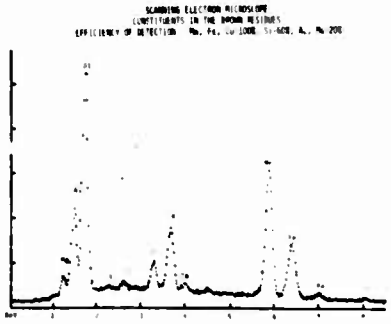


Figure 4. Constituents of the brown residue formed from chlorine treated seawater as determined by the scanning electron microscope.

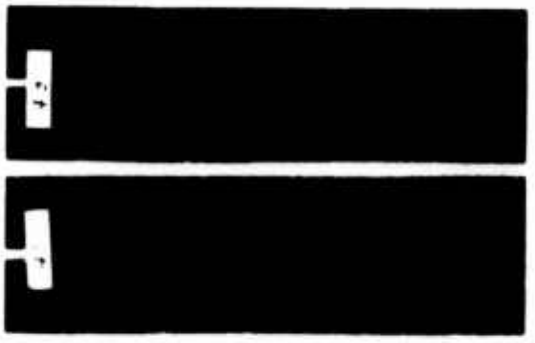


Figure 5. Panels from heat tests: 168 hour cycle; No. 43, 8 hour exposure, 111°F; No. 46, 1/2 hour exposure, 120°F. A few dead barnacles are shown.



Figure 6. Panels from heat test: 84 hour cycle; 1/2 hour exposure; No. 27, 104°F; No. 28, 112°F. Oysters are growing well at the lower temperature.



Figure 7. Test panels after 80 day exposure. No. 56, barnacles growing on an antifouling paint. No. 19, control panel with barnacles and hydroids.

Les Bases Electrochimiques de la Corrosion Localisée en Eau de Mer.

Marcel Pourbaix

Centre Belge d'Etude de la Corrosion CEBELCOR, Bruxelles, Belgique.
Université Libre de Bruxelles, Belgique.
University of Florida, Gainesville, Fla 32601.

De nombreux phénomènes de corrosion se produisent dans des conditions où l'accès de l'électrolyte est restreint, par suite d'une géométrie particulière du matériau ou par suite de l'existence de dépôts solides. Dans chacun de ces cas, la composition chimique de la solution corrodante existant dans des cavités plus ou moins obturées peut être très différente de celle du sein de la solution, du fait principalement de réactions d'hydrolyse. Il doit être tenu compte de ces différences pour toute analyse de tels phénomènes de corrosion, parmi lesquels la corrosion par piqûres, la corrosion caverneuse, la corrosion intergranulaire, la corrosion sous des dépôts et la corrosion fissurante sous tension. Dans chacun de ces cas il est utile d'étudier les phénomènes "anodiques" qui se produisent dans des cavités actives généralement acides et non aérées, et les phénomènes "cathodiques" qui se produisent sur des zones externes généralement alcalines et aérées.

On souligne l'intérêt scientifique et technique d'études approfondies relatives à la thermodynamique et à la cinétique électrochimiques des "cellules de corrosion occluses" et portant sur les points suivants :
- l'électrochimie des surfaces externes passives,
- la morphologie, la chimie et l'électrochimie des cavités internes actives, notamment en ce qui concerne leur pH et leur potentiel d'électrode,
- la cinétique de la corrosion et de sa prévention.

On applique ces considérations à l'étude des quatre cas suivants :
- corrosion par piqûres du cuivre en solution chlorurée, en considérant que la solution au fond des piqûres est saturée à la fois en Cu, en Cu_2O et en CuCl,
- corrosion par piqûres du fer en solution chlorurée, en considérant que la solution au fond des piqûres est saturée à la fois en $FeCl_2.4H_2O$, en Fe_3O_4 et en H_2,
- corrosion par piqûres et corrosion fissurante sous tension d'aciers en solution chlorurée, en soulignant les lacunes qui doivent être comblées pour que soit possible une étude satisfaisante de l'influence des éléments d'alliage. On émet l'hypothèse d'une "fragilité de méthane" due à la décomposition de cémentite existant aux joints de grains,
- corrosion fissurante sous tension d'alliages de titane en solution chlorurée, en considérant que la solution au fond des fissures est saturée en chlorure titaneux instable.

On souligne la possibilité de lutter contre ces différentes formes de corrosion par des traitements cathodiques abaissant le potentiel d'électrode en dessous du "potentiel de protection contre la piqûration".

On termine en énumérant quelques tâches dont la réalisation semble utile en vue d'élucider certains aspects électrochimiques de la corrosion fissurante sous tension

Mots-clefs : Corrosion par piqûres; corrosion caverneuse, corrosion intergranulaire; corrosion sous dépôts; corrosion fissurante sous tension, cellules de corrosion occluses, aération différentielle, cuivre, fer, aciers, titane, cémentite.

---

1. INTRODUCTION CORROSION DANS DES CONDITIONS DE DIFFUSION RESTREINTE. CELLULES DE CORROSION OCCLUSES.

De nombreux phénomènes de corrosion, dont l'importance pratique est considérable, se produisent dans des conditions où l'accès de l'électrolyte est restreint, par suite d'une géométrie particulière du matériau (structures présentant des interstices, telles que des tôles rivées, des assemblages filetés), ou par suite de l'existence de dépôts solides (produits de corrosion, incrustations, salissures marines, etc..). Dans chacun de ces cas, où la corrosion se produit dans des conditions de diffusion restreinte, et que B.F. BROWN a proposé de grouper sous le vocable "occluded cell corrosion O.C.C." (cellules de corrosion occluses C.C.O.), la composition chimique de la solution corrodante existant dans les cavités plus ou moins obturées peut être très différente de la composition chimique du sein de la solution. L'influence de cette différence de composition est tellement importante qu'il doit en être tenu compte pour toute analyse approfondie du phénomène de corrosion.

Ces phénomènes se manifestent notamment dans la corrosion par piqûres, dans la corrosion caverneuse, dans la corrosion intergranulaire, dans la corrosion sous des dépôts, et dans la corrosion fissurante sous tension.

Il est connu depuis de nombreuses années que les solutions à l'intérieur de piqûres de fer et d'aluminium sont acides : en 1925, J.R. BAYLIS (1) a observé un pH d'environ 6 dans des piqûres existant à l'intérieur de tubes en acier pour distribution d'eau; en 1937, T.P. HOAR (2) a signalé l'importance de l'acidification locale, due à une hydrolyse, pour la corrosion de l'étain dans des solutions sensiblement neutres; en 1951, C. EDELEANU et U.R. EVANS (3) ont mesuré, pour des piqûres d'aluminium, des pH voisins de 5,3 en solution de chlorure et voisins de 4,7 en solution de sulfate. Comme indiqué notamment par U.R. EVANS ((4), p.119), cette acidification est due à l'hydrolyse d'ions métalliques : dans le cas du fer, les ions Fe^{+++} s'hydrolysent avec formation de magnétite Fe_3O_4 et de différents composés ferrosoferriques (hydroxydes et sels basiques), qui s'accumulent jusqu'à réalisation d'un équilibre, relatif par exemple à la réaction

$$Fe^{++} + 2\ Fe^{+++} + 4\ H_2O \rightleftharpoons Fe_3O_4 + 8\ H^+$$

Dans le cas de l'aluminium, différentes réactions d'hydrolyse sont possibles, conduisant à différentes variétés d'oxyde ou d'hydroxyde d'aluminium, par exemple selon la réaction globale

$$Al + 3\ H_2O = Al(OH)_3 + 3\ H^+ + 3\ e^-$$

I.L. ROSENFELD et I.K. MARSHAKOV ont présenté en 1963, lors du "Congrès International de Corrosion Métallique" tenu à Moscou, un très important mémoire sur la corrosion caverneuse, où ils attirent particulièrement l'attention sur les modifications de potentiel d'électrode et de pH survenant dans les cavernes de corrosion (5).

Il est probable que, pour chaque forme de "cellule de corrosion occluse" O.C.C. (ou C.C.O.) affectant un métal ou alliage donné lorsqu'il est en contact avec un milieu donné, les caractéristiques chimiques à l'intérieur de la cavité en corrosion sont à peu près les mêmes. Par exemple, lorsqu'un acier au chrome donné se corrode en présence d'eau de mer, la composition de la solution est à peu près la même à l'intérieur d'une piqûre, d'une caverne, ou d'une fissure de corrosion sous tension; par conséquent, les résultats d'études faites en ce qui concerne la chimie des solutions existant à l'intérieur de piqûres et de cavernes peuvent être extrapolés à des fissures. Il va de soi, cependant, qu'une telle extrapolation doit être faite prudemment, sans que soit perdue de vue l'influence spécifique d'autres facteurs, et spécialement l'influence de la tension.

2. REGIONS ANODIQUES ET CATHODIQUES. PHENOMENES ANODIQUES ET CATHODIQUES.

Dans le cas fréquent où la solution corrodante contient de l'oxygène, les surfaces situées à l'extérieur des cavités obturées, et qui sont en contact direct avec cette solution, sont souvent passivées par l'oxygène, et agissent comme cathodes aérées où l'oxygène est réduit en eau et/ou en eau oxygénée avec augmentation du pH, par exemple selon la réaction

$$O_2 + 4\,H^+ + 4\,e^- \rightarrow 2\,H_2O \quad (\text{ou } O_2 + 2\,H_2O + 4\,e^- \rightarrow 4\,OH^-)$$

Les surfaces situées à l'intérieur des cavités sont actives, et agissent comme anodes non aérées où le métal subit une corrosion avec hydrolyse, ce qui conduit à une diminution du pH, par exemple selon les réactions suivantes :

pour le fer : $Fe \rightarrow Fe^{++} + 2\,e^-$

et $3\,Fe^{++} + 4\,H_2O \rightarrow Fe_3O_4 + 8\,H^+ + 2\,e^-$

pour l'aluminium :

$$Al \rightarrow Al^{+++} + 3\,e^-$$

et $Al^{+++} + 3\,H_2O \rightarrow Al(OH)_3 + 3\,H^+$.

Ceci conduit donc, lorsque la solution corrodante est une eau aérée sensiblement neutre, à des cellules d'aération différentielle entre de grandes cathodes passives où la solution est légèrement alcaline, et de petites anodes actives où la solution est nettement acide. Le couplage de ces réactions cathodiques et anodiques provoque un transfert d'anions des cathodes externes vers les anodes internes (qui est associé avec la circulation d'un courant électrique entre ces deux groupes de régions, de telle sorte que soit maintenue l'électroneutralité des solutions dans ces deux compartiments). Si la solution corrodante contient du chlorure, les anions ainsi transférés peuvent être des ions chlorure Cl^-, et l'acide qui se forme à l'intérieur des cavités est en fait de l'acide chlorhydrique, qui est très agressif. Ceci est l'une des raisons pour lesquelles, ainsi qu'il est bien connu, les chlorures favorisent de manière particulièrement nuisible la corrosion par piqûres, la corrosion caverneuse, et la corrosion fissurante sous tension : la solution existant à l'intérieur des piqûres, cavernes et fissures contient de l'acide chlorhydrique.

Il faut aussi être bien conscient de ce que, lorsque la thermodynamique le permet, c'est-à-dire lorsque le potentiel d'électrode du métal à l'intérieur de la cavité en corrosion est inférieur au (plus négatif que le) potentiel d'équilibre de l'hydrogène dans la solution que renferme la cavité, la réaction anodique de corrosion n'est pas la seule réaction possible : une réaction cathodique de dégagement d'hydrogène $2\,H^+ + 2\,e^- \rightarrow H_2$ peut aussi se produire à l'intérieur de la cavité; cette réaction de dégagement d'hydrogène freine l'abaissement de pH et peut éventuellement conduire à une

"fragilité d'hydrogène". Quelques autres réactions cathodiques ou anodiques peuvent aussi se produire, si la thermodynamique le permet, et parmi elles des réactions affectant des carbures et des composés intermétalliques déposés dans la matrice ou le long des joints de grains.

En conclusion, les problèmes de nature électrochimique qui sont associés avec les corrosions qui s'accomplissent dans des conditions de diffusion restreinte peuvent concerner trois groupes de phénomènes :

- sur les surfaces "cathodiques": des réactions électrochimiques et chimiques s'accomplissant à des potentiels relativement élevés, et en milieu généralement alcalin.
- sur les surfaces "anodiques" : des réactions électrochimiques et chimiques s'accomplissant à des potentiels d'électrode relativement bas, et en milieu généralement acide.
- entre les surfaces cathodiques et anodiques : des transferts d'ions et des réactions chimiques.

Chacun de ces trois groupes de phénomènes doit être considéré aux deux points de vue thermodynamique et cinétique. Ceci implique la mesure et l'interprétation :

- des potentiels d'électrode relatifs aux surfaces cathodiques ; ces potentiels d'électrode sont des différences de potentiel entre une surface cathodique et une électrode de référence réversible placée dans la solution jouxtant cette surface, à l'extérieur des cavités,
- des potentiels d'électrode relatifs aux surfaces anodiques : ces potentiels d'électrode sont des différences de potentiel entre une surface anodique et une électrode de référence réversible placée dans la solution jouxtant cette surface, à l'intérieur d'une cavité,
- des potentiels de diffusion entre les solutions à l'intérieur et à l'extérieur des cavités ; ces potentiels sont des différences de potentiel entre les deux électrodes de référence citées ci-dessus.

Il va de soi que l'étude doit être différente selon qu'il s'agit d'étudier l'initiation de la corrosion ou sa progression. Le traitement cinétique peut être différent pour chaque catégorie de O.C.C.; mais le traitement thermodynamique doit être fondamentalement le même.

Dans la suite du présent exposé, après avoir présenté quelques opinions concernant l'initiation de quelques formes de "corrosion en diffusion restreinte" ou "cellules de corrosion obturées" O.C.C., nous examinerons la thermodynamique et la cinétique des phénomènes électrochimiques en jeu.

3. L'INITIATION DE LA CORROSION CAVERNEUSE, DE LA CORROSION PAR PIQÛRES, ET DE LA CORROSION FISSURANTE SOUS TENSION.

3.1 Corrosion caverneuse

Une corrosion caverneuse se produit lorsqu'un métal ou alliage passivable subit une corrosion généralisée en présence d'une solution exempte d'oxygène, avec formation d'ions métalliques qui s'hydrolysent lorsqu'ils viennent en contact avec de l'oxygène, ce qui conduit à la formation d'une solution acide et d'un oxyde ou hydroxyde insoluble.

Sont donc susceptibles de corrosion caverneuse en présence d'une solution neutre donnée les métaux et alliages dont le diagramme potentiel/pH présente un domaine triangulaire de corrosion généralisée s'étendant aux pH supérieurs à 7 (p.ex. le fer et la plupart des aciers au chrome). La figure 1 (6b) montre un tel diagramme pour le fer à 25°C, avec indication des valeurs expérimentales du pH en absence d'oxygène (ligne 1), et en présence d'oxygène (lignes 2a et 2b).

La figure 2 montre l'initiation et la propagation d'une caverne de corrosion du fer dans une eau passivante aérée contenant un peu de chlorure, caverne qui résulte du placement d'une plaque non métallique sur la surface du métal.

Lorsqu'il est en contact direct avec l'eau contenant de l'oxygène, le métal est couvert d'un film protecteur de Fe_2O_3, et présente un potentiel d'électrode voisin de + 0,2 volt par rapport à l'électrode standard à hydrogène (esh). Si une plaque en matière plastique est posée sur une partie de la surface en fer, le potentiel du fer sous cette plaque descend jusqu'environ -0,5 $volt_{esh}$, par suite de l'élimination de l'oxygène dans le mince film de solution qui demeure entre la plaque et le métal (figure 2a).

De ce fait, le film protecteur subit une dissolution par réduction, et le métal devient actif. Des courants d'aération différentielle circulent entre les zones externes passives et la partie active de la surface, où le fer se corrode avec formation de cations Fe^{++}. L'électroneutralité de la solution existant dans la caverne commençante se maintient par diffusion d'anions Cl^- venant du sein de l'eau. Une partie des ions Fe^{++} s'hydrolyse en Fe_3O_4 ou est oxydée en ions Fe^{+++}, lesquels s'hydrolysent en $Fe(OH)_3$, car Fe_3O_4 et $Fe(OH)_3$ sont, selon le diagramme d'équilibres potentiel/pH du système $Fe-H_2O$, les formes stables du fer dans les conditions de potentiel d'électrode et de pH existantes. Ceci conduit à une diminution du pH jusqu'à environ 4 à 3 et à une élévation correspondante du potentiel (le long de la ligne 1 de la figure 1), jusqu'à environ -0,4 $volt_{esh}$ (figure 2b). La corrosion est la plus forte près de la partie interne du dépôt de $Fe(OH)_3$, là où le pH est minimum, environ 3 (figure 2c).

3.2 Corrosion par piqûres

La figure 3 montre l'initiation et la propagation d'une piqûre de fer dans une eau aérée renfermant du chlorure, selon un mécanisme inspiré par les expériences électrochimiques de T.P. HOAR (7) et par les expériences ellipsométriques de J. KRUGER (8). Nous nous référons ici à la figure 4 qui montre schématiquement les conditions expérimentales d'immunité, de corrosion généralisée, de corrosion par piqûres, de passivation parfaite et de passivation imparfaite du fer en présence de solutions renfermant 10^{-2} mole Cl^- par litre (355 ppm). Le point 1 (-0,5 $volt_{esh}$) de cette figure concerne les conditions de corrosion caverneuse déjà considérées en section 3.1.

Considérons le cas où, pour quelque raison que ce soit, due par exemple à la présence d'oxygène, le potentiel d'électrode du fer passif en présence d'eau de pH 8 atteint le "potentiel de rupture" ou "potentiel de piqûration" (point 2 de la figure 4, soit environ + 0,1 $volt_{esh}$). Dans un premier stade, quelques ions Fe^{++} passent à travers le film d'oxyde passivant sans changement perceptible de la morphologie de ce film (ceci se produit lorsqu'est atteint le "premier temps d'induction t_1" de KRUGER, pour lequel HOAR a observé un accroissement du courant anodique sans que KRUGER ait détecté par ellipsométrie aucun changement de la morphologie du film). Dans un second stade, ces ions Fe^{++} sont oxydés par l'oxygène à la surface en ions Fe^{+++}, qui, dans un troisième stade, forment par hydrolyse, à l'intérieur d'un film précédemment protecteur,

une solution acide qui modifie gravement la morphologie de ce film (lorsqu'est atteint le "deuxième temps d'induction t_2" de KRUGER). Ce troisième stade correspond à une véritable piqûration, avec formation d'une cavité acide (zone 3 de la figure 4) qui provoque une chute soudaine du potentiel mixte de la surface. Ce potentiel mixte, qui augmente ensuite au fur et à mesure que la cavité est obturée davantage par la formation de produits de corrosion, subit une nouvelle chute, avec formation d'une deuxième piqûre, lorsqu'est atteint à nouveau le potentiel de piqûration. Le cycle se renouvelle alors, et le potentiel mixte oscille entre deux limites qui sont respectivement le potentiel de piqûration des surfaces passives externes et le potentiel des piqûres actives internes; chaque chute de potentiel décèle l'apparition d'une nouvelle piqûre.

3.3 Corrosion fissurante sous tension

Ainsi que l'a écrit B.F. BROWN (9, fig.1), les fissures de corrosion sous tension s'amorcent à des points faibles de la surface, particulièrement là où des corrosions antérieures, qui peuvent ou non résulter d'une tension, ont conduit à des cavités acides : cavernes, piqûres, etc...

4. THERMODYNAMIQUE ET CINETIQUE DES CELLULES DE CORROSION OBTUREES.

4.1 Généralités

Comme indiqué en section 2, la plupart des "corrosions en cellules obturées" (corrosion par piqûres, corrosion caverneuse, corrosion fissurante sous tension, par exemple) impliquent l'existence simultanée de cathodes passives et d'anodes actives. Elles peuvent donc être considérées, ainsi que l'a dit J. MONTUELLE (10) pour la corrosion par piqûres, comme une "maladie de l'état passif".

S'il en est ainsi, de telles corrosions ne doivent affecter que des métaux et alliages qui peuvent devenir passifs dans leurs conditions d'utilisation. Et comme, parmi les nombreux facteurs qui affectent la passivité et l'activité des métaux et alliages, le potentiel d'électrode et le pH jouent un rôle particulièrement important, il est rationnel, lors de l'étude de l'électrochimie de ces corrosions, d'accorder une attention spéciale à l'influence de ces deux facteurs,et cela tant pour la thermodynamique que pour la cinétique des réactions à considérer. Il va de soi cependant qu'il ne faut pas mésestimer l'influence d'autres facteurs (par exemple l'influence spécifique des anions).

Par conséquent, lorsque l'on est confronté avec un problème déterminé mettant en jeu des "cellules de corrosion obturées" pour un alliage déterminé en présence d'un milieu déterminé, il paraît recommandable d'opérer selon les étapes suivantes (ces étapes seront illustrées dans les sections 4.2 à 4.4, avec exemples concernant la piqûration du cuivre, du fer et d'aciers ainsi que la corrosion fissurante sous tension d'aciers).

4.11 Electrochimie des surfaces externes passives

Réunir autant d'informations que possible concernant l'électrochimie des surfaces passives externes :

a) Quels sont les constituants superficiels des surfaces passives externes ?
b) Quelle est la composition de la solution corrodante ?
c) Quel est le potentiel d'électrode du métal ou alliage en présence de cette solution ?

4.12 Morphologie et chimie des cavités internes actives

Réunir autant d'informations que possible concernant la chimie des cavités internes actives :

a) Quels sont les constituants de l'alliage en corrosion : constituants de la matrice; composés intermétalliques et carbures, spécialement aux joints de grains ?
b) Quels sont les produits de corrosion solides déposés à l'intérieur de la cavité : oxydes ou hydroxydes, hydrures, sels ?
c) Quelle est la composition chimique de la solution à l'intérieur de la cavité : pH, concentrations en différents cations et anions ?
d) Quel est le potentiel d'électrode de l'alliage en présence de cette solution ?

4.13 Electrochimie des cavités actives

4.131 Diagrammes d'équilibres

Sur la base des données accessibles, calculer, si cela n'a pas été fait précédemment, pour les cavités internes (et éventuellement aussi pour les surfaces externes passives), les conditions d'équilibre thermodynamique de tout corps solide existant, en présence de la solution à considérer. Représenter ces conditions d'équilibre graphiquement (diagrammes de solubilité et diagrammes potentiel/pH). Ces diagrammes devraient indiquer, chaque fois que c'est faisable, les domaines théoriques de stabilité et d'instabilité de tout corps solide.

4.132 Valeurs expérimentales de potentiel et de pH à l'intérieur des piqûres actives

Compte tenu des résultats obtenus en section 4.131, essayer de reproduire synthétiquement des solutions semblables aux solutions existant à l'intérieur des cavités, et essayer de produire des cavités artificielles dans des conditions semblables aux conditions existant en pratique. Déterminer la composition des deux solutions ainsi obtenues, ainsi que le potentiel d'électrode du métal dans ces solutions; comparer les résultats de ces deux séries d'expériences avec les diagrammes d'équilibre .

4.14 Cinétique de la corrosion et de sa prévention

En opérant sur des solutions synthétiques et/ou sur les cavités artificielles mentionnées en section 4.132, essayer d'élucider la cinétique de la corrosion à l'intérieur de ces cavités, spécialement en ce qui concerne les conditions d'immunité et de passivation, et les possibilités de prévention de la corrosion.

4.2 Application à la corrosion par piqûres du cuivre

A titre d'exemple de la méthode d'étude décrite en section 4.1, nous décrivons brièvement une étude qui a été faite au sujet de la corrosion par piqûres du cuivre dans l'eau de distribution de Bruxelles froide. Cette étude, qui est certainement imparfaite et incomplète, ne doit nullement être considérée comme un modèle et devrait être poursuivie de manière plus approfondie. Cet exemple est donné essentiellement pour fixer les idées, en suivant les quatre stades considérés en section 3.1. Des détails sont donnés dans plusieurs publications (11, 12, 13).

4.21 Electrochimie des surfaces externes passives

Nous n'avons pas examiné de manière approfondie la nature des constituants superficiels des surfaces externes passives. La solution corrodante était de l'eau de Bruxelles aérée : pH 7,9; dureté totale 33,9 degrés français (26,0° dureté bicarbonique et 7,9 dureté non bicarbonique; 26,0° dureté calcique et 7,9° dureté magnésienne; saturée en $CaCO_3$ (index de Langelier zéro); 229 ppm

CO_2, 46 ppm SO_3, 22 ppm Cl.

Le potentiel d'électrode des surfaces externes variait fortement entre -250 mV par rapport à l'électrode à calomel saturée ecs et environ +50 à +400 mV_{ecs}, selon la durée du contact avec l'eau, les conditions de circulation de l'eau, l'état de surface, la présence ou l'absence de lumière, etc...

4.22 Morphologie et chimie des cavités internes actives

La figure 5 représente une piqûre de cuivre en présence d'eau de Bruxelles froide. Cette piqûre contient, sous une couche de malachite verte $CuCO_3.Cu(OH)_2$, des cristaux blancs de chlorure cuivreux CuCl et un dépôt non adhérent d'oxyde cuivreux rouge Cu_2O. La solution qui existe au fond de la piqûre est donc en contact direct avec Cu, Cu_2O et CuCl; la solution qui existe au sommet de la piqûre est en contact direct avec $CuCO_3.Cu(OH)_2$.

Ceci donne quelques informations concernant le point b de la section 4.12 (produits de corrosion solides). Au sujet du point a (constituants du métal), nous savions uniquement que les constituants principaux du cuivre électrolytique sont du cuivre pur et un peu de Cu_2O, et nous n'avons pas examiné particulièrement les échantillons du métal soumis aux essais. Aucune information n'était accessible à cette époque concernant le point c (composition de la solution à l'intérieur de la piqûre) et le point d (potentiel d'électrode du cuivre à l'intérieur de la piqûre).

4.23 Electrochimie des cavités actives

4.231 Diagrammes d'équilibres

La figure 6 est, pour 25°C, le diagramme d'équilibres potentiel/pH pour le système binaire Cu-H_2O. Elle montre que, en présence d'eau pure de pH voisin de 7, le cuivre métallique Cu est la forme stable du cuivre en absence complète d'oxygène (ligne a), l'oxyde de cuivre CuO est la forme stable en présence d'oxygène (ligne b), l'oxyde cuivreux est stable dans des conditions intermédiaires.

La figure 7 est, aussi pour 25°C, le diagramme d'équilibre pour le système ternaire Cu-Cl-H_2O pour des solutions contenant 10^{-2} at.gr. Cl^-/l. (355 ppm Cl^-). La figure 8 est le diagramme d'équilibre pour le système quinaire Cu-CO_2-SO_3-Cl-H_2O pour des solutions contenant, comme c'est le cas pour l'eau de Bruxelles, 229 ppm CO_2, 46 ppm SO_3 et 22 ppm Cl.

Les figures 7 et 8 montrent que, en présence des solutions considérées, le chlorure cuivreux CuCl ne peut être stable que dans les conditions acides (pH inférieur à 3,66 ou à 2,45 selon la teneur en chlorure). S'il se forme en présence d'eau neutre, CuCl doit donc s'hydrolyser selon la réaction :

$$2\ CuCl + H_2O \rightarrow Cu_2O + 2\ H^+ + 2\ Cl^-$$

jusqu'à ce que les conditions d'équilibre de cette réaction soient atteintes. La solution existant à l'intérieur d'une piqûre active de cuivre, qui est saturée à la fois en CuCl et en Cu_2O, doit donc être acide.

On peut obtenir plus d'informations concernant la chimie et l'électrochimie de la piqûre en considérant que, si l'état d'équilibre est réalisé au fond de la piqûre, la solution existant en cet endroit doit être en équilibre avec CuCl, Cu_2O et Cu; pour des solutions contenant 22 ppm Cl^-, teneur qui est considérée à la figure 9, ceci correspond au point triple n° 4 de cette figure : E = +0,326 $volt_{esh}$ et pH = 2,45.

Cependant, il n'y a pas de raison pour que la concentration en chlorure à l'intérieur de la piqûre soit égale à la concentration à l'extérieur de la piqûre, qui est 22 ppm. Comme l'a montré une étude approfondie des équilibres du système ternaire Cu-Cl-H_2O (11c, 12c), le cuivre se dissout en milieu acide avec formation des cations Cu^+ et Cu^{++} et de l'anion $CuCl_2^-$ et, du fait d'un excédent des cations sur les anions, l'électroneutralité à l'intérieur de la piqûre doit être rétablie par diffusion d'autres anions, principalement des ions chlorure, venant du sein de la solution. La concentration en ions Cl^- existant réellement à l'intérieur d'une piqûre de cuivre doit donc être celle pour laquelle l'électroneutralité de la solution est assurée.

Le tableau ci-après, qui résulte de travaux effectués précédemment (13), indique les réactions qui peuvent se produire à l'intérieur d'une piqûre de cuivre, ainsi que leurs conditions d'équilibre à 25°C (les corps solides sont soulignés) :

(22) $\underline{Cu} = Cu^+ + e^-$ $\qquad E = +0,520 + 0,0591 \log (Cu^+)$

(23) $\underline{Cu} = Cu^{++} + 2e^-$ $\qquad E = +0,337 + 0,0295 \log (Cu^{++})$

(76) $\underline{Cu} + 2\,Cl^- = CuCl_2^- + e^-$ $\qquad E = +0,208 + 0,0591 \log (CuCl_2^-) - 0,1182 \log (Cl^-)$

(55) $\underline{Cu} + Cl^- = \underline{CuCl} + e^-$ $\qquad E = +0,137 - 0,0591 \log (Cl^-)$

(51) $2\underline{CuCl} + H_2O = \underline{Cu_2O} + 2Cl^- + 2H^+$ $\qquad pH = 5,66 + \log(Cl^-)$.

Donc, pour toute valeur de l'activité en ions chlorure Cl^-, que nous supposerons ici égale à la concentration, les formules 55 et 51 donnent respectivement le potentiel d'électrode et le pH d'équilibre, et les formules 22, 23 et 76 donnent respectivement les activités (ou concentrations corrigées) en ions Cu^+, Cu^{++} et $CuCl_2^-$. La valeur de la concentration en Cl^- qui correspond à l'électroneutralité de la solution est la valeur pour laquelle

$$2\,(Cu^{++}) + (Cu^+) + (H^+) = (Cl^-) + (CuCl_2^-) + (OH^-)$$

ou, puisque la concentration en OH^- est suffisamment faible pour être négligée,

$$2\,(Cu^{++}) + (Cu^+) + (H^+) = (Cl^-) + (CuCl_2^-).$$

La figure 9 montre l'influence de la concentration en Cl^- sur les potentiel, pH et concentrations cités ci-dessus. L'électroneutralité de la solution est réalisée lorsque ces données ont les valeurs suivantes :

$\log(Cl^-) = -2,16$ soit 0,00692 at.gr./l., ou 245 ppm Cl^-

$E = +0,265$ volts$_{esh}$

$pH = 3,50$

$\log(Cu^+) = -4,32$ soit 0,00005 at.gr./l.

$\log(Cu^{++}) = -2,46$ 0,00345 at.gr./l.

$\log(CuCl_2^-) = -3,36$ 0,00043 at.gr./l.

Ceci signifie

- pour Cl, une teneur totale de 0,00692 + 0,00086 = 0,00778 gr.at./l., ou 273 ppm Cl
- et pour Cu, une teneur totale de 0,00005 + 0,00345 + 0,00043 = 0,00393 gr.at./l. ou 250 ppm Cu.

Par conséquent, selon ces calculs, le potentiel d'électrode d'équilibre du cuivre à l'intérieur d'une piqûre, à 25°C, est environ + 265 mV_{esh} (par rapport à l'électrode standard à hydrogène), ou, si on adopte + 241 mV_{esh} pour le potentiel de l'électrode à calomel saturée, +24 mV_{ecs}. Le pH de la solution à l'intérieur de la piqûre, près du cuivre, est environ 3,50. Cette solution contient environ 273 ppm Cl et environ 250 ppm Cu. Ces conditions d'équilibre peuvent être représentées approximativement par le point triple $Cu/CuCl/Cu_2O$ de la figure 7, qui concerne toutefois $10^{-2,00}$ at.gr. Cl^-/l (355 ppm) au lieu de $10^{-2,16}$ (245 ppm); mais cette relativement faible différence peut être négligée pour une approche semi-quantitative du problème.

4.232 Valeurs expérimentales de potentiel et de pH à l'intérieur de piqûres de cuivre actives

Afin de vérifier la validité de ces prévisions thermodynamiques (11c, p.7), J. VAN MUYLDER a placé un fil de cuivre dans de l'eau dégazée, à laquelle il a ajouté des quantités croissantes de CuCl, lequel s'est hydrolysé avec formation de Cu_2O et de HCl. Cette addition a été poursuivie jusqu'à stabilisation du potentiel d'électrode du cuivre et du pH de la solution. Ces valeurs stables ont été respectivement E = + 20 mV_{ecs} (au lieu de + 24) et pH = 3,4 (au lieu de 3,5). La solution contenait 207 ppm Cl (au lieu de 273) et 17 ppm Cu (au lieu de 250). Exception faite pour la teneur en cuivre, les résultats de ce rapide essai expérimental sont en accord satisfaisant avec les données calculées. Les raisons de l'écart observé en ce qui concerne la teneur en cuivre n'ont pas encore été recherchées.

Signalons aussi que, le long des surfaces externes passives, ainsi que sur la partie externe des piqûres, le matériau est en contact avec l'eau telle quelle, sans modification sensible, laquelle a un pH égal à 7,9 et contient de l'oxygène.

Comme le montre la figure 9, le dérivé de cuivre stable dans ces conditions est de la malachite, et c'est là la raison pour laquelle la partie externe des piqûres est formée de malachite. Comme l'a montré N. de ZOUBOV (voir 11e, fig.13), la teneur en cuivre d'une eau de pH 7,9 contenant 229 ppm CO_2 ($10^{-2,28}$ molaire) et saturée en malachite est d'environ 10-7 at.gr. par litre (0,006 ppm Cu).

4.24 Cinétique de la corrosion du cuivre par piqûres, et de sa prévention

Lors d'une première série d'expériences, de l'eau de Bruxelles a été mise en circulation pendant plusieurs semaines ou mois sur un grand nombre d'échantillons de cuivre présentant différents états de surface, isolés ou couplés avec différents métaux ou avec du graphite, et dans différentes conditions de circulation de l'eau. Des mesures de potentiels à courant nul ont été faites sur ces échantillons au cours de ces essais.

Il a été trouvé que, sans exception, des piqûres sont toujours apparues lorsque, quelle qu'en soit la raison, le potentiel d'électrode du cuivre est devenu plus élevé qu'une valeur critique, laquelle a été voisine de +170mV_{ecs} pour la surface interne concave des tubes de cuivre (16 mm diamètre), et de + 100 mV_{ecs} pour la surface convexe de fils de cuivre (2mm diamète). Aucune piqûre n'a été observée lorsque le potentiel d'électrode avait une valeur inférieure à ces valeurs critiques.

Par ailleurs, quelques expériences potentiocinétiques ont été faites sur des échantillons de cuivre décapé en présence de différentes solutions : eau de Bruxelles dégazée, solutions de bicarbonate de sodium, ainsi que des solutions exemptes d'oxygène saturées en CuCl mentionnées en fin de la section 4.232 du présent rapport, et censées représenter la solution existant à l'intérieur des piqûres.

Il a été observé que :

- lors d'une polarisation anodique en présence d'eau de Bruxelles exempte d'oxygène, le cuivre se couvre successivement d'une couche de Cu_2O sensiblement protectrice et d'un dépôt non protecteur de CuO,

- dans certaines conditions (teneurs en $NaHCO_3$ voisines de 0.01 à 0.03 molaires, soit 440 à 1.320 ppm CO_2), la malachite peut être complètement protectrice,

- en présence de la solution acide existant à l'intérieur des piqûres (pH voisin de 3,4), la réaction $Cu = Cu^{++} + 2\ e^-$ se produit de manière réversible: il y a corrosion du cuivre dès que le potentiel d'électrode devient supérieur au potentiel d'équilibre (environ + 20 mV_{ecs}), et il y a déposition de cuivre dès que le potentiel d'électrode devient inférieur au potentiel d'équilibre.

Ce fait clarifie la signification scientifique du "potentiel critique de piqûration", dont la valeur observée expérimentalement est voisine de + 170 mV_{ecs} pour la face concave de tubes, et voisine de + 100 mV_{ecs} pour la surface convexe des fils, valeurs qui ne sont que légèrement supérieures au potentiel d'équilibre à l'intérieur de piqûres (+ 20 mV_{ecs}) : une dissolution du cuivre à l'intérieur des cavités acides existantes (c'est à dire une piqûration) se produira chaque fois que, du fait de l'existence de valeurs relativement élevées du potentiel sur les surfaces passives externes, le potentiel à l'intérieur des cavités deviendra supérieur à + 20 mV_{ecs}; au contraire, une déposition de cuivre à l'intérieur des cavités (pas de piqûration) se produira chaque fois que, du fait de l'existence de valeurs relativement basses du potentiel sur les surfaces passives externes, le potentiel à l'intérieur des cavités deviendra inférieur à + 20 mV_{ecs}. La différence entre le potentiel critique de piqûration et le potentiel d'équilibre (150 mV pour les tubes et 80 mV pour les fils) doit correspondre à un potentiel de diffusion.

Pour vérifier ceci nous avons utilisé avec J. VAN MUYLDER le dispositif représenté à la figure 10. Un cylindre en matière plastique B pourvu d'un petit tube C renfermant un peu d'amiante a été fixé par collage sur une tôle de cuivre A. Un peu de CuCl a été introduit à l'intérieur du tube B, qui a été obstrué par un bouchon pourvu d'une électrode de verre et d'une électrode à calomel. On a fait circuler de l'eau de distribution de Bruxelles sur la partie externe de la tôle; de l'eau de Bruxelles a été versée dans le compartiment interne, où elle est demeurée stagnante.

Il a été observé que, après quelques jours, les valeurs de potentiel d'électrode et de pH à l'intérieur du cylindre se sont stabilisées à des valeurs très semblables à celles qui avaient été prédites pour des piqûres. Par polarisation anodique ou cathodique des surfaces externes, après que celles-ci soient devenues sensiblement passives (à des potentiels d'électrode supérieurs à environ + 50 mV_{ecs}) il a pu être possible de réaliser à volonté, dans le compartiment interne agissant comme une piqûre artificielle, des potentiels d'électrode supérieurs ou inférieurs au potentiel d'équilibre à cet endroit (+ 20 mV_{ecs}), et d'y produire ainsi, à volonté, une dissolution du cuivre (aux potentiels supérieurs) ou un dépôt de cuivre (aux potentiels inférieurs).

Suite à ceci, le mécanisme électrochimique de la corrosion du cuivre par piqûres a été élucidé dans une large mesure, et des remèdes scientifiques contre cette corrosion ont été établis.

4.3 Application à la corrosion par piqûres du fer.

Comme deuxième exemple de la méthode d'étude décrite en section 4.1 du présent rapport, nous nous référerons ici à des recherches relatives à la corrosion du fer et d'aciers au carbone.

Comme signalé en section 1, il est très probable que, pour chacune des formes de "corrosion en cellule occluse" se produisant sur un même métal en présence d'un même milieu, les caractéristiques chimiques de la solution existant dans la cellule en corrosion sont à peu près les mêmes. Les résultats de travaux de recherches faites à ce point de vue pour des piqûres ou des cavernes de corrosion peuvent donc être extrapolés pour des fissures. Une raison de plus pour considérer à la fois la corrosion par piqûres et la corrosion fissurante sous tension, est que, comme l'ont établi plusieurs auteurs parmi lesquels S. SMIALOWSKA (14), B.F. BROWN (9, p.2) et nous même (6a, fig.24), une piqûre peut être l'amorce d'une fissure.

4.31 Electrochimie des surfaces externes passives.

Dans la figure 1, la ligne 2b indique les potentiels d'électrode de fer passif électriquement isolé en présence de solutions exemptes de chlorure renfermant de l'oxygène (+ 0.4 à + 0.5 $volt_{esh}$ pour pH 8). A la figure 11 on peut voir que, dans des solutions renfermant 10^{-2} at.gr. Cl^- par litre (355 ppm), le fer ne peut être passif qu'entre deux valeurs critiques du potentiel d'électrode : un "potentiel de passivation" (pour pH 8 : - 0,3 $volt_{esh}$) et un "potentiel de piqûration" (+ 0,1 $volt_{esh}$). De nouvelles piqûres se forment lorsque le potentiel d'électrode est supérieur à ce potentiel de piqûration; les piqûres ainsi formées demeurent actives entre ce potentiel de piqûration et un "potentiel de protection contre la piqûration" (environ - 0,3 $volt_{esh}$).

4.32 Morphologie et chimie des cavités internes actives.

La figure 12 représente schématiquement, d'après U.R. EVANS (4b, p.28), une piqûre de fer formée en présence d'une solution aérée de chlorure de sodium. Comme indiqué par U.R. EVANS, si la solution est initialement neutre, la solution à l'intérieur de la piqûre devient localement acide par suite d'hydrolyse de sel de fer. Encore selon EVANS (4a, p.119), une telle piqûre peut contenir de la magnétite Fe_3O_4 et différents composés ferro-ferriques verts (hydroxyde ou sels basiques). Ainsi qu'il est bien connu, la partie externe d'une piqûre de fer en contact avec une eau aérée contient de l'hydroxyde $Fe(OH)_3$, qui est généralement considéré comme le constituant principal de la rouille.

Nous avons observé avec J. VAN MUYLDER (6b, 6d) des pH compris entre 2.7 et 4.7 et des potentiels d'électrode compris entre - 0,35 et - 0,45 $volt_{esh}$ à l'intérieur des cavernes actives de fer Armco.

4.33 Electrochimie des cavités acides.

4.331 Diagrammes d'équilibre

La figure 13 (15, p.312) donne un diagramme d'équilibres potentiel/pH pour le système binaire Fe-H_2O, à 25°C. A notre connaissance, aucun diagramme digne de foi n'a actuellement été établi pour le système ternaire Fe-Cl-H_2O.

Cependant, on sait que la solubilité du $FeCl_2.4H_2O$ (qui est incolore) dans l'eau à 25°C est voisine de 39 gr $FeCl_2$ dans 61 gr H_2O (environ 5 molaire)*, et que la solubilité du $FeCl_3.6H_2O$ (qui est gris foncé) est voisine de 49 gr $FeCl_3$ dans 51 gr H_2O (soit environ 6 molaire).

Rappelons que, comme indiqué en section 4.2 du présent rapport, une bonne connaissance des constituants solides existant au fond d'une piqûre de corrosion de cuivre active (CuCl et Cu_2O en contact avec du Cu métallique) a rendu possible l'élucidation des phénomènes de piqûration du cuivre aux points de vue thermodynamique et cinétique, et a permis de prévoir des remèdes à cette piqûration. On peut certainement opérer de même, avec les mêmes résultats, pour la piqûration du fer.

Il existe cependant une différence fondamentale entre les piqûres de fer et les piqûres de cuivre : alors que, comme indiqué en section 4.232, une piqûre de cuivre peut exister en état d'équilibre thermodynamique, une piqûre de fer ne le peut pas. Contrairement au cuivre, le fer métallique ne peut jamais être thermodynamiquement stable en présence d'eau dans les conditions usuelles de température et de pression. Parmi les nombreuses réactions qui peuvent se produire à l'intérieur d'une piqûre de fer, quelques unes ne peuvent pas atteindre un état d'équilibre (corrosion de fer actif, dégagement d'hydrogène), mais d'autres le peuvent (par exemple, les réactions d'hydrolyse).

Les dérivés solides du fer qui peuvent exister de manière stable dans des solutions acides et exemptes d'oxygène renfermant des chlorures, telles qu'existant à l'intérieur de piqûres, fissures, etc., sont Fe, Fe_3O_4 et $FeCl_2.4H_2O$ (pour lesquels on possède des valeurs d'enthalpies libres de formation à 25°C), et peut-être de la magnétite hydratée et des chlorures basiques (pour lesquels de telles données ne nous sont actuellement pas connues). Il semble que les ions ferreux Fe^{++} sont la seule forme dissoute stable de fer dans ces conditions.

Admettant les valeurs suivantes d'enthalpies libres de formation

Fe_3O_4	- 242.400 cal	
$FeCl_2$	- 72.200 "	(sous forme de $FeCl_2.4H_2O$)
Fe^{++}_{aq}	- 20.300 "	

on obtient par le calcul les conditions d'équilibre suivantes pour le Fe, Fe_3O_4 et $FeCl_2.4H_2O$ en présence de solutions électriquement neutres (pour lesquelles $(Cl^-) = 2\ (Fe^{++})$) :

$$E = -0{,}368 \text{ volt}_{esh}$$
$$pH = 4{,}80$$
$$\log (Cl^-) = 2{,}745$$
$$\log (Fe^{++}) = 2{,}444$$

La <u>figure 14</u> montre schématiquement les domaines de stabilité thermodynamique de Fe, $FeCl_2.4H_2O$ et Fe_3O_4 ainsi calculés, en présence de solutions électriquement neutres en $FeCl_2$ (pour lesquelles, comme dit ci-dessus, $(Cl^-) =$

* Signalons ici que le sulfate ferreux $FeSO_4.7H_2O$ (qui est vert) est moins soluble que que le chlorure ferreux : environ 33 gr $FeSO_4$ dans 67 gr H_2O (soit environ 2 molaire).

2 (Fe^{++})). Il va de soi que cette figure est donnée uniquement pour fixer les idées et qu'elle ne peut pas être exacte, à cause de la très grande valeur des concentrations en jeu : les activités calculées en ions Cl^- et Fe^{++} sont énormes, et les méthodes thermodynamiques applicables aux solutions diluées ne peuvent absolument pas être valables dans le cas présent.

Par ailleurs, en dessous de la ligne a de la figure 14, les pressions d'équilibre en hydrogène H_2 sont supérieures à 1 atmosphère. Par conséquent, dans les piqûres existant sous pression atmosphérique, seuls les états d'équilibre situés au dessus de cette ligne sont réalisables (par exemple l'équilibre entre $FeCl_2.4H_2O$ et Fe_3O_4); les équilibres entre Fe et $FeCl_2.4H_2O$ et entre Fe et Fe_3O_4, ainsi que l'équilibre entre H_2O et H_2, n'y sont pas réalisables. On peut donc s'attendre à ce que, sauf si le métal y est polarisé cathodiquement en dessous d'environ -0,37 $volt_{ehs}$, le fond d'une piqûre (ou fissure) de fer en milieu chloruré soit constitué par du fer se corrodant avec dégagement d'hydrogène dans une solution environ 5 molaire en fer saturée en $FeCl_2.4H_2O$ et en Fe_3O_4, ainsi qu'en hydrogène.

Si, en première approximation, on admet que la figure 14 est sensiblement exacte, on est conduit à l'opinion que les caractéristiques de la solution existant au fond d'une piqûre (ou fissure) active ayant atteint l'état de régime sont sensiblement celles du point de rencontre de la ligne a (équilibre H_2/H_2O) et de la ligne $FeCl_2.4H_2O/Fe_3O_4$, c'est-à-dire : pH = 4,25, E = -0,25 $volt_{ehs}$, et que le potentiel du fer en corrosion dans cette solution est compris entre cette valeur -0,25 $volt_{ehs}$ et -0,37 $volt_{ehs}$ (potentiel d'équilibre du fer), c'est-à-dire environ -0,3 $volt_{ehs}$.

Nous reviendrons sur ce point en section 4.34.

4.332 Valeurs expérimentales de potentiel et de pH à l'intérieur de piqûres de fer actives.

La figure 1 (16, figure 78) montre l'influence du pH sur le potentiel d'électrode du fer en contact avec des solutions exemptes de chlorure, respectivement en absence d'oxygène (ligne 1) et en présence d'oxygène (lignes 2a et 2b). La figure 11 (6d, figure 3) montre les circonstances de potentiel d'électrode et de pH pour du fer électriquement isolé en présence de solutions de pH 8 10^{-2} molaires en Cl^- (355 ppm Cl^-)*. On voit que, si la solution est exempte d'oxygène (point 1), le fer subit une corrosion généralisée; si la solution est saturée en oxygène (point 2), il se produit des piqûres; dans les piqûres ainsi formées (région 3) la solution est acide (pH 2,7 à 4,7) et le potentiel d'électrode se situe près de la ligne 1 de la figure 1.

Comme on le voit sur cette figure, dans une piqûre, la solution est acide, et le fer se corrode avec dégagement d'hydrogène à un potentiel d'électrode qui est voisin du "potentiel libre" (potentiel à courant zéro) du fer dans cette solution acide.

---

* Un court exposé concernant de tels diagrammes est donné en annexe au présent rapport.

L'examen des données actuellement existantes concernant la thermodynamique du système Fe-Cl-H_2O conduit à considérer comme probable que, dans une piqûre ou une fissure de fer en milieu chloruré, cette corrosion du fer avec dégagement d'hydrogène se produit dans une solution acide saturée à la fois en $FeCl_2.4H_2O$ et en Fe_3O_4. On pourrait donc obtenir des données dignes de foi concernant l'électrochimie des piqûres (et autres formes de O.C.C.) pour le fer de manière très simple, en versant de l'eau exempte d'oxygène sur un mélange de $FeCl_2.4H_2O$, de Fe_3O_4 et de poudre de fer, dans un récipient pourvu d'une électrode de fer, d'une électrode de verre et d'une électrode à calomel, et en mesurant le potentiel d'électrode du fer et le pH de la solution ainsi obtenue, ainsi que sa teneur en ions Cl^- et en Fe^{++} et, si possible, le potentiel d'électrode de Fe_3O_4. Une telle solution reproduirait probablement la solution existant à l'intérieur des piqûres, fissures, cavernes, etc. de fer.

Des expériences de polarisation anodique et cathodique potentiocinétiques et potentiostatiques, réalisées sur du fer en présence de cette solution aideraient à élucider aussi la cinétique de ces corrosions. Pour l'étude de la corrosion sous tension, les électrodes de fer ainsi étudiées seraient utilement soumises à un fluage provoqué par un effort de traction.

4.333 Essai de schéma d'une piqûre, ou fissure de corrosion du fer.

Suite aux exposés faits aux sections 4.321 et 4.322, la figure 15 représente nos conceptions actuelles concernant la chimie et l'électrochimie d'une piqûre de fer (figure 15a) et d'une fissure de fer (figure 15b), en présence d'une eau contenant du chlorure.

Au fond de la piqûre ou fissure, le fer se corrode à environ -0,3 à -0,5 $volt_{esh}$ avec dégagement d'hydrogène dans une solution d'oxygène exempte de pH voisin de 4 très concentrée en ions Fe^{++} et Cl^-, et saturée à la fois en $FeCl_2.4H_2O$ et en Fe_3O_4 existant sous forme de dépôt cristallin au fond de la piqûre.

Au sommet de la piqûre ou fissure, l'oxygène diffusant du sein de l'eau oxyde les ions ferreux Fe^{++} et la magnétite Fe_3O_4 en ions ferriques Fe^{+++} (et $FeOH^{++}$) et en hydroxyde ferrique $Fe(OH)_3$. Le pH atteint une valeur minimale (environ 2,7) aux endroits où se forme le très peu soluble $Fe(OH)_3$, par hydrolyse d'ions Fe^{+++}.

L'existence d'une cellule d'aération différentielle entre les cathodes passives externes (où O_2 est réduit en H_2O à environ +0,2 $volt_{esh}$) et les anodes actives internes (où Fe se dissout avec dégagement d'hydrogène à environ -0,3 à -0,5 $volt_{esh}$) conduit à la circulation de courant électrique : des électrons libres e^- sont transférés à travers le métal de l'anode aux cathodes, et des anions Cl^- sont transférés à travers la couche de rouille des cathodes vers l'anode.

4.34 Cinétique de la corrosion du fer par piqûres, et de sa prévention.

Des études potentiocinétiques faites précédemment (17,6)*, en procédant à des potentiels d'électrode successivement croissants et décroissants, ont conduit à définir un "potentiel de protection contre la piqûration", lequel est sensiblement

* Voir annexe au présent rapport.

égal au potentiel existant à l'intérieur des piqûres actives. Si le potentiel d'électrode des zones externes passives est inférieur à ce potentiel de protection, les piqûres éventuellement préexistantes ne grandissent pas, et deviennent donc inoffensives; en outre, il ne peut pas se former de nouvelles piqûres.

L'appareillage représenté par la figure 16 (6e, figure 5), qui est très semblable au dispositif montré à la figure 10 précédemment utilisé pour la production artificielle de piqûres de cuivre, a été utilisé par J. VAN MUYLDER pour l'étude de cavernes de fer artificielles. Un cylindre de plexiglas percé d'un petit trou renfermant de l'amiante a été fixé par collage sur une tôle de fer Armco ou d'acier au carbone. Cet ensemble a été immergé dans une solution de pH 10.0 contenant un peu de chlorure (0,0010 molaire en NaOH, et 0,0010 molaire en NaCl, soit 355 ppm Cl). Un bouchon supportant une électrode à calomel et une électrode de verre a été placé sur le cylindre, dans lequel on a fait passer un courant d'azote afin d'en chasser l'oxygène. On fait barboter de l'oxygène dans la solution externe qui est agitée en permanence.

Les points marqués 0 à la figure 17 indiquent les conditions existant lorsqu'aucun courant électrique n'est appliqué à la surface externe : environ -100 mV_{esh} et pH 10.0 pour cette surface externe, et environ -350 à -450 mV_{esh} et pH 2.7 à 4.7 pour la cavité interne, laquelle se corrode. En polarisant cathodiquement la surface externe par passage de courants d'intensité croissante entre cette surface et une anode auxiliaire en platine (points 1 à 9), on a observé que :

- lorsque le "potentiel de protection contre la piqûration" (environ -400mV_{esh}, point 3) est atteint sur la surface externe, la solution à l'intérieur de la caverne cesse d'être acide (pH 7) et le potentiel d'électrode dans la caverne est voisin du potentiel d'immunité (environ -500 à -600 mV_{esh}).
- lorsque le potentiel d'électrode externe devient inférieur à -800 mV_{esh}, la solution à l'intérieur de la caverne devient nettement alcaline (pH 10 à 11), du fait d'une réduction importante de l'eau avec dégagement d'hydrogène.

La figure 18 montre des résultats obtenus en 1970 par Antoine POURBAIX au centre de recherches de la compagnie "Union Oil of California", à Brea, Californie (18) en utilisant un dispositif analogue à celui utilisé précédemment par J. VAN MUYLDER et représenté à la figure 16, avec quelques modifications permettant la mesure du courant électrique passant entre les surfaces externes et internes. Dans le cas de cette expérience, une surface externe passive a été soumise à une polarisation cathodique croissante dans une solution 10^{-3} molaire en NaCl et 10^{-3} molaire en NaOH (pH = 9,5); le pH de la cavité interne était voisin de 5,5.

En absence de polarisation cathodique externe (points 0), la cavité interne active agissait comme anode, avec une densité de courant de 2,5 $\mu A/cm^2$. Cette cavité interne cessa d'agir comme anode au point 4, où le potentiel d'électrode interne (potentiel à courant zéro) fut -0,43 $volt_{esh}$. Le potentiel d'électrode externe, qui était alors ce que l'on appelle de manière approchée le "potentiel de protection contre la piqûration" que l'on peut déterminer par la méthode potentiocinétique à potentiels successivement croissants et décroissants (voir annexe) était de -0,31 $volt_{esh}$ (à ce point 4); pour ce point, le potentiel de diffusion entre les électrolytes externe et interne était -0,31 + 0,43 = 0,12 volt. Il y a lieu d'être bien conscient de ce que, dans le cas présent, l'abaissement du potentiel externe à la valeur du "potentiel de protection" ne correspond pas exactement à une absence totale de corrosion

à l'intérieur de la cavité; ceci ne se produira que lorsque, du fait d'une polarisation cathodique plus forte, le potentiel interne deviendra égal au potentiel d'équilibre de la réaction de corrosion qui, à 25°C, est donné par la relation $E = -0,440 + 0,0295 \log (Fe^{++})$ $volt_{esh}$.

Selon des expériences d'orientation, qui devraient être poursuivies de manière plus systématique, la teneur en fer au fond de la caverne (ou piqûre, ou fissure) semble être de l'ordre de 1 molaire (probablement entre 0,5 et 5 molaire). Il est donc probable que ce potentiel d'équilibre dans la cavité est voisin de $-0,44$ $volt_{esh}$; selon la figure 18 le "potentiel de protection" exact en dessous duquel les cavernes, piqûres et fissures cessent de croître et peuvent être le siège d'un dépôt de fer métallique selon la réaction inverse $Fe^{++} + 2\ e^- \rightarrow Fe$ est donc voisin de $-0,38$ mV_{esh} (entre les points 5 et 6 de la figure 18).

Comme le montrent les figures 17 et 18, la corrosion caverneuse du fer, ainsi que les autres formes de "corrosion en cellule occluse" O.C.C. ou "corrosion dans des conditions de diffusion restreinte" peuvent donc être évitées par une "protection cathodique" convenable, abaissant le potentiel d'électrode de la surface externe du métal en dessous de son "potentiel de protection contre la piqûration".

Mais ceci conduit nécessairement à un accroissement du dégagement d'hydrogène dans les cavités et peut donc conduire à un accroissement de la fragilisation par l'hydrogène dans le cas où le matériau est sensible à cette forme de dégradation.

4.4 Application à la corrosion par piqûres des aciers, et à leur corrosion fissurante sous tension.

Dans les deux sections précédentes, nous avons considéré le comportement de cuivre et de fer purs au point de vue de l'électrochimie de leur corrosion dans des conditions de diffusion restreinte O.C.C., dans des solutions renfermant du chlorure. Une étude approfondie du comportement des aciers nécessiterait la connaissance de données thermodynamiques et cinétiques dignes de foi au sujet de tous les constituants des aciers. La plupart de ces données sont actuellement inexistantes.

Toutefois, nous exprimerons ici quelques considérations basées sur nos connaissances actuelles concernant l'O.C.C. d'aciers au carbone et d'aciers au chrome.

4.41 Electrochimie des surfaces externes passives.

La figure 19 (19, figure 15), qui fait partie d'un travail réalisé en collaboration à l'Université de Floride, Gainesville, montre schématiquement les conditions expérimentales d'immunité, de corrosion généralisée, de corrosion par piqûres, de passivation parfaite et de passivation imparfaite pour six alliages fer-chrome en présence de solutions renfermant 0,100 atome-gramme Cl par litre (3.550 ppm). Selon cette figure, les quatre premiers de ces alliages (0,5 à 12,0 % Cr) donneraient lieu à corrosion caverneuse et à corrosion par piqûres en présence d'une solution à 3.550 ppm Cl neutre et saturée en oxygène; l'alliage à 16,0 % Cr ne subirait pas de corrosion caverneuse, mais pourrait subir une certaine corrosion par piqûres; l'alliage à 24,9 % ne subirait aucune de ces deux formes de corrosion.

4.42 Morphologie et chimie des cavités internes actives.

Nous ne possédons pas d'information particulière concernant la morphologie des cavités d'aciers. En ce qui concerne leur chimie, B.F. BROWN et al. (20a, 20b) ont, au cours de leur travail de pionniers, observé à l'intérieur de fissures de corrosion de différents aciers des pH voisins de 3,8 et des potentiels variant entre -0,2 et -0,5 volt$_{esh}$ selon la nature de l'acier.

La figure 20 (19, figure 7) montre l'influence du pH sur les potentiels à courant nul de la série d'alliages Fe-Cr mentionnée ci-dessus. Comme dit en section 4.332, ces potentiels à courant nul sont probablement sensiblement égaux aux potentiels de ces alliages à l'intérieur de fissures ou piqûres actives de même pH. Pour pH = 3,8 ces potentiels sont

0,5	% Cr	-0,42 volt$_{esh}$
2	% Cr	-0,38
5	% Cr	-0,35
12	% Cr	-0,29
17	% Cr	-0,27
25	% Cr	-0,24

Il apparaît donc qu'un accroissement de la teneur en chrome de l'alliage provoque une élévation du potentiel d'électrode à l'intérieur des piqûres et fissures.

4.43 Electrochimie des cavités actives.

4.431 Diagrammes d'équilibres.

A notre connaissance, ce n'est que pour le cuivre (15) qu'ont été établis des diagrammes dignes de foi concernant des systèmes chlorurés. De tels diagrammes n'existent pas pour les autres constituants des aciers.

4.431.1 Système Cr - H_2O

La figure 21 (15, p. 262) donne un diagramme d'équilibres potentiel/pH pour le système binaire Cr - H_2O, à 25°C.

4.431.2 Systèmes C - H_2O et Fe_3C - H_2O

Comme dérivés du carbone nous ne considérerons que le graphite C, la cémentite Fe_3C, le méthane CH_4, le monoxyde de carbone CO et le bioxyde de carbone CO_2. Dans un but de simplification, nous ne considérerons pas d'autres hydrocarbures et autres composés organiques dont la formation a été décelée par D.N. STAICOPOLUS (21) lors d'une polarisation cathodique de la cémentite.

Nous admettrons les valeurs suivantes d'enthalpies libres de formation standard des substances considérées :

Substances solides		Eau et substances dissoutes		Substances gazeuses	
Fe	0 cal	H_2O	- 56.690 cal	H_2	0 cal
Fe_3O_4	- 242.400 cal	H^+	0 cal	O_2	0 cal
Fe_2O_3	- 177.100 cal	Fe^{++}	- 20.300 cal	CO	- 38.808 cal
C	0 cal			CO_2	- 94.260 cal
Fe_3O_4	+ 4.540 cal			CH_4	- 12.140 cal

Du fait de l'absence de données thermodynamiques, nous n'avons pas pu considérer les carbonyles de fer, et particulièrement le $Fe(CO)_5$ qui pourrait probablement être formé comme produit d'oxydation du Fe_3C.

Etant donné que l'enthalpie libre de formation du Fe_3C est positive, ce composé est thermodynamiquement instable, mais il est possible d'en calculer des conditions d'équilibre métastable.

Les valeurs d'enthalpies libres de formation indiquées ci-dessus conduisent aux conditions d'équilibre suivantes pour quelques unes des réactions faisant intervenir ces substances. Les numéros 41 à 43 se réfèrent à la nomenclature utilisée dans la section de notre Atlas relative au carbone (15, p. 453); les numéros 30 à 37 concernent des réactions faisant intervenir Fe_3C, qui n'ont pas été considérées dans l'Atlas.

a) Réactions avec C

(41) $CH_4 = C + 4\,H^+ + 4\,e^- \quad E_o = + 0.132 - 0.0591\ pH - \frac{0.01477}{\log p_{CH_4}}$ (*)

(42) $C + H_2O = CO + 2\,H^+ + 2\,e^- \quad E_o = + 0.518 - 0.0591\ pH - \frac{0.02955}{\log p_{CO}}$

(43) $C + 2H_2O = CO_2 + 4\,H^+ + 4\,e^- \quad E_o = + 0.207 - 0.0591\ pH + \frac{0.01477}{\log p_{CO_2}}$

(*) Dans l'Atlas (15, p. 453 et fig. 7, p. 455), la valeur de -0.132 a été indiquée par erreur au lieu de + 0.132 pour le potentiel d'électrode standard pour la réaction 41.

b) Réactions avec Fe_3C

Réduction de Fe_3C

(30) $3\,Fe + CH_4 = Fe_3C + 4\,H^+ + 4\,e^-$ $\quad E_o = +0.181 - 0.0591\,pH - 0.01477 \log_{P_{CH_4}}$

Oxydation de Fe_3C

(31) $Fe_3C + 4\,H^+ = 3\,Fe^{++} + CH_4 + 2\,e^-$ $\quad E_o = -1.678 + 0.1182\,pH + 0.08865 \log (Fe^{++}) + 0.0295 \log_{P_{CH_4}}$

(32) $Fe_3C = 3\,Fe^{++} + C + 6\,e^-$ $\quad E_o = -0.472 + 0.0197 \log (Fe^{++})$

(33) $Fe_3C + H_2O = 3\,Fe^{++} + CO + 2H^+ + 8e^-$ $\quad E_o = -0.171 - 0.01477\,pH + 0.02215 \log (Fe^{++}) + 0.00739 \log_{P_{CO}}$

(34) $Fe_3C + 2\,H_2O = 3\,Fe^{++} + CO_2 + 4H^+ + 10e^-$ $\quad E_o = -0.201 - 0.02364\,pH + 0.01773 \log (Fe^{++}) + 0.00591 \log_{P_{CO_2}}$

(35) $Fe_3C + 4\,H_2O = Fe_3O_4 + CH_4 + 4H^+ + 4\,e^-$ $\quad E_o = -0.350 - 0.0591\,pH + 0.00148 \log_{P_{CH_4}}$

(36) $Fe_3C + 5\,H_2O = Fe_3O_4 + CO + 10\,H^+ + 10\,e^-$ $\quad E_o = -0.010 - 0.0591\,pH + 0.00591 \log_{P_{CO}}$

(37) $Fe_3C + 6\,H_2O = Fe_3O_4 + CO_2 + 12H^+ + 12e^-$ $\quad E_o = +0.383 - 0.0591\,pH + 0.00492 \log_{P_{CO_2}}$

(38) $2\,Fe_3C + 13H_2O = 3Fe_2O_3 + 2CO_2 + 26H^+ + 4e^-$ $\quad E_o = -0.350 - 0.0591\,pH + 0.00148 \log_{P_{CH_4}}$

Signalons ci-après les conditions d'équilibre du système $Fe\text{-}H_2O$ pour les réactions faisant intervenir des ions Fe^{++} et les corps solides Fe, Fe_3O_4 et Fe_2O_3 (15, p.309-310)

(13) $3\,Fe + 4\,H_2O = Fe_3O_4 + 8H^+ + 8\,e^-$ $\quad E_o = -0.085 - 0.0591\,pH$

(17) $2\,Fe_3O_4 + H_2O = 3Fe_2O_3 + 2H^+ + 2\,e^-$ $\quad E_o = +0.221 - 0.0591\,pH$

(23) $Fe = Fe^{++} + 2\,e^-$ $\quad E_o = -0.440 + 0.0295 \log (Fe^{++})$

(26) $3\,Fe^{++} + 4\,H_2O = Fe_3O_4 + 8H^+ + 2\,e^-$ $\quad E_o = +0.980 - 0.2364\,pH - 0.0886 \log (Fe^{++})$

(28) $2\,Fe^{++} + 3\,H_2O = Fe_2O_3 + 6H^+ + 2\,e^-$ $\quad E_o = +0.728 - 0.1773\,pH - 0.0591 \log (Fe^{++})$

A la figure 22 nous avons montré :

- pour le système $Fe\text{-}H_2O$: les conditions d'équilibre thermodynamique entre les corps solides Fe, Fe_3O_4, Fe_2O_3 et les ions dissous Fe^{++} (réactions 13, 17, 23, 26 et 28)

- pour le système $C\text{-}H_2O$: les conditions d'équilibre thermodynamique entre le C solide et les corps gazeux CH_4 et CO, chacun pour une fugacité (ou pression partielle corrigée) de 1 atm. (réactions 41 et 43).

- pour le système $Fe_3C\text{-}H_2O$: les fugacités (ou pressions partielles corrigées) en CH_4 relatives à la réduction de Fe_3C avec formation de Fe (réaction 30) et à l'oxydation de Fe_3C avec formation de Fe_3O_4 (réaction 35).

Dans un but de simplification, nous n'avons pas considéré les autres réactions.

Il apparaît à la figure 22 que, comme prévu, Fe_3C est toujours thermodynamiquement instable à 25°C. Il apparaît aussi que, thermodynamiquement parlant, Fe_3C peut disparaître avec formation de CH_4, soit par réduction (avec formation simultanée de fer métallique Fe selon la réaction 30, à des potentiels inférieurs à la ligne 13), ou par oxydation (avec formation simultanée de magnétite Fe_3O_4 selon la réaction 35, à des potentiels supérieurs à la ligne 13). Rappelons que D.N. STAICOPOLUS (21) a observé que Fe_3C peut être effectivement réduit par polarisation cathodique avec formation de fer et de différents hydrocarbures, parmi lesquels surtout du méthane; il se forme aussi du CO et H_2.

Il semble donc que la réaction thermodynamiquement possible $Fe_3C + 4\ H^+ + 4\ e^- \rightarrow 3\ Fe + CH_4$ (30) se produit effectivement.

Comme le montre la figure 22, les fugacités d'équilibre de CH_4 pour chacune des deux réactions 30 et 35 sont extrêmement élevées, beaucoup plus élevées que les fugacités correspondantes de H_2 (15, p.101) : la fugacité minimale en CH_4, qui existe le long de la ligne relative à l'équilibre Fe/Fe_3O_4 (ligne 13), est 10^{+18} atm., au lieu de $10^{+2,87}$ pour H_2. Il est donc très possible que, dans les conditions de potentiel d'électrode et de pH qui existent lorsqu'on observe une corrosion et/ou une "fragilité d'hydrogène", du Fe_3C est décomposé avec formation de CH_4 à une pression extrêmement élevée. Et, étant donné que, comme dit précédemment (6d) H peut être dissous dans le fer et CH_4 ne le peut pas, il est probable que ce qui est actuellement considéré comme "fragilité d'hydrogène" peut être en fait, tout au moins dans certains cas, une "fragilité de méthane" résultant de la décomposition de carbures existant le long de joints de grains.

Nous attirons l'attention sur des travaux remarquables entrepris par R.W. STAEHLE (22) qui a montré que la cémentite présente dans la perlite se dissout préférentiellement dans certaines conditions : à pH 14 (-400 mV), à pH 4 (entre environ - 500 et + 800 mV), et à - 100 mV dans des solutions de NaCl.

Des travaux complémentaires à ce sujet sont une urgente nécessité. Il serait utile aussi de clarifier les conditions dans lesquelles Fe_3C (et autres carbures) peuvent disparaître avec formation de CO, et éventuellement de $Fe(CO)_5$.

4.431.3 Solubilité d'oxydes et d'hydroxydes. Hydrolyse.

La figure 23 (16, fig.14) représente l'influence du pH sur la solubilité de quelques oxydes et hydroxydes métalliques, à 25°C.

Cette figure ne tient pas compte de l'existence possible de différentes variétés allotropiques d'oxydes et d'hydroxydes (excepté pour l'aluminium). Elle est relative à des solutions exemptes de chlorure et ne considère donc pas la formation possible de complexes chlorés dissous (par exemple avec Cr, Al) et de chlorures basiques insolubles. Cette figure peut cependant donner une image approchée des phénomènes d'hydrolyse qui peuvent se produire lorsque des métaux se corrodent en solution neutre.

Supposons, pour fixer les idées, que la solution existant à l'intérieur d'une piqûre ou fissure est saturée en un oxyde ou hydroxyde d'un métal déterminé et a une activité (concentration corrigée) en métal dissous égale à 1 atome gramme par litre. Les ions métalliques en solution doivent s'hydrolyser jusqu'à ce que le pH atteigne la valeur correspondant à cette solubilité de l'oxyde ou hydroxyde.

Pour quelques métaux considérés à la figure 23 et dans l'"Atlas" (15) nous indiquons ci-après ces valeurs de pH, chaque fois pour deux oxydes qui sont respectivement la forme allotropique la plus soluble (instable) et la forme la moins soluble (stable) :

Zn^{++} :	$Zn(OH)_2$ am.	6.1 → 5.5	$Zn(OH)_2$ ε
Ni^{++} :	$Ni(OH)_2$	6.1 → 6.2	NiO
Cr^{+++} :	$Cr(OH)_3$ hydr.	4.0 → 1.5	Cr_2O_3
Al^{+++} :	$Al(OH)_3$	2.7 → 1.5	$Al_2O_3.3H_2O$ (Hydrargillite)
TiO^{++} :	$TiO_2.H_2O$	-0.6 → -6.5 ?	TiO_2

Pour le fer les oxydes peuvent être, s'il n'y a pas d'oxygène, du $Fe(OH)_2$ instable et du Fe_3O_4 stable. S'il y a de l'oxygène, ils peuvent être du $Fe(OH)_3$ et du Fe_2O_3 anhydre :

Fe^{++} :	$Fe(OH)_2$	6.6 → 6.0	Fe_3O_4
Fe^{+++} :	$Fe(OH)_3$	0.6 → -0.2	Fe_2O_3

Ce raisonnement, qui est certainement simplifié de manière abusive et qui devrait être vérifié et amélioré, conduit à la classification suivante des éléments considérés par ordre de degré d'acidité croissant qu'ils provoquent lorsqu'ils se dissolvent jusqu'à saturation en oxyde ou hydroxyde :

Ni < Zn < Fe < Cr < Al < Ti

Avant de terminer la présente section de notre exposé, nous désirons insister sur la nécessité de connaissances beaucoup plus approfondies concernant la thermodynamique (et la cinétique) relative aux très nombreux composés des aciers et autres alliages qui présentent une importance technique, en vue de l'étude des réactions qui peuvent se produire lorsqu'ils sont en présence des solutions existant à l'intérieur des cavités actives. Ceci est particulièrement important en ce qui concerne les constituants qui existent le long des joints de grains.

4.44 Cinétique de la corrosion des aciers par piqûres et par corrosion sous tension, et de leur prévention.

La figure 24 montre, d'après B.F. BROWN (20), l'influence d'une polarisation cathodique sur les caractéristiques électrochimiques et sur la vitesse de propagation de fissures de corrosion sous tension d'un acier au chrome.

Si l'on compare cette figure 24 avec la figure 17, qui concerne l'influence d'une polarisation cathodique sur les caractéristiques électrochimiques d'une caverne d'acier au carbone, il apparaît que ces deux caractéristiques sont extrêmement semblables : dans les deux cas, l'application sur les surfaces externes d'un potentiel d'électrode inférieur au "potentiel de protection contre la piqûration" rend possible une suppression de toute dissolution du métal. Dans le cas de corrosion par piqûres et de corrosion caverneuse, ceci

conduit à une protection totale du métal. Dans le cas de la corrosion fissurante sous tension toutefois, la protection n'est assurée que si le matériau n'est pas sensible à la "fragilisation par l'hydrogène"; si le matériau est sensible à la "fragilisation par l'hydrogène", des potentiels aussi faibles peuvent conduire à un accroissement de la fragilité.

Il résulte de ce qui précède qu'une polarisation cathodique à des potentiels inférieurs au "potentiel de protection contre la piqûration" (généralement voisin de -0,2 à -0,4 volt par rapport à l'électrode standard à hydrogène esh) peut conduire à une protection de tous les aciers contre la corrosion par piqûres et contre la corrosion caverneuse. Elle peut aussi protéger contre la corrosion fissurante sous tension les aciers qui ne sont pas sensibles à la "fragilisation par l'hydrogène". Une telle protection cathodique peut être réalisée, soit par un traitement électrique, soit au moyen d'anodes sacrificielles, lesquelles peuvent être mises en oeuvre sous forme de revêtements métalliques : Zn, Cd et Pb (23).

En ce qui concerne les aciers sensibles à la "fragilisation par l'hydrogène", il existe, au point de vue purement électrochimique, un besoin particulier d'études complémentaires. S'agit-il réellement d'une "fragilisation par l'hydrogène", ou s'agit-il, en tout ou partie, d'une "fragilisation par le méthane", due à une action sur la cémentite et/ou sur d'autres carbures, spécialement si des carbures existent le long des joints de grains ?

En tout état de cause, il y a lieu d'examiner avec une attention toute spéciale les idées originales émises lors de la conférence d'Ericeira, par M. BRABERS (24).

4.5 Application à la corrosion du titane.

Les figures 25a et 25b (25) montrent deux diagrammes d'équilibres potentiel/pH pour le système binaire Ti-H_2O à 25°C, qui ont été établis respectivement sans considérer et en considérant l'hydrure de titane TiH_2. Les figures 26a et 26b montrent les diagrammes théoriques correspondants d'immunité, corrosion et passivation du titane. Ces figures montrent toutes deux un "triangle de corrosion" dans leur partie inférieure gauche, dans des conditions acides et très réductrices; comme la plus grande partie de ces triangles se situe loin en dessous de la "ligne de l'hydrogène" a, l'affinité de réduction de l'eau en hydrogène y est considérable. La figure 27 (6a, 6c) représente, pour rappel, un schéma préliminaire montrant les conditions probables de potentiel et de pH pour la corrosion, la passivation et la protection du titane. La figure 28 (6a) est un schéma préliminaire pour l'initiation et la propagation d'une fissure de corrosion sous tension dans un alliage titane-aluminium.

Antoine POURBAIX, Miroslav MAREK et Robert F. HOCHMAN (25) ont présenté en Janvier 1971 à Atlanta un travail de recherche effectué au Georgia Institute of Technology pour vérifier expérimentalement l'existence du "triangle de corrosion" montré aux figures 26 et 27. Des courbes de polarisation cathodique ont été tracées sur du titane en solution de HCl 12 N (pH = -0,5). Une première série d'expériences a été conduite sur des surfaces polies à l'émeri, rincées à l'eau et séchées à l'air avant immersion, et a conduit à la courbe représentée à la figure 29a. Les auteurs indiquent que "les échantillons ont été polarisés jusqu'à -1,0 volt$_{csh}$ dans HCl 12 N et maintenus à ce potentiel. Il en est résulté au début une réaction globale de réduction avec dégagement d'hydrogène, sans signe apparent de corrosion de l'échantillon. Après environ

une demi-heure, et très soudainement, une pellicule blanche s'est séparée de l'échantillon et s'est immédiatement dissoute, l'électrolyte s'est rapidement coloré en bleu foncé par formation de Ti^{+++} dissous, le courant de polarisation est devenu fortement anodique et l'électrode s'est rapidement corrodée avec dégagement d'hydrogène. La polarisation potentiocinétique a alors été reprise, à potentiel décroissant, et le courant anodique de corrosion s'est maintenu jusqu'à un potentiel de -1,65 $volt_{esh}$.".

Une deuxième série d'espériences a été conduite sur des échantillons de titane immergés immédiatement après polissage et rinçage, sans séchage. Ceci a conduit (figure 29b) à un potentiel initial à courant zéro légèrement inférieur au potentiel observé précédemment (-0,50 volt au lieu de -0,43 $volt_{esh}$), et la polarisation cathodique a conduit immédiatement à un courant anodique, associé à une corrosion et à un dégagement d'hydrogène. Lors de cette deuxième série d'expériences, le courant devint zéro à environ -0,8 $volt_{esh}$, et il fut souvent impossible de maintenir un courant anodique en dessous de ce potentiel.

Lors de chacune de ces deux séries d'expériences, la formation de TiH_2 fut décelée par analyse avec diffraction de rayons X. Ce TiH_2 a été trouvé non protecteur.

Parmi leurs conclusions, les auteurs expriment l'opinion suivante en ce qui concerne la corrosion fissurante sous tension : "Lorsque du titane dépourvu d'oxyde (tel qu'il apparaît lors de l'ouverture d'une fissure) se trouve en présence d'un milieu fortement acide, il peut se corroder avec formation de Ti^{++} ou de Ti^{+++} et dégagement d'hydrogène, à très bas potentiel. Il est probable que ces ions, qui sont tous-deux thermodynamiquement instables en présence d'eau, s'oxydent en TiO_2 (éventuellement hydraté) avec dégagement d'hydrogène. La vitesse de corrosion du titane à bas pH et bas potentiel peut être très grande (probablement de l'ordre du cm par heure, mais ce chiffre devrait être précisé). A ces potentiels, TiH_2 peut se former sur la surface du titane et faciliter fortement la réaction de dégagement d'hydrogène.

Il n'est pas exclu que le dégagement important d'hydrogène dans ces conditions permette une diffusion d'hydrogène atomique dans la matrice métallique, à partir de l'extrémité de la fissure et que cet hydrogène précipite au sein du métal en TiH_2, qui est un composant particulièrement fragilisant du titane et de ses alliages".

Nous référant à l'exposé ci-dessus, nous désirons souligner l'utilité de ces travaux effectués à Georgia Tech. Il est probable que, à l'extrémité de la fissure, la solution est saturée en un chlorure titaneux ($TiCl_2$ ou $TiCl_3$?) très soluble et instable; cette solution serait très concentrée et très acide. Des recherches électrochimiques effectuées sur une telle solution de manière semblable à celles suggérées ci-dessus en section 4.33 pour le fer seraient très utiles pour élucider le comportement à la corrosion sous tension du titane et d'alliages de titane. Comme indiqué dans les sections qui précèdent, ces recherches devraient être à la fois de natures thermodynamique et cinétique; elles devraient comporter des courbes de polarisation sur des électrodes non soumises et soumises à fluage sous des efforts de traction.

5. QUELQUES TÂCHES A RÉALISER CONCERNANT L'ELECTROCHIMIE DE LA CORROSION FISSURANTE SOUS TENSION.

5.1 Thermodynamique électrochimique de la corrosion dans des conditions de diffusion restreinte (cellules de corrosion occluses).

Réunir les données thermodynamiques accessibles pour des systèmes métal-chlorure-eau, particulièrement pour le fer, le chrome, l'aluminium, le titane et pour les constituants de leurs alliages. Tracer des diagrammes d'équilibres pour ces systèmes, en considérant particulièrement les solutions concentrées saturées en chlorures métalliques. Appliquer ces diagrammes à l'étude des caractéristiques chimiques et électrochimiques possibles dans les cavernes, piqûres, fissures.

5.2 Expériences électrochimiques concernant les cellules de corrosion occluses

Préparer synthétiquement des solutions semblables à celles existant dans les cavernes, piqûres et fissures actives notamment par saturation d'eau exempte d'oxygène avec des chlorures métalliques. Etudier expérimentalement la cinétique des circonstances de corrosion et de non corrosion dans ces cellules.

5.3 Comportement électrochimique de la cémentite et d'autres carbures.

Etudier expérimentalement les conditions pratiques de stabilité et d'instabilité du Fe_3C et d'autres carbures, particulièrement en ce qui concerne l'influence du potentiel d'électrode, du pH et des anions (par exemple selon les méthodes utilisées par R.W. STAEHLE et par D.N. STAICOPOLUS). Examiner les conditions de formation de CH_4, de CO et de $Fe(CO)_5$.

5.4 Electrochimie de la fragilisation par l'hydrogène.

Poursuivre les études concernant la fragilisation cathodique de métaux purs et d'alliages (par exemple selon les méthodes de B.F. BROWN et de M. BRABERS). Examiner s'il existe une corrélation entre les résultats de ces études et la composition et la morphologie des alliages, notamment en ce qui concerne le comportement des composés existant aux joints de grains.

5.5 Protection électrochimique contre la corrosion caverneuse, la corrosion par piqûres et la corrosion fissurante sous tension.

Vérifier l'efficacité de procédés de protection cathodique contre les "corrosions en cellules occluses" spécialement par mise en oeuvre de revêtements sacrificiels (en plomb, cadmium, zinc, etc.). Examiner la possibilité d'éviter la corrosion fissurante sous tension par des traitements superficiels évitant la formation de cavernes et piqûres.

5.6 Méthodes électrochimiques d'essai en corrosion fissurante sous tension.

Mettre au point des méthodes électrochimiques accélérées pour l'appréciation de la susceptibilité à la corrosion fissurante sous tension, pour différents métaux et alliages et dans des conditions conduisant à des résultats en harmonie avec les résultats du comportement en service. Utiliser ces méthodes pour mettre au point de nouveaux alliages. Une attention particulière est à apporter aux méthodes de fluage à courant nul et dans des conditions potentiostatiques.

ANNEXE : POTENTIEL D'IMMUNITE, POTENTIEL DE PASSIVATION, POTENTIEL DE PIQÛRATION ET POTENTIEL DE PROTECTION CONTRE LA PIQÛRATION.

Nous rappelons que, comme exposé dans des publications précédentes (6a, 6e), la figure 30a représente schématiquement cinq courbes de polarisation potentiocinétique relatives à du fer ARMCO dans des solutions exemptes de chlorure de pH 5, 7, 9, 11 et 13. De ces courbes de polarisation il est aisé de déduire la figure 30b qui représente, en fonction du pH et du potentiel d'électrode, des circonstances expérimentales d'immunité, de corrosion généralisée et de passivité.

Les potentiels qui séparent les régions d'immunité et de corrosion généralisée sont les potentiels d'équilibre C de la réaction de corrosion, en dessous desquels cette réaction est thermodynamiquement impossible. Les potentiels qui séparent les régions de corrosion généralisée et de passivité sont les potentiels de passivation P au dessus desquels un film protecteur est formé sur le métal.

La figure 31a représente schématiquement cinq courbes de polarisation en solutions des mêmes pH 5 à 13, mais renfermant 10^{-2} ion gramme Cl^- par litre (355 ppm). r est le potentiel de rupture (ou de piqûration) au dessus duquel le film de passivation devient localement non protecteur, ce qui conduit à la formation de piqûres. p est le potentiel de protection contre la piqûration, en dessous duquel les piqûres formées cessent de grandir, et deviennent donc inoffensives. La figure 31a permet de tracer la figure 31b qui montre, outre les régions déjà mentionnées d'immunité, corrosion généralisée et passivité, une région de piqûration (située au dessus du potentiel de rupture r, lequel dépend fortement du pH et de la teneur en chlorure); la ligne qui représente le potentiel de protection p (lequel est presque indépendant du pH et de la teneur en chlorure) divise le domaine de passivité en une région supérieure où les piqûres préexistantes éventuelles grandissent (la passivité est alors imparfaite) et une région inférieure où les piqûres préexistantes ne grandissent pas (la passivité est alors parfaite). La figure 31b montre aussi que, pour des pH inférieurs à 6, il ne se produit pas de passivation; seule une corrosion généralisée est alors possible.

La figure 4, qui est semblable à la figure 31b, montre les conditions de potentiel et de pH qui sont possibles lorsque du fer est en présence d'une solution de pH 8 10^{-2} molaire en Cl^-. Si la solution est exempte d'oxygène et d'autres oxydants, le potentiel d'électrode du fer non polarisé se placera au point 1 et il se produira une certaine corrosion généralisée avec dégagement d'hydrogène; si de telles conditions d'absence d'oxygène n'existent que sur une partie d'une structure en fer, la corrosion généralisée ainsi initiée conduira à une corrosion caverneuse. Si la solution renferme de l'oxygène, le potentiel d'électrode peut s'élever au point 2 et ceci conduit à la formation de piqûres. Dans les deux cas (en absence et en présence d'oxygène), les produits de corrosion stables ne sont pas les ions Fe^{++} et Fe^{+++} formés primairement, mais des oxydes et hydroxydes tels que Fe_3O_4 et $Fe(OH)_3$; il se produit donc une hydrolyse à l'intérieur des cavernes et piqûres selon les réactions

$$3\ Fe^{++} + 4\ H_2O \rightarrow Fe_3O_4 + 8\ H^+ + 2\ e^-$$

et

$$Fe^{+++} + 3\ H_2O \rightarrow Fe(OH)_3 + 3\ H^+$$

et si, comme c'est généralement le cas, les cavernes et piqûres sont occluses du fait de dépôts de produits de corrosion solides, cette hydrolyse conduit à une acidification locale à l'intérieur des cavernes et piqûres; si du chlorure est présent, cet acide est de l'acide chlorhydrique, qui est particulièrement agressif.

BIBLIOGRAPHIE.

1. J.R. BAYLIS
Met. Chem. Eng. 32, 874 (1925).

2. T.P. HOAR
The Corrosion of Tin in Nearly Neutral Solutions.
Trans. Faraday Soc. 33, 1152 (1937).

3. C. EDELEANU et U.R. EVANS
Trans. Faraday Soc. 47, 1121 (1951).

4. U.R. EVANS
a) The Corrosion and Oxidation of Metals. - Publ. Arnold, Londres(1960).
b) An Introduction to Metallic Corrosion. - Publ. Arnold, Londres 2e édition (1963).

5. I.L. ROSENFELD et I.K. MARSHAKOV
Mechanism of Crevice Corrosion. - Corrosion 20, 115t-125t (1964).

6. M. POURBAIX
a) Recherches en corrosion. Résultats de travaux récents. Voyages aux Etats-Unis d'Amérique. - Rapports Techniques CEBELCOR 109, RT.157 (1969).
b) Une méthode électrochimique rapide de prédétermination de la corrosion atmosphérique. - Rapports Techniques CEBELCOR, 109, RT.160 (1969).
c) Bases fondamentales de la protection cathodique, et applications. Rapports Techniques CEBELCOR 111, RT.166 (1969).
d) Recent applications of electrode-potential measurements in the thermodynamics and kinetics of corrosion of metals. - Rapports Techniques CEBELCOR 112, RT.167 (1970).
e) Signification of the protection-potential in pitting-corrosion, intergranular corrosion and stress-corrosion cracking. - Corrosion, 26, 431-438 (1970).

7. T.P. HOAR
Nature 216, 1299 (1967).

8. J. KRUGER et J. AMBROSE
Breakdown of passive films on iron by chloride ions. - Rapports Techniques CEBELCOR 112, RT.169, et discussion (1970).

9. B.F. BROWN
Stress-corrosion cracking of high strength steels. - Rapport présenté lors dela Conférence de l'CTAN sur la Corrosion sous Tension, 21 septembre 1970.

10. J. MONTUELLE
Acquisitions récentes au sujet de l'origine et de la prévention des phénomènes de corrosion sous tension. Journées de la Corrosion, Lille, avril 1968

11. M. POURBAIX, J. VAN MUYLDER, P. VAN LAER, A. POURBAIX et N. de ZOUBOV
a) Sur la tension d'électrode du cuivre en présence d'eau de Bruxelles. Influence de la lumière et des conditions de circulation de l'eau. Rapports Techniques CEBELCOR 100, RT.125 (1965).
b) Relation entre la tension d'électrode et les circonstances de corrosion du cuivre électrolytique en présence d'eau de Bruxelles. Influence de l'état de surface du cuivre, des circonstances de circulation de l'eau, de traitements de l'eau, et d'un contact du cuivre avec du graphite ou avec du platine. - Rapports Techniques CEBELCOR, 100, RT.126 (1965).

c) Caractéristiques électrochimiques de piqûres de corrosion du cuivre en présence d'eau et de solutions aqueuses chlorurées. Rapports Techniques CEBELCOR 100, RT.127 (1965).
d) Méthodes accélérées d'appréciation du risque de piqûration du cuivre en présence d'eaux. Application à l'étude de l'influence d'un contact du cuivre avec un autre métal ou avec du graphite. Rapports Techniques CEBELCOR 100, RT.128 (1965).
e) Sur le comportement du cuivre en présence de solutions de bicarbonate de sodium. Rapports Techniques CEBELCOR 101, RT.133 (1965).

12. M. POURBAIX, J. VAN MUYLDER, P. VAN LAER, A. POURBAIX et N. de ZOUBOV.

a) Fundamental research on the electrochemical behavior and the corrosion of copper. Report to INCRA. Publication CEBELCOR E.53 (1964).
b) Electrochemical nature of the pitting of copper in water and in aqueous solutions. (Trad. de R.J.F. THORPE du Rapport Technique CEBELCOR, RT.127). Publication CEBELCOR E.61 (1967).
c) Accelerated test for measuring the susceptibility of copper to pitting in water. Applied to studying the effect of coupling copper with other metals and with graphite. (Traduction de R.J.F. THORPE du Rapport Technique CEBELCOR RT.128) Publication CEBELCOR E.62 (1967).

13. J. VAN MUYLDER, N. de ZOUBOV et M. POURBAIX

Diagrammes d'équilibres tension/pH des systèmes Cu-H_2O et Cu-Cl-H_2O. Rapports Techniques CEBELCOR 85, RT.101 (1962).

14. S. SMIALOVSKA Communication verbale de M. SMIALOVSKI, Bruxelles, 23 Juin 1969.

15. M. POURBAIX et al. Atlas d'équilibres électrochimiques en solutions aqueuses.
a) en français : Publication Gauthier-Villars et CEBELCOR (1963).
b) en anglais : Publication Pergamon Press et CEBELCOR (1966).

16. M. POURBAIX Leçons sur la corrosion électrochimique. Rapports Techniques CEBELCOR RT.57b, 30, 49, 86 et 91.

17. M. POURBAIX et al. Etudes potentiocinétiques et corrosimétriques sur le comportement d'aciers alliés.
a) en français : Rapports Techniques CEBELCOR 103, RT.120 (1962)
b) en anglais : Corrosion Science 3, 239-259 (1963).

18. A. POURBAIX Etude de la corrosion localisée de l'acier en solution chlorurée Rapports Techniques CEBELCOR 118, RT.198 (1971).

19. E.D. VERINK et M. POURBAIX

Use of potentiokinetic methods at successively increasing and decreasing electrode potentials in developing alloys for saline exposure. Rapports Techniques CEBELCOR 117, RT.191 (1971).

20. B.F. BROWN a) en collaboration avec C.T. FUJII et E.Ph. DAHLBERG
Methods for studying the solution chemistry within stress-corrosion cracks. J. Electrochemical Soc. 116, 218-219 (1969).

b) On the electrochemistry of stress-corrosion cracking of high strength steels. Publ. CEBELCOR E.76 (1969).
c) En collaboration avec G. SANDOZ et C.T. FUJII
Solution chemistry within stress-corrosion cracks in alloy-steels. NRL Report (15.08.1969). A publier.

21. D.N. STAICOPOLUS The role of cementite in the acidic corrosion of steel. J. Electrochemical Soc. 110, 1121-1124 (1963).

22. R.W. STAEHLE Dissolution of iron and iron carbide in the pearlite matrix Rapport Technique CEBELCOR 114, RT.177 (1970).

23. M. VAN DROFFELAAR Experiences with the protection of austenitic stainless steels in chloride-containing environments. Rapports Techniques CEBELCOR 112, RT.172 (1970).

24. M. BRABERS Fractographic Analysis of Hydrogen Embrittlement. Rapport présenté à la "NATO Stress-Corrosion Conference" Ericeira, 29 mars - 2 avril 1971.

25. A. POURBAIX, M. MAREK et R.F. HOCHMAN
Comportement électrochimique du titane à bas pH et à bas potentiel d'électrode.
Rapports Techniques CEBELCOR 118, RT.197 (1971).

TABLE DES FIGURES

Figure 1 Potentiel d'électrode du fer en absence (ligne 1) et en présence (lignes 2a et 2b) d'oxygène, en solutions exemptes de chlorure. Circonstances générales d'immunité, de corrosion et de passivité.

Figure 2 Initiation d'une caverne de corrosion du fer.

Figure 3 Initiation d'une piqûre de corrosion du fer.

Figure 4 Circonstances de pH et de potentiel en présence d'une solution de pH voisin de 8 (10^{-2} Molaire en Cl^-, soit 355 ppm.).

Figure 5 Piqûre de cuivre en présence d'eau de Bruxelles froide.

Figure 6 Diagramme d'équilibres potentiel/pH pour le système binaire Cu-H_2O à 25°C.

Figure 7 Diagramme d'équilibres potentiel/pH pour le système ternaire Cu-Cl-H_2O, à 25°C pour une teneur en chlorure libre égale à 10^{-2} M (355 ppm Cl^-).

Figure 8 Diagramme d'équilibres potentiel/pH pour le système quinaire Cu-Cl-CO_2-SO_3-H_2O à 25°C. Solutions contenant 22 ppm. Cl^-, 229 ppm CO_2 et 46 ppm. SO_3.

Figure 9 Influence de l'activité des ions Cl^- sur les caractéristiques chimiques et électrochimiques de piqûres de cuivre, à 25°C.

Figure 10 Dispositif expérimental de production artificielle de piqûres de corrosion.

Figure 11 Potentiels d'électrode du fer en présence d'une solution de pH 8 (10^{-2} Molaire en Cl^-, soit 355 ppm. Cl^-).

Figure 12 Corrosion aux défauts de la pellicule d'oxyde sur du fer en présence d'une solution de chlorure de sodium (d'après U.R. EVANS).

Figure 13 Diagramme d'équilibres potentiel/pH du système $Fe-H_2O$, à 25°C.

Figure 14 Domaine théorique de stabilité thermodynamique de Fe, Fe_3O_4, Fe_2O_3 et $FeCl_2.4H_2O$ en présence de solutions électriquement neutres en $FeCl_2$ (Schéma).

Figure 15 Schéma d'une piqûre et d'une fissure de fer.

Figure 16 Dispositif pour l'étude de la corrosion caverneuse.

Figure 17 Influence d'une polarisation cathodique sur les caractéristiques électrochimiques d'une piqûre (ou caverne) de corrosion (acier au carbone ordinaire en présence de solution aérée de NaOH 0.001 M et NaCl 0.001 M) (Schéma). On a réuni par des traits pointillés les caractéristiques simultanées de la surface non aérée (piqûre) et la surface aérée. Les points marqués 0 correspondent à une absence de polarisation; les points 1 à 9 correspondent à des polarisations cathodiques de la surface aérée.

Figure 18 Courbes de polarisation cathodique pour une électrode de fer duplex en solution NaCl 10^{-3} M et NaOH 10^{-3} M.
pH externe = 9,5
pH interne = 5,5
(d'après Antoine POURBAIX).

Figure 19 Circonstances d'immunité, de corrosion généralisée, de piqûration et de passivation parfaite et imparfaite pour six alliages binaires Fe-Cr en présence de solutions 0.1 M en ions chlorure.

Figure 20 Effet de la teneur en chrome sur les potentiels à courant nul des alliages binaires Fe-Cr, en fonction du pH.

Figure 21 Diagramme d'équilibres potentiel/pH du système $Cr-H_2O$, à 25°C.

Figure 22 Diagramme d'équilibres potentiel/pH du système $Fe-C-H_2O$ à 25°C
Ont été considérés :
pour le système $Fe-H_2O$: Fe, Fe_3O_4, Fe_2O_3 solides et ions Fe^{++},
pour le système $C-H_2O$: C solide (graphite), CH_4 et CO_2 gazeux,
pour le système $Fe-C-H_2O$: les équilibres métastables de réduction de Fe_3C en Fe et CH_4, et d'oxydation de Fe_3C en Fe_3O_4 et CH_4.

Figure 23 Influence du pH sur la solubilité des oxydes et hydroxydes.

Figure 24 Influence d'une polarisation cathodique sur les caractéristiques électrochimiques et sur la vitesse de propagation d'une fissure de corrosion sous tension (d'après B.F. BROWN).

Figure 25 Diagrammes d'Equilibres potentiel/pH pour le système $Ti-H_2O$, à 25°C
a) sans considérer TiH_2
b) en considérant TiH_2

Figure 26 Domaines théoriques d'immunité, corrosion et passivation du titane, à 25°C
a) sans considérer TiH_2
b) en considérant TiH_2

Figure 27 Circonstances théoriques de corrosion, passivation et protection du titane (schéma).

Figure 28 Initiation et propagation d'une fissure de corrosion sous tension dans un alliage titane-aluminium.

Figure 29 Courbes de polarisation cathodique de titane en solution HCl 12 N.
a) échantillon de titane poli, rincé et séché avant immersion dans la solution
b) échantillon de titane immergé immédiatement après polissage (d'après A. POURBAIX, M. MAREK et R.F. HOCHMAN).

Figure 30 Comportement de fer en solutions exemptes de chlorure
a) courbes de polarisation en présence de solutions de pH 5 à 13
b) circonstances expérimentales d'immunité, corrosion généralisée et passivité.

Figure 31 Comportement de fer en présence de solutions renfermant du chlorure (10^{-2} ion gramme par litre, i.e. 355 ppm Cl^-).
a) courbes de polarisation en présence de solutions de pH 5 à 13.
b) circonstances expérimentales d'immunité, corrosion généralisée, passivité parfaite et imparfaite, et piqûration.

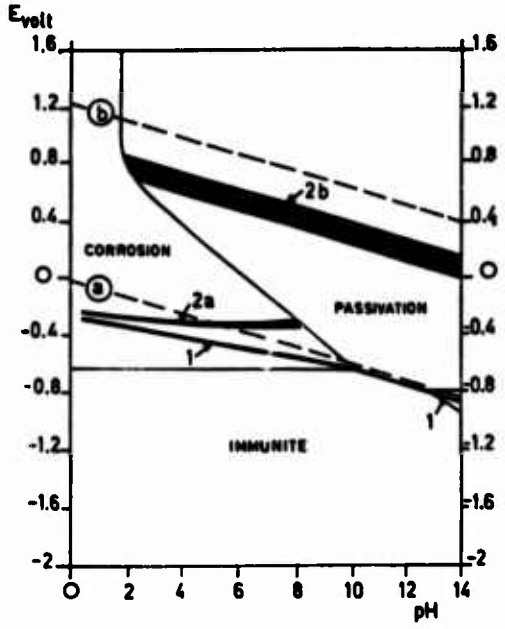


FIGURE 1 : Potentiel d'électrode du fer en absence (ligne 1) et en présence (lignes 2a et 2b) d'oxygène, en solutions exemptes de chlorure. Circonstances générales d'immunité, de corrosion et de passivation.

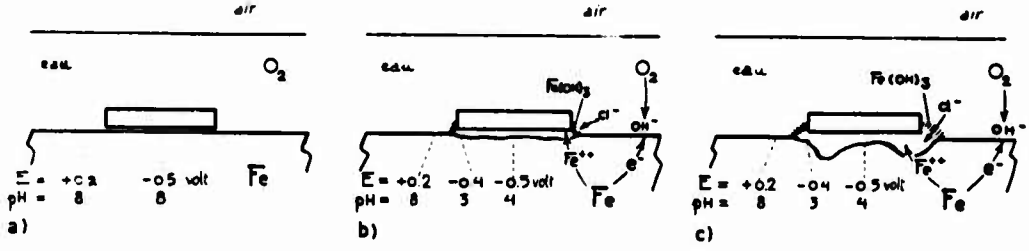
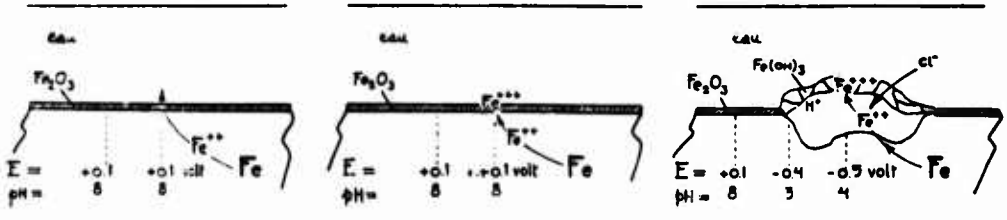


FIGURE 2 : Initiation d'une caverne de corrosion du fer.



a) au temps d'induction t_1 b) entre les temps d'induction t_1 et t_2 c) après le temps d'induction t_2

FIGURE 3 : Initiation d'une piqûre de corrosion du fer.

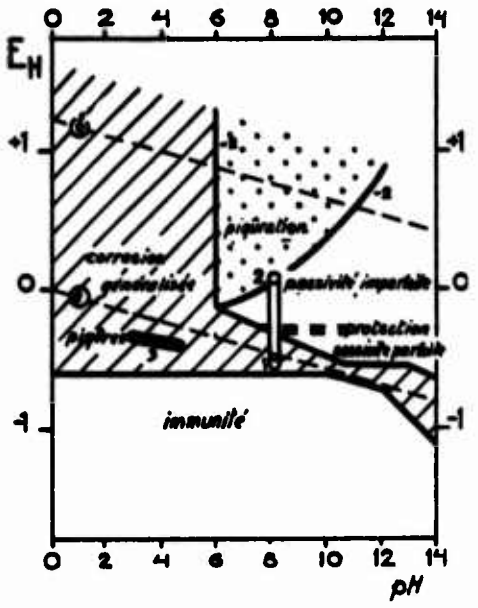


FIGURE 4 : Circonstances de pH et de potentiel en présence d'une solution de pH voisin de 8.
(10^{-2} Molaire en Cl^-, soit 355 ppm Cl^-)

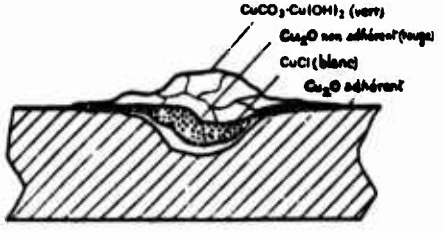


FIGURE 5 : Piqûre de cuivre.

Section montrant la présence de Cu_2O rouge et de CuCl blanc sous une couche de malachite verte.

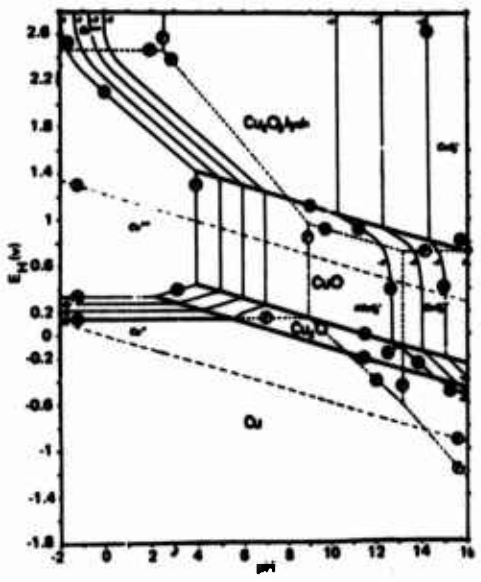


FIGURE 6 : Diagramme d'équilibres potentiel/pH pour le système binaire Cu-H_2O, à 25°C.

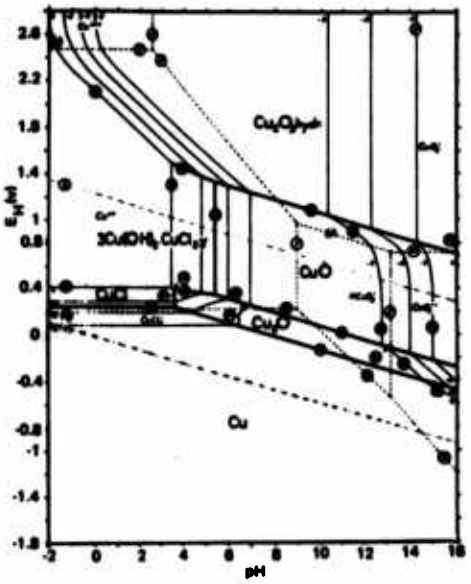


FIGURE 7 : Diagramme d'équilibres potentiel/pH pour le système ternaire Cu-Cl-H_2O, à 25°C, pour une teneur en chlorure libre égale à 10^{-2} (355 p.p.m. Cl^-).

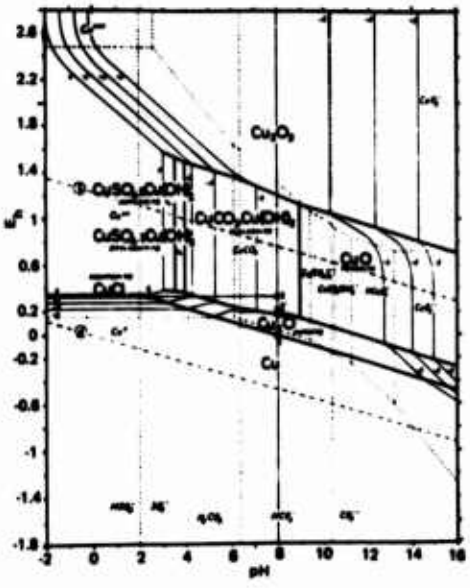


FIGURE 8 : Diagramme d'équilibres potentiel-pH pour le système quinaire Cu-Cl -CO_2-SO_3-H_2O, à 25°C. Solutions contenant 22 p.p.m. Cl^-, 229 p.p.m. CO_2 et 46 p.p.m. SO_3.

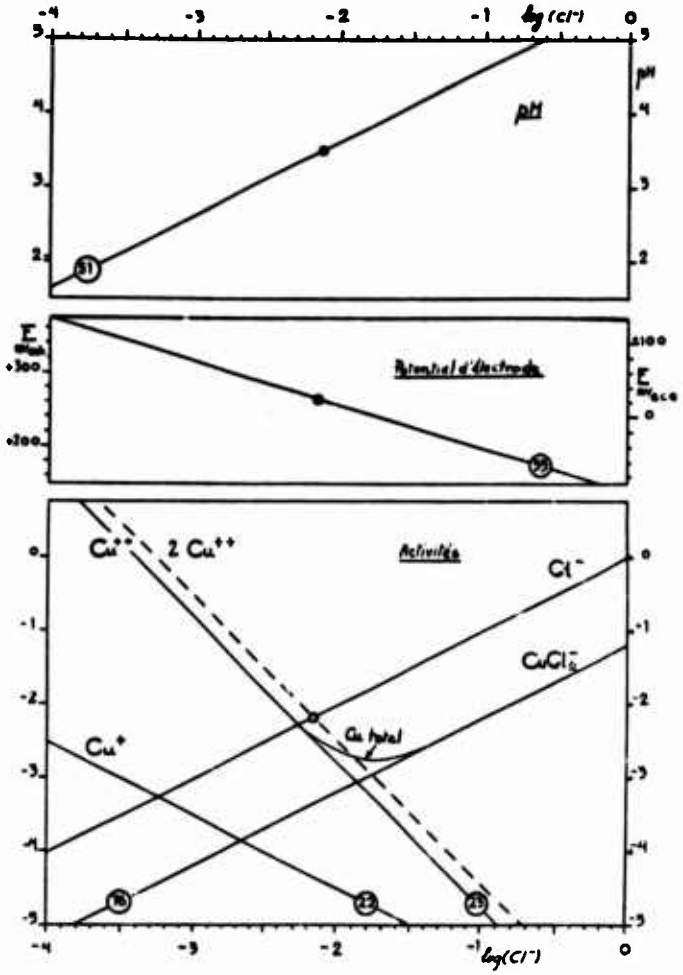


FIGURE 9 : Influence de l'activité des ions Cl⁻ sur les caractéristiques d'équilibre de piqûres de cuivre, à 25°C.

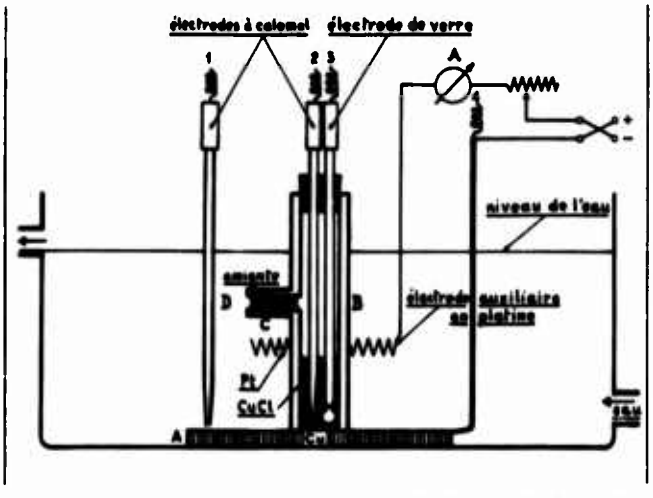


FIGURE 10 : Dispositif expérimental de production artificielle de piqûres de corrosion.

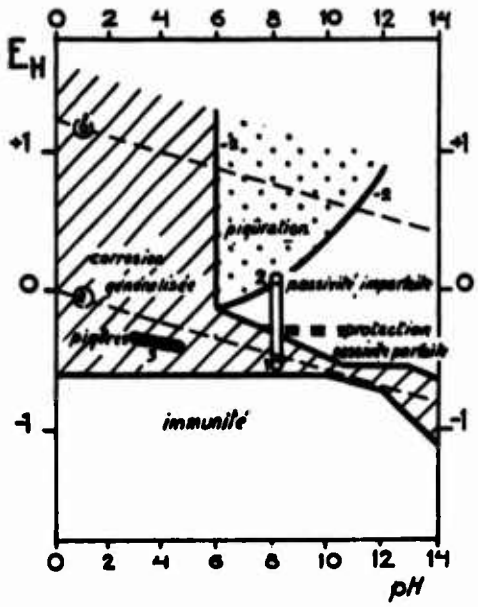


FIGURE 11 : Conditions de pH et de potentiel du fer en présence d'une solution de pH voisin de 8.
(10^{-2} M dans Cl^-, soit 355 ppm Cl^-)

1. fer non polarisé en présence de solution exempte d'oxygène : début de corrosion généralisée.
2. fer non polarisé en présence de solution oxygénée : début de piqûration.
3. piqûres et crevasses actives.

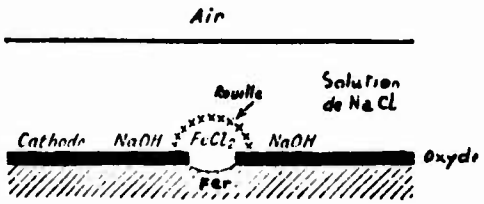


FIGURE 12 : Corrosion aux défauts de la pellicule d'oxyde sur du fer en présence d'une solution de chlorure de sodium.

(d'après U.R. EVANS).

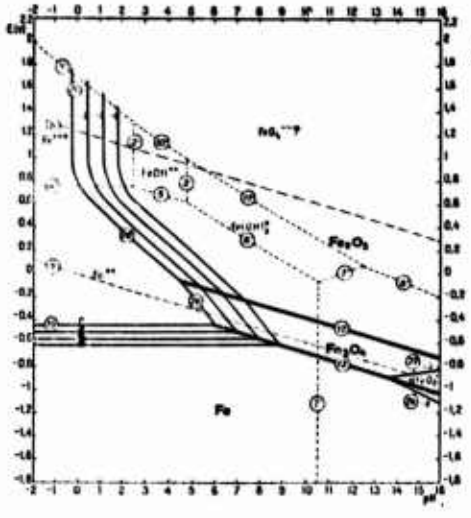


FIGURE 13 : Diagramme d'équilibres potentiel/pH du système Fe-H_2O, à 25°C.

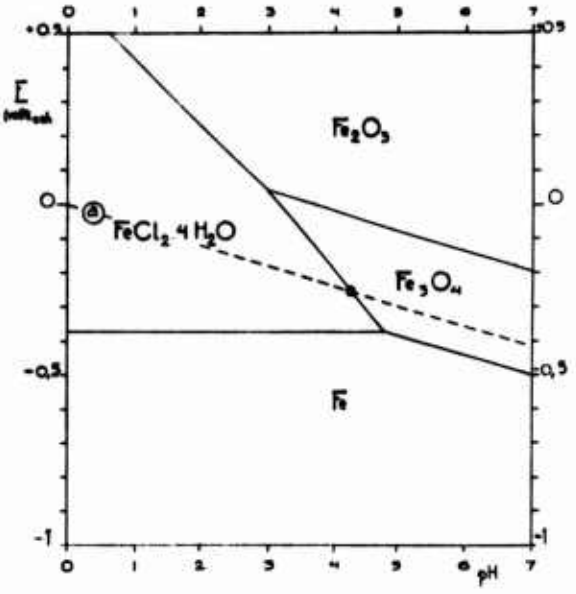


FIGURE 14 : Domaines théoriques de stabilité thermodynamique de Fe, Fe_3O_4, Fe_2O_3 et $FeCl_2.4H_2O$ en présence de solutions électriquement neutres en $FeCl_2$. (Schéma.)

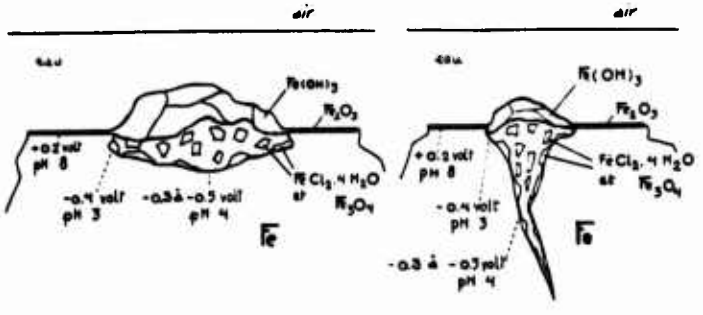


FIGURE 15 : Schéma d'une piqûre et d'une fissure de fer.

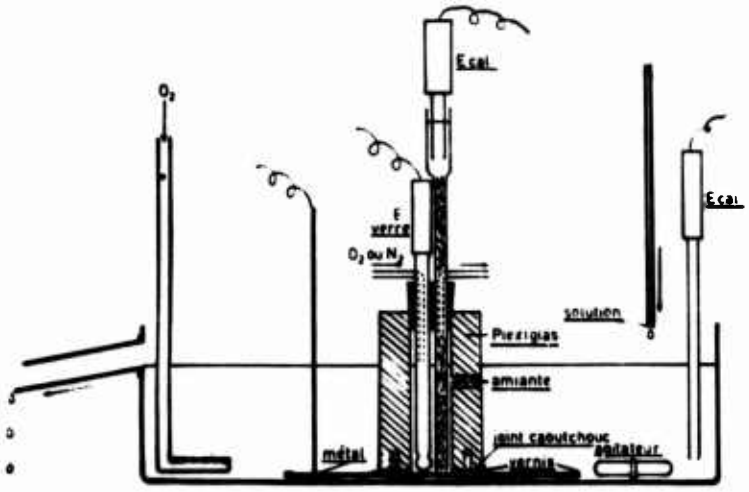


FIGURE 16 : Dispositif pour l'étude de la corrosion caverneuse.

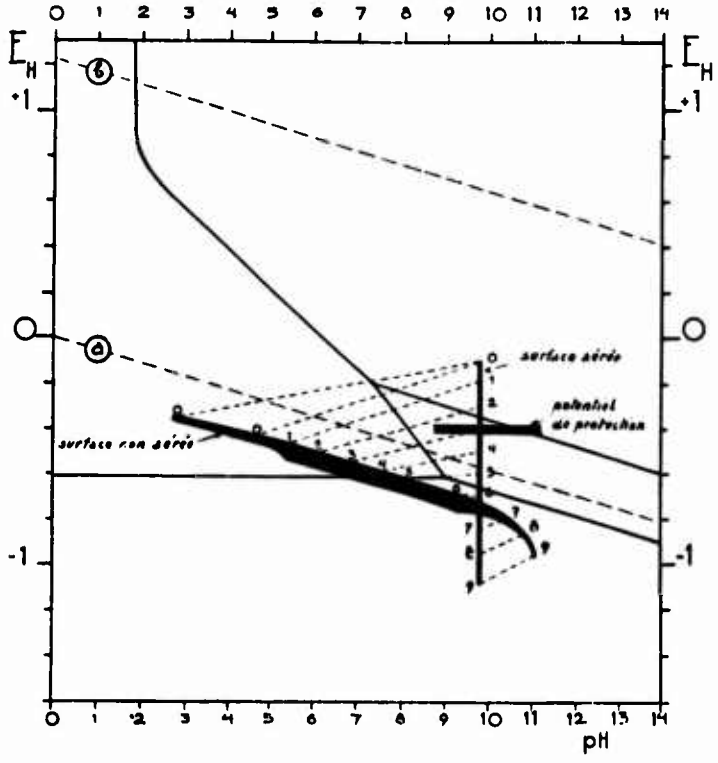


FIGURE 17 : Influence d'une polarisation cathodique sur les caractéristiques électrochimiques d'une piqûre (ou caverne) de corrosion. (Acier au carbone ordinaire en présence de solution aérée de NaOH 0.001 M et NaCl 0.001 M).

On a réuni par un pointillé les caractéristiques simultanées de la surface non aérée (piqûre) et de la surface aérée. Les points marqués 0 correspondent à une absence de polarisation; les points 1 à 9 correspondent à des polarisations cathodiques de la surface aérée.

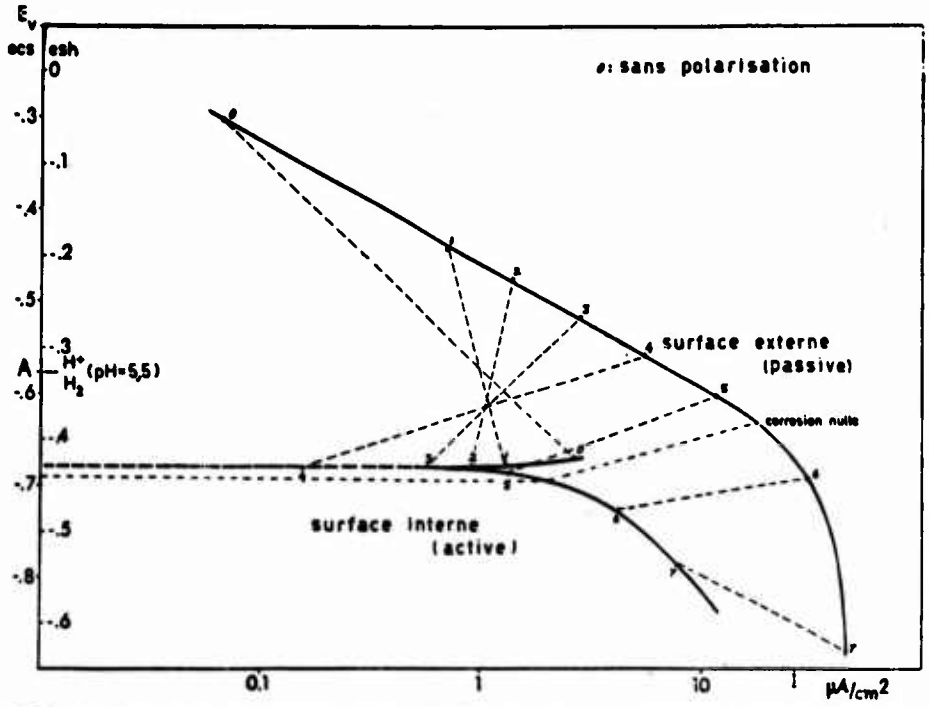


FIGURE 18 : Courbes de polarisation cathodique pour une électrode de fer duplex en solution NaCl 10^{-3} M et NaOH 10^{-3} M. (pH externe = 9,5; pH interne = 5,5).
(d'après Antoine POURBAIX).

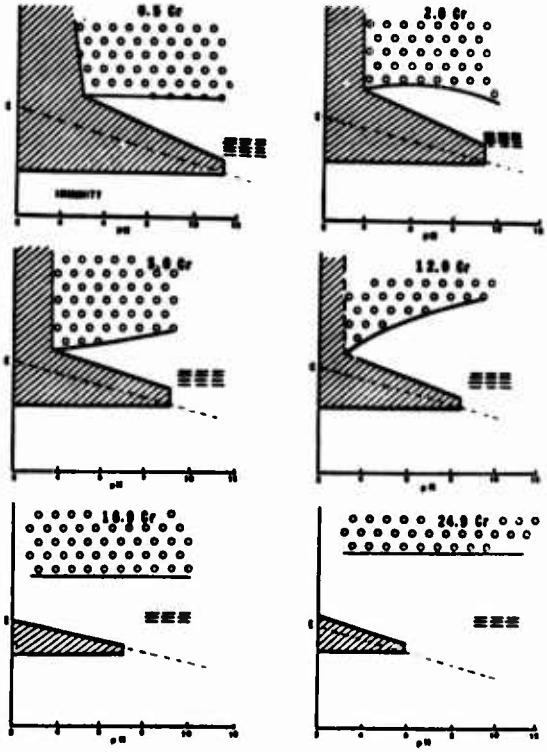


FIGURE 19 : Circonstances d'immunité, de corrosion généralisée, de piqûration et de passivation parfaite et imparfaite pour six alliages binaires Fe-Cr en présence de solutions 0.1 M en ions chlorure.

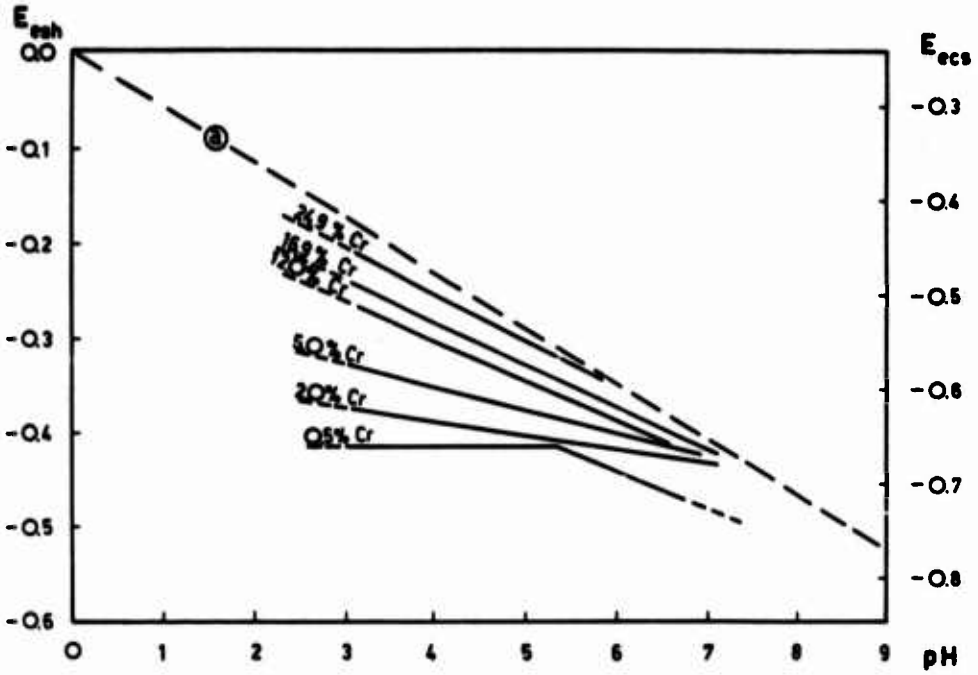


FIGURE 20 : Effet de la teneur en chrome sur les potentiels à courant nul des alliages binaires Fe-Cr, en fonction du pH.

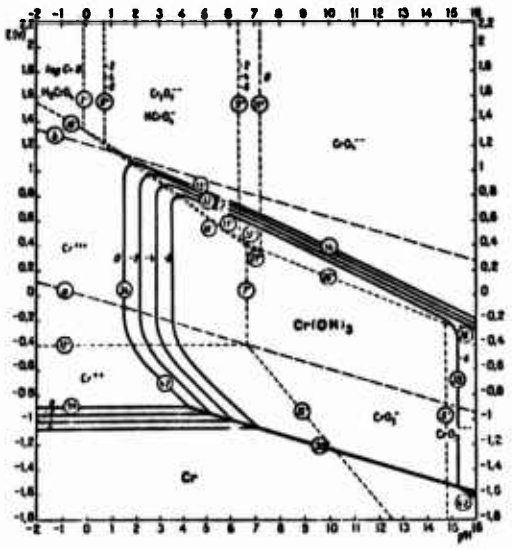


FIGURE 21 : Diagramme d'équilibres potentiel/pH du système Cr-H_2O, à 25°C.

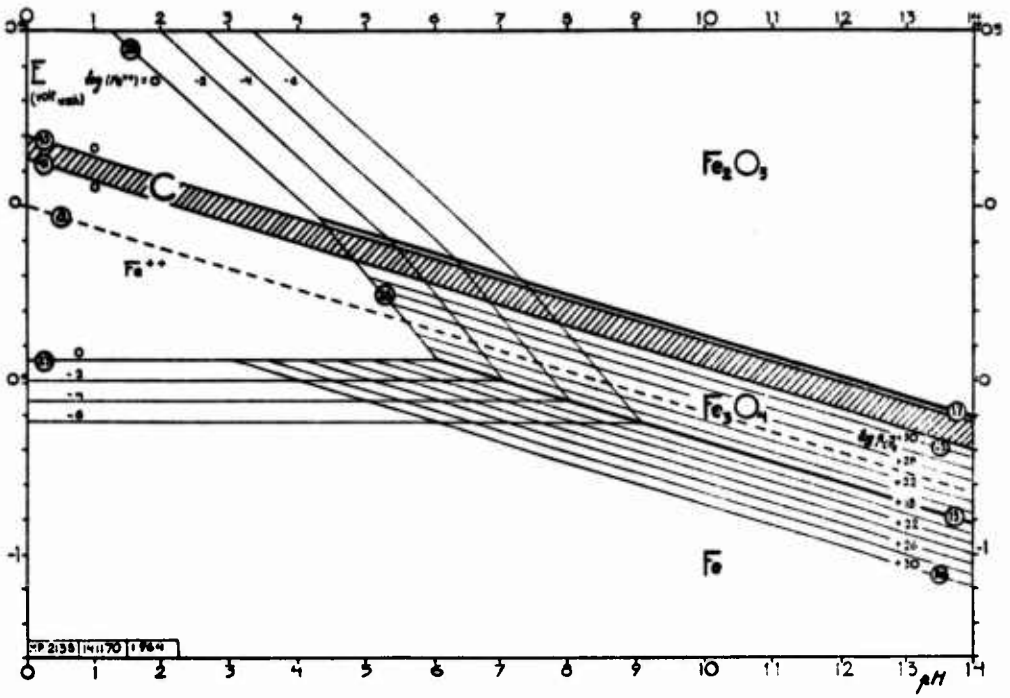


FIGURE 22 : Diagramme d'équilibres potentiel/pH du système Fe-C-H_2O, à 25°C.

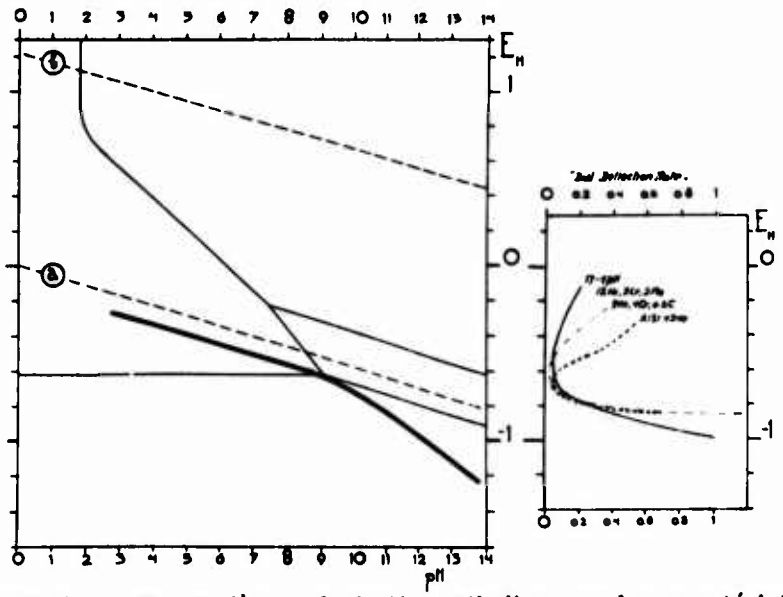


FIGURE 24 : Influence d'une polarisation cathodique sur les caractéristiques électrochimiques et sur la vitesse de propagation d'une fissure de corrosion sous tension. (Acier au chrome AISI 4340 en présence d'une solution de NaCl 3%). (d'après B.F. BROWN).

Le "dial deflexion rate" indiqué dans la partie de droite de la figure mesure la vitesse de propagation de la fissure.

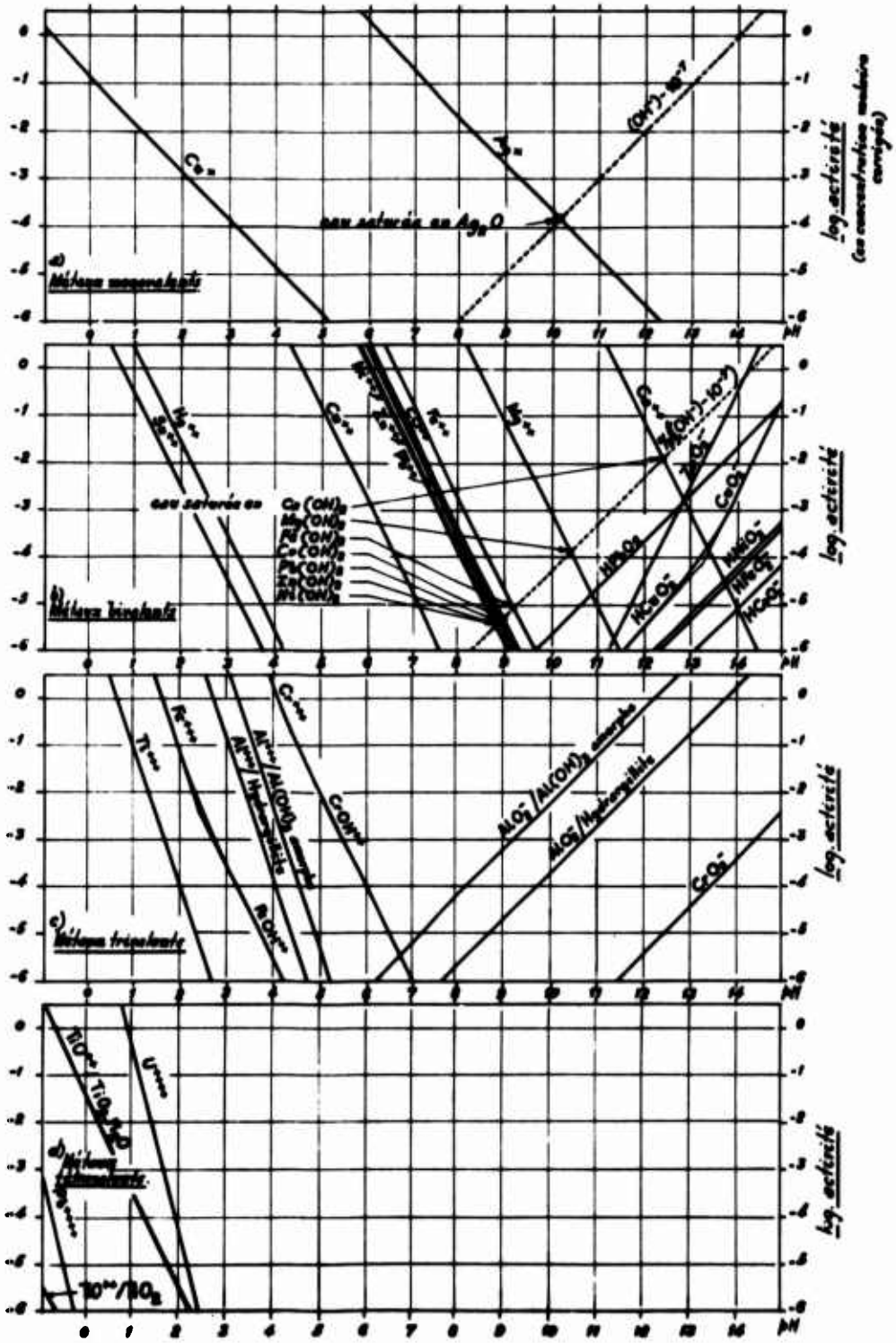


FIGURE 23 : Influence du pH sur la solubilité des oxydes et hydroxydes.

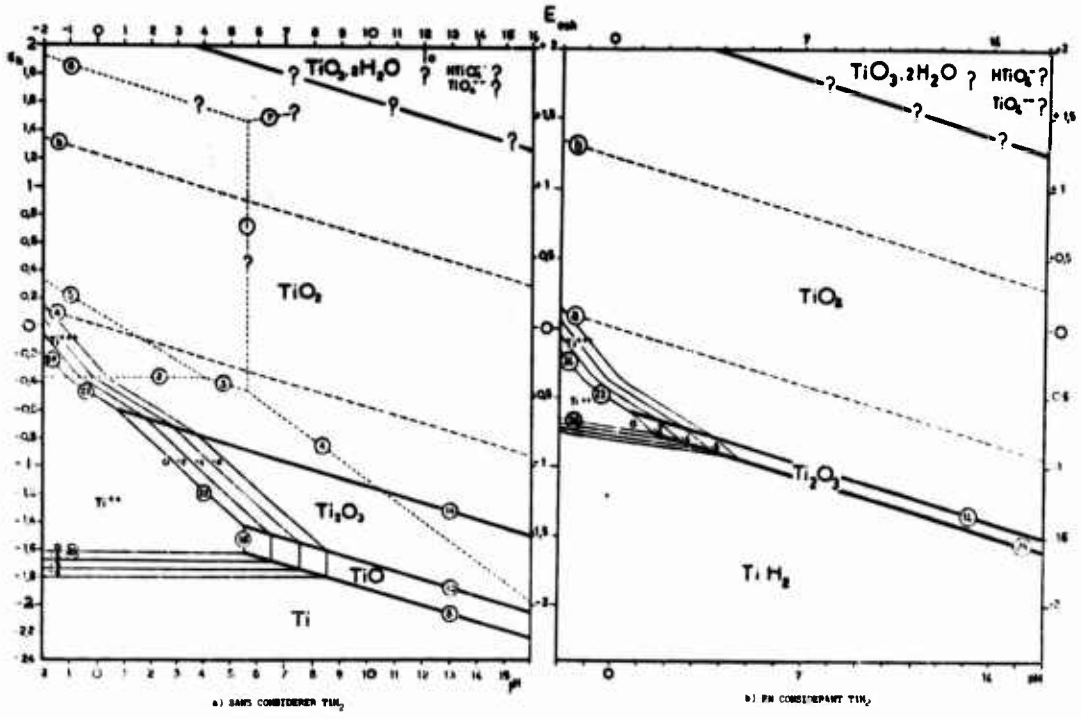


FIGURE 25 : Diagrammes d'équilibres potentiel/pH pour le système Ti-H_2O, à 25°C.

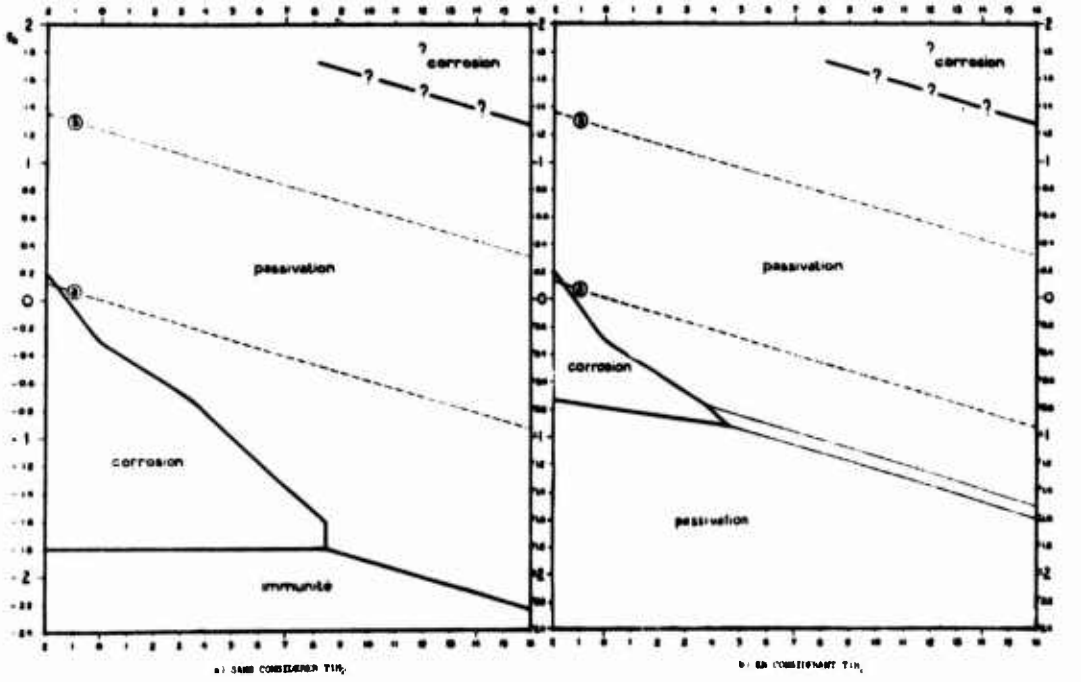


FIGURE 26 : Domaines théoriques d'immunité, corrosion et passivation du titane, à 25°C.

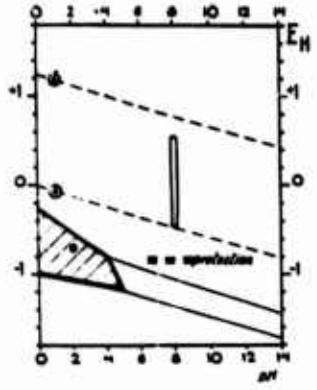


FIGURE 27 : Fissuration et protection du titane. (Absence de piqûration) (Schéma)

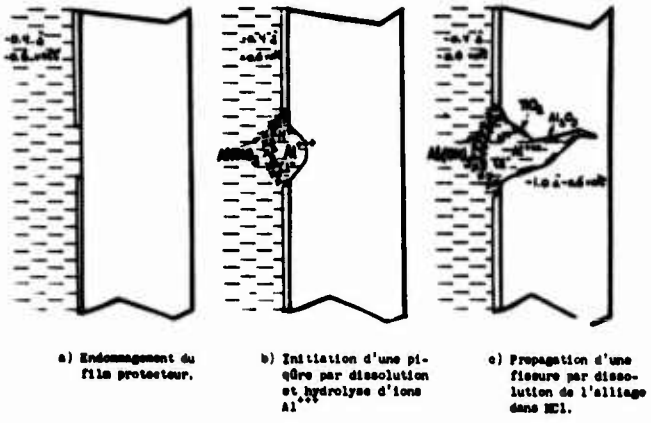


FIGURE 28 : Initiation et propagation de fissures de corrosion sous tension dans un alliage titane-aluminium.

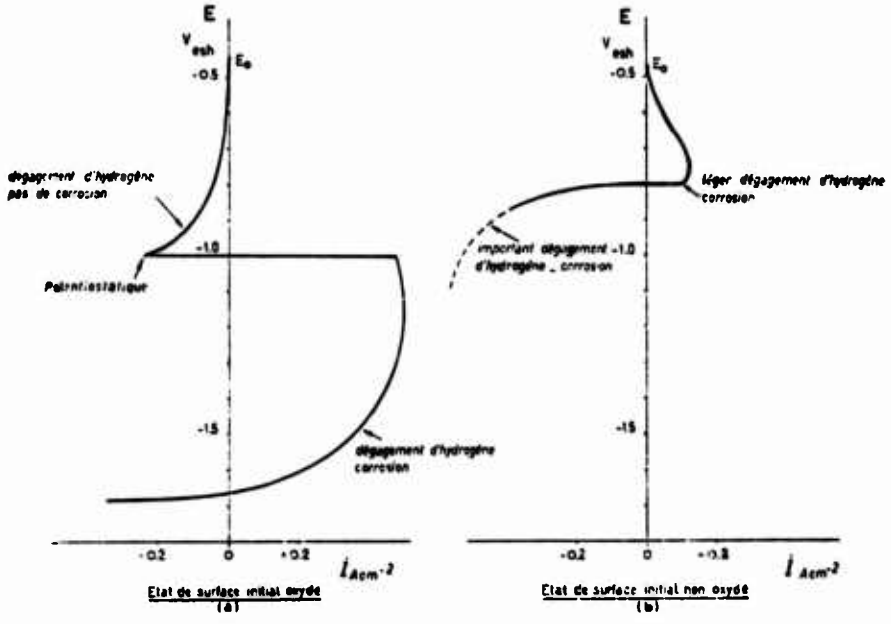
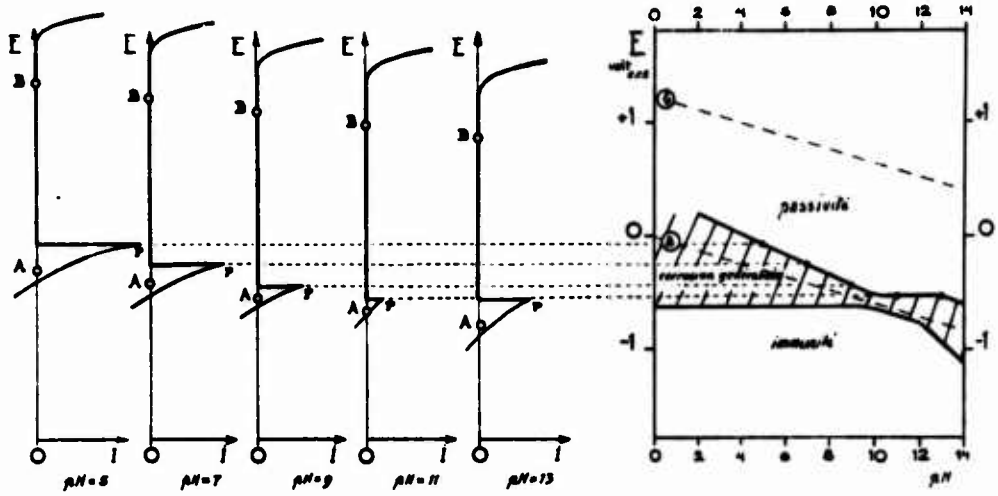


FIGURE 29 : Courbes de polarisation cathodique de titane en solution HCl 12 N.

a) Echantillon de titane poli, rincé et séché avant immersion dans la solution.
b) Echantillon de titane immergé immédiatement après polissage.

(d'après A. POURBAIX, M. MAREK et R.F. HOCHMAN).



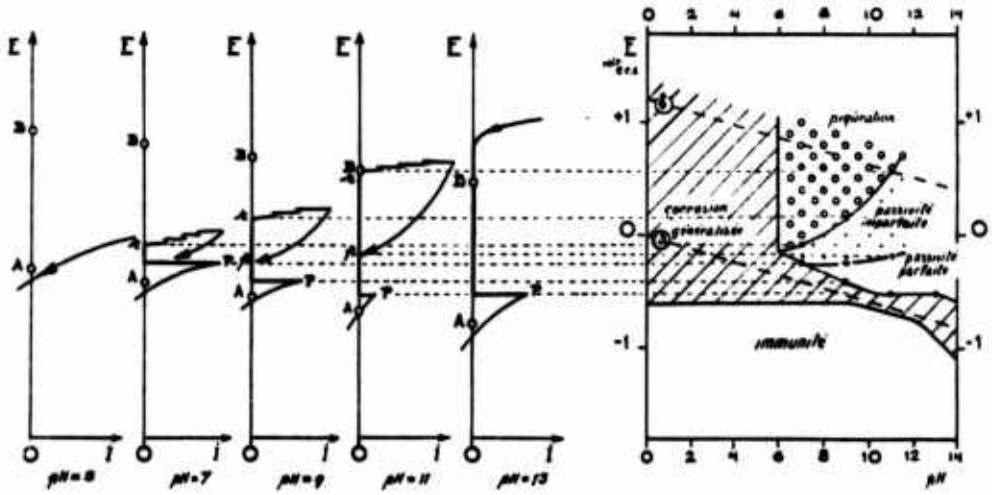
a

b

a) courbes de polarisation en présence de solutions de pH 5 à 13.

b) circonstances expérimentales d'immunité, de corrosion généralisée et de passivité.

FIGURE 30 : Comportement de fer en solution exempte de chlorure. (Schéma)



a

b

a) courbes de polarisation en présence de solutions de pH 5 à 13.

b) circonstances expérimentales d'immunité, de corrosion généralisée, de passivités parfaite et imparfaite, et de piqûration.

FIGURE 31 : Comportement de fer en solution chlorurée. (10^{-2} ion.g par litre, soit 355 ppm Cl^-). (Schéma)

On the Electron-Configuration Theory Of Marine Corrosion[1]

L. H. Bennett, L. J. Swartzendruber, and M. B. McNeil

National Bureau of Standards
Washington, D. C. 20234

The electron-configuration theory of corrosion introduced by Uhlig relates chemisorption and passivity to alloy compositions having favorable d-electron configurations. This theory postulates a critical composition for passivity which coincides with a theoretical filling of the d-band in a "rigid-band" description of these alloys. Recently, detailed knowledge of the electronic structure of Cu-Ni alloys has been greatly increased, and it no longer appears that a strict band model alone can give an adequate description of the disordered alloys. Recent theories and modern spectroscopic methods, including soft x-ray and photoelectron spectroscopy and other techniques, have provided a great deal of new knowledge concerning the electronic structure of Cu-Ni alloys. In light of these experimental and theoretical developments, this paper investigates whether or not there is any evidence to support an electron-configuration theory of corrosion, without regard to the question of passivity, for Cu-Ni alloys in saltwater. The addition of small amounts of Fe has important effects on the corrosion rate in the copper-rich alloys and the relevance of this to the electron-configuration theory is considered. Effects of metallurgical variables and of film properties are noted. The related topic of heterogeneous catalysis is discussed.

Key Words: Alloy theory; catalysis; chemisorption; Cu-Ni alloys; d-bands; electron-configuration; metallurgy; passivity; rigid-band model; saltwater corrosion; surfaces

I. Introduction

Copper-nickel alloys are widely used in saline-water environments where long service life or other desirable properties often justify the expense (1)[2]. The corrosion behavior of these alloys in such environments is highly dependent upon the alloy composition. As is evident from Figure 1, the problem of selecting the optimum composition for a given application is not usually as simple as obtaining the lowest possible corrosion rate consistent with price. In addition, the properties are usually further modified and improved by the addition of small amounts of other elements, notably iron (2,3). A theoretical understanding, even if approximate or imperfect, of the effect of Ni concentration and other element additions on the corrosion behavior could contribute to the development of alloys tailored for specific applications.

The mechanisms involved in the corrosion behavior of the cupro-nickels have been extensively investigated and discussed. The rate determining step in the corrosion process

[1] Supported in part by the Office of Saline Water, U.S. Department of Interior.
[2] Figures in parentheses indicate the literature references at the end of this paper.

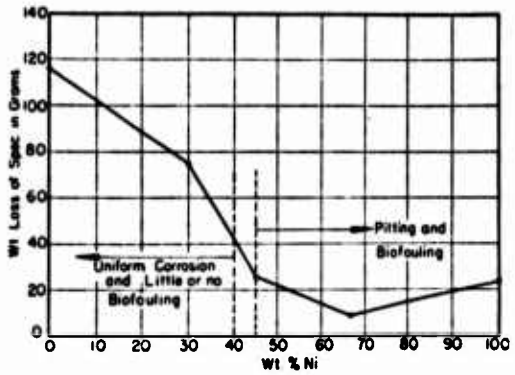


FIGURE 1. Behavior of copper-nickel alloys in sea water (From F. LaQue, J. Amer. Soc. Nav. Engrs. 53, 29 (1941). Biofouling is reduced in the Cu-rich region by the presence of sufficient Cu ions in the water, since copper is toxic to many marine organisms. The origin of the pitting is not known, but pitting is often associated with passivity.

occurs at the "film" or "scale" that forms and separates the base metal from the corrosive solution. There are two interesting directions from which to view this film. The first, which might be considered the electrochemical point of view, or from the outside looking in, is mainly concerned with film properties and film-electrolyte reactions. The second, or alloy theory point of view, is mainly concerned with the electronic structure of the metal and its effect on metal-film interactions. These two views are, of course, not mutually exclusive but arise mainly from the complexity of the problem and the fact that few studies are concerned with all the intricacies of both electrochemistry and solid state physics.

This paper will be concerned mainly with the latter point of view, from the inside looking out. This is an appropriate time to consider this viewpoint since there has recently been a great flurry of activity, both experimental and theoretical, on the electronic structure of copper-nickel alloys. In particular, it is now apparent that the "rigid-band" model, on which many previous arguments have been based, does not give an adequate description of the electronic structure of these alloys.

Practical corrosion situations are very complex, and no one point of view could hope to give predictions for all situations which arise. When conditions are such that very thick adherent films, or "scales" (say $\gtrsim$ 10 μm thick), are allowed to form, the scale properties, both chemical and mechanical, are of overriding importance (4). Under some conditions, the corrosion rates of Cu-Ni alloys in saltwater are greatly reduced and become practically independent of Ni concentration after sufficiently thick films are allowed to form. For thinner films (say $\sim$0.1 μm) the Ni concentration in the alloy is important. The chemical, mechanical and electronic properties of the film are probably the most important factors determining the reaction rate. However, for very thin films (say $<$ 0.1 μm) the chemical reaction between the metal substrate and the film, which in the final analysis determines the protective properties of the film, are of importance. For this case the electronic structure of the alloy must have a strong influence. These very thin films are of importance in the high-nickel region ($\gtrsim$ 40% Ni). They are also important in the high-copper region ($\lesssim$ 40% Ni) when the film is kept very thin by, for example, very high flow rates (5).

The role of the electronic structure of the alloy on corrosion behavior (and in particular, on passivity (6) has been emphasized in a series of papers by Uhlig and his coworkers (7-15). Following earlier work of Tammann, Uhlig (7) proposed the electron-configuration theory of passivity. This theory was advanced to explain the observation that passivity can be achieved in several alloy systems when a critical composition is exceeded. According to this theory, these critical compositions are related to the presence or absence of d-electron vacancies in the electronic structure of the alloys. In this viewpoint the d vacancies are said to favor formation of strongly chemisorbed surface films, which confer passivity and increased resistance to corrosion. In particular, Cu-Ni alloys have been extensively investigated by Uhlig and coworkers using ternary additions to change the critical composition. For these alloys, experimental results, obtained primarily using potentiometric measurements in a 1N H_2SO_4 solution, were in good agreement with Uhlig's electron-configuration theory of passivity. That is, when the electron-configuration described by Mott and Jones (16) predicted the presence of d vacancies, passivation could be

detected in the potentiokinetic curves, whereas it could not be detected if the absence of d holes was predicted.

The electron-configuration theory proposed by Uhlig to explain passivity has been critized on several grounds. First, there is the kind of criticism (6,17) which points out that results used to support Uhlig's arguments can also be accounted for on the basis of various kinetic models involving the electronic properties of the film. Another objection (6) is that attempts to extend the theory to other metals and alloys and other electrolytes appear to give conflicting results. For example, there are a number of transition elements with partially filled d-bands which are not easy to passivate. Conversely, there are non-transition metals, such as Al and Mg, which are readily passivated. It has also been noted (6) that "the critical concentration (15.7 wt %) of chromium required for spontaneous passivation of iron does not agree with the limit for stability of the passive state (about 12%)." Finally, there is the objection (17) that even if passivation is found for Cu-Ni alloys in H_2SO_4, it is not clearly present in NaCl solutions.

In this paper, no attempt will be made to discuss these objections except for Cu-Ni alloys. Much controversy can be generated about whether or not Cu-Ni alloys are passive under given conditions in a given environment. No effort will be made here to enter into this controversy. Whether or not the high Ni alloys are passive, there is no controversy over the fact that Ni additions to Cu reduce the sea-water corrosion rate up to some critical composition. Uhlig (10) notes that the "observed critical composition based on corrosion rates in 3% NaCl at 80 °C is in the neighborhood of 30-40% Ni." Thus it is appropriate to discuss an electron-configuration theory of marine corrosion. The purpose of this paper is to review the electron-configuration theory of corrosion as it pertains to critical compositions in Cu-Ni alloys, and to extend this theory to attempt to correlate the relative saltwater corrosion rates in the high Cu alloys with the electronic structure of the alloys. (The difficult question of the mechanisms by which the electronic state of the base metal may influence the corrosion rate is not explored deeply here.) Correlations are sought in terms of the most modern understanding of the electronic structure of these alloys. The usual description of the electron-configuration theory of corrosion relies on the so-called "rigid-band" model (16), which is no longer felt to adequately describe the electronic structure.

The rigid-band model is described in Section II. In Section III, theories which attempt to give a more realistic description of the electronic properties of alloys are noted. Experimental results on Cu-Ni alloys and their relevance to these theories are given in Section IV. The problem of the relation of bulk and surface properties is considered in Section V. The difficult problem of relating an ideal Cu-Ni alloy to real alloys is considered in Section VI, Metallurgical Considerations. Section VII, Discussion and Summary, includes some consideration of the related topic of catalysis.

II. Band Theory of Metals and the Rigid-Band Model

When the atoms of a metal are brought together to form a solid, the discrete atomic energy levels are spread into continuous regions, called "bands." These bands can be partially characertized by an electronic density of states, N(E), giving the number of electrons per unit energy interval at energy E. For the 3d-transition series, it is usual to describe N(E) by two bands: a wide, low-density, valence-electron band corresponding to the atomic 4s states, and a relatively narrow, high-density band corresponding to the atomic 3d states. These bands are filled up to some maximum energy, E_F, which is determined by the number of 3d + 4s electrons per atom, sometimes referred to as the group valence or the electron-to-atom ratio. The essential difference between Cu and Ni is that in Cu the 3d band is full, whereas in Ni it is not.

The process of forming bands from free-electron states is illustrated in Figure 2, taken from a recent important paper by Hodges et al. (18) This figure illustrates the change in energy levels caused first by "renormalizing" the free-atom wavefunctions to a size appropriate to atoms bound in the solid while maintaining charge neutrality. These renormalized wave functions are then used to construct a potential from which characteristic features of the band structure are calculated. The s level forms a broad conduction band the bottom of which is shown in Figure 2, and the d level a relatively narrow band which is full in Cu but not in Ni. The presence of the unfilled d band is consistent with the observed ferromagnetism of Ni. The actual calculation of the band structure, which is

well understood for pure metals, remains one of the major unsolved problems of metal physics for the case of alloys, though several useful approximations have recently been advanced (19,20).

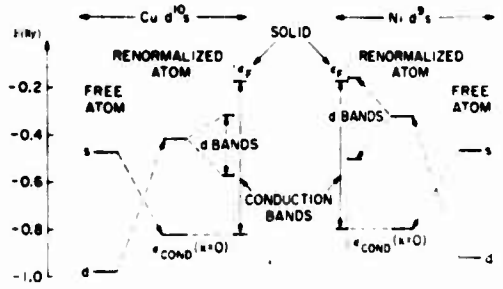


FIGURE 2. Positions of Cu and Ni 4s and 3d energy levels in the free atoms and energy bands in the solid. Only the bottom of the s band is shown. The top of the occupied s band is shown as the Fermi energy, E_F. The top and bottom of the d bands in Cu fall entirely within the conduction band but the top of the d band in Ni is above E_F. [From Hodges et al., ref. 18]

The rigid-band model for transition metals and their alloys was first proposed by Mott (16) almost two generations ago and shown to be in qualitative agreement with many of the known properties of these materials, such as magnetic susceptibility, electrical resistance, and binding energy. In the rigid-band model, all metals of a given transition series (with the same crystal structure) are assumed to have identical band structures, although Mott emphasized that this was only an approximation. A 1935 calculation (21) for the band structure of the first transition series is shown in Figure 3. As Cu is added to Ni, the average electron-to-atom ratio increases and in the rigid-band model the 3d band fills until, at a certain critical composition, it is completely filled with no more "holes" in the 3d band. Above this critical composition the alloy will not become ferromagnetic even at very low temperatures. The filling of the Ni 3d bands by electrons from Cu implies some sort of charge transfer from the Cu to the Ni.

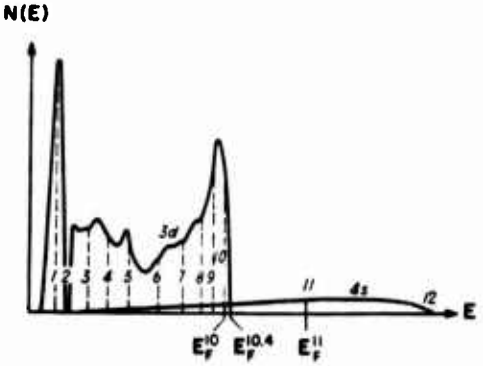


FIGURE 3. The density of levels in the 3d series, as estimated using the rigid-band model from Krutter's calculation (21) on copper [after J. C. Slater, Phys. Rev. 49, 537 (1936)]. The dotted lines indicate the position of the Fermi level for materials with the corresponding number of 3d + 4s electrons. For example, E_F^{10} represents the Fermi level for Ni, which has 9 3d electrons and one 4s electron in the free atom. E_F^{10} falls just below the top of the d band.

This model was shown (16) to give remarkably good predictions concerning the saturation magnetization of Cu-Ni alloys. The measured saturation magnetization in Ni corresponds to 0.6 holes per atom in the Ni 3d band (which is equal to the saturation moment in Bohr magnetons). For an alloy with x parts of Cu and 1-x parts of Ni, the number of holes in the d band is, since Cu contributes one extra electron per atom,

$$\begin{matrix} 0.6-x & (x<0.6) \\ 0 & (x>0.6). \end{matrix}$$

This predicts a saturation moment for Cu-Ni alloys of 0.6-x Bohr magnetons per atom, very close to the experimentally observed value for those alloys that become ferromagnetic.

Kirkpatrick et al. (22) find that this agreement of the rigid-band model with the magnetic behavior of Cu-Ni alloys is not retained when applied to more recently calculated

band structure for pure Ni (23,24). Part of the reason is that, in these calculations, the Ni density of states falls more sharply above E_F than the earlier calculations (for example, Figure 3). Agreement might be restored with "improved" band calculations, or alternately, by permitting the band structure to be deformed upon alloying. Many properties of alloys show good agreement with some kind of "deformable common-band model". Unfortunately, many authors use the term rigid-band model when discussing such a deformable common-band model.

If the common-band picture is extended to the entire 3d transition series, the saturation moment is predicted to be a function only of the number of 3d + 4s electrons. The extent to which this is borne out in practice can be seen in Figure 4. For a large number of alloys a common curve exists, with some breaks in the curve, e.g. Fe-Co, due to a change in crystal structure. There are also a large number of striking deviations. Though the deviations arise in large part from the complications of antiferromagnetic interactions, it is certainly clear that the predictions of the rigid-band model must be carefully scrutinized for each case.

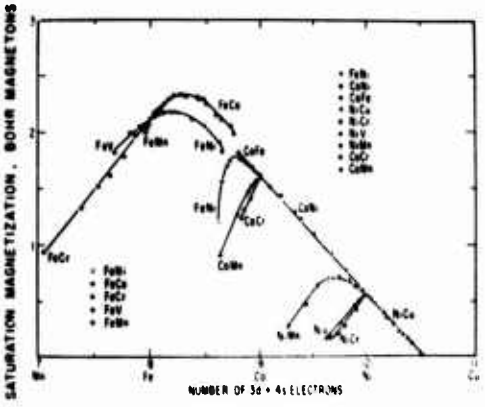
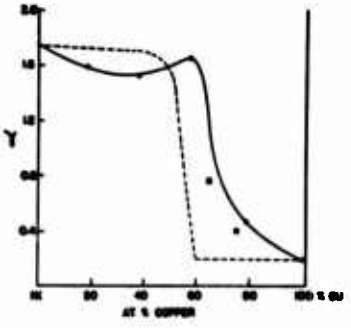


FIGURE 4. The "Slater-Pauling" curves of saturation magnetization versus electron concentration for alloys of the iron transition series. [after H. Hill and B. T. Matthias, Phys. Rev. 168, 464 (1968)]

Despite the success of the rigid-band model in certain cases, it has long been realized that it gives an incorrect description for a number of physical properties (16,25). As an example, the experimentally measured values of the electronic specific heat, γ, which is a measure of the density of states at the Fermi level, are compared with those predicted by the rigid-band model (Figure 5). The high γ values for the Ni-rich alloys reflects the large density of states from the unfilled d-band. However, the γ values for the Cu-rich alloys are much higher than predicted, indicating the presence of virtual d-holes (25) when the d band is "filled" according to the rigid-band picture. The successes and shortcomings of Uhlig's electron-configuration theory as applied to describe the corrosion behavior of Cu-Ni alloys are quite analogous to the successes and shortcomings of the rigid-band model as applied to describe other properties. A reexamination of the electron-configuration theory of marine corrosion in Cu-Ni alloys in terms of modern alloy theory appears to strengthen Uhlig's suggestion of a relationship between the electrochemical behavior and the electronic structure.

FIGURE 5. The electronic specific heat of Cu-Ni alloys. The dashed curved is that expected from a strict application of a rigid-band theory. The solid curve corresponds to experimentally measured values [after J. E. Goldman, Rev. Mod. Phys. 25, 108 (1953)]. More recent measurements [K. P. Gupta, C. H. Cheng, and Paul A. Beck, Phys. Rev. 133, A203 (1964)] are in essential agreement.



III. Alloy Theory

A metal consists of nuclei, atomic-state-like or "core" electrons whose wavefunctions are not greatly different from the corresponding free-atom wavefunction, and electrons ("conduction" electrons) where wavefunctions in the solid are appreciably different from the corresponding free-atom wavefunctions. It is assumed that the total wavefunction can be separated into a suitably symmetrized product of a function of the coordinates of the nuclei plus core electrons only and a function of the coordinates of the conduction electrons only. It is then convenient to transform the problem to one involving normal modes and to obtain solutions in terms of independent "elementary excitations" or "quasi-particles" (26-28). The most familar of these quasi-particles are "electrons", "holes", "phonons", and "magnons". To obtain solutions in these terms, a large number of "many-body effects", such as phonon-phonon, phonon-electron, electron-magnon, and electron-electron interactions are neglected. In the attempt to obtain electronic density of states information (or other features of the band structure) from experiments, it is generally necessary to adjust measured quantities for many-body effects. In many cases, these adjustments are small, but are not precisely known and they may be significant. In the case of electronic specific heats, for example (Figure 5), the measured value of γ does not provide the exact value of N(E), the difference perhaps being as large as a factor of about two. However, the general features and trends revealed by the measurements of γ versus composition are expected to be preserved when corrected to N(E) versus composition. The one-electron method, which treats the wavefunction of the conduction electrons as an antisymmetrized product of independent one-electron wavefunctions , is most used in treating electronic density of states (29). Because of the computational difficulties, many-body effects are not generally included (except in an average or approximate way) in detailed calculations and interpretations of experiments on the electronic structure of metals and alloys.

Progress in high-speed computers and computational methods (30) has allowed more detailed and reliable calculations of band structures than previously. The great detail shown in Figure 6 for a recently calculated (31) density of states cruve for copper can be contrasted with that of Figure 3. The Ni density of states calculations (23,24), while somewhat less detailed than that of Figure 6, show structural features quite similar to those of copper but differ in two important respects that are evident in Figure 2: (1) the width of the d band is greater in Ni and (2) for Cu the center of the d band lies closer to the bottom of the s band.

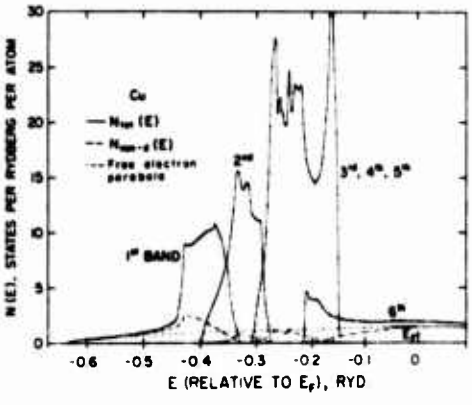


FIGURE 6. Electronic density of states of Cu metal from a recent calculation by Watson et al. [ref. 32]. Each band can accomodate two electrons. The 1st through 5th bands are full. The 6th band is filled to E_F.

Many of the concepts used to understand pure metals, such as the Bloch theorem, Fermi surfaces and Brillouin zones, are valid only for solids with long-range order. The disorder associated with an alloy thus introduces complications in the understanding of the electronic structure. Stern (32) has discussed the basic differences between a theory of pure metals and a theory of disordered alloys. He notes that the concepts associated with a periodic lattice still retain some degree of meaning for disordered alloys, particularly if the atomic potentials of the constituents are nearly the same. However, if the potentials are very different, there will be a non-uniform distribution of the electron charge about the different sites.

A simple case of a disordered alloy is that of a single impurity forming a bound state at an energy above or below the energy bands of the host. Such bound states, familar in doped semiconductors, have the property that the electron or hole wavefunction is localized near the impurity. If a single atom of Ni is placed in a Cu maxtrix, the d state energy of the Ni falls within the Cu d band, forming what is called a virtual bound state (25). The d state is only weakly coupled to the copper band, and is thus only slightly broadened.

For concentrated alloys, there are two extreme contrasting models used to describe the electronic properties. The rigid-band model ignores the differences between the atoms, ascribing the average electron-to-atom ratio to every atom. The alternative extreme, the minimum-polarity model (33,35), assumes that the constituents retain their atomic configuration and hence remain electrically neutral. The maintenance of local charge neutrality in a metal has been called the electroneutrality principle by Pauling (36). Although, as mentioned earlier, the rigid-band model gives poor agreement for the magnetic behavior of Cu-Ni alloys when recent Ni band calculations are used, the minimum-polarity model gives better agreement for the magnetic properties (22). A modified minimum-polarity model, considering charge screening by conduction electrons (25), may provide an improved description. Kanamori et al. (37) have made progress in calculating the electronic structure taking into account the shielding of the impurity charge.

An extremely useful computational technique for the band structure of alloys such as Cu-Ni is known as the coherent potential model (19,20,37). In this model the potentials of all the sites but one are averaged over and replaced by an energy dependent effective potential, known as the coherent potential. Scattering from the atomic Ni and Cu potential shows that (37) instead of a rigid shift of the density of states, the main peaks associated with Cu and Ni sites remain stationary while changing magnitude and shape.

In contrast to the rigid-band model, recent alloy theory and experiments (Section IV) give the following picture for Cu-Ni alloys: (1) The d-holes are not spread uniformly throughout the alloy but are located primarily on the Ni sites. Indeed, there exist "virtual" d holes even in the Cu-rich region. Thus, although their electronic properties are considerably modified by being bound in an alloy, rather than being a free atom, both Ni and Cu retain some of their "atomic-like" individuality. (2) Rather than shifting the Fermi energy within a rigid density of states, the shapes and relative magnitudes of the Cu-like and Ni-like features of the bands are changed upon alloying. There is practically no change in the positions of these features.

IV. Experiments Relevant to the Electronic Structure of Cu-Ni Alloys

The simple rigid-band model applied to Cu-Ni and illustrated in Figure 3 predicts little, if any, change in $N(E_F)$, the electronic density of states at the Fermi level, from pure Cu up to about Cu - 40% Ni. If this model were correct, neither the electronic specific heat nor the magnetic susceptibility should show much change in this region. The specific heat data already discussed in connection with Figure 5 clearly do not follow this prediction [except perhaps (38,39) for <2% Ni] and the susceptibility data [see for example Pugh and Ryan (40) or Robbins et al. (41)] is even in more violent disagreement with rigid-band theory, with the diamagnetism of pure Cu changing to paramagnetism with only 4% added Ni. The susceptibility suggests an increase by a factor of five in $N(E_F)$ for 20% Ni, an error of 500% from the rigid-band prediction! Many-body corrections (e.g., electron-phonon (42) and electron-magnon (43,44) interactions) may reduce the quantitative disagreement, but the conclusion remains: the rigid-band model does not hold for Cu-Ni alloys.

A much employed method to get detailed information about the electronic states in such an alloy is the study of the emission and absorption of electromagnetic radiation. Soft x-ray emission spectroscopy consists of producing vacancies in ion core levels and observing the subsequent spontaneously emitted radiation resulting from electrons in the conduction band dropping into the vacant core states. Clift et al. (45) found that, to a reasonable approximation and in contrast to the rigid-band model, the soft x-ray spectra of Cu-Ni was a compositionally weighted average of the spectra formed for pure copper and pure nickel. Wenger et al. (46), measuring relative integrated intensities of the soft x-ray emission and a characteristic x-ray line, were led to the conclusion that the number of d electrons associated with a nickel site is not changed on alloying, again in sharp contract with the rigid-band model. These experiments (45,46) are not wholly conclusive,

in that important details of the soft x-ray spectra for even pure Cu (47) and pure Ni (48,49) are not seen in these "low-resolution" experiments, but they do give strong support to the existence of a nickel-like band localized at the nickel sites in the predicted filled d-band region of the rigid-band model.

Soft x-ray appearance potentials are much more sensitive to the surface and near-surface conditions. In this technique, core electrons are excited to the unfilled states above the Fermi level, leading to the appearance of small characteristic peaks superimposed on the bremsstrahlung background. Again the results (50) are that there are d holes at Ni sites even for an alloy containing 75% Cu, in contrast to the rigid-band prediction.

The photoelectric effect has been used extensively in recent years to probe the band structure of metals and alloys. The interpretation of ultraviolet photoemission experiments (UPS) is complicated by the contribution of both filled and unfilled density of states with resulting complicated unfolding procedures but again the results (51) are in much better agreement with the presence of vacant d-states at Ni sites in Cu-rich alloys. Figure 7 illustrates two extremes of the theoretical situation. The result of the UPS experiment on a 75% Cu - 25% Ni alloy is close to the virtual-bound state model picture, with an unchanged Cu band superimposed on a broadened Ni d state.

Somewhat less ambiguous in interpretation because of the dependence on only the filled density of states is x-ray induced photoemission (XPS). Hüfner et al. (52), using high-resolution XPS, have shown that the Cu and Ni bands are changed by alloying, but are still distinct bands, not the common bands envisaged in a rigid-band picture.

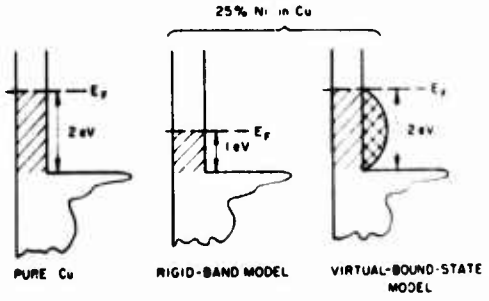


FIGURE 7. Schematic illustration of the filled density of states in Cu and a Cu 75 - Ni 25 alloy, showing the behavior expected from the rigid-band and the virtual bound state models. [after Seib and Spicer, ref. 51].

The angular correlation of positron annihilation radiation probes the Fermi surface in momentum, and unlike other Fermi surface probes, results can be obtained in concentrated alloys. Murray and McGervery (53) found that the Ni atoms in a 77% Cu-23% Ni alloy were contributing 0.8 electrons per atom to the conduction band leaving a d hole of 0.8 electrons at the Ni sites, in contrast to the zero valence assigned to Ni when alloyed into Cu in the rigid-band model.

So far only Cu-Ni binary alloys have been discussed. Of great importance in marine applications, including desalination heat exchangers, are alloys of Cu-Ni that include a small amount of Fe. In this case, the Mössbauer effect has been used to probe the magnetic environment of the Fe atoms. The Mössbauer effect is based on the phenomena of recoilless emission and absorption of γ-rays, and either the radioactive source, or a sample containing non-radioactive iron as an absorber, can be studied. Source experiments probe isolated Fe atoms. Interactions between Fe atoms are studied using absorbers. A source Mössbauer experiment (54) has shown that the Fe atoms maintain their d holes when alloyed in Cu and Cu-Ni alloys. The magnetic environments at the Fe sites depend on the atomic configuration in the neighborhood of the iron. In the Cu-rich region, the magnetic moment is associated with an iron atom and its nearest-nickel-atom neighbors, leading to the linear increase in magnetic moment shown in Figure 8. Near the "critical" region identified by Uhlig for corrosion behavior, the magnetic moment suddenly becomes "giant" and is associated with magnetic polarization clouds extending over many atoms. Mössbauer absorber studies have been made of the interaction between the Fe atoms (55), again requiring a local rather than a common band interpretation.

It is clear that the rigid-band model cannot satisfactorily explain modern experimental data on Cu-Ni alloys. The primary reason for this failure is that the rigid-band model neglects the charge screening discussed by Friedel (25).

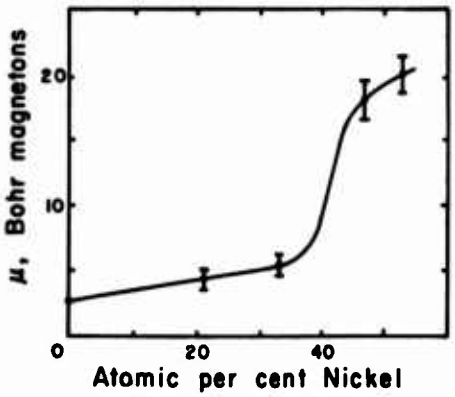


FIGURE 8. Magnetic moment, as measured using the Mössbauer effect, of an isolated iron atom in Cu-Ni alloys. The large increase in moment near the critical composition is caused by the necleation of giant magnetic polarization clouds. [after Bennett et al., ref. 55].

V. The Surface Problem

Uhlig (10,12) treated d-like wavefunctions as well-defined for the surface layer, but ascribed a different electronic structure to the surface than to the bulk alloy. He considered that the surface d-band contains holes so long as other non-transition elements donate fewer electrons than the actual surface holes. The number of surface d holes per atom is found, in this view, by adding one d hole to the bulk value of 0.6 d hole per Ni atom. The additional d hole was assumed to arise from the use of one d electron in the chemisorption process. At the critical composition, when the surface holes become filled by excess electrons provided by alloying components (e.g. one for each Cu atom, two for each Zn atom), passivity is no longer possible. The critical composition was found by equating the number of excess electrons provided by the alloying elements to the number of surface d holes provided by the Ni atoms. Using this view, the observed critical compositions for Cu-Ni alloys with small amounts of ternary alloys could be well described.

Uhlig's technique of adding holes to the d configuration on the surface is not compatible with most of the theories and experiments on surface properties. For example, Waclawski and Plummer (56) argue from photoemission observations on tungsten that an adsorbate (i.e. H_2,O_2, N_2 and CO) covered surface might be more representative of the bulk than a clean surface. Properties of bare Ni surfaces have received increasing theoretical attention in recent months (57). In the absence of a definitive understanding of the electronic configuration appropriate to the surface, it is probably not useful to adopt Uhlig's detailed model for the surface. More recently, Uhlig (58) has shown that it is possible to obtain agreement for the critical compositions without introducing a different electron configuration in the surface than the bulk. Considering the ambiguities, it may be preferable to appeal to experiment to determine critical compositions.

The question of what electronic states <u>are</u> appropriate at a surface has been the subject of a great deal of study (59,60). These studies have been directed toward analyzing surface states arising from free-electron-like states. According to Bloch's theorem, all states in the bulk are of the form $U(r)e^{ik.r}$. For so-called "Cambridge surface states," k will be a complex vector, and the wavefunction will decay away from the surface. Tunneling experiments agree with theoretical predictions on the electronic structure of surface s and d states (61-63).

The problem of a single atom chemisorbed on a metal surface can be treated in a similar way to the theory of localized magnetic moments (61). The electronic states in a surface having a chemisorbed layer has been the subject of many recent investigations (65, 64-67). The electronic structure of an adsorbed atom (or of an adsorbed molecule) has been described in terms of the formation of chemical bonds to its nearest neighbors on the metallic substrate (68,69). This localized picture is called a surface complex or surface molecule (66).

The electron structure of the surface molecule is treated as a diatomic molecule, with the difference that an integral number of electrons are not required in its description. Bennett and Messmer (70) have recently considered the effect of the electronic state of the substrate upon adsorption. They showed that, for various common gases adsorbed on graphite, chemisorption is directly controlled by the detailed electronic state of the surface. It seems unlikely that this work (70) will soon be extended to such complicated cases as chemisorption on Cu-Ni alloys. It might be conjectured, however, that the electronic structure of the Cu-Ni substrate is also important.

Further theoretical and experimental progress has been made in obtaining a detailed knowledge of the physical nature of the chemisorption bond between the alloy and the protective film (71-76). For example, Schrieffer and Gomer (74) have introduced a simple model which gives a rough understanding of the competition of energies which enter into the forming of an "induced covalent" chemisorption bond. In their model the strength of the bond is measured by $J\chi_{loc}$, where J is an antiferromagnetic exchange interaction and χ_{loc} is the local spin susceptibility of the free solid surface. Thus the strength of chemisorption will be large for metals with high local spin susceptibility, accounting for the large heats of chemisorption on transition metal surfaces for which χ_{loc} is largely due to the narrow d bands. Schrieffer (76) notes that even d states below the Fermi level contribute to χ_{loc}. Thus, chemisorption on Cu, even though weak, may have contributions from d states near the Fermi energy, even though the d band is filled in the bulk metal. On this model, whether one uses extreme rigid-band or extreme minimum polarity, as one adds Ni to Cu, the bond strength would be expected to increase because of the increasing number of d states near the Fermi level.

VI. Metallurgical Considerations

Copper and nickel form a continuous series of solid solutions over the whole composition range and there are no known ordered compounds. Thus the phase diagram is very simple. However there is a tendency towards phase separation (clustering) which adds complexity to any experiment, whether probing the electronic structure or the corrosion behavior.

A fundamental problem in interpreting experiments on the surface reactivity of Cu-Ni alloys concerns the actual composition of the surface layer. Sachtler and Van der Plank (77) have concluded that over most of the composition range the adsorbing surface will, in thermodynamic equilibrium, have a composition that deviates strongly from that of the bulk. They have interpreted chemisorption and catalysis data on this basis. On the other hand, experiments on Cu-Ni alloys using Auger electron spectroscopy and LEED (78) have been unable to detect any difference in composition between properly prepared clean metal surfaces and the bulk alloy, although changes in surface composition appear detectable (79) after such treatments as ion bombardment, heating, and annealing.

There has been a recurring controversy over the separation of true bulk effects from those due to clustering in the bulk. It has been claimed, for example, that at least some of the experiments which are regarded as refuting the rigid-band model of Cu-Ni alloys can be explained, instead, in terms of the formation of Ni clusters (80,81). Mozer et al. (82) used neutron scattering to measure the clustering in an almost equiatomic Cu-Ni alloy. The amount of clustering observed was small and could not be responsible for the experimental observation of d-holes in Cu-rich alloys. Depending on the details of the alloy preparation, the resulting clustering could cause variations in the experimentally measured critical compositions. Of more practical importance is whether or not the alloy has been properly homogenized.

Fe is not very soluble in Cu, and clustering as well as phase separation is common. Nonetheless, Mössbauer measurements (83) have shown that appropriate heat treatment and quenching can give essentially random alloys for small Fe concentrations. Coherent precipitates (Guinier-Preston zones) can be formed in some cases and these are recognizable by Mössbauer measurements (55,83). Very finely distributed Fe-Ni precipitates, not detectable by electron-microprobe measurements can drastically affect the corrosion behavior (84).

Comparison of Figures 1 and 8 show that pitting in Cu-Ni alloys occurs at a composition relating to the onset (54) of giant magnetic moments. Whether this correlation is causative or coincidental is not known. Extremely well-prepared and well-characterized alloys would be necessary to investigate the origin of this suggestive correlation.

The element Pd has a similar atomic electronic structure to Ni, with 10 electrons outside of closed atomic shells, but Pd does not increase the density of states as drastically as Ni, acting more like a rigid-band alloy (16). Thus if the relation between corrosion and electron structure were valid, Cu-rich Cu-Pd alloys should be less corrosion resistant in saltwater than Cu-rich Cu-Ni alloys. It was not possible to test the electron-configuration theory of marine corrosion with this alloy system since a wholly different corrosion mechanism (namely, intergranular embrittlement) is dominant (85).

VII. Discussion and Summary

The basis of the electron-configuration theory of passivity is the view that passivity is caused by formation of a chemisorbed protective film of monolayer or multilayer proportions; further, it is conjectured that the formation of this film is related to the presence of unfilled d levels at the surface of the transition metal or alloy. For the case of Cu-Ni alloys with small quantities of ternary additions, Uhlig et al. have presented a considerable amount of experimental evidence which supports this theory. Basically, their results show that the presence or absence of passivation, as detected by polarization measurements in 1N H_2SO_4, can be directly correlated with the presence or absence of an unfilled d band as predicted by the rigid-band model. Although one can argue about fine details near the critical compositions, the fact remains that the electron-configuration theory predicts this critical composition for passivity just as successfully as the rigid-band model predicts the critical composition for the magnetic properties of these alloys. However, strong objections can be made when one attempts to use the electron-configuration theory to describe the corrosion behavior in other alloy-electrolyte systems. Lacking detailed knowledge of the mechanism by which the band structure affects chemisorption, and with the current knowledge concerning the limitations of the rigid-band model, firm conclusions are difficult to draw, but qualitative observations may be made.

It may be preferable to appeal to experiment to determine the critical composition of ternary alloys. Either magnetic data, or electronic specific-heat data, for example, give relatively well defined critical compositions which can be compared with corrosion experiments. The available data on ternary alloys do not appear sufficient to permit detailed comparisons, but some general observations are possible. For example, additions of a non-transition element such as Al shifts the critical composition, as measured by electronic specific heat (42), in approximately the same way as that measured by potentiometric determination of corrosion behavior (12). Similarly, transition metals such as Fe shift the critical composition in the opposite direction to that of Al as measured both by magnetic measurements (86) and by potentiometric measurements (12).

It is possible to extend the electron-configuration theory of corrosion from consideration of critical compositions to the corrosion rates in the high-copper alloys. The minimum-polarity, or the coherent-potential model, and a large number of the experiments previously mentioned show that each Ni atom contributes a small increment of unoccupied d-state to the copper alloy. If the reasonable assumption is made that the presence of these d-holes promotes chemisorption, and further that the tendency for chemisorption is increased when the Fermi level falls within the d-band, then the corrosion behavior of Cu-Ni alloys in saltwater can be rationalized in a semi-quantitative way. In the high-nickel region, the Fermi level lies in the d band with the corrosion rate relatively insensitive to the exact composition. The decline in the corrosion rate in the active region is attributed to the increasing number of d holes. Note that in the high-copper region the decline in the corrosion rate as Ni is added to Cu (Figure 1), closely correlates with the increase in electronic specific heat, (Figure 5). Observations on small Fe additions (84) in the active region are consistent with this picture. An increment of Fe will reduce the corrosion rate by about the same amount as that increment of Ni which provides the same number of d holes in the minimum-polarity model. Fe is shown to be four to five times as effective as Ni in reducing the corrosion rate (Figure 9). The magnetic moment of Fe in Cu-Ni alloys, 2.8 μ_B, is four to five times that of Ni, 0.6 μ_B (54). Experiments with other ternary additions to Cu-Ni in the high-copper region would be desirable.

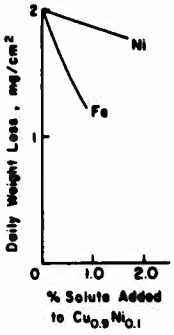


FIGURE 9. Corrosion behavior of a $Cu_{90}Ni_{10}$ alloy in sea water upon adding Fe or additional Ni [after Swartzendruber and Bennett, ref. 84].

It is also interesting to consider related and controversial electron-configuration theories of heterogeneous catalysis by Cu-Ni and similar alloys (87-92). Dowden and Reynolds (87) observed that Cu-Ni catalysts become ineffective for styrene hydrogenation at 38% [illegible] This is in approximate agreement with the critical composition and Dowden proposed an Uhlig-type model for the catalytic process. Many experimental results have been compared with an electron-configuration theory of catalysis, but often using the rigid-band picture. For example, Sachter and van der Plank (77), Hardy and Linnett (93), and Ponec and Sachtler (94) all point out that interpretation of their data in these terms requires the assumption that Ni atoms tend to keep their d holes with them. Since the rigid-band model does not allow d-holes in the high copper-region, these authors viewed this as refuting an electron-configuration theory of catalysis. However, using the minimum-polarity approach, these results are consistent with such a theory.

An interesting set of experiments involving both corrosion and catalysis (but not Cu-Ni alloys) was reported by Hara and Mano (95). They considered the problem of designing tarnish-resistant electrical contacts that can withstand both corrosive gases and organic vapors. In organic vapors, catalytic activity leads to polymer formation and increases contact resistance. They related this catalytic activity to holes in the d band and suggested that the optimum composition is one in which the d band is just full, giving both a low corrosion rate and a low catalytic activity.

In summary, an electron-configuration theory can account on a semiquantitative basis for observations of the corrosion rate of Cu-Ni alloys in saltwater, critical compositions for passivity of Cu-Ni alloys in H_2SO_4, as well as related phenomena such as catalysis on Cu-Ni alloys. Neither the understanding of the electron theory nor the corrosion behavior has been explored sufficiently as yet to ascertain whether observed correlations are more than coincidental. Since Cu-Ni alloys are considered to be the best understood alloy system, it may form a prototype for extension to other alloy systems. As more data and understanding are obtained, the details and complexities become more important requiring interdisciplinary studies involving solid state physics and electrochemistry.

References

1. J. N. Bradley, Int. Met. Rev. 17, 81 (1972).

2. G. L. Bailey, J. Inst. Metals 79, 243 (1951).

3. F. L. LaQue and H. R. Copson, editors "Corrosion Resistance of Metals and Alloys", (Reinhold Publishing Co., New York, 1963).

4. G. D. Bengough and R. May, J. Inst. of Metals 32, 81 (1924).

5. L. J. Swartzendruber and L. H. Bennett, Desalination 9 387 (1971).

6. N. D. Tomashov, (Translated by B. H. Tytell et al.), "Theory of Corrosion and Protection of Metals" (McMillan Co., New York, 1969).

7. H. H. Uhlig and J. Wulff, Trans. A. I. M. E. 135, 494 (1939).

8. H. H. Uhlig, Trans. Electrochem. Soc. 85, 307 (1944).

9. H. H. Uhlig, in "The Corrosion Handbook", (The Electrochemical Society, New York, 1948).

10. H. H. Uhlig, Z. Elektrochem. 62, 700 (1958).

11. H. G. Feller and H. H. Uhlig, J. Electrochem. Soc. 107, 864 (1960).

12. F. Mansfeld and H. H. Uhlig, Corrosion Science 9, 377 (1969); J. Electrochem. Soc. 117, 477 (1970).

13. J. Osterwald and H. H. Uhlig, J. Electrochem. Soc. 108, 515 (1961).

14. N. D. Stolica and H. H. Uhlig, J. Electrochem. Soc. 110, 1215 (1963).

15. H. H. Uhlig, F. Mansfield and M. Kasten, Z. Phys. Chemie Neue Folge 74, 216 (1971).

16. N. F. Mott, Proc. Phys. Soc. 47, 571 (1935); N. F. Mott and H. Jones, "The Theory of the Properties of Metals and Alloys", (Clarendon Press, Oxford, 1936).

17. R. F. North and M. J. Fryor, Corrosion Science 10, 297 (1970).

18. L. Hodges, R. E. Watson and H. Ehrenreich, Phys. Rev. B 5, 3953 (1972).

19. P. Soven, Phys. Rev. 156, 809 (1967); ibid 178, 1136 (1969).

20. P. Soven in, "Energy Bands in Metals and Alloys", L. H. Bennett and J. T. Waber, editors (Gordon and Breach, New York, 1968) p. 139.

21. H. M. Krutter, Phys. Rev. 48, 664 (1935).

22. S. Kirkpatrick, B. Velický, and H. Ehrenreich, Phys. Rev. B 1, 3250 (1970); S. Kirkpatrick, B. Velický, N. D. Lang, and H. Ehrenreich, J. Appl. Phys. 40, 1283 (1969).

23. L. F. Mattheiss, Phys. Rev. 134A, 970 (1964).

24. L. Hodges, H. Ehrenreich, and N. D. Lang, Phys. Rev. 152, 505 (1966).

25. J. Friedel, Phil. Mag. 43, 153 (1952); Adv. in Phys. 3, 446 (1954).

26. D. Pines, "The Many-Body Problem", Benjamin & Co., New York (1961).

27. C. Kittel, "Quantum Theory of Solids", J. Wiley and Sons, New York (1963).

28. S. Raimes, "Many Electron Theory", American Elsevier, New York (1972).

29. L. H. Bennett, editor, "Electronic Density of States," NBS Specl. Publ. 323 (U.S. Govt. Printing Office, 1971).

30. P. M. Marcus, J. F. Janak and A. R. Williams, editors, "Computational Methods in Band Theory," (Plenum Press, New York, 1971).

31. R. E. Watson, A. A. Misetich, and L. Hodges, J. Phys. Chem. Solids 32, 709 (1971).

32. E. A. Stern in "Energy Bands in Metals and Alloys," L. H. Bennett and J. T. Waber, editors (Gordon and Breach, New York, 1968). p. 151.

33. J. H. Van Vleck, Rev. Mod. Phys. 25, 220 (1953).

34. J. H. O. Varley, Phil. Mag. 45, 887 (1954).

35. N. D. Lang and H. Ehrenreich, Phys. Rev. 168, 605 (1968).

36. L. Pauling, "The Nature of the Chemical Bond," (Cornell University Press, Ithaca, New York, 1960).

37. J. Kanamori, K. Terakura and K. Yamada, Prog. Theor. Phys. 41, 1426 (1969); J. Kanamori and K. Terakura, J. Physique Suppl. 2-3, 32, C1-282 (1971).

38. R. Ehrat, A. C. Ehrlich, and D. Rivier, J. Phys. Chem. Solids 29, 799 (1968).

39. H. P. Myers, C. Norris, and L. Wallden, Solid State Communications 7, 1539 (1969).

40. E. W. Pugh and F. M. Ryan, Phys. Rev. 111, 1038 (1958).

41. C. G. Robbins, H. Claus, and P. A. Beck, Phys. Rev. Letters 22, 1307 (1969).

42. P. A. Beck and H. Claus, Journal Res. Nat. Bur. Stds. 74A, 449 (1970).

43. K. H. Bennemann, Phys. Rev. 167, 564 (1968).

44. M. Dixon, F. E. Hoare, and T. M. Holden, Proc. Roy. Soc. A303, 339 (1968).

45. J. Clift, C. Curry, and B. J. Thompson, Phil. Mag. 8, 593 (1963).

46. A. Wegner, G. Bürri and S. Steinemann, Phys. Letters 34A, 195 (1971).

47. R. C. Dobbyn, M. L. Williams, J. R. Cuthill, and A. J. McAlister, Phys. Rev. 2B, 1563 (1970).

48. J. R. Cuthill, A. J. McAlister and M. L. Williams, Phys. Rev. Letters 16, 993 (1966).

49. J. R. Cuthill, A. J. McAlister, M. L. Williams and R. E. Watson, Phys. Rev. 164, 1006 (1967).

50. G. Ertt and K. Wandelt, Phys. Rev. Letters 29, 218 (1972).

51. D. H. Seib and W. E. Spicer, Phys. Rev. Letters 20, 1441 (1968); Phys. Rev. B2, 1676 (1970).

52. S. Hüfner, G. K. Wertheim, R. L. Cohen, and J. H. Wernick, Phys. Rev. Letters 28, 488 (1972).

53. B. W. Murray and J. D. McGervery, Phys. Rev. Letters 24, 9 (1970).

54. L. H. Bennett, L. J. Swartzendruber, and R. E. Watson, Phys. Rev. Letters 23, 1171 (1969).

55. L. H. Bennett, L. J. Swartzendruber, and R. E. Watson, J. Appl. Phys. 42, 1547 (1971).

56. B. J. Waclawski and E. W. Plummer, Phys. Rev. Letters 29, 783 (1972).

57. R. Haydock, V. Heine, M. J. Kelly and J. B. Pendry, Phys. Rev. Letters 29, 868 (1972); R. E. Watson, P. Fulde and A. Luther, Proc. 18th Annual Conf. on Magnetism and Magnetic Materials (to be published); A. Luther, P. Fulde and R. E. Watson, ibid (to be published); K. Levin, A. Liebach and K. H. Bennemann (to be published).

58. H. H. Uhlig, Electrochimica Acta 16, 1939 (1971); H. H. Uhlig, "Corrosion and Corrosion Control", Second Edition (J. Wiley and Sons, New York, 1971) p. 86.

59. E. T. Goodwin, Proc. Camb. Phil. Soc. 35, 205 (1939).

60. J. W. Gadzuk, J. Vacuum Sci. and Tech. 9, 591 (1972).

61. J. W. Gadzuk, E. W. Plummer, H. E. Clark, and R. D. Young, in "Electronic Density of States" L. H. Bennett, editor, N.B.S. Special Publication No. 233, (U.S. Govt. Printing Office, 1972), p. 375.

62. E. W. Plummer, J. W. Gadzuk, and R. D. Young, Solid State Communications 7, 487 (1969).

63. E. W. Plummer, J. W. Gadzuk, Phys. Rev. Letters 25, 1493 (1970).

64. B. Feuerbacher and B. Fitton, Phys. Rev. Letters 29, 786 (1972).

65. D. E. Eastman and J. K. Cashion, Phys. Rev. Letters 27, 1520 (1971).

66. H. D. Hagstrum in "Techniques of Metals Research, Vol. 4, Part 1", edited by E. Passaglia and R. F. Bunshah (Interscience, New York, 1972) p. 309.

67. E. W. Plummer and A. E. Bell, J. Vacuum Sci. and Tech. 9, 583 (1972).

68. T. B. Grimley, J. Vacuum Sci. and Tech. 8, 31 (1971).

69. G. C. Bond, Disc. Faraday Soc. 41, 200 (1966).

70. A. J. Bennett, and R. P. Messmer, Phys. Rev. B 6, 633 (1972).

71. D. M. Newns, Phys. Rev. 178, 1123 (1969).

72. J. W. Gadzuk, Surface Sci. 6, 133 (1967); 6, 159 (1967).

73. A. Van der Avoird, Surface Sci. 18, 159 (1969).

74. J. R. Schrieffer and R. Gomer, Surface Sci. 25, 315 (1971).

75. J. R. Schrieffer, J. Vacuum Sci. and Tech. 9, 561 (1972).

76. J. R. Schrieffer, private communication.

77. W. M. H. Sachtler, and P. Van der Plank, Surface Sci. 18, 62 (1969).

78. G. Ertl and J. Küppers, J. Vacuum Sci. and Tech. 9, 829 (1972).

79. K. Nakayama, M. Ono, and H. Shimizu, J. Vacuum Sci. and Tech. 9, 749 (1972).

80. J. Crangle, in "Electronic Structure and Alloy Chemistry of Transition Element. (AIME Symposium)", edited by P. A. Beck (J. Wiley, New York 1962).

81. A. Kidron, Phys. Rev. B, 1, 939 (1970).

82. B. Mozer, D. T. Keating, and S. C. Moss, Phys. Rev. 175, 868 (1968).

83. L. H. Bennett and L. J. Swartzendruber, Acta Met. 18, 485 (1970).

84. L. J. Swartzendruber, and L. H. Bennett, Scripta Met. 2, 93 (1968).

85. D. B. Ballard, L. H. Bennett, and L. J. Swartzendruber, Corrosion 28, 368 (1972).

86. L. J. Swartzendruber, L. H. Bennett, and R. E. Watson, J. Appl. Phys. 40, 1489 (1969).

87. D. A. Dowden and P. W. Reynolds, Disc. Faraday Soc. 8, 184 (1950).

88. D. A. Dowden, J. Chem. Soc. London 242 (1950).

89. R. L. Moss and L. Whalley, Advances in Catalysis 22, 115 (1972).

90. P. W. Reynolds, J. Chem. Soc. London 265 (1950).

91. A. Couper and D. D. Eley, Disc. Faraday Soc. 8, 172 (1950).

92. G. RienMcker and G. Vormum, Z. Anorg. Allg. Chem. 283, 287 (1956).

93. W. A. Hardy and J. W. Linnett, Trans. Faraday Soc. 66, 447 (1970).

94. V. Ponec and W. M. H. Sachtler, J. Catalysis 24, 250 (1972).

95. T. Hara and K. Mano, I.E.E.E. Transactions on Parts, Materials and Packaging PMP-5, 133-138 (1969).

Discussion by H. H. Uhlig:

I am pleased that Dr. Bennett and his co-workers have given further thought to the relation of electron-configuration in alloy systems to their passive and corrosion behavior. The relations which they have summarized are important to an understanding of how corrosion-resistant metals function, and also how best to establish the optimum route along which any useful research program on better alloys should be directed. Their contribution of modern terminology to the current concepts of the metallic state is welcome.

To whatever extent the idea was at first opposed, our own continuing work in this area has now established, I believe, a definite relation between d band electronic structure within the Ni-Cu alloy system to the possible formation of a passive film. One can always discuss the relative validity of numbers that are predicted by any particular model of electronic states, but quite apart from such details, the critical composition at which passivity initiates [observed divergence of i (critical) and i (passive) at and below 60-70% Cu in 1 N H_2SO_4] is essentially shifted toward higher Ni compositions by alloyed non-transition components (e.g. Al, Zn, Ga, Ge) and toward lower Ni compositions by transition metal components, e.g. Fe, Co, Mn. These shifts are in accord with donor electrons contributed to the alloy by non-transition components, and of electron vacancies by transition metal components. Facts of this kind, plus the relative amount by which each component predictably shifts the critical composition make it extremely unlikely that the reported observations can be merely coincidence.

Independent adsorption studies show that the presence of an unfilled d band in a metal favors the chemisorption of oxygen. Parallel considerations and observations support a model of the passive film based on chemisorbed oxygen. Metal ions may in time penetrate that adsorbed film in nonstoichiometric amounts, accounting for the increased stability of thicker passive films forming in long times or at more noble potentials. For a filled band, on the other hand, bonding of oxygen to the metal is less energetic, and a stoichiometric oxide forms in preference. The latter may act as a diffusion barrier film, but this is not the passive film as presently discussed. The action of the adsorbed passive film is to impede not diffusion, but the rate of metal ion dissolution (e.g. by displacing adsorbed H_2O necessary to ion hydration). Electrochemically speaking, the exchange current density for metal ion dissolution, for whatever cause, is decreased, and anodic polarization is increased, corresponding to the observed polarization behavior of passive metals such as the stainless steels, many nickel-base alloys, titanium, chromium, etc.

The electron interactions responsible for passivity in transition metal alloys such as Fe-Cr, Ni-Cr, Ni-Mo, etc. are not as well established as for the Ni-Cu system but it is assumed that they follow an analogous pattern. It would seem that attention to these systems might well receive attention next by solid state physicists, whose proposed models should benefit from the accumulated empirical data already established on corrosion behavior and passive compositions.

Note Added in Proof to "On the Electron-Configuration Theory Of Marine Corrosion"

L. H. Bennett, L. J. Swartzendruber, and M. B. McNeil

National Bureau of Standards
Washington, D. C. 20234

We are indebted to Professor J. Friedel (of the University of Paris) for the suggestion that some remarks on geometric factors in catalysis and corrosion would be appropriate. This paper has been largely concerned with measurements using polycrystals (though without careful study of possible preferred orientation!) However it has long been known (87) that surface structure is an important factor in catalytic behavior; this has recently been the subject of fairly detailed studies (96,97). For Cu, there is very clear evidence (98) that surface crystallographic orientation has a pronounced effect upon oxide film formation. For Ni, it has been shown that different crystallographic planes show different passivation curves (100), though comparable work has not appeared for Cu-Ni alloys.

In addition to purely crystallographic orientation effects, there are substantial effects due to cold work. This has been shown, for example, for catalysis on Au (96), and it has been noted that not only does corrosion of Cu-Ni polycrystals depend upon the degree of cold work, but also that the effect of cold work on corrosion varies with alloy composition (101). Steps, kinks, facets, etc., on the surface are also known to be important. Clearly more work is needed on the interplay of electrochemical and crystallographic factors in determining both corrosion and catalytic behavior. We thank Drs. J. Kruger, U. Bertocci, and A. W. Ruff, Jr. for their comments.

References

96. S. Kishimoto and M. Nishioka, J. Phys. Chem. 76, 1907 (1972).

97. G. A. Somorjai, Catalysis Reviews 7, 87 (1972).

98. J. Kruger, J. Electrochem. Soc. 106, 847 (1959); ibid. 108, 503 (1961); J. Kruger and J. P. Calvert, J. Electrochem. Soc. 111, 1030 (1964).

100. C. J. Mauvais, R. M. Latanision, and A. W. Ruff, Jr., J. Electrochem. Soc. 117, 902 (1970).

101. L. J. Swartzendruber, unpublished work.

A study of the corrosion products of copper, zinc and some of their alloys

E.D. Mor - A.M. Beccaria

Consiglio Nazionale delle Ricerche
Laboratorio per la Corrosione Marina dei Metalli
Via Mercanzia, 4 - 16123 Genova
Italia

The study of the corrosion products of copper, zinc and their alloys in sea water was made by chemical and physical methods.

X ray diffractometric analysis confirmed the results of chemical analysis, only for long corrosion periods, because, for short corrosion time, only the metal oxydes could be detected.

The following corrosion products were obtained from the various metals:

copper: Cu_2O, CuO, $CuCl_2 \cdot 3\,Cu(OH)_2$, $2\,CuCO_3 \cdot Cu(OH)_2$;

zinc: ZnO, $Zn(OH)_2$, $4\,ZnO \cdot CO_2 \cdot H_2O$, $ZnCl_2 \cdot 4Zn(OH)_2$

OT/67 and OT/58 alloys: ZnO, Cu_2O, CuO, Cu and Zn oxychlorides and basic carbonates.

1. Introduction

The mechanism of the corrosion of copper in slightly alkaline solutions or in sea water was previously investigated by some authors, who examined, the corrosion products by X ray diffractometry. Pourbaix's research on the pitting of copper in solutions containing chlorides (1)(2)(3)[1] or in sea water (4), showed the possible formation of different layers of products in the following order, starting from the metal surface: Cu_2O, $CuCl$, $Cu(OH)_2$, $CuCO_3$.

Compton (5) has found a basic oxychloride having the formula $(Cu^{2+})(OH^-)_n(Cl^-)_y$, that was also confirmed by the results of Uhlig (6). The corrosion products of zinc, studied in water solutions by Uhlig (7), Evans (8) Pourbaix (9) and Johnson (10) are formed by a smaller number of compounds, mainly containing oxydes and hydroxydes. This type of precipitate, following Blok and De Bruyn (11), may be considered as a mixture of $Zn(OH)_2$ and $Zn(OH)_{1.6}X_{0.4}$,

[1] Figures in parentheses indicate the literature references at the end of this paper.

where X represents an anionic impurity adsorbed during the oxyde precipitation. Notwithstanding the number of papers published on the behaviour of Cu-Zn alloys in sea water, very little information was reported concerning the composition of their corrosion products.

The layer, formed by the corrosion products on the surface of metals, may have different thickness and permeability.

The analysis is easier when the thickness of the film is above 1000 Å, while thinner layers lead to serious analytical problems. In the former case, X ray diffractometry may allow the identification of the compounds having a concentration larger than 10%, while, in the latter, with a thickness of about 100 Å, this technique may give poor results. The infrared ATR method, used by Ebiko-Suetaka (12), (13), Pobimer (14) and Poling (15), for the identification of thin oxyde films and the measurement of their thickness, cannot be used with Cu and Zn treated with sea water, due to the roughness of the corroded surface, that does not allow a good optical contact with the ATR crystal.

A good method of investigation must allow the separation and the quantitative analysis of the different components of the corrosion products. Therefore they must be removed from the metallic surface without modifications.

This result is generally achieved by means of a chemical treatment of the metallic matrix with iodo-alcohol (16) or bromo-ether (18 - 17) solutions, or by electrochemical methods (19) (20), that do not modify the metal oxydes (21).

Unfortunately, these methods destroy many products less stable than oxydes, as sulphides, oxychlorides and basic carbonates. For the same reason, the stripping technique, used for electron microscope replicas (22) (23) (24) (25) cannot be satisfactorily used.

A NACE report (26) and the works of Cotton (27), suggest, for the determination of the copper corrosion products in sea water, a separate solution of the various components, without removing the corrosion layer from the metallic surface.

The reagent used (ammonium chloride in NH_4OH solution or hydroxilamine chlorhydrate 10%) has poor selectivity because it dissolves all the copper compounds, without respect to their valence and oxydation degree.

For this reason, we tried to develop a method for the qualitative and quantitative analysis of all the corrosion products of Cu, Zn and their alloys, that also allows the different stages of the corrosion process to be investigated.

We have found a series of treatments, with different solvents at various concentrations and temperatures, that separately dissolves each compound, without modification of the others.

Many solvents were used: methanol (28) to remove sodium magnesium and copper chlorides, glycine (29), that dissolves the bivalent metallic compounds; NH_4Cl (28), that dissolves the metallic compounds other than bivalent. All these reagents do not react with the metallic matrix. After every treatment, to confirm the analytical results, X ray diffractometric analyses were made, both on the layers still adherent to the metal, and when possible, on the removed and pulverized corrosion products.

2. Experimental tecnique

The following metallic materials were used for the experiments: annealed electrolytic copper, 99.8% (codex Erba n.475245), zinc 98% (codex Erba n.493507), and two different Cu-Zn alloys (OT/67 and OT/58), containing respectively the amounts 67/33 and 58/42 of the two metals with 0,2% maximum impurities.

All the test pieces were polished with a series of abrasive papers (180 . 320 . 400 . 500 . 600) and degreased with petroleum ether before immersion into the corrosive solutions. The corrosion tests were made in open cells at 25°C, without agitation, for different lengths of time, carefully maintaining constant both the physico-chemical properties and the concentration of the solutions.

The ratios between the volume of the solutions and the surface of the test pieces were as suggested by Uhlig (30).

The pure metals were placed in various solutions: a very diluted NaOH solution at pH 8.2 [illegible]; NaCl solution 3,5%; $NaHCO_3$ solution 2%; synthetic sea water (Lymann-Fleming); while the two alloys were treated with synthetic sea water only.

Different corrosive solutions with pure metals were used to separately obtain some corrosion products (as oxychlorides and basic carbonates) and test their behaviour with respect to the different reagents.

In fact, the solubility tests directly made on the powders of the possible corrosion products, using the pure crystalline standards normally used for X ray diffractometric identification (atacamite, malachite, Cu and Zn oxydes etc), would only approximately represent the true situation of the corrosion layer.

In is well known that the solubility of a given compound does not depend on its chemical nature only, but is strongly influenced by its granulometry.

To make different tests on the same specimen (chemical methods, X ray analysis, total oxygen), the corroded test pieces were partially covered with adesive Teflon tape, before every chemical treatment.

To determine the best dissolving conditions for Cu and Zn oxydes, the test pieces of the two pure metals, after corrosion in deionized water at pH 8.2 for 100 hours, were washed with methanol, under nitrogen atmosphere, using the apparatus shown in fig. 1.

The treatment with methanol was made at 65°C for 1 hour and the resulting solution was filtered on Millipore membrane UHWPO 2500.

Cu and Zn were absent from the filtrate, where their presence was tested spectrophotometrically, using respectively the Belcker-Crossland method (Cu-cyclohexanone complex: $C_6H_{10}NNHCOCONHNC_6H_{10}$) (31), and the Sadilkova method(32) (zincon complex: $C_2H_{15}N_4O_6SNa.H_2O$).

The experiments showed that copper or zincoxydes formed in the conditions described, are insoluble in CH_3OH.

After treatment with methanol, the test pieces were placed in the apparatus shown in fig. 2 (A), and treated, under N_2 atmosphere, with glycine at different concentrations and temperatures, for 5 minutes. Glycine was introduced in the system, after N_2 flushing, by means of the stopcock 1 [see fig. 2 (A)]

For the comparison, the same treatment was also done on test pieces of copper and zinc, polished and degreased as described above, but without corrosive treatment. The results of these experiments are reported in table 1.

On the same portion of the surface, after rinsing with water, a treatment with NH_4Cl 10% at three temperatures was made using the same apparatus shown in fig. 2, under nitrogen, for 5 minutes.

The results are reported in Table 2.

On the remaining part of the surface, the oxygen combined with metals was determined using the Gurry method (H_2 reduction) (33). The results are shown in Table 3, where the values of oxygen on the non-corroded pieces are not reported, because all the determinations give zero values. On the contrary, the values of oxygen experimentally measured, are compared with those stoichiometrically calculated from the amounts of copper and zinc dissolved with glycine and with NH_4Cl (see Table 1 and 2).

This comparison shows that the treatment with glycine 30% at 80-85°C, followed by NH_4Cl 10% at the same temperature, is the best method for the determination of copper oxydes. The treatment with NH_4Cl, on the contrary, was useless for the zinc compounds. (see Tables 2 and 3).

The X ray diffractometric analysis, confirmed these results.

The same method described above was used to analyse the products formed after corrosion with $NaHCO_3$ 2% and NaCl 3.5%, that mainly consists in basic carbonates and oxychlorides, respectively.

The corrosive treatment lasted from 8 to 350 hours.

In the pieces corroded with $NaHCO_3$, also the CO_2, formed during the glycine treatment, was measured by titration with sodium methanolate in pyridine (Patchornik-Shalitin (34)).

The Cl anion was measured with the Ag iodate method and by spectrophotometric determination of the iodine formed (35).

In both cases, the methanol treatment did not modify either the oxychlorides nor the basic carbonates.

The results are reported in table 4: the composition of the corrosion products depends on the corrosion time. In the first stage of the reaction, only the oxydes are formed, and, subsequently, their precipitate includes anions (Cl^- and/or CO_3^{--}) forming oxychlorides and basic carbonates (Compton (5) Block and De Bruyn (11) Biestek (36) and Pollard (37).

It was possible to determine the stoichiometric composition of the corrosion products by X ray diffractometry, only when the pieces were treated with the corrosive solutions for periods longer than 10 days. For shorter corrosion time oxychlorides, chlorides, or carbonates could not be detected by X ray analysis.

The same analysis method described above was applied to test pieces of Cu, Zn, and their alloys OT/67 and OT/58, corroded in seawater for various times.

The results are shown in table 5.

Also in these circumstances on the primary layer of oxydes, formed in the first stage of the corrosion process, oxychlorides and basic carbonates with variable composition later appear containing some cationic impurities too, as Mg in the case of Zn.

On the contrary, the corrosion products of the alloys OT/67 and OT/58 are practically formed only by copper and zinc oxydes.

Also in these cases, the confirmation of the results was possible by X ray diffractometry, only when corrosion time was longer than 15 days.

Comparing the diffractograms of the corrosion products formed in NaCl solution with those formed in sea water, it could be observed that the latter have broader peaks, that may indicate a finer structure of the compounds, and explain the smaller corrosion of copper and zinc in sea water.

3. - Conclusion

The proposed method of analysis gives therefore good results, allowing the separate solution of the different products of corrosion.

X ray diffractometry, when its application was possible, substantially confirmed the results of the chemical analysis.

Aknowledgment

The Authors aknowledge Mr. Gildo POGGI (C.N.R.) and Mr. ARATA and Dr. MARE' (Research Laboratory of Soc. Italsider) for their cooperation.

References

1. - M. POURBAIX - Corrosion, 26, 431 (1970)
2. - M. POURBAIX - Symp. Coupling Basic Appl. Corros. Res. Dialogue, 67-64, (1966) (Pubb. 1966).
3. - M. POURBAIX - Atlas of Electrochemical Equilibria in Acqueous solutions 384 - 392, Pergamon (1966).
4. - M. POURBAIX - Corrosion Science, 12, 161, (1972).
5. - K. G. COMPTON - Corrosion, 26, 148 (1970).
6. - H. R. UHLIG - The Corrosion Handbook - The electrochemical society Inc. John Wiley - New York , 64, (1953).
7. - H. R. UHLIG - Ibid..... 417, (1953).
8. - U. R. EVANS - Metallic corrosion passivity and protection, E. Atnold ed., 356, (1948).
9. - M. POURBAIX - Atlas of Electrochemical Equilibria in Acqueous solutions, 406-418, Pergamon (1966).
10. - J. W. JOHNSON - Y. C. SUN - W. J. JAMES - Corrosion Science, 2, 153, (1971).
11. - L. BLOK - P. L. DE BRUYN - J. Colloid Interface Sci., 3, 527-32,(1970).
12. - H. EBIKO - W. SUËTANA - Corrosion Science, 10, 110-112, (1970).
13. - H. EBIKO - N. TABATA - W. SUËTAKA - J. Spectroscopy Soc. Japan, 18, (1969).
14. - H. POBIMER - Anal. Chem., 1, 90-2, (1967).
15. - G. W. POLING - Corrosion Science, 10, 359, (1970).
16. - R. ROONEY - S. STAPLETON - J. Iron Steel Inst., 1, 56, (1931).

17. - H. HIGASHIDE - S. HASODA - Tetsu to Hagané, 3, 216, (1956).

18. - H. F. BEEGHLY - Anal. Chem., 24, 713, (1952).

19. - P. KLINGER - W. KOCK - Bertrage zur Metallkundichen Analyse,(1938).

20. - A. CHIPMAN - Trans. Amer. Soc. Metals, 38, 70, (1947).

21. - K. NARITA - A. NIYAMOTO - H. MATUMOTO - Tetsu to Hagané, 9, 846,(1969).

22. - D. H. KAY - Techniques for electron microscopy - Blackell - Oxford (1965).

23. - MURT GULDNER - Progress in Analytical Chemistry, 2, Plenum Press (1969).

24. - H. SAUER - H. ENOCHL - Radex Rundschau, 314, 641, (1967).

25. - K. L. MAURER - Radex Rundschau, 314, 733, (1967).

26. - NACE Technical Committee Report - Publication 59 - 13 Corrosion, 1e, 49, (1959).

27. - J. B. COTTON - Corrosion Technology, 3,(1956).

28. -- HANDBOOK of Chemistry and Physics - 46th Ed. The Chemical Rubber Co. B-173.

29. - D. N. SEN - SANICHIRO MIZUSHIMA - G. CURRAN - J. V. QUAGLINO - J.Am. Chem. Soc., 77, 212, (1955).

30. - H. R. UHLIG - The Corrosion Handbook - The Electrochemical Society Inc. John Wiley - New York, (1953).

31. - R. BELCHER - B. CROSSLAND - T. R. F. FENNEL - Talanta, 17, 639, (1970).

32. - M. SADILKOVA - Mikrochim. Acta, 5, 934, (1968).

33. - R. W. GURRY - Corrosion, 26, 71, (1970).

34. - A. PATCHORNIK - Y. SHALITIN - Analyt. Chem., 33, 1887, (1961).

35. - G. CHARLOT - Dosages Colorimétriques des éléments mineraux, 2me Ed. Masson et Cie, (1961).

36. - T. BIESTEK - J. NIEMIEC - Pr. Inst. Mech Precyz., 2, 38, (1966).

37. - A. J. POLLARD - Rept. NRL Progr., 1-2, (1964).

TABLE 1 - Amounts of copper and Zinc dissolved from apparent surface of samples after 5 minutes of treatment with glycine solutions. In columns a are reported the values obteined from non corroded samples, in columns b the values from corroded samples. Corrosive solution: diluted NaOH (pH 8.2)

Sample n°	Glycine conc. g/100 ml	T °C	Cu $\mu g\ cm^{-2}$		Zn $\mu g\ cm^{-2}$	
			a	b	a	b
1	5	25 - 30	-	20	-	55
2			-	22	-	48
3			-	17	-	47
4		50 - 60	-	25	-	45
5			-	20	-	56
6			-	20	-	52
7		80 - 85	-	30	-	58
8			-	32	-	57
9			-	32	-	65
10	10	25 - 30	-	30	-	60
11			-	32	-	60
12			-	36	-	62
13		50 - 60	-	40	-	65
14			-	42	-	70
15			-	40	-	72
16		80- 85	-	50	2	100
17			-	52	3	105
18			-	56	2	107
19	20	25 - 30	-	40	-	80
20			-	45	-	82
21			-	48	-	88
22		50 - 60	-	50	2	100
23			-	53	4	95
24			-	55	2	88
25		80 - 85	2	80	6	120
26			2	82	7	120
27			3	86	5	125
28	30	25 - 30	2	60	2	100
29			1	65	4	100
30			3	62	3	120
31		50 - 60	4	72	6	132
32			3	74	7	130
33			4	72	9	140
34		80 - 85	3	100	10	150
35			5	106	12	180
36			4	102	9	176

TABLE 2 - Amounts of copper and Zinc dissolved from apparent surface of samples, previously treated with glycine, after 5 minutes of treatment with NH_4Cl 10%. In columns a are reported the values obteined from non corroded samples, in columns b the values from corroded samples. Corrosive solution: diluted NaOH (pH 8.2)

sample n°	Previous treatment*		NH_4Cl 10% treatment T °C	Cu $\mu g\ cm^{-2}$		Zn $\mu g\ cm^{-2}$	
	glycine conc g/100 ml	T °C		a	b	a	b
1	5	25 - 30	25 - 30	-	30	-	-
2			50 - 60	-	70	20	22
3			80 - 85	-	170	30	28
4		50 - 60	25 - 30	-	32	-	-
5			50 - 60	-	75	24	20
6			80 - 85	-	180	28	27
7		80 - 85	25 - 30	-	36	-	-
8			50 - 60	-	78	32	36
9			80 - 85	-	165	28	30
10	10	25 - 30	25 - 30	-	35	-	-
11			50 - 60	-	80	34	32
12			80 - 85	-	163	36	30
13		50 - 60	25 - 30	-	38	-	-
14			50 - 60	-	90	25	28
15			80 - 85	-	155	28	32
16		80 - 85	25 - 30	-	38	-	-
17			50 - 60	-	78	30	31
18			80 - 85	-	130	30	28
19	20	25 - 30	25 - 30	-	36	-	-
20			50 - 60	-	82	26	20
21			80 - 85	-	136	28	29
22		50 - 60	25 - 30	-	33	-	-
23			50 - 60	-	81	27	30
24			80 - 85	-	110	31	36
25		80 - 85	25 - 30	-	35	-	-
26			50 - 60	-	82	37	30
27			80 - 85	-	100	36	34
28	30	25 - 30	25 - 30	-	32	-	-
29			50 - 60	-	75	34	31
30			80 - 85	-	110	38	36
31		50 - 60	25 - 30	-	35	-	-
32			50 - 60	-	76	26	30
33			80 - 85	-	112	28	37
34		80 - 85	25 - 30	-	38	-	-
35			50 - 60	-	65	28	31
36			80 - 85	-	97	29	32

* see Table 1

TABLE 3 - Amounts of oxygen combined with copper and Zinc for apparent surface of sample. Experimental and stoichiometrically calculated values are reported.

Sample n°	Combined O_2 on Cu $\mu g / cm^2$		Combined O_2 on Zn $\mu g / cm^2$	
	exp.	calc.	exp.	calc.
1	37,6	8,9	40,2	13,5
2	35,3	14,3	45,1	11,7
3	38,0	25,5	40,6	11,5
4	40,0	10,3	41,7	11,0
5	32,1	14,5	38,2	13,7
6	35,4	27,7	39,4	12,7
7	37,2	12,0	41,5	14,2
8	39,2	17,9	41,6	14,0
9	42,3	28,7	42,8	15,9
10	42,2	11,9	43,0	14,7
11	45,3	18,3	39,2	14,7
12	38,2	29,7	38,6	15,2
13	47,2	14,9	41,2	15,9
14	44,1	21,0	40,3	17,1
15	42,3	29,6	42,5	17,6
16	40,2	27,4	43,8	24,4
17	35,5	23,0	42,8	25,7
18	38,2	30,5	41,7	26,2
19	37,7	14,5	41,6	19,5
20	35,8	21,6	42,7	20,0
21	33,2	29,2	39,8	21,5
22	32,4	16,7	38,9	24,4
23	36,1	23,5	44,2	23,3
24	35,2	27,7	42,6	21,5
25	35,2	24,4	44,1	29,3
26	37,4	30,9	43,2	29,3
27	36,0	34,2	43,0	30,6
28	35,2	19,1	39,5	24,4
29	32,6	25,8	41,6	24,4
30	36,8	29,6	42,3	29,3
31	34,6	22,6	44,2	32,3
32	33,2	28,3	42,0	31,8
33	35,0	32,1	41,4	34,2
34	37,0	30,0	42,2	36,7
35	38,0	35,0	43,2	44,0
36	37,6	38,0	43,5	43,0

TABLE 4 - Amounts ($\mu g/cm^2$) of various elements obteined from the dissolution of the corrosion products. In column A are reported the formulas of compounds stoichiometrically calculated.

Metal	Corrosive Solution	Corrosion time h	Cu^I	Cu^{II}	Zn	Cl	O	CO_2	A
					$\mu g\ cm^{-2}$				
Cu	$NaHCO_3$ 2%	8	120	80	-	-	35	-	Cu_2O-CuO
		72	100	220	-	-	33	135	Cu_2O-[CuO · $2CuCO_3$]
		120	80	420	-	-	35	218	Cu_2O-[CuO · $3CuCO_3$]
		240	60	1040	-	-	80	475	Cu_2O-[CuO · $2CuCO_3$]
		350	50	2450	-	-	210	1100	Cu_2O-[CuO · $2CuCO_3$]
	NaCl 3,5%	8	140	90	-	-	38	-	Cu_2O-CuO
		72	130	200	-	71	42	-	Cu_2O-[$CuCl_2$ · 2CuO]
		120	120	400	-	142	76	-	Cu_2O-[$CuCl_2$ · 2CuO]
		240	100	800	-	285	134	-	Cu_2O-[$CuCl_2$ · 2CuO]
		350	110	1500	-	535	261	-	Cu_2O-[$CuCl_2$ · 3CuO]
Zn	$NaHCO_3$ 2%	8	-	-	100	-	24	-	ZnO
		72	-	-	300	-	20	147	ZnO · $3ZnCo_3$
		120	-	-	500	-	41	226	ZnO · $2ZnCO_3$
		240	-	-	800	-	98	270	ZnO · $ZnOO_3$
		350	-	-	1500	-	270	260	3 ZnO · $ZnCO_3$
	NaCl 3,5%	8	-	-	200	-	90	-	Zn
		72	-	-	400	71	98	-	6 ZnO · $ZnCl_2$
		120	-	-	700	150	173	-	5 ZnO · $ZnCl_2$
		240	-	-	1100	245	216	-	4 ZnO · $ZnCl_2$
		350	-	-	2000	430	485	-	4 ZnO · $ZnCl_2$

TABLE 5 - Amounts ($\mu g/cm^2$) of various elements obteined from the dissolution of the corrosion products. In column A are reported the formulas cf compounds stoichiometrically calculated. Corrosive solution: synthetic sea water (Lymann and Fleming) at pH 8.2

Metals	Corrosion time h	Cu^I	Cu^{II}	Zn	Mg	Cl	O	CO_2	A
					$\mu g\ cm^{-2}$				
Cu	8	120	80	-	-	-	37	-	Cu_2O-CuO
	72	100	150	-	-	80	28	-	Cu_2O-CuO-$CuCl_2$
	120	120	400	-	-	143	51	45	Cu_2O-3CuO·2$CuCl_2$$CuCO_3$
	240	100	900	-	-	193	144	122	Cu_2O-3CuO·$CuCl_2$·$CuCO_3$
	350	90	1500	-	-	200	236	242	Cu_2O-5CuO$CuCl_2$·2$CuCO_3$
	760	100	2000	-	-	268	340	327	Cu_2O-5CuO·$CuCl_2$·2$CuCO_3$
	1080	90	3000	-	-	329	454	610	Cu_2O-6CuO·$CuCl_2$·3$CuCO_3$
Zn	8	-	-	200	-	-	49	-	ZnO
	72	-	-	500	20	89	102	-	5ZnO·$ZnCl_2$
	120	-	-	900	20	97	172	61	8ZnO·$ZnCl_2$·$ZnCO_3$
	240	-	-	1200	40	198	227	63	10ZnO·2$ZnCl_2$·$ZnCO_3$
	350	-	-	1800	50	148	352	187	10ZnO·$ZnCl_2$·2$ZnCO_3$
	760	-	-	2500	50	206	470	269	10ZnO·$ZnCl_2$·2$ZnCO_3$
	1080	-	-	3000	60	248	565	314	10ZnO·$ZnCl_2$·2$ZnCO_3$
OT/67	8	-	50	80	-	-	32	-	ZnO·CuO
alloy	72	10	50	120	-	37	38	-	4(ZnO·CuO)·($Zn_xCu_yCl_z$)
	120	20	70	250	-	51	56	31	5(ZnO·CuO)·($Zn_xCu_yCl_zCO_{2t}$)
	240	20	70	500	-	87	103	55	5(ZnO·CuO)·($Zn_xCu_yCl_zCO_{2t}$)
	350	20	80	700	-	120	140	75	5(ZnO·CuO)·($Zn_xCu_yCl_zCO_{2t}$)
OT/58	8	-	30	80	-	-	28	-	ZnO·CuO
alloy	72	-	20	100	-	25	25	-	5(ZnO·CuO)($Zn_xCu_yCl_z$)
	120	-	30	200	-	49	69	-	6(ZnO CuO)($Zn_xCu_yCl_z$)
	240	-	40	400	-	59	83	37	6(ZnO·CuO)($Zn_xCu_yCl_zCO_{2t}$)
	350	-	50	500	-	74	100	47	6(ZnO·CuO)($Zn_xCu_yCl_zCO_{2t}$)

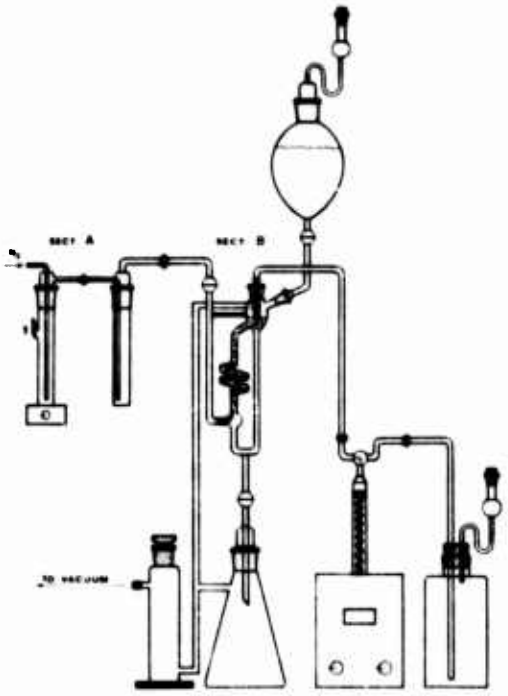


FIG. 2 - Apparatus for treatment with glycine and ammonium cloride

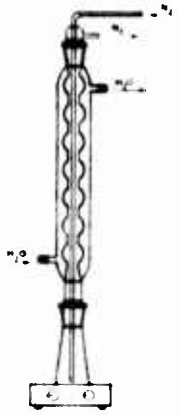


FIG. 1 - Apparatus for treatment with methanol

Erosive Damage-Processes Due to Cavitation

F. Erdmann-Jesnitzer und H. Louis

Institut (B) für Werkstoffkunde
Technische Universität Hannover
Appelstraße 24 A, 3000 Hannover
Federal German Republic

The hydromechanical damage of materials by cavitation is often based on corrosion and always on erosion which is the dominant factor in case of damage of high intensity. Cathodic protection diminishes corrosive damages however without any influence on the erosive part. The kinetics of cavitation damage are examined by observing the initial stages of damage on metallic and non-metallic materials. For this purpose we have developed a testing chamber of flow cavitation with high intensity of erosion. Unscratched and undeformed polished samples show the changes as a result of imploding cavitation bubbles. In some exceptional cases the damage is caused by one bubble only: the surface of soft metals shows plastic deformation waves radiallysymmetric to the centre of damage; in case of brittle materials,however, the initial damages are radiallysymmetric cracks, surrounding a more or less undamaged centre. Heterogeneous metallic materials may show different forms of attack. On soft materials, e.g. wax or pure aluminum, the initial stages of damage are followed by plastic deformation, cracking and finally excavating the material. These different stages of damages can be proved by scanning electron microscope.

Hydromechanical damage by liquid impact has been examined as well. Tests of metallic and non-metallic materials show the similar appearence of surface load in cases of cavitation and liquid impact. Special comparative studies of these forms of loading at pure aluminum (Al 99,99) and plexiglas (PMMA) have proved:

The elementary process of erosive cavitation is the impact of liquid.

From the results of the cavitation tests one can derive basic principles of convenient mechanical properties of metallic materials. They are the guiding-principles for the development of material with high cavitation resistance.

Key Words: flow cavitation, testing chamber,cavitation erosion

---

Damage caused by imploding cavitation bubbles consists of an erosive and a corrosive component. Metallographical studies, referring to the beginning of the destruction demonstrate the effect of corrosion already at a very early stage of loading time. For long periods of loading it is more difficult to determine the part of corrosion. Corrosive as well as erosive damages during the beginning of cavitation damage change the profiles only a little and therewith the cross-section of the channels. Increasing roughness, which may lead to deep damages through the whole workpiece and the corresponding weight loss,show that the erosive component is the dominant factor.

In case of cavitation of low intensity the corrosive damage can be reinforced by mechanical splintering of the layers of corrosion products. Splintering is caused by the mechanical effect of imploding bubbles. This whole process is repeated again and again.

The topic of this report will be the erosion as a mechanical destruction caused by imploding cavitation bubbles. The amount of erosive damage depends on the composition and constitution of the test-material.

To produce an erosive damage by imploding bubbles one can employ the method of vibration. Nevertheless in our institute however, we tried to obtain such a kind of destruction by flow cavitation. The reasons are the following:

1. The production of bubbles by high-frequent vibrations has a relationship to the practical aspects in only a few cases.
2. The specimens are highly loaded, even without the effect of imploding cavitation bubbles at the oscillating nozzle of a vibration equipment.
3. The damage of a great number of specimens seem to be an effect of resonance, as a result of the macroscopical load, and not caused by the imploding bubbles.

If you look at flow cavitation only, using tap water as working fluid, you will find that the destruction of the material consists in general of a corrosive and an erosive part. The erosive part can only be investigated if

1. corrosion is prevented. One possibility to prevent corrosion is the cathodic protection.
2. the erosive damage is highly increased. Thus the duration of experiments have been remarkably shortened and the energy of every imploding bubble has been increased, so that the corrosive part of the whole damage becomes very small and has no further influence on the kinetics of damage.

We, in Hannover, prefer this last mentioned method.
We designed a chamber of flow cavitation similar to that of H. Schröter (1)[1] and J.M. Mousson (2). The possibility of geometrical and hydromechanical variations leads to a chamber of very high intensity of erosive damages. The results of the tests can easily be reproduced. In this chamber the inlet pressure, the reversive pressure, the distance between the barricades and the position of the specimen can be changed.

The chamber is formed by a rectangular channel. The bubbles are caused by the decreasing pressure of the fluid as a result of two cylindrical barricades, called "Wehr" and "Gegenwehr", Fig. 1.

---

[1] Figures in parentheses indicate the literature references at the end of this paper.

The direction of the flow is from the left to right. On both sides there are observation windows, so that you can observe the rate of the damage and the formation of the stream of bubbles. Usually, the specimens are replaced from the top.

The cylindric form of the barricades was chosen because of the easy way of reproduction of the macroscopical and microscopical geometry. Barricades with special forms, as used by H. Schröder, should not be used for these experiments because the reproduction of the microscopical geometry is difficult to realize, however, very important.

The experimental results of cavitation are obtained in the developed chamber of flow cavitation.

When testing soft metals, as for example aluminum, the imploding bubbles lead to a deformation of the specimen surface. As a result of this the roughness and therefore the strengthening increase with duration of test, until the surface does not allow any further plastic deformation.

These changes are the result of many implosions of cavitation bubbles. To examine the elementary process of damage we tried toget only a few bubbles to implode on the specimen surface. Therefore an aluminum specimen has to be checked less than 1 s in the new testing chamber.

The tested specimen shows characteristical changes of the surface which are probably the effect of one single bubble implosion. They appear in form of indentations, some of which are symmetrically surrounded by plastic deformation waves, Fig. 2.

Continuing the cavitation load on this specimen, in the following seconds the initial damages often do not change. This fact may prove that the damage is a result of one imploding bubble only.

In the case of brittle plexiglas (PMMA) the imploding bubbles lead to cylindrical cracks, partly surrounding a more or less undamaged centre, Fig. 3. This damage also seems to be the result of only one bubble implosion.

The initial stages of damage caused by imploding bubbles are the indentations or crackings as shown above. With increasing loading time, e.g. on soft aluminum, craters will be formed. The position and the form of these craters do not depend on the structural constitution of the material.

After a loading time duration up to 5 s the first damages appear scattered all over the whole surface. With increasing test duration (10 s, 20 s) indentations become more and more numerous and extend. Not only indentations, but also glide bands are visible. Even without the help of a microscope the plastic deformation of the specimen surface can be recognized. The cause of this effect is the hydromechanical loading by a great number of imploding cavitation bubbles. This kind of damage is erosion.

Aluminum surfaces loaded for a short time (some seconds only) show radiallysymmetric plastic deformation waves, see Fig. 2. By increasing the testing time and the resulting surface roughness those typical initial cavitation damages do not appear any longer. The reason to this is the changed state of the specimen surface. When typical initial damages in the beginning of the cavitation load appear, the surface is plane. Later on it becomes rougher and rougher, which means that the geometrical and, possibly, the hydromechanical conditions of the surface loading change. As a result of these, the surface becomes strengthened as it is shown in micro-hardness loading time curves (3).

Plastic deformation of the surface leads to bizarre forms of surface profile corresponding with the loading time as shown in Fig. 4 by scanning electron microscope. The testing time of this aluminum specimen amounts to 15, 30, 45 and 60 s. With increasing duration of cavitation load craters will be formed and extend. The position and the form of these craters do not depend on

the structural constitution of the material. The in parts highly deformed surface gives the impression of a viscous flow.

Prodruding parts of the surface are places where cracks start. Fig. 5 shows a damaged aluminum specimen after 60 s of cavitation load. This stage of damage can only be observed by scanning electron microscope.

The prodruding parts of the surface are accompanied by arising cracks. A higher magnification (the picture on the right) shows the ground of those cracks. The appearance of the cracks gives rise to the idea of fracture by alternating stress. It is known that by increasing plastic deformation metals and alloys first show strengthening, called cohesion-strengthening, and then cohesion-destruction with the tendency to the formation of transcrystalline cracks, as for example aluminum. Fig. 6 shows such a crack by high magnification. It is not clear whether the fracture is caused by alternating shear stress or by fatigue.

The appearance of the damaged surface gives rise to the idea that the flow of material is supported by the high frequent pulsation of the load due to the imploding cavitation bubbles.

In the case of brittle materials, i.e. plexiglas (PMMA), the appearance of the damage changes completely. Fig. 3 showed the initial damages caused by an imploding bubble. You will find a more or less undamaged centre in parts surrounded by radiallysymmetrical cracks. Such a typical damage is the result of the implosion of only one bubble. This assumption is based on the fact that these damages generally do not change their appearance during continued cavitation load. With increasing testing duration, the number and the size of the damages will extend, until the whole specimen surface is scattered with cracks, Fig. 7 left. Up to that stage of damage no weight loss is detectable. When continuing the load fragments break out of the surface. Fig. 7 right shows this damage on a surface of PMMA.

For cast iron of different structural constitutions (materials as used in practice) the behaviour under cavitation load has been studied.

The run of these curves typical for this kind of damage gives an idea about the macroscopical behavior of the material against cavitation load. Fig. 8 shows the weight loss of cast iron versus test duration. Analysing the weight loss you will notice the important influence of the structural constitution. From the cavitation tests with a duration from 10 to 70 h the following conclusions can be drawn:

1. Influence of graphite
   The resistance of globular cast iron (called GGG) to cavitation load is better than the resistance of lamellar cast iron (called GGL).

2. Influence of matrix
   The resistance of pearlitic cast iron to cavitation load is better than the resistance of ferritic cast iron.

Microscopical and scanning-electron-microscopical studies about the kinetics of cavitation damage on cast iron have been made. Under cavitation load - independent of the matrix - the graphite was broken out first. The result are holes in the surface. The latitude and the number of these holes are of influence on the further rate of damage. In case of ferritic-globular cast iron the matrix will be deformed by imploding cavitation bubbles. The holes are the beginning of the cracks. A damaged specimen of globular cast iron after 40 h of cavitation load, shows Fig. 9. The whole eroded surface is scattered with cracks.

In the case of cast iron with lamellar arranged graphite the resistance to cavitation damage is lower. A cast iron specimen with lamellar graphite after 15 minutes cavitation load is to be seen in Fig. 10. Cracks seem to start from the ends of the lamellas. In a ferritic matrix, these cracks run faster than in a pearlitic one, leading to better resistance of the latter.

Comparing the damages on lamellar cast iron caused by cavitation with those caused by liquid impact there is no important difference in their appearance to be found, Fig. 11.

It is suggested that in both cases the kind of the load is the same. There are also results about the special behaviour of cavitation bubbles during implosion available (4). Imploding, the bubble forms a small liquid jet which may be the source of the damage. It is very difficult to obtain damages by a single cavitation bubble without interaction of others. Because of these difficulties we tried to obtain the same results by direct liquid impact. Therefore we have built an apparatus, known from publications (5), for producing such liquid jets. The main part of the apparatus is a cylindrical chamber of stainless steel containing the test liquid. After filling, one end of the chamber is sealed by a Polyamid disk. On the opposite side there is an orifice corresponding to the diameter of the jet to be formed. A slug fired from a gun impacts the disk. What follows is that the liquid will be extruded and accelerated as a jet up to velocities of 1000 m/s. The silhouette of this apparatus and the moving jet is to be seen in Fig. 12. Analysing the velocity of the jet and ~~that of~~ the velocity of the spraying water after the impact, you will find that the spraying water moves much faster than the jet.

Two materials with very different mechanical properties were chosen for testing

1. plexiglas (PMMA) as a material without ductility,
2. Aluminum of high purity representing ductile materials.

Fig. 13/1 shows part of a damaged surface of PMMA after liquid impact. The centre of the impact is on the left, on the right there are annullar cracks surrounding the undamaged centre. The impact velocity amounts to 600 m/s, the diametre of the water jet to 3 mm. A topogram (Fig. 13/2) of this part of the surface shows that the cracks, mentioned above, form steps. The vertical surface of each step faces the centre of the impact. To point out the causes of this damage we made further investigations. It could be proved that this kind of damage is only caused by the impact. It corresponds with damages by the implosion of a single cavitation bubble (see Fig. 3). On aluminum of high ductility the damage caused by liquid impact is shown in Fig. 14. In this case there are radially symmetric waves of plastic deformation surrounding a more or less undamaged centre, see also (6). In Fig. 15 part of a damage caused by liquid impact, especially the plastic deformation waves, is to seen by scanning electron microscope. With growing distance from the centre the waves die away.

In contrast to PMMA, the spraying water seems to cause an additional damage in aluminum.

It should be mentioned that the structure of the material (crystalline orientation, grain boundaries etc.) is without influence on the plastic deformation waves.

Comparing a damage caused by one imploding cavitation bubble with one caused by liquid impact, one finds that both kinds of loading will lead to the same change in the appearence of the surface. The following conclusion can be drawn:

erosive cavitation load has the same hydromechanic active component as liquid jet attack.

Finally we want to set up some conditions for material of high resistance to erosive cavitation load resulting from the investigations made in our institute:

1. High flow stress, also at quasi-static high-frequency load,
2. great capacity of strengthening,
3. high rate of elongation without contraction,
4. high fatigue strength, not only of homogeneous but also of heterogenous structures.

Under the current circumstances you can only sketch the way of the systematic investigations made during the last years. With regard to the multiform problems of flow cavitation, cavitation damage and material behaviour, it is easy to recognize that detailed investigations is necessary to gain valuable and secure results.

Valuable and secure results, however, can only be obtained by making use of all modern method of the material science.

The investigations about flow cavitation are sponsored by the German Research Association.

References

1. H. SCHRÖTER; Z. VDI 77 (1933).

2. J. M. MOUSSON; Trans. of ASME 59 (1937)

3. P. Ch. BORBE; Dr. Thesis, Technische Universität Hannover, 1968.

4. A. T. ELLIS; Calif. Inst. of Techn. Hydrodyn. Lab. Rep. 21 - 12, 1952

5. F. P. BOWDEN, F. R. S. and J. H. BR UNTON; Proc. Roy. Soc. Vol 262 (1961), Serie A

6. F. ERDMANN-JESNITZER and R. LASCHIMKE; Archiv für das Eisenhüttenwesen 37 (1966)

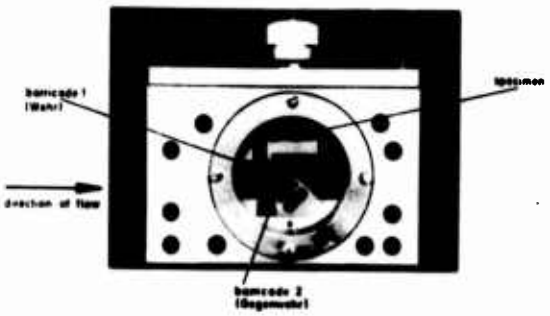


Fig. 1: Cavitation chamber for erosive cavitation damage



Fig. 2: Initial damage caused by one cavitation bubble only



Fig. 3: Initial cavitation damage on PMMA

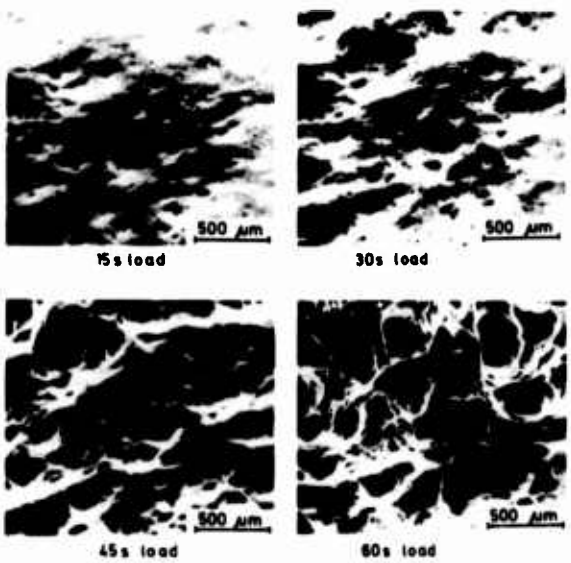


Fig. 4: Cavitation damages after different loading times (Scanning electron microscope)

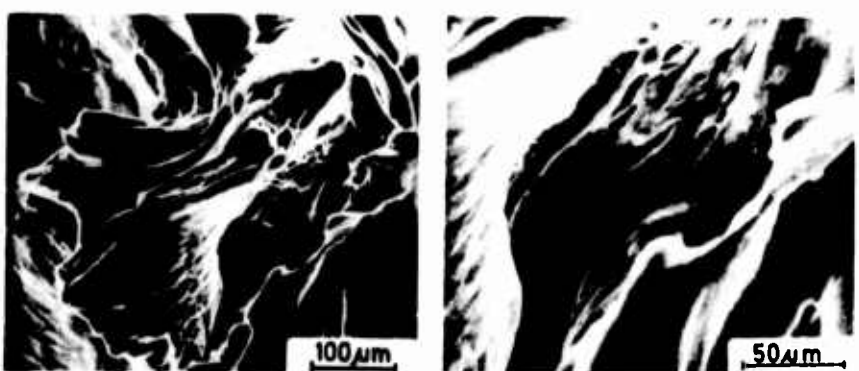


Fig. 5: Plastic deformation and cracks on a cavitated aluminum specimen



Fig. 6: Crack on an aluminum specimen, 60 s cavitated

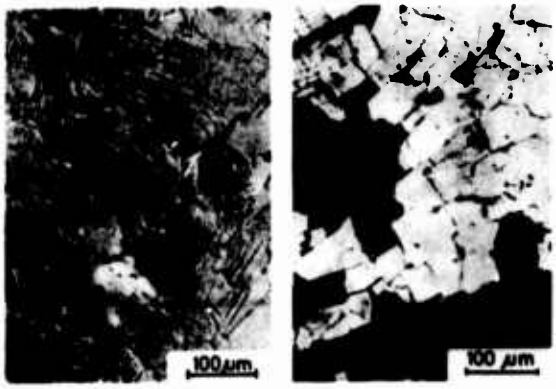


Fig. 7: PMMA specimen at different stages of cavitation damage

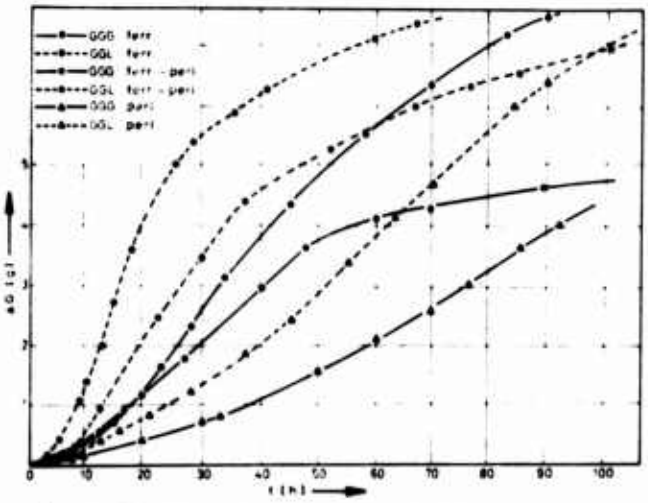


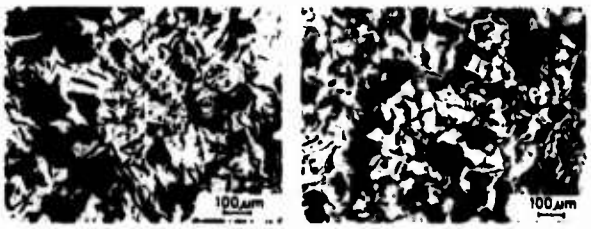
Fig. 8: Cavitation damage on cast iron (influence of structural constitution)



Fig. 9: Cavitation damages on globular cast iron (SEM)



Fig. 10: Cavitation damages on lamellar cast iron (SEM)



impingement of liquid cavitation
Fig. 11: Cavitation and impingement attack on lamellar cast iron

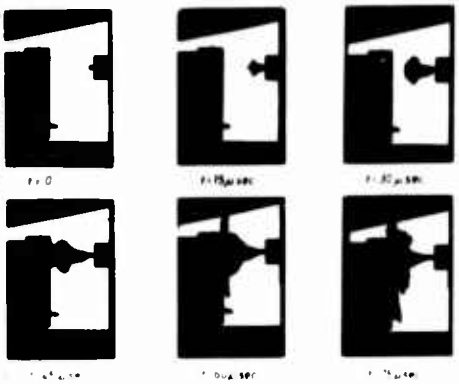


Fig. 12: Water jet of high velocity moving from a cylindrical chamber (right) to a specimen (left)



Fig. 13: Damage on PMMA after liquid impact
1 - Part of the damaged surface 2 - Surface topogram

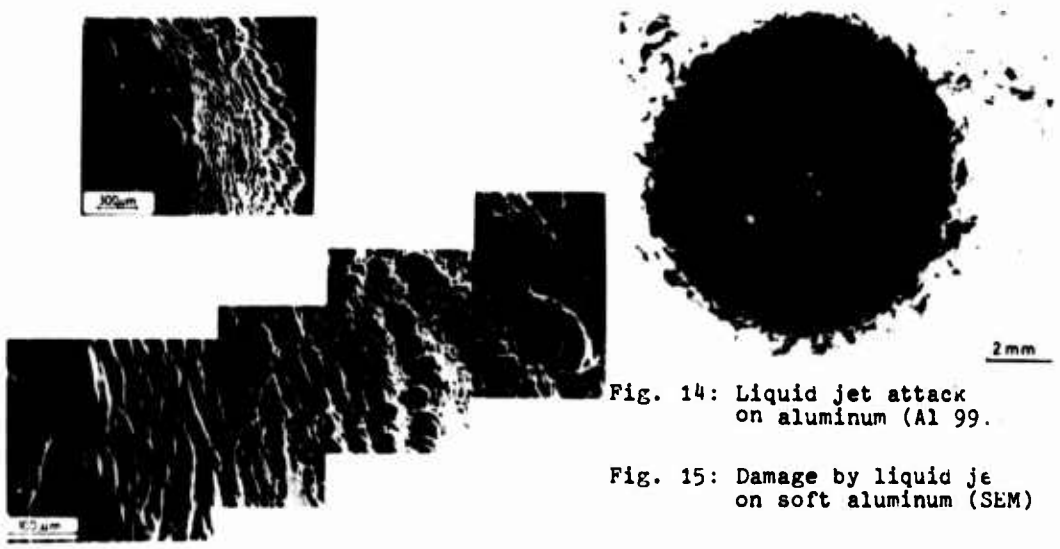


Fig. 14: Liquid jet attack on aluminum (Al 99.

Fig. 15: Damage by liquid je on soft aluminum (SEM)

NATIONAL BUREAU OF STANDARDS SPECIAL PUBLICATION , Proceedings of the 3rd International Congress on Marine Corrosion and Fouling, Held October 2-6, 1972, Gaithersburg, Maryland (Issued).

Short Time Testing of Cavitation Resistance by Liquid Impact

E.-F. Beutin, F. Erdmann-Jesnitzer and H. Louis

Institut (B) für Werkstoffkunde
Technische Universität Hannover
Appelstraße 24 A, 3000 Hannover
Federal German Republic

Nowadays it is generally maintained that the kinetics of destruction of cavitation are similar to those of liquid impact. This is proved by macroscopic as well microscopic forms of initial damage. However, even in advanced stages of damage similarities are to be noticed. These facts can be demonstrated by comparing pictures taken by the scanning electron microscope (SEM) on specimens loaded by cavitation and by liquid impact at different stages of destruction.

As the elementary process of the erosive part of cavitation is the impact of liquid we make use of the conventional liquid impact apparatus to investigate cavitation resistance. This method produces results in very short time.

Weightloss versus time curves on pure aluminum and on pearlitic lamellar cast iron demonstrate this effect as well as microscopic studies of specimen at different stages of damage. As the roughness of the surface of the specimen increases with test duration, one cannot examine the surface under the conventional light microscope. Therefore the scanning electron microscope has proved a very helpful apparatus.

Key words: test equiment for liquid impact, water gun, initial damage, single impact, scanning electron microscope.

In the beginnings, investigations of hydraulic material damage were characterized by the similarity of the macroscopic form of material destruction caused by cavitation and caused by liquid impact. So it was supposed that the same mechanism of attack was the cause for both forms of damage. Further investigations of material destruction by flow cavitation showed an interaction of the mechanical (cavitation-erosion) and

the corrosive (cavitation-corrosion) load (1) [1]. Therefore a common mechanism of attack for flow cavitation and liquid impact was again called into question (2).

In the following time the initial processes of material damage became more and more important (3). By intermittent experiments with test durations shorter than one second we obtained a rather exact picture of surface changes caused by imploding bubbles (4). Using liquid impact we could demonstrate that the initial processes of material destruction were caused by one single impact (5). These experiments showed the identity of material destruction in the microscopic range: the erosive part of cavitation caused by imploding bubbles, and the liquid impact caused by the impact of a spherical or cylindrical liquid volume, on a plane surface (6).

Great effort is needed to generate single bubbles for the damaging of material. Therefore the partial accordance of both of the most important hydraulic material damages - cavitation and liquid impact - led to the simulation of the initial processes of destruction in cavitation through a single liquid impact.

Test equipment for discontinuous liquid impact

In discontinuous working equipment a liquid volume can be accelerated to strike with nigh velocity a specimen surface (7). In this case the kinetic energy of an air-gun accelerates the liquid. To accelerate larger volumes or to reach higher velocities one can use small guns or even 90-mm cannons (8). But also gases or liquids under high pressure serve as a source of energy for high-speed liquid jets.

Another method consists in the acceleration of specimen to strike against a liquid volume hanging on plastic fibres (9), for example, or in shooting through a rain field a specimen fasted to the top of a rocket (10). Both of these test methods need very high financial and apparative effort.

The conventional liquid impact apparatus allows the investigation of the effects of many single impacts as well as the study of the effects of one single impact. By the latter method we obtained significant results with soft lead and soft copper. From these Laschimke deduced the theory of hydromechanical damage by liquid impact (2). He described a test equipment for one single impact with a long rotating arm.

Test equipments for continuous liquid impact

These include test equipment generally used in the field of "jet cutting". One differentiates between a) the common high pressure equipment working with hydraulic pressure intensifiers, b) pneumatic working apparatus not reaching high pressures like that of a), and c) direct working test equipment with maximum pressures lower than those of a) and b).

---

1 - Figures in parentheses indicate references at the end of this paper

Our test equipment

For the investigation of the effects of single impacts on material we have built a water-gun as known from literature. A bullet fired from a small-bore gun (0.22 inch), see fig. 1, left, accelerates a liquid volume in a cylindrical chamber (fig. 1, middle) with a small bore hole, from where the high-speed jet finds its way to the specimen (fig. 1, right). Fig. 2 shows the result of such a jet on soft pure aluminum. The radially symmetric plastic deformation waves are clearly to be seen. These deformation waves are similar to those caused by the implosion of one single cavitation bubble of high energy near a solid surface (4). They differ only in size: while in the case of a single liquid impact the damage has a diameter of some millimeters, depending of the test conditions, in the case of cavitation the damage measures only some percents of a millimeter. To observe the effects of many single liquid impacts we make use of conventional apparatuses (11). See the scheme in fig. 3. We varied this scheme to investigate the effects of one single impact as well as the effects of liquids atomized in a nozzle. Another liquid impact apparatus allows to vary the liquid temperature, the rotating velocity, the gas content of the liquid, the nozzle diameter, and the pressure of the liquid. The test equipment for continuous high-speed liquid jets works directly, i.e. the test liquid, generally tap water, runs from the pump through a metal-lined hose directly to the nozzle. The nozzle is installed in a pistol with closing device, so that it is not necessary to stop the whole apparatus for short-time interruptions. To vary the distance between nozzle and specimen, the pistol can be moved on a rail. The pistol with the closing device in a protection box is shown on the left in fig. 4. On the right you see the water inlet with the pressure gauge. The complete test equipment is enclosed of a protection cover to avoid accidents.

Test results

When a continuous high-speed water jet strikes a plane metal surface there are contradictory phenomena to observe. When the distance between the nozzle and the sample is very short, there is no damage on a smooth aluminum sample. With increasing distance the surface becomes more and more roughened. In a certain distance this roughness increases rapidly which is characteristic for the actual test conditions. This process can often lead to the complete separation of the sample.

The ineffectiveness of a high-speed jet on a plane aluminum surface at short distances seems not cogent because the energy content of the jet is relatively high. Although the energy decreases with the distance from the nozzle, high-speed jets at longer distances show larger effects, even the separation of the sample. This phenomenon we explain as follows: in its periphery the jet scatters into little drops. This scattering begins only in some distance from the nozzle. It is these drops that, we believe, have the destructive power.

The single drop stress the material like a water-hammer. They produce a more or less great roughness depending on the drop diameter. Fig. 5 shows the outer region of a smooth aluminum sample in a high magnification. Craters are clearly to be seen. In a scanning electron microscopic picture one can see the same details in topview (fig. 6). The similarities between the forms of destruction by liquid impact (fig. 6) and those caused by cavitation (fig. 7) are quite evident.

Comparison of cavitation with liquid impact

In addition to the macroscopic similarities of material destruction caused by cavitation and that caused by liquid impact, the microscopic identity of the shape of damage is given, too (3, 4, 5). The test results of liquid impact and cavitation are similar, too, as shown in the following figures. Fig. 8 demonstrates the weightloss versus time curves for pure smooth aluminum loaded by liquid impact (curve A) and loaded by cavitation (curve B). Both curves develop similarly, but curve A shows the higher intensity of destruction expressed by the weightloss. Fig. 9 demonstrates these relations on pearlitic lamellar cast iron. Curve A reflects the destruction by liquid impact, curve B that by cavitation.

These last figures clearly show the advantage of the use of liquid impact over that of cavitation in experiments for cavitation resistance. The advantage lies in a gain of time, i. e. you obtain the same results in a much shorter time with liquid impact than with cavitation.

References

1. Borbe, P.C., Ph. D. Thesis, Hannover 1968
2. Laschimke, R., Ph. D. Thesis, Hannover 1965
3. Erdmann-Jesnitzer, F. and R. Laschimke, Archiv für das Eisenhüttenwesen 37, 1966
4. Erdmann-Jesnitzer, F. and H. Louis, 1. Cong. Nac. d. Corr. y Prot., Madrid 1972
5. Brunton, J.H., Proc. Roy. Soc. London, Ser. A, vol. 260, 1966, London
6. Hammitt, F., Univ. of Michg., Rep. No. 01357-2-I 1969
7. Bowden, F.P. and J.H. Brunton, Proc. Roy. Soc. London, Ser. A, vol. 263, 1961, London
8. Summers, D.A. and R.L. Henry, 1. Int. Symp. Jet Cut. Techn., Coventry, 1972
9. Fyall, A.A., 2. Conf. Rain Erosion, Meersburg, 1967
10. Schmidt, G.F., 2. Conf. Rain Erosion, Meersburg, 1967
11. v. Schwarz, M. and W. Mantel, Z. VDI, Vol. 80, No. 28, 1936

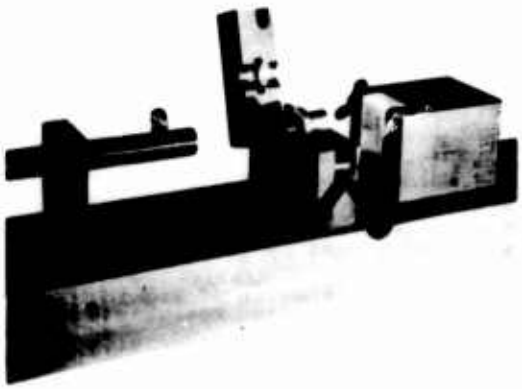


Fig. 1: Test apparatus for high speed liquid jet



Fig. 2: Plastic deformation waves on aluminum

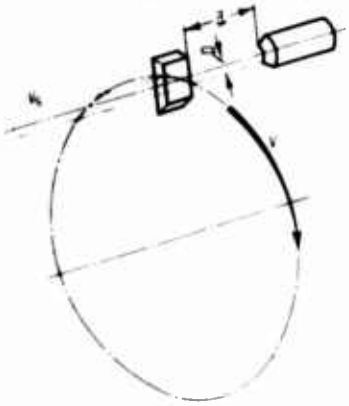


Fig. 3: Scheme of the liquid impact apparatus, v-velocity of the specimen, v_s-velocity of water, D-diameter of nozzle, d-distance specimen - nozzle



Fig. 4: Pistol for continuous water jets

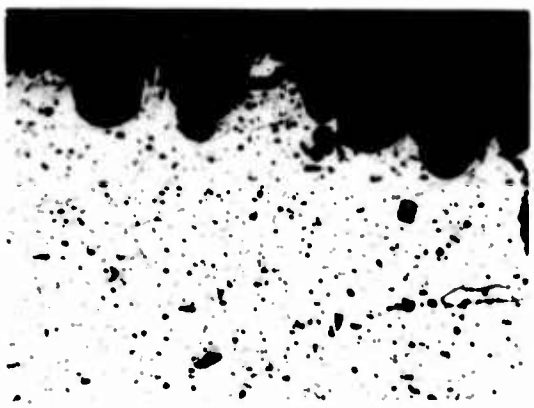


Fig. 5: Aluminium specimen loaded by high speed water drops

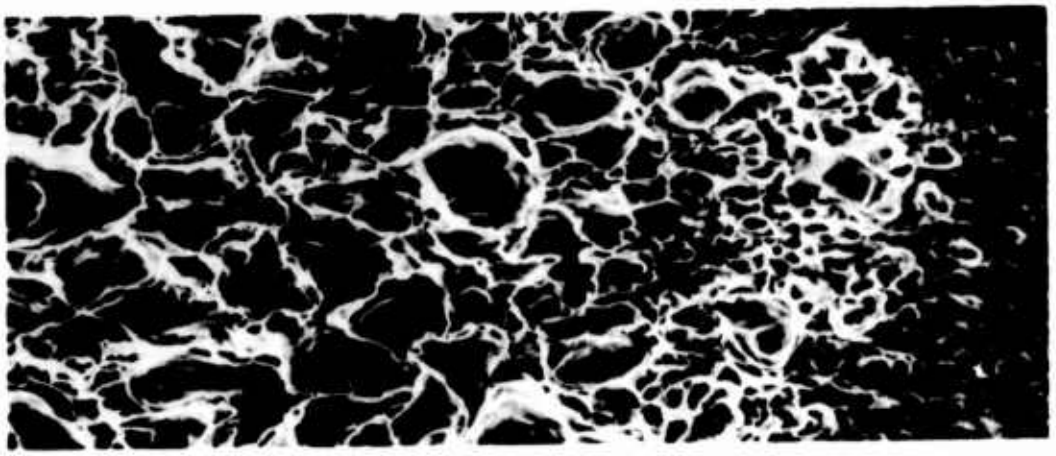
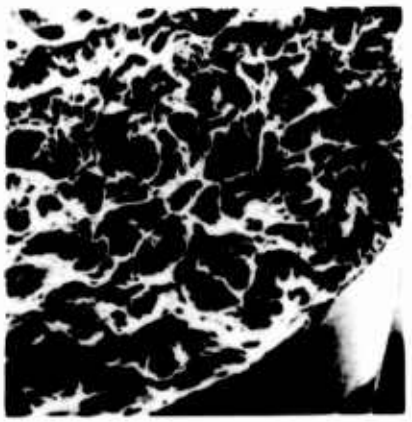


Fig. 6: Aluminum specimen loaded by liquid impact (SEM)

Fig. 7: Aluminum specimen loaded by cavitation (SEM)



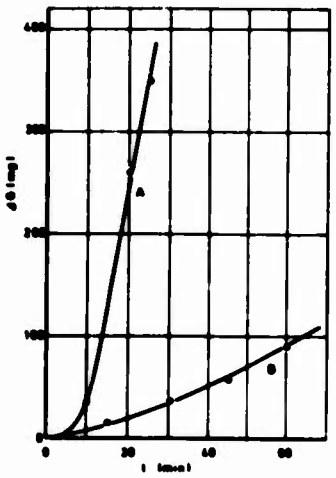


Fig. 8: Weightloss versus time for liquid impact (curve A) and for cavitation (curve B) on pure aluminum

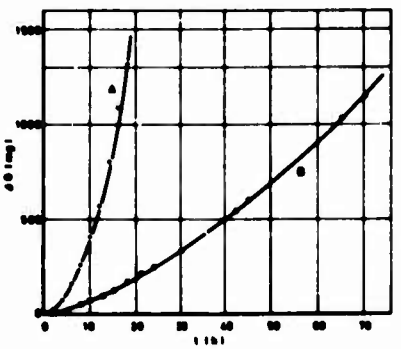


Fig. 9: Weightloss versus time for liquid impact (curve A) and for cavitation (curve B) on pearlitic lamelar cast iron

New testing chamber for cavitation erosion

F. Erdmann-Jesnitzer and H. Louis

Institut (B) für Werkstoffkunde
Technische Universität Hannover
Appelstraße 24 A, 3000 Hannover
Federal German Republic

Cavitation damages, known since the end of the last century, are simulated in several types of test devices. All of these are characterized by the generation of vapour bubbles resulting from changing channel dimensions and the imploding of these bubbles with increasing pressure. The implosion of cavitation bubbles near a surface of a workpiece may lead to damage. The testing devices are classified into 3 types. The different types are characterized. Examinations for the design of a new testing chamber for flow cavitation damages are discussed.

Different geometrical and hydromechanical parameters leading to a high rate of erosive damage are mentioned. The influence of one of these parameters, the distance between the two barricades called "Wenr" and "Gegenwenr", is shown.

Examination to define the inception line of the bubbles at the barricades were not successful. A method to obtain reproducable amount of damage is given. The chosen cylindrical barricades can be reproduced. The influence of their roughness to the rate of damage is shown.

The new testing chamber and the whole test equipment is described.

The weightloss, of Armco-iron specimens for example, gives an idea of the high intensity of damage, in which the cavitation erosion plays the dominant part.

Key words:

classification, testing chamber, flow cavitation, cavitation-erosion, cavitation-corrosion, geometrical and hydromechanical variations, definite bubbles generation, weightloss of different materials, test device.

Since the end of the last century damages in hydraulic machinery caused by imploding cavitation bubbles are known.

Their simulation in special apparatus is achieved since the early thirties. Apparatusses for flow cavitation are characterized by the generation and implosion of bubbles. The generation of bubbles is caused by decreasing the static pressure as a result of changing channel dimensions. When the pressure increases, they will implode. These implosions on the surface of a workpiece cause the cavitation damages. In general there are three sorts of them. Between these ones there are no exact borders, but nevertheless it is usefull to order the numerous testing apparatus into the following three types.

Type 1: konvergent - divergent double nozzle
Type 2: chamber with barricades, called "Wehr" and "Gegenwehr"
Type 3: chamber with obstacle

Fig. 1 shows a scheme of the three different types of channels for investigations in flow cavitation.

Type 1, konvergent-divergent double nozzle

Type 1 is characterized by a typical profile which leads to the generation of bubbles and to their implosion always close to the wall of the chamber.

The intensity of the damage on a specimen fixed in the wall depends on several geometrical and hydromechanical parameters. In general, the reserve pressure is a very important factor.

The test section may be a rectangular double nozzle (1, 2) [1] or a circular nozzle and diffusor, separated by a cylindrical throat (3).

Type 2, chamber with barricades

Type 2 is an improvement of type 1 to increase the damage intensity in order to shorten test duration. This type is characterized by barricades called "Wehr" and "Gegenwehr". The purpose of these barricades is to incept the generation of bubbles and to direct them on to the surface of the workpiece. In general, the barricades in form of special profiles are put into rectangular channel. The surface of the specimen to be tested in the testing chamber may be parallel (4) or in a right angle to the inceptionline of the bubbles at the barricades (5, 6). Chambers of this type were mainly used in the thirties and forties, but are still in use today (7).

Type 3, chamber with obstacle

Starting point for this type were flow channels in which obstacles and profiles were tested in their cavitation characteristics. These

1 - Figures in parentheses indicate the references at the end of this paper

channels can also be used for testing materials. The flow cavitation may cause damages at the obstacle or at the wall in which the specimen is fixed. This last type is mainly used today (8, 9).

In the following, experimental techniques at the Institut (B) für Werkstoffkunde, Technische Universität Hannover, to investigate flow cavitation damages will be described.

In all of these tests the mechanical erosion caused by imploding bubbles is the dominant factor of cavitation damage. The erosive effect of the imploding bubbles leads in the case of soft materials, e.g., to a deformation of the surface of the specimen and is indicated by the resulting changes of the mechanical and physical properties of a certain material.

The corrosive part of the damage is without influence on the kinetics of destruction.

Primarily, the imploding bubbles close to the surface of the specimen are responsible for the destruction of material. Therefore these cavitation bubbles are the principal object for increasing the intensity of the damage, especially in our apparatus for testing cavitation damage.

A maximum destruction can only be obtained when the following three conditions are satisfied:

1. A great number of cavitation bubbles has to be produced.
2. Nearly all the bubbles must implode very close to the surface.
3. The cavitation bubbles must implode with high energy.

We studied all testing chambers for flow cavitation in literature under the aspect of these conditions. For our first tests we chose four different chambers. On the results obtained we based the design of a new chamber, which showed a very high intensity of erosive damage. The results of these tests proved easy to reproduce.

Fig. 2 shows a diagram sketch of our chamber with all geometrical and hydrodynamical variations.

The chamber (type 2) is a rectangular channel. The bubbles are caused by the decreasing pressure of the fluid as a result of two cylindrical barricades, called "Wehr" and "Gegenwehr".

The following parameters can be varied:

1. inlet pressure p_1, i.e. the maximum velocity in the throat.
2. reverse pressure p_2, concerning the lifespan and therefore the energy of the bubble.
3. the distances s between the barricades which form the throat of the channel.
4. the position h of the specimen which determines the mean distance from the line of generation of the bubbles to the place of implosion at a specimen surface.

5. the deflection angle α of the water - bubble stream.

Placing the surface of the specimen parallel to the inception line of the bubbles guarantees a maximum damage.

The influence of the geometrical and the hydromechanical parameters on the intensity of damage was proved. In general, the intensity of damage will be expressed by the weightloss of a specimen versus testing time.

The influence of the throat of the channel, i.e. the distance s between the barricades and their geometry will be briefly discussed.

Great differences in the weightloss led to further tests in which bubbles were to be generated at a definite inception line. Therefore we fixed at the barricade in the area of the decreasing profile a razorblade. The edge of the blade reached into the channel to determine the inception line of the bubbles. With regard to a high-rate damage, these experiments were without success. We tried to use hardened and ground needles of different diameters to receive a definite inception line. These tests were also negative when the bubbles are generated at a definite line on the barricades boundary layer is disturbed in this region. As a result there is only a small amount of weightloss. Besides, the lifespan of the needles was less than 50 h. The load resulting from the generation of the bubbles led to a corrosion attack. Fig. 3 shows these typical damages after 100 h testing time.

As a result of these experiments we chose cylindrical barricades. The macroscopic size of these barricades, i.e. their diameter has no significant influence on the weightloss, so that their dimensions were mainly determined on grounds of construction.

However, the microscopic geometry, i.e. the roughness of the surfaces, is of major importance. Fig. 4 shows the weightloss versus testing time of aluminum specimens in tests with different barricades.

The roughness of the barricades reaches from 0.5 μm up to 8 μm, those of the tested specimens shall not be discussed at this point. With increasing roughness the weightloss decreases. Roughness of more than 10 μm leads to no damage of the specimen in a convenient testing time. This may be, in some cases, of some importance in the development of hydraulic machinery.

To obtain a high rate of damage in the testing chamber, we chose cylindrical barricades with a surface roughness less than 2 μm.

The barricades were hard-chromium plated and polished. The lifespan of the cylindrical barricades was 3 - 5 months; they are easy to reproduce.

At the two barricades, two streams of bubbles are produced. If the distance between them is great enough, they are separated by a zone of water free of bubbles.

Fig. 5 shows schematically the way of the stream in the chamber.

The streams of bubbles which are generated at the barricades are numbered 1 and 3. The zone of water separating them is numbered 2. The main damage of the specimen 4 is caused by the bubble stream 1. The stream 3 only causes traces, but no measurable weightloss.

That means the optimal condi tion can be produced at one stream only.

In the preliminary tests, the barricades were placed at such a distance that the bubble streams were parted by a water stream. This was necessary to get a high rate of damage.

Fig. 6 shows the weightloss versus time of Armco-iron specimens. The test parameter is the distance of the barricades. An increasing distance leads to an increasing weightloss. Distances shorter than 1 mm, show no measurable weightloss during the first 100 h of the test. With increasing distance, the influence decreased.

Fig. 6 gives an idea of the high rate of damage of the new cavitation chamber and the important influence of this parameter. Only a particular combination of all the parameters brings about a maximum of damage.

Some of the new chambers, shown in Fig. 7 are in use at different laboratories.

The new chamber for erosive flow cavitation damage is the main part of the cavitation apparatus, as shown in Fig. 8.

A multistage centrifugal pump sucks the test fluid, generally tap water which has been partially degassed by its circulation, from a container lined with plastic material. The pump presses the water into the test chamber.

The inlet pressure can be regulated by means of a slide valve. The reverse pressure within the area of the imploding bubbles can be regulated by the slide valve behind the test chamber. The water then returns to the container via a by-pass. To maintain temperatures of 15 - 60°C, there are both a heating and cooling device.

To prove that the cavitation-erosion is the main part of the damage in this chamber, comparative studies to chambers of low damage intensity were made.

Fig. 9 shows the results of tests with these chamber. The test material was Armco-iron.

Curve 5 describes the weightloss of a specimen in our new chamber, temperature of liquid 20°C. Curves 1 and 3 show the results in a chamber of low damage intensity at 55 and 20°C. In this case, the main part of damage is cavitation-corrosion. This can be avoided by cathodic protection, which results in a decrease of weightloss, see curves 2 and 4.

Curve 1, in comparison with curve 5, gives an idea of the high-damage intensity of our new chamber in which cavitation-erosion is the dominant part of damage.

References

1. Schröter, H.; Z. VDI 76 (1932)

2. Karpoff, K.P.; U.S. Department of the Interior Bureau of Reclamation, Denver, Colorado, Laboratory Report Nr. C-1070, 1963

3. Hammitt, F.G. and W.J. Walsh; University of Michigan, Internal Report Nr. 8, 1961

4. Schröter, H.; Z. VDI 78 (1934)

5. Mousson, J.M.; Hydraulics, Transactions of the American Society of Engineers 59 (1937)

6. Rata, M.; Symposium de Nice 1960

7. Borbe, P.C.; Ph.D. Thesis, Hannover 1968

8. Varga, J. and G. Sebestyén; Periodica Polytechnica, Engineering Vol. 8 (1964)

9. Govinda Rao, N.S. and A. Thiruvengadam; Journal of the Hydraulic Division 5 (1961)

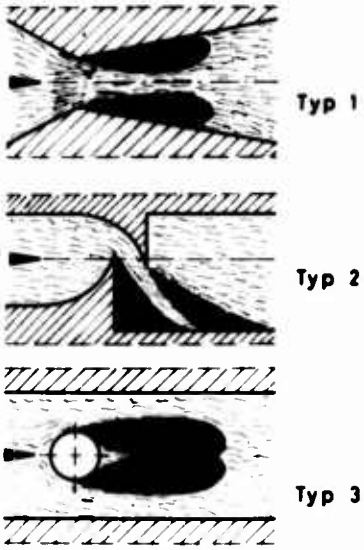


Fig. 1: Different types of chambers for testing material resistance against flow cavitation

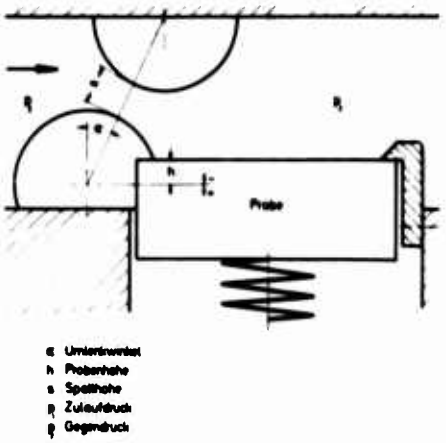


Fig. 2: New chamber for testing flow cavitation damage, (schematically), with geometrical and hydromechanical variations

Fig. 3: Corrosion attack at inception line of bubbles (direction of flow from bottom to top)



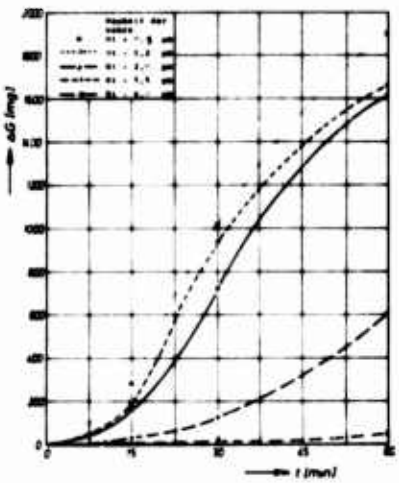


Fig. 4: Weightloss versus testing time, parameter: roughness of barricades

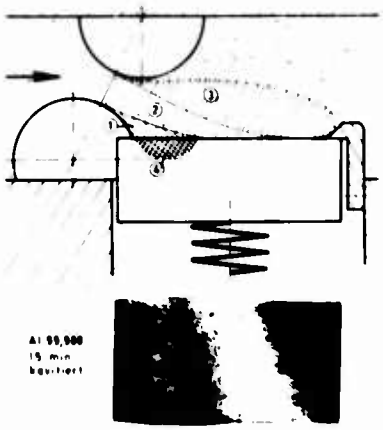


Fig. 5: Way of flow in the testing chamber, (schematically)

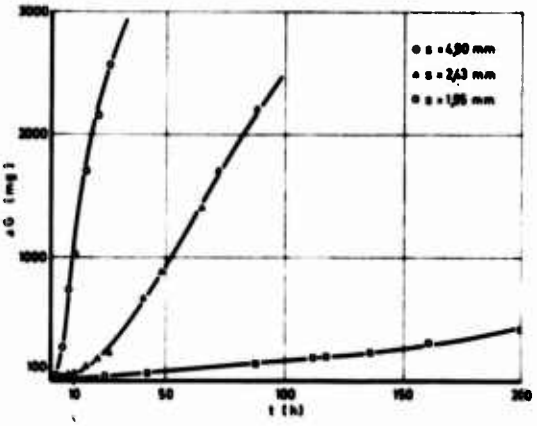


Fig. 6: Weightloss versus testing time, parameter: distance s between barricades

Fig. 7: Cross-section of the new chamber

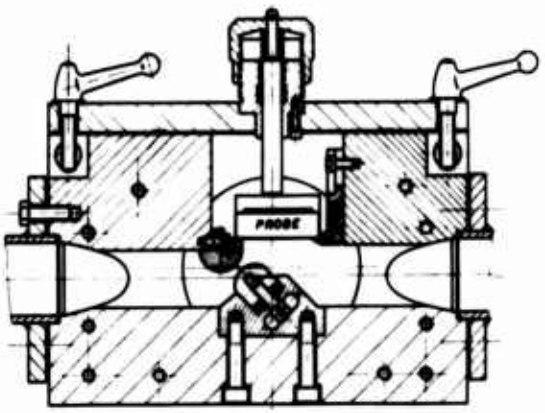
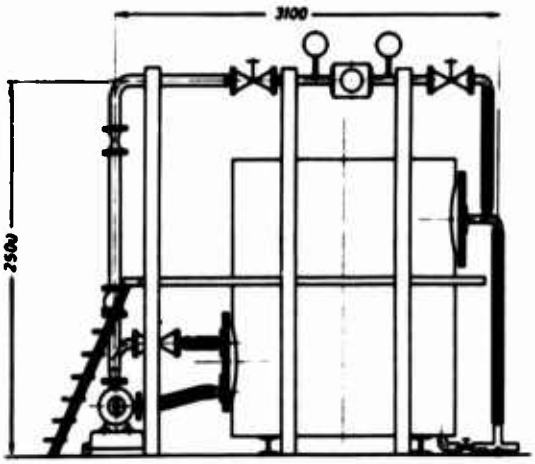


Fig. 8: Test device for flow cavitation (schematically)



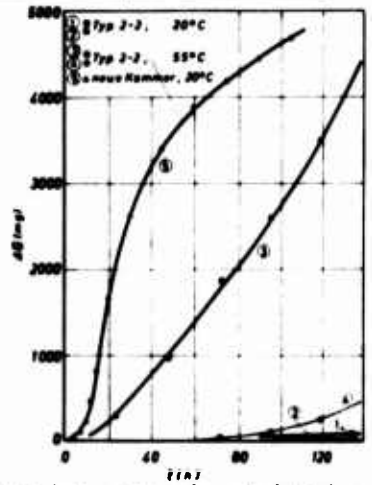


Fig. 9: Comparative tests in cavitation chambers of different damage intensities

Corrosion- and Creep- Induced Instability-Modeling of Fatigue-Cracking in Various Alloys

J. M. Krafft, C. L. Lamb and K. E. Simmonds

Code 8430, Naval Research Laboratory
Washington, D. C. 20390

With concurrence of the Program Chairman, this paper has been dedicated to celebrate the eightieth birthday of Professor Karl F. Herzfeld, February 26, 1972

Crack propagation, the terminal phase of many mechanical-strength failures, is often accelerated by environmental corrosion effects. Data to fully characterize such effects is costly to obtain. Accurate predictive models are needed to provide this from economically limited data collections. In this modeling attempt, stable subcritical crack growth is taken as a means of maintaining a state of plastic flow stability at the crack tip. The condition of discretely sized crack tip micro-ligaments (d_T) are assumed to control; they are strained by the loading of the crack; when the loading ceases their stability is upset by creep induced stress relaxation and/or by environmental surface corrosion; it is restored to equilibrium by an increment of extra straining, which requires an increment of crack growth. The amount of straining required, and thus the crack growth, is estimated from ordinary stress strain curves and transient creep measurements on smooth tensile specimens. Stress corrosion and fatigue crack propagation data on some dozen alloys, from the literature, is examined with respect to uniaxial and cyclic flow properties measured for each. The correlations are encouraging and suggest that a one parameter (V_S) characterization of environmental effects in subcritical cracking is indeed feasible.

Key Words: Fatigue crack propagation; corrosion fatigue; stress corrosion cracking; threshold, fatigue; threshold stress corrosion cracking; low cycle fatigue; plastic instability model.

1. Introduction

In traditional engineering methods, fatigue is treated in terms of the S-N diagram; stress corrosion in terms of the failure time to stressed smooth specimens. A difficulty here is that no useful distinction can be made between cycles or time to initiate a crack, and that for propagation to terminal failure. Experience with smooth specimens usually shows the propagation portion to be relatively short, thus hardly worth discriminating. Yet increasingly it is found that the failure life in realistically constructed engineering structures is largely propagation time. For example, in cyclic flexing of typically welded bridge girders, Fisher et al (1) find that most of the life is expended in fatigue crack

[1] Figures in parentheses indicate the literature references at the end of this paper.

propagation; a nil portion in initiation. The reason appears to be that the stress intensity threshold for fatigue propagation is, after Paris and Bucci (2), so low that undetectably small crack-like flaws can initiate growth. The thresholds are further reduced by elevated mean stress, the ordinary condition of welded structures. Once a crack has grown to a larger size, greater than that for the threshold of stress corrosion cracking, Meyn (3) has shown that corrosion effects can greatly accelerate its "progress".

However well we know these generalities, acquiring data on specific material, loading spectrum and spatial environment combinations is costly and time consuming. Progress could be served by accurate predictive models which permit scant, thus economical data collections to be extrapolated. This paper represents an attempt to establish such a model. It follows an idea proposed by Landes and Wei (4) that creep induced flow can induce tensile instability at a crack tip, and thus crack growth. It expands a subsequent attempt (5) to apply this concept to transient creep in cyclic loading.

2. Creep-corrosion induced instability

Before considering how creep and corrosion can induce tensile instability, it is well to recall how ordinary tensile extension brings it about. An instability may occur at the point in tensile loading at which no further increase in load P is required to continue the deformation; it is the maximum load point, or ultimate tensile strength, or "necking" strain, of the familiar tensile test. If we normalize this load over the supporting sectional area A

$$P = \bar{\sigma} A \tag{1}$$

where $\bar{\sigma}$ is true stress, a function of strain ϵ, then

$$\frac{dP}{d\epsilon} = \bar{\sigma} \frac{dA}{d\epsilon} + A\frac{d\bar{\sigma}}{d\epsilon} \tag{2}$$

The ratio of the areal strain differential dA/A to that of longitudinal strain $d\ell/\ell (= d\epsilon)$ is proportional to Poisson's ratio ν, $dA/d\epsilon = -2\nu A$. Designating the true strain hardening rate as $\bar{\theta}$, the condition for tensile instability, $dP/d\epsilon = 0$, becomes

$$\frac{\bar{\theta}}{\bar{\sigma}} = 2\nu = 1 \tag{3A}$$

for incompressible plastic flow where $\nu = 0.5$. Williams and Turner (6), and Clausing (7) have argued that the instability of material close to a crack tip will be influenced by the locally triaxial stress state. The way of estimating this effect from simple tensile data as proposed by Sachs and Lubahn (8,9) is employed here, where for the maximum effect of triaxiality, the instability is suppressed until the true strain hardening rate $\bar{\theta}$ has decreased to the point where

$$\frac{\bar{\theta}}{\bar{\sigma}} = 1/2 \tag{3B}$$

This means that the strain for fully triaxial instability is larger than that for uniaxial tension of eq. 3A, for which $\bar{\theta}/\bar{\sigma} = 1$.

Since tensile stress-strain curves are experimentally obtained, it is convenient to express the instability condition in terms of tensile measurements. Specifically if $\bar{\sigma}_T = \bar{\sigma}(1-\epsilon_T)$ where $\sigma_T = P/A_o$ is tensile stress and $\epsilon_T = -\Delta A/A_o = \Delta\ell/\ell_o$ is tensile strain, then differentiating σ_T with respect to ϵ_T and letting $\bar{\theta}/\bar{\sigma} = 1$, the uniaxial instability condition corresponding to eq. (3A) becomes

$$\frac{\theta_T}{\sigma_T} - \epsilon_T = 0 \tag{4A}$$

The triaxial instability limit corresponding to eq. 3B becomes

$$\frac{\theta_T}{\sigma_T} - \epsilon_T = -\frac{1}{2} \tag{4B}$$

In calculations for ordinary alloys, ϵ_T below the tensile instability strain is practically negligible compared to θ_T/σ_T, and thus has been neglected so that the instability condition can be summarized,

$$\frac{\bar{\theta}_T}{\sigma_T} + \mathbb{Z} = 0; \qquad \begin{matrix} \mathbb{Z} = 0 \text{ uniaxial} \\ \mathbb{Z} = 1/2 \text{ triaxial} \end{matrix} \tag{4}$$

On the simple tensile curve, the triaxiality effect delays the instability until the slope is decreasing with strain at a rate of $-\sigma_T/2$. In materials exhibiting a "flat top" tensile stress-strain curve, as in two weldable high strength steels and one mild steel to be discussed, this delay has a substantial effect in forestalling fast fracture instability.

If tensile straining is interrupted short of the point of tensile instability, as at a crack tip cycled to a K_I level less than K_{Ic} (i.e. subcritical), the load carrying capacity of a tensile ligament will tend to decrease due to transient creep relaxation. This occurs in ordinary metals even at room temperature. In addition, if the environment is corrosive, the reduction in cross section by surface attack will have a similar effect. As both effects are time dependent it is necessary to express the instability condition in timewise coordinates, whence eq. 2 becomes

$$-\bar{\sigma}\frac{dA}{dt} = A\frac{d\bar{\sigma}}{dt} \tag{5}$$

In tension, the left-hand term of eq. 5 represents strength loss due to sources of areal diminution; the right, increases due to strain hardening but decreases due to creep. Specifically, the areal diminution due to Poisson contraction is expressed as $A(d\epsilon/dt)$, while that due to a corrosion rate V_S (typical units mils/year, in./sec., microns/sec.) is $\pi d_T V_S$ where d_T is the ligament diameter.

The stress relaxation at constant strain is measured directly in these experiments, rather than converted from a measured strain rate sensitivity, $m = d\ln\sigma/d\ln\dot{\epsilon}$, as in the earlier fatigue modeling attempt (5). The transient creep can be characterized by

$$m = -\frac{d\ln\sigma_T}{d\ln t} = \text{constant} \tag{6}$$

where σ_T is the measured (decay in) tensile stress as a function of time t after sudden arrest of the straining machine. For relatively short hold times of the fatigue cycle, the stress relaxation is

$$\Delta\sigma \simeq m\sigma_T\frac{\Delta t}{\tau} \tag{7}$$

where Δt is the dwell time at peak load and τ is Δt plus the loading time t_1, Figs. 1 and 3.

The rationale for converting between measures of strain rate and creep relaxation sensitivities is repeated here from the earlier paper (5) for completeness, Fig. 1. Consider the time required to traverse a path in stress strain space to a fixed strain ϵ at two different strain rates, arriving there with a stress difference, $\Delta\sigma$, approximated by

$$\Delta\sigma \simeq m\bar{\sigma}\frac{\Delta\dot{\epsilon}}{\dot{\epsilon}} \tag{8}$$

Substituting $\dot{\epsilon}_1 = \epsilon/t_1$, $\dot{\epsilon}_2 = \epsilon/t_2$ and $\Delta\dot{\epsilon} = \dot{\epsilon}_1 - \dot{\epsilon}_2$,

$$\Delta\bar{\sigma} \simeq m\sigma\frac{\epsilon/t_1 - \epsilon/t_2}{\epsilon/t_1}, \tag{9}$$

and

$$\Delta \simeq m\sigma_T\frac{\Delta t}{\tau} \tag{10}$$

where $\Delta t = (t_2 - t_1)$ may be regarded as the dwell time at load relative to the total loading plus dwell time $t_2 = \tau$. For sinusoidal fatigue loading $\Delta t/\tau$ would be roughly 1/3, for a square wave, 1.0, and for typical waveforms, somewhere between these limits.

Substitution now of the aforenoted sources of strengthening and of weakening in

the timewise instability equation (Eq. 5),

$$\bar{\sigma}\left(\frac{\pi}{4} d_T^2 \frac{d\epsilon}{dt} + \pi d_T V_S\right) = \frac{\pi}{4} d_T^2 \left(\bar{\theta} \frac{d\epsilon}{dt} - \frac{m\sigma_T}{\tau}\right) \tag{11}$$

whence

$$\Delta\epsilon = \left(\frac{4V_S\Delta t}{d_T} + m\frac{\Delta t}{\tau}\right)\left(\frac{\theta_T}{\sigma_T} \mathcal{E}\right)^{-1} \tag{12}$$

where the triaxiality factor $m = 0$ for thin sheet, and $m = 1/2$ for thick sections. The instability conditions are expressed in terms of the equilibrating strain increment, $\Delta\epsilon$ of Fig. 1, for its convenient conversion into the crack extension required to cause it, now to be discussed.

3. Crack tip plasticity model

Tensile strain at the crack tip is concentrated by the strain singularity effect. The form of this singularity affects both the magnitude of the strain as well as its gradient in distance. The limits of possible singularly strength, Fig. 2, range from the simple Elastic Analogue (EA) of inverse half power, to the McClintock (10) mode III shear Plastic Analogue (PA) which is of inverse first power of distance into the material r. A tendency toward a stronger singularity, particularly when the plastic zone is large, and the strain hardening rate is low, is indicated from analyses of Swedlow and Williams (11), Rice and Rosengren (12) and Hutchinson and Hilton (13). On the other hand, experimental measurement of Liu (14) and of Kendall and Underwood (15) indicate a persistence of the weaker half-power singularity and present results show little reason to assume otherwise. Tentatively then, present calculations are based on the simple elastic-analogue strain singularity,

$$\epsilon = K_I/E\sqrt{2\pi r} \tag{13A}$$

where K_I is the stress intensity factor ($\sigma\sqrt{\pi a}$), E is Young's modulus of elasticity, and, as noted earlier, r is distance from the crack tip into the unfractured material.

Rather than some average effect of the entire field, it has been found useful to assume a constant strain level within a fixed small region, very close to the crack tip, idealized as row of tiny tensile ligaments of a characteristic diameter d_T. The degree of ligament extension in the first (quarter) cycle of loading is taken then as simply

$$\epsilon_T = K_I/E\sqrt{2\pi d_T} \tag{13B}$$

In subsequent cycles of loading ΔK, some of the K-induced excursion in tensile strain will be lost in the obstruction to crack reclosing, and thus to d_T—ligament full strain reversal, due to the residual crack tip plasticity. A characterization of this effect will be discussed in the next section; suffice it here to define its magnitude as ϵ_R whence

$$\Delta\epsilon_T + \epsilon_R = \Delta K/E\sqrt{2\pi d_T} \tag{13C}$$

The straining of d_T-ligaments resulting from the approach of the crack tip, at constant loading (K_I), is a function of the local strain gradient. In prior attempts to explain constant-K subcritical fracturing (16), this gradient was taken as the non-zero portion of the derivative of the strain singularity

$$\Delta\epsilon = \frac{\epsilon_G}{2d_T}\Delta a \tag{14}$$

or

$$\frac{\Delta a}{\Delta\epsilon} = \frac{2d_T}{\epsilon_G} \tag{14A}$$

where ϵ_G, for "gradient strain", represents the K_I- proportional strain level (from eq. 13B) existing at $r = d_T$. Substituting in eq. 12, the growth rate becomes

$$\frac{\Delta a}{\Delta N} \sim \frac{1}{\epsilon_G}\left(8\, V_S\, \Delta t + 2\, m\, d_T \frac{\Delta t}{\tau}\right)\left(\frac{\theta_T}{\sigma_T} + 3\right)^{-1} \qquad (15)$$

In the attempts to match sets of da/dN vs ΔK data for fatigue crack propagation with the predicted values from eqs. 15 and 13, the inverse effect of the $1/\epsilon_G$ factor appears too strong if ϵ_G is taken equal to ϵ_T. Furthermore, in recent stress corrosion crack velocity data (18) the K-proportional ϵ_G effect also appears too strong. Thirdly, with the effect (5), the fatigue growth rate should decrease with increasing mean stress, or stress ratio R, while the reverse is generally observed (19). All of these inconsistencies disappear if we regard the gradient strain ϵ_G as a constant of a material, indicative of a constant value of the strain gradient in the near field of the crack tip independent of the K_I level. The trend in values of ϵ_G will be seen from the data to be reasonable, though lacking for the present, theoretical justification.

4. Effect of mean stress in fatigue

It is evident from work of Hartman and Schive (20) and of Griffiths, Mogford, and Richards (21) that the overall effect of increased mean stress is an increase in crack growth rate relative ΔK. Recent results of Paris and Bucci (22) have shown this effect to be magnified at very low ΔK levels, where the zero growth ΔK-threshold is markedly increased with R. The R-effect can be associated with the effect of the crack tip unloading blockage. Once a crack is initially tensioned, unloading cannot fully compress the plastically extended near-tip enclave to its original size. The importance of this effect has been argued by Paris (23), and Rice (24) and substantiated by experimental results of Elber (25).

A model for estimating the magnitude of the R effect in view of the instability model is illustrated in Fig. 3. It is common experience that the crack opening displacement of a precracked specimen returns short of its origin upon unloading. For a given material, this COD shortage tends to be a constant value, relatively insensitive to the maximum K level. We would assume, as first approximation, this behavior imaged in the strain at d_T, Fig. 3, leaving a characteristic residual ϵ_{RO}. When the maximum K is increased for the same ΔK (right hand side of Fig. 3) only a part of ϵ_{RO}, proportional to the degree of unloading, is felt, so for given ΔK a larger cyclic strain excursion is experienced in the d_T ligament (lower part of Figure 3). The larger strain excursion results in a decreased terminal value of applicable $\theta_T(\epsilon)$, which via eq. 15, involves a greater crack growth increment Δa. From these considerations, the simple form of ϵ_R for use in Eq. (13C) is

$$\epsilon_R = (1 - R)\epsilon_{RO} \qquad (16)$$

The value of ϵ_{RO} should be larger for softer materials, and likely reflected by the "hysteresis" loop in load vs COD records for initially precracked specimens. In present results it is arbitrarily assigned such value as yields a best fit of the data.

Another empirically justified adjustment in the ϵ(at d_T) to K_I relationship is the effect of triaxial stress upon the yield surface. The onset of stress corrosion cracking sensitivity is reasoned dependent on the formation of d_T-ligaments. Using elastic stress field equations and a Tresca yield condition (16) this requires the K level to be augmented by a triaxiality factor.

$$TF = 1/1\text{-}2\nu \qquad (17)$$

where ν is the Poisson ratio. Mulherin (16,26) associates the presence of this beneficial effect with the occurrence of a coherent precipitate phase in non-ferrous alloys, as in aluminums, a brass and titanium alloy; its absence with the non-coherent carbide precipitate of steels. Present results tend to corroborate this rule, as will be apparent later.

5. Fracture flow diagram construction

The manner of converting the stress strain curves to a prediction of subcritical crack propagation behavior is displayed in Fig. 4. The derived curves $(\theta_T/\sigma_T + 3)^{-1}$ vs ϵ_T appears at the top half of Fig. 4. The first cycle, or simple tension result, inflects sharply as a result of first cycle yield point behavior. The triaxiality factor TF will

offset the early elastic ($\nu < 0.5$) portion of this curve to the right by a constant factor. The basic derived cyclic curve, is offset by the R effect strain blockage ϵ_R rather than by a constant factor TF. This gives the appearance of a larger (relative) offset at low ϵ_T levels, increasing the (log) slope of the predicted curve.

The extreme lower limit or threshold of fatigue growth is taken to correspond to the elastic proportional limit of the cyclic stress strain curve. This strain increment, as measured from the zero stress axis of the total cyclic curve, must include the elastic compressive portion of the hysteresis loop, calculated from the tensile stress excursion limits, as σ_T/E, so that

$$\epsilon_T = \Delta\epsilon + \sigma_T/E \tag{18}$$

In the elastic range then, $\epsilon_T = 2\sigma_T/E$, whereas the ordinate "flow" plot is, from Eq. 15, essentially σ_T/E, directly proportional to ϵ_T, i.e. equal to $\epsilon_T/2$. The log-log plot of this is a 1:1 slope of constant ratio X:Y=2:1. This 45° line breaks sharply upward at a strain corresponding to the elastic limit. For strains, vis-a-vis ΔK, in fatigue below this point, the growth rate does not follow the 45° line but goes to zero because the stress relaxation (m) becomes zero for elastic deformation.

The corresponding 45° toe region for the first cycle curve, germaine to stress corrosion cracking and creep, is on a X:Y=1:1 line when longitudinal stress strain curves are employed and on a X:Y = $1/2\nu$:1 1.6:1 for present data where diametral strain was measured, and the strain (but not θ_T) corrected to longitudinal values

$$\epsilon_T = \Delta\epsilon + \sigma_T/M \tag{19}$$

where $1/M = 1/E - 1/\theta_o$, θ_o being the diametral (areal) tensile elastic modulus. Since the stress corrosion cracking is corrosion rate (V_c) dependent rather than creep (m) dependent, the 1:1 elastic limit line need not signal a threshold of SCC crack growth and there is slight evidence in present results to suggest this.

The top end of the derived curves, Fig. 4, represents "limit loading" conditions. For the first cycle the (triaxial) instability point should correspond to K_{Ic}. In the cyclic result, there is evidence that uniaxial ($\bar{z} = 0$) instability pertains to thin sheets. If the tensile curve is of relatively flat top, a "hesitation" shelf at an ordinate value of about 2 (i. e. at the ultimate tensile strength where $\theta_T = 0$, then $(\theta_T/\sigma_T + 1/2)^{-1} = 2$) will forestall the terminal instability. This can be a beneficial effect in some materials, as will be seen in results to follow.

6. Specimen material and experimental procedure

The criteria of alloy selection included: 1) existence of a sufficient range of subcritical crack propagation data; 2) availability, to the authors, of identical fracture specimen material for tensile specimens; and 3) variety of material to typify a good range of structural alloys. Compositions and mechanical properties are collected in Table I, along with some of the results of the study. They comprise thirteen alloys: one carbon steel, two stainless steels, four quenched and tempered steels, one maraging steel, two titanium alloys, and three aluminum alloys. In most cases the tensile coupons were cut from pieces of actual fracture specimens or the same plate stock.

The tensile specimens were made small to allow their fabrication from the oft-times small fracture specimen residuals: 0.170 in. diameter by 0.500 in. long test section, with 1/2 in. 20 threads/in. (NF) ends. A uniform non-tapered test section was utilized. When less than 1/2 inch stock was available, partial threads were employed. The 4340 specimens were smaller; 0.100 D, with 1/4-28 (NF) ends.

The specimens were strained in a small hydraulic testing machine, described elsewhere (27), fitted with an alignment subpress to minimize the buckling tendency in compression. A diametral bi-lobed clip type gage was instrumented with electric resistance foil gage transducers, which with the load signal was recorded with a Hewlett-Packard X-Y recorder. The Tektronix Q-type strain gage preamplifiers employed proved stable enough for the extremely high gains required for the stress relaxation measurement.

The stress relaxation rate was measured by quickly locking the testing machine head and measuring, with grips thus "fixed", the stress decay. Q-unit amplifiers rebalanced, the gain was increased 10-fold, time marks from a Tektronix 181 mark generator superimposed at 1 sec. intervals until 5 seconds after machine arrest, thence at 5 second intervals until the decay in a 5 sec. interval becomes too small to discriminate on the chart. Some of the records (Figs. 10-20) show actual decay traces. A plot of average values for each of the alloys is shown in Fig. 5. The m value is calculated from the slope of the linear $\Delta\sigma_T$ vs log t plot using equation (7) in the form

$$m = \frac{\Delta\sigma_T}{\Delta \log t}/2.303\ \sigma_T \qquad (7B)$$

A linear stress vs log time plot is permissible for the characteristically small values of m of ordinary alloys. The m values, or slope $\Delta\sigma/\Delta\log t$, was found to be constant in most cases, but for cases where it decreases with time, m values for both 1 sec. and 10 sec. slope values are recorded in Table I. The m values are reproducible with $\pm$ 5%.

In the presentation of data to follow, the figures are sequenced in the order of Table I and Fig. 5 to retain the categorical ordering of alloys. The coordinate scale ratio of each fracture data plot is the same as that (published) employed by the authors of the data set, not all 1:1, as it is easier to re-scale the flow derived curves.

7. A533 type B class I pressure vessel steel

The intensive research to which this material has been subjected stems from its importance as a nuclear reactor power plant heavy wall pressure vessel material. Specimens were cut from the 12 in. thick plate, the center region being of fairly uniform properties. Fatigue tests on 1, 2, 3, and 4 inch CTS specimens were undertaken by Clark (28) while on thinner 0.2 inch as well as 1 inch specimens, Paris and Bucci accomplished the feat of establishing the low growth rate region looking for growth thresholds with respect to the stress ratio R. The results reported by Paris, Bucci, Wessel, Clark and Major (29), abbreviated WPMBC, provide a striking resolution of the effect of stress ratio on the growth threshold.

The Fracture-Flow diagram of the WPMBC data, Fig. 6, is coded to distinguish the six stress ratios and two thickness ranges employed. The actual stress strain records, one of several similar test results, is inset along with thus-derived predictive flow curves. The first cycle stress strain curve shows the characteristic upper yield point followed by a strain hardening rate sufficient for a high, about 17%, strain for simple tensile instability. The first cycle instability strain is in reasonable correspondence with measured values of K_{Ic} (30.31).

The cyclic strain excursions showed a rather steady form below about 6% extension, but thereafter a progressive decrease in range of tensile stability. The second and third cycle shapes are believed to best characterize the crack tip material ductility as the fourth cycle, displaced downward 10 ksi on the record, appears curtailed by imminent necking and rupture; the second cycle result is shown. The flatness of the tensile curves developed in these cycles has the effect of causing a large separation between uniaxial and triaxial mechanical instability points. Both second and third cycle curves predict a plane stress growth rate infinity in good correspondence with the thinner plate results of Paris and Bucci. With the triaxial correction, % of Eq. 15 equal to 0.5, both shift to the right to bracket the thick sections results of Clark. There is some questionable overlap here, as the Paris and Bucci data on one in. thick specimens follow the thin sheet prediction in Fig. 6, while that of Clark, the thick plate prediction.

The lower end of the predictive curve permits an assessment of the stress ratio (R) effect for the A533B. Values of the ϵ_R-addition required for best fit of the data were judged from a master plot with a set of equally graded ϵ_R = 0.0010 offset increments. Of the values shown, 0.0020 is best fit for R = 0.8, 0.0033 for R = 0.5, and 0.0060 for R = 0.1. These along with the remaining data fits are cross plotted in Fig. 7, showing a reasonable proportionality of ϵ_R to 1-R as per Eq. 16 and Fig. 3 indicating a value of ϵ_{RO} of about 0.0066 for this alloy. The overall form of the reference curve, as derived from the stress strain curves, can be reproduced from independent test and record measurements to about $\pm$ 5% in either coordinate. After its correction for R effects, the degree of correspondence

with the WPMBC data is encouraging.

The procedure which was used for calculating the "disposable" parameters d_T and ϵ_G implied by the matching is typified here with the A533B. A convenient reference point on the flow diagram is chosen. With English units used for the working sheets, the coordinate $\epsilon_T = 1000 \text{ ksi}/\sqrt{2\pi}\, E$, and $(\theta_T/\sigma_T+R)^{-1} = 1.0$ was marked. At match with the da/dN vs ΔK data, the corresponding value of ΔK yields d_T from Eq. 13: i.e. $\sqrt{d_T} = \Delta K/E\sqrt{2\pi}\ \epsilon = \Delta K/1000$; $d_T = \Delta K^2\ \mu$ in. For the ϵ_G values, through eq. 15, assume a typical loading cycle $\Delta t/\tau = 1/2$; whence $\epsilon_G = m\, d_T/da/dn(\text{ref})$. The m value, taken from data as shown in Fig. 5 and Table I is used. If it is not constant, ϵ_G corresponding to both 1 second and 10 second m values is recorded, then cross plotted against the first cycle ultimate tensile strength in Fig. 8. The match-determined value of d_T is marked on the growth rate scale of each "Fracture-Flow" diagram, and recorded in Table I.

8. 316 and 304 stainless steel

From the studies of effects of high temperature neutron irradiation environments by James (32) and by Shahinian (33), the room temperature data are examined in Figs. 9 and 10. The extraordinary strain hardening capacity of these solution-annealed alloys is evident from the cyclic stress-strain curves, inset in the Fracture-Flow diagrams: first cycle instability strains are of the order of 40 to 50%, which with the indicated d_T value would mean a K_{Ic} of 400 to 500 ksi$\sqrt{\text{in.}}$ (or $\text{MNm}^{-3/2}$), totally unmeasurable. The equilibrium cyclic instability, though still high, is greatly reduced. The ϵ_R shift of 0.008 (i.e. $\epsilon_{RO} = 0.0089$) for the 316, and 0.007 for the 304 brings the prediction into close correspondence with data. These high values of ϵ_R are not unreasonable in view of the initial softness of these materials: a relatively low elastic field outside the yield zone will be available to recompress the cyclicly hardened crack tip region. Like the A533B carbon steel, the "flat-top" cyclic stress strain curves of these alloys leads to prediction of a large separation in ΔK between plane stress and plane strain conditions. However, since the alloys are so soft and tough, and rarely used in thick sections, it is unlikely that the plane strain "bonus" will be realized in practice nor is it indicated in the fatigue data.

The values of the gradient strain ϵ_G needed to match predictions to date are seen in Fig. 8 to be atypically low; in other words the fatigue crack propagation rate is unexpectedly high. Some of this may be attributed to the non-uniform rate of stress relaxation, Fig. 5, as the one second m value is about 50% greater than the 10 second value. This suggests a sensitivity of cyclic growth rate to cyclic frequency, with the atypically high rate for high frequency. James' result on the 316 alloy shows a higher growth rate pattern than that of Shahinian. If the Shahinian data is matched, the value of ϵ_G, Fig. 8, is raised into consistency with other alloys. The process zone size d_T appears identical (530 μin.) for each of these alloys, its relatively high value contributory to their high toughness.

9. 12 and 10% Ni steels

The extensive data of Barsom, Imhof and Rolfe (34) is modeled in this instance: Fig. 11 for the 12Ni, 5Cr, 3Mo alloy; Fig. 12 for the 10Ni, Cr, Mo, Co. In the extensive 10Ni set, a value of $\epsilon_R = 0.002$ is shown, although an even lower value, say 0.001 would fit as well. For such a hard material, a low value might be expected. This suggests a very low sensitivity to stress ratio, which is, in fact, the observation of Barsom et al on their data which shows nil effect on da/dN (ΔK) of a wide range of R values.

The plane strain branch is followed at the top, as would be expected for the relatively thick (1 in.) specimens employed in this high strength material. The difference between thin and thick section branches is not large in the cycled material. Just the opposite is true of the virgin material where the instability point shifts upward by a factor of about three, in both alloys, into correspondence with the measured plane strain fracture toughness K_{Ic}.

From the 12Ni steel data of Barsom et al, Fig. 11, it is possible to discuss corrosion-fatigue effects; their growth rates in salt water was observed to be cyclic frequency sensitive. The model result, Eq. 15, allows for a corrosion rate V_S as a multiplicative factor, operating on the same flow variables. For given corrosion rate V_S, the log-log

growth rate curves should retain the same shape, being simply displaced upward a distance proportional to the log of the cyclic period Δt. This expectation appears to be realized in this data, Fig. 11. The degree of displacement required to make the fit can be used to estimate V_S. If we approximate $\Delta t \simeq 1/4f$, where f is the cyclic frequency, and use reference values of da/dN the same as discussed for the A533B steel (Sec. 7) then from Eq. 15

$$V_S \simeq \epsilon_G \, f/2 \left[\left(\frac{da}{dN} \text{ CF ref} \right) - \left(\frac{da}{dN} \text{ dry ref} \right) \right]$$

where (da/dN CF ref) is the reference growth rate for the corrosion fatigue match, while (da/dN dry ref.) is that for no environmental effect. Values of V_S so calculated (Table I) are fairly consistent, and as will be evident in a later comparison (Fig. 21), too high for use of the material in a marine environment.

10. AISI4340, 9-4-20 and 9-4-?5 steels

Both fatigue and stress corrosion cracking data are available on 4340 steel, Fig. 13. The specimens used for the flow measurements were of Gallagher's stock (35) of a slightly higher tempering temperature than that for Miller's fatigue data (36). Prior experience with tempering temperatures ranging through this region suggest only a small effect of this difference (16). The match of fatigue data is satisfactory. Again as for the high strength 10Ni maraging steels, only a small R correction, $\epsilon_R \simeq 0.002$, is required. The cyclic curve is so rounded that there is little difference between thin and thick section predictions. Unlike A533B and stainless steels, this hard alloy cyclicly softens, as expected after Manson (37), so that the fatigue growth is stable well beyond the K_{Ic} level.

Gallagher's stress corrosion cracking velocity data on this alloy has been fitted by an upward translation of the first cycle flow prediction. The growth threshold for this non-coherent carbide phase steel is not expected to be augmented by a triaxiality factor, as discussed in Sec. (4). The simple fit of the threshold is quite satisfactory, as is that for the K_{Ic} limit. The intermediate velocities fit well except near the threshold where they seem inordinately high and invarient, particularly with the unbuffered salt water. The behavior is more as though the K-proportional ϵ_G should apply. Indeed Sullivan (38) has observed a ratcheting up to and down from this limit in a similar 4340. Further study is needed here. The V_S value emerging this match is noted in Table I.

Only fairly high growth rates, i.e. above 5 μin./cycle are reported for the 9Ni,4Co, 0.20-0.25C steels by Clark (37) and by Crooker et al (40, 41). The fit is as good as can be expected. Crooker's growth rates typically run somewhat faster than Clark's. The fitting has favored Clark's since it is the more extensive of the data sets.

11. Titanium Alloys, 8Al-1Mo-1V and 6Al-4V

The discovery by Brown (42) of the extreme stress corrosion cracking sensitivity of an 8-1-1 titanium plate prompted the in-depth study by Meyn (3) of its corrosion fatigue behavior. The cyclic stress strain curves (Fig. 16) show a progressive trend to a slope inversion, a "two-stage" hardening effect, sometimes observed in first cycle properties of titanium alloys. In the fatigue growth prediction (center plot of Fig. 16) this has the effect of stunting and even reversing the crack growth rate prior to the terminal instability rates. When this portion of the T-C derived curve is superimposed on the Meyn (3) fatigue data (lower figure) the prediction appears substantiated, this particularly evident in his more extensive 2 Hz data set. The fitting required a unexpectedly large R correction factor, $\epsilon_R = .006$, for a material of such high relative strength level.

At the very low cyclic frequencies, the corrosion (V_S) induced growth per cycle has increased by a factor of 30 to well above d_T/cycle. It might be expected here that in each cycle the crack would advance into material less affected by the cyclic straining in such a large constant-load growth increment. The scant data at 1/2 Hz suggests this, where two of the points can be fitted by the first cycle prediction (T), others by the cyclic prediction (T-C) as though the data populations were bimodal.

Meyn (3) has observed that the corrosion effect in fatigue of this alloy disappears for $\Delta K (= K_{max}$ for R = 0) around the (static) stress corrosion cracking threshold K_{Iscc}. The threshold in this coherent precipitate material should be the first cycle result augmented

by a triaxiality factor T.F. = (1/1-2ν) ≃ 2.8. (A corresponding result is observed in the 7075 Al Fig. 18 and 7079, Fig. 19.) If the appropriate transposition is applied to the first cycle curve, it does appear to bound the transition region. The fatigue growth rate in air below the threshold is reasonably well fitted by the predictive curves, although Mayn's vacuum data (not shown) is not. The reference growth rate has been based, as in other alloys of this study, on the high frequency room air data.

The values of V_S implied by the corrosion fatigue frequency effect data fitting are seen in Table I to be internally consistent, and also consistent with the value obtained in matching first cycle predictions with Sullivan's (18) stress corrosion cracking velocity (V-K) data. It should be noted here that the same value of ϵ_G was used for first cycle as for reversed cyclic predictions, implying that the crack tip strain gradient is not only constant with respect to loading level but unaffected by prior strain history. Use of the K-proportional ϵ_G in this instance would reverse the upward slope of the stress corrosion crack velocity prediction, and, as already observed by Sullivan (18), fail to fit the fracture data.

The value of V_S for this 8-1-1 titanium in salt water, Table I (Fig. 21), is higher than for any other material of our experience. A number of less active reagents have been tried by Blackburn, Feeney and Beck (43) the two matched in the upper frame of Fig. 16 appear in reasonable agreement with model prediction as to V-K curve shape.

The 6Al-4V titanium alloy results of Crooker (45) and of Clark (39) are displayed in the Fracture-Flow Diagram form in Fig. 17. The growth limit of first cycle ductility corresponds well with K_{Ic}. As in the 8-1-1 alloy, a strain hardening inflection develops, with corresponding growth rate inversion. Clark (39) has favored us with a single data point which suggests this possibility. The lower tail on Clark's data is believed to be a characteristic start-up surge, not a true threshold.

12. Aluminum Alloys 7075T6, 7079T6 and 5456T321

The long standing propagation data of McEvily and Illg (45), in its Paris ΔK reformulation (47), is nicely fitted by the Fracture-Flow diagram modeling, Fig. 18. The K_{Ic} prediction is slightly higher than usual measured values. A stress corrosion cracking velocity much slower than for 4340 steel or 8-1-1 titanium is indicated by the downward rather than upward shift of the first cycle prediction to fit the data of Hyatt and Speidel (47). A new result here is the tracking of the predicted curve shape in the "tail-off" in growth rate toward the threshold. In the 7079 T6, Fig. 19, the lowest velocity point suggests that some excursion down the elastic 1:1 stability line may forestall the zero growth goal. The scatter in the SCC growth rate above the knee of the curve could be a result of a transitional stage from the triaxially inhibited yielding to a fully plastic ligament condition.

Clark's fatigue propagation data on the 7079-T6 seems to favor the plane strain prediction, Fig. 19, as befits his utilization of thick specimens. This is true also in the softer 5456 Alloy, Fig. 20, whereas Crooker's data tends to favor the plane stress prediction in its emergence to infinite growth rate.

13. Discussion and Conclusions

Specific results have been discussed in connection with preceding particular examples. We believe a general consistency between "theory" and experiment has been demonstrated. Its only conspicously unsatisfactory aspect is the necessity for an arbitrary assignment of the gradient strain ϵ_G. It is possible that this results from deficiencies of the simple elastic analogue plasticity model. However, the general trend in ϵ_G, decreasing with increasing flow strength (UTS), is reasonable. The crack opening displacement varies inversely as the flow strength (YS), so that the transition between its yield strength dependent strains and the yield strength independent plastic strains away from the crack tip should involve a gradient diminished by flow strength. The negative slope of the log ϵ_G vs lot UTS plot suggests an inverse relationship $\epsilon_G \simeq 4$ ksi/UTS.

Some practical results emerging from this study can be listed in conclusion. One of these, quite unexpected, is the fact that the terminal fatigue growth rate instability can be forstalled by conditions of constraint, or plane strain, at the crack tip. It is

to our knowledge the only fracture strength behavior beneficiary of the thick section. Secondly, it appears that the softer materials owe their more substantive fatigue growth threshold levels to a more substantive plastic zone blockage of the strain excursion at the crack tip upon unloading. But much more needs to be learned about the ϵ_p effect, how flow properties are related to it, how it might be measured from COD experiments during cycling. Thirdly, we would remind you of the beneficial effect of triaxiality in displacing upward the K threshold of stress corrosion cracking, apparently a boon to non-ferrous alloys.

A final conclusion can be drawn from a plot of all reasonably well documented assessments of the surface attack rate against tensile yield strength, Fig. 21. The scale at the right is a rough conversion of these rates to lifetimes of a loaded part so beset. The point is not in the correlation; there is none; that is the point. There is an enormous variability, not a factor of three or six as for typical tensile modulus normalized dry fatigue rates, but three or six orders of magnitude. It is the why of this enormous variation, surely corrosion induced, that corrosion experts must address their attentions. We would hope the framework which present results provide will be useful in this quest, by relegating some of the behavioral patterns of stress corrosion cracking to the realm of mechanics.

Discussion

In discussion, the point was brought out that the calculated corrosion rates obtained by Dr. Krafft from his velocity measurements were far in excess of known corrosion rates of steel in sea water.

REFERENCES

1. M. A. HIRT and J. W. FISHER, "Fatigue Crack Growth in Welded Beams", Fritz Engineering Laboratory Rept. 358.35, Jan. 1972.

2. P. C. PARIS, "Testing for Very Slow Growth of Fatigue Cracks", Closed Loop, MTS Systems Corp., Vol. 2, No. 5, pp. 11-14 (1970).

3. D. A. MEYN, "An Analysis of Frequency and Amplitude Effects on Corrosion Fatigue Crack Propagation on Ti-8Al-1Mo-1V", Met. Trans., Vol. 2, pp. 853-865 (1971).

4. J. D. LANDES and R. P. WEI, "Kinetics of Subcritical Crack Growth and Deformation in a High Strength Steel", ASME J. Mat'ls. Engineering, forthcoming 1972.

5. J. M. KRAFFT, "Strain Hardening vs Stress Relaxation Effects on Fatigue Crack Propagation", Report of NRL Progress, July 1971, pp. 1-10.

6. J. G. WILLIAMS and C. E. TURNER, "The Plastic Instability Viewpoint of Crack Propagation", Appl. Materials Res., Vol. 3, p. 144 (July 1964).

7. D. P. CLAUSING, "Effect of Plane Strain State on Ductility and Toughness", Int.J. Fracture Mech., Vol. 6, p. 71 (1970).

8. O. HOFFMAN AND G. SACHS, "Theory of Plasticity for Engineers", McGraw-Hill, New York, 1953, Chap. 14.

9. G. SACHS AND G. LUBAHN, "The Effect of Triaxiality on the Technical Cohesive Strength of Steels", J. Appl. Mech., Vol. 12, p. 211 (1945).

10. J. A. H. HULT and F. A. McCLINTOCK, "Elastic-Plastic Strain Distribution around Sharp Notches under Repeated Shear", 9th Int. Congress Appl. Mech., Vol. 8, Univ. Brussels, 1957, p. 51.

11. J. L. SWEDLOW, M. L. WILLIAMS and W. H. WANG, "Elasto-Plastic Stresses and Strains in Cracked Plates", Proc. 1st Int. Conf. Fracture, Sendai, 1965, Vol. 2, p. 259.

12. J. R. RICE and G. F. ROSENGREN, "Plane Strain Deformation Near the Crack Tip in a Power Hardening Material", J. Mech. Phys. Solids, Vol. 16, p. 1 (1968).

13. J. W. HUTCHINSON, "Singular Behavior at the End of a Tensile Crack in a Hardening Material", J. Mech. Phys. Solids, Vol. 16, p. 13 (1968).

14. H. W. LIU, W. J. GAVIGAN, and J. S. KE, "An Engineering Analysis of Ductile Fractures", Int. J. Fracture Mech., Vol. 6, pp 41-53 (1970).

15. J. H. UNDERWOOD and D. P. KENDALL, "Measurement of Microscopic Plastic Strain Distributions in the Region of a Crack Tip", Exp. Mech. Vol. 9, p. (1969) or see

J. H. UNDERWOOD, J. L. SWEDLOW and D. P. KENDALL, "Experimental and Analytical Strains in an Edge-Cracked Sheet", Engr. Fracture Mech. Vol. 2, pp 183-196 (1971).

16. J. M. KRAFFT and J. H. MULHERIN, "Tensile-Ligament Instability and the Growth of Stress-Corrosion Cracks in High-Strength Alloys", ASM Trans. 62:64 (1969).

17. J. M. KRAFFT and G. R. IRWIN, "Crack Velocity Considerations", ASTM Spec. Tech. Publ. 381, p. 114 (1965).

18. A. M. SULLIVAN, "Velocity of Cracks Extending under Stress in an Adverse Environment", Fracture 1969, Proc. 2nd Int. Conf. on Fracture, Brighton, Chapman Hall Ltd., pp 396-405.

19. R. G. FORMAN, V. E. KEARNEY and R. M. ENGLE, "Numerical Analysis of Crack Propagation in Cyclicly Loaded Structures", ASME Paper Mat. 4, 1966.

20. A. HARTMAN and J. SCHIJVE, "The Effects of Environment and Load Frequency on the Crack Propagation Law for Macro Fatigue Crack Growth in Aluminum Alloys", Eng. Fracture Mech. 1:615, April 1970.

21. J. R. GRIFFITHS, I. L. MOGFORD and C. E. RICHARDS, "The Influence of Mean Stress on Fatigue Crack Propagation in a Ferritic Weld Metal", Metal Sci. J., Vol. 5, pp 150-154 (1971).

22. P. C. PARIS, W. WEISS and A. F. ANDERSON, "On the Threshold for Fatigue Crack Growth", Paper presented at the 5th National Symposium on Fracture Mechanics, U. Illinois, 1 Sept 1971, to be published.

23. P. C. PARIS, "The Fracture Mechanics Approach to Fatigue", "Fatigue, an Interdisciplinary Approach", Proc. 10th Sagamore Army Material Res. Conference, Syracuse Univ. Press, 1964, pp 107-132.

24. J. R. RICE, "Mechanics of Crack Tip Deformation and Extension by Fatigue", in Fatigue Crack Propagation, ASTM STP 415:247 (1967).

25. W. ELBER, "Fatigue Crack Closure under Cyclic Tension", Engr. Fracture Mech., Vol. 2, pp 37-46 (1970).

26. J. H. MULHERIN and H. ROSENTHAL, "Influence of Nonequilibrium Second-Phase Particles Formed During Solidification upon the Mechanical Behavior of an Aluminum Alloy", Met. Trans., Vol. 2 pp 427-432 (1971).

27. J. M. KRAFFT, "Tests for Fracture Strength, Static Impact", Techniques of Metals Research, Vol. 5, part 2, pp 1-102, J.Wiley, New York, 1971.

28. W. G. CLARK, JR., "Effect of Temperature and Section Size on Fatigue Crack Growth in Pressure Vessel Steel", J. Materials, Vol. 6, pp 134-149 (1971).

29. P. C. PARIS, R. J. BUCCI, E. T. WESSEL, W. G. CLARK and T. R. MAGER, "An Extensive Study on Low Fatigue Crack Growth Rates in A533 and A508 Steels", Scientific Paper 71-1E7-FMPWR-P7, Westinghouse Res. Corp., 1971.

30. W. O. SHABBITS, W. H. PRYLE and E. T. WESSEL, "Heavy Section Fracture Toughness Properties of A533 Grade B, Class 1 Steel Plate and Submerged Arc Weldments", Westinghouse Co. Report WC AP 7414, 1969.

31. J. M. KRAFFT, L. R. HETTCHE, A. M. SULLIVAN and F. J. LOSS, "Fracture-Flow Relationship for A533B Pressure Vessel Steel", J. Engr. Industry, Trans, ASME, Vol. 92, p. 330 (1970).

32. L. A. JAMES and E. B. SCHWENK, JR., "Fatigue Crack Propagation Behavior of Type 304 Stainless Steel at Elevated Temperatures", Met. Trans. Vol. 2, pp 491-496 (1971). See also

L. A. JAMES, "The Effect of Elevated Temperatures Upon the Fatigue-Crack Propagation Behavior of Two Austenitic Stainless Steels," Paper WHAN-SA-105; WADCO Corp., 1971.

33. P. SHAHINIAN, H. E. WATSON, H H. SMITH, "Fatigue Crack Growth in Selected Alloys for Reactor Applications", National Symposium on Predictive Testing, Anaheim, Calif., Apr. 1971, ASTM STP forthcoming.

34. J. M. BARSOM, E. J. IMHOF and S. T. ROLFE, "Fatigue-Crack Propagation in High Yield-Strength Steels", J. Eng. Fracture Mech., Vol. 2, pp 319-340 (1971).

35. J. P. GALLAGHER, "Corrosion Fatigue Crack Growth Rate Behavior above and below K_{Iscc} in Steels", J. Materials, Vol. 6, pp 941-964 (1971).

36. G. A. MILLER, "The Dependence of Fatigue-Crack Growth Rate on the Stress Intensity Factor and the Mechanical Properties of High Strength Steels", Trans. Am. Soc. Metals, Vol. 61, pp 442-448 (1968).

37. S. S. MANSON and M. H. HIRSCHBERG, "Fatigue Behavior in Strain Cycling in the Low-and Intermediate-Cycle Range", "Fatigue, an Interdisciplinary Approach", Proc. 10th Sagamore Army Mat'ls. Res. Conf., Syracuse Univ.-Press, 1964, pp 133-172.

38. A. M. SULLIVAN, "Stress Corrosion Crack Velocity in 4340 Steel", Forthcoming in Engr. Fracture Mech.

39. R. C. BATES and W. C. CLARK, JR., "Fractography and Fracture Mechanics", ASM Trans. 62:380 (1969).

40. T. W. CROOKER, J. A. COOLEY, E. A. LANGE and C. N. FREED, "Fatigue Crack Propagation and Plane Strain Fracture Toughness Characteristics of a 9Ni-4Co-0.25C Steel", Trans. Am. Soc. Met., Vol. 61, pp 568-574 (1968).

41. T. W. CROOKER and E. A. LANGE, "Corrosion-Fatigue Crack Propagation Studies of Some New High Strength Structural Steels", Trans. ASME, J. Basic Engr., Vol. 91, pp 570-574 (1969).

42. B. F. BROWN, "A New Stress-Corrosion Cracking Test Procedures of High Strength Alloys", ASTM Mat'l. Res. Std., Vol. 66 p. 129 (1966).

43. M. J. BLACKBURN, J.A. FEENEY and T. R. BECK, "State-of-the-Art of Stress-Corrosion Cracking of Titanium Alloys", Part 4 of Monograph Review, ARPA Order 878 and NAS7-489, 1970.

44. T. W. CROOKER and W. G. CLARK, JR., "Factors Determining the Performance of High Strength Structural Metals", Report of NRL Progress, Mar. 1970, pp 39-41, (see also Ref. 39).

45. A. J. McEVILY and W. ILLG, "The Rate of Fatigue Crack Propagation in Two Aluminum Alloys", NASA TN 4344, (1958).

46. P. PARIS and F. ERDOGAN, "A Critical Analysis of Crack Propagation Laws", ASME Trans. 85D:528 (1963).

47. M. V. HYATT and M. O. SPEIDEL, "State-of-the-Art of Stress-Corrosion Cracking of High-Strength Aluminum Alloys", Part 6 of Monograph Review, ARPA Order 878, 1970.

TABLE 1
COMPOSITION, FLOW PROPERTIES, FRACTURE BEHAVIORS OF VARIOUS ALLOYS

		STEEL	STAINLESS		MARAGE		Q&T			TITANIUMS			ALUMINUMS		
Material		A533B	316 SS	20455	12Ni	10Ni	4340	9-4-20	9-4-25	8-1-1	6-4		7075	7079	5456
		Fe+	Fe+	Fe+	Fe+	Fe+	Fe+	Fe+	Fe+	Ti+	Ti+		Al+	Al+	Al+
Composition	C	0.19	0.060	0.053	0.02	0.123	0.40	(0.20)	0.25	Al	7.4	6.3	Si	0.3	0.14
Wt. %	Mn	1.36	1.77	0.87	0.06	0.17	0.72	(0.30)	0.28	Mo	1.16		Fe	0.4	0.29
	Si	0.25	0.40	0.49	0.06	0.04	0.28	(0.01)	0.01	V	0.06	4.1	Cu	1.5	0.6	0.08
	Al				0.35	0.02				Fe	0.14	0.13	Mn		0.2	0.68
	Ni	0.53	13.3	9.5	12.2	10.11	1.70	(9.0)	8.31	C	0.08	0.023	Mg	2.5	0.3	5.17
	Cr	0.13	17.3	18.3	4.9	2.06	0.80	(0.75)	0.40	O	0.09	0.17	Cr	0.3	0.2	0.08
	Mo	0.62	2.33	0.18	2.9	1.06	0.24	(1.0)	0.48	N	0.004	0.014	Zn	5.5	4.3	0.03
	S	0.017	0.012	0.010	0.009	0.006	0.01	(0.01)	0.008	H		0.004	Ti		0.1	0.03
	P	0.011	0.007	0.019	0.0061	0.009	0.012	(0.01)	0.006							
	Cu	0.16	0.065	0.21	0.35											
	V							(0.10)	0.11							
	Co					8.00			3.78							
No.; Treat		Q&T	An	An	Aq Q	Q&T	Q&T	Q&T	Q&T		An	An		T-6	T-6	H-321
Flow Properties																
E(10^6 ksi)		29	28	27	27.9	28.7	30	28.6	28.6		17	16.5		10.4	10.4	10.4
σ_y (10^3 ksi)		60	44	44	43	52	55	40	46		26.5	27		16	16.0	16
$\nu = E/2\sigma_y$		0.24	0.32	0.31	0.32	0.28	0.27	0.36	0.31		0.32	0.31		0.32	0.32	0.32
TP=1/1-2ν		NA	NA	NA	NA	NA	NA	NA	NA		2.8	2.6		2.8	2.8	2.8
TYS (ksi)		61	40	35	185	180	210	180	178		135	116		75	75	34
UTS (ksi)		87	(95)	(90)	200	210	260	200	196		148	126		89	87	48
ϵ_c B=0		0.16	>0.4	>0.5	0.020	0.042	0.035	0.07	0.07		0.11	0.07		0.11	0.10	0.12
ϵ_c^c B=1/2		(0.17)	ND	ND	0.090	0.085	0.04	0.11	0.12		0.13	0.10		0.12	0.13	>0.15
T-C UTS ksi		71	120	140	190	200	231	195	187		142	120		91	91	51
T-C ϵ_c,B=0		0.072	0.08	0.10	0.07	0.08	0.065	0.09	0.09		0.10	0.10		0.09	0.08	.06
T-C ϵ_c^c,B=1/2		0.087	0.17		0.09	ND	0.050	0.11	0.12		0.11	ND		0.10	0.10	09
$\dot{\epsilon}$ 1 sec.		0.0087	0.0161	0.0161	0.0095	0.0089	0.0070	0.0099	0.0100		0.0118	.0158		0.0138	0.0157	0.0081
$\dot{\epsilon}$ 10 sec.		"	0.0105	0.0105	"	0.0044	"	0.0085	0.0083		0.0105	"		0.0129	0.0115	"
Fracture Behaviors							CNB				CNB	CNB				CTS
Specimen Type		CTS	NCB	CTS-SEN	CTS	CTS	SEN	CNB/CTS			SEN	CTS		CNB	CTS	CNB
Approx. Thick.(in)		0.2,1,2,3,4	0.5	0.5	1.0	1.0	0.15 0.5	0.5/1.0			0.3	0.5/1.0			1.0	0.5/1.0
Crack Direction		ND	LT-TL	LT-TL	ND	ND	----	TL-LT	TL-LT							
Min/Max Stress,R		0-0.8	0-0.05	0.050	0.09	0.1-0.7	0	0	0		0	0		0	0	0
ϵ_{KO}		0.0066	0.009	0.008	ND	(0.002)	(0.002)	(0.002)	(0.002)		0.006	ND		0.002	(0.002)	(0.005)
ϵ_G^c (1 sec.)		0.062	0.016	0.030	0.004	0.0254	0.0094	0.0266	0.0211		0.0262	0.0095		0.0556	0.0536	0.0694
ϵ_G^c (10 sec.)		"	0.009	0.020	"	0.0189	"	0.0228	0.0175		0.0233	"		0.0516	0.0392	"
d_T^G (μ)		4.8	13.4	13.4	26.0	10.9	10.5	8.2	4.0		7.3	19.9		4.0	3.1	5.3
K_T meas.		(200)	ND	ND	215	210	65	165	150		87	110		32	27	ND
K_{Ic} pred.		210	>600	>800	200	190	70	140	125		96	110		45	35	>55
Environment		Air	Air	Air	S	Air	S	Air	Air		S	Air		F	F	Air
Freq(Hz)/V_p(in/sec)		Var/ND	Var/ND	Var/ND	10/-- 1/3.6^{-6} 0.1/1.1^{-6}	Var/ND	0/1.47^{-6}	Var/ND	Var/ND		0/1.37^{-6} Var 10/1.6^{-6} 2/1.9^{-6} 1/2-1.7^{-6} 0/1.2^{-6}(C) 0/1.2^{-7}(CW)			0/1.37^{-6}	0/1.86^{-6}	ND

Var = Varied
ND = Not Determined or Not Available
NA = Not Applicable
( ) = Estimated Value

Environments R. T. Air except
S = Salt Water
F = Fresh Water
C = C H_2Cl_2
CW = C $H_2Cl_2H_2O$ Sat.

Heat treatment
An = Anneal
Au = Austenitize
Ag = Age
N = Normalize
Q = Quench

CTS Compact Tension
SENT Single Edge Notch Tension
CNB Cantilever Notch Bend
CNS Center Notched Sheet

Cracking Direction
L - Longitudinal
T(Width) Transverse
S Short Transverse
1st letter - Crack plane normal
2nd letter - Crack direction

Exponent designates that power of 10

CREEP - GROWTH MODEL

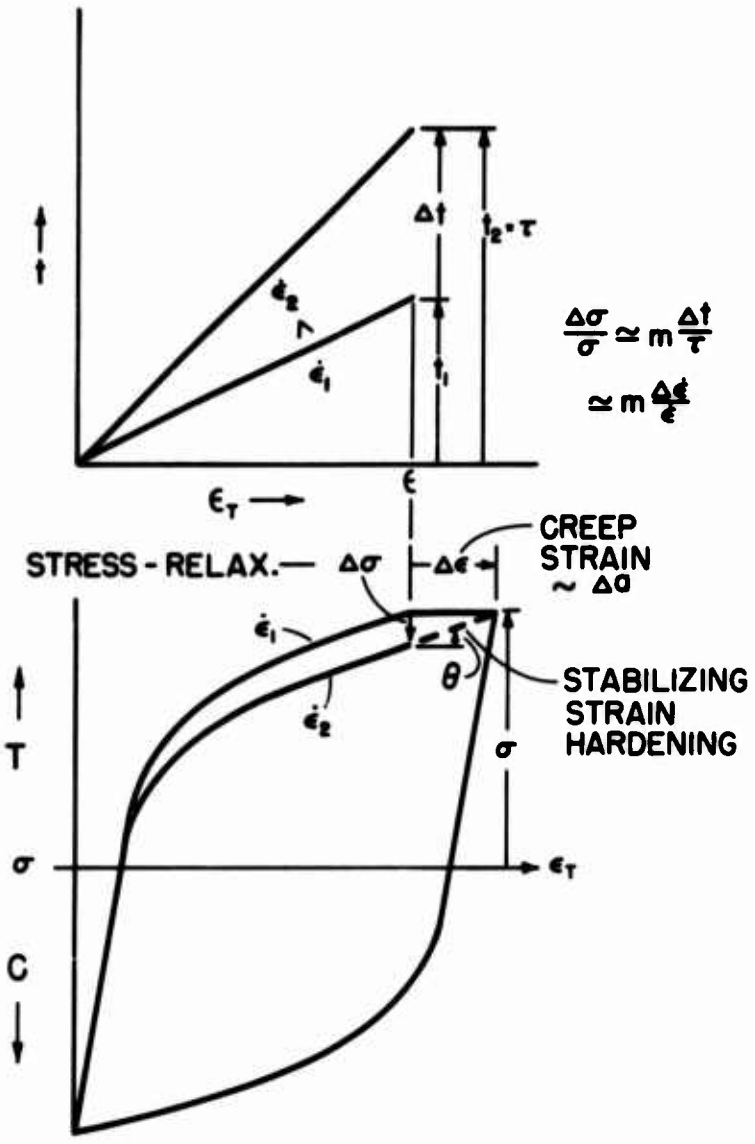
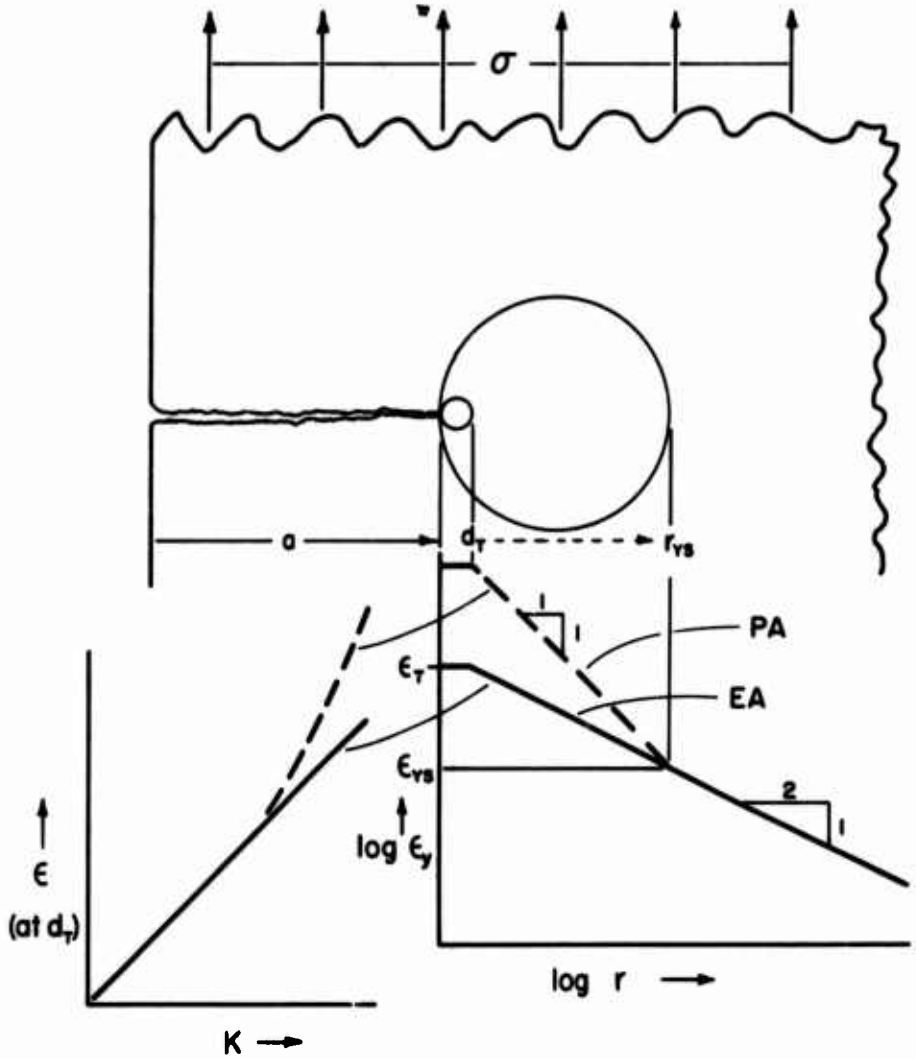


Fig. 1 - Stress relaxation $\Delta\sigma$ in time Δt (upper diagram) is related to the strain rate sensitivity m, and (below) is equilibrated by strain hardening $\theta\Delta\epsilon$ due to crack growth Δa.

CRACK PLASTICITY MODEL



$$K \sim \sigma\sqrt{a} \qquad \epsilon \simeq K/E\sqrt{2\pi r}$$

Fig. 2 - Crack tip d_T - size ligaments undergo plastic strain ϵ when an elastic stress σ is applied because strain field singularity (lower right) concentrates strain. In the elastic analogue model EA, ϵ is proportional to the stress intensity factor K; plasticity models PA predict a larger value.

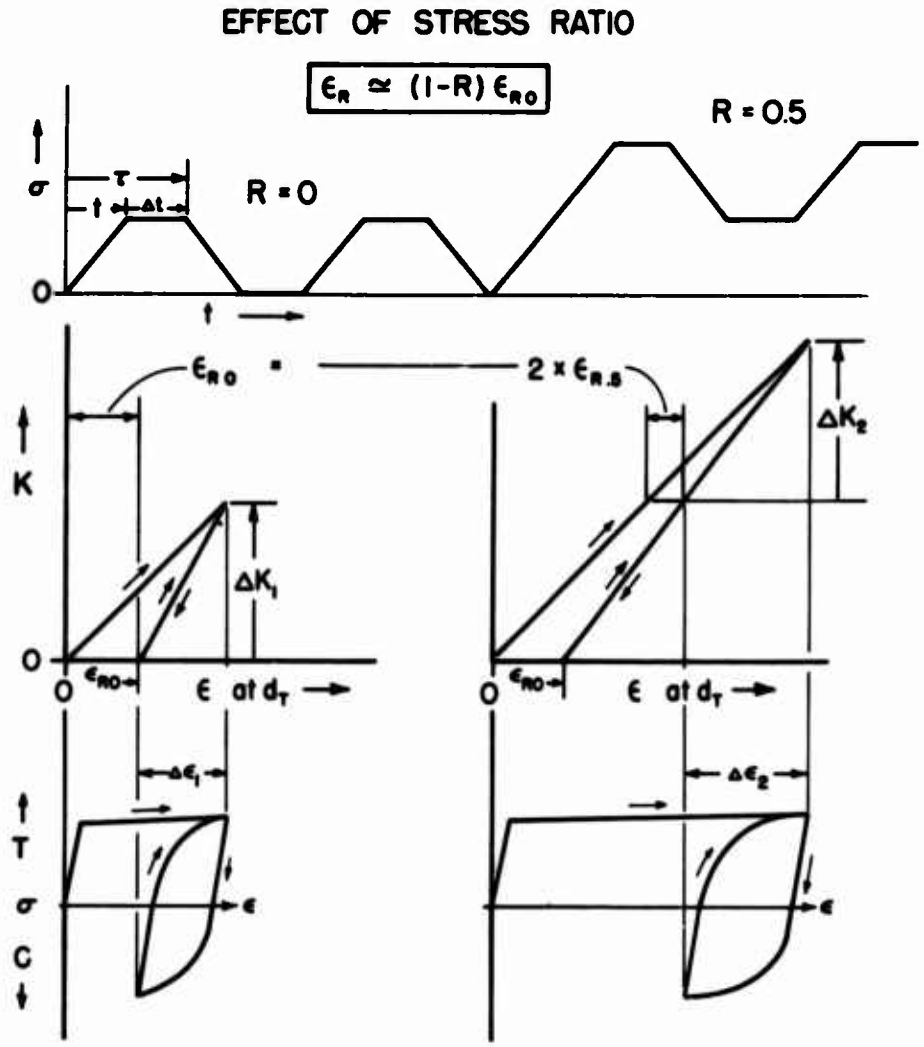


Fig. 3 - Loading, then unloading the crack extends, then compresses the d_T -ligaments. However full compression is blocked by prior tensile distortion, to a degree ϵ_R less for a high stress ratio R than for low.

FRACTURE - FLOW DIAGRAM

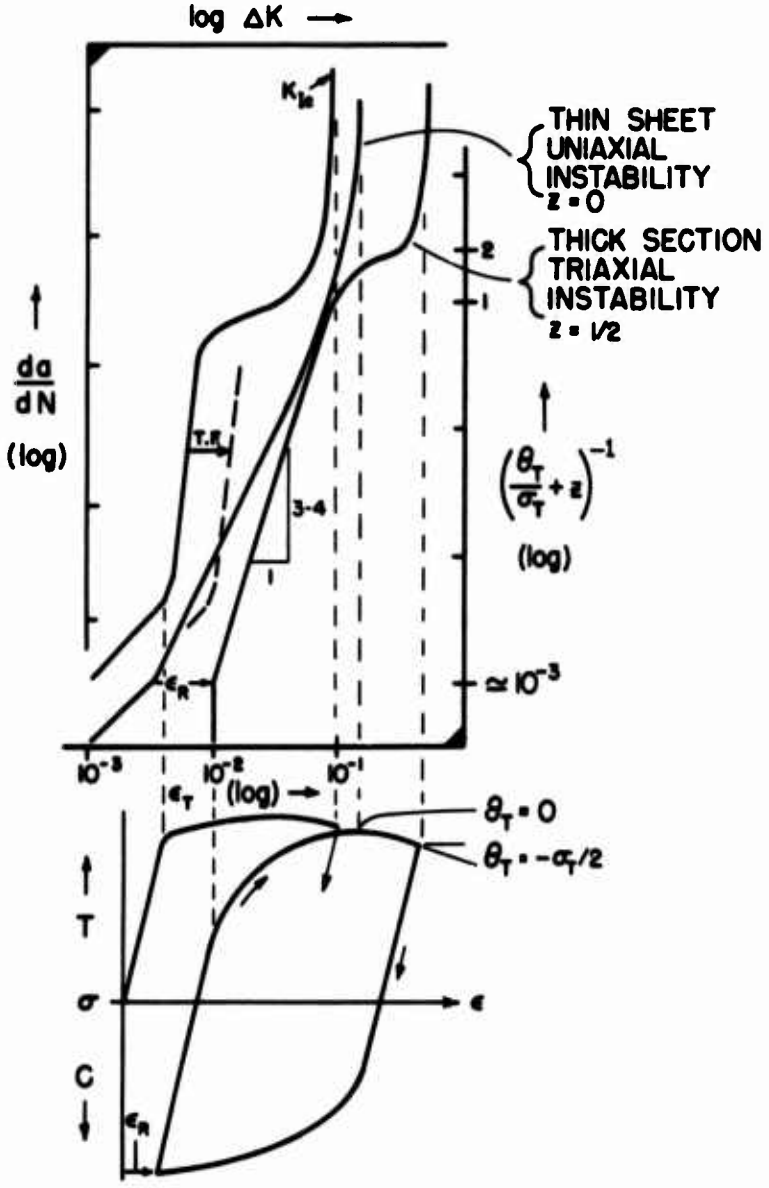


Fig. 4 - Fracture data can be compared to predictions from Flow data by appropriate re-plotting of the stress-strain curves, and allowances for yielding constraint TF and reclosure blockage ϵ_R.

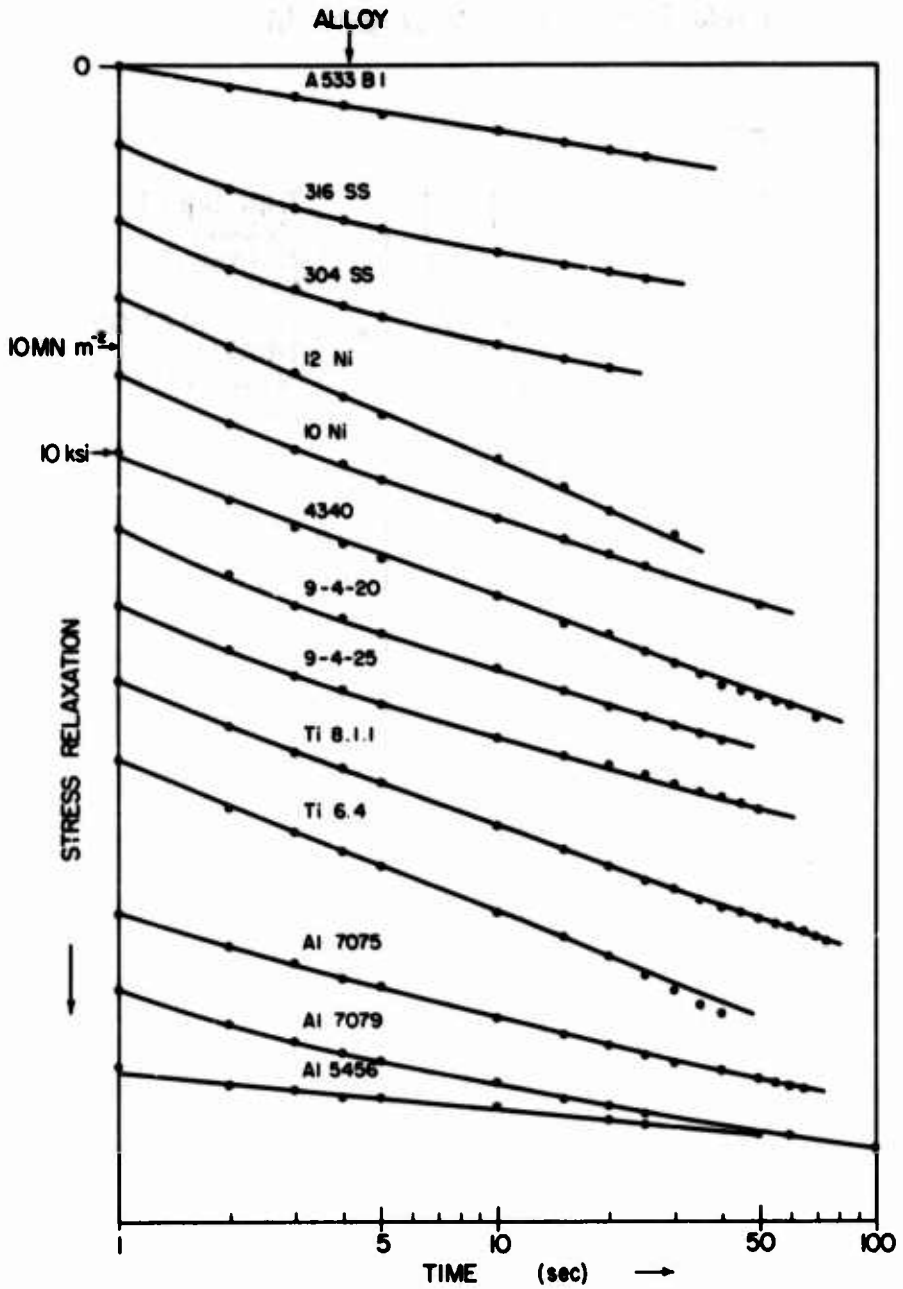


Fig. 5 - Stress relaxation vs log time after sudden arrest of the (hard) testing machine allows assessment of the strain rate sensitivity m for the various alloys.

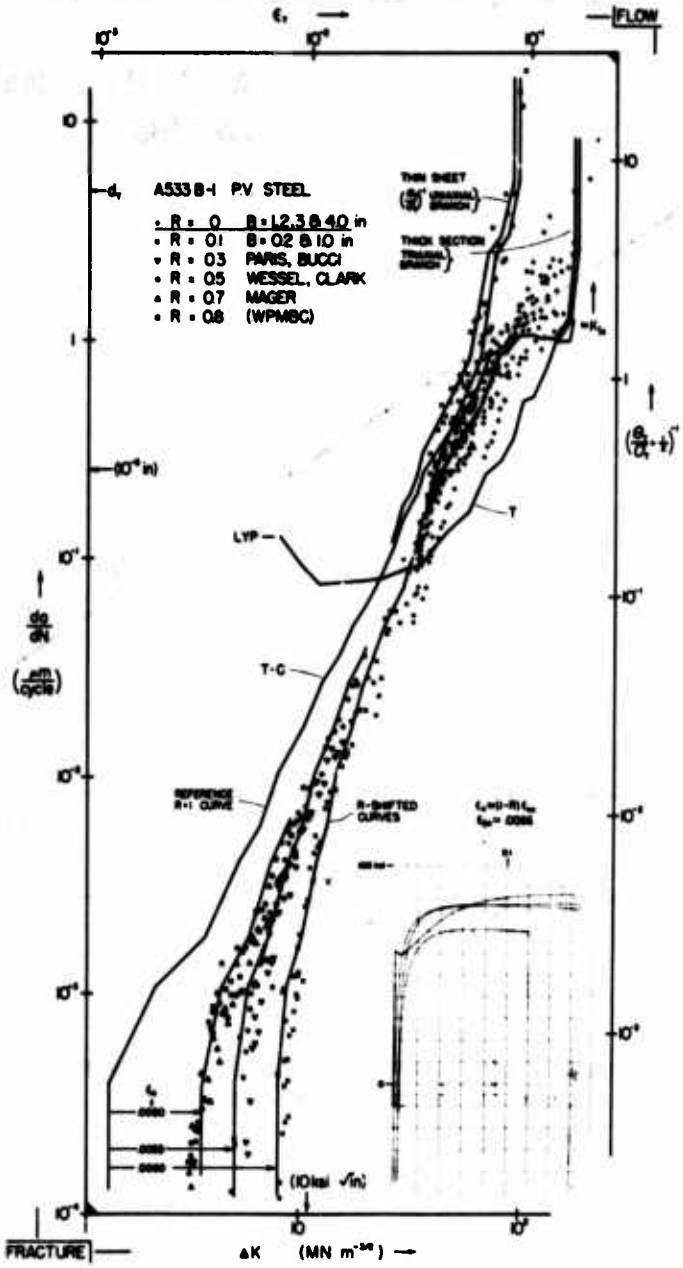


Fig. 6 - The extensive "WPMBC" data on A533B-1 steel is matched to cyclic tension curve (lower right) predictions. The ϵ_R correction shifts the reference curve into agreement with the R-effect at low growth rates. At high rates, the triaxial instability branch fits the thick section fatigue data.

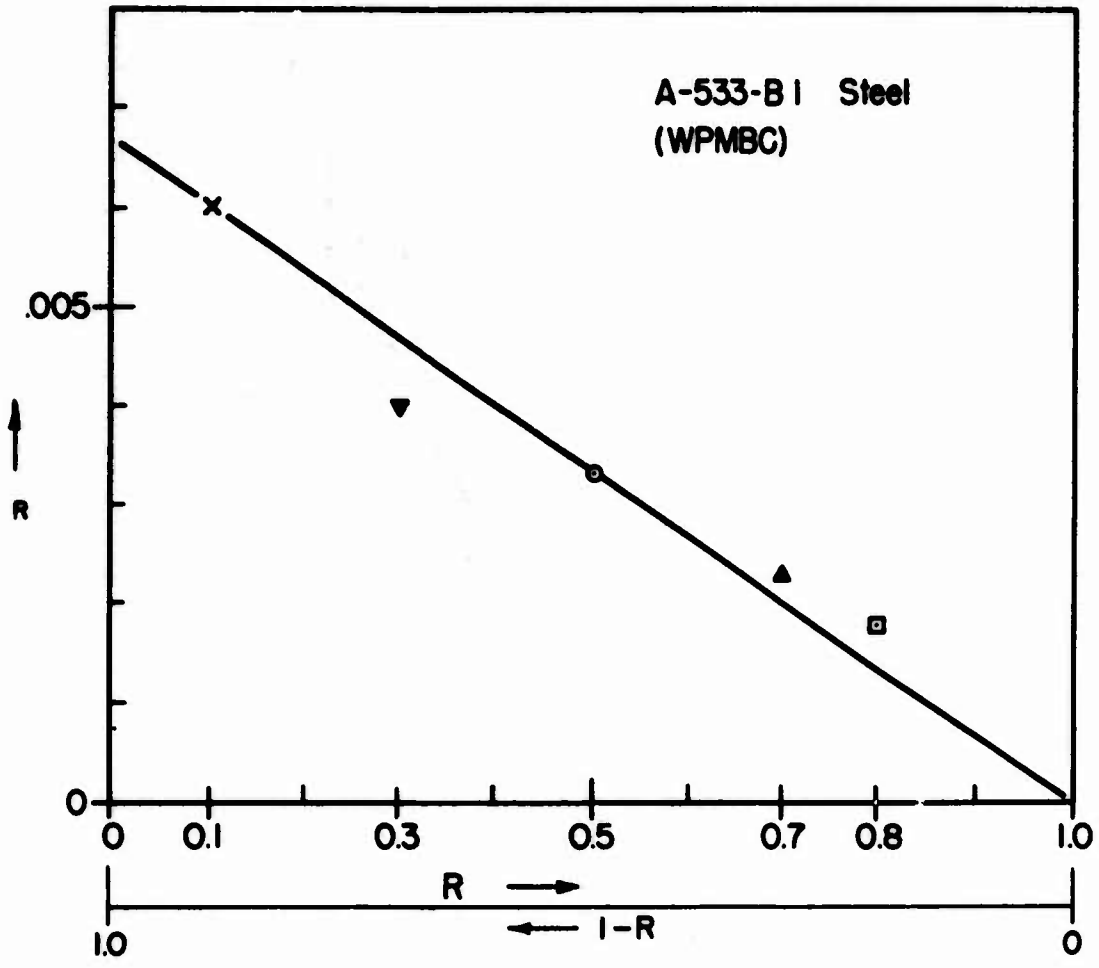


Fig. 7 - The c_R shifts needed to match the A533B-1 data (Fig. 6) conform to the simple model (Fig. 3) trend.

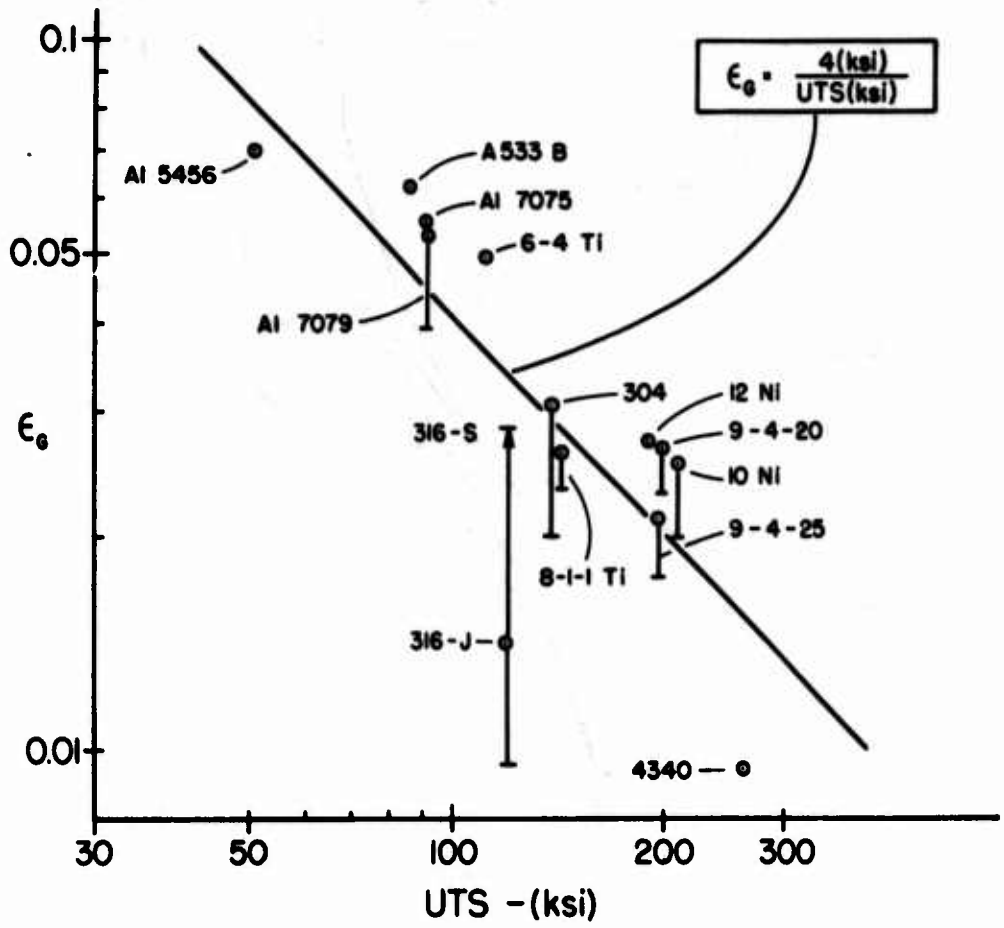


Fig. 8 - Values of the "gradient" strain ϵ_G tend to decrease, inversely, with tensile strength UTS. The lower bars are calculated with 10 sec m values; upper point with 1 sec. Shahinian's stainless steel data 316-S would follow this trend better than James data 316-J which was matched (Fig. 9).

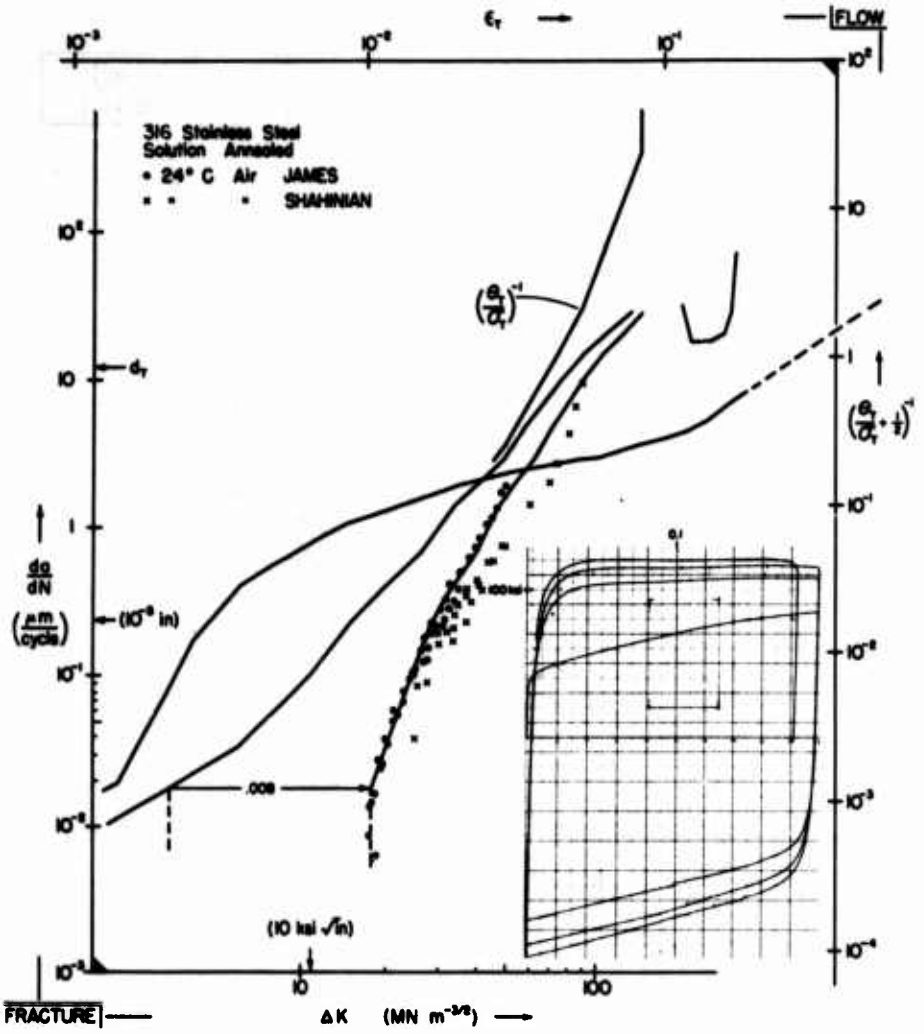


Fig. 9 - Fracture-Flow matching of solution-annealed 316 stainless steel requires a relatively high R effect correction ϵ_R = 0.008, but this is expected for such, soft, cyclicly hardening, material.

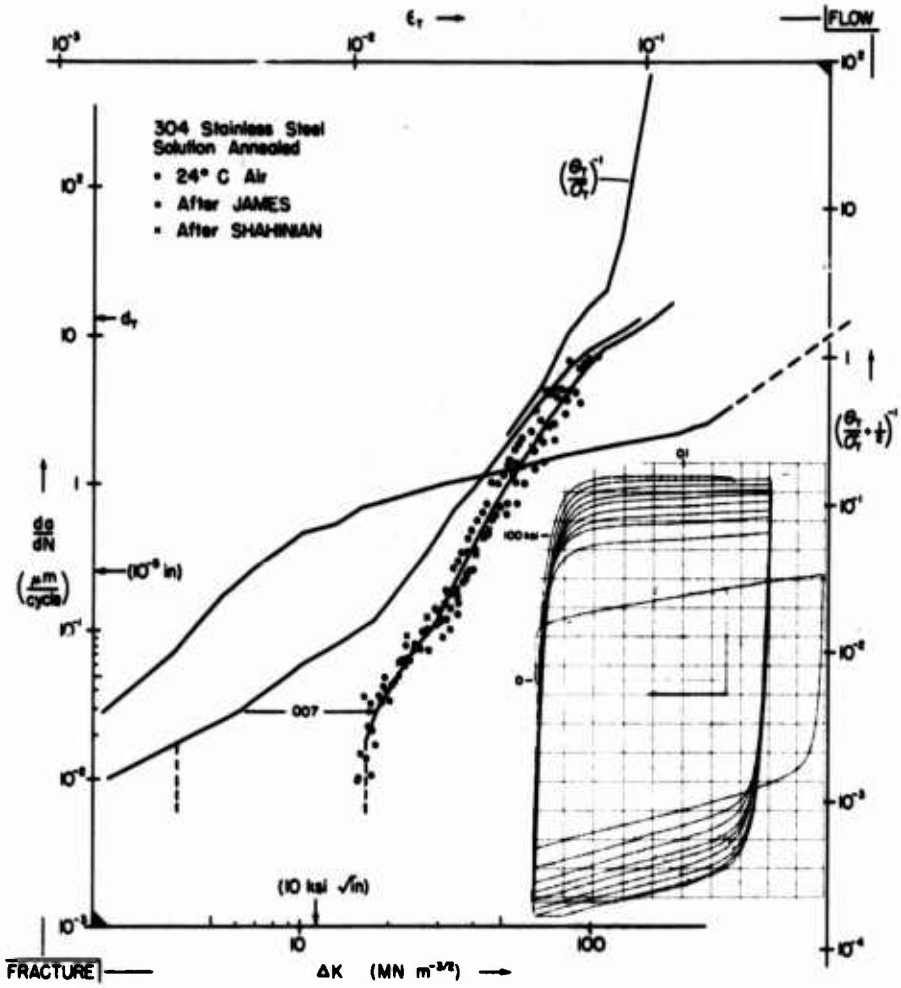


Fig. 10 – For annealed 304 stainless steel, the first cycle tensile instability strain ϵ_c is off scale, indicating, as in 316, an unmeasurably large value of K_{Ic}, yet with cyclic hardening fatigue propagation is normal.

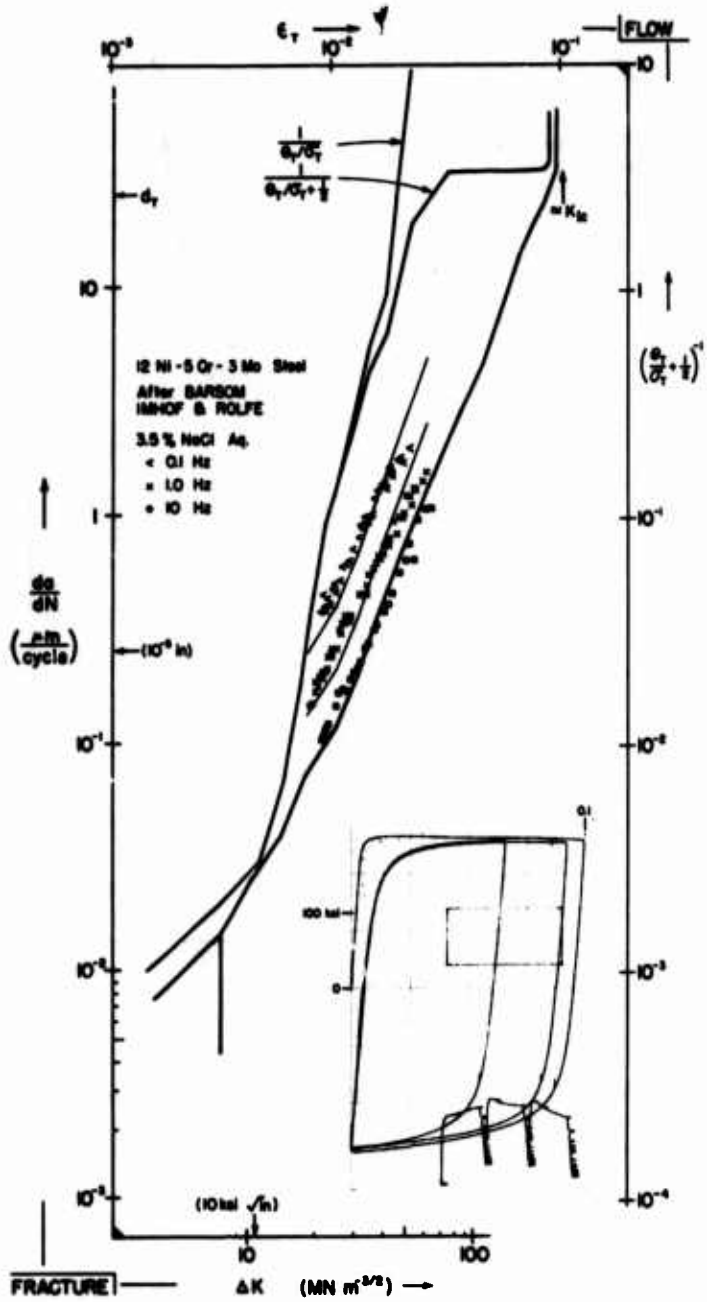


Fig. 11 - Barsom's longer dwell times of lower cyclic frequency of 12Ni steel in salt water exhibited a marked increase in crack growth rate, interpreted as a high V_g - corrosion rate (Table I and Fig. 21). Typical stress relaxation profile at 10X stress gain, are shown in the test record inset.

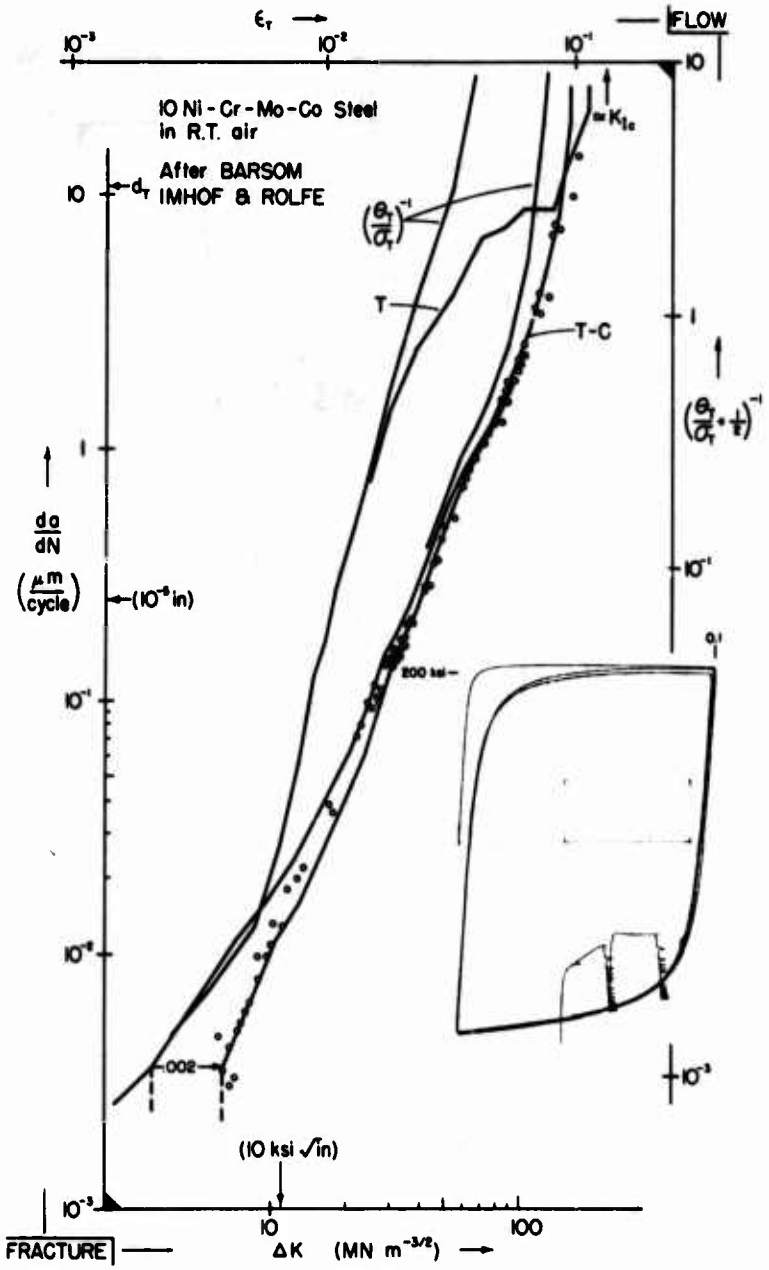


Fig. 12 - The triaxial instability strain of the 10Ni steel, like the 12Ni of Fig. 11, is in agreement with the K_{Ic} value, and far larger than the uniaxial maximum load point.

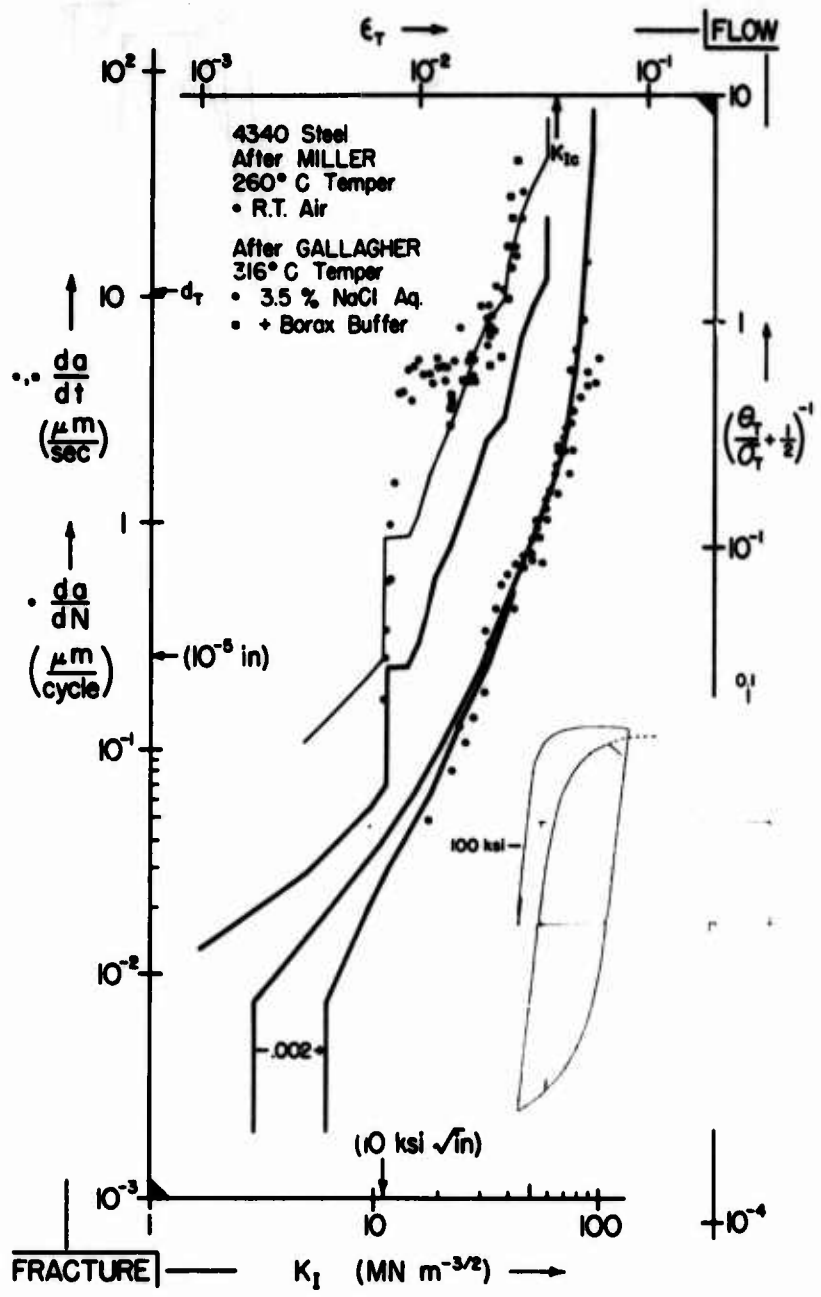


Fig. 13 - The fatigue propagation rate of 4340 steel is fitted by cyclic flow prediction, and stress corrosion cracking by the first tension excursion, The upward shift in matching indicative of a severe environmental sensitivity, high V_g (Fig. 21) in salt water.

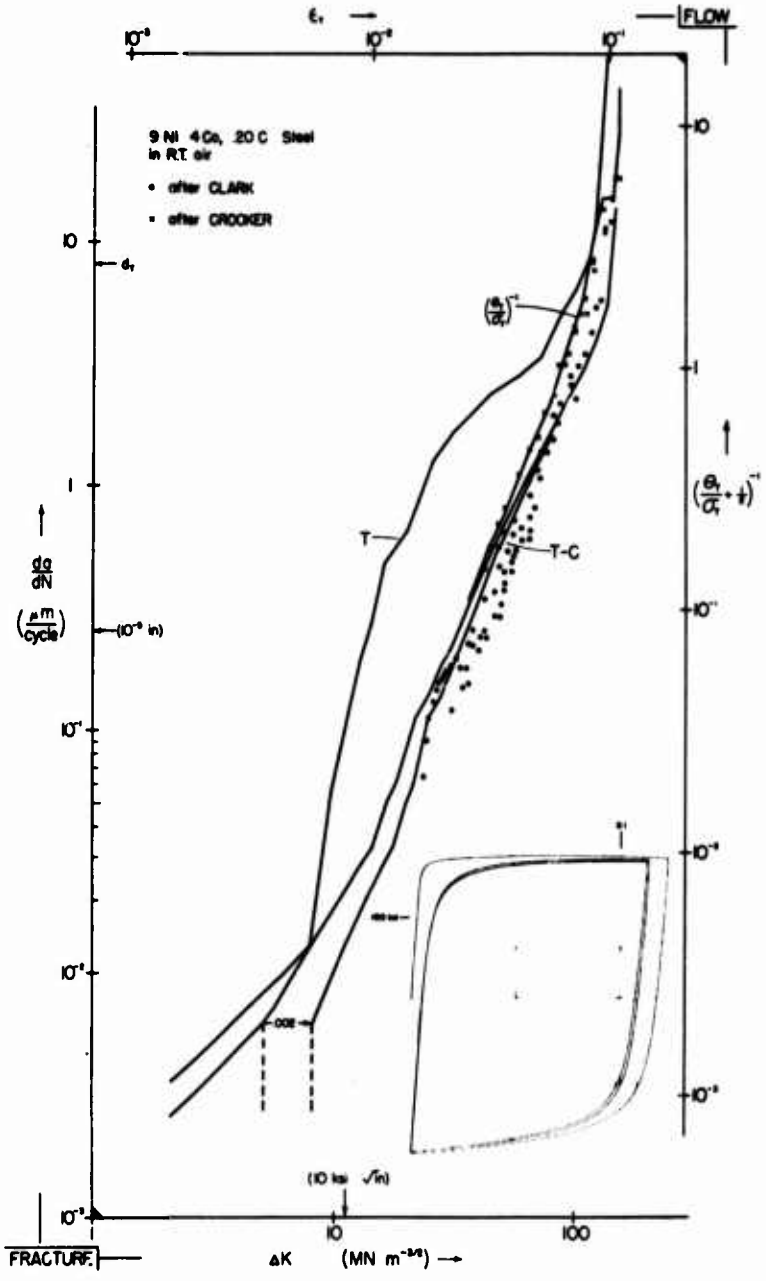


Fig. 14 - Fracture-Flow diagram for 9Ni, 4Co, 0.20C steel.

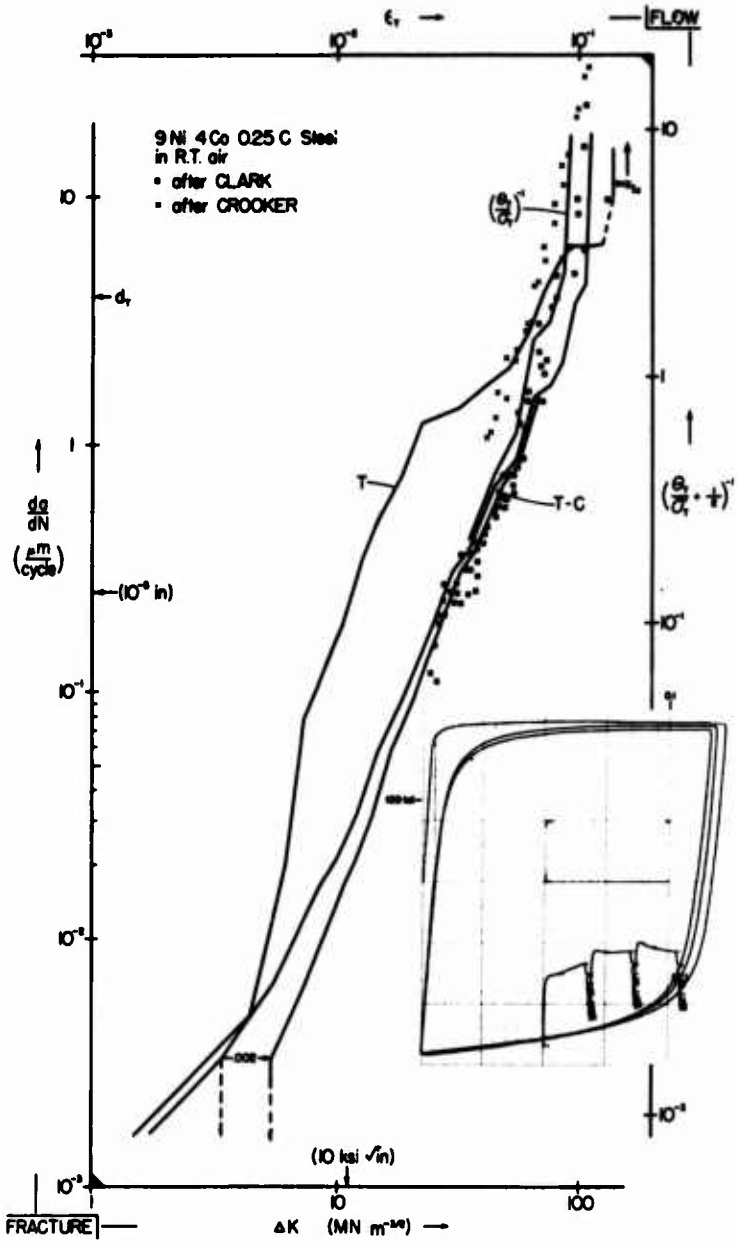


Fig. 15 - Fracture-Flow diagram for 9Ni, 4Co, 0.25C steel.

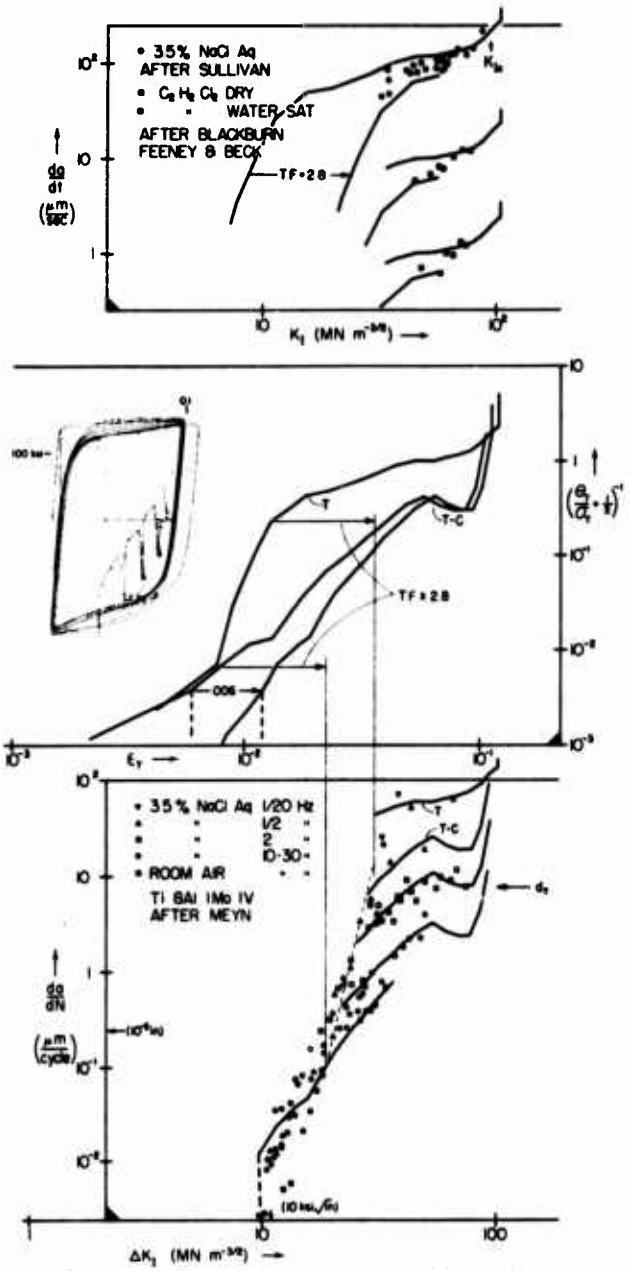


Fig. 16 – The two stage hardening effect in 8-1-1 titanium (center inset) gives an inflection in growth rate (center plot) reflected in Meyn's fatigue data (lower plot). His growth increase with cycle duration yields a V_S value consistent with that for Sullivan's stress corrosion cracking velocity (upper plot). The Blackburn et al data is also matched to first cycle flow prediction with reduced V_S for CH_2Cl_2 environment.

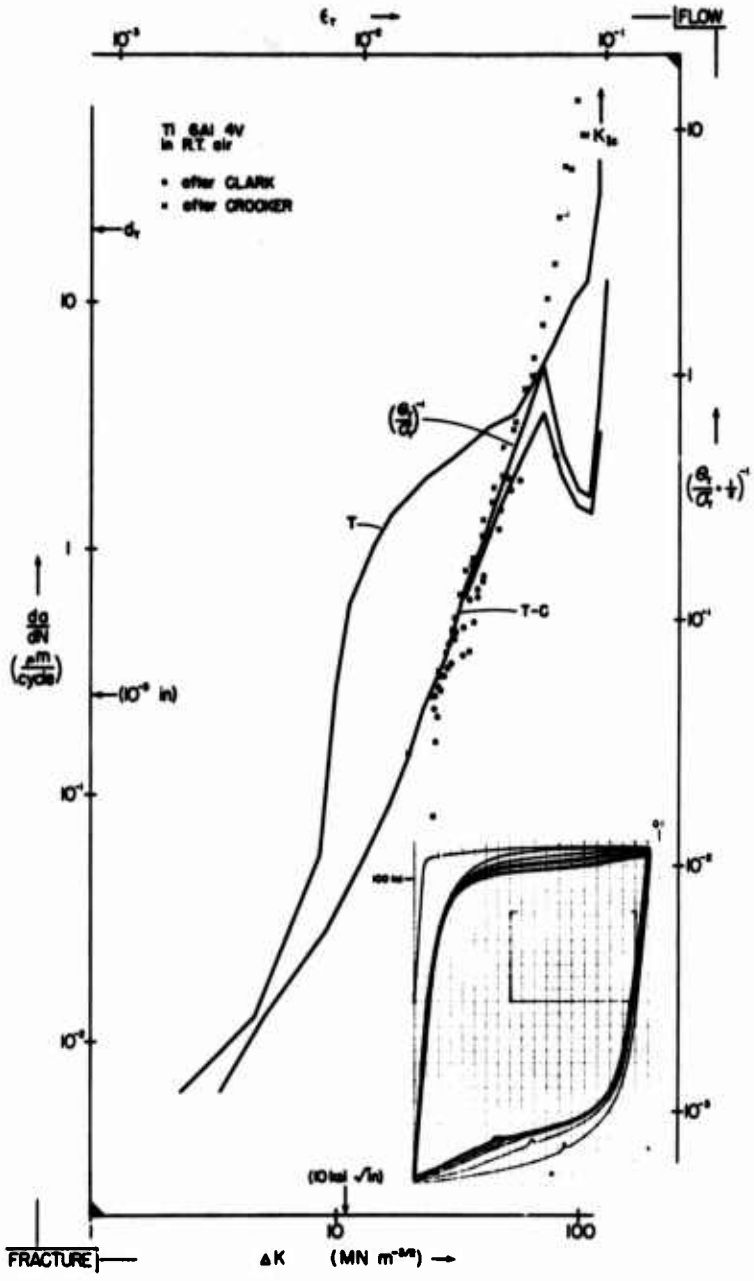


Fig. 17 - Fracture-Flow diagram for 6 Al 4V titanium.

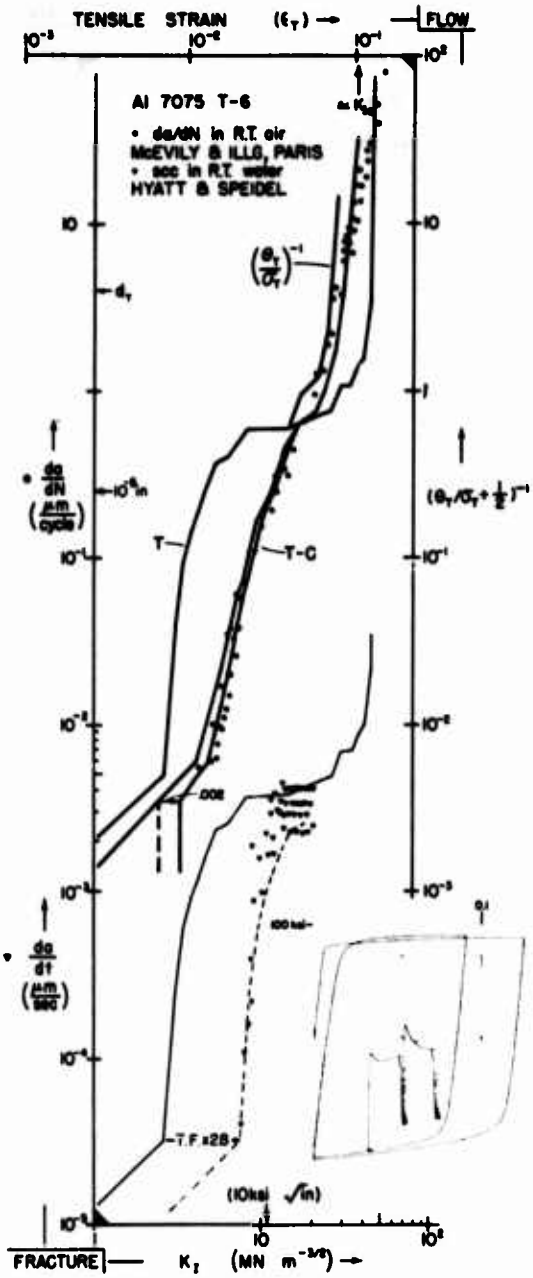


Fig. 18 - The Fracture-Flow diagram match for 7075-T6 aluminum shows agreement with the stress corrosion velocity results of Hyatt and Speidel, the downward translation of first cycle prediction indicative of a slow (V_S) corrosion effect (Fig. 21).

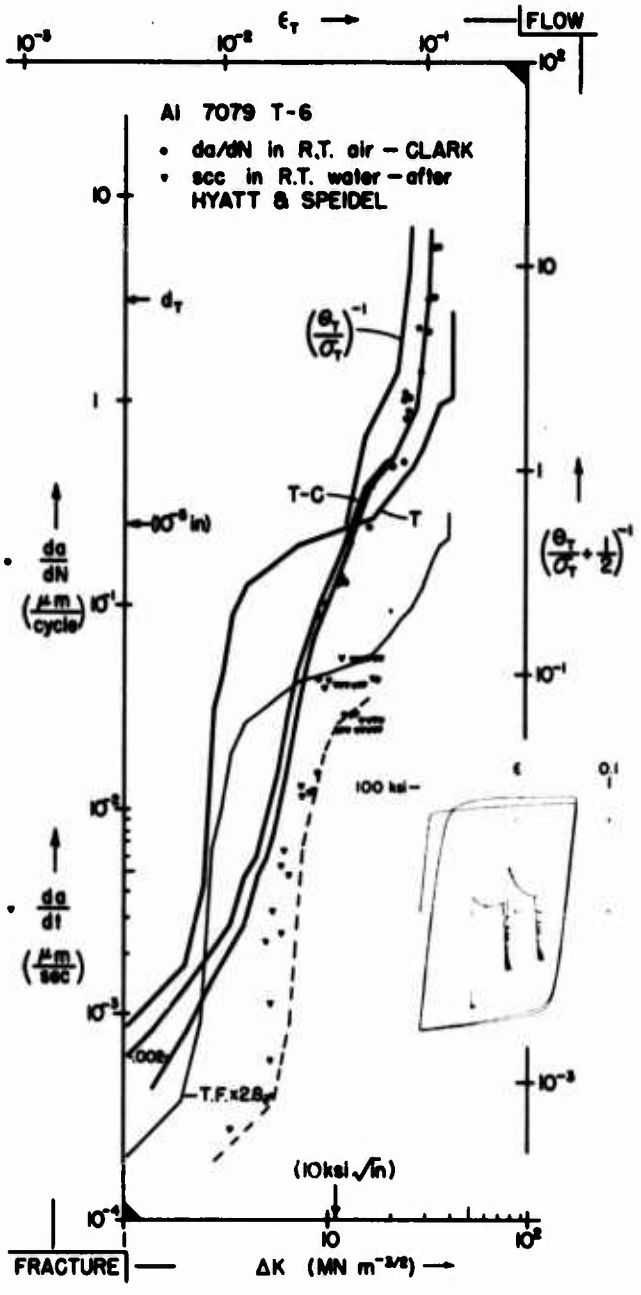


Fig. 19 - The 7079-T6 Aluminum shows somewhat more susceptibility to SCC, or higher V_S than 7075 of Fig. 18.

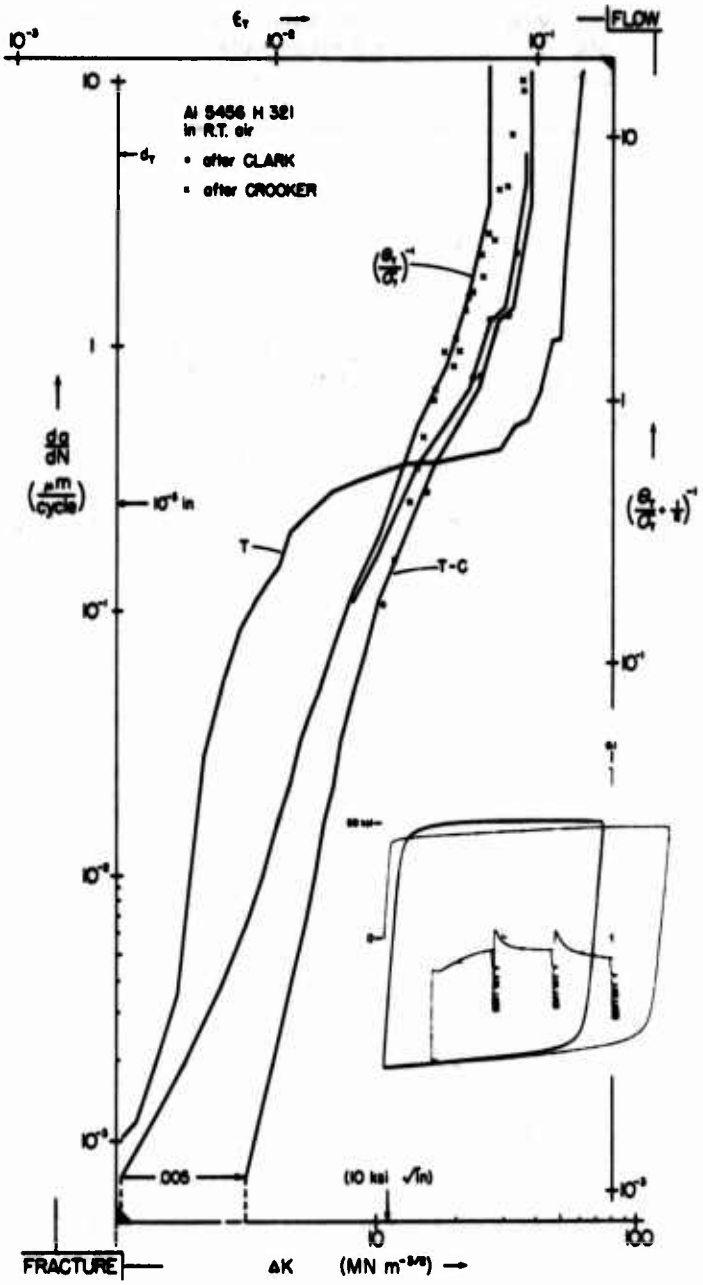


Fig. 20 - Fracture-Flow diagram for 5456-T321 Aluminum.

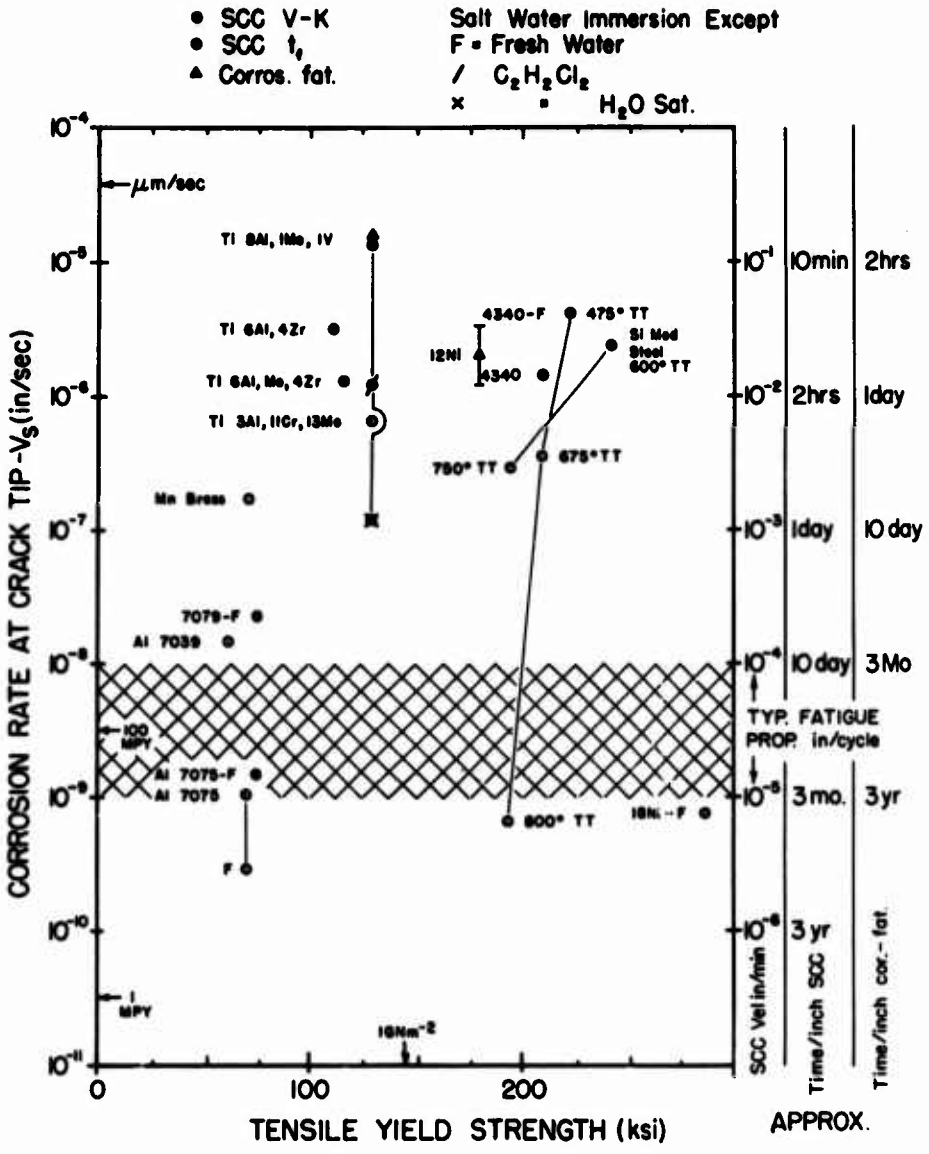


Fig. 21 - The great variability in corrosion-fatigue susceptibility (V_S) is seen in plot, vs tensile yield strength, of data from this paper as well as previous work (16). Consistency among values of V_S by different assessment methods is encouraging. For a structure loaded once a minute, V_S values above band will reduce life expectancy.

Protection contre la corrosion marine sous tension d'alliages d'Aluminium par des revêtements d'oxydes d'Aluminium hydratés ou non et des aciers par des revêtements de Fe_3O_4. I.Alliages d'Al.

Prof. Dr. Ing. Chem. Th. Skoulikidis, Ing. Chem. A. Karageorgos.

Chaire de Chimie Physique et d'Electrochimie appliquée. Université National Technique, Athènes 146, Grèce.

Dans le but de protéger les alliages d'aluminium contre la corrosion marine sous tension, on a préparé sur les surfaces des éprouvettes en alliages d'aluminium par oxydation anodique: γ_1-Al_2O_3, γ_2-Al_2O_3, γ_1-$Al_2O_3 \cdot 3H_2O$, γ_2-$Al_2O_3 \cdot H_2O$. On a varié la densité du courant, l'épaisseur et surtout l'orientation des cristaux envers la direction de la traction future et le temps entre la préparation des oxydes et des hydrates. Sur chaque sorte d'éprouvette, on a pris des courbes potensiostatiques et des courbes poids-temps de fracture (circulation d'eau de mer et charge positive des éprouvettes pour diminuer le temps de fracture; utilisation des éprouvettes mécaniquement et électrolytiquement (dissolution anodique) pre-fracturées (pre-cracked). Des pareilles préparations et mesures ont été faites pour Fe_3O_4 sur des aciers. On a trouvé que les conditions de la préparation des oxydes et leurs hydrates, surtout l'orientation de leurs cristaux, influence considérablement leurs propriétés protectrices et mécaniques et certaines entre eux conduisent à des revêtements, qui protègent les alliages d'aluminium et les aciers contre la corrosion marine sous tension. On discute aussi les propriétés différentes des éprouvettes mécaniquement et électrolytiquement préparées, ce qui peut aider à l'interprétation du phénomène de la corrosion sous tension de ces alliages.

Key Words: γ_1-Al_2O_3, γ_2-Al_2O_3, γ_1-$Al_2O_3 \cdot 3H_2O$, γ_2-$Al_2O_3 \cdot 3H_2O$ orientés; Fe_3O_4 orienté; Eprouvettes mécaniquement pre-fracturées; Eprouvettes électrolytiquement pre-fracturées.

---

1. Introduction

Comme il est connu, les γ_1-Al_2O_3, préparés par oxydation anodique sur la surface d'alliages d'aluminium, exercent une protection contre la corrosion générale et par picures de ces alliages.

Au contraire, l'existence des ces oxydes sur la surface des ces alliages accélère la corrosion sous tension (1-3). Les raisons sont que les pores des ces oxydes et les fractures, qui se produisent à la couche des oxydes, dès qu'on charge une éprouvette par un poids au dessus d'une valeur limite agissent comme si les éprouvettes étaient pré-fracturées (pre-cracked): concentration des tensions mécaniques et augmentation de la densité du courant (phénomène d'une petite anode envers une grande cathode). Alors, la structure secondaire et les propriétés mécaniques des oxydes ne sont pas appropriées pour effectuer une protection contre la corrosion sous tension.

On constate le même comportement (accélération de la corrosion sous tension) pour des éprouvettes revêtées des γ_1-$Al_2O\cdot 3H_2O$ (colmatation) (1-3), mais les résultats sont meilleurs. On trouve dans la bibliographie (1,2,4, 5), que seulement la colmatation des ces oxydes par dichromates conduit à la préparation des couches, qui exercent une protection à la corrosion sous tension (p.).

Mais on constate aussi, par le dépouillement de la bibliographie, que:

a. Pendant la préparation des γ_1-Al_2O_3 et γ_1-$Al_2O_3\cdot 3H_2O$ utilisés, toute la variété des conditions n'a pas été épuisée: densité du courant, temperature, vieillissement avant d'être colmatés, conditions de la colmatation, qui pouvaient conduire à des propriétés structurelles et mécaniques améliorées.

b. N'étaient pas utilisés les γ_2-Al_2O_3-couche d'oxyde, l'existence de laquelle nous avons constaté, il y a plusieurs années, sur la couche de γ_1-Al_2O_3, après une épaisseur de 36µ de celui-ci (6-7), qui possède des propriétés structurelles et mécaniques très différentes des γ_1-Al_2O_3 (8-11)-et γ_2-$Al_2O_3\cdot 3H_2O$.

c. On n'avait pas joué avec l'orientation des grains des oxydes envers la direction de la future traction. Condition, qui influence la structure et les propriétés mécaniques des métaux électrolytiquement déposés (12-14) et pouvant influencer aussi, les propriétés des oxydes, préparés par oxydation anodique.

Ces raisons ont été des arguments suffisants pour reenvisager le sujet.

C'est ainsi que,par des mesures préliminaires, les résultats desquelles ont été présentées à la conférence d'OTAN-AGARD (15), Athènes, 1970 et à la conférence d'OTAN, Ericeira, Lisbone, 1971 (16), on a constaté que, en effet, les conditions ci-haut mentionnées, influencent les propriétés des revêtements et améliorent les résultats au point de vue de la protection des alliages d'aluminium, aussi bien que des aciers (revêtement de Fe_3O_4).

On peut voir ces résultats sur les diagrammes Fig.1a,b et 2a,b où ▮ symbolise des éprouvettes perpendiculaires et ═ horizontales, pendant l'oxydation anodique (p.).

Aux diagrammes 1a,b, on constate la variété des résultats selon la variété des revêtements (γ_1-$Al_2O_3\cdot 3H_2O$: 2,3,4,6,7; γ_2-$Al_2O_3\cdot 3H_2O$: 5,8,9) et du vieillissement préalable des γ_1-Al_2O_3 et γ_2-Al_2O_3 (2,3,5,8), de la méthode de la colmatation (3,4) et de l'orientation (2,6-3,7-8,9). Mais tous les résultats ne sont pas meilleurs que ceux sur l'alliage nu.

Au contraire, aux diagrammes 2a,b, l'influence de l'orientation des oxydes Fe_3O_4 a conduit à un retardement apréciable du temps de rupture envers l'acier nu (15,16).

Malgré l'effet que les résultats pour l'alliage d'aluminium n'étaient pas satisfaisants, on a continué les efforts sur ce sujet et on présente, ce qu'on a optenu, ci-dessous.

2. Partie Experimentale

Ia. Protection d'alliages d'aluminium.

A. Forme des éprouvettes, sortes des revêtements et conditions des mesures.

i. Sorte d'alliage, forme et dimentions des éprouvettes.

Les éprouvettes ont été préparées de l'alliage d'aluminium (H.38), ALCAN: 57S (≙ ASTM: 5052) suivant:

Mg: 2,5%, Cr: 0,25%, Fe+Si: 0,45%, Cu: 0,1%, Mn: 0,1%, Zn: 0,1%, Al: 96,5%.

L'alliage était en forme de bandes d'une épaisseur de 0,25mm. On a coupé les éprouvettes parallelement à la direction du laminage, qui coinci-

dait avec la direction de la future traction. On voit la forme et les dimensions des éprouvettes sur la Fig. 3.

ii. Conditions de la préparation des oxydes γ_1 et γ_2 par oxydation anodique.

L'oxydation anodique des éprouvettes, avec les isolations des surfaces indiquées à la Fig.3, avait lieu dans un bain d'acide sulfurique 15%, sous une temperature constante de 25°C et une densité du courant de 1,5A/dm^2, pendant 35 min. pour la préparation des γ_1 et 110min. (6-9) pour la préparation des γ_2 oxydes (6-9).

Un nombre d'éprouvettes étaient posées pendant l'électrolyse perpendiculairement à la surface du bain: ‖ et un nombre parallèlement, c.a.d. horizontalement: ═.

A cause de la circulation du bain sur les surfaces des éprouvettes, pendant l'électrolyse de bas en haut, due à l'évolution de l'oxygène, les grains des oxydes subissent une orientation parallèle à la gravité. C'est ainsi, que dans le cas ‖ , l'orientation des grains des oxydes est parallèle et dans le cas ═ perpendiculaire à la direction du laminage et de la future traction (14,15).

iii. Conditions de la colmatation.

Les oxydes, préparés sous les conditions ci-haut mentionnées, étaient colmatés par immersion dans de l'eau distillée à une temperature de 100°C et pendant 1,5 min. (15).

iv. Dispositif pour les mesures.

Sur les images 4a, 4b et 4c, on voit la manière avec laquelle, on fixait et on chargeait chaque éprouvette. On voit aussi, la possibilité d'une circulation d'une solution corrosive et la possibilité d'une charge positive de l'éprouvette, à l'aide d'une cathode en aluminium, afin d'accélérer la corrosion sous tension.

A chaque éprouvette appartenait un dispositif (Fig.5a,b) sur lequel, s'enregistrait le temps de rupture et avec lequel chaque éprouvette se chargeait positivement (sous densité du courant anodique constante).

v. Conditions des mesures.

Pendant les mesures des temps de rupture, les éprouvettes étaient immergées dans une solution de 1N NaCl, qui, à l'aide des pompes péristaltiques (dosometriques), circulait avec une vitesse constante de 70ml/h.

A cause du fait que la reproductibilité des mesures avec laquelle nous avons obtenu les courbes 1a,b, n'était pas satisfaisante et que le paramètre actif immédiat de l'accéleration, n'est pas la tension électrique, mais la densité du courant anodique, on a effectué les mesures sous charge positive des éprouvettes, de sorte que la densité du courant anodique restait constante: 2mA/cm^2 (mesures galvanostatiques).

B. Mesures et résultats.

i. Courbe de référence.

Sous les conditions ci-haut mentionnées, on a effectué des mesures sur des éprouvettes d'alliage d'aluminium nu, pour trouver la courbe de référence afin de faire la comparaison avec les résultats des mesures sur des éprouvettes revêtées. On voit les résultats sur les diagrammes 6a,b et c.

ii. Mesures sur des éprouvettes revêtées.

a) Densité du courant anodique: 2mA/cm^2. Densité du courant pendant la préparation des oxydes: 1,5A/dm^2.

On a effectué des mesures sur des éprouvettes revêtées de γ_1-Al_2O_3 ═, γ_2-Al_2O_3 ═, γ_1-$Al_2O_3 \cdot 3H_2O$ ‖ , ═ et γ_2-$Al_2O_3 \cdot 3H_2O$ ‖ , ═ préparées comme ci-haut mentionné et obtenu le diagramme suivant (Fig. 7), où on a aussi présen-

té les résultats sur les γ_1-$Al_2O_3 \cdot 3H_2O$ ‖ , colmatés par dichromates (p.).

On constate à ce diagramme, encore une fois (v.Fig.1a,b et 2a,b), la grande influence de l'orientation des oxydes (comparaison entre 2,3 et 4,5) et les résultats plus satisfaisants de l'orientation ═. Le seul résultat, qui ne coincide pas avec le diagramme 1a,b est, que en diagramme 7 le γ_2-$Al_2O_3 \cdot 3H_2O$ ═ montre des qualités meilleurs que le γ_2-$Al_2O_3 \cdot 3H_2O$ ‖, ce qui n'est pas le cas pour les mêmes hydrates au diagramme (1a,b). On peut donner l'explication, qu'à cause de la plus grande résistance électrique du γ_2-$Al_2O_3 \cdot 3H_2O$ ‖ envers le γ_2-$Al_2O_3 \cdot 3H_2O$ ═, quand on charge tous les deux avec la même tension électrique constante, la densité du courant est plus petite pour ‖ que pour ═. C'est ainsi que le ‖ montre une résistance à la corrosion aux diagrammes 1a,b, plus grande que ═. Mais, quand on charge tous les deux avec la même densité du courant constante le ═ montre une plus grande résistance à la corrosion sous tension que le ‖ . Au contraire, les résistances de γ_1-$Al_2O_3 \cdot 3H_2O$ ‖ et ═ ne sont pas très différentes et c'est pourquoi, potensiostatiquement ou galvanostatiquement, ils montrent le même comportement. La raison de ce comportement différent des γ_2 orientés ‖ ou ═ , au point de vue de leurs résistances électriques à des directions perpendiculaires entre eux, est que le γ_2 est un semiconducteur p-n, beaucoup plus intensif que le γ_1 (11).

On constate aussi au diagramme, que les résultats de toutes les sortes des éprouvettes ne sont pas meilleurs que ceux des éprouvettes nues, y compris celles colmatées par dichromates.

b) Variation de la densité du courant de préparation des oxydes.

On a varié la densité du courant de préparation des oxydes, de sorte qu'elle passait la même quantité du courant: 3150 coul/dm^2 pour γ_1 et 9900 coul/dm^2 pour γ_2 [on a à chaque cas la même épaisseur de la couche (9)] et effectué des mesures pour une charge constante de 10Kg/mm^2. On a obtenu le diagramme suivant (Fig. 8).

On constate au diagramme 8 que, pour toute la variété des oxydes et leurs hydrates, on obtient un maximum des qualités pour une densité du courant de 6A/dm^2, pendant la préparation des oxydes.

Il est intéressant de signaler, que, malgré le fait que les qualités des γ_1-Al_2O_3 et γ_1-$Al_2O_3 \cdot 3H_2O$ au diagramme Fig. 7 (densité du courant de préparation 1,5A/dm^2) sont moins satisfaisantes que les qualités des γ_2-Al_2O_3 et γ_2-$Al_2O_3 \cdot 3H_2O$, préparés sous une densité du courant de 6A/dm^2 montrent des qualités meilleures.

c) Influence du vieillissement des oxydes mêmes et des oxydes avant d'être colmatés.

Nous avons fait les mêmes mesures avec γ_1, γ_2-Al_2O_3 et γ_1, γ_2-$Al_2O_3 \cdot 3H_2O$ et constaté que l'âge des oxydes plus grand que 24h., aussi bien que leur âge avant d'être colmatés, n'était pas en faveur de leurs qualités.

d) Densité du courant de préparation des oxydes: 6A/dm^2.

On a effectué des mesures pour les cas, qui montrent au diagramme Fig. 8, les meilleurs résultats, c.a.d. γ_1-Al_2O_3 ═ et γ_1-$Al_2O_3 \cdot 3H_2O$ ═ sous les mêmes conditions (densité du courant anodique: 2mA/cm^2), mais avec une densité du courant de préparation de 6A/dm^2. On a obtenu le diagramme suivant (Fig. 9), où on a également présenté les résultats sur γ_1-$Al_2O_3 \cdot 3H_2O$ ═ colmatés par dichromates (p.).

Sur le diagramme Fig. 10, on peut faire la comparaison entre tous les résultats obtenus jusqu'ici, y compris les résultats sur γ_1-$Al_2O_3 \cdot 3H_2O$ ‖(1,5A/dm^2) et ═ (6A/dm^2), colmatés par dichromates (p.).

On constate que, malgré les données bibliographiques, les γ_1-$Al_2O_3 \cdot 3H_2O$ (6A/dm^2) colmatés par dichromates, sont pires que toute variété que nous avons préparée pour σ inférieur que 12Kg/mm^2. Ils deviennent meilleurs des quelques variétés par augmentation de σ, mais ils restent toujours pires que γ_1-Al_2O_3 ═ et γ_1-$Al_2O_3 \cdot 3H_2O$ ═ (colmatés dans de l'eau distillée

100°C, 1,5min).

En tout cas, malgré l'amélioration des qualités des couches anodiques, la résistance à la corrosion sous tension des éprouvettes revêtées de ces couches n'est pas meilleure que celle des éprouvettes en alliage nu.

e) Variation de la densité du courant anodique.

Comme il est connu généralement, quand une réaction hétérogène chimique ou électrochimique est accélérée par les conditions, les variétés des propriétés de la surface des corps solides (centre actifs géometriques ou structurals) n'influencent pas la vitesse de la réaction avec le même "poids", que si la réaction était lente.

On attend les mêmes résultats pour les revêtements: si on accélère la rupture au dessus d'une limite, y compris l'effet d'une petite anode envers une grande cathode (p.), on ne pourrait pas révéler les qualités protectrices des revêtements utilisés, qui seraient dissimulées, à cause de la grande vitesse. C'est pourquoi, on a effectué des mesures avec une variété des densités du courant anodique, en employant deux σ (20 et 10Kg/mm^2)[1].

On a constaté que, dans tous les cas, la différence du temps de rupture Δt envers l'alliage nu et celui des différentes couches protectrices entre elles, augmente en faveur des couches protectrices, quand la densité du courant anodique diminue et devient maximum à une densité du courant de 0,5mA/cm^2.

f) Utilisation d'une densité du courant anodique de:0,5mA/cm^2.

C'est sous cette condition qu'on a obtenu le diagramme suivant (Fig.11). On constate que maintenant, les cas γ_1-Al_2O_3 = et γ_1-$Al_2O_3 \cdot 3H_2O$ =, quand les oxydes sont préparés par une densité du courant 6A/dm^2, montrent une protection de la corrosion sous tension envers les éprouvettes nues.

C'est un résultat, le premier, sur lequel on peut baser l'optimisme, qu'avec les mesures, que nous continuons à effectuer, on pourrait améliorer davantage les qualités des ces couches, en précisant l'optimum des leurs qualités dans le cadre de la variation de tout paramètre possible, y compris le paramètre de l'orientation, qui est introduit pour la première fois.

Ib. Contribution au mécanisme de la rupture.

Eprouvettes électrolytiquement pré-fracturées (pre-cracked).

Introduction

Pendant les diverses mesures ci-haut mentionnées, qu'on a effectué pour révéler les qualités mécaniques des couches anodiques, on a constaté:

- Des fractures sur les couches anodiques, dès que les éprouvettes étaient chargées mécaniquement par des valeurs de σ supérieurs d'une valeur limite, correspondante à chaque cas (p.).

- Au dessous de cette valeur limite, la couche restait intacte et après un certain temps, dépendant de la sorte de la couche, de la valeur de σ et de la densité du courant anodique, on pouvait constater des fractures, comme résultat d'une dissolution anodique et de la traction.

- On peut révéler l'existence des fractures aux couches anodiques par le fait que, pour charger les éprouvettes fracturées par une certaine densité du courant anodique, on a besoin d'une tension anodique beaucoup plus petite qu'avant l'apparition des fractures (on peut acquérir la même

[1]Collaboration expérimentale avec Ch. Gryllias et Ch. Spanos, cand.Ing.Chim.

densité du courant avec une tension anodique inférieure), à cause de la résistance électrique des couches intactes.

a. Partie expérimentalle. Résultats préliminaires.

Basés sur ces résultats, on a effectué les mesures suivantes:

i) On a chargé des éprouvettes en alliages d'aluminium revêtées par γ_1-Al_2O_3 = (densité du courant de sa préparation 6A/dm^2) avec un σ=20Kg/mm^2 et par une densité du courant anodique 2mA/cm^2 et mesuré le temps de rupture: valeur moyenne 272 min.

ii) Sous les mêmes conditions, on a chargé des éprouvettes pareilles avec un σ=10Kg/mm^2 et par une densité du courant 2mA/cm^2. Pour cela, on a besoin d'une tension électrique beaucoup plus grande qu'au cas i. On a attendu jusqu'à ce que, par dissolution anodique, les couches des oxydes soient fracturées (diminution de la tension électrique pour avoir la même densité du courant) et à ce moment, on a chargé les éprouvettes par un σ=20Kg/mm^2, soutenu la densité du courant constante et mesuré le temps de la rupture: valeur moyenne 198 min.

En comparant les deux valeurs en i et en ii, on constate, que la rupture en ii a lieu plus vite.

On a pensé, que ce résultat serait peut-être dû au fait, que, au cas ii, il y a un temps de dissolution anodique des couches, pendant lequel les ions d'aluminium migrent vers l'environnement corrosif et qu'à cause de cette migration, il se forme un chemin actif, ce qui accélère la rupture envers le cas i, où les fractures des couches se forment mécaniquement.

Pour prouver cette possibilité, on a préparé des éprouvettes électrolytiquement pré-fracturées (pre-cracked) et comparé avec des éprouvettes mécaniquement pré-fracturées. Les résultats de ces mesures soutenaient l'idée ci-haut mentionnée: les éprouvettes électrolytiquement pré-fracturées accéleraient le phénomène envers les éprouvettes mécaniquement pre-cracked. Ces résultats préliminaires ont été présentés à la conférence d'OTAN-AGARD, Athènes, 1970 et à la conférence d'OTAN, Lisbone, 1971. On présente ci-dessous, les résultats des nouvelles mesures.

b) Mode de préparation des éprouvettes électrolytiquement pré-fracturées.

On met les éprouvettes dans un bain de CH_3OH:HNO_3 (condensé)=2:1 comme anode, après avoir isolé toute leur surface, sauf les endroits destinés pour la préparation des fractures initiales (Fig. 12) de forme triangulaire (hauteur 0,5 mm, base 1 mm) et avec une densité du courant de 30A/dm^2 on provoque par dissolution anodique des fractures, à peu près des dimensions mentionnées. On donne mécaniquement les dimensions précises.

c) Mesures et résultats.

Sur des éprouvettes mécaniquement et électrolytiquement pré-fracturées et sous les mêmes conditions (p.), on a effectué des mesures de temps de rupture. On a constaté (Fig.13) que les éprouvettes électrolytiquement pré-fracturées accélèrent le phénomène, plus que les éprouvettes mécaniquement pré-fracturées, en accord avec les données des expériences de la paragr. a. On a aussi effectué les mêmes mesures sur les deux sortes d'éprouvettes, après avoir coupé les tranches du matériau, qui contenaient les fractures initiales (Fig.14) et obtenu les résultats de la Fig.13. On voit sur ce diagramme, que les éprouvettes préalablement électrolytiquement pré-fracturées accélèrent le phénomène beaucoup plus, que les éprouvettes préalablement mécaniquement pré-fracturées.

On se trouve alors, devant un chemin actif, qui se forme pendant le phénomène initial de la corrosion et la formation des fractures initiales.

On peut prouver l'existence de ce chemin actif par électrographie, par des réactifs colorants et par la méthode d'exo-électrons.

Il faut noter de plus, qu'à des éprouvettes électrolytiquement pré-

fracturées, la rupture a toujours lieu à l'endroit où elles étaient pré-fracturées, même si on enlève les tranches du matériau ci-haut mentionnées, ce qui n'est pas le cas pour les éprouvettes mécaniquement pré-fracturées. De plus, avec elles, on imite la réalité, c.a.d. le mode de la dissolution anodique avec laquelle se forme la fracture initiale.

CONCLUSIONS

1) En utilisant une densité du courant de $6A/dm^2$ pour la préparation, par oxydation anodique, des γ_1-Al_2O_3 et γ_2-Al_2O_3 dans un bain d'acide sulfurique sur les surfaces des éprouvettes en alliages d'aluminium, on constate que ces revêtements montrent des qualités mécaniques satisfaisantes, si leurs oxydes sont orientés perpendiculairement à la direction de la future traction. On peut donner cette orientation aux oxydes si, pendant l'oxydation anodique, les éprouvettes sont posées horizontalement, de sorte que la direction de l'évolution de l'oxygène, coincidente avec la direction de la gravité, soit perpendiculaire à la direction de la future traction.

2) On constate aussi, une amélioration des qualités des γ_1-$Al_2O_3 \cdot 3H_2O$ et γ_2-$Al_2O_3 \cdot 3H_2O$, si les oxydes sont formés de la façon ci-haut mentionnée, vieillis pendant 24h. et transformés en hydrates dans de l'eau distillée de 100°C, pendant 1,5min.

3) Les γ_1-Al_2O_3 = et γ_1-$Al_2O_3 \cdot 3H_2O$ = préparés par la méthode ci-haut mentionnée, possedent les meilleures qualités mécaniques, qui conduisent à une protection de la corrosion sous tension (v. 4).

4) Si on accélère la corrosion sous tension au dessus d'une limite, les différentes qualités des différents revêtements se dissimulent partiellement et, à cause de l'effet d'une petite anode envers une grande cathode, on ne peut pas révéler leurs qualités protectrices envers l'alliage nu. C'est pourquoi, il ne faut pas dépasser les $0,5mA/cm^2$ comme densité du courant anodique pendant les mesures.

5) Le différent comportement des éprouvettes pré-fracturées, préparées mécaniquement et électrolytiquement, y compris les autres expériences déjà décrites, conduit à la conclusion que, pendant la dissolution anodique dirigée au spontanée, à cause de la diffusion des ions du métal, se forme un chemin actif, qui accélère la corrosion sous tension.

On peut alors, ajouter aux causes de l'existence du chemin actif: préexistence, formation à cause de la tension mécanique, formation à cause de la diffusion des substances de l'environnement corrosif, une quatrième cause: formation du chemin actif, pendant le stade initial de la corrosion en forme de dissolution anodique aux centres actifs, géometriques ou structurals, due à la diffusion des ions d'aluminium en état solide.

BIBLIOGRAPHIE

1. F. HAYNIE et W. BOYD: "Stress Corrosion Cracking of Aluminum Alloys", D.M. I.C. Report 228, Battelle Memorial Institut, Ohio, Juillet 1966.
2. H. COLE: "The Influence of Surface and Protective Treatements on Stress Corrosion Behaviour", 29th Meeting of AGARD, Instambul, 1969.
3. D. BRUNGS et W. GRUHL, Werkstoffe and Corrosion 20, 4, 314 (1969).
4. J. JACKSON et W. BOYD: "Stress Corrosion Cracking of Aluminum Alloys",D.M. I.C. Memorandum 202, Battelle Memorial Institut, Ohio, Fevrier, 1965.
5. T. HUMPHRIES: "Stress Corrosion of High Strength Aluminum Alloys", Report No M.T.P.-P et VE M-63-8, NASA/Georges C. Marshall Space Flight Center, Alabama, Juin 1963.
6. TH. SKOULIKIDIS, S. KARALIS et P. MENTOJIANNIS, Kolloid Z.,149, 6 (1956).
7. TH. SKOULIKIDIS, CH. PAPATHANASIOU et J. MARANGOSIS, Kolloid Z.150,54(1957)

8. TH. SKOULIKIDIS, P. MALLIOS et K. KAZANTZIS, Kolloid Z. 159, 130 (1958).

9. TH. SKOULIKIDIS, G. PARASKEVOPOULOS et D. ARGYRIOU, Kolloid Z. 23, 29 (1960).

10. TH. SKOULIKIDIS et P. BEKIAROGLOU, Kolloid Z. 178, 45 (1961).

11. TH. SKOULIKIDIS et K. SARROPOULOS, Disertation (K.S), Université Technique d'Athènes, 1962.

12. TH. SKOULIKIDIS et P. KARADIMOS, Ann. Chim. (Athènes), 22, 147 (1957).

13. TH. SKOULIKIDIS, Ann. Chim. (Athènes), 22, 84 (1957).

14. TH. SKOULIKIDIS et Z. CHANIOTIS, Ann. Techn. (Athènes), 5, (1960).

15. TH. SKOULIKIDIS, A. KARAGEORGOS, K. LAOUDIS, N. KOULOUMBI, 30e Confér. OTAN-AGARD, Athènes, 1970.

16. TH. SKOULIKIDIS, Confér. OTAN, Ericeira, (Lisbone), 1971. (Invited paper).

Discussion

Comment: Il est très intéressant que l'histoire de l'oxydation joue un rôle dominant. Nous avons recherché dans un autre cas l'influence du rapport de pression oxygène/argon sur l'oxydation du fer. On trouve que l'oxyde qui se forme très lentement a une résistance plus élevée aux attaques par corrosion que l'oxyde qui se forme relativement rapidement. Je crois que le défaut aux cristaux de l'oxyde donne la réponse et j'imagine que la vitesse est influencée par l'orientation des cristaux des matériaux.

Skoulikidis: Si j'ai bien compris, vous avez dit que les qualités des oxydes dépendent de la vitesse pendant la préparation. Oui et cà dépend de deux points de vue: vous avez d'abord la grandeur des cristaux qui influence les propriétés mais, de plus, vous avez une augmentation de N semi-oxyde aluminium métal semi-conducteur AP; si vous avez une grande vitesse, la qualité des semi-conducteurs N augmente; alors vous avez ici un genre de protection cathodique car, par le métal, nous avons une diffusion des électrons et des ions. Mais l'oxyde, qui est un semi-conducteur, tend à donner des électrons au métal alors nous avons ici un cas de protection cathodique contre la corrosion et si nous avons une influence aux qualités mécaniques de l'oxyde on augmente la vitesse.

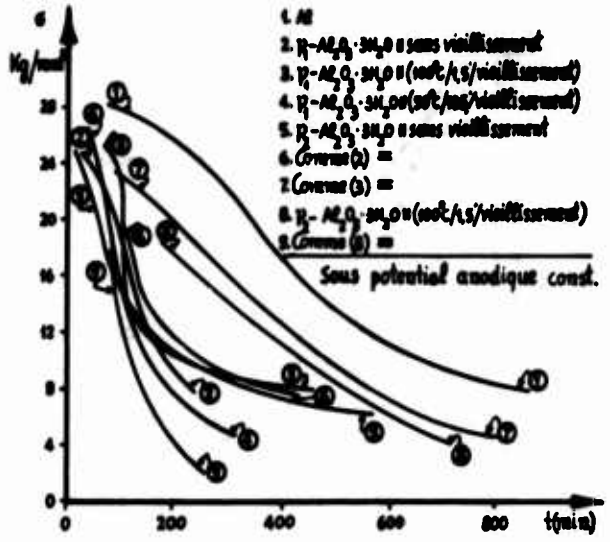

1. Al
2. β_1-$Al_2O_3 \cdot 3H_2O$ sans vieillissement
3. β_1-$Al_2O_3 \cdot 3H_2O$ (100°C/1,5'/vieillissement)
4. β_1-$Al_2O_3 \cdot 3H_2O$ (30°C/10J'/vieillissement)
5. β_2-$Al_2O_3 \cdot 3H_2O$ sans vieillissement
6. Comme (2) =
7. Comme (3) =
8. β_2-$Al_2O_3 \cdot 3H_2O$ (100°C/1,5'/vieillissement)
9. Comme (8) =
Sous potentiel anodique const.
Kg/mm²
t(min)

Fig. 1a

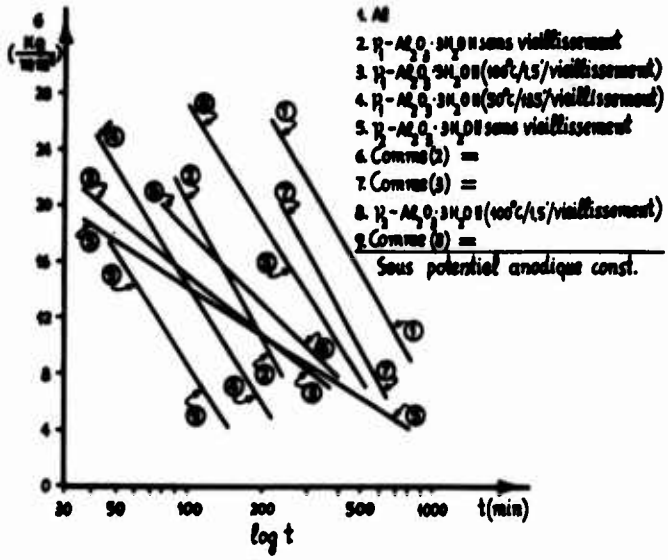

1. Al
2. β_1-$Al_2O_3 \cdot 3H_2O$ sans vieillissement
3. β_1-$Al_2O_3 \cdot 3H_2O$ (100°C/1,5'/vieillissement)
4. β_1-$Al_2O_3 \cdot 3H_2O$ (30°C/10J'/vieillissement)
5. β_2-$Al_2O_3 \cdot 3H_2O$ sans vieillissement
6. Comme (2) =
7. Comme (3) =
8. β_2-$Al_2O_3 \cdot 3H_2O$ (100°C/1,5'/vieillissement)
9. Comme (8) =
Sous potentiel anodique const.
t(min)
log t

Fig. 1b

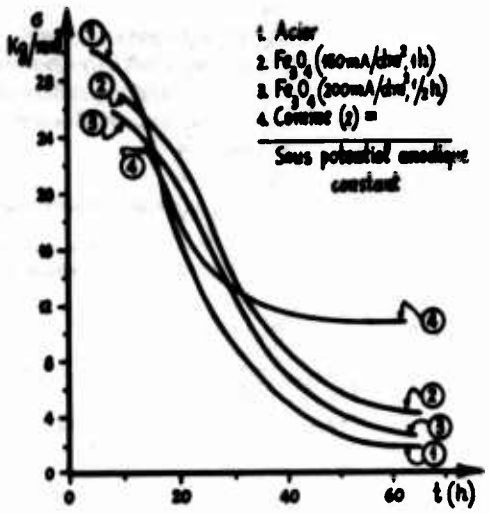

σ
Kg/mm²
28
24
20
16
12
8
4
0
0
20
40
60
t (h)
1. Acier
2. Fe_3O_4 (150mA/dm², 1h)
3. Fe_3O_4 (200mA/dm², ½h)
4. Couche (2) =
Sous potentiel anodique
courant

Fig. 2a

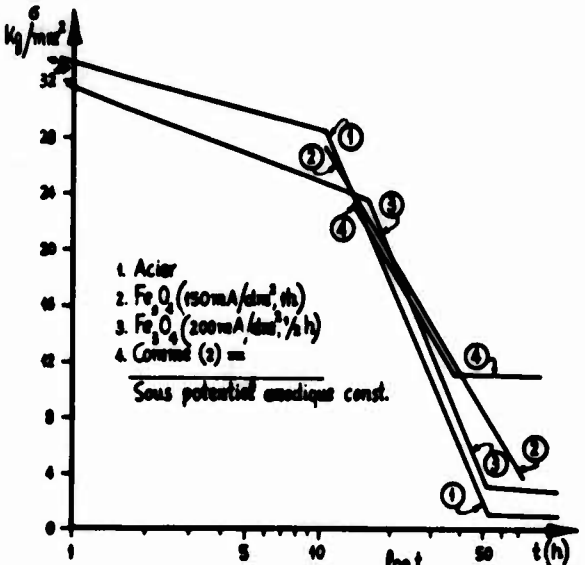

σ
Kg/mm²
32
28
24
20
16
12
8
4
0
1
5
10
log t
50
t (h)
1. Acier
2. Fe_3O_4 (150mA/dm², 1h)
3. Fe_3O_4 (200mA/dm², ½h)
4. Couche (2) =
Sous potentiel anodique const.

Fig. 2b

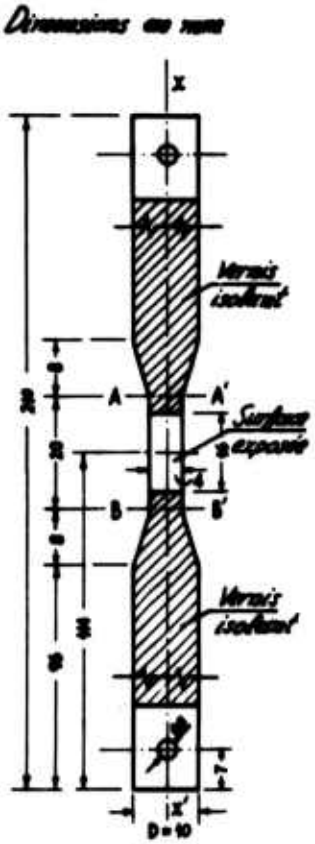
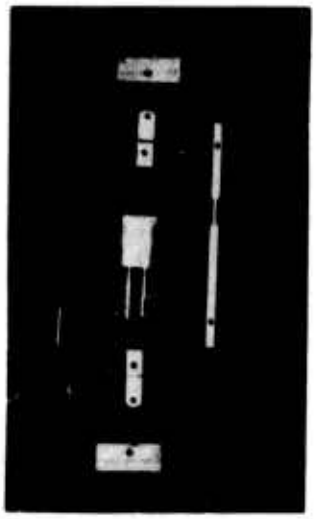
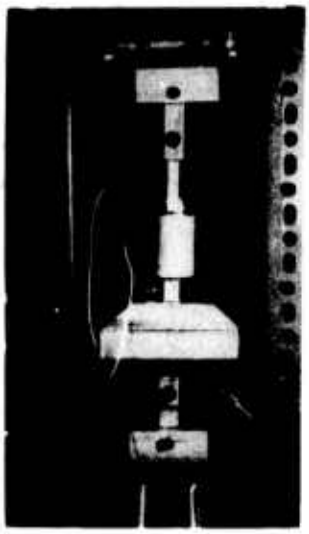


Fig. 3


Fig. 4a


Fig. 4b

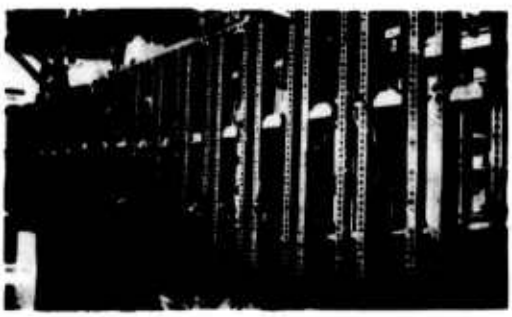

Fig. 4c


Fig. 5a


Fig. 5b

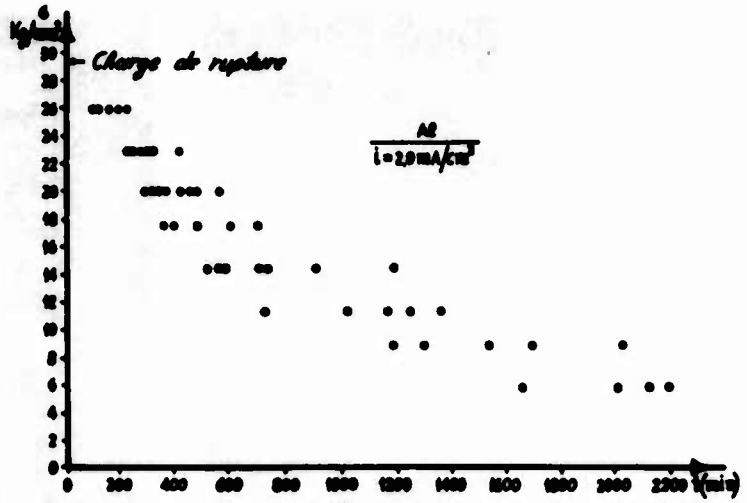
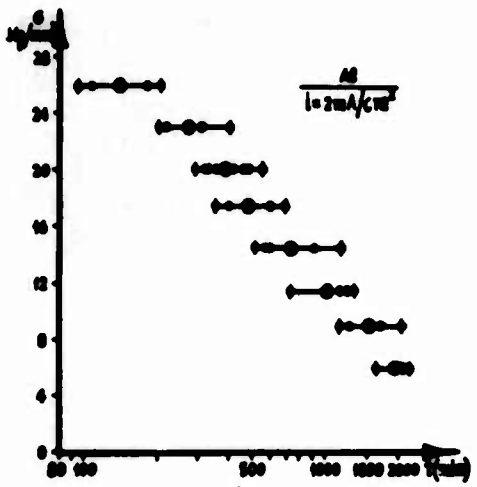
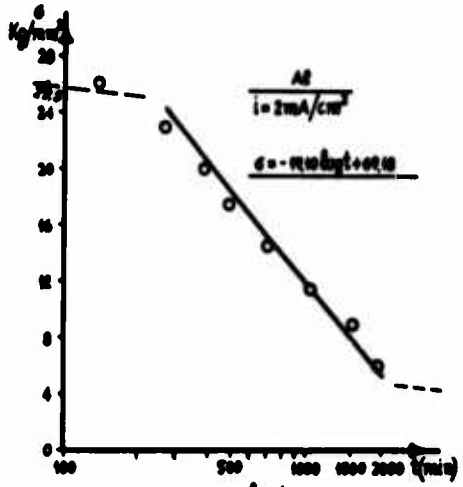


Fig. 6a



log t

Fig. 6b



log t

Fig. 6c

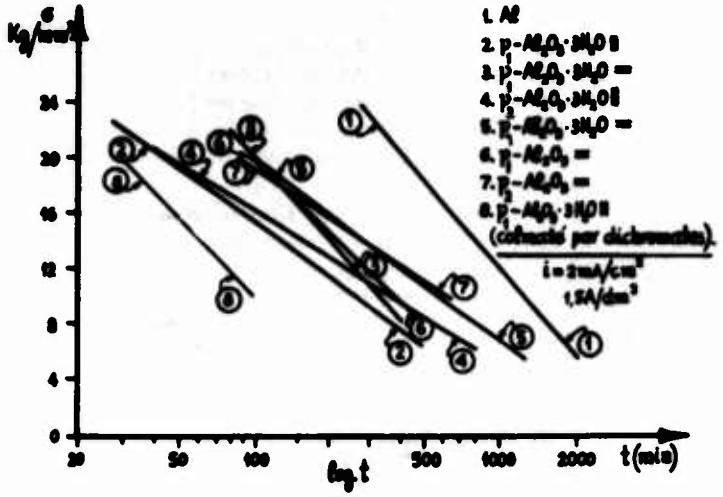


Fig. 7

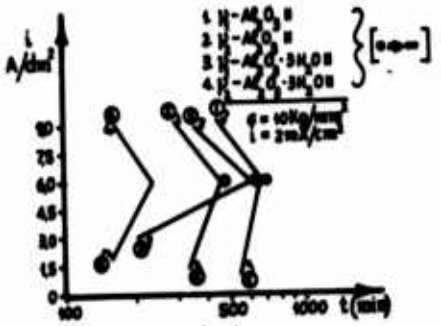


Fig. 8

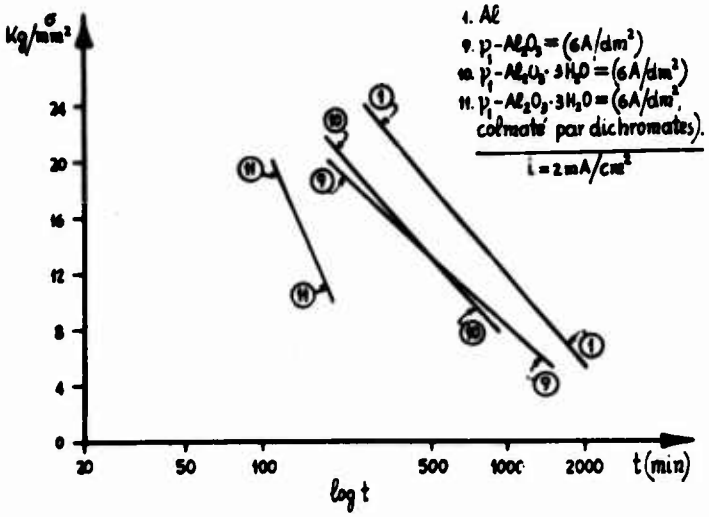


Fig. 9

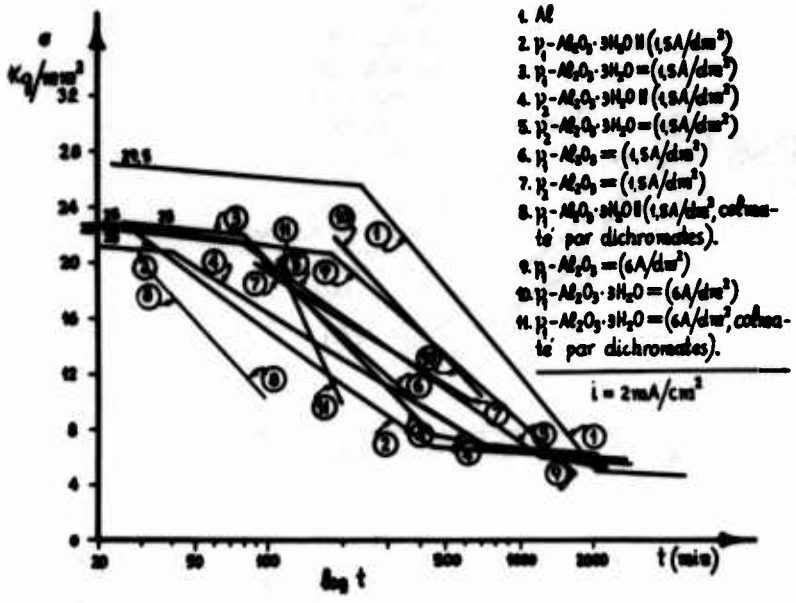

σ
Kg/mm²
32
28
24
20
16
12
8
4
0
20
50
100
500
1000
2000
t (min)
lg t
1. Al
2. γ1-Al2O3·3H2O II (1,5A/dm²)
3. γ1-Al2O3·3H2O = (1,5A/dm²)
4. γ2-Al2O3·3H2O II (1,5A/dm²)
5. γ2-Al2O3·3H2O = (1,5A/dm²)
6. γ1-Al2O3 = (1,5A/dm²)
7. γ2-Al2O3 = (1,5A/dm²)
8. γ1-Al2O3·3H2O II (1,5A/dm², colmatè par dichromates).
9. γ1-Al2O3 = (6A/dm²)
10. γ1-Al2O3·3H2O = (6A/dm²)
11. γ1-Al2O3·3H2O = (6A/dm², colmatè par dichromates).
i = 2mA/cm²

Fig. 10

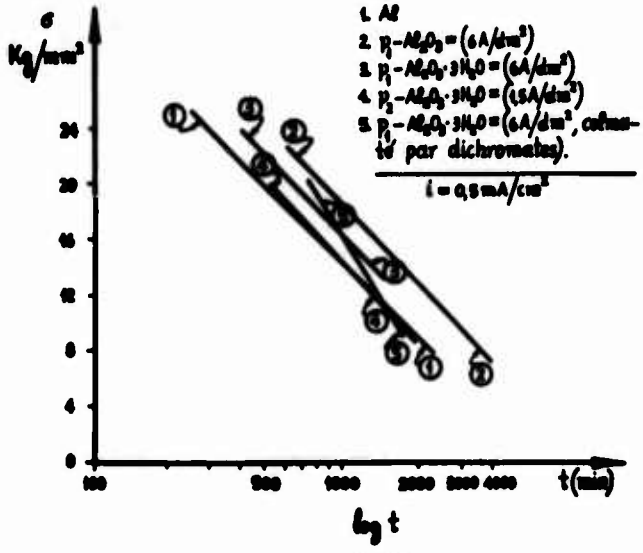

σ
Kg/mm²
24
20
16
12
8
4
0
100
500
1000
2000
3000
4000
t (min)
lg t
1. Al
2. γ1-Al2O3 = (6A/dm²)
3. γ1-Al2O3·3H2O = (6A/dm²)
4. γ2-Al2O3·3H2O = (1,5A/dm²)
5. γ1-Al2O3·3H2O = (6A/dm², colmatè par dichromates).
i = 0,5mA/cm²

Fig. 11.

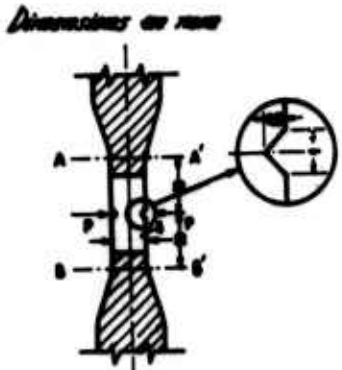


Fig. 12

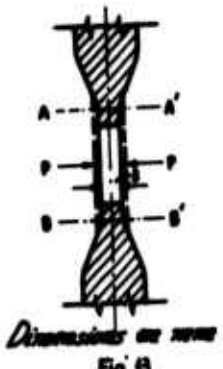


Fig. 13

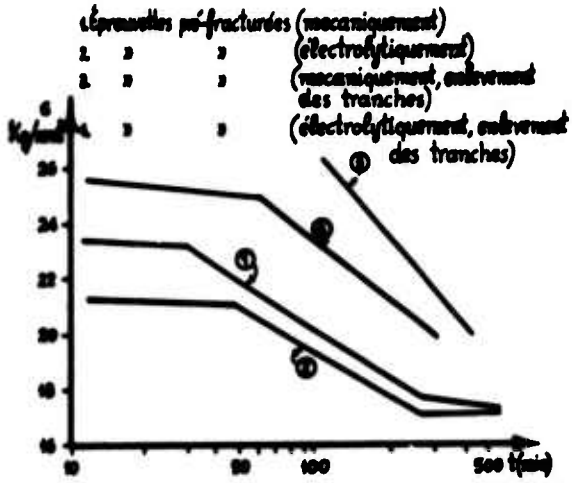


Fig. 14

Stress Corrosion Cracking in Marine Environments

J.C. Scully

Department of Metallurgy

University of Leeds, England

Stress corrosion cracking is observed in a wide range of metallic materials that are employed in marine environments and its occurrence represents a major form of component failure. It can be divided into two separate processes: crack nuclation and crack propagation. Both require chemical conditions arising from highly localized hydrolysis reactions within relatively stagnant regions, for example within crevices, which give rise to a local fall in the solution pH. Such events appear to occur during cracking in ferrous, aluminium and titanium alloys. Notches and cracks exert a mechanical influence upon initiation by causing a localized increase in stress and stress intensity factor (K). Propagation rates are highly dependent upon the value of K, generally up to a maximum propagation rate.

The propagation process can be conceived as a repetitive film breakdown and repair process caused by the interaction of the plastic deformation of the alloy occurring at the crack tip surface with the environment within that region. Electrochemically, the film repair process, repassivation, is of critical importance. It is dependent upon electrode potential, solution composition and pH. Physically, the deformation and tearing behaviour of the alloy is important since these processes create fresh metal area.

The important corrosion reaction may be an anodic or cathodic process. Selective dissolution may occur on a highly localized scale arising from repassivation delay. Alternatively, absorbed hydrogen may cause local embrittlement. It is difficult to distinguish between these two processes for several systems of stress corrosion cracking. Such general ideas on stress corrosion cracking mechanisms are considered with respect to specific alloy systems together with brief indications of protective measures.

Key Words: Repassivation; crack velocity; stress intensity factor; plastic deformation; stress corrosion cracking mechanisms.

---

1. Introduction

Stress corrosion cracking is a form of marine corrosion that has always been of considerable importance. It can occur in a wide range of different alloy systems and often unexpectedly insofar as it is not always accompanied by readily visible localized or general corrosion. The consequence is a history of frustrating failures which represent in some cases considerable economic waste and in a few a loss of human life. Over the last 30 years much money has been spent in attempts to overcome the problem or at least to reduce its occurrence, either by alloy development programmes or through the evolution of protective systems, both subjected to extensive testing programmes. In addition, much effort has been expended in studying the mechanistic aspects of the problem with the objective of solving it by achieving an understanding of the fundamental mechanisms. One result of what has been a prolonged and very costly effort has been to produce improvements

in performance. The critical mechanisms of cracking, however, have not been elucidated although progress has been made in understanding what is a very complex series of reactions. Much of this progress has been described in books (1-3)[1] summarizing and assessing work from a large number of laboratories.

In this paper it is intended to focus attention upon the main mechanistic aspects of the problem and also to indicate likely advances in the future. Together with a general consideration of the problem individual alloy systems are described briefly and possible remedial measures are indicated.

2. General Aspects

For failure of a metal component to occur by stress corrosion cracking certain requirements are necessary. Firstly, the component must be under stress. While the stress may arise from faulty design or from extraordinary demands made upon a component in service, commonly it arises from fabrication, either as a result of a high level of residual stress or from welding, rivetting or any other form of assembly. It is necessary to distinguish between those components in which the initiation of cracking will lead to continuing propagation because of the stress being maintained or increased on the remaining cross-section until complete fracture occurs and others in which the initiation of cracking will result in a lowering of stress with a consequent arresting of the crack propagation process. A highly localized stress arising from an inadequate welding procedure, for example, may only result in very short cracks adjacent to the weld. These considerations emphasize the necessity of being aware of the source of the stress since it will affect the behaviour and life time of a component. Stress corrosion cracking does not necessarily lead to failure. An absence of complete failure is not a useful service criterion, however, since the presence of small stress corrosion cracks which have ceased to propagate is clearly not acceptable in many service situations.

In addition to the presence of a stress the second requirement for cracking is the presence of an environment that can cause cracking. Sea water can cause stress corrosion cracking in some aluminium, copper, magnesium, manganese, titanium and ferrous alloys. On the surfaces of the alloys electrochemical reactions occur, some of which promote failure. Total immersion in sea water is not required. It is a common observation that thin layers of moisture promote corrosion more rapidly than occurs under conditions of full immersion. This arises from the need for dissolved oxygen at the metal surface. The diffusion of this species to the surface from the atmosphere occurs more rapidly through a thin layer than through a much greater distance as would be necessary for an immersed object. Failures between tide levels and in regions accessible by salt-laden moist winds are probably more common than failure in sea water and thereby make the problem of stress corrosion cracking attributable to marine environments more extensive than might otherwise appear.

The process of stress corrosion cracking can be divided into two separate parts: crack initiation and crack propagation. In recent years much attention has been given to the propagation process while the initiation process has been somewhat neglected. For both processes it is important to recognize that what occurs is a complicated sequence of events that are best considered under three different headings: electrochemical, metallurgical and mechanical. The interaction of numerous factors that can be grouped under any one of those headings constitutes the mechanism of crack initiation and crack propagation. To consider one set of factors in isolation is not always productive and may in some situations result in misleading conclusions. To analyze the interaction requires an understand of the kinetics of the various processes and how they may modify each other. Unfortunately data on this dynamic interaction are not plentiful. However this subject has been a region of progress recently and what follows is a pictorial description of the propagation process which in a few years time it can be reasonably expected will be able to be characterized quantitatively. This progress when accompanied by progress on initiation processes will result eventually in predictive precision with respect to failure.

---

[1] Figures in parentheses indicate the literature references at the end of this paper.

3. Crack Initiation

The initiation process can be considered to achieve two conditions which can be described as chemical and mechanical. The chemical condition is that a certain local acidity be achieved by reactions such as:

$$Me^{2+} + H_2O = Me(OH)_2 + 2H^+ \qquad (1)$$

For individual metals other intermediate and probably more complex reactions can be expected. Provided that solution movement is restricted the liquid immediately adjacent to the metal surface will gradually develop a pH dependent upon the hydrolysis constant of the metal chloride or upon a mixture of constants if other anions that are present in sea water participate significantly in this process. Lack of dissolved oxygen is also important in contributing to the development of localized acidity since its presence would counteract the fall in pH through the production of alkali arising from its reduction. Since continuous mixing of the electrolyte will prevent the development of acidity, regions where stagnant conditions are most likely to prevail are of considerable importance in determining initiation sites, within, for example, any kind of crevice and underneath surface deposits such as corrosion products or adherent marine creatures.

Alloys used in marine environments exhibit little or no corrosion either because they develop protective films which resist breakdown, e.g. titanium alloys, or because they are inherently unreactive, e.g. copper alloys, although even with these protective or unreactive layers may develop. Before corrosion reactions like that indicated in equation (1) can occur such films must be broken down, a process that may occur in a number of ways. Breakdown sites may be associated with previous faults in the film arising from the film structure, e.g. grain boundaries in the outer stressed layers, or with poor film formation over faults in the underlying metal surface arising from surface roughness, grain boundaries or edges, or with chemical heterogeneities in the film arising perhaps from heterogeneities in the surface either on an atomic scale or on a larger scale comparable to precipitates or non-metallic inclusions (which may be a cause of poor film adhesion). Such sites and poor mixing conditions of the environment together may lead to film breakdown. The conducting properties of the film and possible galvanic effects between the film and metal are also factors to be considered.

Mechanically stress corrosion crack initiation requires a stress which exerts a tensile component on the surface layers. Improvements in surface life are commonly achieved by putting the surfaces of components into a state of compressive stress by shot peening or grit blasting, although the application of such techniques can be expensive and are only effective if pitting or any other form of corrosion does not occur to a depth comparable to the thickness of the compressed layer. With a tensile stress component and the localized development of acidity the conditions for crack initiation may be achieved. One simple concept is that the incipient pit provides a stress-raising notch, i.e. that at the base of the pit the acting stress is increased as a result of restriction of flow of the material. In highly ductile materials such an idea does not apply because of the easy dissipation of stress concentration and it has been demonstrated that the principle function of pits in such materials is chemical rather than physical (4)[1]. In higher strength materials the conditions under which pits or incipient cracks propagate are best described from considerations of Fracture Mechanics. Propagation occurs when a certain value of stress intensity, K, is achieved and continues until a maximum value of K is reached when tensile overload fracture is then observed, a value dependent upon the toughness of the material. The stress intensity is calculated from specimen dimensions, the acting stress (σ), and the square root of the crack length (c), resulting in an equation of the general form:

$$K = \text{constant} \times \sigma \times \sqrt{c} \qquad (2)$$

---

[1]Figures in parentheses indicate the literature references at the end of this paper.

Below a certain value of the crack tip radius (ρ) K is independent of it and this is commonly implied in describing the crack as sharp. Test specimens are pre-cracked by fatigue to ensure that this condition is met. Under service conditions the incipient crack may be quite blunt. As c increases above a certain value so does K. Blunt cracks are therefore less likely to propagate. What must be avoided in practice are sharp, deep surface flaws, the actual values being dependent upon the toughness of the material. During propagation ρ may become larger than the maximum value to satisfy the condition that K is independent of it. Under such circumstances which may occur in susceptible alloys that undergo appreciable corrosion, e.g. maraging steels, the effect of local acidity in the region of the crack tip is to cause crack blunting. The alloy then undergoes final fracture at a higher K value than in air which under Plane Strain conditions is K_{1c} and thereby appears tougher insofar as the length of crack that can be tolerated in a given component before final fracture occurs is longer than in air. Propagation still occurs, however, until a stress corrosion failure ensues. Such considerations merely emphasize the care that must be exercised in determining the effect of the local corrosion reactions upon the mechanical aspect of the initiation and propagation processes.

The localized acidity referred to above occurs also during pitting corrosion and distinction must be made between pitting and cracking by considering the additional effect of stress upon the chemical process. If the stress is sufficiently high to cause surface straining then film rupture may occur and this appears to be a very important consideration. The effect of such rupture will be to result in rapid attack on the fresh metal surface that is created. This non-random attack represents a particularly complex subject of considerable interest at the present moment. Its description represents also the transition between crack initiation and propagation.

4. Crack Propagation

The situation described above is drawn schematically in Figure 1. It is envisaged that the metal surface is covered with a film that affords some degree of protection to the metal from the environment. As a result of plastic deformation the film is ruptured. On the new unfilmed surface reactions occur more rapidly than on the filmed surface and additional reactions may be initiated that do not occur on filmed surfaces. There are many possible reactions in addition to the reaction described in equation (1):

$$Me = Me^{2+} + 2 \text{ electrons} \quad (3)$$

$$H + \text{electron} = H \quad (4)$$

$$H + H = H_2 \quad (5)$$

$$H_{adsorbed} = H_{absorbed} \quad (6)$$

It is probable that one at least of these reactions represents the primary corrosion reaction that causes crack propagation. Often attempts are made to distinguish between the two reactions (3) and (6), referred to respectively as 'active path' and 'hydrogen embrittlement', which represent the two main mechanisms that are commonly considered to account for crack propagation.

In addition to the reaction responsible for crack propagation there will be a film forming reaction on the freshly created metal surface since the filmed state represents both thermodynamically and kinetically the stable state of the alloy surface. This is of critical importance since the formation of the film will tend to localize the important corrosion reactions on the fresh metal surface as drawn in Figure 1. The cracking process can be usefully considered as arising from two competing processes: fresh metal surface creation and metal surface film formation. A laboratory experiment (5)[1] demonstrating this aspect of cracking is described in Figure 2. Tensile specimens of a Ti-5Al-2.5Sn alloy were strained dynamically at different crosshead speeds while exposed to two

[1] Figures in parentheses indicate the literature references at the end of this paper.

different environments: (a) a 3% NaCl aqueous solution which does not corrode titanium alloys, and (b) a MeOH/HCl/H_2O mixture which does corrode titanium alloys. At high crosshead speeds ductile failure occurred before there was time for stress corrosion crack initiation. At lower crosshead speeds stress corrosion crack initiation and propagation occurred with a consequent lowering in the total elongation to failure. At the lowest crosshead speeds that were employed stress corrosion crack initiation and propagation did not occur in the aqueous solution and it can be concluded that reformation of the protective film, commonly referred to as repassivation (6)[1], occurred before sufficient corrosion damage had occurred to cause crack nucleation. In the methanolic solution, however, since there was no possibility of repassivation because the mixture was aggressive, crack nucleation and propagation occurred and over the longer period of time of the experiments the length of crack developed was greater than in the experiments at higher crosshead speeds and the final elongation to failure was therefore smaller. These experiments illustrate the role of repassivation in determining crack initiation and how it is related to surface strain-rates. The value of the potential is important as has been demonstrated by potentiostatic straining experiments (7)[1]. In practice, it can be expected that in marine environments under constant strain conditions or those of diminishing stress, e.g. around a weld, the effective strain-rate would gradually diminish as a crack propagated and complete repassivation would cause crack arrest.

The requirements for stress corrosion crack initiation and propagation when considered with reference to a repassivation model are quite stringent. The important factor would appear to be the repassivation time. If this is too short insufficient corrosion reaction will occur on the unfilmed metal surface, e.g. insufficient dissolution or hydrogen uptake, whereas if it is too long too much corrosion reaction will take place. Too much dissolution will result in a blunt fissure or pit or too much hydrogen will fail perhaps to localize the weakening effect caused by the absorption. At the tip of the crack the conditions for what must be a narrow, critical range in repassivation time can be expected to be very specific. The pH, potential, temperature and local environmental composition will all be important in determining film formation kinetics while the deformation and fracture mode of the alloy at the local level of stress that is achieved will determine the manner in which fresh metal surface is created. Such considerations demand knowledge of the interaction of electrochemical, metallurgical and mechanical events and the repassivation model provides therefore a very useful working hypothesis that a balance is established during propagation in which the rate of production of new alloy area exceeds slightly the rate of repassivation.

In practice the surfaces of metal components are not strained at constant strain-rates. Strained metals do not generally deform in the manner drawn in Figure 1. At the tips of propagating cracks elaborate deformation and tearing processes occur and these will determine the rate at which fresh metal surface is created. This metallurgical aspect is important and the different tearing modes of alloys may partly determine whether an alloy is susceptible.

Much recent work on propagation studies has provided much new information largely arising from employing techniques of Fracture Mechanics. Once initiation has occurred stress corrosion cracking is only likely to be a problem if the subsequent crack growth rate occurs at a rate that is significant, which will be determined at least in part by the expected or required lifetime of the considered component. Many recent studies have been devoted therefore to measuring crack velocity accurately as a function of mechanical, metallurgical and electrochemical variables. This approach has enabled many such variables to be assessed quantitatively and their relative importance determined. This type of study has followed on the developments of a new test by Brown (8)[1]. In this the initial stress intensity factor is plotted as a function of time to failure (t_f) on several types of standardized pre-cracked notched specimens. A typical result is shown in Figure 3 in which a minimum value of K below which failure did not occur was observed and this is designated K_{Iscc}. Such a value is of potential design value since for a maximum stress value c can be calculated which can be considered as a maximum flaw size that a given proposed structure could tolerate without failure by stress corrosion.

---

[1]Figures in parentheses indicate the literature references at the end of this paper.

Mechanical Variables. The relationship between stress corrosion crack velocity and stress intensity factor has been shown for aluminium (9)[1] and titanium (10)[1] alloys and for high strength steels (11)[1]. It takes the general form in Figure 4. Stage I consists of a logarithmic dependence of crack velocity upon K (or possibly K^2) and in the two non-ferrous alloys occurs with an activation energy of ca. 27kcal/gm.mol (113kJ/mol). Stage II consists of a region in which the velocity is independent of K and occurs with an activation energy of 3-5kcal/gm.mol (12-21kJ/mol). Stage III is rarely encountered and is characteristic of highly susceptible alloys which are not used. While there is some variation according to the specific alloy or heat treatment and environment most systems exhibit Stage II, which represents a maximum velocity, and Stage I except for titanium alloys in sea water.

The lowest velocity observed in Figure 4 might be expected to correspond to K_{1scc}. Accurate measurements for aluminium alloys have shown (9)[1] that the velocity can be as low as 10^{-11}m/sec. and in that situation it is not at all apparent that a K_{1scc} value exists. Instead a value of K might be chosen corresponding to some very low negligible crack velocity. The highest velocity observed is also of significance since there exists the possibility of developing alloys which have low maxima and the use of such alloys might extend the life of components made from susceptible alloys and possibly reduce the incidence of dangerous sudden failures. Beneficial effects achieved by certain heat treatments or by alloying may not only be the result of making initiation more difficult or of raising K_{1scc} if this exists but also may be the result of reducing the maximum velocity.

Metallurgical Variables. Practically all metallurgical variables affect stress corrosion susceptibility and crack velocity. On a large scale, grain size, texture and heat treatment are all important. An example is shown in Figure 5 in which the Stage II velocity has been considerably lowered by overaging treatments. Stage I is generally shifted to higher K values by such treatments. The relative shifts in the two stages cannot be predicted and must be determined for each alloy since there are wide variations. Clearly the determination of such data is a very helpful and necessary aid in alloy selection. On a fine scale, microstructural features, deformation modes and precipitate properties are all of importance. At low plastic strain FCC alloys and hexagonal alloys of titanium that are susceptible to transgranular stress corrosion cracking exhibit coplanar arrays of dislocations. While this observation is not unique to susceptible alloys it does emphasize the importance of deformation mode since such arrays will tend to promote deformation by coarse slip, a process producing on a localized scale relatively large amounts of fresh metal surface. Such arrays are evidence also of restricted slip and the stresses generated at the ends of such long arrays can be expected to be exceptionally high so that they may contribute significantly to the fracture process. At high strain, however, such arrays cannot be seen and it can be argued that localized tearing always generates such high strain that observations made on thin foils are not readily applicable to the propagation process. Stress corrosion cracks are notable for the large amount of tearing that is observed, an example of which is shown in Figure 6. The α titanium alloy lattice has fractured by cleavage, a characteristic stress corrosion fracture mode, yet the cleaved surface represents only a small proportion of the fracture surface. The remaining part of the surface has undergone a process perhaps best described as low energy tearing, a separation process that is mechanical, i.e. is not caused directly by the environment.

Such metallurgical aspects of the fracture must be considered in relation to electrochemical reactions. It is commonplace to attempt to analyze crack propagation by faradaic equivalence. The current density required to dissolve metal at a rate corresponding to the crack velocity is calculated. For some alloys, e.g. of titanium, current densities in excess of 10^2A/cm^2 are required (12)[1] and it is not clear how these might be maintained even if initiated. In reality such high values are not required because large amounts of fractures are torn mechanically. Similar arguments can be made concerning discrepancies between crack velocities and hydrogen diffusion kinetics in analyses (5)[1] of cracking mechanisms in the same alloy system concerning which there is some dispute. While such

---

[1]Figures in parentheses indicate the literature references at the end of this paper.

matters require careful quantitative examination, enough can be seen in fractographs to allow rather simple calculations to be disregarded.

Electrochemical Variables. The effect of variation of electrochemical potential on stress corrosion susceptibility in marine environments is well known for a number of practical alloy systems. Some can be cathodically protected and this may be a practicable solution for components that are immersed continually. Alloys subject to hydrogen embrittlement cannot normally be cathodically protected. High strength steels, for example, are dependent upon strength level which in turn determines the tolerance of the steel for hydrogen. K_{Iscc} is affected mainly by heat treatment and not by the value of the potential, as shown in Figure 7.

The effect of potential upon crack velocity depends upon the alloy system. In aluminium alloys both Regions I and II are lowered (9)[1] as the specimen becomes more cathodic and for titanium alloys (10)[1] similar behaviour is observed as shown in Figure 8 and an approximately linear relationship is observed between the average velocity and potential over a wide range of potential (1500mV). In practice it is conceivable that even partial cathodic protection may prove sufficient to lower the incidence of stress corrosion failures, a point of importance where the alkalinity developed may affect adversely protective paint finishes. In high strength steels moving the potential in either the anodic or cathodic direction from the value of the open circuit potential causes increases in velocity (11)[1].

At the tips of stress corrosion cracks in aluminium, titanium, magnesium and ferrous alloys hydrogen evolution occurs and it is an unresolved question whether the evolution is accompanied by absorption as indicated in equation (6) which causes some form of localized embrittlement contributing to the stress corrosion fracture. In high strength steels hydrogen appears to be the species that causes cracking but in other systems many questions remain unanswered. Cathodic protection may occur in alloys subject to hydrogen embrittlement since film formation may interfere with hydrogen entry (5)[1]. Anodic polarization may promote increases in local acidity and thereby promote hydrogen absorption. The relationship between potential and cracking cannot, therefore, be interpreted without more knowledge of the system under investigation.

5. Discussion

The points discussed above are of a general kind and find application to all systems of stress corrosion cracking. To that extent the systems of cracking have much in common although it must be emphasized that specific mechanisms have not been fully elucidated. Some further simple points can now be made. Since it is necessary for corrosion to occur, alloys resistant to corrosion will show marked resistance to stress corrosion. This is particularly applicable to titanium alloys which for many years were thought to be immune. Cracking in titanium alloys is dependent upon the development of crevices, commonly occurring within pre-existing flaws. In marine environments failures are very rarely encountered in practice. With other alloys similar considerations apply. Protective treatments that prevent pitting or corrosion of any other kind will reduce the occurrence of stress corrosion failures. Coupling to dissimilar metals may prove beneficial or harmful since the result will depend upon the anodic or cathodic polarization characteristics of the alloy as discussed above.

With aluminium alloys pitting occurs in marine environments and stress corrosion susceptibility largely depends upon metallurgical properties, particularly strength as discussed above. Alloy selection is usually based upon strength, alloy content and a protective finish that together exhibit maximum corrosion resistance. Corrosion of aluminium occurs with film thickening accompanying pitting. The presence of the chloride ion may not be necessary for crack propagation. Cracking in Region II can occur in atmospheres with a relative humidity <1% (9)[1] under which condition there is no permanent wetting. It then appears that the velocity is dependent upon the reaction of water molecules with metal atoms at the crack tip. It is possible that the role of the chloride ion under conditions of permanent wetting is to maintain acidic conditions at the crack which maintain the surface in the region of the crack tip bare (or in a poor state of film coverage) for the

[1]Figures in parentheses indicate the literature references at the end of this paper.

critical corrosion reaction and also for the discharge of hydrogen ions which appears to be an important rate determinant (13)[1]. That the Region II velocity increases as the chloride ion concentration is increased (9)[1] may be caused by the influence that the ion has upon the quality of the film maintained at the crack tip. The possibility of adsorbed halide ions promoting the entry of hydrogen atoms into the lattice also cannot be ruled out.

Little work has been reported on the stress corrosion cracking of copper alloys in sea water. High tensile brasses are highly susceptible (14)[1] particularly in the all β condition which is associated with rapid cooling conditions such as occur around a weld. A Cu-Ni-Al has also been observed to crack in the wrought condition but not in the cast condition (15)[1] but since only very slow propagation occurred when specimens were tested at 95% K_{Ic} susceptibility is slight. The alloy appears to undergo localized selective dissolution, possibly of the aluminium. Copper alloys rich in zinc are susceptible to stress corrosion cracking in environments containing ammonia a source for which can be bird droppings (16)[1]. Estuarine waters containing sulphide residues also cause cracking in these alloys. Low temperature stress-relief or annealing both lower susceptibility. The mechanism of cracking in these alloys is out of 'active path' insofar as hydrogen evolution does not occur but whether the principal reaction is dissolution or repeated film formation followed by fracture is not settled in all instances.

Manganese-copper alloys containing additional solute elements such as aluminium are used in marine environments. Because of their high damping capacity they are suitable for use in propellers. The binary alloys 70Mn-30Cu to 90Mn-10Cu are highly susceptible to stress corrosion cracking in sea water (17)[1] but this can be avoided by cathodic protection, a situation that may arise naturally from the proximity of the hull. The failure is mainly intergranular as shown in Figure 9 in which very little plastic deformation can be observed in the fracture surface although the particular alloy is highly ductile when broken in air. The enhanced reactivity of the grain boundary which causes them to be preferentially dissolved may be caused by preferential segregation of manganese to those regions. There is no experimental evidence for such segregation although it could be inferred from the observation that during the aging process that results in a maximum damping capacity a manganese precipitates are formed in the grain boundaries. In aged alloys these are dissolved during cracking. Susceptibility is little affected by the aging process. During cracking manganese and copper are dissolved with copper deposition which provides very efficient local cathodes. The fracture of corrosion product may be part of the cracking process which in stifling localized dissolution can be described as being partly protective and causing localized attack where it is broken. Protection and lower susceptibility can be expected if solute elements are added which will cause the formation of protective films.

6. Conclusion

Considerable progress has been made in the last few years in the understanding of stress corrosion cracking. The increasing emphasis on quantitative analyses is a particularly welcome sign since in addition to providing data which should help in the development of non-susceptible alloys, it should also enable the use of susceptible alloys to be extended. Such progress can be expected to continue over the next few years and this will lead to increased confidence in designing structures and protective systems in which the incidence of stress corrosion failure is minimized.

---

[1]Figures in parentheses indicate the literature references at the end of this paper.

References

1. H.L. LOGAN, The Stress Corrosion of Metals, Wiley, New York (1966).
2. Fundamental Aspects of Stress Corrosion Cracking (ed. R.W. Staehle, A.J. Forty and D. van Rooyen), N.A.C.E. Houston, Texas (1969).
3. The Theory of Stress Corrosion Cracking in Alloys (ed. J.C. Scully), N.A.T.O. Brussels (1971).
4. I.S. McCOLLOUGH and J.C. SCULLY, Corros. Sci., 9, 615 (1969).

5. J.C. SCULLY and D.T. POWELL, Corros. Sci., 10, 371 (1970).
6. J.C. SCULLY, Corros. Sci., 7, 197 (1967).
7. T.R. BECK, ref. 2, p.605.
8. B.F. BROWN, Met. Rev., 13, 171 (1968).
9. M.O. SPEIDEL, ref. 3, p.289.
10. J.A. FEENEY and M.j. blackburn, ref. 3, p.355.
11. B.F. BROWN, ref. 3, p.186.
12. T.R. BECK, ref. 3, p.64.
13. A.J. SEDRIKS, J.A.S. GREEN and D.L. NOVAK, Met. Trans., 1, 1815 (1970).
14. J.N. BRADLEY, Int. Met. Rev., 17, 81 (1972).
15. P. DODD and J.C. SCULLY, work in progress.
16. B.F. PETERS, J.A.H. CARSON and R.D. BARER, Mater. Prot., 4, 24 (1963).
17. R.H. BILLINGHAM and J.C. SCULLY, in preparation.

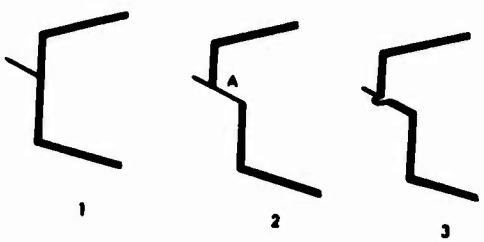


Figure 1. Schematic representation of the crack propagation process. 1. Film-covered crack tip surface. 2. Under the influence of a tensile stress a slip plane moves and creates a slip step (A) which breaks the film. 3. The film reforms on most of the freshly created surface leaving only a small part which is corroded and which may be a site for hydrogen absorption.

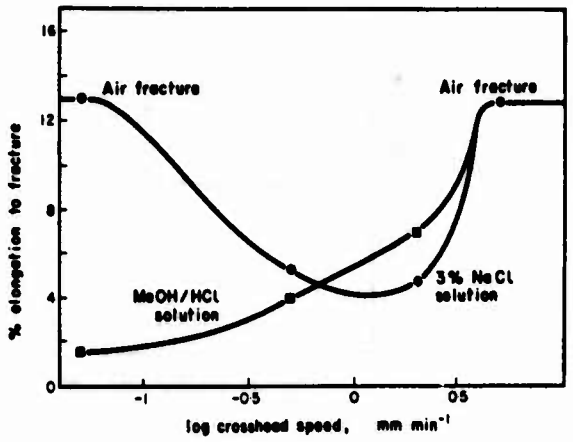


Figure 2. The elongation to fracture of tensile specimens of Ti-5Al-2.5Sn alloy of 3cm gauge length in 3% aqueous NaCl and MeOH+1%HCl environments as a function of Instron crosshead speed (5).

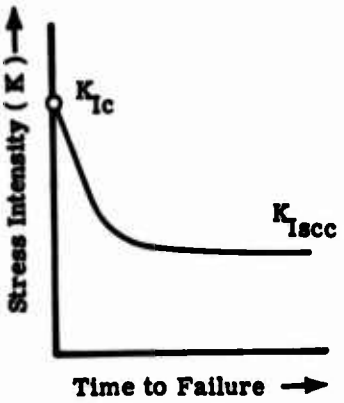


Figure 3. Schematic diagram illustrating the relationship between the initial stress intensity factor and time to fracture in stress corrosion tests. Not all alloy systems exhibit a K_{Iscc} (10).

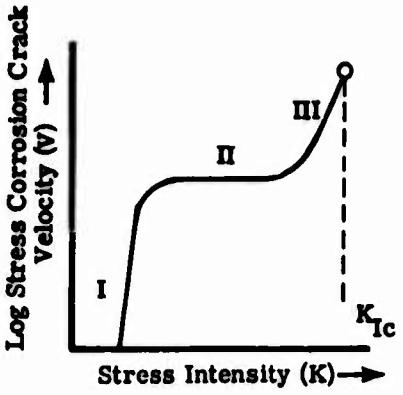


Figure 4. General form of the relationship between stress corrosion crack velocity and stress intensity factor found for a number of different alloy systems. Stage III is not often found (10).

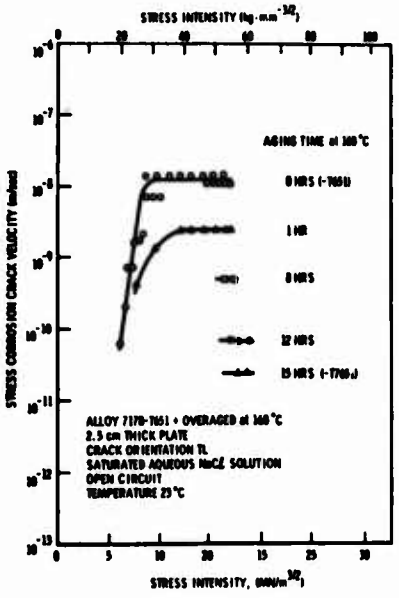


Figure 5. Effect of overaging on stress corrosion crack velocity in Al alloy 7178 (9).

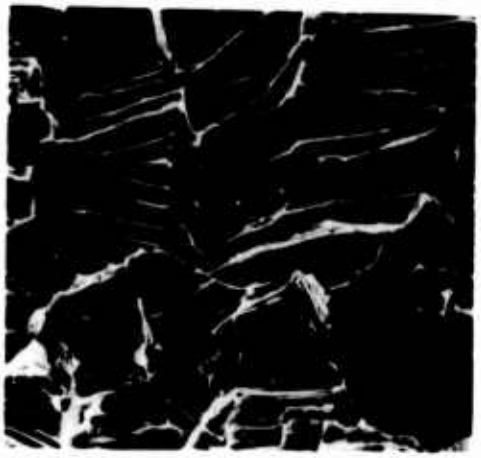


Figure 6. Scanning electron micrograph of part of a stress corrosion fracture surface of Ti-0.29 O alloy. The stress corrosion cleavage represents only a small part of the surface while the rest consists of elongated torn regions. 630X.

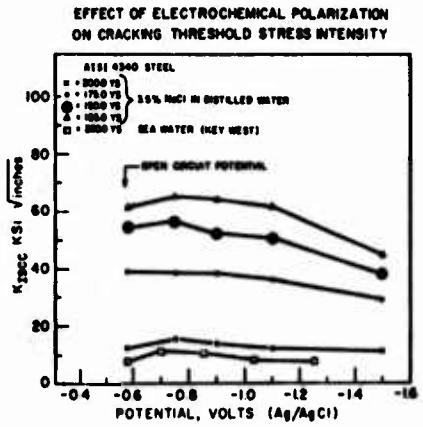


Figure 7. The effect of electrochemical potential on K_{Iscc} for AISI steel heat treated to 5 different strength levels (8).

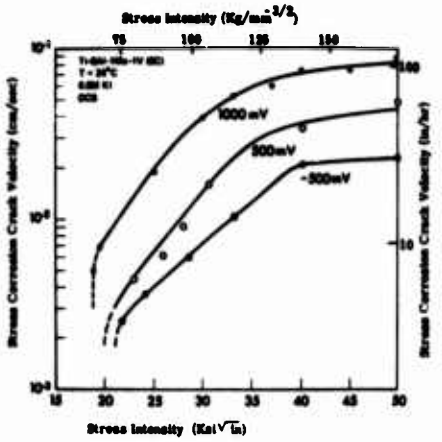


Figure 8. Stress corrosion crack velocity v. stress intensity factor for Ti-8Al-1Mo-1V alloy in 0.6M aqueous KI solution at three different potentials (10).



Figure 9. Scanning electron micrography of part of a stress corrosion fracture surface of 70Mn-30Cu alloy. The stress corrosion intergranular surface exhibits very little deformation (17). 450X.

Discussion

A question on cellular vs. planar dislocation arrays brought the guarded reply that the latter tended to give transgranular cracking while the former tended to give intergranular cracking. Another point concerned the fact that at a potential of plus 1000 mv (SHE) one might infer that H could not possibly be responsible for cracking. The author pointed out however, that much more anodic potentials still produced pits from which H was evolved, and therefore the observation that cracking occurred at plus 1000 mv did not disprove anything with respect to H.

The Development of a High Strength Ductile Stainless Steel of improved corrosion resistance in Marine and Chemical Environments

W.H. Richardson, B.Sc. A.I.M., P. Guha, B.Sc. and
R. Machin, B.Sc. A.R.C.S.T.

Langley Alloys Limited
Langley, Slough, Bucks. England

The development is traced of FERRALIUM(1)[1,2], a duplex ferritic/austenitic precipitation hardening stainless steel, which contains 25% chromium and 5% nickel, with controlled amounts of molybdenum and copper. The significance of chromium, nickel, copper and nitrogen contents on the mechanical properties and corrosion resistance of the basic alloy are demonstrated.

The alloy composition was thereby finalised as -

% Chromium	% Nickel	% Molybdenum	% Copper	% Nitrogen
24.5-25.5	5.0-6.0	2.0-3.0	1.0-3.5	0.13-0.25

Potentiostatic studies using a Wenking potentiostat and stepping motor were used throughout the initial development and production trial stages to examine the effects of compositional and heat-treatment variables on corrosion resistance. These were supported by laboratory immersion tests and by field trials.

The successfully achieved target properties of high strength and ductility, together with good corrosion resistance in sulphuric acid and pitting resistance in chloride solutions are demonstrated.

Data are presented on stress corrosion and corrosion fatigue properties in chloride environments.

Results are included of successful production trials which enabled all common wrought forms of the alloy to be produced in addition to castings.

Significant marine applications of cast, wrought and weld fabricated components are discussed.

Key words : Alloy development; stainless steel; corrosion resistance; pitting resistance; potentiostatic studies; breakdown potential; heat-treatment; microstructure; workability; applications.

Introduction

Traditionally, for critical components in marine engineering, copper and nickel alloys have been used due to their superior corrosion resistance. Recent search for improved combinations of strength, ductility and corrosion resistance has, therefore, been devoted to copper and nickel alloys (2,3,4) and this combination has proved to be difficult to achieve.

Austenitic stainless steels are necessarily low strength alloys and have not been used in marine environments due to their likelihood of suffering pitting and crevice corrosion. Attempts at increasing the strength of these alloys have, as a rule, resulted in sacrifice of some corrosion resistance.

Ferritic-austenitic steels, however, possess superior combinations of strength and corrosion resistance and this paper describes the development of such a duplex steel - FERRALIUM.

---

1. Figures in parentheses indicate the literature references at the end of this paper.
2. FERRALIUM is a registered trademark of Langley Alloys Limited.

High chromium ferritic-austenitic steels have indeed been known for some time and have been used, for example, to handle sulphite in the paper pulp industry. However, due to their inherent lack of ductility and other fabrication problems, as pointed out by Moneypenny(5), duplex alloys have not received wide applications. They were found to be difficult to hot work, their rate of work hardening was excessive, and they were embrittled during welding operations.

Thus, for example, although specifications for cast and wrought stainless steels have been revised by the British Standards Institution in recent years, these specifications include no alloy containing more than 20% chromium and the steels covered are mostly austenitic in structure.

To the best of the authors' knowledge, the only American specification for a wrought stainless steel of the duplex type is AISI 329. This alloy suffers from the shortcomings, previously discussed, of the high chromium duplex steels and is recommended for use only in the fully annealed condition. More recently a cast alloy of this type has been developed which is covered by a tentative Alloy Casting Institute specification CD4MCu. However, certain inherent ductility and quench-cracking problems still exist and no wrought alloys of this nature are available.

The somewhat different situation on the continent of Europe, where ferritic-austenitic steels and high chromium ferritic steels have been more widely used, was probably created by the nickel shortage during World War II. However, most of these alloys still suffer from the shortcomings of the early ferritic-austenitic steels.

Research on the inter-relationship of compositional and microstructural variables on the ductility and formability of high chromium ferritic-austenitic steels has shown that by control of composition and heat-treatment, it is possible to produce a ferritic-austenitic steel which can be easily hot-worked, cold-worked, welded and possesses an excellent combination of corrosion resistance, pitting resistance, high strength and ductility. This paper describes how this was achieved at Langley Alloys Limited in the development of FERRALIUM, a ferritic-austenitic steel, possessing all the above properties, which is now in commercial production, not only as castings, but in all common wrought forms.

STAGE 1

Initially the object of this development was to produce a cast stainless steel of high strength and hardness with corrosion resistance at least equivalent to the high quality molybdenum-bearing austenitic stainless steels of the AISI 316 type. It was believed that the high strength and hardness of such a steel would enhance its performance in many applications handling slurries, aggregates, etc.

At the outset we were well aware of the excellent combination of mechanical properties obtainable in the precipitation-hardening stainless steels containing 13% to 17% chromium and 4% to 7% nickel. These stainless steels in general, however, possessed inferior corrosion resistance to austenitic stainless steels, and were seldom used in chemical or marine industry.

Starting from the known high strength of the duplex austenitic-ferritic steels, plus the addition of a precipitation hardening mechanism, Stage 1 of our development was aimed at a composition and heat-treatment which would give at least a two-fold increase in strength over austenitic steels with no loss of ductility (e.g. BS1632 Grade A covering 18Cr10Ni3Mo steel castings specifies 0.5% Proof Stress of 13.5 Tons/sq.inch (208MN/m^2) and elongation of 22% min.)

Effects of composition on mechanical properties

The initial composition was based on a ferritic-austenitic steel containing 25% chromium, 5% nickel and 1.5% molybdenum. The molybdenum content was raised to 2.5%, the amount considered necessary in austenitic steels for optimum corrosion resistance, and 3% copper was added to assist in producing the desired precipitation hardening mechanism and also for its well-known beneficial effect in resisting corrosion in non-oxidising conditions.

Mechanical properties obtained from all tests in Stage 1 are detailed in table 1, those on the above composition being presented under alloy No.1. Although the strength target had been achieved, low ductility and impact properties were obtained in all conditions of heat-treatment, associated with cleavage fractures. Based on the authors' experience of the beneficial effects of nitrogen additions on the ductility of 28% chromium ferritic steels, this was added to the above composition and alloy Nos. 2 and 3 in table 1 demonstrate the significant improvement in ductility thereby obtained. The effect of nitrogen addition is most pronounced in the as-cast condition, thus providing significant potential advantages in the fettling and welding of castings. Although some reduction in proof stress was shown by the nitrogen-containing steel in the as-cast condition, the target of an excellent combination of strength and ductility had been achieved.

Further experimental compositions were then studied to determine the effects on mechanical properties of varying chromium (alloy Nos. 4 - 7) and nickel (alloy Nos. 8 - 11) contents on the nitrogen-bearing steel.

It will be seen from alloy Nos. 4 - 7 that ductility and impact resistance were reduced as the chromium content was increased beyond 25% - 26%, these reductions being more significant in the case of the lower nickel and nitrogen contents (alloy 5). The results of alloys Nos. 8 - 11 demonstrated that increasing the nickel content per se reduced strength and increased ductility.

Heat-treatment

It is also apparent from table 1 that precipitation hardening temperature also plays an important part in the resultant properties obtainable and that precipitation temperatures of 500°C. or above are necessary to maintain a good combination of strength and ductility.

STAGE 2

Preliminary corrosion tests were carried out during Stage 1 of the development and it soon became apparent that, in addition to the excellent combination of mechanical properties obtained, the alloy range being studied possessed corrosion resistance superior to that of the 18Cr10Ni3Mo austenitic stainless steels in many environments. It was also found that the pitting resistance in chloride solutions was far superior to that of any austenitic stainless steels. This combination of corrosion and pitting resistance led to Stage 2 of the development, which involved a more detailed study of the effects of composition, heat-treatment and microstructural variables on corrosion resistance.

Extensive use was made of potentiostatic techniques, using either breakdown potential or current/time studies at potentials approaching the breakdown potential. The effects of various alloying additions on corrosion and pitting resistance are detailed in Figs.1 - 3.

Effect of composition on corrosion resistance

Potentiostatic studies were carried out using a Wenking potentiostat. The stepping rate during polarisation was maintained at 10mV/min. using a stepping motor. The polarisation cell set-up and electrode holder were as recommended by Greene(6). Polarisation was carried out according to the recommendations of the ASTM G.1 Committee. All test solutions were purged with O_2 free high purity nitrogen.

Fig.1 Shows the results obtained from constant potential tests with varying nickel content, from which it can be seen that pitting resistance was adversely affected by nickel contents outside the range 5% - 6%. Similar tests with varying chromium contents (Fig.2) show that chromium contents below 24.5% can be related to a marked decrease in resistance to pitting.

The results of potentiostatic tests with varying copper contents shown in Fig.3, demonstrated the necessity to maintain a copper content over 0.5% in order to reduce the corrosion rate in chloride solution to an acceptable level.

Effects of heat-treatment and microstructure on corrosion resistance

Having arrived at the composition range for this alloy, further studies showed that heat-treatment and microstructure had a most significant effect on corrosion resistance.

In the relatively slowly cooled as-cast or hot-worked condition, the microstructure consists of grains of austenite in a matrix of ferrite with precipitated intermetallic phases in the ferrite grains (Fig.4). Annealing at 1120°C. followed by water quenching results in a microstructure completely free of such precipitated phases (Fig.5) which can be related to the vast improvement in corrosion resistance as indicated by potentiostatic tests, the results of which are shown in Fig. 6 and 7.

Subsequent precipitation hardening of the pure austenite/ferrite structure has little effect on the corrosion resistance in chloride provided that the precipitation hardening treatment is carefully controlled in order not to cause overageing. Corrosion tests on samples aged at various times and temperatures indicate that 500°C. is the optimum ageing temperature and that the time at temperature should not exceed 4 hours. Fig.8 shows the loss in corrosion resistance on ageing at 530°C.

At this stage it was concluded that an alloy could be produced which when suitably heat-treated would possess the required combination of :

a) Strength
b) Ductility
c) General corrosion resistance
d) Pitting resistance in presence of chloride ions

The composition of this alloy would fall within the following range :

% Chromium	% Nickel	% Copper	% Molybdenum	% Nitrogen
24.5-25.5	5.0-6.0	1.0-3.5	2.0-3.0	0.13-0.25

PRODUCTION TRIALS

This steel was designated FERRALIUM and was subjected to exhaustive trials for the production of castings, forgings, rolled bar, sheet and plate, welded components, extrusions, wire and tube.

Complex castings involving changes of section and welding were successfully produced to radiographic standards.

In spite of the duplex nature of the alloy at hot working temperatures, the steel proved to be amenable to hot working, and rolled, forged and extruded products were successfully produced. Cold-rolled sheet and cold-drawn wire and tube were also made without difficulty. Due to the relatively high strength of the alloy in the annealed condition, the power requirements were found to be higher than for cold working austenitic steels but the rate of work-hardening was comparable. 60% - 70% cold reductions for sheet and tube production and over 95% reduction in wire drawing were achieved.

Corrosion tests carried out during the various stages of production confirmed earlier results that heat-treatment and microstructure played an important part in determining the corrosion resistance of the alloy and that a close control of both was essential to safeguard corrosion and pitting resistance.

ASSESSMENT OF PRODUCTION ALLOY

FERRALIUM produced to optimum composition, heat-treatment, etc. was subjected to extensive laboratory corrosion tests and field trials. Results of these laboratory tests are detailed in Figs. 9 - 12.

General corrosion resistance in sulphuric acid was evaluated not only by potentiostatic tests in 1N and 10N solutions, the latter being illustrated in Fig.9, but also by various immersion tests, results of which are presented as an iso-corrosion chart in Fig.10. Comparative data on 18Cr10Ni3Mo alloy are also given.
The current density peak of FERRALIUM in 10N sulphuric acid is significantly lower than that of the austenitic steel (Fig.9). These results have been confirmed by the immersion test data summarised in Fig.10, which show, over a wide range of concentrations, the superiority of the developed alloy.

Study of the polarisation characteristics of FERRALIUM (Fig. 11) in 3% NaCl solution showed the high breakdown potential at over 800 mV at 20°C which, although it is decreased to 600 mV as the test temperature is raised to 40°C, yet even at that temperature is considerably higher than the 200 mV shown by 18Cr10Ni3Mo at 30°C.

Although the pitting potential of the alloy is reduced at lower pH levels (Fig. 12), it is still around 300 mV at pH of 1.5 at 40°C. The active current density shown in this figure by 18Cr10Ni3Mo indicates a tendency to general corrosion in acid chloride which is not shown by FERRALIUM.

Cast and wrought samples were immersed in Langstone Harbour for a period of two years. One-half of each specimen was held under a perspex gasket to create a crevice condition. There was a total absence of any sign of crevice corrosion after two years. The initial and final weights (grams) of the samples were as follows: cast alloy, solution treated and aged, 69.429, 69.426; rolled plate, solution treated, 86.370, 86.381; and rolled bar, solution treated and aged, 104.165, 104.162. It is of interest to note additionally that inscriptions vibro-etched on the samples before immersion were free of corrosion products after the end of the two-year test.

To provide additional data relating to applications in sea water, a programme of corrosion fatigue and stress corrosion tests was carried out. The satisfactory results of these tests are shown in Figs. 13 and 14.

SUMMARY AND APPLICATIONS

This paper has described the development of a stainless steel which successfully attained the required targets of good corrosion and pitting resistance combined with mechanical strength and ductility, for applications in marine and chemical environments. The data presented herein have been slanted towards marine applications, but the high degree of corrosion resistance shown to many agressive chemicals, has resulted in the extensive use of the alloy in the handling of mineral acids, chloride solutions, hydroxides, etc.

Because of the excellent casting, forming and fabrication characteristics of the steel, it has been utilised in many forms for marine applications. In conclusion, a few significant items are illustrated in Figs. 15 - 17.

Fig. 15 shows a cast FERRALIUM propeller which was in service on a high speed patrol boat for four years, including a long stay in stagnant harbour. The propeller is in excellent condition showing no general corrosion and a complete absence of pitting. The illustration shows dark spots which are, in fact, a form of marine growth. Removal of these has shown bright metal below with no sign of crevice attack, although conditions might be considered ideal for this to have taken place.

Fig. 16 shows some cast rings for a type of marine shaft seal, for which FERRALIUM has become the standard specified alloy.

An inert gas scrubber system for a 250,000 ton dwt. oil tanker has its lower portion, shown in Fig. 17, fabricated from 3/16 in. FERRALIUM plate. This was designed to handle sea water after scrubbing high sulphur-containing boiler flue gases. The resultant solution has a pH of 2.0 - 5.5 at a temperature of 50°C. Most stainless steels would be considered unsuitable to handle this aggressive liquid.

References

(1) U. S. Patent 3,567,434 - 2nd March 1971.

(2) J. N. Bradley and G. Newcombe, Engineer, 1969, 229 (July 10), 28.

(3) P. Guha, D. Brown and G. Littlewood, Journal of Inst. of Metals, May 1971, p. 148.

(4) J. N. Bradley, "Recent Developments in Copper Base Alloys for Naval Marine Applications" International Metallurgical Review, 162, 1972, Vol. 17.

(5) J. H. G. Moneypenny, Stainless Iron and Steel, Vol. 1, p. 87, Chapman and Hall, London (1951).

(6) N. D. Greene, Experimental Electrode Kinetics, Rensselaer Polytechnic Institute, Troy, New York, 1965.

Summarized Discussion

In reply to queries, it was stated that the scrubber depicted in the paper had been in service for about one year with no specific information being reported about corrosion at the welds; that there were no data on crevice corrosion resistance of the alloy in sea water, although crevice corrosion tests had been initiated recently in INCO's Francis L. LaQue Corrosion Lab. at Harbor Island, North Carolina; and that the price per pound would be about $1.50.

A discusser noted that propellers usually receive cathodic protection from the hull of the ship and that this fact must be weighed in interpreting the field trial with the alloy propeller.

Another discusser commented that it was not clear from the paper which of the electrochemical parameters reported were most relevant to corrosion and crevice corrosion in sea water.

Table 1. Effect of composition and heat-treatment on the mechanical properties

Alloy No.	Composition %						Heat-treatment		0.5% Proof Stress		U.T.S		% Elong	Izod	
	C	Cr	Ni	Mo	Cu	N	Solution Treatment	Ageing Temp °C *	MN/m²	1000 psi	MN/m²	1000 psi	L=5D	J	ftlbf
1	0.06	24.9	5.5	2.5	3.3	N.A.	As cast	-	649	94	752	109	3	-	-
							1120°C.	475	680	98	934	135	7	6.7	5
							1120°C.	500	664	96	873	126	15	13.5	10
							1120°C.	525	664	96	828	120	18	20.2	15
Effect of nitrogen addition															
2	0.06	25.4	5.4	2.3	3.5	0.13	As cast	-	541	78	811	117	22	-	-
							1120°C.	475	726	105	988	143	20	17.6	13
							1120°C.	500	726	105	958	138	26	58.3	43
							1120°C.	525	680	98.5	880	127	22	62.3	46
3	0.05	25.9	5.8	2.6	3.6	0.26	1120°C.	475	726	105	988	143	28	23.0	17
							1120°C.	500	664	96	911	132	28	65.0	48
							1120°C.	525	633	91	903	131	32	80.0	59
Effect of chromium															
4	0.07	24.7	4.9	2.2	3.4	0.10	1120°C.	475	664	96	942	136	26	21.7	16
							1120°C.	500	649	94	942	136	26	75.9	56
							1120°C.	525	618	89.5	834	120	35	84.0	62
5	0.05	26.7	4.6	2.0	3.0	0.13	1120°C.	475	865	125	1081	157	20	6.7	5
							1120°C.	500	772	112	965	140	16	10.8	8
							1120°C.	525	726	105	911	132	19	20.2	15
6	0.06	25.2	5.6	2.2	3.7	0.24	1120°C.	475	710	103	973	141	29	29.8	22
							1120°C.	500	664	96	927	134	31	80.0	59
							1120°C.	525	618	89.5	896	130	37	81.4	60
7	0.04	28.6	5.3	2.2	3.2	0.25	1120°C.	475	880	127	1127	163	15	8.1	6
							1120°C.	500	741	107	988	143	25	23.0	17
							1120°C.	525	741	107	927	134	26	33.9	25
Effect of nickel															
8	0.07	25.1	3.7	2.4	3.3	0.15	1120°C.	500	840	122	1012	147	16	9.5	7
9	0.06	25.8	4.6	1.9	3.2	0.12	1120°C.	475	788	114	1004	145	17	8.1	6
							1120°C.	500	741	107	942	136	19	17.6	13
							1120°C.	525	710	103	896	130	25	37.9	28
10	0.06	25.5	5.4	2.3	3.5	0.13	1120°C.	475	726	105	988	143	20	17.6	13
							1120°C.	500	726	105	958	139	26	58.3	43
							1120°C.	525	680	98.5	880	127	22	62.3	46
11	0.07	24.9	8.6	2.3	3.4	0.15	1120°C.	500	568	82	846	123	29	-	-

N.A. = Not added.

* All ageing treatments were carried out at the stated temperature for 4 hours.

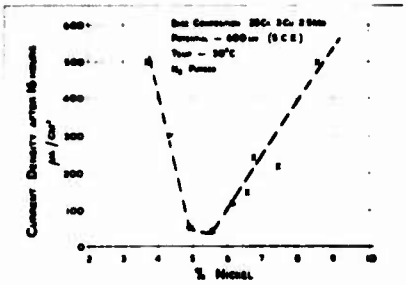


Fig. 1. Effect of Nickel Content on Pitting Resistance in 3% Na.Cl.

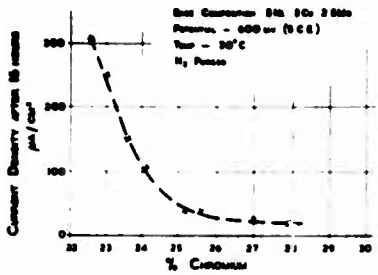


Fig. 2. Effect of Chromium Content on Pitting Potential in 3% Na.Cl.

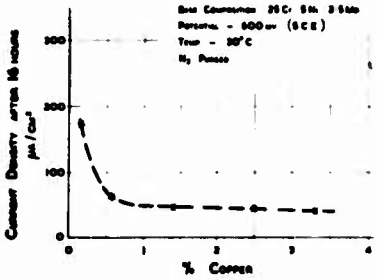


Fig. 3. Effect of Copper Content on Pitting Resistance in 3% Na.Cl.



Fig. 4.

Microstructure of 25Cr. 5Ni. 3Cu 2·5Mo Steel; Slowly Cooled after Hot Working
Magn. x 650



Fig. 5.

Microstructure of 25Cr. 5Ni. 3Cu. 2·5Mo. Steel; Annealed 1120°C, Water Quenched
Magn. x 650

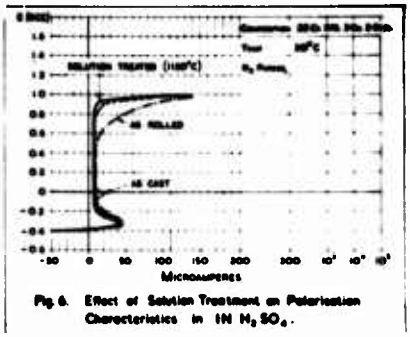


Fig. 6. Effect of Solution Treatment on Polarisation Characteristics in 1N H_2SO_4.

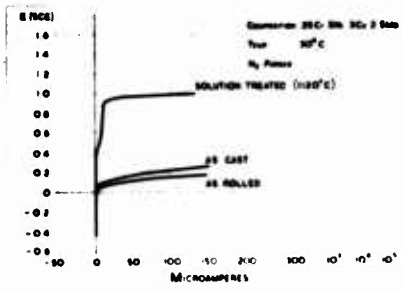


Fig. 7. Effect of Solution Treatment on Polarisation Characteristics in 3% Cl

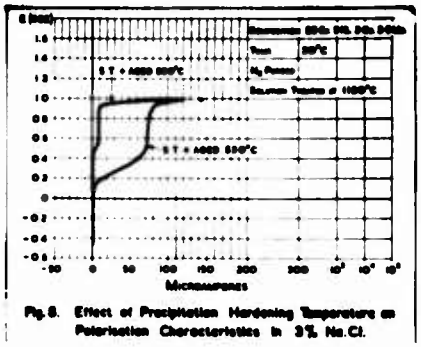


Fig. 8. Effect of Precipitation Hardening Temperature on Polarisation Characteristics in 3% Na.Cl.

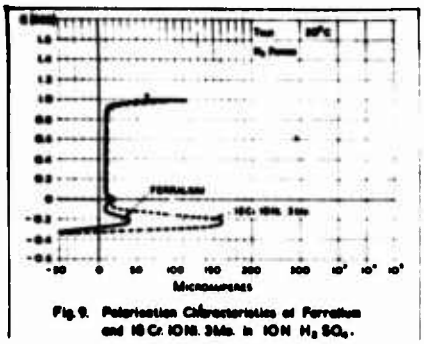


Fig. 9. Polarisation Characteristics of Ferralium and 18 Cr 10 Ni 3 Mo in 10 N H_2SO_4.

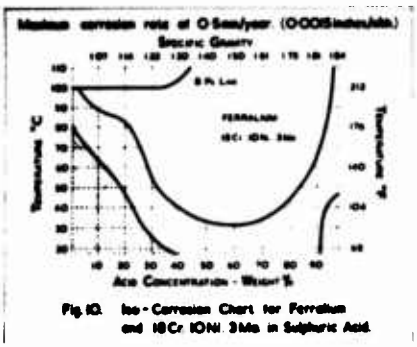


Fig. 10. Iso-Corrosion Chart for Ferralium and 18 Cr 10 Ni 3 Mo in Sulphuric Acid.

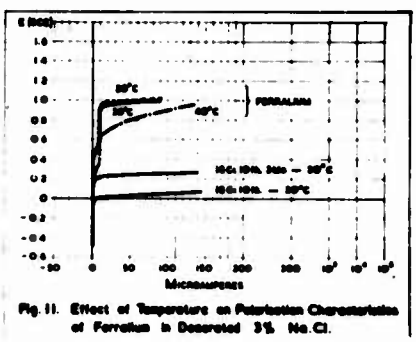


Fig. 11. Effect of Temperature on Polarisation Characteristics of Ferralium in Deaerated 3% Na Cl.

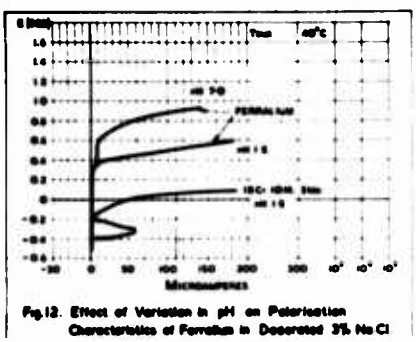


Fig. 12. Effect of Variation in pH on Polarisation Characteristics of Ferralium in Deaerated 3% Na Cl

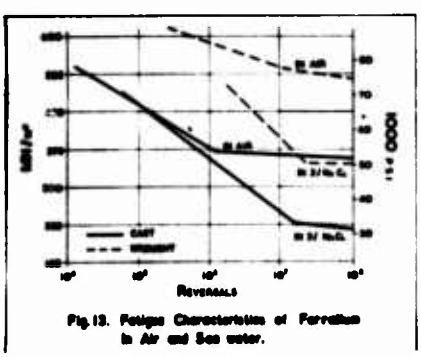


Fig. 13. Fatigue Characteristics of Ferralium in Air and Sea water.

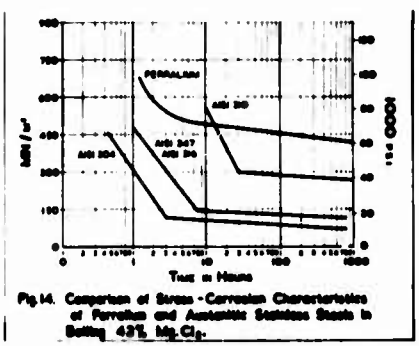


Fig. 14. Comparison of Stress - Corrosion Characteristics of Ferralium and Austenitic Stainless Steels in Boiling 42% $MgCl_2$.



Fig. 15.

Cast Ferralium Propeller after 4 years Marine Service without Corrosion or Pitting. Visible Spots are Marine Growths.



Fig. 16

Cast Ferralium Rings for Marine Shaft Seals



Fig. 17

Part of Inert Gas Scrubber System of Oil Tanker Fabricated from $\frac{3}{16}$" Ferralium Plate

Special Light Metal Alloys and Their Electrochemical Protection for Construction and Decorative Elements Used on Sea-River-Ships

Dr. Paul Csokán

General Design Institute of Machine Industry
Budapest/Hungary

On ships serving for passenger and goods transport, or on hydrotechnical installations, e.g. installation in a sea-river mouth, exposed to sea-water and fresh-water or to the changing effects of sea and continental atmosphere respectively, the component parts made of light metal alloys as constructional or ornamental elements must be provided with a surface-protecting coat that resists increasedly to the corrosional and erosive effect of the surroundings. Protecting coatings with a quality perfectly meeting the demands can be produced with electrochemical methods, traditional or special anodic oxidation processes.

The effectiveness of surface protection may be enhanced in some cases with the help of cathodic-anodic protective methods.

Key Words: Sea-river-ships; factors of sea atmosphere; factors of sea water; anodizing of light metals; conventional-, hard- and direct-colour-anodizing; cathodic-anodic protection of light metals.

---

1. Introduction

Inside the continents the most important routes of international trade have always involved the navigable rivers. Maritime navigation is even today a decisive pre-condition of intercontinental world trade. The goods transported on river waters from inland to the sea are transferred by the traditional method onto sea-going ships at seaports, which does not only mean waste of time but a considerable waste of wages too. Following the development of technics, however, river-ocean-going ships are being produced--in calibres of course determined by the size of the rivers--that are capable of transporting export-import goods from inland to oversea or from overseas to the inside of the continent without trans-shipment but which are just as well apt for passenger-transport.

On the biggest rivers of Europe, as the Danube, Rhine, the Seine, Oder, Vistula, Volga, Don, etc.--but obviously on big rivers of other continents too--more and more sea-river-going ships of this type take part in regular conveyence on seas surrounding the continent, but Hungarian ships for instance transport different goods from the Danube not only to the opposite shores of the Mediterranean but also to more distant ports of South America and Africa. These goods form obviously only a small part of the total amount of goods in maritime trade, but the tendency of development cannot be mistaken, and e.g. one of the most important routes of East-West trade is to become the Rhine-Main-Danube Channel connecting the Atlantic, the North Sea and the Black Sea with the basin of the Mediterranean Sea, after its planned construction in the near future.

The up-to-date shipbuilding industry has made considerable progress beyond the development of transmission machinery as well as equipments of navigation, telecommunication, etc., also in respect of the enlargement of choice in material. That involves, for instance, the wider use of light metals in shipbuilding industry, a fact that can be explained by the following advantageous characteristics:

- The small specific gravity of aluminium metals makes a decrease in dead weight possible to such an extent that in the loading space of ships of a given size--compared to hulls of the same size made of structural steel--sometimes the cargo weight may be increased by approximately 50%. At cargo ships this technical possibility means a considerable financial advantage.

- The favorable solidity properties of most aluminium alloys are even deep below 0°C so stabile that propensity to brittle breach does not appear, as it can be experienced at some kinds of structural steel. In cases of refrigerating cargo ships carrying perishable goods or tankers transporting undercooled liquefied gases or ships going on waters near the artic or antarctic regions the cold resistance of structural materials is a very important requirement.

- The corrosion-resistance of pure aluminium and of different aluminium alloys to mediums of different aggressivity is not always unambigous. Pure aluminium is resistant enough to the effect of sea water, and alloying it with certain metals, e.g., a defined amount of magnesium, still improves considerably the corrosion-resistance. Aluminium metals alloyed with other metals, e.g., copper, nickel, etc., are, however, increasedly sensitive and to the effect of sea water sometimes hole-corrosion in other cases inter-cristalline corrosion occurs. The danger of corrosion is especially big if metals of different kinds get into contact /contact-corrosion/.

- Choosing the kinds of metals for building sea-river-going ships and choosing the methods for the applicable surface finishing operations, utmost care must be taken to the fact that the metal parts of these ships are exposed to sometimes sea atmospheric and sea water, sometimes continental atmospheric and fresh water corrosion and erosion effects with non-predictable periodocity, for non-predictable periods. It is these circumstances therefore that caused us to study more intimately some of the characteristics of the most important medium-effects from the point of view of the applicability of aluminium elements in sea-river-going ships, and considering them to develop the technology of finishing the most suitable surface-protecting ornamental light metal constituents.

2. The Main Characteristics of Medium Effects

2.1 The Effective Factors of Sea Atmosphere

The most important factor determining the characteristics of sea atmosphere are temperature, relative atmospheric humidity and rainfall. According to the types of climate the following approximate values can be taken:

	Temperature	Atmospheric Humidity
Cold climatic area /F, frigidus/	-40...0°C	fog, snow, rain
Moderate climatic area /N, normal/	-20...+35°C	rel. vapour content max. 80%

Tropical climatic area /TH, tropicus-humidus/	over +20°C average	rel. vapour content over 80%

Significant factors are the strength and frequency of wind activity and the amount of rainfall too. Under tropical climate for instance heavy showers of such kind are possible that in ten minutes 100 mm rainfall can occur. The intensity of sunshine must be also seriously considered which under warm climate is often over the value limit of 1,2 - 1,4 cal/cm^2 min.

As a consequence of evaporation and undulation /surf/ the air space is generally contaminated by salty mist or salty water-spray changing between large concentration limits. The drops forming the mist are 90% of a size of 1 - 7 μm, and 1 cm^3 volume of mist contains an average of 2.10^5 - 4.10^6 drops. The composition of the salt contents of the drops as well as their amount follows of course the original composition of the sea-water and the regularities of evaporation.

Pure aluminium and most of the aluminium alloys of commercial quality have proved resistant enough to the effects of sea atmosphere. According to our studies carried out at natural sea-exposure stations on the surface of aluminium objects treated by traditional methods, considerable corrosional damages occurred only at aluminium sorts alloyed with non-ferrous metals apart from matting and the formation of greyish incrustation.

2.2 The Effective Factors of Sea-Water

In the composition of water in the seas of the Earth there is some fluctuation with the geographical position, the average composition is shown in Table 1. 100% salinity is spoken of when the NaCl content of water is 31 g/liter. This value can decrease to 30 - 50% at certain parts of the sea, e.g., at the mouth regions of big rivers.

Very small amounts of boron compounds /max. 0,5 mg-atom/liter B/ and changing amounts of absorbed gases, oxygen in particular /7-8 ppm/liter/ are also to be traced in sea water.

Among the enumerated components the most aggressive are the chlorides and bromides. Hydrocarbonates in solution can in case of losing carbon dioxide precipitate in the form of carbonates with magnesium or calcium in the cathode zone of metal constructions in contact with sea water. According to the change of the hydrocarbonate--carbonate equilibrium the pH value of sea water may fluctuate between 7,5 and 8,4.

Due to its solved electrolite contents of considerable amount sea water has a well measurable specific electric conductivity /k = 1/p, where p = 0,05 ohm^{-1}cm^{2}cm/. The various metals in contact with sea water--according to their material class--will be charged up to different electrode potentials and accordingly galvanic currents occur among the different metal parts, and in the anodic parts of the local galvanic-cells corrosion of different degrees /contact corrosion/ may occur. The electrochemical characteristics as well as the value of the electrode potential of the sea water//aluminium metal interface change between large limits depending on the kinds of electrolites solved in sea water, on their concentration, temperature of water, the rate of flow etc., as well as the composition of the base metal, its metallurgical state and that of its heat-treatment. The potential values measured in flowing sea water at 20 ± 2°C against calomel electrode are shown in Table 2. Comparing the data it is to be seen that from among the usual alloying elements the amount of copper has the biggest influence on the potential of the light metal.

In general, the extent of electrochemical corrosion of each metal type changes according to the developing galvanic cells, too, and this depends

mostly on the amount of the alloying copper to a bigger, and on the alloying zinc to a smaller extent. According to our model experiments carried out in sea water the rate of corrosion can be characterized with the values shown in Table 3 as functions of flow-rate, pH value and temperature of the water. According to the data magnesium has a definitely favourable effect repressing the rate of corrosion, the other alloying materials however, according to their quantity and quality as well as their interaction, increase more or less the liability to corrosion.

The flow rate of sea water does not only influence the grade of electrochemical potential but strength of wave motion has a stress effect on the endurance of coating systems /paint or other coatings/ of the metal parts in the hull. The water motion that goes with the undulation strikes at the metal surface at various parts of the submerged hull, with a very big or slight pressure. Bubbles develop at places where pressure is low, and when they break up a considerable /sometimes in the order of 60,000 psi/ cavitation force appears concentrated to a small part of space, corroding the coating which covers the metal element. Beyond the deterioration of the coatings the cavitation effect of undulation may cause fatigue corrosion fissures in a certain span of time in the base metal itself, too.

Beyond the mentioned effective forms of undulation expressively mechanical erosive affliction is brought about by the sand and other solid alluvial deposits of sea water that are of different degrees of finesses and of different physical properties.

For good measure mention must be made in the line of the effective factors about the bacteria, algae, molluscs and other living inhabitants of sea water, which may cause--according to their species--directly corrosion /e.g., sulfide-corrosion/ or erosion, or uneven damaging of the surface in form of adherences; periodical or constant breakdown at working elements of machines.

2.3 Effective Factors of the Continental Atmosphere

The atmospherical effective factors, i.e., the humid-cold, humid- or dry-hot atmosphere, the extreme value and periodicity of temperature changes, the direction and strength of the dominant wind activity, the amount of rainfall, the corrosive and erosive effects of the sand /dust/ contents whirled along by the wind are function of the geographical facts in each climatic region. The quality of the eventual agressive gases may change according to the type of industrialization of the given area.

2.4 Effective Factors of Fresh Water

In the composition of river waters hydrocarbonate and sulfate compounds of alkali and earth-alkali metals play the main role and their quantitative relation defines the pH value and degree of hardness of water.

River waters are characterized individually by the temperature, flux rate, solid deposit /sand, silt/ contents, the species and amount of biological beings in fresh waters, the quality and quantity of chemical contamination /chemicals, oil and tar products, etc./ derived from the type of the region. The contamination of river waters may change with time. Accordingly, for example the concentration of chemical soiling of the river Rhine increased to such an extent in the last ten years that the fish and other water fauna of the river diminished in a devastating manner, and the water corroded the metal parts of living or industrial installations /bridges, sluice systems, cable ducts, etc./ established in or by the water in an extremely short time and to a very great extent.

2.5 Factors of Construction or Formation

The formation of component part made of light metals /e.g., placing of

bores, bends, notches or other hollow parts collecting the occasionally condensing vapour or rain/, moreover the structural assembling of each mounting part, the welded joints, places of riveting or of other bonds, the rejoint of metal parts of different qualities etc. may play an important part in causing or accelerating corrosion.

Constructions of aluminium of the same quality are anodized generally when mounted ready, because this is the only way of ensuring a damage-free, even quality of the coating. The constructions, however, into which extraneous metal parts are to be built in, must be submitted to electrochemical surface treatment only before assembling, of course, because of danger of contact-corrosion.

3. Special Light Metal Alloys for Construction and Decorative Elements

From the point of view of alternatives in usage-technics and of assortment of material the aluminium products used in ship-building--based on our studies and considering the data adopted from the literature /1/--may be classified into the following types:

- Construction elements: for production of aperture locking devices, floor beams, bridging pieces, panels, wall coatings, rain and sun protection roofs, banisters, grids, etc.: AlMg3, AlMg5, AlMg4,5 Mn, AlMn, AlZn 4 Mg 1, as well as AlCuMg metal cladded with Al 99,5, or AlZnMgCu metal cladded with AlZn.

- Decorative elements: for manufacture of decorative wall coatings, beads, curbings, etc., employed on board or other open air places as well as inside the ship, etc.: Al 99,8 or Al 99,5 pure metals, AlMg and AlMgSi alloys.

- Running machine elements: for production of motors and other transmission machinery parts, parts of installations of electronics, telecommunication technique and ventillation technique, e.g. casting metals of high strength, AlSi and AlMgSi alloys, rolled or pressed /stamped/ goods, etc.

Types of aluminium alloys, hardenable or not-hardenable are employed alike in ship building. The usage of the latter is more advantageous, because they can be worked better and easier at ship building or mounting, and they are just as well weldable without the danger of losing strength. In this respect, too, the AlMg alloys having good strength properties have proved good /AlMg 3 and AlMg 5/, although increasing the magnesium contents over 5% the alloy becomes under certain conditions susceptible to intercristalline corrosion. AlMgSi alloys are used in the biggest quantity from among the sorts of hardenable light metals owing to their favourable strength, ease of working and of anodizing. The AlZn and AlMn alloys have also made considerable progress owing to their advantageous properties in strength, weldability and resistance to corrosion. Alloys of AlSi are used mainly for making casts, different binding elements, fittings. From among the latter the AlMg 4,5 Mn alloy is used in great quantities and with good experience in the ship-building industries.

Pure aluminium, the AlMg, AlMgSi and AlMgZn alloys may be generally produced in a well anodizable quality. In case of employing the traditional anodizing processes the alloying presence of Cu, Mn, Fe, Ni or greater amount of Si will cause a discoloured, grey or black spotted oxide layer of a poorer quality. It is to be emphasised, however, that oxide layers of a quality corresponding to the decorative or technical requirements may be produced on these metals with the so-called integral colour or direct colour anodizing processes, or with the extrahard anodizing processes to be outlined below.

4. Electrochemical Protection of Light Metal Elements Used on Sea-River-Ships

4.1 Conventional Anodizing Processes

The traditional anodizing processes current in the industry are carried out in sulphuric acid or oxalic acid electrolites, occasionally in their mixed solution with direct or alternating current /Eloxal, Alumilite, Anoxal processes, etc./. Disregarding the well-known technological details /2/, let mention be made here of the only fact that the oxide layers obtained this way, generally 30-40 µm thickness, HV = 80-100 kp/mm^2 Vickers hardness and great porosity have, therefore they can be made satisfactorily resistant to corrosion only by special pore-filler after-treatments /sealing/; furthermore, they are colourless, hence the aluminium object in question either remains in its natural colour or the coloured oxide coating having a decorative effect can be produced only with a special painting after-treatment. This oxide layer, however, may fade gradually or become spotted in the open air to the effect of sunshine or as a result of humid air "chalking" /farinage/ may occur. These damages may be eliminated by the up-to-date direct colour anodizing processes.

4.2 Direct Colour Anodizing Processes

In order to eliminate the disadvantages of the traditional anodizing processes have been the direct colour anodizing introduced, permitting the production of oxide coatings, possessing a natural colour, through direct oxidation. Such oxide coatings are lustre- and colour-proof and possess advantageous mechanical properties.

A common feature of such processes, recommended by the patent literature, is that anodizing is carried out in electrolitic solutions of special composition, under specified experimental conditions. In case of processes known up to now /KALCOLOR, DURANODIC 300, VEROXAL, etc./ smaller quantities of sulphuric acid, sometimes alkali metal sulphates, further some aromatic sulphuric acid, e.g., sulfo-salicylic acid or sulfophtalic acid in a higher concentration, or even some other additives, such as maleinic acid, are mixed to the baths. Anodizing is carried out with direct current between the limits of 50 to 120 V, and at a current density of 2,5 to 30 A/sq. dm resp. Alternate current cannot be applied to anodizing in a bath of such type. In order to obtain a proper colour density and intensity resp., an anodizing time of 50 to 60 minutes, in some cases 20 to 40 minutes is required /3/.

The process AUTOCOLOR-HSH /Fémkut/ based upon a Hungarian patent, possesses a great number of advantages, such as:

- the oxide coating having a self-colour can be obtained not only on aluminium qualities of special alloying or heat-treating, but also on any normal commercial grade aluminium;

- the colour-range, obtained by this method, is considerably larger, than those obtained by any other method: the shades are warmer and more pleasant;

- both direct and alternative current can be used for the anodizing bath;

- the technological conditions are more favourable, e.g considerably shorter exposure time as required to obtain a .iate colour intensity and density.

Both alternatives permit to produce a 1 to 30 µm thick coating during 1 to 30 minutes. The oxide coating is extremely lustre- and colour-proof. The variations of colours are shown in Table 4.

The mechanical properties are so advantageous that some aluminium object covered with a not excessively thick coating can be moderately bent, and embossed without damaging the coating itself. Its Vickers hardness corresponds to a value of 200-450 kp/sq. mm.

The porosity of the oxide coating is slight, in case of its indoor application, no pore-filling after-treatment is required, though in case of outdoor appliance, it is advisable to cover the oxide coating AUTOCOLOR with colourless thin lacquer sheating.

4.3 Hard Anodizing Processes

Anodizing processes are also known with the help of which oxide layers much thicker, harder and more wear-resistant than the common coatings may be produced on aluminium and its alloys.

The Alumilite, Martin /MHC/, Sanford, Hardas, Kape, Fémkut-Cs., Langbein-Pfanhauser /LPW/, Tomashov-Bjalobshenski methods and the technical data of other hard anodizing processes can be found in the literature /2,5/.

By most of the processes oxide layers of a thickness of maximum 35-125 µm, poor in pores and of a dense structure may be produced in 60-110 minutes. This coating is generally 350-450 kp/mm² Vickers hardness. The wear-resistance of hard oxide--in case of an originally smooth or mechanically after-refined surface--is 50% better than in the case of hardened steel and 10% better than in the case of hard chrome coating. The breakdown voltage of the layer is around 1000 V, i.e., it has a very good insulating property. The hard oxide coating is somewhat more rough than the original base surface, and with the composition of the base metal it may change from light grey to blackish grey. Alike the customary oxide coating it is hardly or not at all colourable in colouring solutions.

From the point of view of the rate /efficiency/ of oxide formation as well as the physico-mechanical and chemical-corrosion properties of the oxide layer the FÉMKUT Cs-process /6/ is extremely advantageous, according to which the anodization is carried out in a diluted electrolite with special supplements, favourably in a 1-2,5% sulphuric acid solution between temperature limits of +5....-5°C, cell voltage 40-60 V. In 60 minutes a light-coloured, middle grey oxide layer of a possibly slightly rough surface /the layer being 150-250 µm, i.e., considerably thick/ forms on pure aluminium, on AlMg, AlMgSi alloys. The hardness of the layer is HV = 450-600 kp/mm² Vickers units /"extrahard"/, its wear-resistance measured by a Taber abraser and related to the unit of layer-thickness is 30.000-40.000 cycles/µm. A layer like this is much poorer in pores /max. 5-12%/ than the customary oxide, and has even under the aggressive sea circumstances strikingly good resistance to corrosion. An attractive, bright, enamel-looking surface can be produced with slight mechanical grinding or polishing, such a coating, therefore, ensures an expressively decorative effect on the aluminium elements outside and inside the sea-river-ships, too.

4.4 Economical Characterization of the Electrochemical Surface Protection of Light Metals

The principal production costs of the surface-protecting technology of light metal elements is defined by the chemical and energy requirements of the process. The energy consumption of the hard oxide production /high cell voltage and electric liquid-cooling/ is bigger, chemical costs are less; the energy costs as well as the chemical costs of the direct-colouring anodizing are somewhat bigger than the total costs of the oxidation + colouring + pore-filling /sealing/ processes of the traditional anodizing methods.

According to our own statistical data as well as the surveys and calculations published in the technical literature /7/--depending on the

quality of the base metal, the prices of the chemicals and colouring materials, the variants of tooling and the facilities--the expense factors may be expressed by following rations:

Process	Expense Factor
Traditional anodizing in sulphuric acid, without after-colouring	1
Traditional anodizing in sulphuric acid, w ith after-colouring	1,8 - 2,6
Anodizing in oxalic acid, without after-colouring	1,5 - 2,0
Anodizing on oxalic acid with after-colouring	2,3 - 2,8
Direct-colouring anodizing in sulfon-acidic electrolite	2,2 - 2,5
Hard-oxide production by the FÉMKUT Cs-process /100 µm layer/	2,5 - 2,7

5. Other Protection Methods

Let mention be made only as reference on the cathodic-anodic protection method of the corrosion-protection. Sea water--on account of its high salt-contents /salinity/--is an ideal medium for creating an anode-cathode protection system. For the protection of the hull itself and that of the different structure parts made of steel the corrosion protection with magnesium-, zinc- or aluminium-anodes has spread for a long time. In the first place the American technical literature there are several references about the fact that constructions made of AlCu-, AlCuMg-, AlMn-, AlMgMn-type metals as well as castings with higher Cu or Si contents are effectively protected against corrosion in certain mediums with application of anodes produced from pure zinc, aluminium or rather from AlZn or AlZnMg alloys /8/.

Aluminium types that are to a bigger extent alloyed with non-ferrous metals /band or plate products, profiles, etc./ may be protected against corrosive effects by plating with plates of Al 99,5 or AlZn quality; ready assembly units, on the other hand, may be protected with plastic or paint housings, the treatment of these methods, however, is beyond the theme of the present report.

References

1/ W. MUCKLE, Aluminium /Düsseldorf/ 42, 625/1966/
F. E. FALLER, Technische Überwachung 9, 58 /1968/
W. TRÜB, Schweiz. Aluminium-Rundschau 19, 28 /1969/
F. B. PATTEN, A. H. ROEBUCK, Material Protection 7, 31 /1968/
E. ZURBRÜGG, Schweiz. Aluminium-Rundschau 20,33 /1970/
G. FORTINA, M. LEONI, Alluminio 40, 433 /1971/

2/ S. WERNICK, R. PINNER, The surface treatment and finishing of aluminium and its alloys, R. Draper Ltd., Sec. Edit. Teddington/Great Britain, 1959.
S. WERNICK, R. PINNER, E. ZÜRBRUGG, R. WEINER, Die Oberflächenbehandlung von Aluminium, E. G. Leuze Verlag, Saulgau/Württ./Germany, 1969.

3/ H. NEUNZIG, W. RÖHRIG, Metall 18, 590 /1964/
G. E. GARDAM, Aluminium /Düsseldorf/ 41, 423 /1965/
R. D. SHARROCK, Light Metals 7, 47 /1964/
E. BLOCH, E. ZURBRÜGG, Aluminium /Düsseldorf/ 42, 101 /1966/

J. M. KAPE, Galvanotechnik 58, 652 /1967/
J. M. KAPE, The use of integral colour anodizing processes, Paper at the Symposium on Anodizing Aluminium, University of Aston, 1967.

4/ P. CSOKÁN, Metalloberfläche 23, 112 /1969/
P. CSOKÁN and al., Hungarian Patent, Nr. 155.034/Fe-665/1965/Budapest

5/ P. CSOKÁN, Electrochemical surface treatment of light metals /Könnyűfémek elektrokémiai felületkezelése/, Univ. Book-Edition Ltd. /Tankönyvkiadó Váll./, 1965, Budapest/Hungary

6/ P. CSOKÁN and al., Hungarian Patent Nr. 147.102/Fe-438/1959/Budapest
P. CSOKÁN, Corrosion et Anticorrosion /Paris/ 8, 158 /1960/
P. CSOKÁN, Metalloberfläche 15, 113 /1961/
P. CSOKÁN, DECHEMA-Monographien /Germany/ 39, 229 /1960/

7/ P. ARONSON, Metallen /Stockholm/ 21, 67, /1965/

8/ T. J. LENNOX, Jr., M. H. PETERSON, R. E. GROOVER, Materials Protection 7, 33 /1968/
T. J. LENNOX, Jr., R. E. GROOVER, M. H. PETERSON, Materials Protection and Performance 10, 39 /1971/
R. A. HINE, M. W. WEI, Materials Protection 3, 49 /1964/
W. B. BROOKS, Materials Protection 7, 24 /1968/
F. B. PATTEN, A. H. ROEBUCK, Materials Protection 7, 31 /1968/

Discussion

Hector Campbell: There is just two things I would like to ask you. The process that you described right at the finish of your paper--can you apply this no matter what aluminum alloy you are working with or are there any restrictions on the materials on which it can be used? The second point was I noticed when you were in the first part of the paper mentioning the different alloys used for different purposes you mentioned at one point the aluminum magnesium silicon alloys, but as I understand it you mentioned these only for use for decorative purposes and not for structural purposes which surprised me because we in the U.K. and I think here in the U.S.A. also would use these quite extensively as structural materials.

Linder: For the first question the answer is I think that it can be used. It can be applied to any kind of aluminum alloys. There are restrictions according to the oxide or the thickness of the oxide in the air and there are some differences in the method. To the second question, these groups or types of alloys that I read on were just the main groups. There are some other types of course and for instance the aluminum magnesium silicon type of alloys can be used also for construction and they do use it for the river going ships also, but for brevity and for saving time, I did not read it, but these will be also in the proceedings.

Table 1.

Average composition of sea water

Component		Concentration, mg-at/liter
Sodium	Na^{+}	470....471
Potassium	K^{+}	9,9...10,0
Magnesium	Mg^{++}	53,5...52,5
Calcium	Ca^{++}	10,2...10,3
Strontium	Sr^{++}	0,12...0,16
Chloride	Cl^{-}	548....549
Bromide	Br^{-}	0,8....0,85
Sulfate	SO_4^{--}	38,2...38,3
Bicarbonate	HCO_3^{-}	2,3....2,4

Table 2.

Normal electrode potential of light metals in sea water

Metal type	Characteristic alloy components	Normal potential, V
Al 99,99		-1,42
Al 99,99	/0,002% Cu/	-1,21
Al 99,99	/max. 0,02% Cu+0,02% Zn/	-0,92...-0,96
AlMg 0,5	0,4- 0,6% Mg	-1,01...-1,03
AlMg 2,5	2,4 - 2,6% Mg	-1,03
AlMg 3,5	3,4 - 3,6% Mg	-1,04
AlMg 5	4,9 - 5,2% Mg	-1,05
AlCuMg 3	0,04-0,06% Cu+2,9-3,1% Mg	-0,93...-0,96
AlCuMg 1	0,04% Cu +1,2% Mg	-0,77
AlCuMg 1	0,3% Cu +1-1,1% Mg+0,04% Zn	-0,87
AlCu 4,5 Mg 1,5	4,5-4,7% Cu+1,4-1,6% Mg	-0,59...-0,61
AlMg 3,5 Zn 4 Cu 0,5	0,6-0,7% Cu+3,2-3,6% Mg+4-4,5% Zn	-0,75...-0,77
AlMg 2,5 Zn 5,5 Cu 1,5	1,6-1,8% Cu+2,5% Mg+5,5-5,8% Zn	-0,72
AlCu 6,5	6,5% Cu+ max. 0,5% Mg +Zn	-0,69
AlMgSi 1	1-1,2% Mg + Si	-0,80
AlMgSi 2	1-1,5% Mg	-0,80
AlSi		

Table 3.

Corrosion of light metals in sea and river water

metal quality	Corrosion losses mm/year in	
	sea water	river water/Danube/
Pure aluminium	130....280	60....100
AlMg alloys	70....140	50.....90
AlMgZn alloys	100....450	70....290
AlCu alloys	600....1100	220....685
AlMgSi alloys	100....220	100....190
AlSi alloys	180....380	130....880
AlMn alloys	200....360	100....230

Table 4.

Colour of anodic oxide coating to be produced by the AUTOCOLOR-ESA Process on different qualities of aluminium

Type of metal	Type of current	Voltage V				
		5v	10v	15v	20v	25v
Al 99,5	D.C.	-	golden	brown colour	reddish /greyish/	olive brown
	A.C.	-	golden	gold-brown	brownish /ruddy/	brownish black
AlMg 3 AlMg 4	D.C.	light khaki	medium khaki	dark khaki	coffee brown	-
	A.C.	light yellow	old-gold	light brownish	ruddy brown	-
AlMgSi	D.C.	light yellow khaki shade	light khaki	dark khaki	dark grey khaki shade	dark olive green
	A.C.	light yellow	golden	brownish	tobacco brown	dark brown
AlMgSi	D.C.	yellow brown /greyish	dark brown shade/	dark brown	brownish-black	brownish black
	A.C.	-	golden	old-gold	light brownish	medium brown
AlCuMg	D.C.	-	-	yellow	greyish black	bluish grey
		-	-	dark drab	light tobacco brown	-
AlSi 1	D.C.	-	-	light brown /greyish	medium brown shade/	
	A.C.	-	-	light brown	medium brown	-
AlSi 4	D.C.	-	-	medium brownish grey	dark brownish grey	-
	A.C.	-	-	tobacco brown	tobacco brown	-
AlSi 8	D.C.	-	-	dark yellowish grey	greyish brown	-
	A.C.	-	-	dark yellow grey	greyish brown	-
AlMnSi	D.C.	-	-	light grey	medium grey	-
	A.C.	-	-	medium grey	medium grey	-
AlMn 1	D.C.	-	-	light brown /greyish	dark brown shade/	-
	A.C.	-	-	brownish brown	ruddy brown	-
AlCuMg AlZnMgCu AlZnMgCu	D.C.	-	-	dark grey	light grey	light grey
	A.C.	-	-	dark grey	light grey	light grey

Alleviation of Corrosion Problems in Deep Sea Moorings

R. L. Morey[1] and H. O. Berteaux[2]

A number of single point taut moorings have been lost necessitating an analysis of all components in the mooring line. Systematic examination of retrieved components has indicated the presence of corrosion at all stages in the mooring from the surface buoy to the anchor. This includes the various instrument housings and attachments, the mooring line and its terminations, and the interconnecting hardware such as shackles, links and chain. Pitting type corrosion, crevice corrosion, galvanic incompatibility, corrosion fatigue and stress corrosion cracking have been identified and design changes made.

Failure analysis of mooring line specimens exposed in a shallow water experimental array to long term environmental effects has helped the systematic identification and classification of failure modes. Rope specimens which have been tested in this shallow water (120 feet) evaluation program included jacketed and unjacketed carbon steel, modified stainless steel (18-18-2), titanium, Inconel 625, and fiberglass. The characteristics of such materials are evaluated and a comparison made for the newer materials with the standard carbon steels.

The diagnostic capability obtained from this continual analysis has been used to advantage to recommend design and material changes resulting in an improved resistance to environmental deterioration.

Key Word Moorings

1. Introduction

Single point taut-moored systems are used for the placement of instruments of oceanographic and meteorological data. Such buoy systems are deployed each year in the Atlantic Ocean by the Woods Hole Oceanographic Institution for the Office of Naval Research and are retrieved on a regular basis.

These systems sense and record the velocity fields of winds and ocean currents in situ and over long periods of time. Long-term series measurements thus obtained enable the physical oceanographers to establish a correlation between experimental data and the theoretical concepts of oceanic flow.

The type of mooring consists either of a single surface or subsurface float and a taut mooring line. (Fig. 1) Recording instrumentation is placed on the float and inserted in the line at various depths.

C.S. Draper Laboratory[1]
Massachusetts Institute of Technology
Cambridge, MA 02142

Ocean Engineering Department[2]
Woods Hole Oceanographic Institution
Woods Hole, MA 02543

The mooring line is generally part wire rope and part synthetic fibre rope but can be all fibre rope depending on the prevalence of fish bite in a particular area.

The compound mooring line configuration has the advantage of low cost, ease of handling at sea, prevention of possible failures due to fish bites in the upper part of the line, reduced excursion and consequently low noise level on the scientific data.

The reliability of single point moored buoy systems depends on the performance of each of the mechanical components in series in the mooring line - wire rope, chain, hardware, nylon rope, instrumentation casings, etc.

In order to improve this reliability one must positively identify defective parts prior to use and also eventually establish the modes and causes of failure of components while in use. If failure of a component results in failure of the entire mooring a back-up recovery system (1) can be used to recover the remaining part of the failed mooring lying on the ocean floor. The failed component thus retrieved can then be subjected to macro and micro examination to determine the failure mode.

Reliability improvement results in greater mooring life expectancy. This will tend to minimize expensive ship time to retrieve, service and re-implant the systems. Furthermore as the capability for long term data storage increases the demand for longer life of the components that make up the total system is also increasing.

A major cause of mooring failure is corrosion. Other mechanisms of deterioration such as tensile or shear loading effects, fatigue and material defects are often present and must also be considered. Furthermore there is always an interaction between the various failure mechanisms and any one failure may be a combination of one or many factors. For example, a cable may fail by corrosion fatigue, corrosion cells may be set up between an instrument and associated hardware such as shackles, bridles, chains, etc., or can be compounded by tensile effects producing stress corrosion. Failure can be due to mechanical or environmental effects grafted onto tensile fatigue and corrosion factors.

In September 1967 a buoy with a fractured wire rope was found 250 miles off station. This buoy was recovered and an analysis made of the failed cable (2). In this case the conclusion was that deformation had occurred at the point of fracture probably caused by a kink and that subsequent fatigue compounded by corrosion caused the failure of a number of wires in this area. Due to a reduction in the ultimate strength of the wire rope it broke with the balance of the wires failing in tension.

As part of the engineering effort to improve the reliability of deep sea moorings, a continuing program of metallurgical analysis was then inaugurated (3). This paper presents a number of typical case studies, and reviews briefly the theoretical aspects common to most of the failures considered and outlines the corrective means of prevention resulting in increased reliability of deep sea moorings.

2. Environmental Effects

Preponderant environmental effects resulting in accelerated deterioration of mooring components are:

Corrosion: for long life, the corrosion behaviour of a component can be the limiting factor. The intrinsic corrosion resistance is not the only concern but also the often inadvertent coupling that can take place between different materials, e.g. a taut stressed cable in contact with a slack drifting cable has caused failure by galvanic action (4). Corrosion

[1] Figures in parentheses indicate the literature references at the end of this paper.

tendencies are difficult to predict and there is still a need for testing in the ocean prior to use. For simple corrosion one can make allowance for strength reduction due to loss of material but to overlook other factors such as stress corrosion cracking, hydrogen embrittlement, pitting corrosion, galvanic coupling, etc., could be disastorous.

Fatigue: As has been pointed out (5) surface buoy motion can induce repeated bending and torsion stresses in points of attachment of the mooring line as well as cyclic tension stresses in the line itself. Furthermore, in strong currents, vortex shedding can create a strumming situation with high frequency lateral loading. Being in a corrosive medium, the problem is compounded and the effects of corrosion fatigue are greater than the effects produced by either corrosion or fatigue acting singly. Such failures can generally be traced to stress raisers such as sharp edges, pits, nicks, etc.

Biological attack: At the upper portion of the line, fouling is present and can lead to the initiation of pits on surfaces. This problem is actively being studied at W.H.O.I. to determine the mechanism of corrosive attack.

Sharks and several benthic species attack mooring lines, gashing the protective plastic jacket of wire ropes and exposing the underlying steel cable. (Fig. 2) Although some corrosion has occurred at the cuts, wire rope failures due to fish attacks have not yet been identified. As can be expected on synthetic fibre ropes, the problem is more acute and losses of moorings due to fish bites have occurred.

3. Analysis of Retrieved Components

Metallurgical and mechanical analysis was performed on buoy systems components which had been exposed to the environment either as part of regular deep sea moorings or as part of special test moorings deployed in shallow waters. The shallow water test array of the Woods Hole Oceanographic Institution which was implanted seven miles off Cuttyhunk, Massachusetts from 1969 to 1972, enabled specimens of different materials and configurations to be submitted to prolonged environmental exposure. A typical test buoy is depicted in Figure 3. The response of the components evaluated in this way differs from that of components inserted in deep sea moorings of finite duration in that the effects of the environmental exposure extend over a longer period, with a greater prevalence of marine fouling, and with smaller temperature gradients along the line length. This evaluation serves a valuable purpose in that the effects of mechanical loading and corrosive media can be studied, problem areas identified, new materials appraised and modifications incorporated to improve the reliability of deep sea moorings.

Upon recovery of these moorings the components or specimens were examined to determine the degree of deterioration and when applicable establish the mode of their failure. This systematic analysis was performed primarily at the C.S. Draper Laboratory of the Massachusetts Institute of Technology and at the Ocean Structures, Moorings and Materials Section of the Woods Hole Oceanographic Institution.

Components or specimens were visually examined immediately after retrieval to detect gross features of deterioration (corrosion, fish bites, kinks, wire breaks, etc.). The ultimate tensile strength of representative samples were often determined to establish the percentage of strength loss. The bitter ends and/or the fracture faces of components were also subjected to exhaustive macro and micro examination and metallurgical testing in order to understand the mode and ascertain the cause of the failure. In broken wire rope, for example, the strands are carefully disassembled and the fracture face of each wire is examined to determine nature of the break. Samples are photographed in the raw state and after solvent cleaning are inspected by a 100X stereo microscope. Stainless steel specimens are often cleaned in dilute nitric acid.

When necessary, cross-sections of specimens are prepared metallographically for study. A scanning electron microscope has been found useful in determining the fracture path in those instances where subsequent corrosion has not damaged the fracture face.

The following, outlines in the form of a series of case studies, some of the typical and more interesting modes of deterioration and failure so far encountered.

4. Case Studies

1. Wire Rope Assemblies. Wire rope is extensively used in deep sea moorings as it is easy to store and handle, is moderate in cost, has low elongation characteristics and resists fish attack. It is, however, susceptible to mechanical damage (kinks), fatigue and corrosion of the wires. The success of mooring lines using wire rope depend to a great extent on the type of wire rope selected and on the means of protection from the environment (6). Furthermore, wire rope terminations are critical and often are an additional cause of wire rope assembly failure. Deterioration and failure due partly or entirely to corrosion effects has been noted:

a. Deep Sea Moorings: The initial moorings used Nicopress fittings for terminations and bare steel wire rope with a relatively high failure rate. A change to a better termination (Fig. 4), an improved type of rope (torque balanced), and larger size with zinc coated wires, has resulted in a very low failure rate within the limits of present life expectancy (6 months). As an additional protection against corrosion and for better hydrodynamic characteristics, the rope is covered with a plastic jacket. Usually, this is a polyethylene/polypropylene copolymer but other coatings can be used, such as urethane and polycarbonate. Fish bite is still a problem and Fig. 2 shows a severely slashed wire rope jacket retrieved from mooring 314. Fish bite has not as yet caused a cable failure although the inside is flooded. The construction of any wire rope causes the presence of a multitude of crevices which should permit crevice corrosion to occur. This, being like pitting corrosion, an autocatalytic type of corrosion. As noted by Fontana (7), the driving force for the reaction to continue is the need to maintain electroneutrality. The overall reaction involving the dissolution of metal M and the reduction of oxygen to hydroxide is as follows:

$$\text{Oxidation} \quad M \longrightarrow M^{+} + e$$

$$\text{Reduction} \quad 0_2 + 2H_20 + 4\ e \rightarrow 40H^{-}$$

Initially these reactions occur uniformly both within and outside the crevice. Charge conservation must be maintained and a hydroxyl ion is produced for every metal ion in solution. After a short time the oxygen within the crevice is depleted and as dissolution of metal produces an excess of positive charge in the solution, this must be balanced by the diffusion of chloride ions into the crevice to maintain electroneutrality.

For metals commonly used in underwater applications, hydrolysis takes place.

$$M + Cl^{-} + H_2O \longrightarrow MOH + H^{+}Cl^{-}$$

Chloride and hydrogen ions accelerate the dissolution rate and consequently the rate of oxygen reduction on adjacent surfaces also increases. However, as these gashes are generally narrow, it is postulated that there is a limiting exchange of water within the jacket and outside. Corrosion does occur but generally at a very low rate due to the non-availability of replacement ions. On occasions damage to the jacket has occurred during deployment and if severe enough the corrosion can also be severe. The results from the shallow water test site does show that for the same type of rope, jacketed samples outlast bare samples by a factor of approximately 4:1.

Fatigue failure have occurred with the termination fitting. Until recently they were

manufactured from a 1017 carbon steel eyebolt with a drilled hole in the shank. The shank is swaged over the wire rope and the resultant strength of such a bond should exceed the rated strength of the wire rope. Station 374 was set in April 1971 and failed within 7 days at a depth of 500 meters below the surface under generally calm conditions. The individual wires were examined and most had failed in shear leading to the conclusion that an improper swaging operation had taken place. This was not a corrosion problem but only indicates the need for careful examination of each failure. A number of moorings are set at W. H. O. I. site D approximately 100 miles south from Woods Hole with few recent failures in wire rope. Stations 403 and 405 set October 1971 failed at the termination with the shank failing in fatigue, after 14 and 60 days respectively. Occasionally, the Gulf Stream shifts and these particular moorings were subjected to higher currents and consequently greater stress than for which they were designed. The endurance limit was exceeded and the failures were due primarily to fatigue but also compounded by the environmental effects of the ocean. To overcome the fatigue problem in the termination itself, the end fitting had to be redesigned. It is now made of 1040 steel with a heavier wall thickness to increase the endurance limit of the steel. Such fittings are now routinely being used.

b. Shallow Water Array Moorings: Wire rope evaluation has so far been the principal objective of the shallow water tests. For such rope flexibility, resistance to impact loading and resistance to hydrodynamic drag are important features. The latter factor can be reduced somewhat by using a swaged wire rope which has a smaller diameter for a given number of wires. The swaging operation does indent wires and tests in the shallow water array in this configuration showed that fatigue cracks had propagated from such areas.

For long life, the corrosion behaviour of a wire rope can be the limiting factor and this has prompted an evaluation of newer materials.

Two samples of Inconel 625 1/4" - 7x19 aircraft construction wire ropes were tested and retrieved after 279 and 294 days on station. Broken wires were noted and part of the rope had "bird caged." This can happen with a sudden load release or with cyclic loading the rope can rotate and separate the strands. The wires that were broken were not the core wires and examination showed that these wires had broken with brittle type fracture. It appears that this configuration rather than corrosion has caused the failures noted. It would be desirable to test this material in a more standard type of configuration such as a 3x19 torque balanced rope.

Three samples of an 18/18/2 (Cr, Ni, Mo) modified stainless steel have been tested at the shallow water site and failed after approximately 12, 60, and 75 days respectively. All three samples were 3/16" 3x19 torque balanced cable and the first two samples failed at the termination which was a standard swaged steel eye bolt. A defective swaging operation had caused shearing of the wires and premature failure of the first rope tested. The second rope failed at the termination due to fatigue. The third rope utilized stainless steel aircraft type swaged terminations and specialized grips to transfer bending motion away from the termination. The wires failed in brittle fracture and metallographic examination shows cracks in the wire both at the point of failure and away from this zone. It was thus concluded that the problem belonged more to the actual wire drawing process than environmental effects.

A titanium wire rope 1/4" 7x7 configuration consisting of 6 Al 4V wires was tested and failed after 27 days. Each individual wire was resin coated and the end terminations consisted of epoxy filled socket grips. The rope failed completely approximately 1" from one termination in a brittle fracture and partly failed at the other termination. Micro hardness tests indicated that work hardening was not a factor. As has been shown (8) such alloys are susceptible to stress corrosion cracking which can be related to microstructure and the effect of alloying elements such as aluminum. The local embrittlement is generally associated with propagation of stress corrosion cracks and further tests are planned with this rope

to more fully identify cause of failure.

A sample of 1/4" 1x7 jacketed glass fibre rope with epoxy filled end fittings was tested and failed at the end fitting after 146 days. Two samples of Nupaglass monostrand fibre rope were tested and failed after 370 days and 618 days respectively. As this rope shatters on failure, it is difficult to determine the cause but may be due to hydrolytic effects. In comparison, it should be noted that a torque balanced 3 x 19 jacketed mild steel cable set in May 1970 is still on location whereas another sample with deep gashes to simulate fish bite failed after 367 days. Also two samples of 1 x 42 G. A. C. jacketed cable failed after 533 and 581 days respectively by fatigue at the termination.

2. Mooring Line Points of Attachment

a. Attachment to Buoy: Mooring 228 was set in the North Atlantic on December 19th, 1968. The surface buoy had disappeared when time came for recovery on April 17, 1969. Recovery was achieved by use of a back-up recovery system. This compound mooring used 1 x 42 UHS steel cable and 5/8" nylon rope. Failure occurred at a 1" diameter stainless steel bolt on the rigid bridle under the surface buoy which is used as a connection point from the mooring line to the buoy (Fig. 5). The tension record on a tensiometer close to the surface showed the highest recorded tension to be 4,000 lbs. This bolt has been previously used and the actual immersion time is difficult to ascertain.

The fractured face showed a relatively smooth surface, covering approximately seventy percent of the area while the balance had a rough crystalline appearance. The smooth surface was marked with "beach marks" more pronounced at the edge but extended across the surface. Micro examination at 500X showed no signs of ductility in the smooth area but was evident in the region that broke with a crystalline appearance.

It was concluded that the bolt had failed in fatigue and that it had followed the three stages of the fatigue process:-

1. Initial fatigue damage leading to a crack initiation.
2. Crack propagation until the remaining uncracked cross-section of the part became too weak to carry the load imposed upon it.
3. Final sudden fracture of the remaining cross-section.

As this failure occurred in sea water, the failure could more properly be called corrosion fatigue. Microscopic examination was carried out to determine the cause of the initial crack. The presence of sulfide/selenide stringers indicated that this material was a free machining grade steel and was verified by analysis to be Type 303. Surface examination in the vicinity where the crack originated showed the presence of deep pits, often as an extension of the sulfide/selenide stringers. It was concluded that the fatigue crack started at a pit site caused by corrosion due to the inhomogeneities present in the form of the stringers. In corrosion fatigue the rate of crack propagation is enhanced due to the effect of cyclic stresses and corrosion, and also the rate of corrosion is affected by the properties of the surface film. The film on stainless steel once broken in sea water cannot be reformed. The pitting type of corrosion is one form of electrochemical corrosion being an autocatalytic type of anodic reaction. This type of failure being due to corrosion fatigue, step 2 of the classical fatigue process outlined above, could be modified in that the combined action of corrosion and cyclic stresses damages the steel to such an extent that the fatigue process is accelerated and that even if the corrosive environment were entirely removed, fracture would still result.

Unfortunately, the prediction and prevention of fatigue failure is a complex subject and the present state of the art leaves much to be desired on the numerous factors, influencing fatigue behaviour. It is possible, at least in principle, to overdesign a part by overestimating the expected loads and by keeping the design stresses at very low levels. In order to

prevent fatigue failure there are three approaches that can be utilized. An analytical approach, an experimental approach and planned inspection of the component during their life. Due to insufficient data, a purely analytical approach has severe limitations. An experimental approach is expensive and time consuming but an inspection and monitoring method can be beneficial. In this application, the material was changed to a 316 type stainless steel which eliminates the presence of stringers and although they are susceptible to a pitting type corrosion, they are less susceptible than the steels they replaced. The components are routinely inspected after each retrieval.

b. Attachment ot Instruments Inserted in the Line: Another example of a problem with stainless steel is the failure of a bail of a tension meter housing on Station 323. This mooring was set January 4, 1970 and failed March 9, 1970. This bail had previously been used for 4 months. The mooring was on the ocean bottom which caused also the collapse of the instrument housing not being designed to withstand high pressure. As noted in Fig. 7 the bail is in the shape of a U-bolt passing through the end plate of the case and is held in place by nuts on top and bottom of the plate. To prevent nut rotation, they were tackwelded onto the bolt. The fracture face of this bail was examined using a scanning electron microscope which showed that failure had occurred by stress corrosion cracking. The requirements in this case are a tensile stress and a corrosive medium. Different materials are attached by different media and stainless steels are subject to cracking in a chloride environment. Analysis showed that the material was also a free machining grade type 303 stainless steel which after welding is susceptible to intergranular corrosion. This attack is localized at and adjacent to grain boundaries with relatively little corrosion of the grains. Unless stabilized steels are used, welding causes chromium depletion at the grain boundaries. Metallographic sectioning showed that this was the case and that intergranular corrosion was present. Pits were noted at the surface and apparently at least one was deep and sharp enough to initiate a stress corrosion crack. This is generally a very rapid mode of deterioration. Brown has pointed out the problems in quantifying the index of resistance to stress corrosion cracking, an index comparable to the arbitrary 0.2% offset yield strength index of resistance to plastic deformation. It is possible that cathodic protection measures may help in coping with stress corrosion cracking but not enough data is available to generalize.

Another failure occurred in Station 322 and examination of retrieval hardware showed failure was at a current meter utilizing same type of bail. The problem of intergranular corrosion can be overcome and in this case, new bails were made of 316 stainless steel and the nuts were epoxied onto the threaded portion. All instruments were so modified but on station 373 a current meter failed. This bail was also examined by a scanning electron microscope and showed also that the bolt had failed by stress corrosion cracking. In this case, the initial crack had occurred at the root of the thread. These threads are machined, not rolled, and the root in this case was rough and sharp. This was sufficient to form a crevice and a pit had formed and again a stress crack had propagated causing failure. The solution in this case was to redesign the bail and one typical modification was to use a threaded eyebolt and another was to cathodically protect the bail with an expendable block of zinc.

3. Mooring Hardware

a. Shackles: 1/2" round pin anchor shackles with galvanized steel cotter pins were originally used to connect the mooring components. The pin of the shackle is held in place by the cotter pin, but tests run in the shallow water test site showed that the cotter pin could corrode away, allowing the shackle pin to fall out. Corroded and abraded cotter pins were found on the moorings, corrosion being accelerated by motion. Tests were run on alternate materials for cotter pins in both deep and shallow water moorings and a change was made to use type 316 stainless steel. A further modification was made in that the shackle pin was initially replaced by a bolt held by a "stop nut" with a nylon insert. However, the nylon insert created a further problem of crevice corrosion so that the final

configuration is now to use stop-nut without a nylon insert, backed up by a 316 stainless steel cotter pin.

b. Toroid Bands: These bands are used to hold the supporting structure on the syntactic foam surface buoy. Mooring 379 had a band that was completely broken and a second band that had partly fractured. These bands are made of 304 stainless steel and although the cracking had occurred near the welds there was no evidence of improper welding techniques. There is a fibreglass coating over the band and the welded area was rought. It was concluded from the nature of the crack and the presence of further cracks away from the fracture zone that cracking had occurred due to crevice corrosion and failure was due to corrosion fatigue. It was recommended to the manufacturer to smooth the welded areas, by polishing if necessary to reduce the presence of roughened areas.

c. Brummel Hooks: These hooks are used for attaching glass balls to a mooring line having a quick connect/disconnect facility. In this way, glass balls in nylon nets can be quickly attached to a line as it is being paid out from the ship, such balls being essential for buoyancy purposes. These hooks are only available in manganese bronze in a composition that is susceptible to dezincification or selective corrosion. In this type of corrosion, which is noted in brasses and bronzes containing more than 15% zinc, the zinc is corroded away, leaving behind a porous copper mass of little strength. The slow disappearance of zinc from the alloy can be disastrous, as apart from a change in color which can be attributed to tarnishing, there is no marked change indicating that corrosion is taking place. The loss in tensile strength caused the hooks to fracture with the loss of balls. As these hooks are not available in alternate materials, a time limit is now placed on the time of exposure. They are used once on 4 month moorings and if a mooring is expected to remain on station for more than this period, alternate means of attachment of glass balls to the line are used. Such a method is to place the glass balls in polyethylene containers which are then bolted onto chain.

4. Instrument Hardware

The connecting hardware on the instrument cases is usually stainless steel whereas the terminations of the wire rope are mild steel which has led to problems with galvanic corrosion. This problem has generally been alleviated by careful consideration of the general rules:-

a) Use a combination of materials as close together as possible in the galvanic series.
b) If dissimilar metals are to be used, ensure that a large anode is coupled to a small cathode.
c) Coat cathode only and not the anode.
d) If possible, install a third non structural metal, e.g. zinc, anodic to both materials in galvanic contact.

The instrument cases are generally extruded aluminum alloys 7075-T6 or 6061-T6 which are hard coat anodized and then coated with an epoxy paint. Care must always be taken to ensure that this coating is not ruptured as otherwise serious pitting can occur. The fasteners used on such cases are usually 316 stainless steel. For cathodic protection, two methods can be utilized:-

a) All cathodic metal grounded. In this case, all material is electrically at the same potential with a common anode to protect both metals.
b) All cathodic metals electrically isolated from each other and protected by individual anodes.

Both methods are being used and under evaluation for life and cost effectiveness.

5. Review of Corrective Measures

Typical corrections recommended and implemented for increased reliability of moorings were:

- Cathodic protection
- Elimination of galvanic incompatibility
- Precautions in welding
- Precautions in machining (elemination of roughened surfaces)
- Material changes (i.e. 316 S.S. in lieu of 303 S.S. , etc.)
- Coatings (care taken in surface preparation)
- Elimination of crevice corrosion (use of sealants)
- Design for corrosion fatigue and stress corrosion cracking

6. Conclusions

A program instituted by the Ocean Engineering Department of the Woods Hole Oceanographic Institution and carried out primarily at the C.S. Draper Laboratory of M.I.T. has involved the failure analysis of numerous mooring line components. This continual analysis has been used to advantage to recommend design and material changes resulting in an improved resistance to environmental deterioration.

The improved reliability is evidenced by longer moorings and the major causes of problems now are mainly mechanical. This can be due to too much tension in strong currents, vibration, or isolated events such as a weak component. It is imperative that each new mooring or instrumented array be carefully examined for corrosion problems, particularly at the design stage for the various instruments used in line.

The work reported in this paper was supported by the Office of Naval Research under Contract Number N0001 4 - C0241 - NR083 - 004.

References

1. H.O. Berteaux, R. Heinmiller, "Back Up Recovery Systems of Deep Sea Moorings," W.H.O.I., Tech. Memo. 69-7.

2. H.O. Berteaux, E.A. Capadona, R. Mitchell and R.L. Morey, "Experimental Evidence on the Modes and Probable Causes of a Deep Sea Buoy Mooring Failure," P. 671 Trans. Marine Tech. Soc. 1968.

3. R. Morey, "Evaluation of Long Term Deep Sea Effects on Mooring Line Components," M.I.T., C.S. Draper Lab Report (In Press).

4. J.M. Dahlen, "Oceanic Telescope Engineering Program," M.I.T.C.S. Draper Lab Report E-2367 (1970).

5. H.O. Berteaux and R.G. Walden., "An Engineering Program to Improve the Reliability of Deep Sea Moorings," 6th Annual Preprints, M.T.S. (1970).

6. H.O. Berteaux, "A Review of W.H.O.I. Buoy Programs," Collcque Internationale sur L'Exploitation des Oceans," Theme V, Tome II, Bordeaux (1971).

7. H.G. Fontana and N.D. Greene, "Corrosion Engineering," McGraw Hill, New York (1967)

8. T.L. Mackay and N.A. Tiner, "Stress Corrosion Susceptibility of Titanium Alloys in Aqueous Environment," P. 61, Met. Eng. Qtly. (1969).

Summarized Discussion

Discussion from the floor pointed out that stress corrosion cracking, such as might be inferred from the reported cracking failure in the 18% Cr, 8% Ni stainless steel, would not be expected to occur in unheated sea water unless the steel had been severely cold worked.

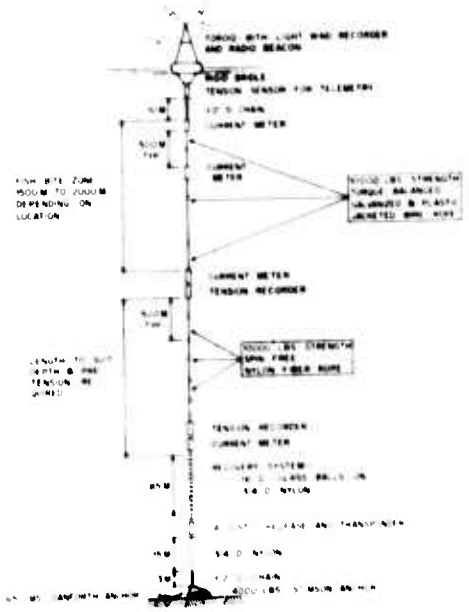


Figure 1. Typical W. H. O. I. Surface Buoy System



Figure 2. Fishbite on Jacketed Wire Rope

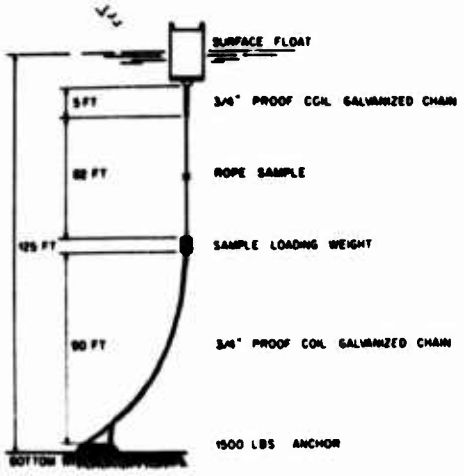


Figure 3. Shallow Water Test Array

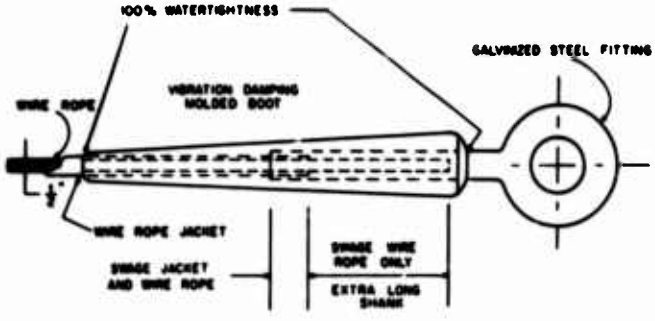


Figure 4. Typical W. H. O. I. Termination



Figure 5. 1" Bolt Failure at Buoy Bridle Connection



Figure 6. Failed U-Bolt from Tensiometer

The Relationship Between the Concentration of Oxygen in Seawater and the Corrosion of Metals

Fred M. Reinhart and James F. Jenkins

Naval Civil Engineering Laboratory
Port Hueneme, California 93043

The research program to determine the effects of deep ocean environments on materials conducted by the Naval Civil Engineering Laboratory over the past ten years has produced much corrosion information on alloys exposed in three seawater environments of differennt oxygen concentrations, which were: an average of 0.4 milliliters per liter at a nominal depth of 760 meters, an average of 1.35 milliliters per liter at a nominal depth of 1830 meters and an average of 5.75 milliliters per liter at a nominal depth of 1.5 meters. The corrosion rates of 169 different alloys after one year of exposure were correlated with the respective oxygen concentrations to determine whether or not any relationships existed between corrosion rates and oxygen concentrations.

It has been shown that for many alloys which corroded uniformly or generally their corrosion rates increased linearly with increasing concentration of oxygen in seawater. This linear relationship indicates that the concentration of oxygen in seawater is a major variable in the corrosion of such alloys.

Generally, there was an erratic relationship between changes in the concentration of oxygen in seawater and the corrosion rates of those alloys whose corrosion resistance is due to passive films on their surfaces. These alloys were the stainless steels, the aluminum alloys and the nickel alloys.

The corrosion rate of copper was not affected by changes in the concentration of oxygen in seawater. The corrosion rates of four aluminum alloys were inversely proportional to changes in the concentration of oxygen in seawater. The corrosion rates of 5086-H34 and 5456-H321 decreased linearly with increasing concentration of oxygen and those of alloys 2219-T81 and 6061-T6 decreased with increasing concentration of oxygen but not linearly or uniformly The titanium alloys were immune to corrosion in seawater of different oxygen concentrations.

Thus, the relationship between changes in the concentration of oxygen in seawater and the corrosion rates varied from immunity to corrosion, to corrosion rates increasing linearly with the concentration of oxygen, to corrosion rates increasing with the oxygen concentration but not linearly, to corrosion rates decreasing with the oxygen concentration, to changes in concentration of oxygen having no apparent effect on corrosion rates.

Key Words: Corrosion; seawater; alloys; oxygen; metals; nickel alloys; aluminum alloys; copper alloys; stainless steels; steels; Deep Submergence; cast irons; titanium alloys.

---

1. Introduction

This investigation was undertaken to determine the effect of the concentration of oxygen in seawater on the corrosion of metals.

During the study on the corrosion of metals in deep ocean environments much information has been collected on the characteristics of seawater at the exposure sites. This study was conducted by the Naval Civil Engineering Laboratory, Port Hueneme, California, and was conducted between 1961 and 1971. The geographical locations of these exposure sites in relation to Port Hueneme, California, are shown in Figure 1 and given in Table 1. Sites I-1 to 4 were at a nominal depth of 1830 meters, sites II-1 and 2 were at a nominal depth of 760 meters and site V was the surface site where the specimens were completely immersed at a nominal depth of 1.5 meters. The seawater characteristics which were determined for each site were temperature, oxygen concentration, salinity, pH, current and

depth. The values of these variables 3 meters above the ocean floor and, in the case of the surface site, 1.5 meters below the surface are given in Table 1. The changes of these variables with depth are shown in Figure 2.

Corrosivity of an environment is determined by its characteristics and by changes in the magnitudes of these characteristics. Changes in the values of these characteristics of the seawater in the Pacific Ocean would be expected to affect the corrosion of metals and alloys exposed in it. The corrosion behavior of alloys is affected by changes in the concentrations of the constituents of seawater with depth. Therefore the corrosion behavior of the alloys cannot be attributed to changes in the concentration of any one characteristic but must be attributed to the combined effects of all characteristics. However, it is possible to show that some variables exert considerably more influence than others on the corrosion of metals.

When changes in the oxygen concentration of seawater vs the corrosion rates of the alloys are discussed it must be understood that the corrosion rates are, in fact, the product of the effects caused by all the corrosive constituents of seawater but in this paper that emphasis is being placed only on the oxygen concentration.

In the area in which these exposures were conducted and at the exposure depths in the Pacific Ocean the concentration of oxygen varied from 0.4 to 5.75 milliliters per liter. The results of the corrosion behavior of the different alloys at the above three exposure sites after one year of exposure were evaluated for the relationships between changes in the oxygen concentration of seawater and their corrosion behavior.

This discussion considers the relationship between changes in the concentration of oxygen in seawater and the corrosion behavior of steels, cast irons, stainless steels, copper alloys, nickel alloys, aluminum alloys and a few miscellaneous alloys.

2. Results and Discussions

Steels. The chemical compositions of the steels are given in Table 2. The relationship between the concentration of oxygen in seawater and the corrosion rates of the steels after one year of exposure is shown graphically in Figure 3.

Since the corrosion rates of the various steels were nearly the same at any one oxygen concentration, the average values for any one oxygen concentration were averaged and used to prepare Figure 3. The curve for these average corrosion rates of all the steels is a straight line with the corrosion rate increasing as the concentration of oxygen in seawater increases. Hence, the corrosion rates of the steels are proportional to the concentration of oxygen.

The average of the corrosion rates of all the carbon and low alloy steels after one year of exposure vs the oxygen content and the temperature of seawater were analyzed using the technique of linear regression analysis. By this technique a relationship between oxygen content, temperature and corrosion rate was obtained for the average of all carbon and low alloy steels. The derived formula is:

$$\text{Corrosion Rate (microns per year)} = 21.3 + 25.4(O_2) + 0.356(T)$$

The corrosion rate is in microns per year, the oxygen content of seawater in milliliters per liter (ml/l) and the temperature in degrees Centigrade (°C).

This derived formula illustrates two important points: (1) the concentration of oxygen in seawater is a major variable and its effect on the corrosion rate of steel in seawater is linear. (2) The temperature of the seawater has much less effect than the oxygen content and its effect is also linear.

This formula, however, cannot be used to predict the corrosion rates of steels in seawater at other locations due to the influences of other variables which may be present.

Walker and his associates[(1)][1] observed the influence of dissolved oxygen on weighed test specimens in distilled water at room temperature and Speller[(1)] made tests in

[1]Figures in parentheses indicate the literature references at the end of this paper.

McKeesport, Pennsylvania, tap water at 72°C in which the oxygen concentration was decreased progressively from 5.0 milliliters per liter to 0.5 milliliters per liter. The results of these two tests showed that the corrosion rate of steel was proportional to the oxygen concentration in nearly neutral solutions. The results of the tests in our investigation in seawater are in substantial agreement with those of Walker and Speller.

It is interesting that the above three tests made in three different electrolytes all indicated the same conclusion. The distilled water was essentially free of variables other than the oxygen concentration and small variations in room temperature which would be expected; the tap water undoubtedly contained dissolved salts and was at an elevated temperature; the seawater contained dissolved salts, was at different temperatures and pressures.

Cast Irons. The chemical compositions of the cast irons are given in Table 3. The relationships between the concentration of oxygen in seawater and their corrosion rates are shown graphically in Figure 4.

The corrosion rates of the three types of cast iron, gray, alloy and austenitic, increased linearly with the concentration of oxygen in seawater. The influence of the concentration of oxygen in seawater on the corrosion of the cast irons was very similar to the behavior of the wrought steels. The slope of the curve for the alloy cast irons is very close to the slope of the curve for the steels. The slopes of the curves for gray and austenitic cast irons are much lower than that for the alloy cast irons; nevertheless their corrosion rates are still proportional to the concentration of oxygen in seawater.

Two cast irons, high silicon and silicon-molybdenum, were uncorroded in seawater after one year of exposure. These two cast irons, probably because of the passive films on their surfaces, were insensitive to changes in the concentration of oxygen in seawater.

Stainless Steels. The chemical compositions of the stainless steels are given in Table 4. The relationship between the changes in the concentration of oxygen in seawater and the corrosion rates of the stainless steels are shown graphically in Figures 5, 6 and 7.

The relationship between changes in the concentration of oxygen in seawater and the corrosion rates of the 200 and 400 Series stainless steels are shown in Figure 5. The corrosion rate of AISI Type 410 stainless steel is proportional to the concentration of oxygen. The corrosion rates of AISI Types 201, 202 and 446 increased slightly as the concentration of oxygen in seawater increased from 1.35 to 5.75 milliliters per liter, but their corrosion rates cannot be considered to be proportional to the concentration of oxygen over its entire range, 0.4 to 5.75 milliliters per liter. Even though the corrosion rate of AISI Type 430 stainless steel was slightly higher at the highest oxygen concentration than at the lowest the effect of oxygen was erratic.

The effects of changes in the concentration of oxygen in seawater on the corrosion rates of the 300 Series stainless steels are shown in Figure 6. The corrosion rates of AISI Types 302, 304, 304L, 316 and 347 austenitic stainless steels were apparently not solely dependent upon the concentration of oxygen in seawater. The corrosion rates of AISI Types 301, 304 sensitized and 325 increased with increasing concentration of oxygen in seawater but not uniformly.

The relationships between changes in the concentration of oxygen in seawater and the corrosion rates of the 600 Series (precipitation hardening) stainless steels are shown in Figure 7. The behavior of these stainless steels is comparable to the behavior of the AISI Types 200, 300 and 400 Series stainless steels.

After one year of exposure in seawater the corrosion rates of the following stainless steels were either less than 2.5 microns per year or zero: AISI Types 309, 316L, 317, 329, 633 and 20Cb-3, 17-14 Cu-Mo, Ni-Cr-Mo and Ni-Cr-Mo-Si. Therefore the corrosion rates of these alloys were unaffected by changes in the concentration of oxygen in seawater.

As is well known oxygen can and does play a dual role in the corrosion of stainless steels in electrolytes. An oxidizing environment (presence of oxygen or other oxidizer) is necessary for maintaining the passivity of stainless steels which is responsible for their high corrosion resistance. However, this same oxidizing environment is necessary to initiate and maintain pitting in stainless steels. Oxygen often acts as the depolarizer

for passive-active cells created by the breakdown of passivity at a specific point or area. The chloride ion (present in abundance in seawater) is singularly efficient in accomplishing this breakdown. Therefore, this dual role of oxygen in seawater can be used to explain the inconsistent and erratic corrosion behavior of stainless steels in this environment.

Copper Alloys. The chemical compositions of the copper alloys are given in Table 5. The relationship between the changes in the concentration of oxygen in seawater and the corrosion rates of copper and the copper alloys are shown graphically in Figure 8.

The corrosion of copper was not affected by changes in the concentration of oxygen over the range 0.4 to 5.75 milliliters per liter. The corrosion rates of all but two of the copper alloys were so comparable that their rates for each oxygen concentration were averaged. These average values were used for constructing the "Copper Alloys" curve in Figure 8. The corrosion rates of the copper alloys increased linearly with the concentration of oxygen in seawater and, hence, were proportional to these changes. Exclusion of the two alloys, Muntz Metal and Manganese Bronze, was because of severe dezincification.

Nickel Alloys. The chemical compositions of the nickel alloys are given in Table 6. The relationships between the changes in the concentration of oxygen in seawater and the corrosion rates of the nickel alloys are shown graphically in Figures 9, 10 and 11. It is shown in Figure 9 that the corrosion rates of Ni-200, Ni-Cu 400, Ni-Cr-Fe 600 and X750 and Ni-Mo 2 alloys increase linearly with the oxygen concentration and, therefore, are proportional to the oxygen concentration.

In Figure 10 the corrosion rates of electrolytic nickel; Ni-201, 211 and 270; Ni-Cu 402, 406, 410, K500 and 45-55; and Ni-Cr 65-35, 75 and 80-20 alloys increase with increasing concentration of oxygen in seawater but not linearly and therefore are not directly proportional to the oxygen concentration. Changes in the concentration of oxygen do not directly affect the corrosion behavior of Ni-Cr-Fe alloys 610 and 88.

In Figure 11 the corrosion rates of Ni-301 and Ni-Mo-Fe-"B" increase with increasing concentration of oxygen in seawater but not linearly. The shapes of the curves for Ni-210, Ni-Cu-505, Ni-Sn-Zn 23 and Ni-Si D show that the relationship between changes in the concentration of oxygen in seawater and their corrosion rates is inconsistent and erratic.

The erratic and inconsistent relationships between changes in the concentration of oxygen in seawater and the corrosion of nickel alloys can be explained by the dual role oxygen plays on these alloys in seawater. Oxygen is necessary for preserving the passive films on the alloys and is also necessary for the formation of passive-active cells when the passive film breaks down locally. This is similar to the effect of oxygen on the corrosion of the stainless steels in seawater.

The passive films on some nickel base alloys were so stable that they did not break down after one year of constant immersion in seawater, even locally, within the range of oxygen concentrations in this investigation. These alloys were: Ni-Cr-Fe-718; Ni-Fe-Cr 800, 804, 825, 825 sensitized, 825cb and 901; Ni-Cr-Mo C,3 and 625; Ni-Co-Cr-Mo 700; and Ni-Cr-Fe-Mo F, G and X.

Aluminum Alloys. The chemical compositions of the aluminum alloys are given in Table 7. The relationships between the changes in the concentration of oxygen in seawater and the corrosion rates of the aluminum alloys are shown graphically in Figures 12 and 13.

As shown in Figure 12 the corrosion rates of Al-Mg alloys 5086-H34 and 5456-H321 decreased linearly with increasing concentration of oxygen in seawater. The corrosion rates of Al-Cu alloy 2219-T81 and Al-Mg-Si alloy 6061-T6 decreased but not linearly, with increasing concentration of oxygen in seawater. This behavior of the above three aluminum alloys can be attributed to the lack of sufficient oxygen to prevent local breakdown of the protective passive films. The local breakdown will cause pitting. In these three alloys the maximum depths of pits at 0.4 milliliters per liter of oxygen were 1040, 1905 and 1980 microns and at 5.75 milliliters per liter they were 340, 405 and 660 microns.

The corrosion rates of the other aluminum alloys 1100-H14, 3003-H14, 2024-0, 5052, 5083-H113 and 5454-H32 were erratic and inconsistent with respect to changes in the

concentration of oxygen in seawater, as shown in Figure 13. This behavior, like that of the stainless steels and some nickel alloys, can be attributed to the dual role oxygen can play with regard to alloys which depend upon passive films for their corrosion resistance.

Miscellaneous Alloys. The chemical compositions of the miscellaneous alloys are given in Table 8. The relationships between changes in the concentration of oxygen in seawater and these miscellaneous alloys are shown graphically in Figure 14. The corrosion rate of lead increased linearly with the concentration of oxygen in seawater. The corrosion rate of solder, (67Pb-33 Sn) also increased with increasing concentration of oxygen in seawater but not linearly or uniformly. The corrosion rates of molybdenum and tungsten were higher at the highest concentration of oxygen in seawater than at the lowest concentration of oxygen but the shapes of the curves between these points cannot be stated since no data are available for an intermediate oxygen concentration. The relationship between changes in the concentration of oxygen in seawater and the corrosion rate of tin was erratic.

Columbium, tantalum and a tantalum alloy, Ta60, containing about 10% tungsten were unattacked by seawater of all three oxygen concentrations after one year of exposure.

Titanium Alloys. Titanium alloys were unattacked by seawater of all three concentrations of oxygen after one year of exposure. The alloys in this investigation were: CP, 75A, Ti-0.15Pd, 5Al-2.5 Sn, 6Al-4V, 7Al-2Cb-1Ta and 13V-11Cr-3Al. It is well known that the passive film on titanium alloys does not break down at ordinary temperatures in chloride ion environments (seawater); hence, its immunity to corrosion.

3. Summary and Conclusions

The purpose of this investigation was to determine the relationships between changes in the concentration of oxygen in seawater and the corrosion of alloys. To accomplish this the corrosion rates of alloys which had been exposed at the three oxygen concentrations (0.4, 1.35 and 5.75 milliliters per liter) in the Pacific Ocean for one year were used to determine the effects of oxygen.

The corrosion rates of the following alloys increased linearly with the concentration of oxygen in seawater: The steels, cast irons, copper alloys except those subject to severe parting corrosion (Muntz Metal and Manganese Bronze A), AISI Type 410 stainless steel, Ni-200 alloy, Ni-Cu 400 alloy, Ni-Cr-Fe alloys 600 and X750, Ni-Mo 2 alloy and lead. Linear regression analysis using the corrosion rates, oxygen concentrations and temperatures of seawater gave the following relationship for the steels:

$$\text{Corrosion Rate (Microns per year)} = 21.3 + 25.4(O_2) + 0.356(T)$$

The corrosion rates are in microns per year, the oxygen contents of seawater in milliliters per liter (ml/L) and temperatures in degrees Centigrade (°C).

This derived formula illustrates two important points: (1) The concentration of oxygen in seawater is a major variable and its effect on the corrosion rate of steel in seawater is linear. (2) The temperatures of seawater has less effect on the corrosion of steel in seawater than the oxygen content and its effect is also linear.

In most cases if the alloy corroded uniformly or generally its corrosion rate increased linearly with the concentration of oxygen - such alloys were the steels, cast irons, copper alloys and lead. The other alloys, AISI Type 410 stainless steel, Ni-200 alloy, Ni-Cu 400 alloy, Ni-Cr-Fe alloys 600 and X750, and Ni-Mo 2 alloy, whose corrosion rates increased linearly with the oxygen concentration were corroded by the pitting and crevice types of corrosion.

The corrosion rate of copper was not affected by changes in the concentration of oxygen in seawater.

The corrosion rates of the following alloys increased with increasing concentration of oxygen in seawater but not linearly or uniformly: AISI Type 201, 202, 301, 304 sensitized, 325, 446 and 632-RH1100 stainless steels; and nickel alloys, electrolytic nickel, Ni-200, Ni-211, Ni-270, Ni-Cu 402, Ni-Cu 406, Ni-Cu 410, Ni-Cu K500, Ni-Cu 45-55, Ni-Cr 65-35, Ni-Cr 75, Ni-Cr 80-20, Ni-301, and Ni-Mo-Fe "B"; and solder composed of 67 percent Pb and 33 percent Sn.

The relationship between changes in the concentration of oxygen in seawater and the corrosion rates of the following alloys were erratic: AISI Type 302, 304, 304L, 316, 347, 430, 630-H925, 631-TH1050 and 635 stainless steels; severely dezincified copper alloys Muntz Metal and Manganese Bronze A; nickel alloys Ni-Cr-Fe 610 and 88, Ni-210, Ni-Cu-505, Ni-Sn-Zn 23 and Ni-Si D; aluminum alloys 1100-H14, 3003-H14, 2024-0, 5052, 5083-H113 and 5454-H32; tin; and zinc.

The corrosion rates of three aluminum alloys were inversely proportional to increasing concentration of oxygen in seawater. The corrosion rates of 5086-H34 and 5456-H321 decreased linearly with increasing concentration of oxygen. The decreases in the corrosion rates of aluminum alloys 2219-T6 and 6061-T6 with increasing concentration of oxygen were not linear.

Many of the alloys in this investigation were uncorroded in seawater containing three different concentrations of oxygen (0.4, 1.35 and 5.75 milliliters per liter) for a period of 1 year of exposure. These alloys were: cast irons containing high silicon and silicon-molybdenum; AISI Type 309, 316L, 317, 329 and 633 stainless steels; specialty stainless steels 20Cb-3, 17-14-Cu-Mo, Ni-Cr-Mo, and Ni-Cr-Mo-Si; nickel alloys Ni-Cr-Fe 718, Ni-Fe-Cr 800, 804, 825, 825 sensitized, 825Cb and 901, Ni-Cr-Mo C, 3 and 625, Ni-Co-Cr-Mo 700 and Ni-Cr-Fe-Mo F, G and X; titanium alloys CP, 75A, Ti-0.15Pd, 5Al-2.5 Sn, 6Al-4V, 7Al-2Cb-1 Ta and 13V-11Cr-3Al; columbium; tantalum and tantalum alloy Ta 60.

The inconsistent and erratic behavior of alloys which depend upon passive films for their corrosion resistance is explained on the basis of the dual role oxygen plays in maintaining these films or in perpetuating passive-active and oxygen concentration corrosion cells.

The corrosion rates of the many alloys which corroded uniformly or generally, increased linearly with increasing concentration of oxygen in seawater. This linear relationship for so many alloys substantiates the major influence of oxygen on their corrosion behavior.

4. References

1. Frank N. Speller, *Corrosion - Causes and Prevention* (2nd Ed.) McGraw-Hill Book Co., Inc. pp 386-387, 1935.

Summarized Discussion

In response to a question whether the authors had considered correlating oxygen concentration with pitting behavior, they replied that they had done this with the finding that generally oxygen concentration correlated better with pitting factor than with overall corrosion rate.

Written Contribution by B. F. Brown:

The authors have performed a valuable service in demonstrating that the oxygen content of natural sea water can play an important role in controlling corrosion rates, and that increasing oxygen content may cause an increasing corrosion rate in some metals and a decreasing rate in others. For the benefit of the engineer who is not a corrosion specialist, it should be emphasized that the research data reported in the paper are <u>average</u> corrosion rates (assuming perfectly uniform corrosion) and that for the great majority of metals which corrode nonuniformly, the data are not appropriate for designing a "corrosion allowance."

Table 1. Exposure Site Locations and Sea Water Characteristics

Site No.	Latitude N	Longitude W	Depth, Meters	Exposure, Days	Temp. °C	Oxygen ml/l[1]	Salinity ppt[2]	pH	Current, Knots, Avg
I-1	33°46′	120°37′	1615	1064	2.6	1.2	34.51	7.5	0.03
I-2	33°44′	120°45′	1719	751	2.3	1.3	34.51	7.6	0.03
I-3	33°44′	120°45′	1719	123	2.3	1.3	34.51	7.6	0.03
I-4	33°46′	120°46′	2066	403	2.2	1.6	34.40	7.7	0.03
II-1	34°06′	120°42′	713	197	5.0	0.4	34.36	7.5	0.06
II-2	34°06′	120°42′	722	402	5.0	0.4	34.36	7.5	0.06
V	34°06′	119°07′	1.5	181-763	12-19	5.75	33.51	8.1	variable

[1] ml/l—milliliters per liter.
[2] ppt—parts per thousand.

Table 2. Chemical Composition of Irons and Steels

Material	C	Mn	P	S	Si	Ni	Cr	Mo	V	Cu	Other
Armco Iron	–	0.02	–	–	–	–	–	–	–	–	–
Wrought Iron	0.02	0.06	0.13	0.01	0.13	–	–	–	–	–	2.5 slag
AISI 1010	0.12	0.50	0.004	0.23	0.060	–	–	–	–	–	–
AISI 1010	–	0.34	0.01	–	0.02	0.02	0.02	–	–	0.03	–
Copper Steel	–	0.40	0.01	–	0.02	0.01	0.03	–	–	0.28	–
ASTM A36	0.20	0.55	0.010	0.020	0.064	–	–	–	–	–	–
HSLA #1[1]	0.18	0.86	0.014	0.023	0.28	0.05	0.64	0.18	0.047	–	B-0.1028 Ti-0.020
HSLA #2	0.12	0.30	0.015	0.025	0.27	2.34	1.25	0.20	–	0.17	–
HSLA #4	–	0.36	0.08	–	0.41	0.32	0.72	–	–	0.38	–
HSLA #5	0.14	0.78	0.020	0.025	0.23	0.74	0.56	0.42	0.36	0.22	B-0.0041
HSLA #5	with mill scale										
HSLA #7	–	0.43	0.12	–	0.13	0.54	–	–	–	1.0	–
HSLA #10	–	0.63	0.01	–	–	0.99	–	–	–	1.42	–
18% Ni-Maraging	0.02	0.10	0.005	0.007	0.14	17.92	–	4.78	–	–	Co-8.75 B-0.003 Ti-0.94 Al-0.17
1.5% Ni	not recorded										
3.0% Ni	not recorded										
5.0% Ni	not recorded										
9.0% Ni	not recorded										

[1] High-Strength-Low-Alloy Steel.

Table 3. Chemical Composition of Cast Irons

Material	C	Mn	Si	Ni	Cr	Mo	Cu
Nickel	–	0.68	2.47	1.56	–	–	–
Ni-Cr #1	–	0.73	1.64	1.66	0.60	–	–
Ni-Cr #2	–	0.86	1.99	3.22	0.98	–	–
Ductile #1	–	0.35	2.50	0.91	–	–	–
Ductile #2	–	0.34	2.24	–	–	–	–
Silicon	–	–	14.5	–	–	–	–
Si-Mo	–	–	14.0	–	–	3.0	–
Austenitic, Type 1	–	1.4	2.05	15.8	1.79	–	6.71
Austenitic, Type 2	–	1.01	2.29	18.2	2.04	–	–
Austenitic, Type 3	–	0.6	1.15	28.4	2.87	–	–
Austenitic, Type 4	–	0.56	5.34	29.7	4.97	–	–
Austenitic, Type 4	2.13	0.79	5.60	29.96	5.02	–	0.16
Austenitic, Type D-2	–	0.94	3.0	21.4	2.26	–	–
Austenitic, Type D-2b	–	0.96	2.0	20.8	3.19	–	–
Austenitic, Type D-2c	2.45	2.12	2.38	22.34	0.08	–	–
Austenitic, Type D-3	–	0.5	1.83	29.8	2.70	–	–
Austenitic, Hardenable	not recorded						

Table 4. Chemical Composition of Stainless Steels

Alloy	C	Mn	P	S	Si	Ni	Cr	Mo	Cu	Other
AISI Type 201	0.08	6.8	–	–	–	4.0	17.1	–	–	–
AISI Type 202	0.09	7.6	–	–	–	4.5	17.8	–	–	–
AISI Type 301	0.11	1.17	0.025	0.021	0.34	6.73	17.4	–	–	–
AISI Type 302	0.11	1.36	–	–	–	9.9	17.3	0.12	0.26	–
AISI Type 302	0.06	1.05	0.020	0.013	0.60	9.33	18.2	–	–	–
AISI Type 304	0.06	1.62	–	–	–	9.5	18.2	0.34	0.16	–
AISI Type 304	0.06	1.73	0.024	0.013	0.43	10.0	18.8	–	–	–
AISI Type 304 Sensitized[1]	0.06	1.62	–	–	–	9.5	18.2	0.34	0.16	–
AISI Type 304L	0.02	1.45	–	–	–	9.5	17.9	–	–	–
AISI Type 304L	0.03	1.24	0.028	0.023	0.68	10.2	18.7	–	–	–
AISI Type 309	0.10	1.60	–	–	–	12.7	23.3	–	–	–
AISI Type 316	0.05	1.73	–	–	–	13.2	17.2	2.60	–	–
AISI Type 316	0.06	1.61	0.021	0.016	0.40	13.6	18.3	2.41	–	–
AISI Type 316L	0.02	1.78	–	–	–	13.6	17.7	2.15	–	–
AISI Type 316L	0.02	1.31	0.012	0.015	0.47	13.7	17.9	2.76	–	–
AISI Type 317	0.05	1.61	–	–	–	13.6	18.7	3.30	–	–
AISI Type 325	0.03	0.7	–	–	–	23.5	9.0	–	–	–
AISI Type 329	0.07	0.46	–	–	–	4.4	27.0	1.40	–	–
AISI Type 347	0.04	1.19	–	–	–	11.3	18.1	–	–	–
AISI Type 410	0.13	0.4	–	–	–	0.2	12.1	–	–	–
AISI Type 410	0.13	0.43	0.019	0.005	0.45	0.1	12.3	–	–	–
AISI Type 430	0.06	0.4	–	–	–	–	17.7	–	–	–
AISI Type 446	0.15	0.8	–	–	–	0.2	30.0	–	–	–
20 Cb-3	–	–	–	–	–	34	20	2.3	3.4	–
Ni-Cr-Mo-Si	–	–	–	–	1.0	23.0	21.0	5.0	–	–
AISI Type 631-TH1050	0.071	0.48	0.017	0.018	0.42	7.42	17.12	–	–	1.19 Al
AISI Type 630-H925	0.031	0.24	0.017	0.011	0.59	4.17	15.29	–	3.23	0.24 Cb
17Cr-14 Ni-Cu-Mo	–	–	–	–	–	14	16	2	3	–
AISI Type 633	–	–	–	–	–	4	17	3	–	–
AISI Type 635	0.05	0.56	0.026	0.009	0.74	6.80	16.8	–	–	0.79 Ti
AISI Type 632-RH1100	0.070	0.50	–	0.016	0.28	7.19	15.05	2.19	–	1.11 Al

[1] Heated for one hour at 1200°F, air cooled.

Table 5. Chemical Composition of Copper Alloys

CDA No.[1]	Material	Cu	Zn	Sn	Ni	Al	Fe	Si	Pb	Other
102	Copper, O free	99.96	–	–	–	–	–	–	–	–
102	Copper, O free	99.9	–	–	–	–	–	–	–	–
172	Be-Cu	97.80	–	–	0.05	–	–	–	–	Be 1.90 Co 0.25
825	Be-Cu, chain, cast	97.5	–	–	–	–	–	–	–	Be 2.0 Co 0.5
220	Commercial Bronze	90	10	–	–	–	–	–	–	–
230	Red Brass	85	15	–	–	–	–	–	–	–
443	Arsenical Admiralty	71.19	27.77	1.00	–	–	0.01	–	–	As-0.027
443	Arsenical Admiralty	70.0	29.0	1.0	–	–	–	–	–	As-0.04
270	Yellow Brass	65.0	35.0	–	–	–	–	–	–	–
280	Muntz Metal	60.69	39.29	–	–	–	<0.02	–	–	–
280	Muntz Metal	60.0	40.0	–	–	–	–	–	–	–
678	Mn Bronze A	56.0	42.0	–	–	1.0	1.0	–	–	Mn-0.01
868	Ni-Mn Bronze, cast	54.58	34.48	0.70	3.77	1.73	1.66	–	0.02	Mn-3.06
–	Al Brass	78.0	20.0	–	–	2.0	–	–	–	–
–	Ni Brass	50.0	40.0	–	8.0	–	2.0	–	–	–
905	G Bronze, cast	88.0	10.0	2.0	–	–	–	–	–	–
903	G Bronze, modified, cast	88.0	4.0	8.0	–	–	–	–	–	–
922	M Bronze, cast	88.2	4.0	6.0	–	–	–	–	2.0	–
–	Leaded Tin Bronze, cast	85.0	5.0	5.0	–	–	–	–	5.0	–
510	Phosphor Bronze A	94.64	<0.10	4.94	–	–	<0.05	–	–	P-0.26
510	Phosphor Bronze A	96.0	–	4.0	–	–	–	–	–	P-0.25
524	Phosphor Bronze D	90.00	<0.10	9.23	–	–	<0.05	–	–	P-0.17
606	Al Bronze 5%	95.0	–	–	–	5.0	–	–	–	–
614	Al Bronze 7%	90.11	–	0.15	–	6.59	3.15	–	<0.02	–
614	Al Bronze 7%	90.0	–	–	–	7.0	3.0	–	–	–
953	Al Bronze 10% cast	89.0	–	–	–	10.0	1.0	–	–	–
954	Al Bronze 11%, cast	86.0	–	–	–	10.0	4.0	–	–	–
–	Al Bronze 13%, cast	83.0	–	–	–	13.0	4.0	–	–	–
–	Ni-Al Bronze #2	80.0	–	–	5.0	10.0	4.0	–	–	Mn-0.5
653	Si Bronze 3%	97.0	–	–	–	–	–	3.0	–	–
655	Si Bronze A	95.49	–	–	–	–	<0.02	3.28	–	Mn-1.18
655	Si Bronze A	95.0	–	–	–	–	–	3.0	–	Mn-1.0
–	Ni Vee Bronze A, cast	88.0	5.0	2.0	5.0	–	–	–	–	–
–	Ni-Vee Bronze B, cast	87.0	5.0	2.0	5.0	–	–	1.0	–	–
–	Ni-Vee Bronze C, cast	80.0	5.0	5.0	5.0	–	–	5.0	–	–
706	Cu-Ni 90-10	89.04	–	–	9.42	–	1.16	–	–	Mn-0.38
706	Cu-Ni, 90-10	89.0	–	–	10.0	–	1.4	–	–	Mn-0.5
962	Cu-Ni 90-10, cast	86.0	–	–	11.0	–	1.4	–	–	Mn-1.3
710	Cu-Ni 80-20	78.62	–	–	20.41	–	0.62	–	–	Mn-0.35
710	Cu-Ni 80-20	80.0	–	–	20.0	–	0.03	–	–	Mn-0.2
715	Cu-Ni, 70-30	68.61	–	–	30.53	–	0.53	–	–	Mn-0.33
715	Cu-Ni, 70-30	69.0	–	–	30.0	–	0.6	–	–	Mn-0.4
716	Cu-Ni, 70-30	64.02	–	–	29.95	–	5.27	–	–	Mn-0.75
–	Cu-Ni, 55-45	54.0	–	–	45.0	–	0.1	–	–	Mn-1.0
–	Cu-Ni-Zn-Pb	62.0	8.0	–	25.0	–	–	–	5.0	–
752	Nickel-Silver	65.0	17.0	–	18.0	–	–	–	–	–

[1] Copper Development Association alloy number.

Table 6. Chemical Composition of Nickel Alloys

Material	Ni	C	Mn	Fe	S	Si	Cu	Cr	Ti	Mo	Other
Electrolytic Ni	99.97+Co	–	–	–	–	–	–	–	–	–	–
Ni-200	99.50	0.05	0.29	0.04	0.006	0.07	0.02	–	–	–	–
Ni-200	99.5	0.06	–	–	–	–	–	–	–	–	–
Ni-201	99.5	0.01	–	–	–	–	–	–	–	–	–
Ni-211	95.0	–	5.0	–	–	–	–	–	–	–	–
Ni-270	99.97	–	–	–	–	–	–	–	–	–	–
Ni-210, cast	95.6	–	1.0	–	–	2.0	–	–	–	–	–
Ni-301	94.0	–	–	–	–	–	–	–	–	–	Al-4.5
Ni-Cu 400	65.17	0.11	1.06	0.90	0.007	0.10	32.62	–	–	–	–
Ni-Cu 400	66.00	0.12	0.90	1.35	0.005	0.15	31.50	–	–	–	–
Ni-Cu 400	66.00	–	0.90	1.40	–	0.20	32.00	–	–	–	–
Ni-Cu 402	58.00	–	0.90	1.20	–	0.10	40.00	–	–	–	–
Ni-Cu 406	84.00	–	0.90	1.40	–	0.20	13.00	–	–	–	–
Ni-Cu 410, cast	66.00	–	0.80	1.00	–	1.60	31.00	–	–	–	–
Ni-Cu K-500	65.00	0.15	0.60	1.00	0.005	0.15	29.50	–	0.50	–	Al-2.80
Ni-Cu K-500	65.00	–	0.60	1.00	–	0.20	30.00	–	–	–	Al-2.80
Ni-Cu 505, cast	64.00	–	0.80	2.00	–	4.00	29.00	–	–	–	–
Ni-Cu 45-55	45.00	–	1.00	0.10	–	–	54.00	–	–	–	–
Ni-Cr-Fe-600	76.00	0.04	0.20	7.20	0.007	0.20	0.10	15.8	–	–	–
Ni-Cr-Fe 600	76.0	–	–	7.0	–	–	–	16.0	–	–	–
Ni-Cr-Fe 610, cast	71.0	–	–	9.0	–	2.0	–	16.0	–	–	–
Ni-Cr-Fe X750	73.0	–	–	7.0	–	–	–	15.0	2.5	–	–
Ni-Cr-Fe 718	52.5	0.04	0.20	18.0	0.007	0.20	0.10	19.0	0.80	3.0	Cb-5.2 Al-0.60
Ni-Cr-Fe 88	71.0	–	–	7.0	–	–	–	10.0	–	–	Sn-5.0 Bi-3.0
Ni-Cr-Mo 3	58.0	–	–	3.0	–	–	–	19.0	–	19.0	–
Ni-Cr-Mo 625	63.0	–	–	–	–	–	–	22.0	–	9.0	–
Ni-Co-Cr-Mo 700	46.0	–	–	1.0	–	–	–	15.0	–	3.75	Co-28.5 Al-3.0
Ni-Fe-Cr 800	32.0	0.04	0.74	46.0	0.007	0.35	0.30	20.5	–	–	–
Ni-Fe-Cr 800	32.0	–	1.0	46.0	–	–	–	20.0	–	–	–
Ni-Fe-Cr 804	43.0	–	–	25.0	–	–	–	29.0	–	–	–
Ni-Fe-Cr 825	41.12	0.05	0.82	30.86	0.01	0.31	1.61	21.12	1.00	2.94	Al-0.14
Ni-Fe-Cr 825	42.0	–	–	30.0	–	–	2.0	22.0	–	3.0	–
Ni-Fe-Cr 825Cb	42.0	–	–	30.0	–	–	2.0	22.0	–	3.0	–
Ni-Fe-Cr 901	43.0	–	–	34.0	–	–	–	14.0	–	–	–
Ni-Fe-Cr 902	42.0	0.02	0.40	48.5	0.008	0.50	0.05	5.4	2.40	–	Al-0.65
Ni-Cr-Fe-Mo "F"	46.0	–	–	21.0	–	–	–	22.0	–	7.0	–
Ni-Cr-Fe-Mo "G"	45.0	–	–	20.0	–	–	2.0	21.0	–	7.0	–
Ni-Cr-Fe-Mo "X"	60.0	–	–	19.0	–	–	–	22.0	–	9.0	–
Ni-Mo-Fe "B"	60.0	–	–	5.0	–	–	–	–	–	26.0	–
Ni-Mo-Cr "C"	55.68	0.05	0.52	6.32	0.009	0.62	–	15.33	–	16.71	W-3.53 Co-0.96 V-0.26 P-0.010
Ni-Mo-Cr "C"	60.0	–	–	5.0	–	–	–	15.0	–	16.0	W-4.0
Ni-Sn-Zn 23	79.0	–	2.0	–	–	–	–	–	–	–	Sn-8.0 Zn-7.0 Pb-4.0

continued

Table 6. Continued

Material	Ni	C	Mn	Fe	S	Si	Cu	Cr	Ti	Mo	Other
Ni-Cr 65-35	65.0	–	–	–	–	–	–	35.0	–	–	–
Ni-Cr 75	78.0	–	–	–	–	–	–	20.0	–	–	–
Ni-Cr 80-20	80.0	–	–	–	–	–	–	20.0	–	–	–
Ni-Mo 2	68.0	–	–	2.0	–	–	–	–	–	30.0	–
Ni-Si D	88.0	–	–	–	–	10.0	3.0	–	–	–	–
Ni-Be	97.5	–	–	–	–	–	–	–	0.50	–	Be 1.95

Table 7. Chemical Composition of Aluminum Alloys

Material	Si	Fe	Cu	Mn	Mg	Cr	Ni	Zn	Ti	Al
1100	–	–	–	–	–	–	–	–	–	99.0
	–	–	4.3	0.6	1.5	–	–	–	–	remainder
2024	–	–	4.3	0.6	1.5	–	–	–	–	remainder
2219-T81[1]	0.20	0.30	6.3	0.30	0.02	–	–	0.10	0.06	remainder
3003	0.15	0.45	0.15	1.25	–	–	–	0.05	–	remainder
3003-H14	0.20	0.58	0.13	1.05	<0.01	<0.01	<0.01	<0.01	–	remainder
5052	–	–	–	–	2.5	0.25	–	–	–	remainder
5083	–	–	0.15	0.6	4.5	–	–	–	–	remainder
5083-H113	0.40	0.40	0.10	0.65	4.5	0.15	–	0.25	0.15	remainder
5086	–	–	–	0.3	4.0	0.15	–	–	–	remainder
5086-H32	0.15	0.25	0.05	0.32	3.75	0.12	–	0.12	0.01	remainder
5086-H34	0.40	0.50	0.10	0.45	4.0	0.15	–	0.25	0.15	remainder
5454	–	–	–	0.03	1.0	0.02	–	–	–	remainder
5456-H321	0.40	(Si&Fe)	0.10	0.75	5.0	0.13	–	0.25	0.20	remainder
6061	–	–	0.25	-	1.0	0.28	–	–	–	remainder
6061-T6	0.60	0.70	0.27	0.15	1.0	0.25	–	0.25	0.15	remainder

[1] Other elements present are: 0.10%V, 0.17% Zr.

Table 8. Chemical Composition of Miscellaneous Alloys, Percent by Weight

Material	Chemical Composition
Chemical Lead	99.9 Pb
Antimonial Lead	94.0 Pb, 6.0 Sb
Tellurium Lead	99 + Pb, 0.04 Te
Tin	99.9 Sn
Zinc	99.9 Zn, 0.09 Pb, 0.01 Fe
Solder	67 Pb, 33 Sn
Molybdenum	99.9 Mo
Tungsten	99.95 W
Columbium	99.8 Cb
Tantalum	99.9 Ta, 0.010 C, 0.010 O, 0.005 N, 0.002 H
Ta-60	88.8-91.3 Ta, 8.5-11 W



Figure 1. Locations of exposure sites.

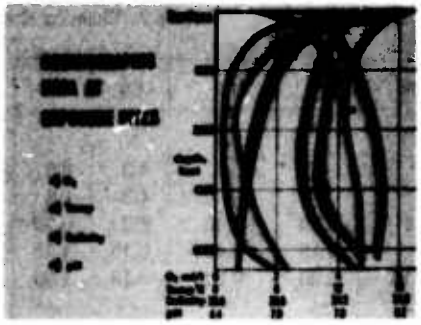


Figure 2. Oceanographic parameters at exposure sites.

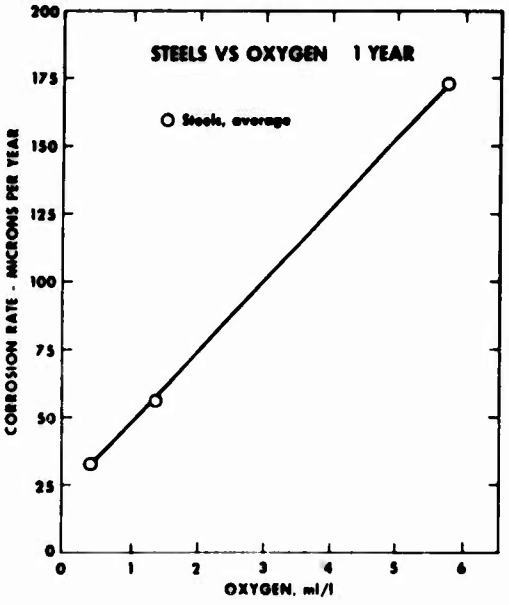


Figure 3. Effect of oxygen concentration of sea water on corrosion of steels after 1 year of exposure.

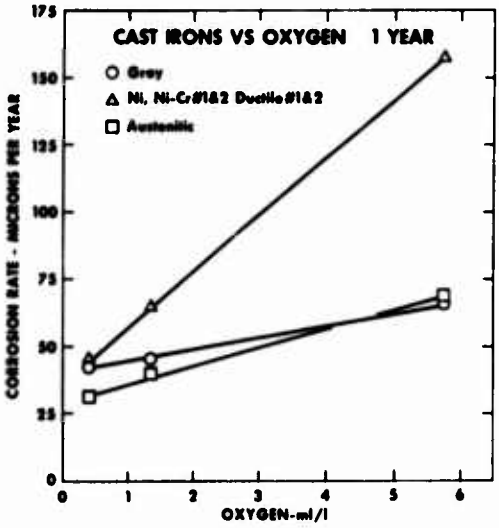


Figure 4. Effect of oxygen concentration of sea water on corrosion of cast irons after 1 year of exposure.

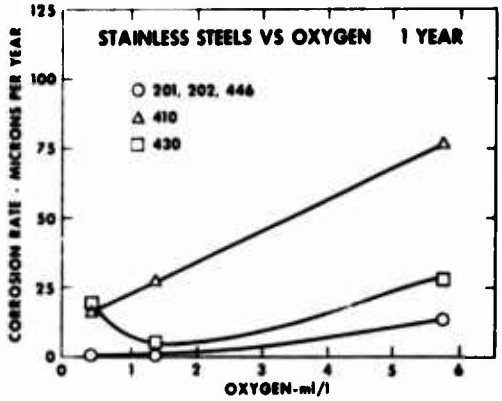


Figure 5. Effect of oxygen concentration of sea water on the corrosion of 200 and 400 Series stainless steels after 1 year of exposure.

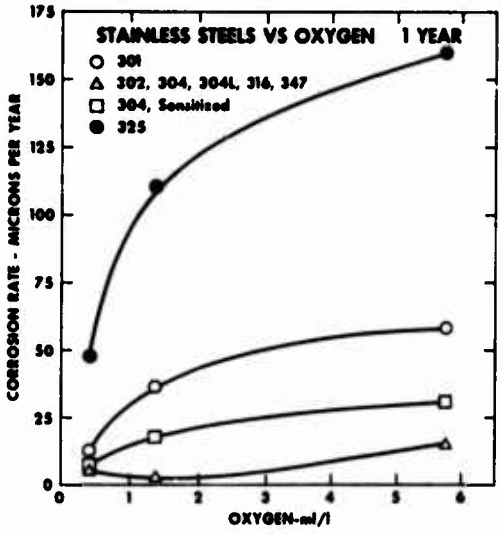


Figure 6. Effect of oxygen concentration of sea water on the corrosion of 300 Series stainless steels after 1 year of exposure.

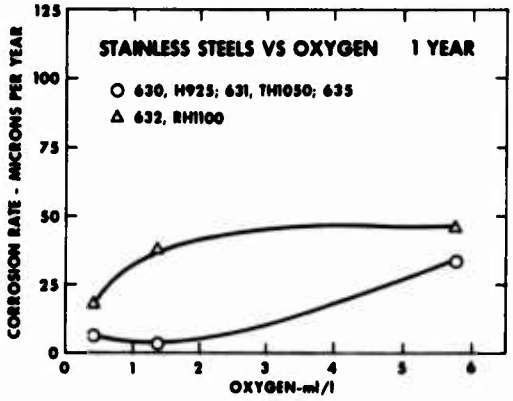


Figure 7. Effect of oxygen concentration of sea water on the corrosion of 600 Series stainless steels after 1 year of exposure.

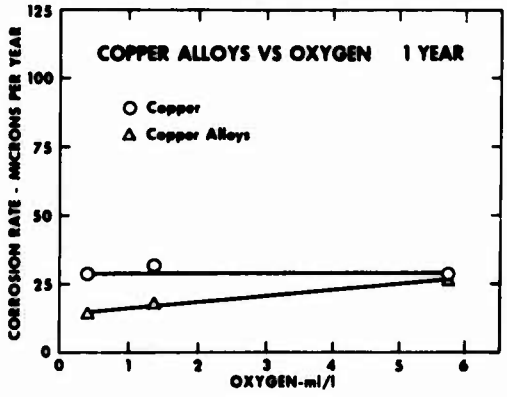


Figure 8. Effect of oxygen concentration of sea water on the corrosion of copper alloys after 1 year of exposure.

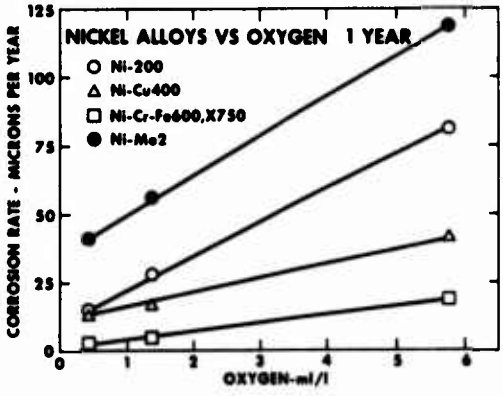


Figure 9. Effect of oxygen concentration of sea water on the corrosion of nickel alloys after 1 year of exposure.

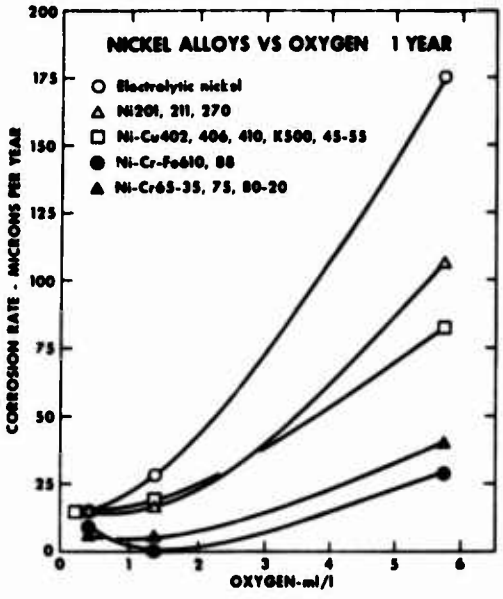


Figure 10. Effect of oxygen concentration of sea water on the corrosion of nickel alloys after 1 year of exposure.

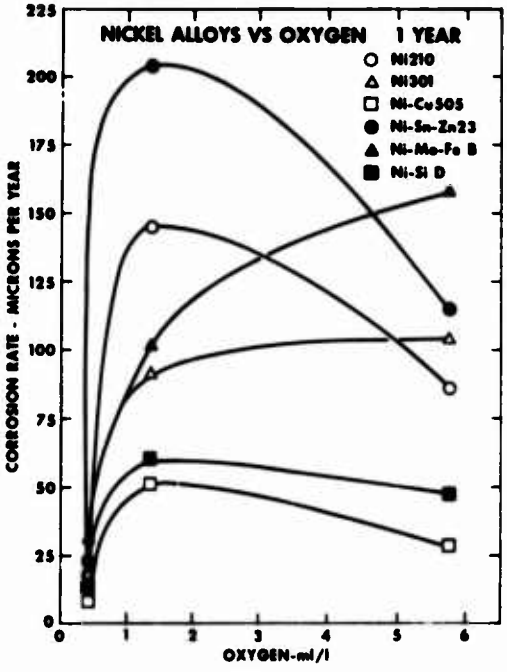


Figure 11. Effect of oxygen concentration of sea water on the corrosion of nickel alloys after 1 year of exposure.

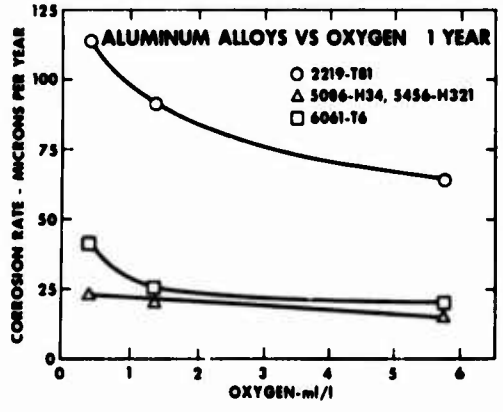
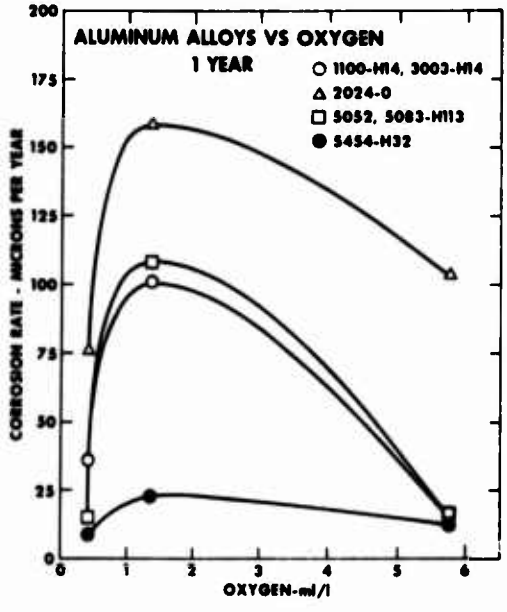


Figure 12. Effect of oxygen concentration of sea water on the corrosion of aluminum alloys after 1 year of exposure.

Figure 13. Effect of oxygen concentration of sea water on the corrosion of aluminum alloys after 1 year of exposure.



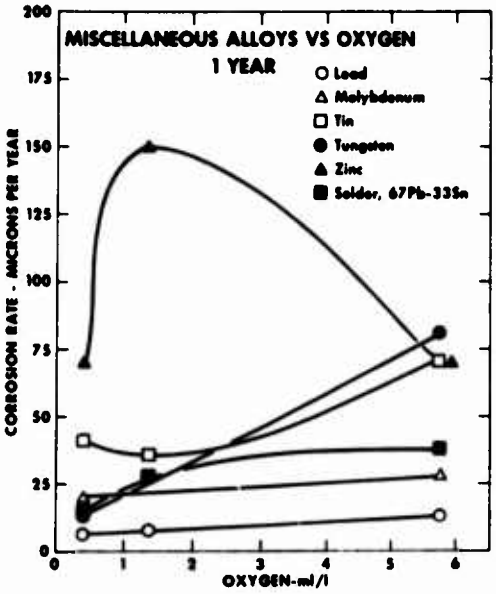


Figure 14. Effect of oxygen concentration of sea water on the corrosion of miscellaneous alloys after 1 year of exposure.

ETUDE DE LA PROTECTION DES STRUCTURES SOUS-MARINES

Cl. Bugéia, Ch. Louis

Compagnie Française des Pétroles
Gaz de France

Cette communication expose les résultats de recherche effectuées entre 1966 et 1971 sur la Protection externe contre la corrosion sous-marine par la COMPAGNIE FRANCAISE DES PETROLES et le GAZ DE FRANCE, sous contrat ELF-ERAP puis CNEXO. Ces recherches portent sur 30 systèmes de revêtements différents dont un grand nombre est à base de résines époxydiques, seules ou associées à une autre résine. L'expérimentation a été orientée plus particulièrement sur les points suivants :

- Comportement des revêtements vis-à-vis de la protection cathodique par courant imposé (-900 mV à -3 000 mV), la durée d'essais étant fixée, en principe, à deux ans ;

- Tenue aux chocs thermiques, 20°C - 100°C, avec surimposition ou non d'une protection cathodique par anode soluble (-1 500 mV), chaque cycle étant répété 1 200 fois environ ;

- Examens de l'état des revêtements, appliqués sur des éprouvettes de grande dimension, après des durées prolongées d'immersions dans différentes mers et à diverses profondeurs, Méditerranée (Antibes), Mer du Nord (Angleterre), Arctique (Labrador), Atlantique (Gabon) et Golfe Persique. On y indique également les principales variétés de salissures rencontrées et leur influence sur la tenue des revêtements.

Les résultats obtenus au cours de cette expérimentation, qui se poursuit toujours en 1972, permettent, dès maintenant, de faire une sélection des meilleurs revêtements pour chacun des essais effectués et donc de pouvoir choisir le système de protection le plus approprié en fonction des caractéristiques de l'ouvrage à protéger : canalisations ou pièces de forme tourmentée, telles que têtes de puits, durée, lieu et profondeur d'immersion, contraintes subies (potentiel, température).

---

1. Introduction et objet de l'étude

La COMPAGNIE FRANCAISE DES PETROLES (C.F.P.) a été chargée en 1965 par l'ENTREPRISE DE RECHERCHES ET D'ACTIVITES PETROLIERES (Société ELF-ERAP), puis par le CENTRE NATIONAL D'EXPLOITATION DES OCEANS (C.N.E.X.O.) à partir du 1er janvier 1970, d'étudier la protection externe contre la corrosion des structures métalliques pétrolières immergées à grande profondeur, canalisations, têtes de puits,...

Ces travaux ont été entrepris avec la collaboration et la participation du GAZ DE FRANCE (G.D.F.) qui avait, dans ce domaine, une grande expérience notamment à la suite des recherches effectuées par ses Services sur les revêtements pour les canalisations sous-ma-

.../...

rines méditerranéennes de transport de gaz.

Les études réalisées entre 1966 et 1971 ont porté sur les points suivants :

- Choix et application des revêtements,
- Comportement des revêtements vis-à-vis de la protection cathodique par courant imposé,
- Tenue aux chocs thermiques avec surimposition ou non d'une protection cathodique par anode soluble,
- Comportement des revêtements après des durées prolongées d'immersion dans différentes mers et à diverses profondeurs.

La présente communication fait le point des résultats obtenus dans ces domaines après plus de 4 ans d'expérimentation.

2. Revêtements étudiés

A la suite des contacts que la COMPAGNIE FRANCAISE DES PETROLES et le GAZ DE FRANCE ont pris avec un grand nombre de fournisseurs entre 1966 et 1971, vingt sociétés ont proposé 30 systèmes de protection qui peuvent être classés en trois catégories :

- Revêtements à base de résines époxydiques, seules ou associées à d'autres produits tels que brai, polyuréthanne, nylon ; dans cette catégorie, qui représente les 2/3 des revêtements retenus, figurent en particulier plusieurs systèmes de réparation sous l'eau ;
- Revêtements à base d'autres matières plastiques : polyamide 11, polychlorure de vinyle, polyester, polyéthylène modifié ou non et polyuréthanne ;
- Revêtements à base de produits hydrocarbonés chargés.

L'application sur les différents types d'éprouvettes a été réalisée par les fabricants eux-mêmes ou par des sociétés spécialisées sous la surveillance et avec la participation de techniciens du GAZ DE FRANCE ; elle a été faite sur métal sablé, en général au moyen de silex, l'état de surface obtenu correspondant au moins au deuxième degré de sablage (sablage "soigné") tel qu'il est défini dans les Spécifications Techniques de Sablage de l'Office National d'Homologation des Garanties de Peinture Industrielle.

Les renseignements relatifs à ces systèmes sont donnés dans le tableau 1 où l'on voit que plusieurs techniques de mise en oeuvre ont été utilisées, à chaud, à froid, sous l'eau, pistolet, brosse, pistolet à flamme, bain fluidisé ; un primaire d'accrochage, en particulier à base de zinc, a été employé dans un assez grand nombre de revêtements. Le nombre total de couches appliquées varie de 1, cas surtout des systèmes obtenus à chaud, à 6 mais un grand nombre de protection en comporte 3. Les épaisseurs obtenues sont également très variables et vont depuis 30 microns jusqu'à plusieurs millimètres.

3. Comportement des revêtements vis-à-vis de la protection cathodique

Le but des essais entrepris dans les laboratoires du GAZ DE FRANCE est d'étudier l'influence, sur la tenue dans le temps dés revêtements, de la protection cathodique par courant imposé qui est susceptible d'être appliquée sur les structures sous-marines pour compléter l'action des protections "passives".

.../...

3.1. Principe des essais et mode opératoire

Ces essais consistent à porter à des potentiels négatifs différents, des éprouvettes métalliques de petite dimension, revêtues des systèmes de protection retenus, immergés dans des bacs remplis d'eau de mer artificielle, maintenus à la température de 20°C ± 2°C, et à mesurer le courant de fuite traversant chaque éprouvette. Des examens visuels de l'état des revêtements sont effectués parallèlement afin de déterminer le début de l'apparition des cloquages ou détériorations.

L'expérimentation porte sur 4 séries de potentiel, -900 mV, -1 200 mV, -1 500 mV et -3 000 mV, potentiels mesurés par rapport à l'électrode de référence argent/chlorure d'argent. Ces potentiels, obtenus par un potentiostat à asservissement électronique à 4 voies sont, en effet, ceux que l'on rencontre le plus couramment dans la protection des métaux en eau de mer : -900 mV correspond ainsi au voisinage du seuil de protection cathodique, -3 000 mV, aux parties d'ouvrages voisines du point d'injection du courant et -1 500 mV enfin, aux parties situées à mi-distance environ entre la source de courant et l'extrêmité de l'ouvrage à protéger. De plus, la tension de -1 200 mV a été retenue, car elle correspond, d'après les travaux antérieurs faits par le GAZ DE FRANCE pour la protection des ouvrages métalliques immergés du barrage de la Rance, au seuil d'accroissement du phénomène de cloquage des revêtements type peinture.

Chacun des bacs d'essai , réalisé en matière plastique, correspond à un potentiel défini ; il comporte des compartiments cathodiques et anodiques séparés par des cloisons en porcelaine poreuse et est relié à l'une des 4 voies du potentiostat. Les éprouvettes, constituées par des cylindres en acier de 40 mm de diamètre et 300 mm de long, terminés par une calotte hémisphérique, sont disposées dans les compartiments cathodiques et reliées électriquement ensemble, leur disposition étant réalisée de manière à éviter les influences réciproques des champs électriques (distance de 120 mm environ entre éprouvettes). Dans chaque compartiment anodique, est placée une anode en graphite.

Les mesures électriques effectuées sont :

- D'une part, la vérification du potentiel imposé au moyen d'un voltmètre électronique placé entre la sortie du potentiel contrôlé par le potentiostat et une électrode de référence argent/chlorure d'argent disposée dans l'un des compartiments cathodiques du bac ;

- D'autre part, la mesure, faite périodiquement, du courant circulant entre l'éprouvette et l'anode en graphite par insertion dans le circuit individuel de chaque éprouvette d'un galvanomètre.

L'eau de mer artificielle, composée selon la formule de Lyman et Fleming , est renouvelée très fréquemment, en particulier dans les bacs à fort potentiel -1 500 mV et surtout -3 000 mV, pour éviter la concentration dans les compartiments cathodiques, de chlore ou d'hypochlorite dû à l'électrolyse de l'eau de mer provoquée par le passage du courant.

La durée des essais est fixée en principe à 2 ans, mais compte tenu des places disponibles dans les bacs d'essais, l'expérimentation est poursuivie au-delà pour les meilleurs systèmes jusqu'à un temps total de 4 années environ.

3.2. Critères de sélection

Les considérations sur lesquelles la sélection des revêtements

... ...

.../...
a été basée sont essentiellement les suivantes :

- Le comportement d'un revêtement sous protection cathodique est d'autant meilleur que la valeur de l'intensité du courant circulant dans l'éprouvette est plus faible. Ce comportement peut donc être considéré comme satisfaisant, compte tenu de la surface immergée des éprouvettes, soit 340 cm2 environ, lorsque l'intensité mesurée est de l'ordre du microampère ; par contre, lorsque la valeur trouvée est de l'ordre du milliampère, la consommation de courant serait, dans la pratique, trop importante et le revêtement est, dans ces conditions, jugé inacceptable ;

- L'état du revêtement doit être également considéré car le passage du courant peut entraîner, même pour des valeurs d'intensité très faibles, l'apparition de cloques ou de détériorations et dans certains cas, la formation de dépôts calco-magnésiens plus ou moins volumineux.

3.3. Résultats obtenus et conclusions qui s'en dégagent

Les résultats obtenus sur les divers revêtements étudiés sont rassemblés dans le tableau 5 ; ils permettent de faire les commentaires suivants :

3.3.1. 13 systèmes sur les 30 retenus initialement donnent satisfaction après 2 ans d'expérimentation ; ils se classent ainsi en fonction de leur tenue sous les différents potentiels imposés :

- Tous potentiels jusqu'à -3 000 mV : résines époxydiques réf. 4 et 19, polyamide 11 réf. 12, résine époxy-brai réf. 21, polyéthylène réf. 23 et hydrocarboné chargé réf. 24.
- Tous potentiels jusqu'à -1 500 mV : hypalon réf. 9, résine époxy-brai réf. 25.
- Tous potentiels jusqu'à -1 200 mV : résines époxy-brai réf. 5 et 7, résine époxy-brai-polyuréthanne réf. 20 et résine époxydique réf. 22.
- Potentiel de -900 mV : polyester chargé réf. 8.

Parmi ces revêtements, il faut remarquer que 4 seulement des systèmes à base de résine époxydique sur les 8 retenus ont donné satisfaction mais, par contre, 4 des 5 résines époxy-brai se sont bien comportées ainsi que l'ensemble des protections appliquées à chaud (réf. 4-12-23).

Un grand nombre de ces systèmes présente toutefois de légers signes de cloquages ou détériorations (cotés Ba dans le tableau 5) ; tel est le cas des revêtements réf. 4-7-8-9-12-19 et 20.

3.3.2. Les systèmes actuellement en essais, réf. 26-27-28 et 30, donnent des résultats très encourageants après un an d'expérimentation sous potentiel imposé.

3.3.3. Il a été observé, au cours de ces essais, que la détérioration du revêtement se traduisait :

- Au potentiel de -900 mV presque uniquement sous forme de rouille ; cette formation s'explique par le fait que la tension -900 mV appliquée à l'éprouvette est un potentiel moyen et qu'en réalité, elle varie autour de cette valeur ; sa valeur absolue peut descendre suivant l'état du revêtement dans certaines zones en- dessous du seuil de protection cathodique, d'où présence de rouille.
- Au potentiel de -1 200 mV à la fois sous forme de rouille et de

.../...

.../...

dépôts calco-magnésiens.

- Aux potentiels de -1 500 mV et -3 000 mV uniquement par des formations calco-magnésiennes.

Tous les revêtements satisfaisants à 24 mois ont été toutefois laissés en essais, à titre comparatif, jusqu'à un temps maximal d'expérimentation de 4 années ; leur état actuel est indiqué dans le tableau 6 où l'on voit en particulier que les revêtements époxydiques réf. 4 et 19 donnent toujours de bons résultats à tous les potentiels après plus de 3 ans d'essais.

4. Comportement des revêtements aux chocs thermiques

Le but des essais, confiés au CENTRE DE RECHERCHES ET D'ETUDES OCEANOGRAPHIQUES (C.R.E.O.) de la Rochelle, est d'étudier le comportement des revêtements sous l'influence des chocs thermiques qui peuvent être supportés par les structures sous-marines, en particulier par les têtes de puits lors du soutirage du pétrole brut, la température pouvant s'élever de la température de l'eau de mer, 3 à 4°C en hiver en Mer du Nord par exemple, à plus de 100°C.

4.1. Principe des essais et mode opératoire

Ces essais consistent à immerger des éprouvettes métalliques, revêtues des systèmes à étudier, dans un bassin d'eau de mer naturelle de 10 m3 renouvelée périodiquement puis à leur faire subir un grand nombre de chocs thermiques de + 20°C à + 100°C environ. Les éprouvettes, montées par groupe de 9 sur un radeau formé d'un cadre en cornière supporté par des blocs de polystyrène expansé, sont constituées essentiellement d'un tube d'acier de 60 mm de diamètre extérieur et de 400 mm de longueur environ, dans lequel est placé un tube d'acier concentrique contenant un cylindre de porcelaine avec résistances chauffantes permettant d'obtenir la température souhaitée par le chauffage d'eau distillée contenue entre les 2 tubes d'acier ; pour éviter une évaporation trop rapide de l'eau, un dispositif de refroidissement de la vapeur dégagée est mis en place au-dessus de chaque éprouvette. La valeur des résistances placées à l'intérieur du cylindre en porcelaine est choisie en fonction de l'épaisseur et de la conductivité thermique du revêtement ; la puissance installée est comprise entre 1 200 W et 2 400 W.

Le cycle auquel est soumis chaque éprouvette est le suivant :

- Montée en température 5 à 10 mn,
- Maintien en température 30 à 35 mn,
- Retour à température ambiante et maintien à cette température 80 mn.

Ce cycle est réalisé à l'aide d'un programmeur qui comporte en plus un système de comptage de cycles. La durée des essais est fixée à 1 200 cycles environ.

Les mêmes essais sont effectués également avec surimposition d'une protection cathodique par anode soluble. L'anode en alliage de magnésium GA 6 Z 3 utilisée se présente sous la forme d'un cylindre de 33 mm de diamètre et de 70 mm de longueur et est disposée à la verticale de l'éprouvette à une distance variant de 0,50 m à 1 m ; son potentiel, mesuré par rapport à une électrode de référence argent/chlorure d'argent, est très voisin de -1,5 volts tandis que celui des éprouvettes

.../...

.../...
varie de -0,6 à -1,2 volts. L'intensité du courant circulant entre l'anode et l'éprouvette est mesurée périodiquement suivant le même principe que pour l'expérimentation en laboratoire sous protection cathodique.

4.2. Critères de sélection

Les considérations sur lesquelles le comportement des revêtements a été jugé sont essentiellement basées sur :

- Les observations visuelles effectuées en cours et à l'issue des essais de choc thermique par les spécialistes de la C.F.P. et du G.D.F: présence de dépôts calco-magnésiens, détérioration du revêtement (éclatement, cloquage, rouille, manque d'adhérence,...)
- Les valeurs des intensités de courant mesurées dans le cas où les essais ont été réalisés avec surimposition d'une protection cathodique. Si l'on se réfère à la surface immergée des éprouvettes, 1 040 cm2 environ, le comportement d'un système peut être considéré comme satisfaisant si l'intensité est de l'ordre du milliampère et comme non satisfaisant si les valeurs trouvées sont de l'ordre d'une cinquantaire de milliampères.

4.3. Résultats obtenus et conclusions qui s'en dégagent

Les résultats obtenus sont rassemblés dans le tableau 2. Son examen permet de constater qu'un certain nombre de revêtements résistent de façon satisfaisante aux cycles de choc thermique effectués, avec ou sans surimposition de la protection cathodique par anode de magnésium (potentiel voisin de -1 500 mV) ; on peut citer le polyamide 11 réf. 12, le polyester chargé réf. 48, le polyéthylène réf. 23, les résines époxydiques seules réf. 4, 19, 22, 26 ou associées à d'autres matériaux réf. 20, 21, 25, 27 et enfin le système de réparation sous l'eau réf. 15/15 bis.

Il convient de signaler également que les revêtements se comportent en général moins bien sous protection cathodique qu'hors protection cathodique, notamment ceux dont la tenue s'est révélée mauvaise précédemment au laboratoire au potentiel de -1 500 mV, cas en particulier des systèmes réf. 1, 5, 7, 8, 15/15 bis et 16.

5. Comportement des revêtements en immersion marine

Le but des essais est d'étudier le comportement des protections dans des conditions aussi proches que possible de la réalité en immergeant des éprouvettes dans différentes mers et à diverses profondeurs.

5.1. Choix des sites retenus

Notre choix s'est d'abord porté sur la station de corrosion située au large d'Antibes où le GAZ DE FRANCE procède depuis de nombreuses années à des essais de tenue des revêtements appliqués sur tubes, puis sur 3 sites, côtes anglaises (Mer du Nord), Gabon (Atlantique) et Das Island (Golfe Persique) où la COMPAGNIE FRANCAISE DES PETROLES possède des permis de recherches d'hydrocarbures. Les principales caractéristiques de ces stations sont consignées dans le tableau 4 ; des mesures océanographiques de chaque milieu ont été effectuées : température, dosage de l'oxygène dissous, Ph, force du courant, sédimentologie et salinité. Par ailleurs, afin d'apprécier l'agressivité du milieu et de connaître le taux moyen de corrosion, des éprouvettes d'acier nu ont été immergées récemment dans chaque station et doivent être normalement prélevées après un an, trois ans et cinq ans d'exposition.

.../...

.../...

5.2. Description des éprouvettes d'essai

Les éprouvettes de corrosion sous-marine présentent une architecture qui simule les diverses formes que l'on peut rencontrer dans une infrastrucutre pétrolière immergée. Elles sont constituées, en fait, de deux tubes d'acier de diamètre différent raccordés par une bride et comportant des cornières et anneaux soudés et, pour certaines, un raccord Grayloc dans la partie médiane du petit tube ; en outre, à sa partie supérieure, un anneau en bronze a été soudé afin de créer un couple de corrosion avec l'acier. La hauteur totale de l'éprouvette est de 1,80 m et son poids de 45 kg.

5.3. Processus de mouillage et de récupération des éprouvettes

Les éprouvettes sont disposées en chapelet le long d'un câble de nylon en position horizontale ou verticale au contact des sédiments, au moyen de flotteurs de 10 et 30 litres en polyéthylène rempli d'essence automobile. Le mouillage de la cordée s'effectue, suivant les stations, soit à partir d'une structure fixe immergée (plate-forme de forage ou de production) soit d'une bouée lumineuse, soit par immersion libre au fond de la mer, la position de la cordée étant alors exactement repérée. Le relevage des éprouvettes, dans ce cas, est réalisé au moyen d'un bateau traînant derrière lui une queue de dragage perpendiculairement à la direction du mouillage.

5.4. Méthodes d'observation des éprouvettes

Après chaque opération de relevage, un contrôle de l'état des revêtements est effectué selon le processus suivant :

- Lavage à l'eau douce des éprouvettes, complété par un brossage,
- Examen visuel approfondi portant, d'un part, sur les détériorations mécaniques subies par les éprouvettes au cours des opérations de relevage et de réimmersion successives, d'autre part, sur le comportement proprement dit du revêtement au cours du temps (présence de cloques, points de rouille, fissures, manque d'adhérence). Pour éliminer, dans la mesure du possible, toute interprétation personnelle, un système de cotation des défauts relevés à été mis au point par le GAZ DE FRANCE et appliqué à chacune des parties constitutives de l'éprouvette, parties "accidentées" comprenant les cornières, les anneaux, la bride, le raccord Grayloc et le fond de l'éprouvette et parties "cylindriques". A partir de ces cotations, une notation d'ensemble de l'état du revêtement est établie.
- Photographie des éprouvettes.

5.5. Résultats obtenus

Les résultats obtenus dans les différentes stations sont rassemblés dans le tableau 3 ; son examen ainsi que les observations faites sur place permettent de faire les commentaires suivants :

a) Les principales variétés de salissures rencontrées sur les éprouvettes sont d'origine animale et peuvent être classées ainsi :

- Organismes à coquille dure : tubes de verre (serpules, pomatocéros, spirorbes), mollusques (huîtres), encroutements calcaires (bryozoaires) et balanes, cette dernière espèce n'étant présente que dans les stations d'Angleterre et surtout du Gabon et du Golfe Persique,
- Organismes à apparence gazonnante ou ressemblant à de petits arbustes : hydraires,
- Organismes mous : ascidies, éponges, actinies.

Le peuplement des salissures et leurs dimensions varie d'une sta-

.../...

.../...

tion à l'autre mais c'est dans les mers les plus chaudes, au large du Gabon et Golfe Persique, qu'on les rencontre en très grande quantité.

Les salissures présentent une adhérence plus ou moins grande au revêtement et ne paraissent pas avoir attaqué celui-ci, à l'exception des balanes qui possèdent, à la base du tronc de cône, une partie coupante qui s'incruste dans les systèmes les plus mous, cas du mastic de réparation sous l'eau réf. 15 bis immergé au Golfe Persique.

b) Parmi les systèmes immergés au large d'Antibes par 100 m de fond, cinq sont dans un état général "assez bon' après le dernier examen effectué ; ce sont le polyester chargé réf. 8 et le polyéthylène réf. 23 (48 mois), la résine époxydique réf. 19 (36 mois) et les résines époxydiques modifiées réf. 20 et 21 (24 mois). Les autres revêtements peuvent se classer ainsi, en tenant compte du temps pendant lequel leur comportement est resté satisfaisant (état général au moins "assez bon") :

- Tenue égale à 36 mois : systèmes réf. 1, 2/15, 4, 12, 15 bis ;
- Tenue égale à 24 mois : systèmes réf. 5, 9 ;
- Tenue égale à 12 mois : systèmes réf. 3, 7, 16 ;
- Tenue inférieure à 12 mois : systèmes réf. 11, 14,14 bis,17,18.

Il y a lieu également de signaler que les revêtements se comportent en général de façon satisfaisante dans les parties "cylindriques" alors que dans les parties "accidentées", plus difficiles à revêtir et plus sensibles aux détériorations mécaniques, ils se présentent en assez mauvais, mauvais ou très mauvais état.

c) Le comportement des revêtements dans les autres stations, Mer du Nord, Gabon et Golfe Persique, est, dans l'ensemble, voisin de celui observé à Antibes.

6. Conclusions

Les résultats obtenus au cours de cette expérimentation qui se poursuit toujours en 1972, permettent, dès maintenant, de faire une sélection des meilleurs revêtements pour chacun des essais effectués et donc de pouvoir choisir le système de protection le plus approprié en fonction des caractéristiques de l'ouvrage à protéger : forme des pièces (canalisations, têtes de puits...), durée, lieu et profondeur d'immersion, contraintes subies (potentiel appliqué, température à laquelle peut être porté l'ouvrage).

Les revêtements expérimentés peuvent ainsi se classer de la façon suivante :

- Ouvrages ou structures uniquement en immersion :
  . Très satisfaisants : ce sont les systèmes réf. 1, 2/15, 4, 8, 12, 15 bis, 19, 23.
  . Satisfaisants : réf. 5, 9, 20, 21.
- Ouvrages ou structures immergés soumis uniquement à une protection cathodique :
  . Très satisfaisants : réf. 4, 12, 19,23
  . Satisfaisants : réf. 9 et 21.
- Ouvrages ou structures immergés soumis uniquement à des chocs thermiques :
  . Très satisfaisants : réf. 1, 4, 8, 12, 15 bis, 19, 23. .../...

.../...

. Satisfaisants : 5, 20 et 21.

- Ouvrages ou structures immergés soumis à la fois à une protection cathodique et à des chocs thermiques :
  . Très satisfaisants : 4, 12, 19, 23.
  . Satisfaisants : 21.

Nous remercions vivement le CENTRE NATIONAL D'EXPLOITATION DES OCEANS (C.N.E.X.O.) de nous avoir permis de présenter cette communication au 3ème Congrès International de la Corrosion Marine et des Salissures.

P.J. 6 tableaux.

Discussion

Question: Have you seen any results in any location that would cause a change in selection of material for either cathodic protection or for materials of coating for another location in the ocean?

Louis: Je crois que, dans les résultats obtenus jusqu'à présent, on n'a pas trouvé de différence dans les effets d'immersion entre le comportement des différents revêtements. Mais il est bien certain que, en dehors des 4 revêtements que j'ai indiqués et qui donnent satisfaction à tous les potentiels, il y en a certains qui sont bons en protection cathodique et qui sont mauvais aux chocs thermiques ou inversement. Donc, il faut faire la synthèse de l'ensemble des résultats pour choisir en fonction du lieu d'immersion celui qui sera choisi.

TABLEAU 1 : NOMENCLATURE DES DIFFERENTS REVETEMENTS ETUDIES

FAMILLE DE REVETEMENTS		REFERENCE REVETEMENT	REFERENCE FOURNISSEUR ou APPLICATEUR	MISE EN PRIMAIRE a	b	c
Hydrocarboné chargé poudre aluminium		24	A			
Polyamide 11		12	B			
Polychlorure de vinyle (plastisol)		13	O			
		13 bis	O	1		
Polyester chargé flocons verre		8	C			
Polyéthylène		23	D			
Polyéthylène chlorosulfoné (hypalon)		9	E	1	à froid	pistolet
Polyéthylène greffé		30	F			
Polyuréthanne		11	G	1	à froid	pistolet
Résines époxydiques		1	H			
		2/15	I	2 (époxy-zinc)	à froid	pistolet
		3	J	2	à froid	pistolet
		4	K			
		14	L			
		19	K			
		22	M			
		26	N	1(zinc silicaté) +1(époxydes)	à froid "	brosse "
Produits à base de résines époxydiques	Résines époxy-brai	5	P			
		7	C	1(à base zinc)	à froid	pistolet
		16	Q	1(zinc silicaté)	à froid	brosse
		21	M	1(à base zinc) +1(à base Al)	à froid "	pistolet "
		25	A	1	à froid	pistolet
	Résine époxy-polyuréthanne	17	R	1	à froid	brosse
	Résine époxy-brai polyuréthanne	20	S	2(à base zinc)	à froid	brosse
	Résine époxy chargé nylon	27	N			
Systèmes de réparation sous l'eau (résines époxydiques)		14 bis	L			
		15 bis	I			
		18	L			
		28				
		29	T			

(1) Les lettres employées ont la signification suivante : a = nombre de couches ; b = réalisation de la protection ; c = mode d'application; d=temps de sèchage entre couches.

O E U V R E (1)					EPAISSEUR TOTALE (2)	ASPECT
R E V E T E M E N T						COULEUR
d	a	b	c	d	mm	
	4	à froid	pistolet	24 h	0,35	Rouge brun
	1	à chaud	pistolet à flamme	-	0,54-0,65	Gris laiteux
	1 1	à froid+cuisson à froid+cuisson	pistolet pistolet		0,03 0,03	Gris Gris
	2	à froid	brosse	24 h	0,96-1,30	Blanc
	1	à chaud	Fluidisation	-	2	Rouge
24 h	3(hypalon) 2(époxydes)	à froid "	pistolet "	24 h "	0,4	Orange foncé
	1	à chaud	fluidisation	-	0,5-0,6	Blanc
15 mn	3	à froid	pistolet	6 h	0,28-0,35	Orange
	1	à froid	brosse	48 h	0,80-1,18	Gris noir
10 mn	3	à froid	brosse (1) pistolet(2)(3)	24 h	0,33-0,41	Gris clair
2 h	2	à froid	pistolet	24 h	0,22-0,29	Gris
	1	à chaud	pistolet à flamme	-	0,32-0,37	Vert foncé
	2	à froid	brosse	24 h	0,08-0,12	Gris
	3	à froid	pistolet	1 h 30	0,67-0,80	Vert
	3	à froid	brosse	24 h	0,15-0,16	Rouge
24 h "	3	à froid	brosse	24 h	0,40-0,50	Blanc
	3	à froid	brosse	72 h	0,50-0,57	Noir
8 h	2	à froid	brosse (1) pistolet (2)	48 h	0,47-0,56	Noir
8 j	2	à froid	brosse	48 h	0,28-0,45	Noir
1 h "	2	à froid	pistolet	24 h	0,29-0,33	Brun rouge
24 h	2	à froid	pistolet	24 h	0,35-0,40	Noir
1 h	2	à froid	brosse	2 h	0,86-1,18	Blanc
12 h	2	à froid	brosse (1) pistolet (2)	24 h	0,34-0,39	Noir
	3	à froid	brosse	24 h	0,7 - 0,8	Gris-beige
	2	sous l'eau	brosse	24 h	0,19-0,23	Jaune
	1	sous l'eau	enrobage manuel	3 j	3,1-4,2	Jaune
	3	sous l'eau	brosse	24 h	0,41-0,66	Gris
	2	sous l'eau	brosse	24 h	0,4-0,5	Jaune
	3	sous l'eau	brosse	24-48 h	0,5-1	Gris

(2) Mesurée sur les éprouvettes de corrosion sous-marine type ANTIBES. **(Tableau 1 - suite)**
(3) Utilisation d'un conditionneur de surface.

TABLEAU 2 : COMPORTEMENT DES REVETEMENTS AUX CHOCS THERMIQUES AVEC OU SANS SURIMPOSITION D'UNE PROTECTION CATHODIQUE (-1 500mV)

FAMILLE DE REVETEMENTS		REFERENCE REVETEMENT	RESULTATS OBTENUS AVEC 1 200 CYCLES ENVIRON (1)	
			SANS PROTECTION CATHODIQUE	AVEC PROTECTION CATHODIQUE
Hydrocarboné chargé poudre aluminium		24		M (643)
Polyamide 11		12	AB	B
Polyester chargé flocons de verre		8	TB	AB
Polyéthylène		23	B	B
Polyéthylène chlorosulfoné (hypalon)		9	M (460)	
Polyéthylène greffé		30		M (400)M(463)
Polyuréthanne		11	M (790)	
Résines époxydiques		1	AB	M (736)
		2/15	M (480)	
		3	M	
		4	E	AB
		14	M (300)	
		19	B	B
		22		AB
		26		B
Produits à base de résines époxydiques	Résines époxy-brai	5	AB	M
		7	AB	M (773)
		16	AB	M
		21		AB
		25		B
	Résine époxy polyuréthanne	17	M (300)	
	Résine époxy-brai polyuréthanne	20	AB	AB
	Résine époxy chargé nylon	27		TB
Systèmes de réparation sous l'eau (résines époxydiques)		14 bis	non appliqué	
		15-15 bis(2)	B	AB (712)
		18	M (230)	
		28		AM
		29 (3)		

(1) Les lettres employées ont la signification suivante :
E: excellent, TB: très bon, B: bon AB : assez bon, AM : assez mauvais, M: mauvais,
Entre parenthèses, nombre de cycles au bout duquel les essais ont été arrêtés.

(2) Eprouvette revêtue avec le système 15 à l'exception d'une zone qui est ensuite protégée sous l'eau par le système correspondant 15 bis.

(3) Essai non effectué en raison d'une mauvaise application sur l'éprouvette de choc thermique.

TABLEAU 3 : COMPORTEMENT DES REVETEMENTS EN IMMERSION MARINE - ETAT GENERAL DES EPROUVETTES

FAMILLE DE REVETEMENTS		REFERENCE REVETEMENT	EPAISSEUR mm	COMPORTEMENT DANS LE TEMPS (1)			
				Méditerranée (ANTIBES)	Mer du Nord (SCARBOROUGH)	Atlantique (GABON)	Golfe Persique (DAS ISLAND)
Polyamide 11		12	0,54-0,65	36	> 43 (AB)	> 38 (AB)	perdue
Polyester chargé flocons verre		8	0,96-1,30	> 48 (AB)	> 43 (AB)	> 38 (B)	> 30 (TB)
Polyéthylène		23 (2)	2	> 48 (AB)	-	-	-
Polyéthylène chlorosulfoné (hypalon)		9	0,4	24	< 21	> 38 (AB)	< 30
Polyuréthanne		11	0,28-0,35	< 12	< 21	< 13	< 17
Résines époxydiques		1	0,80-1,18	36	perdue	13	< 17
		2/15	0,33-0,41	36	> 43 (AB)	> 38 (B)	> 30 (TB)
		3	0,22-0,29	< 12	< 21	< 13	< 17
		4	0,32-0,37	> 36	21	> 38 (AB)	> 30 (AB)
		14	0,08-0,12	12	< 10	< 13	< 30
		19	0,67-0,80	36 (AB)	> 33 (AB)	> 25 (AB)	perdue
Produits à base de résines époxydiques	Résines époxy-brai	5	0,50-0,57	24	> 43 (AB)	> 38 (AB)	17
		7	0,47-0,56	12	perdue	< 13	< 17
		16	0,28-0,45	12	< 11	< 25	< 17
		21	0,29-0,33	> 24 (AB)	perdue	en cours	> 13 (TB)
	Résine époxy-polyuréthanne	17	0,86-1,18	< 12	< 11	< 25	< 17
		20	0,34-0,39	> 24 (AB)	perdue	en cours	> 13 (AB)
Systèmes de réparation sous l'eau (résines époxydiques)		14 bis	0,19-0,23	< 12	< 10	< 13	-
		15 bis	3,1 -4,2	36	> 43 (AB)	13(accidentée)	< 17
		18	0,41-0,66	< 12	< 11	< 25	< 17

(1) Le nombre de mois indiqué correspond au temps pendant lequel le revêtement est resté satisfaisant (état au moins "assez bon"). Pour les systèmes encore satisfaisants à l'issue du dernier examen effectué, l'indication de leur état a été précisée.
(2) Revêtement appliqué seulement sur tronçons de tube droits.

TABLEAU 4 : CARACTERISTIQUES DES STATIONS DE CORROSIONS SOUS-MARINES

MER	LIEU D'IMMERSION	PROFONDEUR D'IMMERSION	ASSISTANCE TECHNIQUE POUR LE MOUILLAGE ET LE RELEVAGE
Méditerranée	Au large d'ANTIBES (France)	90-100 m	C. R. E. O.
Mer du Nord	Au large de SCARBOROUGH (Angleterre)	48 m	TOTAL OIL MARINE
Atlantique	Au large de PORT-GENTIL (Gabon)	30 m	SPAFE (ELF-ERAP)
Golfe Persique	Au large de DAS ISLAND (Abu-Dhabi)	20 m	ADMA (BP, CFP)

TABLEAU 5 - COMPORTEMENT DES REVETEMENTS APRES 24 MOIS D'EXPERIMENTATION SOUS PROTECTION CATHODIQUE

FAMILLE DE REVETEMENTS	REFERENCE REVETEMENT	EPAISSEUR mm (1)	POTENTIEL IMPOSE (2)			
			- 900 mV	- 1200 mV	- 1500 mV	- 3 000 mV
Hydrocarboné chargé poudre aluminium	24	0,35	B	M (5m)*	M (18 m)*	B
Polyamide 11	12	1,1	Ba	Ba	B	Ba
Polychlorure de vinyle (plastisol)	13 13 bis	0,03 0,03	M (3m) M (4m)	M (1m) M (1m)	M (1m) M (1m)	M (0m) M (0m)
Polyester chargé flocons verre	8	0,76	Ba	M (19 m)	M (3 m)	M (1m)
Polyéthylène	23	2	B	B	B	B
Polyéthylène chlorosulfoné (hypalon)	9	0,28	B	Ba	B	M (7 cm)
Polyéthylène greffé	30	0,5-0,6	B après 12 m**	B après 12 m**	B après 12 m**	B après 12 m**
Polyuréthanne	11	0,08	M (20 m)	M (20 m)	M (23 m)	M (1m)

.../...

.../...

Résines époxydiques		1	0,40	M (20 m)	M (4 m)	M (1 m)	M (0 m)
		2/15	0,29	M (17 m)	M (1 m)	M (1 m)	M (0 m)
		3	0,17	M (19 m)	M (23 m)	M (2 m)	M (3 m)
		4	0,37	Ba	B	B	B
		19	0,25	B	Ba	B	B
		22	0,15-0,20	B	B	M (17 m)	M (5 m)
		26	0,4-0,5	B après 12 m**	B après 12m**	B après 12 m**	M (8 m)
Produits à base de résines époxydiques	Résines Epoxy-brai	5	0,45	B	B	M (21 m)	M (5 m)
		7	0,46	Ba	B	M (7 m)	M (0 m)
		16	0,34	M (19 m)	M (14 m)	M (19 m)	M (3 m)
		21	0,2-0,3	B	B	B	B
		25	0,35-0,4	B	B	B	M (5 m)
	Résine époxy polyuréthanne	17	0,75	M (19 m)	M (19 m)	M (15 m)	M (5 m)
	Résine époxy-brai polyuréthanne	20	0,3-0,45	B	Ba	M (19 m)	M (1 m)
	Résine époxy chargé nylon	27	0,7-0,75	B après 12 m**	B après 12 m**	B après 12 m**	B après 12 m**
Systèmes de réparation sous l'eau (résines époxydiques)		14/14 bis (3)	0,03/0,20	M (1 m)	M (0 m)	M (0 m)	M (0 m)
		15/15 bis (3)	0,32/3,5	M (16 m)	M (1 m)	M (1 m)	M (0 m)
		18	0,40	M (1 m)	M (0 m)	M (0 m)	M (0 m)
		28	0,4-0,5	Ba après 12 m**	Ba après 12 m**	B après 12 m**	M (1 m)
		29	0,5-1,0	M (1 m)	M (0 m)	M (0 m)	M (0 m)

(1) Mesurée sur les éprouvettes expérimentées

(2) Les lettres employées ont la signification suivante :
B:bon (intensité de courant de l'ordre du microampère, pour la surface immergée de l'éprouvette, 340 cm2)
Ba:bon mais présentant quelques cloques ou piqûres de rouille
M:mauvais (intensité du courant de l'ordre du milliampère ou présence de nombreuses cloques ou piqûres de rouille)
Entre parenthèses, temps en mois au bout duquel le revêtement est devenu mauvais.

(3) Eprouvette revêtue avec le système 14 ou 15 à l'exception d'une zone qui est ensuite protégée sous l'eau par le système correspondant 14 bis ou 15 bis.

* défaut d'application ** Essai actuellement en cours.

TABLEAU 6 : ETAT ACTUEL DES REVETEMENTS SOUS PROTECTION CATHODIQUE

FAMILLE DE REVETEMENTS		REFERENCE REVETEMENT	POTENTIEL IMPOSE							
			- 900 mV		- 1 200 mV		- 1 500 mV		- 3 000mV	
			Durée d'essais	Etat (1)	Durée d'essais	Etat (1)	Durée d'essais	Etat (1)	Durée d'essais	Etat (1)
Hydrocarboné chargé poudre aluminium		24	25 m	B		*		*	25 m	B
Polyamide 11		12	45 m	Ba	45 m	Ba	45 m	B	36 m	M
Polyester chargé flocons verre		8	33 m	M						
Polyéthylène		23	25 m	B	25 m	B	25 m	B	15 m	B
Polyéthylène chlorosulfoné (hypalon)		9	45 m	B	45 m	Ba	45 m	M		
Résines époxydiques		4	40 m	Ba	40 m	B	45 m	B	42 m	B
		19	37 m	B	39 m	Ba	39 m	B	38 m	B
		22	29 m	Ba	29 m	Ba				
Produits à base de résines époxydiques	Résines époxy-brai	5	45 m	B	37 m	M				
		7	25 m	M	37 m	M				
		21	29 m	B	29 m	B	29 m	B	29 m	B
		25	25 m	B	25 m	B	25 m	B		
	Résine époxy-brai polyuréthanne	20	29 m	Ba	26 m	M				

(1) voir légende tableau 5

* éprouvettes éliminées en raison de défauts d'application

Corrosion Resistance of Metals in the Black Sea Water

F.Tavadze, S.Manjgaladze and M.Vashakidze

Institute of Metallurgy,
15 Pavlov St., Tbilisi 60,
Georgian SSR, U.S.S.R.

Corrosion resistance of a number of metals has been studied in the Bay of Batumi; it has been found that with a complete immersion of samples the corrosion rate of many materials is much higher than that shown in laboratory, both in artificial and natural sea water; in the course of the tests on stainless steel samples, difference is observed in the rate of corrosion as well as in its nature; main reasons accelerating corrosion of metals in the subtropical sea zones are of biological character; in the subtropical zones the highest corrosion resistivity was displayed by the titanium alloys, chrome-nickel austentic and complex alloy chrome-manganese steel samples; the charge of the alloy structures due to the thermal treatment affects their corrosive properties.

This work has been carried out to obtain comparable corrosion characteristics of some metallic materials (table 1) used in the sea. The tests were accomplished in natural (Batumi Bay) and laboratory conditions (3.5% NaCl, artificial and natural sea water). The effect of composition and thermal treatment of alloys has been evaluated.

Experimental technique. The samples of the material under study (rectangles - 100 x 50 x 3 mm and disks - 30 - 50 mm dia.) were polished on a grinding wheel avoiding their overheating. Then the samples were washed in acetone and after drying they were weighed within 0.0001 g.

For the tests in the port of Batumi the samples were fixed into frames by means of nylon strings with the distances of 50-100 mm between them. The frames were immersed at a depth of 5 - 6 m. The corrosion tests were started in summer. Duration of the tests in the sea was 14 and 26 months with the inspections every 3 and 6 months. After each inspection the samples were excluded from further tests. The sea water in the zone under study was characterized by the following average annual data: salinity - 17‰, chlorinity - 9.2‰, oxygen solubility - 5.3 mg/l, density - 11.9, temperature - 18°C, current velocity - 4.2 cm/sec.

Laboratory tests have been carried out in thermostatic conditions at 20 and 40°C. The effect of supply intensity of the corrosion medium to the metal surface was studied through complete immersion of the samples into quiet and stirred electrolyte, as well as through alternative immersion into quiet water. In the latter case the time of exposure to the electrolyte was 0.5 min, and that to the air was 15 min.

The corrosion tests being completed, the samples were cleaned of the corrosion products and of fouling, then washed in running water, dried and weighed. The regular corrosion rate was determined by the weight losses, while the pitting corrosion rate was found by the depth of corrosion [2,3].

Results. After immersion the surfaces of the samples were fouled with various organisms - balanuses, pearlworts, sea worms, water algae. The rate of fouling depended on the composition of the alloys.

Under the fouling the low alloy steel samples revealed black products of corrosion, which are common in the conditions of restricted air access. In the laboratory the samples were coated with friable corrosion products of light brown. The low alloy steel samples in the case of a complete irregular corrosion were destroyed at a rate of 0.072 - 0.100 mm/year (table 1). Maximum corrosion rate was observed on the samples tested in the sea and in 3.5% NaCl, at 40°C, as well as with the alternative immersion into electrolyte. In the latter case the rate of corrosion was even higher than in the sea. The corrosion rates of low alloy steel samples tested by complete and alternating immersion in the quiet water and by ~~alternative~~ immersion into electrolyte, differred due to the different oxygen supply to the metal surface and to the structure of the formed corrosion products.

In 2 - 3 months through pittings were formed on the 5 mm thick samples of chromium ferritic and chrome-nickel martensite steel under the foundations of the Balanus houses. The centers of pitting corrosion were found on the Cr18-Ni9 steel samples after 26 months of tests (table 2).The complex alloy chrome-nickel austentic steel, Cr18-Ni20, and the titanium alloys appeared to be corrosion resistant. The pitting corrosion of stainless steel developing mainly under balanuses seems to depend both on the formation of differential aeration pairs and by the change of pH due to the existence of the marine macro- and microorganisms.

The brass samples were fouled with single balanuses and coated with yellowish-brown deposit,while in laboratory the deposit was greenish-grey with small yellowish-brown spots; after removal of the latter the surface turned out to be partially coppered. The corrosion rate of brass was 0.005 mm/year. to 0.014 mm/year.

The samples of bronze alloys kept in natural conditions and in lab. were covered with corrosion products in the form of green spots after removal of which the Al9Mn2 alloy was covered with fine black rash.Fouling of copper alloys, especially of bronze is negligible. As with the low-alloy steel, maximum rate of corrosion of copper alloy was observed in the marine tests. However, unlike the low alloy steel, alternative immersion into the sea water exerted less influence on copper alloys, for the control process foe copper alloys is anodic. In the sea water copper alloys are liable to the pitting corrosion.

The observed rate of aluminium sample fouling is maximum. Unlike the stainless steel,aluminium under the balanus' house acts as a cathode.The pitting corrosion developed in the foul free places.

The tests in the quiet and stirred electrolyte have shown that the rate of corrosion of alloys in these conditions is much lower than in the sea. Though the electrolyte's stirring increases the corrosion rate of nearly all the alloys, corrosion in the sea is mainly enhanced by biological processes and not by the water movement.

Some metals were tested after various conditions of thermal treatment (table 3). The original ferrit-perlitic structure of low alloy steel seems to be more corrosion resistant than the sorbite one obtained after hardening followed by tempering. For Cr13 and Cr17-Ni2 steel hardening with subsequent tempering decreases the corrosion resistance. Normalization of the aluminium-magnesium alloy at 350°C with 12-hour exposure doubles its resistance.

Conclusions.The corrosion rate of many metallic materials investigated in the sea with their complete immersion is considerably higher than

that in the laboratory conditions.
2. Main reasons accelerating the metallic corrosion in the sea are biological ones, the rate of corrosion depending on fouling.
3. The rate of corrosion of low-alloy samples increases with alternative immersion, while the rate of aluminium alloys corrosion decreases. The rate of corrosion of high alloy steel samples and of copper alloys depends but slightly on the manner of their immersion.
4. The corrosion resistance of alloys depends on the thermal treatment.
5. The highest corrosion resistance in the subtropical zones of the Black Sea is typical for the titanium alloys, the chrome-nickel austenite and complex alloy steel, which are the most desirable for these conditions.

References

1. V.A.Klimova, N.M.Abramskaya, J. *Технология судостроения*. No. 2 (1966)
2. G.V.Akimov, *Теория и методы исследования коррозии металлов*, Proc. Ac.Sci.USSR (1945)
3. I.L.Rosenfeld and K.A.Zhigalova, *Ускоренные методы коррозионных испытаний металлов*, Moscow, Metallurgia Ed.(1966).

Table 1

Rate of corrosion (mm per year) of alloys in the marine water

Name of alloy group	Main elements content, %	Exposure time 3 months	6 months	26 months	K
Carbon-steel	C 0.2	0,208	0.088	0.085	1
Low-alloy steel	C 0.4 Cr	0.463	0.111	0.107	1
"	C 0.3 Cr Mn	0.110	0.077	0.059	1
"	C 0.1 Cr Si Ni Cu	0.132	0.079	(0.073)	1
High-alloy steel	Cr13	0.079x	0.065x	0.030x	20
"	Cr17Ni2	0.088x	0.059x	0.014x	20
"	Cr18Ni10 Ti	0.0002	0.0002	0.0003x	3
"	Cr18Ni10Si3Cu3Mo3 Nb	0.0002	0.0001	0.0001	1
"	Cr15NMn15 Cu Mo Si	-	-	(0.026)	5
Brass	Cu62	0,087	0.042	0.006	1
"	Cu66 Si	0,066	0.051	(0.030)	3
"	Cu80Si3	0,033	0.019	(0.014)	1
Bronse	Be2	0.037	-	(0.019)	1
"	AL9Mn2	0.030	-	(0.011)	0.4
"	AL10Fe3Mn1.5	0.038	0.026	0.010	0.3
Aluminium alloy	Mg6	0.036	0.020	0.020x	1.5
"	Mg6 Mn	0.026	0.016	0.007	0.4
Titanium alloy	Al5Sn3	0.0002	0.0000	0.0000	1

Notes: 1. K- corrosion rate ratio in the natural and laboratory conditions in 3,5% NaCl solution at room temperature in 3 months period
2. Figures in parentheses show the results after 14 months of tests
3. x- samples subjected to pitting corrosion

Table 2

Characteristics of pitting corrosion of alloys in the marine water

Name of alloy group	Main elements content, %	Maximum depth of pittings, mm	Pitting-factor	Rate of corrosion irregul.%
High-alloy steel	Cr13	5.0	185	30
"	Cr17Ni2	5.0	307	17
"	Cr18Ni10 Ti	0,28	9300	10
Bronse	Be2	0,2	10	20
Aluminium alloy	Mg6	0,25	42	30
"	Mg6 Mn	1,16	580	0,5

Table 3

Rate of corrosion (mm per year) of alloys after thermal treatment

Name of alloy group	Main elements content, %	Regime of thermal treatment	Rate of corrosion	K
Low-alloy steel	C 0.4 Cr	Hardening 350°/water, temper- 180°, exposure- 10 min.	0,065	1,7
High-alloy st.	Cr13	Hardening 1000°/water, temper- 600°, exposure- 10 min.	0,062x	0,5
"	Cr17Ni2	Hardening 1120°/water, temper- 300°, exposure- 15 min.	0,035x	0,4
Bronse	Al9Mn2	Annealing 700°, exposure- 30 m.	0,017	0,8
Brass	Cu62	Annealing 750°, exposure- 30 m.	0,031	0,2
Aluminium alloy	Mg6	Normalization 350°, exposure- 12 hr	0,007	3,0

Notes: 1. K- corrosion rate ratio in the original conditions and after thermal treatment
2. x- samples subjected to the pitting corrosion

Microfouling: The Role of Primary Film Forming Marine Bacteria

William A. Corpe

Department of Biological Sciences
Barnard College, Columbia University
New York, N. Y. 10027

When glass slides were submerged in the sea or sea water samples, bacteria became attached and after a week the count/ cm^2 was often larger than $2x10^6$ cells. Common marine chemoorganotrophs, mainly of the genus Pseudomonas were the first organisms to become attached but were replaced as the predominant type after 48-72 hrs, by species of Caulobacter, Hyphomicrobium and/or Saprospira. Diatoms and stalked protozoa became attached and grew only after bacterial films had become established.

Pseudomonas isolates attached and grew at a faster rate, from a small inoculum, in sea water enriched with 0.005%(w/v) yeast extract, than either Caulobacter or Saprospira species. The extent of growth and maintenance of attachment was related to the concentration of nutrients.

All of the periphytic bacteria produced an extracellular, alcohol insoluble material that gave a variety of tests for polyanionic carbohydrates. The polymers formed water insoluble precipitates with Alcian Blue and cationic detergents. They were completely adsorbed by anion exchange cellulose but were eluted with dilute solutions of NaOH into several fractions, each with a different charge density. The ability of polyanions to complex metal ions and aggregate particulate materials, causes them to be of special interest to marine fouling and corrosion.

Key Words: Microfouling; film forming; periphytes; polyanionic carbohydrates.

---

1. Introduction

The attachment of sessile animals and plants to solid surfaces submerged in the sea is commonly referred to as marine fouling and has long been recognized as a biological problem that causes major economic losses to the marine industry since all types of structural materials exposed to sea water will sooner or later become fouled (1).[1]

The identification and study of various organisms concerned with the fouling process (2,3) and the development of various techniques for retarding them have only been partially successful (4) and it seems clear that additional approaches to understanding the process are needed.

Fouling is an accumulative process in which a succession of species become attached and grow over an extended period of time. The development of "Aufwuchs" species is certainly enhanced in polluted areas (3) which suggests that the amount and kind of food available is one of the major factors related to fouling. Since organic and inorganic residues are acted upon and modified extensively by bacteria and other microorganisms, one must consider the relationship of these biologically important agents to the overall process.

ZoBell (5,6) has shown that initially clean surfaces submerged in the sea become populated by periphytic bacteria within a matter of a few hours. Such organisms were not dislodged by washing with sea water. The work of Marshall and associates (7,8) have shown that

[1]The numbers in parenthesis refer to the list of references at the end of this paper.

sorption of marine bacteria to solid surfaces has a reversible and irreversible phase and that irreversible attachment is coincident with the production of fibrilar materials on the bacterial surface which is believed to serve as a bridge between the cell surface and the solid substratum, overcoming the repulsion barrier that exists between the two.

In an earlier work, Corpe (9) described a group of periphytes that produced considerable quantities of extracellular polysaccharide slime which was considered to be at least in part responsible for attachment of the organisms; but was also shown to cause aggregation of other bacteria and particulate debris to the substratum.

The growth and polysaccharide producing properties of some of the periphytic bacteria involved in microfouling will be described in the present work and their possible importance as precursors of the heavy microfouling process discussed.

2. Materials and Methods

Submersion of glass slides in sea water

Sterile glass slides (50x75 mm) were attached to a 6 mm, steel, marine cable and submerged in the sea at various locations at a depth of 1-5 meters below the surface at low tide. Slides were also submerged in large aquaria or water samples while held in glass racks (Wheaton Glass Co., Millville, N. J.). The preparation and handling of slides have been described elsewhere (10). Slides were submerged in the sea from (a) the end of the pier at Scripps Institution of Oceanography (SIO) in LaJolla, Calif; (b) from a U.S. Navy Oceanographic tower one mile off the coast at San Diego, California; and (c) from a floating dock at Point Loma in San Diego Bay. Slides were also submerged in large sea water samples collected at Sandy Hook State Park on the New Jersey shore and at Daytona Beach, Florida, at a test site maintained by Battelle Institute, Columbus, Ohio. Slides were also submerged in a large regulated marine aquarium which has been previously described (10).

Estimation of the number of periphytic bacteria on glass slides

Slides were removed from sea water aseptically after various periods of time then rinsed 5 times with sterile sea water to remove the unattached organisms and swabbed with a sterile Dacron swab (Scientific Products Co., Raritan, N. J.). The swabbings were diluted and plated for determination of viable counts, using Bacto Marine agar (Difco Co., Detroit, Mich.) as the plating medium. The colony counts from duplicate plates were multiplied by dilutions and divided by the area swabbed in centimeters to determine the viable count per cm^2. Rinsed slides were also fixed and desalted with 2%(v/v) glacial acetic acid, in distilled water, for 5 min then rinsed with tap water and stained with Hucker's crystal violet for 1 min or 1%(w/v) aqueous Alcian Blue (8GN, Matheson, Coleman and Bell, East Rutherford, N. J.) for 20 min. Slides were rinsed with tap water and dried in air and examined with the oil immersion lens of a Leitz microscope. The bacterial cells in 20 microscopic fields were counted and the average number of cells per field determined and used to calculate the microscopic count per cm^2. Pairs of slides were usually examined in each determination.

Isolation and characterization of the main periphytic bacteria that form colonies on agar plates

The predominant types of bacteria forming colonies on marine agar were isolated for study. They were mainly gram negative, motile, non-sporeforming rods that grew as periphytes on slides submerged in artificial sea water (Instant Ocean Aquarium Systems, Inc., Wickliffe, Ohio) containing 0.005% Bacto yeast extract of Bacto peptone (Difco, Detroit, Michigan). They were identified as *Pseudomonas*, *Flavobacterium* and *Achromobacter* species which represented over 90% of the total isolates (10).

The organisms described in this paper represented the predominant types from slides submerged at various sites and are listed in Table 1. Plate counts were done on water samples taken at the sites where slides were submerged usually at the beginning and during the experiments; using Bacto Marine agar as the plating medium. Several bacteria isolated directly from sea water were included in certain phases of this study. A representative isolate studied in some detail is listed in Table 1.

Characterization of the bacterial isolates was done following procedures described by

Shewan, Hobbs and Hodgkiss (11) and Shewan (12). Morphology of broth and agar grown cells was examined with the phase microscope and Gram stained by the Hucker modification (13). Motility was determined in young agar and broth cultures and flagella were stained, after fixation with formaldehyde, by the Leifson method (14). Total cell counts were done using a Petroff-Hauser counting chamber by procedure described by Wilson and Knight (15).

Production of extracellular polysaccharides by marine bacteria

The marine isolates were grown aerobically in a medium containing Bacto peptone, 0.5%(w/v) and glucose, 1%(w/v) in artificial sea water diluted to provide 8 parts of sea water to 2 parts of distilled water. The organisms were grown at 25-28C in 500 ml flasks, containing 100 ml of medium and mounted on a shaker rotating at 70 rpm. After incubation for 4 days the cultures were chilled and then centrifuged in a model SS-3 Servall centrifuge with a GSA head (Ivan Serval Co., Norwalk, Conn.) at 9,000 rpm. The cells were washed three times with dilute sea water (8:2), frozen and lyophilized for determination of dry weight. The culture supernatant fluids were added with stirring, to 2 volumes of cold methanol or acetone. The precipitate that formed was allowed to settle in the cold room at 4C and then the clear supernatant fluid decanted and the precipitate recovered by centrifugation at 3,000 xG. The precipitates were desalted by dialysis at room temperature against 4 changes (20 liters) of 0.01N HCl and exhaustively dialysed against distilled water to remove chloride ion. The small amount of precipitate that persisted or that formed during dialysis was removed by centrifugation. The material did not contain carbohydrate and was discarded. The clear supernatant fluid was neutralized to pH 7 with 0.01N NaOH, lyophilized and weighed.

Saprospira grandis Gross (ATCC 23116) was grown in the medium of Lewin (16), and Caulobacter halobacteroides Poindexter (ATCC 15269) was grown in a medium described by Poindexter (17). Polysaccharides were recovered from culture supernatant fluids as described above.

Some analyses of the polysaccharides

The anthrone method described by Neish (18) was used as a general test for carbohydrates and as a quantitative method for neutral sugars by reference to a standard curve prepared with glucose. The uronic acid content of polysaccharides was estimated by the Dische carbazole method according to the procedure given by Kabat and Mayer (19). Glucuronic acid was used to prepare the standard curve. Samples of polysaccharide were hydrolyzed in sealed tubes with $1NH_2SO_4$ for 1,2,4 and 6 hours in a boiling water bath. After the tubes were cooled they were opened, the contents neutralized with 1NNaOH to pH 7 and the reducing values determined by the Park and Johnson procedure as described by Kabet and Mayer (19).

Samples of the polysaccharides were hydrated and suspended in distilled water and diluted to provide concentrations ranging from 1mg/ml to 25 ng/ml. One ml samples were mixed with 0.5 ml of 1%(w/v) Alcian Blue and after 10 min examined for the presence of a water insoluble precipitate. The precipitate was recovered by centrifugation and washed 3 times with distilled water and dissolved in 1N H_2SO_4 and the optical density read at 605 nm against a reagent blank. The dye content was determined by reference to a standard curve prepared with Alcian Blue in 1N H_2SO_4. The test has been found to be quite specific for acid polyanions (Kang and Corpe, unpublished data). The polysaccharides were also tested for the formation of water insoluble complexes with the cationic detergent hexadecyltrimethylammonium bromide (Eastman Kodak Co., Rochester, N. Y.) using the method of Scott (20).

The adsorption of polysaccharides on diethylaminoethyl (DEAE) cellulose in the $-OH$ form was done using the column procedure of Neukom and Kuendig (21). Columns were eluted with distilled water, 0.05, 0.1, 0.5 N NaOH in that order and successively collected 5 ml fractions analyzed for neutral carbohydrates and uronic acids as described above.

3. Results

Comparison of the total and viable counts of periphytic bacteria on glass slides submerged in the sea

The time-course attachment of bacteria to sterile glass slides submerged from the end of Scripps pier in LaJolla are shown in Figure 1. The microscopic count/ cm^2 increased to $2.2x10^6/cm^2$ after 6 days but the viable (plate) count increased to only $1x10^4/cm^2$ during the same period and then fell to $5x10^3/cm^2$ by the end of the 7th day, while the microscopic count

was still increasing. The viable count/ ml of sea water ranged between 50 and 200 during the experiment.

The data represent average counts from pairs of slides. Microscopic counts involved counting of single cells which were often in clumps and microcolonies, whereas the plate counts were estimates of "colony forming units" which could have represented either single cells or large cell masses. The error is enormous in both methods but there are several facts that emerge from this and similar experiments (10) when comparisons are made of the types of bacteria on stained slides with those that form colonies on agar. Bacteria that form colonies on agar are short, coccoid or slightly curved rods, a type which seems to predominate through the first 48 hr of submergence. These were replaced as the predominant type after 48-72 hrs by stalked and filamentous bacteria, which were never observed on Bacto marine agar plates (22).

Slides submerged at other locations gave similar results in which the total counts always greatly exceeded the viable count (10). The first organisms were short rods but were supplanted as the predominant type by stalked, budding or filamentous forms that have been identified as Caulobacter, Hyphomicrobium and Saprospira species which do not form colonies on Bacto marine agar when plated directly from natural environments (10). Other microorganisms such as diatoms, and attached protozoa appeared only after the bacterial films had become well established.

The development of bacterial films on slides submerged in San Diego Bay occurred very rapidly, presumably because of the relatively high concentration of organic nutrients in the water compared to that in waters facing the open sea. After 5 days, various kinds of particulate matter accumulated on the surface of the slides and by the 10th day a large stalked protozoan identified as a species of Zoothamnium were seen in abundance in a living state or heavily encrusted with particulate debris (23).

Identification of the principle periphytic genera isolated from glass slides

The periphytic bacteria isolated from agar plates were mainly gram negative rods. 50-90% of the total isolates were identified as Pseudomonas species (Table 1). They were motile, polarly flagellated rods with single polar flagella, oxidase positive and non-pigmented except in old colonies on agar which became off white or yellow-tan in color. 10-49% were a mixed group of yellow or orange pigmented organisms identified as Flavobacterium spp. or non-pigmented, non-motile rods identified as Achromobacter spp. Gram positive organisms were encountered only rarely and accounted for only 10-15% of the cultures isolated from slides (10).

The Pseudomonas species were studied in greatest detail. All of them oxidized glucose to acid but none grew anaerobically or produced fermentation reactions. None of the isolates grew in broth prepared with distilled water. T6c, Ma71b and 6b produced rather heavy viscosity when grown in PGYE sea water broth after 3 days on a shaker; the other cultures did not. T6c is representative of a number of strains of Pseudomonas atlantica which were described in a previous paper (9).

Growth of bacteria, from a small inoculum, on slides submerged in artificial sea water enriched with 0.005%(w/v)yeast extract

Each of the predominant isolates as well as pure cultures of C. halobacteroides and S. grandis were examined for their ability to attach and grow from small inoculum (3-6,000 cells) on the surfaces of glass slides submerged in 200 ml of artificial sea water enriched with 0.005% yeast extract. Data in Table 2 shows that the microscopic counts usually exceeded the viable counts at both 24 and 68 hrs, often by a very large factor. Some of the organisms grew and attached more rapidly than others. The Caulobacter and Saprospira species did not initiate growth or attachment at a rate, even close to that of the pseudomonads. Culture 103 a sea water isolate became attached to glass slides and grew as a periphyte.

The attachment of several of the bacteria was followed in a time course experiment with more frequent counts made. Such an experiment with culture Ma 8 is shown in figure 2. The microscopic and viable counts/ cm^2 increased until the 36th hour, then both decreased

steadily. The viable count of the organisms in the medium (unattached) followed the same course. Cultures T6c, Ma 13, 6b and 103 showed the same type of growth curves although the rate of attachment, growth and extent to which they became detached were somewhat different. When the nutrient level was increased to 0.1-0.5%(w/v), larger viable and total populations /cm^2 were observed, death and cell detachment was the final result.

The conditions used in this experiment of course are hardly equivalent to what one might occur in the sea, where mixing and aeration and constant supply of fresh nutrients are made available to the attached periphytes, nevertheless it attests to the ability of the organisms to attach and initiate rapid growth in a sea water containing low levels of a complex nutrient. When artificial sea water was supplemented with glucose or succinate and inoculated with the same sort of small inoculum (30-60 cells/ml) no growth or attachment occurred. When the size of the inoculum was increased to 10^5/ml, attachment by only a very small percentage of the cells occurred. Cells that were killed by heat or formaldehyde did not become firmly attached to glass slides irregardless of the medium.

Polysaccharides containing material isolated from cultures of marine periphytic bacteria

As was noted above, slides submerged in natural environments supported organisms that produced Alcian Blue stainable, acid polysaccharide slime which was believed to be concerned with attachment of periphytes to solid surfaces (9). The yield of extracellular, alcohol insoluble, non-dialyzable materials was variable, but the properties of each of the products indicated the presence of polyanionic carbohydrate.

Molar ratios of neutral sugars to uronic acids show wide differences among the various products. T6c and other strains of Ps.atlantica show a ratio of 1:1. 6b, Ma 8 and Ma 13 have a ratio of 2:1 and Ma71b contains 3 times as much uronic acid as neutral sugar. Culture 103, C. halobacteroides and S. grandis products contain much more neutral sugar than uronic acid.

Hydrolysis of the polysaccharides with 1N H_2SO_4 was fairly rapid, as shown in Table 3. Samples containing the greatest proportion of uronic acid (T6c, Ma71b) showed most rapid destruction of reducing sugar when the hydrolysis time was extended. Caulobacter and Saprospira products were more resistant.

All of the polymers gave some precipitate with the cationic detergent hexadecyltrimethylammonium bromide. The ratio of neutral sugar to uronic acid in the precipitate was similar to that of the starting material but that remaining in solution showed a greater proportion of neutral sugar.

The amount of Alcian Blue bound per milligram of polymer seems to be a consistant and reproducible property, but it could not be correlated with either the titratable acidity of the polyanions nor the total amount of uronic acid present.

All of the carbohydrate was adsorbed onto DEAE cellulose and was eluted with increasing molarity of NaOH as shown in Table 3. The fractions eluted with 0.01M NaOH contained a relatively small amount of uronic acid compared with fractions eluted with 0.05 and 0.1M NaOH. The fractions isolated with 0.5 M, presumably are those with the greatest charge density but inasmuch as the amount of uronic acid is considerably less than the amount in the earlier fractions, suggests that other acidic groups may be present, perhaps sulfate. A typical elution pattern is shown in figure 3.

Several of the polysaccharides isolated from periphytic cultures showed some ability to interact with salts of heavy metals either by forming an insoluble precipitate (Table 3) or by showing spectral shifts in the ultraviolet region which was usually accompanied by a slight shift in pH. The interaction of copper sulfate and 7mg/0/ml in 5 ml T6c polysaccharide in mg/ml concentration was particularly dramatic, with an instantaneous formation of a firm gel when the polymer and the salt were mixed. In other cases (Ma8 and C. halobacteroides) a heavy precipitate was formed, which settled to the bottom of the tube.

4. Discussion

The microfouling of glass slides and other solid surfaces submerged in sea water seems to follow a course that can be divided into roughly three phases. (a) Primary attachment by

common, marine, chemoorganotrophs which readily use organic nutrients adsorbed to the solid substratum but are followed by (b) attachment and growth of somewhat more nutritionally specialized, stalked and/or filamentous forms, which become the predominant periphytic flora. When bacterial films have been established (c) diatoms, other microalgae and sessile protozoa appear in large numbers.

Identity and growth of primary periphytes

While various Pseudomonas species were recognized as the principle periphytic bacteria that attach initially, Flavobacterium and Achromobacter species were also commonly encountered (10). Many marine bacteria isolated directly from sea water represented by culture 103 were able to exist as periphytes under experimental conditions which suggests that perhaps most of the common chemoorganotrophs in sea water exist as periphytes, depending on the specific environmental conditions and the nature of the solid substratum. These periphytes grew readily in sea water with low levels of nutrient (Table 2). The extent of their growth seems to be related to the nutrient concentration and probably more specifically to the amount of nutrient adsorbed to the solid substratum. After maximum growth, cell death occurred (Fig. 2) probably because of the exhaustion of nutrients and/or accumulation of wastes; thus initiating autolysis resulting in release of cells from the substratum. In natural environments where mixing, aeration and a more constant supply of fresh nutrients are made available and inhibitory growth products removed, cell death might not occur as rapidly. Results of the plate count which is a measure of the primary periphytes (Fig. 1) show that they do decline after 144 hrs although nutrient exhaustion is not necessarily the cause.

The number of viable cells was always a very small fraction of the total count/cm^2 which is not entirely due to experimental error. The growth and viability of cells in the microenvironment of a surface, is the information that is needed to explain the results, but this is not available.

Secondary periphytes

Bacteria which attach secondarily and become the predominant flora were identified as Caulobacter, Hyphomicrobium and Saprospira species. These organisms did not grow as rapidly as pseudomonads, from a small inoculum in the artificial environment (Table 2). While there is no experimental evidence to suggest the secondary species are dependent on some condition created by the primary periphytes, this possibility can not be ruled out. The stalked, budding and filamentous forms did not form colonies on Difco marine agar, which seemed curious since they are aerobic chemoorganotrophs.

Hirsch and Conti (24) have indicated that Hyphomicrobium does not grow well on common laboratory media and Lewin (25) has pointed out that Saprospira are predatory saprophytes, suggesting that they may require special nutrients provided by other organisms for direct isolation. Caulobacter spp. may be stimulated by secretions from other species (16). It is conceivable that the special growth requirements of these species are not met by the plating medium used.

Microalgae and protozoa

The appearance of numerous diatoms and other microalgae on surfaces of slides only after bacterial films have been developed may be because of the relatively slow growth rate of these periphytes, rather than some stimulatory effect provided by the bacterial film. The development of saprozoic or holozoic protozoa on the other hand may be quite dependent on the bacterial film to supply the amount and kind of nutrients which favor their growth. Periphytic bacteria have been shown to produce a wide variety of hydrolytic enzymes (26) which could catalyze the hydrolysis of bacterial cell material and other organic residues which have been adsorbed to bacterial films. Films of considerable complexity were observed on slides submerged in San Diego Bay (Table 1). Not only attached bacteria but particulate debris accumulated on the surface of slides as well as on the bodies of stalked protozoa which had attached to the surface. The degradation of organic materials by enzymes from the periphytes would be expected to make the surfaces a rich source of nutrients and hence sites of intense biological activity. Holozoic protozoa feed on bacterial cells (27) so their development would be expected to be extensive in the vicinity of bacterial films.

Secretion of polyanions by periphytic bacteria

Polyanions were believed partially responsible for attachment of the organisms to glass (9,22) and as described in the present paper a similar material was found in cultures of all marine periphytes examined, although in variable amount. Marshall and others (7,8) has shown that a marine periphyte identified as a Pseudomonas became irreversibly attached to solid surfaces, and electron micrographs of attached cells displayed fibrillar protrusions which were believed to enable the cells to overcome the repulsion barrier between their surfaces and substratum, causing irreversible attachment. While the composition of the material was not reported, it seems possible that it will be found to contain some carbohydrate polyanion.

The carbohydrate materials contained neutral sugars as well as uronic acid, in quite different ratios. In Ma71b there was a greater amount of uronic acid than neutral sugar. In the products from C. halobacteroides and S. grandis the reverse was true. The total uronic acid content was not related to the titratable acidity of the products nor to their ability to combine with Alcian Blue. The rate of hydrolysis of the products indicated they contain different glycosidic linkages. Rapid destruction of reducing values with extended heating times was reasonably well correlated with the uronic acid content, the latter being more readily destroyed by acid than other reducing sugars (28).

The fact that the various crude products could be separated into several carbohydrate containing fractions, each with a different charge density and a different ratio of neutral sugar to uronic acid suggests (a) several distinct polyanions are produced by the organisms (b) that the native product was partially degraded or depolymerized prior to harvesting or (c) the native polymer was partially hydrolized into large subunits during isolation. The latter seems unlikely since materials isolated by methods avoiding desalting with acid showed similar elution patterns.

The carbohydrate content of washed cells was 5-10%(w/w) and while neutral sugars were present in greatest amount, uronic acid was always present suggesting the presence of a cell bound residue of polyanion (10). Material of this sort may account for the electronegative charge of bacterial cells and envelopes (29). The organized holdfast structure of Caulobacter halobacteroides stains with Alcian Blue but so does the rest of the cell. Cell envelopes of several of the periphytic isolates have been shown to form water insoluble complexes with the dye (Corpe, unpublished observations) but whether polyanionic carbohydrates of the type described here are involved is not known.

While the syntheses of polyanions may facilitate adhesion of cells to solid surfaces, they may be equally important in the formation of aggregates of particulate material (30) and interact with and perhaps actively remove heavy metals from treated or coated surfaces. The concentration of toxic metals in bacterial films on detrital material and other solids which are grazed by invertabrate animals, could serve as a means by which undesirable levels of these metals could be introduced in the marine food chains.

Acknowledgments

The author thanks Rita Heller and Kar Tam for technical assistance and Mr. B. Merrill for providing laboratory facilities at Daytona Beach, Florida. This work was supported in part by a contract with the Office of Naval Research.

References

1. C. E. ZOBELL, J. Bacteriol. 46, 38 (1943).

2. G.PERSOONE, Helgol. wiss. Meeresunters. 12, 448 (1965).

3. G.PERSOONE and N. DEPAUW, Helgol. wiss. Meeresunters. 17, 302 (1968).

4. J. S. MURAOKA, Machine Design. 40, 184 (1968) January.

5. C. E. ZOBELL, Circ. 588, Sci. Sect. Natl. Paint, Varnish and Lacquer Assoc. San Francisco, Calif. (1939).

6. C. E. ZOBELL, J. Bacteriol. 46, 38 (1943).

7. K. C. MARSHALL, RUBY STOUT and RALPH MITCHELL, Can. J. Microbiol. 17, 1413 (1971).

8. K. C. MARSHALL, RUBY STOUT and RALPH MITCHELL, J. Gen. Microbiol. 68, 337 (1971).

9. W. A. CORPE, In "Developments in Industrial Microbiology" (C. J. GORUM, ed.) 11, Chapt. 39 AIBS, Washington, D. C. (1970).

10. W. A. Corpe, In Effect of the Ocean Environment on Microbial Activities. U.S.-Japan Conf. on Marine Microbiology. Aug. 25-30, University Park Press, Baltimore, Md. (1972).

11. J. M. SHEWAN, G. HOBBS and W. HODGKISS, J. Appl. Bacteriol. 23, 379 (1960).

12. J. M. SHEWAN, In Marine Microbiology, p. 499 (C. OPPENHEIMER, ed.), C. C. Thomas Publ. Springfield, Ill. (1963).

13. Society of American Bacteriologists. Manual of Microbiological Methods. McGraw-Hill Book Co., Inc., N. Y. (1957).

14. E. LEIFSON, R. M. COSENZA and R. C. CLEVERDON, J. Bacteriol. 87, 652 (1964).

15. P. W. WILSON and S. G. KNIGHT, Experiments in Bacterial Physiology, Burgess Publ. Co., Minneapolis, Minn. (1947).

16. R. A. LEWIN, Can. J. Microbiol. 8, 555 (1962).

17. J. S. POINDEXTER, Bacteriol. Rev. 28, 231 (1964).

18. A. C. NEISH, Analytical Methods for Bacterial Fermentations, Report 46-8-3, Nat. Res. Council of Canada, Saskatoon, Can. (1952).

19. E. KABAT and M. MAYER, Experimental Immunochemistry, (2nd ed.) C. C. Thomas Co., Springfield, Ill. (1961).

20. J. E. SCOTT, In Methods in Carbohydrate Chemistry, 5, 38 (R. S. WHISTLER, ed.), Academic Press, N. Y. (1965).

21. H. NEUKOM and W. KUENDIG, In Methods in Carbohydrate Chemistry, 5, 14 (R. S. WHISTLER, ed.), Academic Press, N. Y. (1965).

22. W. A. CORPE, In Adhesions in Biological Systems (R. MANLEY, ed.), Academic Press, N. Y. (1970).

23. W. A. CORPE, The attachment of microorganisms to glass slides submerged in San Diego Bay, with special reference to a colonial protozoan. ONR Technical Report No. 8/10/72 (1972).

24. P. HIRSCH and S. F. CONTI, Arch. Mikrobiol. 48, 339 (1964).

25. R. A. LEWIN, Can. J. Microbiol. 11, 77 (1965).

26. W. A. CORPE and H. WINTERS, Can. J. Microbiol. 18, 1483 (1972).

27. B. N. SINGH, J. Gen. Microbiol. 111, 361 (1947).

28. E. ANDERSON and L. SANDS, Adv. in Carbohydrate Chemistry 1, 329 (1945).

29. R. A. NEIHOF and W. H. ECHOLS, Biophysical studies of microbial cell walls. Part 2, Electrophoresis: Apparatus and exploratory experiments. NRL Report 6795 Nov. (1968).

Table 1

Periphytic Pseudomonas species isolated from sea water

Culture	Source	% of viable bacteria*
4b	Slides, submerged 2 days in the sea from SIO pier	80
T6c	Slides, submerged 2 days in the sea from the Navy Tower at San Diego	90
Ma71b	Slides, submerged 2 days in a 10 gal. carboy of sea water from Sandy Hook, N. J.	65
Ma 8	Slides, submerged 3 days in marine aquarium	86
Ma 13	Slides, submerged 1 day in marine aquarium	60
6b	Slides, submerged 2 days in two lite beaker of sea water, Daytona Beach, Florida	60
103	Sea water sample, collected from the south shore of Long Island, N. Y.	50

* Twenty-five percent of the colonies from Difco marine agar plates were isolated and characterized. The other bacteria that formed colonies were mainly Flavobacterium and Achromobacter species.

Table 2

Attachment of periphytic bacteria to slides submerged in artificial sea water containing 0.005% yeast extract

Culture	Bacterial count/cm^2			
	25 hrs		68 hrs	
	Microscopic x10^5	Viable x10^4	Microscopic x10^5	Viable x10^4
T6c	0.09	0	6.10	0
6b	5.40	3.56	1.10	2.52
Ma71b	0.16	0.02	19.73	0.91
Ma 8	3.66	0.53	6.48	4.34
Ma 13	0.15	1.4	0.21	0.42
103	1.76	13.10	2.70	1.68
C. halobacteroides	0.09	nd *	0.19	nd
S. grandis	0.09	nd	0.14	nd

* nd = not determined.

Table 3

Some properties of crude, carbohydrate polyanions from periphytic bacteria*

	Toc	Ma71b	Ma8	Ma13	5b	103	Caulo	Sapro.
1. Yield, mg/ml culture	1.30	0.13	0.21	0.11	0.13	0.13	0.21	0.34
2. Mequiv./100 mg	0.16	0.35	0.41	0.06	0.24	0.10	0.12	0.23
3. Time, hydrolysis (hrs)	1.0	0.5	2.0	1.0	1.0	2.5	2.0	2.5
4. Reducing sugar mg/mg	0.89	0.80	0.62	0.87	0.97	0.68	0.77	0.69
5. Alcian Blue complexed, mg/mg	2.1	1.1	1.1	1.3	1.5	2.8	2.0	1.9
6. Molar ratio Hexose:uronic acid								
a. crude product	1:1	1:3	3:1	2:1	2:1	5:1	6:1	10:1
b. CTAB precipitation	1:1	1:3	2:1	2:1	2:1	4:1	2:1	6:1
7. Precipitation with $CuSO_4$	+	nd	+	nd	nd	+	+	nd

* Caulo, Caulobacter halobacteroides; Sapro, Saprospira grandis; CTAB, cationic detergent hexadecyltrimethylammonium bromide. nd, not determined.

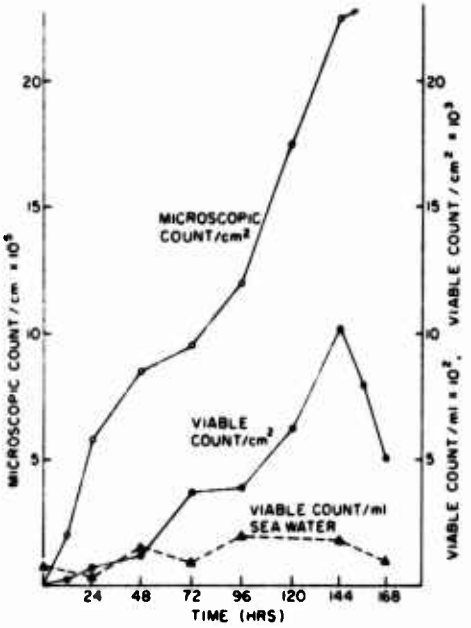


Figure 1. Time-course attachment of bacteria to sterile glass slides, submerged in the sea at SIO.

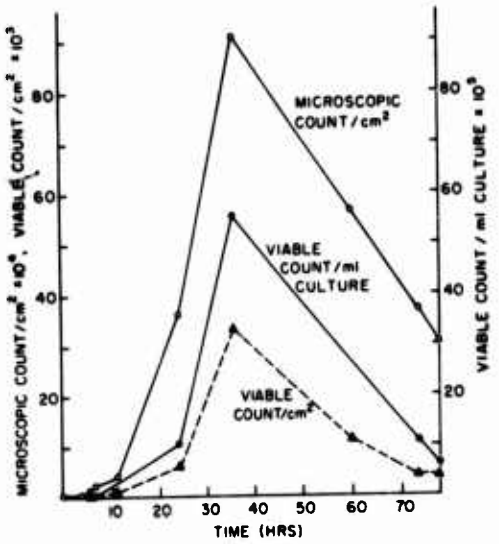


Figure 2. Growth and attachment of Ma8 to glass slides submerged in artificial sea water containing 0.005%(w/v) yeast extract.

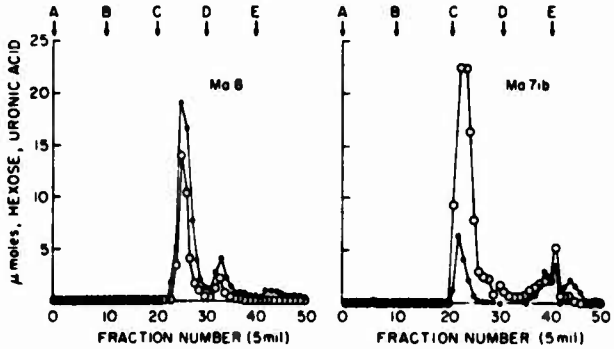


Figure 3. Elution of polyanions from DEAE cellulose columns (2x9 cm) with 50 ml volumes of A. Distilled water, B. 0.01N NaOH, C. 0.05N NaOH, D. 0.1N NaOH and E. 0.5N NaOH. Five ml fractions were analyzed for Anthrone carbohydrate (Hexose) and Carbazole Uronic acid.

Discussion

Question: We have obse ed that old bacteria produce both extracellular capsular material and polymers by leakage of intracellular material, but we have not determined which one was more important in the attachment of the bacteria to the surface. Do you have any thoughts on that?

Corpe: I think that the polymers probably are complexed with other materials at the cell surface, particularly with proteins. This raises the question as to the nature of the specific material that is concerned with the adhesion process. I would not necessarily assign this to these acid polymers, but I think that they must be involved in some way, if not in primary attachment, then maybe in the adhesion of other materials to the surfaces.

Question: I think that the notable discrepancy between the viable and total counts is a major and horrible problem of marine bacteriology. Did you try variable culture media in obtaining your viable counts? Can you reduce this enormous discrepancy?

Corpe: We did try some other media, but we did not spend too much time on this because the success of other people has not been very encouraging. In our counts we probably estimated numbers of pseudomonads and other common organotrophes, whereas the caulobacters, saprospiras and hyphomicrobia do not grow on the medium employed. Use of selective media gave an estimate of some of these fastidious forms, but the numbers observed still did not approach those obtained by total count procedures.

Question: Did you test for any sulfate in the neutral polysaccharides? Are they sulfated or not?

Corpe: Yes, sulfate is present. Those fractions eluted from columns with 0.5N NaOH that were found to contain sulfate did not have much uronic acid.

Role of Surface Chemical Composition on the Microbial Contribution to Primary Films

Gary E. Sechler
and K. Gundersen
Department of Microbiology
University of Hawaii
Honolulu, Hawaii 96822

Primary films forming on a variety of commercially important materials were assayed for bacteria, diatoms and extraneous particulate matter for extended periods. Total counts per unit area from opaque materials were made using a new plastic layering technique which allowed for quantitative removal of the entire primary film in situ. This provided a natural microscopic view of all biotic and abiotic constituents in the microcosm.

Total microscopic counts showed bacterial and diatom growth occurring in nonrandomly distributed microcolonies over the surfaces; surfaces included stainless steel, aluminum, phosphor-bronze, glass, Monel and "plexiglass". Although significant bacterial growth appeared after 1 day of immersion, diatoms showed little tendency toward active growth until approximately 5 days. Similar delays in diatom growth were seen using an assay method based on placing porous Teflon membranes over various test surfaces.

Viable bacterial counts on aluminum, wood, zinc, "plexiglass" and steel showed significant differences at respective time intervals during the first 15 days of immersion. Populations from metals generally proportioned galvanic activity, and metals also attracted a more heterogeneous population. Conversely, the non-metals appeared to attract a more stable bacterial microcommunity from the onset of immersion. Almost all varieties were subsequently lost within the first day of immersion, while a select few "took over" the microcosm with prolific growth. Of the 52 tentative species isolated from all materials tested, 70-75% appeared as transients. No isolate was found to persist during 42 days of continuous immersion and there was no evidence of surface selection by any isolate. All isolates were found to be common heterotrophs.

The results suggest that bacteria may sorb to metals at rates proportionating that which nutrients sorb, a condition predicated by relative galvanic activity. Sorption and colonization of non-metals in this study depended strongly upon surface electrical nature, polarity and toxicity. All immersed materials attracted a similar bacterial microflora, although the pattern of occurrence varied, according to surface chemical nature.

Key Words: Bacteria; diatoms; sorption; surfaces; primary films; metals; non-metals; galvanic activity.

1. Introduction

Transparent materials have classically served as typical surfaces for in situ microscopic studies to determine microbial growth rates, sorption phenomena and qualitative analyses of primary films (1,2,3). Although chemical differences may be quite extreme, opaque

[1] Figures in parentheses indicate the literature references at the end of this paper.

materials appear to have been generally passed by at the comparative microbial level during primary film formation. The scanning electron microscope (SEM) used successfully in laboratory studies may find only limited application in studying surface film microbiota from field experiments; lack of mobility and time factors in processing would necessarily limit routine use.

The goal of the current investigation was to devise a simple method which could be used routinely for large-scale comparative studies on primary films regardless of test surface opacity. With supporting cultural evidence from the same materials, considerable insight could be gained on the qualitative and quantitative aspects of surface microbiological development.

The comparative responses of a large number of common structural materials to biofouling in the sea have been given considerable attention (4,5,6). It is noteworthy that primary films, established as at least a prime determinant in generalized microfouling (7), have not been attacked as vigorously as have the eventual products of unchecked biofouling.

2. Materials and Methods

This investigation was designed to search out basic data on materials' influence on primary film formation in the sea. The test site selected was Kaneohe Bay, Oahu, Hawaii, a reasonably stable marine estuary. Another worker (8) previously found physical and chemical environmental factors in the bay essentially nil during the summer months, the time period selected for these studies. The only significant variable was therefore the test surfaces themselves, which were always immersed concomitantly during a field series.

75 × 25 mm test surfaces of glass, plexiglass, stainless steel 304, aluminum 5052, Monel and phosphor-bronze (A) were thoroughly cleaned, sterilized and immersed in replicate in glass racks at a 3m depth. At 21 intervals ranging from 1 to 120 days, replicate panels were taken from the sea, rinsed, dried and processed to remove the entire surface epilithic layer intact. This was done by immersing test panels into a 10% solution of Parlodion (nitrocellulose), draining, drying in air, excising a portion of the film and stripping it away from the surface (9). The film was then stained in crystal violet and permanently mounted for microscopy. All possible biotic constituents were then noted and counts per unit area were made on all bacteria, diatoms and extraneous particles.

Prior to conducting the Parlodion filming experiments Teflon membranes with 5 μm pores were fixed tightly over a variety of metal and non-metal surfaces. Experiments had previously shown that metal ions freely diffused through the membrane pores, and that the test surfaces could presumably select for microorganisms. To assay, the test surfaces were withdrawn from the water at 1 and 4 days, rinsed, excised, stained and mounted. The membranes were then examined to quantitate and study morphologically the organisms sorbing to Teflon.

Viable bacterial counts and identifications were also made in a supporting study from panels of aluminum, galvanized steel, mild steel, "plexiglass" and wood. These surfaces were marked off in smaller areas of standard size, sterilized and immersed at the test site. Assay was done by a swabbing—millipore filtration—culturation method over periods ranging from 1 hour to 42 days.

3. Results

The Parlodion filming technique quantitatively removed all biotic material from test surfaces, even including very young barnacles. All biological components were easily discernable, including bacteria, diatoms, yeasts, filamentous algae, fungi, protozoa and small invertebrates.

Total bacterial surface populations increased at a generally logarithmic rate until approximately 4-5 days (Figure 1). This was followed by a fairly stable population plateau, which persisted until termination of sampling at 120 days. Note that this general response

[2] Figures in parentheses indicate the literature references at the end of this paper.

does not exclude phosphor-bronze, which is generally toxic to most microorganisms. In addition, surface bacterial populations did not distribute evenly, but rather as steadily-growing microcolonies in large patches. This pattern of surface bacterial growth has been studied *in situ* on glass slides by other workers (1) .

Considerable variability in average numbers of organisms per microcolony from each surface was common at most all sampling intervals. Figure 2 denotes a roughly harmonic growth pattern, including periodic increases and decreases approximately every 10-20 days. Since Figure 1 showed a population plateau on essentially all materials from 10 days, the growth dynamics seen here indicate that much of the population would necessarily be dying concomitantly with the active proliferation. Note that the most galvanically-active metal here, aluminum, has generated extremely large colonies by day 5.

Diatom populations (Figure 3) reached maxima at approximately 7-9 days and were about 10^{-1} per cm^2 less than the maximum bacterial densities attained. Growth also occurred at a generally slower rate than the bacteria. After 16 days all materials responded homogeneously in regard to total cell densities.

Figure 4 shows that the diatom proliferation is also generally harmonic except that the periods are apparently shorter as compared to the bacteria. Morphological examination at almost every sampling interval revealed a new diatom succession. Since active growth extended over the entire sampling period while total populations remained essentially stable, the diatom microcommunity must be considered in a dynamic flux developmentally.

Counts on particulate organic matter consistently showed the greatest homogeneity from surface to surface. Highest particle densities were 10^{-1} per cm^2 less than the diatom populations.

Results on total counts using the Parlodion filming technique suggest that there may be a relationship between diatom population death and subsequent bacterial proliferation and vice versa. In this regard, a considerable number of diatoms were seen on Teflon in various stages of decomposition with closely-associated bacterial microcolonies.

Studies on viable bacterial populations showed a somewhat different response in regard to population development. In Figure 5 populations developed at rates characteristic of each test material. On the average, the viable cell density maximum was about 10^{-1} per cm^2 lower than total counts on Parlodion mounts. Note that before 20 days population maxima on the metals are directly proportional to relative position in the galvanic series.

Plexiglass showed an intermediate population response through the 42-day immersion period. Highest rate of cellular increase to equally significantly high populations, however, was on wood panels. Subsequent tests later showed that none of the resident species of bacteria isolated from wood were obligately cellulolytic but rather common heterotrophs. All 52 isolates representing all five surfaces were found to be heterotrophic. None persisted through the entire 42 day immersion period and less than 30% were considered stable, adjusted members while the balance were likely transients. There was, in addition, no surface selection or specific sensitivity to any of the five test materials.

A surprisingly similar response by all surfaces was found by plotting numbers of isolates present on each surface versus immersion time (Figure 6). In general, maximum numbers of species on any surface were found during the first day of immersion. By the second day, less than half the original number of isolates was present; this number generally stablilized until about 30 days, followed by only a slight decrease. Note that zinc, aluminum and steel again appear in perfect galvanic order according to maximum numbers of isolates recovered.

Reconsidering the viable bacterial growth curve (Figure 5), it is obvious that the maximum numbers of bacterial species correlate with the lowest population levels. Conversely, the highest populations were reached when the number of varieties dropped steeply, suggesting a rapid "take over" by the most competitive species. The nonmetals, wood and plexiglass,

[3] Figures in parentheses indicate the literature references at the end of this paper.

sorbed much fewer varieties than did the metals, yet retained approximately comparable numbers of species.

4. Summary

In summary, surface chemical composition appears to influence the microbial contribution to primary films markedly during the first 2-3 days with regard to total populations and numbers of potential genera sorbing. Since bacteria in the sea generally carry a net negative surface charge, the most important effect from materials immersed in the sea must necessarily be surface electrical nature. Zinc, aluminum and steel should therefore repel bacteria electrostatically during the first few minutes or hours of immersion. Evidence suggests that these metals may sorb organic matter at rates proportional to their relative electronegativity. This abundance of concentrated nutrient must subsequently attract a markedly heterogeneous bacterial population. Highly competitive species soon dominate the microcosm, proliferating at maximum rates until depletion of space or nutrient limits population expansion further.

Organic matter may actively sorb to many nonmetal surfaces, such as glass, and passively to uncharged polymers such as "plexiglass". Because of its high polarity and hence great wettability, wood would be conducive to direct attachment by microorganisms.

When bacterial populations reach the "stable" state, the data has shown that there is a consistentlydynamic flux of cellular material building and decomposing concomitantly. Considerable metabolic residue and slime material would then accumulate and enmesh all the sorbed organisms. Cytolyic products from organisms and organic matter from the environment would also fortify the slime nutritionally.

Sorbed, but non-developing diatoms would now have the opportunity to proliferate freely in the enriched, abundant substrate, and other diatoms contacting the surface would likely find conditions favorable. After diatom generation and subsequent cell turnover, the biomass would increase markedly, attracting both sessile and grazing invertebrates. Passively enmeshing algae spores and invertebrate larvae would likely find the developing microcosm secure and bountiful. And with the maturation of these forms, terminal biofouling is a vivid reality.

References

1. T. L. BOTT and T. D. BROCK. Limnol. Oceanog. 15, 333 (1970).
2. K. C. MARSHALL, R. STOUT and R. MITCHELL. J. Gen. Microbiol. 68, 337 (1971)
3. C. E. ZOBELL. Marine Microbiology. Chronica Botanica Co. (1946).
4. A. A. ALEEM. Hydrobiologia 11, 40 (1957).
5. B. T. SCHEER. Biol. Bull. 103 (1945).
6. WOODS HOLE OCEANOGRAPHIC INSTITUTION, Contrib. No. 580, U.S. Naval Inst., George Banta Pub. Co. (1952).
7. W. A. CORPE. Developments in Industrial Microbiology (Vol. 11), American Institute of Biological Sciences (1970).
8. K. H. BATHEN. Hawaii Institute of Marine Biology, Tech. Rep. No. 14 (1968).
9. G. E. SECHLER and K. GUNDERSEN. Appl. Microbiol. 21, 140 (1971).

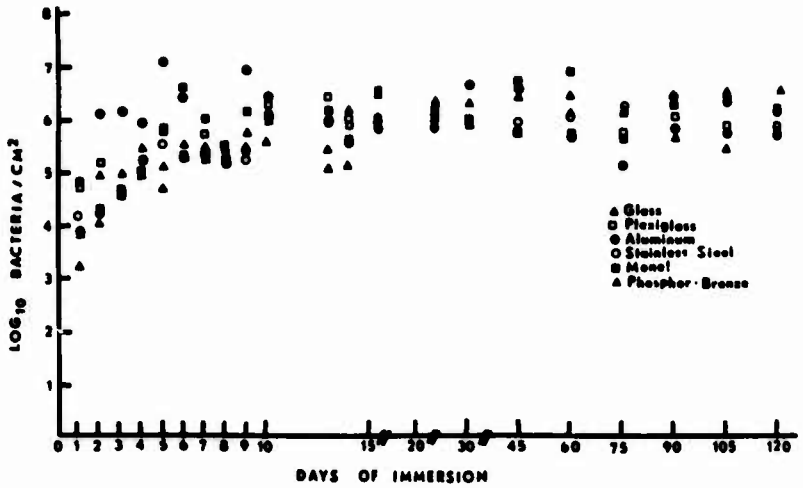


Fig. 1 Total surface bacterial populations on various materials during 120 days of immersion.

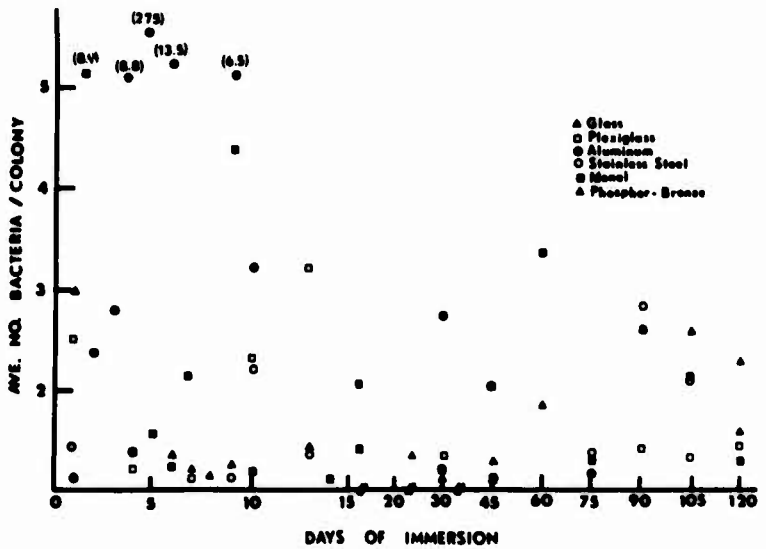


Fig. 2 Bacterial developmental pattern on various materials.

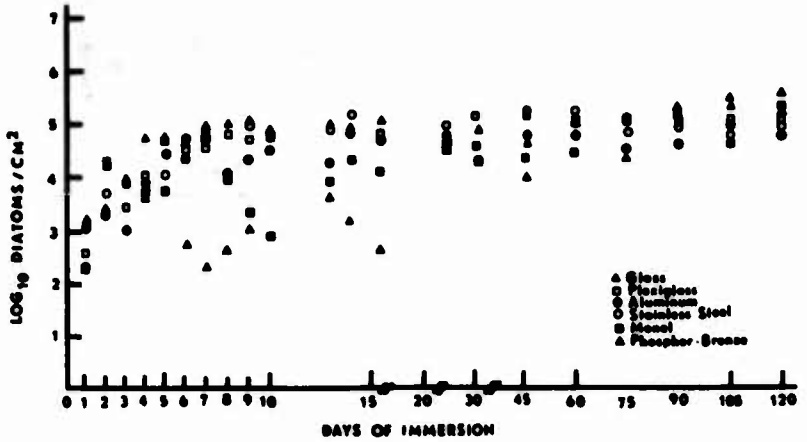


Fig. 3 Total surface diatom populations on test panels during 120 days of immersion.

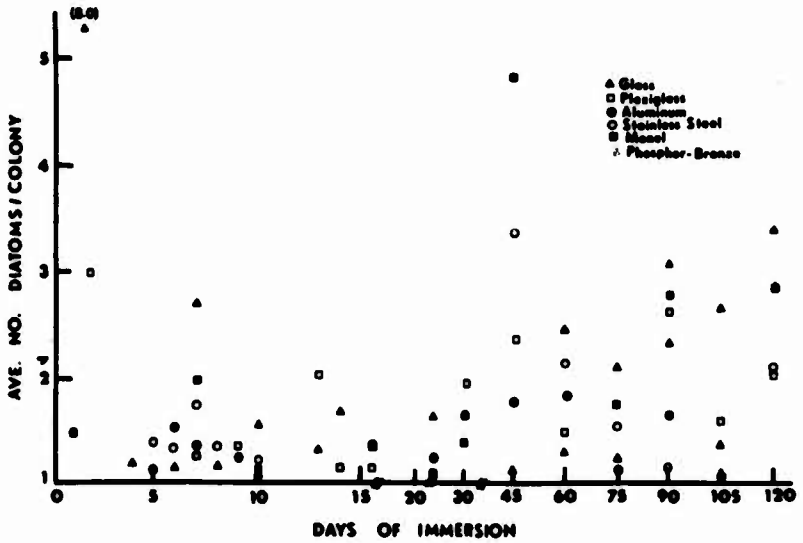


Fig. 4. Diatom developmental pattern on immersed test surfaces

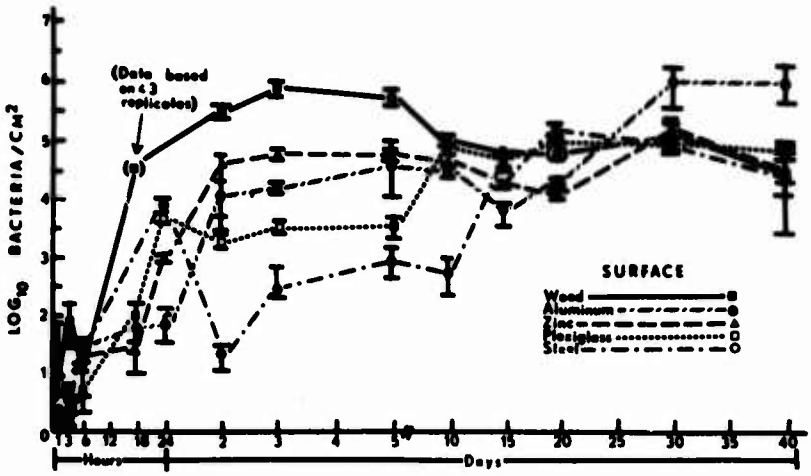


Fig. 5 Developmental pattern of viable surface bacterial populations.

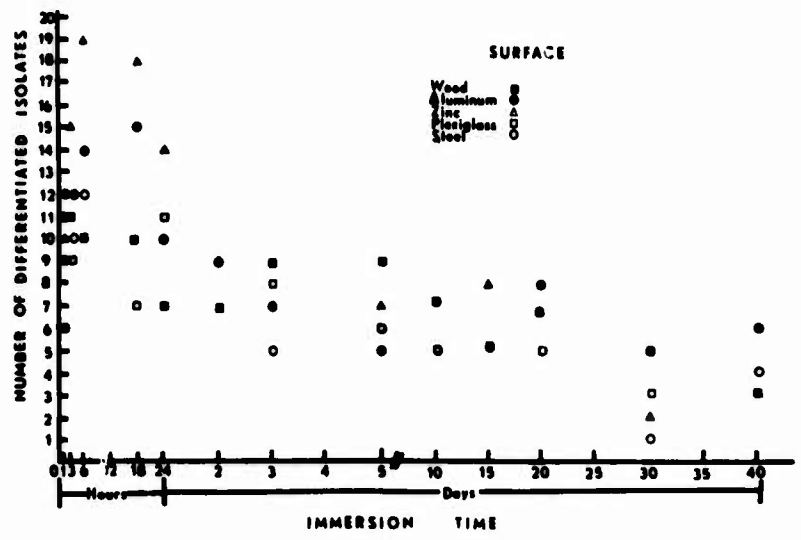


Fig. 6 Number of bacterial isolates present at various sampling intervals

The Role of Chemotactic Responses in Primary Microbial Film Formation

L.V. Young and Ralph Mitchell

Harvard University
Cambridge, Mass. 02138

Isolated strains of motile marine bacteria have been observed to exhibit positive chemotaxis toward favorable compounds and negative chemotaxis away from unfavorable compounds. Using a microcapillary method, positive chemotactic compounds enhanced the rate of attachment and the total number of bacteria which irreversibly affixed to artificial surfaces. Compounds which elicited a neutral response did not enhance attachment. Toxic organic and inorganic compounds, such as chloroform and $CuSO_4$ caused negative chemotaxis. The bacterial cells actively stayed away from regions of toxic concentrations. The negative chemotactic response was not uniform. All bacterial isolates tested were repelled by toxic compounds. However, the concentration required was different for each bacterium. The incorporation of a favorable compound toward which the bacterium normally moves did not alter the negative chemotaxis. The numbers observed were not a result of simple mortality since at non-lethal concentrations negative chemotaxis was still exhibited. These observations suggest that positive chemotaxis plays a role in the attachment of the primary bacterial film to surfaces and negative chemotaxis functions in the prevention of bacterial film formation.

Key Words: Chemotaxis; attachment; microbial fouling; primary film.

---

1. Introduction

The development of microbial populations on surfaces is a widespread phenomenon found in natural waters. In lakes, streams and oceans, microbial populations can be found in association with both animate and inanimate surfaces. The heavy slime layer produced by microorganisms contribute to such problems as increased frictional resistance, anaerobic conditions and corrosion in freshwater and seawater transport systems. The functioning of instrumentation can be impaired as well. In seawater, the microbial population on surfaces creates an additional problem by producing the primary film which is generally thought to be a prerequisite for the attachment and metamorphosis of fouling animals.

The early studies on the attachment of marine bacteria to surfaces has been undertaken extensively by Zobell (1,2). He clearly demonstrated that surfaces in seawater are a region of bacterial concentration. More recently, Corpe (3) showed that a marine pseudomonad with a propensity to attach to surfaces, does so by production of copious amounts of extracellular polysaccharide. The mechanism by which bacteria initially attach to surfaces has been elucidated by Marshall, et al. (4). Investigations by both Zobell (2) and Marshall, et al. (4) suggest that in a low nutrient environment a surface provides an area of nutrient concentration. Since bacteria concentrate in these regions, the implication, therefore, is that the organisms can detect these nutrients.

The study of bacterial chemotaxis, the detection of chemicals by bacteria, has been under investigation recently by Adler (5,6). His work provides us with a methodology by which we can investigate whether chemical attraction or repulsion can influence the attachment of bacteria to surfaces.

Materials and Methods

Organisms: Four marine pseudomonads were used in this investigation. G4 and P2 isolated from a glass surface in seawater; R3 obtained from Dr. K.C. Marshall, University of Tasmania; and MAV obtained from Dr. S. Fogel, Process Research, Cambridge, Massachusetts. All four bacterial strains were heterotrophic, facultatively anaerobic, obligately marine, short rods with a polar flagellum. They differed in their colony morphology, pigmentation, and chemotactic patterns.

Assay for Chemotaxis: Cultures were grown in seawater nutrient broth for 10 to 12 hours and harvested by centrifugation. After washing in artificial seawater, the cells were centrifuged and resuspended in artificial seawater to a concentration of $\sim 10^6$/ml. The method for the chemotaxis assays was modified from Adler (6). The compound to be tested was held in a 5 µl microcapillary sealed at one end. The open end was inserted into an active suspension of bacteria in a chamber consisting of a capillary u-tube on a glass slide and supporting a coverslip. After 10 - 15 min. the contents of the capillary were assayed by serial dilution in artificial seawater and plate counts on seawater nutrient agar.

Chemicals: All the compounds used in the positive chemotaxis assays were diluted in artificial seawater. For the negative chemotaxis assays, the compounds were suspended in artificial seawater nutrient broth.

2. Results

The four marine isolates used for the attachment experiments were subjected to a chemotactic assay toward a series of simple carbohydrates. Under the influence of a positive stimulus such as seawater nutrient broth, bacteria in the bulk solution concentrate in and around the capillary mouth (Fig. 1). As indicated in Table 1, each isolate displays a unique chemotactic pattern toward the compounds. Seawater nutrient broth provided a positive control since all four isolates were strongly attracted to it. An artificial seawater control was used to indicate the number of bacteria which entered the capillary by random activity only. By using this data we could then consider the question whether attractive surfaces possess enhanced attachment of bacteria.

Compounds which elicited opposite chemotactic patterns from 2 different organisms were selected for comparative attachment tests. Equivalent concentrations of the test compounds (10^{-2} to 10^{-3} M) were fixed to glass slides which were then submerged into a suspension of chemotactically active bacteria. At timed intervals the slides were removed, rinsed and the irreversibly attached bacteria were counted. Illustrative of the results obtained are seen in Figs. 2 and 3. Approximately twice as many organisms designated R3 (Fig. 2) attached to surfaces treated with lactose than to those treated with maltose. On the other hand, as seen in Fig. 3, the isolate MAV was found to attach in numbers 3-fold higher on maltose treated surfaces than on lactose treated ones. Referring back to Table 1, it is observed that their attachment preference correlates with their chemotactic response.

In the same manner, the other compounds which elicited a positive chemotactic response also produced an enhanced bacterial attachment on treated surfaces. In all cases, bacterial attachment to untreated surfaces and those treated with compounds producing a neutral chemotactic response provided the control.

We have also observed that bacteria display a negative chemotactic behavior toward toxic organic and inorganic compounds. When a toxic compound is combined with the nutrient borth, bacteria remain outside the capillary and avoid the area immediately adjacent to the capillary mouth (Fig. 4). Often a distinct region free of bacteria is observed. The size of the bacteria-free region varied with the organism and the concentration of toxicant used. Of particular importance is the fact that this negative chemotaxis effect could be observed at non-lethal concentrations.

The effect of chloroform on the isolate, G4, is illustrated graphically in Fig. 5. The lower curve indicates the number of bacteria entering the capillary as a function of toxicant concentration. When there was no toxicant present and only artificial seawater nutrient broth was placed in the capillary, 10^5 bacterial cells ingressed. As the concentration of the toxicant increased, the bacterial numbers sharply decreased by nearly 2 orders of magnitude. The top curve illustrates the viability of the organisms over the concentration range tested. The highest concentrations used were lethal as indicated by the drop in the curve. However, over the concentration range in which negative chemotaxis was found to occur, viability was not affected. Under these non-lethal conditions, approximately 97% of the bacterial cells which otherwise would enter the capillary were prevented from doing so.

Figure 6 illustrates a corresponding set of data for a different bacterial isolate, MAV, and a different toxicant, ethanol. Again the top curve indicates that there was no lethal effect over the concentration range in which negative chemotaxis was observed. In this case the threshold concentration which triggered the negative taxis response is clearly indicated on the bottom curve. The inclusion of 10^{-1} M ethanol along with the nutrient broth in the capillary again inhibited a significant fraction of bacteria, which normally would enter the capillary, from doing so.

A total of 4 hydrocarbon compounds, chloroform, ethanol, benzene, and toluene, and 2 heavy metal compounds, lead and copper, were used as toxicants. The results of their effect on bacterial chemotaxis are summarized in Table 2. The last column of the Table under sub-lethal conditions shows that more than 90% of the cells were inhibited from entering the capillary. In all but one case more than 70% of the bacteria which otherwise would enter the favorable zone in the capillary were prevented from doing so. In terms of the overall effectiveness of the toxic chemicals, no consistent pattern appears to emerge. Of the bacteria tested, G4, MAV, and P2, in general, displayed similar responses to the toxic chemicals (Table 2). However, R3 was repelled to a lesser degree than the other bacteria. Only 70 - 80% were inhibited from entering the capillary by any of the chemicals tested although the concentrations were similar. These data suggest that R3 was more sensitive than the other isolates to sub-lethal effects of the toxicants on bacterial motility.

3. Discussion

Motile bacteria appear to have the ability to detect and respond to both favorable and unfavorable compounds. Their attachment to surfaces can be significantly enhanced by the presence of an attractive material. This suggests that a two step biological process may be involved in bacterial attachment to surfaces: an initial attraction to a favorable vicinity, the surface: then a physiological adaptation by the organism to adhere itself to the surface as described by Corpe (3), Marshall, et al. (4), and Hirsch and Pankratz (7).

The negative chemotactic ability of motile bacterial cells enables them to move away from zones of toxicity. This ability provides a survival mechanism not only at lethal concentrations but at non-lethal concentrations as well. The organism can therefore selectively avoid potentially toxic areas. The incorporation of a food source along with the toxicant in the capillary did not alter the negative response. It therefore appears that negative taxis takes precedence over the positive response. This negative chemotactic ability appears to provide a survival mechanism for bacteria since a) non-lethal concentrations of toxicants are detectable, and b) incorporation of a food source did not alter the response. The evidence, therefore, suggests that toxicity is not the only mechanism operative in the prevention of microbial fouling. Heavy metal paints currently used for control may also be functioning by inhibiting the organism's approach to the surface.

This work was supported in part by Contract # N00014-67-A-0298-0026 between Harvard University and the U.S. Office of Naval Research.

Table 1

Chemotactic Patterns of Some Marine Bacteria

Compound	Bacteria			
	R3	MAV	MI-1	G4
NB	+++	+++	+++	+++
ASW	-	-	-	-
Maltose	-	++	-	++
Lactose	+	-	+	-
Fructose	-	-	+	±
Galactose	++	-	+	-
Glucose	++	+++	+	+
Glucosamine	-			

Table 2

Negative Chemotaxis of Four Marine Isolates Toward Low Molecular Weight Hydrocarbons and Heavy Metal Compounds

Bacteria	Compound	Compound Absent	Compound Present	Effective Non-Lethal Concentration	Degree of Neg. Taxis
R3	chloroform	12,500*	3,550	0.1 %	72 %
	toluene	5,000	1,000	0.1	80
	ethanol	2,500	500	0.2	80
	$CuSO_4$	5,600	180	0.05	70
G4	chloroform	89,000	2,240	0.3	97.5
	toluene	18,000	800	0.1	95.6
	ethanol	80,000	20,000	3.0	75
	benzene	24,000	3,160	0.2	87
	$Pb(NO_3)_2$	17,800	7,940	0.001	56
P2	chloroform	4,000	200	0.5	95
	toluene	35,500	1,100	0.1	95
	ethanol	8,000	320	2.0	96
	benzene	7,940	630	0.2	92
	$Pb(NO_3)_2$	1,780	225	0.001	87
MAV	chloroform	10,000	1,120	0.3	89
	toluene	32,000	2,000	0.5	93.7
	ethanol	80,000	4,200	3.0	95
	benzene	11,200	3,150	0.05	91
	$Pb(NO_3)_2$	17,800	720	0.001	96

*Number of bacteria/5 λ capillary.

4. Literature Cited

1. C.E. Zobell, Biol. Bulletin, 77, 302, (1939).
2. C.E. Zobell, J. Bact., 46, 39, (1943).
3. W.A. Corpe, Develop. Ind. Microbiol., 11, 402, (1970).
4. K.C. Marshall, R. Stout, R. Mitchell, J. Gen. Microbiol., 68, 337, (1971).
5. J. Adler, Science, 153, 708, (1966).
6. J. Adler, Science, 166, 1599, (1969).
7. P. Hirsch and S. H. Pankratz, Z. Allg. Mikrobiol., 10, 589, (1970).

Discussion

Question: It seems quite incredible that an organism as small as a bacterium could detect a concentration gradient. I wonder whether, in fact, they are responding to the presence of the substance by some automation in their movement, as I noticed the bacteria moving up the tube in your experiments seemed to accumulate in the region where there was a change of concentration. I wonder if you have anything to remark about the mechanism by which they achieve this chemotaxis?

Young: Essentially what happens is that the detection of the attractant triggers a reaction in the bacterium causing it to change its direction. This results in a random motion rather than a direct movement from point A to point B along the concentration gradient. Ultimately, the bacteria accumulate in a region of high concentration of attractant because the movements of the bacteria become increasingly less random.

Question: I should like to ask what initial concentrations you had inside your capillary tubes, because if you had a strong enough solution in the tube you might find a negative tactic response with anything?

Young: Yes. If the concentrations are too high it is possible to show a negative response. The observed negative chemotaxis was obtained with initial concentrations in the capillary tube that were much lower than those that would inhibit growth of the organism.

Comment: I object to your proposal of attempting to control fouling by applying sub-lethal concentrations of toxic materials to surfaces to induce a negative chemotaxis. You are assuming that all bacteria approaching a surface are motile. Many bacteria adhering to surfaces even after one hour are not motile, particularly some achromobacters and flexibacters.

Young: Yes, that's true. The chemotactic response, of course, is dependent on the motility of the bacteria. Non-motile bacteria would not give this chemotactic response.

Question: You suggested that once the bacteria become attached, the attachment became irreversible. An interesting experiment would be to generate a negative chemotactic response at the surface to see whether the bacteria can subsequently leave the surface. Have you considered doing this?

Young: Our next step is to actually test negative chemotaxis in relation to a surface. We have not yet begun this study.

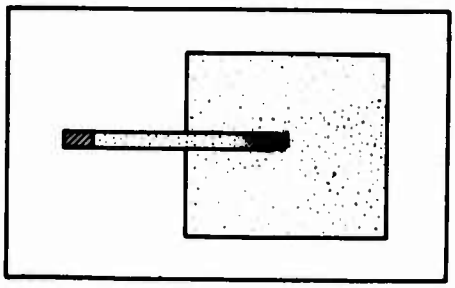


Figure 1: Diagramatic representation of positive chemotaxis observed under the microscope.

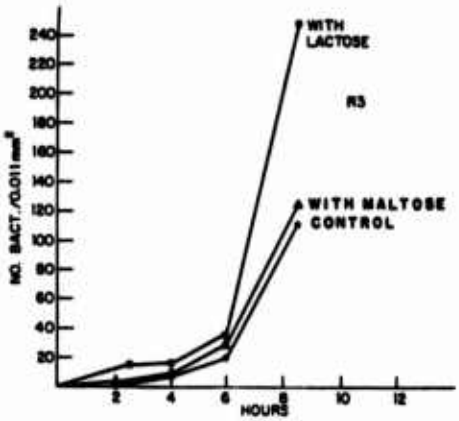


Figure 2: Attachment of isolate R3 to surfaces treated with 0.1 ml 10^{-2} M lactose and maltose.

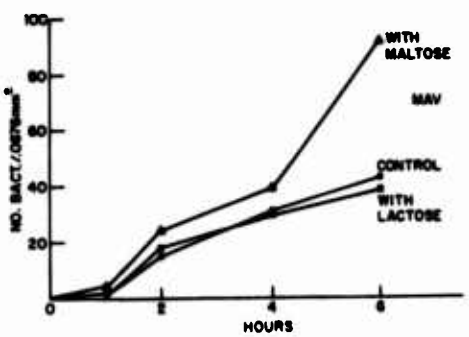


Figure 3: Attachment of isolate MAV to surfaces treated with 0.1 ml 10^{-2} M lactose and maltose.

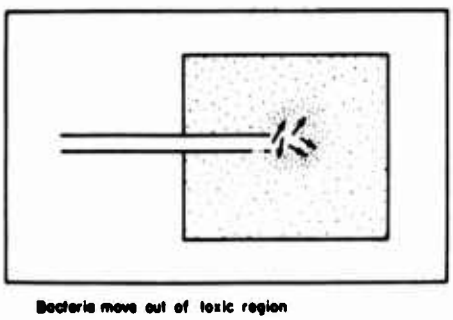


Figure 4: Diagramatic representation of negative chemotaxis observed under the microscope.

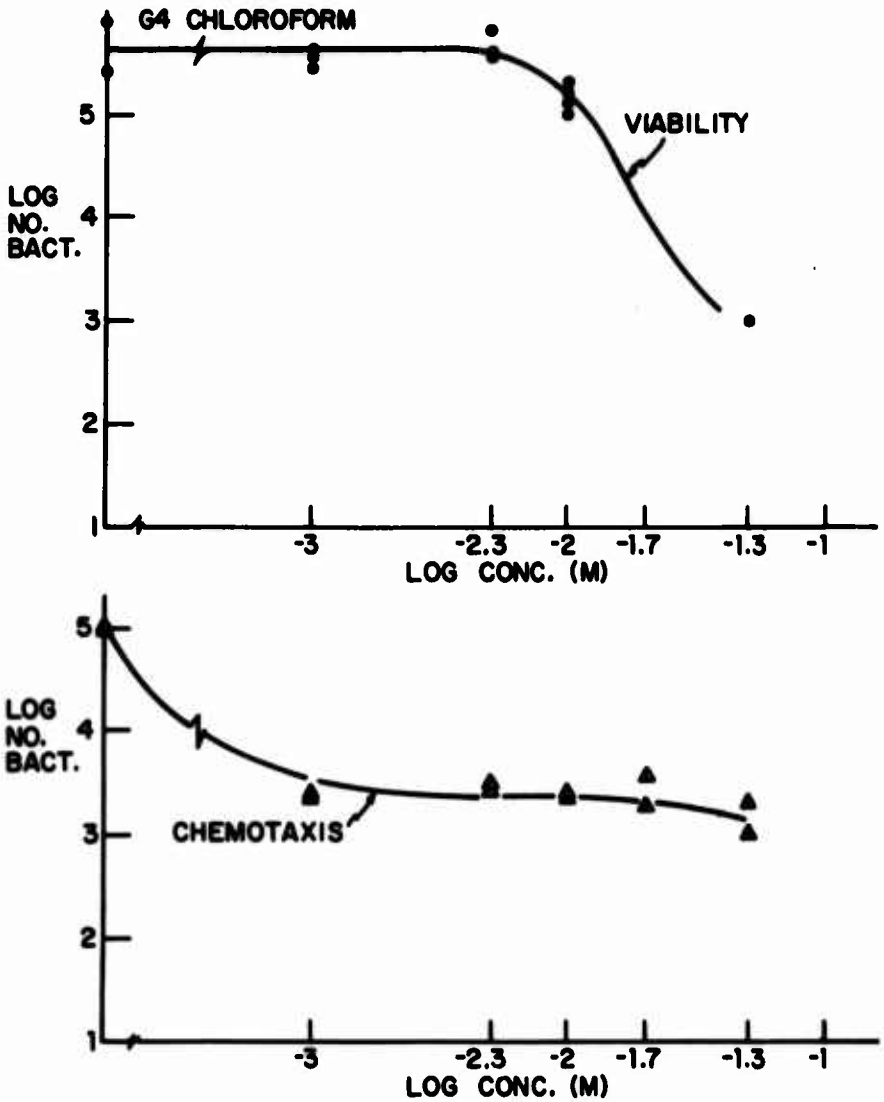


Figure 5: Upper: Viability of isolate G4 in chloroform

Lower: Effect of chloroform concentration on negative chemotaxis of isolate G4

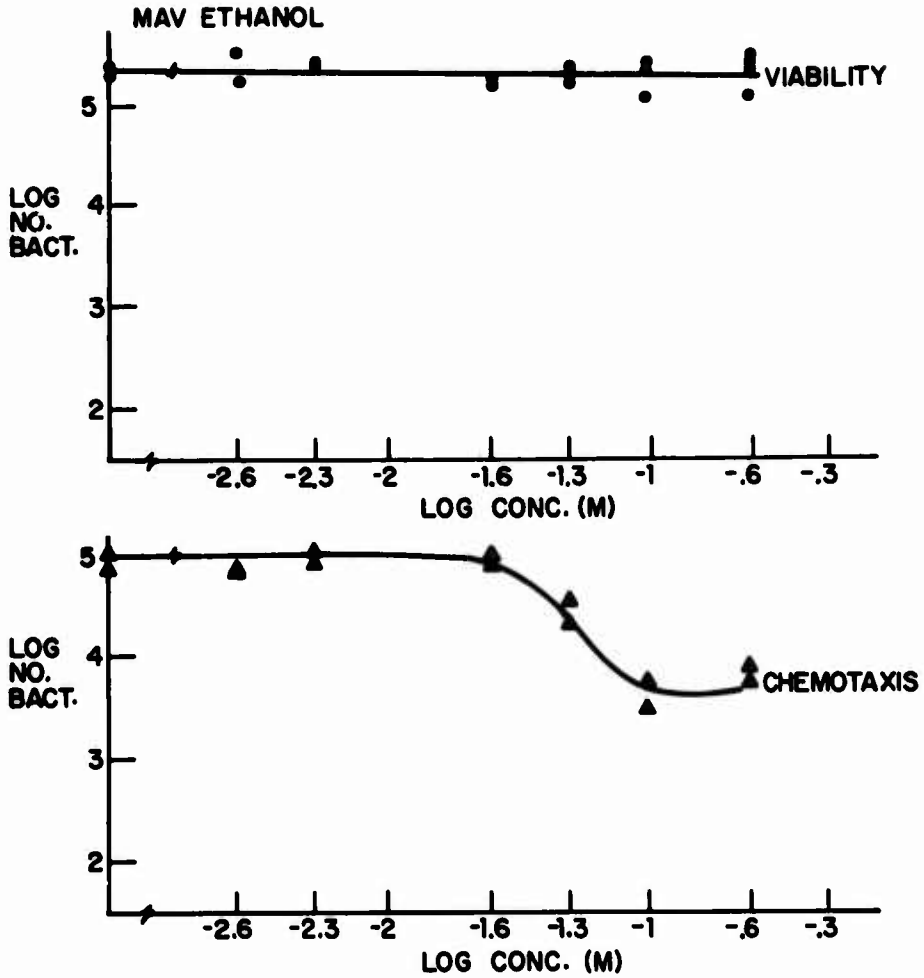


Figure 6: Upper: Viability of isolate MAV in ethanol
Lower: Effect of ethanol concentration on negative chemotaxis of isolate MAV

Mechanism of Adhesion of Marine Bacteria to Surfaces

Kevin C. Marshall

Department of Agricultural Science
University of Tasmania
Hobart, Tasmania, Australia

The behaviour of bacteria at solid surfaces immersed in seawater is considered in terms of their colloidal and biological properties. The sorption process involves two distinct phases; the attraction of a bacterium to a surface and its subsequent firm adhesion to the surface. The initial phase is shown to depend on such factors as chemotactic responses, the balance between electrical double-layer repulsion and van der Waals attraction energies, and the relative hydrophobicity of the bacterial surface. Firm adhesion to a solid surface is a selective process and is shown to be related to the production of bridging polymers by certain bacteria. The polymer fibrils serve to anchor the bacterial cell to the surface. This anchorage may be disrupted by treatment with pyrophosphate and periodate. Firm adhesion to surfaces by many marine bacteria is prevented by an inhibitor of protein synthesis (chloramphenicol).

Key Words: Bacteria, sorption, solid surfaces, electrical double-layer, hydrophobicity, bridging polymers.

1. Introduction

Bacteria are the smallest and, in terms of their ultra-structural detail, the most primitive of all living cellular entities (1)[1]. The majority of bacteria in natural habitats are rod-shaped, but spherical and spiral forms are often encountered along with some rather more complex morphological forms (2). Bacteria range in size from about 0.25 μm (mycoplasmas) to several μm in length; the average size being about 1.0 μm in length or diameter. As a result of their small size, bacteria suspended in an electrolyte exhibit properties that are characteristic of colloidal systems. Consequently, it is possible to consider their behaviour at a surface in terms of classical colloid chemistry, and an insight into the mechanism of firm adhesion of marine bacteria to surfaces has been obtained from such an approach. It must be remembered that bacteria are living organisms and, as such, are capable of growth, metabolism and, in some instances, independent motion. The results presented below demonstrate that these biological characteristics play an important role in the initial attraction of bacteria to surfaces and in the degree of selectivity that is evident in the final adhesion process.

2. The Attraction of a Bacterium to a Surface

One or more factors may be involved in the attraction of marine bacteria to a solid surface immersed in seawater. The most important factors could be chemotactic responses, electrostatic interactions, electrical double-layer phenomena and hydrophobic effects.

[1] Figures in parentheses indicate the literature references at the end of this paper.

(a) Chemotaxis. In a relatively dilute nutrient environment as in normal seawater, certain nutrients are concentrated at a solid surface and motile bacteria may respond by swimming along the nutrient concentration gradient toward that surface. This tactic response is the subject of the preceeding paper by Young and Mitchell. Chemotaxis is of no significance in the case of non-motile bacteria colonizing a submerged surface.

(b) Electrostatic interactions. At normal physiological pH values bacteria possess a net negative surface charge. In some species the ionogenic surface consists exclusively of acidic (carboxyl) groups, while in other species a heterogeneous ionogenic surface of predominantly acidic groups with some basic (amino) groups is found (3).

Most solid surfaces possess a negative charge and it is unlikely that bacteria would be attracted to these surfaces by electrostatic interactions.

(c) Electrical double-layer phenomena. Cations are attracted to negatively-charged surfaces, while anions tend to be excluded. The cations are not held firmly at the surface, but form a diffuse layer (the electrical double-layer) near the surface. The extent or thickness of this diffuse double-layer (1/K) is dependent upon both the concentration and the valency of the electrolyte employed. With increasing concentration or valency of the electrolyte, the thickness of the electrical double-layer decreases. When two negatively-charged bodies (e.g. a solid surface and a bacterium) are in close proximity, their respective cation double-layers overlap and the tendency is for a mutual repulsion of the bodies (= double-layer repulsion energy). Van der Waals attraction energies tend to counteract this repulsion effect. As shown in Fig. 1, the extent of the double-layer repulsion energy varies with the electrolyte concentration while the extent of the van der Waals attraction energy remains constant. At low electrolyte concentrations the resultant is a strong repulsion energy adjacent to the surface, while at higher concentrations a secondary attraction trough occurs away from the repulsion energy barrier closer to the surfaces. Bacteria probably are held at this point of attraction - a finite distance from the solid surface.

The results in Table 1 clearly demonstrate the effect of electrolyte concentration and valency on the attraction of Achromobacter R8 to a glass surface. The bacteria are repelled at low electrolyte concentrations, but are attracted at high concentrations. Divalent cations are more firmly held near a surface and the effective double-layer thickness at a particular concentration is less than for monovalent cations. Hence, rejection of Achromobacter R8 from a glass surface occurs at lower electrolyte concentrations in a divalent than in a monovalent system.

For the interaction between glass and bacterial surfaces in 0.2 M NaCl electrolyte, the secondary attraction trough is at an interparticle distance of greater than 30 Å while the repulsion energy barrier nearer to the surface is of the order of 50×10^{-13} ergs (4). Bacteria held at the point of attraction are readily removed by their own motive power (where motile) or by the shearing force of a jet of water and, consequently, this has been referred to as the reversible phase of sorption (4). Although motile bacteria appear to approach a surface with considerable force, the kinetic energy of the motile Pseudomonas R3 (5.45×10^{-18} ergs) is not sufficient to overcome the repulsion energy barrier quoted above (4).

(d) Hydrophobic effects. The possibility exists that bacteria with a relatively hydrophobic outer surface may be rejected from the aqueous phase at the interface of a two-phase system (air-water, oil-water or solid-water). Preliminary studies with several unusual freshwater bacteria suggested that this mechanism may exist (5). As with these freshwater bacteria, the marine bacterium SW11 exhibits a preferred orientation at air-water, oil-water and solid-water interfaces. The cells are always aligned perpendicularly to the interface (Fig. 2). Some evidence has been obtained suggesting that the end of the cell pointing into the interface is relatively more hydrophobic than the remainder of the cell surface. There is no concentration of positively-charged surface ionogenic groups at the end of the cell (5). The distinct orientation of SW11 cells at a variety of interfaces may be the result of a rejection of the hydrophobic portion of the cell from the aqueous phase. Initially, this phenomenon represents another example of reversible sorption.

3. Firm Adhesion of Bacteria to Surfaces

How does a bacterium eventually overcome the repulsion energy barrier and become firmly

adhered to a surface? Displacement of a relatively large body such as a bacterium by Brownian motion is not sufficient to overcome the energy barrier, but the displacement of extracellular polymeric fibrils produced by a bacterium may be sufficient for such fibrils to bridge the repulsion gap and anchor the cell to the surface. In recent years it has been shown that bacteria can be flocculated by anionic and non-ionic polymers as a result of bridging by the polymers between the cells (6, 7). Corpe (8) has reported the production of an extracellular acid polysaccharide by primary-film forming bacteria, and Marshall et al. (4), presented indirect electron microscopic evidence for the possible role of polymeric bridging in the adhesion process. More direct evidence for such polymeric bridging has been obtained with freshwater bacteria by Marshall and Cruickshank (5), using a technique similar to that employed by Taylor (9). Further studies have now been made with the marine bacterium SW11. Bacteria were allowed to adhere to blocks of solid Spurr's embedding medium, which were then thoroughly washed with 2.5% NaCl, fixed with glutaraldehyde in 2.5% NaCl and re-embedded in fresh Spurr's medium for sectioning. As shown in Fig.3, the bacteria are orientated at right-angles to the original solid-water interface with the end of the cell a short distance from the original surface. The cells clearly are anchored to the surface by means of bridging polymeric fibrils.

In view of Corpe's (8) finding of extracellular acid polysaccharide production by marine bacteria, attempts have been made to remove firmly adhering bacteria from surfaces by periodate treatment. This method has been successful with several freshwater bacteria (5), but periodate failed to remove a range of marine bacteria from surfaces. Treatment with pyrophosphate (10) prior to periodate treatment resulted in the successful removal of the marine Pseudomonas strains R3 and SW1 as well as the marine bacterium SW11 (Fig. 4). Similar results have been obtained in preliminary tests on heterogeneous bacteria firmly adhering to surfaces from natural seawater.

An important consideration in any biological adhesion process is the rapid sorption of proteins and other contaminating monolayers to surfaces immersed in natural waters (11). Critical surface tension measurements have revealed that the wettability of surfaces immersed in marine bacterial cultures is drastically modified prior to bacterial adhesion (12). Such changes in wettability may be of relevance in the sorption of the more hydrophobic portions of those bacteria mentioned above.

Marshall et al. (13) found that the phase of firm or irreversible sorption to a surface was a highly selective process. Many of the bacteria initially attracted to the surface (reversible sorption) did not become firmly adhered to the surface (irreversible sorption). Those bacteria capable of forming some type of extracellular bridging polymer must have a selective advantage in this process. It has been suggested that growth of the bacteria at the surface was a necessary requirement for bridging to occur (4). Recently, I have shown that the inhibition of protein synthesis by the antibiotic chloramphenicol inhibited the irreversible sorption of several marine Pseudomonas species (Fig. 5). However, tests with a freshwater hyphomicrobium and the marine bacterium SW11 showed that chloramphenicol and streptomycin did not prevent firm adhesion, even though streptomycin inhibited growth of the bacteria. Apparently, these bacteria had synthesized the appropriate bridging polymers prior to addition of the antibiotics. In view of this result, it was surprising to find that chloramphenicol drastically reduced the numbers of bacteria firmly adhering to a glass surface immersed in seawater (Fig. 6). Apparently, many of the bacteria in seawater are not actively metabolizing, but in the vicinity of the higher nutrient status at the surface they must begin to metabolize and form extracellular polymers.

4. Conclusions

Based on a concept of regarding a bacterial suspension as a living colloidal system, it has been possible to define some of the mechanisms involved in the initial attraction and the subsequent firm adhesion of marine bacteria to surfaces submerged in seawater. A knowledge of the biological role in the adhesion process gives some insight into possible means of controlling microbial film formation.

Acknowledgments. The investigations reported in this paper have been supported by a grant from the Australian Research Grants Committee. The author is grateful to Mr. R.H.Cruickshank for assistance with the electron microscopy and to Mrs. Robyn Page for technical assistance.

REFERENCES

1. R.Y. STANIER, M. DOUDOROFF and E.A. ADELBERG, The Microbial World (3rd Ed.), p. 34, Prentice-Hall, New Jersey (1970).
2. W.A. CORPE, Symposium on Adhesions in Biological Systems, p. 74, Academic Press, New York, (1970).
3. K.C. MARSHALL, Australian J. Biol. Sci. 20, 429 (1967).
4. K.C. MARSHALL, R. STOUT and R. MITCHELL, J. Gen. Microbiol. 68, 337 (1971).
5. K.C. MARSHALL and R.H. CRUICKSHANK, Submitted for publication.
6. M.W. TENNEY and W. STUMM, J. Water Pollution Control Fed. 37, 1370 (1965).
7. P.L. BUSCH and W. STUMM, Environ. Sci. Technol. 2, 49 (1968).
8. W.A. CORPE, Devel. Industr. Microbiol. 11, 402 (1970).
9. A.C. TAYLOR, Symposium on Adhesions in Biological Systems, p. 63, Academic Press, New York, (1970).
10. R.C. STEPHANSON, Australian J. Soil Sci. 9, 33 (1971).
11. R.E. BAIER, E.G. SHAFRIN and W.A. ZISMAN, Science 172, 1360 (1968).
12. R.E. BAIER, Private Communication, 1972.
13. K.C. MARSHALL, R. STOUT and R. MITCHELL, Canad. J. Microbiol. 17, 1413 (1971).

TABLE 1 - ATTRACTION OF ACHROMOBACTER R8 AND THE APPROXIMATE ELECTRICAL DOUBLE-LAYER THICKNESS (1/K) AT DIFFERENT CONCENTRATIONS OF UNI-UNIVALENT AND DI-DIVALENT ELECTROLYTES.

Electrolyte	Univalent (NaCl)		Divalent ($MgSO_4$)	
conc. (M)	1/K (Å)	Bacteria/mm^2	1/K (Å)	Bacteria/mm^2
10^{-1}	10	3500	5	4100
10^{-2}	31	2280	15	3050
10^{-3}	100	950	50	1920
10^{-4}	310	0	150	810
10^{-5}	1000	0	500	0

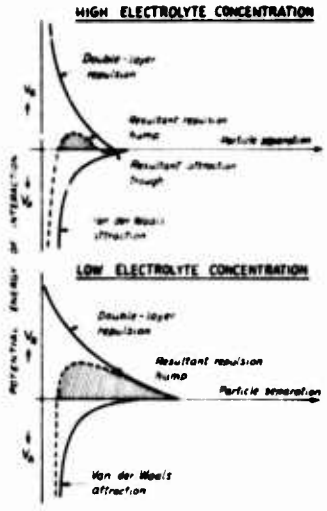


FIG. 1. Idealized curves showing the potential energy of interaction (repulsion or attraction) between solid and bacterial surfaces at low and high electrolyte concentrations.

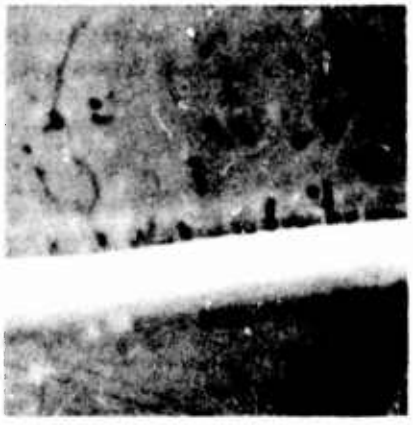
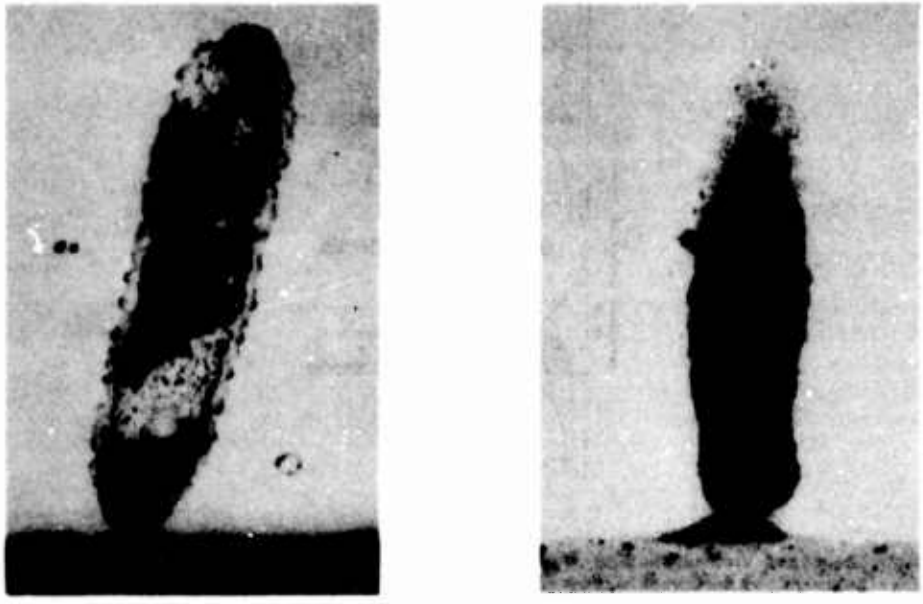


FIG. 2. The orientation of the marine bacterium SW11 at an oil-water interface. Phase-contrast microscopy (2,500 X).



(a) (b)

FIG. 3. Electron micrographs of thin sections of a re-embedded block of Spurr's medium showing the mode of attachment of the marine bacterium SW11 to the solid surface.

(a) Stained with uranyl acetate and lead citrate (55,300 X).

(b) Stained with permanganate and lead citrate (94,800 X).

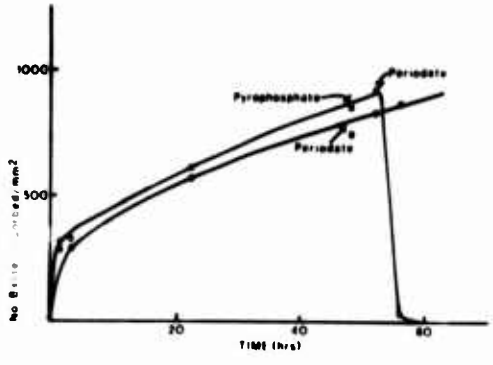


FIG. 4. Effect of pyrophosphate and periodate treatment on the removal of Pseudomonas SW1 from glass surfaces.

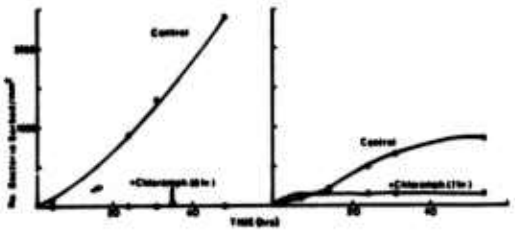


FIG. 5. Effect of chloramphenicol added after 0 or 7 hours on the sorption of Pseudomonas R3 to glass surfaces.

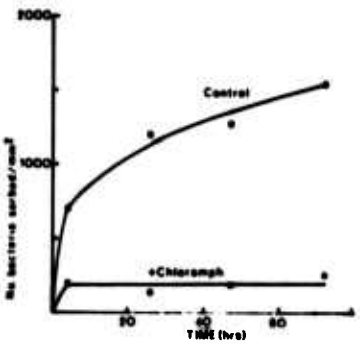


FIG. 6. Effect of chloramphenicol added at time zero on the sorption of bacteria from a natural seawater sample.

Discussion

Question: This question concerns the theoretical interpretation of this reversible phase of adsorption. You observe that the bacteria rotate, but apparently about a fixed axis. If these organisms are really being held a short distance away from the surface, is there anything in this interpretation which would keep them from moving from point to point on the surface?

Marshall: Our observations indicate that the bacteria just rotate around a fixed point. It is a little surprising that they do not drift across the surface, but it is difficult to determine whether they are drifting or not. Certainly, motile bacteria rotating at a surface are able to break away from it and come back to another point.

Question: As a non-bacteriologist, I am curious to know whether you have investigated the interaction between charged bacteria and a potential controlled surface, for example, platinum, where we can alter the charge from positive to negative? The second comment I'd like to make is that the oxygen composition of the solution in which metals are immersed as substrates for adhesion would be extremely important because the freely corroding or natural potential is very sensitive to the oxygen concentration.

Marshall: I have begun some work with reversing charges on platinum electrodes, but I am unable to provide any useful information at this stage. I am sure that by controlling the charge, we might be able to modify the behaviour of certain bacteria at the surfaces. One point I should like to stress is that no matter what surface we immerse in seawater, it is quickly contaminated by monomolecular layers that have different wetting properties and maybe different charge properties. Dr. Baier will have more to say about this point in his paper.

Question: Another way of altering the charge and the hydrophilic-hydrophobic nature of the surface is by the use of a long chain cationic detergent like cetyl ammonium bromide. This should make the bacterium adsorb very strongly because you then have a positive attraction all through the diffusion boundary layer as well as hydrophobic attraction to the surface of the bacterium. Have you tested such materials?

Marshall: We have used the surfactant Tween 80 with air-water interfaces. This prevents the specific perpendicular orientation of flexibacter at an air-water interface, but I have not tried to alter the charge relationships at such an interface.

Question: You said that at low concentrations there should be a repulsion. What is the low concentration?

Marshall: For a monovalent cation, the critical concentration for complete rejection of the bacteria from the surface is about 5×10^{-4}M. For a divalent cation, it is a lower concentration still, almost an order of magnitude lower.

Question: Can you verify it?

Marshall: I'm not quite sure what you mean by verify it. We do not get attachment below these critical concentrations, but in natural fresh waters attachment is observed because the ionic concentrations of the waters are above these critical levels.

Influence of the Initial Surface Condition of Materials on Bioadhesion

Robert E. Baier

Cornell Aeronautical Laboratory, Inc.
of Cornell University
P.O. Box 235
Buffalo, New York 14221

The nature of the events occurring immediately after first exposure of engineering or structural materials to a marine environment can be assessed by a combination of surface chemical tools. These include surface-specific infrared spectroscopy (based upon an internal reflection technique), ellipsometry (based upon external reflection of polarized monochromatic rays), contact angle measurements (leading to an inference of the relative surface free energy of the material and any acquired coating), and contact potential determination (reflecting the initial rest potential of any conductive material and the change in the surface electronic structure by acquired organic films). The earliest phases of biological adhesive events in saline media have been shown to be influenced by the surface chemistry, the surface texture, and surface charge of the solid substrates. The "critical surface tension" of the solid substrates, a parameter easily derived from contact angle data, has been correlated with adhesion of biological entities to organic and inorganic substrates in media as diverse as blood, tissue, the oral and uterine cavities, saliva, and sea water. In each instance, a prerequisite to adhesion of any cellular material at these substrates was the prior accumulation of a predominantly proteinaceous "conditioning" film. Minimum strengths of biological adhesion and maximal degrees of biocompatibility are proposed to correlate most strongly with an initial critical surface tension in the range between 20 and 30 dynes/cm. Substrates with relative surface free energies in this range, although allowing accumulation of initially adsorbed protein films, do not appear to force fouling-inducing denaturation of the protein through significant changes in its adsorbed configuration. With specific reference to biological fouling in the maritime environment, early experiments suggest that the first acquired modifying film on any emplaced foreign surface is a glycoprotein layer. This interface conversion then provides for strong bonding with exuded muco-polysaccharide components from the first arriving cellular species such as those which form primary bacterial films.

Key Words: Surface chemistry, fouling, proteins, primary films, infrared spectra, critical surface tension.

---

1. Introduction

When biologically productive waters first contact a solid surface of an engineering or structural material, a sequence of events is initiated which often ends in gross biological fouling of that solid surface. This process includes those many steps common to the normal life cycle of the fouling organisms and, although a natural process of the maritime

environment, is not very often desired with deliberately emplaced sea-dwelling materials. We have been attempting to define the earliest events occurring when both organic and inorganic solids are first contacted by a variety of biological fluids. We have used simultaneously a group of powerful surface chemical methods which allow the assessment of changes at the surfaces of solid materials within the first few seconds of their initial exposure to biological media.

2. Experimental Techniques

The methods used are multiple attenuated internal reflection (MAIR) infrared spectroscopy (1), [1] ellipsometry (2), critical surface tension determination (3), and contact potential determination (4) supplemented by more traditional surface characterization techniques such as electron microscopic inspection of the surface textures. MAIR infrared spectroscopy is a relatively new optical technique available commercially only since the middle 1960's (5) which allows microscopic amounts of material, especially when present in thin films adsorbed to solid surfaces, to be immediately analyzed by the chemical-structure-sensitive tool of infrared frequency analysis. Ellipsometry is a related optical method known for almost a century which with modern computational methods (6) allows a rapid estimate of the thickness and refractive index of adsorbed films on reflecting solid surfaces. Both optical methods are nondestructive. The critical surface tension of a material is derived from measurements of a series of contact angles of purified liquids on that material's surface. It has been shown to correlate one-to-one with both the outermost chemical constitution of that material and with its relative surface free energy (7). Contact potential measurements allow some information on the electrical asymmetry across the solid interface.

3. Illustrative Results and Their Interpretation

Use of such methods in combination has shown that the initial events in the interactions of blood with a foreign surface, for example, are that within the first 5 seconds most solid surfaces become uniformly coated with strongly adherent proteinaceous films having an average thickness of about 50 Angstroms and having critical surface tensions between 35 and 40 dynes/cm (8). Extension of the contact time of the solid surface with blood to 60 seconds allows a thickening of the acquired coating to between 100 and 200 Angstroms while maintaining both the predominantly proteinaceous identity of the film components and the outermost wettability typical of the initially accumulated film (8). Continuing times of contact allow incorporation of small amounts of lipids and replacement or remodeling of the original protein by other components from the biological milieu (8).

In saline media where bacterial fouling of a solid surface is usually the first discernable microscopic event in the fouling chain, such as in the oral cavity (9) (rich in saliva) or in biologically productive water (rich in microorganism produced exudates), similar experiments show that the first chemical event is a modification of the solid surface by accumulation of a reasonably specific glycoprotein. This is followed by accumulation of a "volume phase" muco-polysaccharide-dominated adhesive substance which becomes anchored to the initially acquired "interfacial" glycoprotein film (10).

Figure 1a and b shows two spectra characterizing the film naturally acquired on a solid surface (of a germanium internal reflection prism) during the spontaneous "sticking" of three mussel attachment disks in an artificial sea water culture (11). Figure 1a shows that the dominant composition of the material was muco-polysaccharide in nature. The major infrared absorption bands at about 3400 cm^{-1}, 1650 cm^{-1} and 1100 cm^{-1} all reflect the hydroxylated polysaccharide component. Buried within these major peaks, however, could be evidences of minor--but more important--constituents that had been adsorbed previously or admixed with the polysaccharide. Figure 1b shows the spectrum of this identical film on its original surface after a lengthy distilled water rinsing. Trace 1b illustrates that the preponderance of the polysaccharide material was easily removable by simple distilled water rinsing but that a remnant, and probably initially adherent, glyco-

---

[1] The numbers in parentheses refer to the list of references at the end of this paper.

proteinaceous film remains as an extraction-resistant "conditioning" layer. Identification of the remaining extraordinarily thin film as a glycoprotein rests upon the modification of the infrared spectral trace from what has been described in Figure 1a to that illustrated in Fibure 1b. The trace given in Figure 1b has the characteristic protein absorptions at 3300 cm^{-1}, 1650 and 1550 cm^{-1} with only a small remaining peak at 1100 cm^{-1} characteristic of polysaccharide. In both traces, Figures 1a and 1b, it is also to be noted that some hydrocarbon bands are exhibited at the region centering around 2900 cm^{-1}. It can thus be demonstrated in this simple example of biological fouling, as it has been in numerous other systems where biological adhesion occurs (12), that a thin proteinaceous "conditioning" film causes the first modification of the initial surface condition of any implanted substrate. It is considered that this film is an obligatory precursor to the adhesion of any formed elements and to the subsequent buildup of a fouling mass of biological cells (13). In the case of specific interactions of blood at nonphysiologic interfaces, evidence has been presented that the first adsorbed constituent is the abundant blood protein, fibrinogen (8). On the other hand, in the complex media of saliva (9) or of cervical mucous fluid (14), it has been demonstrated that the first acquired film is of a glycoprotein character similar to that found in most maritime circumstances.

It is only subsequent to the formation of the adsorbed protein "carpet" that microscopic examination reveals the deposition of the densely populated interfacial layers of bacterial cells (15), blood platelets (16), or somatic cells (in tissue culture) (17) in a variety of biologically adhesive systems. It is our current interpretation that interfacial modification of any engineering or structural material by initially adsorbed protein-dominated films is an absolute requirement for activation of the chain of events in the adjacent liquid volume which allows long term anchoring of formed biological elements to solid surfaces. In those instances when such emplaced materials have remained apparently fouling-resistant for long periods of time, with the exception of circumstances where outright poisoning of organisms is occurring by leachable toxic elements from special paints or coatings, it is not yet clear whether this apparent resistance is due to detachment of the initially adherent organisms after a period of time or to inhibition of the initial activation and anchoring process.

4. Discussion and Conclusions

With respect to discovering the influence of the initial surface condition of materials on bioadhesion, it should be made clear that the following is now the question of overriding importance: How is the influence of differing substrate surface properties transduced and communicated, to the first discrete biological organisms which arrive at that surface, through the initially adsorbed predominantly proteinaceous conditioning films?

We have not discussed here, for the sake of brevity, the important influence of these interfacial films on water structure and the reverse influence of adsorbed water on the surface character of the materials and the adsorbed protein layers (18). Neither have we discussed the benefits that will certainly derive from selection of surface chemical "coupling" agents for maritime surfaces and from attention to surface chemical/physical concepts during fabrication of new improved composite materials for maritime application (19). Nor have we considered all of those major unresolved questions of how one separates the broad term "surface properties" into the definitive specific details of surface chemistry, surface charge, and surface texture and shown the nature of their perturbation in real circumstances by unknown amounts of adventitious contaminants either introduced during manufacturing or in actual deployment situations (20).

We have shown, however, that it is within our technical capability at present to analyze with a great degree of completion the composition and configuration of the thin layers of matter that intervene in the interactions of solid surfaces with biologically rich saline media. Elsewhere, we have reported studies of thin polymeric films in which their conformation in solution was determined, their surface pressure vs. surface area and surface potential vs. surface area relations as spread films at air/water interfaces characterized, and their optical thicknesses, infrared spectra, contact potentials, and critical surface tensions, when transferred to solid surfaces, also determined (21). It is important to note that such parameters could be supplemented, without deterioration of the value of the techniques described, by additional physical measurements such as electron diffraction and electron microscopy. Thus, a multipronged surface chemical/physical approach and,

particularly, a recording of diagnostic infrared spectra for as-acquired specimens of even monomolecular thickness allows a direct correlation between features of the initial solid substrates and the surface properties which it subsequently manifests through the mediation of the acquired polymeric films.

It is our current supposition that the initial common event in the interaction of all biologic elements with foreign surfaces is the rapid deposition of a strongly adherent protein-dominated film. From electron microscopic studies of adherent cells from blood (16) or tissue origin (22), it is suggested that a critical or perhaps limiting thickness of the adsorbed films exists in the neighborhood of 200 Angstroms since, after that thickness is acquired, the first formed cellular elements are seen to deposit. The presence of such living species must change the nature of the adsorption process in their vicinity. This forces the suggestion that a threshold time will exist for cellular adhesion in all circumstances, including maritime circumstances, during which period initially adsorbed conditioning layers are acquired. This threshold time should generally be of the order of a minute or two in the most concentrated "surrounds" (such as blood or saliva) but may extend to many hours in the very dilute, biologically impoverished regions of the sea. It is also noteworthy that the formed elements in biologically adhesive systems do not at any time entirely cover the solid surface (16, 23). Therefore, the fact that these living cells might prevent further deposition of proteins or other modifying polymers in some areas of the substrate does not eliminate the possibility of subsequent fouling by the addition of more acquired proteinaceous layers in other areas on that same surface.

5. Prospects for the Creation of Nontoxic Surfaces Resistant to Marine Fouling

In a series of fundamental studies on protein films adsorbed to solid substrates, it has been shown that the proportion of native structure of the adsorbed macromolecule never reached 100% except in a minority of instances when the relative surface energy of the adsorbing substrate was purposely allowed to be low (13, 24). This result has been shown to be reasonably independent of the makeup of the solutions from which the adsorption occurred, even though it was observed that low solution concentrations favored relatively lower proportions of native structure in the adsorbed films (24). These findings suggest a potential mechanism for achieving resistance of an engineering or structural material to fouling by biological entities in the marine environment. Since, as it seems most likely, the initially adsorbed proteinaceous molecules are drastically modified in conformation and reactivity by the process of their two dimensionalization from their original three-dimensional form in the solution state, it is this transmutation of the protein properties which correlates with its providing the interfacial anchor for subsequently arriving formed elements. Since the extent of this potentially adverse modification of the initially adsorbed molecules has been shown to be capable of diminution by the proper choice of the surface energy of the substrate, it is likely that native conformation of the outermost layer of adsorbed molecules can be obtained on a properly surface-chemically-designed engineering material so that that layer is passive toward the activation or accumulation of cellular elements arriving at that surface.

We have recently demonstrated, along these lines, that a strong, corrosion-resistant alloy of the cobalt-chromium class--when cleaned and polished according to the best manufacturing processes--does not have long term resistance to accumulation of cellular elements from a very rich biological fluid (blood) unless it is first completely coated with a modifying, adherent, waxy layer whose apparent critical surface tension is in the range between 20 and 30 dynes/cm (correlating with the exposure of CH_3 groups outermost) (25). This layer then accumulates a passivating proteinaceous film essentially inert to arriving blood platelets which normally adhere and aggregate to cause massive thrombus--the body's equivalent to gross biological fouling. It has also been shown that benefits of selection of the proper surface chemistry of a series of metals can be overwhelmed by lack of similar attention to their surface charge and/or surface textures (26).

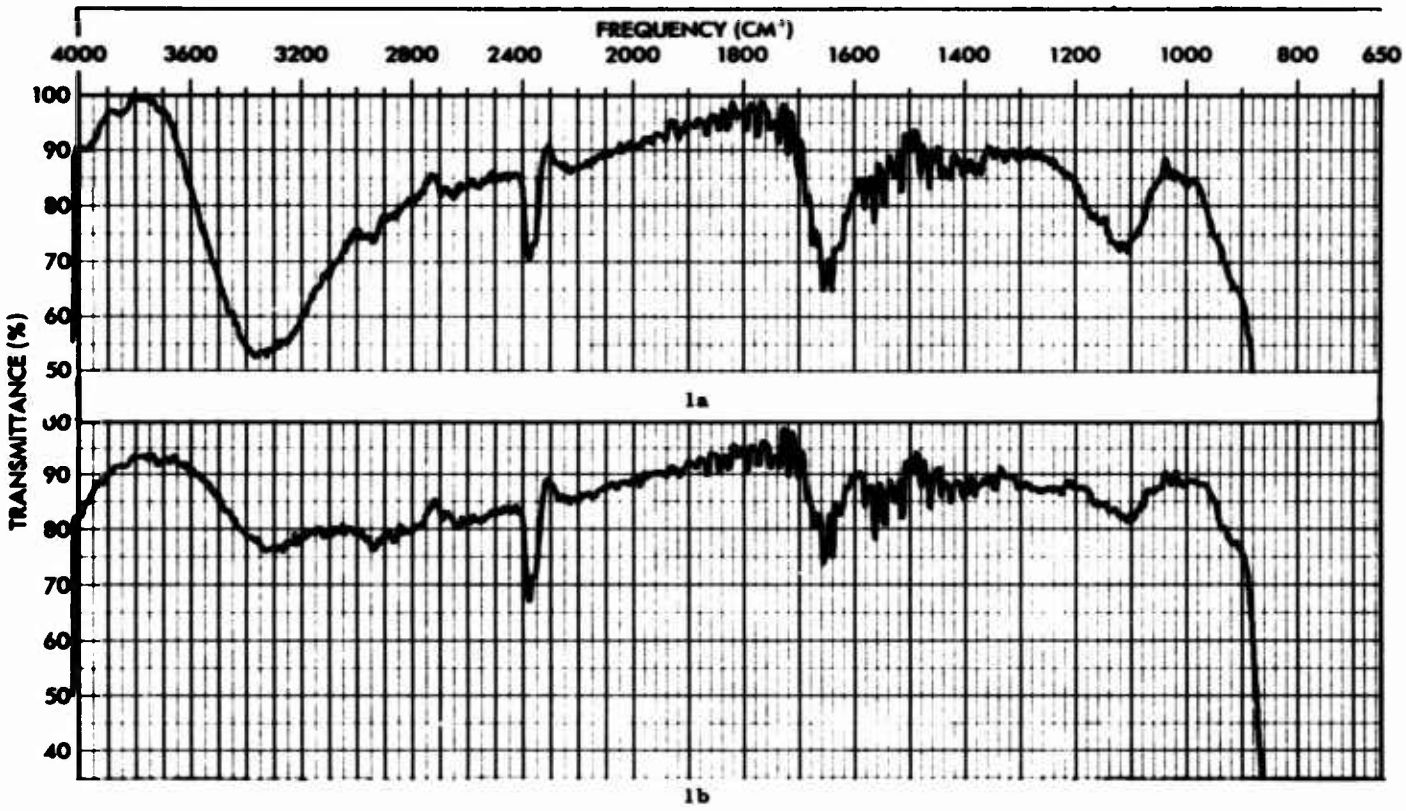


FIGURE 1

INTERNAL REFLECTION INFRARED SPECTRA OF SPONTANEOUSLY DEPOSITED FILMS WHICH PRECEDE BIOLOGICAL FOULING OF INORGANIC SURFACES

References

1. N. J. HARRICK, Internal Reflection Spectroscopy, Interscience Publishers, New York (1967).

2. K. H. ZAININGER and A. G. REVESZ, RCA Review, 25:85 (1964).

3. H. W. FOX and W. A. ZISMAN, J. Colloid Sci., 7:428 (1952).

4. K. BEWIG, "Improvements in the Vibrating Condenser Method of Measuring Contact Potential Differences," Naval Research Laboratory Report 5096 (1958).

5. Harrick Scientific Corporation, Ossining, N.Y., and Wilks Scientific Corporation, South Norwalk, Conn., have equipment available.

6. F. L. McCRACKIN and J. P. COLSON, NBS Technical Note 242 (1964).

7. W. A. ZISMAN, "Surface Energetics of Wetting, Spreading, and Adhesion," Journal of Paint Technology, 44:42-70, (1972).

8. R. E. BAIER and R. C. DUTTON, "Initial Events in Interactions of Blood with a Foreign Surface," J. Biomed. Mater. Res., 3:191-206 (1969).

9. R. E. BAIER, "Occurrence, Nature, and Extent of Cohesive and Adhesive Forces in Dental Integuments and Dental Materials," Surface Chemistry and Dental Integuments (R. P. Quintana and A. Lasslo, Eds.), Charles C. Thomas, Publisher (1972).

10. M. COOK, T. R. TOSTESON, K. MARSHALL and R. E. BAIER, Unpublished Experiments (1972).

11. M. COOK, "Composition of Mussel and Barnacle Deposits at the Attachment Interface," Adhesion in Biological Systems (R. S. Manly, Ed.), Academic Press (1970).

12. R. S. MANLY, Editor, Adhesion in Biological Systems, Academic Press (1970).

13. R. E. BAIER, G. I. LOEB and G. T. WALLACE, "Role of an Artificial Boundary in Modifying Blood Proteins," Federation Proceedings, 30:1523-1538 (1971).

14. R. E. BAIER and J. LIPPES, in preparation.

15. W. A. CORPE, "Attachment of Marine Bacteria to Solid Surfaces," Adhesion in Biological Systems (R. S. Manly, Ed.), Academic Press (1970).

16. R. C. DUTTON, T. J. WEBBER, S. A. JOHNSON and R. E. BAIER, J. Biomed. Mater. Res., 3:13 (1969).

17. L. WEISS, The Cell Periphery, Metastasis and Other Contact Phenomena, John Wiley & Sons, Inc., New York (1967).

18. R. E. BAIER, "Surface Properties Influencing Biological Adhesion," Adhesion in Biological Systems (R. S. Manly, Ed.), Academic Press (1970).

19. R. E. BAIER, E. G. SHAFRIN and W. A. ZISMAN, Science, 162:1360 (1968).

20. R. E. BAIER, "The Role of Surface Energy in Thrombogenesis," Bulletin of the New York Academy of Medicine, 48:257-272 (1972).

21. R. E. BAIER and G. I. LOEB, "Multiple Parameters Characterizing Interfacial Films of a Protein Analogue, Polymethylglutamate," Polymer Characterization: Interdisciplinary Approaches (C. D. Craver, Ed.), Plenum Press (1971).

22. A. C. TAYLOR, "Adhesion of Cells to Surfaces," Adhesion in Biological Systems (R. S. Manly, Ed.), Academic Press (1970).

23. L. I. FRIEDMAN, H. LIEM, E. F. GRABOWSKI, E. F. LEONARD and C. W. McCORD, Trans. Am. Soc. Artificial Internal Organs, 16:63 (1970).

24. G. I. LOEB, "Spectroscopy of Protein Monolayers: A Transition in β - Lactoglobulin Films," J. Polymer. Sci.: Part C, pp. 63-71 (1971).

25. R. E. BAIER, V. L. GOTT and R. C. DUTTON, "Thromboresistance of Stellite 21: The Role of an Adventitious Waxy Contaminant," J. Biomed. Mater. Res., in press (1972).

26. V. A. DePALMA, R. E. BAIER, J. W. FORD, V. L. GOTT and A. FURUSE, "Investigation of Three Surface Properties of Several Metals and Their Relation to Blood Compatibility," J. Biomed. Mater. Res. Symposium, No. 3, pp. 37-75 (1972).

Discussion

Question: Do you assume that these proteins entirely displace the layers of water which have wetted hard surfaces in the sea or is it only a partial displacement?
Baier: I am willing to consider both mechanisms, but my working hypothesis is that the proteins are essentially permanent and efficient interface conversion layers because they scavenge water from the surface, thereby creating that intimate molecular contact between themselves and the substrate that is necessary to form a true adhesive bond. Otherwise, one would expect them to be reasonably labile and erode away from the surface. We are studying this by checking on their degree of lability by exchangeability into solvents.

Question: And they are able to displace water by virtue of their lower surface energy, water being about 72 dynes/cm?
Baier: Well, that's questionable because adsorbed water has already lowered the critical surface tension of the wet metal substrate. Its surface free-energy is in the range of about 22 dynes/cm. It is quite complicated when you recognize that a protein actually orders water around itself and the substrate also orders water at its own surface. It is found that a protein always spontaneously accumulates on any solid surface exposed to the protein solution. Consequently, we now have to adjust our theories to account for observation.

Marine Fungi: Spore Dispersal, Settlement and Colonization of Timber

E.B. Gareth Jones.

Department of Biological Sciences, Portsmouth Polytechnic, Portsmouth, PO1 2DZ, England.

This paper will consider the spore dispersal, settlement and penetration of timber by marine fungi. It will also consider briefly their tolerance of a copper-chrome-arsenate preservative.

Aspects considered under spore dispersal include: spore release from asci and ascocarps, the number of spores in sea water, their distribution with depth and distance from land.

The section on spore settlement will consider the morphology of marine fungal spores, their settlement and germination.

The final section on colonisation will include mode of penetration of timber and a consideration of their cellulolytic activity as measured by weight loss, enzymatic and strength tests. The paper will end with a brief discussion of their tolerance of a copper-chrome-arsenate preservative under laboratory conditions.

Key Words: Lignicolous marine fungi; spore liberation; dispersal; bitunicate asci; deliquescing asci; spore morphology; settlement; attachment; germination; biodegradation; preservative tolerance.

---

1. Introduction

Lignicolous marine fungi were first described by Barghoorn and Linder (1) and their ability to degrade wood is well documented (2). However, Ingold (3) has drawn attention to the lack of information on the dispersal, settlement and subsequent attachment of spores of marine fungi. This paper considers the information available and highlights aspects requiring further study.

The following stages in the colonization of wood will be considered: spore release, dispersal, settlement and penetration of the mycelium into the substrate.

2. Spore liberation

Fungi Imperfecti.

Conidia are released passively. They merely separate or break off from the conidiophores. These conidia may be helicoid (*Zalerion maritima, Cirrenalia macrocephala*), appendaged (*Orbimyces spectabilis, Varicosporina ramulosa*) or without appendages (*Dendryphiella salina, Asteromyces cruciatus*) (See Figure 1).

Ascomycetes.

Some 90 lignicolous marine Ascomycetes have been described (2). In this group, the ascus is usually the structure responsible for the explosive release of the spores. Two basic types of asci are found within the Ascomycetes: unitunicate and bitunicate.

The numbers in parentheses refer to the list of references at the end of this paper.

Unitunicate asci and their ascospores are released from the ascocarps in a variety of ways. The most common method involves the active discharge of spores from asci. The ascus becomes turgid as the result of increased osmotic pressure, the wall is stretched, and this leads to the rupture of the ascus in a definite way with the resultant explosive release of the ascospores. Perhaps it is not surprising that few marine Ascomycetes (e.g. *Chaetosphaeria chaetosa*) release their spores by this method. Presumably the internal osmotic pressure of the ascus would have to be very high to absorb water from the surrounding sea water. Also pressure would affect the success of this method, especially in deep water.

The second mechanism is the passive discharge of asci from ascocarps and the subsequent active release of the spores. This method is rarely found in the marine Ascomycetes but has been reported for *Gnomonia marina* (4).

Most of the marine lignicolous Ascomycetes with unitunicate asci release their spores as follows. The ascus wall is extremely thin (5) and is structurally quite different from the unitunicate asci of some terrestrial genera (6). The ascus wall breaks down and liberates the spores into the centrum. When mature, the tip of the neck opens, sea water may enter the ascocarp and the mucilage around the spores or in the centrum swells. This probably helps to expel the spores up the neck and out of the ostiole into the surrounding water (5, 7, 8, 9). If the spores are appendaged, any mucilage around the spore expands and gets dissolved and then the appendages stretch out (5) (See Figure 2). *Amylocarpus encephaloides* and *Eiona tunicata*, both cleistothecial forms, have deliquescing asci and appendaged ascospores. This suggests that the deliquescing ascus has been evolved in the marine Ascomycetes more than once, e.g. in the Plectomycetes and Pyrenomycetes. Ingold (3) regards the non-explosive asci of *Genea, Chaetomium* and *Ceratocystis* as degenerate. In the sea, this seems an ideal way of releasing ascospores. All that is required is the release of the spores from ascocarps. An explosive mechanism is of limited use due to the greater viscosity of water as compared with that of air. It is therefore significant that no glycogen has been found in the epiplasm of maturing asci of *Cerioseporopsis halima* (5).

The bitunicate ascus has an active method of spore discharge and is well illustrated in *Leptosphaeria discors* (10). The ascus wall consists of an outer rigid layer (ectoascus) and a very thin inner extensible one (endoascus). Just before discharge the ectoascus ruptures apically (sometimes subapically (11)), water is absorbed with the result that the endoascus elongates very rapidly up the neck of the pseudothecium, soon projects through the ostiole, bursts, squirting its ascospores into the air or water. The effectiveness of this method must be very much reduced when the fungus is continuously submerged, due to the increased viscosity of water. The observations made above concerning the internal osmotic pressure of the unitunicate ascus and the effect of pressure with depth, also apply to the bitunicate asci. It is therefore interesting that in a recent study (12) 970 recordings of marine fungi were made on 266 test panels submerged for up to 120 weeks in the sea. Of these, only 12 recordings were of bitunicate species (*Pleospora* sp. (2 recordings), *Leptosphaeria orae-maris* (9) and *Microthelia maritima* (1)).

Basidiomycetes.

The two marine higher Basidiomycetes have appendaged basidiospores, lack sterigmata, and release their spores passively. The resupinate *Digitatispora marina* releases its spores directly into the water. In the Gasteromycete *Nia vibrissa*, the basidia break down and the sporophore then contains thousands of basidiospores immersed in mucilage. Spore release has not been observed but it is probably by the mucilage expanding and rupturing the peridial wall or by the decay of the peridial wall. No spores have been seen to be released when the sporophores are kept in air.

3. Dispersal

There are no figures available for the numbers of spores of lignicolous marine fungi in known volumes of sea water. Both Kohlmeyer (13) and I (unpublished) have observed a variety of spores in scums along the sea shore, but even these are poor in species and number compared to freshwater scums. Millipore filtration techniques have proved disappointing. Large volumes of water has to be filtered and even then the counts are low (5-8 spores/litre). However, Iqbal (personal communication) using similar methods reports 7,000-8,300 spores per litre from freshwater taken from the river Creedy, Devon.

Large numbers of Yeasts and Phycomycetes have been reported from sea water. Fell (14) reports 1-513 yeast cells per litre from samples taken in the Indian Ocean and counts of 1-5,000 cells per litre from samples in the Biscayne Bay (15). Gaertner (16) found that the number of Phycomycetes in sea water off Iceland was low (1.3-12 infective units per litre) but that fine sediments in the German Bay were rich in numbers varying from 230-58,700 fungi per litre(17).However, these workers used specific isolating techniques. Plating out sea water is of limited use in determining the number of lignicolous marine Pyrenomycetes present as so few fruit under laboratory conditions. While some groups of fungi are present in high numbers, it is surprising that lignicolous fungi are so poorly represented. Untreated timber placed in the sea is soon colonised by a variety of species. It has been shown (18) that lignicolous fungi must be well distributed in sea water for they have been observed colonizing polyurethane panels at depths of 437m. (Table 1).

4. Settlement

Spore morphology.

Some 60% of the Ascomycetes, 10% Fungi Imperfecti and both the marine Basidiomycetes have appendaged spores. It has been suggested that these appendages a) help to keep spores afloat by offering increased resistance to settlement; b) to entangle and attach the spores to suitable substrates or c) to catch unorganised eddy diffusion currents (19). However, no quantitative experimental work has been carried out to test these ideas.

No work has been carried out to determine how long a spore takes to settle and attach itself to a substrate, or how effective the adhesion is. This is important as spores have to settle often in turbulent or fast moving waters. Nothing is known of the settlement of non-appendaged spores or their settlement in relation to water movement.

Germination.

If spores are to successfully colonize wood, they must be capable of rapid germination and penetration of their substrate. Spores have been reported as germinating within 24 hours of seeding agar plates (5) but detailed information is lacking. Byrne (20) has shown that temperature affects the germination rate of marine fungi, especially low temperature (Table 2). Most of the fungi tested had a high percentage germination with the exception of *Torpedospora radiata*. These high germination rates may explain why these fungi are so successful in colonizing freshly submerged timber in the sea.

5. Penetration of mycelium into wood

The ability of marine fungi to attack and soft rot wood has been widely reported (1, 2, 21). Their mode of attack and penetration is identical to that of terrestrial species and well documented by Levy and his coworkers (22, 23).

Some seventeen out of the 126 lignicolous marine fungi known have been shown to soft rot wood under laboratory conditions (2). *Corollospora maritima* brings about a 25.7% weight loss of beech test blocks in 18 weeks.

Meyers (24) has shown that the surface layers of wood (1-2 mm) is colonized by a diverse fungal population (e.g. *Cirrenalia* sp., *Ceriosporopsis halima; Corollospora maritima; Torpedospora radiata, Halosphaeria quadricornuta* and *Lulworthia* spp.). However, of these only *Lulworthia* spp. penetrated to any depth (12 mm).

Various methods have been used to determine the intensity of fungal degradation of cellulose and wood. They include: A) weight loss and visual examination (2); B) enzymatic studies (25, 26); C) breaking strength of cordage (27) and D) fungal protein production (28).

The ecology and decay capability of lignicolous marine fungi and their inter relationship with other marine organisms are subjects discussed in the handbook "Marine borers, fungi and fouling organisms of wood" (29). Jones and Irvine (30) have shown that the selected species tested are more tolerant of a copper chrome arsenate preservative than many terrestrial fungi.

While there is an accumulating literature on lignicolous marine fungi, certain aspects warrant further investigation. These include spore liberation, settlement in relation to water movement and germination rates on various substrates. These are subjects under investigation at Portsmouth and Fazzani (31) has produced a film showing spore release in *Sillia ferruginea*. This fungus belongs in the Pyrenomycetes and is found growing on timber in water cooling towers (32). This film is available on loan from Mr. K. Fazzani or myself at the address given above.

I am indebted to Mr. K. Fazzani for allowing me to show his film at the Congress.

References

1. E.S. BARGHOORN and D.H. LINDER, *Farlowia*. 1, 395 (1944).

2. E.B.G. JONES, *Marine Borers, Fungi and Fouling Organisms of Wood*. p.237. O.E.C.D. Paris (1971).

3. C.T. INGOLD, *Fungal spores, their Liberation and Dispersal* pp. 302. Clarendon, Oxford (1971).

4. A.B. CRIBB and J.W. CRIBB, *Univ. Queensland Papers, Dept. of Botany*, 3, 97 (1956).

5. M. LUTLEY and I.M. WILSON, *Trans. Br. mycol. Soc.*, 58, 393 (1972).

6. G.N. GREENHALGH and L.V. EVANS, *Trans. Br. mycol. Soc.*, 50,181 (1967).

7. I.M. WILSON, *Trans. Br. mycol. Soc.*, 37, 272 (1954).

8. E.B.G. JONES, *Trans. Br. mycol. Soc.*, 47, 97 (1964).

9. E.B.G. JONES, *Trans. Br. mycol. Soc.*, 45, 245 (1962).

10. D. TE STRAKE WAGNER, *Nova Hedwigia*, 9, 45 (1965).

11. T.W. JOHNSON, *Bull. Marine Sci. Gulf and Caribean*, 6, 349 (1956).

12. E.B.G. JONES, *Biodeterioration of Materials*, p.460 Elsevier, Barking (1968).

13. J. KOHLMEYER, *Zeitschrift für Allg. Mikrobiologie*, 6, 45 (1966).

14. J.W. FELL, *Bull. Marine Science*, 17, 454 (1967).

15. J.W. FELL, D.G. AHEARN, S.P. MEYERS and F.J. ROTH, *Limnol. Oceanogr.* 5, 366 (1960).

16. A. GAERTNER, *Veroff. Inst. f. Meeresf. Bremerhaven.* 11, 65 (1968).

17. A. GAERTNER, *Veroff. Inst. f. Meeresf. Bremerhaven.* 11, 105 (1968).

18. E.B.G. JONES and T. LE CAMPION-ALSUMARD, *Int. Biodetn. Bull.*, 6, 119 (1970).

19. J. KOHLMEYER and E. KOHLMEYER, *Nova Hedwigia*, 12, 189 (1966).

20. P. BYRNE, *The Physiological Responses of Some Marine, Freshwater and Terrestrial Fungi to Salinity*. Ph.D. Thesis. London University (1971).

21. G. BECKER and J. KOHLMEYER, *J. Timber Dryer's and Preservers, India*, 4, 1 (1958).

22. J.F. LEVY, *Advances in Botanical Research*, 2, p323, Academic Press, London (1965).

23. J.F. LEVY, *B.W.P.A. Annual Convention*, p.1-8 (1969).

24. S.P. MEYERS, *Marine Borers, Fungi and Fouling Organisms of Wood*, p. 217. O.E.C.D. Paris (1971).

25. S.P. MEYERS, *Biodeterioration of Materials*, 1. p.594. Elsevier, Barking (1968).

26. S.P. MEYERS, S.L. CHUNG, and D.G. AHEARN, *Biodeterioration of Materials*, 2, p.121 Applied Science, London (1972).

27. S.P. MEYERS, B. PRINDLE and E.S. REYNOLDS, *Tappi*, 43, 534 (1960).

28. E.B.G. JONES and J. IRVINE, *Biodeterioration of Materials*, 2, p.422. Applied Science, London (1972).

29. E.B.G. JONES and S.K. ELTRINGHAM (eds.), *Marine Borers, Fungi and Fouling Organisms of Wood*, pp. 367 O.E.C.D., Paris (1971).

30. E.B.G. JONES and J. IRVINE, *J. Inst. Wood Science*, 29, 31 (1971).

31. K. FAZZANI, Cooling Tower Fungi I. ASCOMYCETES - *Sillia ferruginea* Black/White film, 10 minutes silent.

32. R.A. EATON and E.B.G.JONES, *Material und Organismen*, 6, 51 (1971).

Table 1.

Distribution of marine fungi with depth

Depth (m)	Zalerion maritima	Corollospora maritima	Lulworthia purpurea	Haligena unicaudata
47				
67				
80	+		+	
86	+		+	
87	+	+	+	
106		+		
126	+	+		
127			+	
130				+
134			+	
180		+		
187				+
210			+	+
230				
237				+
280		+		+
287				+
330			+	+
337				+
380			+	+
387				
430				+ 2
437				+
487				
537				
Total	4	5	8	12

Table 2. Spore germination of some marine fungi at different temperatures.

	C^{o} Temperature.			
	10 hours (%)	15 hours (%)	20 hours (%)	25 hours (%)
Torpedospora radiata	NG.	42 (40)	18 (28)	18 (42)
Corollospora maritima	42 (100)	24 (100)	18 (85)	18 (98)
Zalerion maritima	48 (60)	24 (60)	18 (88)	18 (95)
Asteromyces cruciatus	48 (55)	42 (60)	18 (70)	18 (75)
Dendryphiella salina	48 (60)	24 (88)	18 (86)	18 (78)

NG = No germination after 72 hours.

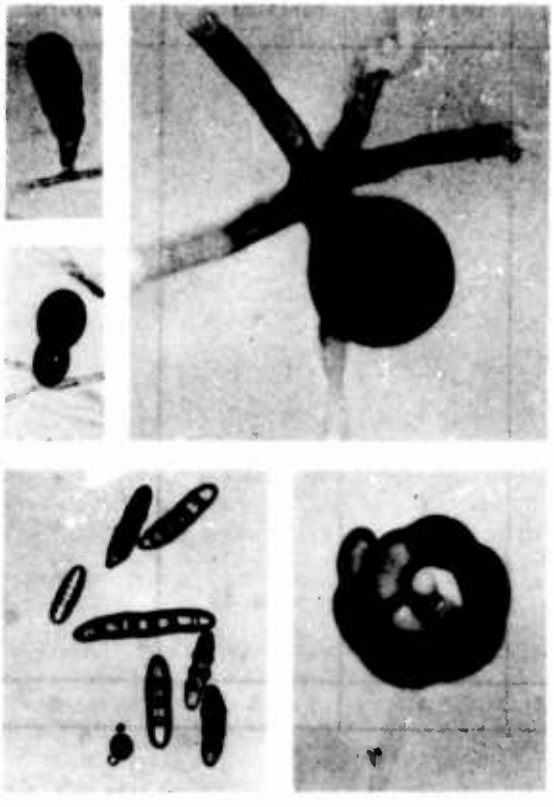


Figure 1. Conidia of some marine Fungi Imperfecti:

(a) *Cremasteria* sp. (x 600); (b) *Humicola alopallonella* (x 600); (c) *Orbimyces spectabilis* (x 1,500); (d) *Dendryphiella salina* (x 500); and *Zalerion maritima* (> 1,000).

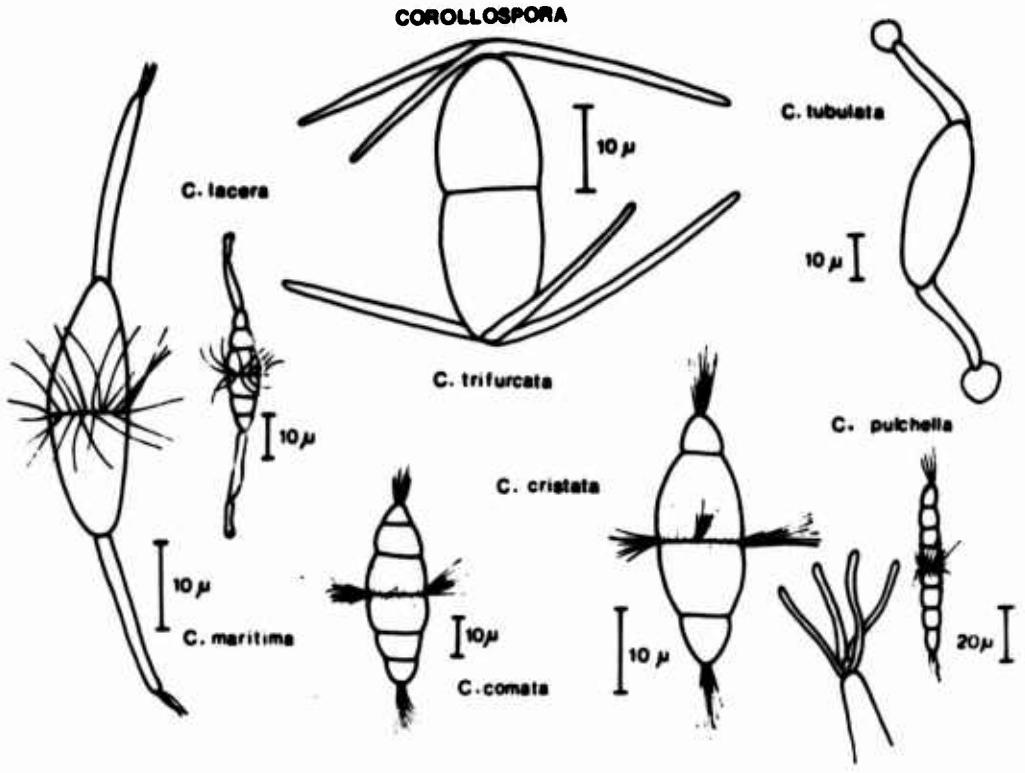


Figure 2. Appendaged ascospores of some species of *Corollospora*.

Fundamental aspects of the problem of antifouling

H. Barnes

The Dunstaffnage Marine Research Laboratory, Oban,
Argyll, Scotland.

The importance of fouling studies to the antifouling problem are outlined. Stress is laid on the necessity to investigate the biology of sedentary organisms as it concerns the solid surface - larval (or spore) interaction: the biology of other stages, larval or adult are largely irrelevant. A distinction is made between two classes of methods to prevent settlement, namely, to prevent contact of spores or larvae so that insufficient time is available for settlement processes to be initiated, or to kill them when in contact with the surface, preferably at a very early stage. Since most settlement takes place when the ship is at rest more attention should be given to strictly 'in-dock' procedures. Contact poisoning - using the term in its widest sense - is far more economical than methods depending upon leaching rate. Attention is directed to some aspects of conventional paints.

Key Words: Antifouling; sedentary organisms; settlement processes

---

I have been asked to give a general introduction to that part of the programme dealing specifically with fouling and its prevention. I shall try to emphasize only the basic chemical and biological problems involved and some possible modes of attacking, if not solving them.

Whilst as a so-called 'academic' I would never wish to decry pure research as a legitimate activity worthy of financial support in any civilized society, and whilst well aware that all too often applied research is often hindered by a lack of fundamental information, it must be clearly recognized that the prevention - and I stress the preventive aspect - of fouling is a problem in applied science: once the problem is stated an end product is defined and, as with all other applied problems, the success of the work must be judged by its practical results: has the object been achieved? has a method of preventing fouling been devised that is capable of being put into practice? In our case the problem, stated in general terms, is to prevent the settlement of marine organisms on materials exposed in the sea: amongst other factors, the kind of materials involved, their use, and their location may affect not only the ultimate solution but also the approach to this solution so that, for example, in our case, the fouling of ships, of harbour structures, of 'permanent' buoys, or of deep-sea structures, pose a series of sub-problems in the antifouling complex. Certain basic aspects will be common to all these sub-problems but each must be approached in its own right and solved in the most appropriate way. We shall be largely concerned with ship fouling.

One of the difficulties of trying to be up-to-date in any discussion of anti-fouling work arises from the secrecy that has surrounded- and to some extent still surrounds - the development of both old and new methods of attack; in the past this was often the result of jealousy between individual firms protecting their own particular formulations and more recently to this has been added the sometimes necessary exigencies of security. It seems unlikely that the difficulties arising from these two sources can ever be avoided.

We should be quite clear at the outset that from the practical point of view the positive aspect of our subject, *i.e.*, the occurrence of fouling as distinct from its prevention, presents no problem at all! - any material if immersed in the sea for a long enough time will eventually collect a settlement of macroscopic marine organisms. If the

surface is in no way repellent to marine organisms then this will happen very quickly: in boreal regions the amount, whether measured by either the area covered or by the weight of material accumulated, will vary greatly according to the season of immersion, but in tropical regions unless the environment is influenced by what may be called 'meteorological' factors such as freshwater run-off arising from, say, monsoon conditions, total settlement may be largely 'non-seasonal'. All this is merely a reflection of the presence of the settling stages of sedentary organisms in the water. In some respects, the study of fouling communities and their development is largely irrelevant to that of anti-fouling since the latter seeks to prevent even the establishment of those species which will give rise to these communities. This is not to argue that the study of fouling - no matter how artificial it may be - is without its own intrinsic interest. The mixture of plants and animals that come to cover immersed surfaces represents an 'isolated' if somewhat artificial community and its development, seasonal changes, the interactions within it, and so forth, are of themselves of considerable biological interest as well as being relevant to studies on the development and structure of communities on hard natural substrata. Most of the work, on what are termed fouling communities has, however, been largely descriptive: much of an experimental nature and also of considerable academic interest to students of community structure and the competition and other factors involved in its development remains to be done. Observations on the development of fouling, if not of fouling communities as such, are nevertheless of some practical importance to antifouling work; in particular, (1) they give information on the seasons and places when and where fouling is particularly prevelant and so indicate the most suitable times and places for conducting tests on the efficiency of any antifouling techniques: it has, for example, long been known that for all-the-year round work tropical testing stations have many advantages; (2) when associated with tests of any antifouling scheme they are able to indicate the relative sensitivity of the various organisms to that technique; in this way it may be possible to select certain key organisms whose reactions to a particular technique may allow an efficient estimate of the antifouling technique to be made; such seems to be the case with regard to the quality of many copper-containing paints since, if barnacle settlement is inhibited, then the leaching rate will be above a certain critical value ($\simeq$ 10μg/cm^2/ day) and other animals are unlikely to settle; rarely,however, do all the settling organisms react in the same relative manner to different antifouling tests; for example, mercury compounds seem to be far more toxic to plants than to animals.

Organisms which become directly attached to a submersed substratum, as distinct from becoming embedded in any microbial or subsequent macroscopic growth, are by nature sedentary in their adult phase and do not, therefore, normally 'arrive' at the surface as adults but in the case of plants as spores, and in the case of animals as larval or juvenile forms. Although in the case of plant spores there must be profound changes - morphological and biochemical - in the transition from spore to sporeling and then to the adult plant and although these are apparently often initiated by contact or events immediately subsequent to contact (about which something will be said by later speakers) in the absence of a nervous system the phenomenon in plants must be far different from that pertaining to animal larvae which usually do have a well-developed nervous system and which on contact with a solid surface may, and in those cases studied do, have a characteristic and complex behaviour pattern during settlement and metamorphosis to the young adult. Even so, it is possible to consider that in both cases there are three fundamental alternatives to the prevention of fouling, namely (a) by preventing the organisms reaching the substratum, (b) by killing them at some larval stage while they are in contact with it, or (c) subsequently as adults. The third alternative is unattractive because (a) growth may be rapid and the effect of even small and low-growing attached organisms is soon felt in terms of ships performance, (b) the adult may - though not necessarily - be more difficult to kill, and (c) even if killed, sufficient residual dead material, either plant or animal, may remain seriously to interfere with performance, and, as a result of gregarious behaviour, to attract larvae when the latter are present: many years ago it was common practice for mariners to take their ships into tropical estuaries and this was often an effective - if from some other points of view rather drastic - antifouling procedure; the lowered salinity killed the fouling and the current, often in such situations carrying much silt, removed the dead remains. We shall consider only the two former possibilities. In passing, it is perhaps not inappropriate to remark that unless mass poisoning of the whole body of water surrounding a ship - say, a whole dock basin - is envisaged, then there is little point in studying the larval

stages preceeding that at which settlement takes place, except in so far as their behaviour and reactions are expected to mirror those of the settling stages. Perhaps one exception may be made to this somewhat sweeping statement; characteristically the action of contact with a solid surface is to inhibit those nerve centres responsible for swimming so that studies of the swimming behaviour might contribute to our knowledge of its inhibition.

Since many of the plant spores involved in fouling are non-motile and since there is no evidence that the motile larvae of sedentary animals actively seek out solid surfaces as distinct from reacting to them once encountered - some of the problems of the prevention of settlement are still common to both groups. The prevention of settlement may be obtained by (a) providing physical conditions near the surface that are inimical to the organisms; this may involve producing conditions, which do not allow sufficient time for any contact stimulus to act or in common parlance, involves 'keeping the organisms away from the surface', or (b) killing them before contact is made e.g., surrounding the substratum with a poisonous 'layer' (one may point out in passing that there is little information on what part this plays in the action of a normal antifouling paint, i.e., whether the larvae are destroyed after settlement or deterred before they come into contact with the surface). The simplest physical procedure to prevent any stimulatory contact is to keep the water over the surface moving at some critical velocity either as a laminar flow or as a turbulent motion. This is the remedy adopted (possibly in combination with other features such as inhibitory slimes) by many marine organisms such as fish and could be adopted by a shipowner if he decided never to dock his ships - in itself rather an unpracticable remedy. From subsequent papers it will appear that the current speed required to prevent the settlement of algae spores is far in excess of that for animal larvae. This does, however, lead to an important aspect of antifouling work, namely, that whether prevention of contact or interference with subsequent events is the selected procedure, they are only particularly needed when a ship is in dock or harbour, so that procedures which run themselves down to no effective purpose while the ship is in motion are, to put it mildly, wasteful; to paint a ship with an antifouling composition in winter in a northern port, dispatch it several thousand miles eventually to dock in a tropical harbour is not good business practice. Perhaps because other aspects of running ships are more important, owners seem to have paid little attention to their schedules in relation to antifouling costs. I am sure that a knowledge of such facts about seasonal fouling conditions in various localities could enable considerable economies to be made in the running of fleets of ships, particularly in a restricted locality.

Although various strictly dockside procedures - mostly unsuccessful - have from time to time been tried at least in a preliminary way - I wonder whether dockside procedures have received sufficient attention either from the scientific or economical point of view. How feasible and, in view of the ever-increasing sophistication of underwater engineering, how attractive could an 'in-dock' antifouling service be? How economical could it be made? How could it be fitted in with other docking facilities? Clearly the answers to these questions depend upon the development of a reliable procedure capable of preventing settlement on a stationery vessel over a restricted period of time. Is it totally impossible that a vessel could not be given a regular 'in-dock' wipe down by mechanical means, perhaps with a poisonous and temporarily adhesive solution? These questions do allow us to stress the advantages or otherwise of treating a ship in dock: on the one hand, extensive dock-side facilities would be available to which recourse is not possible with the ship under way while, on the other, such an antifouling procedure would have to be fitted in with repair work and the like and similar facilities for ships using any such technique would have to be available in all the major ports: the setting up of such, if it were successful, would surely be well within the capacity of a modern business. In this connection one has to remember that current antifouling procedures are low in priority relative to other activities on docking; indeed they are the veritable Cinderella. Of course any such facility depends upon the development of a successful technique and the ones most obvious to explore (it has been done in a preliminary way but with equivocal results) are those preventing contact or killing the organisms before contact. It would hardly be acceptable when the public is concerned - and quite rightly so - with the spread of pollution to suggest a toxic dock - but it is possible. It would be possible to retain the toxic water and destroy its toxicity before release into the general body of the water. More reasonable, are procedures which depend upon a creating turbulent motion at the surface of the hull: a stream of air bubbles has been investigated.

Perhaps, however, it will be necessary for some time to depend upon procedures some of which, however wasteful, depend upon the production of a toxic effect at the surface of the paint. In spite of some assertions to the contrary all the available evidence strongly suggests that if a poison is to be incorporated into a paint it must be released at a certain minimum rate to be effective. In other words, we are dealing with a two-phase system of paint-water: there is little evidence that any successful contact paint - only poisoning the organisms when in contact with the film so that the poison passes, so to speak, directly into the organism - has been developed. More attention should be given to this possibility since it would obviate the necessity for a critical leaching rate with its obvious wasteful loss of poison. The development of any such contact mechanism has clearly to depend upon the passage of material across the cellular boundaries, plant or animal, and the structure and composition of these - about which a great deal is now known - should be carefully considered in relation to the chemical composition and physical structure of the paint. In the development of any such technique it will be necessary to study the surface-larvae (or surface-spore) system as a whole: the behaviour of a barnacle cyprid - and still less the nauplius stage - in the free-living state would be largely irrelevant except perhaps for preliminary tests. The possibility of using lipid-soluble materials immediately comes into question, but the difficulties - not the least of which is that of maintaining a specifically designed paint surface in its original form over long periods under sea water - are severe if not insuperable. If it were to prove possible to interfere with the cementing mechanism, or other adhesive reaction, at the interface between the paint and the animal then material - and only a very small quantity - might be lost from the film: however, once again it will prove difficult to maintain such a carefully designed surface in the same effective condition over a long period. Furthermore, such a mechanism would perhaps have to be species-specific so that more than one contact inhibitor would be required to deal with the variety of fouling organisms normally encountered: one only needs to recall the 'apparent' simplicity of spore adhesion with the complex behaviour of a cyprid and its ultimate cementing to a surface. In some ways this suggestion resembles that put forward by those who advocate the study of marine animals which live in the marine environment and yet do not become fouled and in which the production of inhibitory materials - probably slimes rather than poisons - are supposed to be important. Yet the continuous production (formation) as distinct from release by chemical or physical means, in a solid film such as paint, of compounds such as are continuously generated by living processes would seem to be extremely difficult. Possibly some guides may be obtained from the considerable body of information on the clumping and dispersion of some animal cells under different environmental conditions.

Perhaps for some time, and certainly if some risks are not to be taken, it will be necessary to try to improve the performance of conventional antifouling coatings either in terms of their ability to prevent fouling or their cost relative to a given life. If one is going to accept this position - at least for the time being - it seems that whatever the detailed mechanism involved the necessity to maintain a critical rate of loss of some poisonous material must be accepted. It then becomes even more desirable to define the objective since further investigations are likely to give diminishing returns. Improved coatings with conventional poisons might extend the life of antifouling films by a factor of three: new and more powerful toxins should give even further improvements. Yet, with conventional coatings, the efficiency of the coating is likely to be considerably impaired, of not virtually ruined, if the paint dries out at a dry-docking for whatever purposes it is made. With such coatings - unless one can be developed which will retain its effectiveness after drying out - it is pointless to aim for a longer life than that between anticipated successive visits to dry dock. Improvement of the present position will have to be based on the use of more efficient poisons so that a lower leaching rate is effective (much work goes on in this field), the matching of these poisons to the paint media, combined with an improvement of the adhesion and compatability of the various coatings to one another and to the hull of the ship: much of this is pure paint technology. Related to this conventional approach, since it would have to be based on the leaching principle, is the possibility of developing a totally toxic film as distinct from enclosing a discrete toxin within a more or less conventional film. This could take the form of a metal polymer complex with the required properties or of a completely organic poisonous coating: wastage, in the sense that in a conventional coating a large part of the film must dissolve in order to release the poison, would be eliminated. Even if it proves too difficult to make a totally

poisonous film it may be possible to develop one in which a 'liquid' toxin diffuses through the matrix without dissolution of the latter: this would involve maintaining a concentration gradient between the outside and inside of the film: much is now known of diffusion in and through solids and this possibility should be explored. In the normal copper paint, except when sufficiently loaded with toxin to give so-called contact leaching, release of the poison requires as stated above, the dissolution of part of the paint - usually an acidic component (often rosin) by the alkaline sea water. Many such paints often have a far less useful life than would be expected from their copper content: this is usually ascribed to the deposition of insoluble copper.

From the purely practical point of view there is always the vexed question of accelerated tests: in the case of conventional films it is well known that the effective life in service and that on a test panel exposed from a raft are different by a significant amount and both differ from that calculated from standard leaching rate tests: it is highly desirable to have a test which relates the test performance to that on ships in service. There is little point in merely imitating service conditions in the laboratory since this would not lead to any acceleration: so far, accurate information has only been obtained by comparing the results of exposure tests, leaching rate tests on raft exposed panels, and analysis of samples from the ship's hull at known times during service. The results of any accelerated test must be calibrated against the third kind of information. Any effort to increase the rate of solution of the rosin acidic component must take into account the different effects of the solution - normally an alkali containing a complexing agent for the copper ion - including the solution of insoluble copper compounds deposited in the matrix which are particularly important when thick films are being considered, and also the physical effects of any increased speed of panel relative to the solution used.

To summarize: the possibilities of in-dock treatment should be further explored; attention should be directed to possible methods in which the inhibitory action is only implicated when the settlement stage is in contact with the surface: further improvements in the conventional approach might come from efforts to increase the toxicity of the poison if its solubility can be matched to that of the matrix, or better still if a totally toxic film can be developed: it will be essential to concentrate on those aspects of the biology of sedentary organisms truly relevant to antifouling.

Elek Lindner and Carol A. Dooley

Mare Island Naval Shipyard
Vallejo, California 94592

The adhesive cement of the barnacle Balanus crenatus was studied by histochemical, histoenzymological, chemical, and instrumental analytical methods. The results suggest that the hardening mechanism of the cement is based upon a quinone type crosslinking of the proteinaceous secretion. In such a mechanism, free amino groups of the protein are bound by the very reactive semiquinones which form from o-dihydroxyphenols through phenolase catalyzed oxidation. Melanin formation usually accompanies this mechanism.

In support of this mechanism more than 80% of dry weight of the cement proved to be protein with appreciably high lysine content, as source for free amino groups. In the hardened cement, aromatic crosslinks were indicated with bond strength close to that of C-N covalent bonds; also stable free radicals such as the semiquinones were detected by EPR. The reducing compounds demonstrated both in the cement and the glands can be phenolic precursors of the quinones. UV spectroscopy and evidence for chelated iron suggest o-quinonoid derivatives to be present. Phenolase was demonstrated throughout the secreting apparatus and the secretion. Also, melanin could be detected in the cement. Finally, a comparative study of the barnacle adhesive and a known quinone crosslinked protein, the mussel byssus, showed similarities.

Although the results indicate quinone crosslinking for the hardening mechanism of the barnacle cement, the phenolic precursor of the quinone has not yet been isolated. The facts that there is only one type of gland in the barnacle to secrete the protein, phenolics and enzyme necessary for the quinone crosslinking mechanism and that there is a lack of detectable phenolics could suggest a new type of "strict autotanning," involving a phenolase catalyzed oxidation of the phenolic residues of the phenolase itself, in the absence of other substrates, which in turn crosslinks with free amino groups of other phenolase molecules.

Key Words: Barnacle; cirriped; crosslinking; bonding; histochemistry; spectroscopy; protein; enzymes; quinones; adhesive; hydrolysis

---

1. Introduction

The present paper is a direct continuation of our paper presented at the Second International Congress in Athens, Greece (1)[1] which summarized our biological survey of the attachment mechanism of barnacles and demonstrated a unique method for isolating the barnacle adhesive in relatively high purity.

---

[1] Figures in parentheses indicate the literature references at the end of this paper.

It was shown that the initial attachment of the barnacle is a purely mechanical hold, established by the antennular suction cups of the last larval stage of the barnacle, the cyprid, which is reinforced by adhesive cement. The minute quantity (0.1 microgram) of the cyprid cement makes its collection without contamination very difficult. Although larger amounts of cement are secreted by the growing adult, they are spread in concentric circles between basis and substratum in approximately a five micrometer layer, which makes the collection of this type of the cement for analysis equally difficult. A method for increased cement production was developed in the laboratory by carefully detaching barnacles, which invariably will make an attempt at reattachment (Fig. 1). Reattachment is possible because the ducts are not plugged by hardened cement, but flushed out after the primary secretion to keep the ducts open for emergency repair or reattachment by a secondary secretion (2). This secondary cement can be collected relatively free of contamination in quantities sufficient for analysis.

It was established that the cyprid, the primary, and the secondary cement are histologically and histochemically identical. This was done by locating the cement glands and studying their development and function in relation to the rest of the cementing apparatus. Although the cement glands of the pedunculate barnacles (Lepadidae) were studied by Darwin (3) and their cytological details and functions described by Krüger (4), the first accurate report on the glands of a sessile barnacle (Balanidae) was published only recently (5). Our studies showed that the cement glands are giant unicellular glands (100 to 200 micrometers in diameter) with a large nucleus containing several nucleoli and a dense cytoplasm with several vacuoles (Fig. 2). These permanent, periodically functioning glands develop directly from the cement glands of the cyprid with more and more such glands joining them as the growing animal requires more cement. The knowledge of the exact location of the cement glands permits studies on the cement precursors either by histochemical methods in situ or by chemical and instrumental analysis through extraction, fractionation, and isolation.

Based upon the information gained during the biological phase of our research, the chemical characterization of the hardened cement was undertaken through histochemical, solubility, ultraviolet and infrared spectral, elemental and amino acid analyses methods.

2. Results

Histochemical methods (6, 7, 8) were found convenient for obtaining preliminary information on the chemical character of the cement in situ without time-consuming collection processes and without the danger of contamination. All three types of adhesive cement of the barnacle Balanus crenatus, Bruguière were subjected to the histochemical tests: the cyprid cement, the primary or normally secreted adult cement, and the secondary cement. In addition, these reactions were performed on the cement glands and the results on the cytoplasm and the nucleoli were recorded.

Tests for lipids, carbohydrates and proteins are summarized in Table 1. Neither lipids, nor carbohydrates could be demonstrated with certainty in any type of cement. Direct staining methods (LISON-DAGNELLE, SHEEHAN-STOREY and ELFTMAN-1957) gave negative or very weak positive results with SUDAN BLACK B. BAKER'S ACID HAEMATEIN method gave a stronger color after the lipids were extracted by pyridine; therefore, the test must be considered negative. According to the method by ELFTMAN-1954, after carefully controlled chromation, non-lipids stain with HAEMATOXYLIN only, non-chromated lipids with SUDAN BLACK B only, and chromated phospholipids with both dyes. The barnacle cement showed stronger staining with HAEMATOXYLIN. Based upon the results obtained with controlled chromation by ELFTMAN, phospholipids are indicated in the cytoplasm but there is only a slight indication for lipids in the nucleoli of the cement glands.

The classical PAS (Periodic acid-Schiff) method for carbohydrates gave very weak or no coloration with all types of barnacle cement. Acetylation and deacetylation, techniques designed to improve specificity of the reaction, did not change the results appreciably; therefore, carbohydrate is not indicated. Methods for acid mucopolysaccharide, such as ALCIAN BLUE, METHYLENE BLUE AT pH 4, METACHROMASIA of AZURE A induced by sulfation, and also the METHYL VIOLET method for amyloid were negative with the cement. In the cement gland cytoplasm METHYLENE BLUE and ALCIAN BLUE methods were positive, but the hue with ALCIAN BLUE and the lack of METACHROMASIA after sulfation indicate nucleic acids rather than acid

mucopolysaccharides. In the nucleus, however, sulfated mucopolysaccharide was indicated by autoradiography using sulfur-35 tagged sulfate (Fig. 3).

In contrast to the negative results for lipids and carbohydrates all three types of cement gave positive reactions with histochemical methods for proteins, such as the MERCURY-BROMPHENOL BLUE, MILLON, and MOREL-SISLEY diazotation methods. Unexpectedly, the MOREL-SISLEY method indicated tyrosine only in low concentration in the cytoplasm of the cement glands and no tyrosine in the nucleoli. Unfortunately, these results could not be confirmed by the MILLON reaction because of the destructive nature of its reagents. The results of the reactions for tryptophan are also remarkable. Except for very limited positive results with DMAB (p-dimethylaminobenzaldehyde) on the outside surfaces of the secondary cement (owing perhaps to artifacts) both the DMAB and NED (naphthyl ethylene diamine) reactions showed negative results with the cement. In the cement gland, however, both methods were mildly positive in the nucleoli and in the cytoplasm; and DMAB indicated large local concentrations of tryptophan in the cytoplasm.

Simple histochemical staining reactions based on coupling the colored ions of organic dyes with ionic functional groups of tissue components, which carry an electric charge opposite to that of the dye ion, can be indicative of the chemical character of the functional groups. Table 2 lists some of these staining reactions. All three types of cement stain with anionic dyes such as EOSIN Y, ERYTHROSIN B and ORANGE G, but do not stain with cationic dyes such as ALCIAN BLUE, AZURE A, CELESTIN BLUE, JANUS GREEN, METHYLENE BLUE, NEUTRAL RED or THIONIN. Such staining characteristics would indicate cationic functional groups, such as free amino groups, in the tissue rather than anionic groups, such as carboxyl or sulfate groups. In staining with amphoteric dyes the anionic sulfonate groups of LIGHT GREEN, ACID FUCHSIN and ANILINE BLUE WS dissociate more strongly than do their amino groups, thus they stain barnacle cement as do the anionic dyes, indicating free amino groups. The chemical reaction mechanism of staining with combinations of dyes such as the GALLEGO-GARCIA, MALLORY TRICHROME, MASSON-PATAY, or SCHNEIDAU methods is not sufficiently understood for chemical evaluation of the results. Nevertheless, the results with these dye combinations are included in our table mainly for their historical value. Another popular group of histological stains is the MORDANT HAEMATEINS. Owing to its phenolic hydroxyls the naematein is mildly anionic and forms insoluble salts or lakes with certain trivalent-metallic compounds (mordants). Thus, the dye binds with the tissue components through the metallic mordant and acts similar to the cationic dyes. Accordingly, the DELAFIELD, EHRLICH and HARRIS methods were negative with the cement, but HEIDENHAINS method, using ferric alum as mordant, gave a positive result. This could be the result of the cement's affinity toward iron, which will be shown later.

The cement glands showed more complex staining. As with most of the other histochemical reactions, the coloration produced by the histological stains are not uniform throughout the entire cytoplasm. Such variations indicate concentrations of various materials with different functional groups. The cement gland cytoplasm shows such staining intensity variations with anionic dyes, while the nucleoli stain more strongly and uniformly. Only weak staining can be attained with the cationic dyes THIONIN and AZURE A in the cement gland. Nuclear stains, such as the MORDANT HAEMATEIN technique, readily stain both the cytoplasmic portion and the nucleoli of the cement gland. Staining with the amphoteric dyes deserves notice. While LIGHT GREEN stains cytoplasm but not the nucleoli and ANILINE BLUE WS gives various but intense staining in the cytoplasm but weak staining in the nucleoli, ACID FUCHSIN stains the nucleoli very strongly in aqueous solution but stains the cytoplasm only in strong acidic media.

The behavior of ACID FUCHSIN suggests a low isoelectric point for cytoplasmic structures. Also, the variations in color intensity in the cytoplasm with most of the other single dyes and dye combinations indicate tissue elements with different isoelectric points. By staining the cement gland separately with the anionic ORANGE G and the cationic METHYLENE BLUE dyes buffered to various pH values covering a range from one to ten in 0.2 pH increments, the isoelectric points of the cell elements were determined. While the same method gave an isoelectric point of about 8.2 for the hardened cement and about 5.9 for the nucleolus, different areas in the cytoplasm range from 3.9 to 9 in isoelectric point. Those areas of the cytoplasm where the isoelectric point is approximately six appear to coincide with larger concentrations of tryptophan.

Histochemical reactions for some of the functional groups of the cement are summarized in Table 3. Free amino groups were demonstrated in the hardened cement as well as in the cytoplasm and the nucleoli of the cement gland by the NINHYDRIN-SCHIFF, combined with deamination control, and by the SOLOCHROME CYANINE RS and the ALKALINE FAST GREEN techniques. The SCHIFF reaction was weakly positive for aldehydes in the hardened cement and strongly positive in the cement gland cytoplasm and nucleoli, however, the presence of aldehydes could not be confirmed by the GOMORI HEXAMINE SILVER method. Sulfhydryl groups were demonstrated by the ALKALINE TETRAZOLIUM and SCHMORL ferric-ferricyanide method in the cement, but only weak reactions were obtained in the cytoplasm and the nucleoli of the cement gland. ADAMS thioglycollate-ferric ferricyanide method indicated some disulfide bridges in both the cement and the gland. A weak positive reaction after blocking the sulhydryl groups with phenylmercuric chloride suggests reducing groups other than -SH or -S-S- in the hardened cement. By the method of LILLIE the absorption of iron (II) ions, believed to be chelated by o-quinhydrone type compounds, was demonstrated in the cytoplasm. With the VULPIAN ferric chloride reaction for such o-dihydroxyphenolic compounds, only the primary cement gave a weak positive reaction. The MASSON-FONTANA method designed for detecting melanin, an o-dihydroxyphenol derivative, was positive in the cyprid cement (Fig. 4) but weak in the primary cement.

Based on the histochemical reactions, there is strong indication that the barnacle adhesive has a high content of protein with an abundance of free amino groups; and also some reducing groups or compounds are indicated. In the cement gland cytoplasm, where the precursors of the adhesive are expected, tryptophan was found in high local concentrations, which appear to be concurrent with variations of isoelectric points in various areas throughout the cytoplasm. Also there was some indication for quinhydrone type compounds being present in the cement gland.

A number of conventional analytical techniques on the hardened cement are hampered by its extreme resistancy toward solvents. The chemical and physical stability of the hardened cement, or its resistancy toward dissolution, depends on the crosslinks which hold the individual protein chains together. The weakest of these linkages, produced by the Van der Waals forces, cleave in boiling water. Proteins with a majority of salt linkages will swell or dissolve in dilute acids or alkalis. Dissolution or swelling in salt solution indicates mainly hydrogen bonds. Scleroproteins crosslinked by covalent bonds are the most stable. Disulfide bridges of the keratin type scleroproteins can be disrupted by thioglycollate solution (9). The strength of the C-N bond in crosslinks of collagen derived from Schiff-base type condensations (10) or in the quinone-amine bridges of the arthropod cuticle (11) is quite near to that of the peptide bond, therefore, hydrolysis with strong acids or alkalis will disrupt these bridges simultaneously with the protein backbone. While the C-C bonds in crosslinks of collagen derived from aldol type condensations (10), in di- and trityrosine bridges of resilin (12), and in desmosine crosslinks of elastin (13) appear to be even stronger, these scleroproteins also dissolve in strong acid or alkali because of the hydrolysis of the protein backbone. Proteins with aromatic crosslinks such as the quinone, dityrosine and desmosine types appear to dissolve rapidly in sodium hypochlorite (14) owing to the cleavage of the aromatic ring, although other bonds such as the peptide linkage break as well.

Most solubility tests on the barnacle adhesive gave negative results. The larval cement of the barnacle showed only an extremely slight swelling after one week in 0.2 N NaOH, indicating some salt linkages, but readily dissolved in hypochlorite which indicated aromatic or peptide bridges (Fig. 5). Based on our present knowledge about the synthesis of peptides in nature, peptide crosslinkage does not seem to occur readily outside an organism. Also, indications are that the formation of crosslinks in resilin may require a few days or weeks (15) and desmosine forms even slower (16), therefore, these types of crosslinkages do not seem to be suitable for the barnacle adhesive, which hardens within hours. By elimination, the results of the investigation of bond strength of the crosslinks suggest quinone crosslinking.

Quinone crosslinking appears to be one of the more expected reaction mechanisms for the barnacle cement. The barnacle is an arthropod and quinone crosslinking has been established (11, 17) to be a hardening mechanism used by arthropods in the formation of the epicuticle (Table 4). The hardening of the cuticular protein is accomplished by the penetration of a derivative of the blood tyrosine (11, 18, 19) in which a second hydroxyl is attached by the phenolase enzyme (20) to the aromatic nucleus (21) and the aliphatic chain is

altered (11, 22, 23, 24, 25, 26). This o-dihydroxyphenol is oxidized by the phenolase (27) to a semiquinone free radical (28) which reacts with the free amino groups of the protein (29). The quinone crosslinking mechanism is usually accompanied by melanin formation from phenolic compounds through the catalytic action of the phenolase (30). Semiquinones can form quinhydrone type compounds (31) or dimers of semiquinones (32) which are capable of chelating ferrous ions (33). Since semiquinones are relatively stable free radicals owing to their symmetrical resonance system (34), it was suggested that unreacted free-radicals might be trapped within the cement structure. Electron paramagnetic resonance (EPR) spectroscopy, which is one of the most sensitive methods of detecting free-radicals, did indeed show bands that might be attributed to a quinone type free-radical (Fig. 6). The purified barnacle cement showed a single absorption with a width of 5-10 gauss at approximately $g = 2.01 \pm 0.01$. Although the hyperfine structure of the spectra is not available at this time for more precise analysis, the approximate g value and absorption width corresponds with those reported in the literature for quinone type free-radicals (35, 36).

Besides arthropods, there are other organisms also using quinone crosslinking processes. One of these is a mollusc, the mussel Mytilus edulis, which uses quinone crosslinked protein for attachment (37, 38, 39, 40, 41, 42). The elemental analysis of the barnacle and mussel adhesives show some similarities (Table 5). The major difference is in the nitrogen content, which indicates a somewhat higher protein content for the mussel adhesive. The estimated protein content of the barnacle cement is 87.5% versus 96.4% protein in the mussel byssus. Although the individual amino acid contents of the mussel byssus and the barnacle cement show some differences, general similarities can be observed (Table 6). In general, basic amino acids, lysine in particular, and aspartic and glutamic acids, both dicarboxylic acids which can be hydrolysis products of their amides, are represented in relatively larger quantities (7.0-8.7%) in both secretions. This is in accordance with the quinone crosslinking mechanism since the quinone binds with free amino groups. Both nonpolar and uncharged polar amino acids, on the other hand, are present in moderate quantities (each less than 6.5%). Glycine and, to a certain extent, alanine are exceptions. These amino acids are in relatively much larger quantities in the mussel byssus (22.9% and 8.5% respectively) than in the barnacle cement (6.5% and 4.5% respectively). The high glycine and alanine content is characteristic of structural proteins with considerable tensile strength such as resilin (31% glycine, 11% alanine) (43), collagen (33% glycine, 11% alanine) (44), elastin (36% glycine, 19% alanine) (45), and silk fibroin (45% glycine, 29% alanine) (46). Similarly, the thin threads of mussel byssus which anchor the heavy shell must have high tensile strength. The barnacle cement, however, is spread only in a thin layer between the basis and the substratum, and tensile strength might not play such an important role.

There is a noticeable similarity between the IR spectra of the cement of the barnacle Balanus crenatus and that of the mussel Mytilus californianus (Fig. 7). The major bands around 3300 cm^{-1} (N-H stretching), 1650 cm^{-1} (C-O stretching), and 1550 cm^{-1} (N-H bending) are characteristic bands for proteins and polypeptides. Most other bands such as 3070 cm^{-1} (N-H stretching), 2960 cm^{-1} (C-H stretching) and also 1230 cm^{-1} and 1160 cm^{-1} (backbone vibrations) are always present in polypeptide spectra. The moderate absorption band at 1080 cm^{-1} can be assigned to C-O stretching, O-H bending, or C-O-C stretching in ring structures which could indicate some polysaccharide although a number of other functional groups including ethers, aldehydes, and amines also show absorption in this region.

Since aromatic compounds show absorption in the UV domain, the aromatic crosslinking mechanism was studied by UV spectroscopy on model reactions as well as on the hardened barnacle and mussel secretions (Fig. 8). Model studies using amines, amino acids, peptides, and crystalline proteins reacted with p-quinone indicate that the product of these reactions can be characterized by a strong absorption at 345 nm. Similar reaction products using o-dihydroxyphenol and phenolase enzyme in place of p-quinone produce less intensive absorption around 325-330 nm. In order to study the UV spectra of hardened secretions of the barnacles and mussels, these highly insoluble substances had to be brought into solution without the disruption of the crosslinks. Thin-layer chromatograms (TLC) of substances hydrolyzed by 8N HCl at 40°C indicated that the hydrolysates of the model compounds as well as the mussel byssus contained larger peptides besides amino acids, while the barnacle cement hydrolyzed completely. On the other hand, TLC indicated only partial hydrolysis of the barnacle cement by $Ba(OH)_2$ at 125°C for 48 hours, producing

peptides and amino acids. The UV spectra of the cold 8N HCl hydrolysate of the mussel byssus and the $Ba(OH)_2$ hydrolysate of the barnacle adhesive show absorption at about 325 nm indicating that these proteinaceous substances are crosslinked by o-quinonoid bridges.

In nature aromatic crosslinking of proteins by o-quinones is catalyzed by a phenolase enzyme complex (20), which is believed to hydroxylate monophenols to o-diphenols (21) followed by the oxidation of the latter to o-quinones (27). The same enzyme complex is believed to catalyze the dark melanin pigment formation (30) from 3,4-dihydroxyphenylalanine (DOPA), the o-dihydroxy derivative of the monophenolic amino acid tyrosine. By introducing DOPA into the tissues the location of the phenolase enzyme can be determined by the dark pigment formation which indicates the probability of the quinone crosslinking mechanism, especially in light colored tissues and substances. Using this method, strong phenolase activity was demonstrated in the cyprid cement near the remains of the antennules, where the location of the primary secreting orifices is suspected, and in some portions of the adult duct network (Fig. 9). This histochemical reaction was also positive in sections of primary and secondary adult cement. The presence of the phenolase enzyme was positively demonstrated inside the cement glands (Fig. 10) by using activators such as Cu^{2+} ions or UV radiation, modifying the length and temperature of the incubation, and employing enzyme inhibitors such as cysteine, cyanide or diethyldithiocarbamate. Phenolase activity in the cytoplasm appears to coincide with areas having an isoelectric point of approximately 6. The enzyme concentrates around the secretion collector channels and the dark melanin particles reveal the phenolase to be entering and moving in these channels in high concentration. The demonstration of the phenolase enzyme in the cement glands, secreting ducts and hardened adhesive represents a decisive indication for the quinone crosslinking being involved in the hardening mechanism of the adhesive cement of barnacles.

3. Discussion and Conclusions

The chemical investigation of the barnacle adhesive cement outlined above resulted in the recognition of a hardening mechanism characterized by quinonoid type aromatic crosslinking of proteinaceous substances. Such a mechanism is not entirely unexpected.

As early as 1932, based upon his observations on other Crustacea, Yonge (47) speculated that the secretion of the cement gland of the Cirripedia may be similar to the cuticle. Thomas (48) elaborated on this idea by attempting to show that the cement glands of the Cirripedia are modified tegumental glands, although these glands in the Balanidae were not found and described until much later (5). In the meanwhile, Pryor's classical works (11, 17) elucidated a great deal of the hardening mechanism of cuticular protein by introducing the concept of aromatic crosslinkages. In his scheme, free amino or other reactive groups of the protein are crosslinked by an ortho quinone, which is formed from monophenols via diphenols by a phenolase catalyzed oxidation. Although, based upon the combination of these early results, several authors (49, 50, 51, 52) speculated whether the barnacle cement could be "quinone tanned protein," chemical or histochemical analysis of the adhesive of the Balanidae was not attempted until recently.

In one of these early attempts, Lacombe (53) indicated acid mucopolysaccharide in both the intra- and extracellular secretion, but Lindner and Dooley (54) showed the proteinaceous nature of the cement and determined its amino acid profile. Shortly thereafter, Lindner and Dooley (55) and Saroyan et al. (56, 57) reported results which were already suggesting concurrency with the quinone crosslinking mechanism. The subsequent results of Hillman and Nace (58) and Cook (59) were in agreement with the proteinaceous nature of the barnacle cement. By histoenzymology, Arvy et al. (60) found alkaline phosphatase activity in the cementing apparatus, and Arvy and Lacombe (61) claimed that succinodehydrogenase was demonstrated in young cement glands. Shimony (62) speculated that arylsulfatase found in the mantle tissue could be associated with sulphated mucopolysaccharides in the hardening process of the adhesive. But recently, Lindner et al. (63) demonstrated the enzyme associated with aromatic crosslinking of the adhesives. This type of hardening mechanism of the barnacle adhesive is indicated by a series of results.

1. In support of the histochemical results which indicated a proteinaceous adhesive containing free amino groups and reducing compounds, instrumental analysis showed protein in excess of 80% of the dry weight of the adhesive of the barnacle Balanus crenatus. The relatively high lysine content in the protein fraction is probably the major source of free amino groups for crosslinking.

2. The extreme resistance of the hardened cement toward dissolution is an indication of the character of the crosslinks. Resistancy toward selected salt solutions and dilute acid or alkali solutions rules out weaker than covalent bonds, such as hydrogen or salt bonds, as major stabilizing links. Resistancy toward thioglycollate rules out disulfide bonds also. Complete hydrolysis in strong hot acids and alkalis suggests crosslinks with a bond dissociation energy close to that of the peptide bond and rapid dissolution in strong oxidizing agents (NaOCl) is suggestive of the destruction of aromatic crosslinks.

3. Free radicals were found trapped in the hardened adhesive. Such free radicals have to be relatively stable. Semiquinones are one type of such rare stable free radicals (34) which can survive for an appreciably long time. The EPR spectra of the hardened adhesive shows absorption which corresponds with that reported in the literature for quinone type free radicals (35, 36). Attempts to isolate the crosslinking quinone or its phenolic precursor from the barnacle adhesive have not yet been successful. However, reducing compounds, other than thio compounds, were indicated both in the hardened adhesive and inside the cement glands by histochemical methods. In the cytoplasm of the gland cells a slight absorption of ferrous iron could suggest possibility for o-quinhydrone, which forms an iron complex.

4. Model reactions indicated that the product of the reaction between quinone derivatives and compounds with free amino groups develops characteristic absorption bands in the near UV region between 300 and 360 nm. The characteristics of this absorption are dependent upon the reacting species and the type of resulting bond. TLC of the barnacle adhesive hydrolyzed by $Ba(OH)_2$ indicated only partial hydrolysis. This hydrolysate showed absorption at about 325 nm, typical for proteins crosslinked by enzymatically produced o-quinone.

5. The elemental analysis and the amino acid profile of the barnacle adhesive show similarities to those of the byssus of the mussel Mytilus, a quinone crosslinked protein (37). The mussel byssus is somewhat higher in protein and higher in glycine and alanine content, but the other significant amino acids: aspartic acid, glutamic acid and lysine, appear in about the same ratio in both the barnacle and mussel secretions. The similarity between the IR spectra of the barnacle and mussel adhesives is another indication for the barnacle cement having a chemical composition similar to that of a known quinone crosslinked protein.

6. By incubation with DOPA, phenolase, the enzyme connected with quinone crosslinking mechanism, was demonstrated in the hardened cement, particularly in the cyprid cement, inside the secreting duct network, and most significantly inside the cement glands. Larger phenolase concentrations in the cytoplasm appear to coincide with areas having concentrations of tryptophan and an isoelectric point around 6. Since the optimum activity of phenolase occurs between pH 6 and 7, activation of a proenzyme in these locations is indicated.

7. Phenolase catalyzed crosslinking is usually accompanied by dark melanin formation (30), although light colored sclerotized structures are also known. The barnacle adhesive has a light yellowish color even when dry, nevertheless, traces of melanin type compounds were indicated, at least in the cyprid cement, by their silver reducing characteristics.

Although it is recognized that far more work is necessary for thorough understanding of the hardening mechanism of the barnacle adhesive cement, there is a series of compiled evidence that at least one type of the major crosslinks responsible for its hardening is brought about by a mechanism similar to that of the extensively studied arthropod cuticle sclerotization. Tryptophan may have a possible role in this hardening mechanism, since it appears in large concentrations in the gland itself but not in the hardened cement. In view of the work of Dennell (64, 65), Pryor (66) and Fuzeau-Braesch (67, 68) tryptophan might be a potential candidate as a hardening agent, especially for light colored structures, such as the adhesive cement of the barnacles.

The facts that there is only one type of gland in the barnacle to secrete the protein, phenolics and enzyme and that there is a lack of detectable phenolic precursors raise the question whether this mechanism is not a type of "strict autotanning" speculated by Mason (69) involving a phenolase catalyzed oxidation of phenolase itself in the absence of

other substrates. In this scheme, the phenolase acts upon itself by oxidizing the phenolic groups (tyrosine for example) attached to its peptide backbone. These oxidized phenolics can then react with the free amino groups of other phenolase molecules to produce a crosslinking. The inactivation of the phenolase during catalytical oxidation of diphenol (70, 71, 72, 73, 74, 75) is indicative of the possibility of such a mechanism. The quinones formed by the oxidation of the diphenols are expected to react with any available free amino groups. The nearest amino groups that the quinone molecule comes in contact with are probably the ones attached to the same protein molecule which just created it by catalytical oxidation. Thus, the phenolase molecules become crosslinked by their own quinonoid products, thereby losing their enzymatic activity. The recent findings of Locke and Krishnan (76) that the cuticular protein may be composed of phenolase enzyme is another indication for the phenolase being its own substratum. Also, an "autotanning" or "self-tanning" mechanism was proposed (40, 41, 77, 78, 79, 80, 81) in which there are no separate phenolic precursors, but the protein molecules crosslink through the oxidized phenolic groups of the tyrosine residues of the protein molecules. This mechanism is supported by the observations that phenolase is capable of oxidizing tyrosine residues of some proteins (82, 83, 84, 85, 86, 87, 88). If the phenolase enzyme itself has tyrosine residues in its peptide chain available for such oxidation and also contains free amino groups to react with quinones, there appears to be no reason why the phenolase could not oxidize some of its own tyrosine residues to a reactive quinonoid species which then could react with the amino groups. In such a three-in-one fashion the phenolase could be the activating enzyme, its own substrate and the protein to be crosslinked, thus making a strict auto-crosslinking mechanism possible.

TABLE 1

TESTS FOR LIPIDS, CARBOHYDRATES AND PROTEINS IN BARNACLE ADHESIVE AND GLAND

TEST METHOD	REAGENTS - REACTIONS	OBJECTIVE	ADHESIVE			GLAND	
			CYPRID	PRIMARY	SECONDARY	CYTOPLASM	NUCLEOLUS
		Lipids					
Lison-Dagnelle	Sudan black B		-	-	-	+	+
Sheehan-Storey	Sudan black B		-	-	-		
Baker	Chromation + Acid haematein		+	+	+	-	-
	and after pyridine extraction		+++	+++	++	-	-
Elftman (1954)	Controlled chromation + Sudan black B		+	+	+	V++	-
	Controlled chromation + Acid haematein		+++	+++	++	V++	+
Elftman (1957)	Chromate fix. + Sudan black B		-	-	-	++	++
		Carbohydrates					
P. A. S.	Periodic acid - Schiff reagent		-+	-	-+	+	+
	after acetylation		-+	-	-+	-	-
	after acetylation + deacetylation		-+	-		+	+
Alcian blue	pH 2.8	acid mucopolysaccharids	-	-	-	blue	blue
Methylene blue	pH 4	acid mucopolysaccharids	-	-	-	+++	++
Metachromasia	Sulphation + Azure A	acid mucopolysaccharids	-	-	-	-	-
Methyl violet		amyloid	-	-	-	-	-
		Proteins					
MBPB	Mercury - Bromphenol blue		++	++	++	red	purple
Millon	$Hg(NO_3)_2$ + $NaNO_2$ + cc. HNO_3	tyrosine	++	++	++		
Morel-Sisley	Diazotation	tyrosine	++	++	++	+	-
DMAB	p-dimethylamino bensaldehyde	tryptophan	-	-	+	V++	+
NED	Naphtyl-ethylenediamine	tryptophan	-	-	-	+	+

LEGEND: +++ = strongly positive, ++ = positive, + = weakly positive,
V++ = varying color intensity, -+ = positive in spots,
- = negative.

TABLE 2

STAINING REACTIONS OF BARNACLE ADHESIVE AND GLAND

METHOD	REAGENTS	ADHESIVE			GLAND	
		CYPRID	PRIMARY	SECONDARY	CYTOPLASM	NUCLEOLUS
	Anionic dyes					
Eosin Y		++	++	++	V++	+++
Erythrosin B		++	++	++	V++	+
Orange G		++	++	++	+	++
	Cationic dyes					
Alcian blue	pH 2.8	-	-	-	blue	blue
Azure A		-	-	-	+	+
Celestin blue		-	-	-	-	-
Janus green		-	-	-	-	-
Methylene blue	pH 4.0	-	-	-	+++	+
Neutral red		-	-	-	V++	-
Thionine		-	-	-	+	+
	Amphoteric dyes					
Acid fuchsin		++	++	+++	V++	+++
Aniline blue WS		-+	-	-+	V+++	+
Light green		++	++	++	++	-
	Combination dyes					
Gallego-Garcia	Aniline blue WS + Eosin Y	pink	pink	pink-blue-purple	purple-blue	pink-blue
Mallory Trichrome	Acid fuchsin + Aniline blue WS + Orange G	red-orange-purple-blue			purple-blue	red-purple
Masson-Patay	Haematoxylin + Ponceau 2R + Light green	purple - green			green	purple-green
Schneidau	Acid fuchsin + Thionine	purple - blue			pale green	dark green
	Mordant haematein					
Delafield	Haematein + $NH_4Al(SO_4)_2.12\ H_2O$	+	-	-	++	++
Ehrlich	Haematein + $NH_4Al(SO_4)_2.12\ H_2O$	-	-	-	+++	+++
Harris	Haematein + $KAl(SO_4)_2.12\ H_2O$	-	-	-	++	++
Heidenhain	$NH_4Fe(SO_4)_2.12\ H_2O$, then Haematein	++	++	++	++	++

LEGEND: +++ = strongly positive, ++ = positive, + = weakly positive,
V++ = varying color intensity, -+ = positive in spots,
- = negative.

TABLE 3

REACTIONS FOR FUNCTIONAL GROUPS IN BARNACLE ADHESIVE AND GLAND

METHOD	REAGENTS	OBJECTIVE	ADHESIVE			GLAND	
			CYPRID	PRIMARY	SECONDARY	CYTOPLASM	NUCLEOLUS
Ninhydrin - Schiff	Ninhydrin + Schiff reagent	$-NH_2$ (alpha)	++	++	++	++	++
	after deamination	other than $-NH_2$	-	-	-	-	-
Acid Solochrome Cyanine R	pH 2.1	$-NH_2$	++	++	++	++	++
Alkaline Fast Green	pH 8.0	$-NH_2$ (omega)		+++	+++	V+	+
Schiff	Fuchsin-sulphurous acid	aldehyde	+	+	+	++	++
Gomori	$AgNO_3$	aldehyde	-	-	-	-	-
Alkaline Tetrazolium	Ditetrazolium chloride	-SH	++	++	++	+	-
Schmorl	$K_3Fe(CN)_6 + FeCl_3$	-SH	-	+	++	+	+
Adams	Thioglycollate + $K_3Fe(CN)_6 + FeCl_3$	-S-S-	+		++	+	+
	after blocking -S compounds	other reducer	-	+	+	-	-
Lillie	$FeSO_4 + K_3Fe(CN)_6$	quinhydrone	-	-	-	++	-
Vulpian	$FeCl_3$	phenols	-	+	-	-	-
Masson - Fontana	$AgNO_3$	melanin	++	+	-	-	-
Ziehl - Neelsen	Basic fuchsin + acid alcohol	double bonds	++	+	+	V++	+

LEGEND: +++ = strongly positive, ++ = positive, + = weakly positive,
V++ = varying color intensity, -+ = positive in spots,
- = negative.

TABLE 4

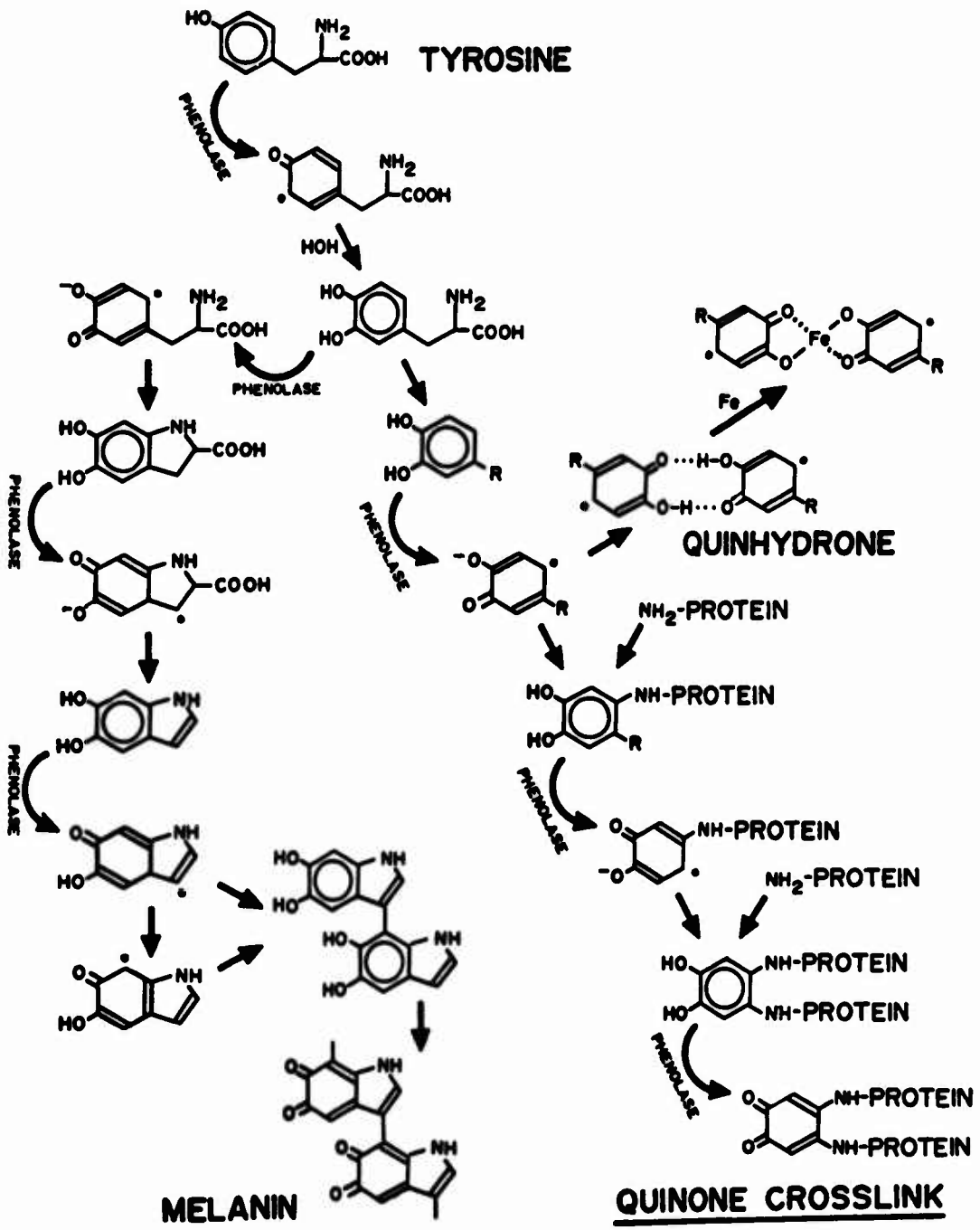

TYROSINE
PHENOLASE
HOH
PHENOLASE
PHENOLASE
PHENOLASE
PHENOLASE
PHENOLASE
Fe
QUINHYDRONE
NH2-PROTEIN
NH2-PROTEIN
MELANIN
QUINONE CROSSLINK

TABLE 5

ELEMENTAL ANALYSIS

ELEMENT	% BY WEIGHT IN SAMPLE	
	Barnacle cement	Mussel byssus
C	44.6	44.1
H	6.45	6.36
N	14.0	15.4
Estimated protein content	87.5	96.4

TABLE 6

AMINO ACID ANALYSIS IN WEIGHT PERCENT

NAME	FORMULA	BARNACLE CEMENT	MUSSEL BYSSUS
	Non-polar amino acids		
alanine	$HOOC-CH(NH_2)-CH_3$	4.5	8.5
valine	$HOOC-CH(NH_2)-CH(-CH_3)_2$	4.5	2.9
leucine	$HOOC-CH(NH_2)-CH_2-CH(CH_3)_2$	6.3	3.4
isoleucine	$HOOC-CH(NH_2)-CH-(CH_3)-CH_2-CH_3$	3.5	2.2
proline	$HOOC-\overline{CH-NH-CH_2-CH_2-CH_2}$	5.3	2.6
phenylalanine	$HOOC-CH(NH_2)-CH_2-C_6H_5$	3.5	1.5
tryptophan	$HOOC-CH(NH_2)-CH_2-\overline{C=CH-NH-C_6H_4}$	not determined	
methionine	$HOOC-CH(NH_2)-CH_2-CH_2-S-CH_3$	0.3	0.4
cystine	$HOOC-CH(NH_2)-CH_2-S-S-CH_2-CH(NH_2)-COOH$	1.2	
	Uncharged polar amino acids		
glycine	$HOOC-CH(NH_2)-H$	6.5	22.9
serine	$HOOC-CH(NH_2)-CH_2-OH$	5.6	3.9
threonine	$HOOC-CH(NH_2)-CH(CH_3)-OH$	5.5	3.4
tyrosine	$HOOC-CH(NH_2)-CH_2-C_6H_4-OH$	2.3	0.9
cysteine	$HOOC-CH(NH_2)-CH_2-SH$	2.7	1.2
	Acidic amino acids and their amides		
aspartic acid	$HOOC-CH(NH_2)-CH_2-COOH$	8.4	7.0
asparagine	$HOOC-CH(NH_2)-CH_2-CO-NH_2$		
glutamic acid	$HOOC-CH(NH_2)-CH_2-CH_2-COOH$	8.7	7.5
glutamine	$HOOC-CH(NH_2)-CH_2-CH_2-CO-NH_2$		
	Basic amino acids		
lysine	$HOOC-CH(NH_2)-CH_2-CH_2-CH_2-CH_2-NH_2$	8.6	8.0
arginine	$HOOC-CH(NH_2)-CH_2-CH_2-CH_2-NH-C(=NH)-NH_2$	6.3	4.7
histidine	$HOOC-CH(NH_2)-CH_2-\overline{C=CH-N=CH-NH}$	2.0	4.3
	Total	68.9	85.3



Figure 1. Adult Balanus crenatus secreting cement in an attempt to reattach itself.



Figure 2. Microtome section of cement gland of adult barnacle, Balanus crenatus.

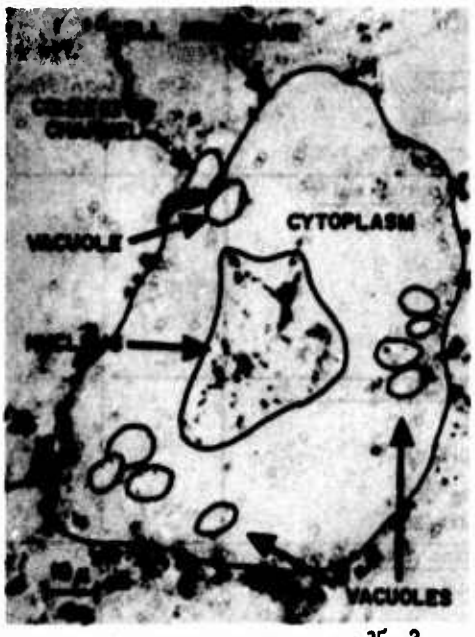


Figure 3. Incorporation of $S^{35}O_4^{2-}$ by cement gland nucleus of Balanus crenatus.

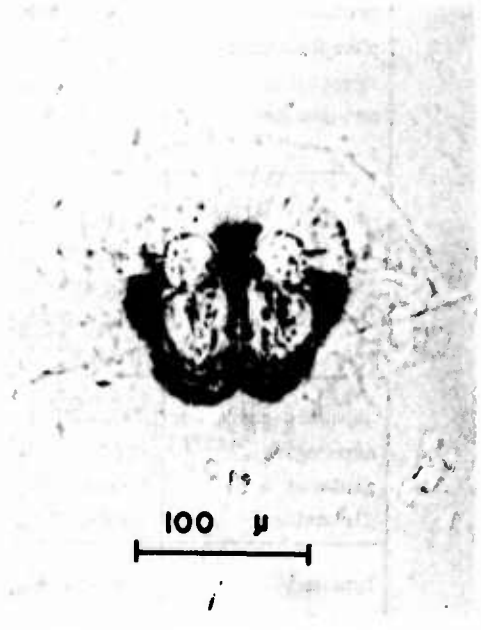


Figure 4. Melanin reaction in larval cement.

OFFICIAL U.S. NAVY PHOTOGRAPHS

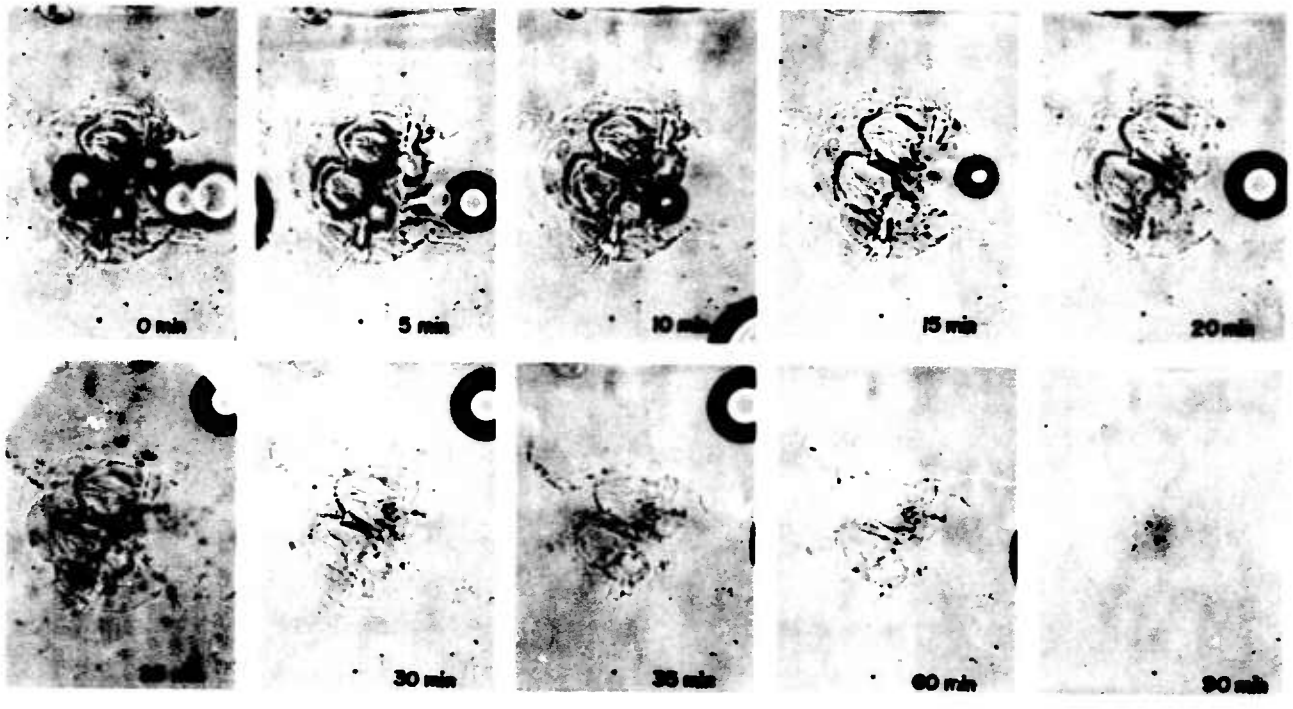


Figure 5. Dissolution of larval cement in hypochlorite.

OFFICIAL U.S. NAVY PHOTOGRAPH

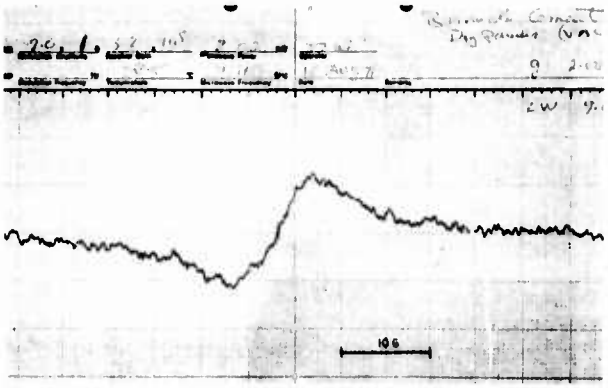


Figure 6. EPR spectrum of secondary cement of Balanus crenatus.

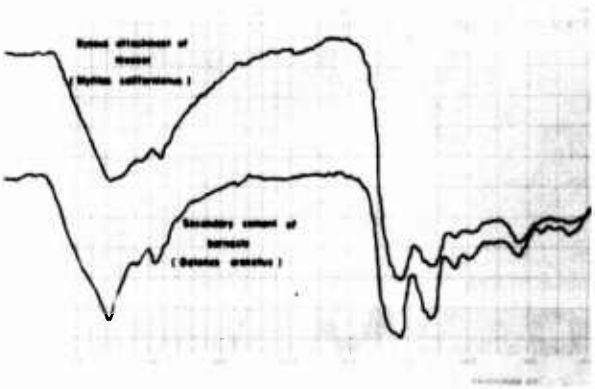


Figure 7. Infrared spectra of barnacle cement and mussel adhesive patch.

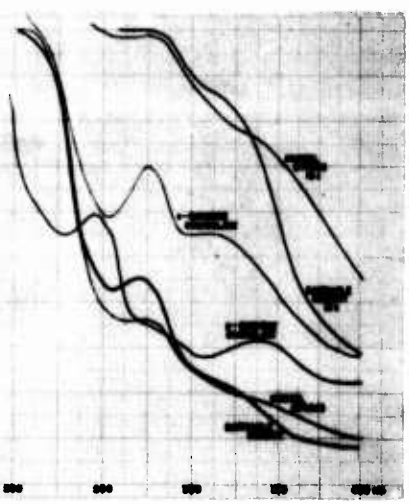


Figure 8. Ultraviolet spectra of 8N HCl hydrolysate of mussel byssus (also shown in tenfold concentration) and of $Ba(OH)_2$ hydrolysate of barnacle cement (also shown in tenfold concentration). Also shown are the spectra of synthetically o- and p-quinone crosslinked model polypeptides.

OFFICIAL U.S. NAVY PHOTOGRAPHS

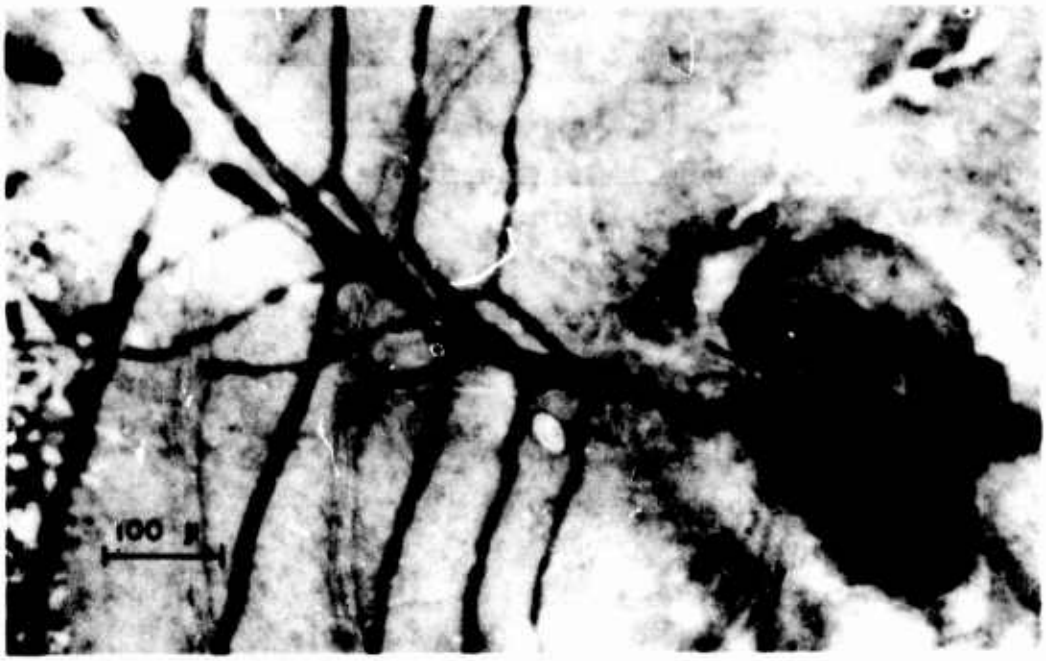


Figure 9. Phenolase ensyme demonstrated in hardened cement and in secretory ducts.



Figure 10. Microtome section through cement glands of Balanus crenatus showing sites of phenolase activity.

OFFICIAL U.S. NAVY PHOTOGRAPHS

References

1. J. R. Saroyan, E. Lindner and C. A. Dooley, 2nd Int. Congr. Marine Corrosion and Fouling, Athens pp. 495-512, Tech. Chamb., Greece (1968).
2. J. R. Saroyan, E. Lindner and C. A. Dooley, Biol. Bull. 139, 333 (1970).
3. C. Darwin, A. Monograph on the Subclass Cirripedia - The Lepadidae. pp. 33-38 (1851).
4. P. Krüger, Arch. Mikr. Anat. 97, 839 (1923).
5. J. Bocquet-Vedrine, Arch. Zool. Exp. Gen. 105, 30 (1965).
6. A. G. E. Pearse, Histochemistry, Theoretical and Applied (2nd Ed.), 998 pp., Little, Brown, Boston (1961).
7. P. Gray, The Microformist's Formulary and Guide, 794 pp., Blakiston, New York (1954).
8. F. M. Weesner, General Zoological Microtechniques, 230 pp., Williams & Wilkins, Baltimore (1960).
9. C. W. M. Adams, J. Histochem. Cytochem. 4, 23 (1956).
10. K. T. Joseph and C. Gowri, J. Sci. Ind. Res., 29A, 504 (1970).
11. M. G. M. Pryor, Proc. Roy. Soc. B. 128, 393 (1940).
12. S. O. Andersen, Acta physiol. Scand. 66, suppl. 263, 1 (1966).
13. J. Thomas, D. F. Elsden and S. M. Partridge, Nature 200, 651 (1963).
14. E. H. Slifer, Sci. 102, 282 (1945).
15. S. M. Partridge, D. F. Elsden and J. Thomas, Nature 209, 400 (1966).
16. E. J. Miller, G. R. Martin and K. A. Piez, Biochem. biophys. Res. Com. 17, 248 (1964).
17. M. G. M. Pryor, Proc. Roy. Soc. B. 128, 378 (1940).
18. G. Fraenkel and K. M. Rudall, Proc. Roy. Soc. B. 134, 111 (1947).
19. R. Dennell, Proc. Roy. Soc. B. 134, 485 (1947).
20. G. Bertrand, Compt. rend. 121, 1215 (1896).
21. H. S. Raper, Physiol. Revs. 8, 244 (1928).
22. P. Karlson and C. E. Sekeris, Nature, 195, 183 (1962).
23. C. E. Sekeris and P. Karlson, Biochim. Biophys. Acta 62, 103 (1962).
24. C. E. Dalgleish, Arch. Biochem. Biophys. 58, 214 (1955).
25. P. Karlson, Nature, 195, 183 (1962).
26. P. Karlson and H. Ammon, Hoppe-Seyl. Z. 330, 161 (1963).
27. M. W. Onslow and M. E. Robinson, Biochem. J. 22, 1327 (1928).
28. L. Michealis, Chem. Revs. 16, 243 (1935).
29. L. Meunier and A. Seyewetz, Compt. rend. 146, 987 (1908).

30. E. Bourquelot and G. Bertrand, Compt. rend. soc. biol. 47, 582 (1895).

31. L. Lison, Histochimie Animale, Gautier-Villards, Paris (1936).

32. L. Michaelis and E. S. Fetcher, J. Am. Chem. Soc. 59, 1246 (1937).

33. R. D. Lillie, J. Histochem. Cytochem 5, 346 (1957).

34. L. Michaelis and M. P. Schubert, Chem. Revs. 22, 437 (1938).

35. M. Bersohn and J. C. Baird, An Introduction to Electron Paramagnetic Resonance, W. A. Benjamin, Inc. (1966).

36. B. Ventkatarman and G. K. Fraenkel, J. Chem. Phys. 77, 2707 (1955).

37. C. H. Brown 6th Int. Cong. Exp. Cytology, Stockholm, p. 351 (1947).

38. C. H. Brown, Exp. Cell Res. Suppl 1, 351 (1949).

39. C. H. Brown, Nature 165, 275 (1950).

40. C. H. Brown, Quart. J. Micr. Sci. 93, 487 (1952).

41. J. D. Smith, Quart. J. Micr. Sci. 95, 139 (1954).

42. K. Ramalingam and M. H. Ravindranath, Acta Histochem., 41, 57 (1971).

43. K. Bailey and T. Weis-Fogh, Biochim. Biophys. Acta 48, 452 (1961).

44. J. H. Bowes, R. G. Elliott and J. A. Moss, Biochem. J. 61, 163 (1955).

45. R. E. Neuman, Arch. Biochem. 24, 289 (1949).

46. F. Lucas, J. T. B. Shaw and S. G. Smith, Advances in Protein Chem., Academic Press N. Y., Vol. 13 p. 107 (1958).

47. C. M. Yonge, Proc. Roy. Soc. B 111, 298 (1932).

48. H. J. Thomas, Quart. J. Micr. Sci. 84, 257 (1944).

49. J. E. Harris, J. Iron Steel Inst. 154, 297 (1946).

50. K. A. Pyefinch, J. Mar. Biol. Assoc., 27, 464 (1948).

51. K. A. Pyefinch and F. S. Downing, J. Mar. Biol. Assoc. 28, 21 (1949).

52. E. W. Knight-Jones and D. J. Crisp, Nature 171, 1109 (1953).

53. D. Lacombe, Publ. Inst. Pesquisas Marinha, No. 017, 1 (1968).

54. E. Lindner and C. A. Dooley, Rept. 69-3, Paint Lab., S.F. Bay Nav. Shipyard, DDC AD856070 (1969).

55. E. Lindner and C. A. Dooley, Rept. 70-5, Paint Lab., Mare Isl. Nav. Shipyard, DDC AD880578-L (1970).

56. J. R. Saroyan, E. Lindner, C. A. Dooley and H. R. Bleile, 158th Meet. Am. Chem. Soc., Org. Coat. Plast. Chem. 29, No. 2, 62 (1969).

57. J. R. Saroyan, E. Lindner, C. A. Dooley and H. R. Bleile, Ind. Eng. Chem. Prod. Res. Dev. 9, 122 (1970).

58. R. E. Hillman and P. F. Nace, Adhesion in Biological Systems (ed. R.S. Manly) Academic Press, N. Y., p. 119 (1970).

59. M. Cook, Adhesion in Biological Systems (ed. R. S. Manly) Academic Press, N.Y., p. 149 (1970).

60. L. Arvy, D. Lacombe and T. Shimony, Am. Zool. 8, 817 (1968).

61. L. Arvy and D. Lacombe, C. R. Acad. Sc. Paris, Ser. D. 267, 1326 (1968).

62. T. B. Shimony, Diss. Abstr. 32 B, 3788 (1972).

63. E. Lindner, C.A. Dooley and C. Clavell, Rept. 72-1, Paint Lab., Mare Island Naval Shipyard, DDC AD900182 (1972).

64. R. Dennell, Proc. Roy. Soc. B 133, 348 (1946).

65. R. Dennell, Proc. Roy. Soc. B 148, 280 (1958).

66. M. G. M. Pryor, Nature 175, 600 (1955).

67. S. Fuzeau-Braesch, Compt. Rend. Soc. Biol. 153, 57 (1959).

68. S. Fuzeau-Braesch, Compt. Rend. Acad. Sci. Paris, 248, 856 (1959).

69. H. S. Mason, Proc. 4th Int. Con. Biochem. Vienna 57 (1959).

70. C. R. Dawson and J. M. Nelson, J. Am. Chem. Soc. 60, 250 (1938).

71. L. P. Kendal, Biochem. J. 44, 442 (1949).

72. I. Asimov and C. R. Dawson, J. Am. Chem. Soc. 72, 820 (1950).

73. C. R. Dawson and W. E. Tarpley, The Enzymes (J. B. Summer and K. Myrback eds.) Vol. 2, pp. 454-491, Academic Press, N. Y. (1951).

74. M. G. M. Pryor, J. Exp. Biol. 32, 468 (1955).

75. P. Karlson and H. Liebau, Hoppe-Seyl. Z. 326, 135 (1961).

76. M. Locke and N. Krishnan, Tissue Cell. 3, 103 (1971).

77. G. Blower, Nature, 165, 569 (1950).

78. G. Blower, Quart. J. Micr. Sci. 92, 141 (1951).

79. R. H. Hackman, Biochem. J., 54, 371 (1953).

80. R. Dennell and S. R. A. Malek, Proc. Roy. Soc. B.144, 545 (1956).

81. B. M. Jones, Proc. Roy. Soc. B 149, 263 (1958).

82. I. W. Sizer, J. Biol. Chem. 163, 145 (1946).

83. I. W. Sizer, J. Biol. Chem. 169, 303 (1947).

84. I. W. Sizer, C. O. Brindley and P. F. Wagley, 1st Int. Congr. Biochem. Abst. p. 361 (1949).

85. W. J. Hass, I. W. Sizer and J. R. Loofbourow, Biochim. Biophys. Acta. 6, 589 (1951).

86. J. G. Cory, Dissert. Abst., p. 954 (1963).

87. M. K. Dabbous, J. Biol. Chem. 241, 5307 (1966).

88. J. G. Cory and E. Frieden, Biochem. 6, 121 (1967).

Discussion

Crisp: I wasn't quite clear of the evidence for autopolimerization by a single molecule. Was it because the phenol was not found to be present in the cell?

Lindner: There is really no evidence for auto-crosslinking. It is just a speculation at this time. This type of crosslinking was first proposed by Blower in 1949, for the same reason, namely, that he could not find a phenotic precurser for the crosslinking. Soon after this, a partial quinone crosslinking was proposed for the mussel bases itself.

Crisp: I asked because Dr. Walker has found that there was a ferric-chloride reaction in the cell which indicated an ortho-phenol so that perhaps there is after all a precurser.

Lindner: Thank you very much. That would be a very interesting--indeed it would help to make this mechanism more understood.

Barnes: Perhaps I might ask a question. I do not think really this problem that you pose of a cell having to provide several things and getting them mixed at the right time is at all peculiar. I think this is one of the mysteries of science how cells can do this sort of thing, and while it's puzzling and one ought to know more I don't think there is any reason to despair if one has to postulate a mechanism which seems to come from one cell. One could suggest that there might be some activation at the time at which a particular secretory product is released from a cell and which takes place only at that time for some reason we do not know. When you speak about primary cement, I take it you mean cyprid cement or are you suggesting that there is yet another primary and secondary cement in the adult?

Lindner: No. What I mean by primary cement is that normally secreted by the adult. We called the secondary cement that which results after detachment and on reattachment. I think we now have enough evidence both histological and histochemical to consider the primary and secondary cement identical as far as chemical composition goes, and this is probably the same as the cyprid cement. A comment on the activation of such materials, that is why I tried to stress the isoelectric point in those areas in which phenolase activity was found in the cytoplasm: any change in the isoelectric point may be an activator for the phenolase.

Barnes: One other point. Did you look for ascorbic acid in these cells? This has been implicated by some people in the process of quinone tanning of integuments. Had you any evidence for this? The presence of ascorbic acid might interfere with other tests because of its intense reducing properties.

Lindner: No, we didn't look for ascorbic acid. This is one question which I can perhaps answer four years from now.

Spore Settlement in Relation to Fouling by Enteromorpha

A. O. Christie

International Red Hand Marine Laboratory, Newton Ferrers, Devon, England.

An investigation into spore settlement as the critical stage in fouling by Enteromorpha has shown that several factors contribute to the success of this fouling alga. Under suitable conditions of surface roughness zoospore attachment can occur in seconds. The rapid sequence of changes shown by electron microscopy to occur during the first few hours of settlement include the elaboration of a comparatively thick protective wall which increases spore resistance to toxic action. The adhesive secreted by the settling zoospore is amenable to enzymatic digestion and offers the possibility of a novel method for control.

Key Words: Enteromorpha intestinalis, fine-structure, settlement, thigmotaxis, zoospore.

---

1. Introduction

Algal fouling has been recognised as a serious economic problem only in comparatively recent years, but nevertheless it is one which is liable to become progressively severe as trends continue towards larger ships and increased periods between drydockings. From the antifouling viewpoint a sound knowledge of the biology of this particular type of fouling is important and this paper presents our approach to fouling by the green alga Enteromorpha.

By the mid-sixties it had become apparent that copper based antifouling compositions were not performing efficiently in tanker operation and demanded a more detailed biological investigation of this situation. A survey of the fouling on twenty oil tankers docking in European waters showed:

(1) Fouling samples were almost entirely algal.

(2) The number of different algal types encountered was limited and independent of routing.

(3) The percentage frequency of occurrence was Enteromorpha 75%, Ectocarpus 13%, Cladophora 5%, Chaetomorpha 5%, others 2%.

The ubiquitity of green algae and the dominance of Enteromorpha immediately singled out this algal genus for special attention. Since the species Enteromorpha intestinalis had been frequently observed in tanker fouling samples and was also locally available, this alga was selected for study in a programme designed to obtain a better understanding of the events taking place during the initial attachment of swarm spores.

Experimental material

Fronds of Enteromorpha are collected from mid-shore level in an area of freshwater drainage at Newton Ferrers, Devon, England. The time of collection of shore material is important since spore release shows a marked tidal

periodicity with maximum spore liberation occurring three to five days before the highest tide of each lunar period (1)[1]. Zoospore liberation reaches a peak about five days before the maximum tide of the bimonthly cycle with the peak in gamete liberation following two to three days later. Fruiting fronds, indicated by the presence of bleaching at their tips, are washed in fresh water, placed individually in specimen tubes and flooded with filtered sea water. Spores are generally released within a few minutes and samples removed for identification. Sporophyte plants produce quadriflagellate zoospores whilst morphologically identical gametophyte plants produce biflagellate male or female gametes. Zoospores and gametes are distinguished by flagellar count and gametes sexed by observation of cross fusion.

Settlement in Enteromorpha - physical aspects.

All three types of swarm spore produced by Enteromorpha are capable of settlement but the rates at which settlement takes place vary greatly. Under certain conditions of light and temperature some swarmers of Enteromorpha can maintain an independent motile existence for up to eight days (2). Laboratory experiments on settlement rates on glass and polystyrene surfaces show considerable individual variations, although the general order of settlement rate, zoospores $\gg$ fused gametes $>$ gametes is invariable. An explanation for these observations lies in the response of zoospores to surface contact (thigmotaxis). Zoospores in suspension in sea water and placed as a convex drop on a smooth hydrophobic surface are reluctant to settle and congregate presumably at a site of preferred light intensity at the air/water interface. If liquid is then removed to facilitate contact between the spores and the surface rapid settlement results. Such a thigmotactic response is known (3) to occur with spores of the filamentous brown alga Ectocarpus allowed to settle overnight on grooved Teflon. A similar but very rapid response to surface contact can be readily demonstrated with zoospores of Enteromorpha. Zoospore suspensions on finely grooved Teflon were brought into surface contact by positioning a coverslip over the convex drop. After one minute the coverslip was removed and the Teflon piece rinsed in sea water. Photomicrographs taken within five minutes of initial contact with the zoospore suspension are shown (Fig.1).

Zoospores from fronds kept under laboratory conditions for some days often show no thigmotaxis, similarily, zoospores held in suspension show a decreasing thigmotaxis with time. Gametes have never been observed to show a thigmotactic response to grooved surfaces, settlement taking place gradually over a period of days. Paired gametes have been observed to settle in Teflon grooves within five minutes of fusion but do not exhibit marked thigmotaxis.

Conditions of light, temperature and salinity also influence settlement (4). On glass surfaces the initial settlement rate was higher in daylight than in darkness and optimum settlement occurred at a temperature of 23°C and a salinity of 26°/$_{oo}$. Successful settlement was recorded over a temperature range of 4-38°C and a salinity range of 2.5-52°/$_{oo}$. These results accord well with the general situation occupied on the shore by Enteromorpha and also serve to demonstrate how conditions on a tanker hull provide a niche for this fouling alga.

Settlement in Enteromorpha - fine structure

Due to the size of the spores (zoospores 10 x 6 μ, gametes 7 x 3 μ) observations by light microscopy are limited. Settlement of zoospores of Enteromorpha has therefore been followed using electron microscopy of thin sections (5). The series of electron micrographs (Fig.2) summarises the

---

[1] Figures in parentheses indicate the literature references at the end of this paper.

ultrastructure of a swimming zoospore and the changes taking place during the first four hours after settlement. The swimming spore (Fig.2, 1 & 2) with a central nucleus is bounded only by a plasmalemma and the basal region is occupied mainly by the chloroplast enclosing the starch grains and pyrenoid. The anterior portion (Fig. 2,2) contains many Golgi-derived electron-dense vesicles which contain adhesive material. On settlement (Fig. 2,3) the adhesive material is secreted as a fibrillar substance attaching the cells to the substratum. A cell wall appears soon after initial settlement and after four hours has thickened considerably. Comparison with the free-swimming stage indicates that considerable physical protection is provided within a short time.

Settlement in relation to the effect of poisons

The ability of zoospores to settle within seconds in response to a high level of surface contact and the rapid sequence of events leading to the development of a thick cell wall suggested that settled zoospores might be more resistant to toxic action than free-swimming zoospores.

This has been tested in toxicity experiments based on sporeling counts after five days growth over a range of poison concentrations. With organo-metallic poisons, spores allowed to settle in the dark for 24 hours before the addition of poison show an increase in LD_{50} (the poison concentration required to kill 50%) between three to five times that obtained using a suspension of zoospores as a control. The rate at which this protection is afforded is of practical importance and was tested in the following experiment. Uniform 1ml aliquots of a freshly obtained suspension of zoospores were rapidly inoculated into a series of Sterilin petri-dishes containing 7ml sea water. After five minutes the dishes were drained and filled with filtered sea water. At 0, 5, 10, 15, 30, 60 and 120 minutes the sea water was discarded and replaced by triphenyl tin chloride at concentrations of .01, .005, .002, .001 and .0005 p.p.m. in sea water supplemented with soil extract, nitrate and phosphate. After five days illumination sporeling counts were taken and the LD_{50} values calculated for poison additions at the different settlement times. The drainage proceedure inevitably introduced more variability than normally experienced in toxicity tests with Enteromorpha but despite this a progressive change in LD_{50} values was obtained. Spores settled for five minutes prior to poison addition gave an LD_{50} value of .002 p.p.m. increasing to .005 p.p.m. when poison was added after sixty minutes.

Since fouling can be initiated by zoospores, gametes and fused gamete pairs it is useful to compare the relative susceptibility of these forms to toxic action. However, the inherent variability associated with results based on a five day germination test in which bacteria and diatoms are unavoidably present as contaminants casts doubt on absolute values. As a generalisation zoospores and fused gamete pairs both allowed to settle for 24 hours prior to the test give comparable LD_{50} values. These values drop by a factor of three to five for swimming zoospores and large female gametes and a further factor of two for the smaller male gametes.

Biochemical aspects of settlement

The biochemical nature of the adhesive secreted by the settling zoospores of Enteromorpha is of considerable interest since an understanding of the mechanism of spore adhesion might lead to alternative practical control methods. Two approaches have been made to this problem both of which lead to the conclusion that the secreted adhesive is mainly proteinaceous. Electron microscopy (5) of spores incubated in trypsin during settlement showed complete digestion of secreted fibrillar adhesive. In a parallel series of experiments (6) the adhesion of zoospores was used as the criterion to test the effects of various enzymes on attachment. Although it is very difficult to make quantitative measurements of the bond strength between spore and surface the use of a standardised water jet provided information on relative adhesion

under different experimental conditions. These experiments showed that adhesion to glass improved rapidly during the first hours after attachment presumably due to physical changes taking place in the secreted adhesive. Certain proteolytic enzymes notably pronase and trypsin and the carbohydrase α-amylase exerted a marked effect on the strength of adhesion and the results were consistent with the interpretation that the adhesive secreted by the settling zoospore is a glyco-protein.

The success of proteolytic enzymes in solution (1mg/ml) in destroying the adhesion of settling zoospores suggested that surfaces carrying covalently linked proteolytic enzymes might offer a novel method for biological control of Enteromorpha. Laboratory investigation by the water jet method required ideally a smooth and transparent surface and this imposed limitations. It is possible (7) to link enzymes to glass and 10mm diameter coverslips theoretically containing 1 - 10μg trypsin were prepared by Dr. Weetall of the Corning Glass Company, New York. No significant difference in the adhesion of zoospores were found between control and experimental surfaces. In further experiments the $TiCl_4$ method (8) has been used to couple pronase to regenerated cellulose micropore filters. It is difficult to observe spores on this type of opaque surface but settled spores remained on experimental surfaces indicating that the surface activity of the enzyme was again insufficiently high. Limited algal control has been achieved by incorporating pronase (1%) into an acrylic binder. With improved enzyme technology biological control might still be possible.

Discussion

The fact that the life cycle in Enteromorpha intestinalis comprises a regular alternation between sporophyte and gametophyte generations (9) presents the added complication of three types of reproductive body. Zoospores, male and female gametes must all be considered along with fused gamete pairs as potential fouling organisms. From the results presented here, the thigmotactic response of zoospores allowing rapid settlement and further rapid development of a protective cell wall might suggest their major involvement in practice. Although the possibility of initiation of Enteromorpha fouling by gametes does exist it would be interesting to know whether gametophyte plants of this alga do predominate in tanker fouling.

One aspect of the present work which is at variance with practice is the susceptibility of zoospores to toxic action determined under laboratory conditions. The example given here of 0.002 p.p.m. as the LD_{50} value for triphenyl tin chloride is typical of the order of toxicity obtained with organotins that are currently used in antifouling compositions. At this level of toxicity it ought to be possible to design antifoulings based on organotin compounds which would be completely effective in controlling Enteromorpha; practical experience is rather different! On this basis there must be additional reasons why Enteromorpha constitutes a fouling problem at all. Perhaps the most important is its filamentous mode of growth. The surface is required only to provide anchorage, once a sporeling has established itself on an antifouling surface and succeeded in growing beyond any boundary layer of poison then continued growth appears inevitable. In practice, settlement is most likely to occur under stationary conditions when leaching from the antifouling surface is at a minimum. Under these circumstances it is probable that the rapidity of zoospore attachment and the development of increased resistance to toxic action play a large part in the success of Enteromorpha as a fouling alga.

The ability of proteolytic enzymes to interfere with spore adhesion offers an alternative method of control of Enteromorpha. Despite the fact that the enzyme-coupled surfaces were not sufficiently active, insolubilized enzymes form an expanding area of technology with many developments in prospect. The practicability of this type of approach is not only dependent on these but also on the nature of the adhesives secreted by the settling

spores of other fouling algae. As far as Ectocarpus is concerned both polysaccharide and protein are present in the secreted adhesive (10). Part of our current fundamental research effort is directed to studies of the biochemical nature of adhesives secreted by settling spores in certain green, brown and red algae. Should the overall picture provide sufficient similarities enzymatic control of algal fouling would provide an exciting prospect.

Acknowledgements

The work presented owes much to our collaboration with the Department of Botany, Leeds University. My thanks are especially due to Dr. L. V. Evans for providing the series of electron micrographs and to the Annals of Botany for their permission to publish these photographs. I would also like to thank my research colleagues Mr. B. W. P. Sparrow and Mr. T. Lovegrove.

References

1. A. O. CHRISTIE and L. V. Evans, Nature, Lond., 193, 193 (1962)
2. W. E. JONES and M. S. BABB, Br. phycol. Bull. 3, 525 (1968)
3. D. G. MÜLLER, Z. Bot. 52, 193 (1964)
4. A. O. CHRISTIE and M. SHAW, Br. Phycol. Bull. 3, 529 (1958)
5. L. V. EVANS and A. O. CHRISTIE, Ann. Bot. 34, 451 (1970)
6. A. O. CHRISTIE, L. V. EVANS and M. SHAW, Ann. Bot. 34, 467 (1970)
7. H. H. WEETALL, Science. 166, 615 (1969)
8. J. M. NOVAIS, Ph.D. Thesis, University of Birmingham (1971)
9. C. BLIDING, Opera Botanica 8, 1 (1963)
10. J. R. J. BAKER, Ph.D. Thesis, University of Leeds (1971)

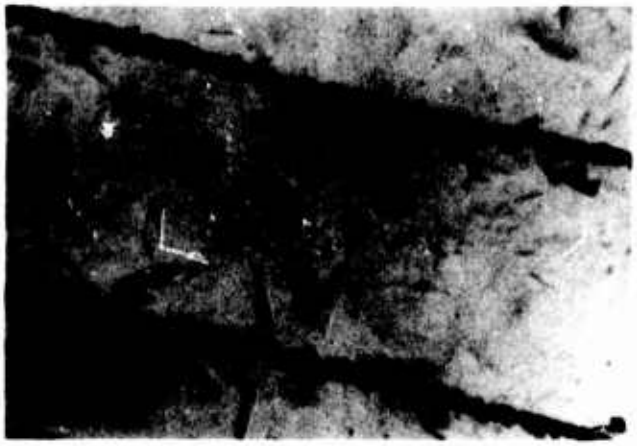


Fig. 1A. Photomicrograph of zoospores settled in parallel grooves on a Teflon surface. The initial contact time with swimming spores was one minute X100.



Fig. 1B. Portion of groove as Fig. 1A x450.

Fig. 1.

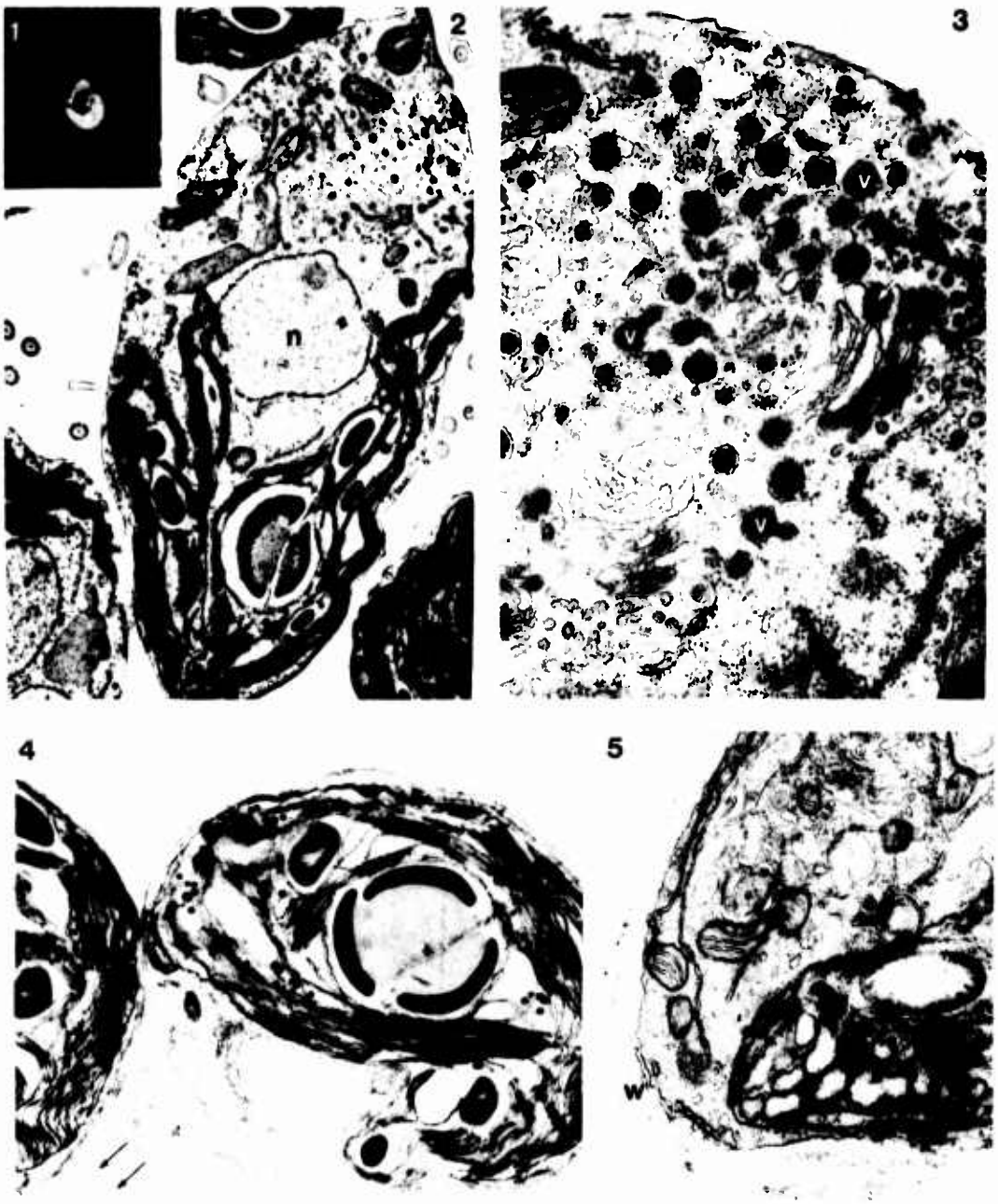


Fig. 2. 1. Swimming zoospore, light micrograph X1000. 2. L.S. zoospore showing chloroplast (c), nucleus (n), Golgi body (g) and dense vesicles of adhesive (arrows) X14000. 3. Part anterior region zoospore with adhesive vesicles (v) and Golgi body (g) showing vesicle production (arrow) X40000. 4. One hour settled zoospores in L.S. with external fibrillar adhesive (arrows) X15000. 5. Part of a settled cell (four hours) showing thick wall (w) X28000.

Discussion

Question: I was wondering whether when you treat the settled spores with pronase you just may not be digesting away the adhesion of the cell itself to the adhesive and not digesting the adhesive at all with pronase.

Christie: We have some additional evidence which I did not show today which concerns the electron microscopical approach. If you remember, one of the slides of the newly settled zoospores showing the fibrillar adhesive, if you allow a spore to settle for about five minutes so that it secretes this adhesive and then you treat it with trypsin and look at the preparation in an electron microscope you will find that the fibrillar adhesive has been etched away. We have done this but I haven't shown the picture; this is collaborative evidence that perhaps it is a digestion of the adhesive. It certainly disappears with this treatment. It is rather difficult to do because it is difficult not to remove the cells altogether, so that you have got to give them just a short time to settle and a short burst of enzyme and we have observed this.

Jones: Just a comment about the fine structure. You showed that in the sections of the spores you had electron dense material in the vesicles. You showed later on when you saw the spore settling or after the spore had settled you had fibrillar material. In sections that we have looked at in both Polysyphonia and also in Enteromorpha, we find that you have electron dense material certainly in some vesicles, but surrounding it is a halo of fibrillar material. Do you have any evidence of this?

Christie: I do not know if it was apparent from the slides, but around these small vesicles which do contain the adhesive, there is a second membrane appearing as a sort of banded granulated margin around them, but we never really thought--or it never appeared to us that this was fibrillar material and we have always assumed that the material inside the vesicle once it was pushed through the plasmalema assumed this fibrillar appearance.

Unknown: We found in working with the secretions of the mussel byssus that similar vesicles appeared in the cell. In our case we saw the fibrillae inside as well as outside the cell and I would like to call to your attention the work of Pygodorf. He pointed out that in the case of actin, soluble globular actin is produced in the cell but this is altered to insoluble fibrillar actin. The fibrillae are insoluble and of course your mucilage or cement in this final stage must be insoluble to withstand sea water, but it may be produced in the cell as a globular protein as I believe you indicated.

Christie: This aspect of physical changes in the material from inside the cell to outside the cell is very, very clear because if you allow spores to settle for several hours before you try the effect of enzymes on them, even pronase, it just doesn't budge them. So there are obviously big changes in the physical nature of that adhesive after it is secreted and which takes place very quickly. I really meant to finish off the paper by summing up the relationships of the biological approach to our interest on the anti-fouling side and of course, I failed to do this, but perhaps I can recapitulate the points. The first point is the thick-cell wall and the apparent increased resistance to toxic action. The second is this very rapid settlement response to the grooved surfaces. The third one, which I did not cover, is the growth of Enteromorpha. If it establishes itself on a surface then, once it grows beyond any boundary layer of poison then you can do nothing to stop it. The fourth one which was brought home to me very forcibly yesterday by Dr. Moss's paper was the fact that these spores when they settle push themselves away from the surface and increase that physical distance. I think, therefore, that when you add everything up together, it perhaps explains this apparently anomalous picture of the great sensitivity of free-swimming spores in laboratory tests to poisons, whereas in practice Enteromorpha is a severe weed to control.

NATIONAL BUREAU OF STANDARDS SPECIAL PUBLICATION , Proceedings of the Congress on Marine Corrosion and Fouling, Held October 2-6, 1972. Gaithersburg, Maryland (Issued).

The Effect of Water Velocity on the Settlement of Swarmers of Enteromorpha spp

David R Houghton, I Pearman, and D Tierney

Central Dockyard Laboratory
H M Naval Base, Portsmouth
Hants PO1 3LZ, England

A number of drying treatments have been investigated and the effect on the production of swarmers observed. Cooling to 5°C gave the best results, after 24 hours, and drying under an infra-red lamp the best at 6 hours. Air drying was also beneficial and preferred because of the large amount of material required for each experiment. The bubbling of the common gases N_2, O_2 and CO_2 through seawater containing the alga did not increase the yield, except for N_2 which first of all stimulated swarmer production but later suppressed it.

Initial experiments provided qualitative results which showed that Enteromorpha swarmers settled at water speeds up to 9.0 knots. In subsequent quantitative experiments, where the panels were washed before culturing, settlement took place at up to 10.7 knots. The conclusion is drawn that settlement of these species can occur when ships are under way at relatively high speeds. It is also concluded that settlement can probably occur at water velocities well in excess of 10 knots.

Key Words: Water velocity; Enteromorpha; Swarmer Settlement.

1. Introduction

Species of Enteromorpha are well known fouling organisms of ships' hulls. These algae belong to the family Ulvaceae and are essentially marine, occurring in nature, mainly in the littoral zone or near low water level. They are, however, found in fresh water, and several of the marine species are capable of existing in a wide range of salinities, often ascending well into estuaries, especially where there is some pollution (1)[1].

Several authors (2)(3)(4) have investigated the effect of water velocity in the attachment of sedentary and boring organisms. Although there is some discrepancy in the literature as to the actual speed which will prevent settlement, it appears that none of these species will attach when the water velocity over the surface is in excess of two knots. It seems to have been generally accepted that a similar water speed would prevent the attachment of algal species. However, experience with 'Tankers' and observations in the field where settlement has occurred in situations where there is a comparatively fast flow, suggests that spores are capable of attachment even under conditions of high water velocities.

It was decided to investigate this phenomenon, in the laboratory, using species of Enteromorpha collected from Langstone Harbour. In order to obtain sufficient material for the experiments various methods were tried to increase the yield of swarmers.

[1] Figures in parentheses indicate the literature references at the end of this paper.

2. Materials and Methods

Because no attempt was made to separate zoospores and zygotes formed from gamete fusion the term swarmer has been used throughout. Thalli of Enteromorpha were brought into the laboratory and placed in fresh seawater and the swarmers collected on release. The number obtained was extremely variable, which may have been due to the lunar rhythm (5) or to some such factor as the length of exposure to air. In an attempt to obtain a more reliable yield, various treatments were applied to the thalli. Two approaches were adopted, one in which the Enteromorpha was kept in air and treated and the other where the treatment was carried out in seawater. These are referred to for convenience as 'dry' and 'wet' treatments respectively.

The freshly collected thalli was divided into a number of samples each of approximately 100g which were given the following 'dry' treatments:

(a) Untreated control

(b) Dried under a 275 watt infra-red lamp placed at a distance of 50 cm for periods of 2, 4 and 6 hours.

(c) Air dried for 2, 6 and 24 hours.

(d) Cooled to 5°C for 2, 6 and 24 hours.

(e) Cooled to -12°C for 2, 6 and 24 hours.

After being treated the samples were placed in 4l beakers containing 300 ml of a seawater Erdschreiber medium and kept at room temperature (c.18°C). Three 5 x 7.5 cm glass slides were placed in each beaker to act as collectors. They were left in the medium for 48 hours to allow swarmers to settle, after which they were removed and kept in large culture trays under constant illumination for one week. The slides were then examined under the binocular microscope and the number of developing thalli recorded. An average figure for the three slides, expressed as number per sq cm, was obtained.

In the 'wet' treatments three 100g samples were placed in separate beakers containing 1 litre of Erdschreiber enriched seawater and a 5 x 7.5 cm glass slide. The beakers were kept in separate compartments and N_2, O_2 and CO_2 respectively was bubbled through the water. The Enteromorpha was removed after 2, 6 and 24 hours. Each slide was left for a further 48 hours before removal to the culture trays. Assessment of swarmer settlement was carried out as described above.

The apparatus used in the settlement experiments is shown in Fig 1. It consisted of two seawater-filled GRP tanks each of approximately 250 gallons capacity. They were connected by a short 7.6 cm diameter pipe line in which was situated a pump capable of delivering a maximum of 300 gallons per minute. On the discharge side of the pump there was a control valve for regulating the flow of water. The tank into which the pump discharged was sealed at the top and when in use was under a positive pressure. The water flowed from one tank to the other via a 15 x 23 x 150 cm perspex channel; a sluice at the upstream end allowed further control of the seawater flow. Turbulence in the system was controlled by a baffle and a perforated inlet in the pressurised tank and by the curvature leading to the perspex channel. In the tank into which the water discharged there were six refrigeration plates of 35,000 BTU/hour capacity thermostatically controlled. Without refrigeration a rapid rise in temperature took place; of the order of 20°C.

A strip of perspex 120 x 15 x 0.3 cm was placed at the bottom of the channel to act as a settlement surface. It was partially cut through at inversals of 7.5 cm so that it could be easily broken without the surface being disturbed at the end of the experiment. The strip was fixed in the channel with the smooth side uppermost by means of a silicone rubber compound. This provided adequate adhesion during the experiment but also allowed the strip to be removed with ease.

The water velocity was measured by two methods. Initially an Aott propeller driven current meter was used but in later experiments velocity was determined using a Casella Pitot-static tube connected to a seawater-filled manometer. Measurements were made approximately 1.5 cm above the perspex strip in the centre line.

At the commencement of each experiment the whole system was filled with seawater which was pumped around the system until it had reached the experimental temperature of 16°C (± 1°). The water velocity along the channel was then measured. Two plastic mesh bags, 91 x 46 cm, half-filled with the thalli of Enteromorpha spp were suspended in the tank containing the cooling elements. Thus the swarmers released by the alga into the water were circulated around the system.

After three days the bags containing the alga were removed and the experiment continued for another 24 hours. When the pump was stopped the sea-water was allowed to drain from the perspex channel, the strip removed and divided into its 7.5 x 15 cm sections. In preliminary experiments these small panels were placed directly into an Erdschreiber medium made up in seawater and cultured under constant illumination for a week at a temperature of 18°C (± 2°). Each panel was then examined under a binocular microscope using ten 5 cm sweeps, at righ angles to the direction of the water flow. The number of thalli per panel was recorded.

In later experiments the panels were washed with tap water or sterile sea-water, after removal from the channel, to remove any unattached swarmers.

To confirm the presence of swarmers in the experimental system, three 50 ml daily samples were taken from the channel and placed in 9 cm diameter petri dishes. They were left for 24 hours under a uniform light intensity to allow swarmer settlement. The water was then discarded, one dish was washed with sterile seawater, one with tap-water and the third untreated; they were then filled with sterile seawater and incubated as described above and scanned under the binocular microscope.

A preliminary series of 4 experiments were carried out in which the water velocity varied from 1.87 to 3.9 knots. This was followed by a second series of three experiments where the water speed was between 8.2 and 9.0 knots. Algal attachment was recorded as being present or absent.

In a subsequent series the actual number of swarmers settling was recorded; the first two experiments were carried out at water velocities between 2.9 to 3.6 knots and the third between 4.4 and 4.9. A further series of experiments was undertaken at relatively high water velocities of between approximately 8 and 10 knots.

Since it took 25-30 seconds for the water to drain from the channel after the pump was shut off it was possible that attachment of swarmers to the experimental panels could have occurred during that period. To investigate this possibility the system was filled with seawater which was then innoculated with swarmers and the pump turned on and left running until the channel was filled with water as in the other experiments. The pump was then switched off and the water allowed to drain from the channel. The collecting strip was treated as before, being separated into small panels, washed and cultured, after which the number of attached specimens was recorded. This experiment was repeated three times. Control dishes were set up to confirm the present of swarmers.

3. Results

The results of both the 'wet' and 'dry' treatments upon spore release from thalli of Enteromorpha spp are summarised in Fig 2. It can be seen that the yield of spores varied considerably from one treatment to another, and in some cases with the duration of the treatment. Bubbling CO_2 through the seawater containing the thalli had an adverse effect on swarmer production, the yield being less than that obtained in the control. Oxygen appeared to have little or no effect upon the yield. Treatment with H_2, however, presented a rather different picture. There was a considerable increase in yield with material kept for 2 hours in seawater through which the gas was bubbled. More than twice

the number of swarmers were obtained if the treatment was continued for 6 hours before return to normal sterile seawater. After 24 hours the yield was below that of the control.

Infra-red drying for 4 hours and six hours respectively, increased the yield of swarmers to almost the same level as was obtained by air drying for 6 and 24 hours. Thalli maintained at -12°C for 2, 6 and 24 hours showed little difference in production to the control material. Cooling to 5°C for the same periods produce a steadily increasing yield with the duration of the treatment, and, after 24 hours, presented the highest yield recorded. Air drying of the material was adopted because of the large quantities of the alga required for each experiment and the ease with which the treatment could be carried out.

In the initial settlement experiments the water velocity in the channel varied from 1.87 to 3.9 knots. In the four experiments settlement was recorded on all the panels. In the second series only the first 40 cm of the collecting strip was examined, the water speed varying from approximately 8.2 to 9.0 knots. Swarmer settlement occurred in all three experiments.

Subsequently the actual number of swarmers settled on the collectors was recorded. In this series the first two experiments were carried out with water velocities varying from 2.9 to 3.6 knots and in the third between 4.4 and 4.9 knots. The numbers settling in each experiment are shown in Table 1 and the daily check on available swarmers in Table 2. Settlement occurred over the whole range of water velocities. There were indications that numbers were slightly higher at the lower as opposed to the higher end of each velocity range. In this series of experiments there also appeared to be a relationship between the number of swarmers available for settlement and the actual number settled.

Four experiments were carried out in which the perspex panels were washed with either tap or sterile seawater. The results are given in Table 3, the water velocity in the first experiment varied from 8.9 to 9.1 and in the remainder from 10.2 to 10.7 knots. The washing procedure appeared to have no adverse effect on the results. The number of swarmers present in the system throughout the four days of each experiment is shown in Table 4. The very considerable differences in the number of swarmers present was not apparently reflected by the actual settlement as appeared to be the case in the previous series. There was also a considerable decrease in the number of swarmers in the water over the experimental period.

The results of the investigation to see whether swarmers settled whilst the water was draining from the channel are given in Table 5 and the availability of spores in Table 6. There was a tendency for swarmers to settle in pairs in the perspex strip but this was not so marked in the petri dish cultures; the respective percentages being 30% and 5%.

4. Discussion

In all the experiments settlement of swarmers took place on the collecting strip at a water speeds up to and including approximately 10.7 knots. Although it was not possible to measure the water speed at the actual point of attachment, the conditions in the channel were reasonably representative of the water flow at least over some parts of a ship's hull. Because of the limitations of the apparatus it was not possible to increase the water velocity beyond the maximum obtained in these experiments.

It is possible that the swarmers, which are approximately 10-12 μ, enter the boundary layer of water adjacent to the surface and are consequently no longer subjected to the forces which may tend to remove them. If this is so then it is likely that settlement would occur at considerably higher speeds.

From the experiments it would appear that the number of swarmers settling is dependent on the number available only when that number is small.

The implication of these results is that as far as weed fouling by Enteromorpha is concerned settlement can occur on a ship's hull even when it is steaming at relatively high speed.

5. References

1. F. E. FRITSCH, The Structure and Reproduction of the Algae, Vol. 1. Cambridge University Press (1956).

2. F. G. W. SMITH, Biol. Bull. mar. biol. Lab., Woods Hole. 90, 51 (1946).

3. H. DOOCHIN and F. G. W. SMITH, Bull. Mar. Sci., Gulf & Caribbean 1, 196 (1951).

4. D. J. CRISP, J. Exp. Biol. 32, 569 (1955).

5. A. O. CHRISTIE, L.V.EVANS and M. SMITH, Ann. Bot. 34, 467 (1970).

TABLE I

NUMBERS OF SWARMERS SETTLING ON PERSPEX SECTIONS DURING FIRST SERIES OF EXPERIMENTS

Panel Number	Speed (knots)	Number settling		Mean	Speed (Knots)	Number settling Expt 3
		Exp 1	Exp 2			
1	2.9	11	1	6.0	4.4	32
2	3.0	8	7	7.5	4.4	106
3	3.1	9	4	6.5	4.5	42
4	3.2	7	2	4.5	4.5	18
5	3.3	11	5	8.0	4.5	15
6	3.3	8	3	5.5	4.5	8
7	3.3	8	* 150	-	4.5	16
8	3.4	4	4	4.0	4.6	0
9	3.5	1	3	2.0	4.6	16
10	3.5	0	0	0.0	4.6	2
11	3.4	1	4	2.5	4.7	0
12	3.5	0	5	2.5	4.7	1
13	3.5	3	0	1.5	4.7	3
14	3.5	1	3	2.0	4.8	8
15	3.6	6	4	2.0	4.9	5
	TOTAL	72	49		TOTAL	182

* Localised clump of swarmers

TABLE 2

SAMPLES OF SEA WATER FROM THE SYSTEM TAKEN THROUGHOUT THE FOUR DAYS OF THE EXPERIMENTS SHOWN IN TABLE I, SHOWING NUMBERS OF SWARMERS SETTLING IN PETRI DISHES

Day	Numbers settling in petri dishes		
	Expt 1	Expt 2	Expt 3
1	54	32	159
2	-	14	139
3	18	14	4
4	3	0	4

TABLE 3

NUMBERS OF SWARMERS SETTLING ON PERSPEX SECTIONS AT VARIOUS VELOCITIES AFTER WASHING TO REMOVE UNSETTLED SWARMERS

Panel Number	Speed (knots)	Number Settling Expt 1	Speed (knots)	Number Settling			Mean
				Expt 2	Expt 3	Expt 4	
1	8.9	32	10.7	0	23	0	7.7
2	8.9	66	10.7	13	7	5	8.3
3	8.9	42	10.4	4	6	15	8.3
4	9.0	18	10.3	5	1	5	3.7
5	9.0	15	10.3	2	19	10	10.3
6	9.0	8	10.3	5	2	9	5.3
7	9.0	16	10.3	5	7	7	6.3
8	9.0	0	10.3	35	5	2	14.0
9	9.0	16	10.2	0	10	7	5.7
10	9.1	2	10.2	27	0	4	10.3
11	9.1	0	10.2	5	27	7	13.0
12	9.1	2	10.2	8	2	10	6.6
13	9.1	5	10.2	5	21	6	10.6
14	9.1	8	10.2	8	6	19	11.0
15	9.1	3	10.2	5	19	10	11.3
	TOTAL	233	TOTALS	127	155	126	

TABLE 4

SAMPLES OF SEAWATER FROM THE SYSTEM THROUGHOUT 4 DAYS OF RUNS DESCRIBE IN TABLE 3. SHOWING NUMBERS OF SPORES SETTLED AND DEVELOPED IN PETRI DISHES

Treatment	Day	Number Settling in Petri Dishes			
		8.9 - 9.1 Knots	10.2 - 10.7 Knots		
		Expt 1	Expt 2	Expt 3	Expt 4
Wash	1	650	1590	3000	1380
	2	223	3000	250	1000
	3	148	2000	-	444
	4	7	450	680	522
Spray	1	680	1020	2000	340
	2	98	3000	420	500
	3	3	2000	-	34
	4	5	740	120	852
Untreated	1	590	2000	660	5000
	2	149	3000	950	3000
	3	278	2000	-	198
	4	6	900	910	600
Mean	1	640	1540	1886	2240
	2	156	3000	873	1500
	3	142	2000	-	225
	4	5	700	570	668

TABLE 5

NUMBERS OF SWARMERS SETTLING ON PERSPEX STRIP AFTER PUMP HAS BEEN SWITCHED OFF (ALL SECTIONS WERE WASHED)

Sections sprayed with tap water				Sections washed in sterile sea water			
Section Number	Numbers settling			Section Number	Numbers settling		
	Expt 1	Expt 2	Expt 3		Expt 1	Expt 2	Expt 3
1	0	0	0	2	0	1	0
3	0	0	0	4	0	0	0
5	0	0	0	6	0	0	0
7	0	0	0	8	0	0	0
9	0	1	0	10	0	1	0
11	0	0	0	12	0	0	0
13	0	0	0	14	0	0	0
15	0	0	0				

TABLE 6

SAMPLES OF SEAWATER FROM THE SYSTEM IMMEDIATELY AFTER CARRYING OUT EXPERIMENT SUMMARIZED IN TABLE 5, SHOWING NUMBERS OF SWARMERS SETTLED

Dish Number	Number settling
1	1140
2	1550
3	1500
4	1100
5	1110
6	1240
7	850
8	1130
Mean	1202

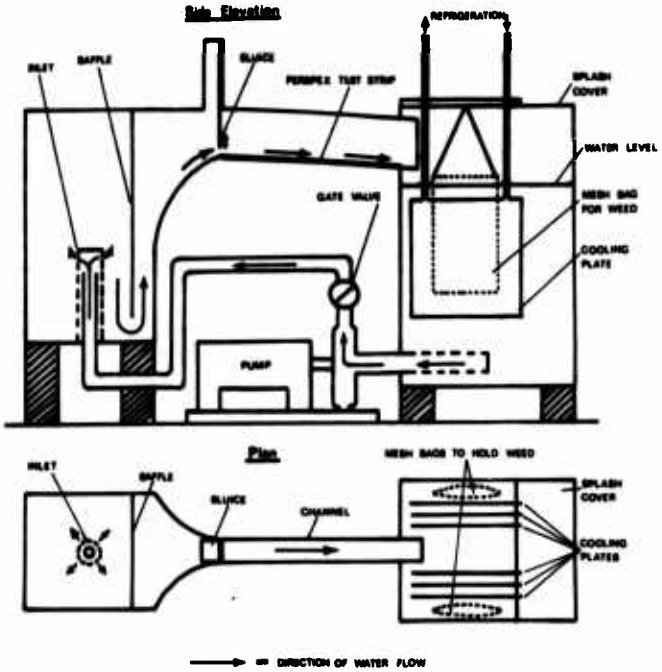


Fig 1. Experimental system for studying the settlement of swarmers of Enteromorpha spp at different water velocities

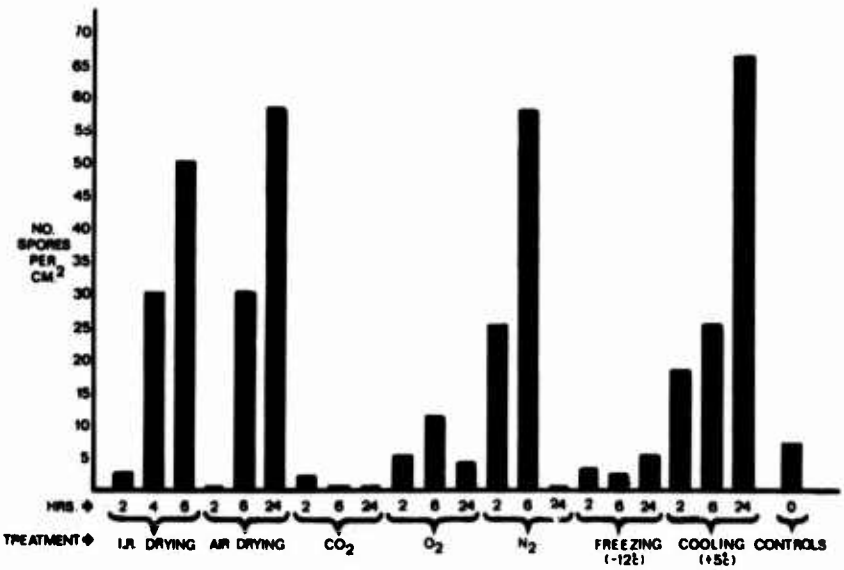


Fig 2. The effect of various shock treatments upon the production of swarmers by Enteromorpha spp.

Mechanisms of Adhesion of Fouling Organisms

D. J. Crisp, FRS

University College of North Wales
N.E.R.C. Unit
North Wales, U. K.

I. Introduction

The adhesion of living tissue to non-living material is not only of interest in marine fouling; it has important applications also in surgery and dentistry (Manly 1970), while the principles underlying the success of biological adhesives which set underwater may have wide significance in the development of artificial cements designed for the same purpose.

Three aspects of bioadhesion can be distinguished: first, cell to cell adhesion; secondly, adhesion between the living tissue and non-living parts of the animal; and thirdly, adhesion between the animal and foreign objects. Cell to cell adhesion is a property of normal growth and organization, involving cell surface structure and compatability; its significance in medicine is immense, but it need not concern us here. The union of living tissue to inert structural elements which are formed by the animal, such as calcium phosphate (bone), calcite (shell) and chitin, appears to require an intermediate macromolecule of rather specific structure; for instance collagen is associated with bone in vertebrates, conchiolin with calcite in molluscs and arthropodin with chitin in arthropods. A bone, shell valve, or piece of arthropod exoskeleton always contains the relevant protein incorporated into its structure. Hence, these specialized proteins not only form bonds between tissues and the skeletal elements but also help to unite the crystals or macromolecules of the skeletal elements into a firmly knit resilient component of the animal's organization. These internal adhesives are not relevant directly to the adhesion of fouling organisms but their structure may prove to be of significance in connection with gregarious pre-settlement behavior. Two of them, arthropodin and conchiolin, have been implicated in the recognition of the presence of adults of their own species by barnacle larvae (Crisp and Meadows, 1962, 1963) and by oyster larvae (Crisp, 1967) respectively. It is possible that recognition is mediated by molecular attraction between a part of the surface of the larva and the surface layer of the structural protein (Crisp, 1965a,1973). If so, they would again have an adhesive function in a somewhat different context.

The fouling problem is clearly concerned with the third aspect of bioadhesion, attachment to foreign objects. Representatives of all the lower plants from bacteria to macroalgae, and of all the animal phyla from protozoa to the lower chordates living in aquatic environments attach themselves permanently or temporarily to extraneous objects or to other organisms. The subject, despite its importance, has been greatly neglected, and the nature of the majority of animal plant adhesives is unknown.

II. Adhesion Mechanisms

The materials used by organisms for attachment to foreign objects may be divided into two classes:

(1) Permanent cements which undergo a setting or curing process, usually a form of chemical cross-linkage of macromolecules. The adhesive force is then related to the strength and number of the chemical bonds which have to be severed.

(2) Temporary adhesives which are not chemically bound, but which hold two surfaces together by the work which has to be done against viscosity when the surfaces are separated.

The phenomenon is well known to all biologists who have attempted to separate a pack of wet microslides, and its underlying principle was expounded by Stefan (1874). Stefan type adhesives are viscous "tacky" fluids, their adhesive 'force' dependent not only on their viscosity but also on the circumstance under which separation is brought about, details of which will be described below.

These two mechanisms have a quite different applicability. The permanent adhesive is ideal for attaching an organism in one position throughout life, or for bonding pieces of substratum to build a permanent tube. Since the cement typically cannot relax without involving complete failure of the adhesion, the mechanism is unsuitable for fixing an animal in a situation where it may need to move or to yield to a superior force. For this purpose, as well as for all types of temporary attachment, Stefan adhesives are required.

It is not generally realized how important, and therefore how widespread, are devices for temporary attachment of organisms living in water. The density of the medium renders the aquatic environment totally different from the terrestrial from the point of view of locomotion over surfaces. Most aquatic organisms have specific gravities not greatly in excess of that of water so that gravitation may be largely or entirely eliminated. Conversely, the force exerted by water currents impinging on aquatic organisms is much greater than the forces due to air currents of corresponding velocity on sub-aerial creatures. The magnitude of such forces approximates to the rate of change of momentum, $a\rho(\Delta u)^2$, where a is the area of impingement, ρ is the density of the medium and Δu the change in fluid velocity after impact. Water having a density so much greater than that of air, the aquatic compared with the terrestrial organisms experience forces augmented by several magnitudes. Hence, the force of friction, which enables all but the smallest terrestrial organisms to resist disturbances and to crawl over horizontal surfaces on land cannot perform this function for small organisms living on surfaces under water. A different force is therefore needed. Adhesion by sticky secretions from the limb tips or body segments appears the most probable substitute available for gravitational friction. Thus, in the interstitial environment of sands, where the animals are invariably small and need to withstand the considerable flow of water through the pores, adhesive organs are almost universal (Delamare de Boutteville, 1960). Organs of adhesion are likely to be equally universal in small organisms (of less than 1 cm) which crawl freely over submerged surfaces, including of course, the larvae of fouling organisms.

Although the distinction between a rigid, permanent cement and a fluid Stefan adhesive appears in principle quite sharp, it may not necessarily be so. If the processes of polymerization and cross-linkage which lead to the formation of the former proceed only to a limited degree, a tacky visco-elastic fluid may be formed which may have rigidity under sudden stress but relax under a steadily maintained force.

III. Permanent Cements

Most examples of animal cements of the permanently setting type utilize a protein-polyphenol oxidase system. The best known are in the

arthropods. The arthropod cuticle itself is composed of chitin and protein, and the latter is normally hardened by o-dihydroxyphenols and phenol oxidases which enter by diffusion. The oxidase converts the dihydroxyphenol to the quinone which then combines with a free amino group on the protein to form a protein-diphenol complex. The latter is again oxidized in the presence of phenol oxidase to form a protein quinone complex which can link with another amino group, so joining two proteins together. It is believed that terminal amino groups are first involved and later the amino groups of the protein side chains. Thus the setting process will first increase the effective chain length of the proteins, making the material more viscous and later cross-link the molecules into a rigid structure. There are clear indications that this mechanism has been adapted by the arthropods for a variety of purposes in addition to hardening of the cuticle, such as cementing the eggs of crustacea to the swimmerets, hardening of insect egg cases after laying, and in the production of cement by barnacles.

A mechanism to delay the onset of the hardening process until the appropriate moment is usually essential. For example, a secretion must remain liquid until it has been discharged from a gland through its ducts. The simplest mechanism of control is by the separate discharge of two components which activate each other on mixing. Prior's description of the hardening of the cockroach ootheca (Prior, 1940, a,b) affords the classic example. The left colleteral gland secrets the protein together with polyphenol oxidase and the o-dihydroxy phenol combined in the form of a glycoside and therefore not vulnerable to the phenol oxidase. The right gland secretes a β glycocidase which liberates the phenol. The hardening process is therefore initiated as the two secretions mix and surround the egg.

Evidence for the existence of similar mechanisms in the attachment cements of fouling organisms exists (Brown, 1950) but is fragmentary since the relevant biochemical studies in invertebrates other than arthropods have not been done. However, the following features may be regarded as indications of the existence of a protein-phenol-phenoloxidase setting mechanism; when all are present simultaneously, the evidence is strong:

(a) Demonstration of phenolic compounds in secretory tissue or in their secretum,

(b) Demonstration similarly of phenol oxidase,

(c) Observed increase in viscosity or rigidity of secreted cement,

(d) Double system of secretory components.

On the basis of these criteria there is strong evidence for the existence of quinone tanning in the byssus of the bivalve Mytilus (Brown, 1952; Smythe, 1954; Ramalingam and Ravindrarath, 1971) and some evidence for it in the setting of the hydrosarc of Tubularia (Hawes, 1955). The reef building tubeworm Sabellaria also appears to possess such a mechanism (Vovelle, 1945). The evidence in regard to barnacle cement will be discussed in more detail below.

It follows that the framework of animal cements is generally of protein, a point which can readily be confirmed by analysis if sufficient material is available in a pure form, as in bivalves and barnacles (Cooke, 1970; Walker, 1972). Where the amounts are insufficient, the technique employed by Evans and Christie (1970) may be useful. They showed that the attachment of the minute spores of Entermorpha intestinalis was vulnerable to proteolytic enzymes, while they were lossened but not detached by carbohydrases. The authors therefore concluded that the adhesive was a protein-carbohydrate complex.

IV. Temporary Adhesion

As argued above, all small surface living invertebrates must have non-gravitational means of temporary attachment, such as suction or Stefan adhesion. The ciliated crawling larvae of many invertebrates such as the metatrochs of Spirorbis, the cypho nautes of Bugula, and the pediveligers of Ostrea lay down a mucus trail as they glide over the surface. The cypris larva has a complex antennulary organ which is used for temporary attachment (Fig. 1a). It is not suitably designed to attach by suction, but probably adheres through the secretion of adhesive produced most likely by numerous unicellular glands which open onto the microvillous attachment pad (Nott and Foster, 1969). Presumably the pad can be detached by "peeling off" from one end, while at the same time being capable of great resistance to a pull normal to the surface. The process of attachment and detachment needs to be observed in detail and interpreted in relation to the complex system of extrinsic and intrinsic muscles operating the appendage.

Stefan predicted the force between two discs of radius R fully immersed in a liquid medium of viscosity η as

$$F = \frac{3\pi\eta R^4}{4t}\left[\frac{1}{x_1^2} - \frac{1}{x_2^2}\right]$$

where x_1 and x_2 are the initial and final distances separating the discs and t is the time taken to effect separation. Reducing the equation to its more convenient differential form

$$F_x = 2K\frac{dx}{dt}\,x^{-3} \qquad (K = 0.75\pi\eta R^4)$$

This equation shows that the force preventing separation of the surfaces is a direct function of the rate of separation. The system will not withstand indefinitely a continuously applied pull, but it will withstand suddenly applied forces with great resistance and without any danger of rupture at a plane of fracture. Furthermore, the adhesion is very sensitive both to the area of contact, rising as its square, and to the distance of separation, being inversely proportional to the cube of the fluid thickness. In contrast, the horizontal drag, F_y, produced when the discs are slid sideways at a given velocity is very much less than the vertical force F_x. For discs separated by a fluid with newtonian viscosity η,

$$F_y = \pi R^2 \eta dy/dt\; x^{-1}.$$

Thus, comparing F_y and F_x for discs of 1 cm radius separated by a 10μ film of water with $dx/dt = dy/dt = 1.0$ cm/sec:

$$F_y = 4.7 \times 10^7 \text{ dynes}$$

$$F_x = 31.4 \text{ dynes.}$$

This form of adhesion is ideal therefore where the animal needs to glide over the surface without losing contact with it.

Perhaps the clearest examples of Stefan adhesion are the limpets. The

characteristically low shell with a very large expanse of foot closely applied to the surface and covered with mucus secreting glands has been evolved independently several times. In the genus Patella the force of adhesion measured by subjecting the animals to a steadily increasing force is greatly in excess of an atmosphere (Driver, 1970), showing that suction alone is not capable of accounting for the force of adhesion. The lateral force required to detach the limpet from a smooth surface is much less than the vertical force needed to lift it off. Indeed pulling it off vertically often causes failure within the structure of the foot, leaving the epithelium still attached. Limpets and other gastropods can progress over surfaces while still attached to them by passing progressive waves of contraction or regressive waves of extension along the length of the foot (Jones and Trueman, 1970). The waves can be seen beneath the foot by observing limpets walking over glass. They appear as dark areas where the epithelium is momentarily raised off the surface. At the forward end of such a wave, the muscles evidently 'peel off' the epithelium, while at the rear end the epithelium is reapplied very closely to the surface probably being pulled down by lowered hydrostatic pressure within the wave. The waves, being sources of adhesive weakness, disappear instantly the limpet is disturbed, the foot spreading out and applying itself more closely to the surface. The mechanism is not immediately obvious, but possibly some of the intervening fluid can be withdrawn into the substance of the foot, so decreasing the separation distance x and greatly increasing the strength of adhesion.

The ascidian tadpole attaches by a sticky secretion at its anterior end, and the material shows no sign of hardening (Lane, 1971). Moreover, colonies of compound acidians are capable of limited mobility (Carlisle, 1961) which would be incompatible with the existence of a rigid cement. Probably a viscid material is utilized by such colonies to maintain contact with the substratum.

V. Barnacle Adhesives

Adhesives for permanent attachment of barnacles to the substratum are secreted at two stages in the life history. Just prior to metamorphosis, the cyprid exudes through canals in the antennulary attachment organ, a quantity of cement originating from the paired larval cement glands, (Fig. 2a,b). This is called the cyprid cement. After a short interval of growth, during which the juvenile barnacle is still dependent for adhesion on the cyprid cement, the adult cement apparatus develops in the form of groups of unicellular glands discharging through collecting ducts which open below the calcareous or membranous base of the animal. The cells and ducts form an intricate pattern, first described by Darwin (1854), which increases in size and complexity with the growth of the animal (Fig. 3). The adult cement is obtainable in much larger amounts than the cyprid cement, hence, its constitution is better known and it will be convenient to describe it first.

(a) Adult Cement

(i) Histology and Histochemistry. The appearance under the light microscope of the unicellular glands secreting adult cement has been described by Bocquet-Védrine (1965) for Elminius modestus and by Lacombe (1966, 1967, 1968) for Balanus tintinnabulum. Lacombe and Liguori (1969) describe differences between B. tintinnabulum and Lepas anatifera in the location of the glands and the arrangement of the collecting ducts. In B. tintinnabulum (as in Elminius modestus) there were two markedly different cytoplasmic regions, one with affinity for basic dyes and the other for acid dyes; it was suggested one was a region of synthesis and the other of accumulation. On the other hand, Lepas gland cells were not regionally differentiated but contained vacuoles varying in size throughout the cytoplasm. Lacombe (1967) correctly found that the cytoplasm was P.A.S. negative and rich in ribonucleic acid but incorrectly postulated from the positive reaction with alcian blue the presence of acid mucopolysaccharide--

even though she noticed that ribonuclease treated controls were less strongly stained. Walker (1970) using adequate controls, showed that in fact the alcian blue reaction was wholely due to the presence of ribonucleic acid in the synthetic region of the cell, and no appreciable carbohydrate or mucin was present. The collecting canals and the regions where they enter the gland cells were shown to be rich in alkaline phosphatase by Arvy et al, (1968).

Walker (1970) described the fine structure of the adult cement glands in three species, Balanus balanoides, Elminius modestus and Balanus hameri. In the first two species (Table 1) there were distinct areas, staining strongly for ribonucleic acid, and containing free ribosomes, mitochondria, and golgi bodies and sometimes lipid globules. All these features are indicative of synthetic activity. Adjacent were areas containing aggregations of vacuoles, the contents of which were protein positive. These regions were presumably for storage. They connected with and presumably discharged through intracellular ducts. The cement secreting cells of B. hameri had a cytoplasm of uniform appearance, containing, however, the same elements that were segregated in two regions of the gland cells of the other two species. Like those of B. tintinnabulum (Liguori, 1970), the cells of B. hameri lacked intracellular collecting ducts but were in intimate contact with the cement duct cells. Walker's findings show clearly that the material synthesized by the cement glands is a protein with no detachable admixture of carbohydrate or lipid.

(ii) Chemical Analysis. The successful analysis of adult cement depends on obtaining sufficient quantities of unadulterated material. Material scraped away from the base could easily become contaminated with ovarian lipid if the base were damaged, and this may account for the large component of lipid in barnacle cement reported by Cooke (1970) but unsupported by other investigators. Walker (1972) devised a method of maintaining barnacles under circulation out of contact with the substratum so that the cement could be collected at intervals in a pure state. Nitrogen determination both by elemental analysis and by the Keldjahl method showed that the material was composed very largely of protein, in agreement with Saroyan et al (1970). Its amino acid composition was also in general agreement with that recorded by Cooke (1970) and by Saroyan et al (1970), but Walker's analyses include additional information on the rather high level of sulphur containing amino acids. Electron probe analysis indicated that not only sulphur but also calcium and phosphorus form an integral part of the matrix. The claim made by Cardarelli (1968) that the cement of B. nubilis is of carbohydrate and lacking almost entirely in nitrogen, differs from the conclusions of all other workers and seems likely to be false. It is improbable that the material of one species of the genus would differ so fundamentally from that of the others.

The adult cement does not appear to harden, but forms an insoluble somewhat plastic coat where exposed to water. When a barnacle is gently pried off a surface, fine strands of sticky material, presumably cement, can sometimes be seen between the base and the substratum.

(b) Cyprid Cement

The suggestion made by Harris (1946) that the fixation of cirripedes might be accomplished by means of a quinone tanned protein was first tested by Knight Jones, and Crisp (1953) who obtained positive reactions for phenols in the cyprid antennule and cement apparatus. Hillman and Nace (1970) detected protein and traces of lipid in the mass of cement surrounding the antennule of settled cyprids of B. elurneus, but obtained no reaction for carbohydrates nor for phenolic amino acids. However, Saroyan et al (1970) not only demonstrated again the protein nature of the cement, but also confirmed the presence of phenolic amino acids.

Walker (1971) made a detailed study by light and electron microscopy of the whole of the cyprid cement apparatus of the cypris larva of B. balanoides. He found two types of cells in the cement gland (Fig. 2b) which he termed the α and β cells (Table 2). Lipids and carbohydrates were both undetectable. The α cells contained granules giving positive reactions for proteins, phenolic compounds, and a polyphenol oxidase system; the β cells gave only a reaction with kromphenol blue and therefore appear to contain only protein. The reactions of the α cell granules could be repeated on the recently discharged cement. It is therefore tempting to suggest that we have here a two component system like that of the cockroach shell gland, which allows polymerization only after the components of the α glands have been activated by mixing with β gland material. It is strange, however, that whereas all the β material appears to be discharged, considerable amounts of α granules are left in the cells. After discharge the duct system is left empty. Possibly the β material is flushed through after the α granules and the process of mixing occurs externally. Like the adult cement, the cyprid cement, when probed, appears plastic and sticky rather than rigid.

VI. Mechanism of Barnacle Adhesion

The mode of growth of a barnacle makes it impossible for the calcareous side walls (parietes) to be firmly bound to the substratum. It is therefore necessary for the base alone to be cemented and the parietes to be held down by muscles which can relax when necessary to allow accretion at the growing basal margin of the shell.

Gutmann (1960) described these as "fixation fibres" (Fig. 4). They are very numerous and have a long tendon stretching to the parietes and a short tendon to the base, with a small muscle between. Thus the mechanical structure of a barnacle is precisely like that of a limpet, the only major difference being the ability of the latter to move voluntarily on rythmic waves of compression or extension (Crisp, 1965b). Despite literary allusions to the contrary (Dickens, 1837), barnacles are capable of lateral movement under sustained pressure (Crisp, 1960), and they can, like limpets, be detached and reset. It is reasonable, therefore, to suppose that the adhesive mechanism of the adult sessile barnacle is also, like that of the limpet, of the Stefan type, dependent on a high viscosity fluid rather than a chemically bound rigid solid for its bond.

The same arguments do not apply to the adhesion of the cyprid, nor of the stalked barnacle. The cyprid attachment cement has only a temporary function; it could be ruptured after the adult glands became functional without the animal's suffering serious harm. The stalked barnacle probably does not need to be able to migrate under pressure. Its cement appears to become hard and waxy; nevertheless, the glands remain active throughout life and the animal can recement itself if detached (Patel, 1959).

References

ARVY, L., LACOMBE, D. and SHIMONY, T., (1968), Am. Zool. 8, 817.

BOCQUET-VEDRINE, J., (1965), Archs Zool. exp. gén. 105, 30-76.

BROWN, C. H., (1950), Nature, Lond. 165, 275.

BROWN, C. H., (1952), Q. Jl microsc. Sci. 93, 487.

CARDARELLI, N. F., (1968), U. S. Dept Health Educ. Welf. Natn. Inst. Health Publication No. 51, 49 pp.

CARLISLE, D. B., (1961), Proc. Zool. Soc. Lond. 136, 141-146.

COOKE, M., (1970), pp. 139-150 in Adhesion in Biological Systems (ed. R. S. Manly). Academic Press, New York and London.

CRISP, D. J., (1960), Nature, Lond. 188, 1208-1209.

CRISP, D. J., (1965b), pp. 99-117 in Ecology and the Industrial Society. Fifth Symposium of the British Ecological Society. Blackwells: Oxford.

CRISP, D. J., (1965a), pp. 51-65 in Botanica Gothoburgensia III. Proc. Fifth Marine Biological Symposium, Göteborg.

CRISP, D. J., (1967), J. Anim. Ecol. 36, 329-335.

CRISP, D. J., (1973), Factors influencing the settlement of marine invertebrate larvae. In: Perspectives in Chemoreception by Marine Organisms (ed. P. T. Grant). Academic Press, New York. (In Press.)

CRISP, D. J. and MEADOWS, P. S., (1962), Proc. R. Soc. Lond. B.156, 500-520.

CRISP, D. J. and MEADOWS, P. S., (1963), Proc. R. Soc. Lond. B.158, 364-387.

DARWIN, C., (1854), A monograph of the sub-class Cirripedia: Balanidae, Verrucidae, etc., Ray Soc. London. 684 pp., 30 pl.

DELAMARE deBOUTTEVILLE, C., (1960), Vie Milieu Suppl. 9, 740 pp.

DICKENS, C., (1837), The Pickwick Papers. 609 pp. Chapman and Hall: London.

DRIVER, P., (1970), Unpublished M.Sc. Thesis, University of Wales.

EVANS, L. V. and CHRISTIE, A. O., (1970), Ann. Bot. 34, 451-66.

GUTMANN, W. F., (1960), Abh. senckenb. naturf. Ges. 500, 1-43.

HARRIS, J. E., (1946), J. Iron Steel Inst. 2, 297-333.

HAWES, F. B., (1955), J. mar. biol. Ass. U.K. 34, 333-346.

HILLMAN, R. E. and NACE, P. F., (1970), pp. 113-121 in Adhesion in Biological Systems (ed. R. S. Manly) Academic Press, New York and London.

JONES, H. D. and TRUEMAN, E. R., (1970), J. exp. Biol. 52, 201-216.

KNIGHT JONES, E. W. and CRISP, D. J., (1953), Nature. Lond. 171, 1109.

LACOMBE, D., (1966), Publčoes Inst. Pesq. Mar. Rio de Janeiro. 32, 1-39.

LACOMBE, D., (1967), Publčoes Inst. Pesq. Mar. Rio de Janeiro. 011, 1-29.

LACOMBE, D., (1968), Publčoes Inst. Pesq. Mar. Rio de Janeiro. 017, 1-22.

LACOMBE, D. and LIGUORI, V. R., (1969), Biol. Bull. mar. biol. Lab., Woods Hole, 137, 170-180.

LANE, D. J. W., (1971), Unpublished M.Sc. Thesis, University of Wales.

LIGUORI, V. R., (1970), pp. 123-138 in Adhesion in Biological Systems (ed. R. S. Manly) Academic Press, New York and London.

MANLY, R. S. (ed.), (1970), Adhesion in Biological Systems 302 pp. Academic Press, New York and London.

NOTT, J. A. and FOSTER, B. A., (1969), Phil. Trans. R. Soc. Lond. B.256, 115-134.

PATEL, B., (1959), J. mar. biol. Ass. U.K. 38, 589-597.

PRIOR, M. G. M., (1940a), Proc. R. Soc. Lond. B.128, 378-393.

PRIOR, M. G. M., (1940b), Proc. R. Soc. Lond. B.128, 393-407.

RAMALINGAM, K. and RAVINDRANATH, M. H., (1971), Acta histochem. 41, 57-61.

SAROYAN, J. R., LINDNER, E., DOOLEY, C. A., and BLEILE, H. R., (1970), Ind. Engng Chem. Prod. Res. Dev. 9, 122-133.

SMYTHE, J. D., (1954), Q. Jl microsc. Sci. 95, 139-152.

STEFAN, J., (1874), Sber. Akad. Wiss. Wien (Math-Naturw. Kl) 69, 713.

VOVELLE, J., (1945), Archs. Zool. exp. gen. 106, 1-187.

WALKER, G., (1970), Mar. Biol. 7, 239-248.

WALKER, G., (1971), Mar. Biol. 9, 205-212.

WALKER, G., (1972), J. mar. biol. Ass. U.K. 52, 429-435.

Table I. Constitution of two regions of cement gland cells of Elminius modestus (Based on Walker, 1970)

Test	Significance	Region of Synthesis	Region of Storage
Azan	---	Blue	Red
Bromophenol blue	Protein	Negative	Strongly positive
Millon's reagent	Tyrosine	Negative	Positive
D.M.A.B.* - nitrite	Tryptophan	Negative	Negative
D.D.D.** - n-ethyl maleimide	Control S.H.	Negative	Weakly Positive
D.D.D.	SH (Cysteine)	Negative	Positive
D.D.D. - Thioglycollic reduction	S=S (Cystine)	Negative	Strongly Positive
P.A.S.***/control	Carbohydrate	Negative	Negative
Lead tetraacetate - Schiff	Carbohydrate	Negative	Negative
Alcian blue/Ribonuclease control	Mucins	Negative	Negative
Mucihaematin/Ribonuclease control	Mucins	Negative	Negative
Hale's Colloidal Iron	Acid Polysaccharide	Negative	Negative
Toluidine blue	Muco-substances with strongly acidic groups give γ (red) metachromasia	β (purple) Metachromasia only	Negative
Azure A			Negative
Alcian Blue	Mucins and ribonucleic acid	Strongly positive	Negative
Mucihaematin		Strongly positive	Negative
Methyl green pyronin/ ribonuclease control	Ribonucleic acid	Strongly positive	Negative

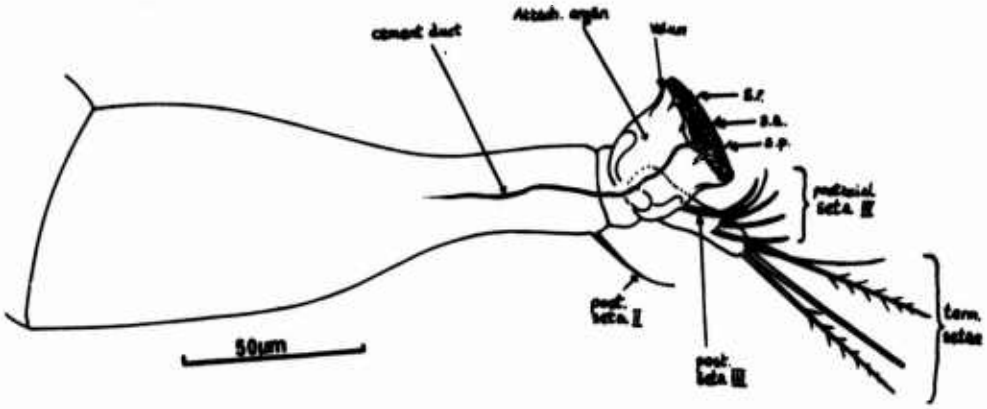
Table I con't.

Test	Significance	Region of Synthesis	Region of Storage
Sudan black B/Methanal: chloroform control	Lipids	Strongly positive. Negative in Balanus balanoides	Negative
Conclusion		High concentration of R.N.A. with lipid	Protein storage only

* Dimethyl aminobenzaldehyde
** Dihydroxy -dinaphthyl-disulphide
*** Periodic acid Schiff reaction

Table II. (From Walker, 1971)

Test	α Cell Granules	β Cell Secretion	Cement	Significance
P.A.S./Control	—	—	—	No carbohydrate
Lead tetraacetate Schiff	—	—	—	
Alcian blue	—	—	—	No mucins
Mucihaematin	—	—	—	
Hale's reagent	—	—	—	No acid polysaccharides
Toluidine blue metachromasia	—	—	—	
Azure A metachromasia	—	—	—	
Bromophenol blue/ de-amination control	+++	++	+++	Protein
Millon's reagent	+++	—	+++	Tyrosine
D.M.A.B. - nitrite	++	—	—	Tryptophan
D.D.D.	++	—	++	SH groups
D.D.D. n-ethyl maleimide	+	—	+	SH block
D.D.D. Thioglycollic reduction	+++	—	+++	S=S groups
Ferric chloride	+++	—	+++	Phenols
Sodium iodate	+	—	++	
Argentaffin	+	—	+	
Acid diazonium	++	—	++	
Polyphenol oxidase/KCN control	+++	—	++	Strong phenolase activity
Sudan black B/control	—	—	—	No lipid
Azan	red	blue	mainly purple red externally	



s.r. radial sense organs

s.a. axial sense organ

s.p. postaxial sense organ

Figure 1a: Structure of the antennule of Balanus balanoides (From Nott and Foster, 1969).

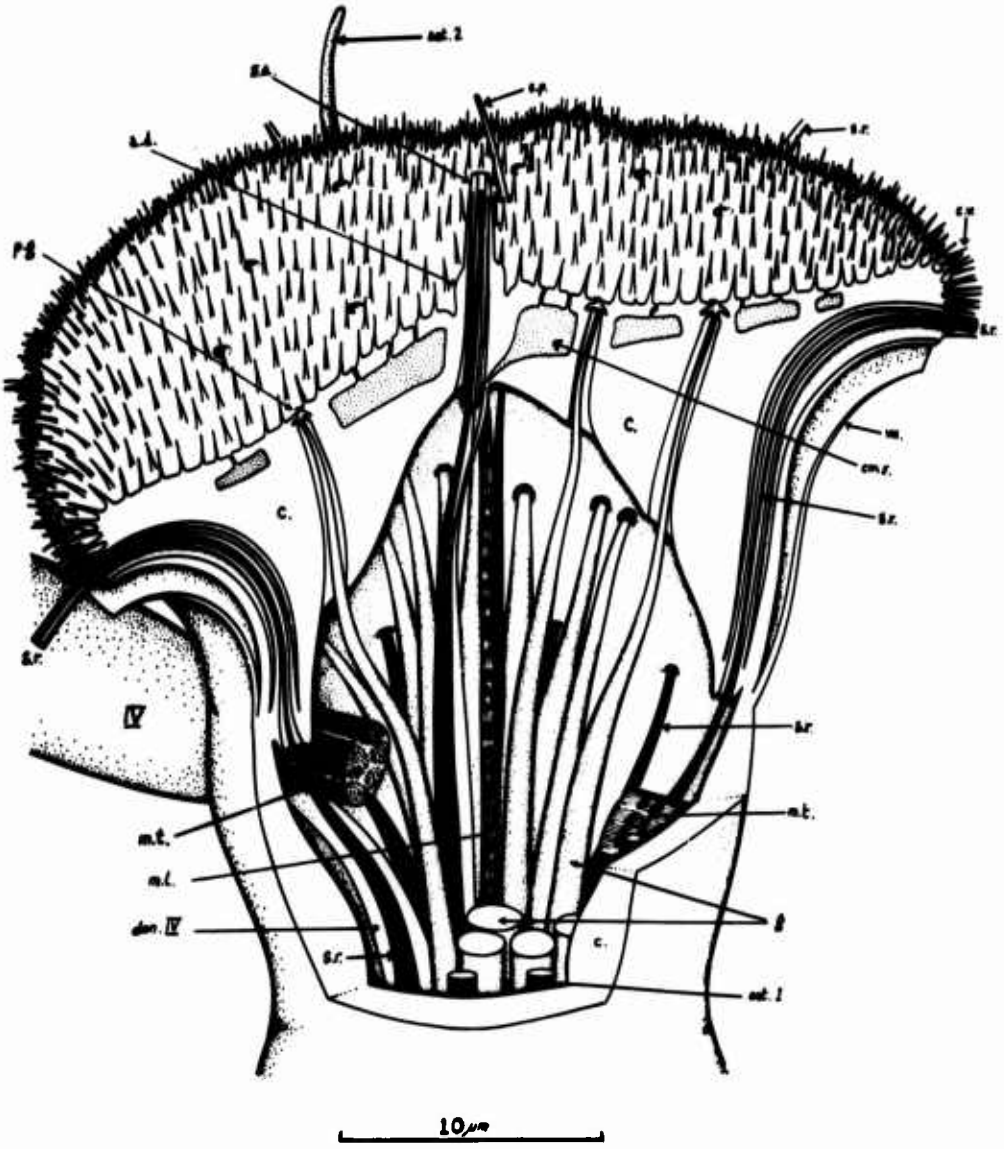


Figure 1b. Structure of the antennulary attachment organ of Balanus balanoides (From Nott and Foster, (1969).

Fig.1b (key to abbreviations used)

a.d.	axial dome
c.	cuticle
c.v.	cuticular villi
cm.	cement duct
den.IV	dendrites to the fourth segment
g.	antennular gland
m.l.	longitudinal muscle
m.t.	transverse muscle
p.g.	pore of antennular gland
s.a.	axial sense organ
s.p.	postaxial sense organ
s.r.	radial sense organ
set.1	preaxial seta
set.2	postaxial seta
vm.	velum

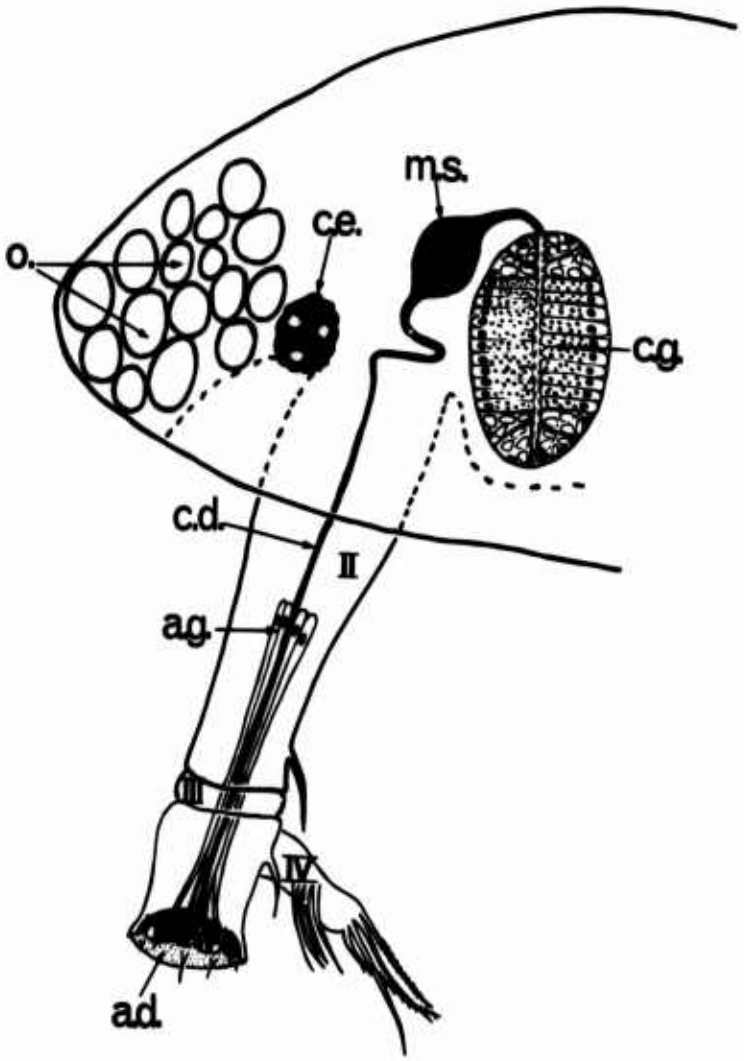


Figure 2a. Cuprid cement apparatus.
Arrangement for the discharge of the contents of the cement gland through the antennulary attachment organ.

a.d. Attachment disc of antennulary organ
a.g. Antennulary glands (for temporary adhesion?)
c.d. Cement gland duct
c.e. Compound eye
c.g. Cement gland
m.s. Muscular sac
o. Oil globules

II, III, IV, Segments of antennule (After Walker)

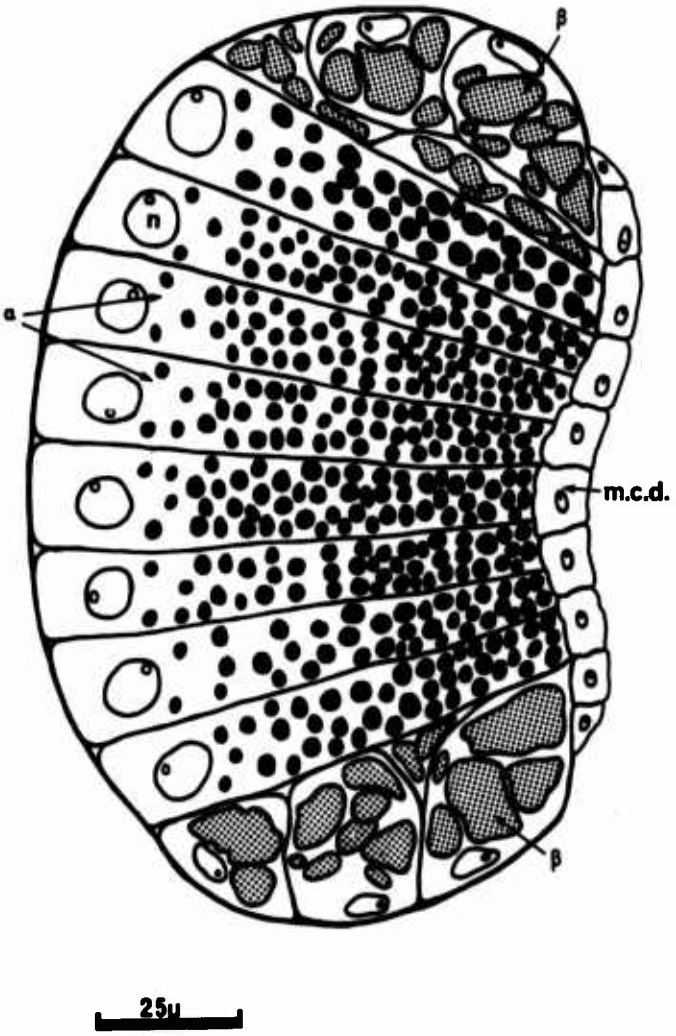


Figure 2b. Cyprid cement apparatus.
Median transverse section through one of the cement glands of the cyprid showing the positions of the two cell types α and β. n - nucleus, m.c.d. - median collecting duct. (From Walker 1971).

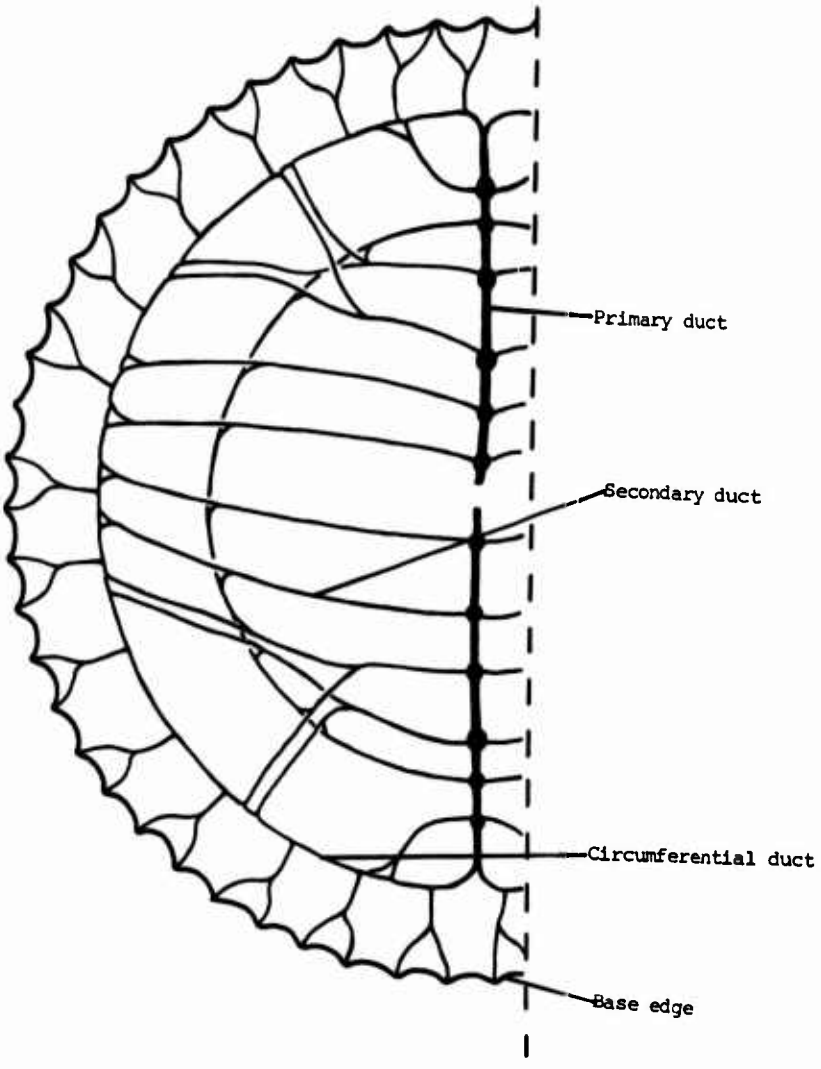


Figure 3. Balanus hameri. Portion of calcareous base showing the adult cement duct system. (From Walker, 1970.)

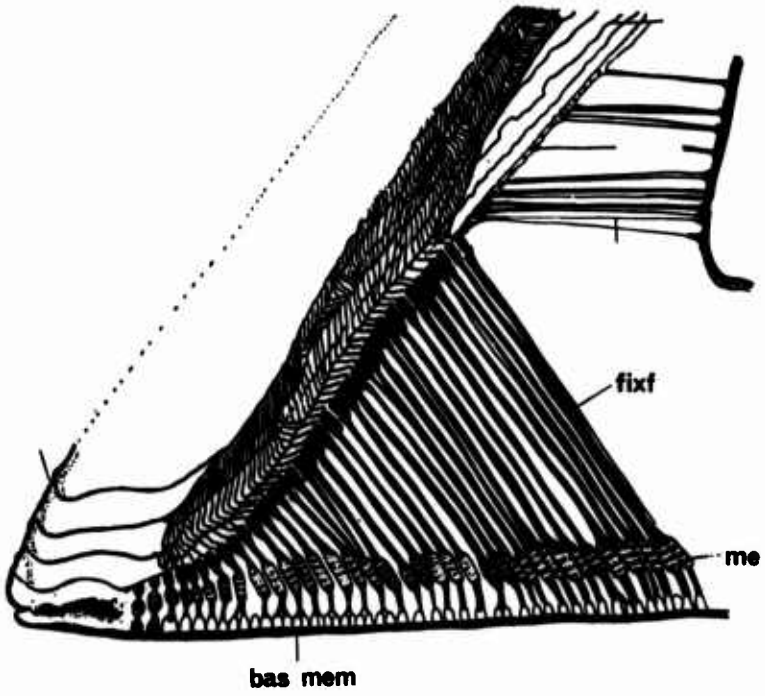


Figure 4. Section of the edge of a growing barnacle. The parietal plate on the left shows the last four growth increments, probably corresponding to moults. A thin slip of tissue (shaded) separates the growing edge of the parietal plate from the growing rim of the base. Fixation fibres (fixf) with small striated muscles (me) and a short tendon hold the parietal plate to the base (bas. mem). The latter is fixed by adult adhesive to the rock surface. (Diagram after Gutmann, 1960)

Discussion

Lindner: You mentioned that your laboratory found some evidence of phenolase or polyphenoloxidase enzyme. My question would be what kind of evidence did you find and if you did in the electron microprobe analysis, did you look for copper since the phenolase enzyme does contain a copper and that would be a very good indication for phenolase enzyme presence.

Crisp: The phenoloxidase was identified by histochemical tests, not for the presence of copper. We looked at the metallic elements present in the cement by means of electron probe, but copper was only present in trace amounts. It was not present in these congregations of material which were largely aluminium, iron and cilicon, but there was really too little of it present for us to be sure whether it was uniformly distributed or was an impurity. So I would not like to say that we have got evidence in the presence of copper of a phenoloxidase. The evidence is solely of the histochemical tests and that was in the cells which are producing--the cement cells, the alpha cells--which are producing the cement material which is discharged down the duct.

Molecular Fouling of Surfaces in Seawater

Rex Neihof and George Loeb

Naval Research Laboratory
Washington, D. C. 20390

As part of an investigation of the initial events occurring on exposure of solid surfaces to seawater, the surface electrical charge of different model particles exposed to various seawater media has been measured by electrophoresis. The importance of traces of dissolved organic matter in imparting the characteristic moderately negative charge generally observed on immersed solids was assessed by using seawater samples treated with ultraviolet light to destroy organic constituents. Model particles of an anion exchange resin, germanium and quartz exhibited surface charges ranging from strongly positive to strongly negative in irradiated seawaters but in untreated seawater converged within a range from zero to moderately negative. The amount of seawater necessary to complete the change in charge on a given number of particles was inversely related to the content of dissolved organic matter. A comparison of results in irradiated natural seawater and a simple artificial seawater indicated that the seven major inorganic ions are responsible for determining the charge of solids in organic-free seawater. Thus the surface charge exhibited by solids in natural seawater is contributed largely by an adsorbed layer of electronegative organic matter. The difficulty with which this material is eluted from surfaces suggests that it is macromolecular.

Key Words: Electrophoresis; Dissolved organics; Surface activity; Seawater; Macromolecular adsorption; Molecular fouling; Surface charge; Organic photodegradation; Seawater immersion.

Introduction

Fouling and corrosion are initiated on the surfaces of materials subjected to marine exposure. An understanding of the mechanisms of adhesion of fouling organisms and of corrosive attack therefore requires a knowledge of the surface properties of materials in contact with seawater. An important factor in these interfacial processes is the electrical charge on the surface. In an earlier investigation we determined the surface charge of various particulate materials with widely different surface properties using a recently improved microelectrophoresis technique (1,2)[1]. These model particles in artificial seawater exhibited surface charges ranging from strongly positive for an anion exchange resin to strongly negative for a clay mineral, but in natural seawater showed a restricted range of moderately negative values of surface charge. This range was similar to that of natural particulate matter such as bacteria, small algae and detritus. These results suggest that solid surfaces adsorb similar, electronegatively charged, minor constituents from seawater.

Experiments with dialyzed seawater indicated that substances with molecular weights both below and above about 12,000 were involved in producing the changes in surface charge observed with model particles. These results together with the observations of Harvey (3), ZoBell (4), Bader, Hood and Smith (5) and others strongly suggest that the constituents

[1] Figures in parentheses indicate the literature references at the end of this paper.

responsible are organic. To evaluate this possibility it is necessary to have as a control, seawater which is free of organic matter. Artificial seawater is not entirely satisfactory for this purpose because of the traces of organic surface active material known to be present even in reagent grade salts of high purity (6). Ultraviolet photo-oxidation as described by Armstrong, Williams and Strickland (7), however, seems to offer an eminently suitable method for ridding seawater of organic matter. It requires no addition of chemicals to the water sample other than a small amount of hydrogen peroxide or other source of oxygen and decomposition appears substantially complete within a few hours. This paper reports on the differences in surface properties of selected materials after exposure to natural and photo-oxidized seawaters.

Experimental

The electrophoresis apparatus, described elsewhere in detail (2) consisted of a flat, quartz observation cell 0.074 x 1.21 cm in cross-section fused through graded seals to Pyrex electrode chambers at each end. The cell was positioned with faces vertical for viewing with a horizontal microscope at 400 x and was immersed in a water bath kept at 25.00°C. Palladium-hydrogen electrodes (8) served to provide the necessary 6 - 10 Ma current.

The electrophoretic mobility, M, in (μm/sec)/(V/cm) was computed from the formula:

$$M = \frac{D\ K\ A}{TI}$$

where T is the time in seconds required for a particle to traverse a distance, D, in μm observed on a calibrated microscope reticule, K is the specific conductance of the suspending medium in $ohm^{-1}cm^{-1}$, I is the current in amperes and A is the cross sectional area of the electrophoresis cell in cm^2. The mean mobility of 20 particles was routinely taken to characterize a suspension. Standard deviations of ±0.05-0.10 were typical.

Conductivities were measured at 25.00°C in a dip cell using a bridge (Beckman RC-18) operating at 1000 Hz. Salinity values were derived from conductivities (9).

Seawater samples were obtained from two sources: the Chesapeake Bay off Patuxent Naval Air Station, Maryland (collected at high tide 3 May, 1972, salinity 9.0‰, pH 7.9) and the Gulf of Mexico about 350 km WNW Key West, Florida (25°50' N; 85°30'W collected 29 March, 1972, salinity 35.4‰, pH 8.1). The latter sample was taken about one meter below the surface through Nytex and polyethylene tubing by suction into 20-liter carboys and was received in the laboratory two days later. Both samples were filtered through 300 μm Nylon plankton nets at the time of collection and stored at 3°C in Pyrex or Teflon FEP containers. Before use, water samples were centrifuged for 30 min at 18,000 g in 150 ml Corex bottles to free them of natural particulate matter. All glassware and Teflon which was to contact seawater was cleaned in a mixture of hot concentrated nitric-sulfuric acids, rinsed in distilled water and dried in an oven or rinsed in the seawater to be used. Teflon storage containers were also steamed for a half hour after cleaning.

Artificial seawater conformed to the formulation of Lyman and Fleming (10), but contained only the salts contributing the seven major ions in seawater. It is referred to as "7-ion seawater". The salinity was adjusted to match the salinity of the natural seawater under study. Water for dilutions and final rinsing of glassware was obtained after an alkaline permanganate distillation, scrubbing of the steam in dilute phosphoric acid and finally distillation in a two-stage quartz still.

The dissolved organic carbon content of water samples was determined by the method of Menzel and Vaccaro (11).

Model particles of quartz, germanium and a strong-base ion exchange resin carrying quaternary ammonium groups (Dowex 21 K)were chosen to exhibit widely differing surface properties. In addition, germanium and quartz are useful materials for companion optical and photometric studies. Germanium from a broken internal reflection prism and transparent quartz were powdered in a Plattner mortar. The ion exchange resin was powdered with a porcelain mortar and pestle. All particles were fractionated by differential

sedimentation to retain those with diameters in the range of about 0.5 - 5 μm. Quartz particles were cleaned in several changes of hot concentrated nitric acid, washed thoroughly in distilled water and ignited overnight at 600°C. Germanium particles were heated overnight at 600°C in an atmosphere of purified hydrogen. The ion exchange resin was washed several times in distilled water. Contact of cleaned particles with laboratory atmosphere and other possible sources of contamination was minimized.

Organic constituents in seawater and 7-ion water were decomposed by ultraviolet photoxidation in an apparatus similar to that described by Armstrong, et al. (7). The samples in stoppered 120 ml quartz tubes were illuminated at a distance of about 5 cm by a 1200 W Hanovia ultraviolet lamp. Forced air cooling kept the temperature of the water near the surface at 60-65°C. Oxygen was supplied by addition of two drops of 30% hydrogen peroxide per tube at three or four intervals during a total illumination period of about 24 hr.

In a typical experiment model particles were suspended in seawater or 7-ion seawater at a suspension density of about 0.4×10^7 particles/ml in 25 ml Corex centrifuge tubes with polypropylene screw caps. The particles were exposed to increasing volumes of seawater by successive centrifugations and resuspensions with 25 ml portions. It was necessary to break up aggregates of particles in fresh suspensions of quartz and germanium and also occasionally after numerous centrifugations by brief treatment with an ultrasonic probe shielded from direct contact with the seawater by a glass test tube filled with water. This treatment did not detectably affect the mobilities.

RESULTS AND DISCUSSION

The electrophoretic mobilities of the model particles of anion exchange resin, quartz and germanium exposed to increasing volumes of two quite different kinds of seawater are shown in Figs. 1 and 2 (left section). The Gulf of Mexico sample had the rather high salinity and low fertility typical of tropical seas while that from the Chesapeake Bay was estuarine and of low salinity. In both samples the mobilities assumed by the model particles after equilibration fell in a rather narrow range: from 0 to -0.6 for Gulf water and -0.55 to -0.80 for Bay water. These results are similar to those obtained earlier with other materials in other seawater samples, namely, that all particles tend to assume similar mobilities (and therefore surface charge) when exposed to seawater (1). As already mentioned a tenable explanation for these results is that the particles become coated with minor, electronegative constituents dissolved in seawater. In such situations it is well known that adsorbed material usually dominates electrokinetic behavior regardless of the nature of the underlying surface (12). We shall discuss the results in terms of this hypothesis.

With quartz and germanium, surface coverage with adsorbed material is apparently complete at the first contact of particles with the smallest volume of water used (5 ml) and no significant changes in mobility occurred with increasing volumes of either sample of natural seawater. With the ion exchange resin, however, there is an indication of less than equilibrium coverage with exposure to small quantities of Bay water and in Gulf water an exposure of about 250 ml is required before a constant surface charge is reached. The greater volume required for equilibration of the resin is probably due largely to its porous nature, which would result in a much larger capacity for interaction with seawater constituents compared to the relatively smooth, non-porous surfaces of glass and germanium. The larger amount of Gulf water needed to reach a constant surface charge compared to Bay water is correlated with its lower content of dissolved organic carbon, 0.75 mg carbon / l versus 2.3 mg carbon / l.

More definitive evidence that organic matter is implicated in contributing a surface charge to the particles in seawater is derived from experiments in photo-oxidized media (middle section, Figs. 1 and 2). Quartz in all cases is observed to carry a negative charge consistent with its behavior in simpler electrolyte solutions (13). In photo-oxidized Bay water, however, the charge is especially high. In this case the adsorption of material carrying only a moderate electronegative charge would be expected to impart a lower charge to the surface. This is the result actually observed in untreated Bay water. In photo-oxidized Gulf water the surface charge of quartz is so similar to that in the untreated water that the formation of an adsorbed

adsorbed film cannot be demonstrated; other techniques would be required. Germanium carries a much lower charge than quartz in photo-oxidized waters. However, adsorption of electronegative constituents from untreated water imparts an increased charge with the result that germanium and quartz show nearly the same surface charge in both Bay and Gulf waters.

The ion exchange resin particles exhibit the most marked differences between photo-oxidized and untreated waters. The high positive mobilities in photo-oxidized seawaters are to be expected if the strongly basic quaternary ammonium groups which it carries are free to dissociate in solutions of non-complexing electrolytes. In untreated Gulf water the charge on the resin particles is lowered only to zero and not to a negative value comparable to that of quartz and germanium. Similarly particle mobilities in the presence of adsorbing protein have been found to vary somewhat with the nature of the particulate material (12,14). This may be due in this case to incomplete coverage of fixed positive groups by negatively charged adsorbing constituents. Whether the more complete coverage apparent in Bay water is due to a greater concentration or chemical difference in adsorbing species, or to still other factors cannot yet be decided.

In the right hand sections of Figs. 1 and 2 are shown the results of transferring the same particles which had been exposed to repeated changes of photo-oxidized seawater (middle section) to untreated water. In all cases there is a change in mobility after comparable washing to the values obtained by direct immersion in untreated water (compare left section). Thus exposure to photo-oxidized seawater produces no irreversible surface changes in any of the model particles.

For reasons which have been discussed by Strickland and Parsons (15) it is not possible to ascertain by available analytical methods whether the photo-oxidation procedure completely destroys all the organic matter in seawater. Our analyses for dissolved organic carbon indicate only that more than 90% has been fully oxidized. We have attempted to compensate for this uncertainty by increasing the time of irradation several fold over the original recommendation of Armstrong, et al. (7). The constancy of the mobility values with exposure to increasing volumes of irradiated water is consistent with the view that any undestroyed organic matter remaining is not surface active.

Additional support for the contention that the surface charge of the particles is not being significantly influenced by residual organic matter in photo-oxidized seawater comes from the mobility data in irradiated 7-ion seawater of the same ionic strength as the natural seawater samples (middle sections, Figs. 1 and 2). The surface charge of all particles in the two kinds of photo-oxidized water is essentially the same. It is extremely unlikely that residual organic material can be producing such similar effects in these two different media. Rather it seems reasonable to conclude that only the seven major ions of photo-oxidized seawater are important in determining the surface charge of these particles. Auxiliary experiments with irradiated 7-ion seawater which had lower than the normal concentration of magnesium indicated that this ion was important in determining the charge of germanium and quartz but not of the ion exchange resin. This is consistent with the observed effects of polyvalent ions on negatively charged surfaces (16).

It will be noted that the mobilities of a given kind of particle are higher in Bay than in Gulf water. This can be largely attributed to the presence of a more expanded ionic double layer outside the surface of shear around the particle in the lower ionic strength Bay water (17). However, the difference in mobility between the two media is not the same for different particles because different materials can be expected to follow different ionic strength mobility relationships as a result of factors such as ion adsorption and particle conductivity (12,17). Therefore it is not yet possible to draw quantitative conclusions about the similarity of adsorbed materials in samples of natural seawater of different ionic strength. Spectral studies may be more helpful in establishing the chemical nature of substances adsorbing from different seawaters.

A rough check on the adequacy of the supply of organic matter of seawater to give substantial surface coverage of the model particles can be made by introducing several approximations and assumptions. The interfacial area in 1 ml of a standard suspension containing about 0.4×10^7 particles of a non-porous material such as quartz and germanium is about 0.25 cm^2 assuming an average particle size of 1 μm and a roughness factor of two (18). A proteinaceous material giving monolayer coverage in this area with about 0.8 x

10^{-4} mg/cm^2 would require a dissolved organic carbon concentration of 0.01 mg/l assuming a carbon content of 50%. This is less than 2% of the amount found even in the more dilute Gulf sample (0.75 mg C/l). An assumption of monolayer coverage by other types of organic compounds would not change this estimate by more than a factor of three. Thus it would appear that the adsorbable constituents could represent a very small fraction of the total organic content.

An assessment of the difficulty of removal of adsorbed constituents was carried out by subjecting particles previously equilibrated with untreated seawater to washing in photo-oxidized seawater. The degree of retention may be estimated from the ratio of the mobility change after washing to the total change possible if reversion to the mobility of fresh particles in photo-oxidized media were attained. After washing with up to eight 25 ml portions over a period of a day, germanium and quartz showed retentions of 70% and 90%, respectively, while the ion exchange resin retained 100% of its mobility. Additional washing in distilled water followed by resuspension in photo-oxidized seawater lowered the retention values of quartz and ion exchange resin to as little as 80% but produced little further change in germanium. The results show that the adsorbed constituents are rather tightly held by the particle surfaces and suggests that they are macromolecular inasmuch as the cooperative nature of the multiple binding sites possible in such materials would readily account for a strong association (19). Other evidence for this has been discussed previously (1).

The results of this study show that materials with electropositive or strongly electronegative surface charges are unlikely to exist in natural seawater. Materials which are capable of exhibiting extreme surface charges in water containing only the inorganic constituents of seawater will take on moderately negative charges when exposed to natural seawater. This occurs as a result of a rapid interaction with dissolved organic material. In view of the variety of materials on which such adsorption has been shown to occur we suggest that it may take place on all surfaces at least to some extent. Dissolved polymeric materials in particular have the required properties for this interaction. Proteinaceous and humic materials and other substances derived from the degradation of natural products of marine and terrestrial origin are predominantly negatively charged polymers and are therefore attractive candidates (20). Adsorbed materials may very well favor the colonization of marine microorganisms (4) and thereby constitute the first step in a sequence of events leading to macrofouling.

References

1. R. A. NEIHOF and G. I. LOEB, Limnol. Oceanogr. 17, 7 (1972).
2. R. A. NEIHOF, J. Colloid Interface Sci. 30, 128 (1969).
3. H. W. HARVEY, J. Mar. Biol. Ass. U.K. 25, 225 (1941).
4. C.E. ZoBELL, Biol. Bull. 77, 302 (1939).
5. R. G. BADER, D. W. HOOD and J. B. SMITH, Geochim. Cosmochim. Acta, 19, 236 (1960).
6. N. L. JARVIS and M. A. SCHEIMAN, J. Phys. Chem. 72, 74 (1968).
7. F.A.J. ARMSTRONG, P. M. WILLIAMS and J.D.H. STRICKLAND, Nature 211, 481 (1966).
8. R. A. NEIHOF and S. SCHULDINER, Nature 185, 526 (1960).
9. P. WEYL, Limnol. Oceanogr. 9, 75 (1964).
10. J. LYMAN and R. H. FLEMING, J. Mar. Res. 3, 134 (1940).
11. D. W. MENZEL and R. F. VACCARO, Limnol. Oceanogr. 9, 138 (1964).
12. H. A. ABRAMSON, L. S. MOYER and M. H. GORIN, Electrophoresis of Proteins and the Chemistry of Cell Surfaces, p. 80. Reinhold, New York (1942).
13. H. A. ABRAMSON, J. Gen. Physiol. 13, 169 (1929).
14. H. B. BULL, Arch. Biochem. Biophys. 98, 427 (1962).
15. J.D.H. STRICKLAND and T. R. PARSONS, A Practical Handbook of Seawater Analysis (3rd Ed.), p. 153. Fisheries Research Board of Canada, Ottawa (1968).
16. H. FREUNDLICH, Kapillarchemie (4th Ed.) Vol. I. p. 361. Akademische Verlagsgesellschaft, Leipzig (1930).
17. Ref. 12, p. 13.
18. J. J. BIKERMAN, Surface Chemistry (2nd Ed.), p. 223, Academic Press, New York (1958).
19. A. SILBERBERG, J. Phys. Chem. 66, 1884 (1962).
20. E. K. DUURSMA in Chemical Oceanography V. 1 (J. P. Riley and G. Skirrow, eds.), p.433. Academic Press, London (1965).

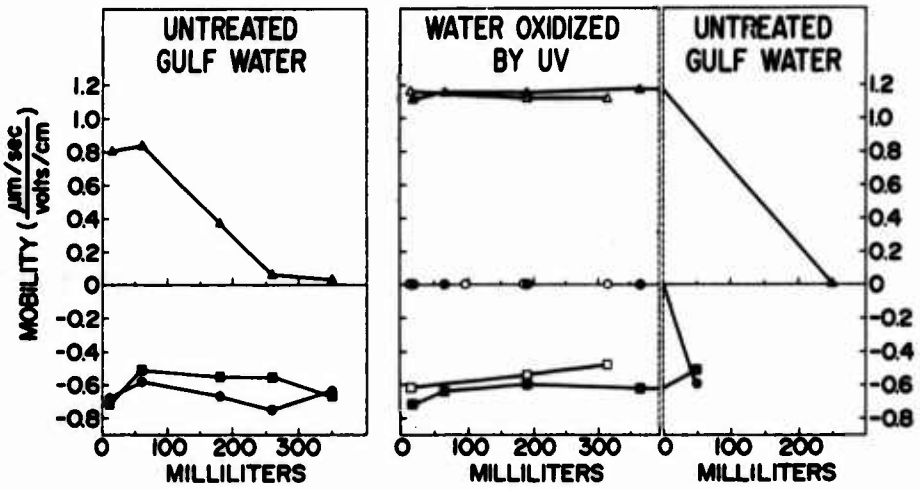


Fig. 1. Electrophoretic mobilities of model particles in artificial and Gulf of Mexico seawaters.

UV-treated 7-ion water	Gulf water	
-○-	-●-	Germanium
-□-	-■-	Quartz
-△-	-▲-	Anion exchange resin

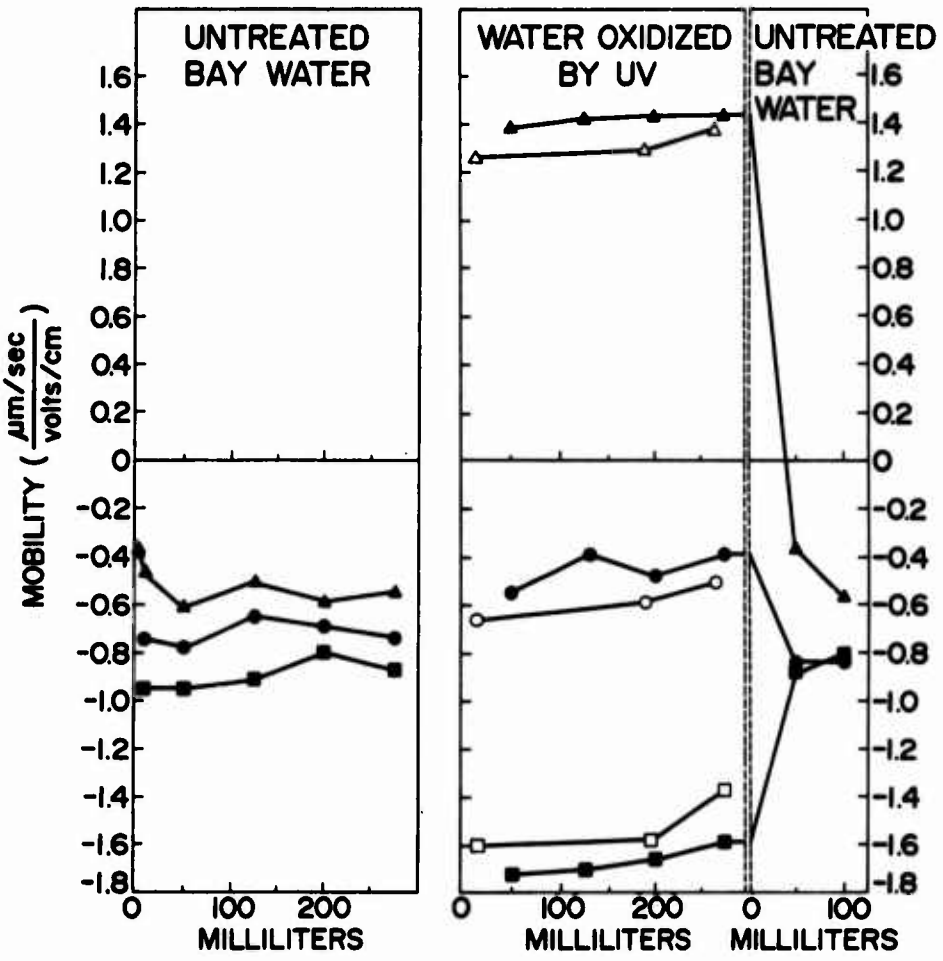


Fig. 2. Electrophoretic mobilities of model particles in artificial and Chesapeake Bay seawater.

UV-treated 7-ion water	Bay water	
-○-	-●-	Germanium
-□-	-■-	Quartz
-△-	-▲-	Anion exchange resin

Discussion

Question: I am not too sure whether to direct this question to Dr. Neihof or Dr. Baier. Both of them might like to consider it; from your results and from the type of thing that Dr. Baier is reporting, you do get these conditioning layers probably organic layers which Dr. Baier was talking about on the surface to which something will adsorb. You are talking about the smaller particles. It is obvious that both the smaller particles and the large surface are both being (or probably being) covered or conditioned by the same material. How is this going to affect their interaction or that between the small particle and the large surface?

Neihof: Well, one can speculate of course. It is easy to see in something like an ion exchange resin that electrostatic interactions are going to be very strong. It is not so easy to see on that basis why something with an electro-negative charge is going to adhere to something else with an electro-negative charge, but I think people like Pethica, for example, have indicated enough possibilities, dipole-dipole interactions, hydrogen bonding, and you, yourself, indicated some possibilities this morning so that it is easy to find mechanisms for the sticking of particles to surfaces even though the electrostatic forces do not appear to be there. There is also the possibility of a mosaic of charges on a surface which itself may look like a negative surface, but positive groups may nevertheless be present and be taking part in binding of an electrostatic nature. There is one thing. I hope I didn't confuse anybody. I did forget to say that in all of these model particle studies the sea water had been previously centrifuged to clarify it of any natural particles. So the work on model particles is completely divorced from that on natural particles. Now, I would like to imply although I have nothing to really prove this, that natural particles may very well have interacted with the materials that contribute this negative charge, although that is not necessary. Many of them are already negatively charged but if in laboratory systems, they do perhaps show extreme electro-negative charges, they are obviously not likely to do so in sea water. I doubt if that answers your question.

Baier: I doubt if I can shed any great light on this interaction between the small particles and the large, but it gives me the opportunity to make the comment that Rex and George have now shown something that has been familiar in other biologically active fluids (in particular, blood, where the surface-charged induced adhesive hypothesis has been invoked time and time again) that a net negative surface might in some way repell net negatively charged cells in a saline media and it has been found by a group led by Lynacker and colleagues many years ago that no matter what the original surface charge as measured by say, resting potential of metals, or zeta potential of insulators, plastics and so on, that, if they are flowed with blood, with serum, with even pure protein solutions, within seconds of contact of the protein-containing medium, they all come to the identical surface state in terms of surface charge. So in terms of implications for biological adhesions, biological fouling, if we are going to continue to think of surface charging having an influence at all, we have, therefore, to think of the original surface charge state as influenced through perterbation of the initially adsorbed organic layer and that once that organic layer has brought everything to the same state of surface charge, the latter can no longer dictate subsequent result. It has to now be mediated through the protein or other organic three-dimensional configuration or chemical groups and I look upon these last couple of slides, especially the Chesapeake Bay water as a beautiful extension of the findings to other biological regimes such as sea water which we can now all consider a very dilute chicken soup.

Ship-fouling as an evolutionary process.

G. Russell and O.P. Morris.

Department of Botany, The University, Liverpool L69 3BX, England

Ectocarpus siliculosus is a cosmopolitan species of brown algae and it occurs naturally in a wide range of habitat conditions. It is also one of the most consistently successful ship-fouling algae, often present in sufficient quantity to cover large areas of hull treated with copper-based antifouling preparations.

Preliminary investigations have shown that ship-borne Ectocarpus has a higher tolerance to copper than plants of the same species collected from an uncontaminated rocky shore (1)[1]. This study has been extended to include a large number of Ectocarpus populations collected from diverse habitats.

Isolates from these populations have been grown in unialgal culture and their performance in the presence of copper has been assessed by means of a new bioassay technique. The technique, which tests early developmental stages as well as adult material, is described in detail.

Our results show that copper tolerance in Ectocarpus is a fairly widespread phenomenon, usually having evolved in populations whose habitat conditions are associated with high copper concentrations.

However, copper tolerance has also been found to arise by spontaneous mutation from an otherwise copper sensitive strain, thereby producing plants of high potential fouling ability. The heritable nature of copper tolerance has been established by culture of many successive generations of plants.

Methods by which population differences are maintained are mentioned and the significance of our findings in relation to fouling problems is discussed.

Key words: Copper tolerance; population; selection; mutation.

---

1. Introduction.

The purpose of this investigation was to examine the ship-fouling properties of Ectocarpus siliculosus. Linked with the success of this species as a fouling alga is its cosmopolitan distribution and capacity to grow in a very wide range of marine and estuarine habitats. On the basis of this information it seemed sensible to consider the possibility that the adaptive properties of E. siliculosus might be genetically determined and that genetic variability might account also for the ship-fouling aptitude of the species. We decided therefore to examine this species on a population basis and in relation to copper, the traditional antifouling toxicant.

---

[1]The numbers in parentheses refer to the list of references at the end of this paper.

2. Methods.

We used the term 'population' in the sense only of a number of Ectocarpus plants growing together within the confines of a recognisable habitat, eg. a ship's hull or a particular area of shore line.

Such plants were isolated and grown in laboratory culture using a relatively inorganic medium based on that of von Stosch (2).

The response of the plants to copper was measured chiefly by growth although observations on fertility and morphology were also made. Growth of adult plant material was assessed by centrifugation in blood sedimentation (Wintrobe) tubes for 10 minutes at 4,000 rpm. Juvenile stages grown from motile zoospores were measured on the basis of cell counts and filament lengths. All material was grown in 100 ml of medium contained in 'Pyrex' crystallising dishes. All cultures received continuous illumination of 2,700 lux from 'White' fluorescent tubes and all were grown at 11°C.

Under these conditions the plants grew well and gave consistent, repeatable results. All experiments were run in duplicate and the results did not indicate a requirement for further replication. Experiments with adult material were terminated after 35 days of growth; sporeling experiments were terminated 21 days after zoospore discharge.

3. Results.

1. Population analyses.

The responses of E. siliculosus populations to copper were compared in two ways:

A. Overall population responses were indicated by the performance of single cultures containing ten plants sampled from each population. This approach was used for both adult and sporeling material.

B. The performances of ten or twenty single plant isolates were measured separately to assess possible variation within populations from different habitats.

A. Overall population responses.

Fig. 1 shows the results obtained for adult plant samples. Ship-fouling populations plus certain others show relatively high tolerance to copper. The most tolerant plants were those collected from habitats with substrates of high copper content, for example on rocks at old copper minings (Bradda) and on the painted surface of a test panel (Salcombe Panel). Some populations show such a high degree of adaptation to a cupriferous environment (eg. Daphnella) that the plants grew better at a copper concentration of 0.10 mgm/litre than in the control medium.

As is shown in Fig. 2, sporelings showed essentially the same response to copper as the adults from which they were derived.

At this point in the investigation it seemed possible that copper tolerance might only reflect differences in vigour of the strains involved. This was overcome by devising an index of copper tolerance which simply related plant performance under treatment with growth under control conditions. Low tolerance indices were given by non-tolerant populations while the more copper-tolerant plants gave higher values, as shown in Figs. 3 & 4. In most cases it was necessary to consult both growth rate and tolerance index values to effect a full comparison of population responses to copper.

The tolerance index also provided a means of comparing adult and sporeling performance; the high correlation between adult and sporeling indices ($p < 0.001$; see Fig. 5) indicates that copper tolerance is under genetic control and is transmitted normally from generation to generation.

B. Individual plant responses.

The observations on sporeling growth suggested considerable variability within populations; this variation has been quantified for adult plant samples of populations from four different habitats on the coasts of England, Wales and the Isle of Man.

1.	Rhosneigr (Wales)	- uncontaminated rocky shore.
2.	Bradda (Isle of Man)	- highly toxic copper mine.
3.	Salcombe Panel (England)	) May be subject to spore immigration from
4.	Port St. Mary (Isle of Man)	) areas of high copper influence.

The results obtained (Figs. 6 and 7) show that at Bradda, where the influence of copper is very strong, natural selection eliminates all but the more tolerant plants. Conversely at Rhosneigr it would appear that in the absence of copper the tolerant genotype is at a selective disadvantage.

Variation may be maintained or enhanced in the remaining populations as a result of one or more factors which may include microhabitat differences in selectivity, spontaneous mutation in established genotypes, or immigration from adjacent copper tolerant populations.

2. Mutation.

Treatment of zoospores from the Rhosneigr strain, a copper-sensitive population, resulted on one occasion in the appearance of a single plant growing in a medium containing 0.10 mgm Cu/l, Fig. 2. This first generation plant, the sole survivor of an inoculum of about 120,000 zoospores, proved capable of growth and reproduction in a copper concentration which was lethal both to its parent material and to its siblings.

The progeny of this plant were subcultured into two different media half were grown - through nine successive generations - in the absence of selection i.e. in control medium, while half were subjected to selection in a medium containing 0.10 mgm copper/litre. The ninth generation sporelings from both regimes were compared by subculturing in control and copper media. Results are given in Fig. 8.

The second and ninth generations of tolerant sporelings did not differ significantly in response to copper whether grown previously in a control medium or in one containing copper. The responses of these sporelings did, however, differ significantly from those of first generation siblings and the parent strain.

This indicates that the solitary first generation survivor of copper treatment is indeed a spontaneous mutant for copper tolerance. The results also show that copper tolerance is a stable character capable of unchanged transmission through at least nine asexual generations.

4. Discussion.

The results have shown that E. siliculosus is not uniform in its response to copper, and the existence of copper tolerant populations - associated with high levels of environmental copper - has been demonstrated.

Inevitably such populations would have a high fouling potential against copper-based antifouling paints, and once established on a ship they would be provided with an excellent means of dispersal so that this metal would, in time, be expected to lose its effectiveness against fouling plants in much the same way as DDT became ineffective against insects and warfarin against rats.

It is highly probable that the variable nature of Ectocarpus is the basis of the unaccountable variation in success of antifouling techniques. A toxic hull may come into contact with a highly tolerant population and be unexpectedly fouled while a susceptible ship may avoid such populations and remain clean for a long time.

Naturally occurring copper-tolerant populations may be associated with mine wastes, cupriferous rock or the long term use of copper as an antifouling toxicant. Although such populations obviously provide the most potent source of further fouling, a chance contact between a mutant spore on a ship's hull could lead to hull colonisation from an otherwise harmless population.

The situation may also be complicated by the chelating effects of EDTA and soil extract, both of which have been shown effectively to reduce the toxicity of copper to Ectocarpus. On the other hand we have found that reduced light intensity, though retarding the growth of Ectocarpus, did not in fact materially affect its intrinsic copper tolerance. Both these observations obviously relate to the conditions in a port system rich in organic pollutants or containing silty water.

In the search for new antifouling preparations and procedures it is clear that all aspects of the proposed shipping route should be known. This formidable objective is probably unrealisable but a more comprehensive bioassay method should at least establish a firmer basis for prediction.

REFERENCES.

1. G. RUSSELL and O. P. MORRIS, Nature, Lond., 228, 288-289. (1970).

2. H. A. von STOSCH, Proc. Fourth Int. Seaweed Symp., pp. 142-150 (1964).

Discussion

R.A. Neihof suggested that an organism adapted to a copper species contained in a freshwater outlet would not necessarily be adapted to the copper species leaking out of antifouling paint. O.P. Morris replied that he had information only on the converse situation: plants growing on antifouling paint were found also to be tolerant to ionic copper in the culture medium.

In reply to the question whether the different developed tolerances to copper were associated with its uptake, O.P. Morris replied that Ectocarpus zoospores display the same resistance as the adult material, though they have no cell wall. It was therefore difficult to conceive of a tolerance mechanism dependant on the exclusion of copper from the cell. The actual copper content of small marine algae had not so far been analysed.

J. Smith observed that although copper paints had been used on ships for years, he had not yet experienced a fouling problem with Ectocarpus, though he had with Enteromorpha. O.P. Morris replied that in his experience, Ectocarpus on ships was confined to the lower half of the hull, where growth is not luxuriant and the plants are inconspicuous. Possibly it was excluded from better lit situations by competition from Enteromorpha. He thought that copper tolerance would by now be firmly established in both of these fouling algae. It was then reported that ships coming into Southampton were fouled not only by Ectocarpus and Enteromorpha, but by Giffordia, Ceramium and Polysiphonia.

Another speaker asked whether there was any relationship between the salinity at the site of collection and the tolerance of the plants to copper. The salinity of the culture medium was between 33 and 35 $^{o}/_{oo}$. The Isle of Man populations at Bradda, Port Erin and Port St. Mary were all growing within a mile of each other. The salinity did not vary significantly, but the copper tolerances were considerably different, so suggesting no correlation.

J.S. Ryland inquired whether Ectocarpus bred asexually or sexually, and whether acquired tolerances were transmitted to sexually produced offspring. O.P. Morris replied that British Ectocarpus, used in his research, reproduces asexually, but that sexually reproducing populations exist in warmer waters, as at Naples for example.

H. Barnes pointed out that the strength of the copper in the solutions utilized exceeded its solubility product in sea water. It was important, therefore, to ascertain what state the copper was in. Was it complexed ? Does its free ion effect copper entry to, and indeed action in, the plant cell ? It was essential to learn more about the physical chemistry of copper in sea water, and in media which contain organic materials, and to know something about the relation between copper inside and outside the cell.

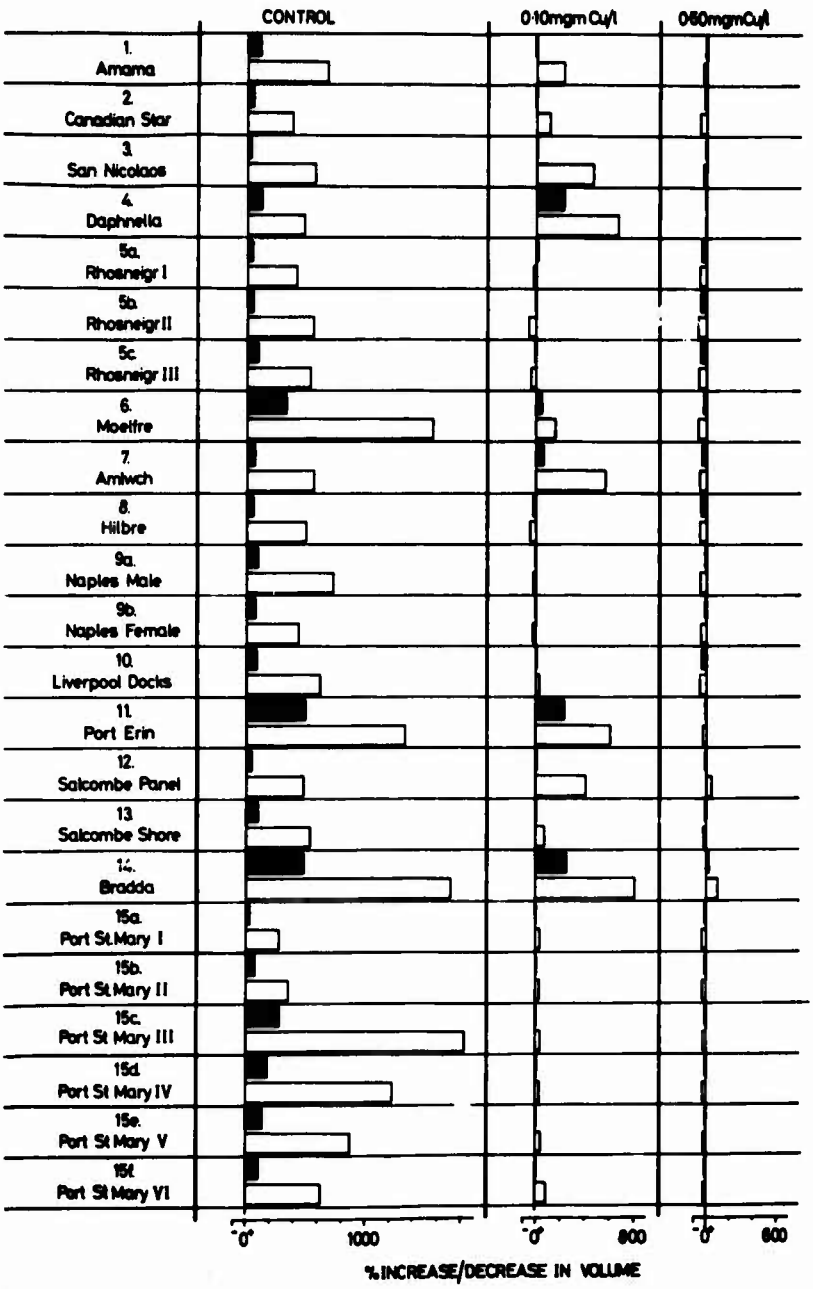


Fig 1. The effect of two copper concentrations on the growth in culture of adult population samples of *E.siliculosus*.

Closed histograms- 14 day results; open histograms- 35 day results.

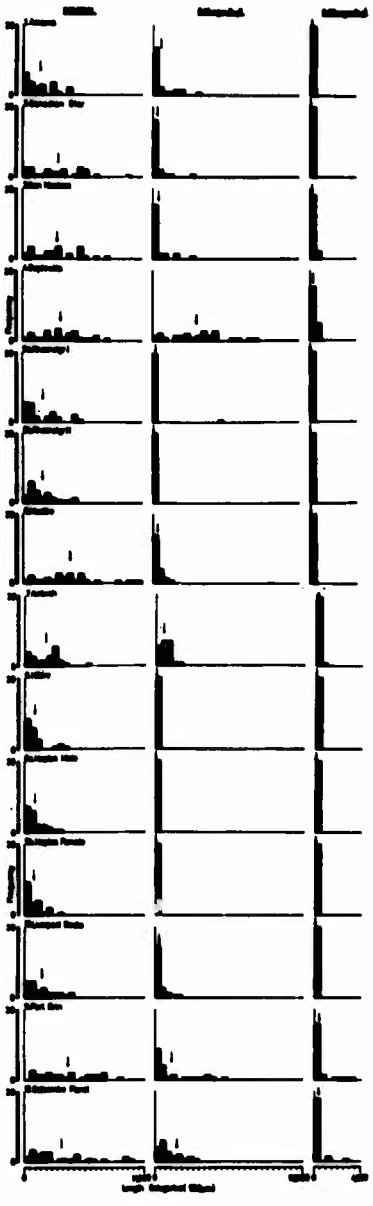


Fig 2. Length distribution diagrams for population sporeling samples of E.siliculosus in control and two copper media,after 21 days.Means are indicated by arrows.

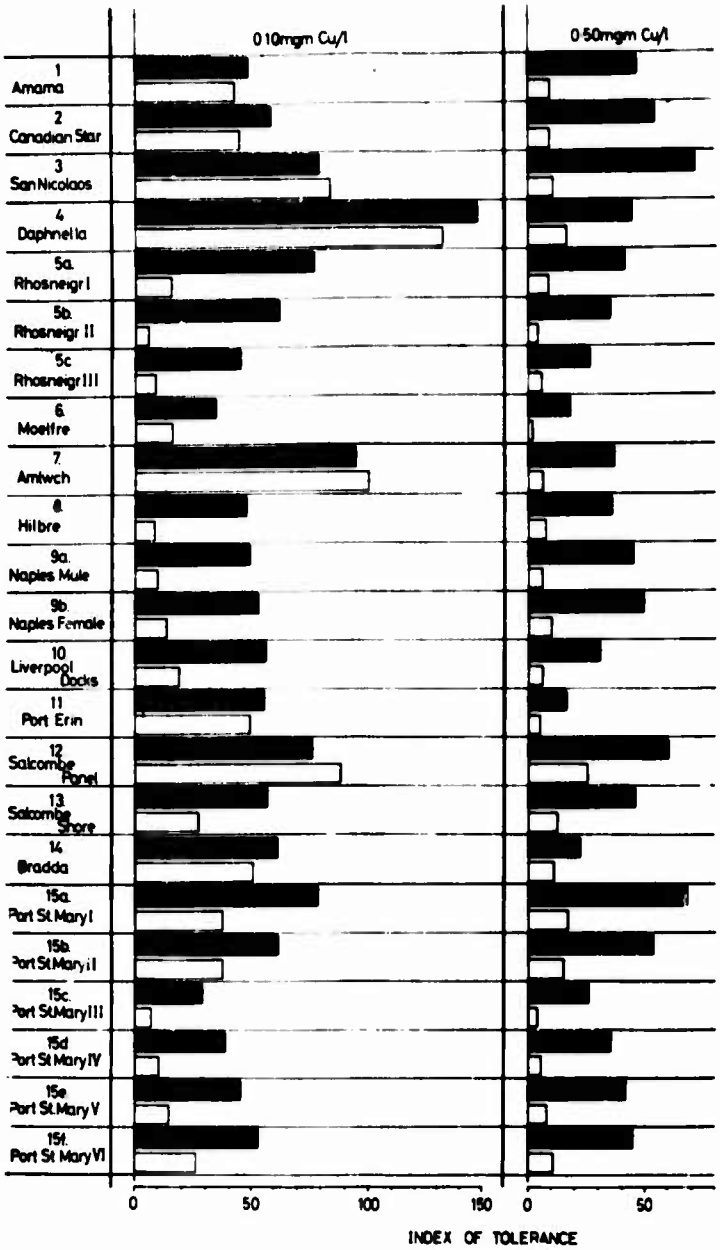


Fig 3. Indices of tolerance of *E.siliculosus* populations calculated for adult plant samples at two copper concentrations.

Closed histograms- 14 day values; open histograms- 35 day values.

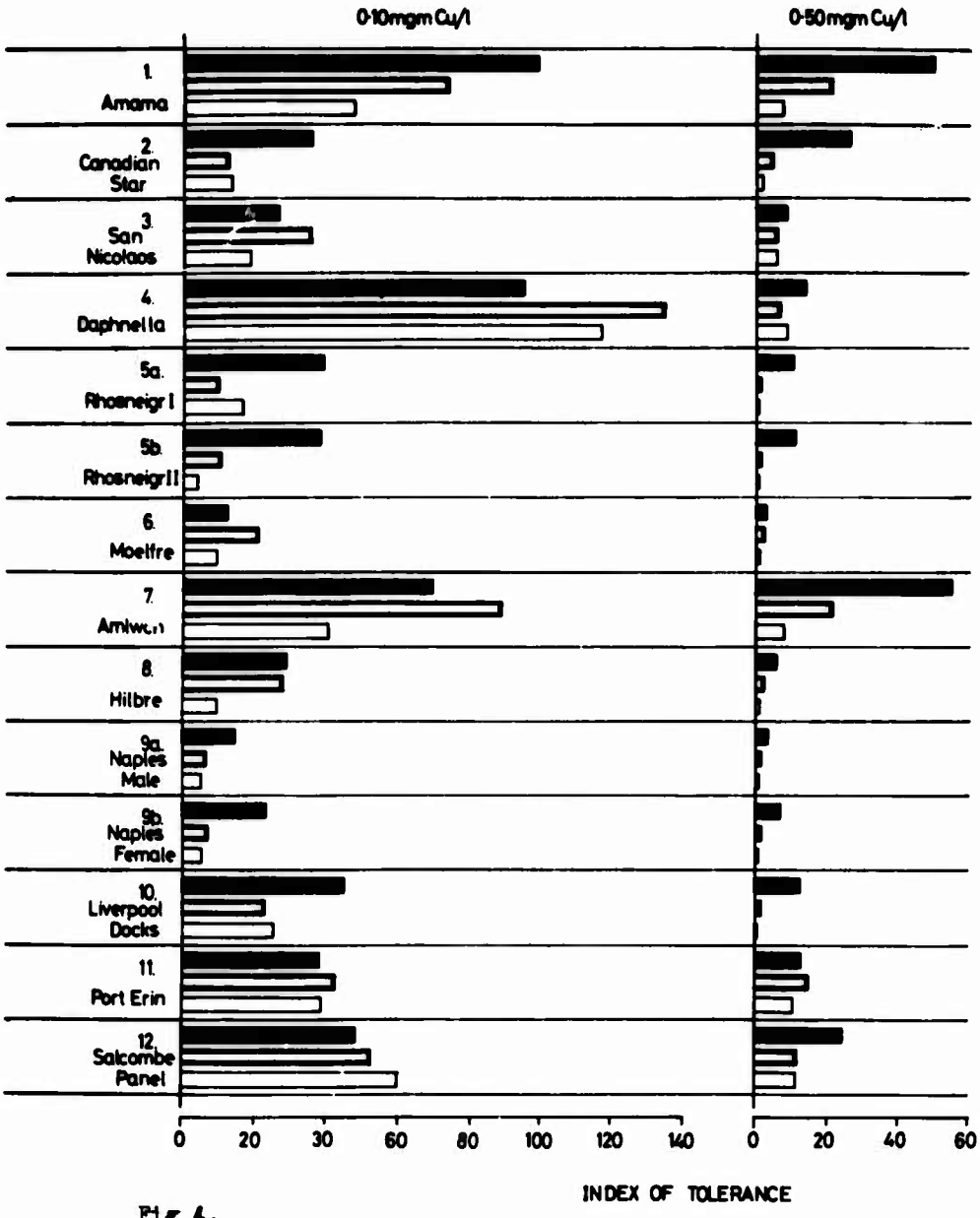


Fig 4.

Mean tolerance indices for populations of E.siliculosus,calculated for sporeling samples at two copper concentrations.

Closed histograms represent 7 day results;open,thick-walled histograms represent 14 day results;open,thin-walled histograms represent 21 day results.

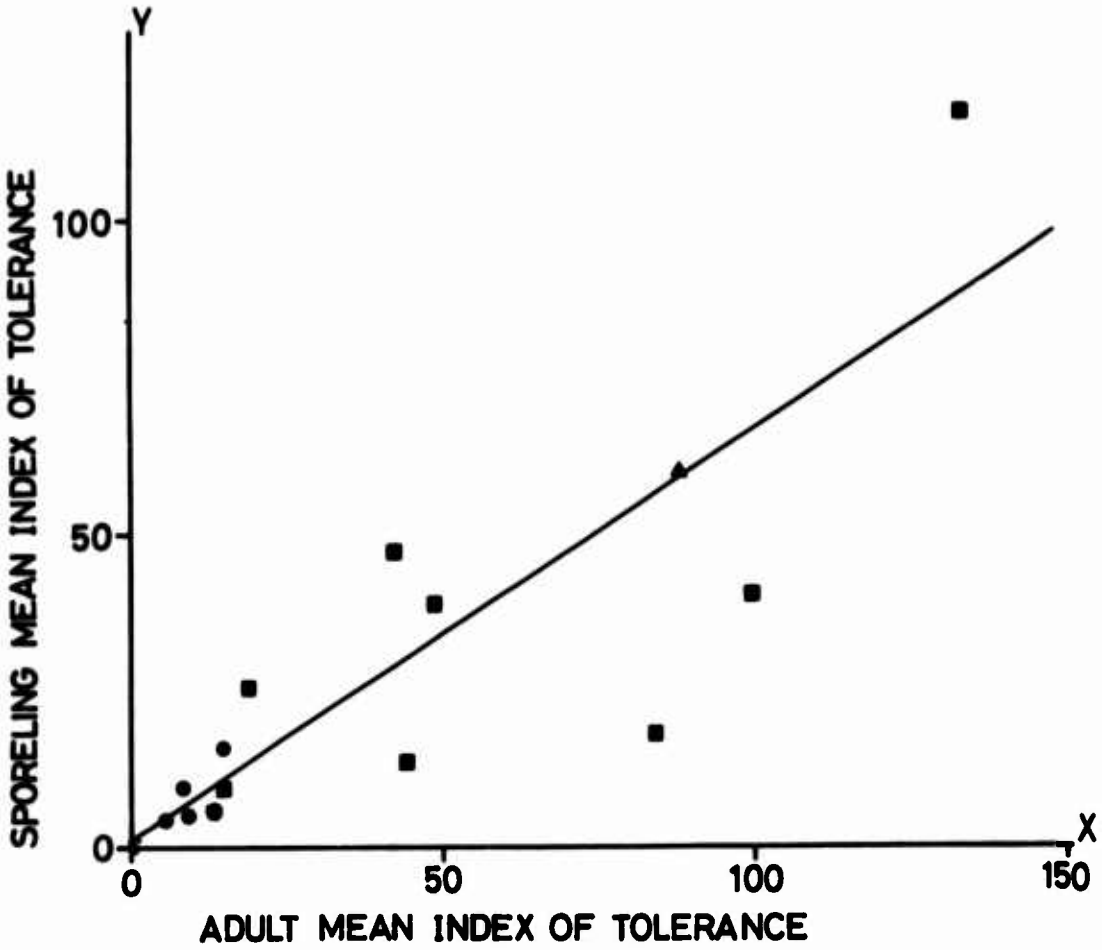


Fig 5.

Correlation: Mean adult/mean sporeling sample index of copper tolerance for 14 populations of E.siliculosus.

$y = 0.63x + 1.16$; $r = 0.835$.

● - non-tolerant populations.

■ - populations tolerant at the 0.10mgm Cu/l level.

▲ - populations tolerant at the 0.50mgm Cu/l level.

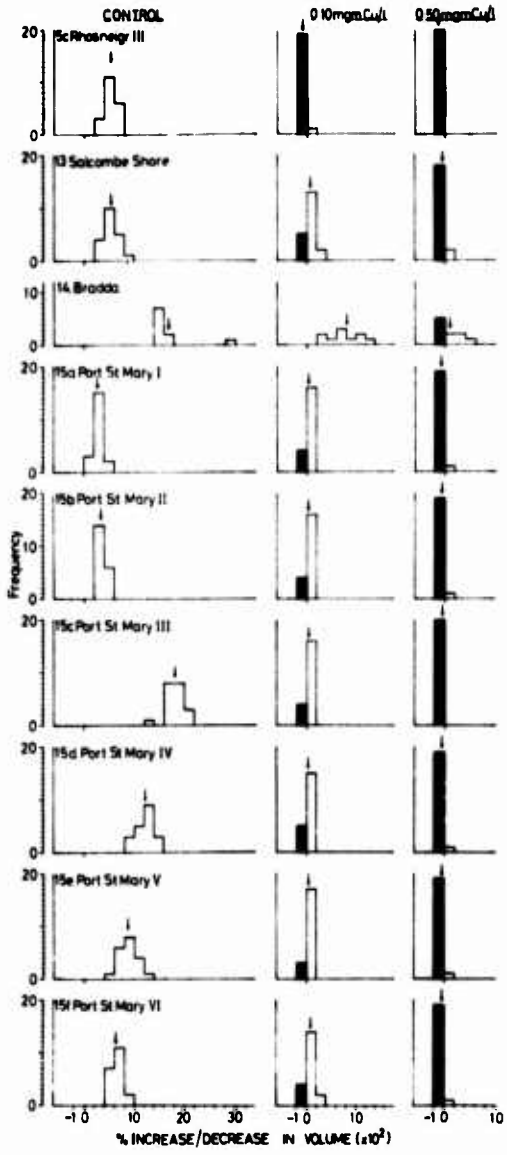


Fig 6.

Growth of individual adult plants of E.siliculosus, sampled from four populations, in control and two copper media after 35 days.

Open histograms represent positive growth; closed histograms denote a decrease in plant volume.

Individual plant performances are represented as means of duplicate treatments; population means are indicated by arrows.

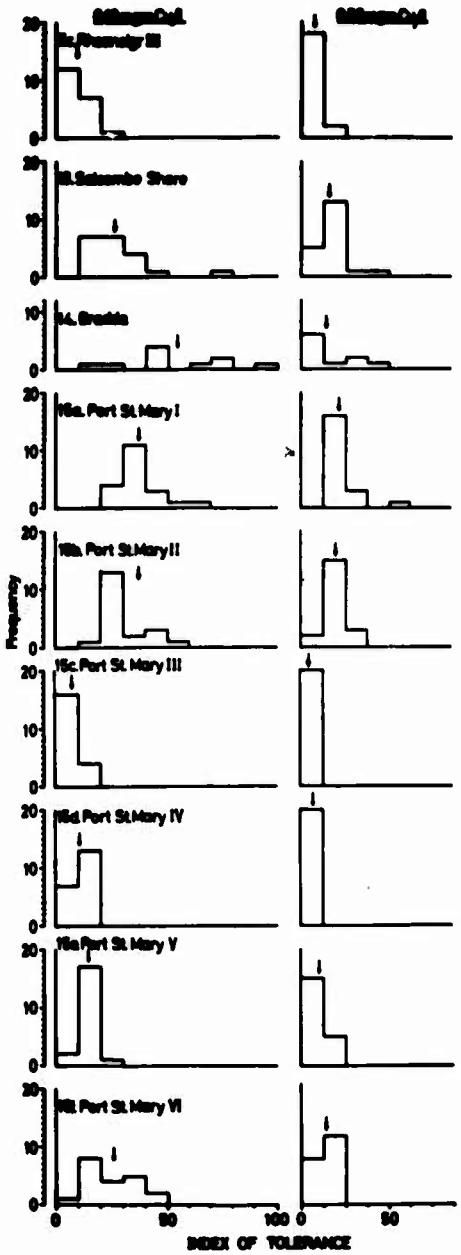


Fig 7. Index of tolerance distribution in adult plant samples of E.siliculosus populations after 35 days. Values for individual plants are means of duplicate treatments;population means are indicated by arrows.

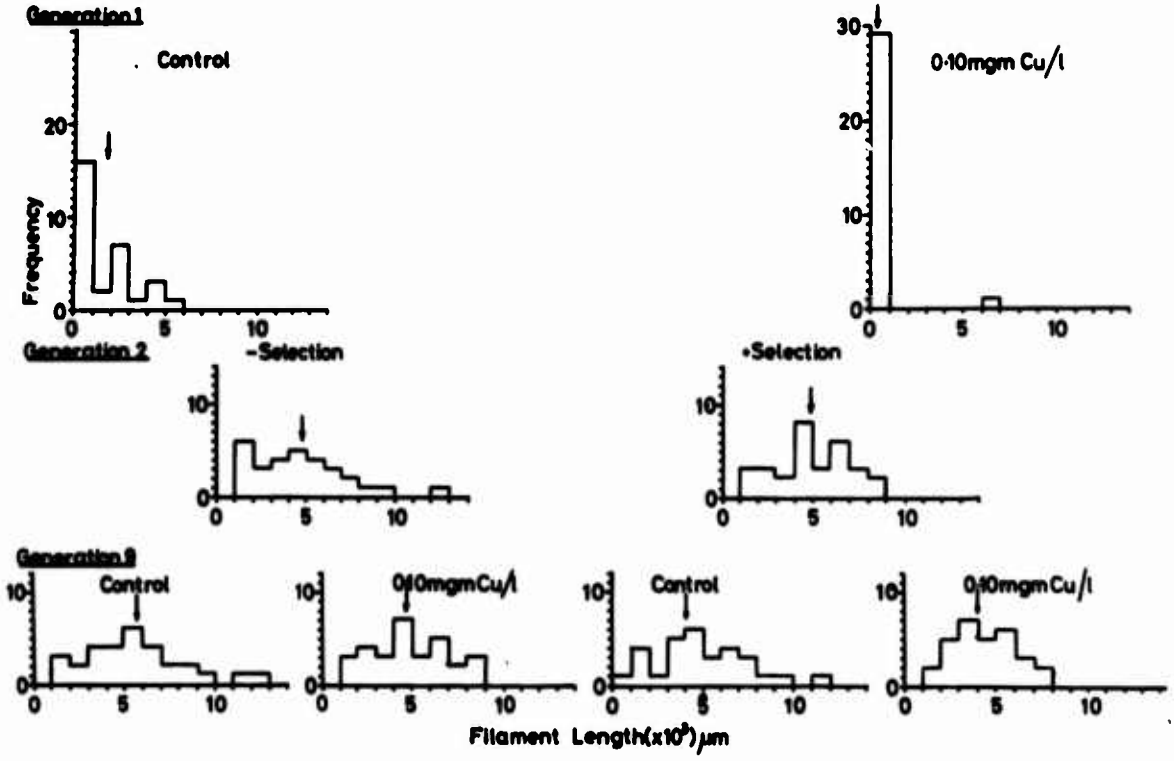


Fig 8.

Selection for copper tolerance in sporelings of E.siliculosus over 9 generations.

Generation 2 sporelings are derived from the single tolerant plant selected for (at 0.10 mgm/l)in the first generation.

Histograms represent the sum of two duplicates for each treatment.Means are indicated by arrows.

Larval Transport, Settlement, and Population Structure of Offshore Biofouling Assemblages in the Northeastern Gulf of Mexico

W. E. Pequegnat and Linda H. Pequegnat

Texas A&M University
College Station, Texas 77843

Results are presented from a two-year study of the development of fouling assemblages on plastic-float arrays anchored in the Gulf of Mexico at 2, 11, and 25 miles offshore from Panama City, Florida. All three arrays carried floats near the surface (4 m) and near the bottom (17, 29, and 44 m), as well as at common depths in between. Floats were harvested and replaced at intervals varying from two weeks to one year.

Differences in depth, distance from shore, season, duration of exposure, and orientation to currents created major differences in species diversity, the complexity of biotal assemblages, and the production of standing crop biomass. The causes of successional changes in predominant species are discussed. Estimates are given of the magnitude of secondary production for some common species.

Differences in species composition and diversity existing among the float-arrays and at different depths on the same array revealed that the water masses bathing the floats had very different histories. Hence, points of settlement of the pelagic larvae of some epifaunal species can aid in identifying different water masses of the water column.

Organotin used here proved to be an effective deterrent to the development of most invertebrates but not to algae. Notations are given on quasi-antifouling effects resulting from biological interactions and manipulation of some environmental parameters.

Key Words: Biofouling assemblages; epifauna; biomass; secondary production; meroplankton; water masses; anti-foulant; barnacles; hydroids.

---

1. Introduction

This paper is based upon data generated by a two-year study of the accumulations of marine organisms upon plastic floats introduced into the NE Gulf of Mexico at three sites offshore from Panama City, Florida (Fig. 1).

The study's principal objectives were (1) to predict the nature of the fouling assemblages likely to develop upon various types of underwater sensors placed at specified locations in the water column, and (2) to test the effectiveness of an organotin chemical at minimizing the rate of development and ultimate mass of the fouling accumulations. The laboratory analyses of the fouling populations required to achieve these objectives produced a wealth of information on the ecology of the shelf waters of this part of the NE Gulf. As the study progressed, it became apparent that some of the biological data helped our understanding of the circulation of these local waters and linked some of these movements with such major circulations as the East Gulf Loop Current.

As a result of these conclusions, we tested the feasibility of using larval transport and settlement as a tool for discerning circulation patterns. In addition, interest was

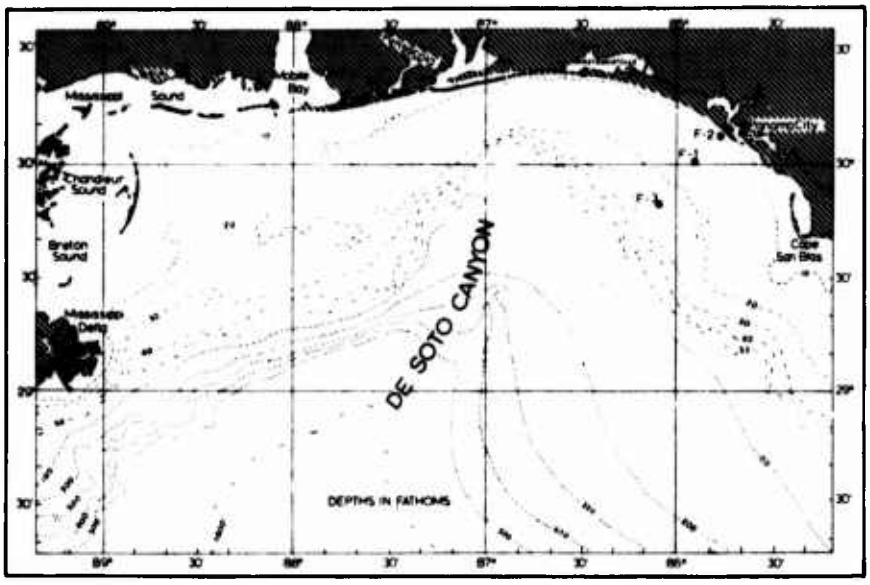


FIGURE 1. Northeastern Gulf of Mexico showing locations of the three fouling stations: F-2 at 2 miles offshore, F-1 at 11 miles offshore and F-3 at 25 miles offshore.

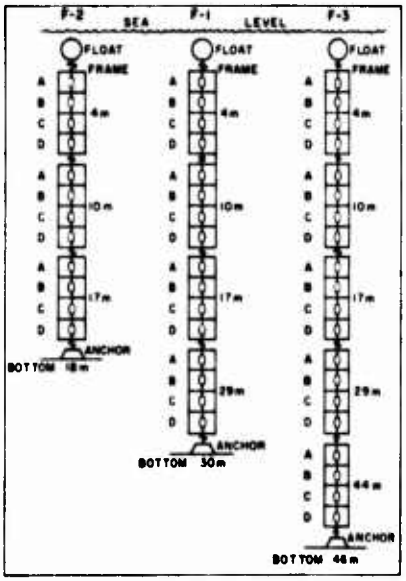


FIGURE 2. Float positions at the three fouling stations: F-2 (2 miles offshore), F-1 (11 miles offshore), and F-3 (25 miles offshore).

heightened in deriving relationships between larval origins, water movements, and population structure of biofouling assemblages produced at specific levels in the water column in the NE Gulf.

2. Field Methods

Surface-to-bottom arrays of peanut floats having surface areas of 600 cm^2 were installed on a line at points 2, 11, and 25 miles offshore from Panama City, Florida (stations F-2, F-1, and F-3 on the map in Figure 1). The respective depths at these stations were 18, 30, and 46 m (Fig. 2). Because the floats were to be harvested at different time-intervals, they were grouped in sets of four (A, B, C, D on Fig. 2) at each depth. Thus, at the 2-mile array three tetrads of floats were exposed at depths of 4, 10, and 17 m by attachment to PVC racks suspended from an anchored glass float. As the depth increased seaward, a fourth tetrad was added at the 29 m depth of the 11-mile array and a fifth tetrad at the 44 m level was added to the 25-mile array. Consequently, all stations had tetrads near the surface and near the bottom as well as at the same intermediate depths. Exposed floats were harvested by divers on regular schedules. They removed the A-floats and exposed new ones either on a bi-weekly or monthly schedule. They serviced the B, C, and D positions on respective schedules of 3, 6, and 12 months. In addition, the divers photographed all floats on each harvest schedule and cleaned or replaced the racks and lines as needed to minimize rack-to-float colonization.

3. Laboratory Methods

Measured samples were taken from all of the 680 floats exposed during the study. Samples were examined microscopically and species were separated, identified, enumerated, measured, oven dried, and ashed. In all, 200 species were detected. After incineration, the weight of dry organic material (biomass) was calculated from weight loss. Total float biomass was computed from sample data for countable species and from areas of float coverage for colonial species.

4. Selected Variations in Fouling Accumulations

Characteristics of float placement and harvesting schedules permitted us to compare qualitatively and quantitatively variations in accumulations of foulers with differences in distance from shore, depth of exposure, duration of exposure, and change of hydrologic season. Time and space limitations permit us to consider only two of these here.

Distance from shore: Substantial reductions of biomass and major changes in species composition occurred with increase in distance from shore (Fig. 3). At the 4-meter depth the sharper break in biomass occurred between the two- and 11-mile station, whereas the larger change in species composition came between the 11- and 25-mile stations. These breaks, however, were depth dependent, as will be noted later.

Depth of exposure: Figure 4 depicts the differences in accumulations due to depth at the 11-mile station. The predominant species in terms of biomass contribution are barnacles at the 10- and 17-meter depths and the gymnoblastean hydroid Bougainvillia carolinensis at the bottom (29 m). The barnacles at the latter depth, although more numerous than at the two shallower points, contribute less to total float biomass because of their small mean size of 1.5 mm. These and the many other observed differences with depth can be accounted for by lower temperatures at the deeper levels during part of the year. But this factor cannot fully explain all depth variations throughout the entire year, because the water column is nearly isothermal at the three stations from November to May. Again we point to the occurrence of different water masses sweeping past the floats at different depth levels, which have different origins and contain the meroplankters of different species of epibenthic organisms able to settle on the float surfaces.

5. Variations in Species Diversity

The numbers of different species found at all depths on floats of the 11-mile station after three months always exceeded those at the 2-mile and 25-mile stations. The totals at any one station, however, were higher in summer than winter. For example, at the 11-mile station, the respective totals were 70 and 50 species on average for 3-month floats (Table 1).



DISTANCE
FROM SHORE: 2 miles
BIOMASS: 15.45 grams
BARNACLES: 3,400 Balanus venustus, 4.9 mm ave.
HYDROIDS: Gonothyraea gracilis



DISTANCE
FROM SHORE: 11 miles
BIOMASS: 5.75 grams
BARNACLES: 400 Balanus venustus, 3.7 mm ave.
HYDROIDS: Gonothyraea gracilis



DISTANCE
FROM SHORE: 25 miles
BIOMASS: 3.82 grams
BARNACLES: 49 Conchoderma virgatum
2 Lepas anatifera
HYDROIDS: Obelia flabellata
OTHER: 50 nudibranch mollusks and eggs

FIGURE 3. Variations in accumulations of organisms due to distance from shore. All three floats were exposed for the same time period (one month) and at the same depth level (4 meters) but at different distances from shore.



DEPTH: 10 meters
BIOMASS: 3.91 grams
BARNACLES: 2,400 Balanus venustus, 3.3 mm ave.
HYDROIDS: Gonothyraea gracilis
AMPHIPODS: Few Jassa falcata
Few Caprella equilibra

OTHER: Few nudibranchs
Few polychaetes
Few small anemones



DEPTH: 17 meters
BIOMASS: 4.60 grams
BARNACLES: 2,900 Balanus venustus, 3.3 mm ave.
4 Balanus merrilli, 2.0 mm ave.
HYDROIDS: Gonothyraea gracilis
AMPHIPODS: Few Caprella equilibra

OTHER: Few polychaetes



DEPTH: 29 meters
BIOMASS: 2.07 grams
BARNACLES: 4,400 Balanus venustus, 1.5 mm ave.
7 Balanus merrilli, 1.3 mm ave.
HYDROIDS: Obelia flabellata
Bougainvillia carolinensis
AMPHIPODS: 500 gammarids (5 species)

OTHER: 4 Ectoproct colonies (Bugula)
Few serpulids
Few small gastropods & pelecypods

FIGURE 4. Variations in accumulations of organisms due to depth at the 11-mile c [illegible] station. All three floats were exposed for the same time period (one month: May [illegible] but were located at different depths.

Although the number of species increased with length of exposure, the simple numerical increase between 2 weeks and 3 months did not reflect the major change in species composition of the fauna that occurred during that interval. Only eight species of animals were found on 2-week floats at all depths at the 11-mile station, and 5 of these were among such pioneering animal groups as suctorians, barnacles, hydroids, and filibranch pelecypods. The number of species increased markedly by 2 months as the result of settlement of serpulids, anemones, errant polychaetes, additional pelecypods, gastropods, and brachyuran crustaceans. The interval between 2 and 3 months was marked not so much by species increase as by population fluctuations. For instance, at the 11-mile station in summer and at 29-m depth, some 29 species were found on 2-month floats and 34 on 3-month floats. Only 15 species were common to both. Hence, in the interval of a month or so 14 species dropped out while 24 new ones settled. Actually, in some cases, a net loss of species occurred. The most important species that dropped out varied but ordinarily were (1) caprellids that had exhausted much of their food supply or had been subjected to heavy predation by anemones, crabs, and fishes; (2) barnacles that were removed by fishes, killed by such drills as Thais floridana, or smothered out by encrusting ectoprocts or anemones; and (3) gammarids that built up populations attractive to fishes and some crabs and then regressed under apparently intense predation.

The reduction of species on the winter versus summer sets appears to be attributable to limited spawning periods plus seasonal changes in water circulation. For example, several species of polychaete annelids in such families as Syllidae, Eunicidae, and Nereidae were found on 11-mile floats in summer but not in winter. Some of these were found on 2-mile floats in both winter and summer. On the other hand, several species of serpulid polychaetes were found on both summer and winter floats at the 11- and 25-mile stations but not at the 2-mile station in winter. This suggests that the serpulids may have originated in the southern Gulf and were carried only as far shoreward as the 11-mile station in winter, and that the errant polychaetes were introduced to the floats from shoreward areas in summer but not in winter.

Data derived from 1-year floats at the 25-mile station indicate that about 30-35 is the maximum number of macroscopic species that will settle on the 600 cm^2 surface of these floats for long periods of time. So far as number alone are concerned, there is a steady increase with time of those species that derive their food from float inhabitants and detrital materials. But the majority of such species contribute only minor amounts to the total of organic matter found on the floats.

6. Larval Transport and Water Circulation

Results of the Panama City study made clear to us the importance of the relationship between the history of water masses or currents and important differences in the fouling assemblages that we were analyzing. Techniques for identifying particular water masses by analysis of holoplankter composition are well known. We believe that the meroplankters of epifaunal species can be even more useful in studying current patterns than holoplankters because once they settle on a surface they remain as a record of the passage at some time or another of a given parcel of water with its particular complement of larval organisms. Moreover, by looking back from the date of appearance of a species on the float by reference to known rates of growth, one can caluclate approximate times of larval settlement. In the following paragraphs consideration will be given to those biological differences, between the 2-mile, 11-mile, and 25-mile stations as well as those between surface and bottom floats at the same stations, that were directly attributed to water circulation. In so doing, some mention must be made of the particular species of animals involved.

Barnacles

There were substantial biological differences between the arrays of floats at the 2, 11, and 25-mile stations, as well as differences on the vertical axis between shallow and deep floats (Tables 2 and 3). Only two barnacle species are shared by all three stations, viz., Balanus venustus and B. improvisus. The 11-mile station appears to be more closely related biologically to the 25-mile station than to the 2-mile station, since it supports B. merrilli and B. calidus that are clearly offshore species here. We note also that these latter two species occur primarily on the bottom floats (Table 3).

Table 1. Variations in the number of species found on floats with time, depth, and season at the 11-mile station. TS = total of all different species found on all floats, TDS shows the total of different species found at each depth. SRD = number of species restricted to that depth.

11-MILE STATION									
	Summer (May-Aug) TS = 70					Winter (Nov-Feb) TS = 50			
Duration of Exposure (wk)	Depth (m)	4	10	17	29	4	10	17	29
2		5	5	4	11	5	5	4	5
4		8	13	10	14	5	8	6	12
8		12	17	21	29	9	12	8	30
14		15	19	16	34	10	17	16	34
	TDS	19	27	24	53	16	27	14	31
	SRD	1	3	2	33	1	3	1	29

Table 2. Occurrence of barnacle species at the three fouling stations.

SPECIES	2 miles	11 miles	25 miles		
Balanus eburneus	+	-	-	May-Jul	all depths
Balanus venustus	+++	+++	+++	all mos.	all depths
Balanus improvisus	+	+	+	May-Dec	above 17 m
Balanus merrilli	-	+	++	May-Aug	below 10 m
Balanus calidus	-	+	+++	Jan-Aug	"
Balanus spongicola	-	-	+	Mar-Aug	"
Conchoderma virgatum	-	rare	+	Apr-Aug	above 10 m
Lepas anatifera	-	-	+	Jun-Dec	4 m only
Lepas pectinata	-	-	rare	Apr	10 m only

Table 3. Depth distribution of barnacle species at 11-mile and 25-mile stations. Numbers in columns are percentages of the species' total sample population.

	Float Depth and Station Position									
	4 m		10 m		17 m		29 m		44 m	
Species	11 mi.	25 mi.	11 mi.	25 mi.	11 mi.	25 mi.	11 mi.	25 mi.	11 mi.	25 mi.
Lepas anatifera	0	100	0	0	0	0	0	0	0	0
Conchoderma virgatum	100	97	0	3	0	0	0	0	0	0
Balanus improvisus	9	90	72	8	19	2	0	0	0	0
Lepas pectinata	0	0	0	100	0	0	0	0	0	0
Balanus venustus	8	1	9	5	25	16	58	33	0	45
Balanus calidus	0	0	0	0	0	0	0	5	100	95
Balanus merrilli	0	0	0	0	0	0	5	15	95	85

Data in the foregoing tables appear to indicate that offshore bottom water penetrates shoreward at least to the 11-mile (F-1) station, but not so far as the 2-mile station. Since B. merrilli appears at 11 miles in greatest numbers from late May through August, this shoreward movement of bottom water may take place then. Figure 5 shows that at the 11-mile station substantial drops in bottom-water temperature occur periodically during this period and that the drops are accompanied by rises of surface temperature. We note here also that bottom salinities increase and surface salinities decrease. The same changes occur at the 25-mile station but not at the 2-mile station.

These observations seem to indicate that there is a shoreward flow of bottom water in summer that does not reach to 2 miles offshore, and that there is a concurrent offshore flow of surface water of low salinity. The latter could account for the observation that the stalked barnacles, Lepas anatifera and Conchoderma virgatum, which are surface forms, do not ordinarily penetrate shoreward of the 25-mile station.

To our knowledge, naither Balanus calidus nor B. merrilli exist along the shore near Panama City. Balanus calidus is known to exist in offshore waters SW of Cape San Blas, Florida, some 65 nautical miles SE of the 25-mile station. This suggests that B. calidus cyprids may be carried to the 25-mile station via northwestward moving bottom water. This may apply also to B. merrilli. The fact that both species exist along the Yucatan Channel suggests a relationship with the East Gulf Loop Current. Since the greatest influx of these barnacles occurs when the Loop Current is running strongest and penetrating farthest north, it may bring cyprids northward rapidly enough that they could be spun off into eddies that sweep past the 25-mile station but not usually shoreward of the 11-mile station. In order to be compatible with known data on length of larval life, such a current would have to average little more than one knot in order to carry viable larvae from well southward of the Yucatan Channel. Leipper (1967) has reported velocities of 2-3 knots for the Loop Current in May and June.

Other lines of evidence reinforce the above indications. The 2-mile and 11-mile stations are more closely related biologically at 4 and 10 meters, whereas the 11-mile and 25-mile stations are more closely related at 17 m and deeper levels. The fact that these total shallow and deep relationships are much more pronounced in summer than in winter suggests that there truly is a net transport of low salinity surface water away from shore at this time with a concurrent shoreward movement of bottom water.

The movement of this bottom water, which we believe is less than 17 m thick 25 miles offshore and perhaps no more than half that thickness at 11 miles, carries a rather unique complement of meroplankters. No less than 24 invertebrate species were found to be characteristic of the bottom water floats at the 25-mile and/or 11-mile stations. Seventeen of these species are shown to have southern or tropical distributions. One of them is the hydroid Bougainvillia carolinensis that occurred primarily on the bottom floats (44 m) at F-3 and at 29 m at F-1. It came in with the bottom water and settled only when a hard surface was presented. As might be suspected from the above, this species was only rarely found at the 2-mile station.

7. Variations in Standing Crop Biomass

The amount of biomass found on the floats varied with duration of exposure, distance from shore, depth, season, and species composition (Figures 3 & 4).

The greatest secondary production occurred at the 11-mile station, followed by the 2-mile station and the 25-mile station. At the 11-mile and 25-mile stations, production was generally greater in spring and summer than in winter, but was sometimes the reverse at the 2-mile station because of the greater growth of barnacles and gammarids there.

The important determiners of the amount of biomass occurring at a particular time were ecological relationships among dominant species in the assemblage. Possible relationships between the barnacle Balanus venustus, the anemone Aiptasia eruptaurantia, the caprellid Caprella equilibra, and various hydroids can be shown in part by reference to Table 4. In summer, barnacles increase rapidly through the 8th week, followed by a precipitant decline. Aiptasia, on the other hand, does not appear until the 8-week harvest, where its numbers have increased explosively from pedal laceration. It appears that the anemone has some as

yet unexplained deleterious effect on the barnacles, for barnacle decline is not severe at 29 m and at all depths in winter at the 11-mile station in the absence of Aiptasia. The anemone feeds upon caprellids and gammarids and both of the latter may feed upon hydroids.

The float assemblages constitute a fairly complex but obviously incomplete ecosystem. Primary producers on the floats cannot supply sufficient organic matter to allow for the development and sustaining of the large standing crops just observed. Plankton must meet the deficit. Some general conception of secondary productivity can be made on the floats. For instance, Caprella equilibra feeds on the hydroids Clytia johnstoni and Clytia fragilis when available. Data derived for these hydroids where neither Caprella nor nudibranchs were present show they can produce 3.84 g of dry organics in 8 weeks. Where both Caprella and Clytia were found together on an 8-week float under the same conditions, the caprellid population contained 0.42 g of dry organic and the hydroid 0.41 g. At 0.25 metabolic efficiency the caprellids would have required 1.68 g or about 43% of the above 3.84 g production of dry organics. But this does not allow for reduction of the caprellid population through predation by Aiptasia. During the same period the anemone accumulated 0.68 g of dry organics. Assuming that about a quarter of this was supplied by caprellids, then Caprella would have produced 0.68 grams of organic material. If most or all of the total caprellid organics came from Clytia then the latter would have had to produce about 4.4 g of dry organics in 8 weeks. This seems a reasonably close approximation of the observed rate of 3.84 g for hydroid production, especially since we don't know the metabolic efficiency of the principal species.

8. Antifouling Effects

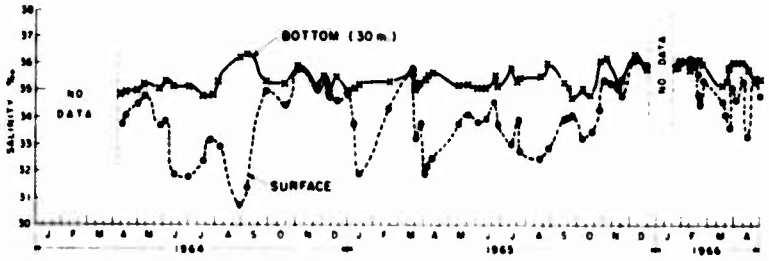
The only chemical antifoulant employed in this study, an organotin, was carried by a thin, teflon band that girdled certain "protected" floats. In practical application, however, other factors, such as grazing and predation by animals, may curtail, control, or completely obliterate fouling developments. Moreover, one may extend the concept of antifouling effects to include season of exposure, depth, and position of installation relative to observed current patterns.

Organotin: In adequate concentrations this material prevented completely the settlement or transgressions of both larval and adult animals (Fig. 6). Even after leaching in the sea for up to nine months, no growth occurred on the band (except for some flat algae), although the "zone of inhibition" usually narrowed as hydroids and barnacles encroached upon it. This particular compound proved to be most effective against polychaete annelids, followed by ectoprocts, anthozoan coelenterates, barnacles, hydroid coelenterates to the least sensitive gammaridean crustaceans.

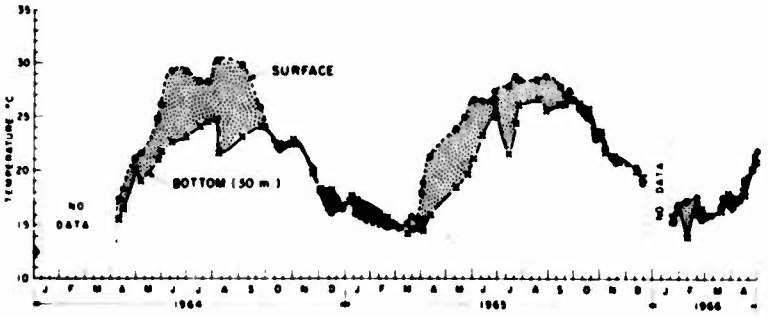
Biological Inhibitor: Evidence gained during this study points to the likelihood that the anemone Aiptasia eruptaurantia produces and emits a substance that both prevents settlement and kills attached acorn barnacles (Balanus venustus). This possibility should be investigated biochemically, since similar action probably applies to other barnacle species.

Reference

1. D. F. Leipper, Tech. Rpt., Ref. 67-9, Dept. of Oceanog., Texas A&M Univ., College Station, Texas (1967).



SURFACE AND BOTTOM WATER SALINITIES AT STATION F-1 MAY 1964 - APRIL 1966



SURFACE AND BOTTOM WATER TEMPERATURE AT STATION F-1 MAY 1964 - APRIL 1966

FIGURE 5. Surface and bottom water temperatures and salinities at the 11-mile offshore station during the two-year study period.

Table 4. Differences in rates of accumulation of biomass with time and depth among the organisms occurring on 16 floats exposed at the 11-mile station in spring-summer (top half of table) and another 16 floats exposed in winter (bottom half). The former were all exposed on 16 May, whereas the winter floats were all exposed on 14 November. But in each case, floats were removed in fours after 2, 4, 8, and 14 weeks at each depth. TFB = total float biomass. DO = dry organic matter.

Depth (m)	Exposure (weeks)	Balanus venustus Ind.	Balanus venustus DO(g)	Aiptasia Ind.	Aiptasia DO(g)	Caprella Ind.	Caprella DO(g)	Hydroids DO(g)	TFB
SUMMER									
4	2	1,410	.21	0	0.00	0	0.00	.08	.3003
	4	1,950	3.29	0	0.00	300	.02	.50	3.8225
	8	1,510	5.79	1,600	.68	6,900	1.25	.42	8.5298
	14	90	.66	1,700	14.83	362	.03	0.00	19.7817
10	2	1,735	.33	0	0.00	10	.001	.03	.3778
	4	1,900	1.66	0	0.00	100	.008	.75	2.4778
	8	1,737	3.41	1,500	.42	19,056	1.200	.14	6.7317
	14	dead	0.00	1,818	16.55	0	0.000	0.00	22.6213
17	2	7,535	.19	0	0.00	0	0.000	.05	.2400
	4	4,666	2.50	0	0.00	10	.001	.15	3.1403
	8	3,600	2.45	1,604	.19	1,430	.040	.53	4.8542
	14	dead	0.00	6,466	20.88	0	0.000	.35	24.4753
29	2	6,900	.51	0	0.00	4	.001	.03	.5941
	4	7,700	1.10	0	0.00	20	.003	.25	1.9411
	8	3,660	.32	0	0.00	2	.002	.82	7.4063
	14	900	.86	0	0.00	0	.000	.40	3.9041
WINTER									
4	2	624	.15	0	--	23	.01	0.00	.1900
	4	533	.61	0	--	2,400	.08	1.50	2.2314
	8	1,200	.71	0	--	25,640	3.61	.60	5.9019
	14	860	.81	0	--	15,000	2.70	.26	4.0663
10	2	1,003	.18	0	--	0	--	.01	.2611
	4	874	1.93	0	--	0	--	.44	3.0934
	8	820	3.11	0	--	20	.015	1.69	4.8470
	14	1,425	5.30	0	--	6,235	.65	.43	6.4953
17	2	975	.13	0	--	0	--	.02	.1637
	4	1,133	3.31	0	--	0	--	.12	3.5034
	8	986	2.34	0	--	1,633	.20	.84	3.4361
	14	1,852	7.78	0	--	8,700	2.28	.06	10.2505
29	2	1,481	.27	0	--	0	--	.00	.2876
	4	1,866	1.90	0	--	28	.01	.10	2.4785
	8	5,983	3.69	0	--	0	--	.10	4.4342
	14	3,260	10.68	0	--	285	.25	.75	14.1238

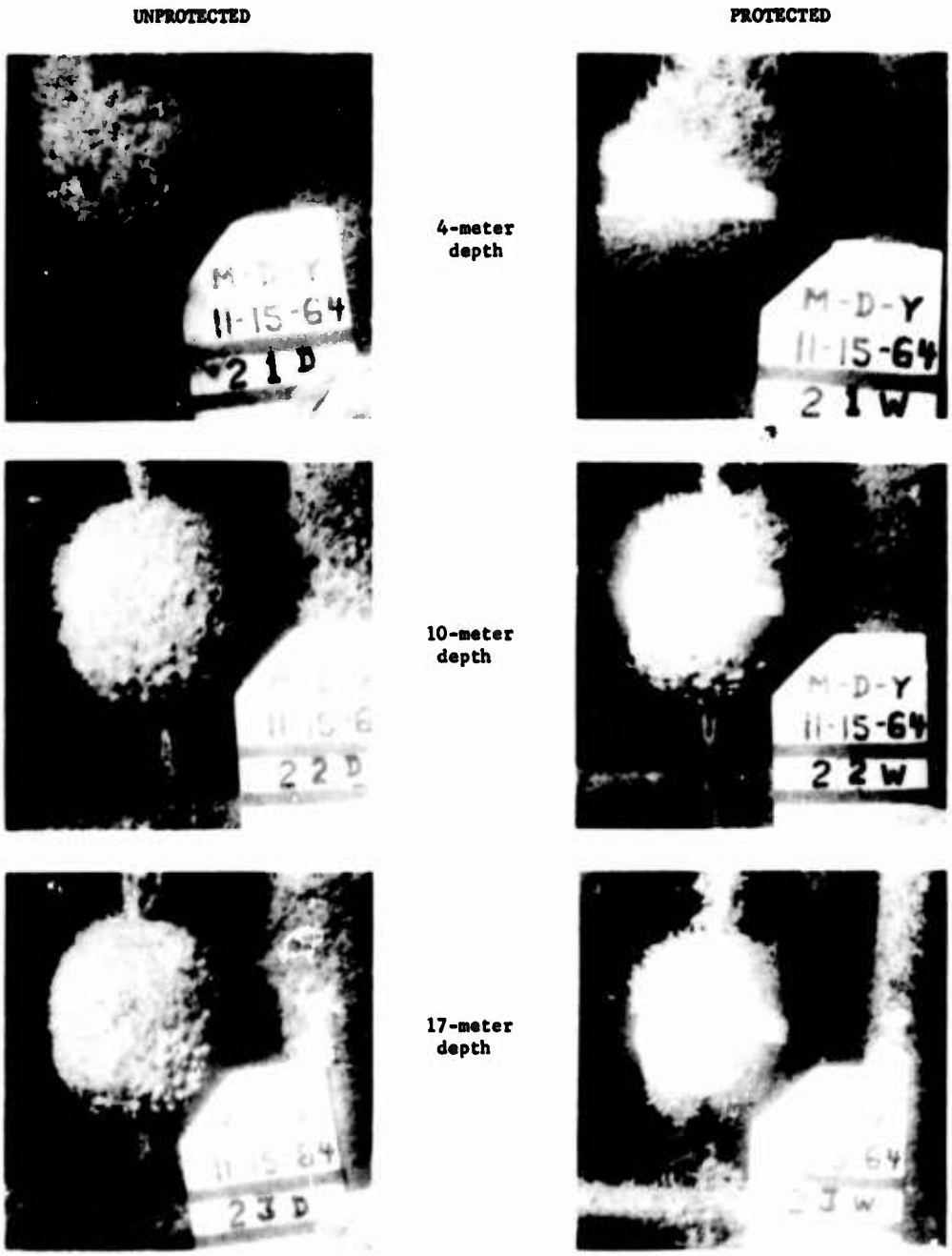


FIGURE 6. Photographs comparing protected and unprotected floats exposed for 3 months from August 22 to November 15, 1964 at the 2-mile station.

Discussion

A questioner asked for the size of the floats. Each had a surface area of roughly 600 cm^2, being about 6 inches high and 4 inches in diameter. There was no control test for antifoulants and no control tests for nature of the substratum and its effect.

It was asked whether the substratum had the same character and supported the same communities at the three stations. The bottom was sandy, not the silt-mud bottom found to the west of the Mississippi delta.

G. Relini asked whether differences in the dominant currents to which the panels were exposed were reflected in the nature of the settlement on the panels. W.E. Pequegnat replied that this was so at the two inshore stations, where there is a complete reversal of the current pattern between summer and winter, and there were very definite differences in the accumulation of organisms established there. This, in fact, was one reason why Itaxia disappeared at the 11 mile station during winter: the current changed completely with reference to the source of the organism. This raised another curious problem, namely, how some of the peracaridan crustaceans such as the gammaridians with no pelagic larvae were able to reach the 25 mile station; the amphipods, particularly the caprellids, seem unlikely to have crawled along the bottom.

Another speaker pointed out the relevance of colonization studies at isolated sites to the study of island biogeography. Particular interest attaches to the colonization curves, which are plots of the numbers of species against a time axis. Thus, at the shallowest float arrays (4 and 10 meters), the colonization curves in summer rose more steeply than did the curves in winter. At the deeper stations (17 and 29 meters), where the annual temperature change is presumably less, the difference between the shape of the colonization curves was not so great.

Crustecdysone Action and the Effects of Light During the Post-Breeding Condition of the Cirripede Balanus balanoides (L)

D. J. Tighe-Ford and D. C. Vaile

Exposure Trials Station, Central Dockyard Laboratory, MM Naval Base, Portsmouth

The action of the arthropod moulting hormone crustecdysone has been studied during the annual post-breeding period of adult Balanus balanoides under day/night conditions and constant illumination. Breeding in this species is followed by a cessation of moulting, termed reproductive anecdysis, after which the tissues of the penis are shed with the exuviae. Doses of 0.02 and 0.2 µg hormone induced marked moulting activity during anecdysis, although the responses differed, and also accelerated moulting during the post-anecdysis period. Furthermore, the injection of hormone during anecdysis apparently interfered with the subsequent shedding of penis tissue. The responses during both physiological states were further influenced by light and it appears that natural production of a moulting hormone may have been stimulated. An early resumption of moulting was also induced by wounding. The possible nature of the biological mechanisms involved in these responses is discussed.

Key Words: Barnacles, crustecdysone, moulting, reproductive anecdysis

1. Introduction

As part of an anti-fouling programme studies are being made of biological systems in barnacles. Moulting is the mechanism which allows development and growth and it has been shown that injections of the arthropod hormone crustecdysone will synchronize and accelerate moulting in adult Balanus balanoides (L.)(1)[1]. There can be little doubt therefore that barnacles possess a hormonal control of moulting, as do other arthropods. The experiments described below are part of studies into the nature of this control.

Moulting is a frequent and recurring activity in adult barnacles and it has been shown in B. balanoides that there is a seasonal variation in the moulting rhythm (2). It was observed that the annual breeding in late autumn is followed by an abrupt cessation of moulting for a period of approximately 6-8 weeks; this was termed anecdysis and attributed to a basic annual rhythm. However it was later suggested (3) that the cessation of moulting arose in part from a depletion of food reserves following breeding and that its apparent duration was related to low availability of food in winter: the term reproductive anecdysis was suggested. It was further observed (2) that in the first moult after this period of non-moulting the barnacles cast their penis tissues. Subsequent casts showed a stump which increased in size as the penis developed during the summer. It was also found that even adults which had been isolated to prevent copulation later underwent a period of non-moulting, provided that they had been sampled from a natural population shortly before breeding. However, adults in which breeding had been inhibited by laboratory conditions continued to feed and moult normally, until fertilization occurred naturally or was induced by a change in the conditions (2, 4): anecdysis then occurred, followed by shedding of penis tissue. These observations appear to support the presence of an endogenous mechanism in B. balanoides which is associated with the breeding condition.

Breeding in this species is induced by critical periods of short photophase and low temperatures, whereas it is inhibited by constant illumination and/or raised temperature (4, 5, 6). It has been shown that light will influence crustacean moulting activities

[1] Figures in parenthesis indicate the literature references at the end of this paper.

(eg 7-10), although the nature of the response varies between species. Moulting during winter anecdysis in the crayfish Orconectes virilis can be induced by periods of long photophase and it was suggested that natural activity was controlled by the action of light through moulting and moult-inhibiting systems (9). It appeared therefore that the post-breeding period of Balanus balanoides might be an interesting area for studying the effects of crustecdysone and light upon moulting activities. Although light was reported to have no effect upon moulting in this species (2), the date of the experiment was not given and it has been reported that the action of light upon crayfish depended upon season (9).

2. Materials and Methods

Studies were made during the winters of 1970/71 and 1971/72 using adult B.balanoides which had settled on panels during the previous spring. Experiments were carried out after breeding had occurred, ie after egg-masses had been laid down. Panels were cut so that small groups of adults of approximately equal size were obtained: the barnacles were cleaned and placed in groups of 10-25 in perspex trays which were divided into parallel compartments. These stood over a sink from which seawater was pumped through an ultra-violet sterilizer into a weir across the head of each tray and returned to the sink after flowing through the compartments. The barnacles were thus continuously submerged in flowing seawater. Exuviae were retained by a nylon mesh screen across the end of each compartment. The systems were continuously replenished with filtered seawater, with an overflow to waste and the temperatures were controlled thermostatically. Throughout the studies no additional food was added to the systems.

With the exception of experiment IV the barnacles were divided into four groups. Two were injected with total doses per animal of 0.02 and 0.2 µg crustecdysone in sterile seawater, as four consecutive daily volumes of 2 µl: two further groups were used as controls, one untreated and the other injected daily with 2 µl seawater for four days. Injections were carried out as previously described (1). Crystalline crustecdysone JL1(11) was used, prepared from the plant Podocarpus elatus (12).

The barnacles were maintained either under laboratory day/night conditions (approximately nine hours photophase, 250 - 800 lux) or under constant illumination and the number of exuviae from each group was recorded daily after the first injections. The adults and the sea-water systems were scrubbed once or twice weekly to remove sediment and any algal growth. Further experimental details are given later as appropriate. For brevity in the text, the non-moulting period which follows breeding is referred to as anecdysis and the period in which natural moulting recommences is termed post-anecdysis.

The results given in all Tables are based upon the daily moulting responses of each group expressed as the number of exuviae/100 animals; these were then summed to give the total moulting activity over a particular period. Dead animals were removed after each daily count of exuviae.

Experiment I (anecdysis period)

A preliminary investigation was made in 1970 of the action of crustecdysone during anecdysis, under conditions of seasonal temperature and laboratory day/night illumination. Adults with a mean carino-rostral diameter of 13.3 ± 0.8 mm were brought into the laboratory in late November, shortly after breeding; 90-95% of those sampled possessed egg-masses. Panels were cut so that approximately 225 adults were obtained in small groups, which were kept in flowing seawater trays for one week. During the first five days a few adults were copulating and 23 exuviae were shed: seven were still attached and those adults were removed. No exuviae were found on the sixth and seventh days and when 20 adults were sacrificed all contained egg-masses. It then appeared reasonable to suppose that all of the experimental animals had bred and entered anecdysis.

Groups of 20 adults were used and the first injections were made on November 30th; the seawater was maintained at a temperature of approximately 10°C.

The nature of the daily moulting activities over seven weeks is shown in Fig 1. No moulting occurred in the untreated adults during the first 24 days, confirming that for the purpose of the experiment the population was in the anecdysis state. Both hormone doses induced moulting responses markedly in advance of the resumption in the untreated and sea-water injected controls. The 0.2 µg dose resulted in a high and synchronized response eight days after first injections, with 18 exuviae shed within a period of four days. However the corresponding response in the 0.02 µg hormone group, although occurring at a similar time, was much less and accompanied by mortality. A similar but higher mortality occurred with this dose in a parallel experiment (unpublished), under non-seasonal conditions of constant illumination at 20°C, in which eight of a group of 20 adults injected with 0.02 µg hormone died within the first 10 days: there was only one death recorded in another group injected with 0.2 µg hormone.

The total moulting activities over seven weeks are summarized in Table I. It can be seen that the overall effect of 0.2 µg hormone during this period was greater than that of the lower dose. The increased and earlier moulting activity in the sea-water injected animals in relation to the untreated controls was apparently a wound response, as discussed later. The increased moulting in the hormone groups was maintained throughout the 12 weeks' duration of the experiment: the activities of the untreated controls, sea-water, 0.02 & 0.2 µg hormone injected groups for weeks 8-12 were 20, 65, 105 and 92% respectively. As discussed later, it appears that the crustecdysone may have stimulated a natural site of production of moulting hormone.

As shown in Fig 1 three exuviae shed during the initial response to 0.2 µg hormone contained no penis tissue, but only the cuticle of the penis: one such exuviae was found in the 0.02 µg group and none in the control groups. In addition, 25 exuviae containing penis tissue were shed by the 20 adults injected with the higher hormone dose. As a barnacle cannot completely cast its penis tissue on more than one occasion after a period of anecdysis, the probable explanation is that some of the exuviae shed early in the experiment contained only a portion of the penis tissue and that the remainder was shed in a subsequent moult(s). Details of the exuviae shed in the various groups are given in Table 2. The results suggest that the partial or complete retention of penis tissue in some exuviae arose from effects of injected crustecdysone, which apparently modified the nature of the moulting activity when compared with the two control groups. The phenomenon appeared to be associated with a dose of 0.2 µg hormone.

Experiment II (post-anecdysis period)

The action of crustecdysone was then examined during the post-anecdysis period, several weeks after the start of the above experiment. Studies were carried out under both laboratory day/night conditions and constant illumination in a light-tight box (2000-2500 lux at the water surface). When adults were brought into the laboratory during mid-December 1970, it was found that they were moulting during the acclimatization period. The exuviae contained penis tissue and it appeared therefore that the population was entering the post-anecdysis state. All the adults sampled possessed egg masses and the mean carino-rostral diameter of the experimental population was 12.5 ± 0.8 mm.

Two parallel experiments were set up, each containing four groups of 20 adults. Both systems shared a recirculated supply of seawater from a common sink, with a continuous replenishment: the mean temperatures under day/night conditions and constant illumination were 9.4 and 9.6°C, respectively. The treated barnacles were injected on three consecutive days, commencing on December 21st. The daily moulting responses throughout seven weeks are shown in Fig 2; in Table 3 the total moulting activity has been divided into the initial response to hormone (during approximately the first two weeks) and the subsequent activity.

The population was moulting when injected and activity was increased in all the treated groups. The effect of the crustecdysone can be seen in Table 3, although the greater activity imposed by the hormone was somewhat masked by the surge of moulting which occurred in all groups during the early post-anecdysis period. There was no apparent difference between the responses to the two doses, as distinct from the results of the

previous experiment. Furthermore, under day/night conditions the complete or partial retention of penis tissue which had occurred after the injection of crustecdysone during anecdysis was not observed.

Moulting activity was increased in all groups under constant illumination. Although the possibility cannot be excluded that this arose from increased algal growth due to light, this is unlikely as the same seawater was circulated through both systems. Further evidence for an influence of light upon moulting activities is obtained from a comparison of the nature of the exuviae shed under the two conditions of illumination over seven weeks (Table 4). With constant illumination it was observed that in the three treated groups the number of exuviae containing penis tissue exceeded the number of animals: this did not occur in any group under day/night conditions. It can be seen in Fig 2 that although 20 penis tissue exuviae were shed in each of the two hormone groups during the initial response under constant illumination, some subsequent exuviae also contained penis tissue. The phenomenon does not appear to be related to the total moulting activity of a group. As in experiment I, the results suggest that the nature of the first moult after anecdysis was somehow modified in the treated groups, although in this case only under constant illumination.

The higher mortality under constant illumination (nine deaths compared with six under day/night conditions) may be another effect of light, as discussed later.

Experiment III (anecdysis period)

A further investigation of the anecdysis period was made the following year, using randomized block systems to allow statistical analysis. B. balanoides were brought into the laboratory on November 30th, 1971 after ascertaining that the majority of the population had bred: 90-95% of the adults removed during "thinning out" possessed egg masses. The panels were cut into 32 groups of 10 barnacles, with a mean carino-rostral diameter of 12.7 $\pm$ 1.0 mm. Two parallel experiments were set up in separate systems, one under constant illumination of approximately 2400 lux at the water surface and the other under laboratory day/night conditions: the mean temperatures were 8.5 and 8.6°C respectively. Each system comprised four, compartmented trays which were supplied with seawater from a constant head unit: care was taken to ensure that the trays in both experiments were supplied at the same flow rates. Each experiment contained 160 adults, as groups of 40. These were further divided into sub-groups of 10, which were placed so that every tray held in random order a sub-group from each of the experimental groups.

During the acclimatization period 23 exuviae were shed in one week by the 320 adults in the trays. All showed normal penis cuticle and were presumably shed by the few adults which had yet to lay down egg masses. Beginning on December 7th the sea-water and hormone groups were injected on four consecutive days. The daily moulting activities of the experimental groups of 40 adults, over seven weeks, are shown in Fig 3: the total activities of the individual sub-groups throughout this period are given in Table 5. The results were subjected to an analysis of variance (Table 6) and difference-of-means tests, etc., as appropriate.

As no moults occurred until the ninth day after the first injections, when the barnacles responded to treatment, it appeared that all of the population were in a state of anecdysis by the start of the experiment.

Moulting activities differed under the two conditions of illumination, although the nature of the responses was broadly the same and similar to that observed during the anecdysis of the previous year (experiment I). Under day/night conditions the crustecdysone induced moulting activity approximately 10 days before this occurred in untreated controls. Although as before there was also an induction of early moulting in the sea-water injected animals (number of moults in first three weeks - Chi Square test, $P < 0.05$) definite activity did not occur until one week after the hormone groups. There was a marked synchrony in the responses to crustecdysone, which was more evident with the 0.2 µg dose. The initial response occurred within the first three weeks: during this period the

mean time to first moult in the 0.2 µg group was 10.9 ± S.E. 0.24 days, which is significantly less than the mean time of 13.4 ± S.E. 0.38 days for the 0.02 µg dose (Fisher - Behrends test (13), P<0.01). Under constant illumination moulting commenced in all four groups at approximately the same time. However, a marked surge of activity was induced by the hormone, with the greater synchrony again imposed by the higher dose. The mean time to first moult (11.0 ± S.E. 0.23 days) in this group was significantly less than that of 14.0 ± S.E. 0.54 days for the 0.02 µg group (P<0.01). These figures are almost identical to those for the day/night conditions and moulting began on the same days under the two conditions. The resumption of moulting in the untreated controls was apparently accelerated under the constant illumination and occurred at approximately the same time as in the sea-water injected controls; although, over a period of seven weeks the total moulting activity was higher in the latter.

Moulting activity in all four experimental groups was increased under constant illumination, as can be seen in Table 5 and from a comparison of the number of second, or penis stump, exuviae under both conditions (Fig 3). Analysis of variance of the results from both conditions of illumination (Table 6) shows the overall effect of light to be highly significant (P<0.01). It is unlikely that this arose from an increased algal growth as the systems were cleaned frequently and the results are similar to those in experiment II in which the barnacles under the two conditions shared a common and recirculated supply of seawater. Table 6 also shows that the relationships between the responses in the four groups of barnacles were the same under both conditions of illumination (P>0.05), thus the barnacles apparently responded to hormone and moulting in the same way under constant illumination as under day/night conditions. Over a further period of five weeks the total moulting activities under constant illumination were as follows: untreated and sea-water controls, 46% and 77%, and 0.02 and 0.2 µg hormone groups, 77% and 82%; whereas the comparable activities under day/night conditions were 10%, 47%, 64% and 52% respectively.

As in experiment I the higher hormone dose group under both conditions of illumination was characterized by moulting responses which were abnormal in relation to the untreated and sea-water controls. Approximately 25% (8) and 35% (13) of the exuviae in the initial response to hormone under day/night and constant illumination conditions, respectively, did not contain penis tissue but only the cuticle. Two such exuviae, only, occurred between all other groups (Fig 3). The effect of the 0.2 µg hormone dose upon the nature of the first moult is significant when compared with the controls (Chi Square test, P<0.01). Although the difference in the number of such exuviae under the two light conditions is not significant (Chi Square test, P>0.05), it was further observed that in the 0.2 µg hormone group under constant illumination three exuviae were shed during the second half of the experiment which possessed very short penes: these contained tissue. It appeared from analysis of the daily moulting activities of the sub-groups that these exuviae followed earlier, presumably incomplete, penis tissue moults: in two of the three sub-groups involved the total number of tissue-containing moults was one more than the number of barnacles. These results appear to be in agreement with the effects of hormone and light during experiments I and II.

Mortality was increased under constant illumination. During the seven weeks of activity shown in Fig 3 there were 8 deaths under day/night conditions and 11 under constant illumination: over a total of 14 weeks' observation the figures were 16 and 28 respectively (Chi Square test, P=0.05-0.06). Similar results were reported in experiments I and II and it is reasonable to suppose that the increased mortality was a result of the non-seasonal light conditions, as discussed later.

Experiment IV (post-anecdysis)

Following the shedding of exuviae containing no penis tissue by barnacles injected during anecdysis with 0.2 µg crustecdysone a further study was made of the effects at this level of hormone action. B.balanoides from the same natural population as those in experiment III were brought into the laboratory on January 5th 1972. The population was apparently entering the post-anecdysis state as moulting was evident when the adults were

placed in the sea-water system and the exuviae contained penis tissue. A group of 25 adults was left untreated and another was injected on four consecutive days with a total dose of 0.2 µg hormone; these were maintained under day/night conditions at a mean temperature of 8.9°C. The daily moulting activities for a period of four weeks after the barnacles were brought into the laboratory are shown in Table 7.

There was a marked moulting response during a period of 9-16 days after the first injection of hormone, in which 23 moults occurred compared with two in the control group. However, although the exuviae possessed either penis tissue or stumps, none showed only penis cuticle and there were no abnormalities. This is in agreement with the results of the post-anecdysis period of the previous year (experiment II) under day/night conditions. Thus the abnormal moulting phenomenon observed in the 0.2 µg hormone groups during the anecdysis of experiments I and III did not occur when the same dose was injected under day/night conditions into a population which had already commenced moulting. It is reasonably certain that a number of the experimental adults must have previously moulted in the sea, as (i) 15 of the exuviae shed during the hormone induced response (days 14-21) had penis stumps, showing that they were second moults: before this response only eight penis tissue or stump exuviae had been shed by this group in the laboratory, and (ii) over eight weeks' observation only 16 and 15 exuviae containing penis tissue were shed by the untreated and hormone groups, respectively.

3. Discussion

The injection of crustecdysone during the post-breeding condition of Balanus balanoides had marked effects upon moulting activities. Although the experiments confirmed the action of hormone previously observed during late summer (1) the nature of the responses differed in several aspects, depending upon whether the animals were in a state of anecdysis or had entered the post-anecdysis state. Moulting activities were also influenced by the illumination. Although the responses during these experiments were complex there were distinct patterns of activity which appear to be similar to those observed in other arthropod species.

Interpretation of the results is facilitated if the responses under day/night conditions are discussed before the effects of non-seasonal illumination. Crustecdysone induced moulting activity during the period of anecdysis markedly before its resumption in untreated controls and the nature of the response was related to the level of injected dose. In both experiments I and III the injection of 0.2 µg hormone resulted in marked and synchronized activity whereas with a dose of 0.02 µg there was either little response or a significantly longer mean time to first moult. The low response to 0.02 µg hormone during the first 2-3 weeks of experiment I indicates that the resultant titre in the animals was insufficient to induce ecdysis in more than 15-25% of the group during this initial period: the associated mortality suggests that some of the barnacles may have initiated moult processes, and then died. It thus appears that the titre arising from this dose was similar to, or slightly below, that which occurred naturally at the end of anecdysis, particularly as the induced activity was comparable with that which later followed in the untreated controls. The reason for the greater response to this 0.02 µg dose in experiment III is uncertain: although it could have arisen from a variation in the experimental conditions over two seasons, there may have been a difference in the stage of anecdysis; the injections were made a week later than the corresponding period for experiment I and the barnacles may thus have been nearer to the end of the anecdysis state. The marked response to 0.2 µg hormone in both experiments strongly suggests that the resultant titre in the barnacles was higher than the natural level which occurs at the end of anecdysis.

Following the injection of 0.2 µg hormone crustecdysone during anecdysis the nature of a proportion of the exuviae shed at the first moult was abnormal in relation to both the two control groups and the observations of previous authors (2), in that penis tissue was completely or partially retained. This was observed in both experiments I and III and indicates that injected hormone can interfere with an apparent natural mechanism at the end of anecdysis. The dependence of these abnormalities upon dose of hormone suggests

that they were related to the ensueing level in the animals during the processes of the first moult. Although there is no direct evidence concerning endogenous seasonal/levels of moulting hormones in barnacles it is reasonable to suppose that the mean titre (and/or sensitivity of target cells) of a population is low during the post-anecdysis period and increases during the summer. It was found that at a time of relatively high natural moulting activity during the summer that there were no apparent differences between the effects of 0.02 and 0.2 µg crustecdysone (1). It may be that the natural shedding of penis tissue at the end of anecdysis is associated with a low level of production of moulting hormone(s) and that as has been suggested (2) the phenomenon is part of a basic physiological rhythm associated with breeding. The mechanism responsible for the abnormal responses induced by the higher dose of crustecdysone is not known. The situation is complicated by a report (14) that untreated barnacles which have been fed during anecdysis may retain all or part of the penis tissue at the first moult and, further, that this phenomenon has been observed in natural populations. It appears significant that under day/night conditions in experiments II and IV no abnormal exuviae were shed after the injection of 0.2 µg crustecdysone during the post-anecdysis period: in these experiments the hormone was acting upon a population which had already commenced moulting. The nature of the moult may therefore be determined by the hormone titre at the initiation of pro-ecdysis or at later, critical, stages: support for this is found in the suggestion that the level of moulting hormone titre in the crab Carcinus maenas determines the nature of the process to be initiated during a moult cycle (15). It can be considered that the experimental addition of food during anecdysis does not reflect the natural condition - thus the observation on complete or partial retention of penis tissue by untreated barnacles fed in the laboratory (13)may reflect an increased production of moulting hormone(s) above that which would occur naturally.

Injection of crustecdysone may also stimulate an endogenous system, as suggested by the results of experiment I in which the increased moulting activity in the hormone groups was sustained for at least 12 weeks. It appears extremely unlikely that this effect could be due to injected hormone persisting in the animals for such a period and furthermore it has been shown that injected ecdysones can stimulate prothoracic glands in insects to produce moulting hormones (16). A similar effect was reported during summer moulting activity in barnacles (1), although the stimulation was only evident for approximately two weeks. The long term nature of the increased moulting after injection of hormone during anecdysis appears to reflect the low natural activity which follows this period and indicates that the duration of the effect may be related to the level of endogenous endocrine activity at the time.

Moulting activities during the post-breeding period were also influenced by light. As seen in experiment II and III the nature of the responses under constant illumination differed in several aspects from those observed in the day/night conditions: (i) moulting activity was increased in all experimental groups, (ii) in experiment III (carried out during anecdysis) there was an earlier resumption of moulting in untreated controls, (iii) although no abnormal exuviae were shed under day/night conditions during either of the post-anecdysis periods of experiment II and IV, there was apparently some retention of penis tissues in the three injected groups under constant illumination in the former experiment, and (iv) mortality was increased. The nature of these responses suggests that they were related to effects of light. Although responses vary between crustacean species it has been shown that increased photophase in winter can induce moulting responses (eg 7, 9, 10). Furthermore, it has been shown that light will control the production of ecdysone via the brain of the silkworm Antheraea pernyi (17). The increased mortality in barnacles subjected to constant illumination in experiments I and III appears to be another manifestation of light as it has been shown that constant light is lethal to crabs in winter (10) and that although during winter anecdysis in crayfish some animals moulted in response to non-seasonal illumination many died at various stages of the moult-cycle (9). It seems therefore that the response to light observed in Balanus balanoides is similar to those observed in other crustaceans and that the production of an ecdysone or moulting hormone(s) may have been stimulated. This contention would appear to be borne out by the similarity of the effects of light to those induced by the injection of crustecdysone.

An early induction of moulting also occurred in sea-water injected controls during anecdysis under day/night conditions. It has been shown previously that wounding will increase moulting activity in barnacles (1) and it was suggested that this arose from a stimulation of an endogenous endocrine system which resulted in increased production of moulting hormones(s). It appears that a similar phenomenon induced the early moulting in the injected controls during anecdysis. Similar wound responses have been observed in insects, eg diapause in various fly species can be broken by pricking, apparently as a result of renewed activity of neurosecretory cells (18).

The results suggest that the annual reproductive anecdysis in Balanus balanoides is part of a basic physiological activity with which light may be associated. This contention is supported by the critical role of photoperiod in the induction of the breeding condition (4, 5, 6): however, the mechanisms involved in this period are still unknown and the suggestions offered are, at best, only partial explanations. Despite a suggestion that only a moult-accelerating hormone (MAH) is involved in the control of moulting in barnacles (19), a moult-inhibiting hormone (MIH) could be involved in the reproductive anecdysis. In crustaceans the production of MAH is typically under the control of MIH which prevents its formation (eg 20, 21) and it has been suggested that light controls the relationship between these hormones (9). The post breeding condition of Balanus balanoides appears to be an interesting field for studying the role of moulting hormones and the biological mechanisms controlling their production and action. Investigations of experimentally induced activities should provide information about endogenous systems and how they may be exploited for anti-fouling purposes.

Acknowledgements

Grateful thanks are given to Mr D R Houghton and Dr R C Reay for advice and encouragement, to Mr S Callaway for advice with statistical interpretation, to Dr D H S Horn for crystalline crustecdysone and to staff who rendered valuable assistance.

4. References

1. D. J. TIGHE-FORD and D. C. VAILE, J. exp. mar. Biol. Ecol. 9, 19 (1972).

2. D. J. CRISP and B. S. PATEL, Biol. Bull. mar. biol. lab., Woods Hole. 118, 31 (1960).

3. H. BARNES, Limnol. Oceanogr. 7, 462 (1962).

4. D. J. CRISP and B. PATEL, Mar. Biol. 2, 283 (1969).

5. D. J. CRISP, Nature, Lond. 179, 1138 (1957).

6. H. BARNES, J. mar. biol. Ass. UK. 43, 717 (1963).

7. G. C. STEPHENS, Biol. Bull. mar. biol. lab., Woods Hole. 108, 235 (1955).

8. D. E. BLISS and J. R. BOYER, Gen. Comp. Endocr. 4, 15 (1964).

9. D. E. AIKEN, Science. 164, 149 (1969).

10. N. G. KURUP, Curr. Sci. No. 7, 149 (1970).

11. D. H. S. HORN, in Naturally Occurring Insecticides, p. 333. Dekker New York (1971).

12. M. N. GALBRAITH and D. H. S. HORN, Aust. J. Chem. 22, 1045 (1969).

13. In R. A. FISHER and F. YATES, Statistical Tables for Biology, Agriculture and Medical Research (5th Ed). Oliver and Boyd Edinburgh (1957)

14. H. BARNES, In Press.

15. D. ADELUNG, Z. Naturforschg. 24b, 1447 (1969).

16. V. J. A. NOVAK, Insect Hormones, p.75. Methuen London (1966).

17. C. M. WILLIAMS and P. L. ADKISSON, Biol. Bull. mar. biol. lab., Woods Hole. 127, 511 (1964).

18. V. J. A. NOVAK, Insect Hormones, p.191. Methuen London (1966).

19. H. BARNES and J. J. GONOR, J. mar. Res. 17, 81 (1958).

20. L. M. PASSANO, in The Physiology of Crustacea, Vol I, p.473. Academic Press London (1960).

21. P. M. JENKINS, Control of Growth and Metamorphosis. Pergamon Press Oxford (1970).

Table 1. Crustecdysone action after injection during anecdysis (over seven week period)

	Total moulting activity	Mortality
Controls	90%	1
Sea-water injected	122%	2
0.02 µg hormone	154%	6
0.2 µg hormone	173%	1

Table 2. Nature of exuviae shed by groups of 20 adults after injection of crustecdysone during anecdysis (over 12 week period)

	Controls	Sea-water	0.02µg	0.2 µg hormone
Total activity	110%	187%	259%	265%
Penis tissue exuviae	18	17	18	25
Penis cuticle exuviae	0	0	1	3

Table 3. Crustecdysone action during post-anecdysis (over seven week period)

Total moulting activities (weeks 1-2)

	Day/Night	Constant illumination
Controls	48%	55%
Sea-water injected	65%	92%
0.02 µg hormone	95%	110%
0.2 µg hormone	99%	110%

Total moulting activities (weeks 3-7)

	Day/Night	Constant illumination
Controls	88%	120%
Sea-water injected	124%	125%
0.02 µg hormone	133%	146%
0.2 µg hormone	65%	151%

Table 4. Number of penis tissue exuviae shed during post-anecdysis by groups of 20 adults (over seven week period)

	Day/Night	Constant illumination
Controls	20*	17
Sea-water injected	16	21
0.02 µg crustecdysone	19	24
0.2 µg crustecdysone	20	24

* out of 26 adults

Table 5. Crustecdysone action after injection during anecdysis (over seven week period).

	Total moulting activities (%)									
	Day/Night				Mean	Constant illumination				Mean
Controls	90,	80,	78,	100.	87	80,	111,	100,	140.	108
Sea-water injected	100,	111,	50,	80.	85	155,	120,	111,	120.	127
0.02 µg hormone	140,	113,	130,	133.	129	138,	150,	164,	160.	153
0.2 µg hormone	170,	113,	135,	167.	146	189,	180,	130,	211.	178

NOTE: each experimental group comprises four sub-groups of 10 adults.

Table 6. Analysis of variance of results in Table 5

Source of variation	d.f.	Sum Sq	Mean Sq	F ratio	P
Illumination (I)	1	6,873	6,873	13.72	<0.01
Treatment (T)	3	21,882	7,294	14.56	<0.001
IxT interaction	3	496	165.3	0.33	notsig.
Residual	24	12,019	500.8	-	-
Total	31	41,270	-	-	-

Table 7. Crustecdysone action during post-anecdysis (over four week period)

Exuviae shed by groups of 25 adults

	Injections													
Days	1	2	3	4	5	6	7	8	9	10	11	12	13	14
Controls	1	1	1	1	1	0	1	3	1	0	0	0	1	2
0.2 µg hormone	0	1	1	1	0	3	1+1*	0	0	0	0	0	0	2+2*
Days	15	16	17	18	19	20	21	22	23	24	25	26	27	28
Controls	0	0	0	0	0	0	0	0	0	0	0	0	0	0
0.2 µg hormone	3+2*	1+6* 2D	4* D	0	1* D	1 2D	1	0	0	0	0	0	0	0

NOTE: unmarked exuviae contain penis tissue, * - penis stump exuviae, D - death

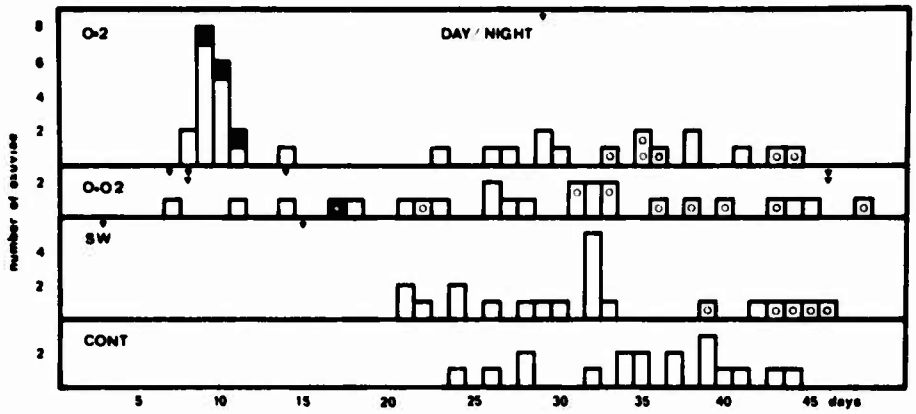


Fig 1. Balanus balanoides: Crustecdysone action during ecdysis period

0,2, 0,02: µg doses of hormone. SW: sea-water injected controls. CONT: untreated controls. Exuviae contain penis tissues, except: ■ : penis cuticle, ○ : penis stump. ▼ : death. Groups of 20 adults.

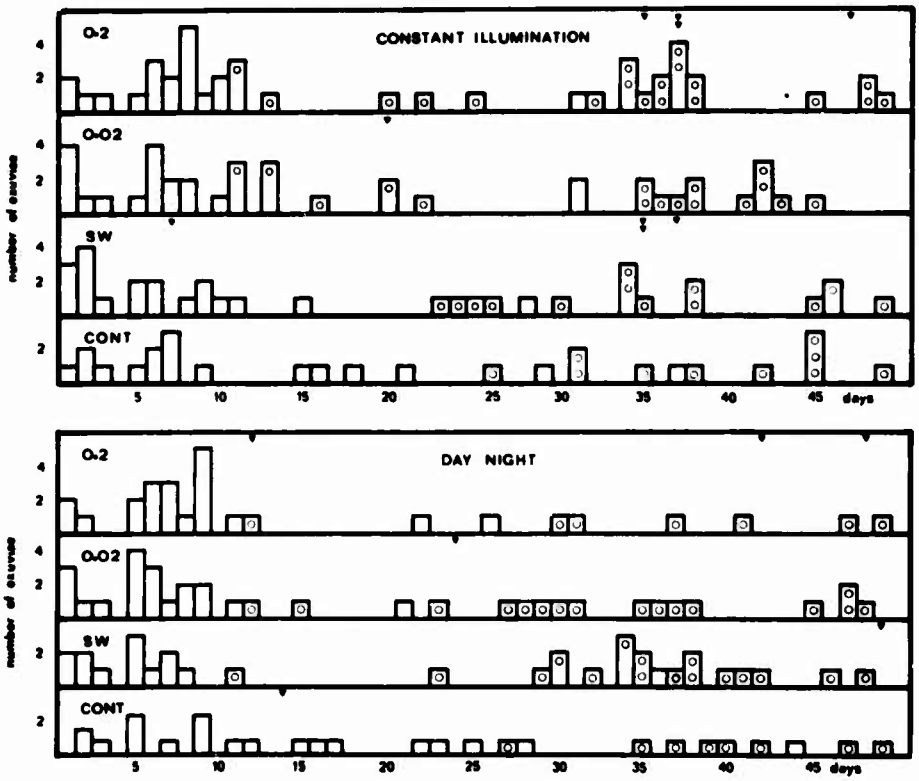


Fig 2. Balanus balanoides: Crustecdysone action during post ecdysis period

See Fig 1 for symbols. Groups of 20 adults, except for 26 untreated controls under day/night conditions (daily moulting activities in this group have been adjusted to allow for this).

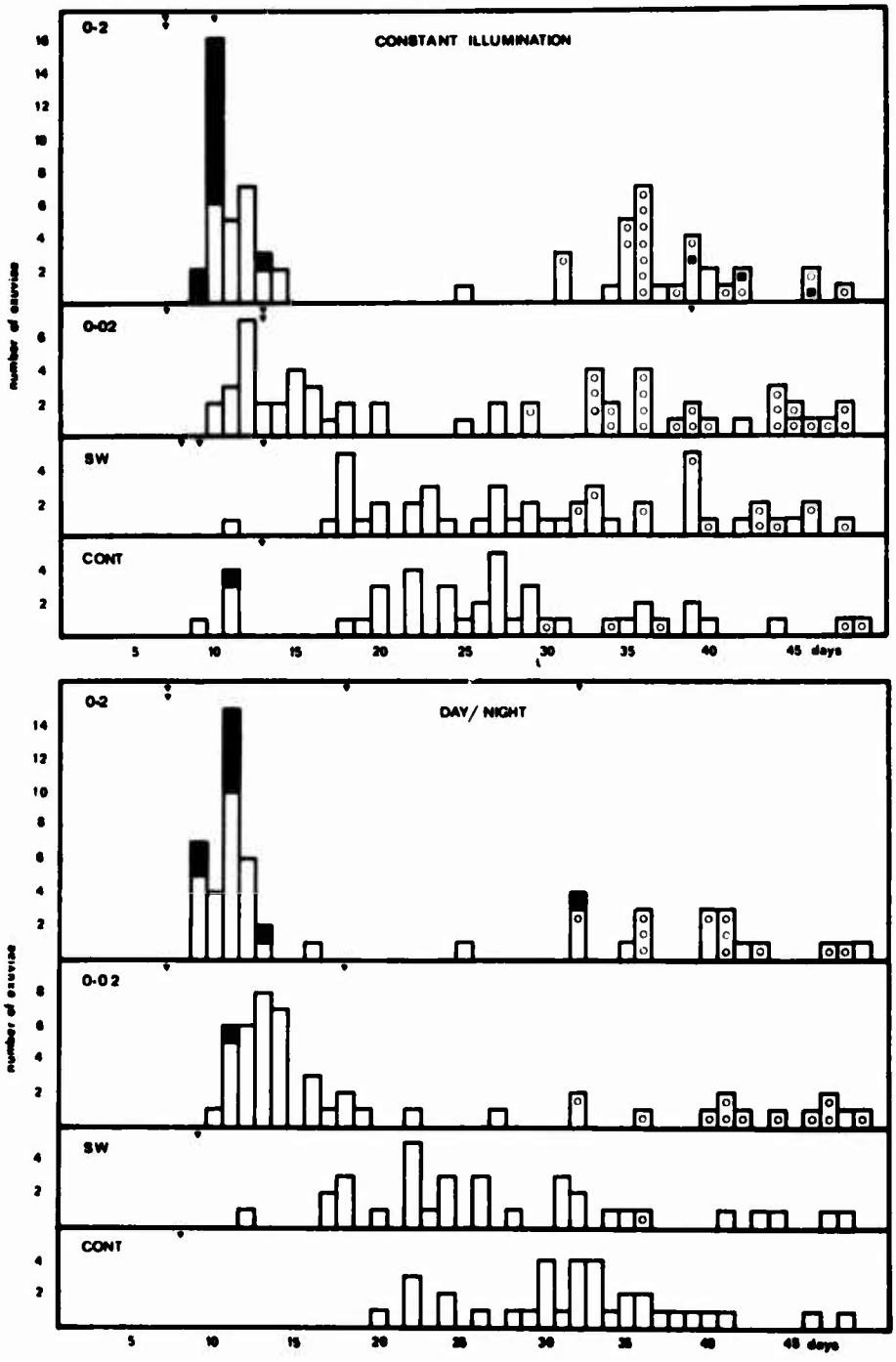


Fig 3. Anlanus balanoides: Crustacyprane action during anastrale period

See Fig 1 for symbols: ▣ short penis exuvia, containing tissue. Groups of 40 adults.

Biological studies on fouling problems in Italy

G. Relini and G. Dabini Oliva

Consiglio Nazionale delle Ricerche
Laboratorio per la Corrosione Marina dei Metalli
Via Mercanzia 4 - 16123 Genova
Italia

Biological studies on fouling from Italian seas, particularly the Lagoon of Venice, Liguria, Sardinia and Civitavecchia have been described with special regard to results obtained during ten years' surveys in the Ligurian sea and mainly in the Genoa harbour. Fouling from harbours, off-shore and from electric power intakes have been investigated (biology-ecology-weights) also in relation to principal antifouling systems used in the intakes. By experimental data on laboratory and industrial plants it was the effectiveness of continuous clorine supply was pointed out as well as the high velocity of water flow to prevent fouling settlement, also from the point of view of pollution control. Distribution, settlement periods, growth rates and mortality of fouling organisms have been studied in several zones having different types and degrees of pollution.

Key Words: Fouling in Italy; harbours; off shore; power stations; intakes; Biology, Ecology, Weight; Pollution; Chlorination; Settlement at different speed of water flow.

In Italy biological studies on fouling (Marine borers excluded)were begun only about 15 years ago and the following localities (fig.1) have been investigated: the Lagoon of Venice (1) (2) (3) (4), the Ligurian sea and particularly the Genoa harbour (5) (6) (7)...(39) (40), Sardinia, off-shore (41) and Civitavecchia (42) (43) (44) (45).

On the fouling from Civitavecchia and the Lagoon of Venice are known: list of species, settlement periods, seasonal sequences and some data about the amount of fouling expressed as wet or dry weight. While new investigations are going on in Trieste and Venice, most of our present knowledge on Italian fouling (biological problems) comes from studies carried out during more than ten years' investigations in the Ligurian sea, where ecology of fouling organisms was examined in relation to principal antifouling systems and different hydrological conditions. The present report deals chiefly with the principal results.

In Genoa harbour fouling six dominant communities (10) (11) are described: 1) Microorganisms 2) Ciona 3) Barnacles 4) Zoobotrion 5) Serpulids and 6) Mussels; only the last one reaches a rather climax situation.

Because of substratum preference they may be divided into three groups:

a) community which appears only on newly exposed panels (microorganisms)
b) communities which appear only on fouled panels as Zoobotrion and Mussels
c) communities present in both the precedent situations (Ciona, Barnacles and Serpulids). A rather different situation was pointed out in the Vado Ligure bay, where Microorganisms and Algae, Hydroids, Barnacles (Serpulids only on monthly panels) and Mussels are dominant communities (36) and generally also the most abundant species are not the same as in the Genoa harbour (15) (22) (23) (24) (25) (27) (28) (29).

In Venice fouling (3) dominant organisms are Microorganisms with Algae, Hydroids (especially Tubularia mesembrianthemum during April and May) Bryozoa (Bugula stolonifera in June) Ascidians (Botryllus schlosseri in July) and Mussels (Mytilus galloprovincialis).

Seasonal quantitative variations of fouling were examined in several Ligurian harbours (37) and in the Genoa harbour variations related to depth (0,1; - 1; - 5; - 9; - 14; - 16 m) were also considered (14) (16) (28) (29). In particular settlement periods of Barnacles and Bryozoans at 6 different depths were described (see fig. 2 and tables 1, 2).

The highest monthly weights of wet fouling were obtained at all depths during summer months, due to the heavy settlement of Barnacles and Serpulids, but weight decreases with depth contemporaneously with the reduction of fouling density.

This weight decreasing with depth does not agree with DePalma's results off Sardinia (41): an average weight (dry) of 5,57 g/dm^2 foot of surface was collected from panels exposed during seven months at 58 m depth and 1,1 g/dm^2 from those exposed at 15 meters.

The maximum one-year accumulation, recorded from Genoa fouling panels (14) was 607 g/dm^2 while the highest monthly weight was found in August 1967: 89 g/dm^2 on a surface panel, while 14 m depth panels, in the same period, showed a weight 18 times lower.

Higher values have been found in Venice: 631,4 g/dm^2 on a 3 month panel in June and 689,2 g/dm^2 on a year's panel in September.

The fouling growing on one year panels immersed in open sea at Vado Ligure (near Savona, -8 m depth) weighed more than 460 g/dm^2 while near Marseille the average higher wet weights after one year was about 20 g/dm^2 (46) at 17-19 m depth.

In Genoa harbour power station intakes have been observed an amount of 289g/dm^2 of fouling on 3 months panels and 716 g/dm^2 on walls after one year (both wet weights) while the highest value recorded in literature is 640 g/dm^2 of Mussels growing in 21 weeks in the salt water intake tunnels of a power-house at Lynn, Massachusets (47).

Ten harbours from western Liguria (also little ones) (37) and seven stations with different types and degrees of pollution in the Genoa harbour were chosen for an evaluation of the correlation between hydrological parameters, pollution and distribution of fouling organisms during a one year survey (fig. 3). In particular the last seven stations, by means of fouling (species settlement period, growth rates, mortality) and physico-chemical parameters (particularly: temperature, pH, dissolved oxygen, salinity, Nitrogen Ammonia, Nitrogen Nitrite, Nitrogen Nitrate, Phosphate, Total iron, Anionic surfactants) have been characterised as follows (21) (26) (31) (32) (33) (34) (35) (38):

Station 1: high content of Nitrogen Ammonia, Nitrogen Nitrate, Phosphate, high turbidity, high surfactants concentration (0,84 ppm), low dissolved Oxygen, fluctuation in pH and Salinity. Minimum of sessile fouling settlement Hydroides elegans, Ciona intestinalis, Balanus amphitrite only on monthly panels, however some Algae (especially Bryopsis plumosa and Enteromorpha spp.)

can resist more than one month and grow vigorously. Within the black slime and mud on the panels, many individuals are of the Polychaetes: Staurocephalus rudolfii Podarke pallida (probably Capitella capitata) and of the Crustacean Nebalia bipes are living.

Station 2: eutrophic waters but less than those of the first station. Ciona intestinalis, Hydroides elegans, Bugula stolonifera are dominant organisms and settle through the year contrary to other stations. A peculiar thing is the heavy presence of the Isopode Sferoma serratum which covers all intertidal substrata (in the Genoa harbour the tide does not exceed 30 cm.).

Station 3: this is the control station, being the best known, the less polluted and the richest as species but not as individuals of Algae and animals.

Station 4: similar to the last one, but with more Nitrogen Nitrate content and shallower.

Station 5: zone with high turbulence and water temperature (over 20°C through the year). Dominant are Ulva, B. amphitrite, Hydroides elegans. Also very common is a small Attinian: Diadomene luciae.

Station 6: in front of the steel-works; high concentration of Iron (up to 7698 µg), Nitrogen Ammonia, low salinity which here reaches its lowest value (28,9 °/$_{oo}$). After the first station this one is the poorest in fouling.

Station 7: polluted by oil and surfactants. Complete absence of intertidal macroorganisms.

Investigations were carried out also on the influence of the substratum pH (13) (48) against settlement and on the behaviour of fouling upon several metal panels (12) (copper, zinc, iron, steel, inox, aluminium) in long and short term experiences.

More and more important and current in Italy too, are the problems concerned with the prevention of fouling in pipes and tunnels because there is an increasing tendency for large industrial installations to be situated on the coast, using seawater as a coolant.

As well-known, (49) (50) such installations are susceptible to heavy marine fouling growing in the cooling systems especially when the intake is in the harbour or other eutrophic water as happened for two (Genoa and La Spezia) out of three electric power stations located in Liguria. For several years we have examined the fouling in the intake tunnels of those two power stations and we have investigated the common antifouling systems with the aim of suggesting the best one for the new power station which was being built in the Vado Ligure bay.

Mussels, Serpulids and Barnacles are by far the most troublesome fouling animals in Ligurian intakes; Serpulids form a peculiar dominant community (30). Such a community of chlorinated water, already known from literature (51)(52), reaches 35 cm thickness in one year and 683 g/dm^2 of wet weight and 258 g/dm^2 of dry weight when the intermittent schedule of chlorination is not good.

Special attention was given to prevention systems based on chlorination and on speed of water flow because of being more effective and less noxious from the pcint of view of pollution control.

In fact in the first method, very little chlorine is discharged to the sea; chlorine and its products are quickly absorbed and active chlorine rapidly disappears from the water. In the second system, the best, no substance is added to the sea water which flows with high speed.

By means of a small experimental pilot plant sited on a pier in Genoa harbour

it was seen that 0,3 ppm of continuous Chlorine (sodium hypochlorite) supply was sufficient to prevent settlement; for killing adult Serpulids (Hydroides and Serpula) in one hour more than 600 ppm are required(38) (53).
So the ineffectiveness of chlorination in some of the Ligurian pipes is due to a bad chlorination schedule and to the shape of intake constructions, in fact the wrongly constructed tunnels have many corners and contain areas where the average speed of flow and renewal of water is low.
These results which agree with literature data (49) (50) were confirmed in a new industrial plant.
The results obtained on fouling prevention by speed of water flow are even more interesting and surprising.
By experimental apparatus (a rectangular tube with three internal sections 300 x 40 mm, 250 x 40 mm, 200 x 40 mm, completely immersed in the sea water and with the pump to the end of the canal containing asbestos panels - size 1000 x 318 x 3 mm -, hydraulically smooth) limiting velocities of water flow for settlement of principal fouling organisms were determined (39), observing settled individuals and not the behaviour of larvae as Prof. Crisp has done (54). Ascidians and Bryozoans in our experimental conditions cannot settle at currents higher than 0,4 m/sec. while Serpulids (Hydroides elegans and Serpula concharum) settle until 0,5 - 0,6 m/sec.
Barnacles (B. amphitrite being the most important species) are able to settle on the panels exposed to a water flow until about 1m/sec.
Really, as pointed out by Crisp (54) (55), the important dynamic feature of water flow relative to settlement is likely to be the velocity gradient, or rate of shear, at the surface rather than the stream velocity within the body of the fluid.
Our colleagues (56), by mathematical and hydrodynamic study of the distribution of velocities within the boundary layer, have been successful in finding a correlation between data obtained with our experimental equipment and those of any other conduit or pipe if the surfaces are smooth and flow with uniform turbulence.
These results had an important confirmation in a new industrial plant built following our advice.
They (56) have found also that, at the same Reynolds number, an increase of fifty per cent in the water flow velocity rises the pressure able to prevent attachment of the cypris by five times.
With the same equipment we have investigated (39) the influence of water current on the growth of fouling organisms which settled on panels before the experiment was begun.
Preliminary results show that Serpulids stop their growth when the velocity of the water current is higher than 2 m/sec.
The growth of settled Barnacles, when they are submitted to a speed of 2, 2,5 ; 3 m/sec, decreases respectively to one half, a quarter and almost completely stops, in comparison with growth of control panel Barnacles.
Though this report is, of course a summarizing and schematic one, we hope we have given a sufficient idea of the research developed in Italy with the aim of contributing to a greater knowledge of fouling problems, also from the point of view of geographical and regional differences in composition and behaviour of world fouling, necessary knowledge for efficient antifouling systems use.

Acknowledgements - We wish to thank for technical assistance: Mr. Giorgio Alabiso, Mrs. Rosa Maria Cannoni and Miss Laura Scotti.

REFERENCES

1. W. NUMANN and K. BETH, Hidrobiol - Instambul (B) 3, 1, 1 (1955).
2. P. FRANCO, Ric. Sci. 33, II-B, 35 (1964).
3. G. RELINI, A. BARBARO and FRANCESCON, Atti Ist. Veneto Sc. Lett. Arti 130, (1972).
4. G. RELINI, A. FRANCESCON and A. BARBARO, Atti Ist. Veneto Sc. Lett. Arti 130, (1972).
5. E. MOR, L'Economia Genovese e la Camera di Commercio negli anni 1955 e 1956, 282, (1957).
6. E. MOR, Hydrobiological and biological conditions in Testing Stations in Europe, Publ. 13425 - O.C.D.E. - (1961).
7. G. RELINI, Doriana 3, 123, 1 (1962).
8. G. RELINI, Arch. Oceanogr. Limn. 13, 2, 281 (1964).
9. G. RELINI, Ann. mus. Civ. St. Nat. Genova 74, 397 (1964).
10. G. RELINI, Natura 57, 136 (1966).
11. G. RELINI, Boll. Zool., 33, 179 (1966).
12. G. RELINI, Boll. Zool., 34, 165 (1967).
13. G. RELINI, Boll. Zool., 38, 349 (1968).
14. G. RELINI, Boll. Mus. Istit. Biol. Univ. Genova 36, 236, 23 (1968).
15. G. RELINI, Boll. Mus. Istit. Biol. Univ. Genova 36, 247, 185 (1968).
16. G. RELINI and E. GIORDANO, Natura (Milano) 60, 4, 251 (1969).
17. G. RELINI and L. RELINI ORSI, Publ. Staz. Zool. Napoli 37, Suppl. 2, 327 (1969).
18. G. RELINI, Publ. Staz. Zool. Napoli 37, Suppl. 2, 311 (1969).
19. G. RELINI and S. GERACI, Publ. Staz. Zool. Napoli 37, Suppl. 2, 317 (1969).
20. G. RELINI, Arch. Bot. Biogeogr. Ital. 14, 4, 168 (1969).
21. G. RELINI, G. DABINI OLIVA and L. FERRETTI, Rev. Inter. Oceanogr. Med. 17, 189 (1969).
22. G. RELINI and G. BAZZICALUPO, Boll. Zool. 36 (1969).
23. G. RELINI, G. BAZZICALUPO and M. MONTANARI, Pubbl. Staz. Zool. Napoli 38, Suppl. 1 (1970).
24. S. GERACI and G. RELINI, Pubbl. Staz. Zool. Napoli 38, Suppl. 1, (1970).
25. D. RAVANO and G. RELINI, Pubbl. Staz. Zool. Napoli 38, Suppl. 1 (1970).
26. G. RELINI, Boll. Zool. 37, 363 (1970).
27. G. RELINI, Rapp. Proc. Verb. C.I.E.S.M. (in press) (1970).
28. S. GERACI and G. RELINI, Boll. Mus. Istit. Biol. Univ. Genova 38, 266, 103 (1970).
29. G. RELINI and D. RAVANO, Atti Soc. Ital. Nat. Mus. Civ. St. Nat. Milano, 112, 3, 301 (1971).
30. G. RELINI, Atti del 1° Simposio Nazionale sulla Conservazione della natura Cacucci, Bari (Italy) - 105 (1971).
31. E. MOR, E. SESSI and G. RELINI, Pubbl. Staz. Zool. Napoli 38, Suppl. 1 (1971).
32. M. MONTANARI and G. RELINI, Pubbl. Staz. Zool. Napoli 38, Suppl. 1 (1971).
33. S. GERACI and G. RELINI, Pubbl. Staz. Zool. Napoli 38, Suppl. 1 (1971).
34. G. ROSSI, G. BAZZICALUPO and G. RELINI, Pubbl. Staz. Zool. Napoli 38, Suppl. 1 (1971).
35. G. RELINI and L. RELINI ORSI, Pubbl. Staz. Zool. Napoli 38, Suppl. 1 (1971).
36. G. RELINI and M. SARA', 6th European Symposium on Marine Biology, Talassia Yugoslavica (in press) (1971).

37. G. RELINI and L. RELINI ORSI, 6th European Symposium on Marine Biology, Boll. Mus. Istit. Biol. Univ. Genova, 39 (1971).
38. G. RELINI, G. DABINI OLIVA and M. MONTANARI, Atti del 2° Simposio Nazionale sulla conservazione della natura - Cacucci, Bari (Italy) - (1972).
39. G. RELINI and G. ROSSI, Pubbl. Staz. Zool. Napoli (in press) (1972).
40. M. MONTANARI and G. RELINI, Pubbl. Staz. Zool. Napoli (in press) (1972).
41. J. R. DE PALMA, Informal manoscript Report O.57.63 (Unpublished Manuscript) Marine Sciences Department - U.S. Naval Oceanographic Office (1963).
42. E. TARAMELLI and C. CHIMENZ, Rend. Acc. Naz. XL - IV, XVI, 1 (1965).
43. E. TARAMELLI RIVOSECCHI and C.CHIMENZ GUSSO, Rend.Acc. Naz. XL, IV, XVIII, 1 (1968).
44. E. TARAMELLI RIVOSECCHI and C. CHIMENZ GUSSO, Boll. Zool., XXXV, 350 (1968).
45. C. CHIMENZ GUSSO and E. TARAMELLI RIVOSECCHI, Rend. Acc. Naz. XL, IV,20, 1 (1970).
46. D. BELLAN - SANTINI, Téthys, 2, 2, 357 (1970).
47. A. C. REDFIELD and E. S. DEEVY Jr., Marine Fouling and its prevention, (3rd Ed.), Chap. 6, 77, U.S. Naval Institute, Annapolis, Maryland (1967).
48. E. MOR, 2nd International Congress on Marine Corrosion and Fouling, (Athens), 445 (1968).
49. A. C. REDFIELD and L. W. HUTCHINS, Marine Fouling and its prevention, (3rd Ed.) Chap. 1 - U.S. Naval Institute, Annapolis, Maryland - (1967).
50. N. HOLMES, Mar. Poll. Bull. 1 (NS) (7), 105 (1970).
51. P. PARENZAN, Riv. Chimico-Sanitaria 3, 1, 3 (1965).
52. H. ZIBROWIUS and G. BELLAN, Téthys, 1, 2, 375 (1969).
53. S. GERACI and V. ROMAIRONE, Pubbl. Staz. Zool. Napoli (in press) (1972).
54. D. J. CRISP, J. Expl. Biol. 32, 569 (1955).
55. H. BARNES, Adhesion in Biological Systems Chap. 5, 89, Academic Press, London, New York (1970).
56. A. MOLLICA and A. TREVIS, L'Energia Elettrica (in press) (1972).

Discussion

G.E. Sechler asked for particulars of the physical and chemical parameters characterizing a "clean" intake pipe. G. Relini replied that the intakes were completely filled with water, and that settlement was prevented solely by the speed of water movement - about 2 meters per second through the pipe - and not by chemical treatment of the surface, though it was important that the walls were smooth. J.S. Ryland asked for a further breakdown of flow velocities, since it was velocity at the surface and not mean flow that was important. G. Relini replied that a mathematical treatment of flow rates in the experimental apparatus and in the intake pipe would be published shortly by some of his colleagues.

A speaker commented that intake velocities greater than 0.5 meters per second usually resulted in fish being forced against the screens and killed; but it was then pointed out that a funnel-shaped intake would combine a relatively narrow pipe, having a high water velocity, with a large screen through which the water flowed slowly enough not to kill fish. Another possibility mentioned was to have the screen set at an angle to the flow, rather than perpendicular to it, so that fish would not be trapped.

K.C. Marshall pointed out that the control referred to by G. Relini was of macrofouling. Even in a high velocity pipeline microbial fouling occurs and will decrease the smoothness of the surface. In hydroelectric pipelines micro-organisms oxidize manganese and deposit it on the surface, and the roughness created causes turbulence troubles.

TABLE 1

Vertical distribution of BRIOZOA settlement on monthly panels from 1966 to 1971

Depths	Bugula neritina		Bugula stolonifera		Bugula flabellata		Schizoporella errata		Watersipora subovoidea		Total
	%	n°	%	n°	%	n°	%	n°	%	n°	
- 0,1 m	33,0	309	15,6	203	1,4	5	1,1	18	3,5	46	581
- 1 m	42,6	455	17,0	221	2,0	7	7,7	124	13,4	177	984
- 5 m	6,3	59	11,3	147	5,7	20	14,0	225	11,4	150	601
- 9 m	6,3	59	17,7	230	37,4	130	20,4	329	32,6	430	1178
-14 m	5,1	48	34,4	448	40,3	140	37,8	608	27,1	357	1601
-16 m	0,5	5	3,8	50	12,9	45	18,7	301	12,0	157	558
Total		935		1299		347		1605		1317	5503

The panel area was about 1200 cm^2

Vertical distribution of total BARNACLES settlement from 1965 to 1971.

Depths	B. AMPHITRITE		B. EBURNEUS		B. TRIGONUS		B. PERFORATUS		Total
	%	n°	%	n°	%	n°	%	n°	
- 0,1 m	7,32	4987	1,16	174	0,62	20	11,41	84	5265
- 1 m	17,55	11947	9,56	1433	1,00	32	31,11	229	13641
- 5 m	28,61	19479	14,30	2143	5,05	161	24,59	181	21964
- 9 m	25,58	17414	24,60	3685	10,45	333	16,98	124	21557
-14 m	15,29	10413	33,13	4963	28,72	915	13,72	101	16392
-16 m	5,61	3821	17,21	2579	54,12	1724	2,17	16	8140
Total		68061		14977		3185		736	86959
		78,26		17,22		3,66		0,8	

One dm^2/ panel was considered

ITALIAN LOCALITIES OF FOULING STUDIES



● Harbours and lagoon ✖ off shore

Fig. 1

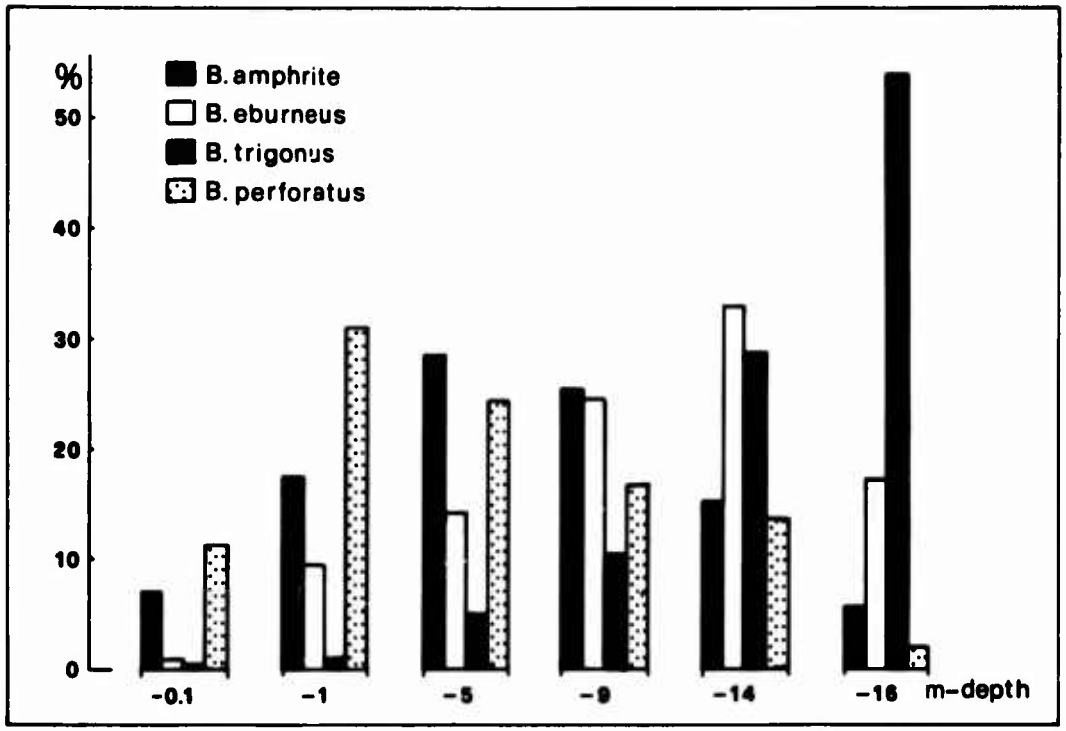
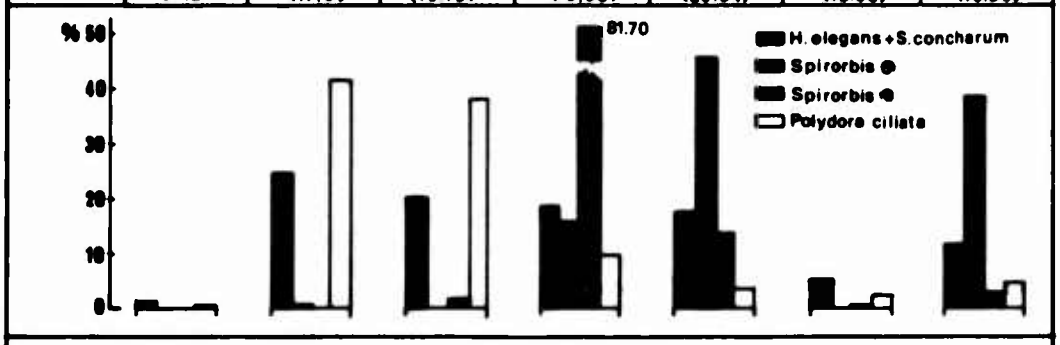


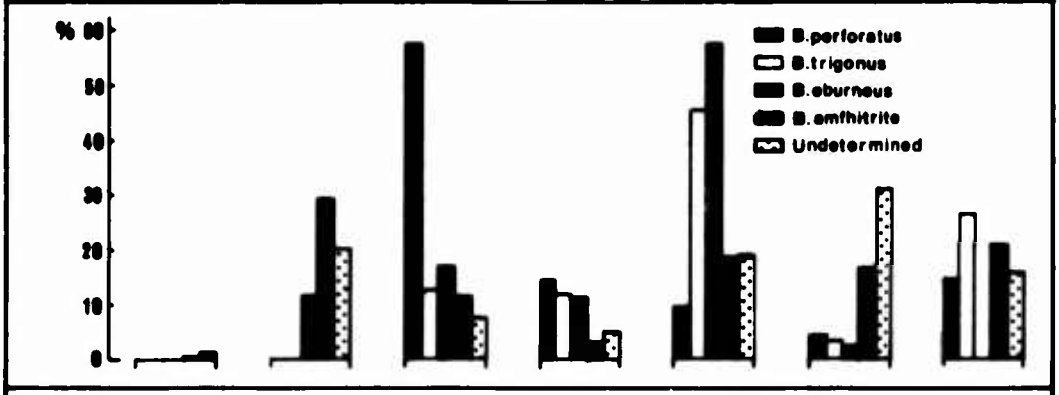
Fig. 2 - Per cent distribution of Barnacles settlement at six depths from August 1955 to December 1971 in the Genoa harbour.

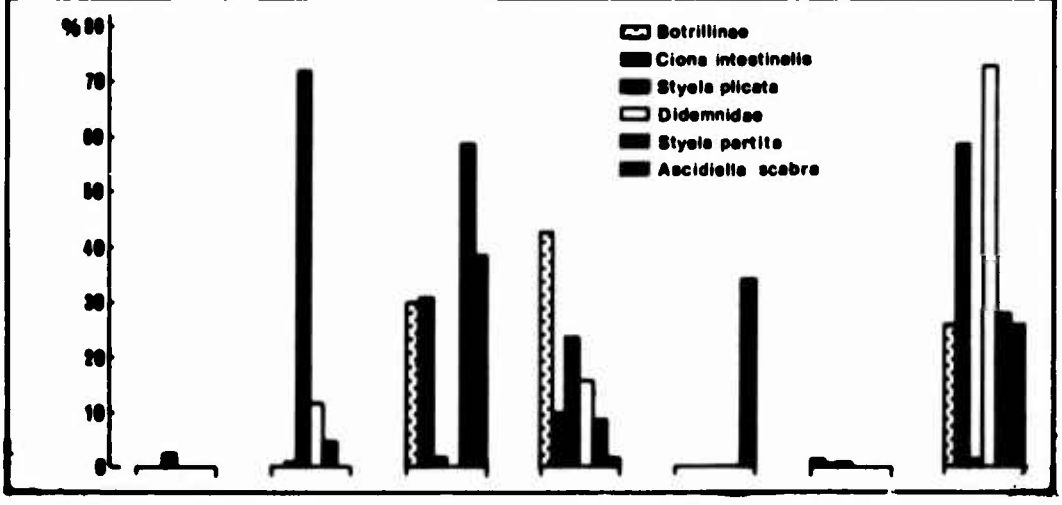
Fig. 3 - (please turn over)

Distribution of the Ascidians, Barnacles and Polichaetes in seven stations of Genoa harbour differently polluted.
For the chemical and physical parameters are reported minimum maximum and mean (in brackets) values of 24 measurements made in one year.

	1	2	3	4	5	6	7
$N\text{-}NH_4$	95 - 1500	83-800	0-400	0-300	0-325	81-1500	0-370
$N\text{-}NO_3$	35.5 - 321 (116.29)	26 - 247 (97.18)	14 - 149 (75.62)	42 - 345 (120.04)	3 - 446 (84.28)	27 - 353 (100.82)	12 - 293 (76.69)
$P\text{-}PO_4$	58 - 313 (179.88)	9.3 - 283 (122.8)	28.5 - 88.6 (57.44)	17 - 144 (73.68)	17 - 75 (45.93)	16 - 134 (42.17	19.2 - 119 (46.13)
O_2 cc/l	0 - 4.21 (2.00)	1.6 - 4.4 (2.9)	3.8 - 6.3 (4.75)	3 - 6.4 (4.45)	3.7 - 5.6 (4.63)	2.8 - 5.9 (4.44)	2.9 - 8.1 (4.91)
t°C	11.5 - 23.5 (17.24)	11.6 - 23.6 (17.9)	11.9 - 25.9 (18.15)	11.7 - 26 (18,06)	20 - 31 (25.34)	12 - 25 (18.56)	11 - 26.9 (18.39)







Metabolism of Mercury Compounds by Bacteria in Chesapeake Bay

J. D. Nelson, Jr. and R. R. Colwell

Dept. of Microbiology
University of Maryland
College Park, Maryland 20742

Biological transformations of mercury in the environment have been identified, but neither the key agents nor the exact processes are well understood. Mobilization of mercury, as a part of the mercury "cycle" in nature, has been given attention because of an increasing mercury load in the environment with resultant hazards to human health, derived in part from microbial activity.

Mercury resistant bacteria isolated from Chesapeake Bay were capable of metabolizing phenylmercuric acetate (PMA) with the production of elemental mercury. The Pseudomonas spp. isolated were resistant to mercury compounds in general and were capable of adaptation to high levels of resistance to specific mercury compounds. The process of biomethylation of inorganic mercury and the observed "reductive decomposition" of organo mercury by mercury resistant marine bacteria may be responsible in part for mercury mobilization and subsequent detoxification of mercury polluted environments, as well as atmospheric transport of mercury.

The decomposition of PMA by a Pseudomonas species was found to be dependant upon adaptation to PMA and was magnesium ion dependant. From the pattern of PMA uptake by cells and effects of inhibitors of oxidative phosphorylation on the PMA metabolic process, it was concluded that degradation of PMA takes place on the cell surface, with production of predominantly inorganic volatile species of mercury.

KEY WORDS: mercury metabolism, PMA decomposition, bacterial mobilization of mercury, Chesapeake Bay and mercury

INTRODUCTION

Mercury in the aquatic environment is transformed by a series of reactions into highly toxic and persistent alkylated forms which accumulate in higher animals and plants (1,2,3)[1]. Participation of bacteria in these events has been documented (4)[1]. The demonstration of reductive decomposition of both inorganic and organic mercury compounds to elemental mercury by mercury resistant bacteria suggests that the aerobic and facultatively

[1]The numbers in parentheses refer to the list of references at the end of this paper.

anaerobic bacteria may be influential in the mobilization of environmental mercury (5,6,7)[1]. Preliminary studies have shown the phenomenon to be inducible (8)[1], and transferable from one cell to another in the form of DNA information (7,8,9)[1].

The investigation of the metabolism of mercury by aerobic, heterotrophic, mercury resistant bacteria has comprised a part of our study of the overall mercury cycling by bacteria in Chesapeake Bay. We have observed a correlation between numbers of mercury resistant bacteria, 60% of which were Pseudomonas species, and environmental levels of mercury (10). Thus, we present in this report the results of our investigation of the mechanisms of resistance and metabolism by a group of Chesapeake Bay bacterial cultures.

MATERIALS AND METHODS

Chemicals. All inorganic chemicals were reagent grade. Phenylmercuric acetate (PMA), methyl mercuric chloride (MeHgCl) and $HgCl_2$ were obtained from Pfaltz and Bauer, Inc., N. Y. Stock solutions of organo mercury in ethanol or $HgCl_2$ in water were made fresh before use. ^{203}Hg labeled PMA in 0.01 M acetic acid was purchased from New England Nuclear Corp.

Growth of Bacteria. A basal medium for the growth of mercury resistant bacteria isolated from Chesapeake Bay consisted of 2.0 gm of glucose, 5.0 gm of Difco (Difco Laboratories, Detroit, Michigan) casamino acids, and 1.0 gm of Difco yeast extract per liter of "three salts solution" containing 10.0 gm NaCl, 2.26 gm $MgCl_2 \cdot 6 H_2O$ and 0.3 gm KCl. The broth was adjusted to pH 7.3 and autoclaved at 121 C for 15 min. A solid medium for enumeration of bacteria and stock culture maintenance was prepared by adding 20.0 gm of Difco agar per liter of broth. Mercury agar was prepared by adding 1000-fold concentrated solutions of PMA or $HgCl_2$ to sterile, molten agar and by spreading plates of solidified agar with MeHgCl. Plates were incubated in darkness at 25 C and liquid cultures were incubated in darkness at 20 C in flasks with aeration. Growth in broth was monitored turbidimetrically with a Klett Sommerson Colorimeter.

Inocula of Pseudomonas 244 for PMA metabolism experiments were prepared by transfer from stock cultures on PMA-containing slants to broth containing 6 ppm PMA and incubating for 24 hours at 25 C. Quantities of PMA-induced cells for resting cell studies were prepared by inoculating the 24 h. broth cultures into 6 ppm PMA containing broth at the rate of 20 ml/100 ml fresh broth and incubating for 1 h. The culture was then chilled, and the cells were centrifuged out of the broth, washed two times with chilled three salts solution, and stored chilled as a suspension in three salts solution until used.

Radioisotope Experiments. Sufficient aqueous ^{203}Hg-labeled PMA was added to three salts or broth to give a final concentration of 6.08 ppm. Samples of 0.1 ml were removed for assay of radioactivity by direct addition to 10 ml of scintillation cocktail consisting of napthalene, 8.23%; PPO, 1.02%; and POPOP, 0.051% in a solution of toluene, 1,4 dioxane, and ethylene glycol monoethyl ether (1:3:3). Cell bound activity was accessed by rapidly filtering 1.0 ml of suspension through a 0.45 micron pore size membrane filter (Millipore Filter Corp., Bedford, Mass.) and washing with two 1.0 ml volumes of three salts solution held at room temperature. For resting cell experiments, labeled PMA was added to pH 7.0 buffered three

[1]The numbers in parentheses refer to the list of references at the end of this paper.

salts containing cells in a total volume 10 ml 5 min. after the start of incubation. Incubation was at 25 C with aeration provided by a magnetic stirrer. A cell density of approximately 0.1 mg dry wt. of freshly grown cells/ml was used in all such experiments. The efficiency of liquid scintillation counting was routinely determined by the channels ratio method.

RESULTS AND DISCUSSION

Properties of Mercury Resistant Isolates. Pure bacterial cultures for study were obtained from routine platings of samples of water and sediment on a solid growth medium containing 6 ppm of $HgCl_2$. Two hundred forty-nine freshly isolated cultures were tested for resistance to a series of types and concentrations of mercury compounds by replica plating. The results (Table 1) indicate that the acquisition of resistance to a single mercury compound may confer resistance to mercury-containing compounds in general.

Resistance to mercury was found to decrease in cultures after several transfers in mercury free media. To investigate resistance as an adaptive phenomenon, thirty of the most resistant cultures were grown in the presence and absence of mercury compounds and then tested for resistance. The results are summarized in Table 2. Growth in the presence of mercury clearly enhanced the resistance of most of the cultures.

A single culture, Pseudomonas 244, was selected for further investigation on the basis of its resemblance to the most commonly isolated group of mercury resistant bacteria (10)[1]. It produces a green fluorescent pigment, which facilitated identification and does not produce H_2S from organic or inorganic sulfur containing compounds. When grown in the absence of PMA, the organism was found to be capable of growth on agar medium containing 3 ppm, but not 24 ppm PMA. However, after growth in a liquid medium containing 6 ppm PMA, the organism grew on 24 ppm PMA agar. Figure 1 shows the comparative kinetics of the gain and loss of resistance to 24 ppm of PMA. A culture previously grown in 6 ppm of PMA medium was inoculated into media with and without 6 ppm PMA which were then incubated with aeration. Cells resistant to 24 ppm PMA increased 200-fold in PMA-containing broth and decreased 30-fold in the PMA-free broth. In either case there was a reproducible transient peak in resistance prior to onset of growth. The experiment was repeated with 5 ppm $HgCl_2$ replacing PMA in the mercury-containing flask. Transient peaks of 24 ppm PMA resistance were observed, but, in contrast, both cultures showed a net decrease in resistance to PMA during the same period. These results and the observations of other investigators suggest that resistance to PMA and other mercury compounds is an inducible response to mercury exposure (8)[1].

When compared with growing cells, buffer suspensions of non-proliferating cells were induced after a longer period of time and were able to maintain their level of resistance to 24 ppm PMA for at least 10 h. in the absence of inducers.

PMA Metabolism. To ascertain the fate of PMA in PMA-resistant cultures, the above experiment was repeated using Pseudomonas 244 grown in ^{203}Hg-labeled PMA media. Duplicate flasks, with and without inoculation, were assayed for cell bound and total radioactivity at hourly intervals (Fig. 2). Samples of culture were acidified to pH 1 with concentrated HCl and extracted with benzene. The extracts were chromatographed on silica

[1] The numbers in parentheses refer to the list of references at the end of this paper.

gel G, developed with petroleum ether: diethyl ether (70:30) (4)[1], and analyzed by autoradiography. During the lag in growth, in which resistance to 24 ppm PMA increased (Fig. 1), a net loss of 39% of the label from the suspension and an accumulation of 4% of the label in the cells occurred. Benzene-extractable PMA correspondingly decreased with no new labeled compounds appearing. The uninoculated control flask showed no significant decreases in activity during the experimental time period. Direct analysis of the vapor phase has shown that the mercury lost from the medium is, at least in part, in the elemental state (W. Iverson and F. Brinckman, personal communication). The concomitant production of benzene and mercury from PMA by a Pseudomonas species from soil has been reported (5)[1]. However, we have not been able to detect benzene in the vapor phase. When ^{203}Hg-labeled cells were subsequently placed in PMA-free broth, further loss of label occurred.

The site of PMA binding was investigated using log phase cells of Pseudomonas 244 labeled for 2/3 of a generation time. The activities of crude sub-cellular fractions obtained by differential centrifugation were assayed after breakage using a French Pressure Cell. Approximately 78% of the activity in the cell free extract was recoverable in a particulate fraction sedimenting at 127,000 X g in 1 h. A fraction sedimentable at 35,000 X g in 15 min., bound nearly 85% of the 127,000 X g pellet activity and was enriched in cell wall material. The latter contained relatively little NADH oxidase, but most of the 2-Keto-3 deoxyoctulosonic acid (KDO), a cell wall specific sugar.

The mechanism of PMA resistance most likely involves the uptake of PMA followed by induction of the enzyme(s) necessary for mercury reduction. Bound inducer is lost from growing cells, and in the absence of a source for replenishment, the levels of enzymes decrease.

Reductive decomposition of mercury compounds by species of Pseudomonas (5)[1] and strains of Escherichia coli (6,7)[1] have been reported. A spectrum of mercury resistant bacterial genera isolated from the Bay were tested for ability to decompose PMA, using a radio-assay (Table 3). Each culture was grown in 0.3 ppm PMA broth, washed and inoculated into a buffered three salts solution as described. The results, though qualitative, indicate that PMA metabolic ability may occur in a number of genera. Several of the species tested did not volatilize significant quantities of Hg. Resistance of these cultures may arise from an unsuspected pathway of mercury metabolism or the induced or fortuitous production of sulfhydryl compounds resulting in mercury mercaptide formation.

PMA Metabolism by Resting Cells. The study of PMA metabolism was simplified by using non-proliferating cells of Pseudomonas 244 in aerated, pH 7.0 buffered three salts solution. Volatilization of Hg label also occurred under these conditions in a reaction which is dependent upon cell concentration. A standard cell density of ca. 0.1 mg dry weight/ml was used which was in the range of cell densities directly proportional to activity. This concentration of cells typically evolved 90% of the label within 2 h. at 25 C in an aerated system.

The comparative kinetics of PMA metabolism and uptake by induced and non-induced cells is presented in Fig. 3. The cells were incubated in broth with and without 6 ppm of PMA to the same stage of growth and inoculated in equal amounts into buffered three salts containing 6.08 ppm of

[1]The numbers in parentheses refer to the list of references at the end of this paper.

labeled PMA. In both cultures there was a rapid uptake of PMA occurring within minutes of the addition of PMA. Label was lost from the induced culture at a rate which was uniformly linear for the first 10 min. Aeration of the mixture was necessary both for uniform sampling and for maximization of the rate of reaction. A culture correspondingly incubated without aeration evolves label at only 22% of the initial rate of the former. The noninduced culture did not evolve detectable amounts of label but accumulated considerably more label than the adapted culture. Increased net binding, presumably related to the inability of the cells to metabolize PMA, was also observed subsequently when metabolically-poisoned or, otherwise, non-metabolizing cells were used. Thus, PMA resistance and metabolism were found to be related and are presumably inducible phenomena. Preliminary experiments using the above experimental protocol indicate that the pH optimum at 25 C is between 6.0 and 7.0, and the Km and V max at pH 7.0 and 25 C are approximately 7.0 ppm and 5 µg/min/mg dry wt. of cells, respectively.

Effect of Salts and Inhibitors on PMA Metabolism. Chesapeake Bay is a dynamic habitat in which extensive seasonal fluctuations in salinity occur. The effect of salinity upon PMA metabolism by Pseudomonas 244 was tested by varying the total concentration of salts in the three salts solution containing NaCl, $MgCl_2$ and KCl. Cells placed in three salts (33% sea water strength) buffered with 0.01 M tris (hydroxymethyl) aminomethane (TRIS)-hydrochloride (pH 7.0) were as active as those in a salts solution at 82% of the strength of sea water (Table 4). However, when a solution 8.2% the strength of sea water was used, the cells were inactive. The inhibition was partially due to decreased salt concentration and to TRIS buffer, for 8.2% salts gave partial activity in the absence of TRIS. When 0.01 M phosphate buffered (pH 7.0) solutions of NaCl, $MgCl_2$ and KCl of equal ionic strength were tested, it was found that Mg^{2+} ion, alone, satisfied the ionic requirement for activity. In phosphate buffered suspensions, concentrations of Mg^{2+} below approximately 10 mM resulted in decreased activity, and a minimum of between 0.11 and 1.2 mM was necessary for detectable activity. Similarly, a Mg^{2+} requirement has been demonstrated for the volatilization of mercury from $HgCl_2$ by cell-free extracts of a mercury resistant strain of Escherichia coli (8)[1]. We have observed that disruption of our cells with a French Pressure Cell destroys activity immediately, even in the presence of various sulfhydroxyl protective agents. This observation and the Mg^{2+} requirement are symptomatic of a structural requirement for mercury reduction. The distribution of bound mercury suggests that mercury attaches to the cell envelope. It is now necessary to compare the cellular structures of induced and non-induced cultures to prove the existence of a specific mercury metabolizing component. However, preliminary investigation of the gross extractable lipid composition and the morphology in thin sections has evidenced no differences in this strain (Wan, Nelson, Colwell, Unpublished Data).

Several inhibitors of oxidative phosphorylation were also tested in the system to see if active transport is essential for the metabolism of PMA (Table 4). Potassium cyanide caused a considerable inhibition of the ititial rate, but none of the inhibitors caused more than a 30% net decrease in PMA metabolized after 30 min. However, the partial inhibitions may have resulted from formation of complexes of phenyl mercuric ions with the inhibitors. Cells tested with sodium arsenate and sodium azide bound considerably more label than the control, but the cyanide treated cells bound

---

[1]The numbers in parentheses refer to the list of references at the end of this paper.

less. In conclusion, from these results and the observed kinetics of metabolism and distribution of binding, we believe that PMA metabolism takes place on or near the surface structure of Pseudomonas 244.

The results of the studies reported here and elsewhere (10)[1] indicate clearly that the bacteria found in the water and sediments of Chesapeake Bay are capable of metabolizing mercury and mercury compounds. In situ experiments are in progress to determine whether the processes observed to occur in the laboratory situation operate in nature.

ACKNOWLEDGEMENTS

This work was supported by EPA Contract # R-800647. Analysis of volatile mercury compounds was performed by Drs. F. Brinckman and W. Iverson, National Bureau of Standards, Washington, D. C. 20234.

REFERENCES

1. U. S. DEPT. OF THE INTERIOR, Geological Survey Professional Paper 713, "Mercury in the Environment", U. S. Govt. Printing Office, Washington, D. C. (1970).

2. R. A. Wallace, W. Fulkerson, W. Shults and W. Lyon, "Mercury in the Environment, the Human Element", Oak Ridge National Laboratory (1971).

3. STUDY GROUP ON MERCURY HAZARDS, "Hazards of Mercury Special Report to the Secretary's Pesticide Advisory Committee, Dept. of Health, Education and Welfare", Environ. Res. 4, 1 (1971).

4. J. M. Wood, F. S. Kennedy and C. G. Rosen, Nature 220, 173 (1968).

5. K. Tonomura and T. Kanzaki, Biochim. Biophys. Acta 184, 227 (1969).

6. I. Komura and K. Izaki, J. Biochem. 70, 885 (1971).

7. A. Summers, "Microbial Methylation Reactions and Heavy Metal Toxicity. Plasmid-Borne Mercury Resistance in E. Coli", 72nd Annual Meeting of the American Society for Microbiology, Apr. 23-28 (1972).

8. I. Komura, T. Funaba and K. Izaki, J. Biochem. 70, 895 (1971).

9. R. Novick and C. Roth, J. Bacteriol 95, 1335 (1968).

10. J. D. Nelson, Jr., H. L. McClam and R. R. Colwell, Proc. 8th Annual Conf. Marine Technol. Soc., Washington, D. C. (1972).

11. J. Shewan, W. Hodgkiss and J. Liston, Nature 173, 208 (1954).

[1]The numbers in parentheses refer to the list of references at the end of this paper.

TABLE 1.

Cross Resistance of Bacterial Cultures to Mercury Compounds

Test Compound [a]	Percent of Cultures Resistant					
	Group [b]					
	24 PMA	15 PMA	3 PMA	3 MeHgCl	100 $HgCl_2$	50 $HgCl_2$
24 ppm PMA	--	--	--	27.9	36.4	9.4
15 ppm PMA	--	--	--	90.8	63.6	20.8
3 ppm MeHgCl	85.8	89.6	6.1	--	100.0	29.2
100 ppm $HgCl_2$	28.6	24.1	0.0	25.6	--	--

[a] Each compound was incorporated into a solid growth medium. See Materials and Methods.

[b] Each culture was classified according to the maximum amount of mercury tolerated (ppm).

TABLE 2.

Adaptation to Mercury Resistance[a]

TEST MEDIUM	Before Growth in Hg		After Growth in Hg	
	Medium grown in	% cultures resistant	Medium grown in	% cultures resistant
3 ppm MeHgCl	Control	20	100 ppm HgCl	63
24 ppm PMA	"	3	" " "	77
"	"	7	50 " "	77
"	"	7	3 ppm PMA	73

[a] Total number of cultures tested = 30

TABLE 3.

Survey of PMA Metabolism by
Mercury Resistant Cultures

Culture	Percent radioactivity remaining[a]	
	1 Hour[b]	4 days[c]
Pseudomonas 244[d]	52.0	45.0
Pseudomonas 100[d]	90.4	80.2
Pseudomonas 127[d]	82.6	63.4
Bacillus 72	95.8	67.0
Achromobacter 187	94.8	92.1
Alcaligenes 94	88.3	78.0
Arizona 132	94.6	69.6
Enterobacter 85	92.8	90.3
Vibrio 21	98.2	92.9
Flavobacterium 119	42.7	45.9

[a]Approximately equal quantities of cells were added to pH 7.0-buffered three salts solution containing 0.4 ppm PMA (5.75×10^5 cpm/microgram) and incubated at 25 C.

[b]With aeration.

[c]Stationary.

[d]Pseudomonas strains 244, 100 and 127 = types I, III and IV, respectively (11)[1].

TABLE 4.

Effects of Salts and Inhibitors on
PMA Metabolism by Pseudomonas 244

Experimental Condition	PMA Metabolized (Percent of Control[a])	
	Initial Rate	Net/30 min
82.0% sea water, Tris buffer	99.3	--
8.2% sea water, Tris buffer	15.0	--
8.2% sea water, no buffer	56.1	--
Tris buffer, alone	5.6	--
NaCl, phosphate buffer[b]	26.1	--
KCl, phosphate buffer[b]	0.0	--
$MgCl_2$, phosphate buffer[b]	99.3	--
0.01M KCN[c]	56.6	74.2
0.02M NaN_3[c]	100.0	82.4
0.01M $Na_2HAsO_4 \cdot 7\ H_2O$[c]	72.0	73.5

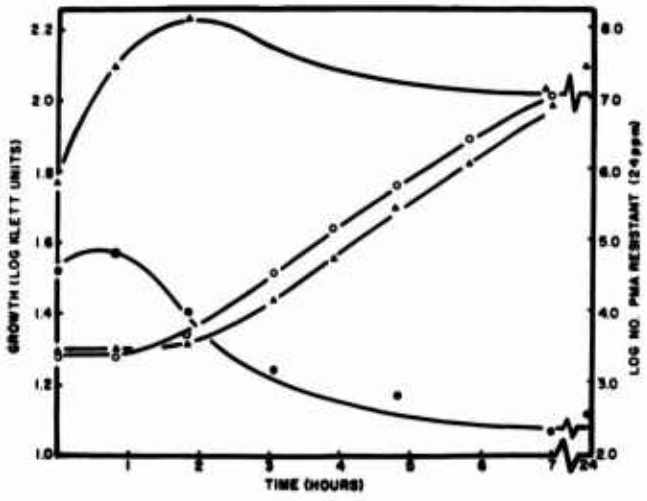
[a]0.01M buffered-"three salts" (pH 7.0) containing 6 ppm PMA and approx. 0.1 gm dry weight of cells/ml, aerated at 25 C.

[b]Concentration equivalent to total ionic strength of "three salts" solution.

[c]Inhibitors incubated with cells 5 min. before reaction started in phosphate-buffered three salts.

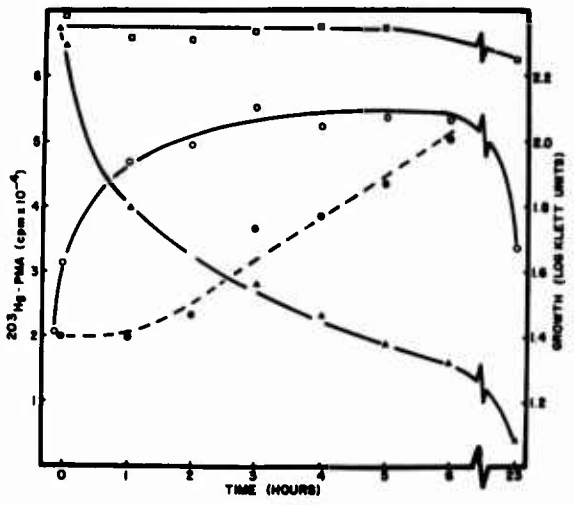
[1]The numbers in parentheses refer to the list of references at the end of this paper.

FIGURE 1.



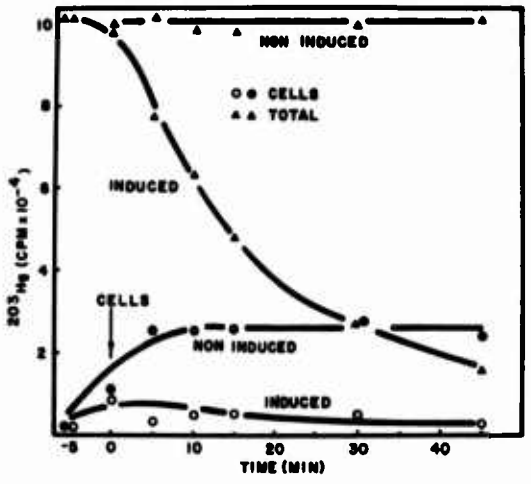
Induction of resistance to PMA by Pseudomonas 244. Broth with (triangles) and without (circles) 6 ppm of PMA was inoculated with cells. Growth was measured turbidimetrically (open symbols), and numbers of cells resistant to 24 ppm of PMA/ml were determined (closed symbols).

FIGURE 2.



Uptake and metabolism of PMA by Pseudomonas 244. Cells were added to broth containing 6.08 ppm of radiolabeled PMA after 5 min. preincubation. Radioactivity in 0.1 ml of cell suspension (△) and in 1.0 ml of cell suspension collected on a membrane filter (○) were determined. 0.1 ml samples of uninoculated broth (□) were also analyzed. Growth was measured turbidimentrically (●).

FIGURE 3.



Uptake and metabolism of PMA by induced and non-induced resting cells of Pseudomonas 244. The reaction was begun when cells were added to the buffered PMA-salts mixture (arrow). 0.1/ml samples of cell suspension were taken at the indicated times.

Discussion

R. F. Acker asked if the formation of filamentous colonies or filamentous cells had been observed as a result of interference with cell division. J. D. Nelson replied that such formations had been looked for but not seen. There are reports in the literature of nickel interfering with cell division, but the authors had not observed this.

The Role of Cellulolytic Bacteria in the Digestive Processes of the Shipworm

Fred A. Rosenberg and Joanne Cutter

Biology Department
Northeastern University
Boston, Massachusetts 02115

Cellulolytic bacteria were isolated from the digestive systems of a number of species of teredine borers. Subsequent investigations, using Teredo navalis, indicated the existence and functioning of two independent cellulase systems in the digestive caecum of the borer; an endogenous caecal cellulase, and a bacterial cellulase. These cellulases differ in several important physical-chemical properties, notably reaction rates and substrate specificity. Markedly enhanced cellulose degradation in the presence of caecal isolated cellulolytic bacteria was shown; and, the requirement for bacterial cellulase in the digestive processes of Teredo navalis was established. The data presented suggests that the bacterial cellulase is the dominating factor in cellulose decomposition and utilization by the borer.

A new concept for the mechanism of cellulose degradation and utilization by the borer is outlined; and two models for the cooperative action of microbial and endogenous cellulases have been proposed.

Key Words: Teredinids, cellulolytic bacteria, bacterial cellulase, borer digestion.

In the past 50 years, a considerable body of evidence has been put forth in support of the presence of cellulases in a number of higher mollusc species. The Teredinids, a family of marine wood boring molluscs, frequently called shipworms, of which Teredo and Bankia are most commonly known, are of particular interest. The Teredinids are exclusively wood boring. Some animals bore into wood for protection only, but the shipworms digest and metabolize the cellulose of the wood into which they bore, exploiting it as a major source of nourishment.

Numerous investigators (1 through 11) have attempted to elucidate the "cellulolytic factor" responsible for the ability of these molluscs to utilize wood as their primary food source.

It has been generally accepted that endogenously produced cellulase, within the tissues of the digestive tract, afforded these molluscs the ability to degrade wood and utilize the cellulose as a nutrient source. However, evidence has been accumulating, which indicates that the presence of gut associated symbiotic bacteria could be an important factor (12, 5,6,13,14, 15). Consequently, the question of whether teredine borers or associated bacteria produce the cellulase responsible for the utilization of wood by the borer has been subjected to considerable investigation.

Additionally, the possibility exists that cellulases produced by both the borer and the gut associated bacteria act in the degradation of cellulose.

The purpose of this investigation was to compare the activity of the two cellulase systems functioning in the digestive caecum of the borer; and to further enumerate some of the properties of the two cellulases, and their methods of isolation (16).

The idea that microorganisms could play a significant role in molluscan digestion has arisen comparatively recently and has yet to be comprehensively treated in the literature.

Boynton and Miller (2) were the first to consider the possibility of cellulose digestion by symbiotic bacteria. However, they dismissed the possibility as they saw no evidence of bacterial action in incubation tubes, and culturing attempts on extracts provided negative

results. Greenfield and Lane (4) also considered the possibility of symbiosis, but could not culture cellulolytic bacteria from fresh tissue homogenates. Liu and Townsley (10) also minimized the possibility of symbiosis because microflora could not be observed in the contents of the caecum using phase contrast microscopy at 980 magnifications.

Saito and Hidaka (13) compared cellulases obtained from isolated bacteria with those obtained from the "liver" of Teredo navalis. They found that cellulose-decomposing bacteria in the intestinal tract of Teredo navalis aid the digestive process by partially digesting the cellulose.

Kadota (14) has reviewed work by a number of investigators concerning the association of cellulose-decomposing bacteria with the teredinids. Cellulolytic bacteria from the digestive organs of Teredo navalis have been successfully cultured in mineral salts media. Cellulase from the bacteria was compared with cellulase from extracts of the digestive diverticula of Teredo navalis. Both were found to decompose regenerated cellulose more easily than native cellulose; wood preparations were attacked in proportion to the degree of delignification.

The objectives of the present investigation were as follows: (a) to determine the presence of cellulolytic bacteria in the digestive system of teredinids; (b) to establish a bacteriological method for the enrichment, cultivation and isolation of cellulolytic bacteria from the digestive organs of Teredo; (c) to compare methodologies for evaluating the presence of cellulolytic activity in either homogenates, or gut associated bacteria, and to report a biochemical method for accurately assessing the degradation of cellulose by either bacterial or endogenous enzymes; (d) to elucidate the role of cellulolytic bacteria in the digestive process of the Teredo; (e) to evaluate the contribution of these bacteria to the cellulose digesting ability of the Teredo; (f) to evaluate the significance of bacterial cellulase activity relative to that of the reported endogenous cellulase; (g) to delineate the source(s) of the cellulase(s) reported to be present in the Teredo; and (h) to propose a functional model of the mechanism by which cellulose is degraded within the digestive system of the Teredo.

Rosenberg and Breiter (15) initially investigated the occurrence and distribution of cellulolytic microorganisms in the digestive system of teredine borers of the species Lyrodus massa (Lamy), Nototeredo knoxi (Bartsch), Teredo furcifera (von Martens) and Teredo malleolus (Turton). Live borers were dissected out of pine boards immersed for varying periods of time in several areas. The stomach, intestine and caecum of the animals was removed, rinsed gently in 95% ethyl alcohol, and the individual organs placed into test tubes containing a sterile minimal salts medium of the following composition:

KNO_3	1.0 g
K_2HPO_4	1.0 g
$CaCl_2$	0.1 g
$FeCl_2$	trace
Artificial sea water	1000 ml (17)

Rectangular pieces of sterilized Whatman No. 1 filter paper were placed into each tube to serve as the sole carbon source. The organs were then gently macerated with a sterile pipette, and the tubes incubated in running sea water of the same temperature as that from which the borers were isolated. Crystalline styles were not incorporated in the studies since there appears to be some evidence of their bacteriolytic activity (18). Browning and eventual shredding of the filter paper at the air-water interphase indicated degradation of the cellulose fibers. Loopsful of the media were gently scraped along the surface of the decomposing filter paper and transferred to plates of Bacto-Marine Agar 2216 E (Difco). These were incubated at 28-30°C. Isolates were streaked onto Marine Agar slants prior to identification.

Finally, all organisms were streaked onto cellulose agar plates, as well as cellulose agar to which either 1% cellobiose or 1% glucose had been added. The composition of the cellulose agar was as follows:

$NaNO_3$	0.5 g
K_2HPO_4	1.0 g

$MgSO_4 \cdot 7H_2O$	0.5 g
$FeSO_4 \cdot 7H_2O$	0.01 g
Powdered cellulose (Sigma)	6.0 g
Bacto-Agar	8.0 g
Lyman and Fleming sea water	1000 ml

These plates were periodically examined for cellulolytic activity, as evidenced by liquefaction or weathering of the medium. Duplicate plates were inoculated without cellulose to determine whether agarolytic bacteria were responsible for liquefaction. No liquefaction occured in the absence of cellulose. Isolates were incubated at 28-30°C.

Fifteen microorganisms, capable of utilizing and digesting filter paper as a sole carbon source were isolated from the intestinal tract of teredine wood borers and from associated marine waters. With the exception of one isolate, all organisms demonstrated cellulose degradation within six weeks on cellulose agar. Four isolates obtained from two different genera of borers as well as from the associated waters exhibit similar characteristics and appear to belong to the genus Cellulomonas.

The information that the gut of Teredo is inhabited by cellulolytic bacteria was indeed gratifying, but merely the knowledge that they are present is insufficient evidence for drawing conclusions as to their importance or relative contribution to their host's digestive processes. It is necessary to demonstrate the dependence of the host on the bacterial population for its utilization of cellulose, and consequently, its survival.

Subsequent studies were performed using borers dissected out of wood collected in Great Bay, New Hampshire and from Nova Scotia. Presently we are working with Bankia setacea obtained from Monterey, California, and Vancouver, B.C. Preliminary experiments show the presence of cellulolytic organisms in caecal extracts of the Bankia.

Several isolation techniques were employed: (a) individual organs were placed into test tubes containing sterile mineral salts medium and a rectangular piece of Whatman #1 filter paper as the sole carbon source; (b) individual organs were placed into test tubes containing 0.6% micro-crystalline cellulose broth. Graying and eventual blackening of the media was indicative of cellulose degradation. (c) Several organs were homogenized in sterile Lyman and Fleming's artificial sea water (17), and the homogenate was streaked directly onto cellulose agar plates (15) modified in that they contained micro-crystalline cellulose and 1% Bacto-agar. All cultures were incubated at 25°C, as this temperature was found to promote optimum growth.

Preparation of the crude caecal homogenate and cellulase extract was done as follows. Caeca were excised from borers. Removal of the caeca was carried out in 10% ethyl alcohol to avoid contamination from bacteria normally found in sea water. The caecal contents were removed by gentle squeezing, and the tissue rinsed serially in alcohol of decreasing strengths to (a) remove contaminating surface bacteria, and (b) to eliminate residual caecal flora.

The collected sterile tissue was homogenized in 30% alcoholic phosphate buffer (4). The homogenate was refrigerated 24-48 hours to allow autolysis to occur. A portion of the homogenate was brought to a total volume of 100 ml by the addition of buffer and Millipore-filtered, using a 0.45 u filter, to collect the crude cellulase extract. To ensure sterility of the extract the filtrate was again filtered using a 0.22 u filter. Crude bacterial cellulase extract was prepared as follows. Cells were collected and washed in deionized water. Washed cells were suspended in 5 ml portions of deionized water and were fractionated by sonification at 20,000 kc/sec for 30 sec. The sonified cells were washed in deionized water and successively filtered through 0.45 u and 0.22 u filters.

Cellulase activity in normal and heat inactivated samples of homogenate and extract was determined by measuring the production of reducing sugar. Reaction mixtures contained cellulose solution and the sample fraction being tested in a ratio of 10:1. All flasks were incubated at 25°C for one week. Reducing sugar was determined daily using the Folin-Malmros method (19). The change in total carbohydrate content was determined for the same time period using the Anthrone method (20). The presence of active cellulase in the bacterial extract was similarly determined.

The optimum pH values for the crude cellulase preparations were compared to that of a commercial cellulase for a pH range from 3.1-8.1. Samples were diluted to a suitable concentration with McIlavine's buffer at various pH values (21). Dilutions were incubated in an equal volume of cellulose solution for 5 hours at 25°C. Reducing sugar was determined using the Folin-Malmros method (19).

To determine thermostability, reaction flasks of each enzyme were incubated at temperatures of 5,18,25,37 and 45°C for 18 hours. Samples were diluted with McIlavine's buffer, adjusted to the optimum pH for the particular cellulase and incubated with an equal volume of cellulose solution for 5 hours at 25°C. The remaining cellulase activities were determined by the Somogyi-Nelson method (22,23).

The saccharifying activity was determined for both crude preparations. Reaction mixtures contained cellulose substrate and the enzyme fraction in equal volume. McIlavine's buffer, at a pH optimal for the activity of the respective cellulase, was added in a volume equal to the total volume of the reaction mixture. Reaction mixtures were incubated at 25°C for four days. Saccharifying activity was determined at 12 hour intervals by measuring increases in glucose production.

To identify the relative specificities of the two crude cellulases, their hydrolytic activity was determined and compared to that of 95% H_2SO_4. Reaction mixtures contained an equal volume of the enzyme fraction and 0.6% micro-crystalline cellulose or 1% cellobiose. Control flasks contained 95% H_2SO_4 and an equal amount of either of the above substrates. All flasks were incubated at 25°C for 48 hours and analyzed for reducing sugar.

The relative enzymatic efficiency of the two cellulase systems was determined, comparatively, using acid hydrolysis. 1 ml of the cellulose solution was subjected to complete acid hydrolysis by heating in 95% H_2SO_4 for 10 minutes. The amount of glucose available for enzymatic hydrolysis was determined by the Folin-Malmros method (19). Calculations were proportional and based on the time interval showing greatest activity.

Detailed results of the individual studies are reported elsewhere (24).

The presence of an active cellulolytic agent in caecal tissue homogenates and extracts, and in the bacterial extract was determined by assaying normal and heat inactivated aliquots of each sample for the production of reducing sugar. Both homogenates and extracts lose their cellulolytic activity upon heating, suggesting denaturation and inactivation of the active component. Thus, in considering the independent activities of the two crude cellulase preparations, it is apparent that both contain active cellulase fraction. The lower activity noted in the endogenous extract can be explained by the fact that the endogenous cellulase is probably tightly bound to the caecal tissue, and was not completely removed upon homogenization and filtration; consequently, all subsequent studies utilized caecal homogenate.

The enzymatic degradation of cellulose was determined by measuring the production of the reducing sugar, glucose, the final hydrolysis product. The Folin-Malmros method (19) was determined to be the most sensitive test for measuring the production of reducing sugars from cellulose degradation, because it is specific for the final degradation product, glucose. The Benedict's Test, used by Harington (1) and other early investigators, also measures reducing sugar production, but it is not specific for glucose. The Somogyi-Nelson Method (22, 23) used by Lane, Greenfield,and Nair, is also specific for glucose; however, an alkaline copper reagent is employed. Strange et al (25) note that copper reagents can interfere with "reductimetric sugar methods" by complexing with various amino acids that might be present, especially cysteine, tyrosine, and tryptophane. Such complex formation causes decreased reduction in the presence of the sugar.

The optimum pH for the saccharifying activity of the two cellulases differs decidedly. The caecal cellulase is optimal at pH 4.6, while the bacterial cellulase exhibits optimum activity at pH 6.6. The observed pH difference is consistent with pH differentials observed by earlier investigators. Greenfield and Lane (4) noted differential pH activity in the "precaecal" and "postcaecal" portions of the gut of T. navalis; activity in the "precaecal" portion was independent of pH, while activity in the "postcaecal" portion exhibited maximal activity between pH 5.6 and pH 6.7. The authors noted that the differential pH activity suggested that more than one enzyme was involved. Kadota (14) also reported pH

differences between a bacterial cellulase and a cellulase from extracts of the digestive diverticula. The pH optimum for the diverticula extract was 5.8, while the bacterial cellulast exhibited optimum activity at pH 6.4 Thus, there appears to be good correlation between the pH activities noted in this investigation and those reported previously. As each enzyme was considered separately, the conclusion became apparent that two cellulases of separate origin were present.

A second activity peak noted for the crude caecal cellulase is thought to represent residual bacterial cellulase in view of its proximity and similarity with the crude bacterial cellulase peak. Kadota (14) reported a similar phenomenon in the whole body extracts of T. navalis, or in mixtures of the diverticula extract and the bacterial cellulase. However, the possibility that the caecal cellulase is a dipolar protein has not been eliminated. Such proteins commonly exhibit two pH optima.

It is also significant to note that the bacterial cellulase has about four times the cellulose-saccharifying activity exhibited by the caecal cellulase and that it remains active and stable 12-24 hours longer than the caecal enzyme. Even after 84 hours, the bacterial cellulase is still active, while the endogenous cellulase has been exhausted.

The comparative activity of the two crude cellulases indicates the rate of bacterial enzymatic hydrolysis to be almost four times that of endogenous enzymatic hydrolysis. When compared with acid hydrolysis, using 95% H_2SO_4, enzymatic hydrolysis by the bacterial cellulast was noted to produce 56% more glucose during exponential activity (about 60 hours) than did enzymatic hydrolysis by the endogenous cellulase.

Insofar as the relative efficiency of the two cellulase systems is concerned the bacterial cellulase was shown to hydrolyze 41.2% of the total amount of glucose available while the caecal cellulase hydrolyzed only 9.2%. This data is consistent with the saccharifying activities and the reaction rates which indicate that cellulose degradation by the bacterial cellulase is almost four times faster than degradation by the endogenous caecal cellulase. Thus, on a purely quantitative basis, the bacterial cellulase is eliciting four times the activity of the caecal cellulase, is producing up to 56% more glucose during exponential growth, and is operating 32% more efficiently than the endogenous caecal cellulase.

It has been previously reported that 80% of the cellulose and 15-56% of the hemicellulose content disappears from wood during its passage through the digestive tract of T. navalis (26). Experimental data obtained in this investigation indicates that such activity could not be attributed solely to an endogenous teredine cellulase, as the activity coefficient, reaction rate, and general efficiency of the system does not allow for such activity. The data obtained suggests a dependence of the borer on bacterial cellulase, as the relative efficiency and much reduced activity of its endogenous cellulase, as compared to the activity of the bacterial cellulase, would not be sufficient to satisfy the nutritional demands of the animal.

Simulated in vivo studies conducted with starved (caecal tissue without contents) and fed (caecum intact with contents) tissue homogenates, under sterile and non-sterile conditions and with the addition of known amounts of caecal isolated cellulolytic bacteria, Cellulomonas sp., confirm the in vitro activity noted for the crude bacterial cellulase, and clearly indicate that the contribution of caecal associated cellulolytic bacteria is to intensify cellulose degradation by the addition of more, or 'symbiotic' bacterial cellulase.

It appears that the borer requires the presence of these cellulolytic bacteria as it is dependent upon the 'symbiotic' bacterial cellulase for sufficient decomposition of wood to justify its utilization as the primary food source. The endogenous caecal cellulase is neither sufficiently active, nor present in large enough quantities to account for the amount of cellulose and hemi-cellulose reported to be removed from wood during its passage through the digestive tract of T. navalis (26).

It thus appears that two independent cellulases are operative in the digestive process of the borer: one of bacterial origin, and one of apparent endogenous origin.

Data presented in Figure 1 and Table 1 suggests that the endogenous cellulase might more accurately be termed a B-glucosidase; and lends further support to the hypothesis that

bacterial cellulase is the predominant factor responsible for cellulose degradation by the borer. Such a conclusion stems from the fact that the endogenous cellulase hydrolyzes 52.1% more cellobiose than cellulose, while the bacterial cellulase hydrolyzes 77.7% more cellulose than cellobiose. In addition, the bacterial cellulase has a total percent hydrolysis (88.2%) equal to that of complete acid hydrolysis (88.3%). The specificity of the bacterial cellulase is therefore apparent. The affinity of the endogenous cellulase, on the other hand, indicates the nature of this enzyme to be more that of a cellobiase or B-glucosidase, than a true cellulase. Hydrolytic activity ratios shown in Table 1 likewise suggest that the endogenous cellulase is more probably a B-glucosidase, and support the dominance of bacterial cellulase in cellulose decomposition and metabolism by T. navalis.

Conclusions regarding the exact specificity of the endogenous cellulase cannot be made on the basis of the experimental data obtained in this investigation; however, several possibilities exist:

(a) The endogenous cellulase is truly a cellulase, but is chain-length specific for the smaller polymeric units of cellobiose. This is unlikely, however, since Mandels and Reese (27) reported that length-specific cellulases act preferentially on the intermediate cellulo-oligosaccharide units, bridging the gap between true cellulases and B-glucosidases.

(b) The endogenous cellulase is actually a stable B-glucosidase (or cellobiase) of bacterial origin. This possibility can be eliminated for two reasons: first, the pH of the bacterial extract shows only one activity peak; and second, the thermostability and thermorecovery properties of this enzyme indicate it to be unstable and rather thermolabile.

(c) The most likely possibility is that the endogenous cellulase is actually a B-glucosidase (or cellobiase) of teredinid origin, secreted into the caecum from the digestive diverticula. This possibility is strongly indicated by the hydrolytic activity ratios presented in Table 1, and the hydrolysis studies presented in Figure 1.

Numerous investigators (3,7,28,29,30,31,32) have reported the presence of cellobiase or B-glucosidase in the digestive diverticula or stomach and crystalline style of the borer (Teredo or Bankia sp.). Also, the pH noted to be optimum for the saccharifying activity of the endogenous enzyme is within 1.0 pH unit of the range reported by Greenfield and Lane (4) as exhibiting maximum activity of the "postcaecal" fraction; and within 0.5-1.0 pH units of that reported by several Japanese investigators (5,6,13,14) to be optimal for activity of the digestive diverticula of T. navalis.

In any case, it is apparent that the endogenous cellulase is not the active principle in hydrolyzing the cellulo-oligosaccharide units to glucose, but more probably acts by hydrolyzing smaller polymeric units of the disaccharide type.

Reese (33) postulated that cellulose degradation occurs in a series of steps, as shown in Figure 2. The first step, carried out by a factor designated as C_1, converts native cellulose into reactive cellulose (B-1, 4-polyanhydroglucose chains). The nature of this action, and even the question of whether it is enzymatic, is unresolved. The reactive cellulose is next acted upon by C_x (the cellulase probably referred to by most investigators), a complex of enzymes that hydrolyze glucosidic linkages producing reducing sugars, such as glucose. Mandels and Reese (27) report the separation of a C_x cellulase, produced by the fungus, Trichoderma viride, into three components which show chain length activity: the A component showed equal activity for both long and short chains, while the B component was more reactive on long chains and the CD component more reactive on shorter chains. Further work by Mandels and Reese (34) has confirmed the presence of a C_1-C_x component cellulase system in fungi that contains length specific cellulase components. Studies on the C_x component by Mandels and Reese (34) and Mandels and Weber (35) substantiate Reese's 1959 (27) proposal for the degradation of cellulose.

Although such a multiple component system has not as yet been demonstrated for bacterial cellulolytic systems, an analogous component system may be speculated to be present in bacterial cellulases.

Much a priori evidence has accumulated concerning the role of marine fungal species in the destruction of wood (36,37). This includes sloughing or softening of the wood surface, penetration and complete vegetative and reproductive infestation of submerged wood panels, and a growth-wise affinity for wood and wood products in pure culture.

The presence of active cellulolytic systems in various species of lignicolous marine Ascomycetes and Deuteromycetes has been demonstrated (38,39,40). Cell free filtrates from species isolated from submerged wood have been shown to produce as much as 3.0 milligrams reducing sugar per milliliter when incubated with cellulosic materials, such as carboxymethyl-cellulose, powdered cellulose, and balsa wood (40,41). Many of these fungi have also been shown to degrade Manila twine, a lignocellulosic material comparable to wood in proximate analysis (41).

Microscopic analysis indicates that the process of wood decomposition by fungi is extracellular; and the growth of wood destroying fungi on lignocellulosic materials depends on the production of extracellular cellulases and xylanases (42).

Meyers and Reynolds (36,37) have implicated the role of marine cellulolytic fungi to be preparatory insofar as a correlation with infestation by boring molluscs is concerned. These authors suggest that cellulolytic fungi "condition" the surface of wood prior to attack by wood borers.

> "The fungal infestation that occurs before borers attack the wood has interesting biological implications. In northern areas, especially, it may facilitate the activities of the borer, not only by making it easier for them to enter the wood, but also by providing them with a source of food."

Implicit in this statement is the suggestion of fungal "preconditioning" of wood cellulosic components prior to marine borer infestation and attack by the enzymatic constituents of the borer's digestive system. This "conditioning", if it is of any effect, surely involves physical and chemical as well as biological factors. Investigators concerned with the role of marine cellulolytic fungi in the decomposition of wood consider the production of extracellular cellulases and xylanases to be an important factor. These enzymes apparently soften ("condition") the wood facilitating the boring activity of the animal, and 'ready' the cellulosic components of the wood for the subsequent action of other enzymes contained within the digestive system of the animal.

Two models for the cooperative action of fungal, bacterial, and endogenous cellulases can be proposed for the degradation of wood and metabolism of its hydrolysis products by Teredo navalis. The distinguishing features between the two proposed models are the speculative nature of the endogenous cellulase (i.e., true cellulase or B-glucosidase) and its specificity (i.e., preferential lengths of B-1, 4-polyanhydroglucose or cellobiose).

Model #1 assumes that the endogenous cellulase is a true cellulase of teredinid origin, and that cellobiase and B-glucosidase are separate enzymes located in the caecum (10,28). According to this model, native wood enters the stomach from the esophagus and is acted upon by three components: (a) amylase and saccharase from the crystalline style (43,3,29,32); (b) alginase and xylanase from the digestive diverticula (3); and (c) cellulase, most probably of the C_1 type, produced either by the digestive diverticula (44,4,45,7,30,31) or by cellulolytic fungi ingested with the wood (36,37,40). It is proposed that the combined activity of these enzymes converts native wood to 'reactive' wood by acting on various extraneous wood components (i.e., non-cellulosic polysaccharides) in such a way as to render the glycosidic linkages of the cellulosic polysaccharides susceptible to enzymatic hydrolysis (46). The activity of the C_1 component is speculative; however, it is an enzyme produced by all actively cellulolytic fungi (34). If C_1 is hydrolytic, its action may be quite random or restricted to weak linkages in non-cellulosic polysaccharides (34). If C_1 is not hydrolytic it might bind directly to the cellulose relaxing the intramolecular bonds so the C_x cellulase can act. Whatever its action, C_1 renders the wood susceptible to attack by the C_x cellulase.

When wood enters the stomach, its presence and/or the presence of the fungal C_1 cellulase, induces the digestive diverticula to secrete cellulase (probably C_1) into the stomach. Here, native cellulose and hemi-cellulose components are acted upon such that the

native wood is converted into 'reactive' wood. The 'reactive' wood is passed into the caecum where it is acted upon by the bacterial C_x cellulase. The production of the bacterial C_x cellulase is thought to be induced by the presence of wood and/or the C_1 cellulase from the fungi or the digestive diverticula. The bacterial C_x cellulase decomposes the 'reactive' wood to cellobiose and glucans (from the hydrolysis of hemi-celluloses). The presence of cellobiose activates cellobiase, present in the caecum, which subsequently converts this disaccharide to the reducing sugar, glucose. The glucans are acted upon by B-glucosidase in the caecum and are converted to other metabolizable sugars. The sugars are absorbed by the caecal tissue and metabolized by Embden-Meyerhof, Pentose Pathway, and Citric Acid Cycle enzymes (10,28) for food and energy.

Model #2 differs from Model #1 in supposing that the endogenous cellulase is really a cellobiase-B-glucosidase, as is suggested by the experimental data presented in this study. Native wood enters the stomach from the esophagus and is acted upon by enzymes secreted by the crystalline style and digestive diverticula, as described in Model #1; endogenous cellulase, however, is absent. As cellulolytic fungi may be present on the wood when ingested, some fungal C_1 cellulase activity may also occur. The combined activity of these enzymes converts native wood into 'reactive' wood. The 'reactive' wood is passed into the caecum, where bacterial C_x cellulase, induced by the presence of wood and/or fungal C_1 cellulase converts it to cellobiose and glucans. The presence of cellobiose activates the endogenous cellobiase-B-glucosidase which is secreted into the caecum from the digestive diverticula. This enzyme converts the cellobiose and glucans into metabolizable sugars, which are absorbed by the caecal tissue. Embden-Meyerhof, Pentose Pathway, and Citric Acid Cycle enzymes are responsible for the conversion of these hydrolysis products into utilizable food and energy within the caecal tissue (10,28).

The main differences between the two models can be summarized as follows:

Nature of Cellulase:

Model #1: Endogenous cellulase is a true cellulase acting preferentially on long chain cellulosic polysaccharides. Its action, in conjunction with the activity of fungal C_1 cellulase and carbohydrases produced by the crystalline style and digestive diverticula, renders the B-1, 4 linkages of polyanhydroglucose chains susceptible to enzymatic hydrolysis by bacterial C_x cellulase.

Model #2: Endogenous cellulase is absent. Carbohydrases from the crystalline style and digestive diverticula, in conjunction with some fungal C_1 cellulase, are responsible for converting native wood to 'reactive' wood, rendering it susceptible to attack by bacterial C_x cellulase.

Nature of Cellobiase and/or B-Glucosidase:

Model #1: Cellobiase and B-glucosidase are separate enzymes located in the caecum. Cellobiase converts cellobiose to glucose, while B-glucosidase acts on other glucans to produce metabolizable sugars, which are absorbed by the caecal tissue.

Model #2: Cellobiase-B-glucosidase is a unit enzyme located in the digestive diverticula, and secreted into the caecum. It is activated by the presence of cellobiose, and converts both cellobiose and glucans into metabolizable sugars, which are absorbed by the caecal tissue.

Figure 3 illustrates this new concept of wood digestion by the Teredinidae. It shows the cooperative action of fungal, bacterial, and endogenous cellulases, and the important role played by symbiotic cellulolytic bacteria in the degradation and metabolism of cellulose and its hydrolysis products within the digestive system of the borer.

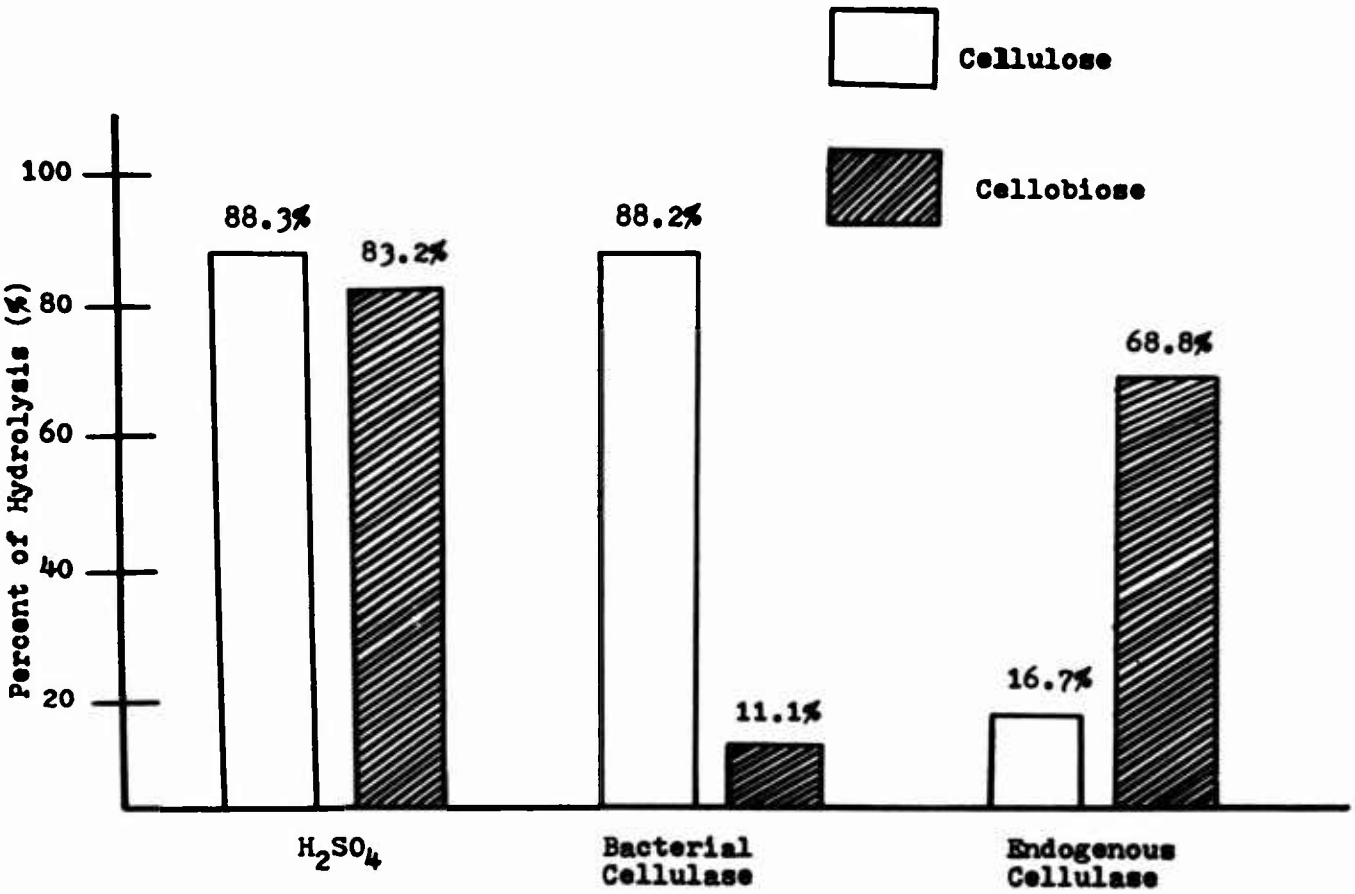
References

(1) C.R. Harington, Biochem. J. 15, 736-741 (1921).
(2) L.C. Boynton and R.C. Miller, J. Biol. Chem. 75, 613-618 (1927).
(3) Y. Hashimoto and K. Onoma, Bull. Jap. Soc. Sci. Fisheries 15, 253-258 (1949).
(4) L.J. Greenfield and C.E. Lane, J. Biol. Chem. 204, 669-672 (1953).
(5) T. Hidaka, Mem. Fac. Fisheries, Kagoshima Univ. 3, 149-157 (1954).
(6) T. Hidaka and K. Saito, Mem. Fac. Fisheries, Kagoshima Univ. 5, 172-177 (1956).
(7) N.B. Nair, Current Sci. 24, 126-127 (1955).
(8) L.J. Greenfield, Proc. Soc. Exp. Biol. Med. 89, 241-243 (1955).
(9) P.C. Trussell, C.C. Walden and E. Wai, Material und Organismen 3, 95-105 (1968).
(10) D. Liu and M.P. Townsley, J. Fish. Res. Bd. Canada 25, 853-862 (1968).
(11) A.A. Imschenezki, Mikrobiologie der Cellulose, p. 354, Akademie-Verlag Berlin (1959)
(12) P. Deschamps, Bull. Soc. Zool. Fr. 78, 174-177 (1953).
(13) K. Saito and T. Hidaka, Mem. Fac. Fisheries, Kagoshima Univ. 3, 50-55 (1954).
(14) H. Kadota, Marine Boring and Fouling Organisms (ed. D.C. Ray), p. 332-341, Univ. Washington Seattle (1959).
(15) F.A. Rosenberg and H. Breiter, Material und Organismen 4, 147-159 (1968).
(16) J. Cutter and F. Rosenberg, Biodeterioration of Materials (vol. 2) pp. 42-51, Applied Science London (1972).
(17) J. Lyman and Fleming, J. Mar. Res. 3, 134-146 (1940).
(18) D. Kuhn and G.L. Lasnik, Bact. Proc. p. 49 (1968).
(19) O. Folin and H. Malmros, J. Biol. Chem. 83, 121-124 (1929).
(20) S. Seifter, S. Payton, B. Novio and E. Muntmyler, Arch. Biochem. 25, 191-198 (1950).
(21) T.C. McIlavine, J. Biol. Chem. 49, 183-190 (1921).
(22) N. Nelson, J. Biol. Chem. 153, 375-382 (1944).
(23) M. Somogyi, J. Biol. Chem. 195, 19-22 (1952).
(24) J. Cutter and F. Rosenberg, Material und Organismen (in press).
(25) R.E. Strange, F.A. Dark, and A.G. Ness, Biochem. J. 59, 172-175 (1955).
(26) W.H. Dore and R.C. Miller, Univ. Calif. Publs. Zool. 22, 383-400 (1923).
(27) M. Mandels and E.T. Reese, J. Bacteriol. 79(6), 816-826 (1959).
(28) D.L. Liu and C.C. Walden, J. Fish. Res. Bd. Canada 27, 1141-1146 (1970).
(29) N.B. Nair, Current Sci. 24, 201 (1955).
(30) N.B. Nair, J. Madras Univ. 26(3), 599-627 (1956).
(31) N.B. Nair, J. Sci. Ind. Res. 15(C), 155-156 (1956).
(32) N.B. Nair, J. Sci. Ind. Res. 16 C(2), 39-41 (1957).
(33) E.T. Reese, Appl. Micro. 4, 39-45 (1956).
(34) M. Mandels and E.T. Reese, Developments in Industrial Microbiology (vol. 5), pp. 5-20, Am. Inst. Biol. Sci. Washington D.C. (1964).
(35) M. Mandels and J. Weber, Advances in Chemistry Series #95, Am. Chem. Soc. (1969).
(36) S.P. Meyers and E.S. Reynolds, Science 126, 969 (1957).
(37) _____, Res. Reviews, Office of Naval Research, Dec. 6-11 (1957).
(38) _____, Bull. Mar. Sci. Gulf Caribb. 9, 441-445 (1959).
(39) _____, Canad. J. Microbiol. 5, 493-503 (1959).
(40) _____, Dev. Ind. Micro. 1, 157-168 (1960).
(41) S.P. Meyers, B. Prindle, and E.S. Reynolds, Tappi 43, 534-538 (1960).
(42) J. Varadi, Biodeterioration of Materials (vol. 2), pp. 129-135, Appl. Sci. London (1971).
(43) R.C. Miller and E.R. Norris, Proc. 6th Pacific Sci. Congr. 3, 615-616 (1940.
(44) C.E. Lane and L.J. Greenfield, Am. J. Physiol 171(3), 741-742 (1952).
(45) C.E. Lane, Marine Boring and Fouling Organisms, pp. 137-144, Univ. Washington Seattle (1959).
(46) R.E. Wise, World Chemistry Monograph Series #97, Reinhold N.Y. (1944).

TABLE I

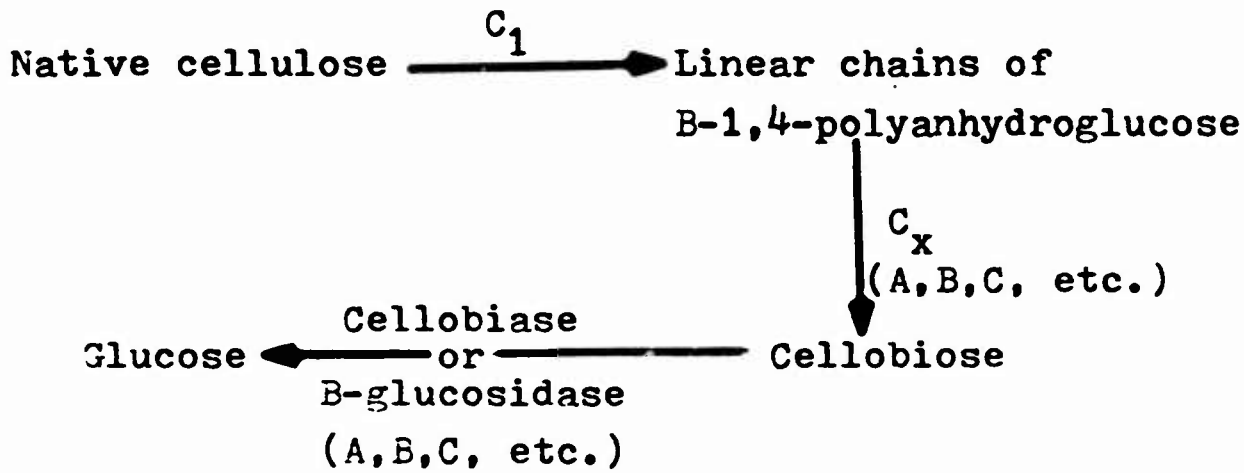
Hydrolytic Activity Ratio*

Hydrolytic Agent	ug/ml glucose Cellulose	Cellobiose	Activity Ratio
Bacterial Cellulase	22.04	3.33	8
Endogenous Cellulase	4.16	20.62	4
H_2SO_4 (95%)	22.06	25.00	1



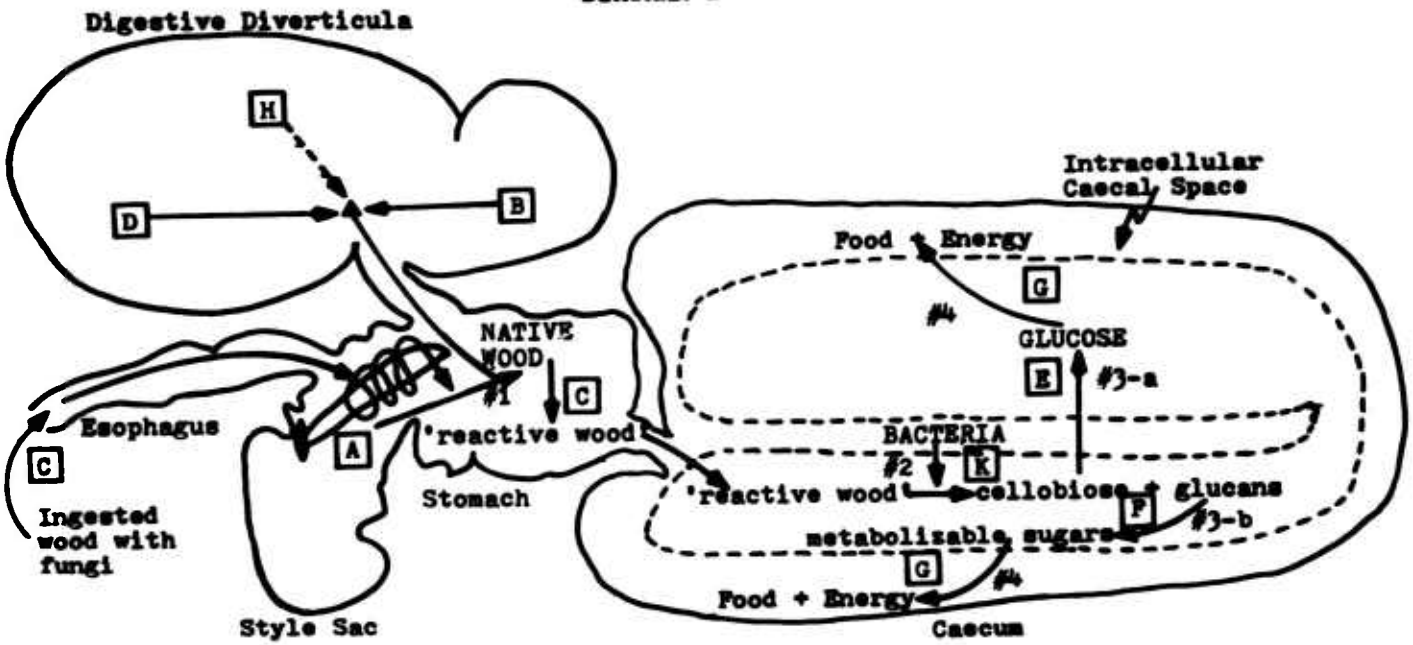
Comparative Substrate Specificity

The following diagram, adapted from Reese (1959), helps to illustrate the concept of enzymatic degradation of cellulose (C_1 and C_x represent enzymes).



DIGESTION OF WOOD BY THE TEREDINIDAE

DIAGRAM 1*



ENZYMES designated with letters:

A = amylase & saccharase
B = alginase & xylanase
C = fungal cellulase (C_1)?
D = cellobiase-B-glucosidase (diverticula)
E = cellobiase (caecum)
F = B-glucosidase (caecum)
G = EMP, CTA, and PP enzymes
H = endogenous cellulase (C_1)?
K = BACTERIAL cellulase (C_x)

REACTIONS designated with numbers:

#1 NATIVE WOOD $\xrightarrow[\text{stomach}]{A,B,C_1(H?)}$ "reactive wood"

#2 'reactive wood' $\xrightarrow{K}$ cellobiose + glucans

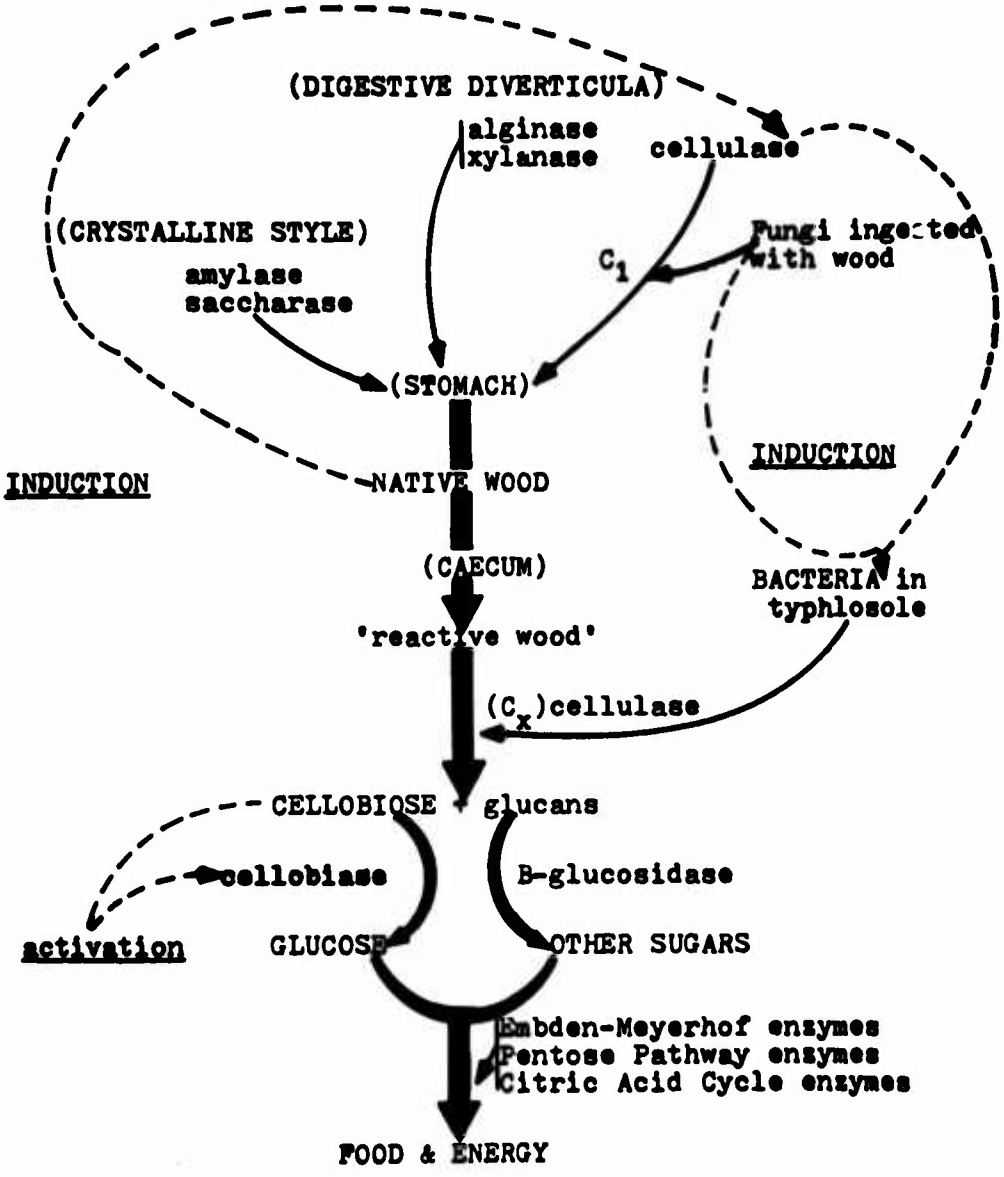
#3-a cellobiose $\xrightarrow{D \text{ or } E}$ GLUCOSE

#3-b glucans $\xrightarrow{F}$ metabolizable sufars other than glucose

#4 ALL metabolizable sugars $\xrightarrow[G]{}$ FOOD & ENERGY

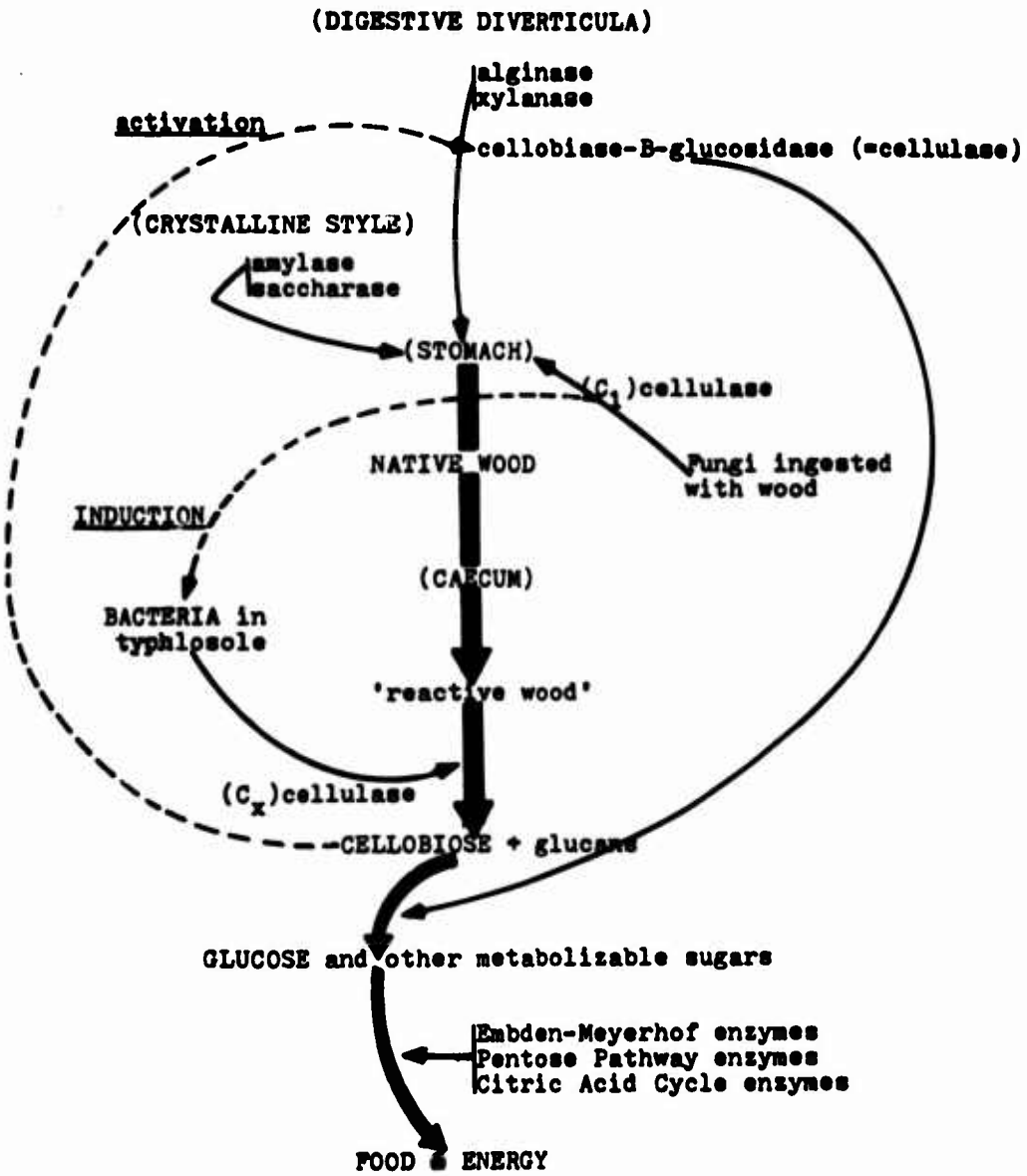
MODEL #1

Endogenous Cellulase is a True Cellulase



MODEL #2

Endogenous Cellulase is a B-Glucosidase



Discussion

Kevin Marshall, University of Tasmania: Dr. Rosenberg, I wonder about your isolation techniques. One would imagine that in the gut of the shipworm the environment is anaerobic and therefore, if you are looking for cellulose decomposers, surely you should be looking for anaerobic decomposers.

Rosenberg: We grew all our isolates under anaerobic conditions and the aerobic isolates were capable of growing anaerobically and vice-versa. We found organisms which were capable of growing under both conditions.

Marshall: My other question concerns your technique of simply rinsing the gut in 95% ethanol. Have you tested the degree of efficiency of sterilization of an external surface with ethanol by this method? I rather doubt that you are removing all the external organisms.

Rosenberg: We ran controls on all of the caecal isolates and we never obtained any growth from the surface of the caecum when we rinsed with 95% alcohol whereas we did obtain organisms from the contents of the caecum.

Robert Dean, Duke University: I have tried your technique of sterilization and, in fact, used multiple washings in both 95% ethanol and sterile sea water and consistently have been able to culture large numbers of bacteria from the external surface of the caecum without puncturing it, though I admit I was working with a different species, namely Bankia gouldi.

Rosenberg: Were you isolating cellulolytic bacteria or just bacteria in general? We were interested only in the fact that cellulolytic bacteria would not grow.

Dean: Yes. I was isolating cellulolytic bacteria. The organisms were first isolated on Di Fio Marine Agar but I was then able to restreak them on cellulose containing media and show that they were indeed cellulose decomposing bacteria. This is why I question your techniques. Furthermore, do you think that enrichment culturing is giving you a valid picture of the microbial constituents of the gut? I ask this because, following your methods, I have consistently obtained three to four species in approximately equal numbers based on colony morphology.

Rosenberg: When we enriched we were trying initially to isolate the cellulolytic bacteria. We were not going on numbers of organisms even though this is open to some question. One can question the relationship between the number of organisms and enzymatic activity, but we were only trying to relate the activity of the bacterial cellulase with that of the caecal cellulase, if one was present. We consistently got four times as much activity from the bacterial isolates as we did from the caecum.

Dean: But you will agree you cannot be sure that the species you get via enrichment is the most important species in the gut because the environment is not quite the same in a test tube.

Rosenberg: That is true but we have consistently isolated Cellulomonas sp. on our cellulose agar.

Dean: With regard to your enzyme assays, I wonder if you express your data as milligrams of glucose liberated from your cellulose substrate per milligram of protein in the assay mixture. What kind of differences did you get between the bacterial extract and the caecum homogenate?

Rosenberg: Can you phrase that slightly differently?

Dean: Commonly in biochemical assays, when one wishes to compare the enzyme activity of various preparations, the data are expressed in terms of milligrams substrate liberated per milligram protein present in the incubation. I wonder if you did this. In other words, after you had done all the processing on your bacterial homogenate and your caecal homogenate, did you measure the amount of protein present in the two mixtures?

Rosenberg: No. We did not.

Dean: So it is quite possible that the greater amount of activity seen with the bacterial extract could be due to the fact that you had several orders of magnitude more protein present in that mixture.

Rosenberg: That is a possibility, but the amount of the caecal homogenate in relation to the amount of bacteria tends to preclude the possibility that we would have that much more protein in the amount of bacteria used than was present in the caecum.

Dean: What was the basis for comparing the two in this regard?

Rosenberg: We simply used a standardized amount of bacteria and a standard amount of caecum.

Dean: All right, you took the bacterial extract from a pure culture of isolated bacteria. Do you know the approximate numbers of bacteria in the culture?

Rosenberg: Yes. I do not have them here but can give them to you later.

Dean: I would think that an enriched culture or pure culture on some medium that had been developing for a day or so would tend to have enormous amounts of protein as compared with a caecal extract. I have found that homogenizing shipworms, large numbers of them, with about equal volume of some medium gives no more than about 500 to 700 micrograms of protein per milliliter and I tend to think that you probably got a far greater amount with the bacterial extract.

Rosenberg: We did not use the bacteria which had been grown on Di Fio Marine Agar. We used the bacteria which had been grown on cellulose agar and the growth on this medium was so slow that it took a number of weeks before we had a sufficient number of organisms to be able to use them.

Dean: Are the bacteria visible in the extracts you prepared?

Rosenberg: When we streaked the extracts back onto cellulose agar plates it took up to six weeks before we detected any bacteria.

Dean: Were they visible when you were preparing the bacterial extracts and you had them in slants or in liquid culture?

Rosenberg: We had some turbidity in liquid, but it was minimal.

Dean: Were they all prepared from liquid culture?

Rosenberg: Yes.

Dean: Fine, but I'm still quite unwilling to accept your data until you check your results in terms of activity per milligram of protein because, to me, efficiency of activity means that benefits greatly exceed costs. It may be that you simply have enormously larger amounts of protein in your bacterial extract.

Levy, Imperial College, London: My interest in the degradation of cellulose concerns the effect of terrestrial fungi in wood. I want to say that I like the ingenuity of your models, but I would add a word of warning about the C_1 - C_x. Recently Dr. Selby, who has been working in this area for some time, gave a review of recent work by T. M. Wood who suggested that the C_1 - C_x sequence was not entirely correct and that there was another twist to the story. Some of the reactions of different types of fungi in wood take a bit of explaining even with the C_1 - C_x areas that we know at the moment.

Rosenberg: Thank you for your comment. May I mention one thing. There are references in the literature to the effect that termites will never act on the wood until it is preconditioned by fungi.

Levy: Yes. I think there are quite a number of references to the interaction between fungi and various micro-organisms. I think this has been suggested for some of the Limnoria though this is a debatable point, but I believe, in certain cases the fungi are supposed to act first.

Gareth Jones, Portsmouth Polytechnique: Dr. Rosenberg, what is the nature of the cellulose material in the caecum when you look at it? Do you find any bacteria? Can you see these visually?

Rosenberg: We have not looked at the contents of the caecum to determine whether bacteria are present. We simply homogenized the caecum and then plated it out and isolated the cellulolytic bacteria from it.

Jones: In your system you assumed that there were fungi present and that the C_1 enzyme was coming from fungi in the wood. Have you found any fragments of mycelium present either in the caecum or the stomach?

Rosenberg: We haven't looked for them. The model was hypothesized after the investigation so we have yet to look for the presence of fungal fragments in the borer itself.

Jones: I asked this because we have extracted cellulose material from the stomach and the caecum using a micro-pipet. We have found no evidence of fungal mycelia and it was extremely difficult to find any bacteria.

Dean: I have spent some time looking at gut contents and have seen numbers of bacteria associated with the material being freshly drawn into the stomach by the crystalline style. However, I have not seen any bacteria in the caecum by looking at squashes on glass slides. If they are present they are either very closely associated with the gut wall or with the particles of wood. I would like to ask one more question concerning your enzyme assays. What form of cellulose were you using as a substrate?

Rosenberg: We used a microcrystalline cellulose. It is from the Sigma Company 0.6% microcrystalline cellulose.

Dean: Recent work on mollusks by a man named Koopmans in Holland showed that Cardium, I believe, was able to readily digest microcrystalline types of cellulose but showed no activity against completely native forms of cellulose such as cotton or wood. This perhaps should be taken into consideration.

The Effects of Temperature and Other Factors on the Tunnelling of *Lyrodus Pedicellatus* and *Teredo Navalis*

P.A. Board

Central Electricity Research Laboratories, Leatherhead,
Surrey, England

A shipworm in wood bathed by a warm seawater effluent will be stimulated to a higher rate of tunnelling than in ambient conditions. It will not necessarily grow any bigger in warm conditions because its form and ultimately its size are determined by the hardness of the wood.

Key Words: Rate of tunnelling; hardness of wood; size; form.

1. Introduction

This report is part of a study of shipworms begun in 1963. Even then it was apparent that we could improve the condition of our rivers. It was, therefore, only a matter of time before shipworms would infest wooden dock and harbour installations that had remained free from attack during the years of pollution. When this happened what would be the effects of warm effluents from coastal power stations?

The conclusions reached here are matters of fact. Readers must make up their own minds whether power stations should be held to account - especially when, at the root of the problem of shipworms, is the driftwood that litters our inshore waters[1].

2. Apparatus

Two perspex channels were supplied by airlift pumps from reservoirs of artificial seawater. The water in one channel was held more or less at 23°C; in the other it was held more or less at 18°C. The heat input was through Pyrex glass coils in the reservoirs. Temperature appreciation was by six resistance thermometers wired to an electronic roll-chart recorder.

3. Methods

The main experiment involved five procedures: 'infestation', 'radiography', 'measurement', 'comparison' and 'analysis'.

Infestation[2]: Two batches of ten spruce, *Picea abies* dowels, each mounted on a weighted perspex frame, were infested each week with settling stages of the shipworm *Lyrodus pedicellatus*. After infestation, frames were placed one in each channel starting at the downstream end of each. During the 98 days duration of this part of the experiment, 120 pairs of dowels were infested and placed in the channels; Fig. 1.

[1]The Port of London Authority removes some 8000 tons annually cast into the River Thames as its report (1) states: "... by a society too affluent to care about wastage and apparently too indifferent to consider the result of its behaviour".

Radiography[2]: Beginning on day 98 with dowels 1-10, radiography was carried out on a weekly basis until day 266. Each week another batch of dowels was added to those being radiographed until eventually all the dowels were being radiographed every week; Fig. 1.
Measurement: Accurate measurements of the negative images of selected shipworms were made with a binocular microscope fitted with an eye-piece scale. The microscope was fixed over a hole in the bench 25 mm in diameter. Beneath the hole was a small fluorescent tube. Above, and mounted on four rubber bungs, was a sheet of clear plate glass. At a working magnification of × 12, the lighted area was just larger than the field on view.
Comparison: This was a process of continual assessment of the radiographic appearances of shipworms and dowels.
Analysis involved the statistical analysis of measurements using a desk calculator and a computer.

4. Results

These were obtained from the radiographic record of growth and development and consisted primarily of measurements of overall lengths and of measurements of the width of tunnel linings at 5 mm intervals of length.

The data on overall lengths were provided by shipworms growing without interference from their fellows or from knots or pins in the ends of dowels. At 23°C sixty-nine *Lyrodus* were found which met these requirements; at 18°C only seven. The sixty-nine yielded 609 measurements; the seven, tunnelling more slowly and taking longer to reach the pins, yielded 126.

The data on tunnel widths at 5 mm intervals of length consisted of 657 measurements provided by the 23°C population and 26 measurements provided by the 18°C population - the same shipworms providing these data as provided those on lengths.

5. Discussion

5.1 Increases in length

Values for mean lengths with 95% confidence intervals were obtained using a program written for a desk calculator. When these were plotted against time it was apparent (Fig. 2) that increase in length could be regarded as linear over the period covered by measurements. (The hiatus after day 130 in the 23°C plot was due to a number of faster growing shipworms having reached the pins at the ends of the dowels in which they were growing.) The relationship between rates of increase in length at the two temperatures was found by performing linear regressions on the data and comparing their slopes (regression coefficients). At 23°C the regression coefficient was 0.5364, at 18°C it was 0.1720. The rate of tunnelling at 23°C was therefore 3.12 times the rate at 18°C.

Another way of comparing increases in length at 23°C and 18°C was to note the times at which the two populations attained the same mean lengths. The following table, based on Fig. 2, shows the time in days taken to reach mean lengths of 12.5, 15, 17.5, 20 and 22.5 mm.

5.2 Changes in form

Although the record of increases in length was incomplete, the record of changes in form was preserved in the radiographic picture of each shipworm. However, only the last set of radiographs was used to obtain measurements of widths at 5 mm intervals of length.

Values for mean widths and 95% confidence intervals were obtained as before and the plot "mean width ($\bar{w}$) × length (l) at 5 mm intervals" is shown in Fig. 3. After a trial plot, the data were converted to the form "log ($\bar{w}$) × log (l)" and linear regressions were

[2]"Techniques of Infestation and Radiography using the Shipworm *Lyrodus pedicellatus* Quatrefages" by P.A.BOARD and M.J.FEAVER (not yet in print) describes fully these two procedures.

carried out on those provided by *Lyrodus* in dowels 1-20 (23°C) and 1-20 (18°C). Subsequently, other regressions were done on data obtained from *Lyrodus* growing in dowels 61-70 (23°C), from *Lyrodus* in 20 mm diameter dowels of Scots pine, *Pinus sylvestris* (which had been well soaked before infestation) and from *Lyrodus* in *Pinus* blocks measuring 150 × 75 × 25 mm. These are all shown in Fig. 4.

Since log width = h. log length + g

$$w = g\, l^{h}$$

where the exponent h, the regression coefficient, is approximately 0.5.

There were no significant differences in tunnel widths in the experimental populations of *Lyrodus* in *Picea* (a, b, c in Fig. 4), but when these were compared with widths of *Lyrodus* in *Pinus* (d and e in Fig. 4), differences in the shape of tunnels apparent to the eye were confirmed by a separation of the means in excess of the 95% confidence limits[3].

The value of the exponent, h, would appear to be a function of the hardness of the wood through which tunnels are made since, when the value of h for *Lyrodus* in *Pinus* is substituted for the hardness (resistance to indentation) in columns B of Table 2 below (based on Appendix B, p.65 (2)[4], the values of h for *Lyrodus* in *Picea* span the required range.

No data are available that relate tunnel widths in the somewhat harder *Pinus* to time and temperature, but there were sufficient examples of shallow and deep tunnelling in *Picea* (notably those of shipworms (a) and (b) Fig. 5) to venture an opinion: that at a temperature suitable for tunnelling, progress is slower in hard wood than in soft wood.

5.3 Hardness and form

At this point, some consideration must be given to the gradients of hardness experienced in the first 5-10 mm of tunnelling for, according Figs 3 and 4, this is where form and size are largely determined.

Settling at a wood/water interface so that its earliest tunnelling is across the grain, a shipworm experiences a more abrupt transition from soft to hard going than it does if it settles on a cut end and follows the grain(3). The result is not only slower progress to begin with, but a wider tunnel. An initially disproportionate increase in width with respect to length (which results in the development of the more powerful adductor muscles required for heavy duty work) is also a feature of the formula $w \propto \sqrt{l}$ (width is proportional to the square root of the length) - as, indeed, is the pattern of subsequent growth.

Once a shipworm reaches conditions of optimum hardness for tunnelling it turns along the grain and with respect to width, begins to increase disproportionately in length. Hardness is still a governing factor. In our spruce dowels, where maximum hardness was reached within a few millimetres of the wood/water interface, *Lyrodus* had no opportunity of attaining optimum hardness for tunnelling. If, however, the pieces of wood used in this experiment had been more substantial - trees or posts, say, instead of dowels, we would have found much bigger *Lyrodus* tunnelling towards the heartwood at a slight angle to the grain - impelled not only by a gradual softening of the wood by water and micro-organisms, but by their own increasing width which would require an increasingly hard substrate for

---

[3]Note, however, the anomalous result of regression analysis on 32 data points provided by *Lyrodus* growing in dowels at 18°C. The restricted range of the measurements (widths from 5-30 mm of length instead of from 5-50 mm) exaggerated the steepening effect of including a group of data points (representing larval size at settlement) until the regression coefficient was 0.51800. At first sight this is similar to values for *Lyrodus* in *Pinus*, but when the 95% confidence level was calculated, there was an overlap between the lower limit for *Lyrodus* in dowels 1-20 at 18°C (0.48128) and the upper confidence limit for *Lyrodus* in dowels 1-20 at 23°C (0.48250).

[4]Figures in parentheses indicate the literature references at the end of the paper.

optimum tunnelling[5].

Growth, which in its secondary phase accentuates length rather than width, is made apparent by the addition of filaments to the ctenidia or 'gills'. In the tertiary phase, when the hardness of the wood is inclined to diminish rather than increase, the gills and the mantle covering are probably all that continue to grow.

5.4 Effects of soft going on size and form

Previously, Board(3) stated that the cross-sectional area of a shipworm's tunnel at any point along its length is always greater than the maximum spread of the valves at the time it was fashioned. In soft going, however, the extent of the excavation can be greater than the outside dimensions of the calcareous lining. Fig. 6 shows this clearly. It is apparent that additions in length to the lining are made by means of annuli each of which is expanded distally to receive the proximal (posterior) end of the one that follows. Probably inflation of the posterior end of the cephalic hood ensures that each annulus is expanded sufficiently to touch the wooden walls of the excavation before it is calcified.

6. Conclusions

(i) Temperature affects the rate of tunnelling.

(ii) Over the period covered by measurements the rate of increase in length was linear and at 23°C approximately three times the rate at 18°C.

(iii) The width of a *Lyrodus* tunnel is roughly proportional to the square root of its length at the point at which width is measured. In spruce dowels the exponent h in the formula $w = g.l^h$ is less than 0.5; in dowels and blocks of Scots pine it is greater than 0.5.

(iv) The exponent h above is a function of the hardness of the wood through which a shipworm is tunnelling.

(v) The width of a shipworm is therefore determined by the hardness of the wood and not directly by temperature.

(vi) Ultimately, however, the size that a shipworm may reach in a piece of wood depends on the gradient of hardness between the point of entry and the centre. Consequently large pieces of wood tend to harbour larger shipworms than small pieces of the same kind.

(vii) Increase in length without a concomitant increase in width is provided for by the addition of new filaments to the gills.

(viii) In soft going the tunnel lining is narrower than the excavation and touches the wooden walls at intervals only.

7. Acknowledgements

The work was carried out at the Central Electricity Research Laboratories, and this paper is published by permission of the Central Electricity Generating Board.

[5]Having regard to these arguments, the larger size attained by some tropical shipworms must be due in part to the fact that tropical woods are generally harder than the so-called "softwoods" or gymnosperms that comprise the driftwood of northern temperate seas, as well as to the fact that higher temperatures result in an extended breeding season and in wood being infested and tunnelled before it has become too soft.

8. References

1. *The Cleaner Thames 1966*, Port of London Authority, (1967)

2. *A Handbook of Home-grown Timbers*, H.M.S.O., London, (1941)

3. P.A. BOARD, *J. Zool, Lond.* 161, 193, (1970)

	12.5	15	17.5	20	22.5
23°C	88.5	93	97.5	102	106.5
18°C	135.5	150	164.5	179	193.5

Table 1. A Comparison of Rates of Growth

At 23°C, in the size range 12.5-22.5 mm, *Lyrodus* in *Picea* dowels grew at the rate of 2.5 mm every 4.5 days. At 18°C, *Lyrodus* in similar *Picea* dowels took 14.5 days to tunnel 2.5 mm. Growth was, therefore, linear and roughly three times as fast at the higher temperature.

		HARDNESS Resistance to Indentation SIDEGRAIN		HARDNESS Resistance to Indentation ENDGRAIN		Wt/cubic foot at 50% moisture content		Wt/cubic foot at 12% moisture content	
		(A)	(B)	(A)	(B)	(A)	(B)	(A)	(B)
Pinus sylvestris	GREEN	430	0.5333	450	0.5333	40	0.5333		
	AIR DRIED	550	0.5333	740	0.5333			30	0.5333
Picea abies	GREEN	340	0.4217	410	0.4859	34	0.4533		
	AIR DRIED	480	0.4654	720	0.5189			27	0.4800

Table 2. Values (heavily outlined) for the physical properties of *Picea* when those of *Pinus* are equated to 0.5333 - the value of (h) for *Lyrodus* tunnelling in *Pinus* blocks.

Note that the regression coefficients of (a) (b) (c) Fig. 4 have similar values.

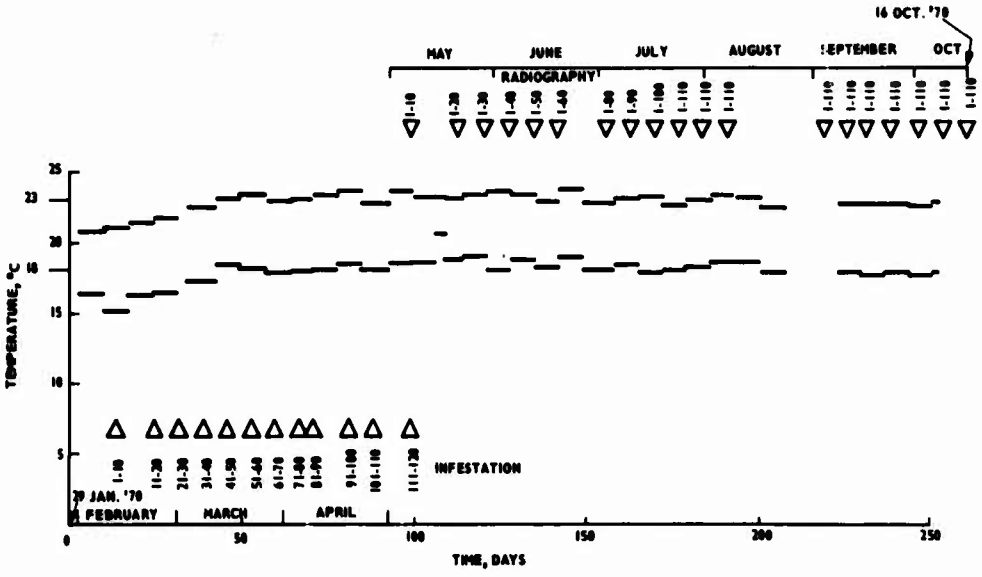


Fig.1 Record of average temperatures on the nominally 18°C and nominally 23°C sides of the experiment, together with the times when frames full of infested dowels were added to the experiment and removed (temporarily) for radiography

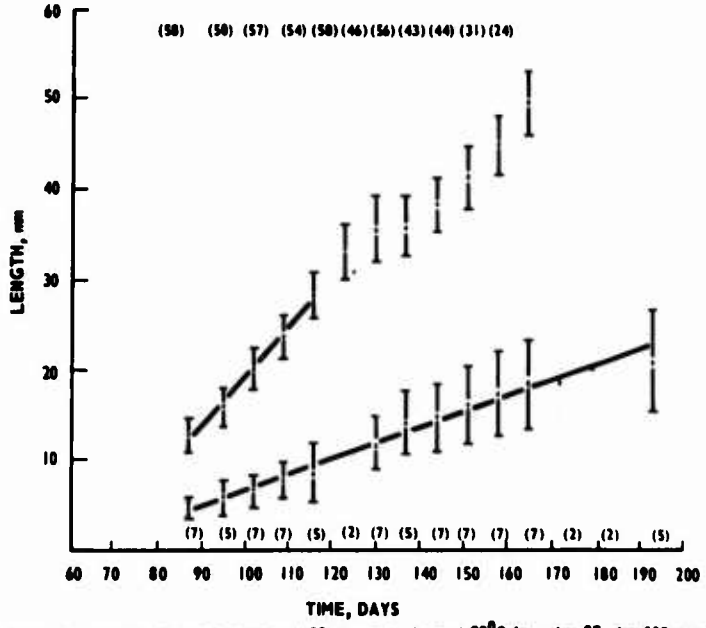


Fig.2 Upper plot: the mean lengths of 69 *Lyrodus* kept at 23°C from day 87 - day 165 with 95% confidence limits placed about the means

Lower plot: ditto for 7 *Lyrodus* kept at 18°C from day 87 - day 193.
Numbers in parentheses = numbers of observations.

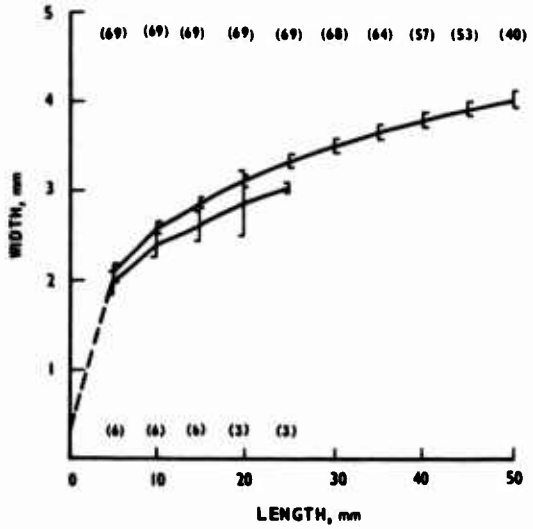


Fig.3 Upper plot: Tunnel widths of 69 *Lyrodus* growing in *Picea* dowels 1-110 at 23°C with 95% confidence limits about the means thus: (E)

Lower plot: Tunnel widths of 6 *Lyrodus* growing in *Picea* dowels 1-20 at 18°C with 95% confidence limits about the means thus: (E)

Numbers in brackets are the number of observations.

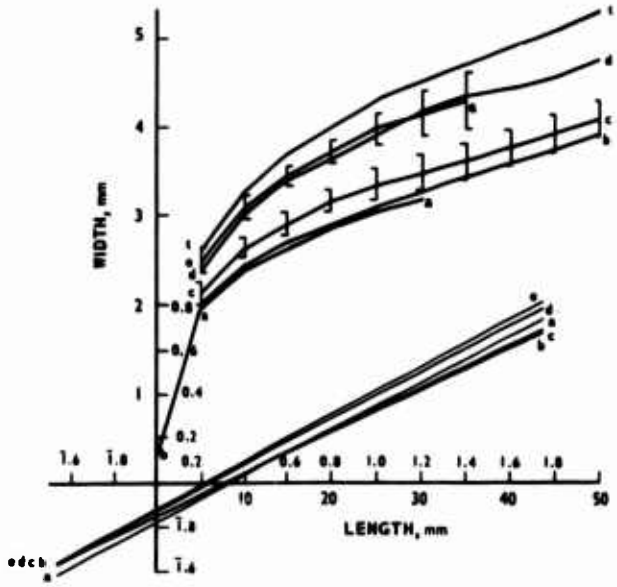


Fig.4 Average width: length relationships of *Lyrodus* and *Teredo* tunnels in *Picea* and *Pinus* - with the corresponding regression lines showing the slight though important divergence in slope associated with hardness of the wood.

(a) *Lyrodus* in *Picea* dowels 1-20 kept at 18°C
(b) *Lyrodus* in *Picea* dowels 1-20 kept at 23°C
(c) *Lyrodus* in *Picea* dowels 61-70 kept at 23°C
(d) *Lyrodus* in *Pinus* dowels
(e) *Lyrodus* in *Pinus* blocks
(f) *Teredo* in *Pinus* dowels



(a) Shallow Tunnelling (b) Deep Tunnelling

Fig.5 The two shipworms (a) and (b) are the same age. For some reason (a) the long, thin one tunnelling just below the surface of the dowel never developed the girth to accommodate adductor muscles as powerful as those of (b) its short fat companion. The latter is able to tunnel through the hard wood near the centre of the dowel (which still contains a residuum of undissolved air), but its progress is slower.

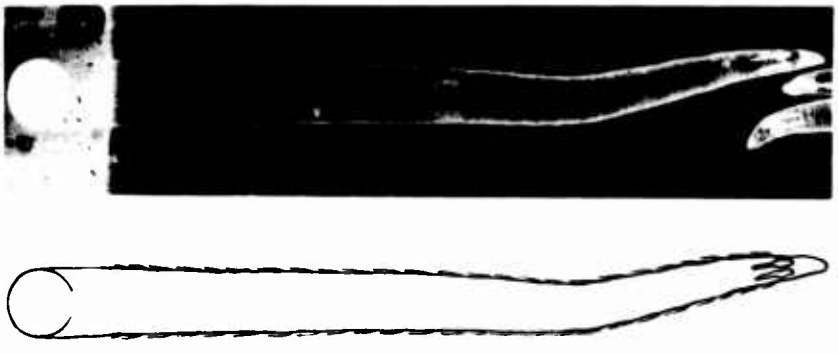


Fig.6 Radiograph and accompanying pen and ink drawing which show that the calcareous lining is not everywhere in contact with the tunnel excavated by *Lyrodus*. This condition is typical of tunnels made in very soft wood.

Note the dense, white, spherical shape of the valves which were moving whilst the radiograph was being taken. Also note the stationary, paired masses of developing larvae associated with the animal's ctenidia or 'gills'.

Inhibition of calcium secretion by chemical inhibitors in shell dwelling organisms

A. A. Karande and K. B. Menon

Naval Chemical and Metallurgical Laboratory
Lion Gate, Bombay 1

Wooden test pieces of Abies pindrow harbouring hundred or more stage 1 pediveligers were exposed to the graded solutions of chemical compounds in 500 ml crystalline jars. The control test pieces were simultaneously maintained in inhibitor-free sea water and in solutions of two more chemical compounds reported as having beneficial effect on the shell building process amongst bivalve molluscs. The degree of inhibitory action of a compound was judged by its ability to prevent or retard the impregnation rate of calcium carbonate in the mucous film lining the entry holes of the veligers. A calcium deposition capacity of the test organisms, as judged by the frequency of occurrence of growth stages, is found to have retarded with the increasing concentration of each of the compounds tested. For instance, at the lowest concentration of 2, 4 dinitrophenol as many as 67 p.c. of the larvae undergo complete transformation and achieve fourth stage of growth whereas at the higher concentration (.000125 M), only about 5 or 6 p.c. of them achieve fourth stage.

In almost all the chemical inhibitors screened here, the test organisms survived as long as 10 days, that being a normal span of life of a veliger, but failed to deposit adequate $CaCO_3$ which is so vital for their metamorphosis and growth. The investigation under report has brought out that the shell growth of the marine organisms is inhibited by certain chemical compounds even at very low concentration. The bioassay method discussed here in greater details may prove of advantage in screening the natural and synthetic chemical compounds for their antifouling efficacy.

1. Introduction

Free swimming larvae of the marine organisms like barnacles, tubeworms or molluscan bivalves become a fouling menace only when they settle and secrete their calcareous shells. It is now well accepted that the toxic elements of the antifouling paint prevent the settlement of the fouling organisms either by repelling these organisms during their exploratory movements on the surface or by impairing their some vital metabolic activity during the post settlement growth. The experience with toxic copper pigment shows that it is the latter mechanism which is more effective in preventing the settlement growth of the marine organisms. This was very fluently explained by the experimental data collected by Crisp and Austin (1)[1] who concluded that the failure of the young barnacles to grow on copper paint was due to the inhibitive action of copper on the cementing of the shell to the substratum. De Wolf (2) while explaining the failure of settlement of barnacles on an effective antifouling paint also assumed that the metamorphosed larva preparing itself for the building of a calcareous shell was poisoned by its contact with the paint coat. Wilbur (3) and others who worked on the shell deposition characteristics of oysters, noted that micro molar concentrations of chemical compounds like 2, 4 dinitrophenol, sulphanilamide and sodium fluoride inhibited calcium deposition rates in these bivalves. Karande (4) who reported on the natural durability of one tropical timber Tetrameles nudiflora also observed that the inability of teredid larvae to grow in this timber was due to their failure to deposit calcareous shells, the latter being very vital for their growth and the sustenance.

[1] Figures in parentheses indicate the literature references at the end of this paper.

In recent years attempts are being made to increase the effectiveness and precise toxic action of the antifouling paints. Experience to-date has shown that the fouling caused by the shell dwelling organisms can be considerably reduced if the shell building mechanism of these organisms is effectively interfered with chemical toxins. A use of more specific chemical inhibitors in antifouling coatings having precise inhibitory action on the shell building capacity of the fouling organisms may therefore prove a very rewarding area of research. With an objective of furthering this view, laboratory studies were carried out on the calcification characteristics of Teredo furcifera larvae exposed to seven chemical compounds reported as having inhibitory effect on molluscan shell growth. It was also the objective of this work to evolve a suitable methodology and technique to study this problem in greater details.

Earlier we have reported our work on wood-borer Teredo furcifera which has bearing on the present investigation. This work which is not fully described here but referred to frequently, includes observations on the breeding of this species in captivity (5), use of its larvae as the test organisms (5), and biology of this species in Bombay harbour (7, 8).

2. Material and methods

Teredid larvae, the test-organisms : In the present investigation our aim was to examine the inhibitory action of toxins on the calcium carbonate deposition ability of the marine organisms. For this, use of teredid larvae (Fig. 1) as the test-organisms was considered very satisfactory. Veliger larvae after initial attachement to the timber substratum undergo rapid metamorphosis and become young worms within five or six days. During its early growth, the larva builds a protective calcareous cone over its entry hole (9). This development of calcareous cone (Fig. 3) which is achieved within first 48 hours of growth since the attachement to the substratum can be used as a precise indicator of the calcium secretory activity of the test-organisms.

Preparation of veliger bearing timber test pieces : Timber panels immersed in the raft for a period of 7 or 8 weeks and harbouring fully matured Teredo furcifera worms were removed and placed in laboratory aquaria with running sea water. Veliger larvae obtained from these worms were used for the present experiments. All quantitative experimental studies were conducted with the "creeping" larvae obtained from worms that had been retained in the tanks for not more than 2 days.

About 1,000 to 1,500 veligers, all measuring 285 μ in size were placed in crystalline jars containing artificial, sterilised and filtered sea water. The larvae were allowed to attack 3"x1½"x½" timber pieces of Abies pindrow (fir) for a period of 24 hours. The larvae and the timber pieces were discarded if the settlement of the former was delayed beyond 24 hours.

Bio-assessment method : For assessing the influence of varying salinity, temperature and calcium levels of the sea water medium on calcification, replicates of the test pieces holding not less than hundred totally uncalcified larvae were immersed in 500 ml crystalline jars, containing artificial sea water. A period of exposure was 48 hours. The larvae in the test-pieces were examined at the end of 48 hours experimental period under Zeiss binocular microscope. This observation involved an examination of the calcareous cone, the development of which proceeded in four stages described below.

Stage I : Totally uncalcified larva, (Fig. 1).

Stage II : Ill-developed cone, entry hole lined with mucous material, (Fig. 2).

Stage III: Partly calcified cone, absence of bridge.

Stage IV : Fully calcified cone, bridge present, (Fig. 3).

Calcium deposition ability was expressed as the percentage incidence of individuals which produced fully calcified cones (i.e. stage IV) in 48 hours.

After ascertaining the laboratory conditions which suited the most for calcification of the cones, the inhibitive actions of chemical compounds were evaluated by a method essentially similar to one detailed above.

3. Results

Effect of salinity on calcification : Samples of artificial sea water having salinity values ranging from 10 ppt to 40 ppt were prepared and veliger bearing timber test-pieces were exposed to these salinities for a period of 48 hours. Table 1 summarises the degree of calcification at the end of experimental period. It is evident from this table that calcification activity is considerably reduced at extreme salinity values. At salinity values ranging from 25 ppt to 35 ppt, over 80 p.c. larvae produce fully calcified cones (Stage IV).

Effect of temperature on calcification : The rate of calcification at various temperatures of the sea water medium was ascertained. It is noted that at 15°C the calcification is completely arrested and almost all larvae continue to remain at veliger stage not only for a period of 48 hours but even longer if allowed to remain at that temperature. At 38°C, the larvae become moribund and perish without showing any signs of calcification. Only 14 p.c. larvae bear fully calcified cone at 35°C. A sustained calcification is supported at 25°C and as many as 87 p.c. larvae bear fully calcified cones.

Effect of calcium levels on calcification : Normal sea water contains 400 mgs. of calcium per litre. Table 2 summarises the rate of calcification in sea water medium having varying levels of calcium. In absence of calcium or in a medium having low calcium level (100 mgs/Ca/lit) calcification is completely arrested. Low calcium, however, does not affect the deposition of mucous material around the entry holes (Fig. 2). Calcification rate rises steeply between 200 mgs/lit to 500 mgs/lit. In hypercalcium sea water (above 600 mgs/lit) calcification rate is considerably arrested.

Effect of timber species on calcification : Our experience, both at the test sites and in the laboratory, showed that the early metamorphosis and growth of teredid larvae considerably depended on the species of timbers the larvae elected to attack. It is seen that in timber Abies pindrow over 90 p.c. larvae build fully calcified cones in 48 hours whereas in timbers Sertulia campanulata and Mangifera indica calcification is delayed for over a period of 4 days. In teredo resistant timber Tetrameles nudiflora (4) calcification is not achieved until the death of the larvae.

Effects of inhibitors on calcification : For assessing an inhibitive effect of chemical compounds on calcification, test pieces of fir holding fully uncalcified larvae were subjected to four graded concentrations of each of seven compounds examined. The salinity of the sea water medium was adjusted to 25 ppt, the temperature was 25°C, pH 8.2 and calcium level was 400 mgs/lit. At the end of the experimental period, percent incidence of each of the four growth stages at varying concentrations was noted. Typical results in respects of two compounds viz. 2, 4 dinitrophenol and sodium fluoride are given in Table 3. It is evident from the table that with the increasing concentrations of inhibitors there has been a reduced calcification activity in the test organisms. For example at lowest concentration of .000125 M of 2, 4 dinitrophenol as many as 70 p.c. larvae show fully calcified cones whereas at the highest concentration mere 5 p.c. larvae show fully calcified cones. A graded physiological response therefore is evident.

Table 4 summarises the percent incidence of only fully calcified cones in four graded concentrations of seven compounds screened. It is observed that with the increasing concentrations there has been a reduced calcification activity in the larvae. As regards two compounds, sodium succinate and sodium maleate, contrary to expectations, no enhancement of the calcification rate is evident. On the other hand it is poorer than that noted in non-toxic controls. A lack of graded response (calcification) to increasing concentration is also evident in respect of these two chemical compounds.

Inhibitors and general toxic action : Chemical compounds screened in the present investigation are reported to have a specific inhibitory action on calcium metabolism and are therefore not expected to have toxic action on the larvae. That they behave as envisaged is amply revealed by the fact that none of these compounds at the concentrations used exert lethal effect on the test organisms. The test organisms having transferred to normal, non-toxic sea water at the end of the experimental period survived for more than three or four days.

4. Discussion

Currently used antifouling paints contain heavy metal toxic compounds of copper, arsenic and mercury which provide a lethal environment that may repel or kill fouling organisms. The newer antifouling paints as envisaged by Saroyan (10) aim at impairement of the initial attachment of larva either by chemical or other means. The latter possibilities are (a) chemical lousing-up of adhesion cement (b) use of wetting or surface active agents interfering with proper adhesion conditions (c) impairement of antennal suction cup adhesion mechanism. All these possibilities aim at killing of the larvae before their transformation into an young adult form. The control of fouling organisms is, however, also possible or perhaps more practical when these organisms are on the verge of fabricating their calcareous basis and shell encasements as a consequence of post settlement activity. Enquiry into the merits of such an approach is possible only when more and more information on the shell building characteristics of these organisms is available.

For the bioassay method used in this study larvae of various fouling organisms were considered for their use as the test organisms. The larvae of teredo, however, were found to be most suitable material by virtue of the fact that their calcification growth under certain predetermined conditions progressed with no or little individual variations.

The rate of calcification of the larvae varied from species to species of the timber and at that stage of growth largely depended upon the density of the timber. Timber Abies pindrow supported uniform calcification growth and over 80 p.c. of the settled larvae could build their calcium carbonate cone within a short period of 48 hours. Quayle (9) who worked on Bankia setacea reported formation of a complete calcareous cone in that species within seven days. Relatively rapid cone formation in T.furcifera proves of considerable advantage since it helps to reduce the experimental period.

About 19 different amino acids are located in the shell matrix of various molluscan species and these are known to influence crystal type formation of the shell (11). Salinity changes which affect amino acid concentrations in many molluscan species (12) may therefore affect shell formation in veliger larvae. Neff (13) who studied mineral regeneration in serpulid worms observed that in these worms mineral regeneration failed when salinity was below 20 ppt. In larvae of T.furcifera also low salinities retarded the calcification of cone. Calcification rate remained unchanged at salinities ranging from 25 ppt to 35 ppt.

A correlation of environmental temperature and crystal type formation of the molluscan shell has been reported by many workers (14). In the present study calcification of the cone at 15°C was found to be completely inhibited, though larvae survived at that temperature for a considerable period. Calcification did not progress satisfactorily at 35°C. At temperature 25°C, corresponding to that of sea water for most part of the year, calcification was rapid and complete.

In a regenerating adult molluscan shell, calcium comes from various sources like mantle (15), digestive glands (16), the kidney, the blood and the medium. In the present study it was observed that in the absence of total calcium in the medium or in a medium having low calcium (100 mgs/lit) there was a complete absence of calcification activity. Normal calcification activity leading to fully developed cone was noted in normal sea water or in hypercalcium sea water (500 mgs/lit). It is of considerable interest to note that lack of adequate calcium in the melium resulted into failure of the calcification process but not the formation of a mucous layer which supports the impregnation of calcium carbonate. Bevelander and Benger (17) also observed absence of calcification activity in a regenerating shell of Isognomon alatum when the latter were exposed to calcium poor sea water. The organic matrix of the shell, however, continued to be formed under this condition.

Wilbur (3) has discussed possible mode of action of a number of chemical agents on calcium deposition activity of molluscs. For instance Iodoacetate and fluoride decrease the production of respiratory intermediates which provide Co_2 for carbonate. Dinitrophenol decreases the high energy phosphate compounds present in the mantle which are required for the secretion of calcium carbonate and protein synthesis. Sulphonamides may inhibit enzyme carbonic anhydrase whose presence and possible participation in shell formation is suggested by Freeman and Wilbur (18). We examined seven of these inhibitors and these at very low concentrations showed appreciable inhibitory effect on calcification of cone in veliger larvae. Interestingly none of these compounds exerted any toxic action on the test organisms and thereby confirmed their specificity as calcium inhibitors.

Wilbur and Jodrey (19) who examined the action of respiratory substrates like succinate, maleate and oxaloacetate observed that only oxaloacetate amongst these increased calcium deposition four-fold. Maleate and succinate had no significant effect on oyster shell regeneration. In our studies we also did not observe any appreciable increase in the shell growth of veliger when these two compounds were added to the sea water medium.

For the bioassay of candidate antifoulants settling or freshly settled larvae such as cyprids (or pediveligers) have been considered an appropriate experimental material (2). In this laboratory cyprids of seven tropical barnacle species including those of Balanus communis (20) and Balanus variegatus (21) were routinely cultured. However, in view of the considerable individual variations in the rate of their growth, these cyprids could not be used with a desired advantage in the present study. In toxicity experiments, where a decided criterion is the shell building ability of the organisms, teredo larvae, as judged by the present experiments, have been proved to be a very useful experimental material.

5. References

1. D.J. CRISP and A.P. AUSTIN, Ann. appl.Biol., 48, 787, (1960).
2. P. De WOLF, T.N.O. Report No. 64 C, Corrosion and antifouling, (1964).
3. K.M. WILBUR, Physiology of Mollusca, p. 243, Academic press (1964).
4. A.A. KARANDE, Nature, 213, 380 (1967).
5. A.A. KARANDE, Science and Culture, 32, 380 (1966).
6. A.A. KARANDE, K. BALASUBRAMANIAN and S. PREMA, Symposium on mollusca, J.M.B.A. (India), 736 (1968).
7. A.A. KARANDE and S.S.PENDSEY, Proc. Ind. Aca. Sci., 70, 223 (1969).
8. A.A. KARANDE, 2nd International congress on marine corrosion and fouling, 563 (1968).
9. D.B. QUAYLE, Marine boring and fouling organisms, p. 159. University of Washington Press (1959)
10. J.R. SAROYAN, 2nd International congress on marine corrosion and fouling, 469 (1968).
11. N. WATABE and K.M. WILBUR, J. Biophys. Biochem. Cytol., 9, 761 (1961).
12. K. ALLEN, Biol. Bull., 121, 419 (1961).
13. J.M. NEFF, Biol. Bull., 136, 76 (1969).
14. J.R. DODD, J. Geol., 71, 1 (1963).
15. A. ABOLINS-KROGIS, Arkiv Zool., 15, 461 (1963).
16. A. ABOLINS-KROGIS, Arkiv Zool., 13, 159 (1961).
17. G. BEVELANDER and P. BENZER, Biol. Bull., 94, 176 (1948).
18. J.A. FREEMAN and K.M. WILBUR, Biol. Bull., 94, 55 (1948).
19. K.M. WILBUR and L. JODREY, Biol. Bull., 108, 359 (1955).
20. A.A. KARANDE and M.K. THOMAS, Current Science, 40, 109 (1971).
21. A.A. KARANDE, Crustaceana, in press.

Table 1 : Effect of salinity on the growth of calcareous cone of Teredo furcifera larvae

Salinity (ppt)	Percent incidence of calcification stages			
	Stage I	Stage II	Stage III	Stage IV
Control	5	1	0	94
10	85	10	0	5
15	71	8	0	21
20	38	12	0	50
25	6	4	0	90
30	11	10	0	79
35	5	1	0	94
40	42	3	0	55

Table 2 : Effect of calcium level in the medium on the growth of calcareous cone of Teredo furcifera

Calcium mg/lit.	Percent incidence of calcification stages			
	Stage I	Stage II	Stage III	Stage IV
Nil	9	91	0	0
100	25	75	0	0
200	38	38	2	22
300	50	0	10	40
400	14	0	0	86
500	0	0	4	96
600	74	4	2	20
Control	7	0	0	93

Table 3 : Inhibitory effect of Sodium fluoride and 2, 4 Dinitrophenol on the growth of calcareous cones of Teredo furcifera

Sodium fluoride (.01 M) dilutions	Percent incidence of calcification stages			
	Stage I	Stage II	Stage III	Stage IV
25%	24	36	0	40
50%	28	29	0	43
75%	21	61	0	18
100%	91	6	0	3
2, 4 Dinitrophenol (.000125 M) dilutions				
25%	30	0	4	66
50%	48	0	6	46
75%	82	5	7	6
100%	84	6	5	5

Table 4 Inhibitory effect of various chemical compounds on the growth of calcareous cones in Teredo furcifera.

Inhibitory compounds	Presumed action	Percent of normal deposition in oysters (5)	Percent occurrence of IV stage at various concentrations			
			25%	50%	75%	100%
Monoiodoacetate (.001M)	Reacts with SH groups	19.6	0	0	0	0
Sodium fluoride (.01M)	Inhibits glycolysis	45.2	40	45	18	3
2,4 Dinitrophenol(.00012SM)	Reduces high energy phosphate concentration	10.8	67	46	6	5
Toluene-p-sulphonamide (50 mg/litre)	Inhibits carbonic anhydrase	65	48	0	3	2
Benzene sulphonamide (50 mg/litre)	- do -	65	83	50	27	46
Sulphanilamide (50 mg/litre)	- do -	68	8	4	14	13
Beryllium nitrate (.0001M)	Inhibits alkaline Phosphatase	13.9	35	5	6	13
Sodium succinate* (0.01M)	Respiratory substrate	110	65	58	76	52
Sodium malate* (.01M)	- do -	120	74	65	82	57

* Accelerators



Fig.1 Pediveliger larvae of Teredo furcifera.



Fig. 2 Mucous lining around the entry holes of larvae of Teredo furcifera



Fig. 3 Fully developed calcified cones guarding entry-holes of the larvae.



Fig. 4 Unguarded entry holes, failure of cone formation as a result of inhibitive action of chemicals.

On the Nutritional Requirements of Wood-boring Crustacea

Helmut Kühne

Bundesanstalt für Materialprüfung (BAM)
1 Berlin 45, Unter den Eichen 87

Wood or cellulose serve as the chief nutrients for the wood-boring marine isopods of the genus Limnoria. Algae (Enteromorpha intestinalis or Dunaliella sp.) have only a low nutritional value for Limnoria tripunctata Menzies and are unable to substitute for wood. Algal-free suspended matter with marine microorganisms do not serve as food for L.tripunctata. The alga E.intestinalis has also only a low nutritional value for the wood-destroying amphipod Chelura terebrans Philippi. The wood-boring Asopods Sphaeroma terebrans Bate and S.quoyana Milne Edwards, however, were able to survive even when they were exclusively fed on E.intestinalis. They fed on algae and wood when they were offered both. The following Australian isopods and an amphipod occurring in brackish water, which have hitherto not been known as wood destroyers, may also feed on wood: Exosphaeroma alata Baker, Syncassidina aestuaria Baker, Cilicaeopsis sp., Iais sp. and Orchestia sp. They could be kept for one year when fed on wood. Iais is a commensal of S.quoyana and S.terebrans.

Key Words: Limnoria tripunctata, Chelura terebrans, Sphaeroma terebrans, Sphaeroma quoyana, Exosphaeroma alata, Syncassidina aestuaria, Cilicaeopsis sp., Iais sp., Orchestia sp.; wood and algae as nutrient sources.

---

1. Introduction

It is known that the wood-boring Crustacea of the genera Limnoria and Chelura feed on wood and that decay of the wood may increase its nutritional value (1, 2)[1]. Vind, Hochman and Muraoka (3) are of the opinion that Limnoria additionally utilises protozoa and marine microorganisms when cleaning their pleopods. Phycolimnoria which is closely related to the genus Limnoria feeds exclusively on sea-weeds (4). The question is still controversial whether the wood-boring species of the sphaeromatids burrow in wood solely for protection or also for feeding (5). Additional algal food seems to be indispensible at least for Sphaeroma terebrans (6).

In order to find an answer to these questions, feeding tests were carried out with selected species of these groups of wood-boring Crustacea. Experiments with Limnoria were concentrated on determining the nutritional value

[1] Figures in parentheses indicate the literature reference at the end of this paper.

of marine microorganisms and algae. Algae were fed also to Chelura, and tests were made with Sphaeroma to find out whether algae constitute an important food source besides timber. In addition, the nutritional requirements of some Australian Crustacea which were found associated with Sphaeroma in wood in brackish water were examined.

2. Materials and Methods

The specimens of Limnoria tripunctata Menzies and Chelura terebrans Philippi used for the experiments, originated from animals of the Mediterranean which had been cultured for some years in the BAM in artificial seawater (salinity 35 ‰) at a temperature of 22-23° C in the dark. The tests were carried out under the same conditions.

Ten medium-sized animals were placed in a Petri dish (Ø 6 cm) containing appr. 15 ml seawater. Samples (appr. 1 cm x 2 cm area) of the substances listed served as nutrient substrates. Data not included in the table 1 are as follows:

Bacterial filter consisting of cellulose nitrate (Sartorius membrane filter SM 11 308); filter paper consisting of α-cellulose, low in nitrogen (Carl Schleicher and Schüll, No.2095); fir sapwood (Abies pectinata DC.) sterilised by autoclaving; Dunaliella sp., a unicellular flagellate alga; Enteromorpha intestinalis, a green alga. For those tests which should be carried out under aseptic conditions, the nutrient substrate and the Petri dishes were sterilised and the seawater autoclaved or filtered with a bacterial filter. Dishes, water and nutrient substrate were changed every two days. The tests lasted for at least 12 weeks, a period that limnoriids free of food materials do not survive.

The Australian wood-boring Crustacea originated from brackish waters ranging between Sydney and Brisbane. Tests with these animals were carried out in aerated 8-l aquaria and in Petri dishes (Ø 6 cm). The Petri dishes and the aquaria containing only wood were set up in the dark at a temperature of 22-23° C; salinity was 25-30 ‰. Part of the newly hatched animals were placed in two aquaria containing algae and wood in full daylight at 22 and 25° C. At 22° C E.intestinalis grew on the wood, and at 25° C the water was rich in Dunaliella. Pine sapwood (Pinus sylvestris L.), E.intestinalis and frass of Lyrodus pedicellatus Qutrfgs. were used as nutrient substrates for those tests which were carried out in Petri dishes (see table 2). The Petri dishes were examined three times a week during the first month and once or twice a week later in the test. Half the water in the aquaria was replaced every two weeks and the frass was partly removed. The species of Crustacea investigated are mentioned in the results.

3. Results

The results of the tests with Limnoria may be seen in table 1. The average period of survival of unfed animals is appr. 5 weeks. It is independent of the amount of microorganisms present in the water and the frequency rate at which the animals are transferred. Neither was the average period of survival of L.tripunctata increased when the animals were fed with suspended matter which was eliminated from the aquaria by means of a bacterial filter and which contained microorganisms but no algae. The bacterial filter of cellulose nitrate could also not be utilised.

When cellulose filter paper was offered, however, the average period of survival increased noticeably. No difference could be observed between those samples which were kept sterile and those which were not kept sterile. On the other hand there was a remarkable difference in the period

of survival between those animals which were transferred every two days and those which were not transferred. These results call for a critical evaluation of the investigations on the influence of microorganisms on Limnoria. When the number of microorganisms with which the animals come into contact is kept as low as possible, the seawater and the nutrient substrate must be replaced quite frequently, i.e. the animals must frequently be transferred. However, on substrates with a nutritional value the adverse effects of repeated transfers are greater than a possible influence of microorganisms.

As can be anticipated wood has a higher nutritional value than filter paper.

When Dunaliella was offered to the animals their average period of survival increased with regard to the starvation controls,but not at the same rate as with filter paper. When algae were offered in addition to filter paper, this did not improve the conditions of survival. The alga Enteromorpha prolonged the period of survival at the same slow rate as Dunaliella.

The average period of survival of the wood-boring amphipod Chelura terebrans could likewise only nearly be doubled with regard to the starvation controls when Enteromorpha was offered. The average period was extended from 12 days (extreme value 20 days) to 20 days (extreme value 40 days).

The results of the tests with the sphaeromatids are presented in table 2. In evaluating these results it should be considered that only newly hatched animals were used which exhibit a high mortality rate, and that the optimum temperatures and ranges of salinity for these species are not known. Moreover, the number of animals available for the tests was less than those of the limnoriids. The values of the longest period of survival are thus more important than the average values. Sphaeroma terebrans Bate, S.quoyana Milne Edwards and Cilicaeopsis sp. survived longer when they were offered Enteromorpha instead of wood. Exosphaeroma alata survived longest on a wood and algae diet. The frass of shipworms with which the species were associated in the wood, was of no nutritional value. The frass was examined, as Chelura is known to be coprophagous (7).

S.terebrans (fig. 1 and 2), the commonest and most important wood destroyer among the sphaeromatids (8) is most difficult to culture. After a period of 6 months individual young animals were still present in the aquaria with wood and with wood and algae. A third generation, however, did not develop.

S.quoyana has also been known as a wood destroyer (9, 10) (fig.3). The species which is bigger than S.terebrans, has an arcuate pleotelson and only 4-5 teeth on the uropods (fig.4). The species lived up to 6 months in the aquaria with wood only. Young animals developed also when they were kept exclusively on algae (fig.5). Fig.6 shows the first signs of burrows of young S.terebrans and S.quoyana. But both speciesfinally settled on a piece of timber with old galleries of Teredo.

E.alata exhibits a marked sexual dimorphism. It is well camouflaged by the wood. The adult males have strongly broadened uropods and a sharply pointed pleotelson (fig.7), while the females have normal uropods (fig.8). The species developed in the aerated aquaria when it was fed on wood alone or on wood and algae. The third gegneration is still surviving after 12 months.

The yet unidentified species Cilicaeopsis (fig.9) seems to prefer algae. It propagated well in the two aquaria containing algae and wood. However, the animals also feed on the softened exterior parts of wood. When a number of newly hatched animals was kept on wood only, one animal survived for more than 150 days.

Unlike the Cilicaeopsis species Cassidina aestuaria Baker (fig.10) which resembles scale insects, clings firmly to the wood surface. It rasps off wood without building galleries. Algae are not eaten. Cassidina develops and propagates in the aquaria with wood as the only food source even after 12 months.

After the same period the small animals of an unidentified species of the genus Iais still lived abundantly with wood as the sole food. In the presence of S.terebrans and S.quoyana Iais is a commensal of these two species (fig.11). Large numbers may populate the ventral side of Sphaeroma species where they profit from the wood rasped off by the host. When they propagate too strongly, however, they adversely affect the hosts, which suffer from lack of oxygen.

The only representative of the amphipods which survived a 12-month wood diet was a species of the genus Orchestia. The animals rasp off wood irregularly and are probably also coprophagous.

4. Conclusions

The test results indicate that marine microorganisms and algae are not important for Limnoria and Chelura, but that they play an important role as additional food sources for sphaeromatids. Wood preservatives acting as stomach poisons alone can therefore be expected to be less effective against Sphaeroma than against Limnoria species feeding exclusively on wood. The number of species of wood-boring Crustacea in subtropical and tropical/brackish waters is probably higher than is so far known.

Acknowledgement

I wish to thank Mrs. Ingeborg Ehlert for conducting the microbiological tests with Limnoria and Miss Heidemarie Reim and Mr. Eduard von Seydlitz-Kurzbach for their assistance in these tests. Furthermore I express my thanks to Miss Rosalie Keirle, Forestry Commission of New South Wales, Sydney, for supplying me with living Crustacea from Australia, and to Mr. Thomas E. Bowman, Museum of Natural History, Washington, D.C., for identification of the Australian species.

References

1) D. L. RAY, In: Marine Boring and Fouling Organisms (Ed. D. L. Ray), p.46. Univ. Washington Press, Seattle (1959).

2) J. KOHLMEYER, G. BECKER und W.-D. KAMPF, Z. angew. Zool. 46, 457 (1959).

3) H. VIND, H. HOCHMAN and J. MURAOKA, Nontechnical Abstract, U.S. Naval Civil Engin. Res. and Eval. Lab., Port Hueneme, California 8, 40PM (1956).

4) R.J. MENZIES, Bull. Mar. Sci. Gulf and Caribbean 7, No.2, 101 (1957).

5) G. BECKER, In: Marine Borers, Fungi and Fouling Organisms of Wood (Ed. E.B. G. JONES and S. K. ELTRINGHAM) Proc. OECD Workshop, 27th March - 3rd April 1968, p.304. OECD Paris (1971).

6) P. A. JOHN, Habits, Structure and Development of Sphaeroma terebrans (a Wood-boring Isopod) p.4 Univ. Kerala Publ., Trivandrum (1968).

7) H. KÜHNE und G. BECKER, Z. angew. Zool., Beiheft 1, (1964).

8) H. KÜHNE, in: Marine Borers, Fungi and Fouling Organisms of Wood (Ed. E. B. G. JONES and S.K. ELTRINGHAM), Proc. OECD Workshop 27th March - 3rd April 1968, p.65. OECD Paris (1971).

9) C. CHILTON, New Zealand J. Sci. Technol. 2, 3 (1919).

10) A. J. MCQUIRE, Proc. New Zealand Wood Pres. Assoc. 4, 12pp. (1964).

Table 1. The effect of nutrient substrates, microorganisms of the seawater and conditions of handling the animals upon survival of Limnoria tripunctata Menzies at 22-23° C. [a]

Nutrient Substrate	Mean time of survival in days (minimal and maximal time of survival) [number of animals surviving at the end of the test]			
	seawater and substrate changed every 2 days			seawater untreated, changed weekly; substrate not changed
	seawater autoclaved	seawater filtered [b]	seawater untreated	
Polyamide [c] fabric (starvation control)	34 (19...65)	41 (13...69)	36 (7...69)	37 (17...79)
bacterial filter [d] + filtered substances	37 (11...61)	NT	NT	NT
sterile bacterial filter [d]	38 (9...73)	NT	NT	NT
filter paper [e]	47 (13...68) [0]	46 (15...63) [0]	47 (9...86) [0]	>78 (9...>148) [5]
fir sapwood (autoclaved)	c.65 (5...>148) [1]	73 (9...148) [0]	NT	>94 (23...>148) [13]
Dunaliella on polyamide [c] fabric	NT	NT	NT	69 (32...106)
Dunaliella on filter paper [e]	NT	NT	NT	>74 (8...>122) [5]
Enteromorpha intestinalis	NT	NT	NT	c.57 (7...>84) [1]

NT = not tested

a) each group consisting of 40 animals
b) with a bacterial filter
c) Perlon
d) consisting of cellulose nitrate
e) consisting of cellulose

Table 2. Survival of some newly hatched Australian sphaeromatids on different nutrient substrates in artificial brackish water. a)

Species	Mean time of survival in days (minimal and maximal time of survival) [number of animals tested]				
	nutrient substrate				
	starvation control	pine sapwood	Enteromorpha intestinalis	pinewood + Enteromorpha	frass of Lyrodus pedicellatus
Sphaeroma terebrans	16 (2...27) [19]	23 (6...49) [11]	36 (7...93) [11]	26 (6...52) [12]	6 (3...16) [6]
Sphaeroma quoyana	21 (9...33) [12]	24 (8...36) [6]	87 b) (54...120) [6]	27 (8...50) [6]	17 (6...29) [6]
Exosphaeroma alata	39 c) (26...58) [6]	32 (3...62) [11]	23 (8...42) [6]	84 (3...175) [3]	13 (3...36) [6]
Cilicaeopsis sp.	15 (4...37) [16]	32 (17...48) [6]	40 (3...113) [6]	54 (42...71) [3]	21 (8...34) [6]

a) Salinity 25...30 ‰, temperature 22...23° C.

b) One of the two surviving animals was kept on wood for a further 30 days and the other for 75 days before they died.

c) These animals were older than the average used and in addition cannibalism occurred.



Fig. 1. Wood infested by Sphaeroma terebrans Bate. - Fig. 2. Sphaeroma terebrans (Sphaeromatidae, Group Hemibranchiatae). - Fig. 3. Wood infested by Sphaeroma quoyana Milne Edwards. - Fig. 4. Sphaeroma quoyana (Sphaeromatidae, Group Hemibranchiatae). - Fig. 5. Sphaeroma quoyana. Young animals feeding on Enteromorpha. - Fig. 6. First traces of boring by young animals of Sphaeroma terebrans and S.quoyana on pine sapwood. - Fig. 7. Exosphaeroma alata Baker, adult male (Sphaeromatidae, Group Hemibranchiatae). - Fig. 8. Exosphaeroma alata, female. - Fig. 9. Cilicaeopsis sp., female (Sphaeromatidae, Group Hemibranchiatae). - Fig. 10. Synassidina aestuaria Baker (Sphaeromatidae, Group Platybranchiatae). - Fig. 11. Sphaeroma terebrans with Iais sp. (Jaeridae).

Discussion

Turner, Harvard University: Did your Sphaeroma terebrans come from Sydney Harbour?

Kuhne: The collections came from six localities between Brisbane and Sydney and Sphaeroma terebrans were found in three of them.

Turner: Styrafoam floats used for our tests in Sydney Harbour were severely attacked by Sphaeroma terebrans. Perhaps you could use this type of inert substrate in your feeding experiments. Specimens living in styrafoam certainly are not getting any wood in their diet. Martesia striata are the only other borers I have found that live in it.

Kuhne: I do not know the optimum temperature for this species and perhaps my temperature, which was 25°C, was too low.

Turner: That should be about right for specimens from that area. They would experience lower temperatures in the winter and perhaps a bit higher in the summer in the Sydney area.

Dean, Duke University: In some of your experiments you were feeding your crustaceans fairly nitrogen deficient substrates which you were changing every two days, so presumably there was no chance for extensive microbial buildup on the surface. Do you think the survival time was limited by the inability of the crustaceans to get sufficient nitrogen or do you think they have some other adaptation for getting adequate nitrogen nutrition even under those conditions?

Kuhne: I believe the main reason for poor survival was frequent disturbance. We had an idea of the concentration of micro-organisms in the water we used for the experiments so we sterilized the water, wood and dishes but we could not sterilize the animals. Consequently at the beginning of the test we had about 200 bacteria per milliliter while normal water had about 1,000 per milliliter. Our 'sterilized' cultures then had about one-fifth as many bacteria as normal water but in two days it nearly reached the level of normal water. Consequently we had to change the cultures every two days and this was harmful to the animals. The question of nitrogen is often mentioned in the literature but I am not sure where they get it.

Settling of Larval Shipworms, Teredo navalis L. and Bankia gouldi Bartsch, Stimulated by Humic Material (Gelbstoff)

John L. Culliney

Museum of Comparative Zoology
Harvard University
Cambridge, Massachusetts 02138

Pediveliger larvae of Teredo navalis and Bankia gouldi show settling and crawling behavior when exposed to humic material (Gelbstoff) in admixtures of bog water and sea water. The behavioral response in this case appears identical to that exhibited when the larvae encounter wood, their natural substratum. These observations imply that shipworm larvae sense dissolved substances derived from the decomposition of wood in terrestrial humic material. Also implied is that under normal conditions, larvae detect wood in the marine environment largely through chemosensory means. However, T. navalis appears to be so sensitive to the presence of Gelbstoff that its normal dispersal may be reduced in estuaries with high concentrations of humic material.

Key Words: Larvae; Teredo; Bankia; Gelbstoff; settling behavior; shipworm

1. Introduction

A number of kinds of marine invertebrate larvae are known to exhibit settling responses to substrata which are suitable for their adult growth. In these cases, settlement appears to be stimulated by a property or small set of properties identifying the particular substratum as one that supports healthy adult populations of the species (1-5)[1].

Implied in these studies is the idea that the mechanism by which a species recognizes its proper substratum has evolved into a nearly foolproof ecological process. However, in this paper, I will present evidence that the settling response of shipworm larvae may be triggered in the absence of wood when the larvae encounter admixtures of sea water and ground water containing high concentrations of humic material (Gelbstoff).

2. Materials and Methods

Larvae were reared following the basic methods of Loosanoff and Davis (6). They were fed small, naked flagellates, chiefly Isochrysis

[1] The numbers in parentheses refer to the list of references at the end of this paper.

galbana Parke at concentrations of 5 x 10^4 to 1 x 10^5 cells/cc. All cultures were approximately two liters in glass jars, maintained at 26 ± 1°C and 32 ± 1 ‰ salinity. Sea water, clean glass jars and food were renewed daily.

Larvae used in experiments were those displaying the foot as they swam, indicating they were ready to settle. T. navalis larvae came from two different female parents. B. gouldi larvae originated from an undetermined number of parents.

Dilutions containing humic material were prepared by mixing filtered sea water with filtered water from a small pool in a cedar bog in Wenham, Massachusetts. The dark, tea-colored water from this pool was quite acidic, pH = 4.2. The bog was situated at the foot of a hill covered with a forest of white pine, Pinus strobus. The bog vegetation was dominated by Atlantic white cedar, Chamaecyparis thyoides, some of which grew in the pool itself. Only fresh bog water was used in experiments which were carried out the same day as the water was collected.

Salinity controls were prepared by substituting distilled water for bog water in the mixture with sea water. pH controls were prepared by adjusting the pH of sea water--distilled water mixtures with HCl.

3. Observations and Results

The Settling Response

In laboratory cultures, swimming pediveliger larvae of a variety of species of teredinids respond to the presence of wood by suddenly retracting the velum and sinking rapidly to the bottom of the culture. They then begin to crawl actively in a characteristic manner superficially resembling the movements of a geometrid caterpillar, a rhythmic series of extensions and retractions of the slender muscular foot.

The dramatic effect of wood in inducing settling and crawling behavior was first noticed when I placed a small piece of sea-water-soaked pine in a culture of swimming Teredo navalis pediveligers. A number of larvae immediately settled to the bottom of the culture vessel and on the wood and began to crawl. Gentle stirring of the culture with the piece of wood caused many more to settle and crawl. The same settling response was then observed with Bankia gouldi. Simple mechanical stimulation was ruled out as a cause of the response, since stirring the culture with a glass rod never caused settling and crawling.

This generalized response to the near presence of wood has since been observed in numerous other species of shipworms, both oviparous and larviparous. In some cases, larvae do not respond until they physically contact the wood; in others, the response is definitely noted when larvae are within a centimeter of the surface of the wood. Individual responsiveness within a species may vary widely. Among species, those with a long-term larviparous life history appear less immediately responsive than others. This same group, on the other hand, shows spontaneous crawling behavior in the absence of wood far more than larvae of oviparous (planktotrophic) species.

The Response to Gelbstoff

Two simple experiments were set up to examine larval reactions to humic material in sea water. In Experiment 1, two parts filtered bog water were added to three parts filtered sea water (40% dilution). Individual pediveliger larvae of Teredo navalis and Bankia gouldi were then pipetted into 250 ml of experimental (bog water dilution) and control (distilled water dilution) solutions and another control, consisting of a small piece

of wood in 250 ml of full-strength sea water. Each larva was then observed for one minute and its behavior was recorded. About halfway through the experiment, the pH in the control solution was reduced to more closely simulate the experimental solution and the "wood control" was discontinued. The results of Experiment 1 are shown in Table 1.

In Table 1, each entry represents the sequential activities of an individual pediveliger during the one-minute period of observation. A positive settling response is designated as C or C^1. This indicates the animal actually crawled or began to crawl. The other categories of activities do not represent a true settling response.

From Experiment 1, it is easy to see that Gelbstoff in sea water is a powerful stimulus to larvae to settle and crawl. Almost no effect can be attributed to reduced salinity and reduced pH. Furthermore, Gelbstoff seems to affect T. navalis far more than B. gouldi.

Experiment 2 tested longer-term effects of the bog water/sea water mixture on the larvae. A lesser dilution (20%) was prepared from one part bog water to four parts sea water, making 250 ml of experimental solution in each of two cultures. Fifteen larvae of each species were pipetted into the separate containers of Gelbstoff solution. Observations were made of crawling activity at intervals for a period of 45 minutes. These observations are summarized in Table 2.

Experiment 2 gives further evidence that T. navalis is more strongly stimulated by the Gelbstoff than is B. gouldi. That the Gelbstoff is apparently non-toxic is shown by the fact that all the larvae in the Experiment 2 containers were alive and most were swimming after two days. None were crawling at this time.

4. Discussion

Gelbstoff in coastal waters appears to be at least partly derived from the decomposition of woody plants in moist forest soils, fresh water lakes and bogs. Another probable source is metabolites of algae, especially the Phaeophyta (7-9). The relationship between decomposing wood and Gelbstoff makes the settling response of shipworm larvae understandable as induced by a chemical stimulus from dissolved wood-derived compounds in sea water.

My field observations (unpublished) of shipworm activity over a three-year period in the Newport Estuary near Beaufort, North Carolina, show that depletions and conspicuous absences of new recruitment, especially T. navalis, are correlated with the presence of Gelbstoff. Dark colored acidic water, rich in humic material, is characteristic of low-lying coastal drainage areas of North Carolina (10). Storms flush this material from surrounding swamps into estuarine waters, staining them dark yellow-red.

After tropical storm Alma in June 1966, recruitment of T. navalis was completely eliminated in most of the Newport Estuary for over five weeks, at a time of year when this species normally shows the heaviest settlement. Bankia gouldi recruitment was much less affected. The effects of the storm were manifested for several days throughout the Estuary in reduced salinity and reddish-colored water. The salinity, however, did not fall low enough to be deleterious to the larvae, as I have determined in experiments to be published elsewhere.

In another example, recruitment of T. navalis at a station near the mouth of a small creek containing highly colored, acidic fresh water was unusually low and much less than that of B. gouldi. At a neighboring station in the center of the broad estuary, T. navalis recruitment was greater by a factor of up to 40, even exceeding that of B. gouldi.

The results of my Experiments 1 and 2 suggest that in an estuary containing high concentrations of Gelbstoff the pediveliger larvae of Teredo navalis may be stimulated to settle in the absence of wood. This would reduce the numbers of larvae eventually reaching wood by inhibiting or retarding their dispersal. Furthermore, larvae settling on a barren bottom would be unnecessarily exposed to predators, parasites and diseases, and potentially deleterious chemical and physical environments.

Further research on the Gelbstoff-induced settling response will involve standardizing the humic material, investigating threshold concentrations, acclimation and other aspects of larval physiology and behavior.

References

1. D. P. Wilson, J. Mar. Biol. Ass. U. K. 32, 209 (1953).
2. _____, ibid 48, 387 (1968).
3. R. S. Scheltema, Biol. Bull. 120, 92 (1961).
4. D. J. Crisp, Botanica Gothoburgensia III, 51 (1965).
5. J. S. Gray, J. Mar. Biol. Ass. U. K. 46, 627 (1966).
6. V. L. Loosanoff and H. C. Davis, Adv. in Mar. Biol. (F. S. Russell, ed.) Vol. 1, 1, Academic, London (1963).
7. K. Kalle, Oceanog. and Mar. Biol., Ann. Rev. (H. Barnes, ed.) Vol. 4, 91, Allen and Unwin Ltd., London (1966).
8. J. McN. Sieburth and A. Jensen, J. exp. mar. Biol. Ecol. 2, 174 (1968).
9. _____, ibid 3, 275 (1969).
10. D. G. Frey, J. Elisha Mitchell Sci. Soc. 65, 1 (1949).

Discussion

Robert Dean, Duke University: If humic materials are derived from the breakdown of plant products then it is possible that they may be responding to a water soluble extractive of wood, perhaps the same one that leads them to respond to the presence of wood. Do you have any thoughts on that and do you think you can get from your work on humic materials an idea of the active ingredient in wood?

Culliney, Harvard University: Yes. It seems likely that similar chemical stimuli, perhaps of the same molecules, are being released from the surface of wood causing the settling response. The response to Gelbstoff in the estuary is simply a biochemical mistake.

Rosenberg, Northeastern University: At the time of tropical storm Alma was there a rise in temperature that might have knocked out Teredo navalis which is a colder water species? Such a rise in temperature might have benefited Bankia gouldi while being fatal to Teredo navalis.

Culliney: That is a good thought, but my laboratory experiments on rearing the larvae of both species showed that both do very well at temperatures as high as 30°C. So I do not think that is the answer.

Turner, Harvard University: Could you elaborate on the possible effects of differences in salinity tolerance of the two species?

Culliney: I ruled out salinity as causing the mass disappearance of Teredo navalis in the estuary because from my experiments, the results of which will be published elsewhere, I found that Teredo navalis is actually better able to tolerate low salinity than Bankia gouldi. Teredo navalis grows well at salinities as low as 10 o/oo while Bankia gouldi begins to show poor development when the salinity goes below 15 o/oo.

Marshall, University of Tasmania: You mentioned the tremendous complexity of the humic substances and I wondered if the techniques of soil scientists would be useful in analyzing it. Perhaps separating the Gelbstoff by gel filtration would give you some idea of the molecular size range of the material. This is essentially molecular filtration through a series of gels of different exclusion capacities which gives you a range of the different molecular sizes. Tests could then be run to get some idea of which fraction was responsible for the settling reaction.

Culliney: I need someone who is a good biochemist for this type of work. My next step is to get in touch with John Sieburth, University of Rhode Island, who has been breaking down humic material and identifying the components. I know that terrestrial humic materials are apparently derived from lignins. These are phenolic compounds which, in sea water, polymerize to form polyphenoles and eventually form additional complex compounds with other dissolved organic matter. Sieburth found some biological activity in his subfractions which seemed to be antibacterial and somewhat toxic to plaice larvae. He did some bioassays on these flat fish larvae but I am not sure how his concentrations relate to what I used in my experiments. It would be exciting if we could pin down the actual material responsible for the settling response.

Marshall: Many of the chemical techniques used for fractionating humic acids actually modify the structure tremendously so some of the toxic effects may actually be artifacts. This is why I mentioned gel filtration, with this technique nothing is modified; you are simply separating out different molecular 'species' by size.

Muraoka, Naval Civil Engineering Laboratory, California: When teredines are expelled in the pediveliger stage they have only a limited amount of time to find wood, after which they are incapable of boring. Did you find 72-73 hours to be the magic number?

Culliney: It is known that long-term larviparous species lose the ability to bore after a relatively short time. I believe Becker was the first to publish on this. After a period of a few hours to a few days, depending on the species, these larvae lose the ability to swim, the vellum degenerates and they go through all the processes associated with metamorphosis. The foot truncates, the siphons develop and the denticulate ridges begin to appear on the edge of the shell. However, there is evidence that short-term larviparous species and oviparous species have the capacity to delay metamorphosis for long periods of time. Dr. Scheltema, of Woods Hole Oceanographic Institution, in his studies on long distance transport of larvae, found larvae of at least two species of shipworm in mid ocean.

Kuhne, Bundesanstalt für Materialprüfung, Berlin: My question concerns the distribution of Bankia gouldi and Teredo navalis in the area you studied. Normally I would expect Teredo navalis to be in the estuary and Bankia gouldi out in the bay. Is it possible that when the Gelbstoff is released into the water, for instance by heavy rains, that those species which occur inshore react more distinctly than those outside the estuary? Also, if wood is swept out of the estuary by heavy rains it would supply the larvae, responding to the Gelbstoff, with a place to settle.

Culliney: Wood undoubtedly is carried into the bay but I think that if the larvae respond wherever they encounter the dissolved humic material many of them would land where there was no wood. Your comment about the distribution of Bankia and Teredo is interesting because experience has shown that the situation is not the same in all estuaries. It is well known from the studies of Kofoid and Miller in the 1920's that in San Francisco Bay Teredo navalis could tolerate very low salinities and that it penetrated into the upper bay where the maximum salinity during the breeding season was only 13 o/oo. My laboratory experiments showed that Teredo navalis grew well in salinities as low as 10 o/oo. However, in the Newport estuary and in Chesapeake Bay, which is similar in that it is surrounded by low-lying, often swampy country, Teredo navalis is restricted to areas very near the sea whereas Bankia gouldi ranges far up the estuary into very brackish water. If, as suggested here, Bankia gouldi is really more tolerant of humic materials, this may account for its distribution in Chesapeake Bay as well as in the Newport estuary. In San Francisco Bay, however, the country is high, well drained and the bay is fed by only a couple of major rivers so there is much less influence of humic material, and the distribution of Teredo and Bankia is reversed. I am most interested in learning about conditions in the Sea of Azov because in the mid 1950's the Russians found that Teredo navalis had penetrated areas where the salinity was about 10 o/oo. It was found that, as increasing quantities of water were drawn from the Don River for irrigation and industrial purposes, salinity in the Sea of Azov began to rise and Teredo navalis began to enter from the Black Sea. I know little about the geography of the area or the occurrence of humic material but on the basis of our observations I would suspect it was not present in any quantity.

Table 1. One minute observations of responses of individual pediveliger larvae of Teredo navalis and Bankia gouldi to humic material (Gelbstoff) in sea water and various controls. All experiments at 23 - 24°C.

Symbols:

C - crawling
C' - incipient crawling, foot contacts substratum briefly
FM - foot movements other than crawling
Q - quiescent, lying on substratum
S - swimming

Teredo navalis			Bankia gouldi		
Gelbstoff bog H_2O 40% S=22°/oo pH=6.2	Distilled H_2O 40% S=21°/oo pH=7.1	Wood S=33°/oo pH=7.2	Gelbstoff bog H_2O 40% S=22°/oo pH=6.2	Distilled H_2O 40% S=22°/oo pH=7.1	Wood S=33°/oo pH=7.2
C',Q	Q,S	C	C,FM,S	FM,S	C
C,S,C	Q	FM,C	FM,S	Q,S	C
FM,S	Q	FM,C	FM,S	FM,Q	C
C',S	Q	C	C,S	Q,S,FM	Q,FM,C
S,FM,S	FM,Q	C	C,FM	Q,FM,S	FM,C
FM,S	S,Q,S	FM,C	FM,S	Q,S	C
FM,S	Q,S	C	FM,C	Q,S	C
Q	S	C	C',S	Q,S	C
FM,S	S	Q,C	Q,S,FM	S,Q,S	FM,C
S,C'	Q	FM,S	C	Q,S	FM,C
	Distilled H_2O 40% plus HCl S=22°/oo pH=6.0			Distilled H_2O 40% plus HCl S=22°/oo pH=6.0	
C',S	Q,S,FM		S,FM	Q,S	
C	S,C'		FM,S	Q,FM,S	
C	Q,S,FM		FM,S	Q,FM,S	
C	Q		FM,S	Q	
C,FM,S	S		Q,S	Q,S	
Q,S	Q,S		S,FM	Q	
C	Q,FM		Q,S	S	
C,FM,S	FM,S		S	S	
C,FM,S	C,FM,S,FM		Q,S	Q,FM	
C',S,FM	Q,S		Q,S	FM,S	
FM,Q	Q,S,Q		Q	FM,S	
C	Q		S	S	
C,S,C	FM,S		FM,S	Q,FM	
Total number of larvae exhibiting crawling behavior= 15/23	2/23	9/10	6/23	0/23	10/10

Table 2. Observations of duration of crawling responses in larval populations of *Teredo navalis* and *Bankia gouldi* exposed to humic material (Gelbstoff) in sea water.

Gelbstoff (bog water) dilution = 20%
T = 23 - 24°C
S = 27°/₀₀
pH = 6.5
Larval populations: N = 15

Teredo navalis		*Bankia gouldi*	
Time	No. crawling	Time	No. crawling
0	9/15	0	3/15
5 min.	7/15	5 min.	1/15
10 min.	3/15	10 min.	0/15
20 min.	4/15	20 min.	0/15
30 min.	4/15	30 min.	0/15
45 min.	4/15	45 min.	0/15

NOTE: Pages 830 through 835 are missing from this text because the manuscript was withdrawn.

Deep water wood-boring mollusks

Ruth D. Turner
Museum of Comparative Zoology
Harvard University
Cambridge, Mass. 02138

Until 1961 knowledge of wood borers in the deep sea was based entirely on material taken from wood dredged by various cruises. The first tests in deep water were those of Muraoka, Tipper and DePalma. These tests were all accomplished by lowering wood panels on racks or moorings from the surface. Tests are now being made using the deep submersible ALVIN.

From these tests it has been shown that: 1) the intensity of the attack increases with time, 2) the attack is most severe at the sea-sediment interface, 3) the free swimming larvae apparently rise only short distances in the water column, 4) the borers are capable of penetrating substances other than wood, 5) settlement of the larvae occurs most commonly in 'protected' area of the panel.

The scarcity of wood in the deep sea and its patchy distribution apparently has led to isolation and speciation. Notes are given on the distribution and ecology of the species as well as aspects of the importance of these borers in relation to man's activities in the deep sea.

Key Words: Wood borers; deep sea; Xylophaga

The only destructive borers in the deep sea belong to the subfamily Xylophagainae (Family Pholadidae). These small bivalve mollusks resemble teredinids superficially and are often confused with them. The Xylophagainae differ from the Teredinidae most strikingly in lacking pallets and apophyses and in having dorsal plates. Typically xylophagids bore into wood but they also penetrate jute, various ropes, guttapercha, and several kinds of plastics. As wood borers they are beneficial for their activity speeds the reduction and recycling of waterlogged wood in the deep sea thus contributing to the nutrients available to other bottom living forms. Xylophaga have been known since 1822 when Turton instituted the genus for Teredo dorsalis Turton 1819 because he recognized the difference between this species and the teredinids. In 1855 telegraph engineers became painfully aware of the 'cable borer' when submarine cables laid in the Mediterranean failed and the culprits, which had penetrated the jute and guttapercha, were identified by Huxley as Xylophaga. Siemens in 1866 (1)[1] wrote one of the first reports on the destruction of the

---

1 Figures in parentheses indicate the literature references cited which are listed at the end of this paper.

outer coverings of deep sea cables, reporting failures in the Mediterranean and Black Seas. Other reports by Preece (1875), Bontemps (1877), Dall (1886), Wünschendorff (1888), Jona (1896, 1913) and Rivera (1915) followed, recording failures in seas all over the world wherever cables were laid. In shallower waters damage was caused by Teredinidae, Limnoria and Sphaeroma but as far as I can determine damage in depths greater than 200 meters was caused by Xylophaga. Unfortunately little if any of this material was saved so it is impossible to check the old identifications. Protection of the cables with various types of metal sheathing soon became routine and interest in the cable borer waned. Between this time and 1961, with the exception of papers by Purchon (2) on the biology of Xylophaga dorsalis (Turton), and R. Turner (3) on the species found in the western Atlantic and eastern Pacific little notice was paid to them. A few species, extracted from wood caught by chance in a dredge, were named and described but that was all. Knudsen (4) reported on the Xylophaga of the GALATHEA expedition, describing 17 new species, thus more than doubling the number of known species. He discussed their reproduction and distribution suggesting that the restricted ranges of the various species were probably related to the patchy distribution of terrestrial plant material in the sea and the less efficient means of dispersal of the juveniles.

The extension of man's activities and man himself to ever increasing depths in the sea has led to systematic testing of materials, improved methods of collecting and even to experimentation at depths of 2000 meters. Interest in this group was sparked when H. Turner (1961) exposed wood panels on a buoy mooring line at depth of 3000 meters at the edge of the continental slope off New York (39°30'N; 69°40'W). When the bottom panels were retrieved they were found to have about 100 young Xylophaga per square centimeter. This was the first time that wood had been carried to the bottom rapidly enough to insure its freedom from attack on the way down. At about the same time the U. S. Navy began testing materials in the deep sea. On the California coast the biological work was under the direction of James Muraoka (5) of the U. S. Naval Civil Engineering Laboratory and his reports appeared between 1964 and 1967. On the Atlantic coast John DePalma (6) of the Naval Oceanographic Office was in charge of the work and his report on the deep tests off Florida and the Bahama Islands appeared in 1969. Both Muraoka and DePalma kindly sent me all of the borers for study. From this and other material, two new genera and eleven new species have been added to the list of known Xylophagainae. During 1966-1967 Ronald Tipper (7) studied the ecology of Xylophaga off the Oregon coast, and in 1970 New England deep sea lobstermen setting their traps at depths of about 1000 feet (305 meters) came to know Xylophaga. The results of this research and the exposure of 'new' wood in depths ranging from 30 to over 2000 meters has confirmed the fact that: 1) the Teredinidae are basically littoral borers, their depth range extending from the intertidal to depths of about 200 meters and 2)that all borer damage below these depths is caused by Xylophagainae. Floating wood may become infested by teredinids and, as it becomes waterlogged and gradually sinks, carries living teredinids to the bottom. The adults may be able to survive at great depths but they are incapable of reproducing and infecting new wood. In colder waters of high latitudes a few species of Xylophaga, for example, X. dorsalis (Turton) and X. praestans Smith of the north eastern Atlantic and X. globosa Sowerby of Chile may occur at depth of only 3 meters below the low tide.

This research also proves the error of the statement that Xylophaga dorsalis (Turton) "occurs chiefly in floating timber" (2) or that "the genus Xylophaga seems to be largely pelagic, occurring mainly in floating and

waterlogged wood" (3). This erroneous impression probably arose from the fact that during heavy storms waterlogged wood containing Xylophaga may be cast ashore but we now know that this wood is brought up from deeper subtidal waters. Whenever testing is done Xylophaga are found only in panels placed near the bottom and, in warm temperate waters, none have been taken in depths less than 30 meters.

Tipper (7) showed that the heaviest settlement of the larvae occurred within 10 cm of the bottom and Muraoka (1966) found that panels 1 meter up on the test rack were much less severely attacked than those set 15 cm off the bottom. In the Tongue of the Ocean, panels in contact with the bottom were severely attacked while those 15 meters off the bottom were completely free of borers. In an array set about 3 miles off Fort Lauderdale, Florida 9 specimens of Xylophaga were taken from a panel set at a depth of 60 meters in water 92 meters deep. This is unusual but it is possible that the larvae were caught in an up-welling current and by chance hit wood and so were able to settle. A bottom panel at this site had 31 Xylophaga. These data suggest that the larvae rise only a short distance off the bottom, and that their dispersal is largely dependent on bottom currents, lending support to Knudsen's theory that the larvae have an inefficient means of dispersal. It has also been noted from these experiments that the larvae usually settle in crevices or other areas where the current is reduced.

Bruun (8) and Knudsen (4) reviewed the data on the presence of terrestrial plant debris in the deep sea pointing out that it was usually found in trenches near land. They also noted the relationship between the presence of such debris and the general richness of the bottom fauna. The scarcity of wood in boreal areas restricts the northern range, and temperature the southern range of shelf species in temperate and boreal zones. Species such as X. dorsalis, X. atlantica and X. globosa are examples of arctic emergence for they may be found in littoral waters at the colder ends of their ranges. Uniform temperatures below the permanent thermocline allow a wider range of distribution for abyssal species though their presence at any given locality is dependent on the presence of wood. Major problems encountered in studying the geographical distribution of the Xylophagainae include 1) the scarcity and patchy distribution of woody material in the deep sea, 2) the chance factors involved in catching a piece of wood in a dredge and 3) the possibility that present records are only a reflection of dredging stations. Until recently, dredging was the only means of obtaining these borers and the stations are usually limited in number and rather widely spaced, so no satisfactory picture could be obtained. Recent collecting using wood panels attached to buoys or special testing units has shown that wherever wood is placed on or near the bottom borers will eventually appear and that the rate of attack increases with the increase in the size of the breeding population. Very little is known about reproduction in the Xylophagainae but we do know that at least 9 of the abyssal species retain the young in the burrow of the parent, usually attached to the dorsal surface of the parent shell near the umbos. This would insure the young being near wood at the time of emergence but would reduce the possibilities of infecting new wood. Many species of deep sea mollusks have a very wide geographic range but this does not appear to be true of the Xylophagainae. The limited ranges of the various species, probably resulting from the patchy distribution of wood on the bottom, may be compared with island populations of terrestrial species.

The subfamily Xylophagainae is composed of 3 genera, Xylophaga (Turton) with 36 species, Xyloredo Turner (9) with 3 species and Xylopholas Turner (10 - in press) with one species. Of the 36 species of Xylophaga 18 are known from the type locality only, 14 are known from 2 to 8 localities, 1 from 14 and 1 each from 18, 19 and 20 localities. Those species known from the most localities, e.g. washington Bartsch, atlantica Richards and dorsalis (Turton), are all northern, relatively shallow water species which are more readily collected. Species of Xylophaga may be arranged in 6 rather distinctive groups, those in each group being allopatric. Species which are known to retain the young in the burrow all belong to groups 2, 3 and 4. Further knowledge of the living animals will probably show that these species groups are, in fact, good subgenera but at present it seems unwise to name them. The three species of Xyloredo are abyssal and they resemble teredinids even more than Xylophaga for they produce long burrows which they line with a thin calcareous tube. They are, however, readily distinguished from the teredinids because they lack pallets and apophyses (9). The single known species of Xylopholas also makes a long burrow but does not line it. This species has siphonal plates which appear to function similarly to the siphonoplax of Penitella but they are located at the base of the siphons rather than being attached to the valves.

From the above discussion it is obvious that we know very little about the Xylophagainae and certainly nothing about the effects of possible population explosions that might occur as a result of man's activities. Continued testing by suspending materials from the surface is important but such testing has its limitations. However, the development of deep submersibles and their working capabilities has made it possible to do far more meaningful research on the biology, physiology and ecology of abyssal organisms. Biologists at Woods Hole Oceanographic Institution with whom I am privileged to cooperate are at present conducting a series of experiments at a permanent test site south of Woods Hole (39°40'N;70°40'W) in 1800 meters using the deep submersible ALVIN. They are making plankton tows just a few centimeters off the bottom, studying metabolic activity, the extent of microbial activity, and the effects of enrichment of the bottom sediments in addition to studying the fauna and the distribution patterns of epibenthic forms which can be observed and photographed from ALVIN.

One of the purposes for this research is to obtain an understanding of the normal situation in the deep sea so that there is a basis for comparison should the offshore disposal of wastes become a common practice. Jannasch et al (11) hypothesize that "the relatively low rates of microbial activity at deep-water conditions appear to render this way of waste disposal very inefficient" and that "it seems possible to trap substantial amounts of nutrients in solid form in the deep sea". Recent experiments suggest that the major attack on material placed in the deep sea results from the activities of 'nibblers' rather than microbes (Jannasch, personal communication). In one experiment various materials including small wooden dowls were placed in a series of plastic tubes in which several small holes had been drilled. The larvae of Xylophaga entered the holes and completely riddled the wood in that portion of the tube extending above the mud-line. The tubes containing wood were the most damaged after a year on the bottom.

Xylophaga have a large wood storing caecum and like the teredinids utilize wood for food. It is generally believed that reduction of the wood depends largely on the activity of bacteria in the gut. It would appear

then that at least some types of bacteria become really active when taken into the gut of the borers, for reduction of the wood by Xylophaga is usually rather rapid. These borers also appear to have one of the most rapid growth rates of all deep sea bivalves, perhaps a result of their ability to utilize this rich source of nutrients. We now have numerous wood panels exposed at the ALVIN station and it is hoped that in the near future we will be able, for the first time, to observe living animals, to study their anatomy, to determine whether there is bacterial activity in the gut and possibly to rear them. Future experiments are planned to determine the varied types of material into which they will bore.

References Cited

1. C. W. Siemens, On the outer covering of deep-sea cables. Rep. British Assoc. Adv. Sci. 35th meeting, Trans. pp. 187-190. (1866).

2. R. D. Purchon, On the biology and relationship of the lamellibranch Xylophaga dorsalis (Turton). J. Mar. Biol. Assoc. U.K. 25: 1-39, figs. 1-16. (1941).

3. R. D. Turner, The Family Pholadidae in the Western Atlantic and Eastern Pacific Part II Martesiinae, Jouannetiinae and Xylophagainae. Johnsonia 3 (34): 65-160, pls. 35-93. (1955).

4. J. Knudsen, The bathyal and abyssal Xylophaga (Pholadidae, Bivalvia). Galathea Report, 5: 163-209, figs. 1-41. (1961).

5. J. S. Muraoka, Deep-ocean biodeterioration of materials, Parts I-VI. Technical Reports U. S. Naval Civil Engineering Laboratory, Port Hueneme, California, R329 (1964), R393 (1965), R428 (1966), R456 (1966), R495 (1966), R525 (1967).

6. J. R. DePalma, A study of deep ocean fouling, Straits of Florida and Tongue of the Ocean, 1961 to 1968. Inf. Rep. IR 69-22, U. S. Naval Oceano. Office, pp. 1-26. (1969).

7. R. Tipper, Ecological aspects of two wood-boring molluscs from the continental terrace off Oregon. Dept. Oceano., Sch. Sci., Oregon State Univ., pp. 1-137, figs. 1-50. (1968).

8. A. F. Bruun, Remnants of plants in the deep-sea. Galathea Report 1 (5): 15-17. (1959).

9. R. D. Turner, Xyloredo, a new teredinid-like abyssal wood-borer (Mollusca, Pholadidae, Xylophagainae). Breviora no. 397: 1-19, pls. 1-6. (1972).

10. R. D. Turner, A new genus and species of deep-water wood-boring bivalve (Mollusca, Pholadidae, Xylophagainae). Basteria 36: 8 pages, 12 figs. (1972, in press).

11. H. W. Jannasch, K. Eimhjellen, C. O. Wirsen and A. Farmanfarmaian, Microbial degradation of organic matter in the deep sea. Science 171: 672-675. (1971).

Discussion

Muraoka, Naval Civil Engineering Laboratory: When the wood disintegrates what happens to the Xylophaga? One wonders how the species survive because from what one reads about the deep-sea wood is not abundant there.

Turner: When the wood disintegrates the Xylophaga undoubtedly fall out and probably die or are eaten within a short time. If sufficient larvae are present in the plankton to settle on newly submerged wood at a rate of over 100 per cm^2, one does wonder what happens if no wood is available. It is possible that the larvae can delay metamorphosis for long periods of time and that the arrival of new wood on the bottom triggers a settling response. The larvae must be rather widely distributed in the deep sea because wherever we have submerged wood it has eventually been attacked. However, the devastation of the wood at the ALVIN station came as a complete surprise because off California and in the Tongue of the Ocean, Bahama Islands, we had panels exposed for much longer periods of time and the wood, though severely attacked, was not on the point of crumbling. I have wondered if specimens could survive in the firm clay nodules on the bottom but only twice in the hundreds of dredge hauls that Dr. Sanders of Woods Hole Oceanographic Institution has made did he get specimens when apparently no wood came up in the dredge. On one of our ALVIN cruises we collected a large number of clay nodules and these were carefully examined for evidence of Xylophaga but none was found. The most logical answers at present are that the larvae can delay metamorphosis until wood is present or that wood is more abundant on the bottom than we thought.

Neuroendocrine regulation of Reproductive cycle in Martesia striata*

R. Nagabhushanam

Department of Zoology, Marathwada University, Aurangabad, INDIA

The present paper deals with the neuroendocrine regulation of reproductive cycle in the wood boring molusc, Martesia striata. Two types of neurosecretory cells were seen in the various ganglia. Cell Type I: The cells are pyriform in shape; the cell bodies range from 18 to 22 u in length and the secretory material stains red with Mallory's and blue-black with chrom-haematoxylin-phloxin. Cell Type II: These cells are smaller and the cell body is oval in shape, measuring 12-18 u in diameter. The fine granules in the cytoplasm stain pinkish with Mallory's and gray with CHP. The vacuolisation of these cells is very striking and the vacuoles do not possess a characteristic shape. Cytochemical observations on the Type I cells reveal that the cytoplasm of the neurosecretory material contains a high concentration of RNA and the positive tests of PAS and lipid seem to be due to the presence of glycolipid.

The number of Type I cells that contained droplets of secretory material showed a distinct seasonal fluctuation. During July, August and September only a few cells contained granules as compared with the other months. The gonads of the same Martesia were sectioned every month and the condition determined. All the specimens collected during the period from July to September had spent gonads. During this period most of the Type I cells did not contain granules. This parallel between Type I cell activity and the reproductive cycle may be interpreted as an effect of these cells on the gonad.

Introduction

While extensive studies were made on the neurosecretory system of Gastropoda, less is known of this system in Lamellibranchiata (1). Gabe (2) mentioned in a short communication about the occurrence of neurosecretory cells in 20 species of bivalves. Lubet (3,4) described secretory cells from the cerebral and visceral ganglia of Mytilus and Chlamys. This author claims the existence of a correlation between the secretory activity and gametogenesis. Nagabhushanam (5) described the neurosecretory cells in American oyster, Crassostrea virginica.

The present paper deals with the structure and distribution of neurosecretory cells and their physiological role in the marine wood borer, Martesia striata.

Material and Methods

Martesia striata were collected from standard test panels which

*Supported by contract N000 14-70-C-0172 from Office of Naval Research, Wash. D.C.

were immersed at Ratnagiri on the West coast of India. The shell valves were carefully removed and the whole body was transferred to Bouin's or Helly's fluid. Serial sections were cut at 6 u. The following staining techniques were employed: (1) Mallory's triple stain (MS), (2) Gomori's chromalum-haematoxylin-phloxin (CHP), (3) Periodic acid-Schiff (PAS) reaction for polysaccharides after diastase digestion, (4) Sudan Black B, mounted in an aqueous medium and (5) Einarson's gallocyanin-chromalum method for nucleic acids.

Results and Discussion

Neurosecretory cells.

There are three-cerebral, pedal and visceral- pairs of ganglia in the central nervous system of Martesia striata. The ganglia are surrounded by a thin capusle of connective tissue. Immediately beneath is the cellular cortex which envelopes the neuropile consisting of nerve fibres. Two types of neurosecretory cells, differing in size and staining ability with CHP and MS, were seen in the various ganglia. These two types of neurosecretory cells are designated as Cell Type I and Cell Type II.

Cell Type I - The cells are somewhat pyriform in shape; the cell bodies range from 18 to 22 u in length and 12 to 15 u in width. The nucleus is round or oval measuring 8 to 10 u in width; it may be either central or eccentric in position. The secretory material stained red with MS and blue-black with CHP. The granules always appear as very fine particles. Vacuoles are generally absent. In certain cells the secretory material could be seen in the axons. This cell type is represented in cerebral, visceral and pedal ganglia.

Under the phase contrast microscope, the secretory granules appeared as dark masses filling the cytoplasm. The nucleus is transparent with low refractive index. The nuclear membrane is distinctly visible. Towards the periphery of the cell the granules showed Brownian movements. Inside the cytoplasm small spheroids of different sizes are visible besides the granules.

Type I neurosecretory material was poorly preserved by alcoholic fixatives. This loss of granules was appreciably prevented by post-fixing in 10 percent formalin after initial fixation in 80 percent ethanol prior to paraffin embedding. This loss of secretory material appears to be due to the solvent action of alcohol. Careful examination of Helly's fixed adjacent paraffin sections of ganglia, one series stained with Mallory's and the other with Sudan Black B, revealed that the Type I neurosecretory material is strongly sudanophilic. The secretory material gave positive test with PAS after digestion with diastase. In sections fixed in Bouin's fluid and stained with gallocyanin-chromalum the cytoplasm of the neurosecretory cells showed blue colouration indicating a concentration of RNA.

Cell Type II - These cells are smaller than the type I cells and restricted to the cerebral and visceral ganglia. The cell body is somewhat oval in shape, measuring 12-18 u in diameter. Their nuclei are similar to those of Type I cells and the fine granules in the cytoplasm stain pinkish with MS and gray with CHP. In certain cells

the neurosecretory granules are particularly concentrated around the nucleus. The vacuolisation of these cells is very striking; the vacuoles do not possess a characteristic shape. Occasionally very fine particles are observed in the vacuoles. Just as in Type I cells the secretory material leaves the perikaryon by way of the axons.

The neurosecretory cells of Martesia striata show resemblances with resemblances with those described earlier in other lamellibranchs. The most exact resemblance is between the cell which are here described as Type I and those designated as grana II by Fahrmann (6) in Unio and the pyriform-shaped cells of Teredo (7). Grana I described by Fahrmann (6) in Unio and cell Type II of Crassostrea (5) agree very closely with Type II cells of Martesia.

Concerning the distribution of the neurosecretory cells, Type I cells are seen in all the ganglia while Cell Type II is observed only in the cerebral and visceral ganglia. Similar observations were made by Nagabhushanam (5). From a study of the histological sections, various authors (3,5,6) concluded that the neurosecretory material is transported along the axons. The observations in Martesia support this view, the secretory material being traced along the axons.

Cytochemical observations on Type I cells of Martesia reveal that the cytoplasm of neurosecretory material contains a high concentration of RNA and the substance may be glycolipid. This is in agreement with the observations made in Crassostrea (5) and Unio (6).

Seasonal activity of neurosecretory cells

To find out whether there is any change in neurosecretory material in the various cell types, the various ganglia of 30 animals were fixed every month, sectioned and observed for a period of one year (1971). The number of Type I cells that contained secretory material showed a distinct seasonal fluctuation. From Table 1 it could be seen that during July to September 1971 only a few cells contained secretory material as compared with the other months. On the other hand, the number of Type II cells that contained secretory material did not change appreciably. The gonads of the same Martesia were sectioned every month and the condition determined. It has been observed that the spawning of Martesia begins in March and extends up to June and majority of them has spent gonads during July to September period (Table 2). During this period the Type I cells did not contain granules. This observed parallel between the activity of Type I cells and reproductive cycle in Martesia might be interpreted as an effect of these cells on the maturity of the gonads. Nagabhushanam (5) also made similar observations in Crassostrea virginica. The Type I neurosecretory cells in the oysters shoed a distinct annual cycle of activity that correlated with the reproductive cycle. Salanki and Baranyi (8) noticed a change in the accumulation of the neurosecretory material in relation to sexual cycle in Anodonta. From these few studies so far made in the lamellibranchs it may be inferred that the reproduction and spawning in lamellibranchs are under the control of hormones produced by the neurosecretory cells.

References

(1). Welsh,J.H. 1961- Neurohormones in Mollusca. Amer. Zoologist,1: 267-272.

(2). Gabe,M. 1955- Particularites histologiques des cellules neurosecretrices chez quelques lamellibranches. C.R. Acad. Sci. Paris, 240: 1810-1812.

(3). Lubet,P. 1955- Cycle neurosecretoire de Chlamys varia et Mytilus edulis. Ibid., 241: 119-121.

(4). Lubet,P. 1956- Effects de l'ablation des centres nerveux sur l'emission des gameted chez Mytilus edulis et Chlamys varia. Ann. Sci. Natur. Zool., 18: 175-183.

(5). Nagabhushanam,R. 1968- Observations on neurosecretion in the central nervous system of Mollusca. Bull. Natl. Inst. Sci. India, No. 36, 1-16.

(6). Fahrmann,W. 1961- Licht- unt electronenmikroskopische untersuchungen des nervensystems von Unio tumidus unter besonderer Berucksichtigung der neurosekretion. Z. Zellforsch., 54: 689-716.

(7). Gabe,M. and P.Rancurel. 1958- Caracteres histologiques des cellules neurosecretrices chez quelques Teredo. Bull. Inst. France Afr. Noire, 20: 73-79.

(8). Salanki,J. and I.Paranyi. 1965- Studies on the relationship between periodic activity and neurosecretion in freshwater mussel, Anodonta cygnea. Annal. Biol. Tihany, 32: 77-82.

Table 1

Showing active neurosecretory cells of Type I and II in the cerebral and visceral ganglia of *Martesia striata*

(Average of 30 animals)

Year and Month	Type I cells	Type II cells
1971		
January	25	21
February	29	19
March	35	24
April	32	18
May	30	23
June	24	20
July	10	18
August	5	23
September	7	21
October	15	24
November	20	19
December	24	25

Table 2: Condition of Gonads in *Martesia*

Year and Month	No. of animals with ripe gonads		No. of animals with spent gonads		Indistinct gonads
	Males	Females	Males	Females	
1971					
January	9	11	0	0	10
February	12	14	0	0	4
March	13	17	0	0	0
April	16	14	0	0	0
May	12	18	0	0	0
June	9	16	2	3	0
July	4	5	11	10	0
August	2	3	12	13	0
September	1	1	15	13	0
October	10	14	2	4	0
November	12	15	1	2	0
December	14	16	0	0	0

STUDIES OF THE FOULING COMMUNITIES ALONG ARGENTINE COASTS

Ricardo Bastida

Laboratorio de Ensayo de Materiales e
Investigaciones Tecnológicas
(LEMIT), La Plata, Argentina

Comprehensive information on investigations of fouling communities made since 1965 along the Argentine coasts is exposed in the present paper. Studies were made on experimental rafts located in two main harbours: Mar del Plata (38°03'17" S, 57°31'18" W) and Belgrano (38°54' S, 62°06' W). Both areas, of temperate-cold waters show very aggressive communities practically during the whole year.

General hydrological conditions of both areas are compared, and attachment cycles of the main fouling species are presented.

Several ecological aspects are considered, such as trophic relations of the community, role and growth rate of certain species, ecological succession, etc. Fouling development on short term panels seems to be regulated by the water temperature in Mar del Plata's area, as other ecological factors do not modify too much during the year. On the contrary, Belgrano's harbor fouling communities are exposed during the year to great variations in several hydrological factors.

Key words: Fouling communities; experimental raft tests; ecological succession; hydrological characteristics of Argentine harbors; powerstation fouling communities.

---

1. Introduction

The Laboratorio de Ensayo de Materiales e Investigaciones Tecnológicas (LEMIT), together with the Instituto de Biología Marina and the economical aid of several institutions, has been conducting marine fouling studies at several sites on the Argentine coasts since 1965. These studies, carried out by a group of biologists and chemists, have been directed at gathering comprehensive information on the fouling communities' dynamics and its control by antifouling paints.

Fouling studies on the experimental raft were begun in Mar del Plata's harbor and

continued without interruptions until the present. Many contributions of that studied area were published in the lastfew years.

Our second experimental raft was anchored in Belgrano's harbor after preliminary studies that indicated the importance of fouling in the area. Recently the first year of raft observations was completed and we intend to continue with the investigations in the area during the next years. Preliminary observations were also made at a powerstation located in Quequen's harbor which had severe fouling problems in its refrigerating system.

Extending our information to southern areas, preliminary data was obtained from Madryn's harbor, in our Patagonian coast. Due to the lack of an experimental raft in that area, fouling samples were obtained from the piles of the wharf (the only harbor construction) and from two wrecks in the surrounding area. These preliminary observations seem to be important, as the patagonian coast is unknown with regards to its fouling communities and at present an important deep-water harbor related with industrial activities is under construction in the same area and will in a few years of service change, without any doubt, the ecological factors of the area.

Our fouling studies will develope in the future not only covering new sites of the Argentine coasts, but also trying to obtain a deeper knowledge of the studied areas. This will be a kind of challenge for our scientific group, as the flora and fauna of our country is not yet deeply known, which is one of the reasons why ecological studies sometime go rather slowly. And of course it is not neccessary to mention the difficulties in many cases to obtain the neccessary economical support.

Due to the justified regulations of the congress regarding contributions, the present paper tries to give only a brief general view of fouling along Argentine coasts that could be extended by any interested person by reading previously published results, and others that will be published in the future.

2. Mar del Plata's harbor

This is the better known area in fouling aspects, as it was the first place choosen for our investigations. This port, one of the most important along our coasts is mainly dedicated to fishery aspects and overseas commercial traffic.

Settlements of special benthic communities are conditioned by the particular environment of the harbor, and are clearly differentiated from those inhabiting the natural surrounding areas. The most distinctive hydrological characteristics of this harbor are: slight turbulence, slightly lower salinity than in neighboring areas, lower pH, dissolved oxygen and a high content of organic detritus. The water temperature varies within a range of about 15° C annually. Full details of the harbor construction and environmental characteristics have been given in previous papers (1, 2).Graphs of the principal hydrological factors in this harbor are included in another paper presented to this Congress (3) and in Fig. 6.

Since the first tests, attachment cycles of the main fouling species have been registered. Summarizing the information, we include in this opportunity some graphs obtained along three consecutive years (1966-69) for the principal species at four different levels, from surface to 2 meters depth (Fig. 2 and 3).

Ecological succession of fouling communities can be clearly observed through long term panel samples. However very important stages in the evolution of the communities also takes place in extremely short periods. In those areas of aggressive foul-

ing they can only be detected by obtaining samples in short periods of around 5-10 days.

Based on our observations on ecological succession of fouling communities (2, 4) we considered it of great importance to determine the several stages forming the period from the moment the substratum is immersed until the destruction of the fouling community. Unfortunately until the moment there has been no universal criteria by which to define the principal stages of evolutionary processes of fouling communities, although this could be very useful for comparing data obtained in different geographical areas. This could be used as another element for comparing grades of aggressiveness, as this characteristic is not only determined by the species involved, but also by the speed in which fouling communities are formed.

Among the scarce information regarding stages of development of these benthic communities, we think that Kawahara's position is one of the best and also corresponds with our conclusions expressed in previous papers (2, 4, 5).

Based on Kawahara's studies (5) and using our own information, we established six stages (I-VI) that include the whole cycle of fouling community development. In the particular case of Stage II we found neccessary to create three Substages: IIA, IIB and IIC (4).

Trying to study the different stages reached by fouling communities on monthly panels (short-term panels) during the whole year, we used the information gathered during three consecutive years (1966-69). Thought it, we could establish that in our area the maximun stage on monthly panels is stage III. By graphing together stages and water temperature, a close correlation can be observed between both factors(Fig. 4). Another interesting fact is that substages of Stage II always precede and follow Stage I, following the oscilations of mean water temperature. In this case, temperature seems to act as an inhibitor or diminisher of the sexual activity rythm of fouling species, rather than to directly affect the larval stages. On the contrary, Stage III is determined directly by the temperature of the same month, or the month before that provokes a massive sexual reproduction and a fast development of larvae and juvenils.

Due to the scarce information about water line level fouling communities and their important action on vessels, we studied the ecological role of Siphonaria lessoni, a Pulmonate Gastropod associated with the algae-belt. This species was simultaneously studied in neighboring natural areas (6), which allowed us to compare that information with that obtained on experimental floating substratum in the harbor area. This gave us interesting information about the importance of substratum slope in the vertical distribution of the species; the vertical distribution of larvae during the previous stage of attachment; the successional stage that the larvae needs for its association with a fouling community; the true limiting factors of vertical distribution of the species; the factors involved with different shapes of individual shells; the trophic spectrum and some other aspects of its ecology, recently published (7).

Among them we have to mention the peculiar role of Siphonaria lessoni as a fouling organism, as this species is not harmful by itself, but creates suitable conditions for the settlement of other organisms which really are harmful and destroy the anticorrosive paint used at this level. The typical algae-belt found at water-line level, due to its density, eliminates or reduces in a great extent the possibilities of attachment of many invertebrates. In our area this fact is very clear with Balanus amphitrite. Adult populations of Siphonaria lessoni tend to reduce the covered surface of the algae-belt in relation with its grazing habits, leaving exposed surfaces for settling and further development of Balanus amphitrite. The harmful action of barnacles of course, is increased at this level by the absence of antifouling paints.

Growths studies of Siphonaria lessoni (Fig. 5) also demonstrate that experimental rafts are excellent places for this kind of study and suggests that it could be used by biologists more often.

The applied methodology also allowed us to determine that growth rings are useless for the growth studies of this species, as they are not directly related to any characteristic biological process in this life, and can appear at an individual level at irregular intervals.

With regards to our interest on water-line panels, we studied the behaviour of antifouling paints at this level (8) trying to establish a long term investigation plan on this aspect. Preliminary results, actually in press, were promising and show a fair control of invertebrates and algae, despite the particular conditions of this interface level.

3. Belgrano's harbor

Belgrano's harbor is situated in the Bahia Blanca sound, at 38° S. Because of its geographical characteristics, this area offers a sheltered place for the establishment of numerous harbors, and at present we can find Galvan's harbor, Ing. White's harbor and Belgrano's harbor, the last one being the most important and located near the mouth of the sound.

High tides in this area reach from 2.6 to 3.6 meters, creating important currents and the exchange of water from the sound with that of the open sea. Although there are no important fresh water affluents, there are conspicuous draining areas during rainy months.

Maximum degrees of surface water temperature are obtained during December and January, reaching over 25° C. Minimum temperatures can be seen in June, with values under 3° C . The maximum monthly range of temperature is around 10°C, correspondig to June (Fig. 6).

Air temperatures reaches maximum readings generally during January, with temperatures above 30° C. Minimum temperatures are registered between June and August with readings under 0° C, the maximum monthly range being 20° C, in June and August.

Salinity shows conspicuous variations along the sound. Sometimes very high values (41.35 °/oo) can be observed, the minimum being 18.86 °/oo. This amplitude is due to the exchange of waters with the open sea, rainfall and evaporation. Also salty terrestrial areas of the environs play an important role as they contribute with important quantities of salt to be sound during rainy months.

The pH is stable during the year and its values (7.8 - 8.6) are similar to those of normal sea water.

The water in this area has an important content of inorganic suspended particles. The highest readings can be acquired during rainy days, as the rain erodes the intertidal muddy bottom increasing the suspended sediments.

The general hydrological conditions of Belgrano's harbor and surrounding areas are quite different from those observed in Mar del Plata's harbor, and consequently differences can be expected in this fouling communities.

The preliminary studies in this area start in 1967 over an experimental raft (9). Samples were taken from 20 x 30 cm acrylic sanded panels, immersed from surface to 1,30 m depth at three different levels. Studied samples of that year belong to 6 and 12 month immersed periods.

These preliminary studies allowed us to detect that fouling communities in Belgrano's harbor were quite aggressive, showing some important variations with regards to those of Mar del Plata's harbor. Some species which were very common and always present in high number (Caprella penantis, Caprella equilibra, Botryllus schlosseri, Bugula neritina, incrusting Briozoa, Plumularia setacea, Eupomatus dianthus, etc.) were never even seen in Mar del Plata or only occassionally. Other species always present in Mar del Plata's harbor (Mercierella enigmatica, Idotea baltica, Balanus trigonus, Siphonaria lessoni, etc.) were not detected in Belgrano's area.

Results obtained during preliminary studies can be observed in the table III.

Based on this studies we planned investigations on a new raft with different characteristics in order to obtain more extensive data. Recently the first year of observations on the new raft have concluded and the results will be published in the near future.

This last cycle indicates that the fouling in Belgrano's harbor is really aggressive, having less effect on monthly panels only during the coldest months. Fouling on long term panels is always important and reaches high biomass values.

4. Powerstation at Quequen's harbor

For the first time a fouling problem was observed in the water refrigerating system of a powerstation on the Argentine coasts. We are asked for information on the biological problem and possible ways of control.

Quequen's harbor is located to the south of Mar del Plata's port, and not very far from it. This area is scarcely known in relation with its benthic communities and its waters are of a mixed type, receiving waters from the open sea and fresh ones from the Quequen River.

Its water temperature is similar to that observed in Mar del Plata, but its salinity goes from normal sea water values to low ones, specially during the rainy months. It also has an important daily variation due to important tidal currents.

pH values do not modify notably during the year, and water oxygen also mantains normal values.

The possibilities of water exchange between the harbor area and the open sea eliminates or reduces the pollution problem, vinculated with the typical activity of that port.

Our observations in the tubing system demonstrated an aggressive action of some foulers, principally of Mercierella enigmatica in the first section where sea water is injected in the system. In that section this species can form incrustations of 30 cm thickness. However the larvae originate in those inner areas were there is a marked influence of fresh water. In those natural bottoms Mercierella enigmatica forms compact aggregations of high density, and even reaches the point of forming stony masses of 50 cm or more in diameter. During the end of spring, summer and the beginning of the autum, this species shows an important sexual activity. In that period when the water current flows in the direction of the sea, lavae penetrates in great number in the refrigerating system. Once attached, they accelerate their normal growth rhythm due to the continuous water flow that transports extra available food; they are able to reproduce in the tubing , but we do not know yet if the larvae can attach once again in the system.

Although we do not have information during the whole year, it is probable that

the incrustations of Mercierella enigmatica diminish totally or in part during the coldest months, at least this happens on the experimental raft in Mar del Plata's area (2, 4).

The inner sections of tubing are colonized by another type of community, characterized by the presence of two Mytilids: Brachyodontes rodriguezi and Mytilus platensis, the last one never reaches the largest size of natural areas. They attach to the tubing wallsforming some areas of great density, but the fouling thickness never exceeds 5 cm. The attachment of these molluscs is mainly produced on the lateral sides of tubings, while the floor and roof are always practically clean. Other species that can be found between Mytilids are Pododesmus rudis, Balanus amphitrite, Cyrtograsus altimanus and Cyrtograpsus angulatus, but always in low densities. Both Cyrtograpsus are always of small size. Bigger individuals probably can not remain attached to the substratum due the water current.

The main problem at the powerstation is created by the presence of specimens of Mytilus platensis in the brass tubes of the condenser, as their presence creates particular currents that destroy those tubes. To replace them the powerstation has to stop for some days, reducing its power production. Until the moment we do not have information regarding whether this problem is created by valves of dead specimens transported by the water flow or if they belong to "in situ" attached specimens.

These general observations allowed us to outline an investigation plan of the fouling of the tubing and surrounding area that probably will be carried out in a near future. The use of doses of chlorine for the control of the fouling in the refrigerating system is suggested.

5. Madryn's harbor

Fouling studies in this area are quite interesting for several reasons. As we mentioned before there is no available fouling information for the Patagonian coast. From the biogeographical point of view it is very important as it is the limit between two biogeographical provinces: the Argentine province and the Magallanic province.

Madryn's harbor is placed in the Golfo Nuevo that covers approximately 2 200 km^2 and its mouth is quite narrow (12 km). Because of its great depth, absence of low extended bottoms and narrow mouth it constitutes an area of peculiar characteristics, different from the greater part of the Patagonian coast. Waters are generally calm, differing notably from the rough sea that predominates in most parts of the exposed Argentine coast.

Tides are of great importance in all the gulf. The vertical range of tides can exceed 4 meters, creating important currents near the mouth. Mean water monthly temperatures go from 9.7° C (in August) to 18.3° C (in February) (Fig. 7). Salinity values ranges around 33.5 °/oo and are stable throughout the whole year. Dissolved oxygen has normal values, while the pH values correspond to those normal of the sea water. Water visibility is very high, mean values are around 10 meters, but sometimes reach more than 20 meters. Suspended organic detritus are in low densities. All these general hydrological characteristics clearly separate this area from the rest that have been studied.

Samples were obtained from vertical metallic wharf piles, from the highest tide level to the bottom, around 10 m depth. Also samples were obtained from two wrecks at 5 and 15 m depth.

Due to the conspicuous tides, the wharf exhibits important intertidal communities. For a better exposition we shall make reference to fouling communities describing them from supralittoral level to infralittoral, based on Pérès's classification.

Supralittoral level.

This level is characterized by a Cyanophyta community where these algae are dominant species (Lyngbia aestuarii, Oscillatoria nigroviridis, Oscillatoria bonnemaisonii, Phormidium fragile, Spirulina labyrinthiformis, Spirulina subtilissima, Calothrix crustacea, etc.). Among these algae and also at lower levels can be found Chironomidae larvae and eggs. Cyanophyta generally form a very thin dark green film.

At lower levels and near to the limits of the midlittoral level, the Gastropod Siphonaria lessoni fringes the upper limit of the Enteromorpha sp. belt over which this species grazes. Individuals of Siphonaria lessoni reach bigger sizes at this latitude than in northern areas. The presence of Siphonaria lessoni over the algae belt confirms the observations made in Mar del Plata where the vertical distribution of the species depends on the algae belt limits (7). Both species, Siphonaria lessoni and Enteromorpha sp. continue their distribution in the following level.

Midlittoral level.

At the upper limit of this level generally is found Brachyodontes purpuratus that replaces Brachyodontes rodriguezi, a typical species of the northern coast of our country. Generally this species creates dense populations that give shelter to different species of invertebrates and also Siphonaria lessoni that grazes on epibiont algae and diatoms. Continuing down Brachyodontes purpuratus populations mixed with another Mytilid, Mytilus chilensis, a replacement species of Mytilus platensis typical of the northern coast.

When Brachyodontes purpuratus disappears in lower levels, and after some extention of pure aggregations of Mytilus chilensis, appears another Mytilus, Aulacomya magallanica (= A. ater), a mollusc of great economical importance that can reach great size. Between the masses created by mussels, generally can be found several species of crabs such as Cyrtograpsus altimanus, Halicarcinus planatus, the isopod Exosphaeroma sp. and the molluscs Fissurellidea hiantula, Patella magallanica and Gaimardia trapeziana. At this level, barnacles of different species also attach, among them the most conspicuous is Balanus psittacus, one of the world's biggest species. However this species is not found at midlittoral level in surrounding areas (10), probably because rocks in those areas are not hard and compact. In these places Balanus psittacus distributes itself in shallow waters in the infralittoral.

The algae of the midlittoral level is very important and such richness has never been registered in northern areas. Its qualitative and quantitative characteristics seen to vary notably during the year, but still manu studies have to be done to establish the seasonal presence of species and also the acute vertical distribution limits.

Among the most common species we can mention: Enteromorpha sp., Ulva lactuca, Cladophora sp., Chaetangium fastigiatum, Nemalion helmintoides, Scytosiphon lomentaria, Polysiphonia spp., Ceramium rubrum, Ceramium sp. and also some of the Cyanophyta mentioned at higher levels but always in lower densities.

During our observations we could not find the two species typical of midlittoral level of the surrounding areas (10): Corallina oficinalis and Hildebrandia lecanellieri. Probably the metallic characteristic of the substratum was the reason for their absence.

Infralittoral level.

As it has been seen in natural areas of our northern coast the upper limit of this level is indicated also by the presence of Chlorophyta of Codium genus. This algae is represented in our sample area by three species: Codium fragile, Codium vermilara and Codium decorticatum, the last one quite uncommon in the wharf piles but more common in deeper water over one of the wrecks.

At this level can also be found the Mytilus chilensis - Aulacomya magallanica community, together with Balanus psittacus. At infralittoral levels is where Aulacomya magallanica reaches its maximum length, over 15 cm.

Associated with Codium fronds generally could be found two typical crabs, Leucippa pentagona and Rochinia gracilipedes and also the mentioned species Cyrtograpsus altimanus and Halicarcinus planatus. Many species of Gastropods are generally found at this level such as Patella magallanica, Tegula orbignyana, Trophon geversianus, Epitonium orbignyi, Fusus acanthodes, the chiton Plaxiphora aurata and several species of Serpulinae and Spirorbinae worms.

Although the richest algae biomass is found at midlittoral level some species go deeper such as Polysiphonia spp., Ceramium rubrum, Ceramium sp., Pterosiphonia sp., Colpomenia sinuosa, etc., reaching a maximum depth due to the clear waters.

In wharf areas of low light intensity it is typical to find the presence of Lithothamnia covering the substratum as a paint film would. Also common in those places are another Rodophyta Rodhymenia sp., the luminescent anemone Corynactis sp. and the tunicates Ciona intestinalis and Ascidea sp.

Over the wrecks is commonly found the brown algae Dictyota spp. and in some occasions isolated specimens of Macrocystis pyrifera.

Our experience in the geographical area indicates that a great part of the Latinamerican coast is scarcely known in relation to fouling and marine wood-borers and the only way of solving this problem seems to be the creation of local investigation groups to carry out these studies in each country.

Perhaps using the last words of an exposition is not exactly the best way to call out for cooperation programs on fouling studies in Latinamerican countries. But anyways it is a means of communication, and if we get possitive results, one of the main objectives of this kind of congress will be obtained.

6. References

1. Bastida R.- Compte Rendu, 2nd. International Congress on Marine Corrosion and Fouling, Athens, Greece: 557-562 (1968).

2. Bastida R.- Rev. Mus. Arg. Cs. Nat. B. Rivadavia, 3 (2): 203-285 (1971).

3. Rascio V.- Communication. 3rd. International Congress on Marine Corrosion and Fouling, Washington, USA, (1972).

4. Bastida R.- LEMIT, serie II (168): 1-55 (1970).

5. Kawahara T.- Rep. Fac. Fish., Pref. Univ. Mie., 4 (2): 27-41 (1962).

6. Olivier S. R. and Penchaszadeh.- Cah. Biol. Mar., 9: 469-491 (1968).

7. Bastida R., Capezzani D. and Torti M. R.- Marine Biology, 10 (4): 297-307 (1971).

8. Rascio V. and Bastida R.- LEMIT, serie II (218): 43-71 (1972).

9. Bastida R. and Torti M. R.- LEMIT, serie II (188): 47-75 (1971).

10. Olivier S., Kreibhom I. and Bastida R.- Bol. Inst. Biol. Mar., 10: 1-74 (1966).

TABLE I

Stage	Substage	Months	Temperature	
I		September 1966 September 1967 September 1968 September 1969		11,2° C
II	II A	June 1967 July 1967 August 1967 June 1968 July 1968 August 1968 June 1969 July 1969 August 1969	10,1° C	
	II B	October 1966 February 1967 April 1967 May 1967 November 1967 May 1968 October 1968 November 1968 October 1969	15,3° C	13,1° C
	II C	November 1966 December 1966 March 1967 October 1967 April 1968 May 1969	15,8° C	
III		January 1967 December 1967 January 1968 February 1968 March 1968 December 1968 January 1969 February 1969 March 1969 April 1969		19,6° C

TABLE II

PRINCIPAL CHARACTERISTICS OF MAR DEL PLATA'S, BELGRANO'S AND MADRYN'S HARBORS

MAR DEL PLATA	BELGRANO	MADRYN
Lat.: 38° 03'18" S Lon.: 57° 31'18" W	Lat.: 38° 54' S Lon.: 62° 06' W	Lat.: 42° 46' S Lon.: 65° 02' W
Biogeographically belongs to the Argentine Province	Biogeographically belongs to the Argentine Province	Biogeographically belongs to the Magallanic Province
Tide amplitude: 0.9-0.6 m	Tide amplitude: 3.6-2.6 m	Tide amplitude: 4.7-2.9 m
Low tidal currents	Important tidal currents	Moderate tidal currents
Low turbulence	Low turbulence	Low turbulence
Reduced midlittoral level with hard bottoms (artificial and natural)	Extended midlittoral level with soft (muddy) and hard (artificial) bottoms	Extended midlittoral level with soft (sandy) and hard (artificial) bottoms
Water temperature with seasonal cycles	Water temperature with seasonal cycles	Water temperature with seasonal cycles
Salinity fairly constant with values near those of normal sea water	Salinity with important monthly variations	Salinity very stable, values similar to those of normal sea water
Dissolved O_2 values under those of normal sea water	Dissolved O_2 values similar to those of sea water	Dissolved O_2 values similar to those of sea water
pH values under the normal ones	pH values similar to those of normal sea water	pH values similar to those of normal sea water
Low water visibility	Very low water visibility	High water visibility
Abundant bioseston	Abundant abioseston	Scarce seston
Intersticial sediment of fouling (organic detritus)	Intersticial sediment of fouling (mudd and clay)	Intersticial sediment of fouling (calcareous and SiO_2)
Fouling communities with several local species	Fouling communities with several local species	Fouling communities with many local species
Fouling communities with a high grade of epibiosis	Fouling communities with a high grade of epibiosis	Fouling communities with a high grade of epibiosis
Growth rhythm of certain species very accelerated, communities of low stability	Growth rhythm of species near normal values, fairly stable communities	Growth rhyth of species normal, with development of very stable communities
Communities with high number of cosmopolitan species	Communities of high number of cosmopolitan species	Communities with very low number of cosmopol.species
High percentage of pollution indicating species	Low percentage of pollution indicating species	No pollution indicating species
Experimental raft on service	Experimental raft on service	No experimental raft

TABLE III

BELGRANO'S HARBOR RAFT. FOULING ORGANISMS REGISTERED IN THE PRELIMINARY STUDIES(1967)

Species	Number of individuals or relative abundance				
	Medium panel	Lower panel	Upper panel	Medium panel	Lower panel
	6 months observations		12 months observations		
ALGAE					
Enteromorpha intestinalis...	-	-	VC	R	-
Enterom. cf. prolifera.....	-	-	R	R	-
Cladophora sp.....	-	-	-	R	-
Petalonia fascia.....	-	-	VC	R	-
Ectocarpus sp.....	-	-	C	R	-
COELENTERATA					
Plumularia setacea.....	C	C	-	C	R
Gonothyraea inornata.....	-	-	-	R	R
NEMERTEA (indet.)	4	-	5	4	3
ANNELIDA					
Hydroides sp.....	8	-	-	-	-
Eupomatus dianthus.....	21	6	-	12	-
Eupomatus plateni.....	5	3	-	2	1
Serpula vermicularis.....	-	1	-	-	-
Halosydnella australis.....	10	31	4	13	18
Syllidae	30	41	12	38	41
Nereidae	-	-	4	-	-
MOLLUSCA					
Pododesmus rudis.....	-	5	-	-	-
Brachyodontes rodriguezi....	-	4	-	1	-
Pyrene paessleri.....	-	1	-	-	-
Littoridina australis.....	-	-	1	-	-
CRUSTACEA					
Balanus amphitrite.....	1580	341	350	1132	386
Corophium sp.....	55	16	> 300	210	93
Gammaridea indet.....	8	28	> 300	50	17
Caprella cf. penantis.....	10	1	5	2	-
Caprella cf. equilibra.....	111	15	-	8	9
Sphaeroma sp.....	-	-	19	-	-
Exosphaeroma sp.....	-	-	1	-	-
Cyrtograpsus altimanus.....	25	89	3	3	1
Pilumnus reticulatus.....	-	1	-	-	-
INSECTA					
Chironomidae larvae.....	-	-	13	-	-
ENTOPROCTA					
Pedellina cernua.....	-	-	-	-	R

TABLE III (cont).

BELGRANO'S HARBOR RAFT. FOULING ORGANISMS REGISTERED IN THE PRELIMINARY STUDIES (1967)

Species	Number of individuals and relative abundance				
	Medium panel	Lower panel	Upper panel	Medium panel	Lower panel
	6 months observations		12 months observations		
BRYOZOA					
Bugula neritina.....	-	C	R	C	C
Bugula sp.....	-	-	-	R	R
Scruparia ambigua.....	-	-	-	R	R
Alcyonidium polyoum.....	-	-	-	-	R
Bowerbankia sp.....	-	C	C	C	R
Cryptosula cf. pallasiana...	A	VC	C	VC	VC
Canopeum sp.....	A	VC	C	VC	VC
TUNICATA					
Ciona cf. intestinalis.....	9	113	-	2	-
Molgula sp.....	-	-	6	17	20
Ascidea sp.....	-	-	2	-	10
Botryllus schlosseri.....	R	R	VC	VC	VC

Key of the table: A Abundant
VC Very common
C Common
R Rare



Fig. 1

Harbors studied in the Argentine coasts

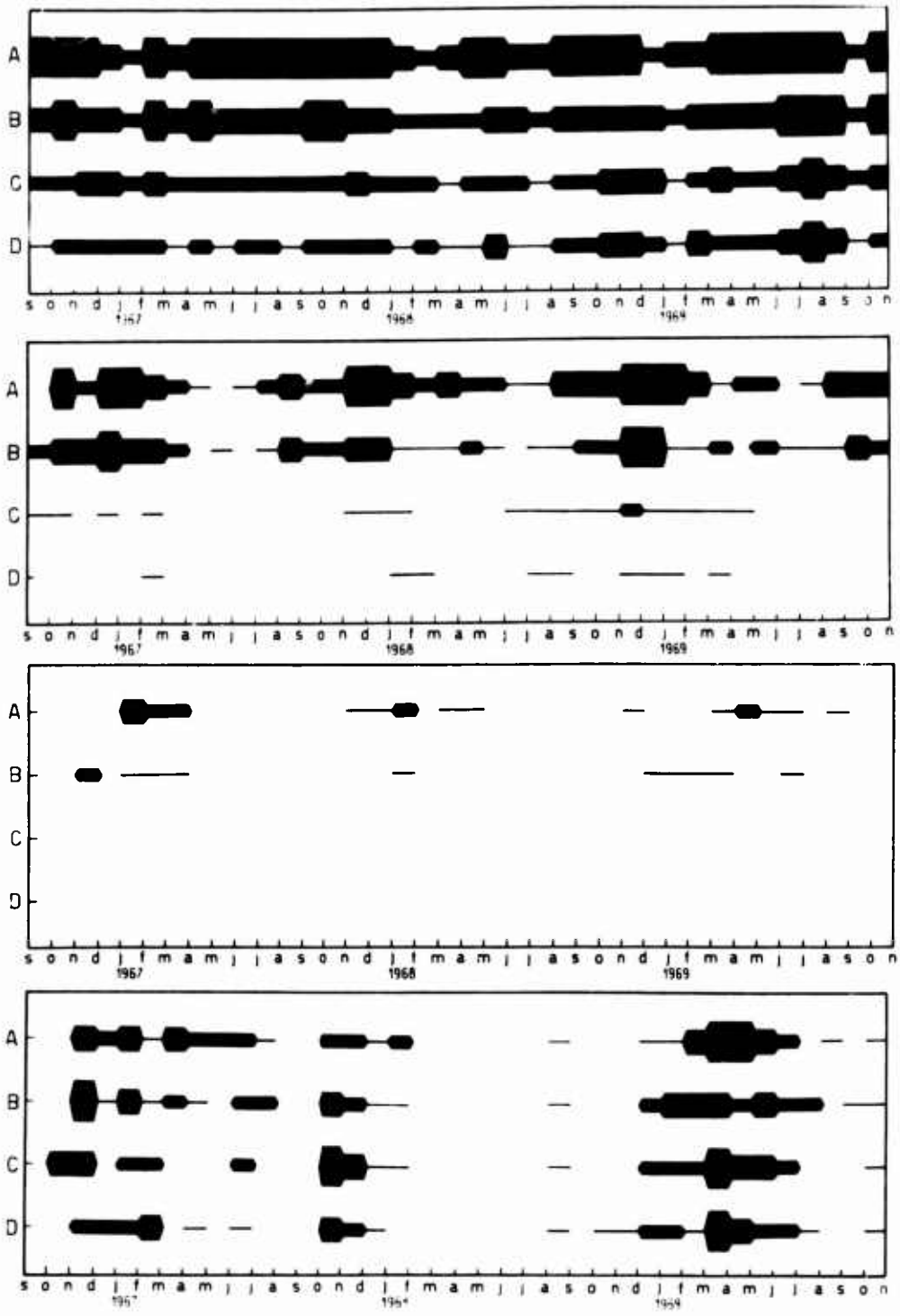


Fig. 2.- Diatoms (I), Enteromorpha intestinalis (II), Ulva lactuca (III) and Tubularia crocea

15

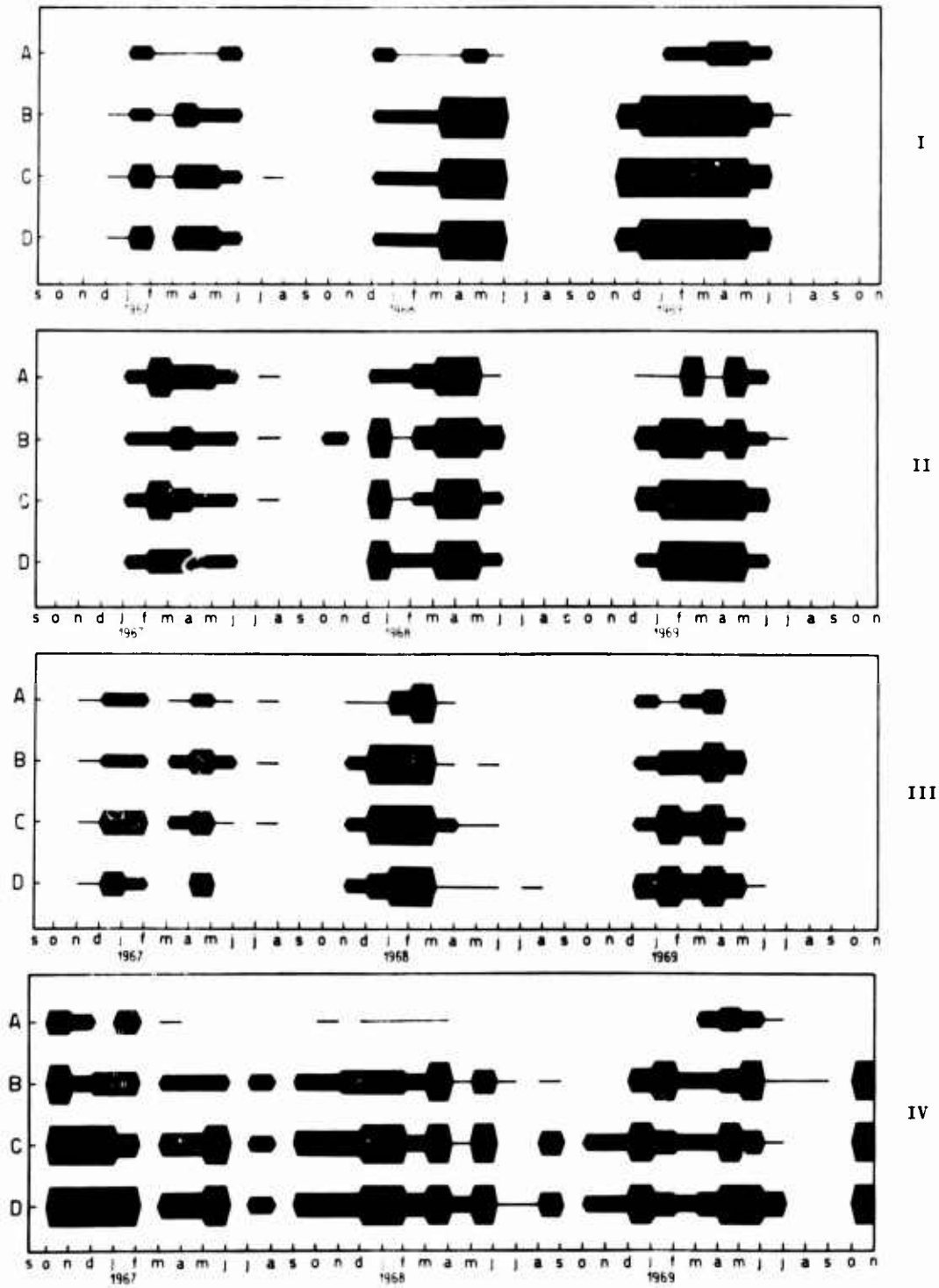


Fig. 3.- Serpulids (I), Balanus amphitrite and trigonus (II), Bugula sp. (III) and Ciona intestinalis (IV)

16

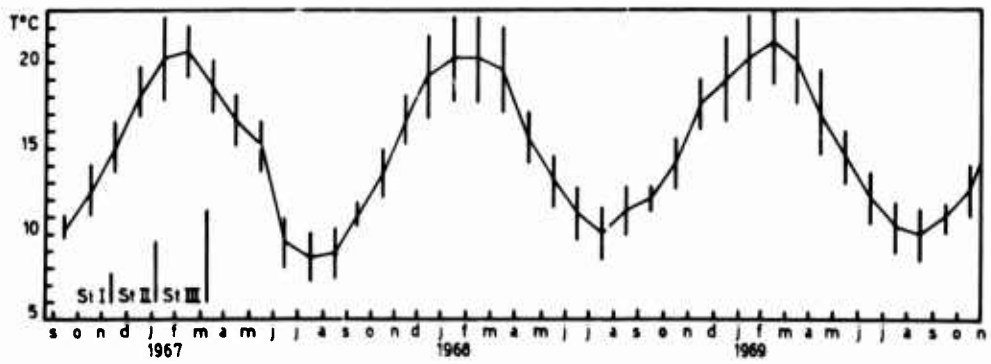


Fig. 4

Relations between stages and water temperature

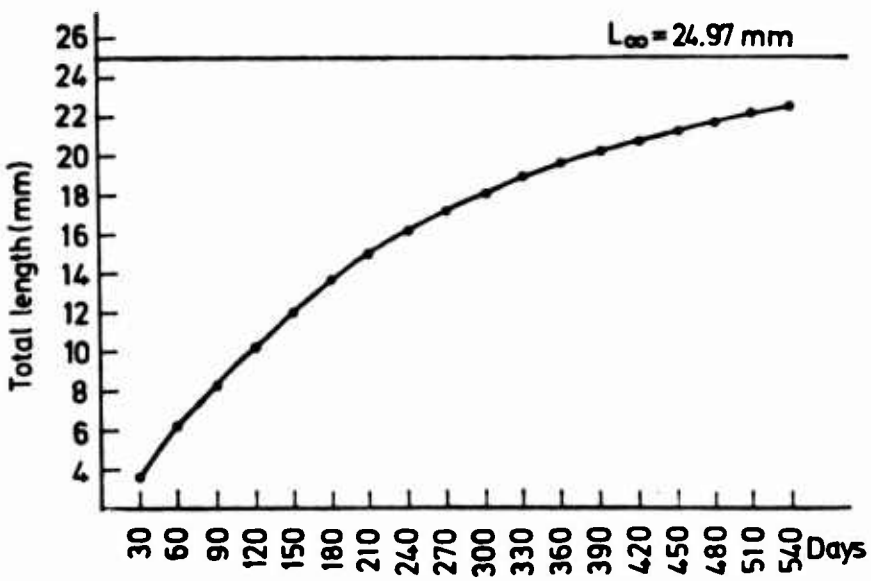
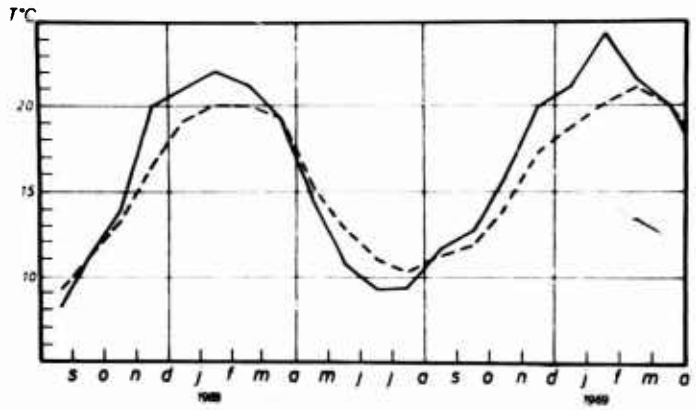
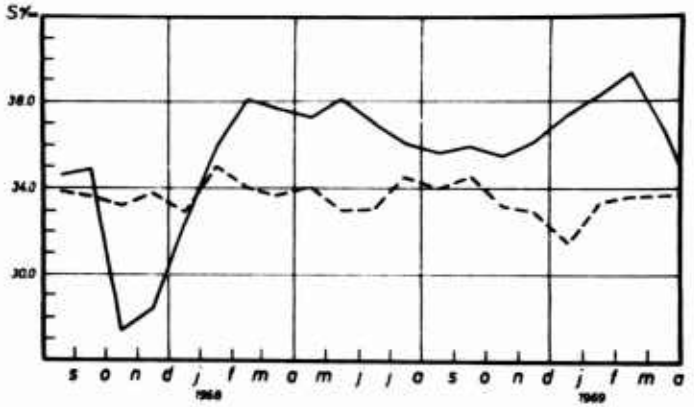


Fig. 5

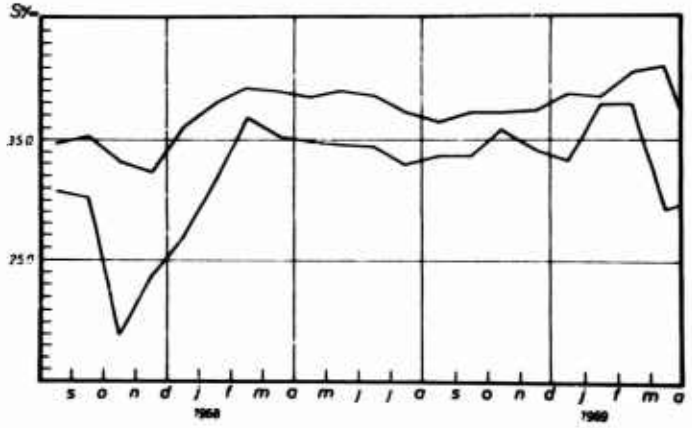
Siphonaria lessoni: growth curve



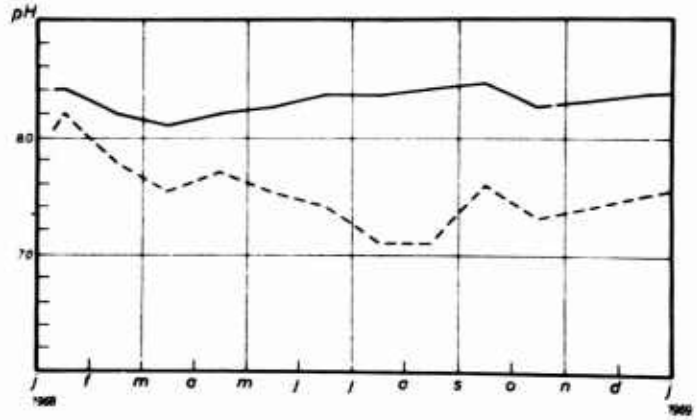
Monthly average temperature of water



Monthly average salinity



Monthly salinity (maximum and minimum)



Monthly average pH of water

Fig. 6.- Hydrological conditions of Belgrano's and Mar del Plata's harbors

—— Belgrano's harbor ------ Mar del Plata

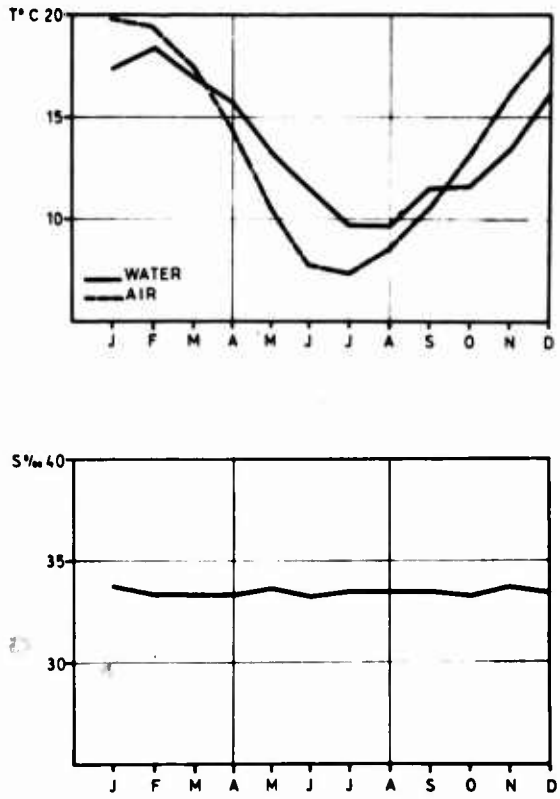


Fig. 7

Temperature of water and air, and salinity, Madryn's port

Fearless Fouling Forecasting

John R. DePalma

Naval Oceanographic Office
Washington, D. C. 20390

A foreknowledge of local marine fouling conditions is required by ocean scientists, engineers, and architects for effective planning and decision-making. At the Naval Oceanographic Office, we are attempting to provide this information in a form that can be readily understood and used. One format that we are developing is the growth curve nomogram, from which fouling rate forecasts can be made within various marine environments. Our initial growth curve nomogram for warm coastal environments makes use of two generally accepted assumptions about coastal fouling organisms; first, that the larvae generally originate in nearshore broodsites, and second, that they are carried to offshore substrates by coastal currents. We believed that if these assumptions were correct and could be quantified, it might be possible to distinguish a pattern of diminishing fouling intensity with increasing depth and distance from shore; and, since coastal currents tend to flow parallel to the shoreline, that this basic pattern should persist wherever local factors are not limiting.

To test this hypothesis, we collected fouling organisms on test panels at a grid of stations off Fort Lauderdale, Florida. Dry weight data from a 12-month series of these test panels were plotted on a cross-sectional map of the test area, and these values were then contoured by percent of maximum accumulation, using the highest value (shoreline station) as 100%. A pattern of decreasing density of settlement away from shore and away from the sea's surface was consistently demonstrated.

We tested the Fort Lauderdale forecasting model at 27 other warm-water coastal stations to see how extensively this pattern persisted. We found our forecasts to be better than 70% reliable at 19 of these stations. However, stations located in regions where the bottom had a very gentle slope-angle produced higher-than-expected fouling rates, and stations located near small, coral-reef fringed islands produced lower-than-expected fouling rates. Forecasting models appropriate for these environments, as well as for cold coastal and open-ocean regions, will be constructed.

Key Words: Marine fouling forecasting, coastal fouling rate; open-sea fouling rate; warm-water fouling growth form; cold-water fouling growth form; mid-ocean island fouling growth form; warm-water fouling test model; fouling rate prediction.

---

1. Introduction

Ocean scientists and engineers require advance information on fouling conditions in different regions of the world's oceans for effective planning, designing, and decision making. To satisfy this requirement, the Naval Oceanographic Office is sampling fouling

communities in the world's faunal provinces and attempting to identify trends that might permit both long- and short-range forecastings. We are now 10 years into this sampling program, and certain regularities of both growth form and concentration that may be predictable are becoming increasingly apparent.

We are now able, in most cases, to distinguish between coastal and open-sea fouling communities on the basis of the dominant organisms comprising each. Within the coastal domain we can detect a warm-water growth form and a cold-water growth form, which seem to meet and mingle at about the 15° C. mean annual surface isotherm (fig. 1). Within the warm-water environment, we sometimes can further differentiate a mid-ocean island modified growth form, the effect of heavy grazing of the fouling community by coral reef fishes, and a shortage of suitable substrates along sandy shores.

We also have noted definite trends in the relative intensity of fouling attachment. We have observed that in open-sea areas the fouling rate diminishes from the surface to approximately the bottom of the mixed layer. Below the mixed layer, fouling organisms do not attach in sufficient numbers to be a problem for most applications, except very close to the bottom at all depths. In coastal areas, the maximum fouling attachment is likely to be found close to shore, with amounts decreasing seaward and with increasing depth. We think that these slightly different patterns of distribution indicate that open-sea fouling larvae originate in floating, oceanic broodgrounds, while coastal fouling larvae originate, for the most part, in permanently fixed shoreline broodgrounds.

Fouling rates are extremely variable within the confines of harbors and estuaries, depending on the relative stress of pollution or other local factors. This variation has been demonstrated by many different pierside fouling studies.

The offshore extent and intensity of settlement in coastal areas seems to be related to the declivity of the bottom; i.e., in regions where the bottom slopes off very gradually, coastal fouling organisms tend to be found attached in greater numbers and farther from shore than in regions with steep slopes. We think this can be accounted for in two ways: First, the circulation of the waters in large shallow basins, usually wind and tide influenced, tends to move fouling larvae rapidly away from shore, and second, there is simply less water available in shallow basins to dilute the numbers of potential fouling larvae produced in nearshore broodstocks.

If the assumptions we are making about the origins of fouling larvae and the mechanisms of dispersal are correct, and if these factors are regulating, and if normal distribution patterns can be quantified -- then, fouling rate forecasts should be possible on a regional basis wherever local factors (pollution, predation, etc.) are not limiting.

To test the above hypothesis, we sampled the local fouling community at a grid of stations off Fort Lauderdale, Florida between 1964 and 1968.

The coastline at Fort Lauderdale is regular and oriented nearly north and south. The bottom within 10 miles of the coastline is generally a calcareous sand, and it slopes rather steeply into the Straits of Florida. The Fort Lauderdale site is described in greater detail in an earlier report (1).

A warm-water site, rather than a cold-water site, was selected for construction of our initial forecasting model because warm-water fouling communities are more easily quantified. Not only do warm, coastal fouling communities enjoy continuous settlement and growth of individual members, but the community tends to establish and maintain a consistently low-profile, hardshelled growth form, extending from the surface to the bottom. Cold-water fouling communities, on the other hand, tend to be layered; i.e., dominated by substantial amounts of bulky forms (mussels and kelps) near the surface and by low-profile, cementing, calcareous forms near the bottom. These bulky forms attaching in the surface layer may produce 100 times as much dry weight per unit area of substrate as can be produced near the bottom.

A coastal site was selected in preference to an open-sea site for construction of the initial model because "blue-water" sampling, particularly over long periods of time, is both more difficult and more expensive.

2. Methods

We exposed standard 15-cm. by 30-cm. wood/asbestos test panels at the stations shown in figure 2 to determine fouling rates at various depths and distances from shore. The term "fouling rate" is here defined as dry weight of attached organisms per unit area of substrate per unit time of exposure. This dry weight value provides a quantitative measure of fouling productivity.

Offshore test panels were hung vertically at 30-meter intervals between 15 meters below the surface and 1 meter above the bottom, mostly from buoyed arrays. Panels were also exposed 1 meter below mean low water at the shoreline. The panels were exposed for monthly and cumulative periods of time up to 12 months. These sampling techniques are standard for Naval Oceanographic Office biofouling studies.

After recovery, the fouling organisms were identified, counted, and measured, and the fouling material was scraped off the asbestos surface, oven-dried to constant weight at 100° C., and weighed.

The dry weight values from a series of 12-month exposures were then plotted on a cross-sectional chart of the test area and contoured by percent of maximum accumulation, using the highest value (shoreline station) as 100% (fig. 3). This contouring revealed, not surprisingly, a regular decreasing density of settlement of fouling organisms with depth and distance from shore. Subsequent testing of this contour chart showed it to be a useful tool for long-range (12-month) forecasts of fouling conditions at Fort Lauderdale.

To obtain short-range forecasts as well, we plotted, one interval at a time on semi-log graph paper, all of the dry weight data (1-month, 2-month, 3-month, etc.) collected during 1964 to 1968 from all of the stations within each contour interval. We then enclosed the scatter of data points for each interval in bands and fitted the bands together to form a scatter diagram (fig. 4). After the scattergram overlaps were resolved, 80 of 102 data points (78%) remained within the appropriate limits of each zone.

This scattergram now provided a quantitative, long- and short-range predictable description of the fouling conditions off Fort Lauderdale, Florida. Still to be determined, however, was how extensively this pattern persisted in other warm-water coastal regions.

3. Testing the Model

To determine the extent of this coastal distribution pattern, we then assembled all of the fouling rate data from 27 other warm-water (15° C. mean annual surface temperature or greater) stations we had sampled since 1961. These stations were located in various coastal environments off Florida, Puerto Rico, the Bahama Islands, Jamaica, Ecuador, Sardinia, Hawaii, Okinawa, Japan, and Thailand. The data bits from each station were plotted as before, and the scatter of values from each station was tested against the Fort Lauderdale scatterband for an equivalent depth and distance from shore.

As expected, data from most of the stations (19 of 27) fit the Fort Lauderdale pattern very well. Taken in total, 74% of 330 data points from these 19 stations fell within predicted limits. Within individual zones, the reliability ranged from a high of 80% in zone D, which had the largest number of data points, to a low of 68% in zone B, which had the second highest number. These 19 stations were all located in regions where the shelf had a moderate to steep gradient (greater than 2°).

It was interesting to note that of the eight stations that did not fit the Fort Lauderdale pattern, dry weight data values from two were off-scale on the high side (more fouling than expected) and values from the other six were off-scale on the low side (less fouling than expected). Both of the stations having unusually high rates of fouling were located well offshore in large, shallow basins (Osaka Bay and the Gulf of Thailand) where the bottom slope angle was less than 2°. The pattern of the plotted data values from these two stations indicated that in shallow regions a modified zone chart will be required, with individual zone limits extending a greater distance from shore. We are presently collecting data which will be used to construct this modification to the basic warm-water coastal fouling rate zone chart.

All of the six stations having the unusually low fouling rates were located on or near coral reefs [Jamaica, the Bahamas, two sites in Puerto Rico, and two sites in the Ryuku Islands]. Many of the recovered test panels from these sites showed evidence of fish predation. There was no apparent pattern to the plotted dry weight data values; variations in the dry weights from individual test panels seemed to be more a reflection of the relative severity of predation rather than of time, depth, or distance from shore.

We then turned to the published literature for other tests of our warm-water coastal fouling rate forecasting model. We were able to locate only two other investigators who had attempted to quantify offshore fouling in terms of dry weight. One of these, Denise Bellan-Santini (2), weighed dried scrapings from a conduit pipe moored normal to the shoreline in 17 meters of water at an unspecified distance from shore, in a region of the western Mediterranean Sea having a moderate shelf slope. She states that the Fort Lauderdale dry weight values were "quite comparable to those obtained on the pipe." Pequegnat, Gaille, and Pequegnat (3) also collected dry weight fouling data from offshore sites in the shallow basin of the northeastern Gulf of Mexico. Their values were high compared to values from equivalent Fort Lauderdale sites. The high values might be either a reflection of the gentle sloping shelf or from the fact that the Gulf of Mexico samples included substantial numbers of secondary foulers (amphipods and other unattached forms). Secondary foulers were not generally harvested at Fort Lauderdale.

4. How to Forecast Warm-Water Coastal Fouling Rates

To forecast warm-water coastal fouling rates, first determine the gradient of the bottom in the area of interest. If the angle is greater than 2° (width and depth of shelf ratio 35:1 or less), then estimate the depth of water, distance from shore, and anticipated length of exposure at the emplacement site. Next, plot a point on the Basic Warm-Water Coastal Fouling Rate Zone Chart (fig. 3) appropriate for this depth and distance from shore. Finally, determine the zone for this point and the relative position within the zone (high side, middle, low side). The width of the appropriate zone, measured along the abscissa for exposure time in the Warm-Water Coastal Fouling Rate Scattergram (fig. 4), is the range of dry weight values that can be expected to accumulate per one-half square foot (450 square centimeters) of vertical surface over this period of time. This range of values can be refined according to the relative position of the point within the zone. For example, if an object is planted on the bottom, one-half mile offshore in 17 meters of water, it will accumulate 85 to 230 grams of dry weight fouling per one-half square foot of substrate in 11 months, with the additional likelihood that this amount will be closer to 230 than 85.

Vertical surfaces are specified in these computations because they represent average fouling conditions. It should be recognized, however, that the lower face of horizontal surfaces will accumulate approximately 10% more dry weight fouling per unit area per unit of time and the upper face approximately 10% less.

Appendix A is a series of photographs which shows the relative accumulation of fouling in the various zones.

5. Concluding Remarks

Although our present forecasting model provides only a range of dry weight values, marine scientists and engineers will find it useful for planning and decision making. So far it has been found to have wide application along continental shelves where the average gradient is greater than 2 degrees (fig. 1). Eventually we hope to be able to forecast fouling conditions in all marine environments.

Within the limits described, we can demonstrate better than 70% reliability for our predictions, which isn't bad for biological phenomena, and puts us just behind the Old Farmers Almanac among FEARLESS FORECASTERS.

References

1. JOHN R. DePALMA, A study of deep-ocean fouling, Proceedings of the Second International Congress on Marine Corrosion and Fouling, Athens, Greece (1968).

2. DENISE BELLAN-SANTINI, Salissures biologiques de substrats vierges artificiels immerges en equ pure, durant 26 mois, dans la region de Marseille, II. Resultats quantitatifs, TETHYS, 2(2):357-364 (1970).

3. WILLIS E. PEQUEGNAT, R. S. GAILEY, and L. H. PEQUEGNAT, Biofouling studies off Panama City, Florida. II. The two-mile offshore station, Reference 67-18T, Texas A. & M. University Research Foundation Report (1967).

Discussion

There were two comments on the differences in abundance of fouling encountered along continental coasts and around oceanic islands. The first was that these differences might be a consequence of the relative concentrations of primary producers. The second credited these differences more to the conflicting mechanisms of larval dispersal around islands, and larval containment in bays.

Mr. DePalma was asked if different water masses did not cause variations in settlement. He answered that he had observed species differences but not significant weight differences in warm-water coastal environments.

There were also two comments on the subject of fish grazing. The first described briefly an experiment recently concluded near the Virgin Islands that did in fact quantify the predation on fouling communities by reef fishes. The other was a reminder that fish grazing is not restricted to coral reefs.

Another person described the effects of current speed on growth rates of fouling organisms, and suggested that more precision could be obtained in the nomogram if this factor could be incorporated.

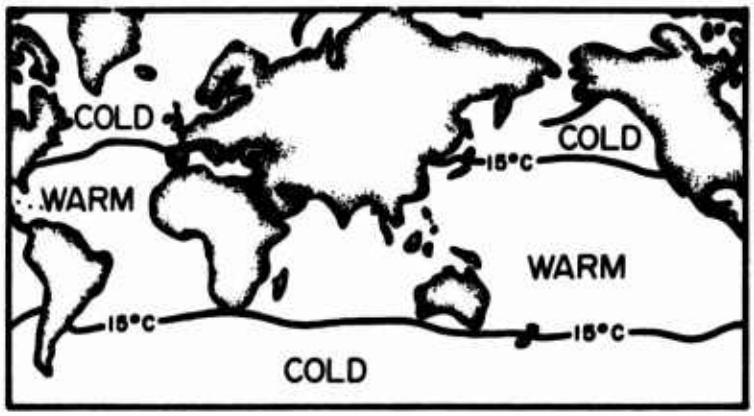


Figure 1. The World, Showing the Generally Accepted Limits of Warm Seas.

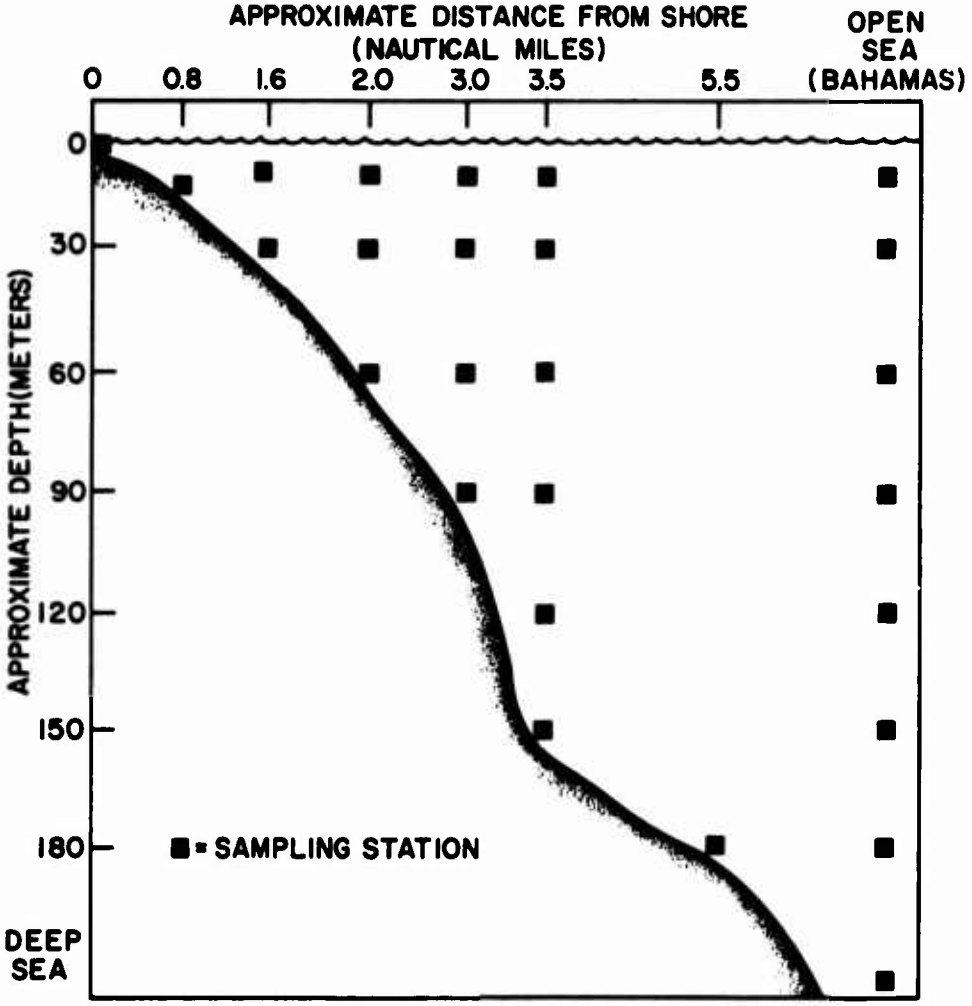


Figure 2. Study area off Fort Lauderdale, Florida showing approximate location of stations where fouling rate data were collected during 1964 - 1968.

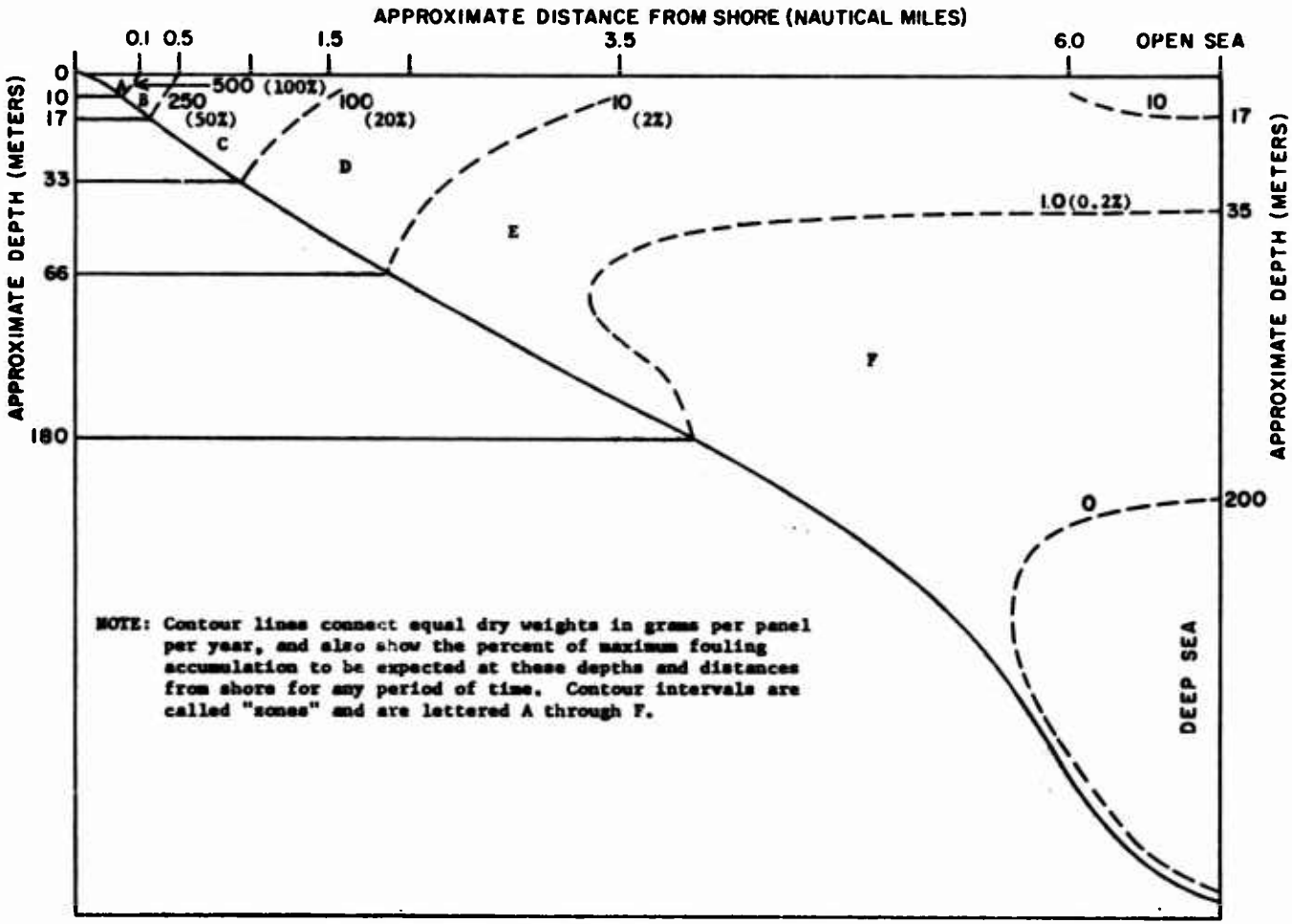


Figure 3. Basic Warm-Water Coastal Fouling Rate Zone Chart.

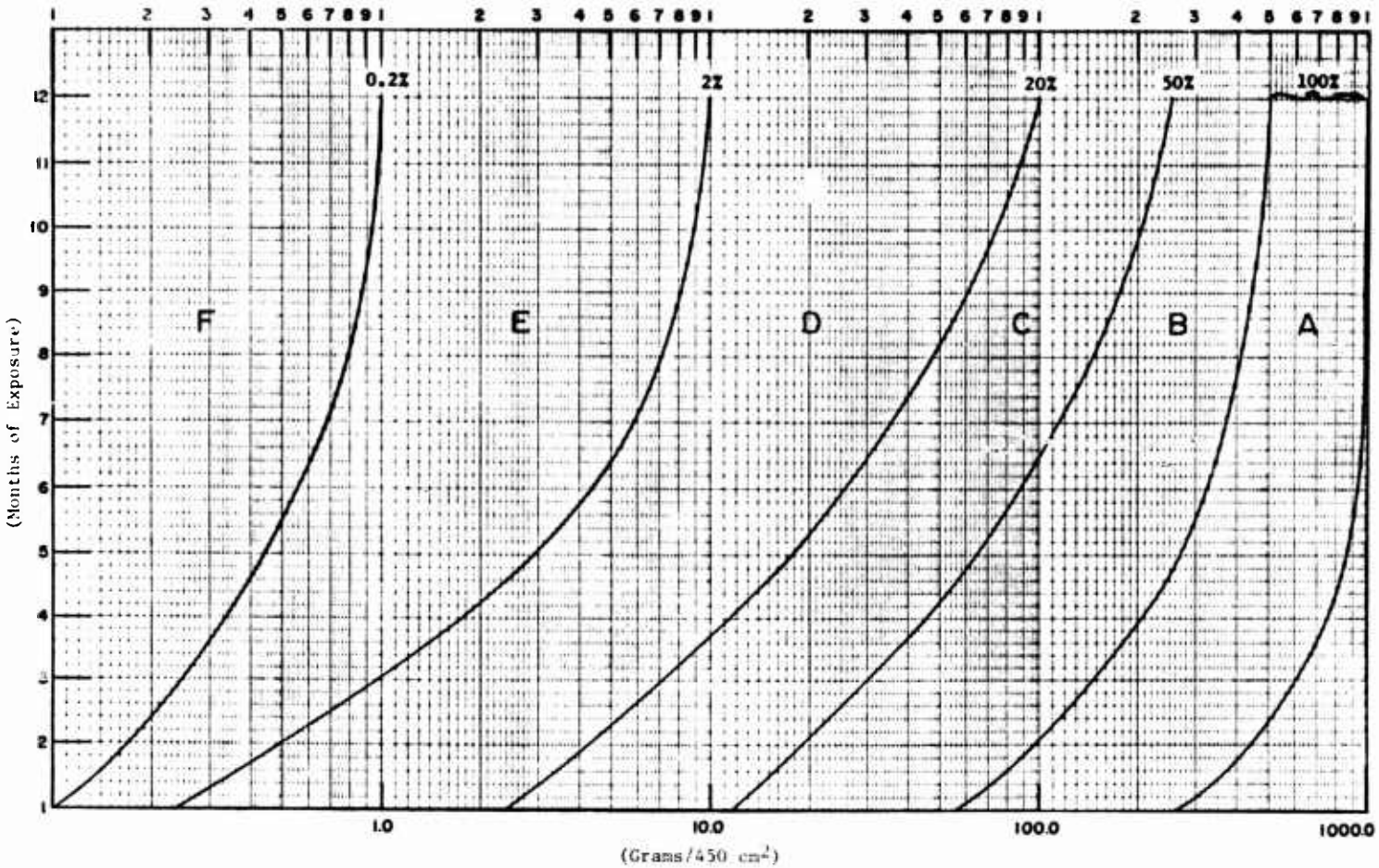


Figure 4. Warm-Water Coastal Fouling Rate Scattergram.

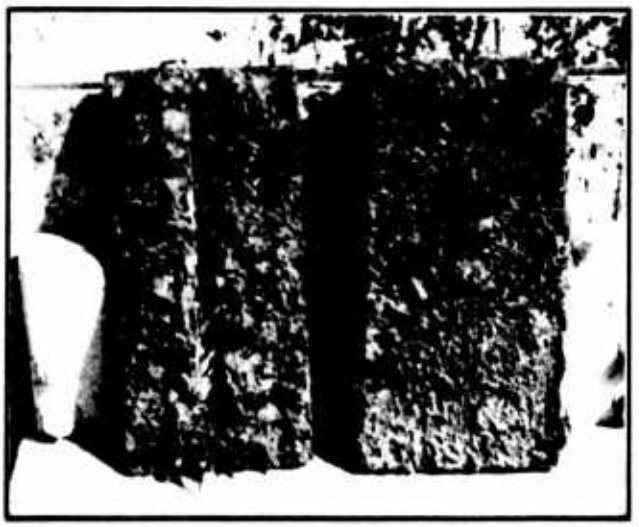
Appendix A

Relative Fouling Accumulation in the Various Zones



12 Months
Dry Weight - 610 grams/panel (450 sq.cm.)

ZONE A



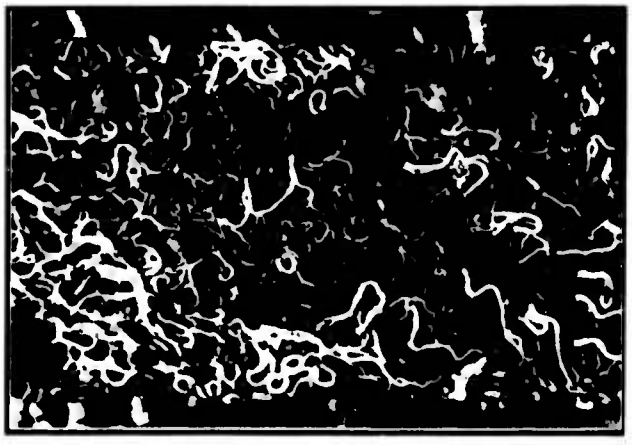
6 Months (Oct-Apr) - Middepth
Dry Weight - 295 grams/panel (450 sq.cm.)



12 Months - Bottom
Dry Weight - 485 grams/panel (450 sq.cm.)

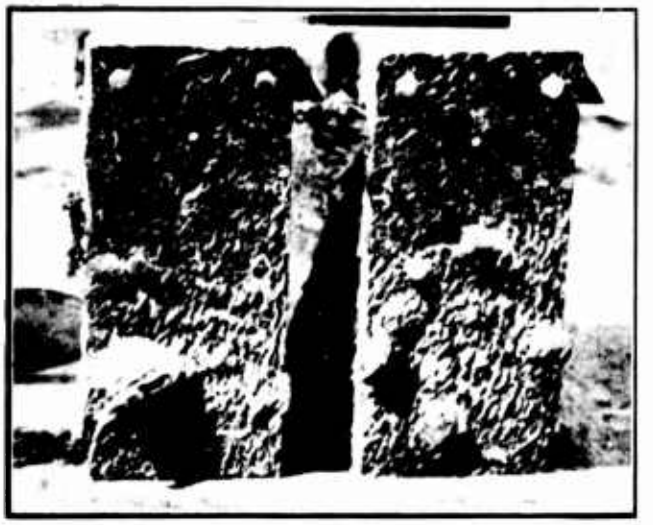


12 Months - Middepth
Dry Weight - 122 grams/panel (450 sq.cm.)

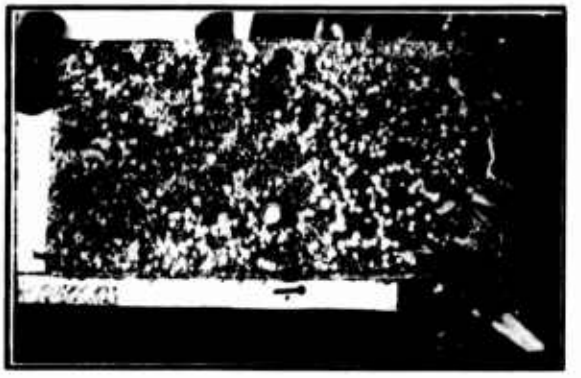


12 Months - Bottom
Dry Weight - 180 grams/panel (450 sq.cm.)

ZONE C



12 Months - Middepth
Dry Weight - 30 grams/panel (450 sq.cm.)

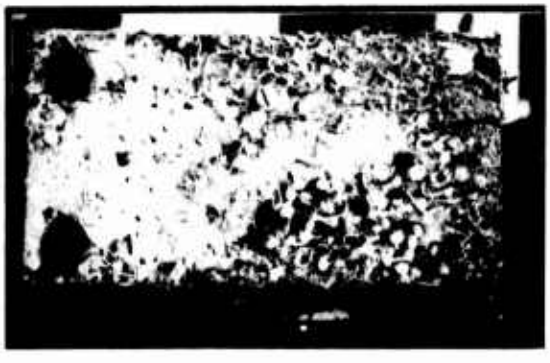


12 Months - Bottom
Dry Weight - 78 grams/panel (450 sq.cm.)

ZONE D



12 Months - Middepth
Dry Weight - 7.5 grams/panel (450 sq.cm.)



12 Months - Bottom
Dry Weight - 9.0 grams/panel (450 sq.cm.)

ZONE E



12 Months - Middepth
Dry Weight - 1.0 gram/panel (450 sq.cm.)



12 Months - Bottom
Dry Weight - 1.0 gram/panel (450 sq.cm.)

ZONE F

Control of Marine Fouling in a Water Cooling System in Tropical Australia

Dale Straughan

Allan Hancock Foundation
University of Southern California
Los Angeles, California 90007

The following is a report on research initiated at a request from engineers at the Northern Electric Authority Power Plant in Townsville (19°S) Australia, for assistance in controlling marine fouling in the water cooling system. A chlorination system using chlorine gas, was already installed. The request was to provide assistance in formulating the optimum chlorination program to control fouling organisms. The aim of this research was to provide biological data to determine:

1. Minimum effective chlorine dose.
2. Frequency at which dose should be repeated.
3. Most effective times of applying dose.

Larval settlement on fouling plates was monitored daily both in a section of the cooling system never exposed to chlorine and in a section of the cooling system where chlorine was administered. Intake chambers exposed and not exposed, to chlorine as well as intake pipes were examined as often as possible. Laboratory experiments were carried out on the tolerance to chlorine of the dominant fouling organisms including the mussel Xenostrobus securis Wilson 1967 and the pearl oyster Pinctada margitifera.

Data is presented to show:

1. Normal fouling patterns in the water cooling system.
2. Effects of chlorination in the water cooling system.
3. Results of laboratory experiments on exposure of tropical organisms to chlorine.

This study lasted from August 1966 to May 1968. By the latter date, an effective chlorination system was in operation.

Introduction

In 1966, shell blockage of the condenser screens at the Northern Electric Authority Power Plant at Townsville, north Queensland became an increasing problem. Each time a blockage occurred, the water main in question was closed down and shell cleaned from the main and condenser screen. This was not only a costly process in terms of man power and money, but with a projected increase in demand for power from this station, could result in power shortages.

The power plant was within the last few years of its projected life. Therefore, while there was a need for increased efficiency in the control of marine fouling, costly reconstruction was out of the question. At this point, the Northern Electric Authority installed a chlorinator and asked the author for assistance in determining the most efficient use of the equipment at the power plant to obtain control of marine fouling.

On the premise that the best way to control the fouling was to prevent larval settlement, the following questions were posed.

1. Were there any distinct temporal larval settlement patterns?
2. What was the effect on larval settlement of pumping water through the cooling system at different rates?
3. What was the effect of chlorination on larval settlement?

The dominant species cleaned from the condensers were the black lip pearl oyster Pinctada margitifera and the mussel Xenostrobus securis Wilson 1967. These species are both considered sessile organisms. However, both are capable of movement, and if dislodged, are able to secrete new bysus threads and reattach themselves to a solid substrate. Hence, it was considered possible that there was some migration of juveniles (as opposed to larval stages) of these species into the water cooling system. Two further questions were also posed.

4. Was there a significant migration of juvenile bivalves into the water cooling system?
5. What was the effect of shlorination on juvenile and adult bivalves?

This paper presents the answers to these questions as determined in a study between August 1966 and June 1968. Data on the formation and comoosition of the fouling community will be presented elsewhere.

Physiography

The Northern Electric Authority Power Station in Townsville (19^{o} 14' S) is situated on Cleveland Bay between Ross Creek and Ross River (Figure 1). The intake chambers are located in Ross Creek. The water is then pumped through 6 water mains each 600 yards (549 m) long and two feet (61 cms) in diameter, to the Power Station. The water is later discharged into Ross River. While there is no provision for returning hot water through the intake lines, water can be flushed back through the water mains from the power station to the intake chambers.

Water enters the Ross Creek intake chambers through mesh screens (Figure 2). The mesh is 13 x 13 mm with an internal diagonal of 16 mm. The chambers are 20 feet (6.1 m) deep and the entrance from the creek is at the bottom of the chamber (i.e. well below low water mark). Water enters the chamber both through pumping and by tidal flow. Water is pumped through the intake chambers as diagramed in Figure 2. It then flows through vertical bars 5 to 10 mm apart to pass from the intake chambers into the water mains to the power station. A third set of screens with fine mesh (in the order of 1 mm diameter mesh) are used to protect the condensers.

The maximum tidal range on spring tides is 12 feet (3.6 m) and the minimum tidal range on neep tides is 5 feet (1.525 m). In general, tides exhibit a diurnal pattern. While there are usually two series of spring tides each month, the series are not evenly spaced out. During the study, there was 11 or 12 days between the peak of spring tides at the new moon and the peak of spring tides at the full moon, while there was a lapse of 16 or 17 days between the peak of spring tides at the full moon and the peak of spring tides at the new moon.

Northern Electric Authority (N.E.A.) engineers recorded the temperature of water entering the intake chamber for the period December 1966 to June 1968. During this period, water temperatures ranged from 19°C to 33°C (Figure 3).

N.E.A. engineers also recorded the rate of water flowing through the test areas of the intake chambers between December 1966 and June 1968. When the pumps were working at maximum velocity, water flow through the water mains was 3.3 knots.

A total of 6 pumps can be used to pump water from Ross Creek to the N.E.A. power station. Each pump has its own water main from the intake chambers to the power station. Pumps 1, 2, 3, 4 each have a capacity of 420,000 gallons per hour while pumps 5 and 6 each have a capacity of 390,000 gallons per hour. During most of this survey from 1 to 4 pumps were in use. However, there were periods of complete shut down and short periods in September and December 1967 when all pumps were operative.

The region is within an arid zone (see (1) for definition)[1] and the entrance to the water cooling system is at the bottom of Ross Creek. Under these conditions, freshwater entered the water cooling system for only one prolonged period in mid February 1968 following 50 inches (1.251 m) of rain between February 5 and 18. The salinity dropped below that of seawater for a few hours only, on February 3, 1967, and March 15, 1967 (H. Fulford, personal communication).

Prior to this study, chlorination was carried out in the water mains. This had generally kept fouling under control with minimal problems of condenser blockage up until 1966 (H. Fulford, personal communication). Chlorination had, however, only been in the water mains and not in the intake chambers.

Materials and Methods

The water intake chambers were examined when they were emptied for cleaning in November 28, 1966, October, 1967, and December, 1967. A comparison of the organisms on fouling plates and on nearby walls of the chamber was made in March, 1967, October, 1967, and December, 1967 to determine if the fouling plates presented a realistic record of fouling in the intake chambers.

Number 1 water main was first examined in September, 1966. The surfaces in the main itself were virtually clean of all fouling organisms. The surfaces between valves separating the intake chamber from the main had not been chlorinated and fouling organisms from this region were sampled. The water mains were inspected and fouling samples collected whenever the mains were opened for servicing. Samples of shell cleaned from the chambers throughout the survey were examined.

Larval settlement and recruitment was studied through the use of asbestos cement fouling plates between December 1, 1966 and May 31, 1968. Asbestos cement was chosen because it provided a surface similar to the concrete walls of the intake chambers. Fouling plates had an exposed surface area of 100 x 80 mm on each side. Fouling plates stood vertically in a horizontal frame of the type described by Straughan (2).

Fouling plates were suspended below low water spring level at C_1 in the intake chamber on December 1, 1966 (Figure 2). These plates were moved to C_2 on May 31, 1967 to insure that these plates would not be influenced by the chlorination program to be

---

[1] Figures in parentheses indicate the literature references at the end of this paper.

commenced at E in June 1967. To further ensure that no chlorine reached the unchlorinated control fouling plates, if no pumps were active at the time of chlorination, chlorine was added at E at the commencement of the flood tide so that flow for the next 6 hours was into the chamber and not out from E towards C_2. Fouling plates in the series were examined at monthly and longer intervals. The establishment of this fouling community will be discussed elsewhere. Fouling plates in this series were compared to nearby walls of the intake chamber to determine if the asbestos plates were accurately indicating the larval settlement possible on the walls of the intake chamber and water mains.

A second series of fouling plates was suspended at C_1 on February 1, 1967 and moved to C_2 on May 31, 1967. Initially fouling plates were examined at different ages in increments of 1 day to determine the optimum period of plate exposure for maximum larval settlement. No settlement was recorded on fouling plates exposed for 1, 2, 3 days, 1 barnacle cyprid was recorded on plates exposed for four days, 3 barnacle cyprids after five days exposure, 5 larvae had settled after six days exposure, 10 larvae had settled after 7 days exposure. When plates were exposed for up to 14 days only one additional larvae settled. Hence, it was considered that the optimum exposure period of the fouling plates to obtain maximum larval settlement was 7 days. One of a series of seven fouling plates was replaced and examined daily on a rotating system so that one plate that had been suspended for seven days was examined daily. This was designed to give a daily record of larval settlement by a comparison of number and size of organisms recorded each day. Fouling plates exposed for less than 7 days did not develop a sufficient layer of micro-organisms to encourage larval settlement of macro-organisms. Aging of fouling plates for 24 and 48 hours in the laboratory prior to exposure to larval settlement did not produce satisfactory results.

A third series of fouling plates were suspended below low water spring level in No. 4 pump chamber (E) July 1, 1967. This was the position where chlorination of the intake chambers occurred. A program of replacement and examination of fouling plates parallel to that in the second series was followed. Five additional plates in the frame were examined at weekly and monthly intervals. A comparison of larval settlement on plates in the second series (unchlorinated) and those in the third series (chlorinated) between July 1, 1967 and May 30, 1968 showed the effects of chlorination on larval settlement.

Chlorine, in the form of calcium hypochlorite was added to the intake chambers at E so that the concentration in pump chambers 1, 2, 3, 4 was 20 ppm chlorine. For a short period in early June 1967, (see Table 4) chlorine was added to give a concentration of 40 ppm.

Fouling plates were returned to the laboratory in a rack in a seawater container. They were usually examined microscopically immediately while all organisms were living. Dominant species were identified while other organisms were classified into major groups. Estimates were also made of species abundance. If it was not possible to examine fouling plates immediately, they were held in seawater aquaria.

Two types of experiments were carried out to determine effects of chlorination on juvenile and adult organisms. Bivalves were used in most of these experiments because this was the dominant group causing problems in the condensers. Smaller organisms such as barnacles and serpulids were also studied in some experiments. In the experiments to determine the effects of the chlorination program, selected organisms were placed in a wire basket suspended with the fouling plates at E. The effects of the chlorination program were determined by daily examination of these organisms.

Tolerance of selected organisms to chlorine was determined in a series of labora-

tory experiments. Organisms were maintained in aerated aquaria and calcium hypochlorite added. The aquaria were covered to reduce the rate of chlorine loss. Organisms were examined daily and the following noted:

1. attachment of bysus threads,
2. gaping animals alive,
3. gaping animals dead.

There was a high mortality of bivalves in the water mains following the entry of freshwater into the water cooling system in February 1967. This suggests that occassional filling of the water mains with freshwater may be an effective means of fouling control. Hence, bivalves were placed in a series of aquaria with a range of salinities from freshwater to seawater. Organisms were examined daily and the following noted:

1. attachment of bysus threads,
2. gaping animals alive,
3. gaping animals dead.

Although most of the problems such as reduced water flow due to fouling growth in the water main and blockage of condenser screens was probably due to the fouling in the water mains, no fouling plates were placed in these water mains. This is because it was impossible to anchor the fouling plates in the water mains. Instead, the water mains were inspected and fouling samples collected whenever the mains were opened for servicing. Samples of shell cleaned from the condersers were also examined. Twenty animals were used in each experiment unless otherwise indicated.

Results

The Intake Chambers

Comparison of fouling plates in series 1 with the nearby walls of the intake chamber revealed no major differences in the fouling community. Fouling developed to a thickness of approximately 3 inches in four months during the summer following the cleaning of the intake chambers (November 1966 to March 28, 1967). Therefore larval settlement on the fouling plates was indicative of larval settlement on the walls of the intake chambers. Few Xenostrobus were recorded either from fouling plates or the intake chamber, whereas, they were removed from the water mains by the ton.

The monthly total of the number of larvae settling daily on fouling plates at the unchlorinated localities (C_1, C_2) is presented in Table 1. Differences in larval settlement numbers in February 1967 and 1968 can be attributed to the effects of freshwater flooding in 1968. The higher rainfall in January 1968 than in January 1967 (3) may likewise have caused reduced larval settlement in 1968. In March 1968, the slightly reduced settlement may have been due to a 'lag' in recovering from the heavy rains in February 1968 (3). However, overall there is little difference in the settlement numbers recorded in March, April, May, 1967 and March, April, May, 1968. As the numbers of settling larvae in 1968 remained comparable to the numbers reported over a similar period in 1967, it was assumed that, as planned, the chlorination program instigated at E was not reducing larval settlement at the control site.

There is some seasonality in larval settlement in that larval settlement was the least abundant in July - 4 - and August - 29. There was a peak in settlement numbers in September - 1419 - and the February-March period (all over 100 per month except during the flood period). A comparison between the number of larvae settling between February 1, 1967 and May 31, 1967, and the maximum tidal height on the day of settlement showed that 69% of all larvae settled during periods when the tidal height ranged from 10 to 12 feet (3.05-3.66 m) and 99% of all larvae settled when the tidal height ranged from 8 to 12 feet (2.46-3.66 m). This data suggests that most larvae settle on spring tides. However,

large numbers of Balanus cirratus settled during spring tide periods in February and March 1967. Therefore, it was important to examine the relationship between the numbers of larvae settling and tidal height for the whole survey because the above correlation could be of a seasonal nature and/or due to one abundant species - namely Balanus cirratus. Such was the case. At the end of the survey only 33% of the larvae settled on days with a maximum tidal height of 10 to 12 feet (3.05-3.66 m), 73% settled on days with a maximum tidal height of 8 to 12 feet (2.44-3.66 m) and 80% settled on days with a maximum tidal height of 7 to 12 feet (2.12-3.66 m). The data did not show any consistent correlation between the number of larvae settling on fouling plates and tidal height.

55% of larvae settled when there were no pumps working while 13%, 12%, 9%, and 11% settled when a total of 1, 2, 3, and 4 pumps respectively were working. Insufficient data were available to consider situations where a total of 5 or 6 pumps were working. However, under conditions of increased water flow, one would expect either a similar or reduced larval settlement to that recorded when a total of 4 pumps were working. However, the operation of a single pump is sufficient to significantly reduce larval settlement in the intake chambers. (Numbers larvae settling/day were compared to obtain this data.)

Comparison of monthly totals of larval settlement per day to the unchlorinated and chlorinated fouling plates between July 1, 1967, and January 31, 1968 reveals over an 80% reduction in larval settlement on the fouling plates (Table 2). Examination of the walls of the chlorinated pump chambers verified that larval settlement was reduced significantly. It also showed a low survival rate among the larvae settling on the walls. Larval settlement on the day following chlorination was less than 5% that of settlement recorded on the unchlorinated plates (Table 3). Only 35% of the unchlorinated fouling plates bore no larval settlement after a weeks exposure while 55% of the chlorinated fouling plates bore no settlement after a weeks exposure. No settlement was recorded on the unchlorinated plates on 55% of the days while no settlement was recorded on the chlorinated plates on 70% of the days.

Newly settled Pinctada are of the order of 1-3 mm wide. However, these were seldom recorded on the fouling plates. Usually Pinctada appeared suddenly on the plates when about 10 mm broad and on occassions appeared up to 40 mm broad. Pinctada also demonstrated their mobility by crawling about aquaria in the laboratory. As the fouling plates were suspended by ropes from a point above water level, Pinctada could not have crawled onto the fouling plates, but must have been carried to the plates by water currents and then settled on the plates. The size of the majority of Pinctada settling on the fouling plates suggested that they have previously been attached elsewhere. The smaller animals could have entered through the mesh from Ross Creek. All could pass from the intake chambers and into the water mains. Therefore, the water mains could be colonised by larval, juvenile and adult Pinctada. Hence, the chlorination program needs to be such to control adult Pinctada as well as preventing larval settlement.

A series of laboratory experiments were conducted on Pinctada margaritifera, Tapes turgida, Balanus cirratus, and Pinna bicolor, all of which occurred in the intake chamber and were found in shell removed from the water mains using the normally recommended chlorine doses. Short exposure periods were used because these low amounts of chlorine would be rapidly absorbed in the water cooling system. Aerated and non-aerated water was used because low oxygen levels probably occurred in sections of the water mains when water was allowed to stand.

Pinctada was exposed for up to 5 hours in 1 ppm, 2 ppm, 3 ppm chlorine in unaerated and aerated seawater. The results -- 100% survival.

Tapes was exposed for up to 5 hours in 1 ppm and 2 ppm chlorine in aerated sea-

water and 1 ppm chlorine in unaerated seawater. The results -- 100% survival.

Balanus was exposed for up to 2 hours in 1 ppm and 2 ppm chlorine in aerated and unaerated seawater. The results -- 100% survival.

Pinna was exposed for 6 hours in 3 ppm chlorine in aerated and unaerated seawater and 2 ppm in unaerated seawater. The results -- 100% survival.

Organisms were also placed in wire baskets at E to determine survival on two occassions (Table 4). The organisms tested without a protective calcareous exterior (anemones and the hydroid Amathia) died first after either one or two days exposure to doses of chlorine of 20 ppm or more. On the other hand the serpulids (Hydroides basispinosus and Pomatoleios kraussii) were still alive 3 days after exposure to such doses 5 times during an 8 day period. All Pinctada died during this period while only 2 out of 6 Balanus were alive at the termination of this experiment. All Pinctada shells were heavily corroded by the chlorine.

When Pinctada were exposed to 40 ppm in the laboratory where there was less loss of chlorine than in the intake chambers, 1 out of 10 animals were gaping after 48 hours exposure, and all were dead after 72 hours exposure.

Xenostrobus were exposed to different doses of aerated chlorinated seawater in the laboratory (Table 5). Animals exposed to 5, 10, 15 ppm chlorine all recovered when placed in clean seawater. Animals exposed to 20 and 40 ppm did not recover. When Xenostrobus were exposed to 40 ppm chlorine in unaerated seawater all animals were still attached to the substrate after 24 hours exposure.

Xenostrobus was also exposed to freshwater in two separate experiments. In both experiments 75% of the animals were dead after 2 weeks exposure and the remaining animals died during the next three days.

The Water Mains

As the water mains were only 2 feet (61 cms) in diameter, fouling samples were only collected at their intake end. Examination of shell removed from the water mains following chlorination was considered an indicator of the condition of the remainder of the water mains.

Initially 95% of the shell removed from the water mains was either Pinctada margitifera or a related species of pearl shell. However, by November 1967, no pearl shell was removed from the pipes, but large amounts of Xenostrobus were collected. These grew in long strings of animals from the sides of the pipes. Those strings eventually became unstable, fell off the walls and were washed downstream to block the condensers. It was apparent that the concentrations of chlorine that kept the water mains clean of Pinctada did not control Xenostrobus.

A chlorination program was instigated in which each main in turn was chlorinated to 15 ppm at the intake end, each week commencing December 26, 1967. The program was interrupted during the heavy rains of February 1968 and the water mains were not examined until April 1968. At this time in main No. 3 there was no settlement on an area that had been cleaned when last examined (December 22, 1967). However, a few small specimens of Xenostrobus were found nearby. Xenostrobus was the dominant organism in the pipe on both occassions. However, density was reduced from approximately 200 per square foot (35 cms square) in December to approximately 100 per square foot (35 cms square) in April. Pinctada was not found on either occassion.

When main No. 2 was examined (April 2, 1968) the density of Xenostrobus at the inspection point was 150 per square foot (35 cms square). The main was chlorinated at the rate of 30 ppm and allowed to stand over each of the following three weekends. After this treatment, over 300 lbs. of shell was removed from the condenser and when the main was opened (April 23, 1968) more shell was washed out. At the inspection point, there were approximately 100 Xenostrobus per square foot (35 cms square). All specimens were very small and at this stage did not cause any obstruction of the main. However, specimens were larger and more abundant further along the main.

The main was then chlorinated at the rate of 50 ppm and allowed to stand on the next weekend. Once again shell was washed out prior to inspection (April 29, 1968). The density of Xenostrobus was approximately 90 per square foot (35 cms square) both at the inspection point and further along the main. More shell probably fell off the substrate subsequently because at this stage the shell was weakly attached to the substrate.

While chlorination rates of 15 ppm kill and stunt Xenostrobus near the injection point, higher chlorination rates of 30-50 pp, were necessary to obtain control further along the main initially.

Discussion

The aim of this study was to provide the optimum control of fouling organisms at minimal expense. Prior to considering actual dosage rates of chlorine, it was considered prudent to consider natural settlement rhythms on a seasonal and/or tidal nature and the effects of water flow on larval settlement. If, for example, settlement peaked consistently on spring tides, chlorination would coincide with periods of spring tides. This would mean an irregular schedule because of the irregular pattern of these tides. It was hoped to reduce the use of chlorine but obtain maximum control by applying it during maximum periods of larval settlement.

There is a seasonal pattern in larval settlement, with reduced larval settlement in midwinter. The reduction in larval settlement in October and November following a peak in settlement in September is initially puzzling. However, this is probably due to a gradual increase in pollution levels in Ross Creek towards the end of the dry season. Larval settlement increased in December 1967 following the onset of summer storms. A similar pattern was found in the larval settlement of Mercierella enigmatica in the Brisbane and Ross Rivers (4, 5). In both river estuaries there is an immediate increase in larval settlement following flushing after rains. 1967 was a year with unseasonal midwinter rains (3). There is probably no September increase in larval settlement in the intake chambers in years when winter rains are absent. It is suggested that the normal seasonal pattern is one of increased larval settlement during the summer months but that this increased larval settlement period does not commence until after the commencement of summer storms.

Periodicity in breeding and larval settlement is the rule in most species. Usually this bears a strong correlation to tidal and/or lunar periodicity (1, 4, 5). Analysis of the data on total numbers of settling larvae during the study period show no such correlation. It is possible that any correlations of the various species (e.g. Balanus cirratus tended to settle on high tides for at least the period February to April 1967, while Mercierella enigmatica settled 23 ± days after the penultimate series of spring tides (1)) with different tidal phases cancelled each other in the longer term.

Increased rates of water flow can reduce larval settlement (6). Some species even require perfectly still water for larval settlement. There was a significant reduction in larval settlement on fouling plates in the intake chamber when one or more pumps were active. This suggests increased settlement in the water mains when there was no water

flow. It also suggests that the intermittent use of the pumps increased larval settlement because each time the pumps were used more larvae would be brought into the water mains to settle during the next quiescent period. Hence, one would predict a reduction in larval settlement in the intake chambers if at least one pump is continually working and reduction of fouling in the water mains during periods when the plant is running at maximum capacity.

Larval settlement was controlled by the periodic application of chlorine at dosages of 20 ppm. This is a much higher rate of application than normally recommended for fouling control. For example control in a similar water cooling system in the Brisbane river was obtained by chlorination at the rate of 1-5 ppm for 20 minutes once during each six week period.

Larval settlement may have been controlled by lower levels of chlorine. However, the migration of juvenile Pinctada into the intake chambers and of juvenile and adult Pinctada into the water mains had to be controlled as well as juvenile and adult Xenostrobus that settled in the water mains during periods when the water mains were not in use.

Application of chlorine to 20 ppm in the pump chamber at E was sufficient to control fouling in this chamber. This should also apply to application in other areas of the intake chambers.

However, experiments showed that Xenostrobus was more tolerant to chlorine than Pinctada. However, while 20 ppm did not kill this species, it resulted in weakened bysus attachment in 24 hours. Maximum back flushing of the water mains was recommended at the end of chlorination periods in the water mains to remove weakly attached mussels. Whether mussels are killed or only detached from the substrate, it is necessary to back-flush and remove them from the water mains or else the shells block the condensers.

Initially higher dosages of chlorine were necessary to obtain control of Xenostrobus than to maintain it. In the initial stages when more fouling organisms were present, the chlorine was more easily absorbed and the dosages were less effective. Resettlement was by smaller specimens than those found prior to control. In the laboratory experiments, the smaller animals were less resistant to chlorine than the larger animals.

To summarize:

1. The fouling in the water cooling system would be significantly reduced if the system was kept operating at a maximum rate.
2. Periodic application of chlorine at the rate of 20 ppm which is allowed to stand for 24 hours at least, is necessary during intermittent operation to control fouling. Application should be very frequent - every week - during periods of infrequent operation in the summer months following the onset of heavy rains, and less frequent - every month to six weeks - during midwinter and/or periods of maximum operations.

Acknowledgements

I wish to thank those responsible for the opportunity to do this work - in particular Mr. H. Fulford of the Northern Electric Authority for his continued support and encouragement.

The Northern Electric Authority paid travling expenses and provided equipment and the opportunity to carry out this research. The Warden of the James Cooke University, Townsville, provided laboratory facilities.

References

1. Straughan, Dale, The Influence of Seasonal Rainfall and Water Temperature on the Population of Mercierella enigmatica (Annelida : Polychaeta) in the Ross River Estuary North Queensland. J. exp. mar. Biol. Ecol., 9 (1972).

2. _____, Intertidal Fouling in the Brisbane River, Queensland. Proc. R. Soc. Qd., 79, 4, p. 25-40 (1967).

3. Straughan, I.R., The Hyla bicolor complex (Anura, Hylidae) in North Queensland. Proc. R. Soc. Qd., 80, 5, p. 43-54 (1969).

4. Straughan, Dale, Ecological Studies of Mercierella enigmatica (Annelida : Polychaeta) in the Brisbane River, Queensland. J. Anim. Ecol., 41, 1, p. 93-136 (1972).

5. Korringa, P., Relations Between the Moon and Periodicity in the Breeding of Marine Animals. Ecol. Monogr., 17, 3, p. 347-381 (1947).

6. Wood, E.J.F., Effect of Temperature and Flow Rate on Some Marine Fouling Organisms. Aust. J. Sci., 18, p. 34-37 (1955).

Table 1.

Total number of larvae recorded each month on fouling plates examined daily.

1967	February	1204
	March	1342
	April	629
	May	351
	June	214
	July	4
	August	29
	September	1419
	October	105
	November	77
	December	208
1968	January	493
	*February	433
	March	1046
	April	788
	May	419

*Period of rain and freshwater flooding.

Table 2.

Monthly total of daily larval settlement on chlorinated and unchlorinated fouling plates.

		Unchlorinated	Chlorinated
1967	July	4	0
	August	29	23
	September	1419	206
	October	105	85
	November	77	22
	December	208	27
1968	January	493	173
	Total	2335	436

Table 3.

Larval settlement the day after the addition of chlorine.

	Unchlorinated	Chlorinated
	9	0
	12	0
	20	0
	16	3
	17	1
	12	0
	6	0
	2	0
	0	0
	1	1
	3	1
	0	0
	0	0
	2	2
	0	0
	84	0
Total	184	8

Table 4.

Effects of chlorine brought up to the strength indicated on organisms placed in cages in the pump chamber. + on the date of commencement of each program indicates that the organism was used but the number was not recorded.

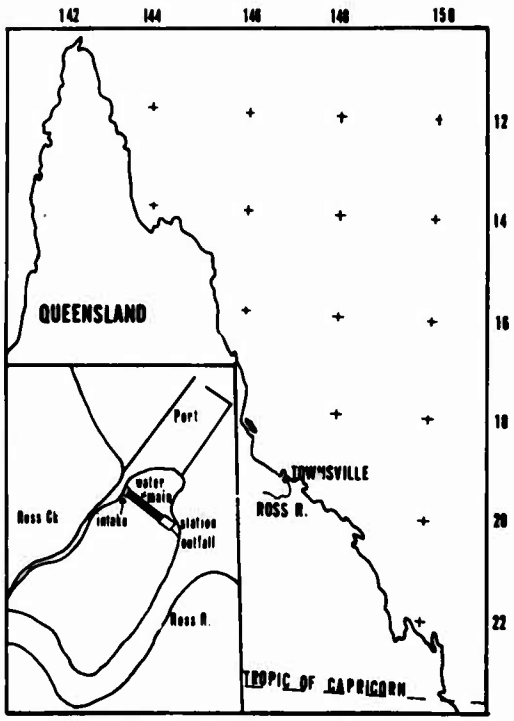
Date	Chlorination Program	Anemones	Amathia	Pinctada	Balanus	Serpulid
May 1967						
3	Chlorine to 20 ppm	+	+	10	3	
4	Chlorine to 20 ppm	Dead	Dead	Alive	Alive	
5	Removed			Alive	Alive	
June 1967						
1	Chlorine to 35-40ppm	+	+	8	6	+
2	Chlorine to 20 ppm	Dead	Alive	Alive	Alive	Alive
3			Dead	Alive	Alive	Alive
4				Alive	Alive	Alive
5	Chlorine to 20 ppm			Alive	Alive	Alive
6	Chlorine to 40 ppm			Alive	Alive	Alive
7				Alive	Alive	Alive
8	(morning residue 10 ppm) Chlorine to 20 ppm			Alive (1 gaping)	Alive	Alive
9				1 Dead 3 gaping	Alive	Alive
10				4 Dead 4 gaping	Alive	Alive
11				8 Dead	4 Dead 2 Alive	Alive

Table 5.

Effects of exposure of Xenostrobus to chlorinated seawater. - no observable ill effects. Except where stated, 20 animals were used in each experiment.

Chlorine °/ooooo	Time of exposure (hours) 3	12	24	27	48
0	–	–	–	–	–
5	–	–	–	–	15/18 detached
10	–	–	bysus loose	bysus loose	all detached
15	–	–	bysus loose	bysus loose	all detached
20	–	–	bysus loose	all detached	
40			all detached		

Figure 1.



Map of north-eastern Australia showing the position of Townsville. Inset diagram showing relationship between Ross Creek, the intake chambers, water mains, N.E.A. station, outfall, and Ross River.

Figure 2.

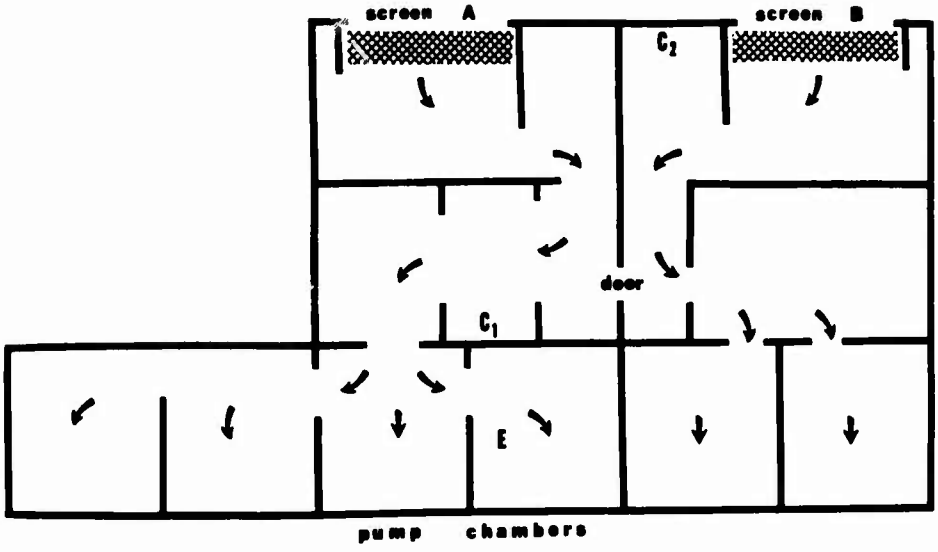
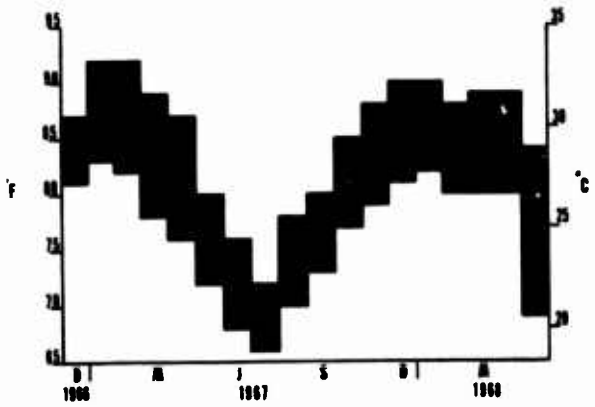


Diagram showing water flow through the intake chambers. Water enters through screens A or B and flows through into one of six pump chambers. It is then pumped through water mains to the power station. At times there is also some flow between the two sides of the power station through the "door".

Figure 3.



Monthly maximum and minimum water temperatures recorded at the N.E.A. power station between December 1966 and May 1968.

THE PROBLEM OF MARINE FOULING IN THE COASTAL WATERS OF INDIA AND ITS ECONOMIC IMPLICATIONS WITH SPECIAL REFERENCE TO FISHING FLEET MANAGEMENT

R.Balasubramanyan, N.Unnikrishnan Nair and A.G.Gopalakrishna Pillai

(Indian Council of Agricultural Research,
Central Institute of Fisheries Technology,
(Craft and Gear Division), Cochin-11,
Kerala, INDIA)

The problem of marine fouling and its prevention is a subject of very great economical importance to all the maritime nations of the world. It is well known that a host of maritime countries bordering the Indian Ocean are at present, actively concerned with the commercial exploitation of the natural marine living resources in their coastal waters as well as off-shore and deep sea areas. A large fleet of fishing vessels comprising of boats of different sizes, types and tonnages are taking part in this tremendous venture. The Indian fishing fleet comprising of innumerable indigenous sailing crafts and a large number (nearly 10,000) of introduced mechanised boats have all assumed a greater responsibility to-day than ever before in the harvesting of the natural food resources of the seas around India. Of the 69 million tons of fish, the world produces to-day (1970), India's annual contribution is about 1.7 million tons. Besides feeding her own millions of people, India has also exported to world markets nearly 36000 tons of marine products valued at about 351 million rupees during 1970-'71. The entire economy and the well being of the Indian fishing industry to-day lies, to a great extent, in the efficient operation and management of her fishing fleet. Apart from the high initial capital investment on the development and the expansion of the fishing fleet, an enormous amount of money is being spent annually on their proper maintenance so as to obtain a prolonged trouble free life and uninterrupted useful service from them. The real weight of the fouling problem in India with an economical background is presented in this paper.

One major problem that constantly interferes with the smooth sailing of fishing vessels in the warm Indian tropical waters, is the intensive settlement of the marine fouling organisms on the boat hulls and their successful prevention.

Settlement of the marine fouling organisms is common on all structures exposed to sea-water, may that be wood, steel, aluminium, fibreglass-reinforced plastics (FRP or GRP) or even ferro-cement either in their static or dynamic conditions. As a result of this accumulated fouling complex on the hull that is always exposed to sea-water, the boat gradually develops undue frictional resistance resulting in the corresponding decrease in its normal speed, increase in its fuel consumption with poor manoeuvrability. Marine fouling also causes the loss of efficiency of all under-water propelling devices and the frequent malfunctioning of all underwater electronic installations. Fishing vessels have to be dry-docked every now and then or atleast once a year to get rid of all the unwanted fouling and refloat them. This means a constant source of recurring expenditure and loss of fishing days, but fouling has to be prevented and the hull below water-line should remain as clean and as smooth as possible and at any cost. There is still no one successful and economical method of preventing marine fouling. The problem of marine fouling has, therefore, attracted the attention of biologists, chemists, engineers, technologists alike and a great volume of literature on this subject has thus accumulated.(1)[1] In India, scientific contributions on this subject of marine fouling have been made from time to time since

[1] Figures in parentheses indicate the literature references at the end of this paper.

the last four decades and very valuable findings have so far been documented (2-9).

Fouling by plants and animals in sea-water is more a biological phenomena well supported by the varied hydrographical features and the geographical position of the location. Though nearly 1400 different species of animals and 600 different species of plants have so far been identified in the marine fouling complex encountered all over the world (1) practically a restricted few of them become a regular menace to all fishing crafts by virtue of their general structure and volume, and by their permanent settlement on hulls under-water. The marine fouling complex along the 5000 km. length of coastal waters of India appears to be a true representative of the typical Indo-West Pacific tropical flora and fauna.

The microscopic fouling forms are the bacteria, diatoms, marine fungi, protozoans and rotifers while the macroscopic forms are the sponges, coelenterates, flat worms, bryozoans, tube-worms, amphipods, barnacles, molluses etc, apart from the marine algae and few other free living planarians, nemertines, polychaetes, isopods, decapods, gastropods and pisces (7). To a small extent the green algae is represented by Enteromorpha, Ulva etc particularly on the wind-water zone of the boats. The cirripede barnacles are mostly and conspicuously represented by Balanus amphitrite varieties communis and variegatus; Balanus tintinnabulam tintinnabulam and chthamalus stellatus stellatus ; the annelidan tube-worms by the ever present Hydroides norvegica; serpula vermicularis and Mercierella enigmatica; the Ectoprocta (Bryozoans or Polyzoans) comprising of both encrusting and erect forms and causing the unique sea-mat by the presence of colonies of Membranipora sp, Electra spp and Bugula nertina , and the Lamellibranch bivalves are well represented by a number of species consisting of Ostrea, Crassostrea, Mytilus and Modiolus(7,9). Plate 2.

The barnacles, tube-worms, bryozoans and mussels are by far the most important forms from the point of view of surface coverage, volume and weight when they a l settle and colonize on boat hulls. Periods of regular breeding and intensive settlement of the fouling forms were carefully investigated which proved to show their quicker growth, early maturity, greater fecundity and greater tolerances in environmental changes in the tropical waters (7,8,10). The tropical marine fouling flora and fauna appeared to be unique in many respects and in particular the heavier and denser growth of protective shells were the noteworthy feature. A supporting investigation on the hydrographical conditions of the aquatic environment brought to light the greater influence of water salinity and only a lesser influence of sea-water temperature on the fouling complex encountered (7). Though fishing trawlers in India maintain an average speed of 7 to 11 knots under normal fishing cruise, they tend to get heavily fouled at the time of their long detention at their ports. The intensity of fouling is mostly confined to few selected zones on the hull below water-line such as at the turn of the bilge, below the keel, rudder surfaces and water-line belt. Displacement hulls with deep draughts had comparatively more of fouling organisms,may be due to the large area exposed. Bronze propellers and copper metallic surfaces were also heavily fouled under their galvanic inactivation. External installations of cathodic protection sometimes interfered with the efficient performance of antifouling coatings. Layers and l yers of marine foulants especially shell bearing forms not only have caused surface damages to wooden fishing boats but also accelerated corrosion of steel hulls after causing damages to the protective paint coatings.

A large number of boat hulls were carefully examined at the time of their dry-docking and it was gathered that on an average an

accumulation of fouling forms weighing 10 to 15 kg. per square meter (dry weight excluding silt and other non-fouling matter) of hull surface exposed to sea-water was present during a period of 7 to 8 months of active service. Sluggish movements and considerable loss of speed were encountered with such vessels. Rudders were inactive and propellers were less efficient in their performance and on an average about 38 to 55% loss of speed in different class of trawlers was also noticed under heavy fouling conditions which of course was more or less regained once the vessels were refloated after hull cleaning and painting. The British Admiralty makes an allowance for design purposes for an increase of frictional resistance due to fouling at the rate of 1/2 percent per day out of dock in tropical waters. Tests on U.S.S. Hamilton showed that as a result of fouling on the propellers, the increase in SHP was two or three times the increase in thrust"(1). Tests carried out on a small training vessel 'YAYOI MARU' indicated that after 15 months when the ship was considerably fouled, the resistance increased over 100% (16). The National Council of American Shipbuilders brought to notice that a ship after being out of dry-dock for 200 days the increase in power required to maintain the same speed was 24%. Extremely light fouling by barnacles growing to approximately 1/8" high and 3/16" across the base alone has increased the total resistance of a ship by almost 30%.(17) It is estimated that as much as 200 tons of fouling may be removed from a ship's bottom at a single docking.(1) "Mussels have been observed to accumulate at a rate of one pound per square foot of surface per month, and barnacles at about half this rate. The maximum accumulation of fouling which has been recorded from navigation buoys is about 25 pounds per square foot in 35 months. In the case of barnacles, the maximum accumulation recorded amounted to 6½ pounds per square foot on a buoy set for a year."(1) Similar detailed observations under Indian tropical conditions have also been made and the final data is under processing.(18) In general, fouling by barnacles, oysters, tubeworms and mussels are comparatively high in the tropical warm waters of India.(18), Plate 1

The systematic examination of the effects of fouling is of comparatively recent origin although the problem has been recognised from ancient times. Even as early as in the 5th century B.C. there are written records of the treatment of ship's bottom and there is no doubt that the maritime nations of the ancient world took measures to prevent fouling (1). Even to-day toxic pigments like Copper, Mercury, Arsenic and other organo metallic, compounds incorporated in paints form the commercial antifouling coatings. Studies in India on the biological evaluation of a number of commercial antifouling paints have only indicated much scope for their improvement as regards the design, formulation toxic loading and actual efficient performance.(12,14,15) Fishing trawlers, as a routine measure in India, are hauled up once a year on the slipway or dry dock for cleaning and painting the hull. Hauling, cleaning, painting, slipway rent and launching accounts for nearly 70 to 80% of the total expenses involved while the cost of paint is only 20 to 30%, obtainable on an average price of Rs.12 to 15 per litre with only 5 months fouling free life. It is roughly estimated that the present Indian mechanised fishing fleet alone would require annually approximately 3,00,000 litres of antifouling paints (exclusive of primers and anti-corrosive paints) valued at Rs.45,00,000 to keep their hulls free from fouling and to have a smooth sailing only for a limited period.

This Institute brought to light the increased efficiency of Copper-aceto-arsenite (7 to 8 months of fouling free life) as a toxic pigment in the antifouling coatings in lieu of the conventional cuprous oxide.(14) For the first time in India, a laboratory formulation of antifouling paint with organo metallic tin (Tri-butyl-tin oxide) was formulated and was put to successful trials (19). The more efficient

expoxy or vinyl based antifouling compositions are not in use now on account of their being highly priced and also that the raw materials have still to be imported into India. Other than antifouling paint coatings, innumerable methods are being suggested from time to time for the successful prevention of the marine fouling from Ship's bottom, like underwater mechanical brushing generating electronic vibrations on the hull, and releasing of highly toxic chemicals when desired through pipe system installed at important locations on the hull under water but unfortunately these suggestions will have considerable resistance from the Indian fishing community on account of their need for higher initial investment and elaborate technicalities. Efficient toxic antifouling paints will have the best reception provided a fouling free life of one to three years are assured both for smaller boats and bigger class of vessels. Any further studies on marine fouling can not be considered as of academic nature any longer but the subject now has immense industrial applicability and the several facets of their prevention techniques have become a technology by itself.

Indian fishing fleet is fast expanding in size as well as in numbers. In the absence of adequate dry-docking facilities at present, the only way is to enhance the effective life of antifouling paints or to bring out a most economical alternate method of preventing fouling. The newer construction materials like fibreglass reinforced plastics, marine quality aluminium and "ferrocement" and their exposed surfaces will in no way be free from fouling in Indian waters. Thus the problem of marine fouling and its successful prevention still baffles the scientific world and will continue to remain a challege to all maritime nations. Plate 3

ACKNOWLEDGEMENT

The present work forms part of a project study on "Marine Fouling and its prevention in Fishing Boats" undertaken at the Central Institute of Fisheries Technology. The authors are thankful to Dr.V.K. Pillai, Director and Mr.G.K.Kuniyan, Head of the Craft and Gear Division of the Institute.

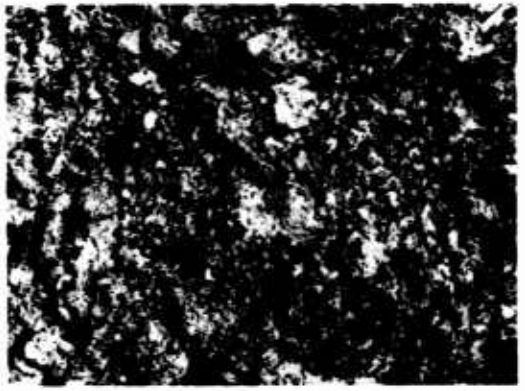
REFERENCES

1. Woods Hole Oceanographic Institution, U.S.A. — Marine Fouling and its prevention", 1-388,(1952)
2. E.W. Erlanson — Curr. Sci, 4, 726, (1942)
3. M.D. Paul — Proc. Indian Acad Sci.15 B, 1 (1942)
4. _____ — Curr. Sci, 5, 478 (1937)
5. G.K.Kuriyan — J. Bomb. nat. Hist. Soc.49, 90 (1950)
6. _____ — J. Zool Soc. India. 4, 157,(1952)
7. R.Balasubramanyan and T.R.Menon — J. Mar. biol. Ass. India. 5, 294, (1963)
8. M.Unnikrishnan Nair — Jour. of Sci & Ind. Res.Vol.24, No.9, 1-6, (1965)
9. A.Purushotham and K.Satyanarayana Rao — "Progress Report" for 1953-1970, Journal of the Timber Development Association of India,Vol.XVII, No.3, 1-71(1971)
10. N. Unnikrishnan Nair — Hydrobiologica, vol.30, Fasc 3-4 503-512 (1967)
11. _____ — Fishery Technology, Vol.VII, No.2, 174-184, (1971)

12.	R. Balasubramanyan	"Paintindia", 7, 19-24, (1969)
13.	_____	"Proceedings of the symposium on Mollusca" - Part III, 730-735, (1970)
14.	_____ & K.Ravindran	"Proceedings of the symposium on Marine Paints, 20-21, (1964)
15.	A.G.Gopalakrishna Pillai, K.Ravindran & R.Balasubramanyan	'Paintindia', 10, (1968)
16.	Annon	Shipbuilding Research Association of Japan, Report No.II, (1952-1953)
17.	_____	British Shipbuilding Research Association, Institution of Naval architects, Transactions, October, (1955)
18.	R. Balasubramanyan	A note on the quantitative study of the marine fouling complex on ship's bottom (unpublished)
19.	A.G.Gopalakrishna Pillai and N.Unnikrishnan Nair	"Fishery Technology" IX, 2, (1972)



A FLEET OF FISHING TRAWLERS



FOULING ON HULL



BEFORE LAUNCHING





AFTER LAUNCHING
FOULING ON RUDDER-7 Months FOULING ON PROPELLER-7 Months

SINDHU KUMARI
COCHIN



15·24M(50') WOODEN TRAWLER



OYSTERS



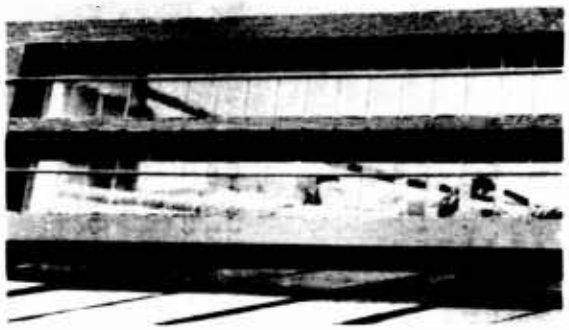
TUBE WORMS



HYDROIDS



MYTILUS MODIOLUS BARNACLES



IMMERSION RACK FOR COLLECTION OF FOULANTS



HEAVILY FOULED RACK - 7 MONTHS



FOULING ON AF COATING



FOULING ON FRP HULL



FOULING (Cleaned) ON 'FERROCEMENT' HULL

Succession and Seasonal Progression in the Fouling Community at Beaufort, North Carolina

John P. Sutherland and Ronald H. Karlson

Duke University Marine Laboratory
Beaufort, North Carolina

In this study, community development (succession) and seasonal changes in species abundance (seasonal progression) were followed on undisturbed substrate at Beaufort, N. C. Substrate was made available at different times of the year to determine the effect of differences in colonizing species composition on these two processes. Organisms were collected on ceramic tile plates (232 cm^2), suspended on a rack approximately 0.3 m below the low tide mark. Those sessile organisms which settled on the lower surface of these plates and were the major competitors for space, constituted the assemblage of organisms studied.

Submergence time had a dramatic effect on colonizing species composition. Plates which were submerged monthly during May-November 1971 were colonized by different species and showed different patterns of initial community development. There was also considerable year to year variation in initial development. However, seasonal progression on undisturbed plates was generally less dramatic than seasonal changes in colonizing species composition. Thus the two processes do not appear to be directly related. Some evidence of succession was indicated on the plates submerged from May-November 1971. By June 1972 these plates were more similar in species composition than they were during 1971, suggesting an approach to a climax state.

We feel the term, seasonal progression, should be applied only to seasonal changes in species abundance on undisturbed substrate, after succession has produced a climax. It should not be synonomous with seasonal changes in colonizing species composition. On this definition we are still unable to determine the extent of progression at Beaufort because we still have not defined the climax community.

1. Introduction

The assemblages of organisms commonly associated with the fouling of man-made structures are prime candidates for the study of natural communities. They have already been the focus of considerable attention (11,19)[1] with the

[1] The numbers in parentheses refer to the list of references at the end of this paper.

result that many of the animals are well known biologically. Many of the dominant organisms are sessile and the communities can be replicated on artificial substrate which is easily examined. As a result they approach laboratory systems in their ease of manipulation and sampling. Although a great deal of study has been conducted on these communities, much of it is taxonomic in orientation (2,5,6,7,16,17,18,19) and relatively little attention has been paid to the long term dynamics of undisturbed communities. The only quantitative information generally consists of counts of organisms settling on substrate exposed for short (1-3 months) periods of time (19).

The dynamics of undisturbed communities are of considerable interest, particularly at Beaufort, N. C., where they have been reported to undergo profound seasonal changes in species abundance (10). Moreover, colonizing species composition varies dramatically at Beaufort, with the time of year when substrate is made available (10). Seasonal changes in species abundance and in colonizing species composition have both been used as evidence for seasonal progression, as opposed to succession towards a climax (6,12,13). Scheer (13) was one of the first investigators who attempted to distinguish between progression and succession in fouling communities. He cited McDougall's (10) work at Beaufort, N. C., as an example of seasonal progression and his own work at Newport Bay, California, as true succession. He concluded that the differences in community dynamics were probably a result of differences in the annual range of temperature, 23°C at Beaufort and 5°C at Newport Bay. Haderlie (6) also reported the absence of seasonal progression at Monterey, California. However, Reish (12) concluded that seasonal progression was more important than succession in Alamitos Bay, California. It is probably true that aspects of both succession and seasonal progression were present at Beaufort and in Southern California, but that they were imperfectly differentiated. In particular, an appropriate time scale must be agreed upon for the evaluation of successional versus progressional stages, and for defining climax (stable) states.

The purpose of this study was to re-examine the processes of succession and seasonal progression on undisturbed substrate at Beaufort, N. C. Substrate was made available at different times of the year to determine the effect of differences in colonizing species composition on these two processes. The present work is the base-line portion of a larger experimental program designed to determine the mechanisms of species replacement in this community.

We wish to thank William Kirby-Smith and Bob Lewis for providing temperature and salinity data. Andre Aucin, Mike Corcoran, Ann Dean, Timmy Green, Wayne Harrington, and Pat Sutherland all helped with the time consuming sampling procedure, some without pay. Marty Farmer prepared the figures. This research has been supported by the Office of Naval Research.

2. Methods

Organisms were collected on the lower surface of unglazed ceramic tile plates (232 cm^2) suspended horizontally on racks beneath the Duke Marine Laboratory dock. The plates were approximately .3 m below the low tide mark and remained continuously submerged. The rack used in 1970 had to be discontinued in April 1971, because it became impossible to remove the plates without disturbing the animals growing on them. In 1971, the rack consisted of 4, 3 m lengths of 5.1 cm diameter PVC pipe, bolted to end pieces so they were parallel and about 40 cm apart. Each plate had a 6.5 mm stainless steel bolt fixed permanently through the center with a cotter pin. These bolts were driven through holes in the PVC pipe and held in place with a removable cotter pin. With this design they could be removed from the rack and handled without disturbing organisms on the lower surface. During 1971, mobile invertebrate predators (e.g., nudibranchs) were found to move from plate to plate along the rack, disrupting the

development of plates submerged at different times. To prevent this in 1972, each plate was bolted to PVC caps which were threaded onto one end of 5.1 cm diameter PVC pipes. The pipes were about 2 m long and the other end was attached to the dock above the high tide mark. Thus in 1972, each plate was suspended independently.

The first series of (3) plates was submerged in October 1970. During 1971, additional series of (3) plates were submerged each month from May through November. In 1972, the number of plates in a series was increased to 4 and new series were submerged each month from April through July. In all cases, series were submerged at approximately the first of their respective months.

The plates were sampled periodically in a non-destructive manner to provide information on recruitment, growth and mortality for each species, and competition for space between species. For each sample, the plates were removed from the rack, brought to the laboratory, and examined in a small aquarium supplied with recirculating, aeriated water. Temperature was maintained within ± 5°C of ambient water temperature. All organisms appeared healthy and unharmed by our handling procedure. From January to November 1971, the position and size of each individual or colony was traced onto a glass pane, placed over the plate. A sighting device was used to reduce problems of parallax. The community map thus produced was retraced onto paper and stored. Percent cover of each species was estimated by measuring the area it occupied on the map with a planimeter accurate to ± 1 mm^2. This method proved to be extremely time consuming and after November 1971, percent cover was estimated by a point sampling technique. A plot of random points was generated by computer on an area equal to that of the ceramic tile plate. These points were traced onto the glass pane which was suspended over the plate. Using the sighting device it was noted which species were under each point. We found that 75 points gave us estimates of percent cover within ± 5% of planimeter estimates (<5% for the more abundant species). We considered this adequate, especially since we were most interested in the more common species (see below). A different set of 75 random points was used for successive samples of the same plate.

Only the area occupied more or less exclusively by a species was sampled. Canopies were not counted as occupying space; only the basal area of attachment was counted. Areas or points where species grew on top of other species were counted twice except when the lower species was a dead barnacle. Dead barnacles were treated differently because organisms grew on them readily and they often persisted for months beneath a layer of tunicates or bryozoans (see below). Thus it was possible to estimate > 100% coverage.

Data analysis was performed by a PDP 11/20 computer, except that planimeter estimates of percent cover were computed on an IBM 1130 computer. The major problem in analysing percent cover data involved the pooling of data from different plates in the same series. Because plates in the same series were not sampled simultaneously, data from a given plate often applied to a different time interval than those of other plates in the same series. In order to pool the data we assumed that events on each plate occurred uniformly throughout the sample interval. Thus, on a given plate if a species increased its percent cover by 50% in 40 days, its increase was considered to have been 1.25%/day. In the computer memory, an array was set aside for each species on each plate and numbered for each day of the study period. The appropriate rate of change (plus or minus) for each species was placed in each of the elements of the array representing a day in the sample interval (e.g., from day 70 to day 110) for that plate. When this was done for all species on a given plate, the percent cover of each species could be estimated at arbitrary intervals by summing the rate of change from day 1 (day of submergence). Since these arbitrary intervals coincided in time for each of the plates in the series, a mean and standard

deviation of % cover could be calculated which applied to a particular time period. The arbitrary interval was chosen to approximate the actual sampling interval, 14 days from May to November 1971, and 30 days for all other time periods.

Details of the analysis of variance on percent cover are included in the appropriate section in Results.

To determine reproductive periodicities, 3 plates were examined at 1-2 week intervals for the number of larval recruits. After being examined, these plates were scraped clean and resubmerged. Three different sets of (3) larval recruitment plates were used to coincide with the series of plates submerged in October 1970, May through November 1971, and April through July 1972. Data were collected from plates on the 1970 rack from 22 April to 6 May 1971. Earlier data from this rack were inadequate because of problems with species identification. Data were collected from plates on the 1971 rack from 13 May 1971 to 13 April 1972, and from plates on the 1972 rack after 20 April 1972. Daily settling rates were calculated for each species on each of the 3 plates. These daily rates were summed over an arbitrary 7 day period to provide weekly estimates of the number of larvae which had settled on each plate. Data from all plates were then used to calculate the mean number (and standard deviation) of larval recruits for each week.

During 1970 and 1971, temperature data were collected at the Duke Marine Laboratory dock, augmented by data collected at the nearby National Marine Fisheries Service dock. Weekly temperature ranges were taken from tables which reported daily maximum and minimum temperatures except when the daily temperature range was less than 2°C. In this case, the tables provided only the noon water temperature. Beginning in January 1972, weekly temperature and salinity ranges were taken from continuous recordings at the Duke Marine Laboratory dock.

3. Organisms in the Community

Reduced sedimentation makes the lower surface of plates the best accumulator of fouling organisms (8,9) and only those sessile organisms which settled on these surfaces were included in this study. Several additional criteria were imposed to separate the "dominant" from the "subdominant" species. A "dominant" species was one which:

1. Was capable of utilizing primary space (4), i.e., attaching to the plate itself. This ruled out species which were only seen growing epizootically, i.e., on secondary space.

2. At some time in the study occupied more than 10% of the primary and/or secondary space in a series.

These criteria reduced the number of dominant species to 10 and these species constitute the community of this study. The species were: Balanus spp - barnacles; Schizoporella unicornis - an encrusting Bryozoan; Bugula neritina - an erect, foliose Bryozoan; Botryllus schlosseri - a colonial tunicate; Molgula manhattensis - a solitary tunicate; Ascidia interrupta - a solitary tunicate; Styela plicata - a solitary tunicate; Bougainvillia sp. - an athecate hydroid; Pennaria tiarella - an athecate hydroid; Tubularia crocea - an athecate hydroid.

The various species of barnacles common to the Beaufort area (B. eburneus, B. amphitrite, B. tintinnabulum, and B. improvisus) have not been distinguished in this study for two reasons. First, they were difficult to identify to species when they were very small, which was always the case on the larval plates because of the short submergence time. Secondly, our major interest was in the mechanisms which determined community structure

and it seemed logical to assume a similar effect for all species of Balanus.

Of all the species, the abundance of Bugula neritina was the most poorly estimated by our method of sampling. This species has an extensive canopy but a very small zone of attachment. However, we feel that although it was abundant, its effect on the community was small because of its growth form. Other organisms in the community grew beneath the canopy with no apparent difficulty.

4. Results

Temperature and Salinity

In the Beaufort area during 1970-1972, temperatures ranged from a minimum of 3-4°C in winter to 28-30°C in summer (fig. 1). The relatively mild winter of 1971-1972 was evidenced by higher water temperatures than in the winters of 1970 and 1970-1971 (fig. 1). However, this mild winter was followed by a spring and early summer which was cooler and more variable in temperature than the other two comparable periods on record. For example, the minimum temperatures in late May 1972, were between 16 and 17°C while the corresponding temperatures for the same period in 1970 and 1971 were 19-21°C and 20-22°C respectively (fig. 1).

The low temperatures in May 1972, were caused by a storm stalled off the Southeast Coast. The month was unusually cool and rainy, a circumstance reflected in low salinity readings as well as cooler temperatures. Thus, the low (20-23‰) salinities in late May and early June (fig. 1) were probably unusual, although comparative data are unavailable. Minimum salinities in the fall of 1971 were also probably lower than in 1970 as a result of two hurricanes which came ashore in the Beaufort area. For example, on 2 September 1971, one week after tropical storm Doria came ashore, surface salinity had dropped to 18‰. At the end of September 1971, hurricane Ginger also passed through the Beaufort area although no salinity records were taken. No hurricanes passed through the Beaufort area in 1970. The low salinities in February 1972, (fig. 1) were probably not unusual as this is a normally stormy period.

Larvae

Balanus: Barnacles were numerically the most abundant settlers on the larvae plates. They settled predominately from March through August or September, although settling was reduced during the cool, early summer of 1972 (fig. 2).

Tubularia: Tubularia typically settled in the cooler periods of the year, in spring, fall, and early winter (fig. 2). The apparent peak in settling during April 1972 resulted from the larval plates still being on the 1971 rack. Larval plates were placed on the 1972 rack on 9 April 1972, and were in a different position under the dock. In contrast to the 1971 rack where Tubularia was abundant on adjoining plates, there was no Tubularia near the 1972 rack. The actinulae larvae of this species are relatively poorly dispersed and the absence of a nearby source of larvae probably reduced settling on the 1972 rack. Some additional data were available from the 1971 rack for early May 1972, and these indicate a higher recruitment than was recorded on the 1972 rack. However, recruitment of Tubularia during the cool spring of 1972 was genuinely lower than for 1971. During the spring of 1971 there were no adult Tubularia close to the 1971 rack and the recruitment was still high (fig. 2). Thus the high recruitment on this rack in April of 1972 was a local phenomenon in a spring of generally low Tubularia recruitment. In addition to fewer recruits in 1972, the recruitment period ended in May 1972 while in 1971 it continued through June (fig. 2).

Solitary tunicates: Solitary tunicates included Styela plicata, Ascidia interrupta, and Molgula manhattensis. These were not differentiated because it was difficult to tell the young stages apart from each other and from another tunicate, Perophora viridis, a species which was not included in this study but which at times settled heavily and confused the counts. In addition, none of the species were common pioneers of newly submerged substrate. For example, in early May 1972, on 8 experimental plates submerged on 9 April, the mean recruitment rate for Styela plicata alone, was 48 individuals in a 7 day period (Sutherland, unpublished). Comparable figures for all solitary tunicates on the newly submerged larval plates were 10 or less (fig. 2). Thus, we believe that the recruitment of solitary tunicates was underestimated on the larval recruitment plates because of an apparent preference of the larvae for older plates. The data do indicate the potential availability of tunicate larvae from May through September, although they settled in October and November as well in 1970 (see below).

Pennaria: Pennaria is a summer hydroid (10) and settled only once during our study, during June and July of 1971 (fig. 2).

Schizoporella: Schizoporella larvae were available from May through November. In 1971, its recruitment was limited to the period from late July into November, while in 1972, recruitment began in May and continued through the summer (fig. 3). Recruitment in 1972 was greater than in 1971 by an order of magnitude (fig. 3), in contrast to that of Balanus and Tubularia which was reduced from the previous year (fig. 2).

Bugula: Bugula was a common recruit to newly submerged plates from May through September (fig. 3). Again, recruitment in 1972 was somewhat higher than in 1971, although the reason for this was not apparent.

Botryllus: Botryllus settled only once during our study, in the spring and summer of 1971 (fig. 3).

Monthly Series

October 1970: No data are available for the initial stages of this series because of procedural difficulties. Tubularia was abundant initially but had disappeared by the time the first map was made in January 1972 (fig. 4). At that time the series was dominated by Styela which occupied almost 50% of the area, but Ascidia and Schizoporella were also common (fig. 4). Both of the latter species gradually lost in the competition for space with Styela and were essentially absent by the end of April 1972 (fig. 4). At this time the series was terminated because of handling difficulties on the 1970 rack.

May 1971: This series was dominated initially by Bugula and Tubularia (fig. 5). In June both Ascidia and Styela settled beneath the former two species and began to grow and displace them. Tubularia is a winter species at Beaufort (10) and may also have disappeared because of increasing temperatures. Nudibranch predation on Tubularia was also heavy. Styela dominated Ascidia in the competition for space and by August the series was dominated by Styela, with Botryllus a common epizootic species (fig. 4). In October and November most Styela died for unknown reasons, particularly interesting in view of their survival over the same months on the October 1970 series. They were observed to be necrotic and often the internal organs were absent. This left much free space, eventually dominated by a regrowth of Tubularia which persisted throughout the winter and spring (fig. 4). The series was once again dominated by Styela during the summer of 1972; by May, Styela occupied almost 50% of the area (and Tubularia declined later in the summer). Schizoporella and Molgula also invaded the series in the spring of 1972 for the first time (fig. 4), and Bugula had become abundant by May but was underestimated by our sampling procedure.

June 1971: Like the previous series, this series was initially invaded by Tubularia and Bugula, although neither became as abundant (fig. 6). In contrast to the May 1971 series, however, Pennaria became abundant in June and July, and Ascidia settled in the absence of Styela. In the absence of competition with Styela, Ascidia dominated about 75% of the primary space by August (fig. 6). Ascidia settled less abundantly than Styela and had a more determinate growth form. Both factors contributed to its inability to dominate 100% of the area and to the high variation in percent cover between plates, which persisted through the summer (fig. 6). They also indicate why Ascidia was unable to compete with Styela on the May series (fig. 5).

Throughout the summer Pennaria occupied most of the remaining space in this series and was abundant on Ascidia as well. The area occupied by Styela represents only a few large individuals. Thus the two series were dramatically different all summer as a result of being started a month apart. The May series was dominated by Styela and Botryllus while the June series was dominated by Ascidia and Pennaria.

There was a distinct species turnover in the fall in this series as well as in the May series. Pennaria is a summer hydroid at Bearfort (10) and disappeared as the water cooled (fig. 1 & 6). In addition, Ascidia suffered a mortality similar to that of Styela on the May 1971 series, although it occurred several weeks earlier (fig. 5 & 6). The free space which remained was dominated by Tubularia as in the May 1971 series and Schizoporella invaded during November (fig. 5 & 6). By June 1972, the May and June series were quite similar with Styela dominating about 50% of the area and the remaining area occupied by Tubularia, Molgula, Schizoporella, (and Bugula) (figs. 5 & 6).

Hydractinia echinata invaded one plate in this series during August 1971, and by mid-November occupied about one-third of that plate. Its abundance remained about the same through June 1972. Although it met the basic criteria for inclusion in the community, it was not included in this analysis because of its restricted occurrence.

July 1971: In contrast to the May and June series in 1971, the July series was dominated initially by Balanus which then gradually decreased in abundance over the winter and spring of 1972 (fig. 7). Pennaria and Bougainvillia were variably abundant in the summer and fall, but largely disappeared by winter. During January through April 1972, the abundance of Schizoporella, Molgula, Styela, and Bougainvillia increased. However, all species except Schizoporella appeared to be losing in the competition for space with Styela by June 1972 (although Bugula was abundant at this time) (fig. 7).

August 1971: After an initial light settlement of Balanus, this series became dominated by Schizoporella (fig. 8). On the basis of our October 1970 series, we had expected heavy Tubularia, and Styela recruitment to this series in the fall, as there was still considerable empty space available by October 1971. We attribute the dominance of Schizoporella and the absence of other species to the lowered salinities caused by rain from tropical storm Doria, which passed through Beaufort in the last week of August. Maturo (9) found that Schizoporella settled well at low salinities and this appears to be substantiated here. Although some Tubularia invaded in November and December of 1971, Schizoporella remained dominant through June 1972. Species which invaded the other series in the spring of 1972, e.g., Styela, Molgula, (and Bugula) did not invade this series at the same time, suggesting they were excluded by Schizoporella (e.g., figs. 7 & 8).

September 1971: This series was invaded initially by Balanus and Bougainvillia, and in October was similar in appearance to the July series (fig. 7 & 9). As for the August series, Tubularia and Styela did not invade

in the fall of 1971. Bougainvillia disappeared in the winter and Balanus was replaced in the spring by Schizoporella, Molgula, Styela, Tubularia, (and Bugula) (fig. 9). The sequence of events was very similar to the July series except for the initial presence of Pennaria and absence of Tubularia in the July series (fig. 7), and the lower density of Balanus in the September series (fig. 9). Thus different submergence times produced similar as well as different sequences of species replacements.

October 1971: The October series was invaded only by Schizoporella, with a small amount of Tubularia appearing in late November (fig. 10). This was strikingly different from the October 1970 series which was dominated by Styela by March 1971 (fig. 4). Schizoporella dominated the October 1971 series through March with some invasion of Tubularia in April, only giving way to Styela (and Bugula) from May to July 1972 (fig. 10). Although no salinity data are available, we again attribute the initial (and thus continued) dominance of Schizoporella to lowered salinities caused by rain from hurricane Ginger, which passed through Beaufort on September 30 to October 2, 1971.

November 1971: The November series remained essentially empty until the arrival of Tubularia and Schizoporella in December and January (fig. 11). Tubularia occupied over half of the area during the spring of 1972, but disappeared with the onset of summer and/or lost in competition for space with Styela (fig. 11). Bugula was also present but underestimated here. Schizoporella remained low in density throughout the study period. Thus, by June 1972, the November series was similar to the May and June series. All three series had much available space in November.

1972 Series: Except for the presence of Balanus in the April series, during 1972 Schizoporella settled essentially in the absence of other species (fig. 12). The striking dominance of Schizoporella, in contrast with the spring of 1971, again appeared to result from the cool spring with its abnormally low salinities (fig. 1). The decline in Balanus in the April 1972 series was a result of being overgrown by Schizoporella (fig. 12).

Analysis of Variance

One way ANOVA (15) was used to detect differences in percent cover for the same species on different series. The analysis was performed only for June 1972 for all 1971 series, as this was the only period when differences between series were subtile enough to require statistical differentiation. Data were normalized with the arcsin $\sqrt{X}$ transformation, where X = % cover of a species on each plate in a series (15). Species included in the analysis were Tubularia, Styela, Schizoporella, Bugula, Molgula, Ascidia, Bougainvillia, and Balanus.

An F-max test for homogeneity of variances (15) revealed no significant differences ($p<.05$) for any species. This result is qualified somewhat by the omission of data for Molgula on the October series, and for Balanus on the May series. In both instances the percent cover of the respective species was zero, as was the sample variance. Using these two samples in the ANOVA would have violated the assumption of equal sample variances.

On the 1971 series in June 1972, ANOVA indicated significant ($p \leq .05$) differences only in the mean area occupied by Balanus, Schizoporella, Molgula, Styela, and Tubularia. In most cases a Student-Newmann-Keuls test (15) was used to detect significant differences between specific means. However, to detect differences between other series and the October series with respect to Molgula, the other series were tested for significant deviations from zero with a t-test. A similar procedure was followed in detecting differences between the other series and the May series with respect to Balanus. All significant differences ($p \leq .05$) are listed in Table 1 for all possible comparisons between series. For instance, in

June 1972, the series beginning in September and June of 1971 were different only with respect to Schizoporella (Table 1).

The major result of the analysis was a strong indication of convergence (i.e., similarity) in the 1971 series by June 1972. This is of particular interest in view of the strikingly different sequence of events on most series, as discussed above. Species composition in the June and November series was not significantly different by June 1972 (except for Hydractinia) (Table 1). During the summer of 1971 the June series was dominated by Ascidia and Pennaria, which, however, both disappeared in October 1971 (fig. 6). This left much free space on this series by November, after which the sequence of events in both series was similar (figs. 6 & 11). A trace of Molgula on the November series in June 1972 was not plotted. A similar convergence was seen in the May series, which in June 1972 only differed from the June and November series in having a greater amount of Tubularia (Table 1 and fig. 5). In 1971, the May series was dominated by Styela until November, when the mass mortality made much free space available (fig. 5). As for the June series, after this mortality the sequence of events was very similar to the November series (figs. 5 & 11).

In contrast to the other 1971 series, the sequence of events in the July and September series was similar (figs. 7 & 9) and by July 1972, there were no significant differences in species composition (Table 1). Interestingly, these similar series were separated by a series (August) which by June 1972 was strikingly different from all other series in the abundance of Schizoporella and the absence of Styela (fig. 8 and Table 1).

A further argument can be made for the convergence of the May, June, July, and November series. By June 1972, both Balanus and Molgula were minor constituents of all series. If these two genera (and Hydractinia) are ignored, by June 1972, there were no significant differences in species composition between these four series except for Tubularia, which, however, was present on all of them (Table 1). Although July and September were identical (Table 1), September had more Schizoporella than May, June, and November (fig. 9 and Table 1) and could not be included in the group of 4 similar series.

A final indication of convergence between series was found in the similarity of abundance of Styela by June 1972 on all 1971 series except the August one (Table 1). If Styela suffers heavy mortality in the fall of 1972 as it did in 1971, a large amount of free space would be made available on all series simultaneously. Thus, the series might further converge by 1973 as the May, June, and November 1971 series converged by June 1972.

5. Discussion

Submergence time had a dramatic effect on initial community development as a result of seasonal reproductive periodicities. During 1971, initial changes in species abundance on each series were different (except perhaps for July and September). The physical environment as well as time of year also appeared to have a direct effect on recruitment and initial development. Thus in October 1970, in the absence of periods of low salinity, the plates were colonized by Tubularia succeeded by Styela. On the October 1971 series, Schizoporella was the dominant organism. It seemed to be the only species capable of reproducing and growing in the low salinities caused by hurricane Ginger. Similarly, Schizoporella became dominant on the August 1971 series apparently as a result of tropical storm Doria. The physical environment also altered the initial development on the 1972 series as compared with the spring and summer of 1971. In 1971, the initial progression on each series was different, while in 1972 it was very similar, dominated by Schizoporella. We again attribute the success of Schizoporella to the unusually cool and rainy months of May and June. The physical

environment apparently suppressed the normal reproductive cycles of many species in 1972, e.g., Tubularia, and greatly altered the initial progression of species. Similar variation in year to year recruitment has been observed on the West Coast of North America by Coe and Allen (3).

The May and June series in 1971 underwent catastrophic changes in species composition in the fall of that year. However, seasonal changes in species abundance on older, undisturbed plates were generally less dramatic than changes in colonizing species composition. Not all larvae could invade the older plates. Thus Pennaria invaded the June but not the May 1971 series. Schizoporella invaded the August 1971 series, but did not invade the May, June, and July series at the same time. Again in October 1971, Schizoporella took over the newly submerged series, but did not invade the September (or earlier) series. In 1972, Schizoporella dominated all new series, but in spite of a very high recruitment, it was relatively unsuccessful at invading the 1971 series. Conversely, however, Schizoporella on the August series prevented the invasion of Styela, Molgula, and Bugula during the spring of 1972. Finally, Balanus larvae were generally available except in winter, but became abundant only on the July and September series in 1971 and the April series in 1972.

In addition to filtering out certain species of potential recruits, undisturbed communities appeared to remain more stable by harboring the vegetative remains of species which appeared to be absent. For example, Tubularia disappeared from the May and June series during the summer of 1971. It appeared again on these series in October, almost two months before it began to settle and grow on the newly submerged fall series. Tubularia was a common colonizer of newly submerged substrate and its absence from the October 1971 series probably resulted from an absence of larvae (because of the fall storms which lowered the salinity). The growth of Tubularia on the May and June series in October could only have come from the vegetative remains of the previous spring's growth.

The August 1971 series remained relatively constant throughout the year, dominated by Schizoporella; there were few seasonal changes in this series. For various reasons, therefore, it appears that the organisms at Beaufort on undisturbed substrate are not as regularly replaced during the year as Scheer (13) and McDougall (10) thought.

Shelford (14) gives some criteria for recognizing succession as follows: "1) Do forms drop out as the development of the community progresses? 2) Are any of the earlier animals essential to the seating of the later ones? 3) Is the second year's aspection like the first? If not succession may be indicated." All three criteria were met to some degree in this study. Balanus appeared to be a form which persisted on primary substrate only during the initial stages of community development. The recruitment of solitary tunicates appeared to require some conditioning of the plates, being much heavier on older plates than on newly submerged ones. Finally, and most importantly, in the second summer most 1971 series were less different in species composition than during the first summer, suggesting an approach to a climax state.

Scheer (13) originally defined seasonal progression as resulting "...from differences in breeding seasons of various organisms", but also included the idea of seasonal changes in species abundance on undisturbed, "mature" substrate ("...most of the organisms which settled in the winter months were dead or moribund by spring, and were replaced by organisms breeding in the latter season."). Previous authors (6,12) have used the term, seasonal progression, synonomously with seasonal changes in colonizing species abundance, implying that such changes are sufficient evidence for progression. In fact the original definition confuses two processes which need not be related; the seasonality of reproduction may have little to do with species replacements on undisturbed substrate. Indeed, during this

study colonizing species composition on new substrate changed much more rapidly over the year than species abundance on undisturbed substrate, suggesting that different processes were involved. We feel the term, seasonal progression, should be applied only to seasonal changes in species abundance in undisturbed, climax communities. With this perspective, initial differences in community development are "noise" in the process of succession and not evidence for seasonal progression. How much "noise" is involved depends on the seasonality of reproduction, but this may have little to do with the eventual presence or absence of progression, i.e., the existence of an oscillatory or stable climax. It seems probable, however, that those systems with the "noisiest" development will also attain climax states of greater seasonal variability. These are the systems in which seasonal progression is the most probable.

The problem of defining a climax is essentially the same as that of defining stability, and is a problem that ecologists still haven't adequately resolved (1). In the present case it appears that the 1971 plates were still changing as well as converging by June or July 1972. Thus, two or more years are required for the Beaufort system to mature and only then can the reality of seasonal progression be determined.

REFERENCES

1. Brookhaven National Laboratory, Brookhaven Symposia in Biology, No. 22 (1969).

2. Dale R. Calder and Morris L. Brehmer, Int. J. Oceanol. & Limnol. 1, 149 (1967).

3. W.R. Coe and W.E. Allen, Bull. Scripps Inst. Oceanog. Tech. Ser. 4, 101 (1937).

4. Paul K. Dayton, Ecol. Monogr. 41, 351 (1971).

5. E.C. Haderlie, 2nd Int. Cong. Mar. Corrosion and Fouling, Athens., pp.1-14 (1968).

6. E.C. Haderlie, Veliger, 12, 182 (1969).

7. E.C. Haderlie, Veliger, 13, 249 (1971).

8. F.J.S. Maturo, J. Elisha Mitchell Sci. Soc. 73, 11 (1957).

9. F.J.S. Maturo, Ecol. 40, 116 (1959).

10. K.D. McDougall, Ecol. Monogr. 13, 321 (1943).

11. Dixy Lee Ray (ed.), Marine Boring and Fouling Organisms, University of Washington Press, 536 pp. (1959).

12. Donald J. Reish, Veliger, 6, 124 (1964).

13. Bradley T. Scheer, Biol. Bull. 89, 103 (1945).

14. V.E. Shelford, Puget Snd. Biol. Sta. 7, 217 (1930).

15. Robert R. Sokal and James Rohlf, Biometry, W.H. Freeman and Co., San Francisco, 776 pp. (1969).

16. Harry W. Wells, Ecol. Monogr. 31, 239 (1961).

17. Harry W. Wells, Mary Jane Wells, and I.E. Gray, Ecol., 45, 752 (1964).

18. Harry W. Wells, Mary Jane Wells, and I.E. Gray, Bull. Mar. Sci. Gulf and Caribbean, 14, 561 (1964).

19. Woods Hole Oceanographic Institution, Marine Fouling and its Prevention, U.S. Naval Institute, Annapolis, Md, 388 pp. (1952).

Discussion

Dr. Sutherland was asked what evidence he had that some species were necessary for the settlement of others that followed. He answered that Styela demonstrated this by its preference for older plates, and its avoidance of newly exposed plates.

In answer to another question, Dr. Sutherland indicated that Schizoporella was able to maintain a fouling-free surface while the colony was alive.

May	May						
June	Tubularia	June					
July	Tubularia Balanus	Tubularia	July				
Aug.	Tubularia Schizoporella Styela	Schizoporella Styela	Schizoporella Molgula Styela	Aug.			
Sept.	Tubularia Schizoporella Balanus	Schizoporella		Schizoporella Styela	Sept.		
Oct.	Tubularia Schizoporella Molgula	Schizoporella Molgula	Tubularia Molgula	Schizoporella Styela	Molgula	Oct.	
Nov.	Tubularia		Tubularia Molgula	Tubularia Schizoporella Styela	Tubularia Schizoporella	Schizoporella	Nov.

Table 1. Species which showed significant ($p \leq .05$) differences in mean percent cover on the 1971 series by June 1972. All possible comparisons between series are listed.

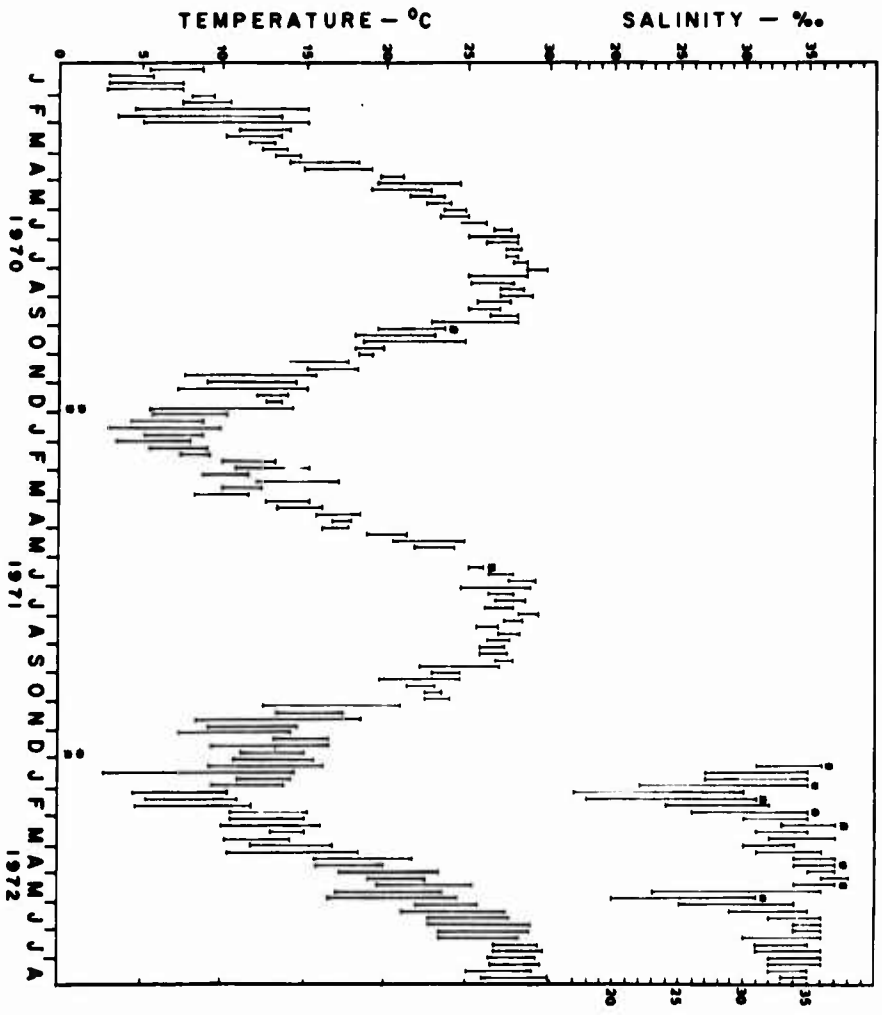


Fig. 1 Weekly ranges of temperature and salinity at the study site.

* - Based on 3-6 days of data. ** - Range based on 8 days.

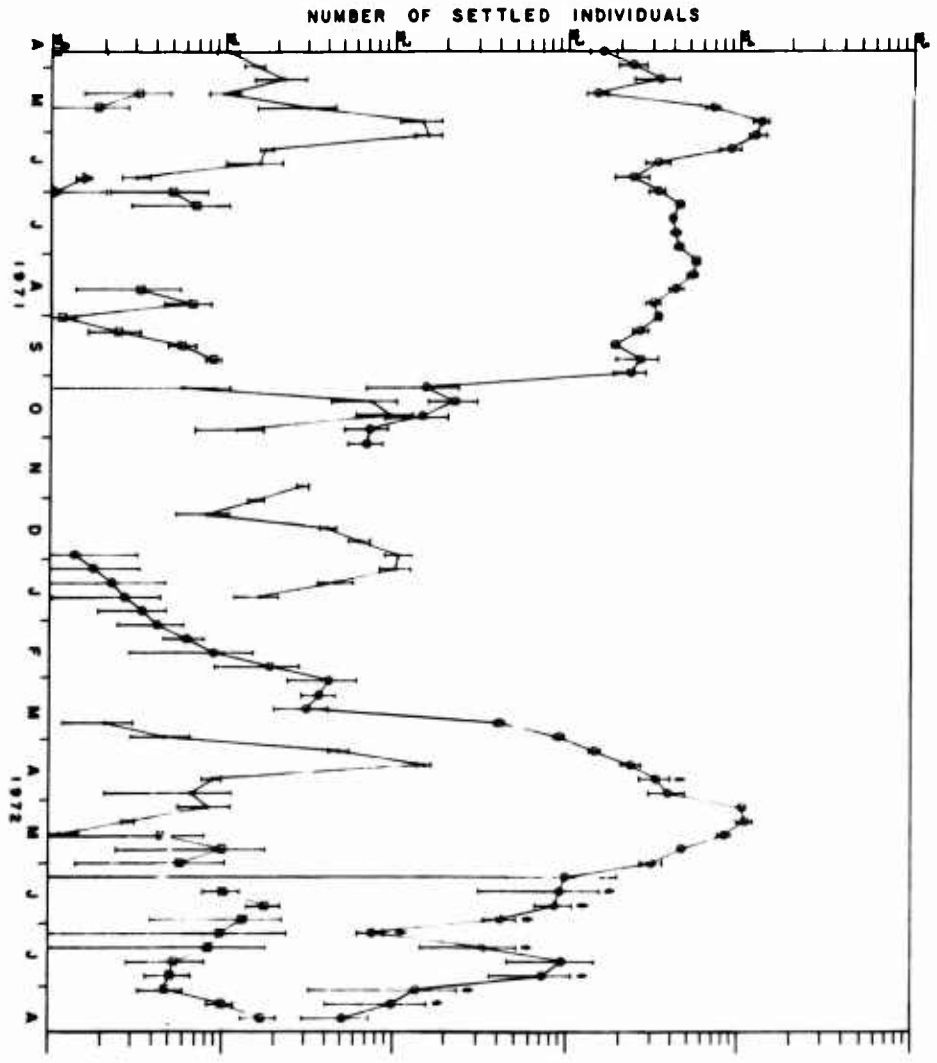


Fig. 2 Estimated mean number (± the standard deviation) of individuals settling during each arbitrary 7 day period. ⊙ - Balanus; ● - Tubularia; ⊡ - Solitary tunicates; △ - Pennaria. ▼ - Data based on 2 plates.

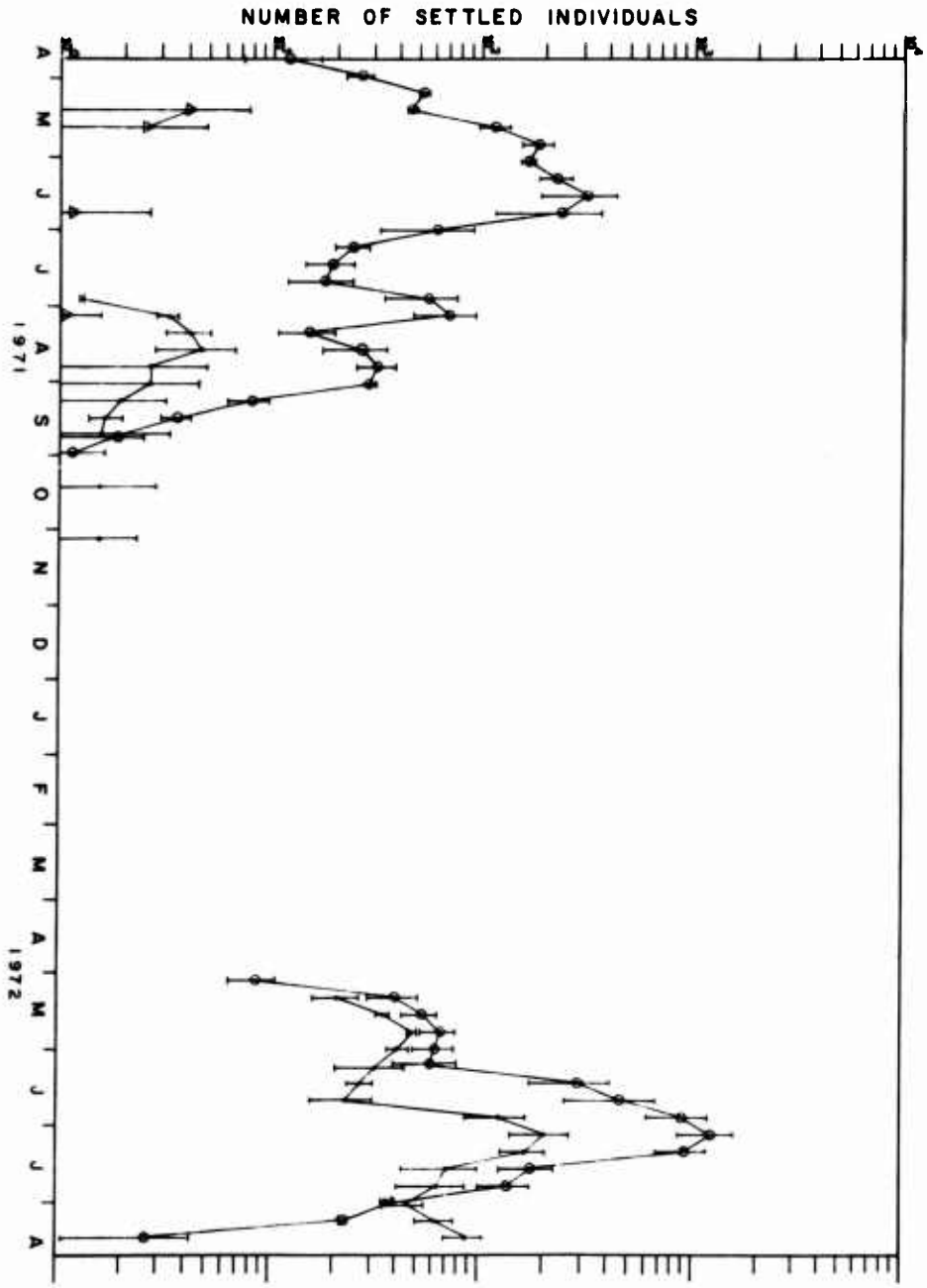


Fig. 3 Estimated mean number (± the standard deviation) of individuals settling during each arbitrary 7 day period. ● - Schizoporella; ⊙ - Bugula; △ - Botryllus.

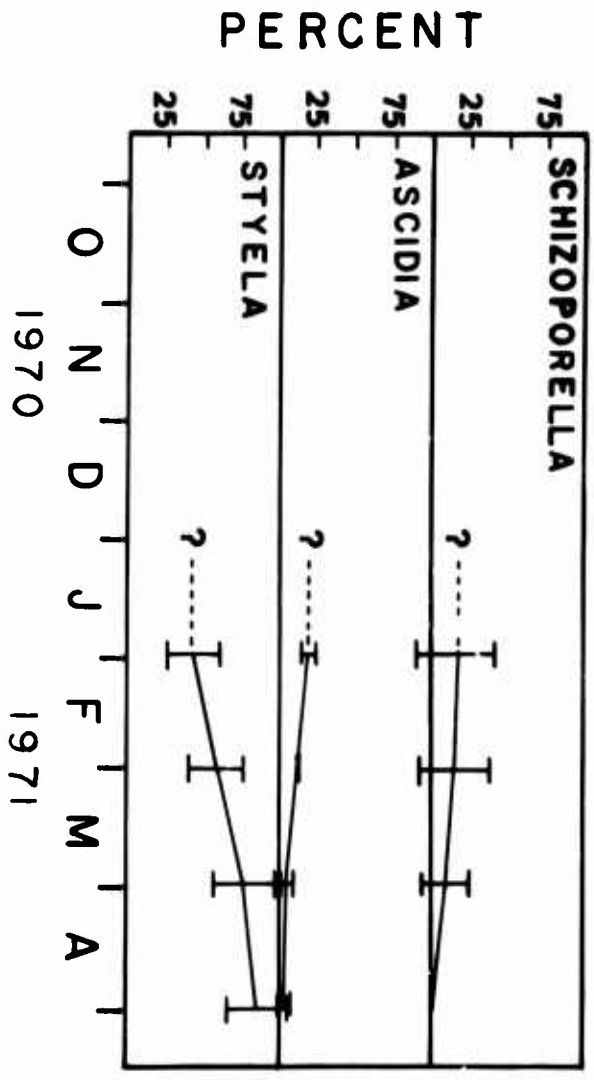


Fig. 4 Estimated mean percent cover (± the standard deviation) for each species at arbitrary intervals. The series was initiated on 2 October 1970.

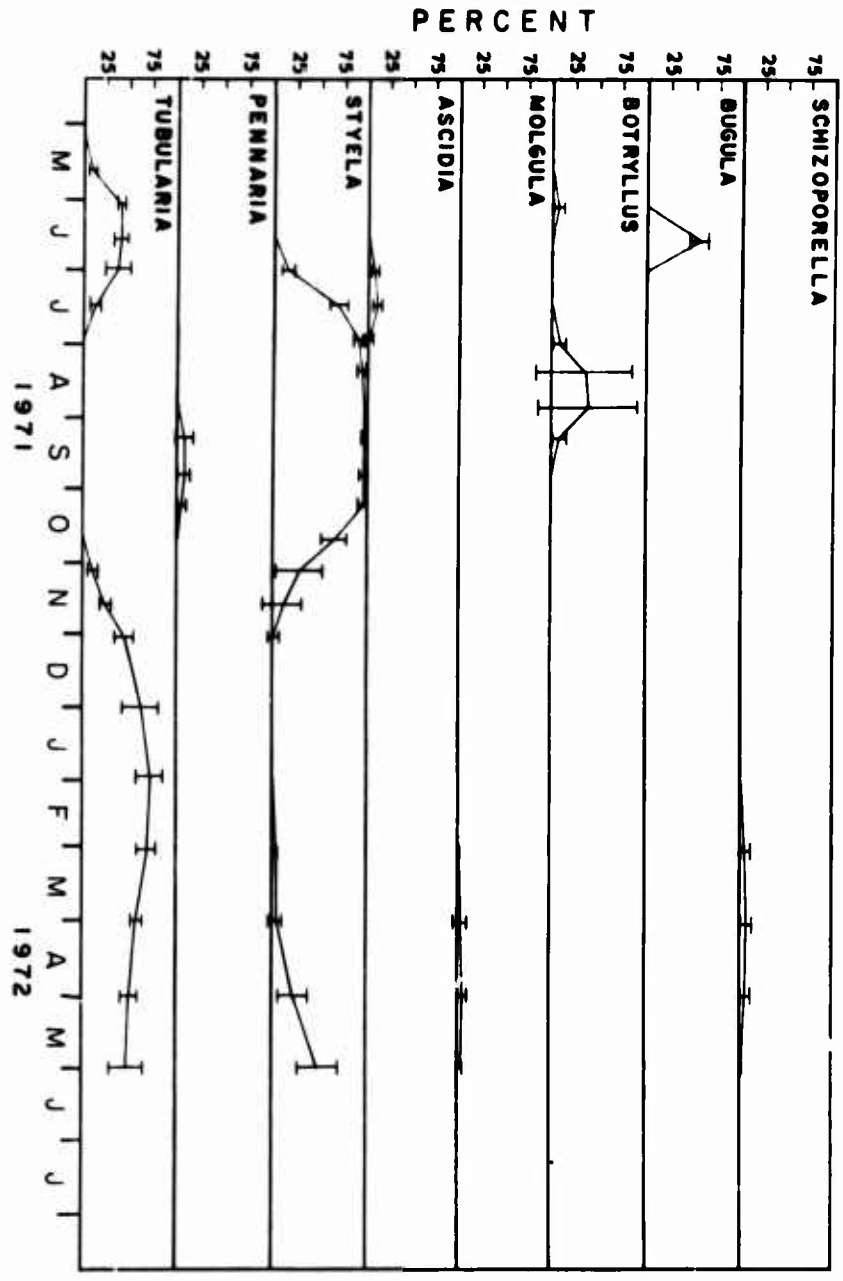


Fig. 5 Estimated mean percent cover (± the standard deviation) for each species at arbitrary intervals. The series was initiated on 6 May 1971.

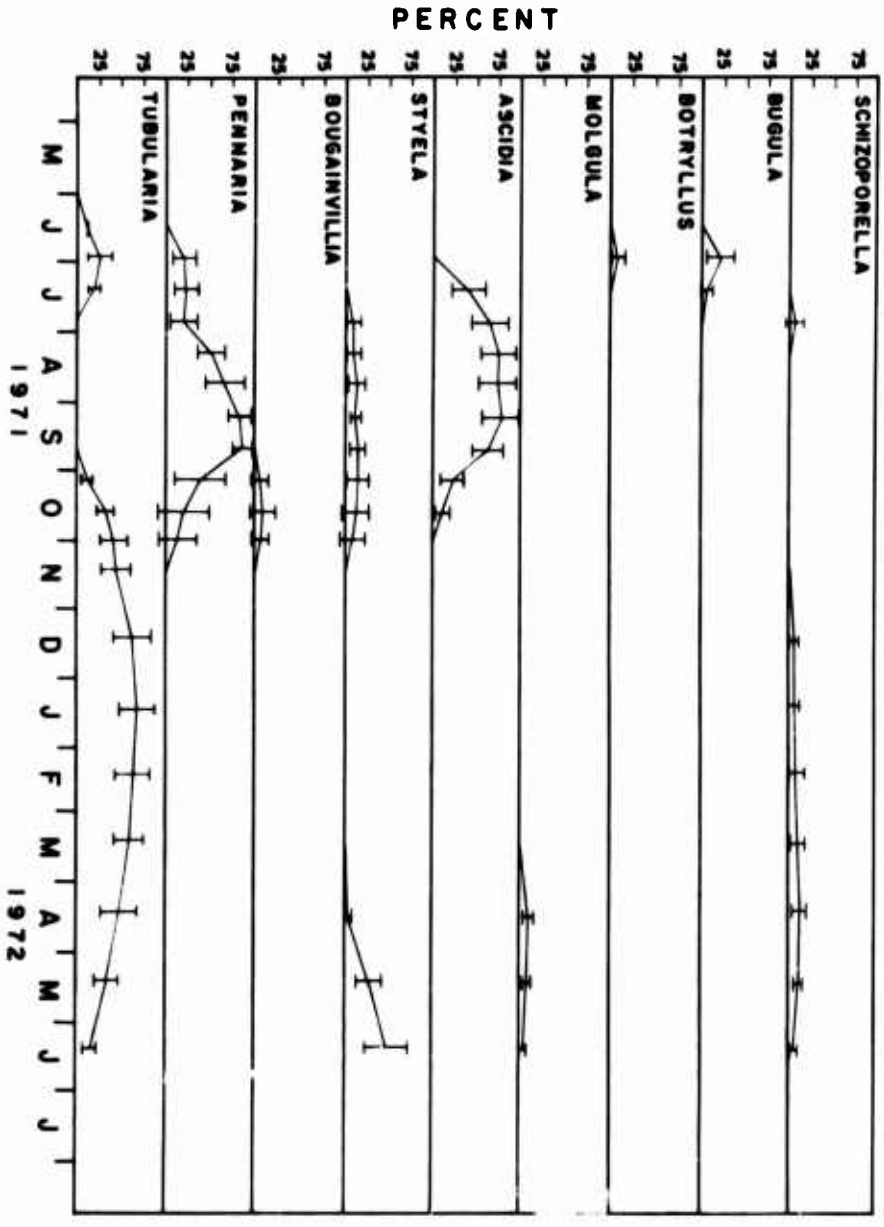


Fig. 6 Estimated mean percent cover ($\pm$ the standard deviation) for each species at arbitrary intervals. The series was initiated on 31 May 1971. (This is the June 1971 series).

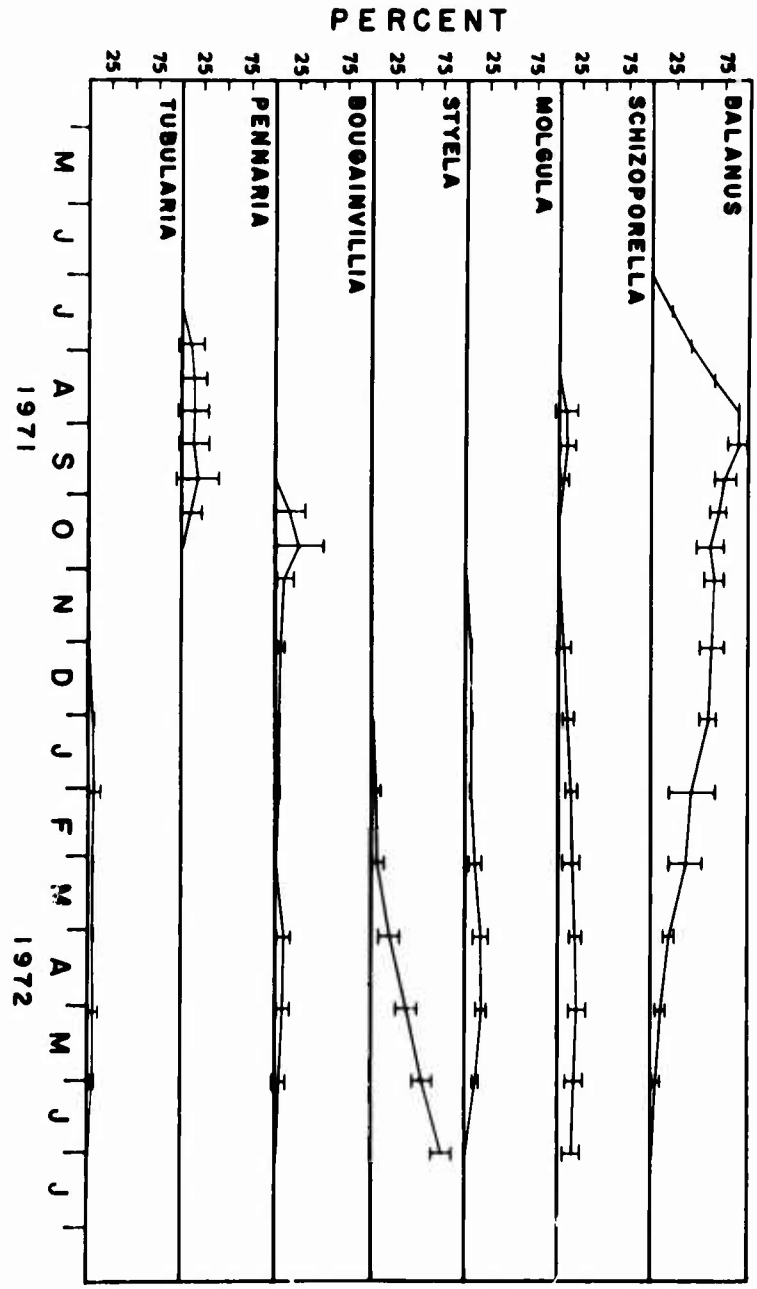


Fig. 7 Estimated mean percent cover (± the standard deviation) for each species at arbitrary intervals. The series was initiated on 1 July 1971.

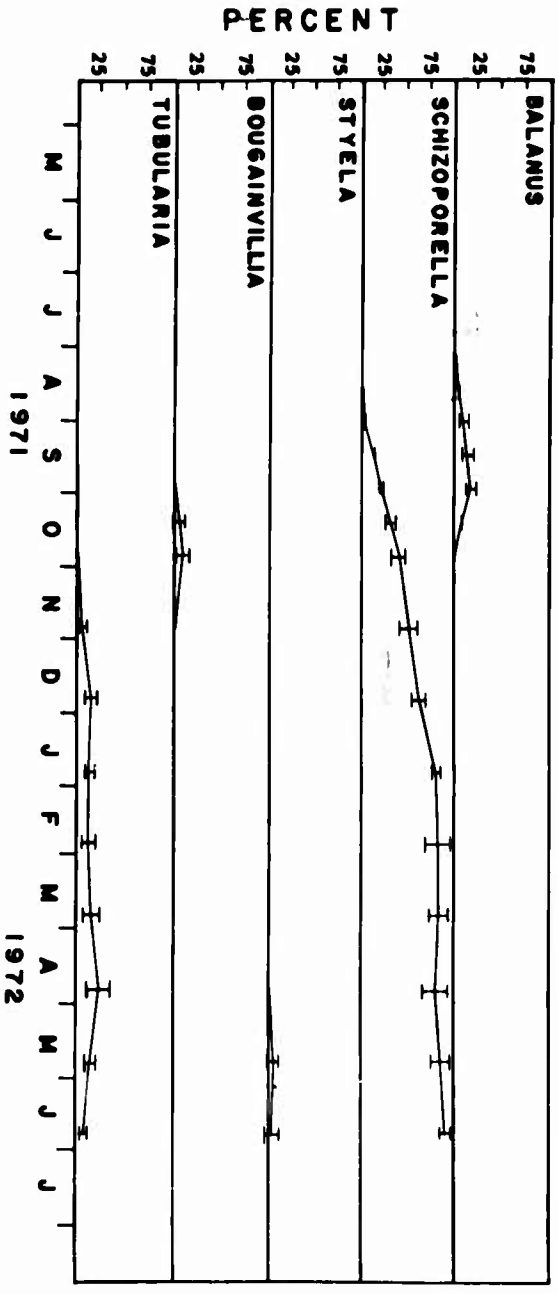


Fig. 8 Estimated mean percent cover (± the standard deviation) for each species at arbitrary intervals. The series was initiated on 2 August 1971.

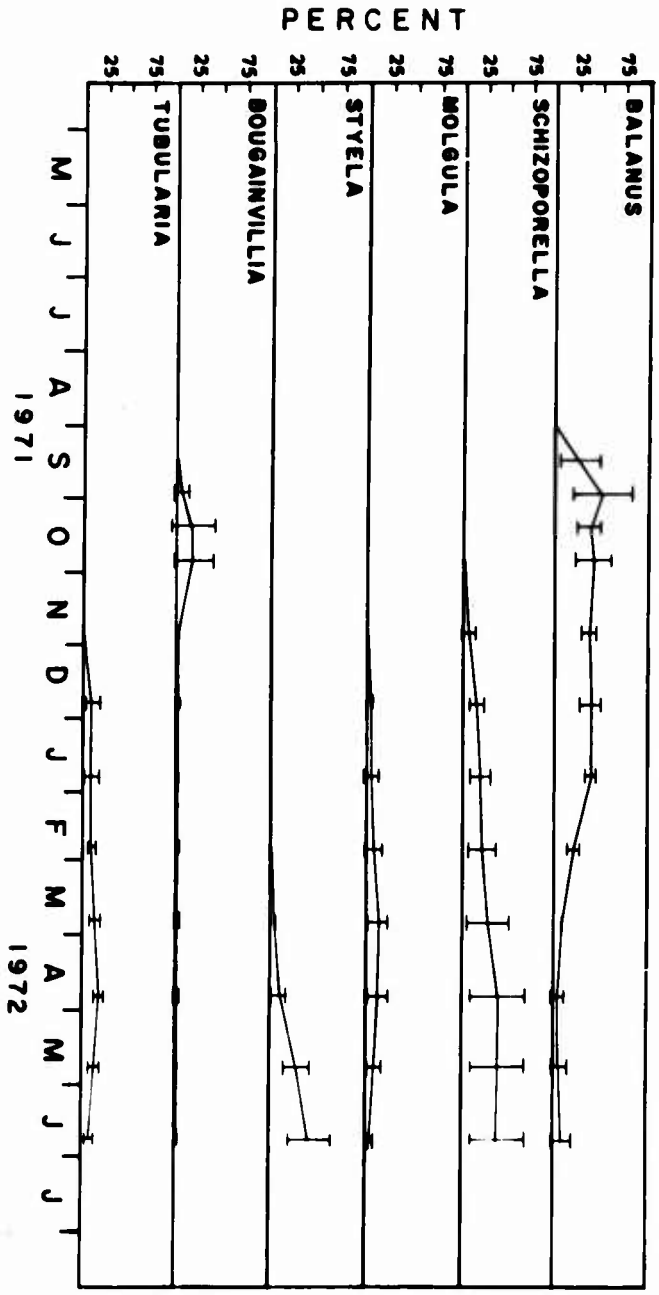


Fig. 9 Estimated mean percent cover ($\pm$ the standard deviation) for each species at arbitrary intervals. The series was initiated on 1 September 1971.

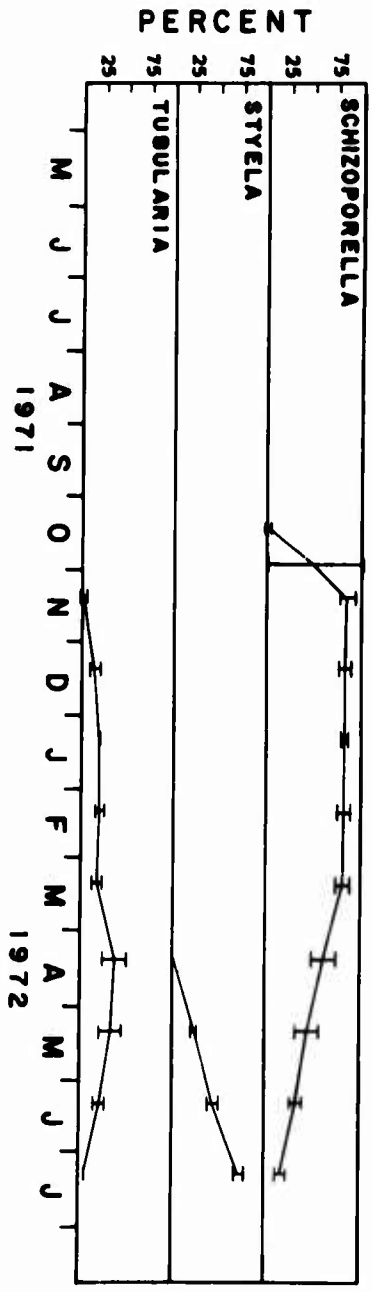


Fig. 10 Estimated mean percent cover (± the standard deviation) for each species at arbitrary intervals. The series was initiated on October 1971.

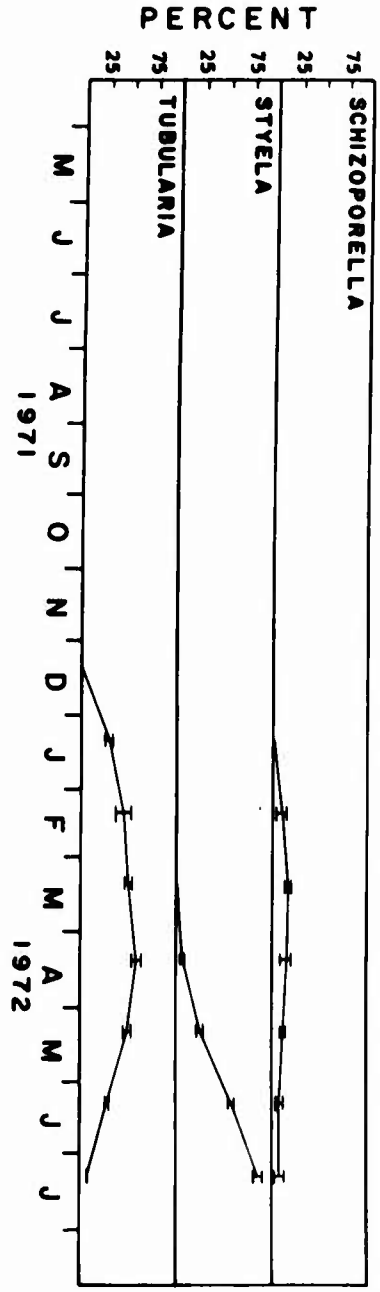


Fig. 11 Estimated mean percent cover (± the standard deviation) for each species at arbitrary intervals. The series was initiated on 12 November 1971.

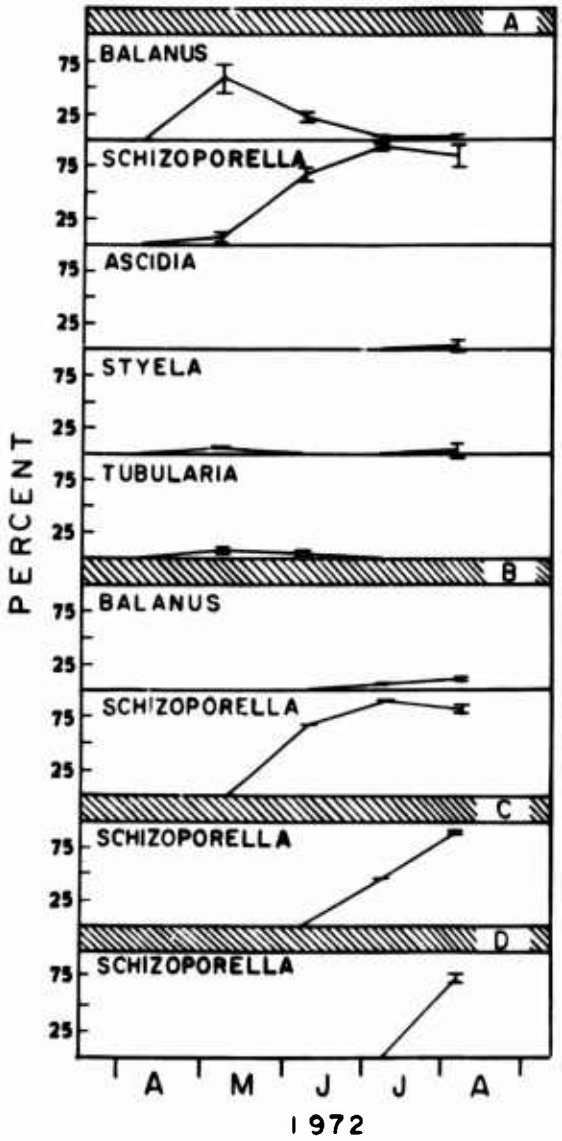


Fig. 12 Estimated mean percent cover (± the standard deviation) for each species at arbitrary intervals. A. Series initiated on 9 April 1972. B. Series initiated on 11 May 1972. C. Series initiated on 9 June 1972. D. Series initiated on 10 July 1972.

Study of Some Variables Affecting Antifouling Paints' Performance

Dr. V. Rascio and Chem. Eng. J. J. Caprari*

*Laboratory for Testing Materials and Technological Research
(La Plata, Argentina) and National Research Council
of the Argentine Republic

1. Introduction

This paper is the fourth and last part of a study about antifouling paints' behaviour in raft trials, started in 1966 in Mar del Plata's port (Argentina). The work was planned between our Laboratory, the National Research Council and the Marine Biology Institute with the collaboration of the Navy. It was the first study on the subject in our country. Up to that date we had only scattered references to the fouling conditions of Argentine's ports and about their influence on the performance of anti-corrosion and antifouling coatings usually employed in the protection of ship's bottoms.

A previous study was made between the Navy and the IRAM (Argentine Institute for Standardisation of Materials) testing commercial paints in three rafts, placed at Belgrano's, Mar del Plata's and Ushuaia's harbours. A specification was prepared, but no work was published on physical and chemical properties of ships' paints and the biological and hydrological characteristics of those ports.

During our investigations, Bastida (1,2,3,4,5)[1] determined the most important fouling species which settle on non toxic plates placed in the experimental raft in Mar del Plata's port and also the relations between fouling and local environment.

A comparison was made with fouling studies previously performed in other countries by Fancutt, Hudson, Harris and Banfield (6,7,8) for the Marine Corrosion Subcommittee of the British Iron and Steel Research Association, by Ketchum and Ayers (9,10) for the Woods Hole Oceanographic Institution and by van Londen and De Wolf (11,12,13,14) for the Verfinstituut T.N.O.

Temperature, salinity and oxygen content were found to be normal for a temperate port [Fig. 1]. Pollution by industrial wastes is appreciable at Mar del Plata's harbour and for this reason pH was periodically recorded; values between 8,3 and 6,7 were found [Fig. 2]. The influence of pH on the properties of antifouling films is very important, because rosin and cuprous oxide solubilities are affected by this variable.

Our experimental scheme was divided into four stages:

a) Influence of the toxic employed and of paint binder solubility (studied between 1-IX-66 and 1-IX-67 (5).

b) Influence of the toxic concentration (1-X-67/1-X-68)(16).

---

[1] The numbers in parentheses refer to the list of references at the end of this paper.

c) A new study of the same variables, but using new mineral toxics, in 18 month's raft trials (1-X-68/1-V-70)(17).

d) Influence of different inert pigments on the toxicity of the film, that is the present paper.

The tested plates were periodically observed for determining the fouling settlement. From 117 paints studied, 60 showed good leaching rate and toxicity throughout the first year's immersion. Leaching rate of the paints decreased very quickly during the second year's exposure [Fig. 3] and only 15 formulations gave good fouling protection at the end of the test (20-24 months).

2. Fouling Organisms Recorded at Mar del Plata's Harbour

Fouling settlement on non toxic panels was determined at four different depths during our studies:

Level A: From surface to 0,30 m
Level B: 0,50 to 0,90 m
Level C: 1,10 to 1,50 m
Level D: 1,70 to 2,10 m

Antifouling paints were only tested at levels B, C and D.

Four different classes of settlement are distinguished at the different depths [Fig. 4,5,6 and 7]:

a) Fouling organisms with similar attachment at the three levels (B, C, D):

Diatoms
Tubularia crocea
Gonothyraea inornata + Obelia angulosa
Mercierella enigmatica + Serpula vermicularis + Hydroides norvegica
Polydora cf. ciliata
Eubranchus sp.
Tisbe furcata + Harpacticus sp.
Corophium sp.
Balanus amphitrite + Balanus trigonus
Cyrtograpsus angulatus
Bowerbankia gracilis
Bugula sp.
Ciona intestinalis

b) Fouling organisms with decreasing settlement from B to D:

Polysiphonia sp.
Enteromorpha intestinalis (with great intensity at level B)

c) Organisms which settle only at levels B and C:

Bryopsis plumosa

d) Organisms which settle only at level B:

Ulva lactuca

The most important differences were represented by the Algae attachment. The Chlorophyte Enteromorpha intestinalis is very common on fouled paints and at level B but is very scarce at levels C and D. Light is necessary for the chlorophylic synthesis. For this reason Enteromorpha is usually restricted to the vicinity of the water line. A study was published recently by one of

the authors about this subject (18).

Ulva lactuca is another Chlorophyte, with slight fixation at level B. As it is a species very sensible to toxic paints (more so than Enteromorpha intestinalis) it is not usually found on painted test plates.

Finally Bryopsis plumosa is the third Chlorophyte registered on non-toxic plates. It is not present on the painted plates.

3. Type of Antifouling Paints Tested

Antifouling oleoresinous and vinyl paints were formulated in such a way as to determine the influence of the following variables: nature of the matrix, solubility of the matrix, nature of the toxic, toxic/inert pigment ratio and nature of the inert pigment.

1. Nature of the matrix

Two different types of binders were used: oleoresinous and vinyl. Forty-eight paints of the first type were formulated with a rosin/phenolic varnish binder (Table I); another 48 paints were prepared with a rosin/linseed standoil 60 poises binder (Table II) and 15 paints with rosin/mercuric oleate binder (mercuric oleate was used as reinforcement toxic and as plasticizer)(Table III). For vinyl paints, 6 samples were formulated using rosin and VYHH vinyl resin (Table IV).

2. Solubility of the matrix

For oleoresinous paints, three different rosin/plasticizer ratios were tested (3/1, 5/1, 7/1). In those paints containing mercuric oleate, the first ratio was fixed at 2,5/1, owing to the content of oleate of the toxic. For vinyl formulations, the rosin/vinyl resin/tricresyl phosphate ratio previously studied (1/1/0,25) was maintained, owing to the good performance of those paints.

3. Nature of the toxic

Cuprous oxide was used as the main toxic. In oleoresinous paints, complementary toxics such as mercuric oleate, mercurous arsenate, cupric acetoarsenite and cuprous arsenite were added. In vinyl samples mercuric oleate was replaced by mercuric oxyde and arsenous trioxyde.

Copper, mercury and arsenic content of the different toxins is tabulated below:

	Cu (%)	Hg (%)	As (%)
Cuprous oxide (Cu_2O)	88,8	-----	-----
Mercuric oxide (HgO)	-----	92,5	-----
Mercuric oleate	-----	41,6	-----
Arsenous trioxide (As_2O_3)	-----	-----	75,0
Mercurous orthoarsenate	-----	72,0	12,5
Cupric acetoarsenite	22,7	-----	40,5
Cuprous arsenite	60,0	-----	23,0

Mercuric oleate, cupric acetoarsenite (Schweinfurt green) and cuprous arsenite were prepared in the laboratory. The other toxins were of

industrial origin.

In oleoresinous paints, 10% of zinc oxide (calculated on the basis of copper oxide content) was also added.

4. Toxin/inert pigment ratio

The antifouling properties of oleoresinous paints formulated with cuprous oxide as only toxin were compared with those of paints prepared with a toxin/inert pigment ratio 3/1.

In vinyl paint formulations inert pigments were not employed.

5. Inert pigments

This is the main variable studied in this paper. Our purpose was to establish the influence of different extenders on the toxicity of the film.

In previous tests the only extender used was ferric oxide. Being a very opaque pigment and giving very resistant films, this pigment in general improves the quality of the paint film.

In this new stage of our work we wanted to compare paints containing ferric oxide with others formulated with calcium carbonate (chalk) and magnesium silicate (talc) and more specially to study the influence of the extenders on the hardness of the film. Barium sulphate was not considered because of its high specific gravity.

4. Preparation and Application

Paint samples were prepared on a laboratory ball mill. The pigments were dispersed during 24 hours, except the cuprous oxide that was added at the end of the milling process (3 hours).

Two coats (about 100μ thickness) were painted on sandblasted steel plates (30 x 40 cm) protected previously with a vinyl wash-primer and a good performance marine anticorrosion paint. Panels were immersed in sea water (raft at Mar del Plata's port) 24 hours after the application of the second antifouling paint's coat.

Observations of the painted plates were made in periods of 75 days. The fouling attachment on non-toxic plates (sandblasted plastics) was monthly registered.

5. Some Observations Related to the Variables Previously Studied

Before analyzing the results obtained in the present experience it is convenient to review the conclusions obtained in previous studies. In some cases they coincide with those presented by other authors but in some cases not.

1. Oleoresinous AF paints (rosin WW/phenolic varnish binder)

important influence on the antifouling properties of the film. It has been demonstrated that as the concentration of ferric oxide increases, the service life of the paint decreases (16).

c) The only complementary toxins which increased the toxicity of the film were mercurous orthoarsenate, cuprous arsenite and mercuric oleate (17). With this last component it is necessary to modify the rosin/plasticizer ratio, because of the presence of the oleic acid. Particularly the use of mercuric oxide gave negative results as antifouling. It is possible that this effect is due to the partial reaction between cuprous oxide and mercuric oxide, giving two slightly soluble compounds (cupric oxide and metallic mercury). The low efficiency of mercuric oxide has been mentioned in our previous papers.

d) Zinc oxide increases the toxicity of the paints. For this reason we added 10 percent with respect to Cu_2O. It has not been tested in higher concentration because of its reactivity with acid binders.

e) Another variable affecting pigment dispersion is the efficiency of the milling operation (the rate of rotation of the ball mill, the size, the quantity and nature of the balls and the amount of consistency of the materials to be milled). All the samples tested were prepared exactly in the same conditions. The influence of this variable is perhaps the cause that sometimes laboratory paints show differences in leaching rate from those of the same formulations prepared on an industrial scale (21,22,23). This aspect of the problem should be thoroughly studied in the future.

f) The influence of the milling time on the activity of the cuprous oxide should be emphasized. A three hours dispersion proved to give very efficient paints. Rosin and cuprous oxide react partially during the milling process, producing copper soaps and modifying the rosin/plasticizer ratio. This reaction reduces the solubility of the binder. Paints of the same composition prepared by dispersing the cuprous oxide for longer periods were less effective.

g) All the effective oleoresinous paints reach after some days of immersion a steady state leaching rate, above the necessary critical value. They show good antifouling properties during exposure periods between 6 and 18 months, and finally the paint film fouls. The effectiveness of the paints is always measured by the time that the film remains without settlement.

h) Slight differences were observed in the behaviour of some effective formulations exposed in different periods. This seems to be related to the sea water pollution of the experimental area. A reduction of the pH values modifies the solubility of some components of the paints (rosin and copper oxide) reducing the release of toxin from the film.

i) Film thickness has an important influence upon the paint coating performance. It is possible to obtain an 80-100μ film of AF paint with two coatings, with brush or roller application. The authors consider that this thickness is the minimum necessary to eliminate the influence of film irregularities due to imperfect application.

j) The test plates actually employed in raft trials are not the most suitable surfaces for testing antifouling paint systems. A great number of samples are annually eliminated due to the fouling settlement at the edges, while the center of the plates is not fouled. The difficulty is to obtain an adequate thickness at the edges, coupled with increased wastage of Cu_2O in that zone, due to the turbulence of the sea water. When fouling attachment begins the film is quickly destroyed and the corrosion processes are accelerated.

2. Vinyl AF paints (Rosin WW/vinyl resin VYHH)

a) Raft trials confirm that vinyl paints are more efficient than oleoresinous antifouling paints, specially in long term exposures (24).

b) Test plates of all antifouling paint samples showed no settlement after one year's immersion. The importance of the use of complementary toxics was established in 18, 24 and 36 month's trials.

c) The use of non-toxic pigments in vinyl paints reduced the leaching rate and the efficiency of the film.

6. Discussion

1. Influence of inert pigments

The existing references dealing with the influence of the inert pigments on the leaching rate of antifouling paint films (9,22,23) do not provide an exact idea about the relation between the paint composition and its efficiency. Babel (9) when discussing the effect of extenders, names a large variety of these substances that give satisfactory results and some others that are not so efficient. Ketchum and Ayers (23) indicate that the fouling resistance of soluble matrix antifouling paints appears to be independent of the presence of non-toxic pigments.

As previously mentioned, the effect of three inert pigments were tested: ferric oxide, calcium carbonate (chalk) and magnesium silicate (talc).

The analysis of the results obtained (settlement of fouling during the immersion period) have established that paints with calcium carbonate showed the best performance:

Extender	Total Samples	Samples without settlement	
		375 days	600 days
Chalk	27	18 (67%)	2 (7%)
Ferric oxide	27	11 (41%)	--
Talc	27	5 (18%)	--

It is possible to compare these results with the service life of antifouling coatings prepared with the same oleoresinous binders and without extenders (cuprous oxide and cuprous oxide + complementary toxins). In this case we have 19 samples (63%) that satisfy the test requirements for a 375 days' immersion period. At the end of a 600 days' raft exposure 7 samples (23%) showed a degree of settlement less than one (see fouling settlement versus efficiency percent in Table VIII).

These results indicate that for any binder solubility used, calcium carbonate (chalk) is the most effective extender for maintaining an adequate leaching rate. Paints with a rosin WW/phenolic varnish binder (3/1) containing this extender and prepared with toxin alone behaved in a similar way at 375 and 600 days' immersion test [Fig. 8]. Differences observed for ratios 5/1 [Fig. 9] and 7/1 [Fig. 10] are of no significance.

Hardness, permeability and an adequate chalking of the film seem to play a part in the antifouling effectiveness of those paints.

The different compositions of oleoresinous paints are presented in Tables I, II and III. Table IV gives the vinyl formulations. The performance of these paints (degree of fouling settlement) in raft trials is shown in Tables V, VI, VII and VIII.

When linseed standoil 60 P was used as plasticizer the influence of the use of calcium carbonate is very marked [Fig. 11,12 and 13]. Samples with this extender were always more efficient than those paints prepared without non-toxic pigments.

The graphs presented are based on the mean values of settlement found for each binder, solubility and pigment composition.

2. Influence of other variables

a) Nature of the toxicant

In order to analyse this variable, we considered as a whole the samples of all the three oleoresinous binders studied, excluded vinyl formulations. For samples without extenders we have:

Toxins, without extenders	Total Samples	Samples without settlement 375 days	600 days
Cu_2O-ZnO-RHg	6	6 (100%)	3 (50%)
Cu_2O-ZnO-AsO_3Cu_3	6	5 (83%)	2 (33%)
Cu_2O-ZnO	6	4 (66%)	---
Cu_2O-ZnO-AsO_4Hg_3	6	3 (50%)	2 (33%)
Cu_2O-ZnO-V.Schw.	6	1 (17%)	---

The samples containing mercuric oleate as complementary toxin showed the highest fouling resistance. The behaviour of these samples was particularly notable in exposure periods up to 20 months.

Considering all the samples with and without extenders the results are in general agreement with those previously obtained:

Toxins with Extenders	Total Samples	Samples without settlement 375 days	600 days
Cu_2O-ZnO-RHg	15	11 (73%)	3 (20%)
Cu_2O-ZnO	24	15 (62%)	2 (8%)
Cu_2O-ZnO-AsO_3Cu_3	24	11 (46%)	2 (8%)
Cu_2O-ZnO-AsO_4Hg_3	24	10 (42%)	2 (8%)
Cu_2O-ZnO-V.Schw.	24	6 (25%)	---

These results confirm that it is possible to formulate good paints with an adequate performance using cuprous oxide only. Fifteen paints of this composition remain unfouled for 12 months, and 2 samples reached 20 months of immersion (paints 417 and 318, Tables I and V). At the end of the exposure period fouling attachment was beginning at the edges of the plates. The results confirm that the use of complementary toxins and specially mercuric oleate, cuprous arsenite and mercuric orthoarsenate is desirable for performances up to one year.

b) Binder composition

The efficiency of the three binders used may be tabulated in the following way:

Binder	Total Samples	Samples without settlement 375 days	600 days
Rosin/oleic acid[1]	15	11 (73%)	3 (20%)
Rosin/ph. varnish	48	26 (54%)	6 (12%)
Rosin/standoil	48	16 (33%)	---

It is very important to remark that samples prepared with mercuric oleate are not strictly comparable with the samples obtained with the other two binders but they are included so as to give an idea of the behaviour of this matrix.

The fourth binder is that of the vinyl paints, used as reference. One hundred percent of these paints remain unfouled after 12 months immersion and 67% after 20 months.

c) Binder solubility

From the examination of the results obtained with the different rosin/plasticizer ratios, we get:

Rosin/plasticizer ratio	Total Samples	Samples without settlement 375 days	600 days
3/1	37	20 (54%)	2 (5%)
5/1	37	22 (59%)	4 (11%)
7/1	37	11 (30%)	3 (8%)

The set of samples that show the highest efficiency as antifouling at 375 and 600 days exposure is that corresponding to a 5/1 rosin/plasticizer ratio. This value is only of statistical interest, because it seems that each toxin requires an individual adjustment of this variable, so as to obtain the best coating performance.

It is important to mention that none of the samples tested showed cracking, blistering, peeling or any other significative failure of the film under the exposure conditions of Mar del Plata's harbour.

7. Summary

1. Calcium carbonate (chalk) provides better antifouling paints than those formulated with ferric oxide or magnesium silicate as extender pigments.

2. After 375 days' immersion, samples containing chalk showed in some cases a lower settlement than others prepared with toxins as only pigment. Two samples with Cu_2O-ZnO-$CaCO_3$ were still unfouled after a 600 days' raft trial.

3. Good antifouling performance can be obtained with cuprous oxide-zinc oxide paints, but if longer lives than one year are required in the hydrological and biological conditions of our experimental area, it is advisable to use complementary toxins. Of all the substances tested for

[1] from mercuric oleate

this purpose only three gave satisfactory results: mercuric oleate, cuprous arsenite and mercurous orthoarsenate.

4. The best performance was obtained with a rosin WW/phenolic varnish binder. Paints formulated with rosin WW/mercuric oleate give good fouling resistance, but the greater toxicity could be due to the mercury content of the paint.

5. A 5/1 rosin/plasticizer ratio provided the highest percentage of paints with excellent performance. A 3/1 ratio gives very satisfactory protection with Cu_2O-ZnO formulations.

6. The good fouling resistance of coatings based on a vinyl acetate-vinyl chloride copolymer resin binder should be noted. Some of these paints were able to withstand exposure periods of up to 600 days in the raft conditions.

References

1. Bastida, R. O.- Preliminary notes on the marine fouling at the port of Mar del Plata (Argentina). Compte Rendu, 2nd. Int. Congr. on Mar. Foul. and Corrosion. Athens, 1968, 557-562 b.
2. Bastida,R.O.- Las incrustaciones biológicas en el puerto de Mar del Plata, período 1966 67. Rev. Mus. Arg. Cienc. Nat. B. Rivadavia, Hidrobiología, tomo III, nº 2, 203-285, 1970.
3. Bastida, R. O.- Las incrustaciones biológicas en el puerto de Mar del Plata. 1a. y 2a. parte. LEMIT, 4-1969, 1-60.
4. Bastida, R. O.- Las incrustaciones biológicas en las costas argentinas. La fijación mensual en el Puerto de Mar del Plata durante tres anos consecutivos. Corrosión y Protección (Espana), 2, nº 1, 21-37, enero-febrero 1971.
5. Bastida, R. O. y M. R. Torti.- Estudio preliminar sobre las incrustaciones biológicas de Puerto Belgrano. LEMIT, 3-1971, 45-75.
6. BISRA, Marine Corrosion Subcommittee.- Fouling of ships' bottoms; identification of marine growths. Paper nº 14, 1944.
7. Fancutt, F. and J. C. Hudson.- The formulation of ships' bottom paints. Iron and Steel Institute, England, 1947.
8. Harris, J. E.- Report on antifouling research, 1942-44. Iron and Steel Institute, England, 1947.
9. U. S. Naval Institute.- Marine fouling and its prevention. Woods Hole Oceanographic Institution, USA, 1952.
10. Ketchum, B. H. and J. C. Ayers.- Action of antifouling paints. Ind. Eng. Chem., 40, 249-253 y 2024-2027, 1948.
11. De Wolf, P. and A. M. van Londen.- Raft trials and ships' trials with some underwater paint systems. T.N.O. Report, 43 C, 1962.
12. Van Londen A. M.- A study of ship bottom paints, in particular pertaining to the behaviour and action of antifouling paints. T.N.O. Report, 54 C, 1963.

13. Van Londen, A. M.- The mode of action of antifouling paints. T.N.O. Report, 62 C, 1964.
14. De Wolf, P.- Barnacle fouling on aged antifouling paints. T.N.O. Report, 64 C, 1964.
15. Rascio, V. et J. J. Caprari.- Contribution a l'étude du comportement des peintures antisalissures. I. Influence du toxique utilisé et de la solubilité du liant. Peintures, Pigments, Vernis (France), 45, nº 2, 102-113, 1969.
16. Rascio, V., J. J. Caprari et R. O. Bastida.- Contribution a l'étude du comportement des peintures antisalissures. II. Influence de la concentration de toxiques. Peintures, Pigments, Vernis (France), 45, nº 11, 724-735, 1969.
17. Rascio, V. y J. J. Caprari.- Contribución al estudio del comportamiento de las pinturas antiincrustantes. III. Nuevas experiencias realizadas en el puerto de Mar del Plata, período 1968/70. Corrosión y Protección (España), 1, nº 4, 19-33, 1970.
18. Rascio, V. y R. O. Bastida.- Contribución al estudio del comportamiento de las pinturas antiincrustantes. V. Acción de los tóxicos a nivel de línea de flotación. LEMIT-ANALES, 3-1972, en prensa.
19. Rascio, V.- El problema de la corrosión submarina y de las incrustaciones biológicas (fouling) en cascos de barcos. NAVITECNIA, 21, nº 2, 281-288, 1967.
20. Rascio, V.- Pinturas antifouling. NAVITECNIA, 22, nº 4, 120-124 y nº 5, 145-150, 1968.
21. Barnes, H.- Studies on antifouling compositions. II.The formation of copper soaps in the preparation of compositions containing cuprous oxyde and rosin. J. Iron and Steel Inst., 157, 1947.
22. Young, G. H., W. K. Schneider and G. W. Seagren.- Antifouling paints. Effect of inert pigments on antifouling action. Ind. Eng. Chem., 36, nº 12, 1130-1132, 1944.
23. Ketchum, B. H. and J. C. Ayers.- Effect of non toxic pigments on the performance of antifouling paints. Ind. Eng. Chem.,40, nº 11, 2124-2127, 1948.
24. Rascio, V. y J. J. Caprari.- Anticorrosion and antifouling paints for ship bottoms with vinyl binder. LEMIT-ANALES, 3-1972 (in press).

TABLE I

CHEMICAL COMPOSITION OF ANTIFOULING PAINTS (Binder resin UV phenolic varnish)

(g/100)

N°	Cu_2O	As_2S_3	Schweinf. Green	As_2Cu_4	ZnO	Fe_2O_3	Chalk	Talc	Alumin. octoat.	Resin	Phenolic varnish	Solvents
404	47,0				4,5				2,5	17,25	5,75	23,0
405	47,0				4,5				2,5	19,15	3,85	23,0
406	47,0				4,5				2,5	20,10	2,90	23,0
410	35,0				3,6	12,9			2,5	17,25	5,75	23,0
411	35,0				3,6	12,9			2,5	19,15	3,85	23,0
412	35,0				3,6	12,9			2,5	20,10	2,90	23,0
416	35,0				3,6		12,9		2,5	17,25	5,75	23,0
417	35,0				3,6		12,9		2,5	19,15	3,85	23,0
418	35,0				3,6		12,9		2,5	20,10	2,90	23,0
420	35,0				3,6			12,9	2,5	17,25	5,75	23,0
421	35,0				3,6			12,9	2,5	19,15	3,85	23,0
424	35,0				3,6			12,9	2,5	20,10	2,90	23,0
440	41,2	6,2			4,1				2,5	17,25	5,75	23,0
441	41,2	6,2			4,1				2,5	19,15	3,85	23,0
442	41,2	6,2			4,1				2,5	20,10	2,90	23,0
446	30,8	4,6			3,1	13,0			2,5	17,25	5,75	23,0
447	30,8	4,6			3,1	13,0			2,5	19,15	3,85	23,0
448	30,8	4,6			3,1	13,0			2,5	20,10	2,90	23,0
452	30,8	4,6			3,1		13,0		2,5	17,25	5,75	23,0
453	30,8	4,6			3,1		13,0		2,5	19,15	3,85	23,0
454	30,8	4,6			3,1		13,0		2,5	20,10	2,90	23,0
458	30,8	4,6			3,1			13,0	2,5	17,25	5,75	23,0
459	30,8	4,6			3,1			13,0	2,5	19,15	3,85	23,0
460	30,8	4,6			3,1			13,0	2,5	20,10	2,90	23,0
464	41,2		6,2		4,1				2,5	17,25	5,75	23,0
465	41,2		6,2		4,1				2,5	19,15	3,85	23,0
466	41,2		6,2		4,1				2,5	20,10	2,90	23,0
470	30,8		4,6		3,1	13,0			2,5	17,25	5,75	23,0
471	30,8		4,6		3,1	13,0			2,5	19,15	3,85	23,0
472	30,8		4,6		3,1	13,0			2,5	20,10	2,90	23,0
476	30,8		4,6		3,1		13,0		2,5	17,25	5,75	23,0
477	30,8		4,6		3,1		13,0		2,5	19,15	3,85	23,0
478	30,8		4,6		3,1		13,0		2,5	20,10	2,90	23,0
482	30,8		4,6		3,1			13,0	2,5	17,25	5,75	23,0
483	30,8		4,6		3,1			13,0	2,5	19,15	3,85	23,0
484	30,8		4,6		3,1			13,0	2,5	20,10	2,90	23,0
488	41,2			6,2	4,1				2,5	17,25	5,75	23,0
489	41,2			6,2	4,1				2,5	19,15	3,85	23,0
490	41,2			6,2	4,1				2,5	20,10	2,90	23,0
494	30,8			4,6	3,1	13,0			2,5	17,25	5,75	23,0
495	30,8			4,6	3,1	13,0			2,5	19,15	3,85	23,0
496	30,8			4,6	3,1	13,0			2,5	20,10	2,90	23,0
500	30,8			4,6	3,1		13,0		2,5	17,25	5,75	23,0
501	30,8			4,6	3,1		13,0		2,5	19,15	3,85	23,0
502	30,8			4,6	3,1		13,0		2,5	20,10	2,90	23,0
506	30,8			4,6	3,1			13,0	2,5	17,25	5,75	23,0
507	30,8			4,6	3,1			13,0	2,5	19,15	3,85	23,0
508	30,8			4,6	3,1			13,0	2,5	20,10	2,90	23,0

TABLE II

CHEMICAL COMPOSITION OF ANTIFOULING PAINTS (Binder resin WW linseed oil/tall oil P)

(g 100)

N°	Cu_2O	Ag_2HgI_4	Rebecca's Green	$AgHgI_3$	ZnO	Fe_2O_3	Chalk	Talc	Aluminium esterat.	Resin	Standoil	Solvent
401	46,9				4,6				2,5	17,25	5,75	23,0
402	46,9				4,6				2,5	19,15	3,85	23,0
403	46,9				4,6				2,5	20,10	2,90	23,0
407	35,0				3,6	12,9			2,5	17,25	5,75	23,0
408	35,0				3,6	12,9			2,5	19,15	3,85	23,0
409	35,0				3,6	12,9			2,5	20,10	2,90	23,0
413	35,0				3,6		12,9		2,5	17,25	5,75	23,0
414	35,0				3,6		12,9		2,5	19,15	3,85	23,0
415	35,0				3,6		12,9		2,5	20,10	2,90	23,0
419	35,0				3,6			12,9	2,5	17,25	5,75	23,0
420	35,0				3,6			12,9	2,5	19,15	3,85	23,0
421	35,0				3,6			12,9	2,5	20,10	2,90	23,0
437	41,2	6,2			4,1				2,5	17,25	5,75	23,0
438	41,2	6,2			4,1				2,5	19,15	3,85	23,0
439	41,2	6,2			4,1				2,5	20,10	2,90	23,0
443	30,8	4,6			3,1	13,0			2,5	17,25	5,75	23,0
444	30,8	4,6			3,1	13,0			2,5	19,15	3,85	23,0
445	30,8	4,6			3,1	13,0			2,5	20,10	2,90	23,0
449	30,8	4,6			3,1		13,0		2,5	17,25	5,75	23,0
450	30,8	4,6			3,1		13,0		2,5	19,15	3,85	23,0
451	30,8	4,6			3,1		13,0		2,5	20,10	2,90	23,0
455	30,8	4,6			3,1			13,0	2,5	17,25	5,75	23,0
456	30,8	4,6			3,1			13,0	2,5	19,15	3,85	23,0
457	30,8	4,6			3,1			13,0	2,5	20,10	2,90	23,0
461	41,2		6,2		4,1				2,5	17,25	5,75	23,0
462	41,2		6,2		4,1				2,5	19,15	3,85	23,0
463	41,2		6,2		4,1				2,5	20,10	2,90	23,0
467	30,8		4,6		3,1	13,0			2,5	17,25	5,75	23,0
468	30,8		4,6		3,1	13,0			2,5	19,15	3,85	23,0
469	30,8		4,6		3,1	13,0			2,5	20,10	2,90	23,0
473	30,8		4,6		3,1		13,0		2,5	17,25	5,75	23,0
474	30,8		4,6		3,1		13,0		2,5	19,15	3,85	23,0
475	30,8		4,6		3,1		13,0		2,5	20,10	2,90	23,0
479	30,8		4,6		3,1			13,0	2,5	17,25	5,75	23,0
480	30,8		4,6		3,1			13,0	2,5	19,15	3,85	23,0
481	30,8		4,6		3,1			13,0	2,5	20,10	2,90	23,0
485	41,2			6,2	4,1				2,5	17,25	5,75	23,0
486	41,2			6,2	4,1				2,5	19,15	3,85	23,0
487	41,2			6,2	4,1				2,5	20,10	2,90	23,0
491	30,8			4,6	3,1	13,0			2,5	17,25	5,75	23,0
492	30,8			4,6	3,1	13,0			2,5	19,15	3,85	23,0
493	30,8			4,6	3,1	13,0			2,5	20,10	2,90	23,0
497	30,8			4,6	3,1		13,0		2,5	17,25	5,75	23,0
498	30,8			4,6	3,1		13,0		2,5	19,15	3,85	23,0
499	30,8			4,6	3,1		13,0		2,5	20,10	2,90	23,0
503	30,8			4,6	3,1			13,0	2,5	17,25	5,75	23,0
504	30,8			4,6	3,1			13,0	2,5	19,15	3,85	23,0
505	30,8			4,6	3,1			13,0	2,5	20,10	2,90	23,0

TABLE III

CHEMICAL COMPOSITION OF ANTIFOULING PAINTS (Binder Resin WW/oleic acid) *

N°	Cu_2O	R.Hg**	ZnO	Fe_2O_3	Chalk	Talc	Aluminium esterate	Resin	Plasticiser	Solvents
425	38,3	3,8	3,8				2,3	24,0	9,5	18,3
426	39,8	2,2	3,9				2,3	27,9	5,6	18,3
427	40,2	1,7	4,0				2,3	29,3	4,2	18,3
428	28,0	3,8	2,6	11,5			2,3	24,0	9,5	18,3
429	29,3	2,2	2,9	11,5			2,3	27,9	5,6	18,3
430	29,8	1,7	2,9	11,5			2,3	29,3	4,2	18,3
431	28,0	3,8	2,6		11,5		2,3	24,0	9,5	18,3
432	29,3	2,2	2,9		11,5		2,3	27,9	5,6	18,3
433	29,8	1,7	2,9		11,5		2,3	29,3	4,2	18,3
434	28,0	3,8	2,6			11,5	2,3	24,0	9,5	18,3
435	29,3	2,2	2,9			11,5	2,3	27,9	5,6	18,3
436	29,8	1,7	2,9			11,5	2,3	29,3	4,2	18,3

* g/100

** as HgO

TABLE IV

CHEMICAL COMPOSITION OF ANTIFOULING PAINTS (Binder Resin VW/Vynil resin)

(g/100)

N°	Cu_2O	MgO	AsO_4Mg_3	Schweinf. Green	AsO_3Cu_3	As_2O_3	Resin	Vynil resin*	Tricresil phosphate	MIBK	Toluene
V-1	60,0						6,0	6,0	1,5	13,5	13,0
V-2	50,0	10,0					6,0	6,0	1,5	13,5	13,0
V-3	50,0		10,0				6,0	6,0	1,5	13,5	13,0
V-4	50,0			10,0			6,0	6,0	1,5	13,5	13,0
V-5	50,0				10,0		6,0	6,0	1,5	13,5	13,0
V-6	50,0					10,0	6,0	6,0	1,5	13,5	13,0

* VYNH Union Carbide

TABLE V

ANTIFOULING PAINTS (Binder resin VW phenolic varnish) - FOULING SETTLEMENT

N°	Pigment	Resin VW/ varnish	Fouling settlement after (days)							
			75	150	225	300	375	450	525	600
606	Cu_2O-ZnO	9 1	0	0	0	0	0-1	1-2	1-2	1-2
607		8 1	0	0	0	0	0-1	1-2	1-2	2
608		7 1	0	0	0	0-1	1	1-2	2	3
609	Cu_2O-ZnO-Fe_2O_3	9 1	0	0	0-1	0-1	0-1	2	2	2-3
611		8 1	0	0	0	0	0	1	1-2	1-2
612		7 1	0	0	0	0	0	2	2	2-3
613	Cu_2O-ZnO-Chalk	9 1	0	0	0	0	0-1	2	2	2
617		8 1	0	0	0	0	0	1	1	1
618		7 1	0	0	0	0	0	1	1	1
622	Cu_2O-ZnO-Talc	9 1	0	0	1	1	1-2	2-3	2-3	2-3
623		8 1	0	0	1	1	1	2-3	3	3-4
624		7 1	0	1	2	2	2	2-3	4	4
630	Cu_2O-ZnO-AsO_4Mg_3	9 1	0	0	0	0	0	0	0-1	0-1
631		8 1	0	0	0	0	0	0-1	0-1	1
632		7 1	0	1	1	1	1-2	2-3	3	3
636	Cu_2O-ZnO-AsO_4Mg_3-Fe_2O_3	9 1	0	0	0-1	0-1	1	1-2	2	2-3
637		8 1	0	0	0	0	0	1-2	2	2
638		7 1	0	0-1	0-1	1-2	2	2-3	3-4	4-5
642	Cu_2O-ZnO-AsO_4Mg_3-Chalk	9 1	0	0	0	0	0-1	2-3	3	3
643		8 1	0	0	0	0	0	1	1-2	1-2
644		7 1	0	0-1	0-1	0-1	1-2	2	2	2-3
648	Cu_2O-ZnO-AsO_4Mg_3-Talc	9 1	0	2	2-3	3	3-4	3-4	3-4	4
649		8 1	0	1-2	1-2	2	2-3	3	4	4
650		7 1	0	2-3	2-3	2-3	2-3	3	4	4
654	Cu_2O-ZnO-Schweinf.green	9 1	0	0	0-1	0-1	0-1	3-4	4	4
655		8 1	0	0	1	1	2	3-4	4	4-5
656		7 1	0	2	2-3	2-3	2-3	3-4	4	5
660	Cu_2O-ZnO-Schw.green-Fe_2O_3	9 1	0	1	1	1	1-2	3-4	4	4-5
661		8 1	0	0	1	1-2	2	3-4	4	4-5
662		7 1	0	1-2	1-2	1-2	2	3-4	4	4-5
666	Cu_2O-ZnO-Schw.green-Chalk	9 1	0	0	0-1	0-1	0-1	3	3	3
667		8 1	0	0	0	0-1	1	3	3	3
668		7 1	0	1-2	1-2	1-2	2	3-4	4	4
672	Cu_2O-ZnO-Schw.green-Talc	9 1	0	1	2	2-3	3-4	4-5	5	5
673		8 1	0	0-1	1-2	2-3	3-4	4-5	5	5
674		7 1	0	1-2	1-2	2-3	3-4	4	4-5	5
678	Cu_2O-ZnO-AsO_4Cu_3	9 1	0	0	0	0	0-1	2	2	2
679		8 1	0	0	0	0	0	0	0-1	0-1
680		7 1	0	0	0	0	0	1	1	1
684	Cu_2O-ZnO-AsO_4Cu_3-Fe_2O_3	9 1	0	1	1	1	1-2	2-3	3-4	3-4
685		8 1	0	0	0-1	0-1	1	1-2	2-3	3-4
686		7 1	0	0-1	0-1	0-1	1	2	3-4	3-4
690	Cu_2O-ZnO-AsO_4Cu_3-Chalk	9 1	0	0	0	0	0	2	3-4	3
691		8 1	0	0	1	1	1	2	3-4	3
692		7 1	0	1	1	1	1-2	2	3-4	3
696	Cu_2O-ZnO-AsO_4Cu_3-Talc	9 1	0	1	1	2	2-3	3-4	4	4
697		8 1	0	0-1	1	1-2	2	3-4	4	4-5
698		7 1	0	1	1	1-2	2	4	4-5	4-5

TABLE 11

ANTIFOULING PAINTS (Binder resin MW linseed standoil 60 P) - FOULING SETTLEMENT

N°	Pigment	Resin MW standoil	Fouling settlement after (days)							
			75	150	225	300	375	450	525	600
688	Cu_2O-ZnO	5:1	0	0	0	0	1	1	1	1
689		6:1	0	0	0	1	2	2-3	2-3	3
690		7:1	0	0	0	1-2	1-2	1-2	1-2	2
687	Cu_2O-ZnO-Fe_2O_3	5:1	0	1	2	2-3	3	4	4	4
688		6:1	0	0	0	0-1	1-2	2	2-3	3
689		7:1	0	0	0	0	0-1	2	2-3	3
615	Cu_2O-ZnO- Chalk	5:1	0	0	0-1	1	1-2	2-3	3-4	4-5
616		6:1	0	0	0	0	0	2	2	2
615		7:1	0	0	0	0	0	1-2	1-2	1-2
619	Cu_2O-ZnO-Talc	5:1	0	0	0-1	0-1	1-2	3	3	3
620		6:1	0	0	0	0	0-1	2	2-3	2-3
621		7:1	0	0	0-1	0-1	1-2	2	2-3	2-3
637	Cu_2O-ZnO-AsO_4Rg_3	5:1	0	1	1	1	1-2	4	4	4-5
638		6:1	0	0	0	0	0-1	2-3	2-3	3
639		7/8	0	0	0-1	0-1	1-2	2-3	2-3	2-3
643	Cu_2O-ZnO-AsO_4Rg_3-Fe_2O_3	5:1	0	0	0	0	2	3	4	4-5
644		6:1	0	0	0	0-1	1-2	2-3	3	3-4
645		7:1	0	0-1	0-1	0-1	1-2	2-3	3	3-4
649	Cu_2O-ZnO-AsO_4Rg_3-Chalk	5:1	0	0	0	0	0-1	1-2	2	2-3
650		6:1	0	0	0	0	0-1	1-2	2	2-3
651		7:1	0	0	0	0-1	1	1-2	2	2-3
655	Cu_2O-ZnO-AsO_4Rg_3-Talc	5:1	0	2	2	3	4	4	4-5	4-5
656		6:1	0	0	1	1	2	2-3	3-4	4-5
657		7:1	0	2	2	2	2	3	4	5
661	Cu_2O-ZnO- Sebw.nfort green	5:1	0	0	0	0-1	1-2	3-4	4	4-5
662		6:1	0	0	0	1	1-2	3-4	4	4-5
663		7:1	0	0	0	0-1	1-2	3-4	4	4-5
667	Cu_2O-ZnO- Sebw.green-Fe_2O_3	5:1	0	1	1	1	1-2	4	4	5
668		6:1	0	0-1	1	2	3-4	4	4	4-5
669		7:1	0	1	1	2	3	4	4	4-5
673	Cu_2O-ZnO- Sebw.green-Chalk	5:1	0	0	0	0	0-1	3	4	4-5
674		6:1	0	0	0-1	1	1-2	3-4	4-5	4-5
675		7:1	0	0-1	0-1	1	1-2	3	4	4-5
679	Cu_2O-ZnO- Sebw.green-Talc	5:1	0	0	0-1	0-1	0-1	3	3	3
680		6:1	0	0	0	0-1	1	3	3	3
681		7:1	0	1-2	1-2	1-2	2	3-4	3-4	4
685	Cu_2O-ZnO-AsO_4Fe_3	5:1	0	0	0	0	0-1	3	3-4	3-4
686		6:1	0	0	0	0	0	1-2	2	3
687		7:1	0	0	0	1	2	2	2-3	3
691	Cu_2O-ZnO-AsO_4Fe_3-Fe_2O_3	5:1	0	0-1	2	2	2-3	3-4	4	4
692		6:1	0	0	0	1	1-2	2	2-3	3
693		7:1	0	1	1-2	1-2	2	2	3	4
697	Cu_2O-ZnO-AsO_4Fe_3- Chalk	5:1	0	0	0	0	0	2-3	3	3-4
698		6:1	0	0	0	0	0	1-2	2	2-3
699		7:1	0	1	1	1	1-2	2	2-3	2-3
703	Cu_2O-ZnO-AsO_4Fe_3-Talc	5:1	0	1-2	1-2	2	2-3	3-4	4	4-5
704		6:1	0	0	0	0-1	1-2	2-3	3	3-4
705		7:1	0	2	2	2	2-3	3-4	4	5

TABLE VII

ANTIFOULING PAINTS (Binder Rosin WW Oleic acid) - FOULING SETTLEMENT

N°	Pigment	Rosin WW/ oleic ac.	Fouling settlement after (days)							
			75	150	225	300	375	450	525	600
425	Cu_2O-ZnO-R.Hg	2,5/1	0	0	1	1	1	1-2	1-2	1-2
426		5/1	0	0	0	0	0-1	1	1-2	1-2
427		7/1	0	0	0-1	0-1	0-1	1	1-2	2
425A	Cu_2O-ZnO-R.Hg	2,5/1	0	0	0	0	0	0-1	1	1
426A		5/1	0	0	0	0	0	0-1	1	1
427A		7/1	0	0	0	0	0	0-1	0-1	0-1
428	Cu_2O-ZnO-R.Hg-Fe_2O_3	2,5/1	0	0	0-1	0-1	1	2	2	2-3
429		5/1	0	0	0	0	0	1	1-2	1-2
430		7/1	0	0	0	0	0	1	1-2	1-2
431	Cu_2O-ZnO-R.Hg-Chalk	2,5/1	0	0	0-1	1	1-2	2-3	3	4
432		5/1	0	0-1	0-1	0-1	0-1	1-2	2	2-3
433		7/1	0	0-1	1	1	1-2	1-2	2	2
434	Cu_2O-ZnO-R.Hg-Talc	2,5/1	0	0-1	0-1	0-1	0-1	2	2-3	2-3
435		5/1	0	0	0	1	1-2	3	4	5
436		7/1	0	0	1	1	1-2	2	2-3	3

TABLE VIII

ANTIFOULING PAINTS (Binder Rosin Wk Vynil Resin) - FOULING SETTLEMENT

N°	Pigment	Fouling settlement after (days)							
		75	150	225	300	375	450	525	600
V-1	Cu_2O	0	0	0	0	0	1	1	1-2
V-2	Cu_2O-HgO	0	0	0	0	0	1	1	1-2
V-3	Cu_2O-AsO_4Hg_3	0	0	0	0	0	0-1	1	1
V-4	Cu_2O-Schweinfurt Green	0	0	0	0	0	0-1	0-1	1
V-5	Cu_2O-AsO_3Cu_3	0	0	0	0	0	0-1	0-1	0-1
V-6	Cu_2O-As_2O_3	0	0	0	0	0	0-1	1	1

KEY FOR TABLES V, VI, VII, VIII:

FOULING SETTLEMENT	EFFICIENCY PER CENT
0	100
0-1	90
1	80
1-2	70
2	60
2-3	50
3	40
3-4	30
4	20
4-5	10
5	0

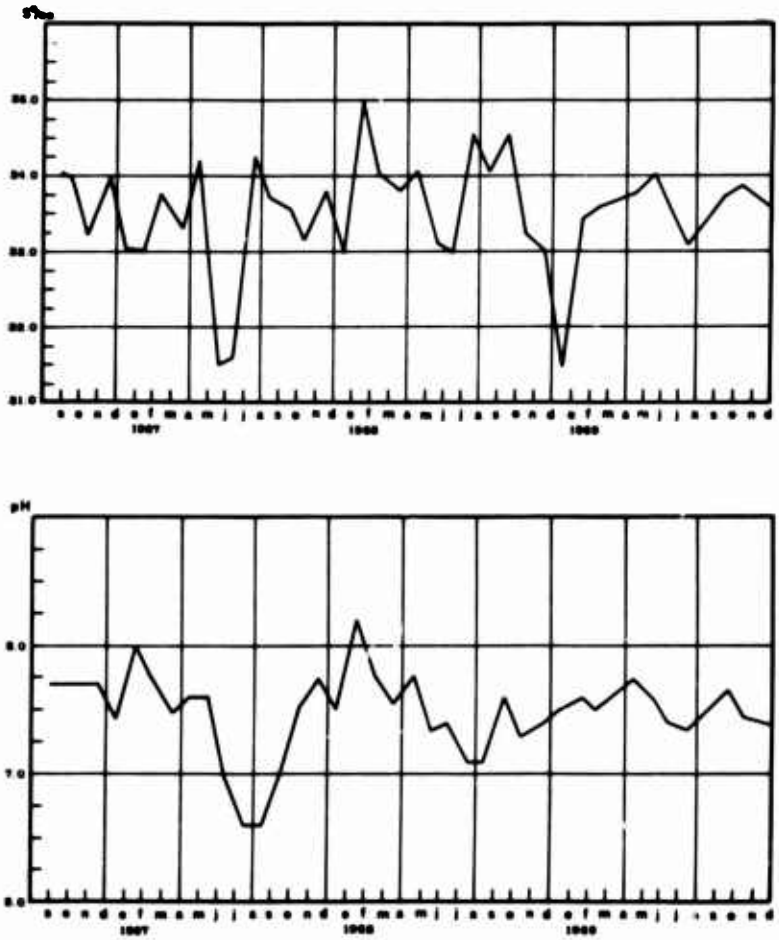


Fig. 1.- Salinity of water (above) and pH, Mar del Plata's harbour (september 1966/september 1969)

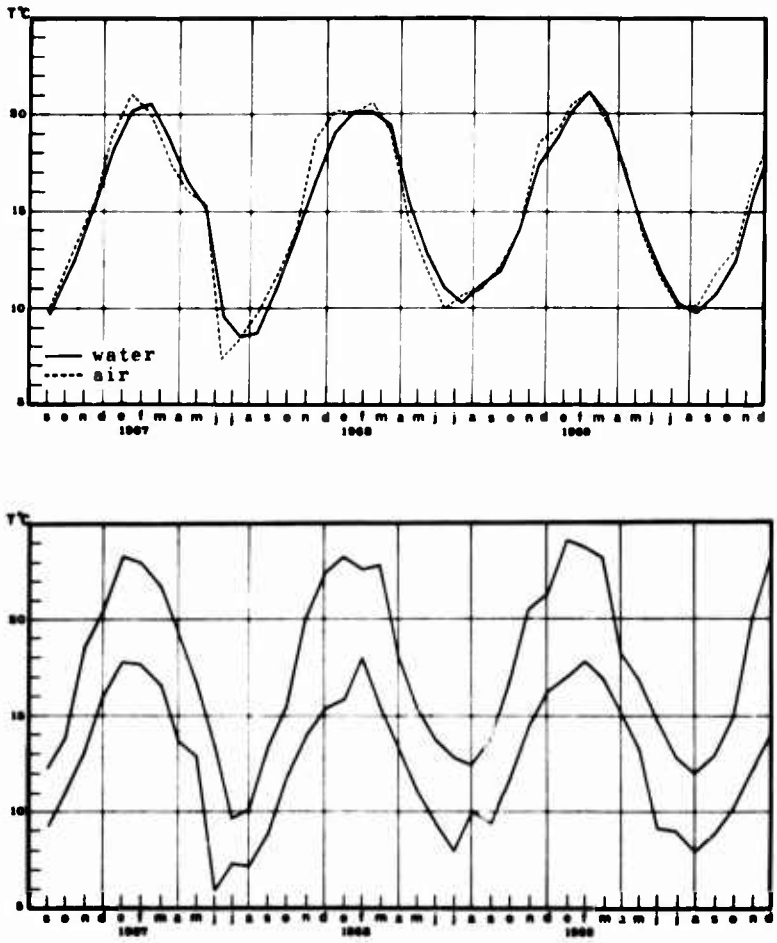


Fig. 2.- Middle temperature of water and air (above) and maximun and minium temperature of water, Mar del Plata's harbour (september 1966/september 1969)

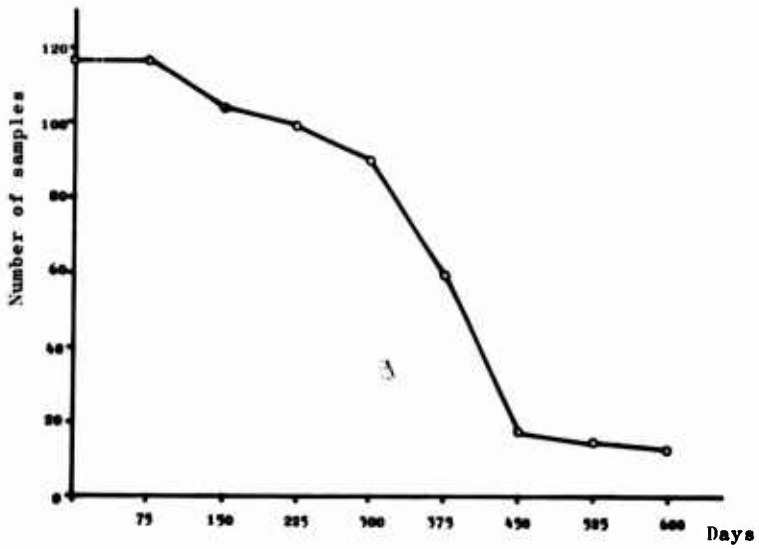


Fig. 3.- Number of samples without settlement of fouling (0 to 600 days exposure)

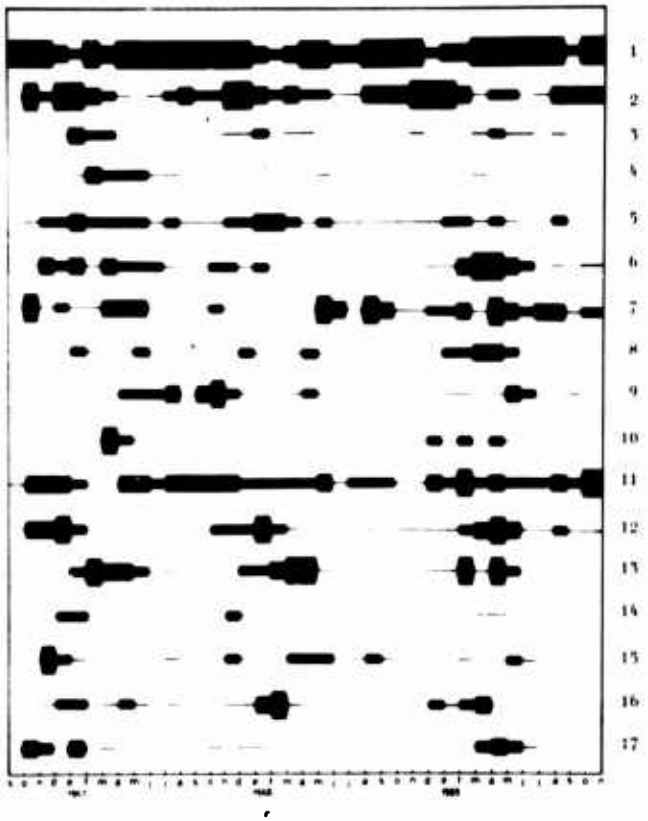


Fig. 4.- Settlement of fouling organisms on non toxic panels: level A, from surface to 0,30 m depth. Mar del Plata's harbour (1966/69)

References (fig. 4 to 7): (1) Diatoms; (2) Enteromorpha intestinalis; (3) Ulva lactuca; (4) Bryopsis plumosa; (5) Polysiphonia sp.; (6) Tubularia crocea; (7) G. inornata + Obelia angulosa; (8) M. enigmatica + S. vermicularis + H. norvegica; (9) Polydora cf. ciliata; (10) Eubranchus sp.; (11) Tisbe furcata + Harpacticus sp.; (12) Corophium sp.; (13) B. amphitrite + B. trigonus; (14) Bugula sp.; (15) Bowerbankia gracilis; (16) Cyrtograpsus angulatus; (17) Ciona intestinalis.

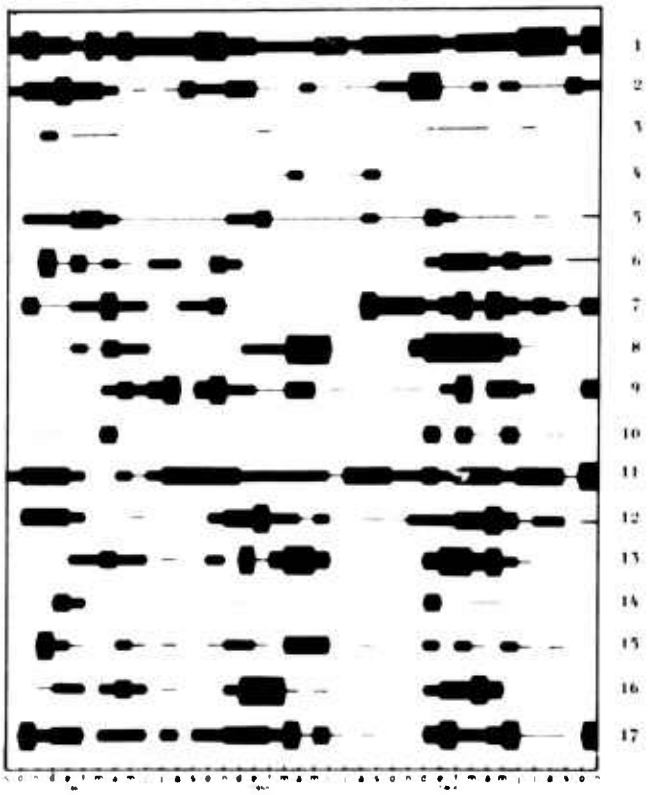


Fig. 5.- Settlement of fouling organisms on non toxic panels: level B, 0,50-0,90 m, Mar del Plata's harbour (1966/69)

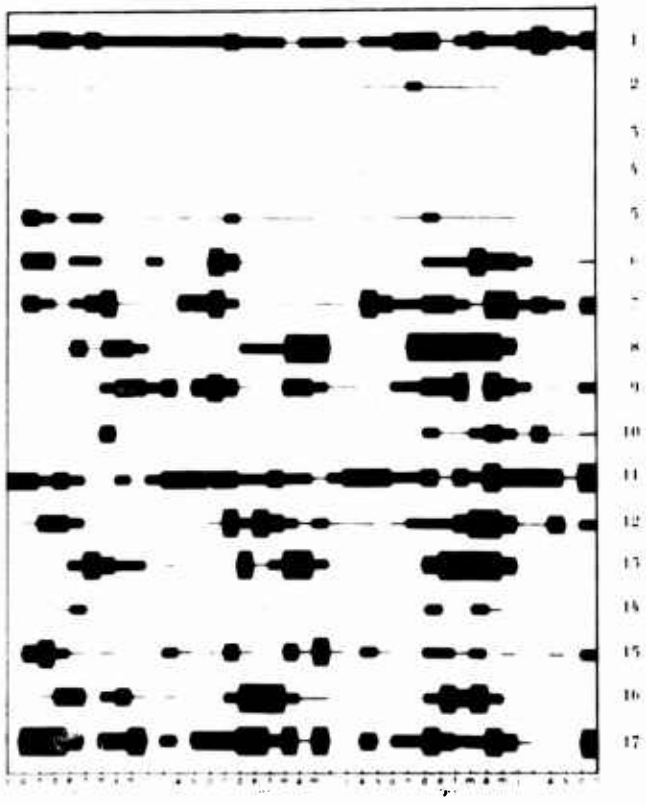


Fig. 6.- Settlement of fouling organisms on non toxic panels: level C, 1,10-1,50 m, Mar del Plata's harbour (1966/69)

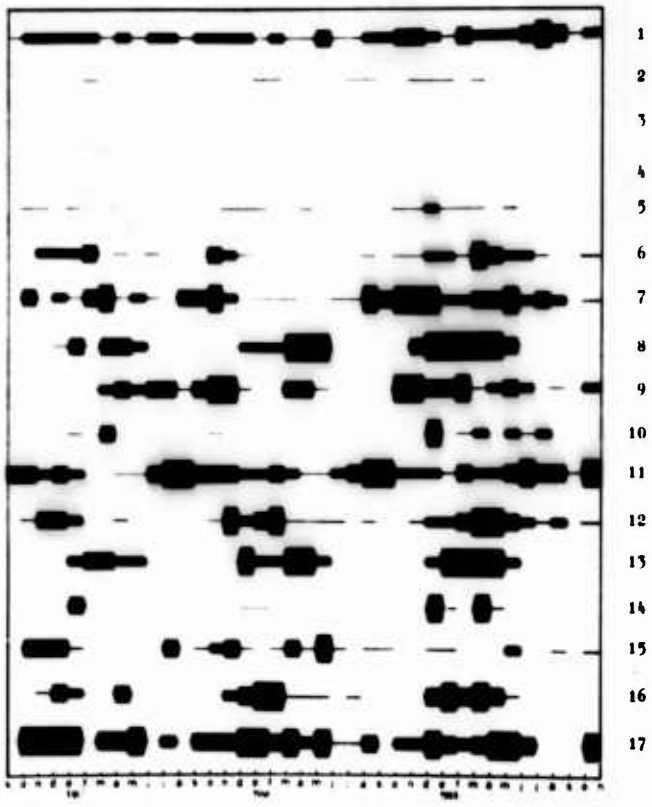


Fig. 7.- Settlement of fouling organisms on non toxic panels: level D, 1,70-2,10 m, Mar del Plata's harbour (1966/69)

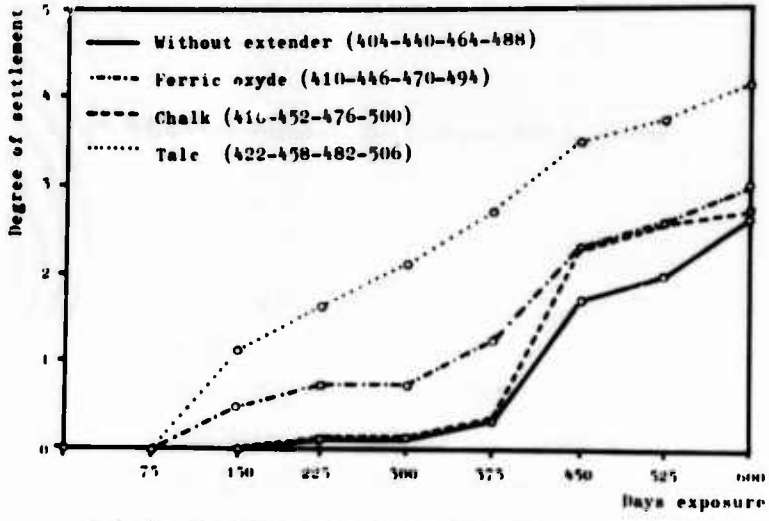


Fig. 8.- Performance (mean values) of paints with and without extenders; binder rosin WW/phenolic varnish (3/1)

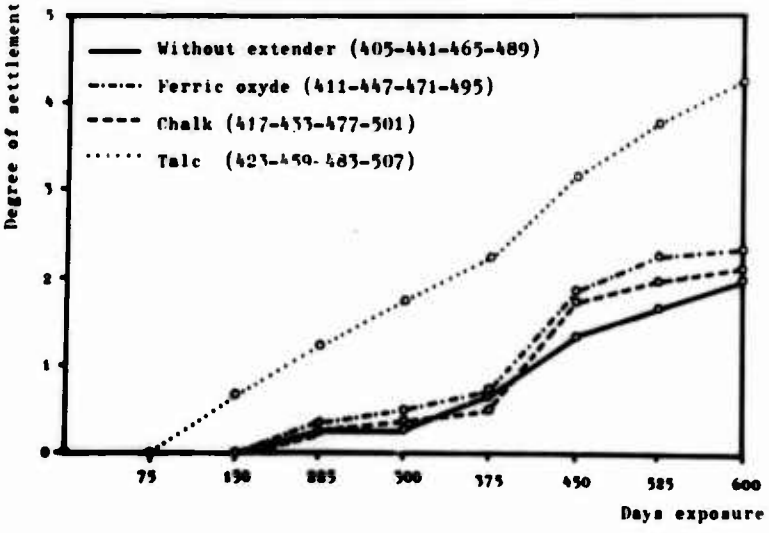


Fig. 9.- Performance (mean values) of paints with and without extenders; binder rosin WW/phenolic varnish (5/1)

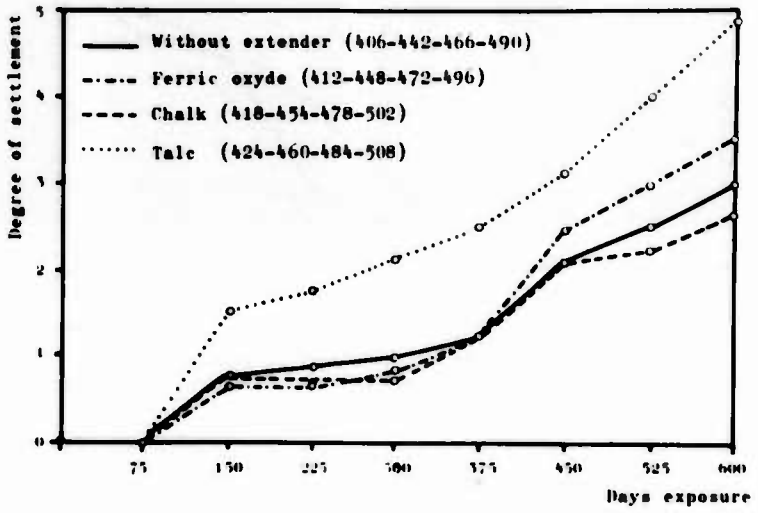


Fig.10.- Performance (mean values) of paints with and without extenders; binder rosin WW/phenolic varnish (7/1)

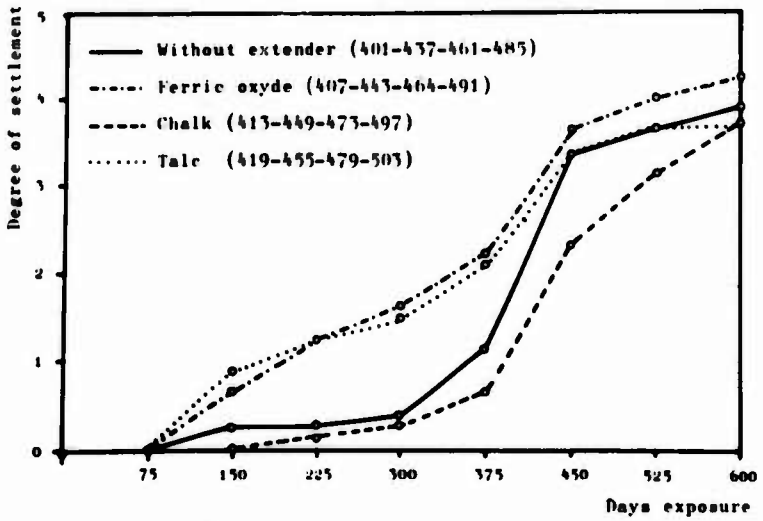


Fig.11.- Performance (mean values) of paints with and without extenders; binder rosin WW/linseed standoil 60 P (5/1)

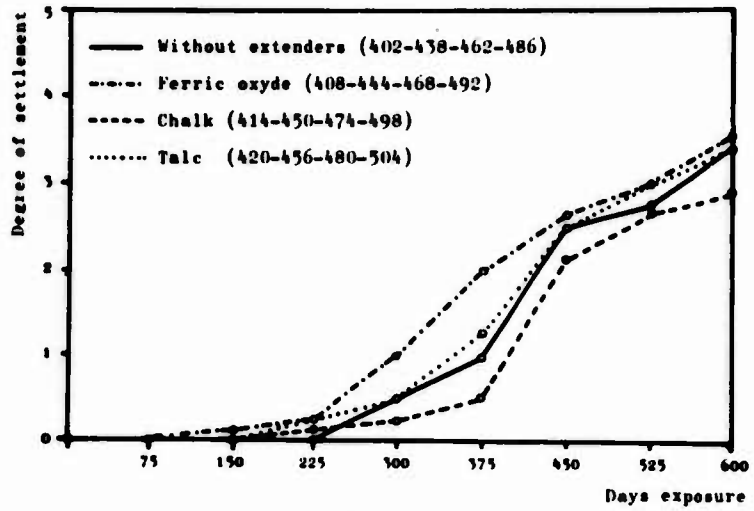


Fig. 12.- Performance (mean values) of paints with and without extenders; binder rosin WW/linseed standoil 60 P (5/1)

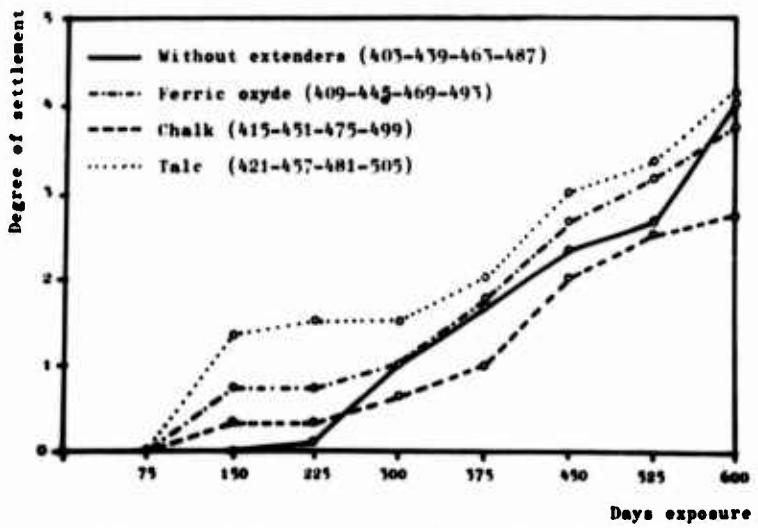


Fig. 13.- Performance (mean values) of paints with and without extenders; binder rosin WW/linseed standoil 60 P (7/1)

Discussion

Birnbaum: Did you maintain a constant pigment volume for all formulations?

Rascio: Yes.

de la Court: I would like to ask you what does it mean two years' exposure in your country? You have always the whole year fouling or is it only for a half a year or three months as in our country?

Rascio: Quand on parle de 1 ou 2 ans de fixation, c'est-à-dire 365 ou 725 jours, la période des salissures dans les ports est d'environ 7 mois pour les balanes, les hydroïdes, les ascidies. C'est à peu près uniforme pendant toute l'année pour les algues.

New Methods of Screening Test of Antifouling Toxicants and Coatings

Shizuo Mawatari

National Science Museum, Tokyo, Japan

Antifouling effect depends partly upon the lethal action of poisonous components and partly upon their leaching rate from paint surfaces. The usual raft tests of painted panels are, in spite of their practical importance, rather incomplete in indicating only the mixed results of these two independent phenomena. Another inconvenience of these tests falls on the fact that the different fouling communities are formed in different seasons. Antifouling coatings must be evaluated on the toxicity of components, rate of leaching and fouling growth on painted surfaces. To elucidate their relationships a consistent research system is needed at present. The author introduced Artemia salina and Chlorella ellipsoidea into his bioassay tests for toxicity of ingredients and leaching rate, and preliminary aquarium treatment to clear the relation between leaching rate and seasonal fouling.

Two or three days old larvae of Artemia salina were added to 100ml of sea-water solution of toxicants prepared in concentration of 1, 5, 10, 25 and 50 ppm. The number of dead individuals was counted after 1, 3, 6, 12 and 24 hours contact. The lethal curve made of the percentage of death at each period showed the characteristic pattern of the toxicants. Monthly change of leaching rate was also studied by the same method.

The unicellular green algae Chlorella ellipsoidea was used as a scale to measure the anti-algal effect of toxicants and coatings. Various concentrations of toxics and leached solution of coatings were tested. Characteristic inhibitive activity was shown as percentage decrease of centrifuged volumes of Chlorella after 1, 3, 5 and 7 days respectively.

A set of large and small panels coated with the same paint was kept in the aquarium of running water from which the larvae of foulers were removed through sand filter. The large panels was transfered to the raft test and the small ones to the leaching study. Bubbled solutions were tested by Artemia- and Chlorella-scale, and obtained results were compared with the fouling communities on the large panels.

By these three methods the author is approaching to realize the consistent research system of antifouling paints.

1. Introduction

As the result of long time researches of many workers Cuprous Oxide has been highly esteemed and is of wide use even at present. Modern chemical analysis has been proved quite sufficient for the quantitative determination of copper released in sea water. A number of works have been accomplished in regard to the relations between leaching rate and

actual anti-fouling activity, and the critical value of 10 $\mu g/cm^2$/day has been confirmed by Ketchum, Barnes and others.

Accompanied with rapid progress of organic synthesis numerous insecticides and fungicides were produced industrially, and some of them proved very useful for antifouling ingredients. The investigation of such compounds has become of urgent necessity in paint manufacture. However, the lethal molar concentration of these organometallic compounds is said to be of the order of 1-30 x 10^{-8}. This extremely low concentration has made the quantitative determination by purely chemical analysis quite difficult or rather formidable.

To overcome the difficulty, various sorts of bioassay methods have been introduced by many workers. The present biological researches were designed to determine the toxicity of antifoulant and also to find the reasonable relations between leaching rate and actual fouling on panels in the sea. The following results were obtained under the collaboration of the Research Institute of Natural Resources, Tokyo, the Research Laboratory of Kansai Paint Co., Ltd. Hiratsuka, and the Marine Laboratory of the Tokyo Mercantile Marine College, Shimizu. The financial aids were given by Japan Light Metal Association and the Shipbuilding Research Association of Japan.

2. Preliminary Investigations

The author tried at first to realize an idea to use the last-stage larvae of actual fouling organisms directly in the bioassay tests. Preliminary works were started in 1966 to find an adequate mass culture method necessary to keep sufficient number of materials for experiments. Larvae of Bugula neritina were released every morning in warmer seasons out of matured colonies in aquarium and used in some tests. Their extremely short swimming period, not exceeding 6 or 7 hours, proved, however, rather inconvenient to check the dilute poison in sea water. Another trials to utilize the larvae of Hydroides yesoensis ended unsuccessful with their unstable hatch and lower survival.

Shelled larvae of Mytilus edulis were obtained about 4 weeks after the artificial fertilization, but the rearing was found somewhat difficult by the long range of larval period and also by the change of food habit on the way of growth. A number of cyprid larvae of two subspecies of Balanus amphitrite were obtained within 1 or 2 weeks in warm seasons, and proved more or less sufficient in the check of low concentration of toxics.

Inevitable difficulties of the use of these larvae exist, however, in their limited breeding season on one hand, and in relatively short

period of the final stage on the other hand. Necessity of skill in culturing food algae was also one of the obstacles against the popular use among technicians and students other than biologists.

Since the direct use of fouler's larvae did not always yield the satisfactory results in the bioassay tests, the troublesome mass culture of final stage larvae seemed to be rather insignificant.

Some trials to utilize the common planktonic crustaceans as the indicator animals were, therefore, carried out next year. Several forms of littoral copepods and freshwater cladocerans such as Calanus, Cyclops, Tigriopus, Daphnia and Moina were brought into use along with the younger stage larvae of above-mentioned fouling species, but rather indefinite results were obtained in various experiments. Cultured younger larvae of foulers and newly collected planktonic materials consist naturally of individuals of different stage of growth. The indefinite results were probably caused by the different physiological activities in successive stage of growth.

These results of preliminary investigations seemed to tell that the most indispensable factor in bioassay tests is not to use the fouling larvae directly, but to use the individuals of the same stage of growth and of the same physiological condition.

3. Artemia-scale Method

In a series of comparative bioassay experiments Artemia-salina showed the nearest results to those of cyprid larvae of barnacles. The author selected it as the most satisfactory indicator animal to determine the low concentration of toxicants in sea water. Dried eggs are easily obtained at any aquarium shop, and it is easy to get numbers of larvae out of eggs even in small vessels. Necessary number of larvae of the same stage and condition are used at any required season of the year. (Fig. 6)

Two or three days old larvae were added to 50 or 100ml of sea water solution of different antifoulant prepared in concentration of 1, 5, 10, 25 and 50 ppm respectively. After 1, 3, 6, 12 and 24 hours contact the number of dead, enfeebled and sunken individuals were carefully counted under the stereoscopic microscope. (Fig. 1) Coefficients 1, 0.7 and 0.3 were applied to the numbers of dead, enfeebled and sunken individuals respectively, and percentages of their sum to the total individuals are regarded as the indices of toxic effect of chemicals at each point of time as follows.

$$\frac{N'(\text{dead})\times 1 + N''(\text{enfeebled})\times 0.7 + N'''(\text{sunken})\times 0.3}{N(\text{total})} \times 100 = \text{percentage death}$$

Obtained curves of organic toxicants are divided into two types of efficiency pattern (Fig. 8). Tin compounds belongs to the fast type and

Triphenarsasin Chloride and DDT to the slow type.

From 1967 to 1969 thorough bioassay tests were carried out on nearly 200 kinds of organic and inorganic compounds, and the results proved the excellent nature of Artemia salina larvae as the indicator animal to determine the antifouling effect.

This method using Artemia as a scale of toxicity will be able to be named "Artemia-scale Method".

4. Chlorella-scale Method

According to the increasing damages by algal fouling on ships, the bioassay tests by some marine algae were started in 1969, and it became clear that the direct use of fouling algae was inconvenient partly by the difficulty of measuring growth and partly by the limited season or period of spore making. The most excellent results were obtained by an unicellular freshwater green algae Chlorella ellipsoidea, and extended researches on a marine species Chlorella ovalis are carrying on at present.

A new culturing equipment (Figs. 2,5) was applied to give constant aeration of CO_2-rich air under definite illumination of 2000 luxes. To absorb light energy effectively and to get constant current b/ bubbling the culture bottles were designed to have flattened parallel walls and specially curved bottom.

After H.Tamiya's celebrated works on Chlorella ellipsoidea the following culture media were used.

Myer's 4N		Arnon's A5	
KNO_3	5.0 g	H_3BO_3	2.86 g
KH_2PO_4	1.25	$MnCL_2.4H_2O$	1.81
$MgSO_4.7H_2O$	2.5	$ZnSO_4.7H_2O$	0.22
$FeSO_4.7H_2O$	0.003	$CuSO_4.5H_2O$	0.08
H_2O	1000 ml	H_2O	1000 ml
		Conc.H_2SO_4	1 drop

In the case of bioassay tests 1 ml of 4N, 0.01 ml of A5 and 0.01 ml of $FeSO_4$ solution were added to 60 ml of toxic solutions with different concentration.

After 2 to 5ml of stock culture of Chlorella was added to the solution in each small bottle, they were set in the equipment. Every other day 5 to 10 ml of the cultures were centrifuged and declining value of haematocrit scale was used as the antifouling potential of chemicals at each concentration. (Fig.10) When the leaching rate was concerned, 60ml of bubbled leachates from painted panels were used in the same procedure. Experiments on about 100 kinds of organic chemicals were carried out and satisfactory results were obtained.

5. Preliminary Aquarium Treatment

Results of usual raft tests of painted panels indicate the mixed effects of two independent factors, the toxicity of antifouling chemical itself and the solubility of vehicles of the paint. The life of an antifouling paint, therefore, comes to end when the leaching rate has declined under the critical point of solubility. The relation between the leaching rate at a certain time and actual antifouling effect of the coating is a very important subject to be studied. However, the quantitative determination of leaching rate of the coating in the sea is almost impossible by the indefinite decrease of exposed surface caused by the attachment and growth of various foulers. Another difficulty regarding the antifouling potential is the unequal effect against different foulers in different seasons. To getover these two difficulties, the paint surface must be kept clear for many months and also the immersion time must be adjusted to the breeding season of different organisms. The preliminary aquarium treatment was originally applied to deal with this situation, and fairly good results were obtained.

A set of large-and small-size panels was coated with a kind of antifouling paint of the same constitution. The set was kept in the aquarium provided with running sea water through the sand filter (Fig. 3), then the coating was thoroughly soaked just like in the sea and the surface was kept clean with no macroscopic fouling organisms. When the appropriate season had come, the large-size panel was transfered into the sea and the small-size panel with 200 cm^2 of exposed surface was put into the study of leaching rate. (Fig. 4) Development of fouling community on the panel and the result of bio-assay test of leachate were compared. (Fig. 7) The results of these tests were indicated in the Table 1.

About 120 sets of these panels were coated with five kinds of antifouling paints containing Tributyltin oxide, Arsenic, Zinc thiocarbamate, DDT and Pentachlorphenol respectively. As many as 24 sets of panels were divided into five groups each adjusted to the different seasons. Preliminary aquarium treatments ranging 1 to 12 months were applied along the definite schedule. (Fig. 9) The toxicity of these leachates was studied by Artemia- and Chlorella-scale methods. Behaviors and activities of toxicants were thus studied comparatively and the close relation between leaching rate and actual fouling was fairly determined.

Fig. 10 indicates the results of comparative study on Cuprous Oxide, TBTO and Triphenarsazin Chloride by Chlorella ellipsoidea after the preliminary aquarium treatment ranging 2 to 11 months. The study showed the long rangeservice of Triphenarsazin Chloride in antialgal activity.

Table 1. Seasonal change of relation between Artemia scale and actual fouling. (by preliminary aquarium treatment)

Al= Algal fouling An=Animal fouling Art=death rate of Artemia

	May			Jul			Oct			Jan			Apr		
	Art	Al	An	Art	Al	An	Art	Al	An	Art	Al	An	Art	Al	An
TBTO	100	0	0	96	0	0	93	4	0	93	4	0	91	4	2
TPC	87	0	2	89	0	4	87	0	0	84	0	0	80	0	2
STC	65	0	4	64	0	6	61	8	2	45	4	0	41	4	9
DDT	55	0	5	53	0	20	52	10	3	42	8	0	37	6	3
PCP	55	0	17	44	0	23	43	4	10	33	8	0	24	6	9

Fouling is shown in grade value of community.

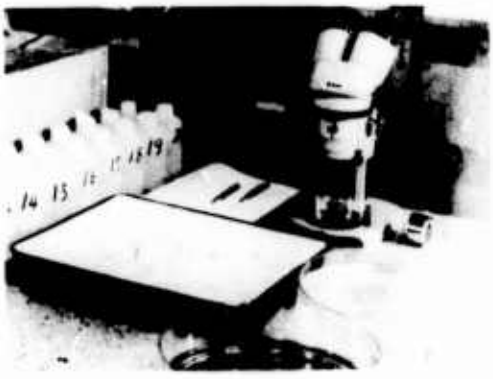


Fig. 1 Couting Artemia individuals

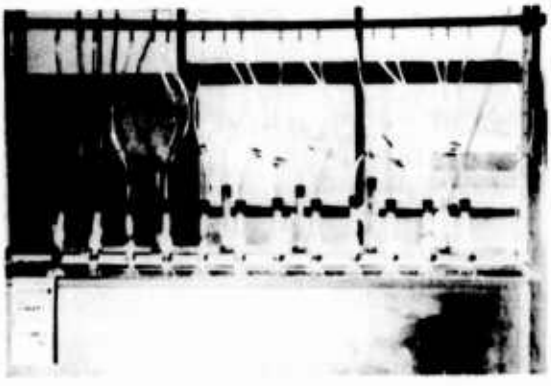


Fig. 2 Apparatus for culturing Chlorella



Fig. 3 Sandfilter and aquarium for preliminary immersion of panels

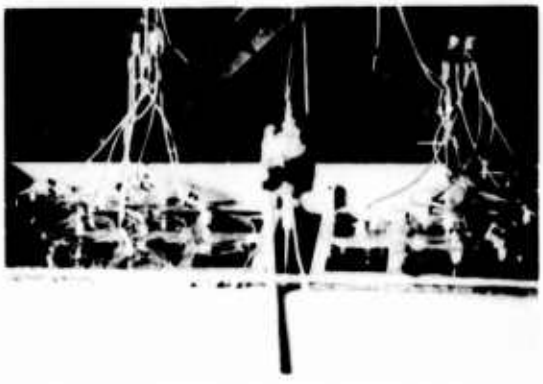


Fig. 4 Bubbling treatment for leaching out of small panels

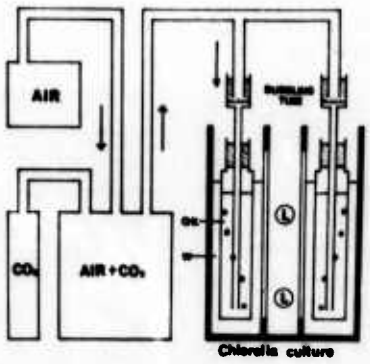


Fig. 5 Plan of Chlorella culture

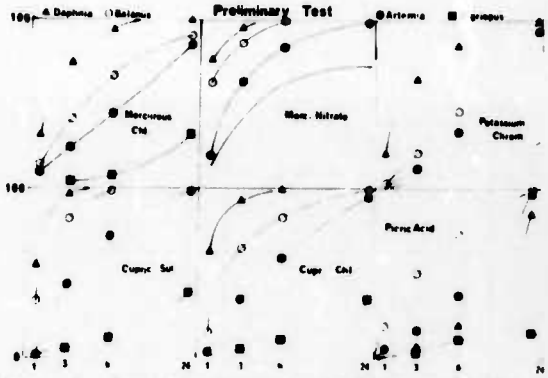


Fig. 6 Lethal curves of four animals compared

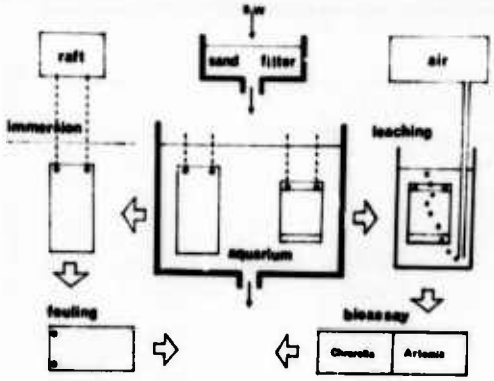


Fig. 7 Plan of preliminary aquarium treatment

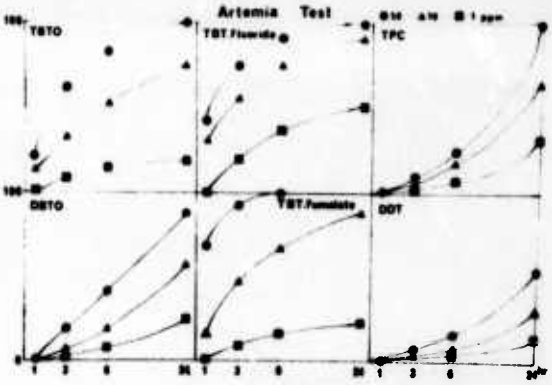


Fig. 8 Artemia test showing two types of lethal curves

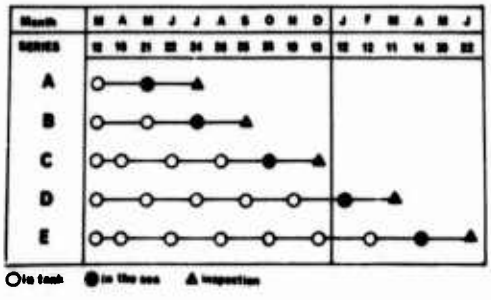


Fig. 9 Schedule of aquarium immersion and raft test

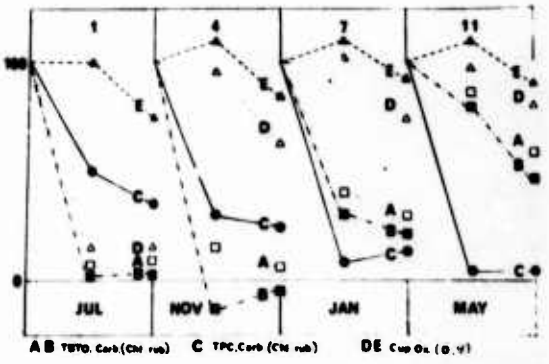


Fig.10 Chlorella test of five kinds of ingredients shown by percentage decrease of volume

Discussion

Christie: I would like to draw attention to some earlier work of Cornell and Sparral on the toxicity of inorganic compounds and organic metallic compounds to barnacle larvae and to artemia larvae. Based on that work, there is some question concerning the conclusion that the initial results on the toxicity of inorganic compounds is representative of the effect you get with organic metallic compounds and that artemia is comparable to the barnacle larvae. With regard to your chlorella work, similar techniques have been published. How do you achieve solubility of the toxicants? Some of the concentrations that you appeared to achieve are inconsistent with my experience.

Mawatari: I made a solution of these compounds using solvents.

Ship Hull Anti-Fouling System Utilizing Electrolyzed Sea Water

Jitsu Shibata* Mitsuhiko Kimura* Kenji Ueda** Yajuro Seike***

Nagasaki Shipyard & Engine Works , MITSUBISHI Heavy Industries, Ltd.
1-1, AKUNOURA-MACHI, NAGASAKI 850-91, JAPAN

Mitsubishi Heavy Industries, Ltd., has recently developed a new anti-fouling system for protection of ships' hulls.

In this system, electrolyzed sea water is mixed with air and released from nozzle pipes which are fitted to the bilge parts of a ship's hull, so that the mixture of electrolyzed sea water and air rises up to the water surface along the ship's side shells.

A test unit with a capacity large enough to cover a 100 m long ship's shell plate was built and operated continuously for five months producing and issuing the electrolyzed sea water over a 4 m x 10 m steel plate immersed in sea water for confirmation of its efficiency and durability.

On the basis of the above test results and the preliminary designs of the system worked out for several different ship applications, it is confidently believed that the system offers a great benefit to shipowners.

Key Words: Ship Hull Anti-fouling; Electrolyzed sea water; Electrolyzer; Nozzle pipe; A/F Economy

1. Introduction

When such marine growth as serpulae or lavers adhere to the exterior of ship's hull and grow there, the hull's frictional resistance increases to reduce the speed of the ship which in turn adversely affects her operational economy. The usual method to overcome this trouble is by coating the hull with anti-fouling paint in which toxic substances are mixed. However, this method has the following disadvantages:

(1) The coating, even if applied twice, is only about 100 μ thick and therefore does not contain sufficient quantity of poison to be fully effective.
(2) Even when there is no possibility of such marine growth adhering to the hull, the poisonous content would continue to dissolve due to contact with sea water, and
(3) Powerful poisons, such as organic arsenites, are difficult to be used because of the harmful effect to humans.

Consequently, as it is difficult to develop a paint which remains effective for a long period on the hull, ships are obliged to dry-dock for recoating every year or so.

* Development Coordinators Section, No.1 Ship Designing Department, Nagasaki Shipyard, MHI
** Chemical Research Laboratory, Nagasaki Technical Institute, Technical Headquarters, MHI
*** Machinery Research Laboratory, Nagasaki Technical Institute, Technical Headquarters, MHI

Figures in parentheses indicate the literature references at the end of this paper.

While strenuous efforts have been made to develop a better anti-fouling paint, different anti-fouling systems, including one using ultrasonic waves[1], which are expected to dispense with the disadvantages of the coating system, are being studied.

Mitsubishi earlier conducted basic experiments on an anti-fouling system utilizing electrolyzed sea water[7], and such a system for sea water piping (MGPS) is already commercially available.

With a view to developing a new anti-fouling system superior to anti-fouling paint system, Mitsubishi started experiments around 1965 to study the feasibility of adapting the electrolytic method for shell plating and have now devised two practicable methods which are the belt-shaped electrode system and the electrolyzer system.

(1) Belt-shaped electrode system

Belt-shaped electrodes, cathode and anode, are attached to the bilge part of the shell plating to electrolyze sea water, and minute bubbles are jetted from a nozzle pipe laid beneath the electrodes to direct the electrolyte up along the shell plating.

(2) Electrolyzer system

Sea water is electrolyzed in an electrolyzer installed on board, and the electrolyte and bubbles are spouted from a nozzle pipe laid along the bilge part of the hull.

Basic experiments on the belt-shaped electrode system (1) were conducted at first with small vessels (70 GT and 100 GT), and later, using 50-meter long electrodes, with the "Houn Maru" (a 50,000-ton class ore carrier) of Nippo Kisen K.K.. The anti-fouling effect of this system was confirmed. However it was found to consume too much electric power and required sophisticated techniques to protect the shell plating from corrosion by the electric stray current. Therefore it was decided to develop the electrolyzer system (2).

For practical use, it was necessary to confirm
(1) required concentration and quantity of the electrolyte for anti-fouling;
(2) characteristics of the nozzle pipe from which the electrolyte and air are spouted;
(3) performance of an electrolyzer that would be compact and highly efficient, and
(4) durability of accessories and piping.

Though designing data of each elements had been accumulated from the various basic experiments, including those on a small electrolyzer and nozzle tests in a 30 cubic meter water tank, the effects of scaling up and system performance had yet to be ascertained.

Consequently a large test plant was built to confirm the overall performance.

2. Overall tests with the large test plant

2.1 Components of the electrolytic anti-fouling system

The electrolytic anti-fouling system, as illustrated in Fig. 1, is principally composed of
(1) a sea water pump with piping,
(2) an electrolyzer,
(3) a rectifier,
(4) a cyclone,
(5) an air compressor with air piping, and
(6) a nozzle pipe.

The electrolyzer, as shown in Fig. 2, is built of a number of parallel spacing plate type electrodes with the intention of making it, as well as the power rectifier, as compact as possible. The cyclone, intended for separating magnesium hydroxide and hydrogen gas formed as by-products of electrolysis, is needed for preventing the choking of nozzles and

ensuring from the gas explosion.

The nozzle pipe is so designed as to mix the electrolyte and air, spout up the mixture in minute bubbles, and evenly distribute the electrolyte over the hull surface. Adequate resistors are applied to the nozzles so that the spouting may be uniform, and remain unaffected by changes in the trim of the hull.

2.2 Outline of the test plant

The test plant, illustrated in Fig. 3, was installed on the jetty of Dock No. 2 at Nagasaki Shipyard. The anti-fouling capacity of the plant was intended to cover a 100-meter length of simulated ship's broadside. A part of the electrolyte generated is spouted together with air from a nozzle pipe laid at the bottom of a panel, 4 meters wide and 10 meters deep, to flow up along the panel surface in minute bubbles.

Another panel of the same size, unprotected from fouling, was soaked in sea water so that the anti-fouling effect could be compared. The first and second tests were conducted in this manner, and afterwards the two panels were joined to make an 8-meters wide anti-fouling test panel for the third test.

The pressurized sea water fed by the pump goes through a strainer and a flow meter, and reaches the electrolyzer where it is electrolyzed. The electrolyte contains magnesium hydroxide and hydrogen gas, which are removed at the cyclone. As the hydrogen gas is ejected together with a small amount of the electrolyte from the top of the cyclone, it is dehydrated in a secondary cyclone. Then it passes through a flow meter and an anti-explosion filter, and enters a ventilator fan duct, where it is diluted. The magnesium hydroxide comes out of the underflow of the cyclone, goes through a flow meter and enters a magnesium hydroxide depositing tank, at the bottom of which it is precipitated.

A part of the electrolyte from the outlet of the cyclone is sent to the nozzle pipe attached to a panel passing through a flow meter and then spouts together with air from an air compressor. Though not indicated in Fig. 3, a mercury manometer is fitted to measure resistance in the strainer, electrolyzer and cyclone.

Major part of the electrolyte is discharged sufficiently far from the panel. A valve is provided halfway on the discharge pipe so that the pressure on the plant can be regulated. Another part of the electrolyte is poured into a water level control tank and by the level switch installed there, the power supply is cut off when the water feed is stopped. Test pieces of various materials are submerged in the water level control tank for subsequent comparison with similar pieces soaked in sea water to determine their respective resistance in highly concentrated electrolyte.

2.3 Results of the tests

(1) Anti-fouling performance

Figs. 4 and 5 indicate the difference in fouling between the electrolytically protected panel and the unprotected one. The distribution of residual chlorine on the panel surface is diagramed in Fig. 3. As Fig. 3 shows, the electrolyte rises in the form of a film approximately 200-mm thick along the panel surface, and quickly starts to disperse as it reaches the surface of the water. Its concentration is slightly lower on the left side perhaps due to the influence of the tidal current. Comparison of the distribution curve in Fig. 3 and the photographs of the electrolytically protected panel in Fig. 5 suggests that about 0.03 ppm is the limit of the anti-fouling effectiveness.

Table 1 lists the results of the weighing of organisms collected from the panel surface. Although the immersion for the third test lasted for five months, the air compressor failed to work for some time and consequently the marine growth was slightly more than would have been otherwise. Fig. 6 shows comparison of the effect of the electrolytic method with that of A/F paint, indicating the superiority of the former.

(2) Electrolyzer

The electrolyzer was in operation for about five months (3,400 hours) without overhauling. Although it was possible to continue the operation further, the test was stopped to inspect the inside of the electrolyzer. It is calculated that five months of continuous operation is equivalent to approximately three years of an actual vessel[8].

The electric current efficiency remained almost invariably at around 80 per cent, and the inter-electrode voltages were about 5 volts. Since the efficiency of the rectifier was about 90 per cent, the electric power required to produce 1 ton chlorine can be calculated in the following way:

$$W = 1/1.323 g \cdot Cl_2/A.h \times 5\ V \times 1/0.8 \times 1/0.9$$

$$= 5.25\ Wh/g \cdot Cl_2 = 5,250\ kWh/ton \cdot Cl_2$$

Judging from the condition of the original 1-micron thick platinum coating of the titanium electrode plates after the completion of the operations, the plates could be used for four to five more months. Thus, if the platinum coating is 1½ micron thick, the plates will last for about 15 months of uninterrupted use or, when installed on an actual ship, 8 to 10 years of normal operation[5][6].

(3) Cyclone

The cyclone separated magnesium hydroxide at a rate of 95 per cent or more, and its pressure loss in practical use was insignificant.

Since the separation of hydrogen gas was insufficient because of its dissolution in water under pressure, a secondary cyclone was provided to isolate the hydrogen gas. On board an actual vessel, it would be necessary to place a cyclone as high as possible to reduce pressure, and thereby, to minimize the dissolution of hydrogen gas in water and facilitate its separation.

(4) Nozzles

After five months of continuous operation, neither abrasion nor choking by magnesium hydroxide was observed on the hard vinyl chloride nozzles.

(5) Durability of the other components

After the uninterrupted operation, no defect was found in the galvanized steel pipes, Butyl rubber lined valves, hard glass made rotor type flow meters, bronze ball valves as well as hinge type simplified flow meters, (important parts of which were made of SUS 32) for the electrolyte piping. Carbon had been deposited on the surface of the neoprene rubber which showed sign of slight deterioration, but presumably not to such an extent as would pose any practical problem.

(6) Effect on paint coating

Although the electrolytically protected panel, as shown in Figs. 4 and 5, looked brown in color near the nozzles, normal anti-corrosive paint (A/C paint) appeared when the top layer of the paint coating was removed. The coloring was due to superficial oxidation of the coating, but does not seem to have affected the paint film strength.

On the other hand, small plates coated with A/C and A/C + A/F paints of oily, chlorinated rubber, tar epoxy and pure epoxy were immersed for 1,200 hours in a highly concentrated electrolyte and ordinary sea water for comparison and the results were as follows:

A/C: The coatings underwent a strip test by a crosscutting method, indicating no difference between the pieces immersed in the electrolyte and those in sea water.

A/F: Cuprous oxide changed to oxidized copper in highly concentrated electrolyte, and no toxic efflux occurred. The resin in the A/F was dissolved by the electrolyte action and softening of the coatings was observed to some extent. However, the A/C undercoatings were found unaffected.

Thus, it was recognized that even a highly concentrated electrolyte hardly affects A/C coatings and therefore would cause no trouble in practical use.

3. Outline of tentative designs for actual vessels

Tentative designs were prepared with respect to 10,000-ton class general cargo vessels, 50,000-ton class ore carriers and tankers of various classes up to 500,000 tons. As an example, the application of the electrolytic anti-fouling system to a 250,000-ton tanker is described in this report.

Fig. 7 illustrates the whole system, Fig. 8 the nozzle pipe, composite pipe and strainer flow-meter unit, and Fig. 9 the electrolyzer unit.

3.1 Whole system

The electrolyzer unit, housed in a container having a capacity of about 3½ meters cube, is installed on the deck or in the upper part of the engine room. The container also houses rectifiers, electrolyzers, cyclones, an air tank, strainers, a switchboard and various gauges. The electrolyzer unit treats the sea water and air supplied respectively by the sea water pump and air compressor installed in the lower part of the engine room, and feeds them into the main electrolyte and air pipes respectively.

The main pipes for electrolyte and air are laid in a longitudinal direction on the upper deck, and branch pipes diverge from them and are connected to strainer flow-meter units provided on ships' broadsides. Provision has been made to allow for the removal of rust and magnesium hydroxide from the inside of the main and branch pipes for the electrolyte and air, and at the same time regulate the rate of flow through the pipes.

Each composite pipe, consisting of two pairs each of large and small vinyl chloride tubes set in position with filler, is contained in a thick steel pipe which runs from the upper deck through a tank to the shell plate. Each composite pipe connects a strainer flow-meter unit on the deck to the nozzle pipe fitted to the shell plating.

As the maximum length of a nozzle pipe is about 25 meters, composite pipes are spaced at intervals of about 50 meters along the hull.

3.2 Nozzle pipes, composite pipes and strainer flow-meter units

Since little marine growth takes place on bottoms of modern large vessels, nozzles are installed along the circular portion of the bilge so that the broadsides can be protected from fouling.

The outside dimensions of the nozzle pipe, made of neoprene, is 205 millimeters wide and 65 millimeters thick. The section of the nozzle pipe is divided into three chambers, top, middle and bottom, and the electrolyte runs through the bottom chamber while the air is fed through the middle. The electrolyte and air are mixed and then jet through nozzles made of hard vinyl chloride into the upper chamber where the mixture remains in a turbid state until it is discharged through the holes of the chamber. At the lower end of the bottom chamber, there are holes for discharging residual magnesium hydroxide which the cyclone and strainer failed to remove.

The outer component of the composite pipe is an STPT Sch 160 tube, joined by sleeve welding.

Each strainer flow-meter unit is housed in a steel plated container 1,250 millimeters long, 900 millimeters wide and 610 millimeters high, to protect the unit from the impact of waves.

3.3 Sea water electrolyzing system

Table 2 lists, as an example, the particulars and electric power consumption of principal units of the system for a 250,000-ton tanker. With one rectifier provided for each of the three electrolyzers, a sudden overload on the generator would automatically switch off one, two or all three rectifiers when required, depending on the seriousness of the overload. They would then be switched on again automatically, when the overload on the generator is relieved.

Due to the flexibility of the electrolyzers in which the chlorine concentration varies in proportion to the amperage, rectifiers with somewhat larger capacities than are normally needed may be designed to permit operation at a slightly higher concentration of electrolyte when the generator is working below its full capacity.

If an electrolyzer is actuated without sea water in it, not only will its insulators burn but hydrogen and oxygen may also accumulate causing fire and explosion. To prevent such dangers, the electrolyzers are so designed that they cannot be switched on unless the sea water pump is operating and there is a difference in pressure between their inlets and outlets.

It is planned to remove the magnesium hydroxide, by the continuous blowing of about 10 per cent of the underflow of the cyclone. To remove hydrogen gas, it is extracted together with a small quantity of the electrolyte through the top of the cyclone, and separated with a smaller secondary cyclone. The gas passes through an anti-explosion filter, is adequately diluted and then discharged by a ventilator fan.

Those portions of the inner surface of the electrolyzer unit which may come into contact with the electrolyte are lined with plastic or neoprene. As the whole unit is housed in a sturdy container, pipes and valves could be of hard vinyl chloride.

Double sea water strainers, with 16-mesh nets and slightly larger in diameter than the piping, will be provided.

3.4 Main and branch electrolyte pipes

The main and branch electrolyte pipes laid on the upper deck are of galvanized steel at least 5 millimeters thick.

4. Operational economy of the electrolytic anti-fouling system

4.1 Present situation on fouling

Fig. 10 shows the speed-reducing effect due to fouling on tankers serving the Japan/Persian Gulf route and ore carriers plying between Japan and South America. The average reduction in speed of tankers for every 12-month period of operation between dockings is 0.5 knot, while that of ore carriers over the same period is 1.0 knot.

4.2 Increase in cruising speeds by electrolytically protected system

The effect of electrolytic anti-fouling is measured by an increase in the cruising speed of the ship. However assuming that the decline in speed diagramed in Fig. 10 is wholly attributable to fouled hulls, and the efficacy of the electrolytically anti-fouling system is perfect, large tankers and ore carriers, if docked at 12-month intervals, would gain 0.5 and 1.0 knot respectively in service speed due to electrolytic protection.

If the drop in speed due to the increased resistance caused by the roughening of the coating surface or by the fouling of the slime, as covered by Fig. 10, is 0.3 to 0.4 knot immediately before docking after every 12 months of operation, the average service speed of a large tanker or an ore carrier with electrolytic protection, is calculated to rise by 0.3 or 0.8 knot respectively. When docking intervals are longer, the electrolytic anti-fouling system will obviously give even a greater advantage in speed.

4.3 Economy of electrolytically protected vessels

Although recent A/F paints have greatly improved, they remain effective for only six months or one year at the most, and their anti-fouling characteristics suddenly deteriorates after that. On the other hand, since the electrolytic anti-fouling system may prevent marine growth on hulls semi-permanently, dock-intervals can be extended.

The aforementioned increase in service speed and the extension of docking intervals would result in a gain in annual freight earnings. Even if their docking intervals remain as they are, a 250,000-ton tanker would earn ¥150 million more, and a 50,000-ton ore carrier, ¥40 million more, on an annual basis. The corresponding increase in operating costs is only the additional fuel for the generating plant to supply power to the electrolytic anti-fouling system. Assuming that the extra power consumption is 209 kilowatts for 50 days a year at anchor, fuel consumption 260 grams per kilowatt of power generated and fuel cost ¥8,500 per ton the operating cost of ¥550,000 a year is trivial for a 250,000 ton tanker when compared with the gain in freight earnings. (refer Table 3)

If docking intervals are extended, the number of idle days will be further reduced.

One of the generally applied criteria upon which to decide whether or not an additional equipment should be used is whether it will pay for itself in three years. Fig. 11 gives an estimated increase of freight income by electrolytically protected vessels over a three-year period, which can be used as a criterion to assess the economic value of this electrolytic anti-fouling system.

5. Summary

With a view to the development of a hull anti-fouling system utilizing electrolyzed sea water for practical use, a test plant on such a scale that would allow enlargement for application to an actual ship, was built, and overall tests were conducted to confirm the practicability of the system and its anti-fouling effect. As a result, a remarkable anti-fouling effect was ascertained as well as the practicability of the electrolyzers, nozzle pipes and accessory units.

On the basis of results obtained from the tests, trial designs of the system were prepared for some types of vessels and their economic aspects were studied. The results envisaged a significant economic advantage for the system.

Since no final evaluation of the system can be achieved until it is tested on board an actual ship, the cooperation of all concerned for its realization, is desired.

References
(all in Japanese)

(1) Mori et al., "A study on ultrasonic anti-fouling of ship's hull", Mitsubishi Juko Giho, VI, 6 (1969).
(2) Beppu et al., "On the operational performance of the SS. Oriental Giant", Seibu Zosenkai Kaiho, 39 (1970).
(3) Yamazaki and Tachiki, "On sea margin", Seibu Zosenkai Kaiho, 39 (1970).
(4) Kitajima, "On the operational record of iron ore carriers viewed through the analysis of entries on the abstrated logbook", Zosen Kenkyu, Feb.(1968).
(5) Tasaki and Urata, "Formation of chlorine by electrolysis of sea water", Karyoku Hatsuden, Mar. (1969).
(6) Taniguchi et al., "A study on a chlorine generator based on electrolysis of sea water", Kogyo Yosui, July (1969).
(7) Yoshii et al., "A study on a system to prevent marine growth on ship hulls", Mitsubishi Juko Giho, IV, 3 (1967).
(8) Sakae et al., "A study on an anti-fouling system for water power equipment for sea water pumping-up power stations", Mitsubishi Juko Giho, II, 2 (1965).

Table 1 Quantity of marine growth after immersion test

Panel	Protected against fouling or not	Position of sample collection (depth from top)	Amount of marine growth (g/m^2)				
			First test (for 35 days)		Second test (for 30 days)		Third test (for 5 months)
			Living	Dried	Living	Dried	Dried
Blank panel	Unprotected surface (A/C only)	2 m	–	–	–	–	–
		3	6 850	1 550	1 207	285	–
		4	900	250	–	–	–
		5	400	100	669	210	–
		6	420	170	–	–	–
		7	5 780	130	424	122	–
		8	2 500	550	–	–	–
		9	3 100	300	246	73	–
Electrolytically protected test panel	Side	2	–	–	–	–	–
		3	1 700	800	–	–	–
		5	1 700	800	–	–	–
		7	450	300	–	–	–
		9	90	80	–	–	–
	Electrolytically protected surface (A/C only)	2	–	–	–	–	80
		3	330	190	Minute serpulae, 1 000~2 000 bodies/m^2		540
		4	70	60	Minute serpulae, 500~1 000 bodies/m^2		380
		5	20	10	0	0	120
		6	3~5 mm serpulae about 4 500 bodies/m^2		0	0	0
		7	0	0	0	0	0
		8	0	0	0	0	0
		9	0	0	0	0	0

Notes: (1) The mean low tide level was about 3m below the panel top.
(2) Organisms were collected from an area of the panel surface 100mm square, and weighed.

Table 2 Particulars of equipments and power consumption (250,000 DWt tanker)

Item	No. of units	Particulars	Power consumption
Rectifier	3	75~150V x 660A	126 kW
Electrolyzer	3	Platinum-coated titanium plate (Pt 1.5μ)	–
Sea water pump	1	280 m^3/h x 500 m TH.	54 kW
Air compressor	1	250 m^3/h (F.A.) x 7 kg/cm^2	28 kW
Air tank reservoir	1	800 ℓ x 7 kg/cm^2	–
Ventilator fan	1	10 m^3/min x 60 mm H_2O	0.6 kW
		Total	209 kW

Table 3 Estimated increase in freight income resulting from use of anti-fouling system

Rout, type of ship			Japan/P.G. large tanker		Japan/S. America ore carrier	
Deadweight capacity			250 000	DWt	50 000	DWt
Round-trip distance			13 600	sea miles	20 000	sea miles
Average service speed	Clean		16.0	kt	16.0	kt
	As it is		15.5	kt	15.0	kt
	Electrolytically protected		15.8	kt	15.8	kt
No. of days at sea per voyage	As it is		36.5591	days/voyage	55.5556	days/voyage
	Electrolytically protected		35.8650	days/voyage	52.7426	days/voyage
No. of days at anchor per voyage			4	days/voyage	6	days/voyage
No. of days required per voyage	As it is		40.5591	days/voyage	61.5556	days/voyage
	Electrolytically protected		39.8650	days/voyage	58.7426	days/voyage
No. of idle days per year due to docking	Once a year		Including transfer time for gas freeing	15 days/year	Including transfer time	12 days/year
	Once every other year			7.5 days/year		6 days/year
No. of voyages per year	As it is	Once a year	8.6294	voyages/year	5.7347	voyages/year
		Once every other year	8.7796	voyages/year	6.0093	voyages/year
	Electrolytically protected		8.9678	voyages/year	6.1114	voyages/year
Increase in cargo volume carried by electrolytically protected ship per year		Once a year	37 550	tons/year	13 730	tons/year
		Once every other year	84 600	tons/year	18 835	tons/year
Freight rate per ton (according to Kaiun, Feb. 1971)			As of Dec. 1970 11.01 dollars/ton (Interscale + 63.64%)		As of Dec. 1970 8.12 dollars/ton	
Increase in freight income per year	Docked once a year		149 000	thousand yen/year	40 100	thousand yen/year
	Docked once every other year		335 000	thousand yen/year	55 100	thousand yen/year

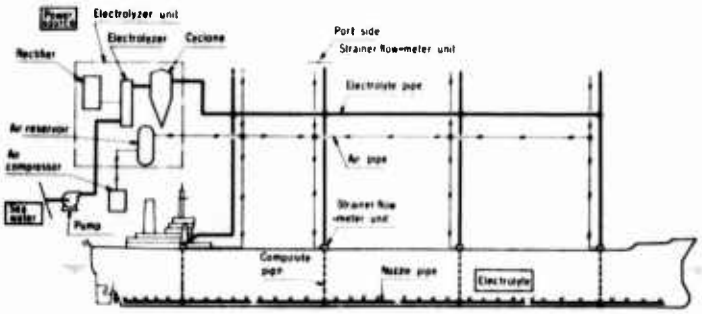


Fig. 1 Outline diagram of ship hull anti-fouling system

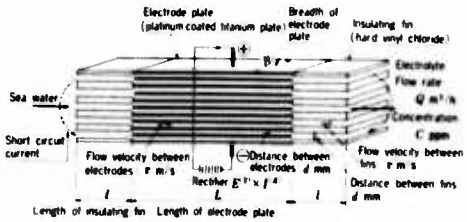


Fig. 2 Interior construction of electrolyzer

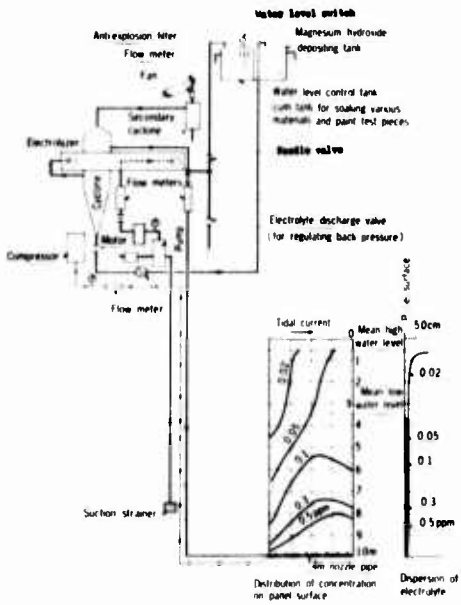
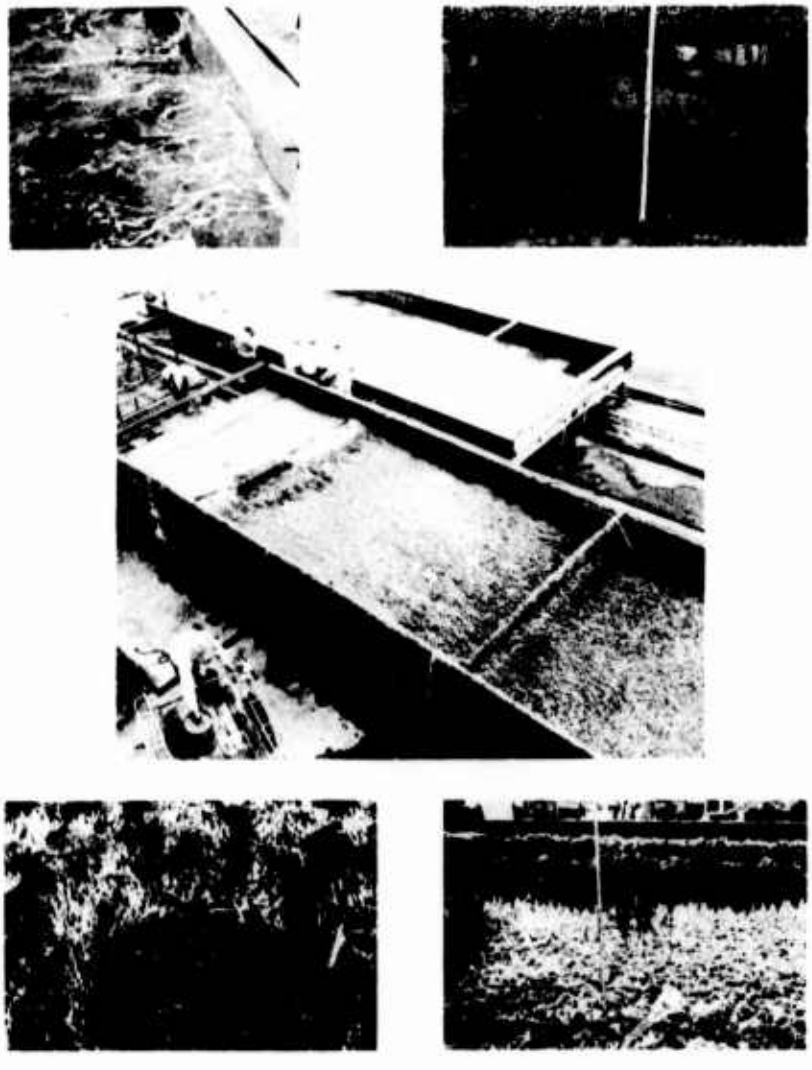


Fig. 3 Arrangement of test unit and steel panel (Figures on steel panel denote distribution of Cl_2)



Dimension of panel	4 m wide, 10 m high
Paint applied	Oily A/C in both cases
Period of immersion	From August 3, 1968 Until September 7, 1968 (for 35 days)

Fig. 4 Steel panel after 1st immersion test

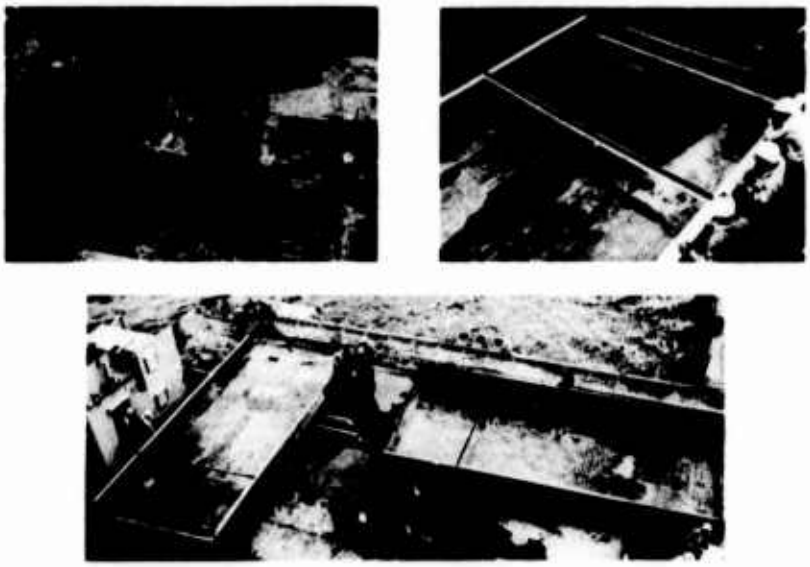
Captions

Top left The mixture of electrolyte and air released from the nozzle pipe installed about 9 m under water, rises straight up and disperses at water level.

Top right Apart from the area approximately 1 m below the water surface, no slime has accumulated on the electrolytically protected panel. Marine growths were conspicuous on angular reinforcements that had been fitted at a distance of 400 mm from the panel surface.

Center Of the two panels, the upper one was equipped with an electrolytic anti-fouling nozzle pipe through which the electrolyte was discharged. A small quantity of slime has accumulated on the panel approximately 1 m below the water surface. (See the top left photo of Fig. 5)

Bottom left and right Contamination of the unprotected panel. Serpula, Barnacles, Ascidians and Bryozoa.



Paint applied: Only A/C in both cases
A 1.5 m high by 1 m wide portion of that part of the electrolytically anti-fouling was remmersed without removing the slime which had accumulated during the first test

Period of immersion: From September 8, 1968
Until October 7, 1968
(for 30 days)

Weather condition when the photos were taken: Drizzling

Fig. 5 Steel plate after 2nd immersion test

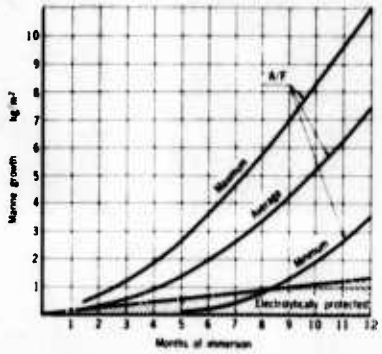
Captions

Center: Of the two panels shown, the one on the left was equipped with an electrolytic anti-fouling nozzle pipe through which the electrolyte was discharged. Chlorine content was 1½ times of that in the first test.

Top left: Contamination of the portion affected during the first test has increased slightly.

Top right: Although the A/C paint near the electrolyte nozzles turned brown, the change was only superficial and had not affected the coating any deeper.

Bottom left and right: The water temperature was lower than in the first test and this resulted in less marine life accumulating. Nevertheless it did foul the unprotected panel as can be seen on the photos. Note the central part in the bottom right photo which was brushed while the panel was still immersed.



- The fouling curve representing the marine growth on the electrolytically protected panel indicates around the mean low tide level (see Table 1) where the electrolytic anti-fouling is least effective.
- Latest informations concerning A/F paints coated on actual ship's hull are desired. A/F paint data on small test pieces are usually better than on actual conditions.

Fig. 6 Immersion test period and quantity of marine growth

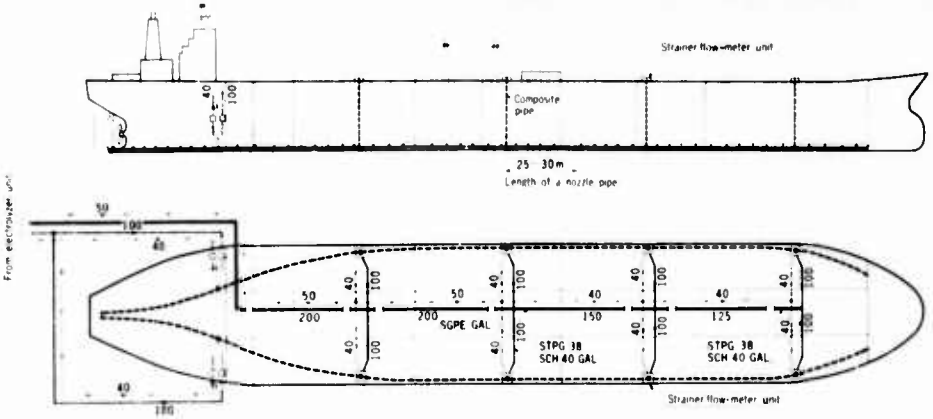
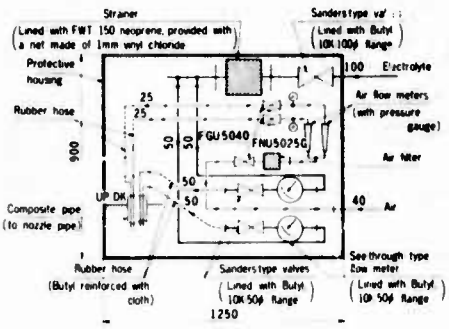


Fig. 7 Arrangement of anti-fouling system on board a 250,000 DWt tanker

Fig. 8 (a)

Strainer Flow-Meter unit



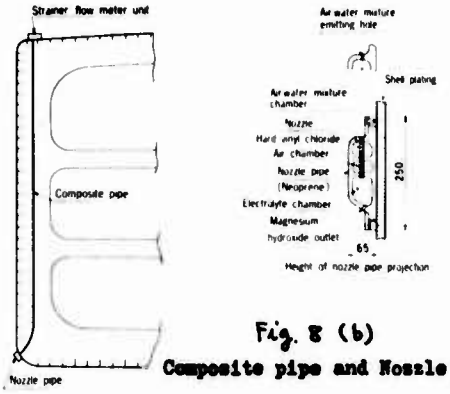


Fig. 8 (b)

Composite pipe and Nozzle pipe

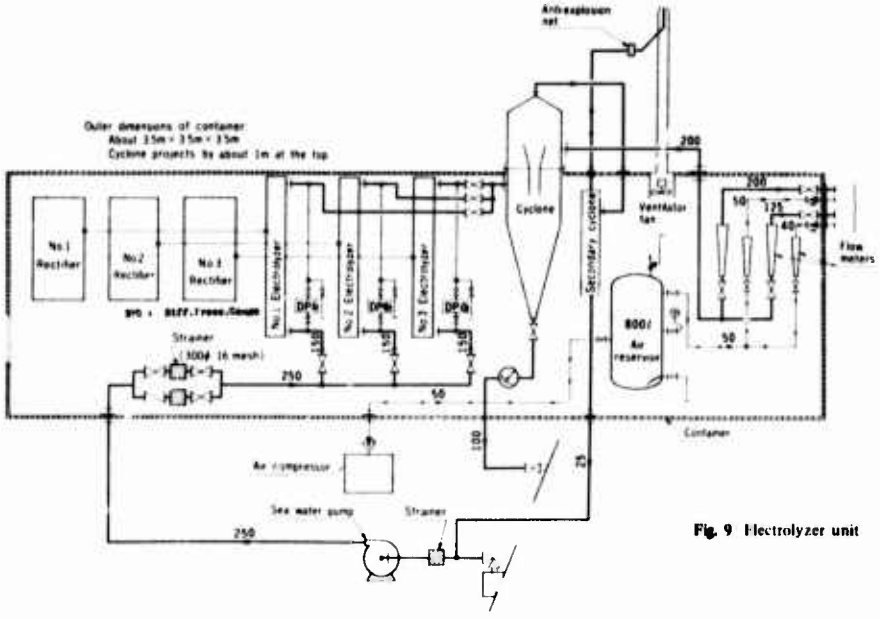
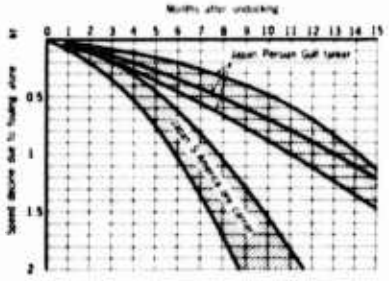


Fig. 9 Electrolyzer unit



Japan/Persian Gulf tanker: Beppu et al., Seibu Zosenkai Kaiho, 39[8] Yamasaki et al., Seibu Zosenkai Kaiho, 39[9]
Japan/South America ore carrier: Taizo Kitajima, Zosen Kenkyu, Feb. 1968[4]

Fig. 10 Decline in ship speed due to hull fouling alone

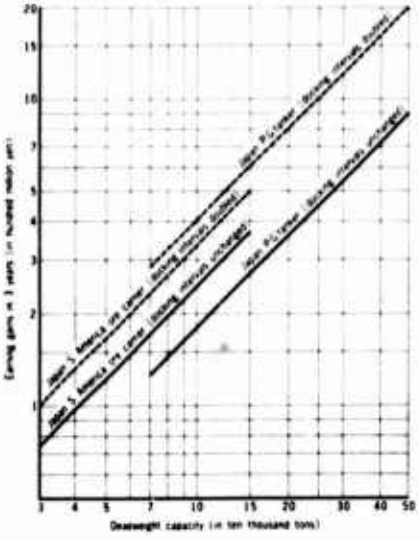


Fig. 11 Estimated increase in freight income over a 3-year period

Discussion

Morgan: In the operation of the system using air, do you think that the trim of the ship will affect the distribution of the electrolyte?

Shibata: The unit has a valve that controls the amount of air going out.

Question: Will the chlorine layer be evenly distributed over the ship hull? Will you be allowed to use this system in ports?

Shibata: The nozzle can control the air to provide even distribution. The system should not be objectionable.

Birnbaum: What is chlorine concentrations in parts per million?

Shibata: Parts per million of chlorine is very low and indicated in figure 3 of the paper.

Smith (U.K.): U.K. experience with an injection system using kerosene plus toxin on merchant ships indicated that the major problem was distribution and results were unsatisfactory because of ship contours. Although tankers may be easier to protect, how would you deal with a complex hull form such as Naval ships?

Shibata: Additional sections would be required.

Smith (U.K.): As you increase the complexity, you increase cost. This has to be traded off against effectiveness of anti-fouling paint or other techniques which perhaps can achieve the same job at a much lower cost. Also, U.K. experience with a piping system with a series of holes or nozzles resulted in a fan shape distribution and areas between the nozzles weren't protected.

Shibata: The electrolyte is pumped and mixed with air to facilitate distribution.

Birnbaum: There is apparently a difference of opinion which can be resolved only by ship trial. We do not have sufficient time to pursue this discussion.

Poretz: What provisions could you incorporate into the system to assure that the system would work all the time, and do you think that this would reflect significantly in the total cost of the system?

Birnbaum: The author indicated that he would not expect to get protection while the ship was underway. When you say all the time, do you mean all the time that the ship is stationary?

Poretz: Anytime the ship is going less than four knots. What is the reliability? That is, how sure are we that the system will operate 100% of the time even with nozzle clogging or how would the system compensate for some other malfunction?

Birnbaum: We are talking about a concept that has just been evaluated and you are asking for data on engineering reliability. Don't you feel this question is premature?

Poretz: No. All I am saying is that to provide this reliability may significantly affect the cost of the system over that indicated in the presentation.

Shibata: In this system, there are three units. If one unit goes bad or malfunctions, the other two units would work, so there is a built-in spare.

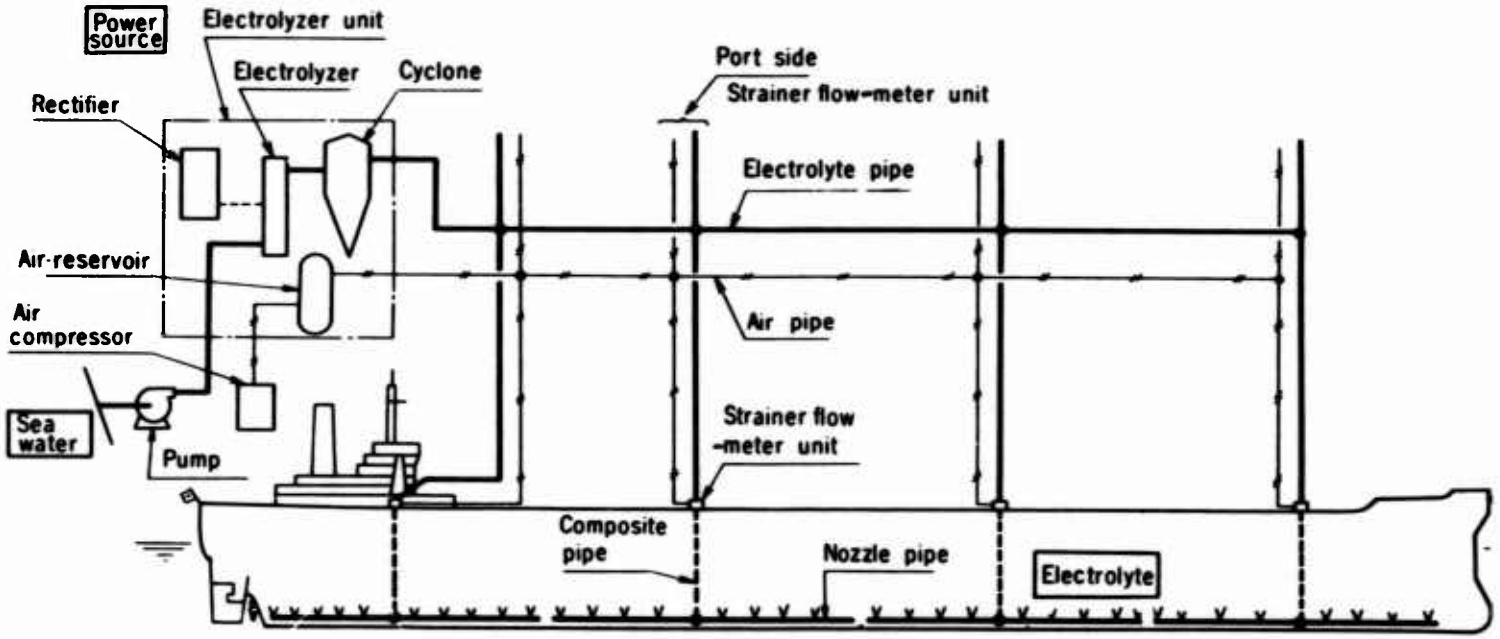


Fig. 1 Outline diagram of ship hull anti-fouling system

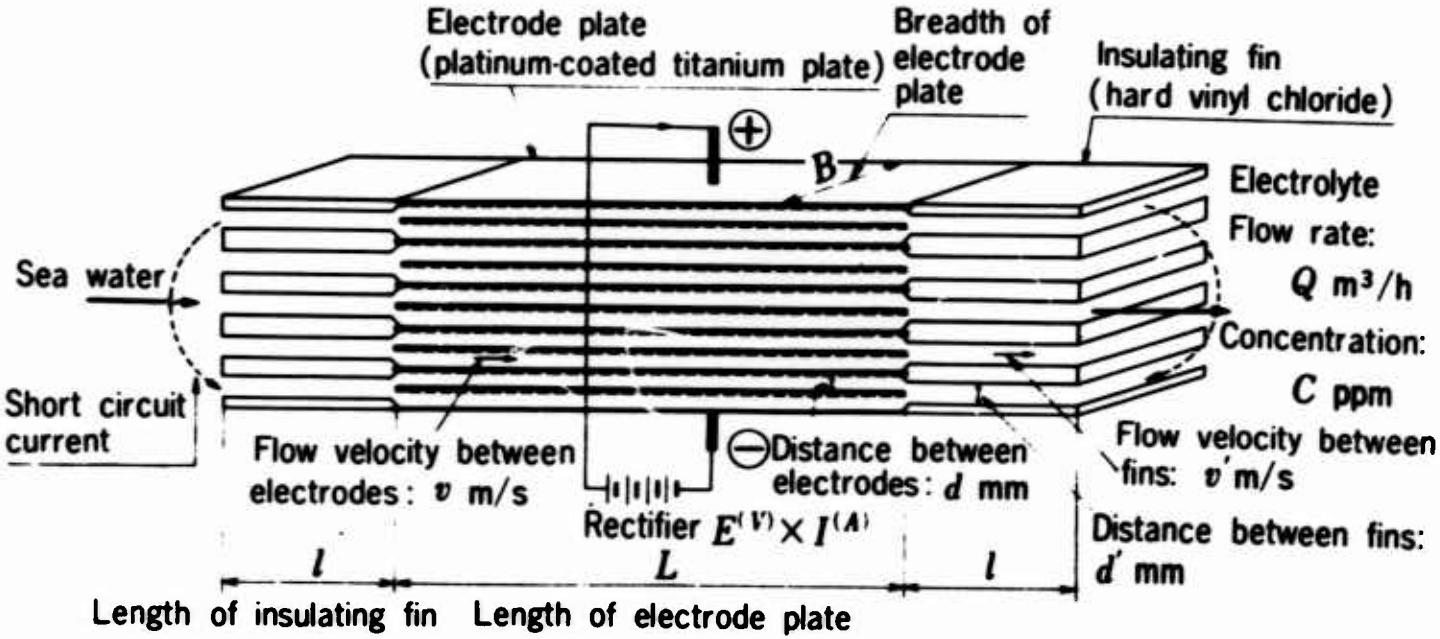


Fig. 2 Interior construction of electrclyzer

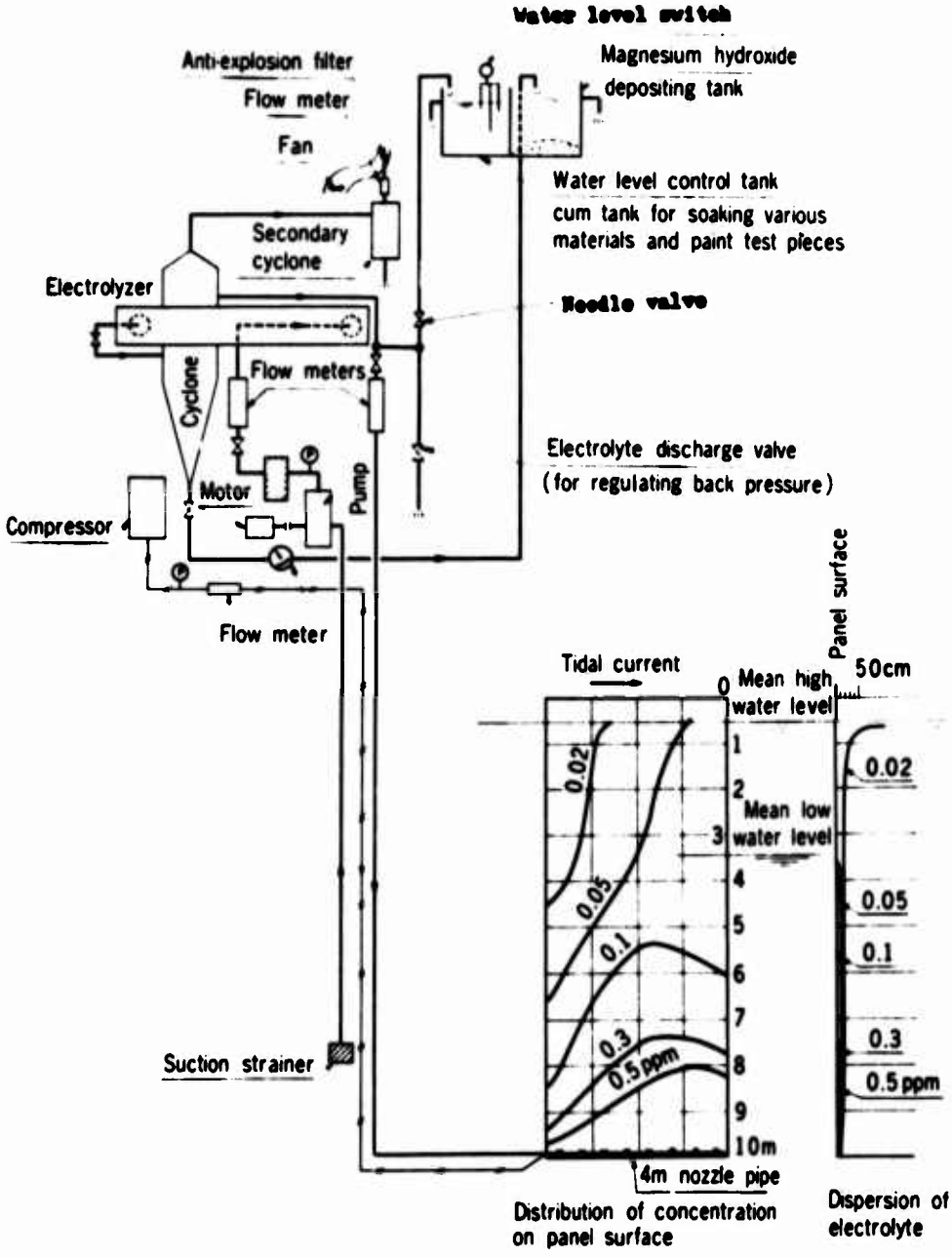
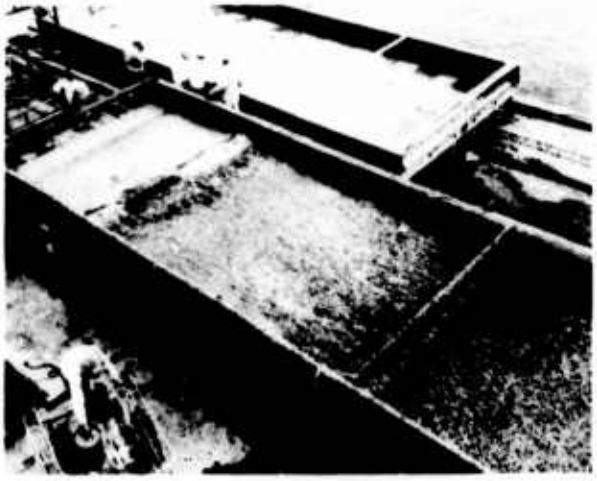


Fig. 3 Arrangement of test unit and steel panel (Figures on steel panel denote distribution of Cl_2)











Dimension of panel	4 m wide, 10 m high
Paint applied	Oily A/C in both cases
Period of immersion	From August 3, 1968 Until September 7, 1968 (for 35 days)

Fig. 4 Steel panel after 1st immersion test

Captions

Top left: The mixture of electrolyte and air released from the nozzle pipe installed about 9 m under water rises straight up and disperses at water level.

Top right: Apart from the area approximately 1 m below the water surface, no slime has accumulated on the electrolytically protected panel. Marine growths were conspicuous on angular reinforcements that had been fitted at a distance of 300 mm from the panel surface.

Center: Of the two panels, the upper one was equipped with an electrolytic anti-fouling nozzle pipe through which the electrolyte was discharged. A small quantity of slime has accumulated on the panel approximately 1 m below the water surface. (See the top left photo of Fig. 5.)

Bottom left and right: Contamination of the unprotected panel. Serpula, Barnacles, Ascidians and Bryozoa.











Paint applied: Only A/C in both cases
A 1.5 m high by 1 m wide portion of that part of the electrolytically anti-fouling was reimmersed without removing the slime which had accumulated during the first test

Period of immersion: From September 8, 1968
Until October 7, 1968
(for 30 days)

Weather condition when the photos were taken:
Drizzling

Fig. 5 Steel plate after 2nd immersion test

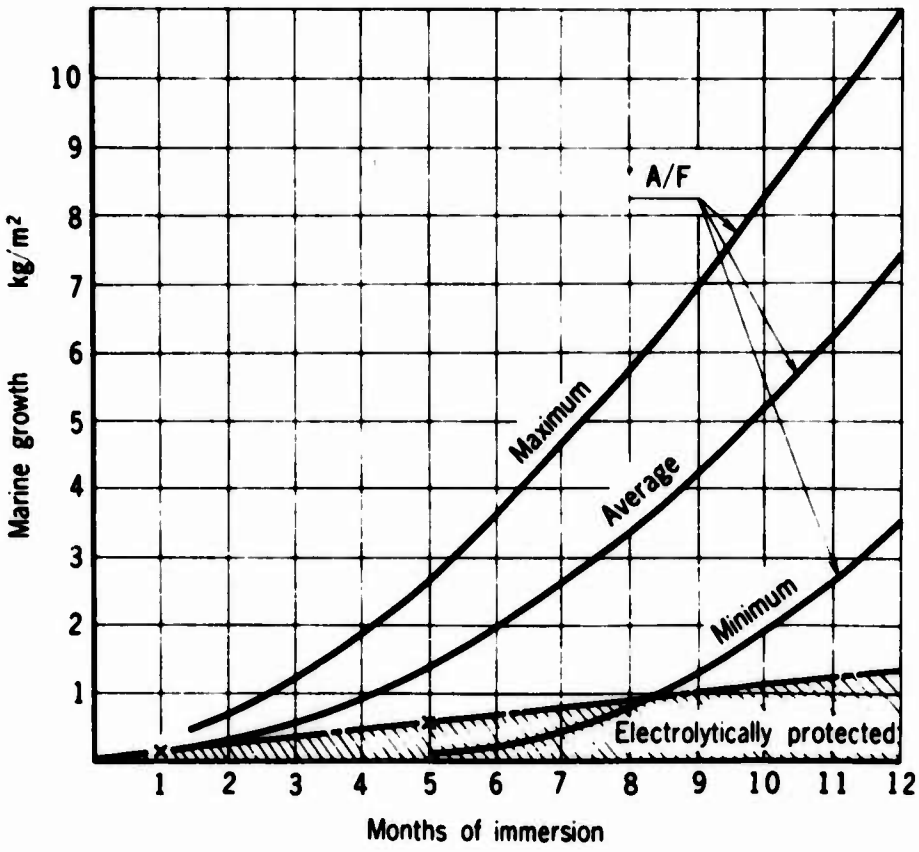
Captions

Center: Of the two panels shown, the one on the left was equipped with an electrolytic anti-fouling nozzle pipe through which the electrolyte was discharged. Chlorine content was 1½ times of that in the first test.

Top left: Contamination of the portion affected during the first test has increased slightly.

Top right: Although the A/C paint near the electrolyte nozzles turned brown, the change was only superficial and had not affected the coating any deeper.

Bottom left and right: The water temperature was lower than in the first test and this resulted in less marine life accumulating. Nevertheless it did foul the unprotected panel as can be seen on the photos. Note the central part in the bottom right photo which was brushed while the panel was still immersed



- The fouling curve representing the marine growth on the electrolytically protected panel indicates around the mean low tide level (see Table 1) where the electrolytic anti-fouling is least effective.
- Latest informations concerning A/F paints coated on actual ship's hull are desired.
  A/F paint data on small test pieces are usually better than on actual conditions.

Fig. 6 Immersion test period and quantity of marine growth

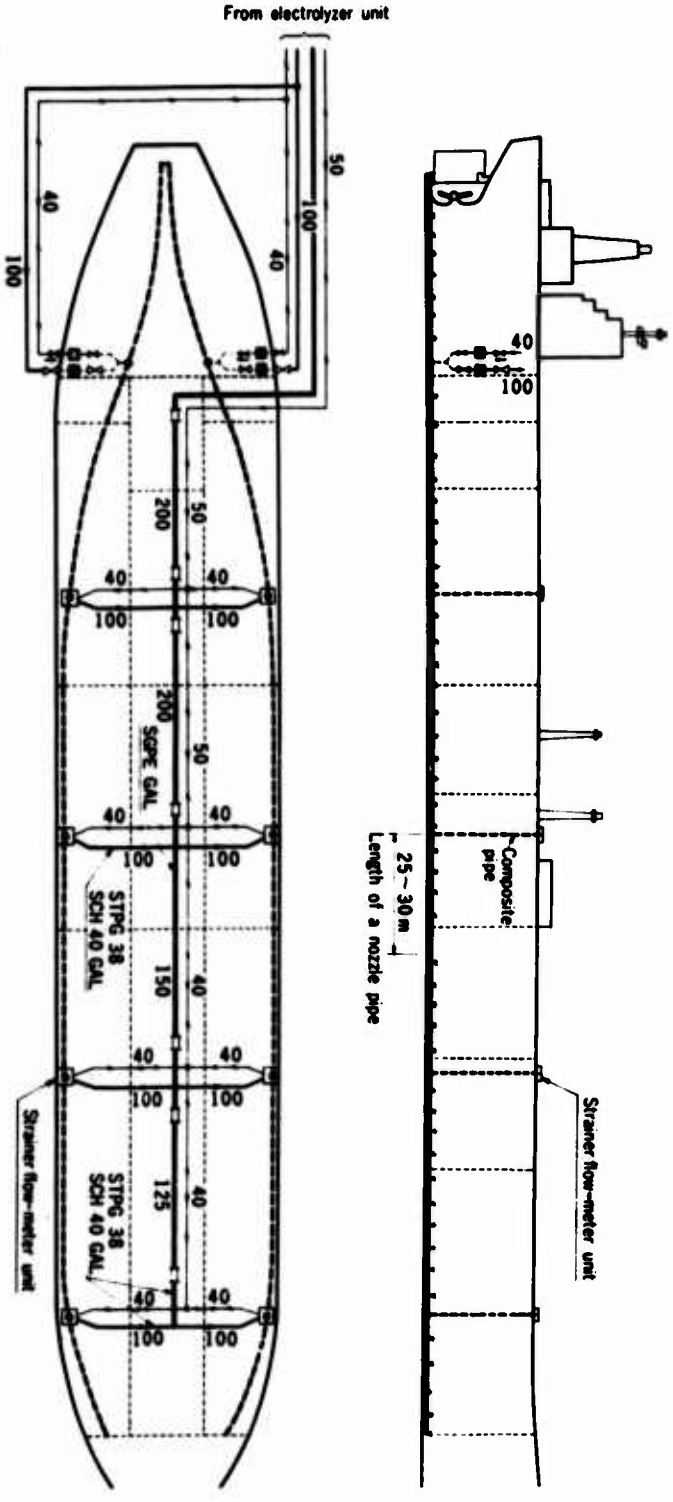


Fig. 7 Arrangement of anti-fouling system on board a 250,000 DWt tanker

Strainer Flow-Meter unit

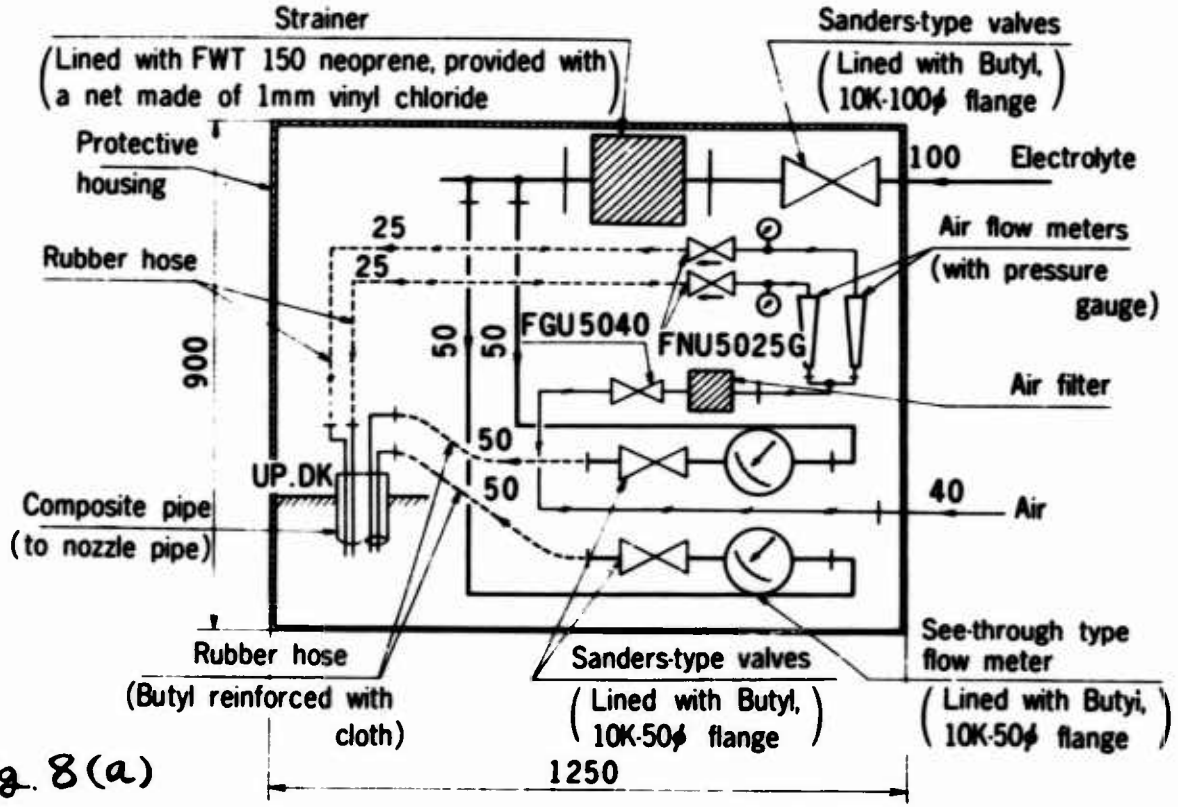


Fig. 8(a)

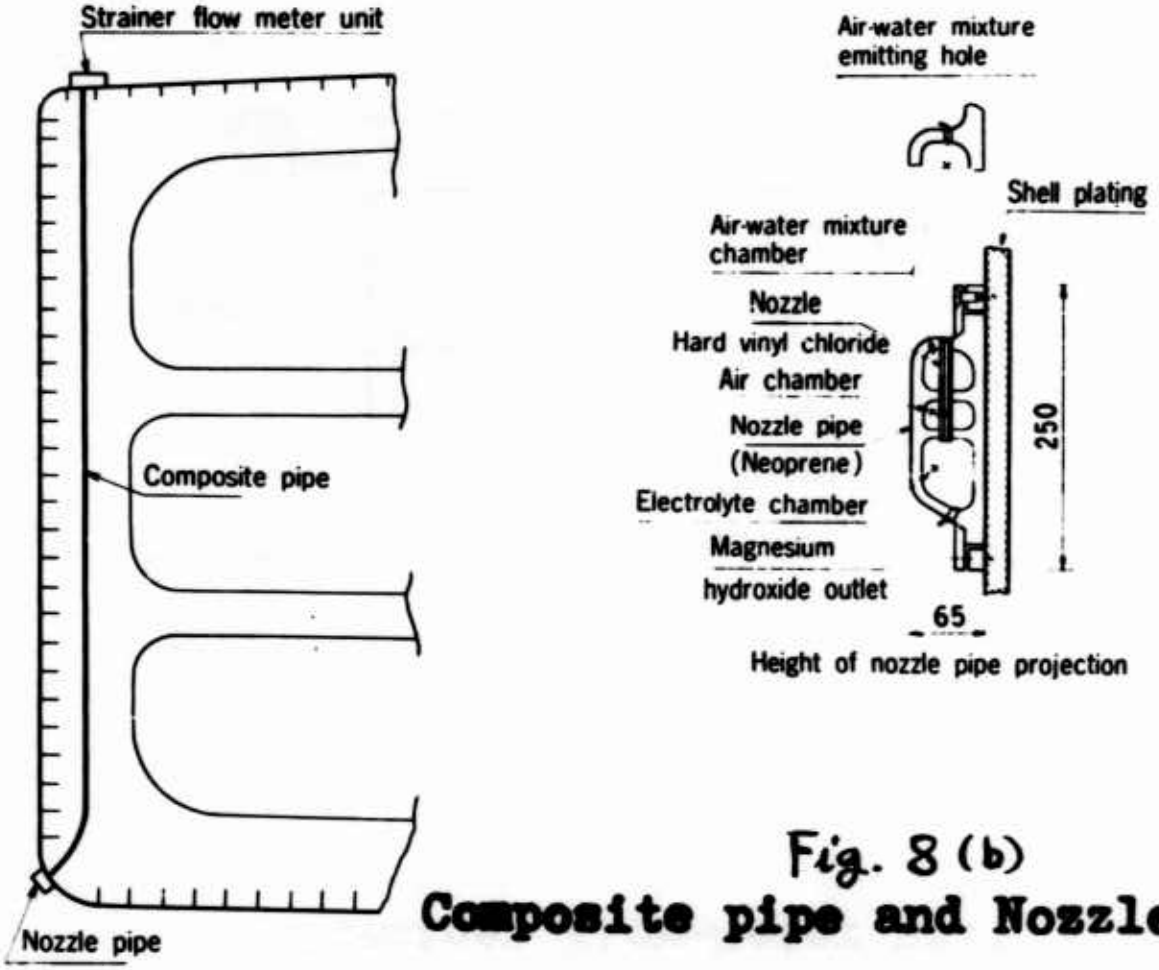


Fig. 8 (b)

Composite pipe and Nozzle pipe

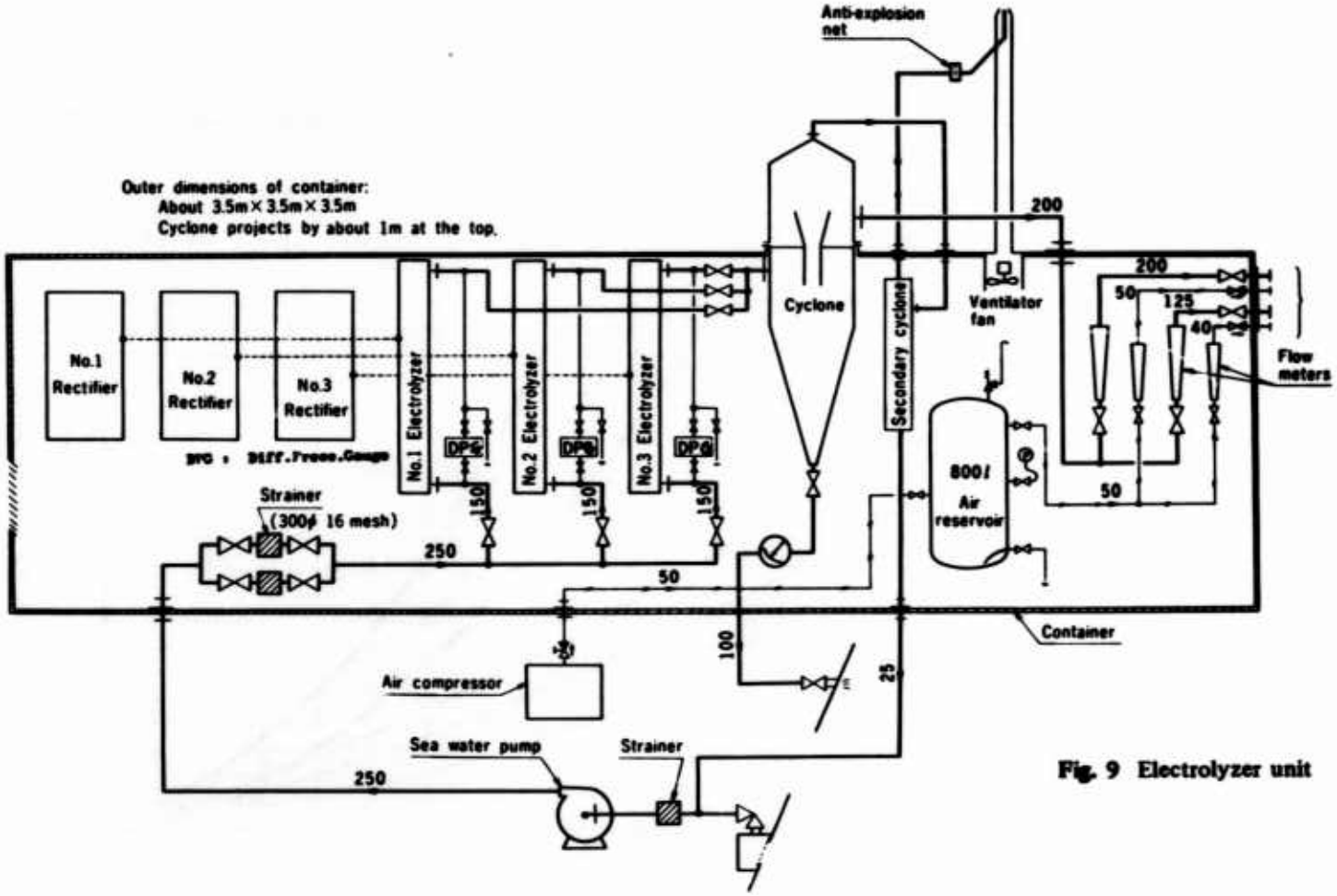
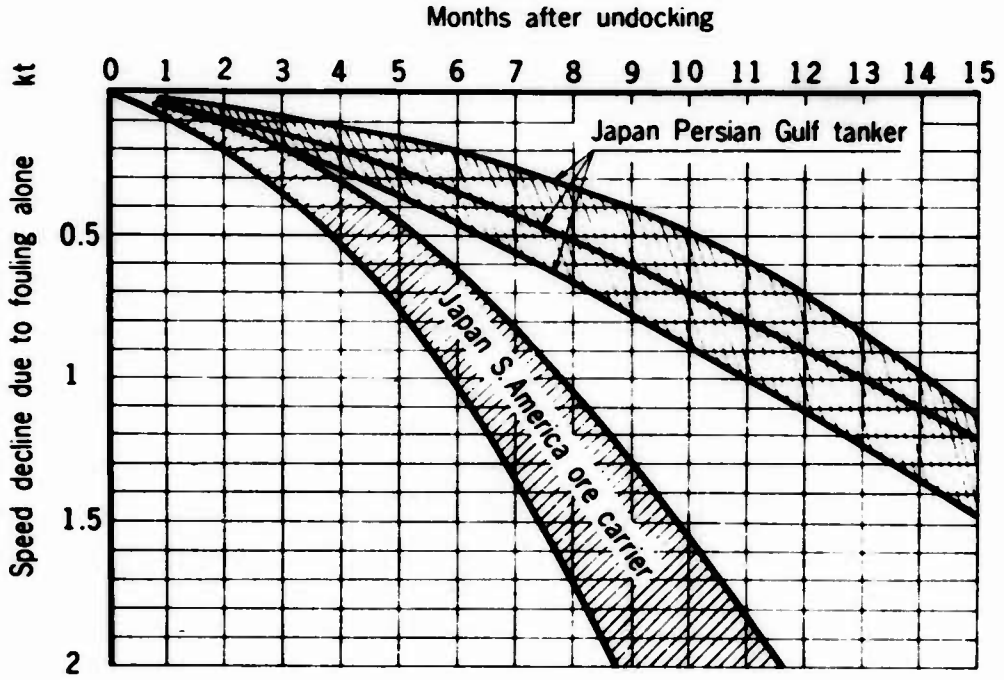


Fig. 9 Electrolyzer unit



Japan/Persian Gulf tanker: Beppu et al., Seibu Zosenkai Kaiho, 39[2] Yamasaki et al., Seibu Zosenkai Kaiho, 39[3]
Japan/South America ore carrier: Taizo Kitajima, Zosen Kenkyu, Feb. 1968[4]

Fig. 10 Decline in ship speed due to hull fouling alone

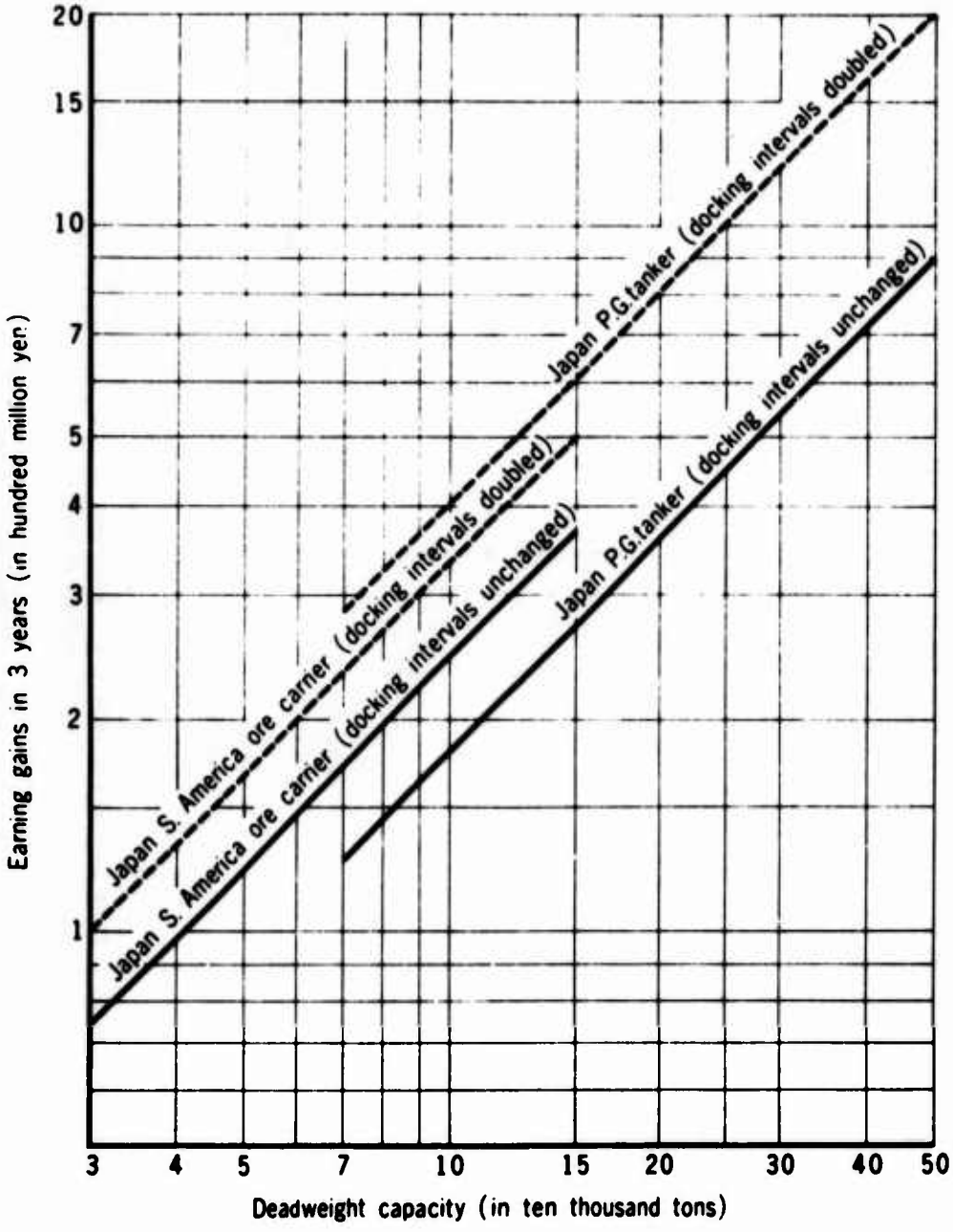


Fig. 11 Estimated increase in freight income over a 3-year period

Table 1 Quantity of marine growth after immersion test

Panel	Protected against fouling or not	Position of sample collection (depth from top)	Amount of marine growth (g/m²)				
			First test (for 35 days)		Second test (for 30 days)		Third test (for 5 months)
			Living	Dried	Living	Dried	Dried
Blank panel	Unprotected surface (A/C only)	2 m	–	–	–	–	–
		3	6 850	1 550	1 207	285	–
		4	900	250	–	–	–
		5	400	100	669	210	–
		6	420	170	–	–	–
		7	5 780	130	424	122	–
		8	2 500	550	–	–	–
		9	3 100	300	246	73	–
Electrolytically protected test panel	Side	2	–	–	–	–	–
		3	1 700	800	–	–	–
		5	1 700	800	–	–	–
		7	450	300	–	–	–
		9	90	80	–	–	–
	Electrolytically protected surface (A/C only)	2	–	–	–	–	80
		3	330	190	Minute serpulae, 1 000~2 000 bodies/m²		540
		4	70	60	Minute serpulae, 500~1 000 bodies/m²		380
		5	20	10	0	0	120
		6	3~5 mm serpulae about 4 500 bodies/m²		0	0	0
		7	0	0	0	0	0
		8	0	0	0	0	0
		9	0	0	0	0	0

Notes: (1) The mean low tide level was about 3m below the panel top.
(2) Organisms were collected from an area of the panel surface 100mm square, and weighed.

Table 2 Particulars of equipments and power consumption (250,000 DWt tanker)

Item	No. of units	Particulars	Power consumption
Rectifier	3	75~150V x 660A	126 kW
Electrolyzer	3	Platinum-coated titanium plate (Pt 1.5μ)	–
Sea water pump	1	280 m^3/h x 500 m TH.	54 kW
Air compressor	1	250 m^3/h (F.A) x 7 kg/cm^2	28 kW
Air tank reservoir	1	800 ℓ x 7 kg/cm^2	–
Ventilator fan	1	10 m^3/min x 60 mm H_2O	0.6 kW
		Total	209 kW

Table 3 Estimated increase in freight income resulting from use of anti-fouling system

Rout, type of ship			Japan/P.G. large tanker		Japan/S. America ore carrier	
Deadweight capacity			250 000	DWt	50 000	DWt
Round-trip distance			13 600	sea miles	20 000	sea miles
Average service speed	Clean		16.0	kt	16.0	kt
	As it is		15.5	kt	15.0	kt
	Electrolytically protected		15.8	kt	15.8	kt
No. of days at sea per voyage	As it is		36.5591	days/voyage	55.5556	days/voyage
	Electrolytically protected		35.8650	days/voyage	52.7426	days/voyage
No. of days at anchor per voyage			4	days/voyage	6	days/voyage
No. of days required per voyage	As it is		40.5591	days/voyage	61.5556	days/voyage
	Electrolytically protected		39.8650	days/voyage	58.7426	days/voyage
No. of idle days per year due to docking	Once a year		Including transfer time for gas freeing	15 days/year	Including transfer time	12 days/year
	Once every other year			7.5 days/year		6 days/year
No. of voyages per year	As it is	Once a year	8.6294	voyages/year	5.7347	voyages/year
		Once every other year	8.7796	voyages/year	6.0093	voyages/year
	Electrolytically protected		8.9678	voyages/year	6.1114	voyages/year
Increase in cargo volume carried by electrolytically protected ship per year		Once a year	37 550	tons/year	13 730	tons/year
		Once every other year	84 600	tons/year	18 835	tons/year
Freight rate per ton (according to Kaiun, Feb. 1971)			As of Dec. 1970 11.01 dollars/ton (Interscale + 63.64%)		As of Dec. 1970 8.12 dollars/ton	
Increase in freight income per year	Docked once a year		149 000	thousand yen/year	40 100	thousand yen/year
	Docked once every other year		335 000	thousand yen/year	55 100	thousand yen/year

Marine Fouling Control by Electrolytic Hypochlorite Generation

Thomas J. Lamb

Engelhard Minerals & Chemicals Corporation
205 Grant Avenue
East Newark, New Jersey 07029

A fouling problem existed on a long sea water line and various types of antifouling methods were investigated. These methods included liquid chlorine, sodium hypochlorite and calcium hypochlorite.

The method selected for this test was electrolytic sodium hypochlorite to study its effects on fouling and corrosion. In addition, the effects of constant chlorination versus intermittant treatment in heavier concentrations was investigated.

Tests were conducted over a two year period and fouling organisms were controlled by less than 1 PPM dosage of equivalent chlorine when the system was in constant operation. It was not found necessary to treat to the chlorine demand of the water, nor was it essential to show a residual in the effluent in order to control the fouling.

Potential problems of cell blockage due to calcareous deposits were also investigated. Cell design was shown to prevent deposits and constant operation could be obtained without having to shut down for cleaning.

Electrode life was also investigated. It was found that previous tests showing the consumption rate of platinum in sea water of 6 mg/amp years were valid.

Workable systems were shown for the safe and complete dessipation of hydrogen gas evolution.

Key words: chlorine; hypochlorite; residual; calcareous

Marine fouling is a problem which has been recorded in the earliest histories of the sea. Although written records of the treatment of ships bottoms as early as the 5th Century B.C. have been found,[1] the search for an antifouling surface undoubtedly began with even earlier ships about which little is written.

---

[1] Superscript figures indicate the literature references at the end of this paper.

Historically, the development of these antifoulants falls into four parts: (1) the repeated introduction and use of metallic sheathing, culminating in the discovery of copper sheathing as an effective antifoulant surface; (2) the invalidation of the use of copper on iron hulls because of galvanic effects; (3) the development of antifouling paints and (4) the use of toxicants in the form of liquid or gases. In general, the systems all operated with one thing in common - that it had the ability to emit some substance which was toxic or undesirable to the fouling organism.

The several factors which determine the tendency of a surface to foul when exposed in the sea may be divided into two main groups: (1) those which determine the numbers of larvae coming in contact with the exposed surface and (2) those which limit the ability of these larvae to attach to the surface and grow.

The factors which control the numbers of larvae are primarily (1) geographical (2) seasonal and (3) the level of pollutants. The factors which control the ability of the larvae to attach themselves are many, such as the texture of the surface, velocity of the water, level of illumination, toxicity, temperature and others. These latter factors are generally those that are controllable while the former are not. Of these latter factors, the one that is most easily controlled is toxicity because it is the only factor which will not require changes in the system design perameters and can be added from outside the system. Many toxics have been tested through the years. These include salts of many metals and many uncompounded metals as well as gases and organic compounds. One of the most convenient of these toxics from a cost and availability standpoint is chlorine. Its toxicity is well known and shown by the fact that the 1971 Occupational Safety and Health Act lists 1 PPM exposure for 8 hours as the current national standpoint for humans.[2] Concentrations in air above about 0.3 PPM can be detected by smell by most persons. Because of the toxicity, chlorine has become one of the most effective of fouling control chemicals. The vital organisms of most marine animals are more sensitive than humans and thus it would be expected they are quite vulnerable to very low concentrations of chlorine. It has been shown that some fishes are killed with doses as little as .05 PPM.[3]

With the knowledge that chlorine was an effective antifoulant, the purpose of this study was to first identify what form of chlorine was most effective and secondly, to design equipment which would produce the desired product and do so automatically and economically.

The methods of chlorine release that were considered were liquid chlorine, calcium hypochlorite and sodium hypochlorite. The chemistry of the reactions of each is as follows:

$$Cl_2 + H_2O \longrightarrow HOCl + HCl$$

$$Ca(OCl)_2 + H_2O \longrightarrow CaOH + HOCl$$

$$NaOCl + H_2O \longrightarrow NaOH + HOCl$$

Each of these forms releases chlorine as hypochlorous acid (HOCl) or ionized as the hypochlorite ion. It can be seen that all forms produce the same end product which is defined as free available chlorine or free residual chlorine. It is chlorine in this form that will be referred to throughout this paper.

Since sea water is the source of marine fouling organisms, it would follow that it also be the source of the salt for the formation of sodium hypochlorite which was decided to be used in these tests. Liquid chlorine was rejected because of the dangers in handling and difficulty in isolating in aqueous solution. Calcium hypochlorite was not considered because of the unavailability of economical calcium chloride and lack of same in sea water. The breakdown of

salt water by electrolysis is shown as follows:

$$NaCl + H_2O \longrightarrow NaOCl + H_2\uparrow$$

The tests were conducted at a sea water inlet which pumped water through an 18" line (45.6 cm) to its delivery point. The total pumping capacity of this line was 6.9 Mg/d (26,200 M^3/d); however, the average water pumped was about half that amount.

Prior to these tests, this line was treated with liquid chlorine with batch treating twice a day for a total of 25 pounds (55 Kg) per day. This treatment gave marginal results because large collections of shells were accumulated at strainers at the end of the line on a regular basis. Also fouling was noted in some distribution lines as shown in Figure 1.

The water was drawn from a lagoon off the Atlantic Ocean with a salinity of about 32 PPT, and a summer time chlorine demand of 2 - 3 PPM.

The design of the equipment for this test was completed in about three months and the two test units were installed in June 1970. Two one pound/hour chlorine units were installed; each of a different design with each capable of equaling the liquid chlorine output used previously.

The two designs employed were for analysis of the geometrical effects on collection of calcareous deposits. One design employed a tube within a tube with the water flowing between the annulus between the tubes. The alternate design employed two parallel plates with the water passing between the plates. These designs are shown in Figures 2 and 3. Previous designs that had a series of plates in parallel have been explained in the literature.[4] Earlier tests on this arrangement showed that the plates clogged with calcareous deposits due to the close spacing and alternate paths open to passage by the water. This previous design is shown in Figure 4. The major goals of this study were to (1) combat the previous deposit buildups and inevitable need for shuting down the equipment for cleaning; (2) design cells which could be used in series in order to generate higher capacities (3) determine the life of the anodes; (4) assess the consequences of the buildup of hydrogen gas within the system and (5) determine the amount of hypochlorite which would control antifouling.

The method chosen for elimination of deposits was velocity combined with a single flow channel for the water. This did not permit alternate paths for the water which when available will permit deposits to build up between some of the plates and eventually decrease the output and require cleaning. Velocity was maintained at 5 ft/second (153 cm/second) or greater. Both designs shown in Figure 2 are single pass configurations.

The cell length was 16 inches (40.5 cm) and with 50 amperes of current at 7 VDC was capable of generating 1/8 pound (.28 kg) of chlorine per hour. Eight of these cells were placed in series to obtain the desired 1 pound/hour (2.2 kg/hour). Total power consumption at the cells was 2.8 KW for 1 pound (2.2 kg) of chlorine capacity. This power consumption was obtained when the water resistivity was 30 ohm-cm in the warmer months. Power consumption was higher during the colder months. In order to maintain constant chlorine output for the changes in resistivity caused by seasonal changes, a power supply was used which employed a saturable reactor. This type supply would maintain a constant current output with changes in resistivity of the water due to seasonal changes.

For the total flow capacity of the system of 6.9 million gallons per day (26,200 M^3/d) of chlorine output would give a concentration of .83 PPM of chlorine to the entire flow. However, during most the test, only two of the three available pumps were used for a total 4.6 mg/d (17,400 M^3/d) and the 1 pound (2.2 kg) generator units were alternated giving a total of .63 PPM total. At the outset of the test, the fouling in the distribution line was

similar to that shown in Figure 1. The large 18" (46 cm) line was apparently lined with shell fish as witnessed by large collections of shells which were collected during the first few months of the test. These shells were collected in a strainer at the delivery point and the numbers decreased sharply after several months to the point that almost none were in evidence during the last year of the test. The generator was allowed to run unmanned for the duration of the test with checks made daily at first, then every other day and finally once per week. These checks were to measure power consumption, chlorine output and flow through the generator. Internal checks on the equipment were made at about 6 - 8 week intervals during required maintenance periods.

The results of the test can be categorized into two areas; (1) the operation of the equipment and (2) results of the hypochlorination on the fouling control program. The equipment performed satisfactorily, giving approximately 90% current efficiency based on Faraday's Law.The inefficiencies appear to be in the generation of small quantities of oxygen and chlorine as determined from laboratory generated samples.

During the duration of the tests, a residual at the outfall, which is .5 miles(.8 km) from the injection point, was never obtained. The chlorine demand of the water which was 2 - 3 PPM had never been attained; however, complete fouling control was obtained. This is significant for two reasons: (1) residual chlorine discharge into estuaries is not required, thus the deleterious effects of residual chlorine can be avoided; and (2) lower quantities of chlorine usage are possible in many cases than would be required if chlorinating to a residual at the outfall.

Prior to the tests, chlorination was done on a batch method twice a day using 10 - 12 pounds (22 - 26 Kg) of chlorine and showing a residual of 2 - 3 PPM. This method proved unsatisfactory because shell fish could survive this type of treatment due to the abilitiy of some of them to close their shells for several hours and not suffering any ill effects from the chlorine.[5] However, continuous chlorination will remedy this situation because the animal must open up to feed at some time, and the low level chlorination will still be sufficient to kill. Electrolytic generators are particularly adaptable to continuous operation and thus constant chlorination is easily attained. If batch treatment is desired, additional storage facilities are required and due to the low concentration (300 PPM) large storage facilities would be required plus additional personnel or timing equipment when pump out of the stored liquid was desired.

Anodes used in the tests were ASTM 338-65 Grade 2 titanium with 100 micoinches of platinum plate. The current density was 250 amperes/ft^2 and the voltage was maintained at 7 volts DC across a waterfilled gap of .185 inches. Platinum consumption was 6 - 7 mg/amp-yr which with a controlled platinum plate thickness can predetermine the anode life to a well defined time frame. The 100 micro in this case would give a life of 3.8 years.

During the tests, the feasibility of adding addition cells to the system was also investigated. This was feasible providing no interruption to the flow was introduced which provided stagnation points which allowed calcareous deposits to build up. It was shown that 10 pounds/hour (22 Kg) generating capacity was the most that could be generated in series before the buildup of hydrogen gas was sufficient to cause a decrease in efficiency.

Hydrogen gas buildup is at the rate of .16 $ft.^3$(4.5 l)/pound of chlorine generated. When this volume is diluted with the hypochlorite at a rate of 1 PPM, the hydorgen concentration is .028 PPM. If this amount of hydrogen is carried in the effluent, it is harmless unless allowed to collect. In case of this test, the hydrogen was vented in a deaerating unit prior to its use. This concentration could also be easily vented in a small holding tank or a colling canal or any other area which allowed a short residence time (3 minutes minimum) and has free access to the open atmosphere. It was shown from this test

that the hydrogen gas can be safely injected into the system without the employment of any specialized removal equipment. In the case of use indoors, however, the evolved gas must be vented to the atmosphere.

The conclusions of this test are:

(1) Sodium hypochlorite is as effective as liquid chlorine as an antifoulant.

(2) Sodium hypochlorite can be efficiently and economically generated from ocean water, brackish water or artificial brine.

(3) Calcareous deposits can be eliminated in generating cells to eliminate cleaning and down time.

(4) A residual is not required in an outfall to guarantee complete fouling control.

(5) 1 PPM at the source of the sea water system completely controls fouling in the system.

(6) The chlorine demand of the water is independent of concentration required for fouling control.

(7) The safety inherent in on-site hypochlorite generation warrants serious consideration as a replacement for liquid chlorine usea.

(8) Continuous chlorination is completely effective for fouling control while intermittant or shock treatment is not.

(9) Logistics problems are eliminated with an on-site sodium hypochlorite generation.

(10) Hydrogen gas evolution can be safely and completely controlled within the system.

REFERENCES

(1) "Marine Fouling and Its Prevention," 221, United States Naval Institute.

(2) R.J. Baker, L.J. Carroll, E.J. Laubusch:" Water Chlorination Handbook," 9, American Water Works Association.

(3) John A. Zillich, "Toxicity of Combined Chlorine Residuals to Fresh Water Fish," J. WPCF, 44, 213 (February 1972).

(4) A.F. Adamson, B.G. Lever and W.F. Stone, "The Production of Hypochlorite by Direct Electrolysis of Sea Water: Electrode Materials and Design of Cells for the Process," J. Applied Chem., 483, 13, November 1963.

(5) D.B. Anderson and B.R. Richards "Chlorination of Sea Water - Effects on Fouling and Corrosion," J of Engineering for Power, 204, July 1966.

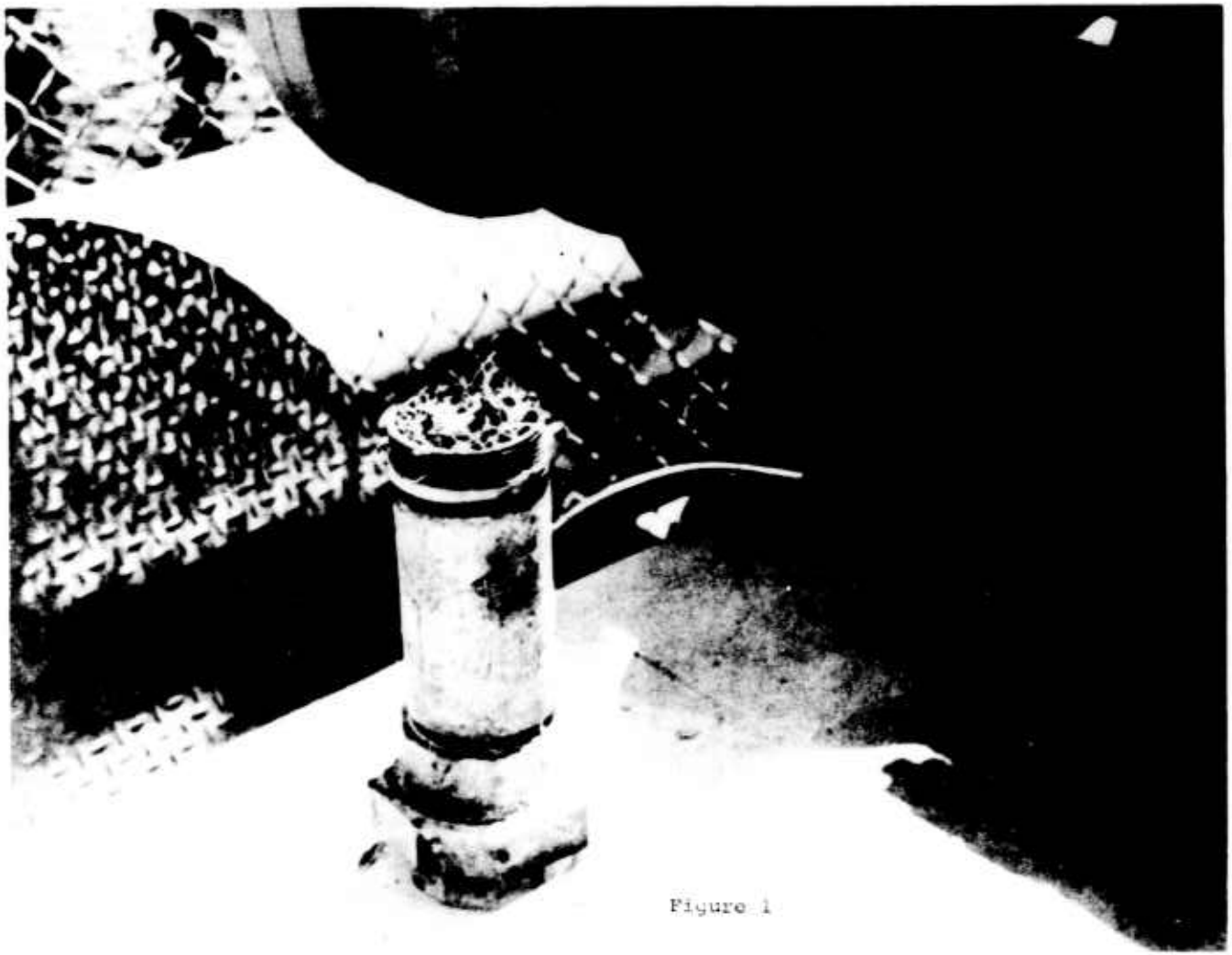


Figure 1

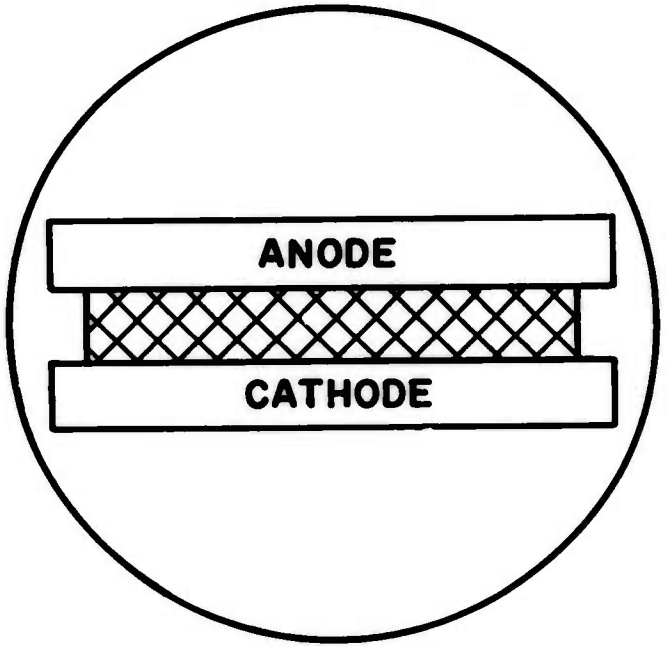
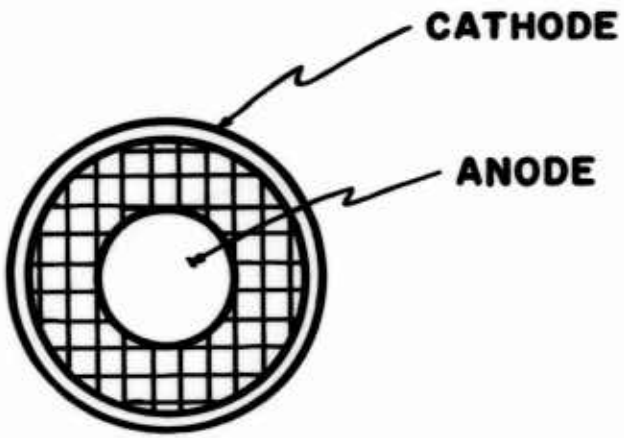


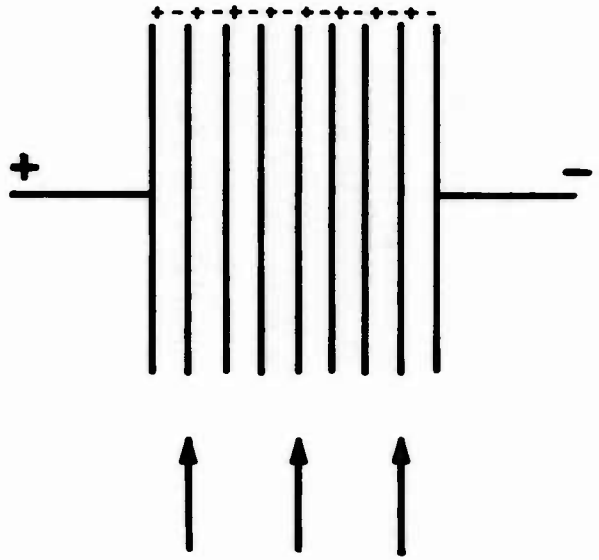
PLATE ASSEMBLY

FIG. 2



TUBE ASSEMBLY

FIG. 3



BIPOLAR ASSEMBLY

FIG. 4

Discussion

Bowen, Franklin Institute: A U. S. Patent was granted a few years ago to an individual named Green for the application of chlorine gas to ships' hulls electrolytically generated. If you are familiar with the claims and results, would you give them to us particularly with respect to resulting corrosion?

Lamb: I am not familiar with the specific patent; however, the shipboard tests that we have done are very limited. Some remarks made by our keynote speaker earlier in the week showed some corrosion results as a result of chlorine concentrations. I am not familiar specifically with this work. Our tests were strictly piping tests. The corrosion in our tests showed that there was no increased corrosion on the hypochlorite side than there was with normal sea water corrosion. The only materials difference we noticed was in the use of threaded PVC. The hypochlorite embrittled the PVC threads and we had failures with threaded PVC. The cemented stock of PVC worked all right.

Neihof, NRL: The biocidal effect of hypochlorite is very pH sensitive in the range from seven to nine. Was the effluent from your electrolytic generators more alkaline than normal sea water?

Lamb: Yes. The sea water we were testing was at a pH of 7.5 at the inlet and at 8.5 at the outlet. Chlorine produces hypochlorous acid and hydrochloric acid which tends to lower the pH. Our system tends to increase the pH because of the hydroxide generation.

Neihof: The effectiveness is probably somewhat less at pH 8.5 than it is at 8. If you could figure out some way of keeping it at around neutrality, you might be able to lower your concentrations still more.

Lamb: The pH I am referring to is at the outflow of the generator. You further dilute that 300-fold so the pH effect on the system is negligible.

Agawall, Dupont: The biocide when you put chlorine in sea water is not chlorine, but bromine because sea water has 60 parts per million bromide ions which is oxidized. When you say that with one part per million chlorine, you completely eliminate fouling, are you saying that you are eliminating only macrofouling, but not microfouling?

Lamb: When this test first started, this line was heavily fouled with shellfish. We collected thousands of oyster shells at the end of the line. It was surprising that they grew in the dark. This was a half-mile long line, but they did. They were much smaller than mature oysters. It took several months before these shells finally stopped coming. At the larvae level, we believe that they are killed on contact upon entrance. So, if you can start this system up then the first time you put water into a pipe you should not have any problems, but in this case it was retro-fitted into a line that was heavily fouled. After about three months the line was clean.

A Study Of The Performance Of Selected Premium Marine Coatings Systems

Richard J. Dick[1] and Willard M. Lawall[2]

(1) Battelle Columbus Laboratories, 505 King Avenue, Columbus, Ohio 43201
(2) United States Coast Guard, 400 Seventh Street, S.W., Washington, D. C. 20590

Eighteen premium antifouling marine coatings systems are being examined in a comprehensive study to determine extended service life potential. The average service life of today's premium shipbottom coatings system is about two years. The U. S. Coast Guard is concerned with extending this time to five years, not only for the protection of vessels but for navigational aids as well. The premium coatings systems in this study were selected to contain combinations of (1) substrate (steel plate, aluminum alloy 6061, fiberglass); (2) pretreatments (wash primers, flame-sprayed aluminum); (3) anticorrosive tiecoats (vinyl-red lead, polyester-flake glass, self-cure and postcure zinc silicates, epoxy, high-build vinyl, epoxy-coal tar, chlorinated rubber); (4) antifouling topcoats (rosin-vinyl, rosin-fish oil, epoxy-coal tar, chlorinated rubber); and (5) toxicants incorporated into antifouling topcoats (cuprous oxide, cupric hydroxide, organotin, organolead). The program for evaluating these systems is concerned mainly with seawater immersion studies, including both dynamic and static exposures. The dynamic exposure procedure presents an improved and acceptable method for evaluating coatings under actual exposure conditions for the simulation of ship activity periods (underway and at anchor). Static exposure conditions are represented by conventional raft-type immersion in subtropical ocean waters. To date, dynamic (simulated service) studies have been in progress for five cycles (one cycle equals two months, one month of activity at a speed of 22 knots and a second month of resting). Static immersion studies have been in progress for 22 months.

Data indicate that the performance of four of the 18 systems is outstanding. Best of this group is a system topcoated with a vinyl-rosin antifouling which contains organotin (TBTF) toxicant. The performance of another five coating systems appears excellent but is somewhat poorer than that of the above four. From rotor apparatus data it is possible to forecast an earlier failure date for this second group. Thus, several coatings systems appear to possess the potential for meeting the desired extended service life.

The performance of a third group of seven coatings systems is demonstrating definite failure trends. There appears to be a good correlation between data obtained from both dynamic and static exposures. Failure trends range from trace fouling to complete failure and the accelerated aspect of rotor apparatus data is constant throughout this performance range. Thus, the validity and usefulness of the rotor studies is confirmed.

An antifouling topcoat containing cupric hydroxide toxicant appears interesting because of its excellent performance. However, this shipbottom coating possesses a problem of fouling in the first few exposure months. Performance of the coating was excellent after this early fouling was sloughed.

Three anticorrosive midcoats appear to have improved the performance of the Type 121 Vinyl-Rosin topcoat. These three systems contain (1) epoxy-coal tar, (2) self-cured zinc silicate, and (3) postcured zinc silicate. All three systems are performing somewhat better than the control system which contains vinyl-red lead anticorrosive.

Key Words: Marine Coating Systems; Antifouling Coatings; Toxicants for Antifouling Coatings; Organometallic Toxicants; Marine Anticorrosive Coatings; Rotor Apparatus; Accelerated Evaluation of Marine Coating Systems.

---

1. INTRODUCTION

Recent improvements in aids to navigation have increased the demands for longer life antifouling and anticorrosive coatings. The paramount need is understood to be for longer-lived antifouling paints.

In 1963, Battelle conducted a survey of the U. S. Coast Guard's buoy-maintenance problem, giving major emphasis to protective coatings. This study culminated in a state-of-the-art report concerning the prevention of deterioration of navigational buoys.

As a logical extension of this early work, the present study was drafted for evaluating newer coating systems for ships and offshore structures as well as for buoys. It was decided that the studies should be limited initially to test panels, the objective being to recognize longer-lived paint systems among the new developments.

The Coast Guard desires to obtain coatings having a 5-year life so that the present 2 to 3-year maintenance cycle can be extended. This places a severe requirement on the antifouling part of the organic coating systems. Consequently, the research program was centered around antifouling coatings, although it also included new approaches to obtaining longer protection against corrosion.

The objective of this program has been the (1) evaluation of selected coating systems believed to have a high potential for long-term protection of ships, buoys, and offshore structures and (2) identification of those coatings that most nearly meet the Coast Guard's requirements for a 5-year protective system.

2. EXPERIMENTAL STUDIES

Eighteen complete marine coating systems of pretreatment, anticorrosive primer, and antifouling topcoat were selected as candidate materials. These systems were applied to either steel, aluminum, or fiberglass panels and then examined for long-term potential in providing protection to underwater areas of ships, buoys, and offshore steel structures. Sixteen systems were placed on static, raft-type immersion and two additional systems were added to the series for study on a specially-designed rotor apparatus. The rotor study offers an accelerated procedure for evaluating coating systems for buoys and also offers a simulated-service procedure for evaluating coatings for ships.

Panel Preparation

Steel panels used in the study were cut from 1/8-inch hot-rolled stock to a panel size of 6 x 12 inches. All edges were well-rounded to remove any roughness that might adversely affect the performance of the paint systems. The panels were sandblasted to white metal SSPC No. 6 and immediately spray-coated with pretreatment (e.g., 0.5 mil, dry, Formula 117 wash primer) or appropriate primer as noted below.

Aluminum panels were cut from marine grade Series 6061 to a size of 6 x 12 x 0.125 inches. The panels were edge-sanded similar to the steel panels above.

Fiberglass panels were cut from sheet stock of 0.635 cm thickness. The glossy surface was scuff-sanded before the application of coatings.

Painting Procedure

All paints were spray-applied to the panel face to conform to the desired dry-film thickness. In addition to coating the panel face, all panels were also backed and edged according to the above procedure.

All panels were marked for identification by stamping a 1/2-inch number into the upper right corner of the panel front. The finished panels were further identified on the back with 6-inch numbers, using Type 129/63 black antifouling paint.

Static Seawater Immersion Studies

The static raft-type exposures were conducted at the Florida Marine Research Facility of Battelle's Columbus Laboratories near Daytona Beach. Duplicate panels of each coating system were secured in standard exposure racks by narrow strips across the 6-inch ends of each panel. The panels were placed in the ocean with the panel surface parallel to the direction of tidal currents. The duplicate panels were mounted on different exposure racks to obtain a truer picture of each coating system's potential. Blank control panels were used throughout the program. These were uncoated 6 x 12-inch Masonite panels which were either (1) exposed during entire period (i.e., placed on exposure at the same time as the painted panels) or (2) periodic controls (new panels each season to observe the presence and character of the fouling community).

To date, the panels have been inspected after 3, 6, 9, 12, and 22 months, and have been examined for blistering, checking, cracking, or peeling of the coatings and for corrosion. Antifouling performance was rated with respect to total fouling and in terms of specific types of fouling (barnacles, mollusks, annelids, filamentous and encrusting bryozoa, hydroids, and algae). Color photographs were taken for recording coating performance.

Accelerated, Simulated-Service Exposure Studies

A test procedure for evaluating antifouling properties was desired which would (1) be conducted in a natural seawater environment; (2) simulate actual ship service conditions; and (3) accelerate the breakdown of coatings for buoys and navigational aids. To avoid an artificial laboratory environment, a rotor apparatus was constructed which allowed the coated panels to be immersed in seawater and be quickly depleted of toxicant by rotating them at speeds comparable to those of ships. This was accomplished by mounting 6 x 6-inch curved panels on a plastic drum which was 3 feet in diameter. After placement in the ocean, the drum was spun at speeds up to 22 knots for a period of four weeks. After this time, the rotor apparatus was shut down and was left on static-immersion for another four weeks to permit the establishment of a fouling community on panels deficient in toxicant. This procedure of one month spinning and one month resting was considered one cycle. Complete inspections were made after 1, 3, and 5 cycles.

Coating Systems

Complete descriptions of the eighteen marine coating systems comprising this study are listed in Table 1, appended. A brief notation of the important features of each system follows.

System No.	Descriptive Feature
1.	Type 121 Standard Vinyl-Rosin control
2.	Type 121/63 Vinyl-High Rosin control
3.	Polyester-flake glass anticorrosive, Type 121 antifoul
4.	Self cure zinc silicate, high-build vinyl, Type 121 antifoul
5.	Postcure zinc silicate, high-build vinyl, Type 121 antifoul
6.	Organolead-modified Type 121 antifoul
7.	Cupric hydroxide antifoul

System No.	Descriptive Feature
8.	Epoxy anticorrosive, rosin-fish oil antifoul
9.	Epoxy anticorrosive, Type 121 antifoul
10.	Chlorinated rubber primer, midcoat, and antifoul
11.	Epoxy primer, epoxy-coal tar anticorrosive, Type 121 antifoul
12.	Epoxy primer, epoxy-coal tar anticorrosive, epoxy-coal tar antifoul
13.	Epoxy primer, epoxy-coal tar anticorrosive, rosin-fish oil antifoul
14.	Vinyl-rosin with organotin (TBTF) antifoul on aluminum substrate
15.	Vinyl-rosin with organotin (TBTF) antifoul on fiberglass substrate
16.	Flame-sprayed aluminum pretreatment, vinyl primer, vinyl-rosin with organotin (TBTF) antifoul
17.	Elastomeric sheet with organotin antifoul
18.	Vinyl with high loading of lead pigment, Type 121 antifoul

Performance of Coating Systems

The two control coating systems (Nos. 1 and 2) were selected because of their known performance records and because of their current wide usage. After five cycles on the rotor apparatus and 22 months of static immersion, the performance of these two controls and that of the other 16 coating systems can be divided into four groups.

Group 1 contains four coating systems which contain essentially no corrosion or fouling after 5 rotor cycles and 22 months of static immersion. That is, on an overall rating scale of 0 - 10 where 10 = perfect, all ratings have been at least 10-. These systems were rated as follows.

Systems Rated as Outstanding

Coating System No.	Overall Performance Ratings After Rotor Cycles 1	3	5	Months Static Immersion 3	6	9	22
14	10	10	10	10	10	10	10
15	10	10	10-	10	10	10	10
17	10-	10-	10		(not evaluated)		
2	10	10-	10-	10	10-	10-	10-

The performance of system No. 14 (vinyl-rosin with TBTF organotin antifoul on aluminum substrate) is outstanding. This is especially significant when considering its performance after 5 rotor cycles. It will be seen below that the rotor ratings consistently project reliable performance patterns on an accelerated basis compared to the static tests.

The other three systems in this group are No. 15 (vinyl-rosin with TBTF organotin antifoul on fiberglass substrate), No. 17 (elastomeric sheet with organotin), and No. 2 (Type 121/63 control). The performance of these three systems can also be considered outstanding, but with the reservation that trace fouling has been observed in the rotor study. Two observations relative to the performance of this premium group are noteworthy. First, the outstanding performance of No. 14 is validated by that of No. 15 which contains the same antifouling topcoat. Second, it is encouraging to find the performance of the Type 121/63 control meeting its expected potential. This performance and that of the Type 121 control, below, tend to validate the results of the entire study.

Group 2 contains five coating systems which have demonstrated only slight amounts of fouling. Their collective performance, as shown below, must be considered excellent.

Systems Rated as Excellent

Coating System No.	Description	Overall Performance Ratings After Rotor Cycles 1	3	5	Months Static Immersion 3	6	9	22
11	epoxy-coal tar/ Type 121	10	10	10-	10-	9	10-	10
4	self cure zinc silicate/Type 121	10	8	10-	10-	9	10-	10-
5	postcure zinc silicate/Type 121	10	8	10-	10-	9	10-	10-
7	cupric hydroxide antifoul	10	8	10-	4	9	10-	10-
16	flame sprayed aluminum/vinyl-rosin with organotin	10	10	10	9+	9+	8	3

The anticorrosive components in system Nos. 11, 4, and 5 appear to be improving the performance of the Type 121 topcoat over that of the control which contains the specification vinyl-red lead barrier coat. It will be of interest to compare the performance of the systems containing self cure and postcure inorganic zinc anticorrosives as they fall into their respective fouling patterns during the coming months.

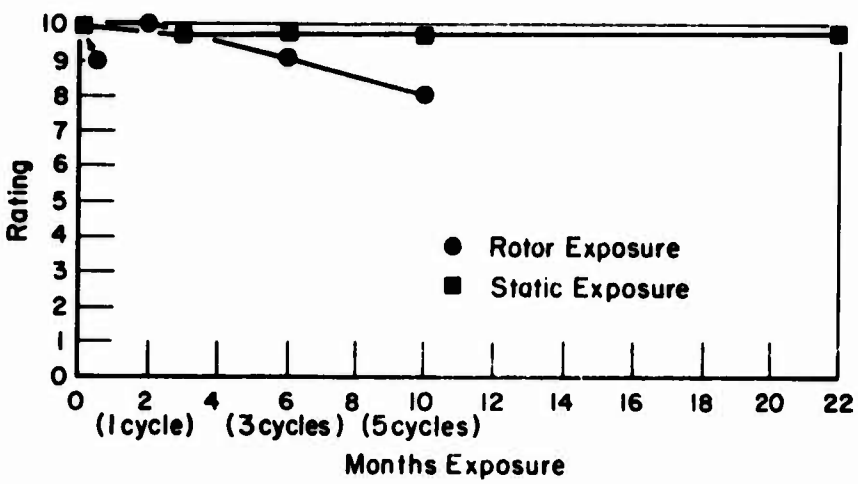
System No. 16 contains the same antifouling topcoat as Nos. 14 and 15 which were rated outstanding above. The static immersion panels for system No. 16 were observed to contain increasing amounts of peeling and edge corrosion at the 3, 6, and 9 month inspections and severe fouling was present after 22 months. Since the rotor panel was consistently rated perfect (10), it is logical to assume that (1) some problem or error in application occurred with the static panels, and (2) the outstanding performance of the vinyl-rosin topcoat with organotin is further substantiated.

The performance of the coating containing the cupric hydroxide toxicant (No. 7) is extremely interesting. $Cu(OH)_2$ is less soluble in seawater than Cu_2O and it could be assumed that it would provide little initial fouling protection during the first months of immersion. This is verified by the 3 month static rating of "4". After an effective leaching rate or concentration of toxicant was present, the paint sloughed the initial fouling and quickly improved to an impressive performance level. Contrary to this pattern, the rotor panel of the $Cu(OH)_2$ paint had undoubtedly leached sufficient toxicant after one month of spinning to maintain a perfect performance rating throughout the study. At this point in time, antifouling topcoat with $Cu(OH)_2$ toxicant appears interesting. If its excellent performance continues, it will be worthwhile to refine the formulation by formulating for an added measure of initial protection from a second toxicant.

Group 3 contains seven coating systems which are demonstrating definite fouling patterns and which have been rated "very good" to "poor". Of interest in this group is the comparison of the accelerated (rotor) and normal (static) performance ratings. In each of these seven systems there is a good correlation between data from the two immersion studies. This correlation confirms the usefulness of the rotor study.

Four of these seven systems must still be considered as "very good" in overall performance. However, data from the accelerated exposure (rotor) study indicate that all of these four systems will be accumulating fouling sooner than will the systems discussed above in Groups 1 and 2.

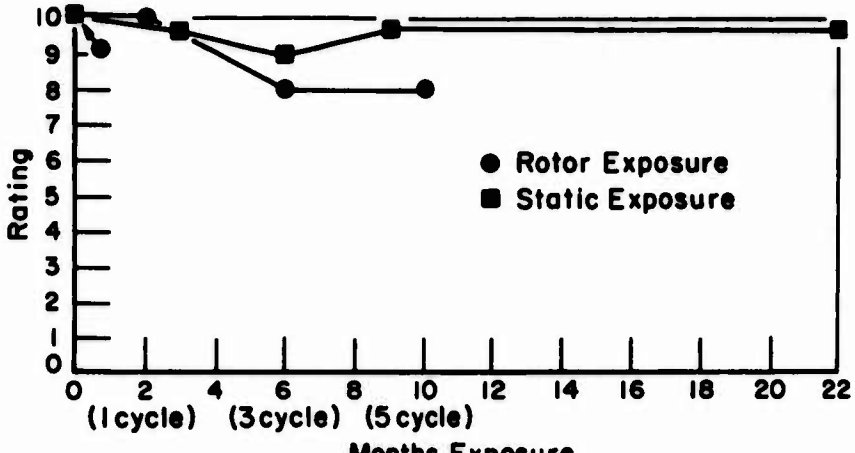
These four systems are as follows:



COATING SYSTEM NO. 9

(Epoxy Barrier Coat under Type 121)

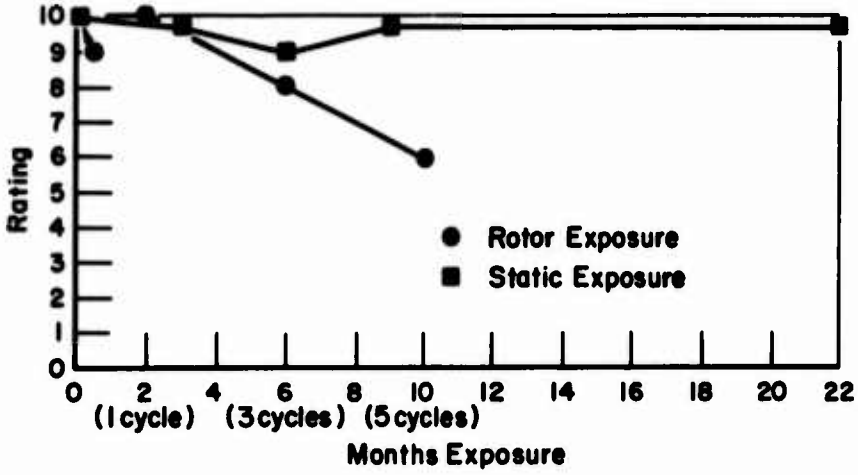
Although the Type 121 antifouling topcoat is performing as well as should be expected, the combination of it with the epoxy barrier coat is apparently not equal to the performance of system Nos. 11, 4, and 5, above.



COATING SYSTEM NO. 1

(Type 121, Vinyl-Rosin Control)

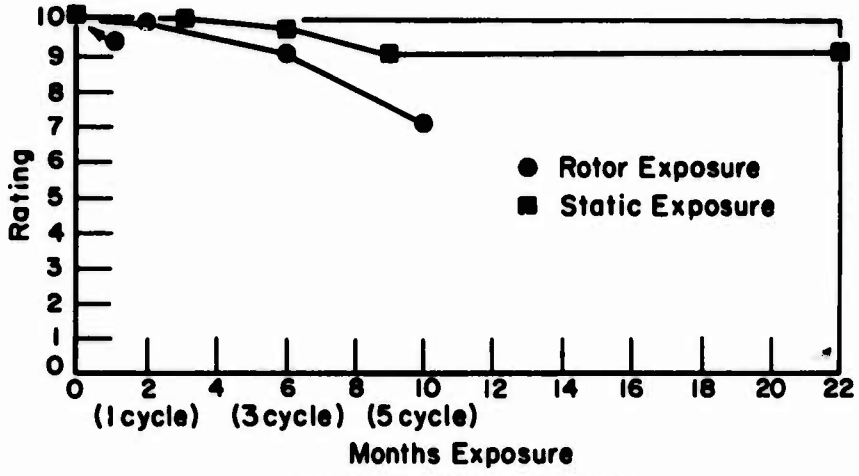
This control specification system is also performing according to expectations. The fact that this Type 121 control is performing slightly poorer than the Type 121/63 control (No. 2), above, is another reliable index to the validity of the overall study.



COATING SYSTEM NO. 3

(Polyester-Flake Glass/Type 121)

It should be emphasized that the above accelerated rating of "6" only expresses topcoat fouling and does not indicate the potential of the underlying anticorrosive barrier coat.

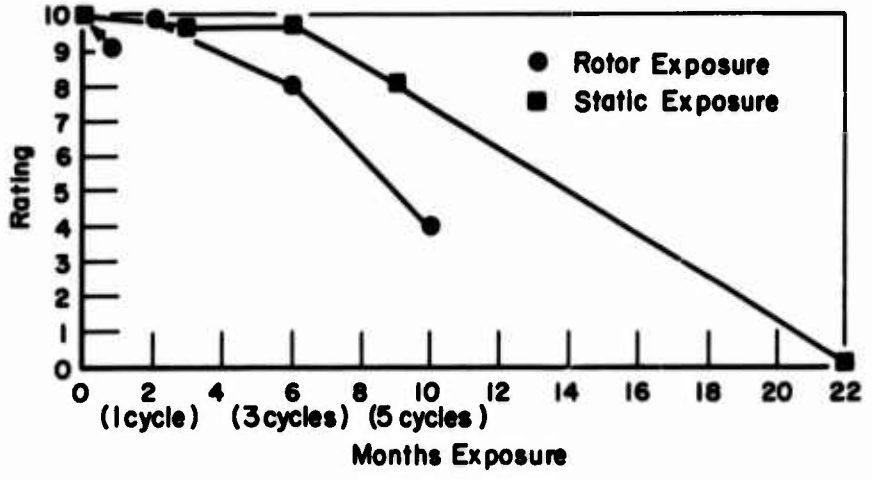


COATING SYSTEM NO. 6

(Organolead-Modified Type 121)

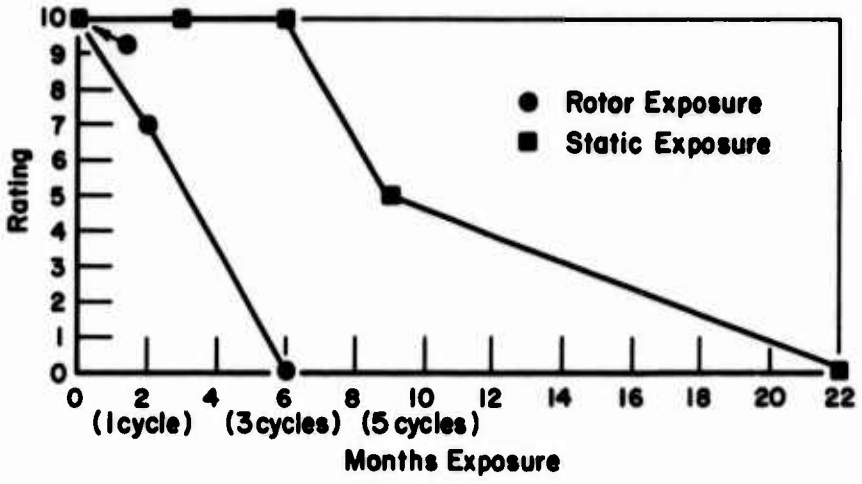
The performance of this system is slightly poorer than was expected. It will be interesting to observe whether the coating will improve and ultimately out-perform the control paints or, as these rotor data now indicate, will fall short of the performance of the controls.

The remaining three systems in this group of seven have all failed in the static immersion study. Each of these failures was correctly forecasted by rotor data obtained early in the program.



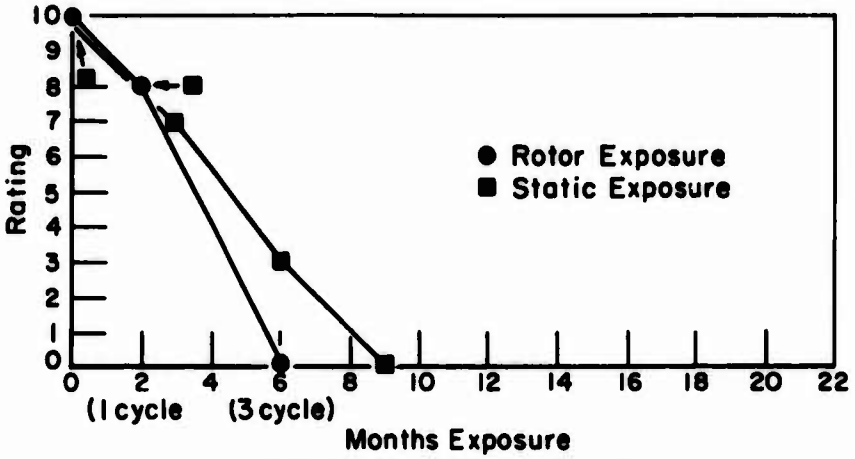
COATING SYSTEM NO. 12

(Epoxy-Coal Tar Barrier and Antifoul)



COATING SYSTEM NO. 8

(Epoxy/Rosin-Fish Oil Antifoul)



COATING SYSTEM NO. 10

(Complete Chlorinated Rubber System)

The final two coating systems (Group 4) failed soon after being placed on immersion. These two are as follows.

Coating Systems Rated as Early Failures

Coating System No.	Description	Overall Performance Ratings After Rotor Cycles 1	3	5	Months Static Immersion 3	6	9	22
13	epoxy-coal tar/ rosin-fish oil	10	0	0	0	0	0	0
18	lead-pigmented vinyl/Type 121	10	0	0	(not evaluated)			

No reasons are apparent for the poor performance of these two coating systems in this program.

3. SUMMARY AND CONCLUSIONS

After 5 rotor cycles of dynamic exposure and 22 months of static exposure in natural seawater, the performance of four of eighteen coating systems has been rated outstanding. The performance of another five coating systems has been rated excellent. Many of these nine systems show promise of meeting the goal of a service life of 3-5 years.

During the exposure period of this study, the performance of a proprietary vinyl-rosin type antifouling coating with TBTF organotin toxicant was rated as best within this premium group, regardless of substrate, primer, or anticorrosive. Longer exposure times are necessary to verify these results. When applied over a wash primer on 6061 aluminum (system No. 14), performance was rated as the best of the 18 systems. When applied over a special primer on scuff-sanded fiberglass (system No. 15), performance was rated as the second best of the 18 systems. When applied over a system of flame-sprayed aluminum/ vinyl primer/clear sealer (system No. 16), performance was perfect on the rotor apparatus. The static panels failed by edge peeling and corrosion indicating faulty preparation or mechanical damage. Other materials whose performance has indicated outstanding antifouling properties are (1) a proprietary elastomeric sheet containing an organotin toxicant and (2) the Type 121/63 Vinyl-High Rosin control containing 14.4 pounds per gallon of cuprous oxide toxicant.

The Type 121 standard Vinyl-Rosin topcoat with 8 pounds per gallon of cuprous oxide toxicant was applied over five anticorrosive barrier coatings. None of these systems have performed as well as the nine premium systems above. The performance of the Type 121 antifouling over an epoxy anticorrosive (system No. 9) was similar to that of the control which contains vinyl-red lead anticorrosive (system No. 1). Superior to both of these has been the performance of the Type 121 topcoat over (a) epoxy-coal tar, (b) self-cure zinc silicate, and (c) postcure zinc silicate anticorrosive coatings (system Nos. 11, 4, and 5, respectively). From this, it can be concluded that the performance of the vinyl-rosin antifouling topcoat can be upgraded by the proper selection of anticorrosive barrier coating.

The antifouling topcoat containing cupric hydroxide toxicant appears to have potential in long-lived marine protective coating systems. However, a problem of poor initial fouling resistance is associated with this material. Both the good performance and the problem of early fouling appear to be related to the limited solubility of $Cu(OH)_2$ in seawater.

Another group of seven coating systems is now showing definite fouling patterns and their performances have been rated from "very good" to "poor". The performance ratings of all of these systems show a definite correlation between static and accelerated

(rotor apparatus) immersion data. The validity and the usefulness of the rotor studies in predicting the expected service life of marine coatings is confirmed by these data. It is felt that the biggest advantage for this research tool is the simulation of actual service conditions since the test procedure is conducted in natural seawater.

ACKNOWLEDGMENT

The authors appreciate the sponsorship of this research by the Department of Transportation, United States Coast Guard. The opinions or assertions contained herein are the private ones of the writer and are not to be construed as official or reflecting the views of the Commandant or the Coast Guard at large.

TABLE 1. EXPERIMENTAL AND CONTROL MARINE COATING SYSTEMS

Coating System Number[a]	Pretreatment	Primer or Anticorrosive	Antifouling Topcoat
1	MIL-P-15328B (Formula 117 Wash Primer)[b] 0.5 mil--1 coat	MIL-P-15929B Formula 119, Vinyl Red Lead, 7 mils in 4 coats	Type 121 Vinyl-Rosin, MIL-P-15931A (3 mils, 2 coats of 1.5 mils each)
2	MIL-P-15328B (Formula 117 Wash Primer)[b] 0.5 mil--1 coat	MIL-P-15929B Formula 119, Vinyl Red Lead, 7 mils in 4 coats	Type 121/63 Vinyl-High Rosin, MIL-P-15931B (3 mils, 2 coats of 1.5 mils each)
3	None	Polyester Glass Flake 30-32 mils--1 coat	Type 121 (4.5 mils, 3 coats of 1.5 mils each)
4	None	(1) Self-cure Zinc Silicate 3 mils--1 coat (2) Primer-Tie Coat 1.5 mils--1 coat (3) Vinyl High Build 4 mils--1 coat	Type 121 (3 mils, 2 coats of 1.5 mils each)
5	None	(1) Postcure Zinc Silicate 2.5 mils--1 coat (2) Tie Coat (3) Vinyl High Build 4 mils--1 coat	Type 121 (3 mils, 2 coats of 1.5 mils each)
6	MIL-P-15328B (Formula 117 Wash Primer)[b] 0.5 mil--1 coat	Formula 119, Vinyl Red Lead, 7 mils in 4 coats	Similar to Type 121 (Cu_2O/Organolead[c]-2/1) (3 mils, 2 coats of 1.5 mils each)
7	Proprietary Wash Primer[b] 0.5 mil--1 coat	Anticorrosive Barrier Coat, 8-9 mils, 3 coats of 3 mils each	Proprietary Cupric Hydroxide Antifouling Paint (3 mils, 2 coats of 1.5 mils each)

TABLE 1. (Continued)

Coating System Number[a]	Pretreatment	Primer or Anticorrosive	Antifouling Topcoat
8	None	(1) Epoxy Anticorrosive (2 mils--1 coat) (2) Epoxy Anticorrosive Intermediate (4 mils, 2 coats of 2 mils each)	Type 105 Cold Plastic (3 mils, 2 coats of 1.5 mils each)
9	None	(1) Epoxy Anticorrosive (2 mils--1 coat) (2) Epoxy Anticorrosive Intermediate (4 mils, 2 coats of 2 mils each)	Type 121 (3 mils, 2 coats of 1.5 mils each)
10	None	(1) Chlorinated Rubber Primer (3-4 mils--1 coat) (2) Midcoat (5-6 mils--1 coat)	Proprietary Chlorinated Rubber (2-3 mils--1 coat)
11	None	(1) Epoxy Primer (0.5 mil--1 coat) (2) Coal Tar-Epoxy Intermediate (6 mils--1 coat)	Type 121 (3 mils, 2 coats of 1.5 mils each)
12	None	(1) Epoxy Primer (0.5 mil--1 coat) (2) Coal Tar-Epoxy Intermediate (6 mils--1 coat)	Proprietary Epoxy-Coal Tar Antifoul (12 mils--1 coat)
13	None	(1) Epoxy Primer (0.5 mil--1 coat) (2) Coal Tar-Epoxy Intermediate (6 mils--1 coat)	Type 105 Cold Plastic (3 mils, 2 coats of 1.5 mils each)
14 (Aluminum 6061 Panel)	MIL-P-15328B (Formula 117 Wash Primer[b]) 0.5 mil--1 coat	None	Proprietary Organotin Antifoul (3 mils, 2 coats of 1.5 mils each)

TABLE 1. (Continued)

Coating System Number[a]	Pretreatment	Primer or Anticorrosive	Antifouling Topcoat
15 (Polyester-fiberglass Panel)	Scuff Sanding	Proprietary Primer for Fiberglass	Proprietary Organotin Antifoul (3 mils, 2 coats of 1.5 mils each)
16	Flame-Sprayed Aluminum--3 mils	(1) Vinyl Primer (1 mil--1 coat) (2) Clear Sealer (2 mils--2 coats)	Proprietary Organotin Antifoul (3 mils, 2 coats of 1.5 mils each)
17[d]	None	Proprietary Adhesive System (1) Adhesive (2) Tiecoat (3) Adhesive	Elastomeric Sheet (1 layer--80 mils)
18[d]	MIL-P-15328B (Formula 117 Wash Primer[b]) 0.5 mil--1 coat	(1) Formula 119 Vinyl, Red Lead (2) High Build Vinyl with High Loading of Lead Pigment (6 mils, 2 coats of 3 mils each)	Type 121 (3 mils, 2 coats of 1.5 mils each)

(a) Panels for static immersion studies are 6 x 12 x 0.125 inches; panels for rotor apparatus immersion studies are 6 x 6 x 0.062 inches. All metal panels are sandblasted to white metal.

(b) Film thickness measured on smooth surface sprayed alongside the blasted panels.

(c) Triphenyllead acetate. Toxicant loading is Cu_2O and TPLA, 4 and 2 pounds per gallon, respectively.

(d) Coating Systems evaluated on rotor apparatus only.

Discussion

Question: On these test panels, you get a coating of fine sediment after you expose it for a long time. Does this fine sediment over these panels have anything to do with antifouling?

Dick: The sediment that you are seeing is basically mud. We took a bucket of sea water and washed it off. Sometimes we'll take a swipe right through the middle of the panel with a very light brush and most of it comes off. I am not discounting the fouling succession establishment of the community through slime and bacteria and soft-fouling, etc. I think it is probably a combination of both.

De La Coure: You indicated you could improve the anti-fouling paint by changing the anti-corrosive primer. From a fouling point of view, this is not understandable, except for loss of adhesion and other similar phenomena. Can you amplify this? For a cuprous oxide paint, the chlorine content of the sea water is very important. Did you make chlorine measurements?

Dick: No. I do not have chlorine data. However, I can get it for you. I cannot explain why anti-corrosive primers affect performance. We know that if we put some top coats over old established films versus freshly applied films, there is a difference in leaching rates of the top coats. So it is possible that a superior anti-corrosive coating might upgrade performance or affect the leaching rate of the antifouling paint. I wish I could tell you why, but I really don't know. I am just reporting the information.

Birnbaum: I have the same doubts about reported differences. I would prefer to see some more replicates. My experience with natural sea water exposures show appreciable variation in results. With respect to poor performance of formula 105 on the rotor test, this would be expected. Although formula 105 test panels perform well for as much as two or three years in Miami, it does not last more than a year on a ship. I think the reason is that formula 105 is a soft film which erodes and leaches very rapidly. I believe considerably more data must be collected for correlation between rotor tests and predictability of ship performance. I do feel that rotor test data is valuable because it simulates ships in motion.

Question: I just want to make one more remark from a theoretical point of view. It is only sensible to do rotor testing because the flow of the sea water along the paint surface on a raft is very low. Thus the diffusion of the cuprous oxide is determined by the laminal layer on the surface of the paint and on a ship that laminal layer is turbulent.

Christie: To what extent are algae present at your test site?

Dick: Very limited because if you have a strong hard fouling community, you do not have soft fouling which is more prevalent in cooler waters.

Christie: We find that in general algae fouling is more difficult to control than the hard fouling.

Dick: In proceeding to the second step of this study, we would make comparable exposures in cooler waters at Doxbury, Mass., perhaps Long Beach, California. We have many exposure stations. These were only conducted at Daytona in the sub-tropical.

Birnbaum: How far below the surface were the rotor panels exposed?

Dick: About two feet. All that we are doing is depleting toxicant. We are trying to get it out as quickly as possible so I do not think that depth is going to be important as long as they stay wet.

Crisp: The problem of the interaction of the anti-corrosive and the anti-fouling coat can be overcome if you put your anti-fouling directly onto a non-corrosive material like phenolformaldahyde. This enables you to tell especially in comparison between a system based on anti-corrosives whether or not your failure is due primarily to the corrosion failure or to the fouling failure.

Kühne: You pointed out the good performance of the paint containing organic tin compounds. It is said that they are susceptible to ultra-violet radiation. Have you any evidence that ultra-violet radiation could affect this performance?

Dick: Ultra-violet falls off quickly as a function of depth. I do not think it is applicable in this circumstance at least to the point where it would affect the results of the study. I do not have specific information, but I do not think it would be germane.

Smith: Paint technologists have two problems. One is to test AF's and one is to test anti-corrosives. While your method I think is very good for anti-fouling, one of the major problems in the coating field to my mind is an accelerated test for anti-corrosive paints. Could I have your comments on how far you think this method does provide really good data on high performance or the differences in performance on high performance anti-corrosive systems?

Dick: If you would allow me the assumption that you can test anti-corrosives without an anti-fouling on them and I am not really convinced you can, then I would say putting them on the rotor just as a physical deterioration mechanism will on an accelerated basis predict the life of the anti-corrosive part of the system. But as I say, I do not think you can legitimately do that. You have to have that anti-fouling paint on it because that is what you see in service.

Smith: I agree you must have anti-fouling. Say you wanted to compare vinyls versus epoxy pitches versus urathane pitches as anti-corrosives. Is your method going to be useful if you topcoated these with standard anti-fouling and thus eliminated the AF factor that way, and what sort of acceleration factor do you reckon you are getting for the anti-corrosive performance alone?

Dick: No accelerated test by my standards is ever going to give you an index, a definite index to performance. Your idea of using one standard anti-fouling certainly is legitimate and I probably would buy that if the focus of your study is to test just the anti-corrosive. In this study, it was to test the entire system as it was applied to a navigational device.

Poretz: You stated that the rotor is in dynamic action for a month and static for a month. I would presume you chose this sequence because of convenience. Is that the reason or did you have any other?

Dick: It was convenience.

Poretz: Now if you leave it static for a month and the samples are very close to each other, you are going to get some sort of diffusion. Do you think this can affect results?

Dick: To test that, I made an initial run of panels with little windows in with no anti-fouling top coat. There was no throwing power even within one panel to that square that did not have anti-fouling. Therefore, I think it is legitimate that the current of the river is giving it a fresh bath constantly and that there is no complementary action from one system to another.

Poretz: That is what I was concerned with, but how far apart were your window panels?

Dick: The rotor panels are side by side.

Poretz: The other test you just mentioned to test diffusion?

Dick: Well, they are exposed in duplicate on different racks so that one might be in one bay, its duplicate might be 40 feet away.

Poretz: But they were not subjected to the dynamic action that you had on each of the panels. It is not the same condition--it is different. It is possible that you might get different results.

Birnbaum: Based on Navy experience over the past twenty years we have come to the conclusion that if you take static panels and keep them at least three inches apart there is no effect on adjacent panels with cuprous oxide containing AF paints. However, we do not have sufficient data on organo-metallic containing paints.

SUMMARY OF THE CONGRESS

by Monsieur V. Romanovsky

International Chairman for the Congress

and Chairman of the Permanent International Committee for Research on Preservation of Materials in the Marine Environment (international sponsoring organization for these quadrennial congresses).

Monsieur Romanovsky kindly agreed to serve as Rapporteur General for the Third International Congress on Marine Corrosion and Fouling. His summarizing comments are found on the pages which follow.

Rapport général prononcé le jeudi 5 octobre 1972

par V. ROMANOVSKY

Président du Comité International Permanent
pour la Recherche sur la Préservation des Matériaux en Milieu Marin

Messieurs les Président,
Mesdames, Messieurs,

Contrairement à mon habitude, et je vous prie de m'en excuser, je ferais appel à quelques feuilles de papier pour vous parler car j'ai eu très peu de temps pour rédiger ce rapport, les dernières communications viennent tout juste de prendre fin.

Je n'ai peut être pas pu assimiler correctement toutes les idées qui ont été émises, mais j'essayerai de faire de mon mieux. Je sollicite toute votre indulgence en ce qui concerne l'imperfection de ce rapport général.

Toutes les communications que j'ai entendues étaient bonnes, certaines excellentes. Malheureusement je n'ai pas pu les entendre toutes car je n'ai pas la faculté de me partager en deux pour participer aux travaux de deux salles. J'ai été aidé par mes amis Messieurs B. Callame et G. Decheux qui m'ont apporté des résumés et leurs impressions générales. Je tiens à les remercier ici.

Je ne me propose pas d'analyser les diverses communications, ce serait trop long, trop fastidieux et je n'ai pas la compétence pour cela. Je me contenterai de développer quelques idées, d'indiquer les tendances générales qui se sont manifestées au cours de ce Congrès et de mettre l'accent sur les progrès qui ont été réalisés depuis huit ans, c'est-à-dire depuis le 1er Congrès de Corrosion Marine et des Salissures qui avait été organisé à Cannes en 1964.

Pour faciliter mon exposé et ne pas dépasser le temps qui m'a été imparti, je diviserai mon rapport en deux parties, relatives respectivement à la corrosion et aux salissures. Les couleurs des salles formant des couleurs complémentaires, je pense que les travaux qui y furent poursuivis le sont aussi.

En ce qui concerne la corrosion, il faut noter que les recherches de base ont fait l'objet de nombreuses communications. Dans l'étude des métaux, les auteurs se sont surtout attachés à celles des alliages de cuivre et des alliages d'aluminium. Au cours des séances, des idées nouvelles ont apparu et des dispositifs originaux et ingénieux ont été proposés. Dans la théorie de la corrosion sous tension, une synthèse générale a même pu être élaborée. Il faut noter que depuis le dernier congrès, les progrès dans les recherches fondamentales ont été très rapides. Nous avons, entre autres, entendu une remarquable communication sur la cavitation avec d'excellentes photographies obtenues au microscope électronique à balayage de champ. Dans le domaine de la protection cathodique, si certaines communications n'ont été consacrées qu'à des observations fragmentaires, d'autres très importantes ont abordé des idées générales et nous ont proposé la description d'appareils pratiques et efficaces.

En ce qui concerne les revêtements, on pourrait déplorer que relativement peu de communications ont été consacrées à ce sujet. Nous avons écouté de très bonnes communications à caractère commercial, mais nous pourrions regretter que le secret, qui s'y attache toujours, leur enlève une grande partie de leur portée scientifique.

Les matériaux sont appelés à travailler en mer à faible, moyenne ou grande profondeur, aussi avons-nous entendu de très intéressantes communications sur les observations réalisées dans ces milieux.

Il y eut également quelques communications consacrées à la tenue du béton dans l'eau de mer et à la corrosion des matériaux dans les installations de dessalement de l'eau de mer.

Pour terminer avec la section de la corrosion et pour reprendre l'observation d'un éminent conférencier, je dirais que la recherche de base est, après ce Congrès, très avance sur l'expérimentation et sur les applications pratiques.

Dans la session réservée aux salissures, on a beaucoup parlé également de recherches fondamentales, mais celles-ci ont souvent été envisagées comme devant aboutir à des applications pratiques à plus ou moins longue échéance.

L'étude du processus de fixation des salissures, et surtout des balanes, a été abordée sous un aspect très scientifique, faisant appel à des notions de chimie et de physique. Ces études permettront certainement un jour d'améliorer les procédés anti-salissures.

En écologie de nombreux documents ont apporté des connaissances sur la répartition, les périodes de fixation et l'abondance des salissures. Comme pour la corrosion, le domaine offshore n'a pas été oublié.

Un certain nombre de communications de très grande valeur a été consacré au rôle du film primaire. Les microbiologistes, qui nous ont exposé leurs idées, n'ont pas hésité à faire appel à la chimie et même à rechercher des analogies avec ce qui se passe dans le milieu sanguin.

Dans le domaine des perforants, nous avons pu admirer un film magnifique et entendre des exposés sur les conditions d'attaque du bois, sur la biologie des tarets et sur leur répartition. Il s'agit là d'un problème dont l'intérêt ne peut échapper à personne.

Certains conférenciers ont proposé des procédés de protection contre les salissures sur les carènes, dans les conduites et sur les structures immergées.

L'examen des communications de la session des salissures suggère quelques idées générales :

1. Très grande importance des recherches fondamentales.
2. Utilisation de techniques nouvelles telles, par exemple, le microscope électronique à balayage de champ ou la cinématographie microscopique.
3. Le peu de communications consacrées à des procédés nouveaux de protection.
4. L'importance de la microbiologie et ses applications à la fixation des salissures.

***
*

Si l'on examine enfin les résultats des travaux de l'ensemble de ce Congrès, on peut constater qu'il a été surtout celui de la recherche fondamentale sans laquelle nul progrès ne peut être réalisé dans les applications pratiques. On remarque aussi que relativement peu de communications ont été consacrées aux revêtements et aux carènes des navires. Il y a là très nettement une différence par rapport aux congrès précédents. On assiste, je pense, à une évolution dans nos recherches. D'empiriques d'abord à l'origine, elles tendent de plus en plus à se rattacher à des bases fondamentales. Je suis persuadé que, dans quatre ans, les progrès de la recherche fondamentale vont se poursuivre, mais on assistera également à une progression des applications de la recherche de base dans des domaines expérimentaux.

Je souhaite que des liens étroits s'établissent et s'intensifient entre laboratoires de divers pays pour promouvoir une recherche coopérative et éviter les dispersions.

***
*

Il ne me reste plus qu'une tâche très agréable à accomplir, celle de remercier tous ceux qui nous ont accueillis ici.

Je voudrais, à titre de Président du Comité International Permanent, promoteur de ce Congrès, être l'interprète de tous les Congressistes pour remercier les organisateurs. Il m'est agréable de souligner que l'organisation de ce Congrès a été absolument parfaite. J'ai pu apprécier dans les salles, dans les couloirs ou dans la cafeteria, la satisfaction totale inscrite sur les visages des participants. Ce Congrès a été une réussite totale. J'ai été très sensible à la gentillesse des organisateurs, cette gentillesse allait surtout aux Européens qui, venus de loin, certains pour la première fois, pouvaient se trouver un peu dépaysés. Les organisateurs ne les ont jamais laissés dans l'embarras. Même les frontières des langues ont été abolies. Vous avez accueillis vos ancêtres européens avec une gentillesse et une compréhension vraiment touchante. Personnellement j'ai été comblé car, lorsque je demandais quoi que ce soit, mon désir était immédiatement exaucé.

Il m'est impossible de remercier individuellement tous les organisateurs et j'aurais bien trop peur d'en oublier, aussi je demanderais à mes amis les Docteurs R. Acker, J. de Palma et W. Iverson d'être mes interprètes auprès de tous ceux qui les ont aidés. Je ferai peut être une exception, et je suis sûr que vous ne m'en voudrez pas, pour remercier Madame S. Torrence qui a été responsable de toutes les réceptions et qui avait organisé le banquet d'hier soir.

C'est donc avec une grande tristesse que nous allons nous quitter mais cette séparation nous sera moins pénible car nous garderons de cette réunion un souvenir inoubliable.

Il ne me reste plus qu'à vous donner rendez-vous au prochain congrès, le 4ème, qui aura lieu à Athènes, en Grèce, en 1976.

Acrylic resin, hydrophilic, 14
Adhesives, 653,691
Adhesion mechanisms, 691
Algal fouling, 88,719,757,898
Alloys, 2,125,594
Alloys, aluminum, 125
Alloys, stainless steel, 2
Alloy theory, 410
Aluminum, 499
Aluminum alloys, 125
Aluminum craft and boat hulls, 125
Aluminum radar antennas, 125
Anaerobic corrosion, 61
Anodes, 176,331
Anodes, galvanic, 176
Anodizing light metals, 538
Anticorrosion, 930
Antifoulant, 731,956
Antifouling, 14,648,731,757,880,898 930,956,964,995,1005
Antifouling coatings, 898,956,1005
Antifouling efficacy, 14
Antifouling, electrolytic 331,964,995
Antifouling paints, 898,930,956,1005
Antifouling screening test, 956
Antifouling test, 956,1005
Antifouling toxicants, 956,1005
Argentina, 842,930
Arrays, 48
Artemia salina, 956
Attachment, 617,625,633,640

Bacteria, 2,61,598,610,625,633,767, 778,898
Bacterial cellulase, 778
Bacterial corrosion, 61
Bacterial mobilization of mercury, 767
Balanus, 48,88,653,691,731,744,806
Bankia, 48,822
Barnacle adhesives, 691
Barnacles, 48,88,653,691,731,744,806
Beaufort, North Carolina, 906
Bioadhesion, 633,691
Bioassay, 956
Biodegradation, 640
Biofouling assemblages, 731,906
Biomass, 731
Bitunicate asci, 640
Bonding, 653
Borer digestion, 778
Breakdown of substrate, 39
Bryozoa, 88,757,898
Burrowing clams (Martesia), 2,842

Calcium secretion, 806
Cargo/ballast tanks, 191
Cathodic-anodic protection, 538
Cathodic protection, 103,176,191, 202,322,338,578
Cavitation, 439
Cellulase, 778
Celluloytic bacteria, 778
Chelura terebrans, 814
Chemical inhibitors, 806
Chemisorption, 410
Chemotaxis, 617
Chesapeake Bay, 767
Chesapeake Bay and mercury, 767
Chlorella ellipsoidea, 956
Chlorination, 357,757,880
Chlorine injection, 88
Chromium in copper-nickel alloys, 264
Cilicaeopsis sp., 814
Cirrepede (cirreped), 653,898
Coastal fouling rate, 865
Coating index, 103
Coatings, antifouling, 898,930,956, 1005
Coatings, inhibitive, 125
Coatings for low carbon steel, 158
Coatings, metallic, 158
Cold-water fouling growth form, 865
Concrete, 215,226
Concrete, reinforced, 215,226
Concrete, steel corrosion in, 215
Condenser tube test, 313
Condensers, 322
Copper, 427
Copper alloys, 299
Copper casting alloy, 277
Copper-nickel alloys, 241,264,285,410
Copper-nickel alloys, erosion, 285
Copper-nickel alloys, velocity testing, 277,285
Copper-nickel base quinary alloy, 277
Copper tolerance, 719
Corrosion fatigue, 462,549
Corrosion products, 427
Corrosion, oxygen effects in, 562
Corrosion testing, 578
Crack velocity, 514
Crevice corrosion, 313
Critical surface tension, 633
Crosslinking, 653
Crustecdysone, 744
Crude oil tankers, 191
Cupro-nickel boat hull, 2
Current meters, 48

Dam Neck, Virginia, 103
d-Bands, 410
Deep sea corrosion, 562,578
Deep sea wood borers, 836
Deliquescing asci, 640
Depolarizing agent, 61
Desalination, 331,338,357
Design concepts for marine construction, 234
Desulfovibrio desulfuricans, 2,61
Dezincification of brasses, 311
Diatoms, 610,898
Dissolved organics, 710
Drag reducing polymers, 14

Ectocarpus, 39,88,674,682
Electric power intakes, 757
Electrochemistry of corrosion, 365
Electrolytic antifouling, 331,964,995
Electrolyzed sea water, 964
Electrophoresis, 710
ENKOTAL process, 311
Enteromorpha, 39,88,674,682
Enteromorpha intestinalis, 674
Enzymes, 653
Epifauna, 731
Epoxy resin repairs, 226
Erosion, 285,439
Exfoliation, 125
Exosphaeroma alata, 814

Film forming, 598,610,617,625,633
Fine-structure, 674
Fishing fleet, fouling of, 898
Fouling community, 906
Fouling of fishing fleet, 898
Fouling forecasting, 865
Fouling growth form, mid-ocean island, 865
Fouling growth form, warm water 865
Fouling, molecular, 710
Fouling test model, warm water 865
Frictional resistance, 14,898

Galvanic anodes, 176
Galvanized steel reinforcement, 215
Gelbstoff, 822
Germination, 39,640

Heat exchangers, 322
Heat transfer, 313
Heating, intermittent, 88,357
Histochemistry, 653
Hydroblasting, 33
Hydroids, 88,731,757,898
Hydrolysis, 653
HYDRON (R), 14
Hydrophilic acrylic resin, 14
Hypochlorite, electrolytic, 995

Iais sp, 814
Impingement, 264,313,338
Impressed current, 338
Infrared spectra, 633
Intermittent chlorination, 357
Intermittent heating, 88,357
Iron injection, 322

Laminar sublayer, 14
LaPlata, Argentina, 930
Larvae, 822
Light metals, 538
Lignicolous marine fungi, 640
Limnoria tripunctata, 814
Localized corrosion, 365
Lyrodus pedicellatus, 797

Macromolecular adsorption, 710
Macro-roughness, 14
Marine borers, 48,778
Marine boring and fouling mollusks, 83,836
Martesia striata, 2,842
Materials for marine construction, 234
Mercury metabolism, 767
Meroplankton, 731
Metal oxides, 427
Microbial fouling, 598,610,617, 625,898
Microfouling, 598,898
Micro-roughness, 14
Molecular fouling, 710
Mollusks, marine boring and fouling, 83,836
Moorings, 549
Moulting, 744
Mutation, 719
Mytilus, 88

Neuroendocrine regulation, 842
North Carolina, Beaufort, 906

Oceanic stalk barnacles (Lepas sp.), 88
Open sea fouling rate, 865
Orchestia sp., 814
Organic photodegradation, 710
Oxide films, 499
Oxygen concentration, 562
Oxygen effects in corrosion, 562

Paints, antifouling, 898,930,956,1005
Periphytes, 598
Phenylmercuric acetate (PMA), 767
Pinctada margitifera, 880
Plastic deformation, 514
PMA decomposition, 767
Polarization techniques, 103
Polyanionic carbohydrates, 598
Population, 719
Port Alfred Harbor, 202
Power stations, 757,847,880
Pre-fracturees, electrolytiquement, 499
Pre-fracturees, eprouvettes, 499
Pre-fracturees, mecaniquement, 499
Preservative tolerance, 640
Primary films, 598,610,617,625,633
Protective coatings, 103,578
Protective coatings for aluminum, 125
Protective coating, underwater, 120
Proteins, 633,653

Quinones, 653

Reference electrodes, 176
Reinforced concrete, 215,226
Reinforced concrete repairs, 226
Reinforcement, galvanized steel, 215
Repassivation, 514
Reproductive anecdysis, 744
Reproductive cycle, 842
Residual resistance, 14
Rhizoids, 39
Rigid band model, 410

Scale prevention, electrolytic, 331
Scanning electron microscopy, 39
Seasonal progressir , 906
Seasonal succession, 906
Secondary production, 731
Sedentary organisms, 648
Selection, 719
Settlement, 640,648,674,682,757, 822,930
Ship bottom smoothness, 14,33
Ship fouling algae, 39,719
Ship resistance, 14
Shipworm, 83,778,797,814,822
Sorption, 610,617,625
Spectroscopy, 653
Speed effects in settling, 757
Sphaeroma, 814
Spirorbis (tubeworm), 88
Spore dispersal, 640
Spore liberation, 640
Spore morphology, 640
Stainless steel, 2,528,594
Stainless steel alloys, 2,528
Steel corrosion in concrete, 215
Stress corrosion cracking, 462,499,514, 549
Structure, fouling, 757,847
Structures sous-marines, 578
Substrate penetration, 39
Sulfate reducing bacteria, 2,61
Surface activity, 710
Surface charge, 710
Surface chemistry, 633
Surface preparation, 88
Surface roughness, 14
Surface roughness, causes of, 33
Surfaces, 38
Swarmer settlement, 682
Syncassidina aestauria, 814

Teredindae control, 83,778
Teredinidae life history, 83
Teredinids, 83,778
Teredo, 822
Teredo navalis, 797,822
Test concepts, 234
Thigmotaxis, 674
Titanium, 2
Toxic surfaces, 357
Tubeworm (Spirorbis), 88
Tunneling, 797

velocity testing, 357

Warm water fouling growth, 865
Warm water fouling test, 865
Water cooling system, fouling of, 880
Water masses, 731
Water velocity, 682
Wood and algae as nutrients, 814
Wood borers, 83,778,797,814,836,842

Xenostrobus securis, 880
Xylophaga, 48,836
Xylophaga washingtona, 48

Zinc, 427
Zoospores, 39,674
Zygotes, 39